

THERMAL ENERGY SYSTEMS

Design and Analysis

SECOND EDITION



Steven G. Penoncello



CRC Press
Taylor & Francis Group

Thermal Energy Systems

Design and Analysis

Second Edition



Taylor & Francis

Taylor & Francis Group

<http://taylorandfrancis.com>

Thermal Energy Systems

Design and Analysis

Second Edition

Steven G. Penoncello

*Professor Emeritus
University of Idaho
Moscow, Idaho, USA*



CRC Press

Taylor & Francis Group
Boca Raton London New York

CRC Press is an imprint of the
Taylor & Francis Group, an **informa** business

CRC Press
Taylor & Francis Group
6000 Broken Sound Parkway NW, Suite 300
Boca Raton, FL 33487-2742

© 2019 by Taylor & Francis Group, LLC
CRC Press is an imprint of Taylor & Francis Group, an Informa business

No claim to original U.S. Government works

Printed on acid-free paper

International Standard Book Number-13: 978-1-138-73589-7 (Hardback)
International Standard Book Number-13: 978-1-315-18626-9 (eBook)

This book contains information obtained from authentic and highly regarded sources. Reasonable efforts have been made to publish reliable data and information, but the author and publisher cannot assume responsibility for the validity of all materials or the consequences of their use. The authors and publishers have attempted to trace the copyright holders of all material reproduced in this publication and apologize to copyright holders if permission to publish in this form has not been obtained. If any copyright material has not been acknowledged please write and let us know so we may rectify in any future reprint.

Except as permitted under U.S. Copyright Law, no part of this book may be reprinted, reproduced, transmitted, or utilized in any form by any electronic, mechanical, or other means, now known or hereafter invented, including photocopying, microfilming, and recording, or in any information storage or retrieval system, without written permission from the publishers.

For permission to photocopy or use material electronically from this work, please access www.copyright.com (<http://www.copyright.com/>) or contact the Copyright Clearance Center, Inc. (CCC), 222 Rosewood Drive, Danvers, MA 01923, 978-750-8400. CCC is a not-for-profit organization that provides licenses and registration for a variety of users. For organizations that have been granted a photocopy license by the CCC, a separate system of payment has been arranged.

Trademark Notice: Product or corporate names may be trademarks or registered trademarks, and are used only for identification and explanation without intent to infringe.

Library of Congress Cataloging in Publication Data

Names: Penoncello, S. G. (Steven G.), author.
Title: Thermal energy systems : design and analysis / Steven G. Penoncello.
Description: Second edition. | Boca Raton : Taylor & Francis, CRC Press, 2018. | Includes bibliographical references and index.
Identifiers: LCCN 2018014278 | ISBN 9781138735897 (hardback : alk. paper) | ISBN 9781315186269 (e-book)
Subjects: LCSH: Heat engineering. | Heat--Transmission. | Thermodynamics--Data processing.
Classification: LCC TJ260 .P38 2018 | DDC 621.402--dc23
LC record available at <https://lccn.loc.gov/2018014278>

Visit the Taylor & Francis Web site at
<http://www.taylorandfrancis.com>

and the CRC Press Web site at
<http://www.crcpress.com>

Contents

Preface to the Second Edition.....	xiii
Acknowledgments	xvii
Author	xix

1. Introduction	1
1.1 Thermal Energy Systems Design and Analysis	1
1.2 Software.....	2
1.2.1 Engineering Equation Solver (EES).....	2
1.2.2 REFPROP.....	2
1.2.3 CoolProp	3
1.2.4 User-Written Libraries.....	3
1.2.5 Software Approach Taken in This Book.....	3
1.3 Thermal Energy System Topics.....	3
1.4 Units and Unit Systems	4
1.5 Properties of Working Fluids in Thermal Energy Systems	6
1.5.1 Thermodynamic Properties	7
1.5.1.1 Thermodynamic Properties in the Two-Phase Region.....	8
1.5.1.2 Important Thermodynamic Property Relationships	9
1.5.2 Evaluation of Thermodynamic Properties.....	10
1.5.2.1 The Real Fluid Model	10
1.5.2.2 The Incompressible Substance Model	11
1.5.2.3 Estimation of Liquid Properties	13
1.5.2.4 The Ideal Gas Model	16
1.5.3 Transport Properties.....	22
1.5.3.1 Dynamic Viscosity	22
1.5.3.2 Kinematic Viscosity	23
1.5.3.3 Newtonian and Non-Newtonian Fluids.....	24
1.5.3.4 Thermal Conductivity	25
1.6 Engineering Design and Analysis.....	26
1.6.1 Workable Designs	27
1.6.2 Optimum Designs	29
1.6.3 Engineering Design and Environmental Impact	30
References	31
Problems.....	31

2. Engineering Economics.....	41
2.1 Introduction	41
2.2 Engineering Economics Nomenclature	41
2.3 The Cash Flow Diagram	42
2.4 The Time Value of Money.....	43
2.4.1 Future Value of a Present Sum: The Single Payment Compound Amount Factor.....	44
2.4.2 Present Value of a Future Sum: The Present Worth Factor.....	46
2.4.3 Future Value of a Uniform Series: The Compound Amount Factor.....	46

2.4.4	An Equivalent Uniform Series That Represents a Future Value: The Uniform Series Sinking Fund Factor.....	48
2.4.5	Present Value of a Uniform Series: The Uniform Series Present Worth Factor	48
2.4.6	An Equivalent Uniform Series That Represents a Present Value: The Capital Recovery Factor.....	49
2.4.7	Present Value of a Uniform Linearly Increasing Series—The Gradient Present Worth Factor	49
2.4.8	Summary of Interest Factors	50
2.5	Nominal and Effective Interest Rates	51
2.6	Time Value of Money Examples.....	51
2.7	Using Software to Calculate Interest Factors	55
2.8	Economic Decision Making.....	56
2.8.1	Present Worth Analysis	57
2.8.2	Annual Cost Analysis	61
2.8.3	Selection of Alternatives	64
2.9	Depreciation and Taxes	64
2.9.1	After-Tax Cash Flow	64
2.9.2	Straight-Line Depreciation (SLD).....	65
2.9.3	Sum of the Years' Digits (SYD).....	65
	Reference	70
	Problems.....	70
3.	Analysis of Thermal Energy Systems	79
3.1	Introduction	79
3.2	Nomenclature	79
3.3	Analysis Procedure.....	80
3.4	Conserved and Balanced Quantities.....	81
3.4.1	The Generalized Balance Law	81
3.5	Conservation of Mass.....	82
3.6	Conservation of Energy	86
3.7	The Entropy Balance (The Second Law of Thermodynamics).....	94
3.7.1	The Reversible and Adiabatic Process	96
3.7.2	Isentropic Efficiencies of Flow Devices.....	97
3.7.2.1	Turbines	97
3.7.2.2	Compressors, Pumps, and Fans	98
3.7.2.3	Nozzles.....	99
3.7.2.4	Diffusers	100
3.7.3	Heat Exchanger Effectiveness	103
3.7.3.1	Effectiveness of a Counter Flow Heat Exchanger.....	109
3.7.3.2	Effectiveness of a Parallel Flow Heat Exchanger.....	113
3.7.3.3	Significance of the Pinch Point Temperature Difference and Effectiveness.....	115
3.8	The Exergy Balance—The Combined Law.....	116
3.8.1	What Is Exergy?	117
3.8.1.1	The Thermodynamic Definition of Exergy	118
3.8.2	The Exergy Balance	118
3.8.3	Exergy Accounting and Exergy Flow Diagrams.....	122

3.8.4	Exergetic Efficiencies of Flow Devices.....	123
3.8.4.1	Turbines	123
3.8.4.2	Compressors, Pumps, and Fans	123
3.8.4.3	Heat Exchangers.....	123
3.9	Energy and Exergy Analysis of Thermal Energy Cycles	126
3.9.1	Cycle Energy Performance Parameters	127
3.9.1.1	Maximum Thermal Efficiency of a Cycle	129
3.9.2	Exergetic Cycle Efficiency	132
3.9.2.1	Power Cycles	132
3.9.2.2	Refrigeration and Heat Pump Cycles.....	134
3.9.2.3	Significance of the Exergetic Cycle Efficiency.....	135
3.9.2.4	The Energy/Exergy Conundrum.....	136
3.10	Analysis of Thermal Energy Systems	137
3.10.1	Analysis of an Engine and Radiator System.....	138
3.10.2	Analysis of a Brine Chilling System for Ice Rink Manufacture.....	143
3.10.3	Analysis of a Gas Turbine System for Power Delivery	149
	References	157
	Problems.....	157
4.	Fluid Transport in Thermal Energy Systems	175
4.1	Introduction	175
4.2	Piping and Tubing Standards.....	175
4.3	Fluid Flow Fundamentals.....	177
4.3.1	Head Loss due to Friction in Pipes and Tubes	179
4.4	Valves and Fittings.....	190
4.4.1	The Hooper 2K Method	192
4.4.2	The Darby 3K Method.....	195
4.4.3	Reducers and Expansions.....	198
4.4.4	Check Valves.....	198
4.4.5	Branch Fittings—Tees and Wyes	200
4.5	Design and Analysis of Pipe Networks.....	204
4.5.1	Parallel Pipe Networks.....	208
4.6	Economic Pipe Diameter.....	213
4.6.1	Cost of a Pipe System	214
4.6.2	Determination of the Economic Diameter	214
4.6.3	Cost Curves.....	221
4.6.4	Economic Velocity Range	223
4.7	Pumps.....	225
4.7.1	Types of Pumps.....	225
4.7.2	Dynamic Pump Operation.....	225
4.7.2.1	Dynamic Pump Performance.....	227
4.7.3	Manufacturer's Pump Curves.....	230
4.7.4	The System Curve.....	231
4.7.4.1	System Curve for a Two-Tank System Open to the Atmosphere.....	231
4.7.4.2	System Curve for a Closed-Loop System.....	234
4.7.5	Pump Selection.....	235
4.7.6	Cavitation and the Net Positive Suction Head	240
4.7.6.1	Calculating the NPSHa	241

4.7.7	Series and Parallel Pump Configurations	245
4.7.8	Affinity Laws.....	249
4.8	Design Practices for Pump/Pipe Systems	253
4.8.1	Economics	254
4.8.2	Environmental Impact	254
4.8.3	Noise and Vibration.....	254
4.8.4	Pump Placement and Flow Control	254
4.8.5	Valves.....	255
4.8.6	Expansion Tanks and Entrained Gases.....	255
4.8.7	Other Sources for Design Practices.....	255
	References	256
	Problems.....	256
5.	Energy Transport in Thermal Energy Systems	277
5.1	Introduction	277
5.2	Heat Transfer Analysis of Heat Exchangers.....	277
5.2.1	Thermal Resistance.....	279
5.2.2	The Convective Heat Transfer Coefficient.....	284
5.2.2.1	Entry Length.....	285
5.2.2.2	Forced External Cross Flow over a Cylindrical Surface	286
5.2.2.3	Forced Internal Laminar Flow—Combined Entry.....	286
5.2.2.4	Forced Internal Laminar Flow—Thermal Entry	287
5.2.2.5	Forced Internal Turbulent Flow	287
5.3	Fouling on Heat Exchanger Surfaces	289
5.4	The Overall Heat Transfer Coefficient	289
5.5	Heat Exchanger Types	294
5.5.1	Double Pipe Heat Exchanger.....	294
5.5.2	Shell and Tube Heat Exchanger	295
5.5.3	Plate and Frame Heat Exchanger.....	297
5.5.4	Cross Flow Heat Exchanger	297
5.6	Design and Analysis of Heat Exchangers	298
5.6.1	A Heat Exchanger Design Problem.....	299
5.6.2	A Heat Exchanger Analysis Problem.....	300
5.6.3	Heat Exchanger Heat Transfer Analysis.....	300
5.6.3.1	Logarithmic Mean Temperature Difference	301
5.6.4	The LMTD Heat Exchanger Model	306
5.6.5	Effectiveness-NTU Heat Exchanger Model	308
5.7	Special Application Heat Exchangers	315
5.7.1	Counter Flow Regenerative Heat Exchanger	315
5.7.2	Heat Exchangers with Phase Change Fluids: Boilers, Evaporators, and Condensers.....	320
5.8	Double Pipe Heat Exchanger Design and Analysis.....	327
5.8.1	Double Pipe Heat Exchanger Diameters	327
5.8.2	Overall Heat Transfer Coefficients for the Double Pipe Heat Exchanger	330
5.8.3	Hydraulic Analysis of the Double Pipe Heat Exchanger	330
5.8.3.1	Hydraulic Consequences of Fouling	331
5.8.3.2	Pressure Drop through the Inner Tube.....	333
5.8.3.3	Pressure Drop through the Annulus	333

5.8.4	Fluid Placement in a Double Pipe Heat Exchanger	340
5.8.5	Double Pipe Heat Exchanger Design Considerations	340
5.8.6	Computer Software for Design and Analysis of Heat Exchangers	341
5.8.7	Double Pipe Heat Exchanger Design Example.....	342
5.8.7.1	Fluid Properties	342
5.8.7.2	Fluid Placement	343
5.8.7.3	Determination of Pipe and/or Tube Sizes	344
5.8.7.4	Calculation of Annulus Diameters.....	346
5.8.7.5	Calculation of Reynolds Numbers.....	346
5.8.7.6	Calculation of Friction Factors	346
5.8.7.7	Calculation of Nusselt Numbers.....	346
5.8.7.8	Calculation of Convective Heat Transfer Coefficients	346
5.8.7.9	Calculation of Overall Heat Transfer Coefficients.....	346
5.8.7.10	Application of the Heat Exchanger Model	347
5.8.7.11	Heat Exchanger Length.....	348
5.8.7.12	Calculation of Pressure Drops through the Heat Exchanger..	349
5.8.7.13	Design Specifications of the Heat Exchanger.....	349
5.8.8	Double Pipe Heat Exchanger Analysis Example.....	350
5.8.8.1	Initial Guess of the Fluid Outlet Temperatures	350
5.8.8.2	Fluid Properties	350
5.8.8.3	Calculation of Annulus Diameters.....	350
5.8.8.4	Calculation of Fluid Velocities.....	351
5.8.8.5	Calculation of Reynolds Numbers.....	351
5.8.8.6	Calculation of Friction Factors	351
5.8.8.7	Calculation of Nusselt Numbers.....	351
5.8.8.8	Calculation of Convective Heat Transfer Coefficients	351
5.8.8.9	Calculation of Overall Heat Transfer Coefficients.....	351
5.8.8.10	Calculation of the UA Values.....	352
5.8.8.11	Application of the Heat Exchanger Model	352
5.8.8.12	Calculation of the Pressure Drops.....	352
5.8.8.13	Heat Exchanger Specifications and Performance	352
5.9	Shell and Tube Heat Exchanger Design and Analysis	352
5.9.1	LMTD for Shell and Tube Heat Exchangers	357
5.9.2	Tube Side Analysis of Shell and Tube Heat Exchangers	357
5.9.3	Shell Side Analysis of Shell and Tube Heat Exchangers	358
5.9.4	Shell and Tube Heat Exchanger Design Considerations.....	361
5.9.4.1	Tube Side Considerations	361
5.9.4.2	Shell Side Considerations.....	361
5.9.4.3	General Considerations	361
5.9.5	Shell and Tube Heat Exchanger Design.....	362
5.9.6	Shell and Tube Heat Exchanger Analysis.....	362
5.9.6.1	Initial Guess of the Fluid Outlet Temperatures	362
5.9.6.2	Fluid Properties	363
5.9.6.3	Shell and Tube Parameters.....	363
5.9.6.4	Fluid Velocities	364
5.9.6.5	Calculation of Reynolds Numbers.....	364
5.9.6.6	Calculation of Friction Factors	364
5.9.6.7	Calculation of Nusselt Numbers.....	365
5.9.6.8	Calculation of Convective Heat Transfer Coefficients	365

5.9.6.9	Calculation of the Overall Heat Transfer Coefficients	365
5.9.6.10	Calculation of the UA Values.....	365
5.9.6.11	Application of the Heat Exchanger Model	366
5.9.6.12	Calculation of Pressure Drops.....	367
5.9.6.13	Design and Analysis Checks.....	368
5.9.6.14	Summary of Results.....	369
5.10	Plate and Frame Heat Exchanger Design and Analysis.....	369
5.10.1	Plate and Frame Heat Exchanger Dimensions	371
5.10.2	Thermal Performance of a Plate and Frame Heat Exchangers.....	373
5.10.3	Hydraulic Performance of a Plate and Frame Heat Exchanger.....	375
5.10.4	Plate and Frame Heat Exchanger Analysis.....	376
5.10.4.1	Initial Guess of the Fluid Outlet Temperatures	377
5.10.4.2	Fluid Properties	377
5.10.4.3	Calculation of the Hydraulic Diameter of the Channel	378
5.10.4.4	Calculation of the Fluid Mass Velocities.....	378
5.10.4.5	Calculation of Reynolds Numbers.....	378
5.10.4.6	Calculation of Nusselt Numbers.....	379
5.10.4.7	Calculation of Convective Heat Transfer Coefficients	379
5.10.4.8	Calculation of the Overall Heat Transfer Coefficients	379
5.10.4.9	Calculation of the UA Values.....	379
5.10.4.10	Application of the Heat Exchanger Model	380
5.10.4.11	Calculation of Pressure Drops.....	381
5.10.4.12	Checks.....	382
5.10.4.13	Summary of Analysis Results	383
5.11	Cross Flow Heat Exchanger Design and Analysis.....	383
	References	389
	Problems.....	390
6.	Simulation, Evaluation, and Optimization of Thermal Energy Systems.....	407
6.1	Introduction	407
6.2	Thermal Energy System Simulation.....	407
6.2.1	Simulation Example: A Pump and Pipe System	408
6.2.2	Modeling Thermal Energy System Equipment.....	414
6.2.2.1	Exact Fitting Method	415
6.2.2.2	Method of Least Squares.....	419
6.2.3	Simulation Example: Modeling of an Air Conditioning System	422
6.2.4	Advantages and Pitfalls of Thermal Energy System Simulation.....	425
6.3	Thermal Energy System Evaluation.....	426
6.4	Thermal Energy System Optimization.....	429
6.4.1	Mathematical Statement of Optimization	429
6.4.2	Closed-Form Solution of an Optimization Problem.....	430
6.4.3	Method of Lagrange Multipliers.....	431
6.4.3.1	Significance of the Lagrange Multipliers.....	438
6.4.4	Formulation and Solution of Optimization Problems Using Software.....	439
	Problems.....	440

Appendix A: Conversion Factors and Constants.....	455
Appendix B: Thermophysical Properties.....	459
Appendix C: Standard Pipe Dimensions.....	527
Appendix D: Standard Copper Tubing Dimensions.....	533
Appendix E: Pump Curves.....	535
Index	595



Taylor & Francis

Taylor & Francis Group

<http://taylorandfrancis.com>

Preface to the Second Edition

This book represents a collection of topics that the author has consistently taught in a senior-level mechanical engineering course on thermal energy system design. Many years of research notes, course notes, and computer code have been distilled into this manuscript.

The design and analysis of thermal energy systems has seen a significant transformation since the advent and widespread availability of the digital computer. Before computational power was at the fingertips of engineers, the design of such systems required extensive hand calculations, plotting performance and system curves, looking for intersection points, etc., to arrive at a design that might work as expected. Digital computing has changed this. Now, engineers can model a thermal system including detailed component performance and system characteristics to solve for operating points without the laborious hand calculations required in the past. Simulation techniques applied to a system model allow the engineer to confidently predict the performance of the system before components are purchased and the system is built. Optimization techniques allow the engineer to consider changing certain system components or parameters to achieve a system that operates with respect to lowest cost, highest thermal efficiency, highest exergetic efficiency, etc. Today's engineer can accomplish all of this using computer software.

This book is intended for senior students in mechanical or chemical engineering. However, it is also appropriate for practicing engineers as a reference. The book is written assuming that the reader has an introductory background in engineering thermodynamics, heat transfer (conduction and convection), and fluid mechanics. Several improvements to the book have been incorporated into this edition based on the feedback of colleagues who adopted the first edition for their courses. The author wishes to thank all of those who provided critical evaluation of the first edition.

Perhaps one of the most significant changes in this edition is the elimination of the Engineering Equation Solver (EES) code for the solution of several of the example problems. Feedback from the first edition made it abundantly clear that other software platforms are preferred. Therefore, the approach in this edition of the book is to focus on the development of the equation set required to conduct a complex thermal energy system design and/or analysis. The solution of the equation set is left to the reader using whatever favorite software is appropriate. Some software options for solving thermal energy system problems are discussed in Chapter 1.

In addition to the software discussion, Chapter 1 introduces the topic of thermal energy systems design and analysis. In this edition, a review of thermodynamic property models used in thermal energy system design and analysis has been moved from Chapter 3 to Chapter 1. Also included in Chapter 1 is an expanded discussion and group-based homework problems on workable and optimum design.

Except for additional end-of-chapter problems, Chapter 2 is virtually unchanged from the previous edition. It provides an introduction to engineering economics. Topics include the time value of money, discrete interest factors, economic decision making, depreciation, and taxes. The goal of this chapter is to give the reader a very basic understanding of the time value of money and how engineering economics plays a role in system design. While these concepts can be stand-alone, there are several places in subsequent chapters where the engineering economy concepts are used.

Chapter 3 provides a brief review of thermodynamic analysis of thermal energy systems, and has been updated to include the concept of heat exchanger effectiveness. The concept of heat exchanger pinch point temperature difference is also introduced in this edition. Chapter 3 also includes an introduction to the concept of exergy and its role in environmental impact and sustainability.

There are *many* types of thermal-fluid energy systems. In fact, there are far too many to include all of them in this book. Therefore, the approach taken in this book is to discuss the basics of fluid and energy transport in thermal energy systems. Chapter 4 covers the basics of fluid transport; the focus is on hydraulic systems including pipe networks, both gravity feed and pump feed. Chapter 4 includes a brief review of the fundamental governing equations for the most common fluid flow scenarios seen in thermal energy systems. In the previous edition of this book, minor losses due to valves and fittings followed the well-known method in Crane Technical Publication 410. This edition of the book replaces the Crane method with the Hooper 2K and Darby 3K methods. The Hooper and Darby methods are preferred in industry because they accommodate a wide range of Reynolds number flows including laminar and transition. By contrast, the Crane method is valid for fully developed turbulent flow.

Chapter 5 covers energy transport in thermal energy systems. The discussion centers around heat exchangers. This chapter provides a brief review of heat exchanger analysis methods including the logarithmic mean temperature difference (LMTD) method and the effectiveness-NTU (ϵ -NTU) method. This chapter also goes into considerable detail for four specific types of heat exchangers commonly seen in industrial applications: double pipe (tube-in-tube), shell and tube, plate and frame, and cross flow. A general heat exchanger model is developed for each of these heat exchanger types including the thermodynamic, heat transfer, and hydraulic performance. Heat exchangers for specialized applications are also discussed including counter flow regenerative heat exchangers, condensers, evaporators, and boilers. This edition includes a significant revision on the topic of plate and frame heat exchangers. The revision provides a much more general approach to the analysis of these types of heat exchangers.

Chapter 6 is an introduction to simulation, evaluation, and optimization of thermal energy systems. Here, many of the concepts in previous chapters are brought together to show how a complete system can be modeled.

More end-of-chapter homework problems have been added to all six chapters in the book.

The material in this book can be covered in a typical 3-credit, 15-week semester (45 class meetings). A typical semester schedule is shown below.

Class Periods	Topics Covered
3	Introductory material (Chapter 1)
5	Engineering economics (Chapter 2)
3	Application of conservation and balance laws (Chapter 3)
1	Review of fluid flow fundamentals (Chapter 4)
2	Minor losses (Chapter 4)
1	Series and parallel pipe networks (Chapter 4)
2	Economic pipe diameter (Chapter 4)
2	Pump performance and selection (Chapter 4)
1	Cavitation (Chapter 4)

(Continued)

Class Periods	Topics Covered
1	Series and parallel pump systems (Chapter 4)
1	The affinity laws for pumps (Chapter 4)
5	Heat exchangers, LMTD, and e-NTU methods (Chapter 5)
1	Regenerative HX, condensers, evaporators, boilers (Chapter 5)
2	Double pipe heat exchangers (Chapter 5)
2	Shell and tube heat exchangers (Chapter 5)
1	Plate and frame heat exchangers (Chapter 5)
1	Cross flow heat exchangers (Chapter 5)
2	Thermal energy system simulation (Chapter 6)
1	Fitting component performance data (Chapter 6)
3	Optimization using Lagrange multipliers (Chapter 6)

This schedule will leave about five open class periods that can be used for exams, quizzes, homework discussion, or project work. When the author teaches this course, a project is usually assigned after the engineering economics discussion. Student teams work on their projects throughout the semester. The final exam period (2 hours) is used as a poster session where the student design teams display their results. This type of project work and final presentation can accommodate a fairly large group of students provided there is enough space available for the poster session.

The appendices in this text provide a variety of information that is useful in solving problems in the book. The appendices also are useful as reference material for design and analysis work. Appendix A provides common conversion factors. Appendix B contains thermophysical properties of many different substances including liquids, refrigerants, air, and metals. Appendix C shows the dimensional information of pipes. Appendix D contains dimensional data for tubing. Finally, Appendix E contains two complete centrifugal pump booklets, complete with performance maps.

Additional information in a download format is available on the book's CRC Press webpage at <https://www.crcpress.com/Thermal-Energy-Systems-Design-and-Analysis-Second-Edition/Penoncello/p/book/9781138735897>



Taylor & Francis

Taylor & Francis Group

<http://taylorandfrancis.com>

Acknowledgments

This edition of the book incorporates many suggestions from users and reviewers of the first edition. The editorial process would be incomplete without the constructive suggestions of colleagues. The author thanks all of those who provided input.

The publishing team at Taylor & Francis/CRC Press has been a pleasure to work with during the publication of this book; Jonathan Plant, Executive Editor for Mechanical, Aerospace, and Nuclear Engineering; Hector Mojena, Ryan Farrar and Sarah Head, Editorial Assistants; and Iris Fahrner, the Project Editor. This team was quick to respond and resolve the author's questions and concerns. Adel Rosario, Project Manager at the Manila Typesetting Company (MTC), was also very responsive and helpful during the production phase of this project.

The cover photograph for this book was provided by Mr. Benjamin Juhnke of Karges-Faulconbridge, Inc. in St. Paul, Minnesota. Permission to use this photograph has been granted by Karges-Faulconbridge, Inc.

This book was written in the presence of the peaceful serenity of Big Lake in north central Minnesota, after the author's retirement from academia. Working on the manuscript of this book while taking an occasional glimpse of the sun sparkling on the waters of the lake provided inspiration beyond all imagination.

The author wishes to express his most heartfelt and sincere thanks to his wife, Jean. Your past and continued love and support through this project made it all worthwhile.



Taylor & Francis

Taylor & Francis Group

<http://taylorandfrancis.com>

Author

Steven G. Penoncello, PhD, earned his BS and MS in mechanical engineering from the University of North Dakota in 1978 and 1980, respectively. He earned his PhD in mechanical engineering from the University of Idaho in 1986. He has been a registered professional engineer in mechanical engineering in the state of Idaho since 1993.

Dr. Penoncello has held academic positions at the University of North Dakota (instructor from 1980–1983, assistant professor from 1986–1988, and associate professor from 1988–1990), and the University of Idaho (visiting assistant professor from 1985–1986, associate professor from 1990–1995, professor from 1995–2015, and professor emeritus since 2015). He has also served in administrative positions at the University of Idaho (Mechanical Engineering Department Chair from 1995–1999, Associate Dean for Research and Graduate Studies in the College of Engineering from 1999–2005, and Director of the Center for Applied Thermodynamic Studies [CATS] from 2005–2015).

Dr. Penoncello has taught undergraduate and graduate courses in thermodynamics, heat transfer, fluid mechanics, air conditioning, solar engineering, refrigeration engineering, internal combustion engines, energy technology, and thermal energy systems design. His research involves the development of standard reference quality formulations for the calculation of the thermophysical properties of fluids and fluid mixtures of scientific and engineering interest.

Dr. Penoncello has been an active member of the American Society of Mechanical Engineers (ASME) since 1978. He became a Life Member of the ASME in 2015. He has served as a member of the K-7 Committee on Thermophysical Properties in the Heat Transfer Division of the ASME from 1988–2013. He has also served as a mechanical engineering program evaluator for the Accreditation Board on Engineering and Technology (ABET), representing the ASME from 1999–2012.

Dr. Penoncello's background in thermal energy systems design and analysis started during his master's research at the University of North Dakota. His master's thesis topic was the analytical modeling and experimental verification of an innovative heat pump system designed for cold climates. This work took a full system approach and involved the simultaneous application of thermodynamics, fluid mechanics, and heat transfer.

In 1991, the faculty of the University of Idaho Department of Mechanical Engineering undertook the task to critically evaluate and update their undergraduate curriculum. During this process, a conscious decision was made to revise the curriculum to allow the undergraduate students to have a significant design experience in several areas of the discipline including solid mechanics and thermal sciences. This process resulted in several new design-based courses including the senior capstone design experience (two courses), an updated machine design course, and a new course in thermal energy systems design. Dr. Penoncello took the lead in the development of the thermal energy systems design course. This book represents a collection of the topics that he has taught in his course since 1992. Dr. Penoncello has coauthored one book, two book chapters, and more than 35 technical papers in the area of thermophysical properties.



Taylor & Francis

Taylor & Francis Group

<http://taylorandfrancis.com>

1

Introduction

1.1 Thermal Energy Systems Design and Analysis

Thermal energy systems are abundant in the industrial, commercial, and residential sectors. They are *thermal* because they often involve the transfer of heat. They typically use working fluids to transport *energy*. They are *systems* because there are several components connected together to form some sort of process or cycle. Some examples of *thermal energy systems* are as follows:

- A heating and cooling system for a commercial or residential building
- A network of pipes and pumps used to transport a fluid to and from various processes within an industrial facility
- A vapor power cycle used to deliver electrical power
- A vapor compression or absorption refrigeration cycle used for cooling or heating

In the design of such systems, the engineer seeks to select components of the system such that the system performs as required while minimizing cost. For the engineer to analyze or design thermal energy systems, it is important to understand the fundamental concepts expressed in terms of various conservation laws and balances. In addition, phenomenological rate equations such as Fourier's law of heat conduction or Newton's law of cooling are required. To complete the picture, the real performance of various components in the system must be known. This is often obtained from equipment manufacturer's specifications. Once all these equations are determined for a specific system, they form the mathematical model of the system. The challenge is to solve these equations to find the system's operating point.

In the era before modern computing technology became widely available, the solution of the mathematical model was done by constructing many graphs representing the equations and looking for intersection points. As an example, consider two straight lines in the x - y plane on a Cartesian coordinate. If the lines are not parallel, there will be a single intersection that can be easily determined graphically. Now take this example and extrapolate it to multiple equations with multiple unknowns. The task becomes daunting and time-consuming if done graphically.

The advent and availability of modern computing technology has reduced the cumbersome task of graphical solutions to simply solving an $n \times n$ system of equations. Modern equation-solving software makes this task quite easy, even for the most complex set of equations. Solution of $n \times n$ systems of equations can even be done in many spreadsheet

applications that include a solver add-in. In thermal energy systems, an added feature that enhances the equation-solving software is the ability to calculate thermophysical properties of the fluids involved in real time within the software. The topic of software is discussed further in Section 1.2.

Having a working mathematical model of a thermal system based on physics and equipment performance information allows the engineer to start thinking about optimization of the system. Optimization techniques allow a system to be designed for minimum cost while still meeting required constraints. Many computer software packages incorporate optimization algorithms to allow studies similar to this.

1.2 Software

As mentioned in Section 1.1, there are many different software packages available that are capable of solving simultaneous nonlinear equations in addition to performing optimization. In thermal energy system design and analysis, it is imperative that the software package used has the capability to retrieve thermophysical properties of the working fluids involved in the system. In order to accomplish this, the software must have the capability to calculate thermophysical properties, (1) internally within the software itself, (2) from a linked external library, or (3) from a linked user-written library. In addition, the formulations used for the thermophysical properties must be of the highest quality. This is important because it eliminates one level of uncertainty in the thermal system design and/or analysis. There are many assumptions made as a system model is constructed and each of those assumptions adds a level of uncertainty. Using internationally accepted, state-of-the-art, modern reference-quality property formulations reduces the uncertainty due to the properties and results in a more reliable solution.

1.2.1 Engineering Equation Solver (EES)

There may be several equation solvers that calculate properties internally. However, the recommended software package in this category is Engineering Equation Solver (EES), available from F-Chart Software (fchart.com/ees). EES contains standard reference-quality formulations for the thermophysical properties of many solids, liquids, and gases. System equations are entered into the software in a free format, with the exception of subprograms which require programming in a structured framework. EES also includes the ability to conduct optimization studies in addition to a plethora of other analyses. As a stand-alone software package, EES is perhaps the most versatile available and very well suited for thermal energy system design and analysis.

1.2.2 REFPROP

The National Institute of Standards and Technology (NIST) has developed a reference fluid thermodynamic and transport properties database known as REFPROP (nist.gov/srd/refprop). This software package contains standard reference quality formulations for many fluids and fluid mixtures. Many of these formulations are incorporated into the EES software package mentioned in Section 1.2.1. REFPROP is not an equation solver; it is simply a fluid property calculator. However, REFPROP is distributed with a dynamic link

library (REFPROP.DLL) that can be used to interface with a variety of software packages including Excel, MATLAB®, Visual Basic, and C++.

1.2.3 CoolProp

An open-source alternative to REFPROP is a software package known as CoolProp (coolprop.org) developed by Bell et al. (2014). CoolProp has an extensive database of state-of-the-art, modern reference-quality formulations for the calculation of the thermophysical properties of fluids. CoolProp is similar to REFPROP in that it is not an equation solver. However, CoolProp has a dynamic link library (CoolProp.DLL) that can be used to interface with a variety of software packages. CoolProp also has the ability to access REFPROP if a user has both CoolProp and REFPROP installed.

1.2.4 User-Written Libraries

It is possible for a user to create a property calculation library, programmed in any language, create a dynamic link library (DLL), and access that DLL from a variety of software packages. In order to do this, the user must be familiar with the formulations used to compute the properties and how to extract the needed property information from the equations given. Most publications that discuss modern equation of state formulations show the accompanying thermodynamic relationships required to determine various properties.

1.2.5 Software Approach Taken in This Book

In this book, no specific software will be discussed. Instead, the focus will be on defining the set of equations required to solve the problem. Solutions to example problems will be reported, but no software code will be shown. This allows the user to adopt any software solution including those discussed in Section 1.2. The companion website for this book will include EES code and Excel files for the solution of many example problems. In addition, course instructors will also be able to have access to a protected area of the website that has EES and Excel files for the solution of most homework problems in the book. Whenever appropriate, Excel solutions will be solved using the REFPROP and CoolProp add-ins.

1.3 Thermal Energy System Topics

There are far too many different types of thermal energy systems to include in a single book. In this book, hydraulic systems will be considered in addition to systems utilizing heat exchangers. The last chapter in the book includes a discussion on thermal energy system simulation and optimization. The working fluids considered are mostly liquids, but there will be examples where gas flows and condensing and/or boiling flows are considered.

It is assumed that readers of this book already have a fundamental background in fluid mechanics, thermodynamics, and heat transfer. The first few sections of Chapters 3, 4, and 5 provide a brief review of these subjects pertinent to thermal energy systems design and analysis. While it is recommended that these review sections be read by students

taking a course in thermal energy systems, instructors may elect to not include them in their course but rather use them as a reference.

1.4 Units and Unit Systems

Units are a very important part of any engineering analysis. Far too often, units are not written down because they seem obvious in a problem. However, countless errors in design and analysis can be traced to a lack of proper unit analysis. As tedious and mundane as it may seem, careful unit analysis should be carried out in *all* engineering problems.

There are five dimensions used in most engineering unit systems; mass (M), force (F), length (L), time (T), and temperature (θ). From physics, it is understood that force and mass are related through Newton's second law of motion. Newton stated that force is proportional to mass and acceleration,

$$F \propto ma \quad (1.1)$$

The proportionality constant in this equation is $1/g_c$. Using this proportionality constant, Equation 1.1 can be converted to an equality and written as,

$$F = \frac{ma}{g_c} \quad (1.2)$$

The magnitude and units of g_c depend on the unit system being considered. In most unit systems, either force or mass are considered *fundamental*, and the other is *derived* from Newton's second law of motion. Table 1.1 shows four common unit systems used in engineering and scientific analysis. The base unit for each of the dimensions along with the $MLT\theta$ units for each dimension is given.

In the four unit systems shown, the length unit is always designated as L and the time unit as T . However, the mass and force units have different $MFLT$ designations (e.g., mass is not always designated as M and force is not always F). This is because Newton's second

TABLE 1.1

Four Common Unit Systems Used in Engineering Analysis and Their Base $MFLT\theta$ Units

Unit	SI ^a System	IP ^b System	British Gravitational System	CGS ^c System
Mass	kg (M)	lbm (M)	slug ($FL^{-1}T^2$)	g (M)
Force	N (MLT^{-2})	lbf (F)	lbf (F)	dyne (MLT^{-2})
Length	m (L)	ft (L)	ft (L)	cm (L)
Time	s (T)	s (T)	s (T)	s (T)
Temperature	K or °C (θ)	R or °F (θ)	R or °F (θ)	K or °C (θ)
g_c	1	$32.174 \frac{\text{lbm-ft}}{\text{lbf-s}^2}$	1	1

^a SI = Système Internationale d'Unités (International System of Units).

^b IP = Inch-Pound (English System).

^c CGS = Centimeter-Gram-Second.

law is used to derive mass from force (British Gravitational System) or force from mass (SI and CGS systems). In the IP unit system, force *and* mass have fundamental units of F and M , respectively, which brings up the need for the proportionality constant $1/g_c$ in Newton's Second Law.

Notice that in all systems except the IP system, $g_c = 1$ (dimensionless). In the IP system, g_c has a value and units; $32.174 \text{ lbm}\cdot\text{ft}/\text{lbf}\cdot\text{s}^2$. The reason for this strange constant is because both mass and force are considered fundamental in the IP unit system. The value of g_c is used to make $1 \text{ lbm} = 1 \text{ lbf}$ at sea level where the acceleration due to gravity is $32.174 \text{ ft}/\text{s}^2$. This is problematic in the sense that while the international community has adopted the SI unit system, many U.S. industries still use the IP system. One of the major points of confusion related to unit systems is how to write equations containing force and mass dimensions. In the past, before the SI system became an international standard, many engineering textbooks incorporated g_c in equations that required a force-mass conversion. For example, in many older engineering textbooks Newton's second law of motion was written as shown in Equation 1.2. In the SI system, $g_c = 1$. Therefore, once the SI system became the international standard, Newton's second law is written as,

$$F = ma \quad (1.3)$$

It should be noted that Equations 1.2 and 1.3 are the same in every unit system shown in Table 1.1 *except* the IP system. In this book, equations will be written *without* the constant g_c to be consistent with modern engineering and science books. However, it is important to understand that when working in the IP system, the constant g_c may need to be incorporated. Careful unit analysis will reveal this as shown in the following example.

Example 1.1

A mass of 10 lbm is at sea level where the acceleration due to gravity is $g = 32.174 \text{ ft}/\text{s}^2$. Determine the force (in lbf) that this mass exerts at sea level.

Solution

The force-mass relationship is governed by Newton's second law of motion. Using Equation 1.3,

$$F = mg = (10 \text{ lbm}) \left(32.174 \frac{\text{ft}}{\text{s}^2} \right)$$

When the units are multiplied through, it is clear that the units are *not* lbf, as expected. This suggests that the force-mass conversion constant in the IP system, g_c is needed. Dividing by g_c results in,

$$F = mg = \frac{(10 \cancel{\text{lbm}}) \left(32.174 \frac{\cancel{\text{ft}}}{\text{s}^2} \right)}{32.174 \frac{\cancel{\text{lbm}} \cdot \cancel{\text{ft}}}{\text{lbf} \cdot \text{s}^2}} = \underline{10 \text{ lbf}}$$

Careful unit analysis revealed the need to use g_c in this problem. In fact, when working in the IP system, one should always be vigilant to the possibility of needing g_c for a force-mass conversion.

It is important to understand that g_c is *nothing but a constant*. It is *not* the acceleration due to gravity. It is the reciprocal of the proportionality constant in Newton's second law of motion when working in the IP system. It came about because the IP system declares both force and mass as fundamental units.

Conversion between units is often required. The official publication for conversion factors is published by the National Institute for Standards and Technology (NIST) (Thompson and Taylor 2008). Appendix A lists several common conversion factors based on this publication. The conversions in Appendix A were computed using EES, which uses the NIST conversion recommendations. There are many online websites offering interactive conversions. The recommended website for interactive conversion is onlineconversion.com. The conversions used on this website are based on the conversion factors suggested by NIST.

Example 1.2

A fluid with a density of 58 lbm/ft³ is flowing through a pipe at a rate of 2000 lbm/hr. Determine the volumetric flow rate of the fluid in U.S. gallons per minute (gpm) and L/s.

Solution

The volumetric flow rate can be found by,

$$\dot{V} = \frac{\dot{m}}{\rho}$$

Solving for the volumetric flow rate in gallons per minute,

$$\dot{V} = \frac{\dot{m}}{\rho} = \frac{\left(2000 \frac{\text{lbm}}{\text{h}}\right)}{\left(58 \frac{\text{lbm}}{\text{ft}^3}\right)} \left| \frac{\text{gpm}}{8.02083 \frac{\text{ft}^3}{\text{h}}} \right| = \underline{4.3 \text{ gpm}}$$

Solving for the volumetric flow rate in liters per second,

$$\dot{V} = \frac{\dot{m}}{\rho} = (4.3 \text{ gpm}) \left| 0.0630902 \frac{\text{L}}{\text{s-gpm}} \right| = \underline{0.265 \frac{\text{L}}{\text{s}}}$$

Careful, meticulous analysis of units is important in any engineering calculation. It is good practice to conduct unit analysis as shown above, no matter what experience level you feel you have.

1.5 Properties of Working Fluids in Thermal Energy Systems

Thermal energy system design and analysis ultimately requires knowledge of the thermophysical properties of the working fluids and materials involved in the system.

Thermophysical properties include the *thermodynamic* and *transport* properties of a substance. Thermodynamic properties are those that can be determined from an *equation of state* for the fluid. Typical thermodynamic properties used in thermal energy systems analysis are pressure, temperature, density, specific volume, internal energy, enthalpy, entropy, isobaric heat capacity, and isochoric heat capacity. Transport properties are properties of a substance that help describe the transport of energy or momentum, such as thermal conductivity or viscosity.

There are countless handbooks and book appendices that contain tables of thermophysical properties of substances. In addition, there are many software packages available that can be used to calculate thermophysical properties. Often, tables of properties or values calculated from software are accepted as fact. The real fact is that behind each table or software calculation is some sort of mathematical *formulation*. This formulation is a collection of equations used to compute the properties. The development of a property formulation ultimately requires experimental data. For some substances such as water or nitrogen, there is an abundance of excellent experimental data over a wide range of pressure and temperature. However, for some substances, the data are very limited. Moreover, as time marches on, experimental measurement techniques improve to the point where experimental data for a fluid measured today may be orders of magnitude more accurate compared to the same data measured several decades previous. Therefore, the *source* of the thermophysical property formulation is important in the design and analysis of thermal energy systems. Using the most current information for thermophysical properties removes a level of uncertainty in the design or analysis.

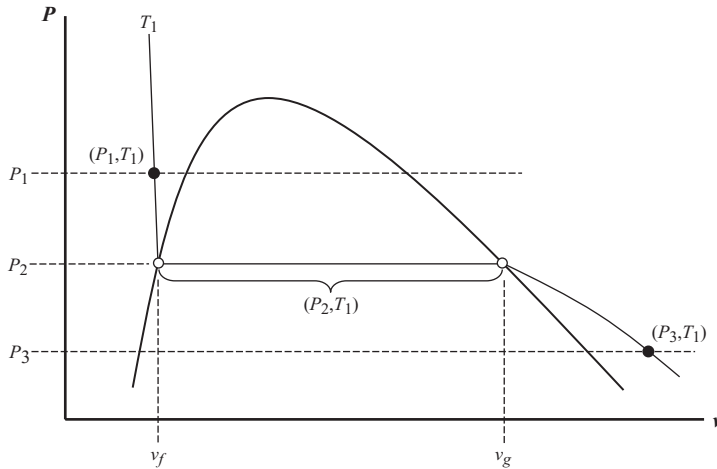
The most current state-of-the-art information on thermophysical properties of substances can be found in scientific and technical journals. In the REFPROP, CoolProp, and EES software packages referenced in Section 1.2, every effort is made to ensure that the formulations used for thermophysical property calculation represent the current standards. Thermophysical properties of several substances, are given in Appendix B.

1.5.1 Thermodynamic Properties

At any given thermodynamic state, there are a myriad of properties. Quite often, the properties required in a thermal energy system analysis are not explicitly known. Therefore, they need to be determined from knowledge of other properties at the state in question. The *state postulate* is important in helping identify how many properties are needed to fix the thermodynamic state. The state postulate may be paraphrased as follows,

Two independent, intensive properties are required to fix the thermodynamic state of a pure substance.

Two properties, x and y are independent if they are represented by a *single point* on a thermodynamic property diagram. Consider the pressure-volume (P - v) diagram shown in Figure 1.1. This figure shows the liquid and vapor behavior of a typical pure fluid. There are three *isobars* indicated on this diagram, P_1 , P_2 , and P_3 . In addition, there is a single *isotherm*, T_1 . Recall that isotherms on a P - v diagram for a pure fluid are rather steep in the liquid phase, are parallel to the isobars in the two-phase region, and curve downward in the vapor phase. Two *single phase* points are identified on this diagram. (P_1, T_1) is a point in the liquid phase and (P_3, T_1) is a point in the vapor phase. These are unique

**FIGURE 1.1**

A pressure-volume diagram for a typical pure fluid.

points that identify a thermodynamic state. Therefore, (P_1, T_1) and (P_3, T_1) are *independent* property pairs. They are also *intensive* because they do not depend on the mass of the substance.

By contrast, (P_2, T_1) are *not* independent because they are coincident in the two-phase region. There are an infinite amount of states that exist at (P_2, T_1) . For example, if you were interested in finding the *specific volume* at (P_2, T_1) , you would have to conclude that there are an *infinite* number of specific volumes at this pressure and temperature, bounded by the *saturated liquid* specific volume, v_f , and the *saturated vapor* specific volume, v_g . Recall that the pressure P_2 is known as the *vapor pressure* or the *saturation pressure* of the fluid at temperature T_1 .

1.5.1.1 Thermodynamic Properties in the Two-Phase Region

Referring to Figure 1.1 again, it can be seen that in the two-phase region of a pure fluid that (P, v) or (T, v) are properties that fix a state somewhere between the saturation specific volumes, v_f and v_g . Consistent with thermodynamic nomenclature, the subscripts *f* and *g* are used to indicate saturated liquid and saturated vapor, respectively. In this two-phase region, there is another thermodynamic property that can be used as one of the independent properties required by the State Postulate; the *quality* of the fluid.

The quality of a fluid in the two-phase region is defined as the ratio of the mass of the saturated vapor in the two-phase mixture to the total mass of the two-phase mixture,

$$x = \frac{m_g}{m} = \frac{m_g}{m_f + m_g} \quad (1.4)$$

From this definition, it can be seen that the quality is somewhere between 0 and 1. On the saturated liquid line, where there is no saturated vapor present, $x = 0$. Likewise, on the saturated vapor line $x = 1$.

The quality can be used to determine a variety of thermodynamic properties in the two-phase region. It can be shown that the specific volume, internal energy, enthalpy, and entropy (v , u , h , and s , respectively) in the two-phase region can be found by,

$$\begin{aligned}v &= (1-x)v_f + xv_g \\u &= (1-x)u_f + xu_g \\h &= (1-x)h_f + xh_g \\s &= (1-x)s_f + xs_g\end{aligned}\tag{1.5}$$

Notice that these equations do not violate the state postulate because either pressure or temperature is required to fix the saturation values (subscripts f and g). Therefore, (T,x) or (P,x) are independent, intensive properties that fix the thermodynamic state in the two-phase region of a pure fluid.

1.5.1.2 Important Thermodynamic Property Relationships

There are several important thermodynamic relationships that are used to determine fluid properties. Perhaps the most important relationship between properties is the *equation of state*. This equation contains a wealth of thermodynamic information. Often times the equation of state is expressed by pressure (P) as a function of temperature (T) and specific volume (v),

$$P = P(T, v)\tag{1.6}$$

The functional form of the equation of state depends on the substance being modeled. In the case of the real behavior of the fluid, the equation of state can be quite complex. On the other hand, if the substance is modeled as an ideal gas, the equation of state is simple,

$$P(T, v) = \frac{RT}{v}\tag{1.7}$$

In Equation 1.7, R is the gas constant for the fluid. The choice of equation of state depends on how the fluid properties are being modeled. This is discussed in detail in the next section.

In addition to pressure, temperature, and specific volume, other properties of interest in thermal energy system analysis are internal energy (u), enthalpy (h), entropy (s), and heat capacities (c_v and c_p). The internal energy and enthalpy are related to the heat capacities of the fluid. The *isochoric heat capacity*, c_v , is defined as,

$$c_v = \left(\frac{\partial u}{\partial T} \right)_v\tag{1.8}$$

Partial derivatives in thermodynamics are often written with subscripts to indicate the property that is being held constant during the differentiation. In Equation 1.8, the specific volume, v , is being held constant. This is why c_v is known as the isochoric (constant volume) heat capacity.

In a similar fashion, the *isobaric heat capacity*, c_p , is defined as,

$$c_p = \left(\frac{\partial h}{\partial T} \right)_p \quad (1.9)$$

In this case, the derivative is calculated while the pressure is held constant. Therefore, the heat capacity calculated using Equation 1.9 is known as the isobaric (constant pressure) heat capacity.

Entropy is related to internal energy and enthalpy through *Gibbs equations* (often referred to as *Tds equations*). Gibbs equations can be derived from the first and second laws of thermodynamics. There are several forms of the Gibbs equations. However, the relationships between internal energy, enthalpy, and entropy for a pure fluid are given by the following forms of the Gibbs equations,

$$Tds = du + Pd v \quad (1.10)$$

$$Tds = dh - v dP \quad (1.11)$$

Equations (1.8) through (1.11) will be used in the next section to derive expressions for changes in thermodynamic properties based on different fluid property models.

1.5.2 Evaluation of Thermodynamic Properties

There are three thermodynamic property models that are often used in a thermal energy system analysis: (1) the real fluid model, (2) the incompressible substance model, and (3) the ideal gas model. The next sections show how these three models are developed and when they can be used in design and/or analysis.

1.5.2.1 The Real Fluid Model

The real fluid model is the most accurate representation of the thermodynamic properties of a fluid. This model includes an equation of state for the fluid developed from experimental data. Often, the equation of state is of the form $P(T,v)$. However, modern equations of state are typically cast in terms of the *Helmholtz energy* of the fluid as a function of temperature and volume, $A(T,v)$. Independent of the form used for the equation of state, thermodynamic property relationships can be derived that allow for the calculation of properties at a given state. Often, these calculations can be quite tedious, depending on the complexity of the equation of state. The resulting properties can be compiled in a table of properties or the calculations can be embedded in software, such as REFPROP, CoolProp, or EES.

While the real fluid model is meant to represent the real behavior of a fluid, it is entirely possible that an equation of state is *not* accurate. Consider the case of water. There have been several equations of state published for water over the years. The International Association for the Properties of Water and Steam (IAPWS) is an international consortium that reviews equations of state for water and recommends which one will be used as the international standard. The current IAPWS equation of state for water (Wagner and Pruss 2002) is much more accurate compared to equations of state 40 to 50 years previous. However, there are still tables of water properties available based on the old formulations. When designing or analyzing thermal energy systems, the most accurate model should always be used.

1.5.2.2 The Incompressible Substance Model

The incompressible substance model is meant to *estimate* the *solid* or *liquid* properties of a substance. Notice that this model is only an estimate of the properties. This model is used quite often in the case where an equation of state is not valid in the liquid phase (some older equations of state are only valid in the vapor phase). The equation of state of an incompressible substance is given by,

$$v = \text{constant} \quad (1.12)$$

In addition, the internal energy of an incompressible substance is only a function of temperature,

$$u = u(T) \quad (1.13)$$

Together, Equations 1.12 and 1.13 formulate the incompressible substance model. Properties of incompressible substances can be calculated using Equations 1.8 through 1.11 along with Equations 1.12 and 1.13.

In the analysis of thermal energy systems, the *difference* in internal energy, enthalpy, or entropy between two thermodynamic states is usually required. When a *single* value of internal energy, enthalpy, or entropy is used, (e.g., in combustion calculations) it is important that all formulations used to determine the properties have the same *datum* or *reference* state.

For the incompressible substance model, the internal energy change can be determined by using Equation 1.8. The internal energy is only a function of temperature in the incompressible substance model. Therefore, Equation 1.8 can be rewritten as,

$$\tilde{c}_v = \frac{du}{dT} \quad (1.14)$$

In Equation 1.14, a tilde (\sim) is used to indicate the incompressible substance model's value of the heat capacity. This equation can be integrated between any two states to determine the change in the substance's internal energy,

$$u_2 - u_1 = \int_{T_1}^{T_2} \tilde{c}_v dT \quad (1.15)$$

For an incompressible substance, it is often reasonable to assume that the heat capacity is constant at the average temperature of the process. This simplifies Equation 1.15 to the following form,

$$u_2 - u_1 = \tilde{c}_{v,avg}(T_2 - T_1) \quad (1.16)$$

The enthalpy change of an incompressible substance can be determined by considering Equation 1.9. Since $h = u + Pv$, the partial derivative in Equation 1.9 can be expanded as shown in the following equation,

$$\tilde{c}_p = \left(\frac{\partial h}{\partial T} \right)_p = \left(\frac{\partial u}{\partial T} \right)_p + \left(\frac{\partial (Pv)}{\partial T} \right)_p = \tilde{c}_v + \left(\frac{\partial (Pv)}{\partial T} \right)_p \quad (1.17)$$

The partial derivative of the Pv product in Equation 1.17 can be written as,

$$\left(\frac{\partial(Pv)}{\partial T} \right)_P = P \left(\frac{\partial v}{\partial T} \right)_P + v \left(\frac{\partial P}{\partial T} \right)_P = 0 \quad (1.18)$$

This derivative is equal to zero because both partial derivatives on the right hand side of Equation 1.18 are zero. The partial derivative of v is zero because v is constant for the incompressible substance model. The pressure derivative is also zero because pressure is being held constant during the differentiation. Substituting this result into Equation 1.17 reveals that.

$$\tilde{c}_p = \tilde{c}_v \equiv \tilde{c} \quad (1.19)$$

Equation 1.19 implies that the isobaric and isochoric heat capacities are equal for the incompressible substance. Therefore, Equation 1.16 can be rewritten as,

$$u_2 - u_1 = \tilde{c}_{avg}(T_2 - T_1) \quad (1.20)$$

The enthalpy change using the incompressible substance model can be determined by substituting $u = h - Pv$ into Equation 1.20,

$$h_2 - h_1 = \tilde{c}_{avg}(T_2 - T_1) - v(P_2 - P_1) \quad (1.21)$$

Notice that the enthalpy of an incompressible substance is a function of both temperature and pressure. However, if the pressure difference between the two thermodynamic states in question is small, the last term on the right hand side of Equation 1.21 is very small. In these cases, the enthalpy difference can be estimated by,

$$h_2 - h_1 \approx \tilde{c}_{avg}(T_2 - T_1) = u_2 - u_1 \quad (1.22)$$

The entropy change of an incompressible substance between two thermodynamic states can be determined by applying Equation 1.10. For the incompressible substance, $dv = 0$. Therefore, Equation 1.10 can be written as,

$$Tds = du \quad (1.23)$$

Substituting Equations 1.14 and 1.19 into Equation 1.23, results in,

$$ds = \frac{\tilde{c}}{T} dT \quad (1.24)$$

This equation can be integrated between the two states resulting in,

$$s_2 - s_1 = \int_{T_1}^{T_2} \frac{\tilde{c}}{T} dT \quad (1.25)$$

Considering the heat capacity to be constant at the average temperature, Equation 1.25 can be written as,

$$s_2 - s_1 = \tilde{c}_{avg} \ln \frac{T_2}{T_1} \quad (1.26)$$

Equation 1.26 indicates that the entropy of an incompressible substance is only a function of temperature. When Equation 1.26 is used to compute entropy changes, the temperatures must be expressed on the *absolute* temperature scale (K or °R).

1.5.2.3 Estimation of Liquid Properties

Equation 1.12 implies that the volume of an incompressible substance is independent of temperature and pressure. This is why engineers might consider the density of liquid water to be 1000 kg/m³ or 62.4 lbm/ft³. Notice, no temperature or pressure is specified. However, in reality, it is understood that the density of a liquid is really a function of temperature and, to a lesser extent, pressure. Appendix B.1 shows saturated liquid properties of water over a range of temperatures. Notice that the density of the saturated liquid (and thus the specific volume) varies with temperature. This raises an interesting question, “What good is the incompressible substance model when estimating liquid properties?” The answer to this question can be seen by considering Figure 1.2. In this figure, the specific volume (v), isobaric heat capacity (c_p), dynamic viscosity (μ), thermal conductivity (k), and the Prandtl number (Pr) of liquid water at 50°C and a variety of pressures are compared to the saturated liquid values at the same temperature. The vertical axis of this plot represents the percent deviation between the properties calculated at the saturated liquid state compared to the real-fluid liquid state,

$$\% \Delta(\text{property}) = 100 \frac{[\text{property}(P, T) - \text{property}(T, x = 0)]}{\text{property}(P, T)} \quad (1.27)$$

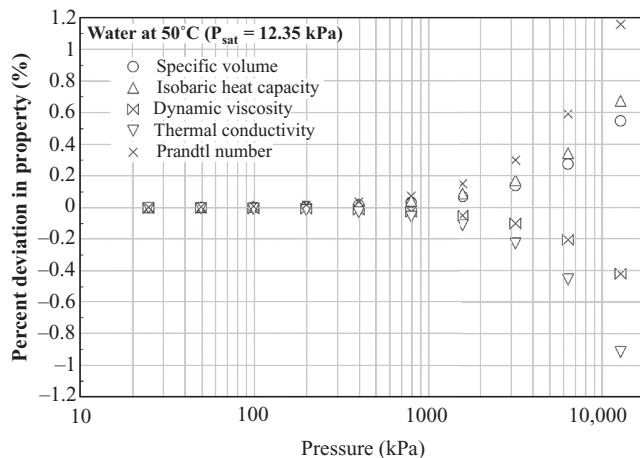


FIGURE 1.2

Comparison of properties of water at 50°C calculated on the saturated liquid line compared to the liquid values defined by ($P, T = 50^\circ\text{C}$).

Notice that the percent deviations are all within $\pm 0.2\%$ at pressures up to 2000 kPa (~ 290 psia). As the pressure gets larger, the deviation from the saturated liquid value becomes greater. However, even at 10,000 kPa (~ 1450 psia), the percent deviations are within 1%. This exercise indicates that as long as the pressure is not excessive, the liquid properties of a fluid can be reasonably estimated by evaluating them on the saturated liquid line *at the given temperature*; no pressure is required.

Example 1.3

Liquid water is flowing through a pipe at 150°F, 100 psia at a volumetric flow rate of 60 gpm. The pipe's inside diameter is 2.067 inches. Determine the Reynolds number of this flow using (a) single-phase water data in Appendix B.2, and (b) estimated liquid properties at saturation from Appendix B.1. Compare the two calculations.

Solution

The Reynolds number is used in a variety of hydraulic and heat transfer calculations. The Reynolds number for flow in a circular pipe is defined as,

$$\text{Re} = \frac{\rho V D}{\mu}$$

The volumetric flow rate of the water is given. The volumetric flow rate is related to the velocity of the fluid and the pipe diameter,

$$\dot{V} = AV = \left(\frac{\pi D^2}{4} \right) V \rightarrow \therefore V = \frac{4\dot{V}}{\pi D^2}$$

Substituting this expression for velocity into the Reynolds number calculation and simplifying results in the following,

$$\text{Re} = \frac{4\rho\dot{V}}{\pi D\mu}$$

- a. From Appendix B.2 at 150°F, 100 psia, the single-phase water properties are given as,

$$\rho = 61.211 \frac{\text{lbm}}{\text{ft}^3} \quad \mu = 1.0393 \frac{\text{lbm}}{\text{ft-hr}}$$

The Reynolds number can now be calculated,

$$\text{Re} = \frac{4\rho\dot{V}}{\pi D\mu} = \frac{4 \left(61.211 \frac{\text{lbm}}{\text{ft}^3} \right) (60 \text{ gpm}) \left(\frac{8.02083 \text{ ft}^3}{\text{gpm-hr}} \right)}{\pi (2.067 \text{ in}) \left(1.0393 \frac{\text{lbm}}{\text{ft-hr}} \right) \left(\frac{\text{ft}}{12 \text{ in}} \right)} = \underline{\underline{209,513}}$$

- b. The liquid properties can be estimated by using the saturated liquid properties at the given temperature. From Appendix B.1 at 150°F (interpolation required),

$$\rho = 61.188 \frac{\text{lbm}}{\text{ft}^3} \quad \mu = 1.0444 \frac{\text{lbm}}{\text{ft-hr}}$$

The Reynolds number can now be calculated,

$$\text{Re} = \frac{4\rho\dot{V}}{\pi D\mu} = \frac{4\left(61.188 \frac{\text{lbm}}{\text{ft}^3}\right)(60 \text{ gpm})\left(\frac{8.02083 \text{ ft}^3}{\text{gpm-hr}}\right)}{\pi(2.067 \text{ in})\left(1.0444 \frac{\text{lbm}}{\text{ft-hr}}\right)\left(\frac{\text{ft}}{12 \text{ in}}\right)} = \underline{208,411}$$

The percent deviation between these two values is,

$$\%\Delta \text{Re} = 100 \left[\frac{(209,513 - 208,411)}{209,513} \right] = \underline{0.053\%}$$

This comparison verifies that the estimated properties can be used resulting in a very accurate calculation of the Reynolds number.

As demonstrated in Example 1.3, using saturated liquid properties to estimate the single-phase liquid properties is a way to determine liquid properties when only the temperature is given. As previously stated, one must always be cognizant of the pressure and ensure it is not excessive. The following example uses the liquid property estimation technique to compute differences in thermodynamic properties.

Example 1.4

A 40% ethanol-water solution enters a heat exchanger at -12°C and leaves at 12°C . The pressure drop of the solution through the heat exchanger is 30 kPa. Determine the change in the internal energy, enthalpy, and entropy of the solution as it passes through the heat exchanger.

Solution

The property changes are calculated using Equations 1.20, 1.21, and 1.26. All of these equations require the heat capacity of the 40% ethyl alcohol solution. Using the brine properties listed in Appendix B.4, the average heat capacity of the solution is found to be,

$$T_{\text{avg}} = \frac{T_1 + T_2}{2} = \frac{(-12 + 12)^\circ\text{C}}{2} = 0^\circ\text{C} \rightarrow \tilde{c}_{\text{avg}} = 3.4342 \frac{\text{kJ}}{\text{kg-K}}$$

Therefore, the internal energy change of the solution through the heat exchanger is,

$$u_2 - u_1 = \tilde{c}_{\text{avg}}(T_2 - T_1) = \left(3.4342 \frac{\text{kJ}}{\text{kg-K}}\right)[12 - (-12)]\text{K} = \underline{82.421 \frac{\text{kJ}}{\text{kg}}}$$

The calculation of the enthalpy difference requires the density of the solution. From Appendix B.4, $\rho_{avg} = 1060.4 \frac{\text{kg}}{\text{m}^3}$. Therefore, the enthalpy difference of the solution is,

$$\begin{aligned} h_2 - h_1 &= \tilde{c}_{avg}(T_2 - T_1) - v_{avg}(P_2 - P_1) = (u_2 - u_1) - \frac{(P_2 - P_1)}{\rho_{avg}} \\ &= 82.421 \frac{\text{kJ}}{\text{kg}} - (-30 \text{ kPa}) \left(\frac{\text{m}^3}{1060.4 \text{ kg}} \right) \left(\frac{\text{kN}}{\text{kPa} \cdot \text{m}^2} \right) \left(\frac{\text{kJ}}{\text{kN} \cdot \text{m}} \right) = \underline{\underline{82.449 \frac{\text{kJ}}{\text{kg}}}} \end{aligned}$$

The entropy change of the solution as it passes through the heat exchanger is,

$$s_2 - s_1 = \tilde{c}_{avg} \ln \frac{T_2}{T_1} = \left(3.4342 \frac{\text{kJ}}{\text{kg} \cdot \text{K}} \right) \ln \left[\frac{(12 + 273.15) \text{K}}{(-12 + 273.15) \text{K}} \right] = \underline{\underline{0.30194 \frac{\text{kJ}}{\text{kg} \cdot \text{K}}}}$$

Notice that the enthalpy difference is very close to the internal energy difference. Therefore, if the pressure drop was unknown, but assumed to be small, then the enthalpy difference could be estimated to be the same as the internal energy difference, as shown in Equation 1.22.

1.5.2.4 The Ideal Gas Model

The ideal gas model is meant to provide an *estimate* for the properties of gases and vapors. The equation of state of the ideal gas can be written in its most universal sense as

$$P\bar{v} = \bar{R}T \quad (1.28)$$

The overbars are used to indicate *molar* quantities. For example, the units of the molar specific volume can be written in different unit systems as,

$$\bar{v} [=] \frac{\text{cm}^3}{\text{gmol}} \quad (\text{CGS}) \quad \bar{v} [=] \frac{\text{m}^3}{\text{kmol}} \quad (\text{SI}) \quad \bar{v} [=] \frac{\text{ft}^3}{\text{lbmol}} \quad (\text{IP}) \quad (1.29)$$

In Equation 1.29, the symbol [=] means *is dimensionally equal to*. The molar value of \bar{R} is the *universal gas constant*. Table 1.2 shows the value and units of the universal gas constant

TABLE 1.2

Values of the Universal Gas Constant in Different Units

Unit System	\bar{R}
SI	$8.314 \frac{\text{kJ}}{\text{kmol} \cdot \text{K}} = 8314 \frac{\text{J}}{\text{kmol} \cdot \text{K}}$
IP	$1545 \frac{\text{ft} \cdot \text{lbf}}{\text{lbmol} \cdot ^\circ\text{R}} = 1.986 \frac{\text{Btu}}{\text{lbmol} \cdot ^\circ\text{R}}$
CGS	$8.314 \times 10^7 \frac{\text{dyne} \cdot \text{cm}}{\text{gmol} \cdot \text{K}}$

in several different unit sets. The equation of state can also be expressed on a *mass* basis by introducing the molecular mass of the gas, M ,

$$Pv = \left(\frac{\bar{R}}{M} \right) T = RT \quad (1.30)$$

In Equation 1.30, R is not universal; it depends on the molecular mass of the gas being analyzed.

In addition to the equation of state, the internal energy of an ideal gas is only a function of temperature. Therefore, the complete ideal gas model can be formulated by,

$$Pv = RT \quad \text{and} \quad u = u(T) \quad (1.31)$$

Figure 1.3 shows a pressure-internal energy diagram for cyclohexane. In this figure, it can be seen that the isotherms are nearly vertical for a good share of the liquid and vapor regions. The nearly vertical behavior of the isotherms in these regions indicate that the internal energy is only a function of temperature, $u = u(T)$. This plot demonstrates the validity of using the incompressible substance model in the liquid phase and the ideal gas model in the low-pressure vapor phase.

The internal energy change of an ideal gas can be determined using Equation 1.8. Since the internal energy of an ideal gas is only a function of temperature, the ideal gas isochoric heat capacity can be written as,

$$c_v^0 = \frac{du}{dT} \quad (1.32)$$

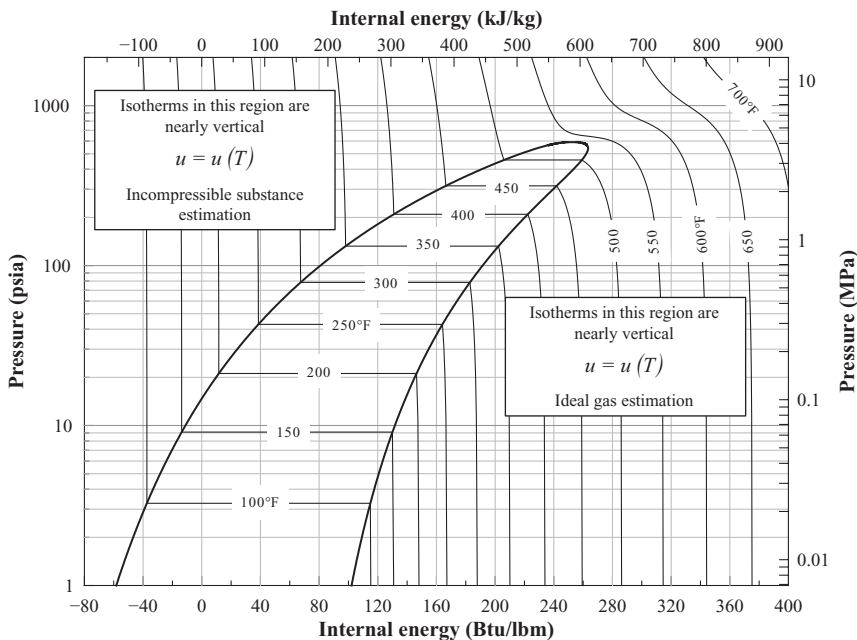


FIGURE 1.3

A pressure-internal energy diagram for cyclohexane.

A superscript “0” is used to identify the heat capacity as an ideal gas value. This equation can be integrated to determine the internal energy change of the ideal gas,

$$u_2 - u_1 = \int_{T_1}^{T_2} c_v^0 dT \quad (1.33)$$

The enthalpy change of an ideal gas can be determined from Equation 1.9. For an ideal gas, the enthalpy can be expressed by,

$$h = u + Pv = u + RT \quad (1.34)$$

According to Equation 1.34, the enthalpy of an ideal gas is only a function of temperature. Therefore, Equation 1.9 can be written as,

$$c_p^0 = \frac{dh}{dT} \quad (1.35)$$

The enthalpy change of the ideal gas can be determined by integrating Equation 1.35 between the temperature limits of the process,

$$h_2 - h_1 = \int_{T_1}^{T_2} c_p^0 dT \quad (1.36)$$

The entropy change of an ideal gas can be determined by either of the Gibbs equations; Equations 1.10 or 1.11. Rearranging Equation 1.10 to solve for ds gives,

$$ds = \frac{du}{T} + \frac{P}{T} dv \quad (1.37)$$

Substituting Equation (1.32) for du and the ideal gas equation of state for P/T results in,

$$ds = \frac{c_v^0}{T} dT + \frac{R}{v} dv \quad (1.38)$$

The entropy change of an ideal gas between two thermodynamic states can be found by integrating Equation 1.38,

$$s_2 - s_1 = \int_{T_1}^{T_2} \frac{c_v^0}{T} dT + R \ln \frac{v_2}{v_1} = \int_{T_1}^{T_2} \frac{c_v^0}{T} dT + R \ln \left(\frac{P_1}{P_2} \frac{T_2}{T_1} \right) \quad (1.39)$$

Manipulating the second Gibbs equation, Equation 1.11, in a similar manner gives an alternate expression for the entropy change of an ideal gas,

$$s_2 - s_1 = \int_{T_1}^{T_2} \frac{c_p^0}{T} dT - R \ln \frac{P_2}{P_1} \quad (1.40)$$

Recall that for an ideal gas, the internal energy and enthalpy are functions of temperature only. However, the entropy of an ideal gas is a function of *both* temperature and pressure as indicated by Equations 1.39 and 1.40.

Equations 1.33, 1.36, 1.39, and 1.40 are the expressions required to compute internal energy, enthalpy, and entropy differences of an ideal gas between two thermodynamic states. All of these equations contain an integral involving the ideal gas heat capacity.

The heat capacity of ideal gases can vary significantly over a given temperature range. The exception to this behavior is seen in the noble gases; the last column of the periodic chart of the elements. For the noble gases (He, Ne, Ar, Kr, Xe, Rn) the ideal gas isobaric heat capacity is constant and given by,

$$c_p^0 = \frac{5}{2}R \quad (\text{Noble gases only}) \quad (1.41)$$

For all other substances, the ideal gas isobaric heat capacity can be modeled using an empirical relationship known as the Shomate equation,

$$c_p^0 = A + B\theta + C\theta^2 + D\theta^3 + \frac{E}{\theta^2} \quad (1.42)$$

In Equation 1.42, θ is a dimensionless temperature usually defined as the actual temperature divided by some arbitrary value. Values of the constants A , B , C , D , and E for several ideal gases are given in Table 1.3.

If the heat capacity dependence on temperature is known, then the equations for internal energy, enthalpy, and entropy changes can be integrated. However, for many thermal energy system calculations, it is often sufficient to assume that the heat capacity is constant at *the average temperature* between the two states being analyzed. In this case, the ideal gas property changes can be written as,

$$\begin{aligned} u_2 - u_1 &= c_{v,avg}^0 (T_2 - T_1) \\ h_2 - h_1 &= c_{p,avg}^0 (T_2 - T_1) \\ s_2 - s_1 &= c_{v,avg}^0 \ln \frac{T_2}{T_1} + R \ln \frac{v_2}{v_1} \\ s_2 - s_1 &= c_{p,avg}^0 \ln \frac{T_2}{T_1} - R \ln \frac{P_2}{P_1} \end{aligned} \quad (1.43)$$

In the equations representing the entropy change of an ideal gas in Equation set 1.43, the temperatures must be on the absolute scale. For the internal energy and enthalpy changes, the temperatures can be either relative or absolute since the equations contain a temperature difference.

The ideal gas heat capacities are related to each other. This can be demonstrated by considering the differential of Equation 1.34,

$$dh = du + RdT + TdR = du + RdT \quad (1.44)$$

TABLE 1.3Shomate Equation^a Constants for Several Ideal Gases in Molar SI Units

Fluid	<i>M</i> (g/mol)	A	B	C	D	E
Nitrogen	28.0134					
(100–500 K)		28.98641	1.853978	−9.647459	16.63537	0.000117
(500–2000 K)		19.50583	19.88705	−8.598535	1.369784	0.527601
Oxygen	31.9988					
(100–700 K)		31.32234	−20.23531	57.86644	−36.50624	−0.007374
(700–2000 K)		30.03235	8.772972	−3.988133	0.788313	−0.741599
Water	18.0153					
(500–1700 K)		30.09200	6.832514	6.793435	−2.534480	0.082139
(1700–6000 K)		41.96426	8.622053	−1.499780	0.098119	−11.15764
Carbon Monoxide	28.0101					
(298–1300 K)		25.56759	6.096130	4.054656	−2.671301	0.131021
(1300–6000 K)		35.15070	1.300095	−0.205921	0.013550	−3.282780
Carbon Dioxide	44.0095					
(298 – 1200 K)		24.99735	55.18696	−33.69137	7.948387	−0.136638
(1200 – 6000 K)		58.16639	2.720074	−0.492289	0.038844	−6.447293
Methane	16.0425					
(298–1300 K)		−0.703029	108.4773	−42.52157	5.862788	0.678565
(1300 – 6000 K)		85.81217	11.26467	−2.114146	0.138190	−26.42221
Ethane	30.0690					
(200–700 K)		3.646182	170.61315	−44.27281	−8.731863	0.230599
(700–2000 K)		−8.489090	211.48703	−98.02772	16.98405	0.745419
Propane	44.0956					
(300–1000 K)		−12.0000	341.54512	−211.2408	55.59196	0.037898
(1000–3500 K)		78.68445	146.45600	−47.23175	5.303024	−9.300454

$$^a \quad c_p^0 \left[\frac{\text{J}}{\text{mol-K}} \right] = A + B\theta + C\theta^2 + D\theta^3 + \frac{E}{\theta^2} \quad \theta = \frac{T[\text{K}]}{1000[\text{K}]}$$

Substituting Equations 1.32 and 1.35 into Equation 1.44 gives,

$$c_p^0 dT = c_v^0 dT + R dT \quad (1.45)$$

This equation can be simplified to,

$$c_p^0 - c_v^0 = R \quad (1.46)$$

Example 1.5

A sample of krypton gas (molecular mass, $M = 83.8 \text{ kg/kmol}$) is initially at 300°C , 400 kPa . The gas undergoes a process and ends up at a pressure of 200 kPa . Determine the change in enthalpy of the gas if the process is (a) isothermal (constant temperature) and (b) isentropic (constant entropy)

Solution

- a. The enthalpy of an ideal gas is a function of temperature only. Therefore, if the process is isothermal, the enthalpy change of the substance must be,

$$h_2 - h_1 = 0 \frac{\text{kJ}}{\text{kg}}$$

- b. Krypton is a noble gas. Therefore, its heat capacities are constant. The isobaric heat capacity of the gas can be found from Equation 1.41,

$$c_p^0 = \frac{5}{2}R = \frac{5}{2} \left(\frac{\bar{R}}{M} \right) = \frac{5}{2} \left(\frac{8.314 \frac{\text{kJ}}{\text{kmol-K}}}{83.8 \frac{\text{kg}}{\text{kmol}}} \right) = 0.248 \frac{\text{kJ}}{\text{kg-K}}$$

The enthalpy change of the gas can be determined from the enthalpy difference equation in Equation set 1.43,

$$h_2 - h_1 = c_p^0(T_2 - T_1)$$

Since the entropy is constant, the last equation in Equation set 1.43 can be written as,

$$c_p^0 \ln \frac{T_2}{T_1} = R \ln \frac{P_2}{P_1}$$

Solving this equation for the final temperature, T_2 ,

$$T_2 = T_1 \left(\frac{P_2}{P_1} \right)^{R/c_p^0}$$

The exponent on the pressure ratio can be rewritten as,

$$\frac{R}{c_p^0} = \frac{R}{5R/2} = \frac{2}{5}$$

The final temperature in the isentropic process can now be found,

$$T_2 = T_1 \left(\frac{P_2}{P_1} \right)^{R/c_p^0} = (300 + 273)\text{K} \left(\frac{200 \text{ kPa}}{400 \text{ kPa}} \right)^{2/5} = 434.25 \text{ K} = 161.3^\circ\text{C}$$

Therefore, the enthalpy change of the krypton gas during the isentropic process is,

$$h_2 - h_1 = c_p^0(T_2 - T_1) = \left(0.248 \frac{\text{kJ}}{\text{kg-K}} \right) (161.3 - 300)\text{K} = \underline{\underline{-34.4 \frac{\text{kJ}}{\text{kg}}}}$$

1.5.3 Transport Properties

Transport properties of interest in thermal energy systems design are those properties that help quantify the transport of momentum and energy within the fluid stream. *Viscosity* is a property that is related to momentum transfer while *thermal conductivity* is related to energy transfer in the form of heat. Viscosity can be expressed as either *absolute* or *dynamic* viscosity, or *kinematic* viscosity. Unlike thermodynamic properties, transport properties cannot be derived from an equation of state. Instead, they are often computed from theoretically-based equations or empirical equations based on experimental data.

1.5.3.1 Dynamic Viscosity

Most thermophysical properties are fairly intuitive. For example, the density of a substance is expressed in mass per unit volume. Viscosity is one of those properties that can be expressed with several different units which may make it a confusing property to understand. From a purely intuitive perspective, the viscosity of a substance is related to how easily it flows. For example, when the oil in your car's engine is cold, it takes more pumping power to move it compared to oil that is warmed up. Therefore, the viscosity of the cold oil is higher than the viscosity of the warm oil.

To understand what viscosity represents, consider a Newtonian fluid under laminar flow in the x -direction as shown in Figure 1.4. The momentum flux in the y -direction (known as the shearing stress) is directly proportional to the x -velocity gradient (known as the strain rate). The proportionality constant is known as the *absolute* or *dynamic* viscosity, μ .

The relationship between the shearing stress and velocity gradient in a Newtonian fluid is known as Newton's law of viscosity,

$$\tau_{yx} = \mu \frac{dV_x}{dy} \quad (1.47)$$

The units of absolute viscosity can be determined from this expression. In the SI system, the dynamic viscosity has units of Pa-s or N-s/m² as demonstrated in the following equation,

$$\mu = \tau_{yx} \frac{dy}{dV_x} [=](\text{Pa}) \left(\frac{\text{m-s}}{\text{m}} \right) = \text{Pa-s} = \frac{\text{N-s}}{\text{m}^2} \quad (1.48)$$

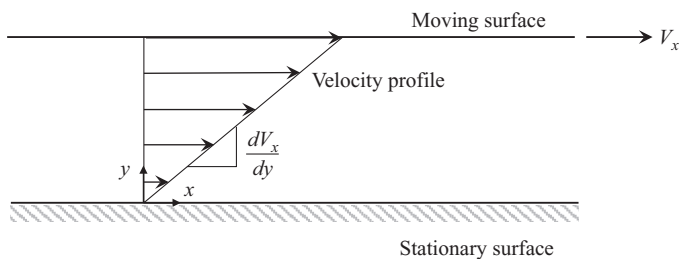


FIGURE 1.4

Velocity profile of a Newtonian fluid under laminar flow between two parallel surfaces.

By expanding the definition of the newton, an alternative unit for absolute viscosity can be determined as,

$$\mu [=] \frac{\text{N}\cdot\text{s}}{\text{m}^2} = \left(\frac{\text{kg}\cdot\text{m}}{\text{s}^2} \right) \left(\frac{\text{s}}{\text{m}^2} \right) = \frac{\text{kg}}{\text{m}\cdot\text{s}} \quad (1.49)$$

Equation 1.48 has units based on force whereas Equation 1.49 has units based on mass. Another often-used unit of dynamic viscosity is developed from the CGS system,

$$\mu = \tau_{yx} \frac{dy}{dV_x} [=] \left(\frac{\text{dyne}}{\text{cm}^2} \right) \left(\frac{\text{cm}\cdot\text{s}}{\text{cm}} \right) = \frac{\text{dyne}\cdot\text{s}}{\text{cm}^2} = \text{P (poise)} \quad (1.50)$$

The poise, P, is named after Jean Louis Poiseuille (1799–1869) who did much work in the area of fluid mechanics.

In the IP unit system, the force-based units of dynamic viscosity can be derived as follows,

$$\mu = \tau_{yx} \frac{dy}{dV_x} [=] \left(\frac{\text{lbf}}{\text{ft}^2} \right) \left(\frac{\text{ft}\cdot\text{s}}{\text{ft}} \right) = \frac{\text{lbf}\cdot\text{s}}{\text{ft}^2} \quad (1.51)$$

This set of units can be converted to a mass-based unit by,

$$\mu [=] \frac{\text{lbf}\cdot\text{s}}{\text{ft}^2} g_c = \frac{\text{lbf}\cdot\text{s}}{\text{ft}^2} \left(32.174 \frac{\text{lbm}\cdot\text{ft}}{\text{lbf}\cdot\text{s}^2} \right) [=] \frac{\text{lbm}}{\text{ft}\cdot\text{s}} \quad (1.52)$$

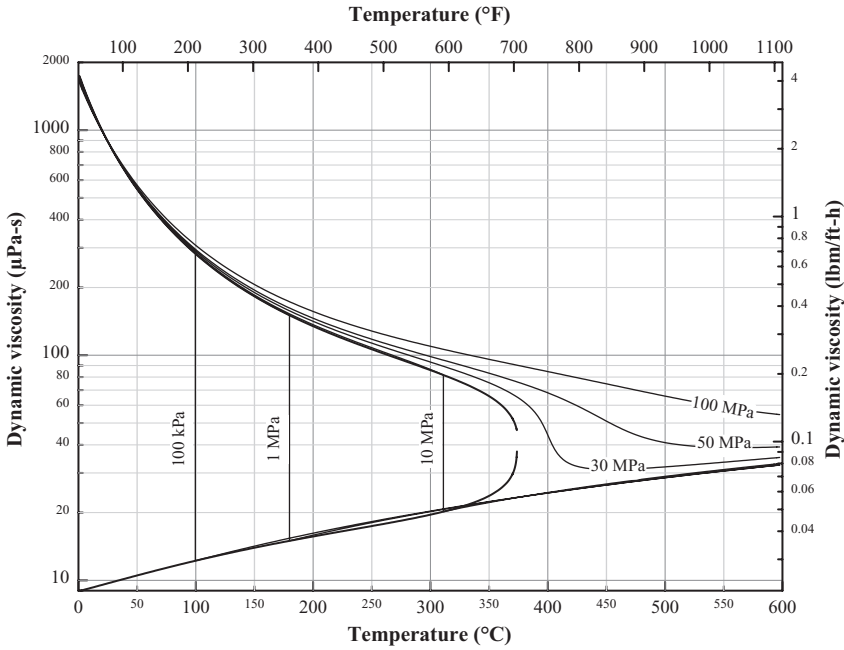
Notice that to convert the absolute viscosity from a force-based unit to a mass-based unit in the IP unit system the force-based value must be multiplied by g_c .

The viscosity of a fluid is truly a function of temperature and pressure. In liquids and low-pressure vapors, the viscosity is only weakly dependent on pressure and is often considered a function of temperature only. For gases and supercritical states, the pressure may have a significant effect on the viscosity in addition to the temperature. This is demonstrated in Figure 1.5 which shows a dynamic viscosity vs. temperature plot for water. This plot shows the behavior of the dynamic viscosity over a wide temperature range for a range of pressures. Notice that in the liquid and vapor regions, the subcritical isobars basically collapse onto one another, especially at lower temperatures, making the viscosity a temperature function. As the pressure and temperature increase, then the isobars start to separate indicating that pressure, in addition to temperature, influence the dynamic viscosity.

1.5.3.2 Kinematic Viscosity

Another measure of viscosity is the *kinematic* viscosity. The kinematic viscosity is defined as,

$$\nu = \frac{\mu}{\rho} \quad (1.53)$$

**FIGURE 1.5**

Dynamic viscosity behavior for water.

Kinematic viscosity is a measure of the resistance of the flow under the influence of gravity. The units of kinematic viscosity can be derived based on the definition shown in Equation 1.53. In the SI system, the kinematic viscosity has units of m^2/s as shown in the following equation,

$$\nu = \frac{\mu}{\rho} [=] \frac{\text{kg}}{\text{m}^3} \frac{\text{m}^2}{\text{s}} = \frac{\text{m}^2}{\text{s}} \quad (1.54)$$

In the IP unit system, the kinematic viscosity has units of ft^2/s ,

$$\nu = \frac{\mu}{\rho} [=] \frac{\text{lbm}}{\text{ft}^3} \frac{\text{ft}^2}{\text{s}} = \frac{\text{ft}^2}{\text{s}} \quad (1.55)$$

In the CGS unit system, the stoke (St) is defined as a cm^2/s ,

$$\nu = \frac{\mu}{\rho} [=] \frac{\text{g}}{\text{cm}^3} \frac{\text{cm}^2}{\text{s}} = \frac{\text{cm}^2}{\text{s}} = \text{St (stoke)} \quad (1.56)$$

1.5.3.3 Newtonian and Non-Newtonian Fluids

Fluids that behave according to Newton's law of viscosity, Equation 1.47, are known as *Newtonian* fluids. Many industrial fluids are Newtonian such as water, light oils, gasoline,

brines, and organic solvents. However, there are many other substances that do not obey Equation 1.47. These are known as non-Newtonian fluids. Examples of non-Newtonian fluids are suspensions, slurries, gels, colloids, and polymers. The study of non-Newtonian fluids is a complex subject within the broader science of *rheology*.

Non-Newtonian fluids can be generally classified into one of two categories; *shear-thinning* or *shear-thickening*. Shear-thinning fluids are substances that experience a decrease in their resting viscosity and flow easier when agitated by a shear stress. In contrast, a shear-thickening fluid behaves just the opposite of shear-thinning fluids. In a shear-thickening fluid, the viscosity of the fluid increases when an external shearing stress is applied.

Shear-thinning fluids can be further classified as *pseudoplastic*, *thixotropic*, or *Bingham plastic*. A pseudoplastic substance experiences a viscosity decrease with an applied shearing stress. When the applied stress is removed, the fluid reverts back to a more solid-like phase. Tomato ketchup is a good example of a pseudoplastic fluid. Squeezing the ketchup out of its container requires an applied force to make it run. However, once the applied force is removed, the ketchup becomes thicker. A thixotropic substance experiences a decrease in viscosity with an applied shear stress, but its viscosity continues to decrease with time as the shear stress is applied. An example of a thixotropic fluid is spun honey. The more it is stirred, the more liquid-like it becomes. A Bingham plastic behaves like a Newtonian fluid once the initial yield stress of the fluid is exceeded. Bingham plastic fluids include toothpaste, blood, molten chocolate, and mashed potatoes.

Shear thickening fluids can be classified as *rheopectic* or *dilatant*. A rheopectic substance experiences an increase in viscosity over time. Examples of rheopectic fluids include gypsum pastes and printer inks. A dilatant substance experiences an increase in viscosity with an applied shear stress, but it does not change over time. Examples of dilatant fluids include cornstarch paste and silly putty.

Ultimately, the viscosity of a fluid determines the frictional effects within the passage it is flowing. Treating a non-Newtonian fluid as Newtonian can lead to significant error in the determination of friction effects, resulting in a system that does not perform as expected. A treatise on rheology is beyond the scope of this text. Therefore, in this book, only thermal energy systems that utilize Newtonian fluids are considered.

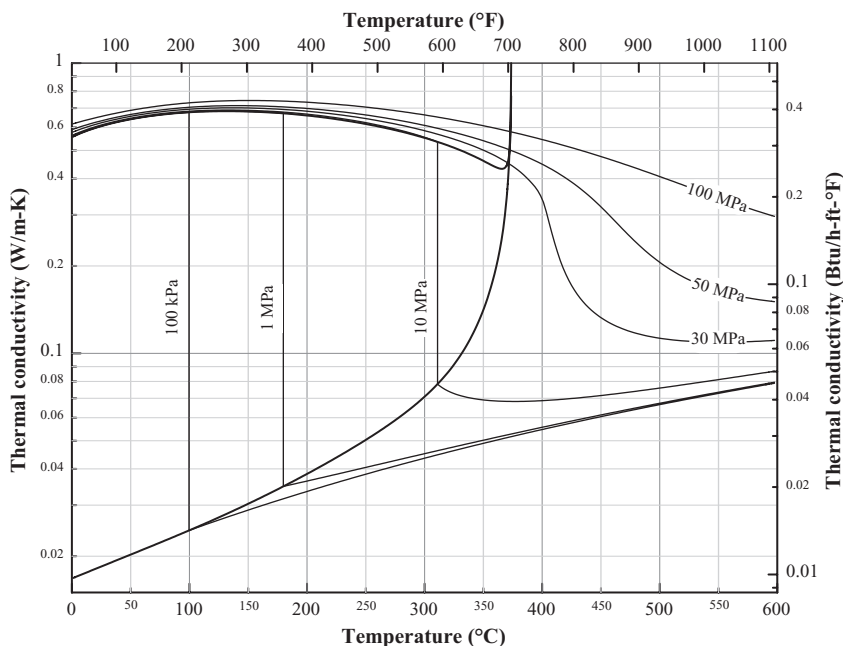
1.5.3.4 Thermal Conductivity

In quantifying energy transport by heat, thermal conductivity is analogous to dynamic viscosity in momentum transport. The thermal conductivity is related to the heat flux and temperature gradient through a material as described by Fourier's law of conduction. For one-dimensional (e.g., the x -direction in a Cartesian coordinate system) conduction heat transfer, this relationship is given by,

$$\frac{\dot{Q}_x}{A} = q_x'' = -k \frac{dT}{dx} \quad (1.57)$$

From Equation 1.57, the units of the thermal conductivity in the SI unit system are,

$$k = -q_x'' \frac{dx}{dT} [=] \left(\frac{\text{W}}{\text{m}^2} \right) \left(\frac{\text{m}}{\text{K}} \right) = \frac{\text{W}}{\text{m-K}} \quad (1.58)$$

**FIGURE 1.6**

Thermal conductivity behavior for water.

In the IP unit system, the units of thermal conductivity are,

$$k = -q_x'' \frac{dx}{dT} [=] \left(\frac{\text{Btu}}{\text{h-ft}^2} \right) \left(\frac{\text{ft}}{\text{°F}} \right) = \frac{\text{Btu}}{\text{h-ft-°F}} \quad (1.59)$$

As with dynamic viscosity, the thermal conductivity of a substance is a function of temperature and pressure. For the liquid and low-pressure vapor phase, the thermal conductivity is only weakly dependent on pressure and is often considered a function of temperature only. In the gas and supercritical phases, the temperature and pressure dependence is much more pronounced. Figure 1.6 shows the thermal conductivity of water over a wide range of pressures and temperatures.

1.6 Engineering Design and Analysis

Design and analysis are two different activities taken on by engineers. They are often performed simultaneously. However, they are distinctly different. Consider a situation where the engineer is charged with devising a system to meet a certain need subject to constraints. This activity is known as *design*. On the other hand, *analysis* is the determination of the performance of a system or component based on physical principles. Analysis, by itself, is not design. However, design requires intermediate analysis of various subsystems or components. Engineering students spend a considerable amount of time becoming adept at analysis. This is because it is such an integral part of design.

There are many things in engineering that have definite answers. For example, adding $2 + 2$ gives 4 with complete certainty. Engineering design, on the other hand is not as straightforward. Design is the *art* of engineering. As engineers, we tend to rely on a series of steps to achieve a goal. The design process is something that is very difficult to quantify let alone delineate in a list of steps. Engineering design is often thought of as the place where art and experience meet science and technology.

1.6.1 Workable Designs

By its very nature, design is open-ended. For example, for any given thermal energy system task, there may be *many* designs that accomplish the task. The systems may look very different and contain different equipment, but they accomplish a required task while being subject to a set of constraints. These many different design solutions are called *workable designs*. Due to the large variability in these workable designs, their costs may be vastly different. Some systems may be of reasonable cost while others are very expensive. Some systems may result in more pollution and have a larger environmental impact than others. As with cost, environmental impact is something industries are concerned about and in many cases, environmental regulations exist that must be followed.

Example 1.6

A rural homeowner is looking into ways to irrigate a small family garden. One possibility being considered is to use the water from a small creek that is 125 ft away from the garden and 25 ft lower than the garden as shown in Figure E1.6. Determine the specifications for a pump and pipe system that would provide irrigation water to the garden at a specified flow rate of 5 gpm.

Solution

In order to deliver the irrigation water to the garden, the pump must develop enough pressure to overcome (1) the elevation difference, and (2) the friction effects in the pipe network,

$$\Delta P_{\text{pump}} = \Delta P_{\text{elevation}} + \Delta P_{\text{friction}}$$

The pressure increase required to overcome the elevation difference is,

$$\Delta P_{\text{elevation}} = \rho g z$$

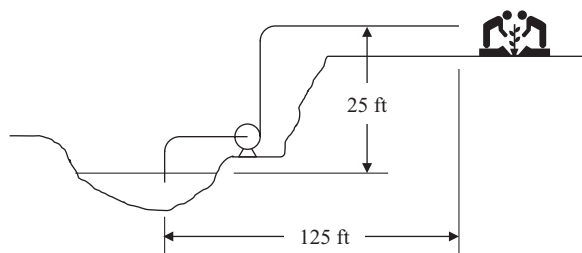


FIGURE E1.6
Schematic of proposed pump and pipe system for irrigation.

Assuming that the density of the water is 62.4 lbm/ft³, the elevation pressure increase required is,

$$\Delta P_{\text{elevation}} = \rho g z = \left(62.4 \frac{\text{lbm}}{\text{ft}^3} \right) \left(32.174 \frac{\text{ft}}{\text{s}^2} \right) (25 \text{ ft}) \left(\frac{\text{lbf} \cdot \text{s}^2}{32.174 \text{ lbm} \cdot \text{ft}} \right) \left(\frac{\text{ft}}{12 \text{ in}} \right)^2 = 10.8 \text{ psi} \approx 11 \text{ psi}$$

g_c

The pressure increase required due to friction can be calculated by conducting a friction analysis of the pipe,

$$\Delta P_{\text{friction}} = f \frac{L}{D} \frac{\rho V^2}{2}$$

The velocity in the pipe is a function of the flow rate and the pipe diameter,

$$V = \frac{\dot{V}}{A} = \frac{4 \dot{V}}{\pi D^2}$$

Substituting this expression into the friction pressure drop equation results in,

$$\Delta P_{\text{friction}} = f \frac{8 \rho L \dot{V}^2}{\pi^2 D^5}$$

The friction factor calculation can be quite detailed. However, a value of $f = 0.02$ will be assumed for the initial design. In reality, the friction factor is a function of the diameter of the pipe. In the final design, it is necessary to determine the real friction factor to ensure that the design is reliable and the system will perform as expected. The total pipe length is (125 + 25) ft = 150 ft. For an arbitrary diameter, say 1-inch, the pressure drop in the pipeline due to friction is,

$$\begin{aligned} \Delta P_{\text{friction}} &= f \frac{8 \rho L \dot{V}^2}{\pi^2 D^5} \\ &= (0.02) \frac{8 \left(62.4 \frac{\text{lbm}}{\text{ft}^3} \right) (150 \text{ ft}) (5 \text{ gpm})^2}{\pi^2 (1 \text{ in})^5} \left(\frac{8.02083 \text{ ft}^3}{\text{gpm} \cdot \text{h}} \right)^2 \left(\frac{12 \text{ in}}{\text{ft}} \right)^5 \left(\frac{\text{lbf} \cdot \text{s}^2}{32.174 \text{ lbm} \cdot \text{ft}} \right) \left(\frac{\text{h}}{3600 \text{ s}} \right)^2 \\ \Delta P_{\text{friction}} &= 145.6 \frac{\text{lbf}}{\text{ft}^2} \left(\frac{\text{ft}}{12 \text{ in}} \right)^2 = 1.01 \text{ psi} \approx 1 \text{ psi} \end{aligned}$$

Therefore, the pump must be able to develop a pressure rise of at least (11 + 1) psi = 12 psi at a flow rate of 5 gpm through a 1-inch pipe. Manufacturer's pump performance curves can now be consulted to find a pump that meets these specifications. This is one workable solution.

There are many other workable designs for this system. For example, if the pipe diameter is varied, the friction pressure drop can be recalculated and thus a new pump pressure increase can be found for a flow rate of 5 gpm. The result is shown in Table E1.6.

All ten of these designs are considered workable designs. However, some of them may be very expensive. For example, 0.25-inch diameter pipe results in an excessive pressure drop due to friction. This means the pumping power required to overcome the friction effects would be excessive, leading to a very expensive design.

TABLE E1.6

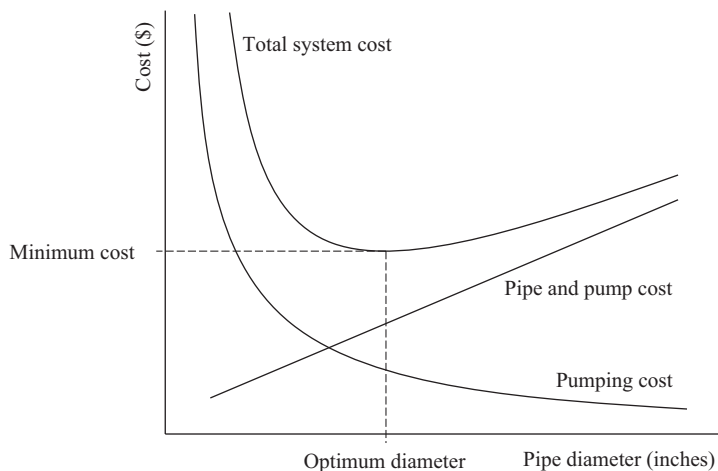
Ten Workable Designs for the Pump and Pipe Network of Example 1.6

D (in)	$\Delta P_{\text{elevation}}$ (psi)	$\Delta P_{\text{friction}}$ (psi)	ΔP_{pump} (psi)
0.25	10.83	1,036	1,046
0.50	10.83	32.36	43.20
0.75	10.83	4.26	15.10
1.00	10.83	1.01	11.84
1.25	10.83	0.33	11.16
1.50	10.83	0.13	10.97
1.75	10.83	0.06	10.90
2.00	10.83	0.03	10.87
2.25	10.83	0.02	10.85
2.50	10.83	0.01	10.84

1.6.2 Optimum Designs

An *optimum design* is the design that reflects some quantifiable criterion such as minimum cost, minimum environmental impact, maximum thermal efficiency, or maximum exergetic efficiency, to name a few. For a specified criterion, there is only one optimum design, which often requires the rigorous mathematical analysis associated with finding the minimum point of a multidimensional function subject to mathematical constraints.

Consider Example 1.6 again. Table E.1.6 indicates that small diameter pipes have a larger friction pressure drop compared to the larger pipes. Small pipes are inexpensive, but a larger, more expensive pump is required to move 5 gpm of water through the pipes. This results in a higher pumping cost. Conversely, larger pipes require a smaller, less expensive pump to move 5 gpm of water through the pipes leading to a smaller pumping cost. However, the initial cost of the larger pipe is higher compared to a smaller pipe. This discussion leads one to believe that there must be an optimum design that minimizes the total cost of the pump and pipe system. Figure 1.7 indicates one way that the optimum design can be determined for this system.

**FIGURE 1.7**

Optimum design condition for the pump and pipe system of Example 1.6.

This figure shows three curves. The “Pipe and Pump Cost” curve represents the initial cost of the pipe and pump for the system. The “Pumping Cost” curve represents the cost of the power required to operate the pump over an arbitrary period of time (e.g., a year). The “Total System Cost” curve is the sum of the other two curves. Notice that this curve indicates there is a minimum cost point associated with an optimum diameter. The pump selected for this diameter pipe will result in the optimum design based on minimizing system cost. Many pump and pipe systems can be optimized using this type of an analysis. The concept of the optimum *economic diameter* is fully developed in Chapter 4 (Section 4.5). Advanced optimization concepts are presented in Chapter 6.

Optimum designs can be determined by minimizing one of many criteria. However, in engineering design, the optimum design is often based on minimizing total system cost; an *economic* criterion. Referring to Example 1.6 again, the costs involved in the pump and pipe system occur at different times. The initial cost of the pump and piping are one-time investments occurring at the beginning of the project. The pumping cost occurs over a period of time. These two investments occur at different times over the life of the system, therefore, they cannot be directly added at any time due to the time value of money. Economic interest factors must be used to equate these costs at a common point over the life of the system. Chapter 2 is an introduction to engineering economics and discusses this issue.

1.6.3 Engineering Design and Environmental Impact

Engineers are expected to conduct themselves in an ethical manner. The American Society of Mechanical Engineers (ASME) maintains an ethics website where a Code of Ethics for Engineers which can be found. The ever-increasing role of the engineer with regard to environmental impact and resource sustainability is an important ethical topic. The Eighth Fundamental Canon of the ASME Code of Ethics for Engineers states,

Engineers shall consider environmental impact and sustainable development in the performance of their professional duties. (ASME n.d.)

In this canon, the role of the engineer with respect to environmental impact is clearly delineated. As thermal energy system designers, engineers must strive to consider environmental impact and sustainability in every aspect of their work. Considering environmental impact means more than just a passing thought. This canon implies that the engineer must strive to minimize the environmental impact of his/her design.

The relatively recent trends in *exergy* analysis can be used to determine the environmental impact of a thermal energy system. The concept of exergy may be enigmatic to many engineers because the topic of exergy may have not been addressed, or only briefly mentioned in their undergraduate coursework. Chapter 3 (Section 3.8) presents the concept of exergy.

Unfortunately, designing a thermal energy system to minimize environmental impact often may be counter to the profit motive of industry. Systems optimized to minimize environmental impact may look very different compared to systems optimized to minimize cost. It is a coincidence if the economic optimum design and environmental impact optimum design are the same. Companies are in business to make money, and the economic optimum design often wins. However, this does not relieve the engineer of his/her ethical duties regarding environmental impact and sustainability. These issues need to be

brought to the attention of middle and upper management. It is ultimately their decision on how to proceed, but the engineer has fulfilled his/her ethical responsibility by bringing the matter to their attention.

References

- ASME. *Ethics in Engineering*. n.d. <https://www.asme.org/about-asme/advocacy-government-relations/ethics-in-engineering>.
- Bell, Ian H., Jorrit Wronski, Sylvain Quoilin, and Vincent Lemort. "Pure and Pseudo-pure Fluid Thermophysical Property Evaluation and the Open-Source Thermophysical Property Library CoolProp." *Industrial & Engineering Chemistry Research*, 2014: 2498–2508.
- Thompson, A., and B. N. Taylor. *Guide for the Use of the International System of Units (SI)*. Gaithersburg, MD: National Institute of Standards and Technology, 2008.
- Wagner, W., and A. Pruss. "The IAPWS Formulation 1995 for the Thermodynamic Properties of Ordinary Water Substance for General and Scientific Use." *Journal of Physical and Chemical Reference Data*, 2002: 387–535.

Problems

Units and Unit Systems

- 1.1 At sea level, a person has a mass of 175 lbm. Determine the weight of this person in newtons (N).
- 1.2 At sea level on the earth, an astronaut weighs 700 N. Determine the astronaut's weight in newtons (N),
 - a. On the surface of the moon where $g = 1.6 \text{ m/s}^2$
 - b. On the surface of Mars where $g = 3.7 \text{ m/s}^2$
- 1.3 An empty hot tub has a mass of 320 kg. When filled, the tub holds 600 gallons of water ($\rho = 62.4 \text{ lbm/ft}^3$). The local acceleration due to gravity is 32 ft/s^2 . Determine the total weight of the hot tub and water in pounds-force (lbf).
- 1.4 A 100-W incandescent light bulb in a lamp is turned on for a period of 12 hours each day for a month (30 days). If the cost of electrical energy is \$0.083/kWh, determine the total cost required to light the bulb for a month.
- 1.5 A residential natural gas furnace in a home has an average daily heat output of 32,000 Btu/h during the month of December to maintain the home at 70°F. The natural gas being used has a density of 0.044 lbm/ft^3 and a volumetric heating value of 1000 Btu/ft^3 . The cost of the natural gas is \$3.29/MBtu. For the month of December, determine the following:
 - a. The total number of cubic feet of natural gas used
 - b. The total cost of the natural gas used

- 1.6 A steam power plant has an average monthly net power delivery of 740 MW over the course of a year. This power delivery is accomplished by burning coal in the boiler. The coal has a heating value of 9150 Btu/lbm. The cost of the coal is \$14.20/ton. The overall thermal efficiency of the plant is,

$$\eta_{th} = \frac{\dot{W}_{net}}{\dot{Q}_{boiler}} = 0.26 = 26\%$$

Determine the annual cost of the coal required to deliver the given average monthly power.

- 1.7 A pump is being used in a system that is circulating liquid hexane at 80°F ($\rho = 40.9 \text{ lbm/ft}^3$). The volumetric flow rate of the hexane through the pump is 125 gallons per minute (gpm). Determine the flow rate of the hexane through the pump in,
- liters/s (L/s)
 - m^3/s
 - lbm/hr
 - kg/s

- 1.8 The net thermal efficiency of an internal combustion engine is given by,

$$\eta_o = \frac{1}{(HV)(sfc)}$$

where HV is the heating value of the fuel and sfc is the specific fuel consumption of the engine. Consider an engine operating with a sfc of 248 g/kWh whose fuel has a heating value of 42 MJ/kg. Determine the overall efficiency of the engine for these operating parameters (%).

- 1.9 The net thermal efficiency of an internal combustion engine is given by,

$$\eta_o = \frac{1}{(HV)(sfc)}$$

where HV is the heating value of the fuel and sfc is the specific fuel consumption of the engine. Consider an engine operating with a sfc of 0.4077 lbm/hp-h whose fuel has a heating value of 18,057 Btu/lbm. Determine the overall efficiency of the engine for these operating parameters (%).

- 1.10 An operating parameter often used by power plant engineers is the *heat rate*. The heat rate is defined as,

$$HR = \frac{\dot{Q}_{boiler}}{\dot{W}_{net}}$$

where \dot{Q}_{boiler} is the heat transfer rate (Btu/h) to the water in the boiler due to combustion of a fuel and \dot{W}_{net} is the net power (kW) delivered by the plant. In comparison, the thermal efficiency of the power plant is defined as,

$$\eta_{th} = \frac{\dot{W}_{net}}{\dot{Q}_{boiler}}$$

where the numerator and denominator have the same units. Consider a power plant that is delivering 1000 MW of power while utilizing a heat transfer rate of 3570 MW at the boiler. Determine the heat rate and thermal efficiency of this power plant.

Properties of Working Fluids

1.11 The Reynolds number of a flow in a circular pipe is defined as,

$$Re = \frac{\rho V D}{\mu}$$

where V is the fluid velocity, D is the pipe diameter, and ρ and μ are the fluid's density and dynamic viscosity, respectively. Consider a 15% calcium chloride solution (by mass) flowing in a 1.61-inch diameter pipe. The calcium chloride solution is at a temperature of 30°F and flows with a velocity of 2.7 ft/s. Using the property data from Appendix B.4, determine the Reynolds number associated with this flow.

1.12 The Prandtl number is a fluid property defined as,

$$Pr = \frac{c_p \mu}{k}$$

where the fluid properties are c_p (heat capacity), μ (dynamic viscosity), and k (thermal conductivity). Using the property tables in Appendix B.3 and the definition of the Prandtl number, verify that the value of the Prandtl number for liquid hexane at a temperature of 10°C is correct as shown in the table.

1.13 The specific energy of a flowing fluid is defined as,

$$e = \underbrace{u}_{\text{internal energy}} + \underbrace{\frac{V^2}{2}}_{\text{kinetic energy}} + \underbrace{gz}_{\text{potential energy}}$$

where u is the internal energy of the fluid, V is its velocity, and z is its elevation relative to an arbitrary datum. Consider a flow of low-pressure steam in a pipeline.

The steam is at a temperature of 300°F and a pressure of 50 psia. The steam is flowing at a mass flow rate of 2500 lbm/h through a pipe with an inside diameter of 11.983 in. The pipe runs horizontally at an elevation of 15 ft above the floor. The elevation of the floor is considered to be $z = 0$ ft. Using the property data from Appendix B.2, determine the following,

- a. Specific energy of this steam flow in Btu/lbm
 - b. The percentage makeup of each component of the specific energy
- 1.14 The Graetz number is used to determine the thermal entry length for developing flow in pipes. The Graetz number for flow in a circular pipe is defined as,

$$\text{Gz}_L = \frac{D}{L} \text{RePr}$$

where D is the inside diameter of the pipe, L is the length from the pipe entrance, Re is the Reynolds number of the flowing fluid, and Pr is the Prandtl number of the fluid. The Reynolds number and Prandtl number are defined as,

$$\text{Re} = \frac{\rho V D}{\mu} \quad \text{Pr} = \frac{c_p \mu}{k}$$

In these equations, the fluid properties are ρ (density), c_p (specific heat), μ (dynamic viscosity), and k (thermal conductivity). V is the fluid's velocity in the pipe and D is the inside diameter of the pipe. Determine the Graetz number for liquid dodecane flowing at 20°C, with a velocity of 0.05 m/s in a pipe with an inside diameter of 5.25 cm at a location that is 0.5 m from the entrance of the pipe.

- 1.15 The enthalpy of a fluid is defined as,

$$h = u + Pv$$

where u , P , and v , are internal energy, pressure, and specific volume, respectively. Consider a sample of saturated vapor water at 380°F. Using the property data from Appendix B.1, calculate the enthalpy of the water at this state in Btu/lbm. Compare this value to the tabulated value of the enthalpy in Appendix B.1.

- 1.16 A sample of carbon dioxide gas is subject to a process where its temperature changes from an initial temperature of 300 K to a final temperature of 900 K. Determine the enthalpy change of the carbon dioxide,
- a. Using the Shomate equation for the ideal gas isobaric heat capacity
 - b. Assuming the ideal gas isobaric heat capacity is constant at the average temperature of the process

Express your answers in kJ/kg. Compare the two approaches and comment on the validity of assuming constant heat capacity in this problem.

- 1.17 The manufacturer of synthetic motor oil lists the viscosity of their 0W20 oil as 47.0 cSt and 8.8 cSt at 40°C and 100°C, respectively. The 0W20 product data sheet

also indicates that the specific gravity of the oil is 0.844 at 15.6 C. The specific gravity of a fluid is defined as,

$$\text{spgr} = \frac{\rho}{\rho_{\text{water}}}$$

where ρ is the density of the fluid in question, and ρ_{water} is the density of liquid water at 4°C. Determine the dynamic viscosity of the 0W20 oil at 40°C and 100°C in mPa-s.

- 1.18 Heat is being transferred through the wall of a furnace at a flux of 160 Btu/hr-ft². The temperatures on each side of the furnace wall are 1200°F and 300°F. The furnace wall is 12 inches thick. If the temperature profile through the wall is linear, determine the thermal conductivity of the furnace wall using Fourier's law of conduction, Equation 1.57.

Engineering Design

(These problems are well-suited as group exercises.)

- 1.19 The top view of a processing line in an industrial facility is shown in Figure P1.19A. The processing line machinery and thermal equipment are located in the gray area. Water is to be supplied to the processing line at points A, B, and C. The water source is an elevated tank that is kept full by a pump controlled by a water-level sensor in the tank. The water source is available at point S. Points A, B, C, and S are all at the same elevation.

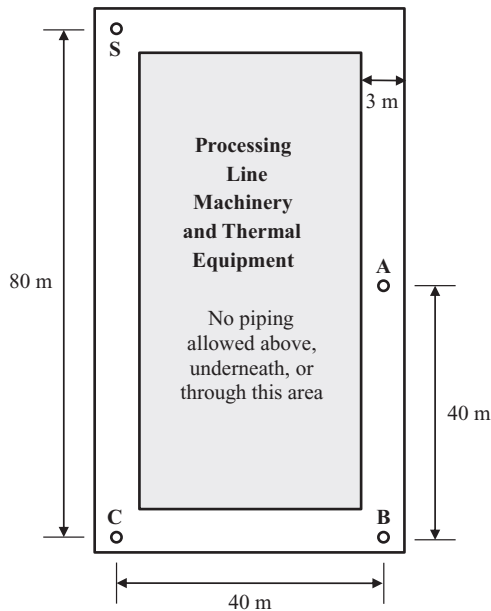


FIGURE P1.19A

Industrial processing facility layout.

The water demand at each point is, 2.5 L/s at A, 3.5 L/s at B, and 1.5 L/s at C. The water demand for points A and C occur intermittently, although they may coincide. The demand at points A and C occurs only during the working shifts. The water demand at point B occurs during the non-shift hours and is also intermittent. Piping can only be installed in a 3-m wide space around the processing line. No piping is allowed above, underneath, or through the processing area.

The calculated friction pressure drop (kPa/m) for various pipe diameters is shown in Figure P1.19B. These curves are computed for horizontal pipes. Losses due to fittings can be considered negligible. The performance curves of nine potential pumps for this application are shown in Figure P1.19C. These curves show the pressure increase across the pump as a function of the flow rate through the pump. The pump performance curves are drawn over a range of acceptable operating efficiency.

Design a pipe system for this application. Provide a sketch of the piping network and specify the information about the system by completing a table similar to Table P1.19.

- 1.20 The cross-section of a steam boiler is shown in Figure P1.20. Water is boiled inside of tubes using combustion gases flowing over the tubes. The tubes are arranged in a square array that is eight rows high. The tubes may be bare on the outside or equipped with circular fins. The inside width of the boiler is 1.9 m.

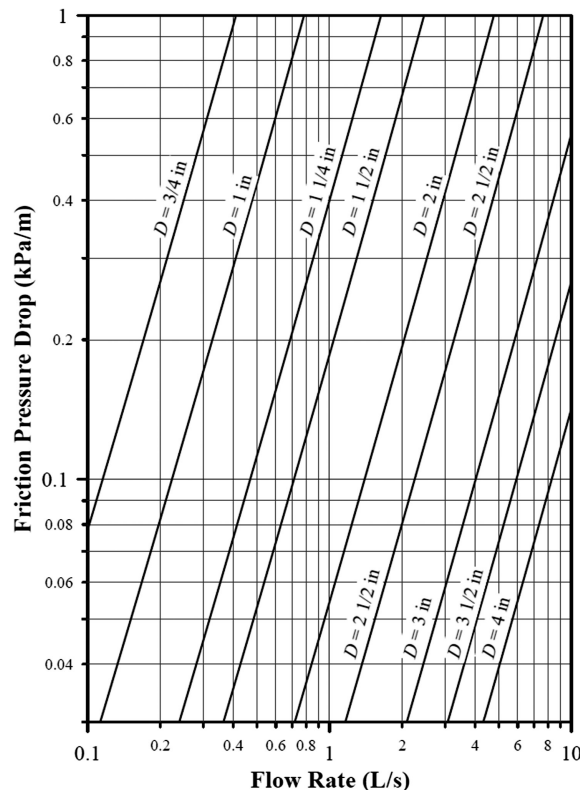


FIGURE P1.19B

Pressure drop data for several horizontal pipes.

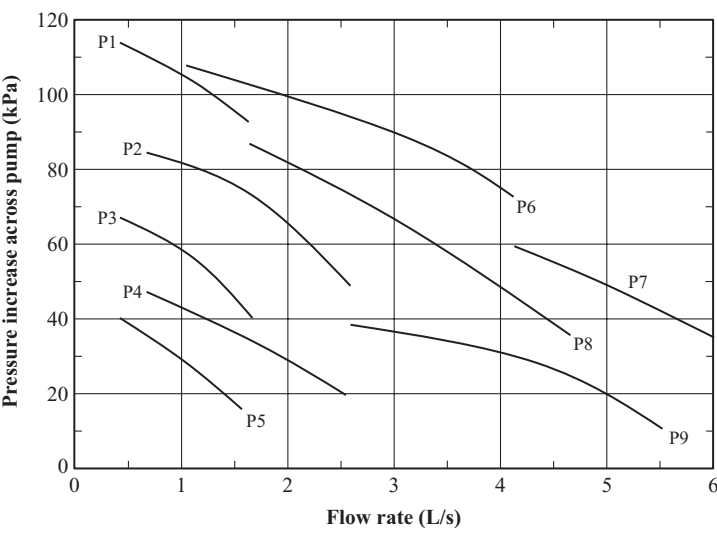


FIGURE P1.19C
Operating characteristics of nine pumps.

TABLE P1.19
Design Specifications for the Pipe Network

Pipe Section	Pipe Size (in)	Design Flow Rate (L/s)		Pressure Drop (kPa)	
		Working Hours	Non-Working Hours	Working Hours	Non-Working Hours

Pump selected: _____
Elevation of water surface in supply tank: _____

Table P1.20A shows the technical data for the tubes and fins (if any). The tubes are connected together by U-bends. The smallest U-bend available results in a centerline distance of 125 mm between adjacent tubes. Larger U-bends are available and can be used in this design.

Water is boiling inside the tubes at a pressure of 800 kPa, corresponding to a saturation temperature of 170.4°C. The combustion gases enter the furnace at $T_{gas} = 580^{\circ}\text{C}$. The following design constraints are relative to the tubes and fins,

1. There must be a minimum of 3 mm of clearance between fins of adjacent tubes and between fins and the boiler walls.
2. For metallurgical purposes, the hottest part of the fin (i.e., the fin tip) must not exceed 400°C.

Another design constraint on the boiler is that it must have a minimum UA product of 23,500 W/K. The overall heat transfer coefficient, based on the steam side (i.e., the *inside*) of the tube, is given by,

$$\frac{1}{U} = R''_{total} = R''_{steam} + R''_{tube} + R''_{gas}$$

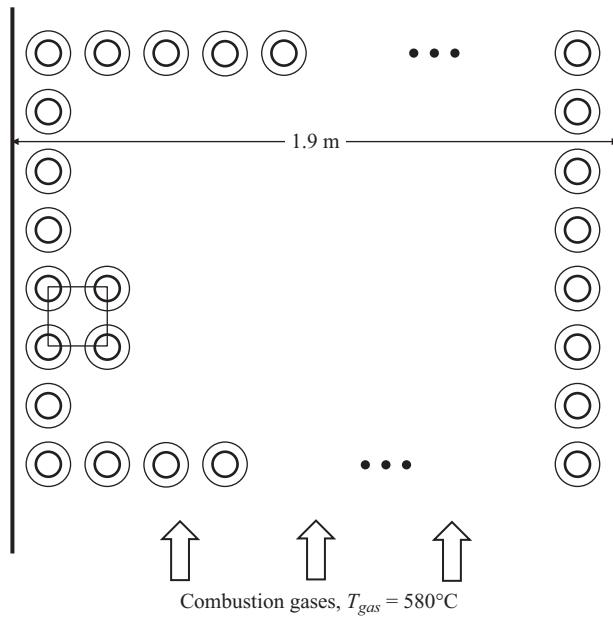


FIGURE P1.20
Sketch of a steam boiler with square array tubes.

TABLE P1.20A

Technical Data for Tubes and Fins to Be Used in the Steam Boiler

Parameter	Value
Outside diameter of tubes	76 mm
Tube wall thickness	4 mm
Length of tubes	2 m
Thermal conductivity of tubes	36 W/m-K
Fin thickness	2 mm
Fin spacing along the tube	6 mm
Fin thermal conductivity	36 W/m-K

The thermal resistances in this equation are,

$$R''_{steam} = \frac{1}{h_{steam}} = \frac{1}{5640 \text{ W/m}^2\text{-K}} = 0.000177305 \frac{\text{m}^2\text{-K}}{\text{W}}$$

$$R''_{tube} \approx \frac{(OD - ID)}{k_{tube}} = \frac{(4 \text{ mm}) \left(\frac{\text{m}}{1000 \text{ mm}} \right)}{36 \frac{\text{W}}{\text{m-K}}} = 0.00011111 \frac{\text{m}^2\text{-K}}{\text{W}}$$

The thermal resistance on the combustion gas side of the tube depends on the fin geometry. An expression for computing the gas side thermal resistance is,

$$R''_{gas} = \frac{1}{h_{gas} \left(\frac{A'_{prime}}{A'_{steam}} \right) + h_{gas} \left(\frac{\eta A'_{fin}}{A'_{steam}} \right)}$$

In this equation,

h_{gas} = combustion gas convective heat transfer coefficient = 70 W/m²-K

A'_{prime} = non-finned tube area per unit tube length = 0.1592 m²/m

A'_{fin} = finned tube area per unit tube length (see Table P1.20B)

A'_{steam} = steam-side tube area per unit tube length = 0.2136 m²/m

η = fin efficiency (see Table P1.20B)

Table P1.20B shows the fin data for available fin heights required to calculate the combustion gas resistance along with an expression to compute the fin tip temperature.

The base temperature of a fin can be calculated by equating two alternate expressions for the heat transfer rate from the combustion gases to the boiling steam,

$$\frac{T_{base} - T_{steam}}{R''_{steam} + R''_{tube}} = \frac{T_{gas} - T_{steam}}{R''_{total}}$$

Design the boiler by specifying the number of tubes in each horizontal row and the fin height such that the tube bank fits into the boiler while maintaining the

TABLE P1.20B

Fin Data

Fin Height (mm)	A'_{fin} (m ² /m)	η	$\frac{T_{gas} - T_{tip}}{T_{gas} - T_{base}}$
0	0.080	1.000	1.000
12	1.211	0.962	0.945
18	1.889	0.924	0.891
25	2.776	0.867	0.811
31	3.618	0.811	0.735
37	4.535	0.752	0.656
44	5.701	0.683	0.567

specified clearances, maintaining a UA product of at least 23,500 W/K, and limiting the tip temperature of the fins to 400°C or less.

Engineering Design and Environmental Impact

- 1.21 Pick a topic in the general area of thermal energy systems of interest to you and research the ethical issues associated with environmental impact and/or sustainability related to subject you selected. Write a short paper summarizing your findings. Cite all of your references. Use *reliable* references (Wikipedia is *not* considered a reliable source).

2

Engineering Economics

2.1 Introduction

It may seem odd to find a chapter on engineering economics in a textbook that deals with thermal energy systems design and analysis. However, this chapter is germane since the optimization of thermal energy systems is often done to minimize the total system *cost*. This cost is generally made up many individual costs including the initial cost of the system components, labor costs, operating costs, maintenance costs, replacement costs, and salvage value. In addition, inflation, depreciation, taxes, and insurance also play a role in the system cost. The costs listed above come at different times during the life of the system. Since money has a time value due to interest, the design of a cost optimized system requires some way to convert all of the expenditures and incomes to a common point in time. This is the challenge in engineering economic analyses.

The value of money is determined by two factors; the actual face value of the money, and the time value of the money. The time value of money is a result of the “cost” of money, i.e., the *interest rate* or *rate of return*. The cost of money can be viewed from two perspectives. From the borrower’s perspective, the cost of money is the *interest* paid. From the point of view of the investor, the cost of money is the *rate of return* required before an investment is viewed as viable.

Engineering economics is often taught as a semester-long course. The presentation in this chapter is not meant to be a substitute for such a course. It is, however, a summary of the salient features of engineering economic analysis that will allow users of this book to apply these concepts to thermal energy systems. For more in-depth coverage of these topics and others not included in this chapter, the reader is encouraged to consult one of several excellent references on this subject.

2.2 Engineering Economics Nomenclature

Throughout this chapter, several economic variables are used. Table 2.1 defines some of the common variables used in economic analysis.

TABLE 2.1

Common Variables Used in Engineering Economic Analysis

Variable	Definition
A	Uniform periodic payments or incomes
AC	Annual cost
AT	After-tax cash flow
BT	Before-tax cash flow
D	Depreciation cost
F	Money considered at a future time
G	Uniform cost or income gradient
i	Interest rate or rate of return
I or IC	Initial cost of an item or investment
M	Maintenance costs
MARR	Minimum acceptable rate of return
n	Number of time periods considered in an analysis
O	Operation costs
P	Money considered at the present time
PW	Present worth
S	Salvage value of an item
t	Tax rate

2.3 The Cash Flow Diagram

The *cash flow diagram* is a useful tool for visualizing an engineering economics problem. The cash flow diagram is akin to a free-body diagram in statics or dynamics, or identifying a system boundary in thermodynamics. Consider the following example:

A heating system for a multi-tenant dwelling has an initial cost of \$20,000. The yearly operation and maintenance charges are \$1,000. Increased rent (to help defray the cost of the heating system) results in an extra \$5,000 per year of income. The heating plant has a life of 10 years, at which time it can be sold for \$7,000.

The cash flow diagram for this scenario is shown in Figure 2.1.

Notice in Figure 2.1 that,

- The costs (or disbursements) are pointing down.
- The incomes are pointing up.
- The uniform yearly incomes and costs are indicated at the *end* of the year, even though they may be distributed throughout the year. This may be confusing, especially in year 10. Even though the system will be sold for \$7,000 at the end of year 10, there must be income received and maintenance costs from year 9 to 10. These cash flows are indicated at the end of year 10.

The incomes and costs are additive *at any point in time* on the cash flow diagram. This means that the cash flow diagram from Figure 2.1 can be equivalently drawn as seen in Figure 2.2

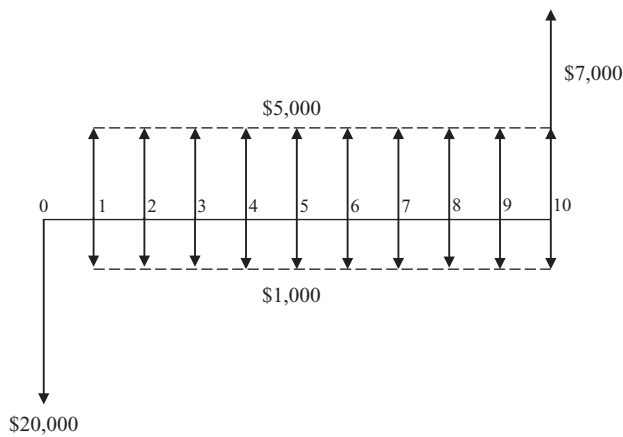


FIGURE 2.1
Cash flow diagram.

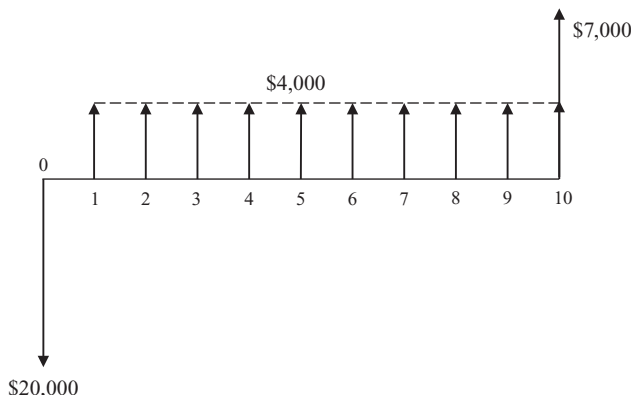


FIGURE 2.2
An equivalent version of the cash flow diagram shown in Figure 2.1.

In most engineering economic analysis problems, the task is to determine how to transform *all* of the incomes and costs on a cash flow diagram to a single point in time. Since \$1 today is not worth the same as \$1 in the past or the future due to inflation and other economic factors, money has *time value*. In order to collapse a cash flow diagram to a single point in time requires that the time value of money be considered.

2.4 The Time Value of Money

If there were no such thing as an interest rate, economics would be fairly simple (and banks would be out of business). For example, if you were to borrow \$12,000 from a bank and pay it back over a year in equivalent monthly installments at 0% interest, your monthly payment would be $\$12,000/12 = \$1,000$. This is easy. However, in the real world, money costs money. If you borrow money, you are expected to pay for the borrowed money over time.

Likewise, if you invest money, you expect a return on your investment over time. The cost of money over time is known as *interest*. The return on an investment over time is called the *rate of return*. Often, the word *interest* is used for both scenarios. In a business or engineering setting, company fiscal and/or project managers determine a *minimum acceptable rate of return* (MARR) for a project. This represents the minimum rate of return that the company can accept before the project is approved.

If the interest were *simple interest*, then the interest payment could be figured into the principal borrowed and divided over the number of payment periods. In the example above, if you were to borrow the \$12,000 at a simple interest rate of 10% per year, your total interest payment would be $(12,000)(0.10) = \$1,200$. This means you would have to pay the bank a total of $\$12,000 + \$1,200 = \$13,200$. The monthly payment would then be $\$13,200/12 = \$1,100$.

Neither of the scenarios given above is common in the economic world. In reality, interest is *compounded*. Compounding means that interest is charged (or paid) on the principal and the previously charged (or accrued) interest. For example, consider an investment of \$10,000 at an annual interest rate of 6%, compounded annually. At the end of the first year, the current \$10,000 would be worth $(\$10,000)(1.06) = \$10,600$. At the end of the second year, the original \$10,000 would be worth $(\$10,600)(1.06) = \$11,236$. At the end of the third year, $(\$11,236)(1.06) = \$11,910$, and so on. Notice in this case, the interest earned gains interest in addition to the principal. This is the idea behind compounding.

2.4.1 Future Value of a Present Sum: The Single Payment Compound Amount Factor

Using the \$10,000 investment example in Section 2.4, a mathematical expression can be derived that will allow us to determine the value of a single payment at any time in the future. The value of the \$10,000 investment at the end of the first year was given as

$$(\$10,000)(1.06) = \$10,600$$

At the end of the second year,

$$\begin{aligned}(\$10,600)(1.06) &= \$11,236 \\ [(\$10,000)(1.06)](1.06) &= \$11,236 \\ (\$10,000)(1.06)^2 &= \$11,236\end{aligned}$$

Notice the recursion here. If we are interested in the future value (F) of the \$10,000 at any year n , and the interest rate is compounded annually at 6%, this can be found by

$$F = (\$10,000)(1.06)^n$$

This thinking can be generalized even further. Notice that the factor 1.06 is equal to $(1 + 0.06)$ where 0.06 is the interest rate, expressed as a decimal rather than a percent. Therefore, using this concept, we can calculate the future value, F , of an initial investment made at the present time, P , at any time period, n , for the interest rate, i (expressed as a decimal), as:

$$F = P(1 + i)^n \quad (2.1)$$

The expression $(1 + i)^n$ is known as an *interest factor*. In particular, this interest factor is called the *Single Payment Compound Amount Factor*. In economic analyses, this factor is written in shorthand notation as $(F/P, i, n)$. Therefore, Equation 2.1 can be written as,

$$F = P \left(\frac{F}{P}, i, n \right) \quad (2.2)$$

Given the expression for this factor, values or tables of values of the Single Payment Compound Amount Factor for various interest rates and compounding periods can be constructed.

Annual compounding was used to develop this interest factor. However, compounding periods may not necessarily be on a yearly basis. They may be quarterly, monthly, daily, or even continuous. When calculating the interest factor, it is important that the interest rate, i , is consistent with the compounding period, n . The following example demonstrates this concept.

Example 2.1

An investment opportunity that provides an annual rate of return of 6% is available. Determine the future value of a \$1,000 investment 10 years from now if the interest is compounded (a) annually and (b) monthly.

Solution

For both cases, the future sum can be found using the single payment compound amount factor,

$$F = P \left(\frac{F}{P}, i, n \right) = \$1,000 \left(\frac{F}{P}, i, n \right)$$

For annual compounding, the interest rate, $i = 0.06$, and the number of compounding periods, $n = 10$. Therefore, the interest factor is,

$$\left(\frac{F}{P}, 0.06, 10 \right) = (1 + 0.06)^{10} = 1.79085$$

The value of the future sum for this annual compounding scenario can then be found,

$$F = \$1,000 \left(\frac{F}{P}, 0.06, 10 \right) = \underline{\underline{\$1,791}}$$

1.79085

For monthly compounding, the interest rate is divided equally over 12 months. Therefore, $i = 0.06/12 = 0.005$, and the number of compounding periods is $n = (10)(12) = 120$. Then,

$$\left(\frac{F}{P}, 0.005, 120 \right) = (1 + 0.005)^{120} = 1.81940$$

$$\therefore F = \$1,000 \left(\frac{F}{P}, 0.005, 120 \right) = \underline{\underline{\$1,819}}$$

1.81940

From an investment perspective, more frequent compounding results in a larger future sum because the interest is gaining interest.

2.4.2 Present Value of a Future Sum: The Present Worth Factor

The *present worth factor* is an interest factor that allows for the conversion of a future sum to a present value at a given interest rate for a number of compounding periods. This interest factor is helpful in determining how much money should be invested at a given interest rate to achieve a future goal. Recall that the single payment compound amount factor was used to convert a present sum to a future value at a given interest rate. The present worth factor is used to do just the opposite. Therefore, it is simply the reciprocal of the single payment compound amount factor,

$$(1+i)^{-n} = \left(\frac{P}{F}, i, n \right) \quad (2.3)$$

Using this interest factor, the present value of a future sum can be found by,

$$P = F(1+i)^{-n} = F \left(\frac{P}{F}, i, n \right) \quad (2.4)$$

2.4.3 Future Value of a Uniform Series: The Compound Amount Factor

In many situations, uniform payments or disbursements occur in an economic scenario. For example, when money is borrowed from a bank for a car loan, the payments are uniform monthly payments. These payments can be converted to an equivalent future value using the *compound amount factor*. This conversion allows one to compute how much interest is paid over the life of the loan. A similar scenario can be envisioned for an investment fund where uniform disbursements are paid out on a regular basis (e.g., a retirement fund).

To develop the expression for the compound amount factor, envision the loan payback scenario shown in Figure 2.3.

Each of the uniform payments, A , can be envisioned as a present value at its respective position on the cash flow diagram. Therefore, the single payment compound amount factor can be used to move that value to the future. For the scenario shown in Figure 2.3,

$$F = A(1+i)^9 + A(1+i)^8 + A(1+i)^7 + A(1+i)^6 + A(1+i)^5 + A(1+i)^4 + A(1+i)^3 + A(1+i)^2 + A(1+i)^1 + A(1+i)^0 \quad (2.5)$$

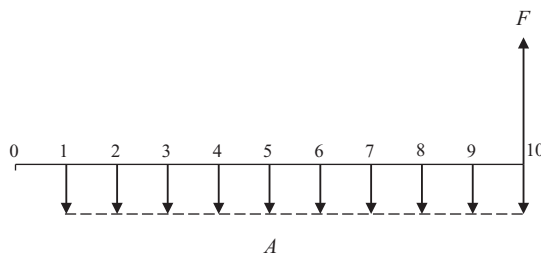


FIGURE 2.3

Cash flow diagram showing the equivalence between a uniform series, A , and a future sum, F .

Since A is uniform, the above equation can be written as,

$$F = A[(1+i)^9 + (1+i)^8 + (1+i)^7 + \dots + (1+i) + 1] \quad (2.6)$$

In general terms of any time period, n , Equation (2.6) becomes,

$$F = A[(1+i)^{n-1} + (1+i)^{n-2} + (1+i)^{n-3} + \dots + (1+i) + 1] \quad (2.7)$$

The term in brackets in Equation (2.7) converts the uniform series, A , to an equivalent future value. The term in brackets is known as the *compound amount factor*,

$$\left(\frac{F}{A}, i, n\right) = (1+i)^{n-1} + (1+i)^{n-2} + (1+i)^{n-3} + \dots + (1+i) + 1 \quad (2.8)$$

Equation 2.8 is not a particularly convenient way to write this factor. However, with some algebra, the factor can be written in a more useful way. Multiplying both sides of Equation 2.8 by $(1+i)$ results in,

$$\left(\frac{F}{A}, i, n\right)(1+i) = (1+i)^n + (1+i)^{n-1} + (1+i)^{n-2} + \dots + (1+i)^2 + (1+i) \quad (2.9)$$

Subtracting Equation 2.8 from Equation 2.9 gives,

$$\left(\frac{F}{A}, i, n\right)[(1+i) - 1] = (1+i)^n - 1 \quad (2.10)$$

Solving Equation 2.10 for the interest factor,

$$\left(\frac{F}{A}, i, n\right) = \frac{(1+i)^n - 1}{i} \quad (2.11)$$

Therefore, the conversion of a uniform series to an equivalent future value is given by,

$$F = A \left[\frac{(1+i)^n - 1}{i} \right] = A \left(\frac{F}{A}, i, n \right) \quad (2.12)$$

Notice that the time period of the uniform series is not specified in this development. It could be years, months, or days. A common mistake is to assume that A refers to a uniform *annual* series. Using the variable A is perhaps an unfortunate misnomer in engineering economic analysis. However, the time period of the series is dictated by n , the number of time periods being considered.

2.4.4 An Equivalent Uniform Series That Represents a Future Value: The Uniform Series Sinking Fund Factor

Given a future value, F , it is possible to find an equivalent uniform series that has the same cash equivalence. This is the reciprocal problem described in Section 2.4.3. Therefore, the conversion F to A can be accomplished by,

$$A = F \left[\frac{i}{(1+i)^n - 1} \right] = F \left(\frac{A}{F}, i, n \right) \quad (2.13)$$

The interest factor is known as the *uniform series sinking fund factor*.

2.4.5 Present Value of a Uniform Series: The Uniform Series Present Worth Factor

Figure 2.4 shows a cash flow diagram that demonstrates the equivalence of a uniform series to a present value. There are several ways to develop the interest factor to convert a uniform series to a present value. One strategy is to use the compound amount factor and convert the uniform series to a future value. Then, the present worth factor can be used to convert to a present value. Using this strategy,

$$P = \left[A \left(\frac{F}{A}, i, n \right) \right] \left(\frac{P}{F}, i, n \right) \quad (2.14)$$

Substituting the interest factors into Equation 2.14 gives,

$$P = A \left[\frac{(1+i)^n - 1}{i} \right] (1+i)^{-n} = A \left[\frac{(1+i)^n - 1}{i(1+i)^n} \right] = A \left(\frac{P}{A}, i, n \right) \quad (2.15)$$

The interest factor developed here is known as the *uniform series present worth factor*,

$$\left(\frac{P}{A}, i, n \right) = \frac{(1+i)^n - 1}{i(1+i)^n} \quad (2.16)$$

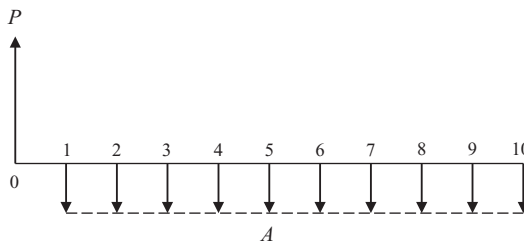


FIGURE 2.4

Cash flow diagram showing the equivalence between a uniform series, A , and a present value, P .

2.4.6 An Equivalent Uniform Series That Represents a Present Value: The Capital Recovery Factor

Given a present value, an equivalent uniform series can be found using the reciprocal of the uniform series present worth factor. This reciprocal is known as the *capital recovery factor*,

$$\left(\frac{A}{P}, i, n \right) = \frac{i(1+i)^n}{(1+i)^n - 1} \quad (2.17)$$

Using the capital recovery factor, the uniform series, A , which is equivalent to a present value, P is given by,

$$A = P \left(\frac{A}{P}, i, n \right) = P \left[\frac{i(1+i)^n}{(1+i)^n - 1} \right] \quad (2.18)$$

2.4.7 Present Value of a Uniform Linearly Increasing Series—The Gradient Present Worth Factor

There are instances in an industrial scenario where costs are incurred uniformly over time (e.g., every year), but the costs increase each time period. Consider the cash flow diagram shown in Figure 2.5. In this figure, the frequency of the series is uniform in time. However, the magnitude of the series increases linearly as time goes on. In addition, notice that the linear increase of the uniform series starts at the end of the *second* period. The value G in this figure is called the *gradient*. It represents the linear increase in the uniform series over time. To determine the equivalent present value of this series, each series value can be treated as a future sum and brought back to the present using the present worth factor,

$$P = \frac{G}{(1+i)^2} + \frac{2G}{(1+i)^3} + \frac{3G}{(1+i)^4} + \dots + \frac{9G}{(1+i)^{10}} \quad (2.19)$$

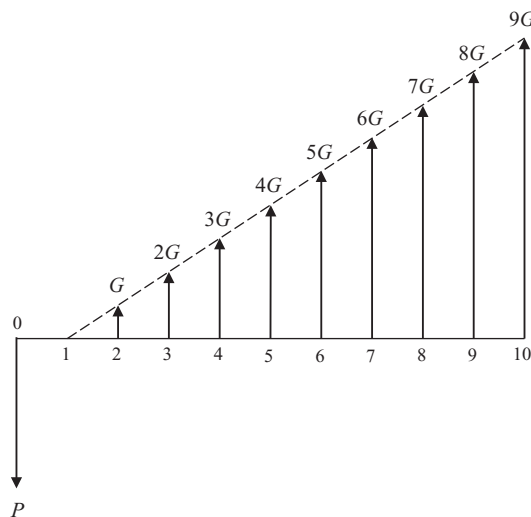


FIGURE 2.5

Cash flow diagram showing the equivalence of a uniform linearly increasing series and a present value.

Writing this equation for any cash flow diagram with n periods,

$$P = \frac{G}{(1+i)^2} + \frac{2G}{(1+i)^3} + \frac{3G}{(1+i)^4} + \dots + \frac{(n-1)G}{(1+i)^n} \quad (2.20)$$

Factoring out the value of the gradient, G , results in,

$$P = G \left[\frac{1}{(1+i)^2} + \frac{2}{(1+i)^3} + \frac{3}{(1+i)^4} + \dots + \frac{(n-1)}{(1+i)^n} \right] \quad (2.21)$$

The term in the brackets is an interest factor known as the *gradient present worth factor*. However, this form of the factor is not very convenient to work with. After performing several algebraic manipulations, Equation 2.21 can be written as,

$$P = G \left[\frac{(1+i)^n - 1}{i^2(1+i)^n} - \frac{n}{i(1+i)^n} \right] = G \left(\frac{P}{G}, i, n \right) \quad (2.22)$$

2.4.8 Summary of Interest Factors

The interest factors developed in this section are known as *discrete* interest factors since the interest compounding occurs over specific finite time periods. These interest factors are summarized in Table 2.2 for convenience and quick reference.

TABLE 2.2
Interest Factors for Discrete Compounding

Name	Converts	Symbol	Computed by
Single Payment Compound Amount	P to F	$\left(\frac{F}{P}, i, n \right)$	$(1+i)^n$
Present Worth	F to P	$\left(\frac{P}{F}, i, n \right)$	$(1+i)^{-n}$
Uniform Series Sinking Fund	F to A	$\left(\frac{A}{F}, i, n \right)$	$\frac{i}{(1+i)^n - 1}$
Compound Amount	A to F	$\left(\frac{F}{A}, i, n \right)$	$\frac{(1+i)^n - 1}{i}$
Capital Recovery	P to A	$\left(\frac{A}{P}, i, n \right)$	$\frac{i(1+i)^n}{(1+i)^n - 1}$
Uniform Series Present Worth	A to P	$\left(\frac{P}{A}, i, n \right)$	$\frac{(1+i)^n - 1}{i(1+i)^n}$
Gradient Present Worth	G to P	$\left(\frac{P}{G}, i, n \right)$	$\frac{(1+i)^n - 1}{i^2(1+i)^n} - \frac{n}{i(1+i)^n}$

2.5 Nominal and Effective Interest Rates

When a financial institution quotes an interest rate to you, they are quoting what is known as a *nominal* annual rate. Sometimes, they may also quote you a compounding period. For example, 6% compounded monthly means that the nominal annual rate is 6% while the compounding period is monthly.

When the compounding period is more frequent than annual, the nominal interest rate does not reflect the true rate due to the interest itself being compounded. In other words, the compounded interest is subject to the time value of money. In this case, the interest that more accurately reflects the time value of money is known as the *effective* interest. The *effective* interest rate for a nominal rate of i for m compounding periods in *one year* can be determined by,

$$i_{\text{eff}} = \left(\frac{F - P}{P} \right) = \frac{1}{P} \left[P \left(\frac{F}{P}, \frac{i}{m}, m \right) - P \right] = \left(\frac{F}{P}, \frac{i}{m}, m \right) - 1 \quad (2.23)$$

For example, the effective interest rate for an investment scenario of 6% compounded monthly is,

$$i_{\text{eff}} = \left(1 + \frac{i}{12} \right)^{12} - 1 = \left(1 + \frac{0.06}{12} \right)^{12} - 1 = 0.0618 = \underline{\underline{6.18\%}} \quad (2.24)$$

Notice in Equation 2.24, the interest rate is expressed as $(i/12)$ because the interest is compounded monthly in this example ($m = 12$).

2.6 Time Value of Money Examples

In this section, several examples will be presented that demonstrate how the discrete interest factors developed in Section 2.4 can be applied in various economic analyses.

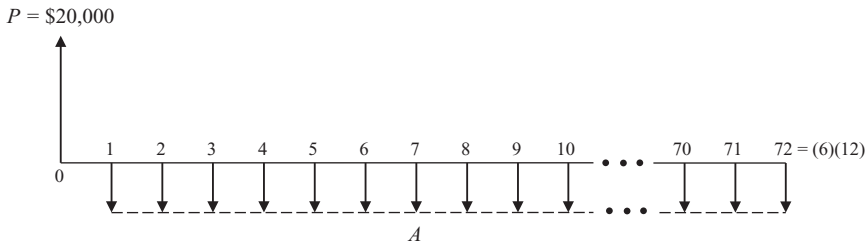
Example 2.2

A bank is advertising new car loans at a nominal rate of 3.5%. Consider a situation where \$20,000 is borrowed from this bank to buy a new car. The loan is to be paid back in equal monthly installments over a 6-year period. Determine the monthly payment and the effective interest rate of the loan.

Solution

In most economic analysis problems, it is a good idea to start with a cash flow diagram to help visualize the problem. The cash flow diagram for this problem is shown in Figure E2.2.

The \$20,000 that the bank lends for purchase of the car is viewed as an income received. The monthly payments are expenses. Notice that there are 72 periods in this cash flow diagram because the life of the loan is 6 years, which is equivalent to 72 months.

**FIGURE E2.2**

Cash flow diagram for car purchase described in Example 2.2.

Based on this scenario, the interest rate paid per month is $i = 0.035/12$. The monthly payment can be found by applying the capital recovery factor,

$$A = P \left(\frac{A}{P}, i, n \right) = (\$20,000) \left(\frac{A}{P}, \frac{0.035}{12}, 72 \right) = \underline{\$308.37}$$

0.0154184

The capital recovery factor was calculated using the expression developed in Section 2.4.6 and shown in Table 2.2. There are many online loan calculators. There are also many loan calculator applications for smart phones and tablets. These calculators use the expressions shown in this example to determine loan payments.

For this loan, the bank advertises an interest rate of 3.5%. This is the nominal annual interest rate. The effective rate of this loan is,

$$i_{\text{eff}} = \left(\frac{F}{P}, \frac{i}{m}, m \right) - 1 = \left(\frac{F}{P}, \frac{0.035}{12}, 12 \right) - 1 = 0.03557 = \underline{3.56\%}$$

1.03557

As expected, the interest rate advertised by the bank is slightly lower than the actual interest rate being paid because of the monthly compounding. If the compounding period was yearly, then the effective rate is equal to the nominal rate.

With installment loans, it is interesting to see how the monthly payment is distributed between payment of interest and repayment of the principle. Many banks offer a payment schedule known as an *amortization* schedule. The following example shows how to develop an amortization schedule.

Example 2.3

Develop an amortization schedule for the car loan described in Example 2.2.

Solution

From Example 2.2, the monthly payment is \$308.37. In the first month, the interest paid is the initial loan amount multiplied by the monthly interest rate,

$$I_1 = P \left(\frac{i}{12} \right) = (\$20,000) \left(\frac{0.035}{12} \right) = \$58.33$$

The balance of the payment is used to retire the principal,

$$P_1 = A - I_1 = \$ (308.37 - 58.33) = \$250.04$$

Therefore, at the end of the first year, the principal balance on the loan is,

$$\text{Bal}_1 = \$20,000 - P_1 = \$20,000 - 250.04 = \$19,749.96$$

The second payment results in,

$$\begin{aligned} I_2 &= P_1 \left(\frac{i}{12} \right) = (\$19,749.96) \left(\frac{0.035}{12} \right) = \$57.60 \\ P_2 &= A - I_2 = \$308.37 - 57.60 = \$250.77 \\ \text{Bal}_2 &= P_1 - P_2 = \$19,749.96 - 250.77 = \$19,499.19 \end{aligned}$$

This process repeats for subsequent years. For any time period, m , during the loan period,

$$I_m = P_{m-1} \left(\frac{i}{12} \right) \quad P_m = A - I_m \quad \text{Bal}_m = P_{m-1} - P_m$$

This type of calculation can be easily adapted to a spreadsheet. The various columns can be totaled to determine the total payments made and the interest paid over the life of the loan. Figure E2.3 is an abridged table that shows the resulting amortization schedule for this example.

The interest paid each month decreases while the amount paid to the principal goes up. The life of the loan, and thus the total amount of interest paid can be reduced significantly by paying down the principal *early* in the life of the loan.

The total amount of interest paid for this loan is \$2,202.49. The longer the term of the loan, the more interest is paid. However, the longer loan term allows for a smaller payment. The consumer must balance both of these issues when deciding what loan term to select.

The following example shows how interest factors are used to manipulate a complex cash flow scenario.

m	Payment = \$308.37		Balance
	Interest	Principle	
0			\$ 20,000.00
1	\$ 58.33	\$ 250.03	\$ 19,749.97
2	\$ 57.60	\$ 250.76	\$ 19,499.20
3	\$ 56.87	\$ 251.50	\$ 19,247.71
4	\$ 56.14	\$ 252.23	\$ 18,995.48
5	\$ 55.40	\$ 252.96	\$ 18,742.51
⋮			
68	\$ 4.46	\$ 303.91	\$ 1,224.53
69	\$ 3.57	\$ 304.80	\$ 919.73
70	\$ 2.68	\$ 305.69	\$ 614.04
71	\$ 1.79	\$ 306.58	\$ 307.47
72	\$ 0.90	\$ 307.47	\$ (0.00)
	\$ 2,202.49	\$ 20,000.00	

FIGURE E2.3

Amortization schedule for the car loan from Example 2.2.

Example 2.4

A company is considering investing in some new equipment to enhance one of their production lines. It is estimated that the addition of this new equipment will increase annual profits by \$50,000. Annual maintenance costs are anticipated to be \$1,000, increasing by \$1,000 each subsequent year. The equipment is expected to last 10 years, at which time it can be sold for \$5,000. The company's fiscal managers have specified that a MARR of 20% annually must be realized from the equipment investment. Determine the maximum amount of money that the company can spend to meet this investment scenario. Assume annual compounding.

Solution

Based on the information given in the problem, the cash flow diagram for this problem is shown in Figure E2.4.

There are several ways to determine P which depend on the common point in the cash flow diagram where all incomes and expenses are referred to. In this case, the present value is desired. Therefore, bringing all incomes and expenses to the present (year 0) results in,

$$P + A_o \left(\frac{P}{A}, i, n \right) + G \left(\frac{P}{G}, i, n \right) = A_p \left(\frac{P}{A}, i, n \right) + S \left(\frac{P}{F}, i, n \right)$$

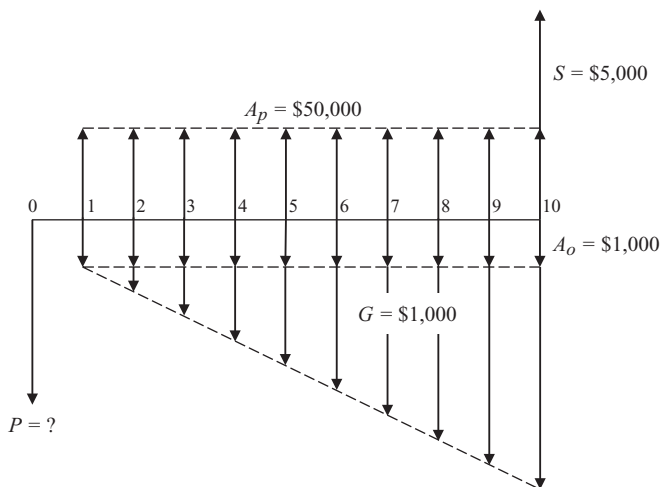
The interest rate and number of periods are known. Therefore, the interest factors can be found using the expressions in Table 2.2. Rearranging algebraically, and solving for P ,

$$P = (A_p - A_o) \left(\frac{P}{A}, i, n \right) - G \left(\frac{P}{G}, i, n \right) + S \left(\frac{P}{F}, i, n \right)$$

$$P = (\$50,000 - \$1,000) \left(\frac{P}{A}, 0.20, 10 \right) - (\$1,000) \left(\frac{P}{G}, 0.20, 10 \right) + (\$5,000) \left(\frac{P}{F}, 0.20, 10 \right)$$

4.19247
12.88708
0.16151

$$P = \underline{\underline{\$193,352}}$$

**FIGURE E2.4**

Cash flow diagram for equipment investment.

This calculation indicates that an investment in the equipment of \$193,352 will meet the company's MARR of 20%. If the equipment is less expensive than this, the rate of return would be higher than 20%. Conversely, if the equipment is more expensive than \$193,352, then the rate of return drops below 20% and the improvement is viewed as financially unacceptable.

In certain instances, it is desirable to determine the interest rate or the rate of return for a given scenario. This is demonstrated in the following problem.

Example 2.5

Suppose that the equipment cost for the processing facility in Example 2.4 has an initial cost of \$225,000. Keeping all other parameters as defined in Example 2.4, determine the corresponding rate of return on this equipment investment.

Solution

The cash flow diagram for this scenario is the same as in the Example 2.4 with the exception that the present value of the equipment is known, $P = \$225,000$. Therefore, the balancing of incomes and expenses at year 0 results in the same equation for the present value, P , as seen in Example 2.4.

$$P = (A_p - A_o) \left(\frac{P}{A}, i, n \right) + S \left(\frac{P}{F}, i, n \right) - G \left(\frac{P}{G}, i, n \right)$$

The interest factors cannot be directly computed because the interest rate is unknown. Writing out the interest factors and substituting the known values results in,

$$\$225,000 = (\$50,000 - \$1,000) \left[\frac{(1+i)^{10} - 1}{i(1+i)^{10}} \right] + \$5,000(1+i)^{-10} - \$1,000 \left[\frac{(1+i)^{10} - 1}{i^2(1+i)^{10}} - \frac{10}{i(1+i)^{10}} \right]$$

The only unknown in this equation is the interest rate, i . However, the difficulty is that the equation cannot be solved explicitly for the interest rate. Therefore, the solution is iterative. Solving this equation results in $i = 0.1562$. Therefore, the annual rate of return for an initial investment in the equipment of \$225,000 is 15.62%. This result substantiates the conclusion drawn in Example 2.4; an equipment investment greater than \$193,352 results in a rate of return less than 20%.

2.7 Using Software to Calculate Interest Factors

Without software, interest factors must be calculated using the expressions shown in Table 2.2. Alternatively, tables of calculated interest factors can be used. However, this often requires interpolation.

Spreadsheet programs are very versatile. Many of the modern programs have built-in interest factor functions. Each spreadsheet program may vary in how the interest factor calculation is called, so the user is encouraged to carefully read the help menu to understand if the factors being used are those needed in the analysis. Having interest factors accessible with a function call is very convenient. Combined with solver capability,

Example 2.5 - Using Microsoft Excel			
GIVEN:	$A_p =$	\$ 50,000.00	Annual profit increase due to equipment
	$A_o =$	\$ 1,000.00	Annual operation cost
	$S =$	\$ 5,000.00	Salvage value of equipment at year n
	$G =$	\$ 1,000.00	Maintenance gradient
	$n =$	10	Number of periods in the analysis (years)
FIND:	$i =$	15.62%	Rate of return (interest rate)
			Calculated with Goal Seek
	$P + A_o \left(\frac{P}{A}, i, n \right) + G \left(\frac{P}{G}, i, n \right) = A_p \left(\frac{P}{A}, i, n \right) + S \left(\frac{P}{F}, i, n \right)$		
COSTS:	$P =$	\$ 225,000.00	Initial cost of equipment
	$A_o^*(P/A, i, n) =$	\$4,902.40	Calculated with PV function
1	$G^*(P/F, i, 1) =$	\$0.00	Calculated with PV function
2	$G^*(P/F, i, 2) =$	\$748.06	Calculated with PV function
3	$G^*(P/F, i, 3) =$	\$1,293.99	Calculated with PV function
4	$G^*(P/F, i, 4) =$	\$1,678.76	Calculated with PV function
5	$G^*(P/F, i, 5) =$	\$1,935.96	Calculated with PV function
6	$G^*(P/F, i, 6) =$	\$2,093.02	Calculated with PV function
7	$G^*(P/F, i, 7) =$	\$2,172.30	Calculated with PV function
8	$G^*(P/F, i, 8) =$	\$2,191.97	Calculated with PV function
9	$G^*(P/F, i, 9) =$	\$2,166.67	Calculated with PV function
10	$G^*(P/F, i, 10) =$	\$2,108.21	Calculated with PV function
	PV COSTS =	\$ 246,291.34	
INCOMES:	$A_p^*(P/A, i, n) =$	\$245,120.11	Calculated with PV function
	$S^*(P/F, i, n) =$	\$1,171.23	Calculated with PV function
	PV INCOMES =	\$246,291.34	
	PV(COST - INCOME) =	\$ (0.00)	Set to zero in Goal Seek

FIGURE 2.6

Microsoft Excel solution of Example 2.5.

iterative problems can easily be solved. As an example, the Microsoft Excel solution of Example 2.5 is shown in Figure 2.6. Notice that all of the interest factors were calculated using the “PV” function (the Help Menu shows how to use this function). The maintenance gradient costs were calculated using the PV function for each individual year since there is no gradient function available.

Using equation solving software is another convenient way to calculate interest factors, especially in an iterative problem such as Example 2.5. Most equation solving software allows the user to develop functions or subroutines that can be stored in a library. This allows for very easy retrieval of the function value by simply providing a function call within the equation set.

2.8 Economic Decision Making

Interest factors allow for the conversion of money in a cash flow diagram to a common point in time. This provides the basis for decision making. In the corporate world, decisions to proceed with a project are often influenced by which alternative is best from the

economic point of view (i.e., which is cheapest, which makes more profit, etc.). There are several different methods used to compute the best economic alternative. In this chapter, the present worth (PW) and annual cost (AC) analyses will be considered.

2.8.1 Present Worth Analysis

In the PW analysis, all expenditures and incomes in the cash flow diagram are converted to an equivalent present worth. When the present worth of each alternative is compared, a decision can be made by selecting the alternative with the numerically highest present worth (e.g., less negative or more positive). Consider the following example, where the lives of two alternatives are equal.

Example 2.6

Two machines are being considered for a manufacturing process. Machine A has an initial cost of \$800 with operating costs of \$600 per year. Machine B costs \$1,000 with operating costs of \$500 per year. Both machines have a 5-year life with no salvage value. If MARR is 15%, compounded annually, which machine should be purchased?

Solution

Assuming that each machine results in the same profit, the only difference between alternatives is the initial and operating costs of each machine. A cash flow diagram for each machine is shown in Figure E2.6.

Assuming annual compounding, the present worth of each alternative is,

$$PW_A = -P_A - A_A \left(\frac{P}{A}, i, n \right) = -\$800 - \$600 \left(\frac{P}{A}, 0.15, 5 \right) = -\$2,811$$

3.52155

$$PW_B = -P_B - A_B \left(\frac{P}{A}, i, n \right) = -\$1,000 - \$500 \left(\frac{P}{A}, 0.15, 5 \right) = \underline{\underline{-\$2,676}}$$

3.52155

The alternative with the highest present worth is Machine B, therefore it should be selected in this case.

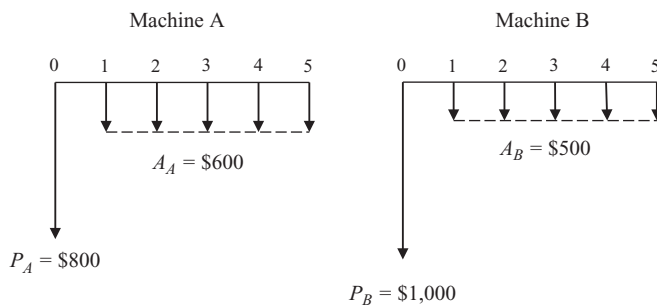


FIGURE E2.6
Cash flow diagrams for machines A and B.

Alternatives with unequal lives require special consideration when using the PW analysis. An unfair comparison can result when unequal-life alternatives are considered without making adjustments. In order to make a fair comparison, one possibility is to consider the lives of the alternatives to be equal at the least common multiple of all alternatives by creating a replacement scheme. For example, if two alternatives are being compared, one with a 3-year life and one with a 6-year life, a 6-year scenario can be envisioned for both alternatives where the equipment, incomes, and cost of the 3-year alternative repeat at the end of the third year. This is demonstrated in the following example.

Example 2.7

A company is considering purchasing a machine for a short-term project. A vendor has two possible machines that would be suitable for the project. Machine X has an initial cost of \$14,000 with a salvage value after 6 years of \$3,000. Machine X results in an annual savings of \$900. Machine Y has a cheaper initial cost of \$9,000. The annual savings using Machine Y is \$700. Machine Y has a life of only 3 years, at which time it can be sold for \$2,000. The MARR for this project is 15%. Determine which machine should be selected based on economics using a Present Worth analysis.

Solution

The cash flow diagrams for Machine X and Machine Y are shown in Figure E2.7A. The lives of each machine are different. Therefore, it would be an unfair comparison to consider the present worth of each machine to make an economic decision on which to purchase.

Since Machine X has a 6-year life and Machine Y has a 3-year life, the least common multiple is 6 years. Therefore, by considering a complete replacement of Machine Y at

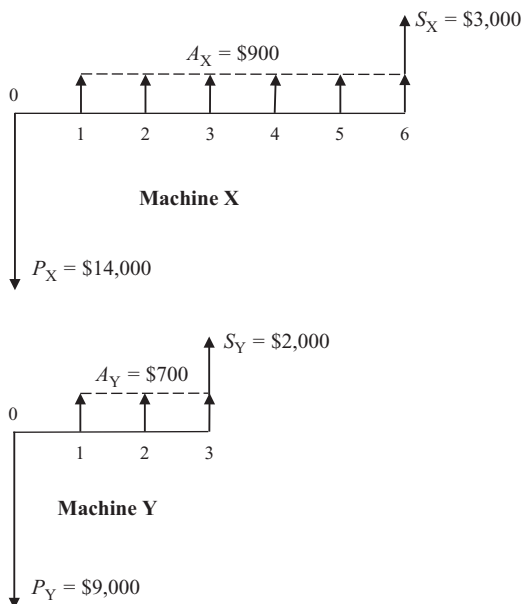
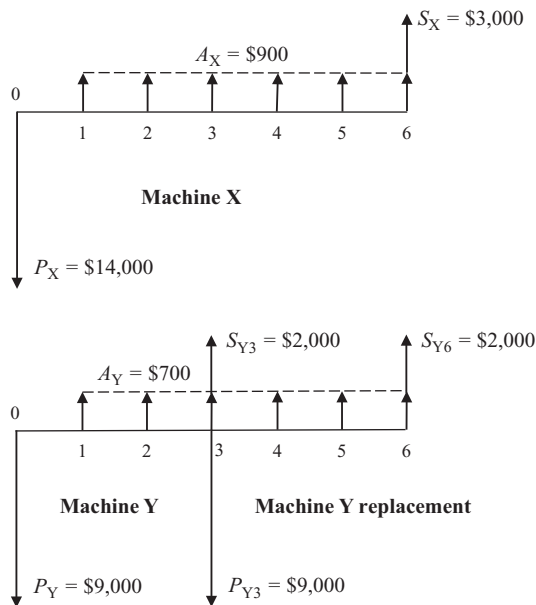


FIGURE E2.7A

Cash flow diagrams for machines X and Y.



Cash flow diagrams for Machines X and Y for the least common multiple life of six years.

Using the cash flow diagrams shown in Figure E2.7B, the present worth of each alternative can be computed. For Machine X:

$$\begin{aligned} PW_X &= -P_X + A_X \left(\frac{P}{A}, i, 6 \right) + S_X \left(\frac{P}{F}, i, 6 \right) \\ &= -\$14,000 + \$900 \left(\frac{P}{A}, 0.15, 6 \right)_{3.78448} + \$3,000 \left(\frac{P}{F}, 0.15, 6 \right)_{0.43233} \\ &= -\$9,297 \end{aligned}$$

$$\begin{aligned}
 PW_Y &= -P_Y - P_{Y_3} \left(\frac{P}{F}, i, 3 \right) + A_Y \left(\frac{P}{A}, i, 6 \right) + S_{Y_3} \left(\frac{P}{F}, i, 3 \right) + S_{Y_6} \left(\frac{P}{F}, i, 6 \right) \\
 &= -\$9,000 - \$9,000 \left(\frac{P}{F}, 0.15, 3 \right) + \$700 \left(\frac{P}{A}, 0.15, 6 \right) + \$2,000 \left(\frac{P}{F}, 0.15, 3 \right) + \$2,000 \left(\frac{P}{F}, 0.15, 6 \right) \\
 &\quad \qquad\qquad\qquad \text{0.65752} \qquad\qquad\qquad \text{3.78448} \qquad\qquad\qquad \text{0.65752} \qquad\qquad\qquad \text{0.43233} \\
 &= -\$10,089
 \end{aligned}$$

The machine with the highest present worth is Machine X. Therefore, based on the economic analysis, Machine X should be purchased for the project.



The present worth of Pump 2 for the same 10-year period is,

While these two present worth values are fairly close, Pump 2 provides a slight economic advantage, therefore Pump 2 should be selected for the application.

In the AC analysis, all expenditures and incomes are converted to an equivalent annual series. When the value of this series is known, a decision can be made based on the alternative with the lowest annual cost. Since *costs* are being compared in this method, it is common to consider costs as positive and incomes as negative.

The AC method can be used to compare alternatives with unequal economic lives. If the lives are different, it is assumed that the shorter-life alternative will be replaced with identical equipment (unless otherwise specified).

Example 2.9

Two machines are being considered for a manufacturing process. Machine A has an initial cost of \$800 with operating costs of \$600 per year. Machine B costs \$1,500 with operating costs of \$500 per year. Machine A has a 5-year life and Machine B has a 10-year life. Neither machine has a salvage value. If the MARR is 8%, which machine is the best economic alternative?

Solution

Assuming that both machines return the same profit, the only costs that are different in each scenario are the initial and operating costs of each machine. The cash flow diagrams for each machine are shown in Figure E2.9A.

For annual compounding, the annual cost of each of these cash flows is,

$$AC_A = \$800 \left(\frac{A}{P}, 8\%, 5 \right) + \$600 = \$800$$

0.25046

$$AC_B = \$1500 \left(\frac{A}{P}, 8\%, 10 \right) + \$500 = \underline{\underline{\$724}}$$

0.14903

This analysis indicates that Machine B has the lowest annual cost and should be selected.

The alternatives, A and B, have different economic lives in this example. As stated above, the AC method can be used in this situation by assuming that the shorter-lived alternative is replaced with identical equipment. To verify that this assumption is valid, consider the replacement of Machine A with identical equipment at the end of its 5-year life as shown in the cash flow diagram shown in Figure E2.9B. The annual cost of this scenario is,

$$AC_A = P_{A0} \left(\frac{A}{P}, i, 10 \right) + \left[P_{A5} \left(\frac{P}{F}, i, 5 \right) \right] \left(\frac{A}{P}, i, 10 \right) + A_A$$

$$AC_A = \$800 \left(\frac{A}{P}, 8\%, 10 \right) + \left[\$800 \left(\frac{P}{F}, 8\%, 5 \right) \right] \left(\frac{A}{P}, 8\%, 10 \right) + \$600 = \$800$$

0.14903

0.68058

0.14903

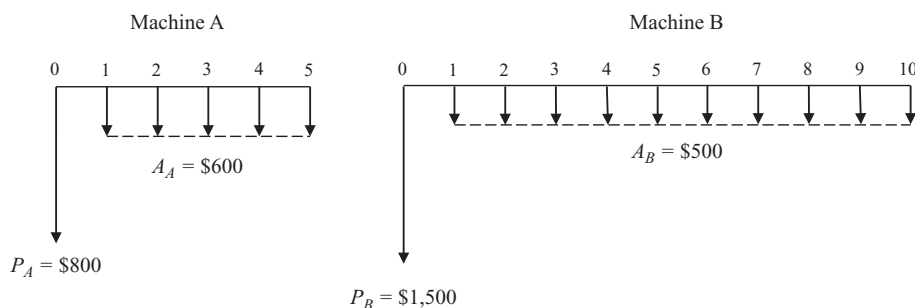
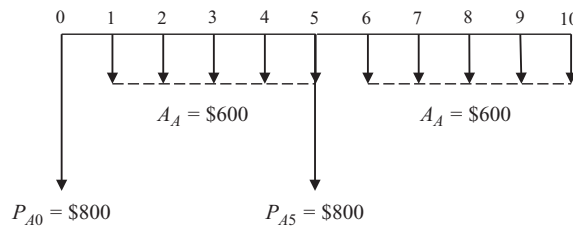


FIGURE E2.9A

Cash flow diagrams for Machines A and B.

**FIGURE E2.9B**

Cash flow diagram for Machine A with a replacement scenario.

Notice that the annual cost of this 10-year scenario consisting of an exact replacement at year 5 is identical to the 5-year single machine scheme. This justifies the notion that the economic life of the alternatives does not need to be the same when using the AC method so long as the shorter-lived alternative is replaced with identical equipment.

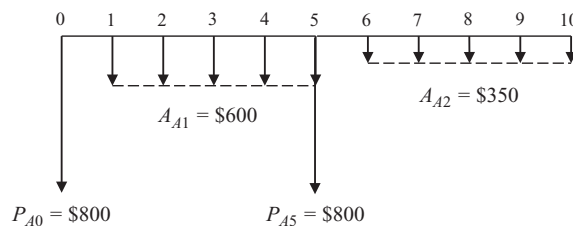
It may be possible to replace Machine A with a different machine at the end of 5 years. For example, consider the replacement scheme where Machine A is replaced with another machine costing \$800 at year 5, but due to improvements in the machine, its operating costs have dropped to \$350. The cash flow diagram for this scenario is shown in Figure E2.9C. The annual cost of this cash flow diagram is,

$$\begin{aligned}
 AC_A = & \$800 \left(\frac{A}{P}, 8\%, 10 \right) + \left[\$800 \left(\frac{P}{F}, 8\%, 5 \right) \right] \left(\frac{A}{P}, 8\%, 10 \right) \\
 & + \left[\$600 \left(\frac{P}{A}, 8\%, 5 \right) \right] \left(\frac{A}{P}, 8\%, 10 \right) + \left[\$350 \left(\frac{F}{A}, 8\%, 5 \right) \right] \left(\frac{A}{F}, 8\%, 10 \right) = \$699
 \end{aligned}$$

0.14903 0.68058 0.14903
3.99271 0.14903 5.86660 0.069029

In this case, it is more economical to purchase Machine A, and install a new machine at year 5 that has cheaper operating costs.

This example demonstrates that the AC method can be used to compare alternatives with unequal lives assuming that the shorter-lived alternative is replaced with identical equipment. However, if the shorter-lived alternative can be replaced with better equipment in the future, the resulting analysis may change the decision. The engineer must carefully consider potential replacement schemes when implementing the AC analysis.

**FIGURE E2.9C**

Cash flow diagram for an improved Machine A at Year 5.

2.8.3 Selection of Alternatives

The methods of decision making presented in this section are based solely on economics. In the selection of alternatives, there are other factors that contribute to the final decision. Some of these factors include environmental concerns, political issues, choice of vendors, etc. As an example, consider a company that is doing the things to gain the public's respect by how it treats the environment. This company may select a more expensive alternative that leads to smaller levels of pollution. This could be an important factor in winning over new customers to purchase the company's products.

2.9 Depreciation and Taxes

Capital outlay (CO) items such as buildings, automobiles, airplanes, equipment, etc., decrease in value over the years due to wear and/or obsolescence. This devaluation can be considered a production cost which reduces a company's earnings. Therefore, considering the devaluation of CO items can reduce taxes and increase profits.

Depreciation is a way to account for the devaluation of CO items and reflect a more accurate picture of earnings. Depending on what is being depreciated, the U.S. Internal Revenue Service (IRS) allows several different methods to calculate the yearly amount allowed.

Taxes are paid by corporations on profit. Corporate rates are generally much higher than consumer tax rates. The corporate tax rate is a composite of federal, state, and local rates. It is common for corporate tax rates to be in the neighborhood of 50% and higher. Since depreciation represents an equivalent cost due to the devaluation of CO items, it reduces profit. The reduction in profit reduces the tax burden.

2.9.1 After-Tax Cash Flow

Profits realized by a company are taxable. Depreciation reduces the taxes because the depreciation can be deducted from the profits before taxes are calculated. In any year k , the after-tax profit realized is given by,

$$A_{AT,k} = A_{BT,k} - T_k \quad (2.25)$$

In this equation, $A_{AT,k}$ and $A_{BT,k}$ are the annual profit after taxes and before taxes, respectively, and T_k is the tax imposed in year k . The tax imposed on the annual earnings can be written as,

$$T_k = t(A_{BT,k} - D_k) \quad (2.26)$$

In Equation 2.26, t is the tax rate and D_k is the depreciation allowed in year k . Substituting Equation 2.26 into Equation 2.25 results in,

$$A_{AT,k} = A_{BT,k} - t(A_{BT,k} - D_k) \quad (2.27)$$

This equation shows the tax advantage provided by depreciation.

The IRS allows depreciation to be determined for CO items based on when the equipment was put into service, what type of equipment it is, and what recovery period is expected for the equipment. For equipment put into service from 1981 to 1986, the Accelerated Cost Recovery System (ACRS) is used. For equipment put into service after 1986, the Modified Accelerated Cost Recovery System (MACRS) is used. The details of how depreciation is calculated using ACRS and MACRS are detailed in IRS Publications 534 (ACRS) and 946 (MACRS). The details of these methods are beyond the scope of this text and are often covered in most textbooks on engineering economy. However, the methods are *accelerated* depreciation schemes which give the companies a better tax advantage early in the depreciation scenario with decreasing depreciation as time goes on. The following sections show two depreciation schemes; straight line depreciation, and an accelerated scheme known as the sum of the year's digits depreciation.

2.9.2 Straight-Line Depreciation (SLD)

In the straight-line depreciation (SLD) model, the amount that can be depreciated annually is constant. The annual depreciation allowed in any year k for an item is given by,

$$D_k = \frac{IC - S}{N} \quad (2.28)$$

In this expression IC is the initial cost of the item being depreciated, S is the salvage value of the equipment at the end of its life, and N is the service life (or tax life) of the item. From this equation, it can be seen that depreciation rate is $1/N$.

2.9.3 Sum of the Years' Digits (SYD)

This is an accelerated depreciation scheme, allowing a larger deduction in the early years of the life of the item being depreciated. The depreciation allowed in any year, k is given by,

$$D_k = \frac{2(IC - S)(N - k + 1)}{N(N + 1)} \quad (2.29)$$

From this expression, the annual decrease in the depreciation is given by the *arithmetic gradient*,

$$\frac{2}{N(N + 1)} \quad (2.30)$$

It is interesting to note that the reciprocal of this gradient is the sum of the years' digits. For example, if $N = 5$,

$$\frac{N(N + 1)}{2} = \frac{5(5 + 1)}{2} = 15 = 5 + 4 + 3 + 2 + 1$$

This is where the depreciation method gets its name.

The following example shows the application of the SLD and SYD depreciation models and their effect on a company's profits, including taxes.

Example 2.10

A company is considering adding a new machine to one of its processing lines. The initial cost of the machine is \$300,000. The addition of the machine is expected to increase the company's profit by \$85,000 per year. The service life of the machine is 10 years and there is no salvage value. The company's corporate tax rate is 51%. Determine the rate of return provided by this machine for the following scenarios,

- Before taxes with no depreciation
- After taxes with no depreciation
- After taxes using SLD
- After taxes using SYD

Solution

- Figure E2.10A shows the cash flow diagram before taxes without considering any type of depreciation scheme. The rate of return for this cash flow diagram can be found by solving,

$$IC = A \left(\frac{P}{A}, i, n \right)$$

$$\$300,000 = (\$85,000) \frac{(1+i)^{10} - 1}{i(1+i)^{10}} \rightarrow i = \underline{25.38\%}$$

- Figure E2.10B shows the cash flow diagram after taxes, but without including any depreciation model. The rate of return for can then be found as follows,

$$IC = A_{AT} \left(\frac{P}{A}, i, n \right)$$

$$\$300,000 = (\$41,650) \frac{(1+i)^{10} - 1}{i(1+i)^{10}} \rightarrow i = \underline{6.46\%}$$

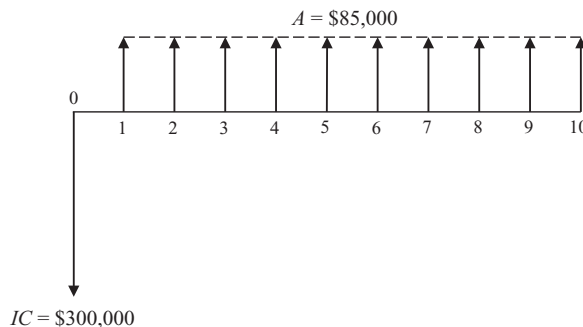
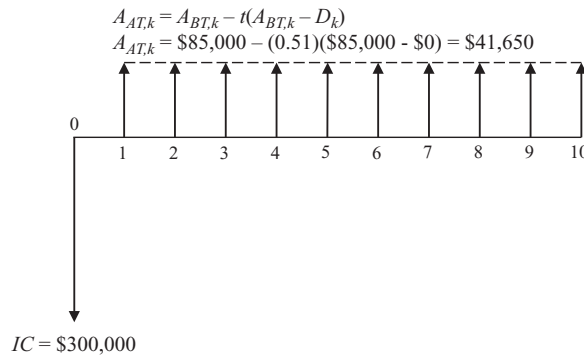


FIGURE E2.10A

Cash flow diagram before taxes with no depreciation.

**FIGURE E2.10B**

Cash flow diagram after taxes without depreciation.

Notice that the rate of return has dropped substantially due to taxes. Parts (c) and (d) demonstrate the advantage of using depreciation schemes.

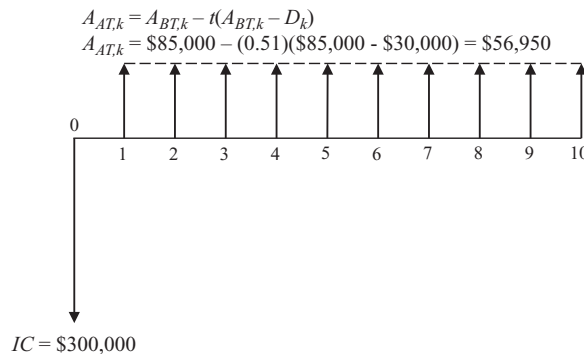
- c. Using SLD, the constant annual amount that can be deducted from the profits using the SLD model is given by,

$$D_k = \frac{IC - S}{N} = \frac{\$300,000 - \$0}{10} = \$30,000$$

This amount can be deducted from the before-tax profit. Figure E2.10C shows the cash flow diagram for this scenario. Solving for the interest rate,

$$IC = A \left(\frac{P}{A}, i, n \right) \rightarrow \$300,000 = (\$56,950) \frac{(1+i)^{10} - 1}{i(1+i)^{10}}$$

$$i = \underline{13.75\%}$$

**FIGURE E2.10C**

Cash flow diagram after taxes using straight line depreciation.

- d. With the SYD method, the depreciation changes each year according to the expression,

$$D_k = 2 \frac{(IC - S)(N - k + 1)}{N(N + 1)}$$

Since the depreciation decreases each year, the after-tax cash flow will also decrease each year. For example, the depreciation for the first two years can be found by,

$$D_1 = 2 \frac{(\$300,000 - \$0)(10 - 1 + 1)}{10(10 + 1)} = \$54,545.45$$

$$D_2 = 2 \frac{(\$300,000 - \$0)(10 - 2 + 1)}{10(10 + 1)} = \$49,090.91$$

The after-tax cash flow for the first two years can then be found,

$$A_{AT,k} = A_{BT,k} - t(A_{BT,k} - D_k)$$

$$A_{AT,1} = \$85,000 - (0.51)(\$85,000 - \$54,545.45) = \$69,468.18$$

$$A_{AT,2} = \$85,000 - (0.51)(\$85,000 - \$49,090.91) = \$66,686.36$$

The yearly decrease in the after-tax cash flow due to the linearly decreasing depreciation is given by,

$$G = A_{AT,1} - A_{AT,2} = \$69,468.18 - \$66,686.36 = \$2,781.82$$

This is the linear gradient value that reduces the after-cash flow each year by this amount. The cash flow diagram can be envisioned as shown in Figure E2.10D.

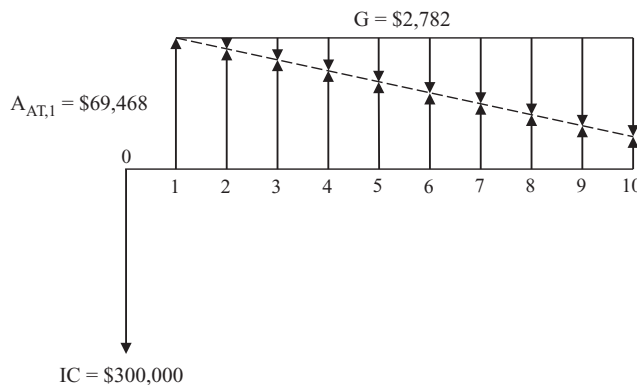


FIGURE E2.10D

Cash flow diagram after taxes using sum of the years' digits depreciation.

This cash flow diagram shows the effect of the linear gradient decreasing the annual after-tax profits each year. This demonstrates the advantage provided by an accelerated depreciation scheme. More after-tax cash is available early in the life of the equipment. This provides businesses the opportunity to make more money early. For a new startup business this may be very important to the success of the company. For businesses that are established, this provides more money early that can be used for future product development, etc.

This gradient can be moved to the baseline of the cash flow diagram as shown in Figure E2.10E. Using this cash flow diagram, the rate of return can be found,

$$IC + G \left(\frac{P}{G}, i, n \right) = A_{AT,1} \left(\frac{P}{A}, i, n \right)$$

$$\$300,000 + (\$2,781.82) \left[\frac{(1+i)^{10} - 1}{i^2(1+i)^{10}} - \frac{10}{i(1+i)^{10}} \right] = (\$69,461.18) \frac{(1+i)^{10} - 1}{i(1+i)^{10}}$$

$$i = \underline{15.13\%}$$

Table E2.10 summarizes the results of this problem. The results of Example 2.10 reveal several important concepts:

1. If there were no taxes, the rate of return on the investment of the machine is very attractive! Paraphrasing the words of Benjamin Franklin, "In this world nothing can be said to be certain, except death and taxes." Therefore,

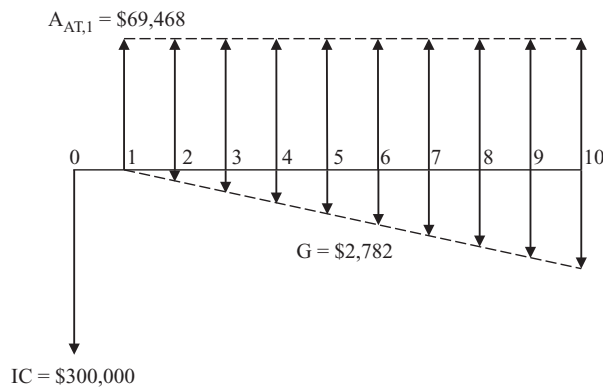


FIGURE E2.10E

Equivalent cash flow diagram to Figure E2.10D.

TABLE E2.10

Summary of Results

Tax and Depreciation Scenario	Rate of Return
(a) No taxes or depreciation	25.38%
(b) Taxes with no depreciation	6.46%
(c) Taxes with SLD	13.75%
(d) Taxes with SYD	15.13%

the result of Part (a) is unrealistic. However, it does indicate the maximum possible rate of return.

2. Depreciation provides a significant tax break. In Part (b) it is seen that without depreciation, the rate of return drops significantly. However, using the different depreciation schemes, the rate of return increases by more than a factor of two over the no depreciation scenario.
3. The depreciation schemes considered in this example result in about the same rate of return. The difference in the rates of return is due to the time value of money. In this instance, it appears that the SYD model gives a slight advantage.

Reference

Corripio, Armando B., Kaherine S. Chrien, and Lawrance B. Evans. 1982. "Cost Estimation Of Fixed Roof (Cone) Carbon Steel Storage Tanks." *Chemical Engineering*.

Problems

Unless otherwise stated, assume interest compounding is annual

Time Value of Money

- 2.1 Using computer software as assigned by your course instructor, develop a program that will allow you to quickly compute the discrete interest factor shown in Table 2.2. Use this program to calculate the interest factors for a nominal annual interest rate of 4.5% compounded monthly for a period of four years. Express the interest factors to six decimal places. The program that you develop will be helpful in finding interest factors for other problems in this chapter.
- 2.2 A small-scale silver mine in north Idaho is up for sale by bid. A mining engineer estimates that at current production levels, the mine will yield an annual net income of \$80,000 for 35 years, after which the silver will be exhausted. If an investor's MARR is 15%, what is the maximum amount that the investor can bid on this property?
- 2.3 A company has a short-term storage need. A proposal is brought forth to build a temporary warehouse at a cost of \$18,000. The annual operating and maintenance (OM) cost of the facility is estimated to be \$900 per year. Using the temporary storage space saves the company \$3,750 per year. If the company's MARR is 12%, how many years must the warehouse last?
- 2.4 The engineering supervisor in a company is recommending the purchase of a new machine for a production line. The machine has an initial cost of \$310,000 and is expected to be functional for 25 years. At the end of its life, it can be sold for \$90,000. The addition of this machine will increase production which results in an increase in annual income of \$85,000. The machine will require uniform annual

operation and maintenance costs. If the company's MARR is 21%, how much can be spent on annual operation and maintenance?

- 2.5 In a chemical processing plant, liquid cyclohexane ($\rho = 48.5 \text{ lbm/ft}^3$) flows through a piping system (pump, piping, valves, etc.) at a rate of 1000 gpm as it is being transported from one process to the next. The pressure drop through the pipe system is 6.2 psi. The facility is automated and runs 24 hours/day, 7 days/week all year long. The cost of energy to operate the pump in the system is \$0.11/kWh. Annual maintenance costs for the piping system are estimated to be 5% of the annual operating cost. The annual income resulting from the piping system is \$18,000. The initial cost of the piping system is \$62,000. The system is expected to last for 15 years with no salvage value. Determine the rate of return that this piping system provides.
- 2.6 Proud parents wish to establish a college savings fund for their newly born child. Monthly deposits will be made into an investment account that provides an annual rate of return of 4.5% compounded monthly. Four withdrawals from the savings fund will be made to help pay for college expenses. The estimated need is \$28,000 when the child turns 18 years old, \$30,000 at 19 years, \$34,000 at 20 years, and \$38,000 at age 21. The last monthly payment to the investment occurs when the child turns 21. This is also the time that the last withdrawal is made. Determine the monthly deposit required to meet this goal.
- 2.7 Joan Johnson and Steve Smith, two mechanical engineers working for the ACME Machine Company were having lunch together one day. They were lamenting the fact that the United States Social Security fund may not be solvent when they retire, leaving a financial hole in their retirement plans. It turns out that the ACME Machine Company has a pretty good pension plan for retirees. However, Joan and Steve would like to have an additional \$2,000 per month on top of their pensions when they retire. To make sure that enough money is available, they both anticipate their life span to be 95 years (both having genetic longevity in their family lines). They both plan to retire at age 65. Joan's current age is 25. Steve is 32 years old. They have identified an investment opportunity that is estimated to earn 4% annually, compounded monthly. Determine how much money Joan and Steve must deposit into their investment accounts monthly, from now until retirement age, to attain their goal.
- 2.8 A high-tech company wants to have \$2.5 billion available in 5 years to develop a new product. The company expects to invest uniformly increasing amounts of money each year to meet this goal. At the end of the first year, the company will deposit \$50 million in an account that is expected to earn 10% annually. Determine how much the uniformly increasing deposit must be each year thereafter to meet this goal.
- 2.9 An electric utility is considering a photovoltaic (PV) solar panel system to provide power to water conditioning pumps within the power plant. The project will be done in two phases. Phase 1 has an initial cost of \$2.5 million. Phase 2 will cost \$2 million at the beginning of year 3. The system will be put into service at the beginning of year 4. The annual savings using the PV panels is estimated to be \$800,000, increasing by \$150,000 per year through year 10. The utility's MARR is 12%.
- Determine if the cost of the PV system is justified. (Hint: Consider comparing the present worth of the costs and present worth of the savings.)
 - What is the actual rate of return for this project?

TABLE P2.10

Expected Yearly Maintenance Cost

Year	Expected Maintenance Cost
2	\$1,000
3	\$1,400
4	\$1,900
5	\$2,600

- 2.10 A company has invested in a new machine for its production line. The initial cost of the machine is \$12,000 and it is expected to last for five years with no salvage value at that time. Annual operation costs are anticipated to be relatively constant at \$750 per year. However, due to heavy use and degradation, the maintenance costs are expected to increase each year. A best guess for the annual maintenance costs are shown in Table P2.10. Determine how much money should be invested in a fund that earns 6% annually, compounded monthly, in order to completely pay for this machine.
- 2.11 The initial cost of a proposed heat recovery system is \$375,000. The annual operation and maintenance costs are projected to be \$12,000. The salvage value of the system at the end of its useful life (projected to be 30 years) is \$60,000. The annual savings in fuel costs resulting from this system are estimated to be \$55,000 per year
- Assuming annual compounding, determine the rate of return for this heat recovery system.
 - If management has set the MARR to be 15% for a heat recovery system like this, what is the maximum initial cost that can be spent on the system (assuming that all other costs and incomes are the same)?
- 2.12 A manufacturing firm entered into a 10-year contract for raw materials. The contract required an initial payment of \$14,000 and \$22,000 per year beginning at the end of the fourth year. The company has made higher profits than anticipated and asked that it be allowed to make a lump sum payment at the end of the third year to pay off the remainder of the contract. Determine the lump sum required if the interest rate is 9%.
- 2.13 A storage tank for toxic chemicals has an initial cost of \$20,000. The tank is expected to last for 25 years, at which point it is discarded with no salvage value. Every five years during its use, the tank must be drained and relined at a cost of \$8,000. Plant managers want to invest a lump sum of money now to cover the cost of the tank and the relining. Determine the amount of money required to be invested at an annual rate of 12% compounded monthly to completely pay for tank and relining.
- 2.14 Two electric motors are available to satisfy a continuous demand of 85 kW. Motor 1 has an initial cost of \$5,500 with an operating efficiency of 91%. Motor 2 has an initial cost of \$4,000 with an operating efficiency of 89%. Each motor has a life of 10 years with no salvage value. The annual cost of electricity to run the machines is \$19.20 per kW of demand plus \$0.12 per kWh of energy use. Determine the

number of runtime hours that makes these two motors economically equivalent to each other if the MARR is 22%.

- 2.15 A company has data that indicates the annual expenditures on a robotics manufacturing line are uniform at \$100 per unit produced for the first four years. This cost has shown to increase by \$50 per unit for the next four years. Determine the equivalent present worth of these per-unit costs if the MARR is 18%.
- 2.16 The WMHX (We Make Heat Exchangers) company has created an investment plan to fund the next generation heat exchanger they plan to develop. The plan calls for an initial investment of \$7 million, decreasing by \$1 million per year through year 5. During years 6 through 10, no deposits or withdrawals will be made. At the end of year 10, \$20 million will be withdrawn to initially fund the development program. Subsequent withdrawals will decrease uniformly each year thereafter through year 15. An investment opportunity has been identified that will return 10% per year, compounded monthly. Determine the withdrawals in years 11–15 that will completely exhaust the funds by the end of year 15.
- 2.17 A company that manufactures food-grade oil is considering a proposal to construct a large tank to store raw, unrefined oil. This will permit the company to buy raw oil at a more favorable price and stockpile it. The cost of the tank is \$150,000. The tank is expected to last for 30 years with a salvage value of \$10,000 at that time. The anticipated annual savings resulting from stockpiling the raw oil is estimated to be \$25,000. Determine the rate of return for this proposal.
- 2.18 In a paper mill, a new conveyor system is being considered to move the freshly chipped wood to the next stage in the production line. The cost of the new conveyor is \$55,250. Yearly operating and maintenance costs for the conveyor are estimated to be \$13,260. The conveyor is expected to last for 20 years with no salvage value. Because of the new conveyor's design, more paper product can eventually be produced by the mill. This new production level results in an increase in annual income of \$28,500. Determine the rate of return on the investment in the new conveyor.

Economic Decision Making

- 2.19 Two different labeling machines are being considered for a canned food processing plant. Machine X has a first cost of \$46,500, a service life of 5 years and a salvage value of \$5,000. The annual operating cost of the machine is \$28,300, increasing by \$2,600 per year after the first year. Machine Y has an initial cost of \$53,100, and a salvage value of \$8,300 after 5 years. The annual operating cost of the machine is \$17,000, increasing by \$1,800 per year after year 1. The MARR is 12%. Determine which labeling machine should be selected based on a present worth analysis?
- 2.20 Solve Problem 2.19 using an annual cost analysis instead of a present worth analysis.
- 2.21 A pipeline engineer is considering alternative natural gas pipeline routings. The first route is mostly over land and the second is primarily undersea. Both pipelines will need some valve and fitting replacements in year 25. Cost data for each route is shown in Table P2.21. Notice that the undersea route has a higher initial cost due to higher installation costs and extra corrosion protection for the pipeline. However, the undersea route has cheaper security and maintenance

TABLE P2.21

Pipeline Cost Data

Parameter	Over Land	Undersea
Initial cost	\$215M	\$350M
Expected life	50 yr	50 yr
Valve and fitting replacement in year 25	\$30M	\$70M
Annual operating and security cost	\$22M	\$2M

costs which substantially reduces annual costs. The MARR for the project is 15%. Determine which route should be pursued based on a present worth analysis.

- 2.22 Solve Problem 2.21 using an annual cost analysis instead of a present worth analysis.
- 2.23 The Automated Assembly Company is considering three different methods for assembly of parts in a production line. Method 1 has an initial cost of \$40,000, an annual cost of \$9,000, and a two-year life. Method 2 has an initial cost of \$80,000, with a 4-year life and an annual operating cost of \$6,000. Method 3 is a longer-life alternative, lasting 8 years with an initial cost of \$160,000 and annual operating costs of \$2,000. Methods 1 and 2 have no salvage value. However, the equipment used in Method 3 can be sold for \$12,000 at the end of its life. The MARR is 12%. Determine which method should be selected based on a PW analysis.
- 2.24 Solve Problem 2.23 using an AC analysis instead of a PW analysis.
- 2.25 A nominal 36-inch pipeline can be installed for \$216,600. The annual cost of the 36-inch pipeline including pump operating costs and maintenance is estimated to be \$48,600. A nominal 30-inch pipeline can be installed to provide the same flow rate for \$161,300. However, the annual operating and maintenance costs are \$68,500. The pipeline is expected to last for 20 years with a salvage value equal to 10% of the initial cost. The MARR is 20%. Based on an economic analysis, which diameter pipeline should be installed?
- 2.26 Two engines are being considered for a power delivery of 500 hp. Engine A has an initial cost of \$15,700 while engine B costs \$22,500. The specific fuel consumption rate of each engine is 0.42 lbm/hp-h for engine A and 0.40 lbm/hp-h for engine B. Both engines burn the same fuel which costs 0.329 \$/lbm. Engine A is expected to last 14 years while engine B has a life of 20 years. At the end of their lives, engine A can be sold for \$5,000 and engine B can be sold for \$6,000. The power demand requires that the engine must operate 4 hours/day for 280 days annually. The MARR is 18%. Determine which engine should be selected for this job based on an economic analysis.
- 2.27 A railroad track runs down a street of a manufacturing complex and the freight cars frequently halt all movement on another company street which crosses it. The traffic holdup adds up to an hour each day and the total daily cost of idle labor caused by the delay is estimated to be \$130. The factory works 250 days each year. An underpass costing \$125,000 will completely eliminate these delays. The useful life of the structure is 25 years with no salvage value. The cost of operating the underpass is estimated to be \$4,400 per year. The MARR for this project

TABLE P2.28

Compressor Drive Cost Data

Parameter	Gasoline Engine	Diesel Engine
Initial cost	\$9,000	\$16,000
Expected life	12 yr	18 yr
Salvage value	\$3,200	\$5,800
Annual maintenance cost	\$1,400	\$2,300
Fuel consumption	0.48 lbm/hp-h	0.38 lbm/hp-h
Fuel cost ^a	x_g \$/gal	x_d \$/gal
Fuel density	43.7 lbm/ft ³	46.7 lbm/ft ³
Parameter	Electric Motor	
Initial cost	\$10,400	
Expected life	22 yr	
Salvage value	\$2,400	
Annual maintenance cost	\$1,900	
Motor efficiency	91%	
Electricity cost ^a	x_e \$/kWh	

^a For fuel costs and electricity cost, obtain values of x_g , x_d , and x_e locally, or use values provided by your instructor.

at 25%. Conduct an economic analysis and determine if the underpass should be built.

- 2.28 A company has a need for compressed air in one of its factory operations. A compressor has been selected for this task. The company is now considering three options to drive the compressor. These options are (a) a gasoline engine, (b) a diesel engine, and (c) an electric motor. The required input to the compressor is 100 hp and the compressor must operate 8 hours/day for 230 days each year. The economic and operating data of the engines and motor are shown in Table P2.28. If the MARR is 18%, determine which option should be selected.
- 2.29 Three alternatives are being considered for an air cleaning system. All three systems have a life of 10 years with no salvage value. System A has an initial cost of \$29,000. During the first five years of operation, the annual costs to operate system A are \$5,000. During the second five years, the annual cost of system A increases to \$16,000. System B has an initial cost of \$43,000. The annual cost to operate system B is \$4,000, however after the first year, this cost increases by \$1,600 per year. System C has an initial cost of \$58,000 with an annual cost of \$2,400. System C requires two upgrades; one during year 4 which costs \$6,000, and the other during year 8 which costs \$3,000. The MARR for this project is 17%. Determine which air cleaning system should be installed based on an economic analysis.
- 2.30 Conduct a parametric study of the economic selection problem given in Problem 2.29. Plot the annual cost of systems A, B, and C as a function of the MARR for the range $0 \leq \text{MARR} \leq 25\%$. Discuss the results.
- 2.31 Two heat treating systems are being considered for a metal forming process. System A has an initial cost of \$121,400 with annual costs of \$8,000. After the first

TABLE P2.33

Vendor Costs for Installation of an Automated Assembly Line

Vendor	System Life (yr)	Initial Cost	Annual Operating Cost	Annual Maintenance Cost	Additional Yearly Maintenance Cost after First Year	Salvage Value
WERBST	20	\$2.3M	\$100,000	\$6,500	\$3,000	\$325,000
PIKUS	30	\$3.4M	\$90,000	\$4,400	\$2,500	\$550,000
BSTDEAL	15	\$1.8M	\$190,000	\$9,000	\$5,500	\$210,000
GR8SYS	40	\$3.9M	\$50,000	\$2,000	\$0	\$720,000

year an additional \$1,000 of maintenance is required each year thereafter. The profits at the end of the first year after installing system A are \$75,000, reducing linearly to \$5,000 in year 15. System A has a 15-year life with no salvage value. System B has an initial cost of \$206,000 with annual operating costs of \$5,000. Installation of system B results in a uniform annual profit of \$54,000. System B has a life of 15 years with no salvage value. The MARR for the project is 12%. Determine which heat treatment system should be installed based on an economic analysis.

- 2.32 Two injection molding systems are being considered for a production line. Use of an injection molding system will reduce the manual time spent on the production line which increases annual profits. System A has an initial cost of \$30,000 with annual operating costs of \$10,000 and a life of 8 years. The salvage value of System A is \$10,000. An alternative system, System B, has an initial cost of \$21,000 with annual operating costs of \$10,000 and a salvage value of \$7,000 at the end of its 4-year life. In both cases, the annual increase in revenue due to the addition of the heat treatment process is expected to be \$20,000. The MARR for this project is 10%. Determine which system should be installed.
- 2.33 A company is converting a mostly manual assembly line to a completely automated, robotic assembly line. A bid package is written asking potential vendors to propose the costs required to automate the assembly line. All vendors are asked to provide the equipment and installation cost, annual operating and maintenance cost, increasing yearly maintenance cost (if any), expected life of the equipment, and salvage value (if any). Four vendors have responded with the data shown in Table P2.33. The MARR for the project is 16%. Determine which vendor should be selected based on an economic analysis.

Depreciation and Taxes

- 2.34 The annual profit realized from a production line in a manufacturing company is \$250,000. Annual depreciation, based on the straight-line model, is determined to be \$125,000. The company's tax rate is 50%. Determine the annual after-tax cash flow.
- 2.35 The annual income received from a production line in a manufacturing company is \$1 million. The annual operating cost for the production line are \$150,000 and the annual maintenance cost is \$50,000. Annual straight-line depreciation is found to be \$425,000. The resulting after tax cash flow is \$630,000. Determine the company's tax rate.

- 2.36 A company has purchased a piece of equipment for \$300,000. Tax codes indicate that the service life of this piece of equipment is 8 years with a salvage value of \$50,000 at the end of the service life. Determine the depreciation amount allowed for this equipment in each of the years 1–8 using SYD depreciation.
- 2.37 The initial cost of a machine for a production facility is \$225,000. The machine is expected to last for 10 years with no salvage value. The company's tax rate is 49% and SLD is used to depreciate the machine. For this type of depreciation, the tax life of the machine is considered 8 years and its salvage value is \$5,000. The after-tax rate of return is 14.3%. Determine the uniform annual before-tax cash flow.
- 2.38 An empirical expression that is sometimes used to estimate the base cost of a shell and tube heat exchanger is (Corripio, Chrien, and Evans 1982),

$$c_{HX} = \exp \left[8.202 + 0.1506 \ln A + 0.06811 (\ln A)^2 \right]$$

In this equation, c_{HX} is the heat exchanger cost in U.S. dollars, and A is the heat transfer area in square meters. Consider a shell and tube heat exchanger with a heat transfer area of 400 m². The heat exchanger has a life of 25 years, with a salvage value equal to 5% of its initial cost. The annual operation and maintenance costs are anticipated to be 15% of the initial cost. The after-tax rate of return is 14.1%. The company's tax rate is 52% and SLD is used for depreciation. For this heat exchanger, the tax life is 20 years and the salvage value is \$6,500. Determine the uniform annual savings resulting from this heat exchanger.

- 2.39 Solve Problem 2.5 including the effect of taxes and depreciation. For tax purposes, the economic life and salvage value are the same as given in Problem 2.5. The pipeline equipment is depreciated using the SLD method and the company's tax rate is 50%.
- 2.40 Solve Problem 2.5 including the effect of taxes and depreciation. For tax purposes, the economic life and salvage value are the same as given in Problem 2.5. The pipeline equipment is depreciated using the SYD method and the company's tax rate is 50%.
- 2.41 Solve Problem 2.18 including the effect of taxes and depreciation. Tax regulations indicate that the economic life of the conveyor is 20 years with a salvage value of \$4,000. The conveyor system is depreciated using the SLD method. The company's tax rate is 52%.
- 2.42 Solve Problem 2.18 including the effect of taxes and depreciation. Tax regulations indicate that the economic life of the conveyor is 20 years with a salvage value of \$4,000. The conveyor system is depreciated using the SYD method. The company's tax rate is 52%.



Taylor & Francis

Taylor & Francis Group

<http://taylorandfrancis.com>

3

Analysis of Thermal Energy Systems

3.1 Introduction

Thermal energy systems can be thought of as providing two basic functions: (1) deliver power or (2) transport energy using a fluid (or fluids) to provide heating and/or cooling. The thermodynamic analysis of such systems is a critical part of their successful design. Chapter 3 presents some of the fundamental concepts in thermodynamic analysis of thermal energy systems. It is assumed that the reader has had a formal course in engineering thermodynamics. Because of this, much of what is contained in this chapter may be review. Chapter 3 is not meant to be a substitute for a full course in thermodynamics. Where material is considered review, the presentation will be brief.

3.2 Nomenclature

Perhaps one of the more frustrating things experienced by an engineering student is the inconsistent nomenclature seen in the three engineering sciences of fluid mechanics, thermodynamics, and heat transfer. There are certain unavoidable variable duplications that are used to represent different quantities. A few of the more common variable duplications are shown in Table 3.1. This variable duplication is unfortunate because it tends to “compartmentalize” each subject in the student’s mind.

The analysis and design of thermal energy systems often requires the simultaneous application of all of these engineering sciences. Therefore, a consistent nomenclature is advantageous. As nomenclature is introduced throughout this text, it will be defined and used consistently throughout. However, there will be cases where variable duplication cannot be avoided.

In many instances, variables specified in capital letters are *total* values. For example, W is the total work done in a process. Typical units for W are kJ in the SI system or Btu in the IP system. On the other hand, variables specified on a per unit mass basis are often written in lowercase letters and termed *specific*. For example, the specific work, w , is the work done per unit mass, W/m . This convention is used for most thermodynamic properties. For example, U is the total internal energy of a substance (an *extensive* property) at a given state whereas $u = U/m$ is the specific internal energy (an *intensive* property). Of course, there are exceptions to this convention. For example, temperature, T , is an intensive property, but it is commonly written in an uppercase letter. The nomenclature in this book will strive to follow the *total* and *specific* convention used in many engineering thermodynamics textbooks.

TABLE 3.1

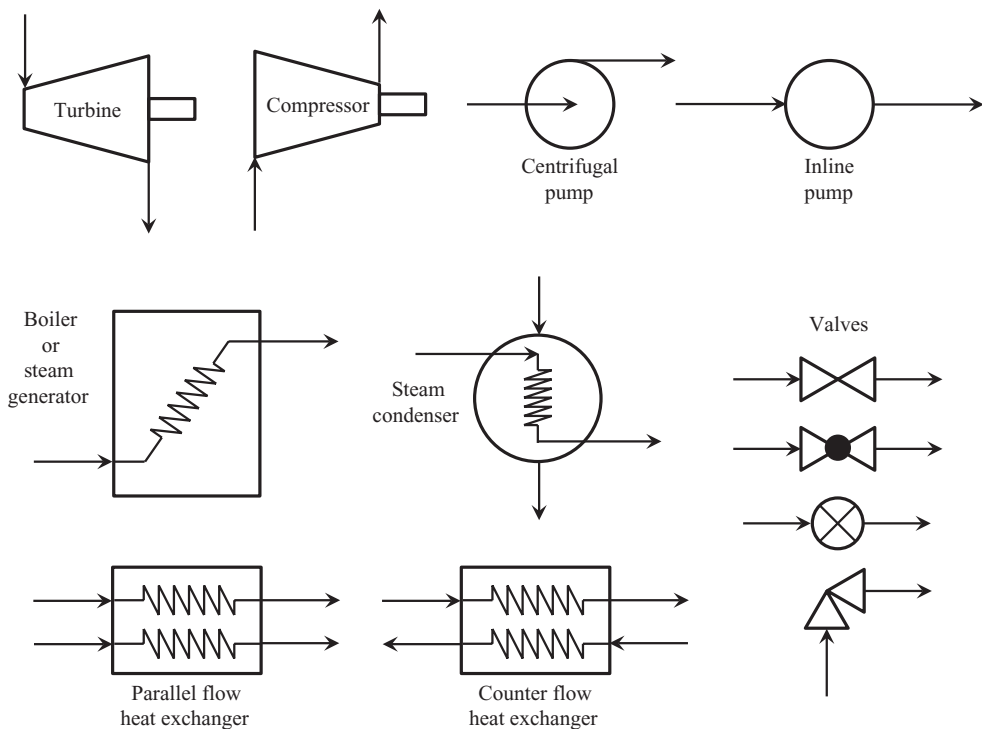
Some Common Variable Duplication Found in Three Basic Engineering Sciences

Variable	Fluid Mechanics	Thermodynamics	Heat Transfer
h	–	Specific enthalpy	Convective heat transfer coefficient
Q	Volumetric flow rate	Total heat transfer	–
q	–	Specific heat transfer	Heat transfer rate
U	–	Total internal energy	Overall heat transfer coefficient

3.3 Analysis Procedure

Thermal energy systems range from very simple to quite complex. Independent of the complexity of the system being studied, the procedure to analyze thermal systems is fairly consistent from system to system. A suggested procedure for thermal energy system analysis is outlined below.

1. Draw a sketch of the thermal energy system being analyzed. This sketch does not have to be terribly artistic, but it should contain common symbols used in system sketches. Some of the more common engineering sketches of equipment found in thermal energy systems are shown in Figure 3.1. Sketches found in this figure will be used throughout this book.

**FIGURE 3.1**

Common sketches used to identify thermal energy system components.

2. Label the sketch with the known information. This will help when it comes time to begin the actual analysis of the system.
3. Draw a *system boundary* to identify what is being analyzed. This is perhaps one of the most important aspects of thermal energy system analysis, and one that is often overlooked. Conservation and balance laws that are needed to conduct the system analysis are meaningless unless a system boundary is drawn. The location of the system boundary is completely up to the engineer. Wise selection of the system boundary can make the analysis quite simple, even for a complex thermal system. On the other hand, some system boundaries may complicate the analysis to the point where it cannot be completed because information about fluid properties, flow rates, or energy transfers is unknown.
4. Once the system boundary is identified, then the proper conservation and/or balance laws can be applied to solve the problem. Conservation and balance laws are discussed in subsequent sections of this chapter.

A good, structured procedure is important in thermal energy system analysis. The procedure outlined above is only a suggestion. Each individual may approach the analysis a bit differently, but the items above will likely be included in the analysis.

3.4 Conserved and Balanced Quantities

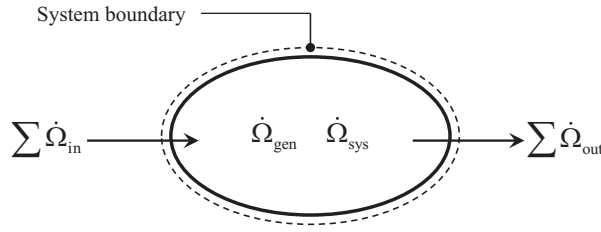
The laws of fluid mechanics, thermodynamics, and heat transfer required to conduct a system analysis are formulated to define some sort of quantity. For example, the first law of thermodynamics quantifies *energy*, and the second law of thermodynamics quantifies *entropy*. A physical quantity can be classified as *conserved* if it cannot be created or destroyed. There are four physical quantities that are conserved; *mass* (in a non-nuclear reaction), *energy*, *momentum*, and *electrical charge*. Quantities that are not conserved are *balanced*. Examples of balanced quantities pertinent to thermal energy systems are *entropy* and *exergy*.

3.4.1 The Generalized Balance Law

Figure 3.2 shows an instantaneous picture of a system and a generalized balanced quantity, Ω . Dots are used above the quantity Ω to indicate a time rate. The quantities $\dot{\Omega}_{\text{in}}$ and $\dot{\Omega}_{\text{out}}$ represent the rate of flow of Ω into and out of the system, respectively. The flow may be the result of Ω being carried into and out of the system with mass, or it may be the result of Ω being directly transferred into the system (e.g., heat or work).

Since the quantity Ω is balanced, it must be true that,

$$\left[\begin{array}{l} \text{time rate of } \Omega \text{ crossing} \\ \text{the system boundary and} \\ \text{passing into the system} \end{array} \right] - \left[\begin{array}{l} \text{time rate of } \Omega \text{ crossing} \\ \text{the system boundary and} \\ \text{passing out of the} \\ \text{system} \end{array} \right] + \left[\begin{array}{l} \text{time rate of } \Omega \text{ being} \\ \text{generated within the} \\ \text{system} \end{array} \right] = \left[\begin{array}{l} \text{time rate of storage} \\ \text{of } \Omega \text{ in the} \\ \text{system} \end{array} \right]$$

**FIGURE 3.2**

A generalized system.

The first two terms represent the *net* rate of Ω entering the system. If the *generated* term on the left-hand-side is positive, the quantity Ω is literally generated within the system. On the other hand, if the generated term is negative, the quantity Ω is actually *destroyed* inside the system. If the *storage* term on the right-hand-side is positive, the quantity Ω is being built up inside the system. Conversely, if the storage term is negative, Ω is being depleted inside the system. In equation form, this expression can be written as,

$$\sum \dot{\Omega}_{in} - \sum \dot{\Omega}_{out} + \dot{\Omega}_{gen} = \dot{\Omega}_{sys} \quad (3.1)$$

A more common way to express Equation 3.1 is to write the storage term on the right-hand side as a time derivative. The result is the *generalized balance law*,

$$\sum \dot{\Omega}_{in} - \sum \dot{\Omega}_{out} + \dot{\Omega}_{gen} = \frac{d\Omega_{sys}}{dt} \quad (3.2)$$

Equation 3.2 is the starting point for the development of any of the equations that are commonly used in thermal energy systems analysis and design.

3.5 Conservation of Mass

The conservation of mass equation can be developed by making the substitution, $m = \Omega$ in Equation 3.2. Mass is a conserved quantity. Therefore, the generation term is zero. This results in the following expression,

$$\sum \dot{m}_{in} - \sum \dot{m}_{out} = \frac{dm_{sys}}{dt} \quad (3.3)$$

The mass flow rates in Equation 3.3 can be expressed in terms of the fluid density, ρ , the cross-sectional area of the flow passage, A , and the mean velocity of the fluid flow, V . In addition, the mass stored in the system is a function of the density of the fluid and the volume enclosed by the system boundary. Incorporating these ideas into Equation 3.3 gives,

$$\sum (\rho AV)_{in} - \sum (\rho AV)_{out} = \frac{d(\rho V)_{sys}}{dt} \quad (3.4)$$

If the mass flow rate entering the system is the same as the mass flow rate leaving, then there can be no mass stored inside the system. A system operating under this condition is said to be operating at a *steady flow* condition. For a steady flow condition, Equation 3.3 can be written as,

$$\sum \dot{m}_{in} = \sum \dot{m}_{out} \quad (3.5)$$

To this point, the equations developed for the system are *rate* equations. They are describing the condition of the system *at an instant in time*. If the behavior of the system over a specified period of time is required, then any of these equations can be integrated over time. For example, to investigate how a system's mass might change over time, Equation 3.3 can be integrated over time, resulting in,

$$\sum m_{in} - \sum m_{out} = (m_2 - m_1)_{sys} \quad (3.6)$$

Example 3.1

Consider the tank and water supply system as shown in Figure E3.1A. The diameter of the supply pipe is $D_1 = 20$ mm, and the average velocity leaving the supply pipe is $V_1 = 0.595$ m/s. A shut-off valve is located at $z = 0.1$ m, and the exit pipe, $D_2 = 10$ mm. The tank diameter is $D_t = 0.3$ m. The density of the water is uniform at 998 kg/m³.

- Find the time to fill the tank to $H_0 = 1$ m assuming the tank is initially empty and the shut-off valve is closed. Neglect the volume associated with the short pipe connecting the tank to the shut-off valve.

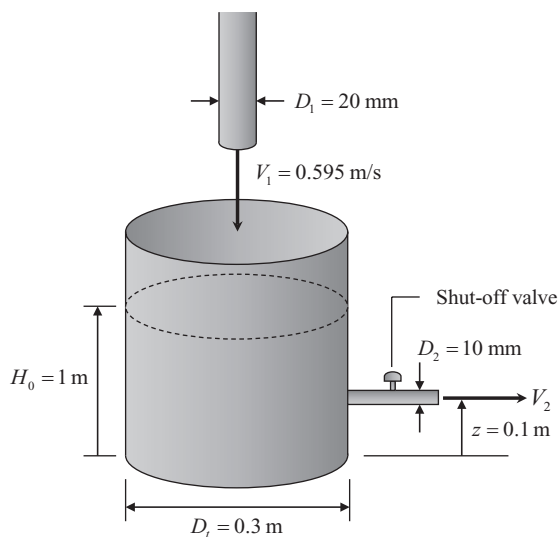


FIGURE E3.1A

Tank and water supply system.

- b. At the instant the water level reaches $H_0 = 1$ m the shut-off valve is opened. The instantaneous average velocity of the outflow depends on the water depth in the tank and can be expressed by,

$$V_2 = 0.85\sqrt{g[H(t) - z]}$$

where g is the acceleration due to gravity. Determine whether the tank continues to fill or begins to empty immediately after the valve is opened.

- c. Determine the steady flow value of the water depth.

Solution

Part (a) of this problem asks how long it takes to fill the empty tank to a height of $H_0 = 1$ m. An appropriate system boundary for this analysis is one that encompasses the inside of the tank up to a height of 1 m as shown in Figure E3.1B. During the time required to fill this system, a total mass, m_{in} enters and the mass inside the system changes by an amount, $m_2 - m_1$. From this analysis, it is clear that we are investigating what is happening inside the system over a finite period of time. Therefore, the appropriate form of the conservation of mass is given by Equation 3.6,

$$\sum m_{in} - \sum m_{out} = (m_2 - m_1)_{sys}$$

For the filling process, this equation reduces to,

$$m_{in} = (m_2 - m_1)_{sys} = m_2$$

Each of the terms in this equation can be expanded as follows,

$$\begin{aligned} (\rho A_1 V_1)t &= \rho V_2 \\ \frac{\pi D_1^2}{4} V_1 t &= \frac{\pi D_t^2}{4} H_0 \end{aligned}$$

The only unknown in this equation is the time required to fill, t . Solving for t gives,

$$t = \frac{H_0}{V_1} \left(\frac{D_t^2}{D_1^2} \right) = \frac{1 \text{ m}}{0.595 \text{ m/s}} \frac{(0.3 \text{ m})^2}{(0.020 \text{ m})^2} = \underline{\underline{378.2 \text{ s} = 6.3 \text{ min}}}$$

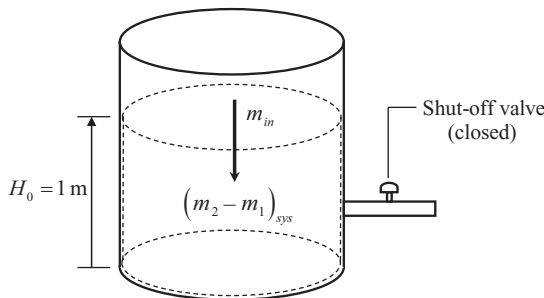
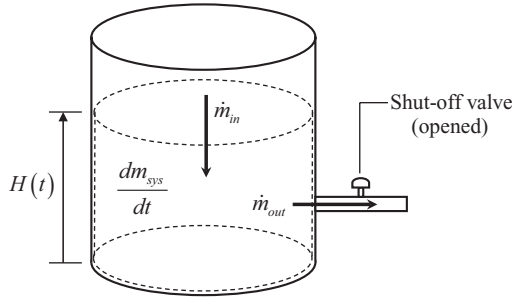


FIGURE E3.1B

Identification of the system boundary.

**FIGURE E3.1C**

System when the valve is opened.

Part (b) asks whether the water level rises or falls when the shut-off valve is opened. In order to determine this, the system must be analyzed at the instant in time when the valve is opened. When the valve is opened, water will flow across the system boundary at the outlet as indicated in Figure E3.1C. At that instant, we are interested in what happens to $H(t)$, the instantaneous height of the water in the tank. This analysis is not conducted over time, but rather at an instant in time. Therefore, Equation 3.3 is appropriate. Since there is one mass flow entering and one mass flow leaving the system, Equation 3.3 is written as,

$$\dot{m}_{in} - \dot{m}_{out} = \frac{dm_{sys}}{dt}$$

If the sign of the storage term dm_{sys}/dt is positive, then the tank continues to fill. On the other hand, if the storage term is negative, the tank begins to drain. The mass flow rates on the left-hand side of this equation can be rewritten in terms of the density of the fluid, cross-sectional areas, and velocities,

$$\rho A_1 V_1 - \rho A_2 V_2 = \frac{dm_{sys}}{dt}$$

The velocity, V_2 , is given in the problem statement in terms of the height of the water in the tank. Substituting this into the above equation and simplifying,

$$\begin{aligned} \rho \frac{\pi D_1^2}{4} V_1 - \rho \left(\frac{\pi D_2^2}{4} \right) (0.85 \sqrt{g[H(t) - z]}) &= \frac{dm_{sys}}{dt} \\ \frac{dm_{sys}}{dt} &= \rho \left(\frac{\pi}{4} \right) \left[D_1^2 V_1 - 0.85 D_2^2 \sqrt{g(H_0 - z)} \right] \end{aligned}$$

The value of H_0 is used for $H(t)$ because this is the height of the water in the tank at the instant the valve is opened. Performing the calculations,

$$\begin{aligned} \frac{dm_{sys}}{dt} &= \left(998 \frac{\text{kg}}{\text{m}^3} \right) \left(\frac{\pi}{4} \right) \left[(0.020 \text{ m})^2 \left(0.595 \frac{\text{m}}{\text{s}} \right) \right. \\ &\quad \left. - (0.85)(0.010 \text{ m})^2 \sqrt{\left(9.81 \frac{\text{m}}{\text{s}^2} \right) (1 \text{ m} - 0.1 \text{ m})} \right] \\ \frac{dm_{sys}}{dt} &= \underline{\underline{-0.0114 \frac{\text{kg}}{\text{s}}}} \end{aligned}$$

Since the storage term is negative, the tank will begin to empty when the shut-off valve is opened.

Part (c) of this problem asks for the water depth resulting in a steady flow scenario. The value of the derivative computed in part (b) is instantaneous. Since the velocity of the water leaving the tank through the bottom pipe is a function of the depth of the water, this derivative will change with time. For a steady flow condition, $dm_{\text{sys}}/dt = 0$. This allows for the solution of the height, H . From the analysis in part (b),

$$\begin{aligned}\frac{dm_{\text{sys}}}{dt} &= 0 = \rho \left(\frac{\pi}{4} \right) \left[D_1^2 V_1 - 0.85 D_2^2 \sqrt{g(H-z)} \right] \\ 0.85 D_2^2 \sqrt{g(H-z)} &= D_1^2 V_1 \\ g(H-z) &= \left(\frac{D_1^2 V_1}{0.85 D_2^2} \right)^2 \\ H = z + \frac{1}{g} \left(\frac{D_1^2 V_1}{0.85 D_2^2} \right)^2 &= (0.1 \text{ m}) + \frac{1}{(9.81 \text{ m/s}^2)} \left[\frac{(0.020 \text{ m})^2 (0.595 \text{ m/s})^2}{0.85(0.010 \text{ m})^2} \right] \\ H &= \underline{0.90 \text{ m}}\end{aligned}$$

When the valve is opened, the water depth will decrease from 1 m to 0.9 m, at which point, the incoming flow balances the outgoing flow and a steady flow scenario is achieved.

3.6 Conservation of Energy

The law of conservation of energy is also known as the *first law of thermodynamics*. The conserved quantity here is energy. Therefore, in Equation 3.2 $\Omega = E$, where E represents the total energy. For non-reacting systems, the total energy (extensive form) of a substance is made up of *internal energy* due to molecular activity, *kinetic energy* due to motion, and *potential energy* due to elevation. Therefore,

$$E = U + \frac{mV^2}{2} + mgz \quad (3.7)$$

The energy of a substance per unit mass, the intensive form, is given by,

$$e = \frac{E}{m} = u + \frac{V^2}{2} + gz \quad (3.8)$$

Making the substitution $\Omega = E$ into Equation 3.2 results in the rate form of the conservation of energy,

$$\sum \dot{E}_{\text{in}} - \sum \dot{E}_{\text{out}} = \frac{dE_{\text{sys}}}{dt} \quad (3.9)$$

For flow systems, it is convenient to separate the energy inputs and outputs due to heat and work transfer from the energy inputs and outputs carried by mass flow of the fluids involved,

$$\sum (\dot{E}_{in} - \dot{E}_{out})_{HW} + \sum (\dot{E}_{in} - \dot{E}_{out})_{flow} = \frac{dE_{sys}}{dt} \quad (3.10)$$

The first term in Equation 3.10 represents the net energy transfer rate associated with heat and/or work transfer to/from the system. This term can be written as,

$$\sum (\dot{E}_{in} - \dot{E}_{out})_{HW} = \sum (\dot{Q} + \dot{W})_{in} - \sum (\dot{Q} + \dot{W})_{out} \quad (3.11)$$

The second term on the left hand side of Equation 3.10 represents the net energy transfer rate resulting from the fluid entering and leaving the system. This term can be rewritten as,

$$\sum (\dot{E}_{in} - \dot{E}_{out})_{flow} = \sum \dot{m}_{in}(e + Pv)_{in} - \sum \dot{m}_{out}(e + Pv)_{out} \quad (3.12)$$

In this equation, e is the specific energy of the fluid as given in Equation 3.8 and Pv is the specific work required to move the fluid across the system boundary. The quantity Pv is often referred to as *flow work*. Substituting Equation 3.8 into Equation 3.12 gives,

$$(\dot{E}_{in} - \dot{E}_{out})_{flow} = \sum \dot{m}_{in} \left(u + \frac{V^2}{2} + gz + Pv \right)_{in} - \sum \dot{m}_{out} \left(u + \frac{V^2}{2} + gz + Pv \right)_{out} \quad (3.13)$$

This equation can be rewritten by realizing that $u + Pv$ is the enthalpy, h , of the fluid. Therefore,

$$(\dot{E}_{in} - \dot{E}_{out})_{flow} = \sum \dot{m}_{in} \left(h + \frac{V^2}{2} + gz \right)_{in} - \sum \dot{m}_{out} \left(h + \frac{V^2}{2} + gz \right)_{out} \quad (3.14)$$

Substituting Equations 3.11 and 3.14 into Equation 3.10 gives,

$$\left[\sum (\dot{Q} + \dot{W})_{in} - \sum (\dot{Q} + \dot{W})_{out} \right] + \sum \dot{m}_{in} \left(h + \frac{V^2}{2} + gz \right)_{in} - \sum \dot{m}_{out} \left(h + \frac{V^2}{2} + gz \right)_{out} = \frac{dE_{sys}}{dt} \quad (3.15)$$

This is the general conservation of energy equation. While this may seem fairly complex, it can be simplified for many common engineering applications.

One of the more confusing issues in many thermodynamics textbooks is the sign convention for heat and work. Most textbooks adopt the convention that positive energy transfers are heat into a system and work out of a system, whereas negative energy transfers

are heat out of a system and work into a system. In the generalized approach taken here, the sign of heat and work transfers are always considered positive in sign, independent of direction. In cases where a heat transfer or work transfer term is unknown, it can be assumed to be either into or out of the system. If the algebraic sign of the term turns out to be negative, this means that the assumed direction is opposite of the actual direction; the magnitude of the result is correct. This generalized approach takes the sign mystery out of the calculation. It allows one to focus on the result without worrying if a sign error was made somewhere in the analysis. Several examples of application of the conservation of energy equation follow.

Example 3.2

Steam at 1.6 MPa and 350°C enters a steam turbine at a flow rate of 16 kg/s. The steam leaves the turbine as a saturated vapor at 30°C. The turbine delivers 9 MW of power. A schematic of the turbine and its operating conditions are given in Figure E3.2. Determine the heat transfer rate from this turbine.

Solution

In many analyses, turbines are considered to be adiabatic (no heat transfer). However, this problem asks for the heat transfer rate. This means the turbine is losing heat, perhaps a result of the insulation around the turbine casing degrading.

The system boundary to be analyzed is shown in Figure E3.2. Since the flow rate is given as a constant value, the turbine must be operating in a steady flow mode. For turbines, it is common to consider the kinetic and potential energy changes to be negligible. Under these conditions, Equation 3.15 reduces to,

$$\left[0 - (\dot{Q} + \dot{W})_{out} \right] + \dot{m}(h_1 - h_2) = 0$$

Solving this equation for the heat transfer rate,

$$\dot{Q} = \dot{m}(h_1 - h_2) - \dot{W}$$

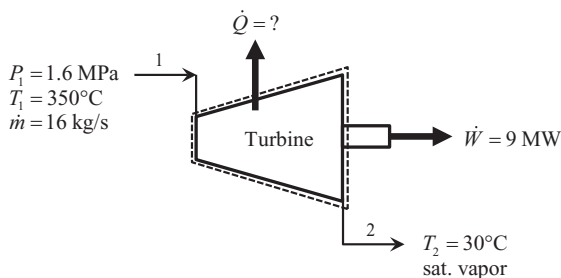


FIGURE E3.2
Steam turbine operating parameters.

Given the input and exhaust conditions specified in the problem, the enthalpy values* of the steam are: $h_1 = 3146.0$ kJ/kg, and $h_2 = 2555.6$ kJ/kg. Therefore, the heat transfer rate from the turbine is,

$$\dot{Q} = \left(16 \frac{\text{kg}}{\text{s}} \right) (3146.0 - 2555.6) \frac{\text{kJ}}{\text{kg}} \left| \frac{\text{kW} \cdot \text{s}}{\text{kJ}} \right| - (9 \text{ MW}) \left| \frac{1000 \text{ kW}}{\text{MW}} \right| = \underline{446.4 \text{ kW}}$$

The sign of the heat transfer rate (+) is consistent with the assumed direction (out of the system). Notice that the magnitude of this heat loss represents about 5% of the power output of the turbine. Better insulation on the turbine casing would increase the power output.

Example 3.3

Water flows through a shower head steadily and exits at a volumetric flow rate of 2.6 gpm. An electric resistance heater placed in the water pipe heats the water from 61°F to 110°F as shown in Figure E3.3A. Determine the electrical power required by the heater.

Solution

The heater is a device that has electrical current flowing through it. The flow of electrical current is analogous to power. Therefore, the electrical resistance heater can be replaced by a power transfer that crosses the system boundary as shown in Figure E3.3B. With negligible kinetic and potential changes between the inlet and outlet of the system, the conservation of energy Equation 3.15 applied to the system boundary shown in Figure E3.3B becomes,

$$\dot{W} + \dot{m}(h_1 - h_2) = 0$$

Since the water remains in the liquid phase and the pressure drop through the system is relatively small, a reasonable approximation to the enthalpy change is $\Delta h \approx \tilde{c}_{p,avg} \Delta T$. Substituting this approximation into the above equation and solving for the power input gives,

$$\dot{W} = \dot{m} \tilde{c}_{p,avg} (T_2 - T_1)$$

The average isobaric heat capacity of the water can be estimated at the average temperature on the saturated liquid curve,

$$T_{avg} = \frac{T_1 + T_2}{2} = \frac{61^\circ\text{F} + 110^\circ\text{F}}{2} = 85.5^\circ\text{F}$$

$$\tilde{c}_{avg}(T_{avg} = 85.5^\circ\text{F}, x = 0) = 0.9984 \text{ Btu/lbm} \cdot \text{R}$$

* Throughout this book, thermodynamic properties are computed using Engineering Equation Solver (EES) <http://www.fchart.com>, REFPROP <https://www.nist.gov/srd/refprop>, or CoolProp <http://www.coolprop.org/>.

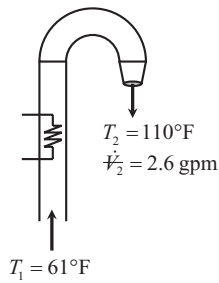


FIGURE E3.3A
Water flowing through a shower head.

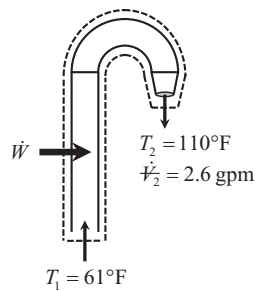


FIGURE E3.3B
Thermodynamic representation of the power transfer to the electrical heater.

The mass flow rate of the water needs to be determined. In the problem statement, the volume flow rate is given at the outlet of the shower. This can be converted to a mass flow rate since the temperature of the water is known at that point,

$$\dot{m} = \rho_2 \dot{V}_2$$

Using the incompressible substance model for a liquid, the density of the water at the outlet can be estimated as the density of the saturated liquid at T_2 ,

$$\rho_2(T_2 = 110^\circ\text{F}, x = 0) = 61.86 \text{ lbm/ft}^3$$

Now, the mass flow rate of the water can be found,

$$\dot{m} = \left(61.86 \frac{\text{lbm}}{\text{ft}^3} \right) \left(2.6 \frac{\text{gal}}{\text{min}} \right) \left| \frac{0.133680556 \text{ ft}^3}{\text{gal}} \frac{60 \text{ min}}{\text{hr}} \right| = 1290 \frac{\text{lbm}}{\text{hr}}$$

The power required can then be found,

$$\dot{W} = \left(1290 \frac{\text{lbm}}{\text{h}} \right) \left(0.9984 \frac{\text{Btu}}{\text{lbm-R}} \right) (110 - 61) \text{ R} \left| \frac{\text{kW-h}}{3412.1415 \text{ Btu}} \right| = \underline{18.5 \text{ kW}}$$

Example 3.4

A 4-ft³ rigid tank contains saturated R-134a at 100 psia as shown in Figure E3.4A. Initially, 20% of the volume is occupied by liquid and the rest by vapor. A valve at the top of the tank is now opened, and saturated vapor is allowed to escape slowly from the tank. Heat is transferred to the refrigerant such that the pressure inside the tank remains constant. The valve is closed when the last drop of liquid in the tank is vaporized. Determine the total heat transfer for this process.

Solution

In this problem, it is helpful to envision the process on a thermodynamic diagram. Figure E3.4B shows a pressure-volume (P - v) diagram for this process. The end state of the process can easily be identified as the saturated vapor state at 100 psia, labeled “2” on the diagram. State 1 is not known at this point. However, since 20% of the volume of the tank is occupied by liquid with the rest being vapor, State 1 must lie somewhere in the two-phase region on the 100 psia isobar.

The energy entering the system is the heat transfer, and there is only one mass flow (out of the system). The mass flow rate leaving the tank is not constant in this example.

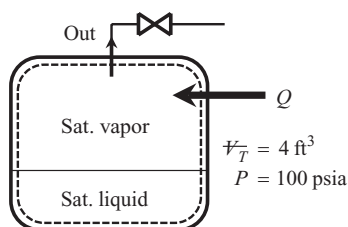


FIGURE E3.4A
R-134a pressure tank.

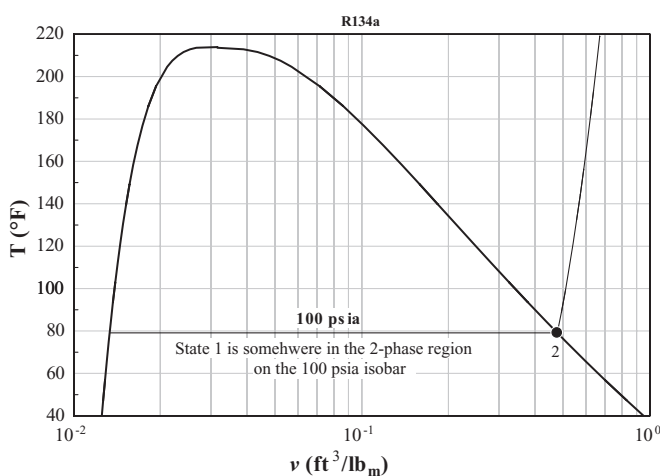


FIGURE E3.4B
 P - v diagram for R-134a showing the end state of the process.

Therefore, this is not a steady flow process. Assuming the kinetic and potential effects are negligible, the conservation of energy equation, Equation 3.15, reduces to,

$$\dot{Q} - \dot{m}_{out} h_{out} = \frac{dE_{sys}}{dt}$$

This equation can be integrated between the initial state defined in the problem, and the end state (when the last drop of liquid vaporizes),

$$\int_{t_1}^{t_2} \dot{Q} dt - \int_{t_1}^{t_2} \dot{m}_{out} h_{out} dt = \int_{E_1}^{E_2} dE_{sys}$$

The first integral on the left-hand side of this equation represents the total amount of heat transferred to the R-134a during the process,

$$\int_{t_1}^{t_2} \dot{Q} dt = Q$$

The R-134a in the vessel is maintained at a constant pressure of 100 psia due to the heat transfer. This means that the temperature of the fluid leaving the system, and thus the enthalpy, is constant. Therefore, the conservation of energy equation can be written as,

$$Q - h_{out} \int_{t_1}^{t_2} \dot{m}_{out} dt = \int_{E_1}^{E_2} dE_{sys}$$

The integral containing the mass flow rate can be modified using the conservation of mass, Equation 3.3, applied to the system,

$$-\dot{m}_{out} = \frac{dm_{sys}}{dt}$$

Substituting this expression into the conservation of energy equation results in,

$$Q - h_{out} \int_{t_1}^{t_2} \left(-\frac{dm_{cv}}{dt} \right) dt = \int_{E_1}^{E_2} dE_{sys}$$

$$Q + h_{out} \int_{m_1}^{m_2} dm_{cv} = \int_{E_1}^{E_2} dE_{sys}$$

Integrating both sides results in,

$$Q + h_{out}(m_2 - m_1) = E_2 - E_1$$

The energy terms on the right-hand side represent the energy of the R-134a inside of the system. Neglecting differences in kinetic and potential energies,

$$E_2 - E_1 = m_2 e_2 - m_1 e_1 = m_2 u_2 - m_1 u_1$$

Substitution of this expression into the previous equation and solving for the heat transfer gives,

$$\begin{aligned} Q + h_{out}(m_2 - m_1) &= m_2 u_2 - m_1 u_1 \\ Q &= m_2(u_2 - h_{out}) - m_1(u_1 - h_{out}) \end{aligned}$$

During the process, the R-134a is in a saturation condition inside the tank. At any time, the mass of the R-134a in the tank is,

$$m = m_g + m_f$$

In this equation the subscript g represents the saturated vapor, and f is the saturated liquid. These masses are related to the volume occupied by each phase,

$$m_g = \rho_g V_g \quad \text{and} \quad m_f = \rho_f V_f$$

Therefore, the total mass of R-134a in the vessel at any time is,

$$m = \rho_g V_g + \rho_f V_f$$

The initial mass in the tank (State 1) is,

$$m_1 = \rho_g V_{g,1} + \rho_f V_{f,1}$$

At the end of the process, there is no saturated liquid left. The mass at that point is,

$$m_2 = \rho_g V_{g,2} = \rho_g V_T$$

Therefore, the initial and final masses are,

$$\begin{aligned} m_1 &= \left(2.094 \frac{\text{lbm}}{\text{ft}^3} \right) \left[(0.80)(4 \text{ ft}^3) \right] + \left(75.05 \frac{\text{lbm}}{\text{ft}^3} \right) \left[(0.20)(4 \text{ ft}^3) \right] \\ m_1 &= \underset{\text{sat vapor in the tank}}{6.70 \text{ lbm}} + \underset{\text{sat liquid in the tank}}{60.04 \text{ lbm}} = \underset{\text{total initial mass in the tank}}{66.74 \text{ lbm}} \\ m_2 &= \left(2.094 \frac{\text{lbm}}{\text{ft}^3} \right) (4 \text{ ft}^3) = \underset{\text{final mass in the tank}}{8.375 \text{ lbm}} \end{aligned}$$

The enthalpy of the R-134a leaving the vessel is the saturated vapor enthalpy at 100 psia can be found to be $h_{out} = 113.83 \text{ Btu/lbm}$. The internal energies, u_1 and u_2 , are the specific internal energies of the R-134a in the vessel at the initial and end states, respectively. The internal energy in the final state is the saturated vapor internal energy at 100 psia and can be found to be $u_2 = 105.0 \text{ Btu/lbm}$. The R-134a in the vessel in the initial state is a mixture of saturated liquid and saturated vapor. Therefore, the internal energy at that state can be found using the quality relationship,

$$u_1 = u_f + x_1 u_{fg} = u_f + x_1 (u_g - u_f)$$

The quality in the initial state is,

$$x_1 = \frac{m_{g,1}}{m_{total}} = \frac{6.70 \text{ lbm}}{66.74 \text{ lbm}} = 0.10$$

Then, the internal energy at the initial state can be found,

$$u_1 = 37.62 \frac{\text{Btu}}{\text{lbm}} + (0.10)(105.0 - 37.62) \frac{\text{Btu}}{\text{lbm}} = 44.39 \frac{\text{Btu}}{\text{lbm}}$$

Now, the required heat transfer can be computed,

$$Q = (8.375 \text{ lbm})(105.0 - 113.83) \frac{\text{Btu}}{\text{lbm}} - (66.74 \text{ lbm})(44.39 - 113.83) \frac{\text{Btu}}{\text{lbm}}$$

$$Q = \underline{4561 \text{ Btu}}$$

Even though only 20% of the vessel is occupied by liquid in the initial state, a significant amount of energy in the form of heat is required to vaporize it.

3.7 The Entropy Balance (The Second Law of Thermodynamics)

The entropy balance is an expression of the second law of thermodynamics that is particularly useful in analysis of thermal equipment and processes. The second law of thermodynamics helps identify irreversibilities in a process or system. Entropy is not a conserved quantity since it can be *generated* by a process. *Entropy generation* occurs as a result of irreversibility. There are many things that cause irreversibility in a process. Common causes of irreversibility in thermal equipment are mechanical friction (e.g., bearings supporting a rotating shaft), fluid friction due to flow, heat transfer through a finite temperature difference, abrupt expansion or contraction, and fluid mixing.

Making the substitution $\Omega = S$ into Equation 3.2 results in the *entropy balance*,

$$\sum \dot{S}_{in} - \sum \dot{S}_{out} + \dot{S}_{gen} = \frac{dS_{sys}}{dt} \quad (3.16)$$

Entropy can be carried into and out of a system by heat and by virtue of the mass flow crossing the system boundary. Therefore, it is convenient to separate the entropy rates due to heat transfer from the entropy rates due to flow,

$$\sum (\dot{S}_{in} - \dot{S}_{out})_Q + \sum (\dot{S}_{in} - \dot{S}_{out})_{flow} + \dot{S}_{gen} = \frac{dS_{sys}}{dt} \quad (3.17)$$

The term \dot{S}_{gen} is the *entropy generation rate* or *entropy production rate*. The magnitude of the entropy generation gives an indication of the irreversibility associated with a thermal

component or a process. The sign of the entropy generation is an indication of the *type* of process. By its very nature, entropy generation can never be negative. For real-world, irreversible processes, the entropy generation is always positive. If the component or process is thermodynamically reversible (an ideal process), then the entropy generation is zero. This can be quantified by Equation 3.18 shown below,

$$\dot{S}_{gen} \begin{cases} > 0 \text{ for all real-world processes} \\ = 0 \text{ for reversible processes} \\ < 0 \text{ is impossible} \end{cases} \quad (3.18)$$

The reversible process is of particular interest to engineers. Even though a reversible process does not exist in the real world, it serves as a performance benchmark that can be used in thermal system design. The reversible process is used in defining *isentropic efficiencies* of various devices (e.g, pumps or turbines). The isentropic efficiency is reviewed in the Section 3.7.2.

The entropy transfer rate due to heat transfer across the system boundary, the first term on the left-hand side of Equation 3.17, can be written as

$$\sum (\dot{S}_{in} - \dot{S}_{out})_Q = \sum \left(\frac{\dot{Q}}{T_b} \right)_{in} - \sum \left(\frac{\dot{Q}}{T_b} \right)_{out} \quad (3.19)$$

In Equation 3.19 the temperature, T_b is the temperature on the system boundary where the heat transfer is taking place. This temperature must be expressed on the *absolute scale* (K or °R). Notice that Equation 3.19 is written to accommodate different boundary temperatures for a given system corresponding to where the heat is crossing. Substituting Equation 3.19 into Equation 3.17 gives,

$$\left[\sum \left(\frac{\dot{Q}}{T_b} \right)_{in} - \sum \left(\frac{\dot{Q}}{T_b} \right)_{out} \right] + \sum (\dot{S}_{in} - \dot{S}_{out})_{flow} + \dot{S}_{gen} = \frac{dS_{sys}}{dt} \quad (3.20)$$

Writing the entropy transfer rates due to mass flow as a function of the mass flow rate, a general expression for the entropy balance can be written,

$$\left[\sum \left(\frac{\dot{Q}}{T_b} \right)_{in} - \sum \left(\frac{\dot{Q}}{T_b} \right)_{out} \right] + \left[\sum (\dot{m}S)_{in} - \sum (\dot{m}S)_{out} \right] + \dot{S}_{gen} = \frac{dS_{sys}}{dt} \quad (3.21)$$

Entropy is a thermodynamic property. Therefore, it is a function of state. On the other hand, entropy generation is *not* a property. It depends on the process. If the path taken by the process is reversible, then the entropy generation is zero. If the process is irreversible, then there are several possible paths that can be taken, depending on the severity of the irreversibility. Because of this, entropy generation is considered a *path* function similar heat and work.

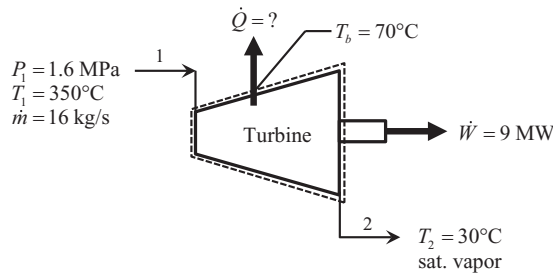


FIGURE E3.5
Steam turbine operating parameters.

Example 3.5

Steam at 1.6 MPa and 350°C enters a steam turbine at a flow rate of 16 kg/s. The steam leaves the turbine as a saturated vapor at 30°C. The turbine delivers 9 MW of power. The turbine is insulated, but not perfectly. The average temperature of the insulation on the outer surface of the turbine is 70°C. Figure E3.5 shows this turbine and its operating conditions. Determine the entropy generation rate for the turbine.

Solution

This is the same turbine that was analyzed in Example 3.2. For the conditions given, the entropy balance Equation 3.21 can be written as,

$$-\frac{\dot{Q}}{T_s} + \dot{m}(s_1 - s_2) + \dot{S}_{gen} = 0$$

$$\therefore \dot{S}_{gen} = \dot{m}(s_2 - s_1) + \frac{\dot{Q}}{T_s}$$

The heat transfer rate in Example 3.2 was found to be 446.4 kW. This is a heat loss from the turbine. The inlet and exhaust entropy values can be found since the states are fully identified; $s_1 = 7.0713$ kJ/kg·K and $s_2 = 8.4520$ kJ/kg·K. With these values,

$$\dot{S}_{gen} = \dot{m}(s_2 - s_1) + \frac{\dot{Q}}{T_s}$$

$$\dot{S}_{gen} = \left(16 \frac{\text{kg}}{\text{s}}\right)(8.4520 - 7.0713) \frac{\text{kJ}}{\text{kg}\cdot\text{K}} + \frac{446.4 \text{ kW}}{(70 + 273.15)\text{K}}$$

$$\dot{S}_{gen} = 22.09 \text{ kW/K} + 1.30 \text{ kW/K} = \underline{\underline{23.39 \text{ kW/K}}}$$

Notice that the entropy generation due to the fluid flow is $22.09/23.39 = 0.94 = 94\%$ of the total. The entropy generation due to the heat transfer is only 6%. Therefore, any engineering efforts to eliminate irreversibility should be focused on the flow process within the turbine.

3.7.1 The Reversible and Adiabatic Process

A thermodynamic process is considered reversible if the system can be returned back to its original state without any changes in the system or the surroundings that the system

interacts with. In reality, reversible processes cannot occur. However, they serve as a benchmark in engineering design. If the flow process through the component is reversible, there is no entropy generation. Therefore, Equation 3.21 becomes,

$$\left[\sum \left(\frac{\dot{Q}}{T_b} \right)_{in} - \sum \left(\frac{\dot{Q}}{T_b} \right)_{out} \right] + \left[\sum (\dot{m}s)_{in} - \sum (\dot{m}s)_{out} \right] = \frac{dS_{sys}}{dt} \quad (3.22)$$

Now consider a reversible process that has one flow entering, one flow leaving, and is operating at steady flow conditions. For this special case, Equation 3.22 becomes,

$$\left[\sum \left(\frac{\dot{Q}}{T_b} \right)_{in} - \sum \left(\frac{\dot{Q}}{T_b} \right)_{out} \right] + \dot{m}(s_{in} - s_{out}) = 0 \quad (3.23)$$

Consider the case where the process is also adiabatic. For this situation, Equation 3.23 simplifies to,

$$s_{in} = s_{out} \quad (3.24)$$

Equation 3.24 implies that for a steady flow, single flow device, a reversible *and* adiabatic process is *isentropic*. This is an important discovery in the thermodynamic analysis of many flow devices.

3.7.2 Isentropic Efficiencies of Flow Devices

The concept of an isentropic process is particularly helpful in defining a performance parameter of a flow device known as the *isentropic efficiency*. The definition of the isentropic efficiency is dependent on what purpose the device is serving.

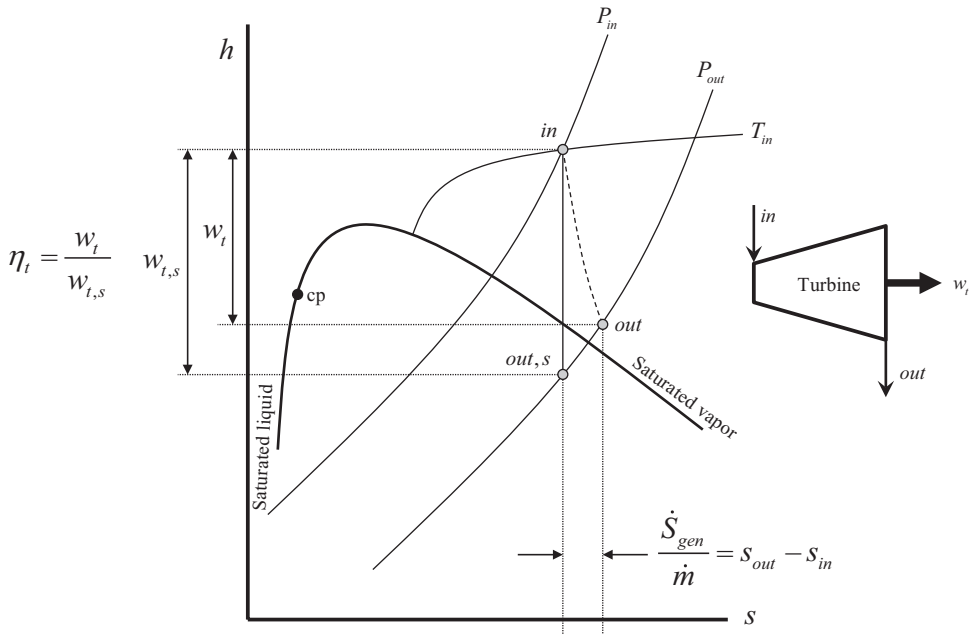
3.7.2.1 Turbines

The purpose of a turbine is to deliver power. The maximum power that can be delivered from a turbine occurs when the flow process through the turbine is isentropic. In the real-world, we expect that the turbine delivers less power due to irreversibilities. Therefore, the isentropic efficiency of a turbine can be expressed as,

$$\eta_t = \frac{w_t}{w_{t,s}} \quad (3.25)$$

In Equation 3.25, w_t is the actual work produced by the turbine and $w_{t,s}$ is the work produced by an isentropic turbine. Applying the conservation of energy to a steady state, adiabatic turbine, the work production is simply the difference in enthalpy between the inlet and outlet. Therefore, the isentropic efficiency can be expressed as,

$$\eta_t = \frac{w_t}{w_{t,s}} = \frac{h_{in} - h_{out}}{h_{in} - h_{out,s}} \quad (3.26)$$

**FIGURE 3.3**

Mollier diagram showing the isentropic efficiency and entropy generation for an adiabatic turbine.

Application of the entropy balance to a steady flow, adiabatic turbine results in,

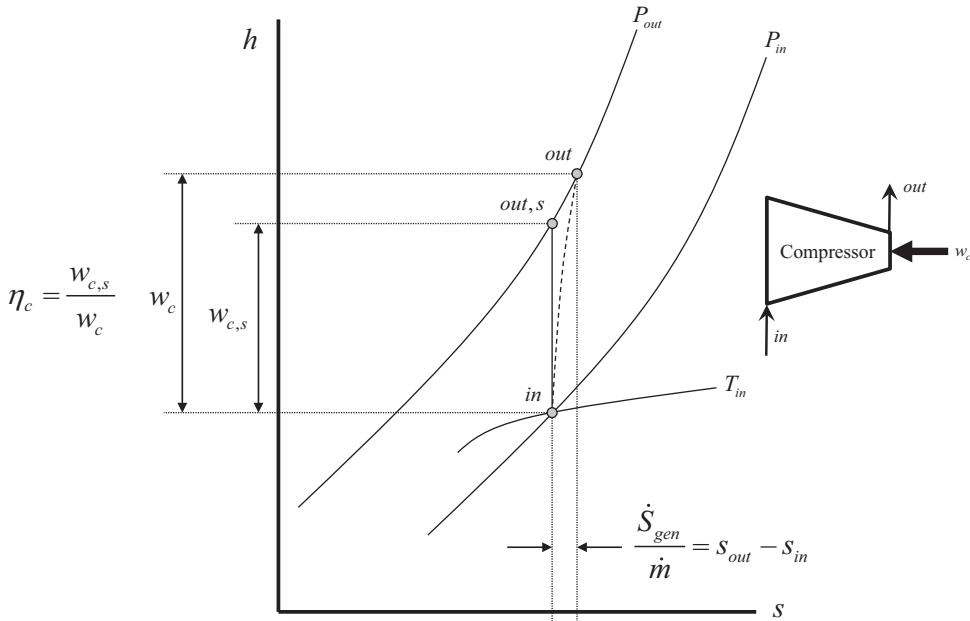
$$\frac{\dot{S}_{gen}}{\dot{m}} = s_{gen} = s_{out} - s_{in} \quad (3.27)$$

The h - s diagram, commonly known as the Mollier diagram, is particularly useful in visualizing the isentropic efficiency and entropy generation in a turbine, as shown in Figure 3.3. This figure shows that the exhaust state of the isentropic expansion and the actual expansion through the turbine are the same pressure, P_{out} .

3.7.2.2 Compressors, Pumps, and Fans

Compressors, pumps, and fans are designed to move fluids. Compressors and fans move gases while pumps move liquids. These devices accomplish fluid movement by utilizing an energy input. If the device is reversible and adiabatic, then all of the input energy can be focused on moving the fluid. In the case of a real-world device, the major sources of irreversibility are mechanical friction and fluid friction. Therefore, to move the fluid at the same rate, more energy is required in the real case. Using this reasoning, the isentropic efficiency of a compressor, fan, or pump can be expressed by,

$$\eta_m = \frac{w_s}{w} = \frac{h_{out,s} - h_{in}}{h_{out} - h_{in}} \quad (3.28)$$

**FIGURE 3.4**

Mollier diagram showing the isentropic efficiency and entropy generation for an adiabatic compressor.

The subscript m is used to indicate a device that *moves* a fluid. Application of the entropy balance to a steady state, adiabatic compressor, fan, or pump, results in,

$$\frac{\dot{S}_{gen}}{\dot{m}} = s_{gen} = s_{out} - s_{in} \quad (3.29)$$

Figure 3.4 shows the h - s diagram for a compressor. As with the turbine, the isentropic efficiency and entropy generation can be seen graphically. h - s diagrams for the fans and pumps are similar. For the pump, the process occurs in the liquid phase. Figure 3.4 indicates that the exhaust state of the isentropic compression and actual compression are at the same pressure.

3.7.2.3 Nozzles

Nozzles are utilized in many different systems. Perhaps the most well-known, large-scale application is in rocketry. However, nozzles also play an important role on the small-scale. For example, nozzles are used in turbines to increase the kinetic energy of the fluid before impinging on the turbine blades, causing a transfer of momentum resulting in a rotating shaft. From these two examples, it becomes clear that the purpose of a nozzle is to increase the fluid's kinetic energy.

Nozzles are generally considered to be adiabatic. If the flow is frictionless, then the velocity at the exit of the nozzle will be at a maximum. Since the purpose of a nozzle is

to increase the kinetic energy of the fluid passing through it, the isentropic efficiency of a nozzle can be expressed as,

$$\eta_n = \frac{ke}{ke_s} = \frac{V^2/2g}{V_s^2/2g} = \frac{V^2}{V_s^2} \quad (3.30)$$

In the evaluation of Equation 3.30, the isentropic exhaust of the nozzle is at the same pressure as the actual exhaust.

3.7.2.4 Diffusers

The diffuser uses a decrease in the fluid's velocity to affect a pressure increase. Like nozzles, diffusers are considered to be adiabatic since the fluid passes through the device quickly, leaving very little time to transfer heat. Since the purpose of a diffuser is to increase the fluid's pressure, its isentropic efficiency is defined as,

$$\eta_d = \frac{\Delta P_d}{\Delta P_{d,s}} = \frac{P_{out} - P_{in}}{P_{out,s} - P_{in}} \quad (3.31)$$

In Equation 3.31, P_{out} is the actual outlet pressure of the diffuser and $P_{out,s}$ is the exit pressure from the isentropic diffuser evaluated at the same exit velocity as the actual diffuser.

Example 3.6

GIVEN:

Air at 25°C, 100 kPa enters the compressor of a gas turbine power plant and is compressed to 460°C, 1600 kPa. After compression, the air is cooled to 300°C with a negligible change in pressure as it passes through a heat exchanger, as shown in Figure E3.6A. Cold water flowing at 2 kg/s cools the air in the heat exchanger. The water enters at 25°C, 200 kPa, and leaves at 110°C with no appreciable drop in pressure. Determine the

- Isentropic efficiency of the compressor
- Compressor's power draw
- Entropy generation in the compressor and heat exchanger

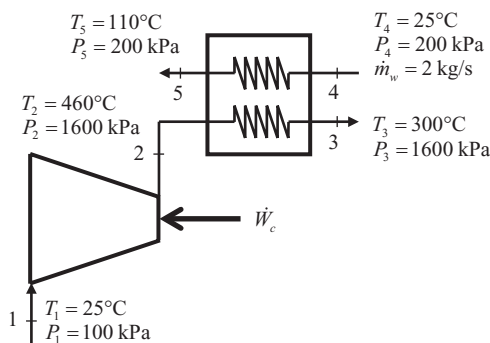


FIGURE E3.6A

Compressor with aftercooler heat exchanger.

Solution

The thermodynamic properties of the air and water for the states given in this problem can all be found, since two independent, intensive properties are known at each state. The properties are shown in Table E3.6. The two independent properties that fix the thermodynamic state are identified in **bold** type. Notice in Table E3.6 that state 2s has been calculated using *pressure* and *entropy* as known input variables.

a. The isentropic efficiency of the compressor can be found using Equation 3.28,

$$\eta_c = \frac{h_{2s} - h_1}{h_2 - h_1} = \frac{(659.59 - 298.45) \text{ kJ/kg}}{(750.13 - 298.45) \text{ kJ/kg}} = 0.7996 = \underline{80.0\%}$$

b. To compute the power draw of the compressor, a system boundary is drawn around the compressor as shown in Figure E3.6B and the conservation of energy equation is applied to the resulting system.

TABLE E3.6
Working Fluid Properties

Thermodynamic Properties of Air					
	<i>P</i>	<i>T</i>	<i>v</i>	<i>h</i>	<i>s</i>
State	kPa	°C	m ³ /kg	kJ/kg	kJ/kg-K
1	100	25	0.85575	298.45	6.86412
2s	1600	375.9	0.11728	659.59	6.86412
2	1600	460	0.13246	750.13	6.99523
3	1600	300	0.10356	579.22	6.73249

Thermodynamic Properties of Water					
	<i>P</i>	<i>T</i>	<i>v</i>	<i>h</i>	<i>s</i>
State	kPa	°C	m ³ /kg	kJ/kg	kJ/kg-K
4	200	25	0.001	105.01	0.36718
5	200	110	0.00105	461.46	1.41878

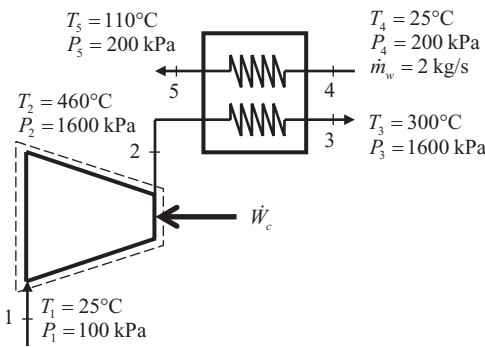


FIGURE E3.6B
System boundary drawn around the compressor.

For steady flow, the conservation of energy equation can be written as,

$$\begin{aligned}\dot{W}_c + \dot{m}_a(h_1 - h_2) &= 0 \\ \therefore \dot{W}_c &= \dot{m}_a(h_2 - h_1)\end{aligned}$$

The enthalpy values can be found since the thermodynamic states are identified at all states, but the mass flow rate of the air is unknown. However, the mass flow rate of the air can be found because it is related to the heat transfer rate in the heat exchanger. Figure E3.6C shows a system boundary surrounding the heat exchanger. For this system boundary, the conservation of energy is written as,

$$\begin{aligned}(\dot{m}_a h_2 + \dot{m}_w h_4) - (\dot{m}_a h_3 + \dot{m}_w h_5) &= 0 \\ \dot{m}_a(h_2 - h_3) &= \dot{m}_w(h_5 - h_4) \\ \therefore \dot{m}_a &= \dot{m}_w \left(\frac{h_5 - h_4}{h_2 - h_3} \right) = \left(2 \frac{\text{kg}}{\text{s}} \right) \left[\frac{(461.46 - 105.01) \text{ kJ/kg}}{(750.13 - 579.22) \text{ kJ/kg}} \right] = 4.17 \frac{\text{kg}}{\text{s}}\end{aligned}$$

Now, the power requirement for the compressor can be found,

$$\dot{W}_c = \dot{m}_a(h_2 - h_1) = \left(4.17 \frac{\text{kg}}{\text{s}} \right) (750.13 - 298.45) \frac{\text{kJ}}{\text{kg}} \left(\frac{\text{kW-s}}{\text{kJ}} \right) = \underline{1884 \text{ kW}}$$

- c. The entropy generation in each of the devices can be found by applying the entropy balance equation to the system boundary surrounding the device. For the compressor, the entropy balance results in,

$$\dot{S}_{gen,c} = \dot{m}_a(s_2 - s_1) = \left(4.17 \frac{\text{kg}}{\text{s}} \right) (6.99523 - 6.86412) \frac{\text{kJ}}{\text{kg-K}} \left(\frac{\text{kW-s}}{\text{kJ}} \right) = \underline{0.5469 \frac{\text{kW}}{\text{K}}}$$

For the heat exchanger, there are multiple flows in and out. Applying the entropy balance equation to the heat exchanger results in,

$$(\dot{m}_a s_2 + \dot{m}_w s_4) - (\dot{m}_a s_3 + \dot{m}_w s_5) + \dot{S}_{gen,HX} = 0$$

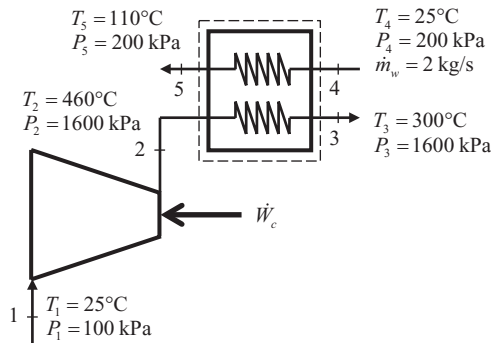


FIGURE E3.6C

System boundary drawn around the heat exchanger.

Solving for the entropy generation,

$$\begin{aligned}\dot{S}_{gen,HX} &= (\dot{m}_a s_3 + \dot{m}_w s_5) - (\dot{m}_a s_2 + \dot{m}_w s_4) = \dot{m}_a (s_3 - s_2) + \dot{m}_w (s_5 - s_4) \\ \dot{S}_{gen,HX} &= \left[\left(4.17 \frac{\text{kg}}{\text{s}} \right) (6.73249 - 6.99523) \frac{\text{kJ}}{\text{kg-K}} \right. \\ &\quad \left. + \left(2 \frac{\text{kg}}{\text{s}} \right) (1.41878 - 0.36718) \frac{\text{kJ}}{\text{kg-K}} \left(\frac{\text{kW-s}}{\text{kJ}} \right) \right] \\ \dot{S}_{gen,HX} &= \underline{\underline{1.007 \text{ kW/K}}}\end{aligned}$$

These calculations reveal that the heat exchanger has nearly twice the entropy generation as the compressor. The magnitude of the entropy generation is a result of irreversibility. In the compressor, the main source of irreversibility is primarily fluid friction. In the heat exchanger, the primary source is the heat transfer through a finite temperature difference.

3.7.3 Heat Exchanger Effectiveness

When developing the expression for the isentropic efficiency of a device, the actual performance of the device is compared to an imaginary device that is completely reversible. By removing fluid friction, mechanical friction, and heat transfer effects; the reversible counterparts to turbines, compressors, nozzles, and diffusers can easily be understood. However, envisioning a reversible heat exchanger is much more difficult. In fact, it is impossible.

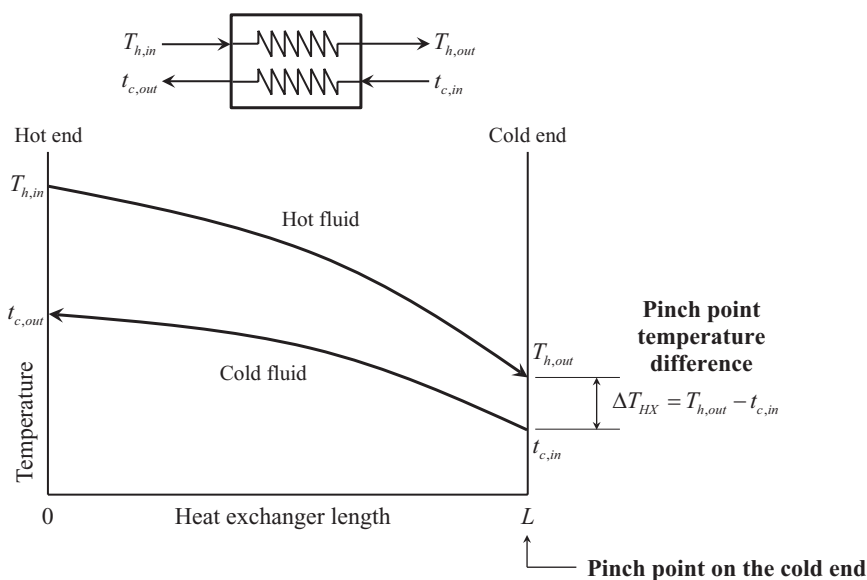
Fluid friction and irreversibility caused by sudden expansions and/or contractions in a heat exchanger are causes of irreversibility. However, these are not the major irreversibilities in a heat exchanger. Even if one could envision frictionless flow, there is still a temperature difference between the fluids which makes the heat exchanger irreversible (heat transfer through a finite temperature difference is irreversibility). This implies that even in an idealized reversible scenario, heat exchangers cannot exist. Therefore, the concept of an isentropic efficiency for a heat exchanger is meaningless.

An alternative way to determine the performance of a heat exchanger is by its *effectiveness*. The effectiveness of a heat exchanger, ϵ , is defined as,

$$\epsilon = \frac{\dot{Q}}{\dot{Q}_{\max}} \quad (3.32)$$

In Equation 3.32, \dot{Q} is the actual heat transfer rate between the fluids in the heat exchanger, and \dot{Q}_{\max} is the maximum heat transfer rate theoretically possible between the fluid streams. To further develop Equation 3.32, two additional heat exchanger parameters are introduced; the *pinch point*, and the *pinch point temperature difference*.

Consider a counter flow heat exchanger where both fluids remain in the single phase (gas or liquid) as shown in Figure 3.5. In this figure, uppercase T and a lowercase t are used to designate the hot and cold fluids, respectively. The plot in Figure 3.5 also shows the temperature profiles of the hot and cold fluids as they travel through the heat exchanger. Since the fluids remain in the single phase, the smallest temperature difference between the hot and cold fluids must be on either end of the heat exchanger. Figure 3.5 shows the case

**FIGURE 3.5**

Counter flow heat exchanger with the pinch point on the cold end.

where this smallest temperature difference occurs at the cold end of the heat exchanger. The smallest temperature difference between the hot and cold fluids is known as the *pinch point temperature difference* (PPTD), and is usually given the symbol ΔT_{HX} . The location of the PPTD in the heat exchanger is known as the *pinch point*. In Figure 3.5, the pinch point occurs at the cold end of the heat exchanger.

The shape of the fluid temperature profiles is dependent on the mass flow rate and thermodynamic properties of each fluid. Therefore, it is entirely possible that the pinch point could occur at the hot end of the heat exchanger. This scenario is shown in Figure 3.6. Comparing Figures 3.5 and 3.6, it can be seen that the definition of the PPTD is dependent on which side (hot or cold) the pinch point is.

If one of the fluids undergoes a phase change within the heat exchanger, then it is possible that the pinch point can occur *within* the heat exchanger. This scenario is what can happen inside of a steam boiler as demonstrated in Figure 3.7.

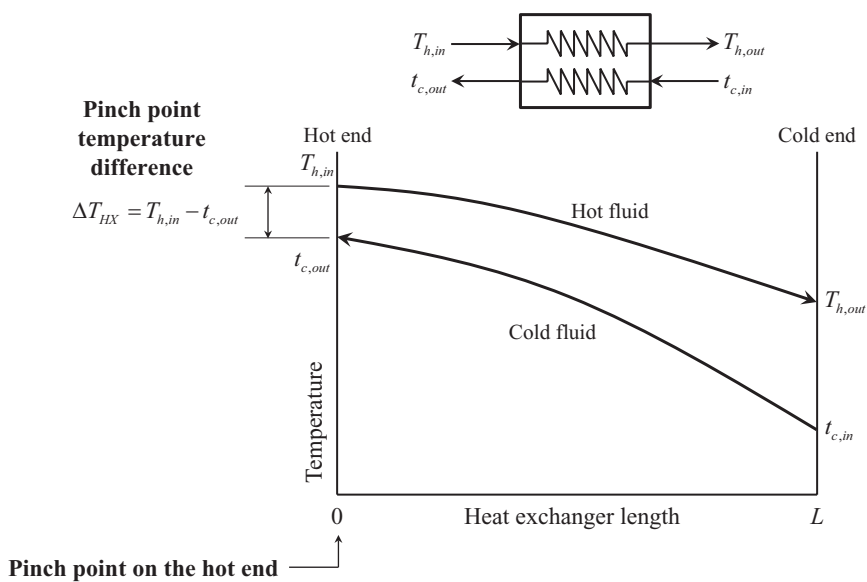
Example 3.7

Liquid acetone enters a counter flow heat exchanger at 80°C with a volumetric flow rate of 10 L/s, and exits at 60°C as shown in Figure E3.7. The acetone is being cooled by water entering the heat exchanger at 20°C and a flow rate of 3.5 L/s. Determine the PPTD and location of the pinch point for this heat exchanger.

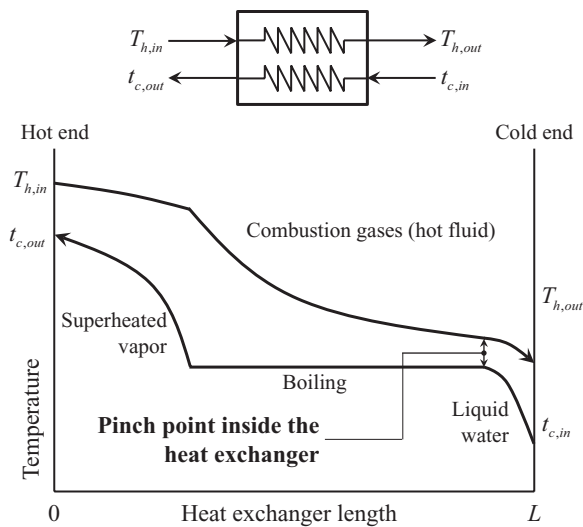
Solution

Since both of the fluids in this heat exchanger remain in the liquid phase, the pinch point will occur on either the hot or cold end. The cold end temperature difference can be found immediately,

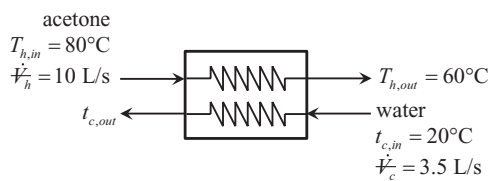
$$\Delta T_c = T_{h,out} - t_{c,in} = (60 - 20)^\circ\text{C} = 40 \text{ K}$$

**FIGURE 3.6**

Counter flow heat exchanger with the pinch point on the hot end.

**FIGURE 3.7**

Counter flow heat exchanger with the pinch point inside.

**FIGURE E3.7**

Counter flow acetone-water heat exchanger.

In order to determine the hot end temperature difference, the temperature of the cold fluid (water) leaving the heat exchanger must be found. Application of the conservation of energy to the heat exchanger results in,

$$\dot{m}_h(h_{h,in} - h_{h,out}) = \dot{m}_c(h_{c,out} - h_{c,in})$$

The enthalpy differences can be approximated by $c_p\Delta T$. Therefore, the above equation can be rewritten as,

$$\dot{m}_h c_{p,h}(T_{h,in} - T_{h,out}) = \dot{m}_c c_{p,c}(t_{c,out} - t_{c,in})$$

In this equation, the isobaric heat capacity of each fluid is evaluated at the average between the inlet and outlet temperatures.

The volumetric flow rate and the inlet temperature of each fluid are known. Therefore, the mass flow rate can be determined by,

$$\dot{m} = \rho \dot{V}$$

The temperatures of the fluids change as they traverse the heat exchanger, therefore the fluid density changes as well. However, in this problem, the volumetric flow rates are given at the *inlet* to the heat exchanger. Therefore, the densities of each fluid can be found using their respective inlet temperatures. From Appendix B.3,

$$\text{acetone: } \rho_h = 719.79 \text{ kg/m}^3$$

$$\text{water: } \rho_c = 998.16 \text{ kg/m}^3$$

The mass flow rate of each fluid can now be found,

$$\dot{m}_h = \rho_h \dot{V}_h = \left(719.79 \frac{\text{kg}}{\text{m}^3} \right) \left(10 \frac{\text{L}}{\text{s}} \right) \left(\frac{\text{m}^3}{1000 \text{ L}} \right) = 7.1979 \frac{\text{kg}}{\text{s}}$$

$$\dot{m}_c = \rho_c \dot{V}_c = \left(998.16 \frac{\text{kg}}{\text{m}^3} \right) \left(3.5 \frac{\text{L}}{\text{s}} \right) \left(\frac{\text{m}^3}{1000 \text{ L}} \right) = 3.4936 \frac{\text{kg}}{\text{s}}$$

The average heat capacity of the acetone can be found since the inlet and outlet temperatures are known. Using the property values in Appendix B.3 for acetone,

$$T_{h,avg} = \frac{(80 + 60)^\circ\text{C}}{2} = 70^\circ\text{C} \rightarrow c_{p,h} = 2.2756 \text{ kJ/kg-K (interpolation required)}$$

The average heat capacity of the water cannot be found because the outlet temperature is unknown. As a first estimate, the heat capacity will be assumed to be equal to the inlet heat capacity. From Appendix B.3 for water,

$$t_{c,in} = 20^\circ\text{C} \rightarrow c_{p,c} \approx 4.1844 \text{ kJ/kg-K}$$

Now, the conservation of energy equation can be solved for the outlet temperature of the water,

$$t_{c,out} = t_{c,in} + \frac{\dot{m}_h c_{p,h}}{\dot{m}_c c_{p,c}} (T_{h,in} - T_{h,out})$$

$$t_{c,out} = 20^\circ\text{C} + \frac{\left(7.1979 \frac{\text{kg}}{\text{s}}\right) \left(2.2756 \frac{\text{kJ}}{\text{kg}\cdot\text{K}}\right)}{\left(3.4936 \frac{\text{kg}}{\text{s}}\right) \left(4.1844 \frac{\text{kJ}}{\text{kg}\cdot\text{K}}\right)} (80 - 60)^\circ\text{C} = 42.41^\circ\text{C}$$

Recall that this result was obtained by assuming the heat capacity of the water at the inlet temperature. Using this calculated outlet temperature, the average heat capacity can now be calculated, which allows for the recalculation of the outlet temperature (i.e., an iterative process). Using the calculated outlet temperature and the property data for water in Appendix B.3,

$$t_{c,avg} = \frac{(20 + 42.41)^\circ\text{C}}{2} = 31.2^\circ\text{C} \rightarrow c_{p,c} = 4.1800 \text{ kJ/kg}\cdot\text{K} \text{ (interpolation required)}$$

Recalculating the water outlet temperature,

$$t_{c,out} = 20^\circ\text{C} + \frac{\left(7.1979 \frac{\text{kg}}{\text{s}}\right) \left(2.2756 \frac{\text{kJ}}{\text{kg}\cdot\text{K}}\right)}{\left(3.4936 \frac{\text{kg}}{\text{s}}\right) \left(4.1800 \frac{\text{kJ}}{\text{kg}\cdot\text{K}}\right)} (80 - 60)^\circ\text{C} = 42.43^\circ\text{C}$$

The difference between the two calculated outlet temperatures is insignificant. Therefore, no further iteration is required.

Knowing the water outlet temperature allows for the hot side temperature difference,

$$\Delta T_h = T_{h,in} - t_{c,out} = (80 - 42.43)^\circ\text{C} = 37.6 \text{ K}$$

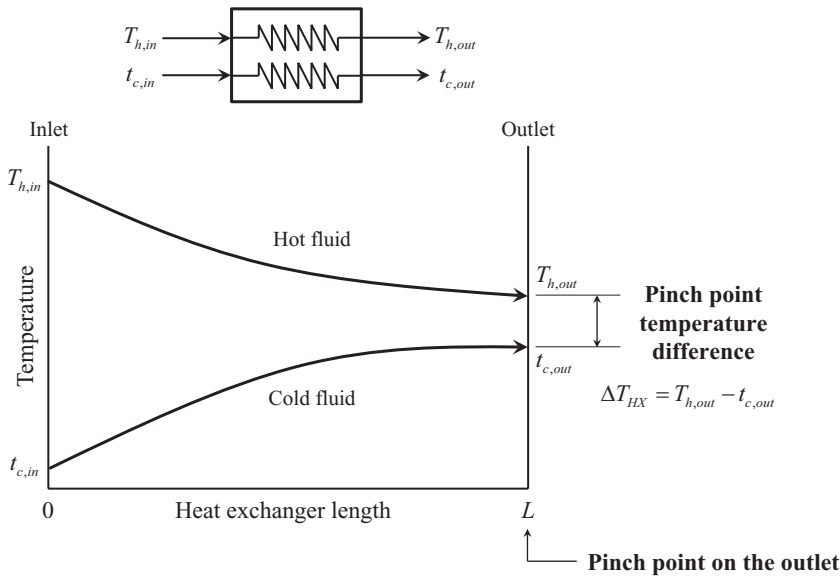
The PPTD is the smaller of the two temperature differences on each end of the heat exchanger. This is also the location of the pinch point. Therefore,

$$\Delta T_{HX} = \Delta T_h = \underline{37.6 \text{ K}} \quad (\text{pinch point on the hot end})$$

Example 3.7 demonstrates that for a counter flow heat exchanger with single phase fluids, the PPTD can be determined by,

$$\Delta T_{HX, \text{counter flow}} = \min \left[(T_{h,in} - t_{c,out}), (T_{h,out} - t_{c,in}) \right] \quad (3.33)$$

If the heat exchanger has a parallel flow configuration, then both fluids enter on the same side (the inlet) and leave on the other side (the outlet). Rather than identify a “hot” or “cold” side, it is easier to consider the “inlet” and “outlet” sides of a parallel flow heat exchanger. Figure 3.8 shows a parallel flow heat exchanger with the accompanying temperature

**FIGURE 3.8**

Fluid temperature profiles in a parallel flow heat exchanger.

profiles for single-phase fluids. Figure 3.8 shows that the pinch point will always occur at the outlet of a parallel flow heat exchanger. Therefore, the PPTD for a parallel flow heat exchanger is given by,

$$\Delta T_{HX, \text{parallel flow}} = T_{h,out} - t_{c,out} \quad (3.34)$$

Example 3.8

Consider a parallel flow heat exchanger operating with the same fluids, temperatures, and flow rates as given in Example 3.7. Determine the PPTD for this heat exchanger.

Solution

Equation 3.34 indicates that the PPTD for a parallel flow heat exchanger is,

$$\Delta T_{HX, \text{parallel flow}} = T_{h,out} - t_{c,out}$$

The conservation of energy applied to the parallel flow heat exchanger will lead to the same water outlet temperature that was calculated in Example 3.7 (i.e., the result of the application of the conservation of energy is independent of the flow configuration). Therefore, the PPTD of the parallel flow heat exchanger is,

$$\Delta T_{HX, \text{parallel flow}} = T_{h,out} - t_{c,out} = (60 - 42.43)^{\circ}\text{C} = \underline{\underline{17.6 \text{ K}}}$$

The magnitude of the PPTD is an indication of the heat transfer area (and therefore the size) of the heat exchanger. Large PPTDs tend to indicate smaller heat exchangers, whereas small PPTDs indicate larger heat exchangers. This concept will help determine the effectiveness of the heat exchanger as defined by Equation 3.32.

The actual heat transfer rate between the two fluids in a heat exchanger, the numerator of Equation 3.32, can be determined by applying the conservation of energy to either fluid,

$$\dot{Q} = \dot{m}_h(h_{h,in} - h_{h,out}) = \dot{m}_c(h_{c,out} - h_{c,in}) \quad (3.35)$$

For fluids remaining in the single phase, it has been shown that Equation 3.35 can be written as,

$$\dot{Q} = \dot{m}_h c_{p,h}(T_{h,in} - T_{h,out}) = \dot{m}_c c_{p,c}(t_{c,out} - t_{c,in}) \quad (3.36)$$

The product $\dot{m}c_p$ is often written as \dot{C} and is known as the *thermal capacity rate* of the flowing fluid. Therefore, Equation 3.36 can be written as,

$$\dot{Q} = \dot{C}_h(T_{h,in} - T_{h,out}) = \dot{C}_c(t_{c,out} - t_{c,in}) \quad (3.37)$$

The maximum heat transfer rate theoretically possible between the fluid streams, the denominator of Equation 3.32, occurs when the PPTD of the heat exchanger goes to zero. This occurs when the heat exchanger is envisioned as being infinitely large. In order to develop an expression for the maximum heat transfer rate, and therefore the effectiveness, the flow configuration of the heat exchanger must be considered.

3.7.3.1 Effectiveness of a Counter Flow Heat Exchanger

In an infinitely large counter flow heat exchanger, one of the fluids must experience the largest possible temperature change,

$$\Delta T_{\max} = T_{h,in} - t_{c,in} \quad (3.38)$$

To determine which fluid experiences the maximum possible temperature change, the thermal capacity rate of each fluid must be considered. There are three possibilities; $\dot{C}_h < \dot{C}_c$, $\dot{C}_c < \dot{C}_h$, or $\dot{C}_h = \dot{C}_c$. The case of equal thermal capacity rates usually occurs in a *regenerative* heat exchanger. The topic of regenerative heat exchangers is deferred until Chapter 5. The remaining two cases will be examined further here.

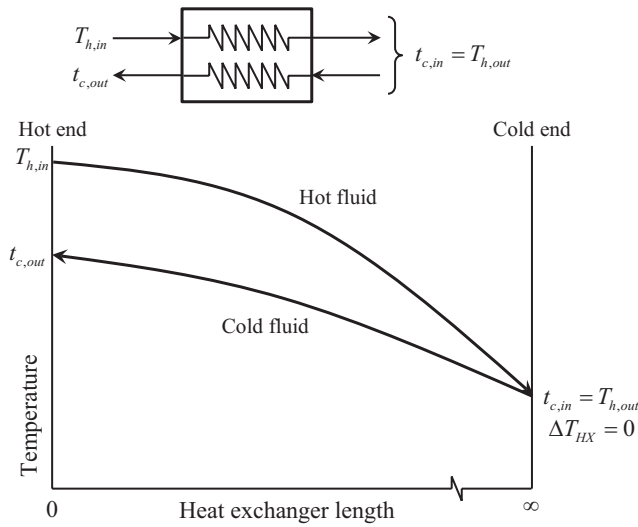
Figure 3.9 shows the temperature profiles for the case where the PPTD goes to zero on the cold end. In this case, the hot fluid experiences the maximum temperature difference. The heat transfer rate between the fluids can be written in two ways,

$$\dot{Q}_{\max} = \dot{C}_c(t_{c,out} - t_{c,in}) = \dot{C}_h \Delta T_{\max} \quad (3.39)$$

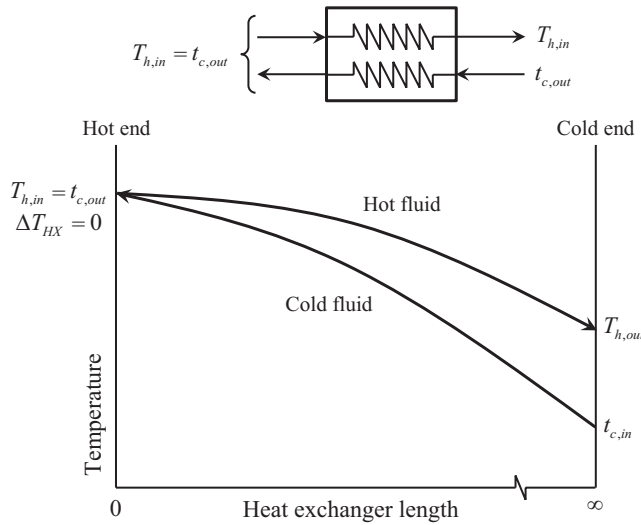
Equation 3.39 implies that $\dot{C}_h < \dot{C}_c$. In this scenario, the fluid with the *minimum* thermal capacity rate (the hot fluid) experiences the largest possible temperature change.

Another possibility is the pinch point occurring on the hot side of the heat exchanger. This is shown in Figure 3.10. In this scenario, the cold fluid experiences the maximum temperature change. Therefore, the heat transfer rate between the two fluids can be written as,

$$\dot{Q}_{\max} = \dot{C}_h(T_{h,in} - T_{h,out}) = \dot{C}_c \Delta T_{\max} \quad (3.40)$$

**FIGURE 3.9**

Fluid temperature profiles in an infinitely large counter flow heat exchanger where the pinch point occurs on the cold end.

**FIGURE 3.10**

Fluid temperature profiles in an infinitely large counter flow heat exchanger where the pinch point occurs on the hot side.

Equation 3.40 indicates that $\dot{C}_c < \dot{C}_h$. In this case, the fluid with the *minimum* thermal capacity rate (the cold fluid) experiences the largest possible temperature rise.

This analysis reveals that in a counter heat exchanger, the fluid with the minimum thermal capacity rate will experience the maximum possible temperature change in an infinitely large heat exchanger. Therefore, the maximum theoretical heat transfer rate for the counter flow heat exchanger can be written as,

$$\dot{Q}_{\max} = \dot{C}_{\min} \Delta T_{\max} = \dot{C}_{\min} (T_{h,in} - t_{c,in}) \quad (3.41)$$

This analysis allows for the formulation of the effectiveness of a counter flow heat exchanger. The resulting expression can be written in two ways, depending on how the actual heat transfer rate, \dot{Q} , is expressed,

$$\varepsilon_{CF} = \frac{\dot{Q}}{\dot{Q}_{\max}} = \frac{\dot{C}_h(T_{h,in} - T_{h,out})}{\dot{C}_{\min}(T_{h,in} - t_{c,in})} = \frac{\dot{C}_c(t_{c,out} - t_{c,in})}{\dot{C}_{\min}(T_{h,in} - t_{c,in})} \quad (3.42)$$

Example 3.9

Liquid ammonia enters a counter flow heat exchanger at a temperature of 0°F and a flow rate of 50 gpm. The ammonia is heated by a flow of water entering the heat exchanger at 140°F and a flow rate of 30 gpm. The water leaves the heat exchanger at a temperature of 40°F. Determine the effectiveness of this heat exchanger.

Solution

A sketch of this heat exchanger is shown in Figure E3.9. In order to find the effectiveness of this heat exchanger, the fluid stream with the minimum thermal capacity rate must be identified. The thermal capacity rates are given by,

$$\dot{C}_h = \dot{m}_h c_{p,h} = \rho_h \dot{V}_h c_{p,h} \quad \text{and} \quad \dot{C}_c = \dot{m}_c c_{p,c} = \rho_c \dot{V}_c c_{p,c}$$

The densities are evaluated at the inlet temperature of each fluid, and the heat capacities are evaluated at the average temperature of the fluid. In order to evaluate the heat capacity of the ammonia (cold fluid), the outlet temperature needs to be determined. Applying the conservation of energy to each fluid stream,

$$\dot{C}_h(T_{h,in} - T_{h,out}) = \dot{C}_c(t_{c,out} - t_{c,in})$$

The density of each fluid at the inlet temperature can be found in Appendix B.3,

$$\text{ammonia:} \quad \rho_c = 41.344 \text{ lbm/ft}^3$$

$$\text{water:} \quad \rho_h = 61.377 \text{ lbm/ft}^3$$

The heat capacity of the water can be found since the inlet and outlet temperatures are known. The cold fluid outlet temperature is unknown, so an initial guess will be made using the cold fluid inlet temperature to evaluate the heat capacity.

$$T_{h,avg} = \frac{(140 + 40)^\circ\text{F}}{2} = 90^\circ\text{F} \rightarrow c_{p,h} = 0.99911 \text{ kJ/kg-K (interpolation required)}$$

$$t_{c,in} = 0^\circ\text{F} \rightarrow c_{p,c} \approx 1.0814 \text{ kJ/kg-K}$$

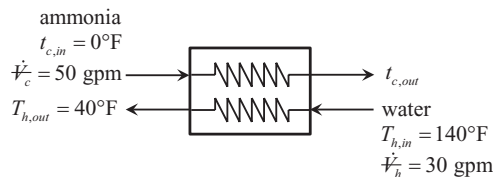


FIGURE E3.9
Counter flow ammonia-water heat exchanger.

Therefore, the thermal capacity rates are,

$$\dot{C}_h = \rho_h \dot{V}_h c_{p,h} = \left(61.377 \frac{\text{lbm}}{\text{ft}^3} \right) (30 \text{ gpm}) \left(0.99911 \frac{\text{Btu}}{\text{lbm-R}} \right) \left(\frac{8.02083 \text{ ft}^3}{\text{gpm-h}} \right) = 14,756 \frac{\text{Btu}}{\text{h-R}}$$

$$\dot{C}_c = \rho_c \dot{V}_c c_{p,c} = \left(41.344 \frac{\text{lbm}}{\text{ft}^3} \right) (50 \text{ gpm}) \left(1.0814 \frac{\text{Btu}}{\text{lbm-R}} \right) \left(\frac{8.02083 \text{ ft}^3}{\text{gpm-h}} \right) = 17,930 \frac{\text{Btu}}{\text{h-R}}$$

The outlet temperature of the ammonia (cold fluid) can now be calculated. Solving the conservation of energy equation for the cold fluid outlet temperature results in,

$$t_{c,out} = t_{c,in} + \frac{\dot{C}_h}{\dot{C}_c} (T_{h,in} - T_{h,out})$$

$$t_{c,out} = 0^\circ\text{F} + \frac{14,756 \frac{\text{Btu}}{\text{h-R}}}{17,930 \frac{\text{Btu}}{\text{h-R}}} (140 - 40)^\circ\text{F} = 82.30^\circ\text{F}$$

Performing an iteration,

$$t_{c,avg} = \frac{(0 + 82.23)^\circ\text{F}}{2} = 41.14^\circ\text{C} \rightarrow c_{p,c} = 1.1104 \text{ (interpolation required)}$$

Recalculating the water outlet temperature,

$$\dot{C}_c = \rho_c \dot{V}_c c_{p,c} = \left(41.344 \frac{\text{lbm}}{\text{ft}^3} \right) (50 \text{ gpm}) \left(1.1104 \frac{\text{Btu}}{\text{lbm-R}} \right) \left(\frac{8.02083 \text{ ft}^3}{\text{gpm-h}} \right) = 18,411 \frac{\text{Btu}}{\text{h-R}}$$

$$t_{c,out} = 0^\circ\text{F} + \frac{14,756 \frac{\text{Btu}}{\text{h-R}}}{18,411 \frac{\text{Btu}}{\text{h-R}}} (140 - 40)^\circ\text{F} = 80.15^\circ\text{F}$$

Performing another iteration to update the ammonia heat capacity,

$$t_{c,avg} = \frac{(0 + 80.15)^\circ\text{F}}{2} = 40.07^\circ\text{F} \rightarrow c_{p,c} = 1.1095 \text{ (interpolation required)}$$

Recalculating the water outlet temperature a second time,

$$\dot{C}_c = \rho_c \dot{V}_c c_{p,c} = \left(41.344 \frac{\text{lbm}}{\text{ft}^3} \right) (50 \text{ gpm}) \left(1.1095 \frac{\text{Btu}}{\text{lbm-R}} \right) \left(\frac{8.02083 \text{ ft}^3}{\text{gpm-h}} \right) = 18,396 \frac{\text{Btu}}{\text{h-R}}$$

$$t_{c,out} = 0^\circ\text{F} + \frac{14,756 \frac{\text{Btu}}{\text{h-R}}}{18,396 \frac{\text{Btu}}{\text{h-R}}} (140 - 40)^\circ\text{F} = 80.21^\circ\text{F}$$

The difference between the two most recent calculated outlet temperatures is insignificant. Therefore, no further iteration is required.

The minimum thermal capacity rate is that of the hot fluid,

$$\dot{C}_{\min} = \min(\dot{C}_h, \dot{C}_c) = \dot{C}_h = 14,756 \frac{\text{Btu}}{\text{h} \cdot ^\circ\text{R}}$$

Therefore, the effectiveness of this heat exchanger is,

$$\epsilon_{\text{CF}} = \frac{\dot{Q}}{\dot{Q}_{\max}} = \frac{\dot{C}_h(T_{h,\text{in}} - T_{h,\text{out}})}{\dot{C}_{\min}(T_{h,\text{in}} - t_{c,\text{in}})} = \frac{T_{h,\text{in}} - T_{h,\text{out}}}{T_{h,\text{in}} - t_{c,\text{in}}} = \frac{(140 - 40)^\circ\text{F}}{(140 - 0)^\circ\text{F}} = \underline{0.7143}$$

This effectiveness suggests that the heat exchanger is functioning quite well.

Higher values of effectiveness are reflected in smaller PPTDs, indicating a larger heat exchanger. A parametric study of the heat exchanger described in Example 3.9 can be helpful to verify this idea. In order to conduct this study, the water (hot fluid) outlet temperature is varied from 32°F to 140°F. This allows for the calculation of the ammonia (cold fluid) outlet temperature, heat exchanger effectiveness, PPTD, and the location of the pinch point. The resulting plot is shown in Figure 3.11. As suggested, this plot indicates that higher effectiveness values lead to smaller PPTDs which indicates a larger heat exchanger. As the PPTD increases (i.e., the size of the heat exchanger becomes smaller), the effectiveness decreases and eventually goes to 0 at a PPTD of 140°F. At that point, there is no heat exchanger and no heat transfer occurs between the fluids.

3.7.3.2 Effectiveness of a Parallel Flow Heat Exchanger

For an infinitely large parallel flow heat exchanger, the fluid outlet temperatures are equal. This is shown in Figure 3.12. In this figure, the outlet temperature of each fluid is signified as $T_{\text{out},\infty}$.

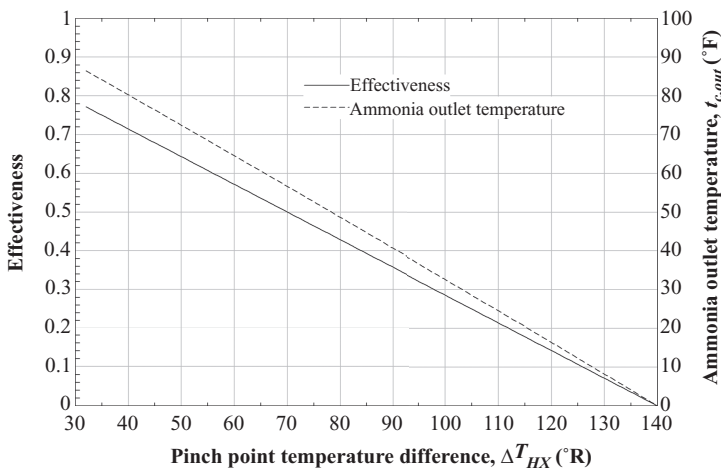


FIGURE 3.11

Parametric study of the heat exchanger described in Example 3.9.

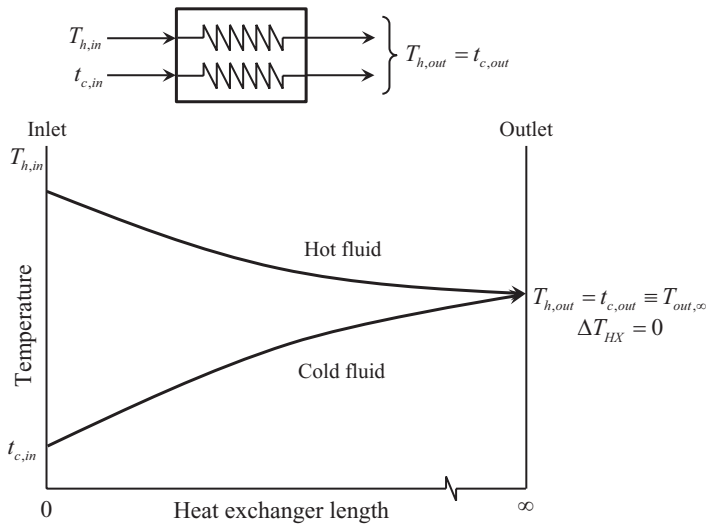


FIGURE 3.12
Fluid temperature profiles in an infinitely large parallel flow heat exchanger.

The maximum heat transfer rate can be written in terms of either fluid,

$$\dot{Q}_{\max} = \dot{C}_h (T_{h,in} - T_{out,\infty}) = \dot{C}_c (T_{out,\infty} - t_{c,in}) \quad (3.43)$$

Equation 3.43 can be solved for the outlet temperature of the infinite heat exchanger,

$$T_{out,\infty} = \frac{\dot{C}_h T_{h,in} + \dot{C}_c t_{c,in}}{\dot{C}_h + \dot{C}_c} \quad (3.44)$$

Therefore, the effectiveness of a parallel flow heat exchanger can be expressed as,

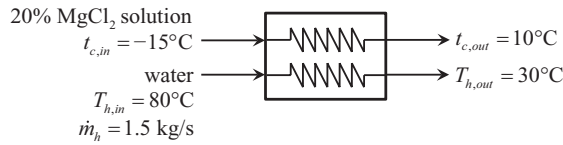
$$\varepsilon_{PF} = \frac{\dot{Q}}{\dot{Q}_{\max}} = \frac{T_{h,in} - T_{h,out}}{T_{h,in} - T_{out,\infty}} = \frac{t_{c,out} - t_{c,in}}{T_{out,\infty} - t_{c,in}} \quad (3.45)$$

Example 3.10

A parallel flow heat exchanger is being used to warm a 20% magnesium chloride-water solution using hot water. The magnesium chloride solution enters the heat exchanger at -15°C and leaves at 10°C . The hot water enters the heat exchanger at 80°C , leaves at 30°C , and flows at a rate of 1.5 kg/s . Determine the effectiveness of this heat exchanger.

Solution

Figure E3.10 shows a sketch of this heat exchanger. In order to determine the effectiveness of this heat exchanger, the thermal capacity rate of each fluid needs to be determined.

**FIGURE E3.10**

Parallel flow magnesium chloride solution - water heat exchanger.

The mass flow rate of the hot fluid (water) is known. In addition, the inlet and outlet temperatures are given. Therefore, the thermal capacity rate of the hot fluid can be found,

$$\dot{C}_h = \dot{m}_h c_{p,h} = \left(1.5 \frac{\text{kg}}{\text{s}} \right) \left(4.1833 \frac{\text{kJ}}{\text{kg} \cdot \text{K}} \right) = 6.275 \frac{\text{kW}}{\text{K}}$$

Appendix B.3
(interpolation required)

The thermal capacity rate of the cold fluid (the magnesium chloride solution) can be found by applying the conservation of energy to the heat exchanger,

$$\begin{aligned} \dot{C}_c (t_{c,out} - t_{c,in}) &= \dot{C}_h (T_{h,in} - T_{h,out}) \\ \dot{C}_c &= \dot{C}_h \frac{(T_{h,in} - T_{h,out})}{(t_{c,out} - t_{c,in})} = \left(6.275 \frac{\text{kW}}{\text{K}} \right) \frac{(80 - 30) \text{K}}{[10 - (-15)] \text{K}} = 12.55 \frac{\text{kW}}{\text{K}} \end{aligned}$$

The outlet temperature in an infinitely large parallel flow heat exchanger can be calculated using Equation 3.44,

$$T_{out,\infty} = \frac{\dot{C}_h T_{h,in} + \dot{C}_c t_{c,in}}{\dot{C}_h + \dot{C}_c} = \frac{\left(6.275 \frac{\text{kW}}{\text{K}} \right) (80^\circ\text{C}) + \left(12.55 \frac{\text{kW}}{\text{K}} \right) (-15^\circ\text{C})}{(6.275 + 12.55) \frac{\text{kW}}{\text{K}}} = 16.67^\circ\text{C}$$

Notice that the units of the thermal capacity rates are given in kW/K and the temperatures are in °C. This may seem confusing since the K and °C scales are different. However, Equation 3.44 is derived from the conservation of energy, Equation 3.43 where temperature *differences* are used. Since temperature differences are the same on the Celsius and Kelvin scales, there is no need to convert the temperatures in Equation 3.44 to the absolute scale. Knowing the maximum outlet temperature, the effectiveness of the parallel flow heat exchanger can be found,

$$\varepsilon_{\text{PF}} = \frac{T_{h,in} - T_{h,out}}{T_{h,in} - T_{out,\infty}} = \frac{(80 - 30)^\circ\text{C}}{(80 - 16.67)^\circ\text{C}} = \underline{\underline{0.7895}}$$

This high value of effectiveness indicates that this is a good heat exchanger for the application.

3.7.3.3 Significance of the Pinch Point Temperature Difference and Effectiveness

Using the PPTD as a known parameter in a thermal energy system is akin to specifying the size of the heat exchanger without actually designing the heat exchanger. The actual

design of the heat exchanger requires a complex analysis that is discussed in detail in Chapter 5. However, knowing the required PPTD allows for the detail design of the heat exchanger to proceed.

The effectiveness is an indicator of how well the heat exchanger is suited for the given application. High values of effectiveness imply that the heat exchanger is functioning closer to the point of maximum theoretical heat transfer. It has also been demonstrated that the effectiveness is related to the PPTD and the size of the heat exchanger (i.e., the heat exchanger area). Therefore, knowledge of the effectiveness from a thermodynamic analysis using Equation 3.32 can ultimately lead to the required heat transfer area. For example, in Chapter 5 it will be shown that the effectiveness of a parallel flow heat exchanger can also be written as,

$$\epsilon_{PF} = \frac{\dot{Q}}{\dot{Q}_{\max}} = \frac{1 - \exp\left[-\frac{UA}{\dot{C}_{\min}}\left(1 + \frac{\dot{C}_{\min}}{\dot{C}_{\max}}\right)\right]}{1 + \frac{\dot{C}_{\min}}{\dot{C}_{\max}}} \quad (3.46)$$

In this equation, UA is the so-called “ UA product” of the heat exchanger where U is the overall heat transfer coefficient, and A is the heat exchanger area. Therefore, if the effectiveness of a parallel flow heat exchanger can be computed using Equation 3.45, then the UA product, and ultimately the area, can be computed using Equation 3.46. The required heat exchange area is critical information in the design of the heat exchanger and complete thermal energy system.

3.8 The Exergy Balance—The Combined Law

Envisioning thermodynamic quantities requires abstract thought. For example, we can physically sense heat, but how can it be quantified? From your previous course(s) in thermodynamics, you learned that heat is a form of energy that is transferred due to a temperature difference. However, heat was not always considered energy. From 1697 to 1703, German chemist Georg Stahl proposed the *phlogiston theory*. Stahl theorized that heat was a fire-like element called *phlogiston*. Phlogiston was contained within substances and was released during combustion which produced the sensation of heat. The phlogiston theory was superseded by the *caloric theory*, developed by French chemist Antoine Lavoisier with a series of papers published from 1768 to 1787. Lavoisier proposed that heat was actually a fluid called *caloric* and it flowed from one substance to another. As caloric entered a substance, it would expand. The caloric theory eventually gave way to the concept of heat as energy.

In 1845, James P. Joule published a paper entitled, “On the Mechanical Equivalent of Heat”. Joule’s work was the foundation for the first law of thermodynamics. From 1850 to 1865 several individuals including Sadi Carnot, William Thomson (Lord Kelvin), William Rankine, and Rudolph Clausius developed the ideas that would eventually become the second law of thermodynamics. In 1865, Clausius proposed a new *transformational property*, entropy, and its relationship to heat as energy. These famous works are the basis of how we understand heat (as energy) in the first and second laws of thermodynamics today.

In 1953, Slovene mechanical engineer Zoran Rant introduced the word “*exergy*” in his Ph.D. dissertation, “Exergy: A Useful Concept”. Rant’s work was based on the earlier works of American engineer J. Willard Gibbs on *available energy* in 1873, the concept of *free energy* developed by German physicist Hermann Helmholtz in 1882, and the idea of the *possibility of doing work* developed by French physicist Louis Gouy in 1889.

This section expands on the concept of *exergy*; its definition and practical application to thermal energy systems analysis and design. As demonstrated by the brief history given above, exergy is a relatively new idea. It is an abstraction, just like energy. However, it is perhaps one of the more practical abstractions that has risen from thermodynamics.

3.8.1 What Is Exergy?

A paraphrase of the first and second laws of thermodynamics is given below.

Energy cannot be created or destroyed [the first law]. Energy can only be transformed. The transformation of energy always happens in such a way that the useful energy content is diminished [the second law].

Exergy (also called *available energy* or *availability*) is the *useful energy* content of a substance. Like energy, exergy is a commodity that is present in all substances. However, the difference between energy and exergy is that exergy can be destroyed in a process. This idea can be demonstrated by considering a natural energy resource, such as coal, oil, or natural gas. Figure 3.13 shows the energy and exergy content of such an energy reserve as a function of time. Notice that the energy content of the resource never changes, even as the reserve is utilized. This is a demonstration of the first law of thermodynamics; energy is conserved. The exergy content of the resource, however, decreases with time as a result of using the resource. Figure 3.13 shows that the exergy content of the resource will reach zero at some time. This must be true because exergy is destroyed in all real-world processes. Figure 3.13 also shows a second exergy curve that reaches the zero axis further in the future. This curve represents the exergy content of the resource with improved designs. This curve represents the exergy content of the resource with improved designs

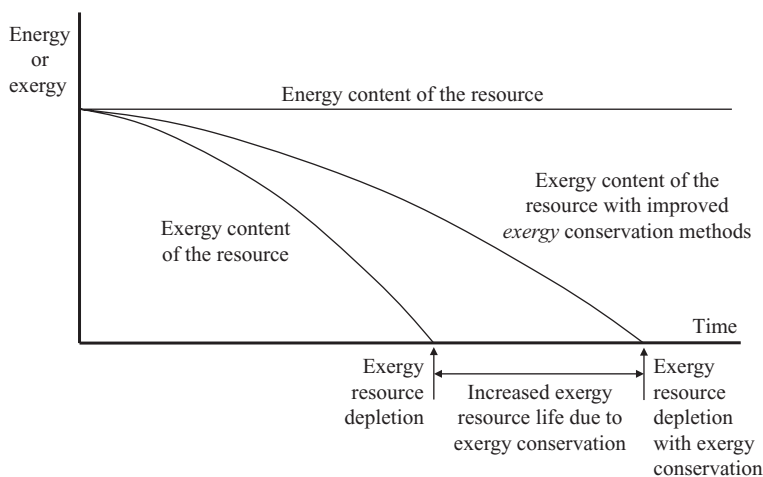


FIGURE 3.13

Energy and exergy content of an energy resource as a function of time.

meant to reduce the exergy destruction. By improving system designs to reduce the exergy destruction, the life of the resource can be extended. This is the *ethical responsibility* of engineers, as referenced in Section 1.6.3. Improving designs to reduce exergy destruction prolongs the life (sustainability) of the natural resource being used. This has a direct relationship to *environmental impact*.

From this discussion, it can be seen that exergy is a commodity. However, it is a commodity that is also destroyed in all real processes. Therefore, it is the responsibility of the engineer to design systems resulting in *exergy conservation*. Notice that the often-heard phrase *energy conservation* is a misnomer. Energy is *automatically* conserved according to the first law of thermodynamics. Engineers strive to conserve *exergy*.

3.8.1.1 The Thermodynamic Definition of Exergy

Exergy is defined as the maximum theoretical work that can be done as a system interacts and achieves equilibrium with its surroundings. The surroundings are often called the *dead state*. At the dead state (specified by P_0, T_0), the substance has no exergy content. From this definition, it can be seen that exergy is analogous to work. Work is the form of energy that we seek in our engineering systems. Work is pure exergy.

3.8.2 The Exergy Balance

Exergy is a quantity that is destroyed in a process by irreversibility. Therefore, an equivalent way to write the general balance Equation 3.2 is,

$$\sum \dot{\Omega}_{in} - \sum \dot{\Omega}_{out} - \dot{\Omega}_{des} = \frac{d\Omega_{sys}}{dt} \quad (3.47)$$

The subscript “des” signifies a destroyed quantity (like exergy). Notice that this term is opposite in sign to a quantity that is generated (like entropy). Making the substitution $\Omega = X$ into Equation 3.47 results in the exergy balance,

$$\sum \dot{X}_{in} - \sum \dot{X}_{out} - \dot{X}_{des} = \frac{dX_{sys}}{dt} \quad (3.48)$$

The variables X or x will be used in this book to specify total or specific exergy, respectively. Subscripts will be used, particularly in the case of specific exergy, x , so it is not confused with quality.

Exergy is carried in and out of a system by energy (heat and work), and by mass flow. Rewriting Equation 3.48 to reflect this results in,

$$\sum (\dot{X}_{in} - \dot{X}_{out})_Q + \sum (\dot{X}_{in} - \dot{X}_{out})_W + \sum (\dot{m}_{in} x_{f,in} - \dot{m}_{out} x_{f,out}) - \dot{X}_{des} = \frac{dX_{sys}}{dt} \quad (3.49)$$

To apply Equation 3.49 to a system, the exergy terms need to be quantified. The equations that follow in the remainder of this section are presented without derivation. The interested reader is encouraged to consult an undergraduate-level textbook in mechanical engineering thermodynamics for the details of these derivations such as, Moran (2014), Cengel (2011), or Klein (2012).

The exergy transport rate due to heat transfer, the first term on the left-hand side of Equation 3.49, can be written as,

$$\sum (\dot{X}_{in} - \dot{X}_{out})_Q = \sum \left[\dot{Q}_{in} \left(1 - \frac{T_0}{T_b} \right)_{in} - \dot{Q}_{out} \left(1 - \frac{T_0}{T_b} \right)_{out} \right] \quad (3.50)$$

In Equation 3.50, T_b is the system boundary temperature where the heat is being transferred, and T_0 is the dead state temperature.

The exergy transferred to and from the system by work, the second term on the left-hand side of Equation 3.49, is given by,

$$\sum (\dot{X}_{in} - \dot{X}_{out})_W = \sum (\dot{W}_{in} - \dot{W}_{out}) + P_0 \frac{dV}{dt} \quad (3.51)$$

In Equation 3.51, the term $P_0 (dV/dt)$ represents the rate that work that is done on or by the surroundings due to a change in volume of the system over time. If the time derivative of the system volume is negative, then the system is being compressed by the surroundings. This is a “free” source of exergy that can be capitalized upon. If the system is expanding, then the volume derivative is positive. This represents work that is done on the environment and is not useful work. Therefore, it ends up reducing the exergy output in the form of work. In a steady flow scenario or the case where the system volume does not change, the volume derivative vanishes.

The third term on the left-hand side of Equation 3.49 is the net exergy transported by mass as it crosses the system boundary. In this equation, x_f is known as *flow exergy* and it is defined as,

$$x_f = (h - h_0) - T_0(s - s_0) + \frac{V^2}{2} + gz \quad (3.52)$$

The subscripts “0” in Equation 3.52 represent the properties at the dead state, which are defined by P_0 and T_0 .

The fourth term on the left-hand side of Equation 3.49 is the exergy destruction rate. Exergy destruction is related to entropy production. Exergy destruction is also called *irreversibility*. The exergy destruction rate term is given by,

$$\dot{X}_{des} = T_0 \dot{S}_{gen} \quad (3.53)$$

The magnitude of the exergy destruction in a process is of great interest to engineers. Equation 3.53 shows how the abstract concept of entropy generation is used in a very practical sense to design and analyze systems.

If the flow of exergy into and out of a system is unsteady, then there will be storage of exergy in the system. This is represented by the derivative on the right-hand side of Equation 3.49. The exergy of a system is given by,

$$X_{sys} = (U - U_0) - T_0(S - S_0) + P_0(V - V_0) + \frac{V^2}{2} + gz \quad (3.54)$$

Using Equation 3.54, the rate of exergy storage inside the system can be written as,

$$\frac{dX_{sys}}{dt} = \frac{d}{dt} \left[(U - U_0) - T_0(S - S_0) + P_0(V - V_0) + \frac{V^2}{2} + gz \right] \quad (3.55)$$

As with previous equations, the subscript “0” refers to the dead state properties.

Substituting Equations 3.50 through 3.55 into Equation 3.49 would make a very complex equation. Therefore, in exergy analysis, it is easier to start with Equation 3.49 and substitute Equations 3.50 through 3.55 as needed. Fortunately, for most exergy analyses, the resulting exergy balance equation is quite manageable.

In the development of the exergy balance, notice that there are terms that are representative of the first and second laws of thermodynamics. The equations above contain enthalpy and internal energy (first law properties) and entropy (a second law property). This happens because the equations for the exergy balance were derived using a combination of the first and second laws. Therefore, the exergy balance is sometimes known as the *combined law*.

Example 3.11

Steam at 1.6 MPa and 350°C enters a steam turbine at a flow rate of 16 kg/s. The steam leaves the turbine as a saturated vapor at 30°C. The turbine delivers 9 MW of power. The turbine is insulated, but not perfectly. The average temperature of the insulation on the outer surface of the turbine is 70°C. The environment surrounding the turbine can be considered to be the dead state at 25°C, 100 kPa. Figure E3.11 shows this turbine. Determine the exergy destruction rate in the turbine.

Solution

This is the same turbine that was considered in Examples 3.2 and 3.5. In Example 3.2, the turbine was analyzed from a first law point of view. Example 3.5 considered the turbine from a second law perspective. In this example, the performance of the turbine will be considered relative to exergy.

There are several ways to determine the exergy destruction. Perhaps the simplest is to consider Equation 3.53. The entropy generation rate has previously been determined in Example 3.5. Therefore,

$$\dot{X}_{des} = T_0 \dot{S}_{gen} = (25 + 273.15) \text{K} \left(23.39 \frac{\text{kW}}{\text{K}} \right) = \underline{6,974 \text{ kW}}$$

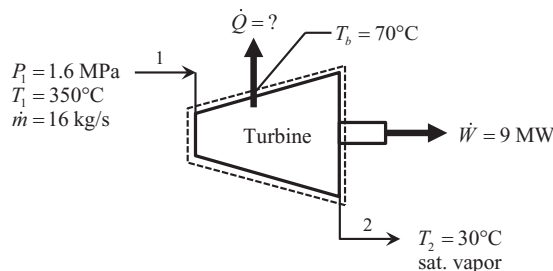


FIGURE E3.11

Steam turbine operating parameters.

Notice that the temperature used in this calculation must be on the *absolute* scale. While this provides the required answer, it really does not reveal much about the turbine. More can be learned by considering application of Equation 3.49 to the turbine,

$$\begin{aligned} -\dot{X}_{out,Q} - \dot{X}_{out,W} + \dot{m}(x_{f1} - x_{f2}) - \dot{X}_{des} &= 0 \\ \therefore \dot{X}_{des} &= \dot{m}(x_{f1} - x_{f2}) - \dot{X}_{out,Q} - \dot{X}_{out,W} \end{aligned}$$

This formulation is particularly informative because each term has significance to how the turbine is performing as shown below,

$$\dot{X}_{des} = \underbrace{\dot{m}(x_{f1} - x_{f2})}_{\text{Net exergy flow input}} - \underbrace{\dot{X}_{out,Q}}_{\text{Exergy loss due to heat}} - \underbrace{\dot{X}_{out,W}}_{\text{Exergy output}}$$

This equation is helpful because it shows the magnitude of each of the exergy components of the turbine; the net incoming exergy, the exergy loss due to heat transfer, the exergy output (power), and the exergy destruction.

The net exergy transfer rate due to mass flow can be written as,

$$\begin{aligned} \dot{m}(x_{f1} - x_{f2}) &= \dot{m} \left[(h_1 - h_0) - T_0(s_1 - s_0) \right] - \left[(h_2 - h_0) - T_0(s_2 - s_0) \right] \\ \dot{m}(x_{f1} - x_{f2}) &= \dot{m} \left[(h_1 - h_2) - T_0(s_1 - s_2) \right] \end{aligned}$$

Using the property values determined in Examples 3.2 and 3.5, the net exergy transfer rate into the turbine is,

$$\begin{aligned} \dot{m}(x_{f1} - x_{f2}) &= \left(16 \frac{\text{kg}}{\text{s}} \right) \left[(3146.0 - 2555.6) \frac{\text{kJ}}{\text{kg}} - (298.15\text{K})(7.0713 - 8.4520) \frac{\text{kJ}}{\text{kg-K}} \right] \\ \dot{m}(x_{f1} - x_{f2}) &= 16,033 \text{ kW} \end{aligned}$$

The rate that exergy is lost from the turbine due to heat transfer is given by,

$$\dot{X}_{out,Q} = \dot{Q} \left(1 - \frac{T_0}{T_b} \right) = (446.4 \text{ kW}) \left[1 - \frac{(25 + 273.15)\text{K}}{(70 + 273.15)\text{K}} \right] = 59 \text{ kW}$$

The heat transfer rate from the turbine was determined in Example 3.5. The exergy transfer rate from the turbine is the power delivered,

$$\dot{X}_{out,W} = \dot{W} = 9,000 \text{ kW}$$

Therefore, the exergy destruction rate in the turbine is,

$$\dot{X}_{des} = \dot{m}(x_{f1} - x_{f2}) - \dot{X}_{out,Q} - \dot{X}_{out,W} = (16,033 - 59 - 9,000) \text{ kW} = \underline{6,974 \text{ kW}}$$

This is the same result that was found using the simpler equation, $\dot{X}_{des} = T_0 \dot{S}_{gen}$. However, this result is more meaningful because the relationship between the net exergy input and the exergy destruction is clearly seen. Due to the steam flow entering and leaving,

the turbine is provided with 16,033 kW of flow exergy. This exergy rate is converted to power (9,000 kW), an exergy transfer due to heat (59 kW), and the remainder is destroyed (6,974 kW).

As demonstrated in Example 3.11, the exergy destruction rate is more physically meaningful than the entropy generation rate. For example, the entropy production rate of the turbine in Example 3.5 is 23.39 kW/K. But, what does this really mean? Unfortunately, the only thing this indicates is that there are irreversibilities in the turbine (the entropy generation rate is positive). However, the number, by itself, does not tell us how bad the irreversibility is. On the other hand, the full exergy analysis of the turbine clearly reveals how much exergy is input to the turbine, and how it is distributed. The exergy analysis gives a much clearer and meaningful picture to how the turbine is operating.

3.8.3 Exergy Accounting and Exergy Flow Diagrams

Performing a full exergy analysis of a device as was done in Example 3.11 reveals much information about how the device is utilizing its exergy *resource* to complete its exergy *task*. Exergy accounting is a way to summarize the results of a full exergy analysis. Consider the turbine that was analyzed in Example 3.11. A full exergy accounting of the turbine is given in Table 3.2.

This table indicates that 56.1% of the incoming exergy to the turbine is ultimately delivered as power. Only 0.4% of the incoming exergy is lost due to the heat transfer. The remaining 43.5% of the exergy is destroyed.

Another useful way to visualize the flow of exergy through the turbine is to construct an *exergy flow diagram* based on the results of a full exergy analysis. An exergy flow diagram for the turbine analyzed in Example 3.11 is shown in Figure 3.14. The block arrows in the

TABLE 3.2

Exergy Accounting for the Turbine of Example 3.11

Exergy Input	Value	Percent of Total
Net exergy flow rate provided by the steam	16,033 kW	100%
Exergy Outputs	Value	Percent of Total Input
Power	9,000 kW	56.1%
Heat loss	59 kW	0.4%
Exergy Destruction (Input–Output)	6,974 kW	43.5%

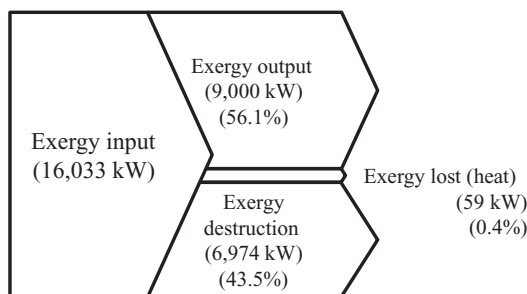


FIGURE 3.14

Exergy flow diagram for the turbine analyzed in Example 3.11.

exergy flow diagram are drawn somewhat to scale. When this is done, a graphical depiction of what happens to the incoming exergy can be easily visualized.

3.8.4 Exergetic Efficiencies of Flow Devices

A full exergy accounting of a flow device allows for the determination of the *exergetic efficiency* (sometimes called the *second law efficiency*) of the device. The exergetic efficiency of a flow device is given by,

$$\eta_x = \frac{\text{Exergy output (exergy task)}}{\text{Exergy input (exergy resource)}} \quad (3.56)$$

This indicates that the exergetic efficiency is a task/resource index. It indicates how well the device is utilizing its exergy resource to perform the required task.

3.8.4.1 Turbines

As seen in Example 3.11, the exergy output of a turbine is the power delivered. The exergy input to the turbine is the net exergy flow rate. Therefore, the exergetic efficiency of a turbine can be expressed as,

$$\eta_{x,t} = \frac{\dot{W}_{out}}{\dot{m}(x_{f,in} - x_{f,out})} \quad (3.57)$$

For the turbine analyzed in Example 3.11, the exergetic efficiency is 56.1%.

3.8.4.2 Compressors, Pumps, and Fans

The exergy output of a device that moves a fluid (a compressor, pump, or fan) is to increase the flow exergy of the fluid passing through it. The exergy input to the device is power. Therefore, the exergetic efficiency of a compressor, pump, or fan can be expressed as,

$$\eta_{x,m} = \frac{\dot{m}(x_{f,out} - x_{f,in})}{\dot{W}_{in}} \quad (3.58)$$

The subscript “*m*” is used to indicate a device that moves a fluid.

3.8.4.3 Heat Exchangers

Heat exchanger performance can also be quantified with an exergetic efficiency. Consider the case where hot and cold fluids do not mix in the heat exchanger. As the hot fluid passes through the heat exchanger, it gives up its exergy to the cold fluid. Therefore, the exergy input to the heat exchanger is the exergy decrease of the hot fluid. The exergy output can be thought of as the exergy increase of the cold fluid. Therefore, a suitable expression for the exergetic efficiency of a heat exchanger where the fluids are unmixed can be written as,

$$\eta_{x,HX} = \frac{\dot{m}_c(x_{f,out} - x_{f,in})_c}{\dot{m}_h(x_{f,in} - x_{f,out})_h} \quad (3.59)$$

Recall that there is no expression for the isentropic efficiency of a heat exchanger (Section 3.7.3). This is because the fluids in a heat exchanger always exist at different temperatures. Even if one could envision frictionless flow, there is still a temperature difference which makes the heat exchanger irreversible. This shows the very practical nature of the exergy analysis compared to second law (entropy) analysis. Given a device, one can always devise its exergy “task” and identify its exergy “resource.”

Example 3.12

Water enters the tubes of a boiler in a power plant at 1200 psia, 120°F, as shown in Figure E3.12. Steam exits the tubes at 1400°F with virtually no drop in pressure. The water is boiled by combustion gases entering the boiler at 2300°F, 1 atm. The combustion gases flow through the boiler with a negligible pressure drop. The mass flow rates of the steam and combustion gases are 1.4×10^6 lbm/hr and 1.13×10^7 lbm/hr, respectively. The combustion gases can be modeled as air. The flows are steady and there is no stray heat transfer from the boiler. The dead state temperature can be taken as 70°F. Determine,

- The exergy destruction rate in the boiler
- The exergetic efficiency of the boiler

Solution

Figure E3.12 shows a system boundary drawn around the boiler. A full exergy analysis will be done on the boiler which will facilitate the calculation of the exergy destruction rate and the exergetic efficiency.

The exergy balance, Equation 3.49, applied to the boiler results in the following,

$$(\dot{m}_w x_{f1} + \dot{m}_g x_{f3}) - (\dot{m}_w x_{f2} + \dot{m}_g x_{f4}) - \dot{X}_{des} = 0$$

$$\dot{X}_{des} = \dot{m}_g (x_{f3} - x_{f4}) - \dot{m}_w (x_{f2} - x_{f1})$$

The flow exergies can be expanded using Equation 3.52, which results in,

$$\dot{X}_{des} = \dot{m}_g [(h_3 - h_4) - T_0(s_3 - s_4)] - \dot{m}_w [(h_2 - h_1) - T_0(s_2 - s_1)]$$

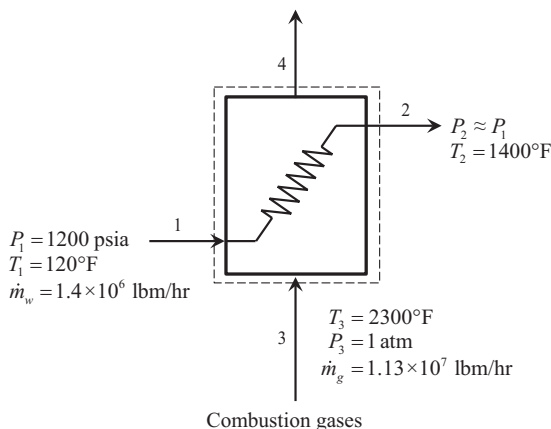


FIGURE E3.12

Steam boiler operating parameters.

While this equation is easier to work with, the flow exergy values will be determined in this example to demonstrate how flow exergy values are calculated. Using this approach is helpful to demonstrate what happens to the flow exergy of each fluid as it passes through the boiler.

States 1, 2, and 3 can be identified since two independent, intensive properties are known. The resulting properties are shown below.

$P_1 = 14.696 \text{ psia}$	$P_2 = 1200 \text{ psia}$	$P_3 = 14.696 \text{ psia}$
$T_1 = 120^\circ\text{F}$	$T_2 = 1400^\circ\text{F}$	$T_3 = 2300^\circ\text{F}$
$h_1 = 91.131 \text{ Btu/lbm}$	$h_2 = 1731.7 \text{ Btu/lbm}$	$h_3 = 721.43 \text{ Btu/lbm}$
$s_1 = 0.16388 \text{ Btu/lbm-R}$	$s_2 = 1.77096 \text{ Btu/lbm-R}$	$s_3 = 2.06441 \text{ Btu/lbm-R}$

State 4 cannot be identified without a thermodynamic analysis of the boiler. Application of the conservation of energy equation to the boiler gives,

$$\begin{aligned}
 (\dot{m}_w h_1 + \dot{m}_g h_3) - (\dot{m}_w h_2 + \dot{m}_g h_4) &= 0 \\
 \dot{m}_g (h_3 - h_4) &= \dot{m}_w (h_2 - h_1) \\
 \therefore h_4 &= h_3 - \frac{\dot{m}_w}{\dot{m}_g} (h_2 - h_1) \\
 h_4 &= 721.43 \frac{\text{Btu}}{\text{lbm}} - \frac{1.4 \times 10^6 \text{ lbm/hr}}{1.13 \times 10^7 \text{ lbm/hr}} (1731.7 - 91.131) \frac{\text{Btu}}{\text{lbm}} \\
 h_4 &= 518.16 \frac{\text{Btu}}{\text{lbm}}
 \end{aligned}$$

State 4 is now identified by enthalpy and pressure. Therefore, the entropy at State 4 can be found,

$$\begin{aligned}
 P_4 &= 14.696 \text{ psia} \\
 h_4 &= 518.16 \text{ Btu/lbm} \\
 s_4 &= 1.97928 \text{ Btu/lbm-R}
 \end{aligned}$$

In order to compute the flow exergy values, the dead state enthalpy and entropy of each fluid must be found. The dead state pressure and temperature are known. The resulting dead state enthalpy and entropy values are given in Table E3.12. The flow exergy values can now be computed using Equation 3.52,

$$\begin{aligned}
 x_f &= (h - h_0) - T_0 (s - s_0) \\
 x_{f1} &= (91.131 - 38.141) \frac{\text{Btu}}{\text{lbm}} - (70 + 459.67)^\circ\text{R} (0.16388 - 0.074639) \frac{\text{Btu}}{\text{lbm-R}} = 5.7250 \frac{\text{Btu}}{\text{lbm}} \\
 x_{f2} &= (1731.7 - 38.141) \frac{\text{Btu}}{\text{lbm}} - (70 + 459.67)^\circ\text{R} (1.77096 - 0.074639) \frac{\text{Btu}}{\text{lbm-R}} = 795.12 \frac{\text{Btu}}{\text{lbm}} \\
 x_{f3} &= (721.43 - 126.71) \frac{\text{Btu}}{\text{lbm}} - (70 + 459.67)^\circ\text{R} (2.06441 - 1.63650) \frac{\text{Btu}}{\text{lbm-R}} = 368.07 \frac{\text{Btu}}{\text{lbm}} \\
 x_{f4} &= (518.16 - 126.71) \frac{\text{Btu}}{\text{lbm}} - (70 + 459.67)^\circ\text{R} (1.97928 - 1.63650) \frac{\text{Btu}}{\text{lbm-R}} = 209.89 \frac{\text{Btu}}{\text{lbm}}
 \end{aligned}$$

TABLE E3.12

Dead State Properties of Water and Air

Water	Air
$P_0 = 14.696$ psia	$P_0 = 14.696$ psia
$T_0 = 70$ F	$T_0 = 70$ F
$h_{0w} = 38.141$ Btu/lbm	$h_{0a} = 126.71$ Btu/lbm
$s_{0w} = 0.074639$ Btu/lbm-R	$s_{0a} = 1.63650$ Btu/lbm-R

Therefore, the exergy destruction rate in the boiler is,

$$\begin{aligned}\dot{X}_{des} &= \dot{m}_g(x_{f3} - x_{f4}) - \dot{m}_w(x_{f2} - x_{f1}) \\ \dot{X}_{des} &= \left(1.13 \times 10^7 \frac{\text{lbm}}{\text{h}}\right)(368.07 - 209.89) \frac{\text{Btu}}{\text{lbm}} - \left(1.4 \times 10^6 \frac{\text{lbm}}{\text{h}}\right)(795.12 - 5.7250) \frac{\text{Btu}}{\text{lbm}} \\ \dot{X}_{des} &= 6.822 \times 10^8 \frac{\text{Btu}}{\text{h}}\end{aligned}$$

The exergetic efficiency of the boiler is determined from Equation 3.59,

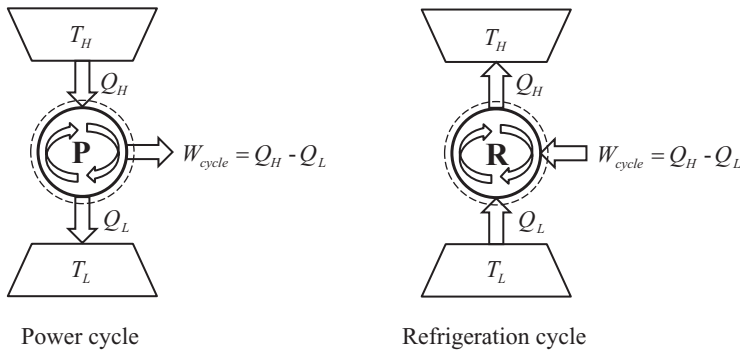
$$\begin{aligned}\eta_{x,\text{HX}} &= \frac{\dot{X}_c}{\dot{X}_h} = \frac{\dot{m}_w(x_{f2} - x_{f1})}{\dot{m}_g(x_{f3} - x_{f4})} \\ \eta_{x,\text{HX}} &= \frac{\left(1.4 \times 10^6 \frac{\text{lbm}}{\text{h}}\right)(795.12 - 5.7250) \frac{\text{Btu}}{\text{lbm}}}{\left(1.13 \times 10^7 \frac{\text{lbm}}{\text{h}}\right)(368.07 - 209.89) \frac{\text{Btu}}{\text{lbm}}} = \underline{0.6183 = 61.83\%}\end{aligned}$$

This result indicates the boiler utilizes nearly 62% of the incoming exergy from the combustion gases to boil the water. The remaining 28% of the exergy is destroyed in the process. This exergy destruction is related to the large temperature difference between the water and combustion gases in the boiler.

3.9 Energy and Exergy Analysis of Thermal Energy Cycles

Components and devices are often connected together, forming a cycle. There are many different cycles. However, they can be generally categorized as cycles that (1) deliver power (e.g., a steam power cycle), or (2) transport energy (e.g., a heat pump cycle). The individual components of the cycle can be analyzed using any of the conservation or balance laws discussed in Sections 3.4 through 3.8. In addition to component performance, we are also interested in how the *cycle* performs.

Figure 3.15 shows a sketch of power and refrigeration cycles. The actual cycle is inside of the circle labeled either “P” (for power cycle) or “R” (for refrigeration cycle). The cycle can take on many different configurations. Figure 3.15 indicates that the cycle must communicate thermally with energy reservoirs. In the case of a power cycle, the energy reservoirs are required by the second law of thermodynamics. In the case of a refrigeration

**FIGURE 3.15**

Sketches of a power cycle and a refrigeration cycle.

cycle, the second law requires a work input to move heat from a low temperature to a high temperature.

Figure 3.15 also shows a system boundary drawn around the cycle. These systems allow for the application of the conservation and balance laws without knowing anything about the details of the cycle. For example, the conservation of energy equation can be used to determine the work output of the power cycle and the work input to the refrigeration cycle as a function of the heat transfer interactions with the thermal energy reservoirs.

3.9.1 Cycle Energy Performance Parameters

There are many ways to quantify the performance of a thermodynamic cycle. The most common cycle performance index is the *thermal efficiency*. The thermal efficiency of any cycle is defined as,

$$\eta_{th} = \frac{\text{energy sought}}{\text{energy that costs}} \quad (3.60)$$

As seen from Equation 3.60, the thermal efficiency is an *energy*-based efficiency. Applying this equation to the power cycle shown in Figure 3.15 results in,

$$\eta_{th, power} = \frac{W_{cycle}}{Q_H} \quad (3.61)$$

Power delivery cycles, particularly vapor power cycles, often use the *heat rate* as a performance index. The heat rate, HR , of a power cycle is defined as,

$$HR = \frac{\text{heat transfer rate into the cycle}}{\text{net power delivery from the cycle (kW)}} = \frac{\dot{Q}_H}{\dot{W}_{cycle}} [=] \frac{\text{energy/hr}}{\text{kW}} = \frac{\text{energy}}{\text{kWh}} \quad (3.62)$$

At first glance, the heat rate appears to be the reciprocal of the thermal efficiency of the power cycle. This is true, except that it is *dimensional*. Notice that it carries units of energy/kWh. The energy can be expressed in terms of Btu or an SI equivalent (e.g., kJ). Power plant

engineers prefer to use the heat rate because it gives them a better sense of how much fuel is required (energy) per kWh of energy delivered by the plant.

Example 3.13

The thermal efficiency of a steam power cycle is determined to be 36%. Determine the heat rate of the cycle.

Solution

The heat rate is simply the reciprocal of the thermal efficiency, modified by the proper unit conversion to result in energy/kWh. In the SI system, the heat rate of this cycle is,

$$HR_{SI} = \frac{1}{0.36} \left(\frac{\text{kJ}}{\text{kW}\cdot\text{s}} \right) \left(\frac{3600 \text{ s}}{\text{hr}} \right) = \underline{10,000 \frac{\text{kJ}}{\text{kWh}}}$$

In the English (IP) unit system,

$$HR_{IP} = \frac{1}{0.36} \left(\frac{3412.1 \text{ Btu}}{\text{kW}\cdot\text{hr}} \right) = \underline{9,478 \frac{\text{Btu}}{\text{kWh}}}$$

As shown, the calculated heat rates reveal how much energy (kJ or Btu) must be used to deliver a single kWh of energy.

For the refrigeration cycle shown in Figure 3.15, the “energy that costs” is the work input to the cycle. However, the “energy sought” depends on what the refrigeration cycle is being used for. If the goal is to keep a space cool, then the energy sought is the low temperature heat transfer, Q_L . Then the thermal efficiency of the cycle is,

$$\eta_{th, \text{refrig}} = \frac{Q_L}{W_{cycle}} \equiv COP_C \quad (3.63)$$

The thermal efficiency of a refrigeration cycle is more commonly expressed in decimal form, rather than a percent. In this case, it is called the *cooling coefficient of performance* (COP_C). The reason for this is that the thermal efficiency of a refrigeration cycle is often in excess of 100%. It is not uncommon to see refrigeration systems operating with thermal efficiencies of 200% to 400% (which translates to a COP_C between 2.0 and 4.0).

An alternative performance parameter used by the U.S. refrigeration industry is the *energy efficiency ratio* (EER). The energy efficiency ratio of a refrigeration cycle is defined as,

$$EER = \frac{\text{refrigeration rate (capacity)}}{\text{power input}} = \frac{\dot{Q}_L}{\dot{W}_{cycle}} [=] \frac{\text{energy/hr}}{\text{W}} = \frac{\text{Btu}}{\text{W}\cdot\text{hr}} \quad (3.64)$$

Comparing Equations 3.63 and 3.64 reveals that the only difference between the COP_C and the EER is that the COP_C is dimensionless, whereas the EER has units. Most often, the refrigeration rate (also known as the *capacity*) of the cycle is expressed in Btu/hr. Higher values of EER correspond to less operating cost.

Example 3.14

A small window air-conditioner has an Energy Star label that indicates it has an *EER* of 11.6 with a power input of 800 W. Determine the cooling capacity of the air conditioner (Btu/hr) and its cooling coefficient of performance.

Solution

The cooling capacity of the air conditioner can be calculated using Equation 3.64,

$$EER = \frac{\dot{Q}_L}{\dot{W}_{cycle}} \quad \therefore \quad \dot{Q}_L = \dot{W}_{cycle} (EER) = (800 \text{ W}) \left(11.6 \frac{\text{Btu}}{\text{W-hr}} \right) = \underline{9,280 \frac{\text{Btu}}{\text{hr}}}$$

The cooling coefficient of performance can be found by using the proper conversion factor,

$$COP_C = \left(11.6 \frac{\text{Btu}}{\text{W-hr}} \right) \left(\frac{\text{W-hr}}{3.4121 \text{ Btu}} \right) = \underline{3.40}$$

Although a misnomer, this air conditioner would probably be marketed as a 9,000 Btu unit.

It is possible to use a refrigeration cycle to provide heating. In this case, the energy sought is Q_H (refer to Figure 3.15). This type of cycle is called a *heat pump* cycle. The heat pump cycle operates in the same cycle as the refrigeration cycle. The only difference is that the heat rejected to the high temperature reservoir is the energy sought. Therefore, the thermal efficiency of a heat pump cycle is given by,

$$\eta_{th,hp} = \frac{Q_H}{W_{cycle}} \equiv COP_H \quad (3.65)$$

As with the refrigeration cycle, the thermal efficiency of the heat pump cycle is often greater than 100%. Therefore, the *heating coefficient of performance* (COP_H) is commonly used rather than the thermal efficiency. As with the refrigeration cycle, the COP_H is the decimal form of the thermal efficiency.

3.9.1.1 Maximum Thermal Efficiency of a Cycle

Refer, once again to the power cycle shown in Figure 3.15. The work delivered by the cycle is given by,

$$W_{cycle} = Q_H - Q_L \quad (3.66)$$

Substituting this into the power cycle thermal efficiency Equation 3.61 and simplifying results in,

$$\eta_{th,power} = 1 - \frac{Q_L}{Q_H} \quad (3.67)$$

Equation 3.67 shows that the thermal efficiency of a power cycle can *never* reach 100%, even in an ideal scenario. This is because Q_L must always be present due to the second law of thermodynamics. When efficiency is expressed in terms of a percent, we tend to automatically assume that 100% is the best possible efficiency. However, as demonstrated, this is not true for the power cycle.

A similar conclusion can be drawn for the refrigeration cycle shown in Figure 3.15. Substituting the expression for the cycle work into the cooling coefficient of performance equation and simplifying gives,

$$COP_C = \frac{Q_L}{Q_H - Q_L} = \frac{1}{Q_H/Q_L - 1} \quad (3.68)$$

Likewise, the heating coefficient performance of the cycle can be expressed as,

$$COP_H = \frac{Q_H}{Q_H - Q_L} = \frac{1}{1 - Q_L/Q_H} \quad (3.69)$$

Equations 3.68 and 3.69 indicate that there is really *no bound* on the COP_C and COP_H . They depend on the ratio of the heat transferred to/from each thermal reservoir. In fact, they can be (and often are) in excess of 1.0.

The second law pioneers, Sadi Carnot, William Thomson (Lord Kelvin), and William Rankine helped solve the problem of the maximum thermal efficiency of a cycle. Carnot proposed that the maximum thermal efficiency of a cycle occurs when all processes are *reversible*. Concurrently, Kelvin and Rankine stated that for a reversible cycle, the ratio of the heat transfers is equivalent to the ratio of the *absolute temperatures* of the thermal reservoirs,

$$\left(\frac{Q_H}{Q_L} \right)_{rev} = \frac{T_H}{T_L} \quad (3.70)$$

Expressions for the maximum thermal efficiency of a cycle can now be developed by substituting Equation 3.70 into Equations 3.67, 3.68, and 3.69. The resulting equations are known as *Carnot efficiency* expressions. For a power cycle, the Carnot efficiency is given by,

$$\eta_{th,Carnot} = 1 - \frac{T_L}{T_H} \quad (3.71)$$

Likewise, the Carnot cooling coefficient of performance can be written as,

$$COP_{C,Carnot} = \frac{1}{T_H/T_L - 1} \quad (3.72)$$

For the heat pump cycle, the Carnot heating coefficient of performance is given by,

$$COP_{H,Carnot} = \frac{1}{1 - T_L/T_H} \quad (3.73)$$

Example 3.15

Ocean Thermal Energy Conversion (OTEC) technology exploits the temperature gradient in the ocean to drive a power cycle. Consider a case where the warm surface waters are at a temperature of 28°C. The low temperature reservoir for the power cycle is located at a depth of 500 ft, where the water temperature is 10°C. During normal operation, the power cycle is delivering 50 MW of power, while transferring 1600 MW of heat to the low temperature reservoir. Determine the thermal efficiency of this OTEC power cycle. How does this compare with the maximum thermal efficiency of the cycle?

Solution

A sketch of the cycle is shown in Figure E3.15. The thermal efficiency of the power cycle is given by Equation 3.61,

$$\eta_{th, power} = \frac{W_{cycle}}{Q_H}$$

The conservation of energy equation applied to the system boundary surrounding the cycle allows for the calculation of the heat transfer rate from the high temperature reservoir,

$$\dot{Q}_H = \dot{W}_{cycle} + \dot{Q}_L = (50 + 1600)\text{MW} = 1650 \text{ MW}$$

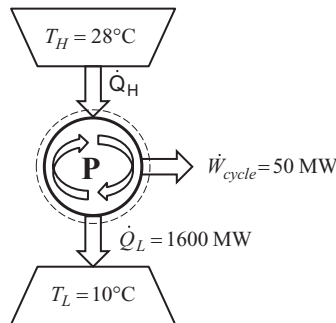
Therefore, the thermal efficiency of the cycle is,

$$\eta_{th, power} = \frac{50 \text{ MW}}{1650 \text{ MW}} = 0.0303 = \underline{\underline{3.03\%}}$$

The maximum thermal efficiency of the power cycle is the Carnot efficiency given by Equation 3.71,

$$\eta_{th, Carnot} = 1 - \frac{T_L}{T_H} = 1 - \frac{(10 + 273.15)\text{K}}{(28 + 273.15)\text{K}} = 0.0598 = \underline{\underline{5.98\%}}$$

This example demonstrates the problem with the “100% is best” thinking. The calculated thermal efficiency of 3.03% seems dismal until it is realized that the best possible efficiency for a cycle of this type under the conditions given is 5.98%.

**FIGURE E3.15**

An OTEC cycle operating between two temperature reservoirs.

3.9.2 Exergetic Cycle Efficiency

The use of the cycle thermal efficiency is well understood. However, Section 3.9.1 demonstrated that the maximum value of the thermal efficiency is not 100%, but rather the Carnot efficiency. The concept of exergy and the *exergetic efficiency* provides an alternate framework for determining the performance of a cycle.

The exergetic efficiency of a cycle is defined in the same way that it was for a device, Equation 3.56, which is repeated below.

$$\eta_x = \frac{\text{Exergy output (exergy task)}}{\text{Exergy input (exergy resource)}} \quad (3.74)$$

3.9.2.1 Power Cycles

Consider a power cycle operating between two thermal reservoirs as shown in Figure 3.16. This figure indicates that the low temperature reservoir is at the dead state temperature. If the dead state is considered the atmosphere, then this depiction of the power cycle is accurate; the ultimate low temperature sink is the atmosphere.

An alternative expression for the exergetic efficiency can be developed based on Figure 3.16. For a power cycle, the exergy task is the delivery of the cycle work. The exergy input is the exergy associated with the heat transfer from the high-temperature reservoir. Therefore, the exergetic efficiency of a power cycle can be written as,

$$\eta_{x, \text{power}} = \frac{W_{\text{cycle}}}{X_{Q_H}} \quad (3.75)$$

Application of the exergy balance Equation 3.49 to the system boundary that encloses the complete power cycle results in,

$$X_{Q_H} - X_{Q_0} - X_{W_{\text{cycle}}} - X_{\text{des}} = 0 \quad (3.76)$$

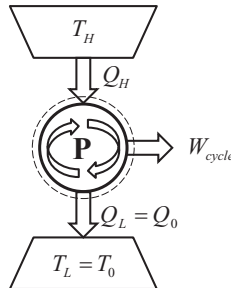


FIGURE 3.16

A power cycle operating between T_H and the dead state.

From Equation 3.50, the exergy associated with a heat transfer is given by,

$$X_Q = Q \left(1 - \frac{T_0}{T_b} \right) \quad (3.77)$$

The heat being transferred at the dead state occurs at a boundary temperature of T_0 . Therefore, the exergy associated with this heat transfer must be zero,

$$X_{Q_0} = Q_0 \left(1 - \frac{T_0}{T_0} \right) = 0 \quad (3.78)$$

Substituting Equation 3.78 into 3.76 and solving for the cycle work gives,

$$X_{W_{cycle}} = W_{cycle} = X_{Q_H} - X_{des} \quad (3.79)$$

Substitution of Equation 3.79 into 3.75 results in,

$$\eta_{x,power} = 1 - \frac{X_{des}}{X_{Q_H}} \quad (3.80)$$

Equation 3.80 is an important equation because it demonstrates that the maximum exergetic efficiency of a power cycle *is* 100% for the case of a reversible cycle with no exergy destruction. Unlike the thermal efficiency which is bounded by the Carnot efficiency at the upper limit, the exergetic efficiency *does* reach a maximum of 100% in the case of an ideal cycle with no irreversibility.

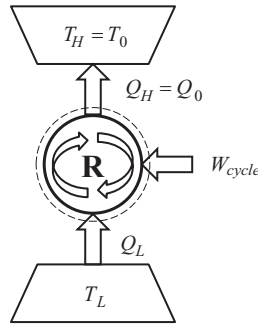
The exergy content of the heat transfer from the high temperature reservoir relative to the dead state at T_0 is,

$$X_{Q_H} = Q_H \left(1 - \frac{T_0}{T_H} \right) \quad (3.81)$$

Substitution of Equation 3.81 into Equation 3.75 results in,

$$\eta_{x,power} = \frac{W_{cycle}}{Q_H \left(1 - \frac{T_0}{T_H} \right)} = \frac{\eta_{th,power}}{\left(1 - \frac{T_0}{T_H} \right)} = \frac{\eta_{th,power}}{\eta_{th,Carnot}} \quad (3.82)$$

Equation 3.82 indicates that the exergetic efficiency of a power cycle operating between T_H and T_0 is directly proportional to the thermal efficiency and inversely proportional to the Carnot efficiency. In addition, since the Carnot efficiency of a power cycle is less than 1, the exergetic efficiency of a power cycle must be larger than the thermal efficiency.

**FIGURE 3.17**

A refrigeration cycle operating between T_L and the dead state.

3.9.2.2 Refrigeration and Heat Pump Cycles

Consider a refrigeration cycle operating between a low temperature source, T_L , and the dead state, T_0 , as the sink. This cycle is shown in Figure 3.17. The exergetic efficiency of this cycle can be determined by applying Equation 3.74,

$$\eta_{x,refrig} = \frac{-X_{Q_L}}{W_{cycle}} \quad (3.83)$$

A negative sign must be used in the numerator of Equation 3.83 because the exergy “output” defined in Equation 3.74 is really an input to the refrigeration cycle.

The exergy balance applied to the system boundary surrounding the cycle shown in Figure 3.17 results in,

$$X_{Q_L} + X_{W_{cycle}} - X_{des} = 0 \quad (3.84)$$

Solving Equation 3.84 for the exergy transferred due to Q_L and substituting into Equation 3.83 reveals the following,

$$\eta_{x,refrig} = 1 - \frac{X_{des}}{W_{cycle}} \quad (3.85)$$

Similar to what was seen for the power cycle, Equation 3.85 indicates that the exergetic efficiency of a refrigeration cycle has an upper limit of 100% in the case of a completely reversible cycle with no exergy destruction.

The exergy associated with the heat transfer from the low temperature sink is given by,

$$X_{Q_L} = Q_L \left(1 - \frac{T_0}{T_L} \right) \quad (3.86)$$

Substituting Equation 3.86 into Equation 3.83 results in,

$$\eta_{x,refrig} = \frac{-Q_L \left(1 - \frac{T_0}{T_L} \right)}{W_{cycle}} = \frac{Q_L}{W_{cycle}} \left(\frac{T_0}{T_L} - 1 \right) = \frac{COP_C}{COP_{C,Carnot}} \quad (3.87)$$

Following similar thinking, the exergetic efficiency of a heat pump cycle can also be developed. The result, shown in Equation 3.88, is left as an exercise for the reader.

$$\eta_{x, hp} = \frac{Q_H}{W_{cycle}} \left(1 - \frac{T_0}{T_H} \right) = \frac{COP_H}{COP_{H, Carnot}} \quad (3.88)$$

3.9.2.3 Significance of the Exergetic Cycle Efficiency

As demonstrated in Sections 3.9.2.1 and 3.9.2.2, the exergetic efficiency of any cycle is always bounded by 0 and 1 (0 to 100%). This makes the exergetic cycle efficiency a much more intuitive index for cycle performance compared to the thermal efficiency. This fact, coupled with the definition of the exergetic cycle efficiency, Equation 3.74, demonstrates the task/resource nature of the exergetic efficiency. High values of exergetic efficiency indicate that the exergy resource is well matched for the exergy task the cycle is providing.

Example 3.16

Two refrigeration systems are being considered for a cold storage application; a standard vapor compression refrigeration system and an absorption refrigeration system. In both cases, the cold space must be maintained at -5°C . To maintain this temperature, heat must be removed from the cold space at a rate of 35 kW. The vapor compression system requires an electrical input of 10 kW to accomplish the refrigeration. The absorption refrigeration system utilizes a 58 kW heat input at 50°C to drive the cycle instead of electricity. Both cycles sink to the atmosphere, which can be considered the dead state, at 22°C . Determine the cooling coefficient of performance and exergetic efficiency of each refrigeration cycle.

Solution

A sketch of the two refrigeration cycles is shown in Figure E3.16. For the vapor compression system, the cooling coefficient of performance is given by,

$$COP_{C, vap} = \frac{\dot{Q}_L}{\dot{W}_{cycle}} = \frac{35 \text{ kW}}{10 \text{ kW}} = 3.50$$

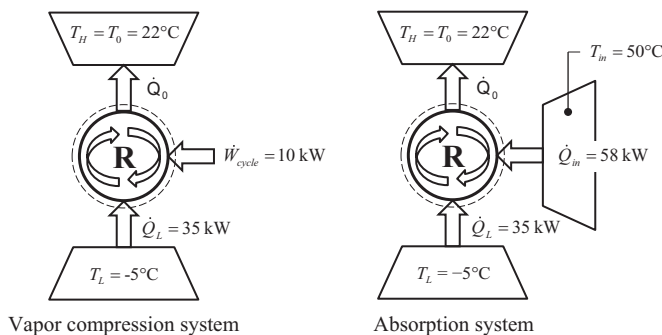


FIGURE E3.16

Two refrigeration cycles that provide 35 kW of refrigeration capacity.

The energy input to the absorption cycle is heat. Therefore, the cooling coefficient of performance is determined by,

$$COP_{C,abs} = \frac{\dot{Q}_L}{\dot{Q}_{in}} = \frac{35 \text{ kW}}{58 \text{ kW}} = 0.60$$

The calculated values of the COP_C for each cycle indicate that the vapor compression cycle is performing better, relative to energy. The higher COP_C of the vapor compression cycle indicates that more refrigeration can be accomplished per kW of energy input compared to the absorption cycle.

The exergetic efficiency of the vapor compression cycle can be found using Equation 3.87,

$$\eta_{x,vap} = \frac{\dot{Q}_L}{\dot{W}_{cycle}} \left(\frac{T_0}{T_L} - 1 \right) = COP_C \left(\frac{T_0}{T_L} - 1 \right) = (3.5) \left[\frac{(22 + 273.15) \text{ K}}{(-5 + 273.15) \text{ K}} - 1 \right] = 0.352 = \underline{35.2\%}$$

The exergetic efficiency of the heat-driven absorption cycle can be derived from Equation 3.74 and is given by,

$$\eta_{x,abs} = \frac{-\dot{X}_{\dot{Q}_L}}{\dot{X}_{\dot{Q}_{in}}} = \frac{\dot{Q}_L \left(\frac{T_0}{T_L} - 1 \right)}{\dot{Q}_{in} \left(1 - \frac{T_0}{T_{in}} \right)} = COP_{C,abs} \left(\frac{\frac{T_0}{T_L} - 1}{1 - \frac{T_0}{T_{in}}} \right) = 0.60 \left[\frac{\left[\frac{(22 + 273.15) \text{ K}}{(-5 + 273.15) \text{ K}} - 1 \right]}{\left[1 - \frac{(22 + 273.15) \text{ K}}{(50 + 273.15) \text{ K}} \right]} \right] = \underline{69.7\%}$$

While the vapor compression cycle is the better cycle at transporting and utilizing *energy*, it is the absorption cycle that is almost twice as efficient at utilizing the *exergy* input to achieve the refrigeration task. In this section, the exergetic efficiency was referred to several times as a task/resource index. The task of the refrigeration cycle (independent of what type it is) is to move heat, \dot{Q}_L . With the vapor compression system, this is accomplished with work, \dot{W}_{cycle} . With the absorption system, the cooling is accomplished with a heat input, \dot{Q}_{in} . The low value of exergetic efficiency for the vapor compression cycle indicates that the exergy input (work) is not well matched to the exergy output (heat). On the other hand, the exergetic efficiency of the absorption system is much higher because the exergy input is *heat* and the exergy task is movement of *heat*. Using heat to move heat is a much better exergetic solution than using work to move heat.

3.9.2.4 The Energy/Exergy Conundrum

Example 3.16 reveals an engineering tradeoff between thermal efficiency and exergetic efficiency. Recall that thermal efficiency is the ratio of energy sought to *energy that costs*. Therefore, systems with high thermal efficiency are less expensive to operate. On the other hand, systems with high exergetic efficiency are making the best use of the exergy resource to perform a task. Therefore, designing a thermal system to have a high thermal efficiency is good from the economic point of view, while designing a system to have high exergetic efficiency is good from the environmental (exergy resource) perspective. As demonstrated in Example 3.16, what is good for high thermal efficiency (minimum cost) is not necessarily good for the environment (exergy resource). This is the conundrum consumers and the industry face.

Businesses are in business to make money. Therefore, it seems logical for a business to design systems that maximize thermal efficiency, thereby reducing operating costs. However, what impact does this practice have on the environment? Even if exergy is not a consideration in system designs, it is *still being destroyed* in the system. The problem that industry faces is that designing to maximize exergetic efficiency may not result in a good profit margin to keep the company in business. However, for an industry to gain various certifications, minimum levels of performance must be met. For example, the Energy Star program was created by the United States Environmental Protection Agency in 1992 under authority of the Clean Air Act. The Energy Star program is voluntary, but minimum standards have been established that industries must meet for various types of systems to have a product worthy of the Energy Star certification. These requirements are meant to minimize environmental impact by reducing air pollution. Consumers then have a choice between products that have achieved the Energy Star certification or products that do not carry the certification. Industries that certify their products through the Energy Star program are practicing good *exergy conservation*.

Consumers are faced with many energy/exergy decisions. For example, should you heat your home with electric resistance heating or air-cooled solar collectors? Electric resistance heating is 100% efficient in that all the electricity (work) entering the heater leaves as heat. However, this is a device that uses work to move heat. As seen in Example 3.16, this is not a very exergetically efficient method of heating. Of course, this also depends on where the electricity originates. If you live in a region where electrical energy is delivered from a hydroelectric plant, then you are relying on the hydrological cycle, which can be considered renewable. However, if you live in a region where electrical energy is delivered from a fossil fuel-fired power plant, then as the electricity is used to run the electric heater, the exergy resource (the fossil fuel) is being depleted. From an environmental point of view, you would be much better heating your home with the air-cooled solar collectors because of their high exergetic efficiency (heat moving heat). Of course, the conundrum is that air-cooled solar collectors cost quite a bit more than electric resistance heaters.

The purpose of this presentation is not to solve the energy/exergy conundrum. Instead, it is meant to provoke some high-level, exergy-based thinking in the engineers who will shape the future of the world.

3.10 Analysis of Thermal Energy Systems

In Section 3.10, the concepts discussed in this chapter will be applied to several types of thermal energy systems. The examples shown in this section are only a small subset of the many different types of thermal energy systems. However, the strategy and solution technique is the same in all types of thermal energy system analyses. There may be many different ways to analyze a given thermal energy system. The techniques shown here represent one possible solution strategy. Studying through the examples in this section and solving several homework problems pertinent to this section will help engineers develop their own unique solution strategies.

As thermal energy system analysis becomes more and more complex, it is incumbent that computer software is utilized to solve the problems and learn more about the system. Several software solutions are presented in Section 1.2. The reader is encouraged to use his/her own favorite software to solve the problems presented in this section.

3.10.1 Analysis of an Engine and Radiator System

Figure 3.18 shows a drawing of an automobile engine with the cooling system for heat removal from the engine block. The analysis in this section will focus on the engine block and the radiator.

Figure 3.19 shows an engineering schematic of the engine block and radiator. Several known system operating parameters are shown on this schematic. As shown in Figure 3.19, the engine coolant is a 40% ethylene glycol–water solution. The coolant enters the radiator at 30 gpm at a temperature $T_{h,in}$ and leaves the radiator at $T_{h,out}$. The air enters the radiator at $t_{c,in} = 20^\circ\text{C}$ with a volumetric flow rate of 3,000 cfm. The air leaves the radiator

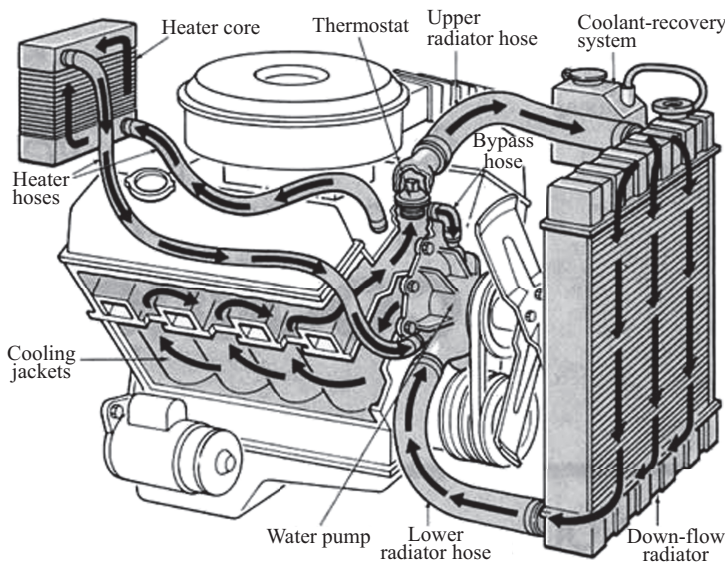


FIGURE 3.18
Drawing of an engine and cooling system.

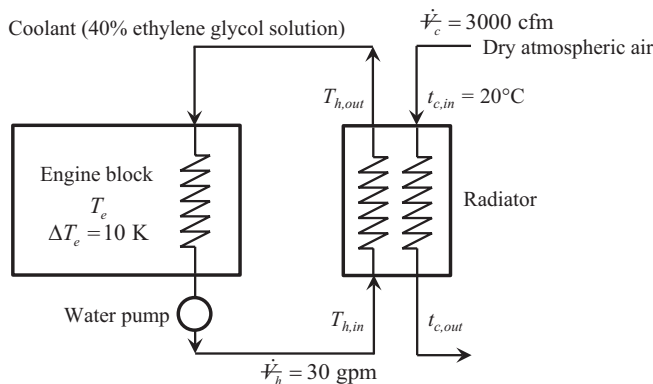


FIGURE 3.19
Engineering schematic of the engine block and radiator.

at $t_{c,out}$. The radiator has a PPTD of $\Delta T_{radiator} = 25$ K. The engine block is at a temperature of T_e . The engine block heat exchanger (water channels flowing through the engine block) has a PPTD of $\Delta T_e = 10$ K, and an effectiveness of 0.55.

The goal of this analysis is to determine the coolant temperatures $T_{h,out}$, $T_{h,in}$, the air temperature out of the radiator $t_{c,out}$, the heat transfer rate between the coolant and the air $\dot{Q}_{radiator}$, and effectiveness of the radiator, and the engine block temperature T_e .

The following assumptions will be made to analyze this thermal energy system.

- The radiator is a cross flow heat exchanger. However, in this analysis the radiator will be treated as a counter flow heat exchanger. While the performance of counter flow and cross flow heat exchangers is slightly different, this assumption should provide a reasonable approximation to cross flow behavior.
- The power requirement of the water pump will be considered negligible. In addition, the temperature of the coolant will be considered constant from the outlet of the radiator to the inlet of the engine at $T_{h,out}$, and from the outlet of the engine to the inlet of the radiator at $T_{h,in}$.
- The engine block temperature will be considered to be uniform.
- There is no stray heat transfer in the lines connecting the radiator to the engine block.
- The air entering the radiator will be assumed to be dry and considered to be at the standard atmospheric pressure of 1 atm (101.325 kPa or 14.696 psia).

This analysis becomes complex rather quickly because only one of the four temperatures entering the radiator is known. This indicates that the solution will be iterative. Therefore, this problem is best solved using computer software. When developing a computer software solution, the best strategy is to develop a set of n equations with n unknowns that fully describes the system. A good bookkeeping method will help to aid in the development of the $n \times n$ equation system. Simply writing equations down without keeping track of unknowns can quickly lead to confusion. There are many ways to keep track of equations and unknowns. One method is to count each equation, the number of *new* unknowns that show up in the equation and keep track of the *cumulative* equations and unknowns as you proceed. This technique will be used in the analysis of this system.

The heat transfer rate between the fluids in the heat exchanger can be written in terms of either fluid by applying the conservation of energy. Considering the air (cold fluid),

$$\dot{Q}_{radiator} = \dot{C}_c(t_{c,out} - t_{c,in}) \quad \dot{Q}_{radiator}, \dot{C}_c, t_{c,out} \quad \begin{array}{l} 1 \text{ eq} \quad 3 \text{ unk} \\ \text{cumulative equations} \\ \text{and unknowns} \end{array} \quad (3.89)$$

The heat transfer rate in the radiator can also be written in terms of the coolant (hot fluid),

$$\dot{Q}_{radiator} = \dot{C}_h(T_{h,in} - T_{h,out}) \quad \dot{C}_h, T_{h,in}, T_{h,out} \quad 2 \text{ eq} \quad 6 \text{ unk} \quad (3.90)$$

The thermal capacity rates of each fluid can be written as,

$$\dot{C}_c = \rho_c \dot{V}_c c_{p,c} \quad \rho_c, c_{p,c} \quad 3 \text{ eq} \quad 8 \text{ unk} \quad (3.91)$$

$$\dot{C}_h = \rho_h \dot{V}_h c_{p,h} \quad \rho_h, c_{p,h} \quad 4 \text{ eq} \quad 10 \text{ unk} \quad (3.92)$$

The density of each fluid is evaluated at the inlet condition (this is where the volumetric flow rate is known), and the heat capacities are evaluated at the average temperature,

$$\rho_c = \rho(P_{amb}, t_{c,in}) \quad \text{no new unknowns} \quad 5 \text{ eq} \quad 10 \text{ unk} \quad (3.93)$$

$$\rho_h = \rho(T_{h,in}, x = 0) \quad \text{no new unknowns} \quad 6 \text{ eq} \quad 10 \text{ unk} \quad (3.94)$$

$$c_{p,c} = c_p(P_{amb}, t_{c,avg}) \quad t_{c,avg} \quad 7 \text{ eq} \quad 11 \text{ unk} \quad (3.95)$$

$$c_{p,h} = c_p(T_{h,avg}, x = 0) \quad T_{h,avg} \quad 8 \text{ eq} \quad 12 \text{ unk} \quad (3.96)$$

The average temperatures of each fluid are,

$$t_{c,avg} = (t_{c,in} + t_{c,out})/2 \quad \text{no new unknowns} \quad 9 \text{ eq} \quad 12 \text{ unk} \quad (3.97)$$

$$T_{h,avg} = (T_{h,in} + T_{h,out})/2 \quad \text{no new unknowns} \quad 10 \text{ eq} \quad 12 \text{ unk} \quad (3.98)$$

In the radiator, the PPTD is the minimum between the cold-side temperature difference or the hot-side temperature difference,

$$\Delta T_{radiator} = \min[(t_{c,in} - T_{h,out}), (T_{h,in} - t_{c,out})] \quad \text{no new unknowns} \quad 11 \text{ eq} \quad 12 \text{ unk} \quad (3.99)$$

The coolant is in contact with the engine block, which is assumed to be at a constant temperature of T_e . The coolant temperature must increase as it passes through the engine block. Therefore, the PPTD of the engine block heat exchanger must occur on the hot end,

$$\Delta T_e = T_e - T_{h,in} \quad T_e \quad 12 \text{ eq} \quad 13 \text{ unk} \quad (3.100)$$

The heat transfer rate to the coolant as it flows through the engine block heat exchanger must be the same as the heat removal rate in the radiator. Therefore, the effectiveness of the engine block can be written as,

$$\varepsilon_e = \frac{\dot{Q}_{\text{radiator}}}{\dot{Q}_{\text{max},e}} \quad \dot{Q}_{\text{max},e} \quad 13 \text{ eq} \quad 14 \text{ unk} \quad (3.101)$$

The maximum possible heat transfer rate in the engine block occurs when the coolant leaves the engine at the engine block temperature. Therefore,

$$\dot{Q}_{\text{max},e} = \dot{C}_h (T_e - T_{h,\text{out}}) \quad \text{no new unknowns} \quad \underline{14 \text{ eq} \quad 14 \text{ unk}} \quad (3.102)$$

Equation 3.102 indicates that the equation set developed to this point has 14 equations and 14 unknowns. Therefore, it can be solved. Adding the equations required to compute the effectiveness of the radiator results in,

$$\varepsilon_{\text{radiator}} = \frac{\dot{Q}_{\text{radiator}}}{\dot{Q}_{\text{max},\text{radiator}}} \quad \varepsilon_{\text{radiator}}, \dot{Q}_{\text{max},\text{radiator}} \quad 15 \text{ eq} \quad 16 \text{ unk} \quad (3.103)$$

$$\dot{Q}_{\text{max},\text{radiator}} = \dot{C}_{\text{min}} (T_{h,\text{in}} - t_{c,\text{in}}) \quad \dot{C}_{\text{min}} \quad 16 \text{ eq} \quad 17 \text{ unk} \quad (3.104)$$

$$\dot{C}_{\text{min}} = \min(\dot{C}_h, \dot{C}_c) \quad \text{no new unknowns} \quad \underline{17 \text{ eq} \quad 17 \text{ unk}} \quad (3.105)$$

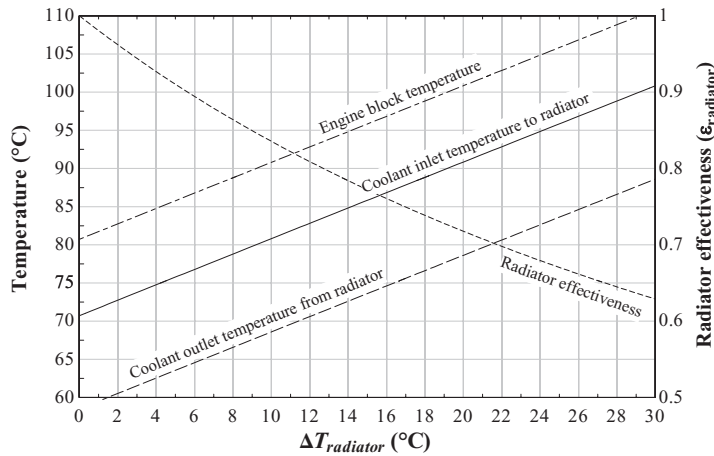
At this point, all of the parameters required in the analysis have been identified. The main system operating variables resulting from the solution of this set of equations is shown in Table 3.3. The result of this analysis indicates that the pinch point of the radiator occurs on the hot end.

Identifying the set of equations that define the thermal energy system allows for the engineer to start thinking about how the system might perform as one or more of the system operating parameters change. This is known as a *parametric study*. In the case of the

TABLE 3.3

Solution to the Engine/Radiator Thermal System Analysis

Variable	Value and Units
Air temperature leaving the radiator	$t_{c,\text{out}} = 70.9^\circ\text{C}$
Coolant temperature entering the radiator	$T_{h,\text{in}} = 95.9^\circ\text{C}$
Coolant temperature leaving the radiator	$T_{h,\text{out}} = 83.6^\circ\text{C}$
Heat transfer rate in the radiator	$\dot{Q}_{\text{radiator}} = 87.3 \text{ kW}$
Radiator effectiveness	$\varepsilon_{\text{radiator}} = 0.67$
Engine block temperature	$T_e = 105.9^\circ\text{C}$

**FIGURE 3.20**

Result of a parametric study investigating the effect of the radiator size on system performance.

engine/radiator thermal energy system, it is of interest to see how the system responds to different sized radiators. This can be accomplished by varying the PPTD of the radiator, calculating the operating parameters, and plotting the results. Figure 3.20 shows the result of a such a parametric study where $0 \text{ K} \leq \Delta T_{\text{radiator}} \leq 30 \text{ K}$. This figure indicates that for a radiator with a larger heat transfer area (i.e., a smaller value of $\Delta T_{\text{radiator}}$), the engine runs cooler, and the coolant temperatures in and out of the radiator are also cooler. It is also noted that the effectiveness of the radiator increases as the radiator's heat transfer area increases. While this result is qualitatively expected, the solution of the parametric study *quantifies* the effect of the radiator size. This is important information for the engineer who is designing the radiator.

Figure 3.20 shows that there are many *workable* solutions. However, which one should be selected? At some point, the design engineer must address economics. Clearly, a radiator with more surface area will be more expensive. Therefore, there is an economic trade-off between a cooler running engine and cost. An *unconstrained optimum* that minimizes the engine block temperature exists where the PPTD of the radiator is zero. However, this represents an infinitely large radiator, and thus only theoretical. The *optimum* radiator PPTD that minimizes the engine block temperature could be identified if temperature limits are placed on the engine block and/or the coolant.

It should be pointed out that the computer solution to this analysis requires that the properties of dry air and 40% ethylene glycol can be found. Some software packages have this capability built in (e.g., EES). However, if the software does not have access to properties, it is a simple enough matter to curve-fit the fluid property data and develop empirical equations that represent the properties shown in Appendix B.4 (secondary heat transfer fluids), and B.5 (dry air). For example, using property information from Appendix B.4 in the range from $0 < T < 120^\circ\text{C}$, the following empirical equation represents the density of 40% ethylene glycol,

$$\rho = a_1 + a_2 T + a_3 T^2 \quad (3.106)$$

Since this is an empirical equation, it is important to note that the coefficients have units that make the equation dimensionally homogeneous. For densities in kg/m^3 and temperatures

in °C, the resulting coefficients are; $a_1 = 1060.7 \text{ kg/m}^3$, $a_2 = -0.41473 \text{ kg/m}^3\text{-}^\circ\text{C}$, and $a_3 = -0.0018467 \text{ kg/m}^3\text{-}^\circ\text{C}^2$. In the same range, the isobaric heat capacity of 40% ethylene glycol can be estimated by,

$$c_p = b_1 + b_2T + b_3T^2 \quad (3.107)$$

The coefficients of Equation 3.107 are $b_1 = 3.4333 \text{ kJ/kg-K}$, $b_2 = 0.0045216 \text{ kJ/kg-K-}^\circ\text{C}$, and $b_3 = -9.7054 \times 10^{-6} \text{ kJ/kg-K-}^\circ\text{C}^2$. Development of these two equations is fairly straightforward using modern computer software.

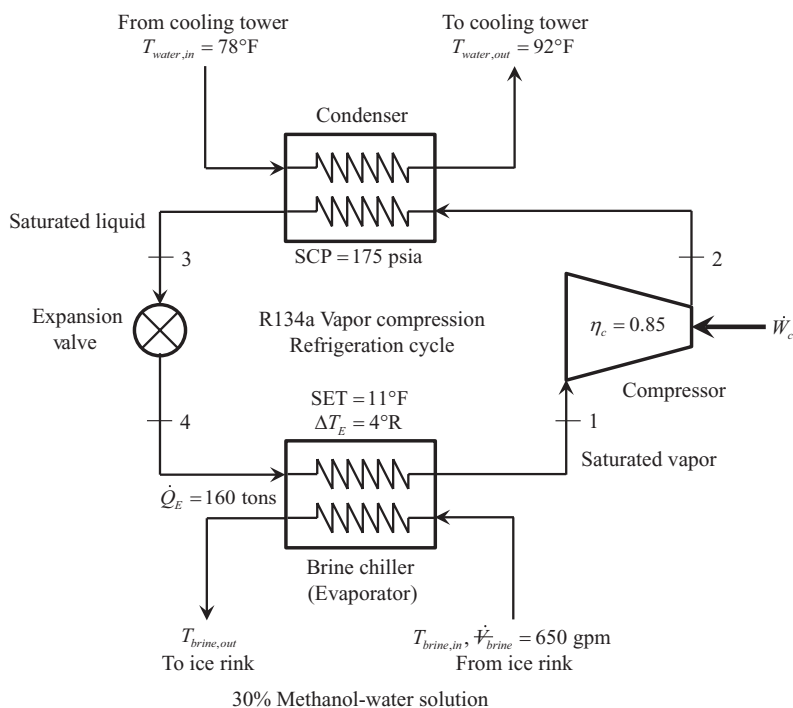
Finally, it is important to be purposefully deliberate with respect to units. Notice that the description of the engine/radiator system includes SI units and IP units. While this may not be desirable, it is sometimes unavoidable in engineering practice. If unit analysis is incorrect, then the computer software may be unable to find a solution (i.e., convergence errors), or the solution may seem unreasonable. This problem is exacerbated as the number of equations and unknowns increases.

3.10.2 Analysis of a Brine Chilling System for Ice Rink Manufacture

The ice in an ice rink can be *natural* or *artificial*. Natural ice is ice that is frozen by virtue of the ambient temperature, without the aid of mechanical refrigeration. The majority of outdoor ice rinks are natural ice. Ice made for indoor ice rinks is manufactured and maintained by a vapor compression refrigeration system. Even though the ice manufactured with a refrigeration system is the same as natural ice (both are frozen water), it is called *artificial* since it is made by mechanical refrigeration.

Figure 3.21 shows a schematic of a vapor compression refrigeration system used to chill a secondary heat transfer fluid that is circulated in tubes underneath the floor of the ice rink. The ice could be manufactured and maintained by simply circulating the refrigerant under the floor of the ice rink. However, the cost would be prohibitive. It is much cheaper to chill a secondary heat transfer fluid. The secondary heat transfer fluids have been historically known as *brines* because the first secondary fluids were salt-based water solutions (calcium chloride–water or sodium chloride–water). The mixture of a salt with water depresses the freezing point of the solution which keeps the fluid in the liquid phase at a temperature below the freezing point of water. There are still salt-based brines in use today. However, the secondary heat transfer fluids have expanded to alcohol–water solutions and glycol–water solutions. While these types of secondary fluids do not contain salt, many still refer to these fluids as *brines*.

Figure 3.21 indicates that the refrigerant used in the vapor compression cycle is R134a. The cycle is operating such that the saturated evaporating temperature (SET) is 11°F. Assuming that there are no pressure drops through the heat exchangers, the SET is the temperature of the refrigerant as it boils in the chiller (notice that the refrigerant leaves the chiller as a saturated vapor). The brine used in this system is a 30% methanol–water solution (by mass). The brine enters the chiller at a volumetric flow rate of 650 gpm. The chiller has a pinch point temperature difference of 4°R. In order to maintain the ice in the rink, the refrigeration system must provide a *capacity* of 160 tons. The capacity of a refrigeration cycle is the heat transfer rate occurring in the evaporator. In the refrigeration industry, the *ton* unit indicates a heat transfer rate equal to 12,000 Btu/h. Historically, this is the steady state heat transfer rate required to melt 1 ton of ice at 32° in 24 hours. The compressor of the refrigeration cycle is operating at a condition where its isentropic efficiency is 85%.

**FIGURE 3.21**

Vapor compression refrigeration cycle used to manufacture and maintain ice in an ice rink.

The saturated condensing pressure (SCP) of the cycle is 175 psia. This terminology indicates the pressure at which the refrigerant condenses. This is the high pressure in the cycle. In this cycle, the refrigerant leaves the condenser as a saturated liquid. The condenser of the refrigeration cycle is cooled by water. The water enters the condenser at 78°F and leaves at 92°F. The water is then circulated to a cooling tower where it is cooled back down to 78°F.

The goal of this analysis is to determine the coefficient of performance (COP), horsepower per ton (HPT), and exergetic efficiency of the refrigeration cycle, the flow rate of the cooling water required (gpm), the temperature of the brine leaving the chiller (to the ice rink), the temperature of the brine entering the chiller (returning from the ice rink), and the effectiveness of the chiller.

The following assumptions will be made to conduct this analysis.

- Heat exchangers in a system like this are typically of the shell-and-tube type. In this analysis, the heat exchangers will be treated as counter flow.
- There are no pressure drops in any of the fluids as they pass through the heat exchangers.
- There are no stray heat transfers in any of the thermal equipment.
- The COP of the refrigeration cycle does not include the pumping power required to move the brine through the chiller or the water through the condenser.
- The dead state temperature is standard atmospheric temperature, $T_0 = 77^{\circ}\text{F}$.

In order to analyze the refrigeration cycle, the properties of the refrigerant are required at all four state points identified in Figure 3.21. The properties at State 1 can be found since

the temperature, $T_1 = \text{SET}$, and quality, $x_1 = 1$ are known. To determine State 2, an analysis of the isentropic efficiency of the compressor must be conducted. The isentropic efficiency of the compressor is defined by Equation 3.28. For the compressor of the given refrigeration system this equation can be written as,

$$\eta_c = \frac{h_{2s} - h_1}{h_2 - h_1} \quad (3.108)$$

This equation has two unknowns, h_{2s} , and h_2 . The enthalpy at the end of an isentropic compression process, h_{2s} , can be found since the pressure at the compressor discharge is known (the SCP), and the entropy must be the same as State 1,

$$h_{2s} = h(P_2 = \text{SCP}, s_{2s} = s_1) \quad (3.109)$$

Using the value of h_{2s} computed from Equation 3.109, the value of h_2 can be calculated from Equation 3.108. At this point, two properties are known at State 2; P_2 and h_2 . Therefore, the remaining properties can be found. State 3 is fully identified with pressure, $P_3 = P_2$, and quality, $x_3 = 0$. State 4 is the exit of the expansion valve. Since valves are isenthalpic, $h_4 = h_3$. In addition, the pressure at State 4 is known, $P_4 = P_1$. Therefore, State 4 is fully identified with pressure and enthalpy. The thermophysical properties of R134a are found in Appendices B.6 and B.7. These appendices are abbreviated tables, so substantial interpolation must be conducted to determine the properties at each state. An alternative is to use computer software to find the properties. Table 3.4 shows the resulting table of thermodynamic properties of the R134a in the system. The entries that are listed in **bold** are the independent pair used to determine the rest of the properties at the given state.

Knowing all of the properties in the refrigeration cycle allows for the COP and HPT to be calculated.

$$\text{COP} = \frac{\dot{Q}_E}{\dot{W}_C} = \frac{\dot{m}_r(h_1 - h_4)}{\dot{m}_r(h_2 - h_1)} = \frac{(168.49 - 114.55) \text{ Btu/lbm}}{(188.15 - 168.49) \text{ Btu/lbm}} = \underline{\underline{2.744}} \quad (3.110)$$

The HPT is the dimensional reciprocal of the COP with units of horsepower per ton of refrigeration. Therefore,

$$\text{HPT} = \frac{\dot{W}_C}{\dot{Q}_E} = \frac{1}{2.744} \left(\frac{1.341 \text{ hp}}{0.284345 \text{ ton}} \right) = \underline{\underline{1.719 \frac{\text{hp}}{\text{ton}}}} \quad (3.111)$$

TABLE 3.4

Thermodynamic Properties of R134a in the Brine Chiller System of Figure 3.21

State	P (psia)	T (°F)	h (Btu/lbm)	s (Btu/lbm-°R)	x
1	27.23	11	168.49	0.41457	1
2s	175	128.58	185.20	0.41457	Vapor
2	175	139.50	188.15	0.41953	Vapor
3	175	115.75	114.55	0.29185	0
4	27.23	11	114.55	0.29996	0.3947

This performance indicator tells the design engineer how much power needs to be input to the cycle through the compressor to affect 1 ton of refrigeration, allowing for the selection of an appropriate compressor for the system.

The exergetic efficiency of the cycle can be found using Equation 3.83. The exergy transfer rate associated with the chiller is given by Equation 3.86. Substituting into Equation 3.83 and simplifying,

$$\eta_{x, \text{chiller}} = \frac{\dot{Q}_E}{\dot{W}_C} \left(\frac{T_0}{T_4} - 1 \right) = \text{COP} \left(\frac{T_0}{T_4} - 1 \right) = 2.744 \left[\frac{(77 + 459.67) \text{ R}}{(11 + 459.67) \text{ R}} - 1 \right] = \underline{\underline{0.3848}} \quad (3.112)$$

Comparing the COP and the exergetic efficiency of the cycle, it can be seen that from an energy point of view, the cycle performs extremely well. This is due to the “free” energy source entering the cycle as heat in the chiller (i.e., heat given up by the brine as it passes through the chiller). However, the exergetic efficiency is low, indicating that only 38.5% of the exergy input to the cycle (electrical energy to the compressor) is used to perform the exergy task (chilling the brine).

The flow rate of the cooling water flowing through the condenser can be determined by applying the conservation of energy to a system boundary surrounding the heat exchanger,

$$(\dot{m}_r h_2 + \dot{m}_w h_{w, \text{in}}) - (\dot{m}_r h_3 + \dot{m}_w h_{w, \text{out}}) = 0 \quad (3.113)$$

Rearranging Equation 3.113,

$$\dot{m}_w = \frac{\dot{m}_r (h_2 - h_3)}{c_{p, w} (T_{w, \text{out}} - T_{w, \text{in}})} \quad (3.114)$$

In Equation 3.114, the enthalpy change of the liquid cooling water is approximated with $c_p \Delta T_w$. The average heat capacity of the water can be found since the inlet and outlet temperatures are known. From Appendix B.3, the average heat capacity is found to be $c_p = 0.99909 \text{ Btu/lbm-R}$. The mass flow rate of the refrigerant can be found by applying the conservation of energy to a system boundary surrounding only the refrigerant as it flows through the chiller,

$$\dot{m}_r = \frac{\dot{Q}_E}{h_1 - h_4} = \frac{(160 \text{ ton}) \left(\frac{12,000 \text{ Btu}}{\text{ton-h}} \right)}{(168.49 - 114.55) \frac{\text{Btu}}{\text{lbm}}} = 35,595 \frac{\text{lbm}}{\text{h}} \quad (3.115)$$

From Equation 3.114, the mass flow rate of the cooling water is found to be,

$$\dot{m}_w = \frac{\left(35,595 \frac{\text{lbm}}{\text{h}} \right) (188.15 - 114.55) \frac{\text{Btu}}{\text{lbm}}}{\left(0.99909 \frac{\text{Btu}}{\text{lbm-R}} \right) (92 - 78) \text{ R}} = 187,298 \frac{\text{lbm}}{\text{h}} \quad (3.116)$$

The volumetric flow rate of the water entering the condenser can be found by using the density at the inlet temperature. At 78°F, the density of liquid water is found in Appendix B.3 to be 62.232 lbm/ft³. Therefore, the volumetric flow of the cooling water entering the condenser is,

$$\dot{V}_w = \frac{\dot{m}_w}{\rho_w} = \frac{\left(\frac{187,298 \text{ lbm}}{\text{h}} \right)}{\left(\frac{62.232 \text{ lbm}}{\text{ft}^3} \right)} \left(\frac{\text{gpm} \cdot \text{h}}{8.02083 \text{ ft}^3} \right) = \underline{\underline{375.2 \text{ gpm}}} \quad (3.117)$$

This information allows the engineer to begin thinking about the pump required to circulate the cooling water. Pump selection is one of the topics discussed in Chapter 4.

The temperature of the brine leaving the chiller can be determined from knowledge of the pinch point temperature difference of the chiller. The refrigerant travels through the chiller at a constant temperature as it boils from a wet mixture to a saturated vapor. The brine cools as it passes through the chiller. Therefore, the pinch point must occur on the cold end of the chiller. This allows for the calculation of the brine temperature leaving the chiller,

$$\Delta T_E = T_{b,out} - T_4 \rightarrow \therefore T_{b,out} = \Delta T_E + T_4 = (4 + 11)^\circ\text{F} = 15^\circ\text{F} \quad (3.118)$$

The temperature of the brine entering the chiller can be found by applying the conservation of energy to a system boundary surrounding the brine as it passes through the chiller. The resulting equation is,

$$\dot{Q}_E = \dot{m}_b(h_{b,in} - h_{b,out}) = \dot{m}_b c_{p,b}(T_{b,in} - T_{b,out}) \quad (3.119)$$

The mass flow rate of the brine can be written in terms of the density and the volumetric flow rate entering the chiller,

$$\dot{Q}_E = \rho_b \dot{V}_b c_{p,b}(T_{b,in} - T_{b,out}) \quad (3.120)$$

Since the inlet brine temperature is unknown, the density and heat capacities are also unknown. However, they are a function of the inlet temperature,

$$\rho_b = \rho(T_{b,in}) \quad c_{p,b} = c_p(T_{b,avg}) \quad (3.121)$$

The process in determining the inlet brine temperature is iterative. To begin the iteration, evaluate the properties at an assumed brine inlet temperature, say $T_{b,in} = 20^\circ\text{F}$. This allows for the determination of the density and heat capacity from Appendix B.4.

At 20°F, $\rho_b = 60.101 \text{ lbm/ft}^3$. At an average temperature of 17.5°F, $c_{p,b} = 0.90834 \text{ Btu/lbm-R}$. Now, the brine inlet temperature can be calculated from Equation 3.120,

$$T_{b,in} = T_{b,out} + \frac{\dot{Q}_E}{\rho_b \dot{V}_b c_{p,b}}$$

$$= 15^\circ\text{F} + \frac{(160 \text{ ton}) \left(\frac{12,000 \text{ Btu}}{\text{ton-h}} \right)}{\left(60.101 \frac{\text{lbm}}{\text{ft}^3} \right) (650 \text{ gpm}) \left(0.90834 \frac{\text{Btu}}{\text{lbm-R}} \right) \left(\frac{8.02083 \text{ ft}^3}{\text{gpm-h}} \right)} = 21.75^\circ\text{F} \quad (3.122)$$

Since this is not the same as the initial guess of 20°F, the calculation is repeated using the new calculated value of $T_{b,in} = 21.75^\circ\text{F}$. From Appendix B.4 at 21.75°F, $\rho_b = 60.078 \text{ lbm/ft}^3$. At an average temperature of 18.38°F, $c_{p,b} = 0.90941 \text{ Btu/lbm-R}$. Repeating the calculation for the brine inlet temperature,

$$T_{b,in} = 15^\circ\text{F} + \frac{(160 \text{ ton}) \left(\frac{12,000 \text{ Btu}}{\text{ton-h}} \right)}{\left(60.078 \frac{\text{lbm}}{\text{ft}^3} \right) (650 \text{ gpm}) \left(0.90941 \frac{\text{Btu}}{\text{lbm-R}} \right) \left(\frac{8.02083 \text{ ft}^3}{\text{gpm-h}} \right)} = 21.74^\circ\text{F} \quad (3.123)$$

The successive values of $T_{b,in}$ are within 0.01°F which indicates that no further iteration is needed. Therefore, the brine temperature leaving the chiller is $T_{b,in} = 21.74^\circ\text{F}$

The effectiveness of the chiller is defined by Equation 3.32. The maximum heat transfer rate would occur when the pinch point temperature difference goes to zero (the chiller becomes infinitely large). At this point, $T_{b,out} = T_4 = 11^\circ\text{F}$. The heat capacity of the brine at an average temperature of 16.37°F is found in Appendix B.4 as 0.90700 Btu/lbm-R. Therefore, the maximum heat transfer rate would be,

$$\dot{Q}_{E,\max} = \rho_b \dot{V}_b c_{p,b} (T_{b,in} - T_4)$$

$$= \left(60.078 \frac{\text{lbm}}{\text{ft}^3} \right) (650 \text{ gpm}) \left(0.907 \frac{\text{Btu}}{\text{lbm-R}} \right) (21.74 - 11) \text{R} \left(\frac{8.02083 \text{ ft}^3}{\text{gpm-h}} \right) \quad (3.124)$$

$$= 3.0511 \times 10^6 \frac{\text{Btu}}{\text{h}}$$

This results in a chiller effectiveness of,

$$\varepsilon_{\text{chiller}} = \frac{\dot{Q}_E}{\dot{Q}_{E,\max}} = \frac{(160 \text{ ton}) \left(\frac{12,000 \text{ Btu}}{\text{ton-h}} \right)}{3.0511 \times 10^6 \frac{\text{Btu}}{\text{h}}} = \underline{0.6293} \quad (3.125)$$

3.10.3 Analysis of a Gas Turbine System for Power Delivery

Gas turbine systems are widely used for power delivery. They have a much higher power output to weight ratio when compared to vapor power cycles (e.g., a steam power plant). Because of this, gas turbine systems are well suited for both stationary and mobile applications. Gas turbine systems can be quite complex. In this section, a simple gas turbine system will be analyzed. The analysis methods demonstrated in this section can easily be extended to more complex systems.

Consider the simple gas turbine system shown in Figure 3.22. This may appear different compared to the way most undergraduate textbooks in thermodynamics treat a gas turbine cycle. In this system, the heat transfer in the combustion chamber is replaced with fuel (in this case, natural gas) flowing into the chamber. The heat of combustion and chemical exergy of the fuel are known. Another modification to the standard cycle is the turbine expansion. In Figure 3.22, the turbine expansion is split into two stages. The *gasifier* turbine delivers the power required by the compressor. The *power* turbine delivers the net power required. In some gas turbine systems, the gasifier turbine and power turbine are collinear on the same rotating shaft. In other cases, as shown in Figure 3.22, the turbines are on separate shafts. This allows for each turbine to operate at a different rotational speed.

For the system in Figure 3.22, dry air is drawn into the compressor at 22°C, 1 atm. It is compressed at a pressure ratio of 5.2 through the compressor which has an isentropic efficiency of 84%. After compression, the air is mixed with a flow of natural gas in the combustion chamber and burned. The combustion products leave the combustion chamber at 1150°C with a negligible drop in pressure. The combustion products then pass through the gasifier turbine which has an isentropic efficiency of 87%. After the gasifier turbine expansion, the combustion products pass through the power turbine where 250 kW of power are delivered. The combustion products are expanded through the power turbine to a pressure of 1 atm. The isentropic efficiency of the power turbine is 81%.

The goal of this analysis is to determine the air-fuel ratio in the combustor, the mass flow rate of the fuel, the specific fuel consumption of the system, the thermal and exergetic efficiencies of the system, and the distribution of the fuel's exergy throughout the system.

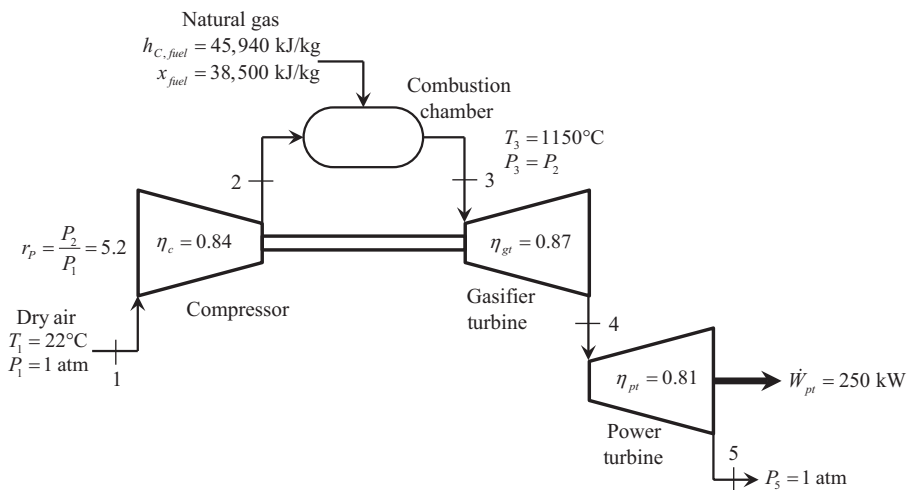


FIGURE 3.22

A simple gas turbine system for power delivery.

In order to proceed with the analysis, the following assumptions will be made.

- The compressor and turbines are adiabatic.
- There is no appreciable drop in pressure through the combustion chamber.
- The combustion products will be modeled as dry air. This will give a reasonable approximation to the performance of the system without having to go through a combustion analysis to determine the actual makeup of the products leaving the combustion chamber. This assumption greatly simplifies the calculation of the properties at States 3, 4, and 5.
- For the purpose of exergy analysis, the dead state will be considered the atmospheric condition entering the compressor.

The properties of dry air are found in Appendix B.5. However, this analysis turns out to be iterative, which makes manual retrieval of properties cumbersome. An alternative is to use computer software for system analysis and property calculation. State 1 is fully identified with pressure and temperature, 1 atm, 22°C. Therefore, the rest of the properties can be found. At State 2, the pressure is known since the pressure ratio across the compressor is given,

$$r_p = \frac{P_2}{P_1} \rightarrow P_2 = r_p P_1 = (5.2)(1 \text{ atm}) \left(\frac{101.325 \text{ kPa}}{\text{atm}} \right) = 526.9 \text{ kPa} \quad (3.126)$$

The enthalpy at State 2 can be found from knowledge of the isentropic efficiency of the compressor,

$$\eta_c = \frac{h_{2s} - h_1}{h_2 - h_1} \rightarrow h_2 = h_1 + \frac{h_{2s} - h_1}{\eta_c} \quad (3.127)$$

The enthalpy at the end of an isentropic compression, h_{2s} , can be determined since the pressure, P_2 and entropy, $s_{2s} = s_1$, are known. Once h_2 is determined from Equation 3.127, the remainder of the properties at State 2 can be found. State 3 is fully identified by pressure and temperature, $P_2 = P_3 = 526.9 \text{ kPa}$, $T_3 = 1150^\circ\text{C}$. Therefore, the rest of the properties at State 3 can be found. Table 3.5 shows the thermodynamic properties of the States 1–3 resulting from these calculations. The independent properties used to calculate the other properties at a given state are shown in **bold** type. The end of the isentropic compression process is shown in *italic* type.

TABLE 3.5

Thermodynamic Properties of States 1–3 for the Gas Turbine System of Figure 3.22

State	<i>P</i> (kPa)	<i>T</i> (°C)	<i>h</i> (kJ/kg)	<i>s</i> (kJ/kg-K)
1	101.325	22	295.43	6.8502
2s	526.9	198.3	473.84	6.8502
2	526.9	231.3	507.82	6.9198
3	526.9	1150	1544.3	8.0741

Applying the conservation of energy to a system boundary surrounding the combustion chamber results in,

$$\dot{m}_a h_2 + \dot{m}_f h_C = (\dot{m}_a + \dot{m}_f) h_3 \quad (3.128)$$

Dividing Equation 3.128 through by the mass flow rate of the fuel, \dot{m}_f ,

$$\frac{\dot{m}_a}{\dot{m}_f} h_2 + h_C = \left(\frac{\dot{m}_a}{\dot{m}_f} + 1 \right) h_3 \quad (3.129)$$

The ratio of the mass flow rate of the dry air to the mass flow rate of the fuel is known as the air-fuel ratio, AF . Making this substitution, Equation 3.129 can be rewritten as,

$$(AF) h_2 + h_C = (AF + 1) h_3 \quad (3.130)$$

Since all the enthalpy values in Equation 3.130 are known, the AF can be found,

$$AF = \frac{h_C - h_3}{h_3 - h_2} = \frac{(45,940 - 1,544.3) \text{ kJ/kg}}{(1,544.3 - 507.82) \text{ kJ/kg}} = \underline{\underline{42.83}} \quad (3.131)$$

This value indicates that for every kg of fuel burned, 42.83 kg of air are required in the combustion process. This is the first parameter required to determine the mass flow rate of the fuel.

Since the gasifier turbine runs the compressor,

$$\dot{W}_c = \dot{W}_{gt} \quad (3.132)$$

Applying the conservation energy to the compressor and gasifier turbine, respectively, Equation 3.132 can be rewritten as,

$$\dot{m}_a (h_2 - h_1) = (\dot{m}_a + \dot{m}_f) (h_3 - h_4) \quad (3.133)$$

The mass flow rates and h_4 are unknown. However, the AF has been determined in Equation 3.131. Dividing Equation 3.133 by \dot{m}_a and solving for h_4 results in,

$$h_4 = h_3 - \frac{h_2 - h_1}{1 + \frac{1}{AF}} = 1544.3 \frac{\text{kJ}}{\text{kg}} - \frac{(507.82 - 295.43) \frac{\text{kJ}}{\text{kg}}}{1 + \frac{1}{42.83}} = 1336.7 \frac{\text{kJ}}{\text{kg}} \quad (3.134)$$

This identifies one property at State 4. The other property that can be found is the pressure at State 4 by using the isentropic efficiency of the gasifier turbine,

$$\eta_{gt} = \frac{h_3 - h_4}{h_3 - h_{4s}} \quad (3.135)$$

$$\therefore h_{4s} = h_3 - \frac{h_3 - h_4}{\eta_{gt}} = 1544.3 \frac{\text{kJ}}{\text{kg}} - \frac{(1544.3 - 1336.7) \frac{\text{kJ}}{\text{kg}}}{0.87} = 1305.7 \frac{\text{kJ}}{\text{kg}}$$

State 4s represents the exhaust of an isentropic expansion in the gasifier turbine. Equation (3.135) gives the enthalpy at that condition. Another property that is known at this state is the entropy, $s_{4s} = s_3 = 8.0841 \text{ kJ/kg-K}$ (Table 3.5). This combination of h_{4s} and s_{4s} represent an independent property pair that fully identifies State 4s, including the pressure, P_4 . To determine this value manually using a property table requires excessive interpolation. Using computer software, the pressure P_4 is found to be 281.1 kPa. Now, pressure and enthalpy are known at State 4 which allows for calculation of the remaining properties.

State 5 can be found from knowledge of the isentropic efficiency of the power turbine,

$$\eta_{pt} = \frac{h_4 - h_5}{h_4 - h_{5s}} \rightarrow h_5 = h_4 - \eta_{pt}(h_4 - h_{5s}) \quad (3.136)$$

In Equation 3.136, the enthalpy at the end of the isentropic expansion through the power turbine, h_{5s} , can be found since the pressure, $P_5 = 1 \text{ atm}$, and entropy, $s_{5s} = s_4$, are known. This allows for the calculation of the properties at State 5 knowing pressure, P_5 , and enthalpy, h_5 . Table 3.6 shows the result of these calculations added to Table 3.5. All five state points and the three isentropic end states are shown in this table.

The power delivery from the power turbine is known. Applying the conservation of energy to a system boundary surrounding the power turbine results in,

$$\dot{W}_{pt} = (\dot{m}_a + \dot{m}_f)(h_4 - h_5) \quad (3.137)$$

TABLE 3.6

Thermodynamic Properties for the Gas Turbine System of Figure 3.22

State	P (kPa)	T (°C)	h (kJ/kg)	s (kJ/kg-K)
1	101.325	22	295.43	6.8502
2s	526.9	198.3	473.84	6.8502
2	526.9	231.3	507.82	6.9198
3	526.9	1150	1544.3	8.0741
4s	281.1	949.9	1305.7	8.0741
4	281.1	976.2	1336.7	8.0992
5s	101.325	697.2	1012.9	8.0992
5	101.325	751.1	1074.4	8.1609

Dividing Equation 3.137 by the fuel flow rate results in,

$$\frac{\dot{W}_{pt}}{\dot{m}_f} = (AF + 1)(h_4 - h_5) \quad (3.138)$$

The AF is also known from Equation 3.131. Substituting Equation 3.131 into Equation 3.137 and solving for the mass flow rate of the fuel,

$$\dot{m}_f = \frac{\dot{W}_{pt}}{(AF + 1)(h_4 - h_5)} = \frac{(250 \text{ kW}) \left(\frac{\text{kJ}}{\text{kW-s}} \right)}{(42.83 + 1)(1336.7 - 1074.4) \frac{\text{kJ}}{\text{kg}}} = 0.02174 \frac{\text{kg}}{\text{s}} \quad (3.139)$$

The specific fuel consumption, sfc , of the gas turbine system is defined as the mass of fuel consumed to deliver a unit of energy. Expressing the energy in terms of kWh, the sfc can be found by,

$$sfc = \frac{\dot{m}_f}{\dot{W}_{pt}} = \frac{\left(0.02174 \frac{\text{kg}}{\text{s}} \right) \left(\frac{3600 \text{ s}}{\text{h}} \right)}{(250 \text{ kW})} = \underline{\underline{0.313 \frac{\text{kg}}{\text{kWh}}}} \quad (3.140)$$

The thermal efficiency of the gas turbine system can be determined using Equation 3.60. For the gas turbine system, the energy sought is the energy delivered by the power turbine. The energy that costs is the energy input to the system by the fuel. These terms can be expressed as rates resulting in,

$$\eta_{th} = \frac{\dot{W}_{pt}}{\dot{m}_f h_C} = \frac{(250 \text{ kW}) \left(\frac{\text{kJ}}{\text{kW-s}} \right)}{\left(0.02174 \frac{\text{kg}}{\text{s}} \right) \left(45,940 \frac{\text{kJ}}{\text{kg}} \right)} = \underline{\underline{0.250}} = \underline{\underline{25.0\%}} \quad (3.141)$$

This indicates that roughly one-fourth of the energy provided by the fuel ends up as useful power. It is prudent to withhold judgement on whether this is an acceptable value. Recall, that the thermal efficiency is not limited by 100%. The limiting thermal efficiency of a power cycle is the Carnot efficiency, defined by Equation 3.71. Assuming that the high temperature in the cycle is at State 3 and the low temperature is the atmospheric condition entering the compressor, the Carnot efficiency of the gas turbine system can be estimated as,

$$\eta_{th,Carnot} = 1 - \frac{T_L}{T_H} = 1 - \frac{T_1}{T_3} = 1 - \frac{(22 + 273.15) \text{ K}}{(1150 + 273.15) \text{ K}} = \underline{\underline{0.793}} = \underline{\underline{79.3\%}} \quad (3.142)$$

Now, there is enough information to conclude that the gas turbine system may not be effectively utilizing the energy input from the fuel. What is causing this? Why is this system

not operating closer to the Carnot efficiency? These are excellent questions! The exergy analysis allows the engineer to pinpoint where major problems are within the system.

In a similar manner, the exergetic efficiency of the gas turbine system can be determined using Equation 3.74. The exergy input to the gas turbine system is the chemical exergy flow rate associated with the fuel. The exergy output is the power delivered from power turbine. Therefore, the exergetic efficiency of the gas turbine system is,

$$\eta_x = \frac{\dot{W}_{pt}}{\dot{m}_f x_{fuel}} = \frac{(250 \text{ kW}) \left(\frac{\text{kJ}}{\text{kW-s}} \right)}{\left(0.02174 \frac{\text{kg}}{\text{s}} \right) \left(38,500 \frac{\text{kJ}}{\text{kg}} \right)} = \underline{0.299} = \underline{29.9\%} \quad (3.143)$$

Recall that the upper limit of the exergetic efficiency is 100%. Therefore, the result shown in Equation 3.143 substantiates the conclusion drawn by comparing the thermal efficiency with the Carnot efficiency.

The exergy flow rate entering the gas turbine system with the fuel is the denominator of Equation 3.143,

$$\dot{X}_{in} = \dot{m}_f x_{fuel} = \left(0.02174 \frac{\text{kg}}{\text{s}} \right) \left(38,500 \frac{\text{kJ}}{\text{kg}} \right) \left(\frac{\text{kW-s}}{\text{kJ}} \right) = \underline{837.0 \text{ kW}} \quad (3.144)$$

The exergy output rate of the cycle is the power delivered by the power turbine. Therefore,

$$\dot{X}_{out} = \dot{W}_{pt} = \underline{250.0 \text{ kW}} \quad (3.145)$$

To determine where the major losses are in the gas turbine system, a component-level exergy analysis will be conducted. The exergy balance, Equation 3.49, will be applied to each component to determine the exergy destruction rate. To quickly compute the exergy destruction rates, it is helpful to calculate the flow exergy values of the air at the five states in the system. This can be done using Equation 3.52 once the dead state is identified. Using the atmospheric conditions entering the compressor as the dead state, the dead state enthalpy and entropy are found to be $h_0 = 295.43 \text{ kJ/kg}$ and $s_0 = 6.8502 \text{ kJ/kg-K}$ (identical to State 1 in Table 3.6). Using these dead state values, and further assuming that kinetic and potential effects are negligible, the flow exergy at each state can be found. The results are added to the thermodynamic property table and shown in Table 3.7.

In the application of the exergy balance to the system components, the mass flow rate of the air is needed. The mass flow rate of the fuel and the AF have been previously found. Therefore, the mass flow rate of the air is,

$$\dot{m}_a = (AF)\dot{m}_f = (42.83) \left(0.02174 \frac{\text{kg}}{\text{s}} \right) = 0.93112 \frac{\text{kg}}{\text{s}} \quad (3.146)$$

In addition, the total flow rate at states 3, 4, and 5 can be computed,

$$\dot{m}_a + \dot{m}_f = \left(0.93112 + 0.02174 \frac{\text{kg}}{\text{s}} \right) = 0.95286 \frac{\text{kg}}{\text{s}} \quad (3.147)$$

TABLE 3.7

Thermodynamic Properties and Flow Exergy Values for the Gas Turbine System of Figure 3.22

State	<i>P</i> (kPa)	<i>T</i> (°C)	<i>h</i> (kJ/kg)	<i>s</i> (kJ/kg-K)	<i>x_f</i> (kJ/k)
1	101.325	22	295.43	6.8502	0
2s	526.9	198.3	473.84	6.8502	178.41
2	526.9	231.3	507.82	6.9198	191.83
3	526.9	1150	1544.3	8.0741	887.62
4s	281.1	949.9	1305.7	8.0741	649.06
4	281.1	976.2	1336.7	8.0992	672.67
5s	101.325	697.2	1012.9	8.0992	348.83
5	101.325	751.1	1074.4	8.1609	392.14

Applying the exergy balance to a system boundary surrounding the compressor allows for the calculation of the exergy destruction rate,

$$\dot{X}_{des,c} = \dot{W}_c + \dot{m}_a(x_{f1} - x_{f2}) = \dot{m}_a[(h_2 - h_1) + (x_{f1} - x_{f2})] = \underline{19.15 \text{ kW}} \quad (3.148)$$

Applying the exergy balance to a system boundary surrounding the combustion chamber,

$$\dot{X}_{des,cc} = \dot{m}_a x_{f2} + \dot{m}_f x_{fuel} - (\dot{m}_a + \dot{m}_{fuel})x_{f3} = \underline{169.8 \text{ kW}} \quad (3.149)$$

Likewise, for the gasifier turbine and power turbine,

$$\begin{aligned} \dot{X}_{des,gt} &= -\dot{W}_{gt} + (\dot{m}_a + \dot{m}_{fuel})(x_{f3} - x_{f4}) \\ &= (\dot{m}_a + \dot{m}_{fuel})[-(h_3 - h_4) + (x_{f3} - x_{f4})] = \underline{7.06 \text{ kW}} \end{aligned} \quad (3.150)$$

$$\dot{X}_{des,pt} = -\dot{W}_{pt} + (\dot{m}_a + \dot{m}_{fuel})(x_{f3} - x_{f4}) = \underline{17.36 \text{ kW}} \quad (3.151)$$

Equations 3.148 through 3.151 represent are the exergy destruction rates within the system components due to irreversibility such as fluid friction, mechanical friction, and heat transfer through a finite temperature difference. The sum of the system's exergy output rate and the component exergy destruction rates is 463.4 kW. However, the fuel is providing an exergy input rate of 837.0 kW. Somewhere, 373.6 kW of exergy is unaccounted for. Close investigation of the gas turbine system reveals that the flow leaving the power turbine is at the dead state pressure, but the temperature is quite high, $T_5 = 751.1^\circ\text{C}$. This represents a significant amount of exergy that is simply vented to the atmosphere. This rate of exergy *loss* from the system can be found by,

$$\dot{X}_{lost} = (\dot{m}_a + \dot{m}_{fuel})x_{f5} = \underline{373.6 \text{ kW}} \quad (3.152)$$

At this point, all of the exergy entering the system in the fuel is accounted for. Table 3.8 shows a summary of the distribution of the fuel's exergy input rate in the gas turbine system. This analysis reveals that the two largest contributors to the low exergetic efficiency

TABLE 3.8

Distribution of the Incoming Fuel Exergy in the Gas Turbine System

Exergy Rate	kW	% of Input
Entering with the fuel	837.0	—
Output of the gas turbine system	250.0	29.9%
Compressor destruction	19.1	2.3%
Combustion chamber destruction	169.8	20.3%
Gasifier turbine destruction	7.1	0.8%
Power turbine destruction	17.4	2.1%
Lost leaving the power turbine	373.6	44.6%

of the system are the exergy destruction rate in the combustion chamber and the rate at which exergy is lost from the system leaving the power turbine. These two exergy transfer rates represent 64.9% of the fuel's exergy input rate to the system. The irreversibilities in the compressor and turbines are only a small part of the exergy destruction, totaling only 5.2% of the fuel's exergy input rate. This analysis provides a framework for the engineer to consider modifications to the system to reduce the exergy destruction and loss by focusing on the two major contributors; the combustion chamber and the exergy vented to the atmosphere at the exhaust of the power turbine.

The combustion process is inherently irreversible. Research into new combustion methods may eventually result in reducing the exergy destruction in a combustion chamber. However, the improvement is likely to be small. The exergy destruction rate in the combustion process is something that engineers must accept. The largest waste of the exergy resource in the gas turbine system analyzed here is venting the hot combustion products to the atmosphere. There are many other uses for this wasted exergy and if they are implemented in a larger scheme (e.g., using the hot combustion gases to provide space heating and/or water heating), then the *system* must be expanded and analyzed to include the additional equipment. This will result in higher exergetic efficiency and a more favorable

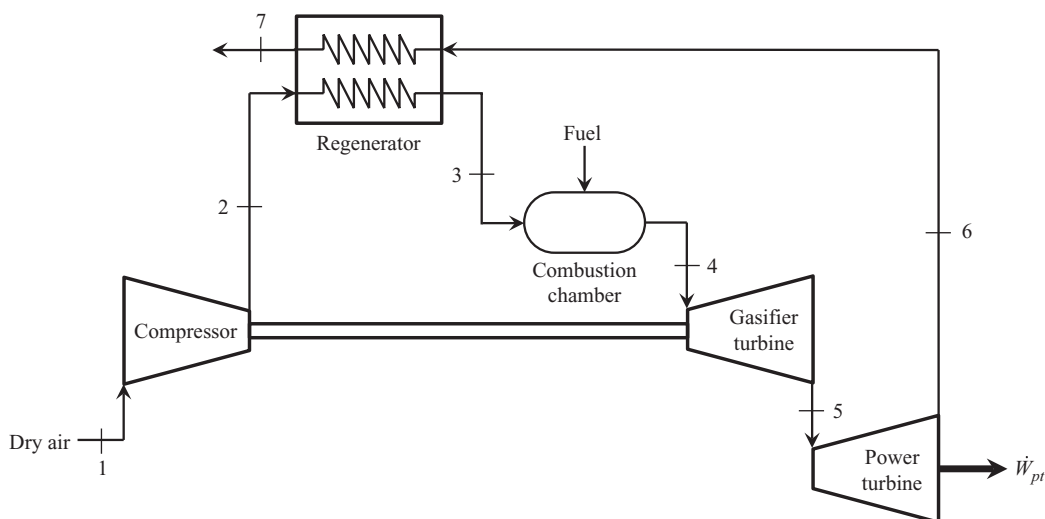


FIGURE 3.23

A gas turbine cycle with a regenerator used to preheat the combustion air.

view of the system as whole. Another possibility is to redesign the gas turbine system itself and use the hot combustion gases to preheat the air entering the combustion chamber, as shown in Figure 3.23. The heat exchanger used to preheat the combustion air is known as a *regenerator*. The regenerator is an effective way to capture the otherwise lost exergy at the power turbine exhaust and transfer it back into the system resulting in higher thermal and exergetic efficiencies; a better use of the fuel's exergy resource.

References

- Cengel, Y. and Boles, M.A. 2011. *Thermodynamics: An Engineering Approach*. New York: McGraw-Hill.
- Klein, S. and Nellis, G. 2012. *Thermodynamics*. Cambridge: Cambridge University Press.
- Moran, M.J., Shapiro, H.N., Boettner, D.D., and Bailey, M.B. 2014. *Fundamentals of Engineering Thermodynamics*. 8th ed. John Wiley & Sons.

Problems

Conservation and Balance Laws

- 3.1 The open water tank shown in Figure P3.1 is filled through Pipe 1 with a velocity of 7 ft/s and through Pipe 3 at a volumetric flow rate of $0.2 \text{ ft}^3/\text{s}$.
- Determine the velocity through Pipe 2 required to maintain a constant water level, H .
 - If the valve in Pipe 1 is suddenly opened to allow a velocity of 12 ft/s, find the instantaneous rate of change of the depth in the tank with time, dH/dt .
- 3.2 Water enters the rigid, covered tank shown in Figure P3.2 with a volumetric flow rate of 0.32 L/s . The water line has an inside diameter of 6.3 cm. The air vent on the tank has an inside diameter of 4.5 cm. The water is at a temperature of 30°C and the air in the tank is at atmospheric pressure (1 atm) and 30°C . Determine the air velocity leaving the vent at the instant shown in the figure.

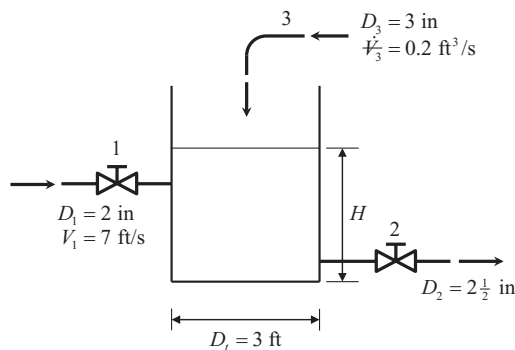
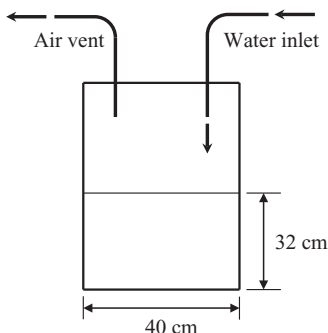


FIGURE P3.1

Water tank with two inlets and one outlet.

**FIGURE P3.2**

Water entering a partially filled, closed tank.

- 3.3 Refrigerant 134a enters a tube in the evaporator of a refrigeration system at 132.73 kPa and a quality of 0.15 at a velocity of 0.5 m/s. The R134a exits the tube as a saturated vapor at -21°C . The tube has an inside diameter of 3.88 cm. Determine the following,
- The pressure drop of the R134a as it flows through the tube (kPa)
 - The volumetric flow rate at the inlet of the tube (L/s)
 - The mass flow rate of the refrigerant through the tube (g/s)
 - The volumetric flow rate at the exit of the tube (L/s)
 - The velocity of the refrigerant at the exit of the tube (m/s)
 - The heat transfer rate to the refrigerant (kW) as it flows through the tube
- 3.4 A pressurized propane tank is fitted with a valve on top that allows saturated vapor to escape when the valve is opened. When the valve is first opened, the mass flow rate of the propane leaving the tank is 0.05 kg/s. As the propane vapor escapes, the mass flow rate varies with time according to the following relationship,

$$\dot{m}_e = \dot{m}_{e,initial} e^{-at}$$

where t is in seconds, and $a = 0.01 \text{ s}^{-1}$. Determine how long the valve must be open to allow 3 kg of propane vapor to escape from the tank.

- 3.5 Water enters a tank through a 10-cm diameter pipe at a velocity of 3 m/s, as shown in Figure P3.5. At the bottom of the tank, water exits at 6 m/s through a 5.25-cm diameter pipe. The depth of the water in the tank is 1.5 m. The tank has a diameter of 1.25 m and a height of 2.5 m. Determine how long it will take for the tank to either overflow or drain.
- 3.6 Refrigeration systems incorporate an expansion process between the condenser and evaporator. Consider the case where Refrigerant 134a enters an expansion valve as a saturated liquid at 65°C with a mass flow rate of 6 kg/min and is steadily throttled to a pressure of 1 bar.
- Determine the rate of entropy production for this process (in kW/K)
 - Determine the rate of exergy destruction for this process (kW). The dead state can be taken to be $T_0 = 25^{\circ}\text{C}$.
 - If the valve were replaced by a power-recovery turbine operating at steady state, determine the maximum theoretical power that could be developed (in kW)

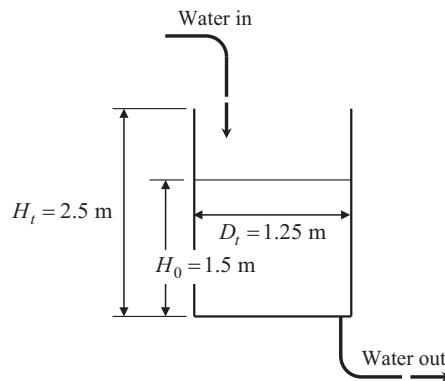


FIGURE P3.5
Water tank with a drain.

3.7 Air enters the adiabatic nozzle of a turbojet engine at 230 kPa, 600°C with a velocity of 60 m/s as shown in Figure P3.7. At the nozzle exit, the air is at 70 kPa, 450°C. The dead state is 100 kPa, 20°C. Determine the following information,

- The exit velocity of the air (m/s)
- The isentropic efficiency of the nozzle
- The exergy destruction per kg of air flowing through the nozzle (kJ/kg)
- Devise and calculate an exergetic efficiency for the nozzle

3.8 An industrial facility needs a flow of 100 gpm of hot water at 180°F, 50 psia. Two designs are being considered to make the hot water as shown in Figure P3.8. In Design 1, the hot water is produced by injecting steam into an insulated



FIGURE P3.7
Nozzle of a turbojet engine.

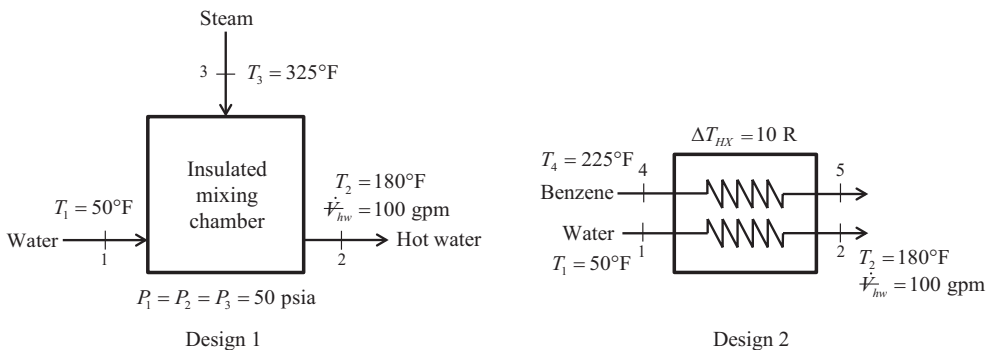


FIGURE P3.8
Two designs for producing hot water.

mixing chamber through which the water passes. The water enters the chamber at 50°F, 50 psia. Steam is injected into the chamber at 325°F, 50 psia. The hot water leaves at the required flow rate and temperature. For this system determine,

- The mass flow rate of the water entering the chamber (lbm/h)
- The mass flow rate of the steam injected into the chamber (lbm/h)
- The exergy destruction rate in the chamber (Btu/h)
- The exergetic efficiency of the chamber

The second design, Design 2, the water is heated in a heat exchanger with a stream of hot liquid benzene that is available from another process in the facility. The heat exchanger is a parallel flow configuration with a pinch point temperature difference of 10°R. The water enters the heat exchanger at 50°F and leaves at the required flow rate and temperature. The hot benzene enters the heat exchanger at 225°F. For this system determine,

- The required mass flow rate of the benzene (lbm/h)
- The exergy destruction rate in the heat exchanger
- The exergetic efficiency of the heat exchanger
- The effectiveness of the heat exchanger

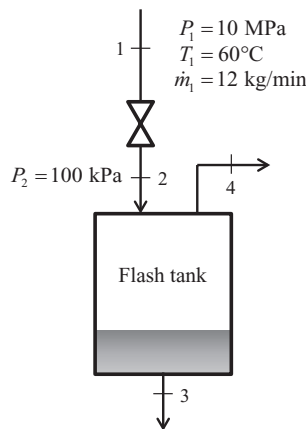
Assuming that the steam and hot benzene flows are readily available in the facility, discuss the tradeoffs between energy, exergy, and economics relating to these two designs.

- 3.9 Dry atmospheric air enters an adiabatic compressor at a 20°C, 1 atm and a mass flow rate of 0.3 kg/s. The air is compressed to 1 MPa. The exhaust temperature of the air is 70 degrees hotter compared to the exhaust of an isentropic compression. Determine,
- The exhaust temperature of the air (°C)
 - The volumetric flow rate (L/s) at the inlet and exhaust of the compressor
 - The power required to accomplish the compression (kW)
 - The isentropic efficiency of the compressor
 - An accounting of the exergy entering the compressor (complete Table P3.9) assuming that the dead state is the same as State 1 (dry atmospheric air)
 - The exergetic efficiency of the compressor
- 3.10 A flash tank is a common component found in refrigeration systems. A refrigerant enters the flash tank as a wet mixture. The saturated liquid portion of the

TABLE P3.9

Exergy Accounting for Part (e)

Exergy Rate	kW	% of Input
Exergy rate input to the compressor		
Flow exergy rate increase of the air		
Exergy destruction rate in the compressor		
TOTAL =		100%

**FIGURE P3.10**

Ammonia flash tank in a refrigeration system.

flow is drawn off at the bottom of the tank and the saturated vapor leaves at the top. Consider the flash tank shown in Figure P3.10. The refrigerant is ammonia and it enters an expansion valve at 10 MPa, 60°C with a flow rate of 12 kg/min and is throttled to a pressure of 100 kPa before it enters an insulated flash tank. Determine,

- The temperature of the ammonia entering the flash tank
- The mass flow rate of the saturated liquid and saturated vapor leaving the tank (kg/min)

Now, consider the case where the flash tank has been in operation for several years and its insulation layer has degenerated causing heat to be transferred to the tank at a rate of 20 kW. Under this condition, determine,

- The mass flow rate of the saturated liquid and saturated vapor leaving the tank (kg/min)
- Two streams of dry air come together and mix in an insulated mixing box. One of the air flows enters the mixing box at 60°F with a volumetric flow rate of 400 cfm. The second stream enters the mixing box at 130°F at 600 cfm. The mixed air leaves the mixing box at a rate sufficient to maintain a steady state. The pressure throughout the system is atmospheric (1 atm). Determine the,
 - Temperature of the mixed air stream leaving the mixing box (°F)
 - Entropy generation rate associated with the mixing process (Btu/min-°R)
 - Exergy destruction rate for the mixing box assuming that the dead state conditions are atmospheric; 70°F, 1 atm (Btu/min)
 - Dry atmospheric air (70°F, 1 atm) enters a compressor at a flow rate of 120 lbm/h. The inlet pipe on the compressor has an inside diameter of 0.5 inch. The air leaves the compressor at 175 psia, 100°F. The diameter of the exit pipe leaving the compressor is large compared with the inlet pipe. Therefore, the kinetic energy of the exit flow is negligible, but the inlet kinetic energy is not. The power input to the compressor is 4.75 hp. Determine,

- The heat transfer rate for the compressor (Btu/h). Is this heat transferred to the compressor or from the compressor?
- The increase in the flow exergy rate of the air as it flows through the compressor (Btu/h)
- The exergetic efficiency of the compressor

If the compressor was adiabatic and operated with an isentropic efficiency of 80%, determine,

- The power input to the adiabatic compressor (hp)
 - The increase in the flow exergy rate of the air as it flows through the adiabatic compressor (Btu/h)
 - The exergetic efficiency of the adiabatic compressor
- 3.13 A pump is being used to move a liquid 30% ethylene glycol-water solution. The pump is connected to a pipe system as shown in Figure P3.13. The pressure on the suction side of the pump is 70 kPa. The pressure at the outlet of the pipe, which is 5 m above the pump discharge, is 550 kPa. The ethylene glycol solution is at a constant temperature of 20°C. The power input to the pump is 10 kW. Determine,
- The volumetric flow rate of the ethylene glycol solution (L/s)
 - The percentage of the pump power input that is required to raise the fluid's pressure from 70 kPa to 550 kPa
 - The percentage of the pump power input that is required to lift the fluid through an elevation of 5 m.

Hint: After writing the conservation of energy equation for the system boundary extending from Point 1 to Point 2, rewrite the enthalpy terms by substituting $h = u + Pv$ and applying the incompressible fluid model.

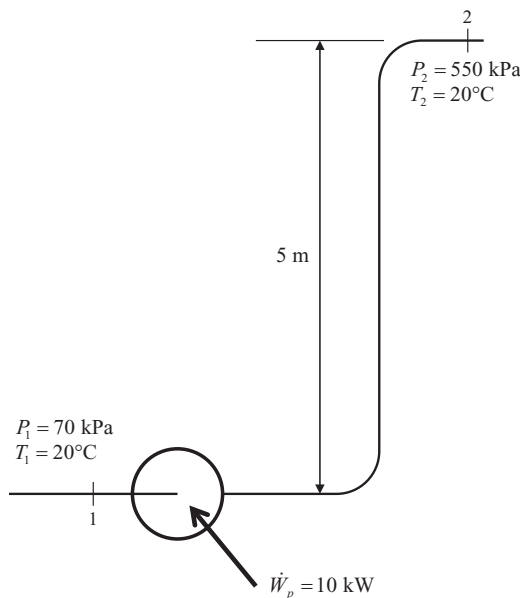


FIGURE P3.13

A pump and pipe system.

- 3.14 A counter flow heat exchanger is being used to cool a flow of cyclohexane from 110°C to 62°C. The cyclohexane enters the heat exchanger at a flow rate of 14 L/s. The cyclohexane is cooled by water entering the heat exchanger at 48°C with a flow rate of 10 L/s. Determine,
- The outlet temperature of the water
 - The pinch point temperature difference and its location (hot or cold end)
 - The effectiveness of the heat exchanger
 - The exergetic efficiency of the heat exchanger if the dead state temperature is 20°C

The effectiveness of a counter flow heat exchanger is related to the heat transfer surface area by the following relationship,

$$\varepsilon = \frac{1 - \exp \left[-\frac{UA}{\dot{C}_{\min}} \left(1 - \frac{\dot{C}_{\min}}{\dot{C}_{\max}} \right) \right]}{1 - \left(\frac{\dot{C}_{\min}}{\dot{C}_{\max}} \right) \exp \left[-\frac{UA}{\dot{C}_{\min}} \left(1 - \frac{\dot{C}_{\min}}{\dot{C}_{\max}} \right) \right]}$$

- Determine the UA product for this heat exchanger (kW/K)

Energy and Exergy Analysis of Thermal Energy Cycles

- 3.15 A household refrigerator-freezer sold in the U.S. has a refrigeration capacity of 0.14 ton. The Energy Star label on the refrigerator indicates that it has an EER of 10.8. Determine,
- The power draw of the refrigerator (W)
 - The cooling coefficient of performance of the refrigerator
- Modern refrigerator-freezers have compressors that are designed to operate 80% of the time. If the cost of electricity is 0.08 \$/kWh, determine,
- The annual cost of running the refrigerator
- 3.16 A steam power plant has an instantaneous net power delivery of 462 MW with a heat rate of 11,827 Btu/kWh. For this operating condition determine,
- The boiler heat transfer rate (MBtu/hr)
 - The thermal efficiency of the cycle
- The heating value of the coal used in this power plant is 28,300 kJ/kg. If the plant operates continuously (24 hr/day) at the rate defined above, determine,
- The number of tons of coal required per day
- 3.17 The initial stages of a power plant design involve analyzing the plant from a cyclic perspective. Consider a steam cycle power plant with a net power output of 1000 MW and an estimated thermal efficiency of 28%. Heat is transferred to the cycle from a reservoir at 800 K and rejected from the cycle to a reservoir at 275 K. If the heat transfers to and from the cycle are considered reversible (an ideal scenario) and the dead state temperature is 275 K, determine,
- The exergy destruction rate of the power plant (MW)

Assume that the power output, thermal efficiency, and reservoir temperatures remain the same but the model is now modified to make it more realistic. Consider the case where the power plant receives heat at 740 K and rejects heat at 300 K. In other words, the heat transfers now occur due to a finite temperature difference making them irreversible. For this modified model determine,

- b. The exergy destruction rate for the high temperature heat transfer process (MW)
- c. The exergy destruction rate of the power plant (MW)
- d. The exergy destruction rate for the low temperature heat transfer process (MW)
- e. The sum of parts (b), (c), and (d). How does this compare to the result computed for part (a)?

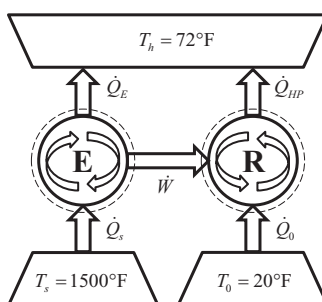
From the viewpoint of one of the power plant design engineers, what does the preceding analysis reveal?

- 3.18 A heat pump is operating between a low temperature reservoir of 270 K and a high temperature reservoir of 340 K. The heat pump receives heat at 255 K from the low temperature reservoir and rejects heat at 355 K to the high temperature reservoir. The heating coefficient of performance of the heat pump is 3.2. The heat transfer rate from the low temperature reservoir is 30 kW. The dead state temperature is 270 K. Determine the,

- a. Power input to the heat pump (kW)
- b. Heat transfer rate to the high-temperature reservoir (kW)
- c. Exergy destruction rate associated with the low temperature heat transfer (kW)
- d. Exergy destruction rate of the heat pump (kW)
- e. Exergy destruction rate associated with the high temperature heat transfer (kW)
- f. Exergetic efficiency of the heat pump itself

- 3.19 An engineer wishing to live off the grid has devised a scheme for heating a residence. The system is a small engine that directly drives a heat pump. This system is shown schematically in Figure P3.19. The engine receives heat from a combustion process at 1500°F and rejects heat to the house which is at a temperature of 72°F. All of the power delivered by the engine drives the heat pump, which receives heat from the environment at 20°F and rejects it to the house. The total heat transfer rate required to maintain the house at 72°F is 65,000 Btu/h. This is provided by the engine and the heat pump. To determine the best possible performance for this system, consider the case where both the engine and the heat pump are operating at the maximum possible thermal efficiency. For this ideal heating system determine the,

- a. Heat transfer rate from the combustion source to the engine (Btu/h)
- b. Heat transfer rate from the outdoor source to the heat pump (Btu/h)
- c. Heat transfer rate from the engine to the house (Btu/h)
- d. Heat transfer rate from the heat pump to the house (Btu/h)
- e. Power required to run the heat pump (hp)

**FIGURE P3.19**

An off-the-grid residential heating system.

- f. Devise and calculate the overall thermal efficiency of this system keeping in mind that the energy transfer from the environment to the heat pump is a “free” energy source.

In an effort to make a more realistic estimation of this system’s performance recalculate parts (a) through (f) assuming that the engine has a thermal efficiency of 36% and the heat pump has a coefficient of performance of 3.50. What is your engineering assessment of this off-the-grid heating system?

- 3.20 Show that the COP_C and the COP_H of a refrigeration cycle are related by the following expression,

$$COP_H = COP_C + 1$$

Start with a sketch of the refrigeration cycle as shown in Figure 3.10 to develop your solution.

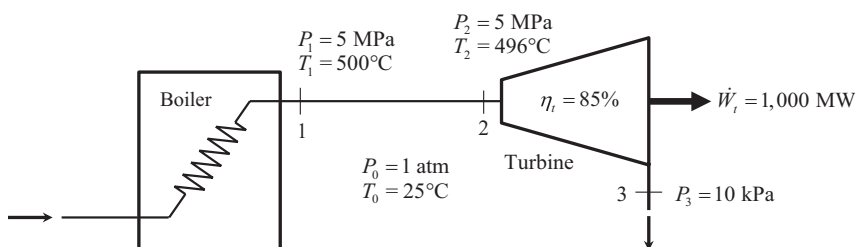
- 3.21 A refrigeration cycle is operating as a heat pump. The source temperature is at the dead state, T_0 , and the sink is at T_H . Show that the exergetic efficiency of this heat pump cycle can be written as,

$$\eta_{x, hp} = \frac{Q_H}{W_{cycle}} \left(1 - \frac{T_0}{T_H} \right) = \frac{COP_H}{COP_{H, Carnot}}$$

Analysis of Thermal Energy Systems

(The following problems are best suited for solution using computer software.)

- 3.22 Steam leaves the boiler of a power plant at 5 MPa, 500°C as shown in Figure P3.22. As the steam passes to the turbine, the temperature drops to 496°C before it enters the turbine due to a heat loss through the pipe’s insulation. The pressure drop in the pipe connecting the boiler to the turbine is negligible. The steam then passes through an adiabatic turbine and exits at 10 kPa. The turbine has an isentropic efficiency of 85% and is delivering 1000 MW of power. Determine the following,

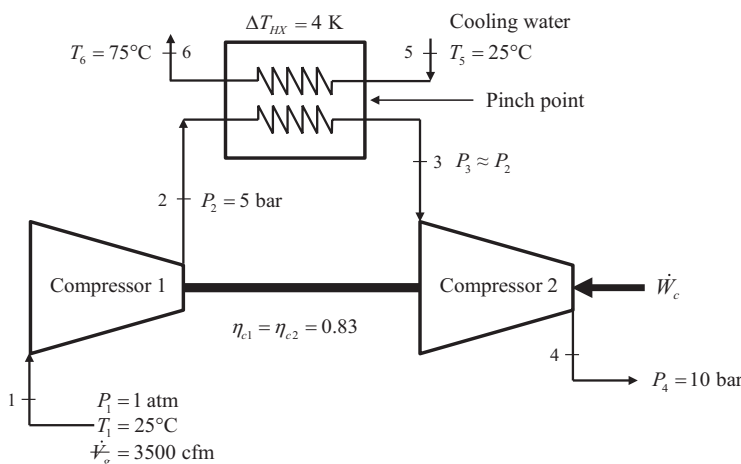
**FIGURE P3.22**

Boiler and turbine of a steam power plant.

- The heat transfer rate from the pipe connecting the boiler to the turbine (in MW)
 - The change in flow exergy rate as the steam flows through the pipe (MW). This represents exergy that is lost to the environment and unavailable for power delivery. Comment on the magnitude of this exergy loss compared to the power delivered by the turbine. What factor(s) would warrant better insulation on the pipe to reduce this exergy loss?
- 3.23 A two-stage air compressor with inter-stage cooling is shown in Figure P3.23. The dry air enters the first compressor stage at 1 atm, 25°C, a volumetric flow rate of 3500 cfm, and is compressed to 5 bar. The air then passes through a heat exchanger with no appreciable drop in pressure, after which, it is compressed in the second stage to 10 bar. The isentropic efficiency of both compression stages is 83%. The heat exchanger is a counter flow heat exchanger where the air is being cooled by water. The water enters the heat exchanger at 20°C and exits at 75°C. The pinch point temperature difference of the heat exchanger is 4 K and the pinch point occurs on the cold end.

Determine the following,

- The volumetric flow rate of the cooling water entering the heat exchanger (gpm)
- The total power draw of both compressors (kW)
- Investigate the effect of the intermediate pressure P_2 by constructing a plot that shows the total power draw as a function of P_2 for the range, $2 \text{ bar} \leq P_2 \leq 5 \text{ bar}$

**FIGURE P3.23**

Two-stage air compressor with inter-stage cooling.

- d. One reason for multistage compression with intercooling is to reduce the total power requirement in an overall compression process. Verify that this idea is correct by calculating the power draw for a single compressor used to compress 3500 cfm of air from 1 bar to 10 bar with an isentropic efficiency of 83%.
- 3.24 Consider the two-stage air compressor with inter-stage cooling described in Problem 3.23. For this thermal system determine the following,
- The exergy destruction rate in each component (kW)
 - The exergetic efficiency of each component.

The dead state can be considered as atmospheric conditions; 1 atm, 25°C.

- 3.25 An industrial furnace used to heat treat carbon steel is shown in Figure P3.25A. The carbon steel stock ($c_{ps} = 0.12$ Btu/lbm-R) passes through the furnace at a rate of 13,200 lbm/h. The steel enters the furnace at 70°F and exits at 550°F. The furnace is fueled by natural gas. The density of the fuel entering the furnace is 0.0456 lbm/ft³ and its heat of combustion is 23,000 Btu/lbm. Dry air for combustion is drawn into the furnace at 70°F. The furnace is operating with a mass-based air-fuel ratio of 33. Hot combustion products leave the furnace at 1100°F. The pressure throughout the system can be assumed to be 1 atm everywhere.

Determine the,

- Volumetric flow rate of the fuel (cfm)
- Cost to run the furnace per day (assuming continuous 24-hour operation) if the industrial cost of natural gas is \$4.90 per 1000 ft³
- Thermal efficiency of the furnace

In an effort to increase the thermal efficiency and save money on fuel costs, it is proposed that a counter flow heat exchanger be used to preheat the dry air entering the furnace as shown in Figure P3.25B. The heat exchanger utilizes the hot combustion products as an energy source to preheat the air entering the furnace. The temperature of the combustion products must be kept well above the dew point temperature to avoid acidic condensation in the heat exchanger. The system designer has specified that this temperature must be no lower than 300°F.

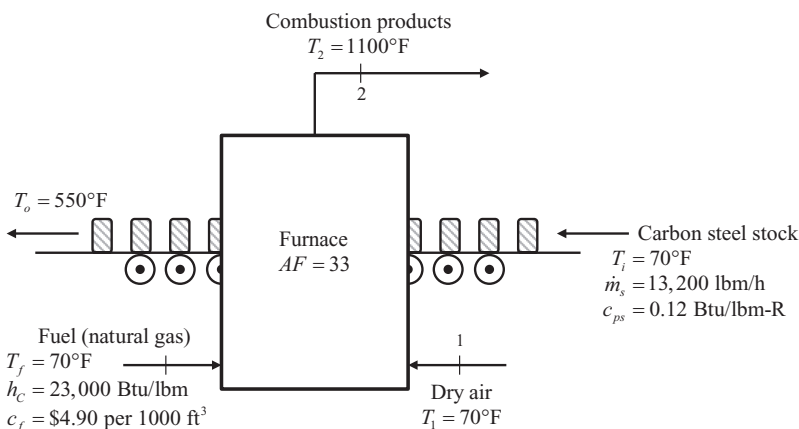
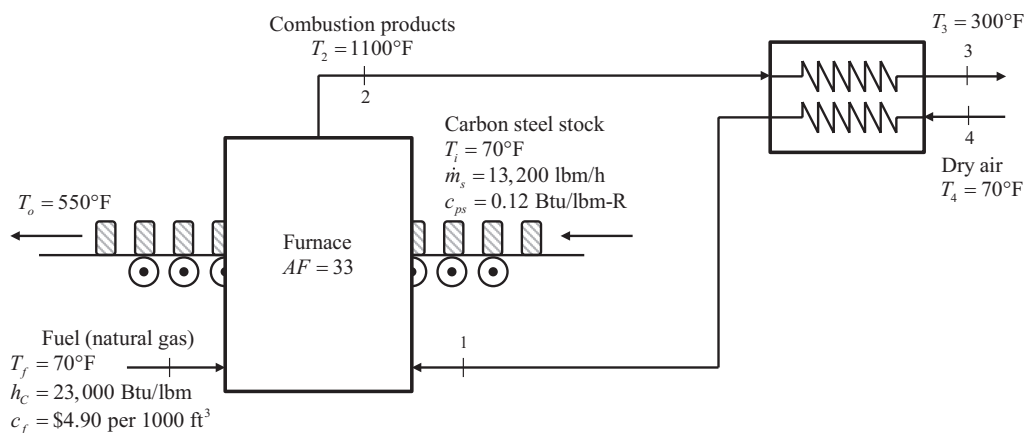


FIGURE P3.25A

Carbon steel heat treating furnace.

**FIGURE P3.25B**

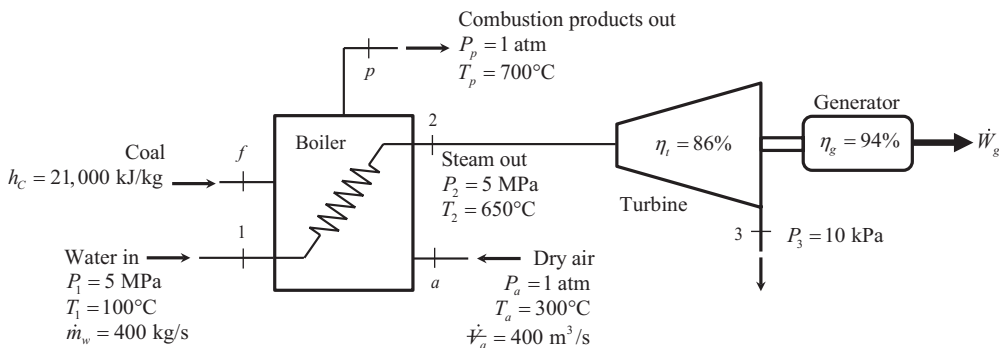
Carbon steel heat treating furnace with air preheater.

With this heat exchanger added to the system, compute the quantities in (a), (b), and (c) above and compare the results with the values for the furnace without the preheater. In addition, determine,

d. The effectiveness of the heat exchanger for this system

- 3.26 Figure P3.26 shows a boiler and turbine from a coal-fired steam power plant. Water enters the boiler at 5 MPa, 100°C at a mass flow rate of 400 kg/s. Steam leaves the boiler at 5 MPa, 650°C . The steam then passes through a turbine with an isentropic efficiency of 86% and exhausts to a pressure of 10 kPa. The turbine is connected to an electrical generator with an efficiency of 94%. The boiler is fired using coal with a heat of combustion of 21,000 kJ/kg. The coal is combusted with dry atmospheric air entering the furnace after passing through a preheater. The air enters the furnace at 1 atm, 300°C at a volumetric flow rate of $400 \text{ m}^3/\text{s}$. The products of combustion leave the furnace at 1 atm, 700°C . Determine the

- Power delivered by the electrical generator (MW)
- Mass-based air-fuel ratio in the boiler

**FIGURE P3.26**

Boiler and turbine in a steam power plant.

- c. Total mass of coal used in one year, assuming the plant runs continuously all year long and the power delivery is constant at the value computed in part (a). Express your answer in tons.

The cost of delivered coal to the plant is \$48.52/ton, and the utility company sells energy at a rate of \$0.10/kWh. Assuming that the power delivery remains constant year-round at the value computed in part (a), and all of the energy delivered by the generator can be sold, determine the following,

- d. The annual cost of coal to operate the power plant
 e. The annual income realized from the sale of energy delivered by the generator
 f. The annual profit made by the utility company due to the sale of energy
- 3.27 In the manufacture of paper, large amounts of electricity, process steam, and hot water are required. While these three needs could be met by individual thermal energy systems, it is prudent to develop a *single* system that can provide all three needs with one fuel source. A thermodynamic cycle that accomplishes this is called a *cogeneration* cycle. Consider a cogeneration cycle in a paper mill as shown in Figure P3.27. A fuel is combusted in the boiler and steam is produced at 600 psia, 700°F. This steam runs through a high-pressure turbine with an isentropic efficiency of 78% and exhausts to a pressure of 170 psia. At the high-pressure turbine exhaust, 50,000 lbm/hr of steam are extracted for process heating (labeled *cogen* in Figure P3.27). The process steam makes its way through several heating processes in the mill and condenses to 18 psia, 180°F. This flow is then combined with saturated liquid water leaving the condenser before being pumped back into the boiler.

The balance of the steam from the high-pressure turbine exhaust passes through the low-pressure turbine and exhausts at a pressure of 20 psia. The isentropic

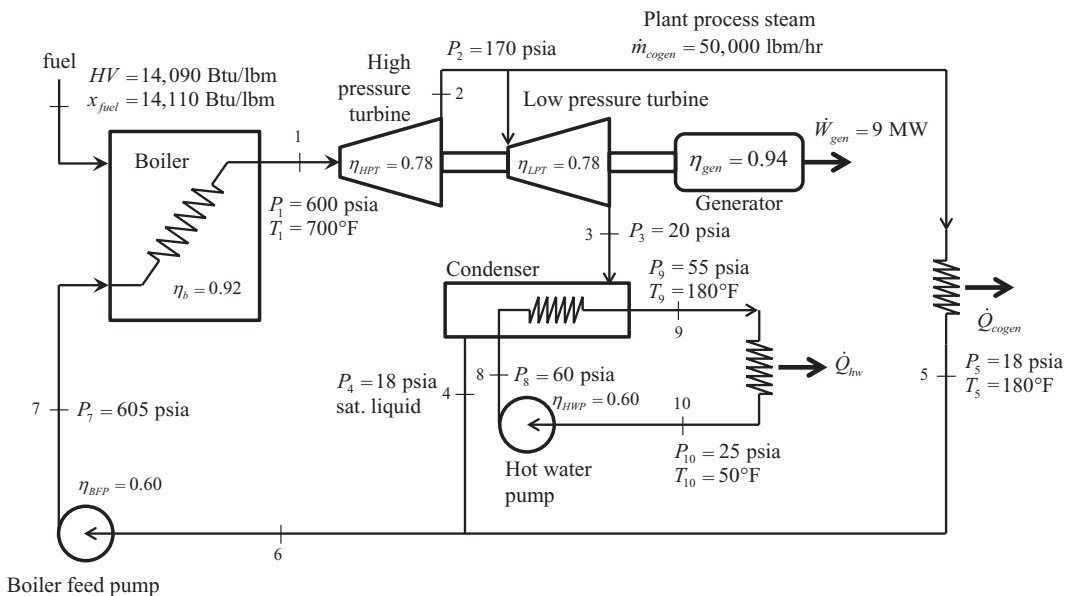


FIGURE P3.27

A cogeneration cycle for a paper mill.

efficiency of the low-pressure turbine is 78%. The turbines deliver power to an electrical generator that has an efficiency of 94%. The generator delivers 9 MW of power to the mill. This power is used for all mill operations including the operation of the pumps in the cogeneration cycle.

The low-pressure turbine exhaust is purposely kept high so the plant hot water needs can be satisfied. The plant hot water enters the condenser at 60 psia and exits at 55 psia, 180°F. The hot water returns from the mill at 25 psia, 50°F before being pumped to 60 psia through the hot water pump that has an isentropic efficiency of 72%. After the saturated liquid from the condenser and hot water from the process heating combine, they pass through the boiler feed pump with an isentropic efficiency of 60%. The boiler feed pump isentropic efficiency is 60% and the water exits at a pressure of 605 psia. The fuel used in the boiler is natural gas with heating value (HV) of 14,090 Btu/lbm and an exergy content of 14,110 Btu/lbm. The boiler has an efficiency of 92%.

Determine the,

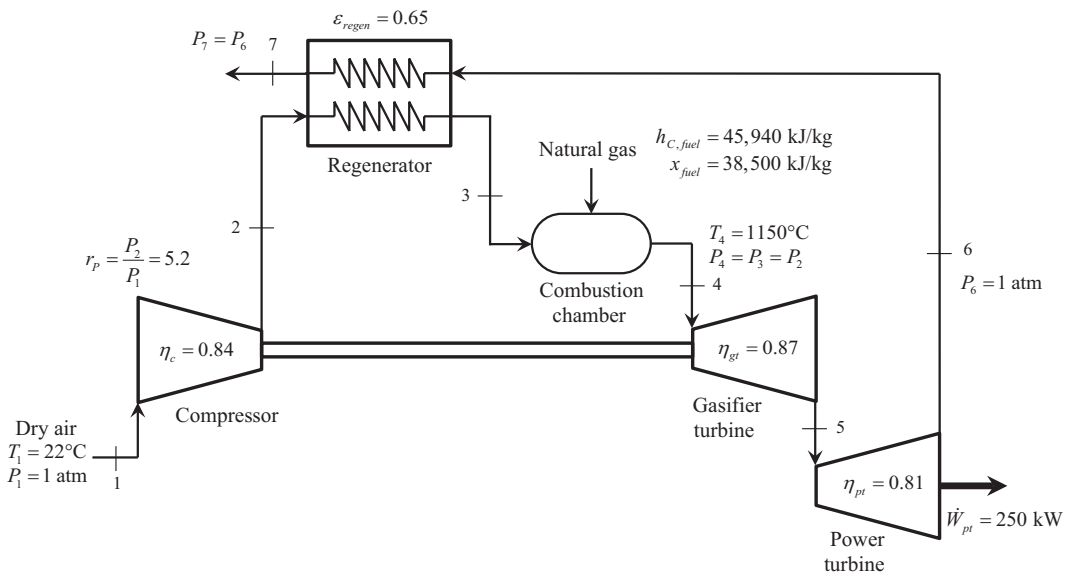
- Mass flow rate of the steam passing through the high-pressure turbine (lbm/hr).
- Mass flow rate of steam passing through the low-pressure turbine (lbm/hr)
- Mass flow rate of the hot water delivered to the plant (lbm/hr)
- Required mass flow rate of the fuel (lbm/hr)
- Heat transfer rate that is provided to the mill by the process steam (Btu/hr)
- Heat transfer rate that is provided to the mill by the hot water (Btu/h)
- Thermal efficiency of the cycle based on (energy sought)/(energy that costs)
- Exergy transfer rate from the exergy resource input to the cycle (Btu/hr)
- Exergy transfer rate representing the exergy task of the cycle (Btu/hr). When considering the exergy task associated with the heat transfers from the cogeneration cycle, it will be difficult to determine the exergy transfer rate associated with the heat transfers because the boundary temperatures are unknown. Therefore, when considering the exergy task associated with the heat transfers, assume the task to be the decrease in flow exergy of the water as it passes through each process.
- Exergetic efficiency of the cycle based on the (exergy task)/(exergy resource)

You should discover that the thermal efficiency of this cycle is very high, but the exergetic efficiency is very low. What you have discovered is that this cogeneration cycle is very good at utilizing energy but is not doing so well with the exergy it has been given by the fuel. To decipher why this is happening, determine the following,

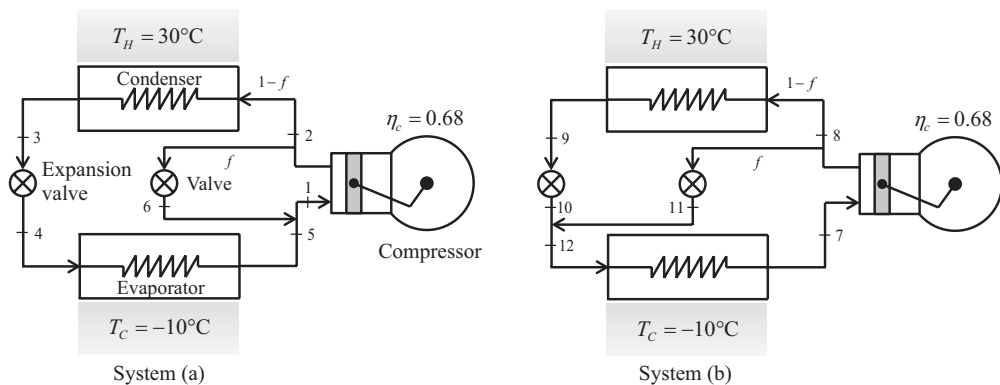
- The exergy destruction rate in the boiler, high pressure turbine, low pressure turbine, condenser, boiler feed pump, and hot water pump (Btu/hr)
- Now, convert the exergy destruction answers in parts (k) to a percent of the exergy resource input rate to the cycle,

$$\%X_{des,component} = 100\% \left(\frac{\dot{X}_{des,component}}{\dot{X}_{resource}} \right)$$

- m. The result of this problem demonstrates the energy/exergy conundrum. Based on the results of your analysis, you should have discovered that the boiler exergy destruction rate is responsible for the low exergetic efficiency of the system. What do you think is causing this large exergy destruction rate? Is there anything that the engineer can do to reduce the exergy destruction in the boiler and increase the exergetic efficiency of the cycle? Is it possible to make the exergetic efficiency better and resolve the energy/exergy conundrum?
- 3.28 Consider the gas turbine system analyzed in Section 3.10.3. The system is modified to include a regenerator as shown in Figure P3.28. The regenerator is a counter flow heat exchanger and has an effectiveness of 0.65. The other operating parameters are the same as in Section 3.10.3 and have been repeated in Figure P3.28. For this modified gas turbine system determine,
- The mass-based air-fuel ratio (AF)
 - The specific fuel consumption (kg/kWh)
 - The thermal efficiency of the system
 - The exergetic efficiency of the system
 - The exergy accounting of the fuel's input exergy transfer rate to the system.
- Construct a table similar to Table 3.8, adding a line for the exergy destruction rate in the regenerator.
- 3.29 Refrigeration equipment is often installed with more cooling capacity than is needed. The best way to operate the equipment when the cooling load is lower than the capacity is to reduce the compressor speed with a variable speed motor. However, variable speed motors and controllers can be quite expensive. In lieu of a variable speed motor, the capacity of the refrigeration cycle can be controlled using a refrigerant bypass line. Figure P3.29 shows two possible ways of accomplishing

**FIGURE P3.28**

Gas turbine system with regenerator.

**FIGURE P3.29**

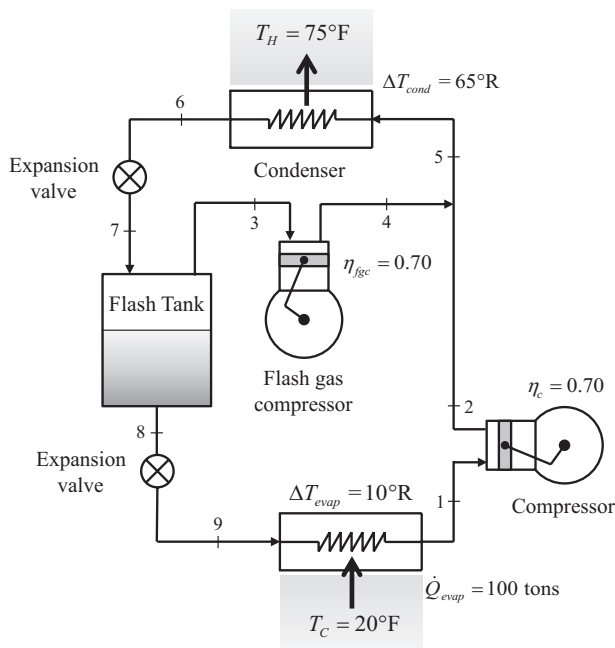
Two possible scenarios for refrigeration capacity control.

this. Both systems are based on a standard vapor compression refrigeration cycle. System (a) recycles a fraction, f , of the compressor discharge back to the compressor suction line. System (b) directs a fraction, f , of the compressor discharge to the evaporator inlet.

Other than the bypass modification, both systems are identical in every other respect; the cold space is being maintained at -10°C while the condenser sink temperature is 30°C , the refrigerant is ammonia, and the compressor isentropic efficiency is 68%. The refrigerant leaving the evaporator is a saturated vapor at -15°C . Leaving the condenser, the refrigerant is a saturated liquid at 40°C . The compressor is a single speed reciprocating compressor with a volumetric efficiency of 75%. The volumetric displacement rate of the compressor is 20 L/s. The volumetric efficiency of a reciprocating compressor is defined as,

$$\eta_{\text{vol}} = \frac{\text{volumetric flow rate at the suction port of the compressor}}{\text{volumetric displacement rate of the compressor}} = \frac{\dot{V}_{\text{suction}}}{\dot{V}_{\text{displacement}}}$$

- Determine the cooling capacity (tons), the cooling COP, HPT, and exergetic efficiency when the bypass is closed (i.e., determine these performance parameters for a standard vapor compression refrigeration cycle operating at the given conditions). The dead state can be taken as 1 atm, $T_0 = T_H = 30^{\circ}\text{C}$.
 - Determine the value of f at which the cooling capacity is 80% of the full-load value found in part (a) for both systems. Calculate the quantities indicated in part (a) for each system under this part-load scenario.
 - Which capacity control system do you recommend and why?
- 3.30 A multistage vapor compression refrigeration system with flash gas removal is being used to maintain a cold space at $T_C = 20^{\circ}\text{F}$ for frozen food storage as shown in Figure P3.30. The system utilizes R134a as the working fluid. The cycle is providing 100 tons of cooling capacity to the cold space. Heat is rejected to the surroundings at $T_H = 75^{\circ}\text{F}$ in the condenser. The pinch point temperature differences for the condenser and evaporator are $\Delta T_{\text{cond}} = 65^{\circ}\text{R}$ and $\Delta T_{\text{evap}} = 10^{\circ}\text{R}$, respectively. The refrigerant enters the compressor as a saturated vapor and it leaves the condenser

**FIGURE P3.30**

A refrigeration system with flash gas removal.

as a saturated liquid. The isentropic efficiency of the main compressor is $\eta_c = 0.70$ and the isentropic efficiency of the flash gas compressor is $\eta_{fgc} = 0.72$. The flash tank is operating at an estimated optimum pressure given by,

$$P_{flash} = \sqrt{P_{high} P_{low}}$$

where P_{high} and P_{low} are the highest and lowest pressures in the system, respectively. For this system, determine the following,

- The total power draw of the compressors (hp)
- The cooling COP and HPT of the system

Verify that the flash gas removal cycle is more efficient than a single-stage vapor compression refrigeration cycle providing 100 tons of cooling and operating between T_C and T_H by calculating,

- The power draw of the compressor for the single-stage cycle (hp)
- The cooling COP and HPT of the single-stage system

The operating pressure of the flash tank is controlled by the expansion valve directly after the condenser. Modern expansion valves are adjustable, offering a wide range of pressure drops across the device,

- Investigate the effect of adjusting the expansion valve by constructing a plot that shows the cooling COP as a function of the flash tank pressure. You should discover that there is an optimum flash tank pressure. Is the flash tank pressure estimate a reasonable approximation to this optimum pressure?



Taylor & Francis

Taylor & Francis Group

<http://taylorandfrancis.com>

4

Fluid Transport in Thermal Energy Systems

4.1 Introduction

In thermal energy system analysis and design, the primary calculations involving fluid transport include the application of the conservation of mass, conservation of energy, and the determination of head losses in pipes, tubes, ducts, valves, and fittings. The conservation laws are presented in Chapter 3, Sections 3.5 and 3.6. The determination of pressure losses is based on energy conservation principles and presented in subsequent sections of this chapter. The flow of a fluid in a thermal energy system can be affected in one of two ways; gravity or forced by a pump. This chapter covers both types of fluid flow systems.

Fluid transport systems can be very simple or quite complex. Independent of the complexity of the design, the engineer strives to maintain a cost-optimized system. Piping systems that have large diameters may result in a very reasonable operating cost (e.g., small power requirements for pumps), but the capital cost of the pipe system may be prohibitive because of the large diameter. On the other hand, a pipe system with a small diameter may have a very reasonable capital cost, but the pumping costs may be overwhelming. Chapter 4 develops equations that can be used to optimize a piping system with respect to cost.

4.2 Piping and Tubing Standards

Pipes are generally designed for high-pressure service. They are made of a variety of materials including steel, cast iron, wrought iron, clay, or plastic. Independent of material, pipe sizes are standardized and are referenced based on their *nominal diameter*. The thickness of the pipe wall is designated by the *schedule* number. The steel pipe schedule is usually expressed as a number (e.g., schedule 40). Stainless steel pipe schedules are usually expressed with a “S” after the schedule (e.g., schedule 10S). For iron pipes, the pipe schedule is usually expressed as *std* (standard), *xs* (extra strong), or *xxs* (double extra strong). Pipes are specified based on their nominal diameter and schedule. For example, a pipe that is specified as “2-nom sch 40” has a nominal 2-inch diameter and the thickness of the pipe wall is consistent with the standard specified for schedule 40. Appendix C lists the standardized pipe dimensions.

Example 4.1

Determine the flow area and wall thickness of the following pipes; 3-nom sch 10S (stainless steel), 3-nom sch 40 (plain carbon steel), and 3-nom xxs (cast iron).

Solution

The flow area of the pipe is its cross-sectional area based on the inside diameter (ID) of the pipe,

$$A = \frac{\pi(ID)^2}{4}$$

The thickness of the wall of the pipe can be determined from the outside and inside diameters of the pipe,

$$th = \frac{OD - ID}{2}$$

Appendix C lists the standard outside and inside diameters of pipes. Using the expressions above, the flow area and thickness of each pipe can be found. The results are shown in Table E4.1.

TABLE E4.1Flow Area (A) and Wall Thickness (th)

Pipe	OD (in)	ID (in)	A (in ²)	th (in)
3-nom sch 10S	3.5	3.260	8.347	0.120
3-nom sch 40	3.5	3.068	7.393	0.216
3-nom xxs	3.5	2.300	4.155	0.600

This result indicates that all 3-nom pipes are not the same. They have different flow areas and wall thicknesses depending on the schedule.

Pipes can be connected by a variety of joints including threaded, flanged, welded, or bell and spigot. Joints for pipes that are 2-nom or smaller are often threaded. For pipes larger than 2-nom, the joints are often flanged or welded. In the bell and spigot joint, one end of the pipe is enlarged just enough to accept another pipe. In this type of joint, a gasket is used to keep a fluid-tight seal. Bell and spigot joints are usually used in larger-diameter iron and PVC pipes.

Tubing has thinner walls compared to an equivalent diameter pipe and are meant for low-pressure service. Tubing can be made of a variety of materials. The most common are copper, steel, and plastic. Tubing is specified by its *standard diameter* and its *type*. The type specification is analogous to the schedule specification in pipes. There are many tubing types available. The most common copper tubing types are K, L, and M. A type K tube has a thicker wall than a type L tube. Type L tubes are thicker-walled compared to a type M tube. Appendix D lists the dimensions of standard copper tubing. The various uses of the different types of copper tube are listed in Table 4.1.

Tubing can be joined and connected to fittings in a variety of ways including soldering and brazing. Other tubing fittings include compression fittings and flare fittings.

TABLE 4.1

Common Uses of Different Types of Copper Tubing

Application	K	L	M
Underground water distribution systems		X	X
Above ground water distribution systems			X
Hydronic heating		X	X
Fuel oil and natural gas distribution systems		X	
Nonflammable medical gases	X	X	
Air conditioning and refrigeration systems		X	
Ground source heat pump systems		X	
Fire sprinkler systems	X	X	X
Compressed air	X	X	X

4.3 Fluid Flow Fundamentals

Consider a pipe transporting a fluid, as shown in Figure 4.1. In this figure, a system boundary has been identified that encompasses the pipe and cuts it at two points identified as 1 and 2. In the general case where friction is considered, there is a possibility of heat being transferred from the system due to the friction effects.

For the case of steady state flow the conservation of energy applied to this system,

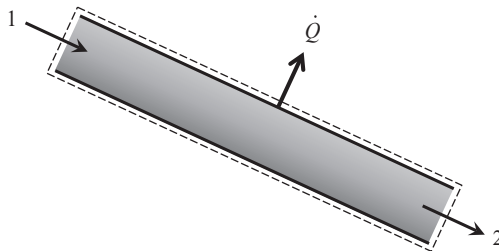
$$\frac{-\dot{Q}}{\dot{m}} + (h_1 - h_2) + \frac{1}{2}(V_1^2 - V_2^2) + g(z_1 - z_2) = 0 \quad (4.1)$$

The enthalpy terms can be written in terms of $h = u + Pv$. Making this substitution in Equation 4.1 results in,

$$\frac{-\dot{Q}}{\dot{m}} + [(u_1 + P_1v_1) - (u_2 + P_2v_2)] + \frac{1}{2}(V_1^2 - V_2^2) + g(z_1 - z_2) = 0 \quad (4.2)$$

The specific volume is the reciprocal of density. Therefore, the Pv terms can be rewritten as P/ρ . Making this substitution and rearranging the equation results in,

$$\frac{P_1}{\rho_1} + \frac{V_1^2}{2} + gz_1 = \frac{P_2}{\rho_2} + \frac{V_2^2}{2} + gz_2 + \left[(u_2 - u_1) + \frac{\dot{Q}}{\dot{m}} \right] \quad (4.3)$$

**FIGURE 4.1**

A pipe transporting a fluid.

The term in brackets in Equation 4.3 represents the change in the fluid's internal energy and any accompanying heat transfer rate due to friction. This can be expressed as the product of the acceleration due to gravity, g , and the *head loss* due to friction, l_f

$$\left[(u_2 - u_1) + \frac{\dot{Q}}{\dot{m}} \right] = gl_f \quad (4.4)$$

Notice that the units of the head loss are length and the product gl_f has units of specific energy. For example, in the SI unit system,

$$gl_f [=] \frac{\text{m}}{\text{s}^2} \cdot \text{m} = \frac{\text{m}^2}{\text{s}^2} \left| \frac{\text{N} \cdot \text{s}^2}{\text{kg} \cdot \text{m}} \right| = \frac{\text{N} \cdot \text{m}}{\text{kg}} = \frac{\text{J}}{\text{kg}}$$

If the fluid is considered incompressible, then its density is constant. Combining this idea along with the head loss represented by Equation 4.4, Equation 4.3 can be rewritten as,

$$\frac{P_1}{\rho} + \frac{V_1^2}{2} + gz_1 = \frac{P_2}{\rho} + \frac{V_2^2}{2} + gz_2 + gl_f \quad (4.5)$$

This form is known as the *specific energy* form of the conservation of energy because each term has units of energy per unit mass. If Equation 4.5 is divided through by g , the conservation of energy equation can be written in *length form* as,

$$\frac{P_1}{\rho g} + \frac{V_1^2}{2g} + z_1 = \frac{P_2}{\rho g} + \frac{V_2^2}{2g} + z_2 + l_f \quad (4.6)$$

The product ρg is known as the *specific weight*, γ , of the fluid. Making this substitution in Equation 4.6,

$$\frac{P_1}{\gamma} + \frac{V_1^2}{2g} + z_1 = \frac{P_2}{\gamma} + \frac{V_2^2}{2g} + z_2 + l_f \quad (4.7)$$

Each of the terms in Equation 4.7 represents a *head* value; pressure head, velocity head, elevation head, and head loss due to friction.

Multiplying Equation 4.5 through by the fluid density gives the *pressure form* of the conservation of energy equation,

$$P_1 + \frac{\rho V_1^2}{2} + \gamma z_1 = P_2 + \frac{\rho V_2^2}{2} + \gamma z_2 + \gamma l_f \quad (4.8)$$

If the flow is assumed to be frictionless, then Equation 4.7 can be written as,

$$\frac{P_1}{\gamma} + \frac{V_1^2}{2g} + z_1 = \frac{P_2}{\gamma} + \frac{V_2^2}{2g} + z_2 \quad (4.9)$$

Equation 4.9 is known as *Bernoulli's equation*. This equation represents the ideal condition of an incompressible fluid flowing in a pipe without friction. While this situation does not exist in the real world, the application of this equation can be useful in providing a benchmark for engineering design.

4.3.1 Head Loss due to Friction in Pipes and Tubes

For fluid flow in circular pipes or tubes, the head loss due to friction is expressed as,

$$l_f = f \frac{L}{D} \frac{V^2}{2g} \quad (4.10)$$

In this equation,

- f = Moody friction factor (sometimes called the Darcy-Weisbach friction factor),
- L = length of pipe,
- D = inside diameter of the pipe,
- V = average velocity of the fluid in the pipe, and
- g = acceleration due to gravity.

If a non-circular pipe is used, the diameter in Equation 4.10 can be replaced with the hydraulic diameter,

$$D_h = \frac{4A_c}{P} = \frac{4 \text{ (cross sectional area)}}{\text{wetted perimeter}} \quad (4.11)$$

The friction factor, f , can be determined graphically using the Moody diagram, shown in Figure 4.2, or it can also be computed using empirical expressions.

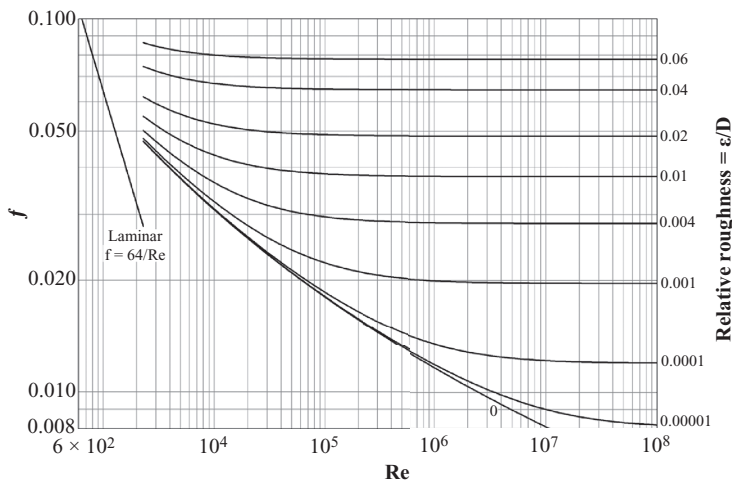


FIGURE 4.2
The Moody diagram.

In the laminar flow regime ($Re_D < 2300$), the friction factor is given by,

$$f = \frac{64}{Re_D} \quad (4.12)$$

The *Reynolds number*, Re , is given by,

$$Re_D = \frac{\rho VD}{\mu} = \frac{VD}{\nu} \quad (4.13)$$

In this equation, μ is the dynamic viscosity (Section 1.5.3.1), and ν is the kinematic viscosity (Section 1.5.3.2) of the fluid.

In the transition and turbulent regions, the friction factor can be computed using one of several correlations shown in Table 4.2. Any of these correlations are sufficient for engineering calculations. In this book, the *Swamee-Jain correlation* will be used for friction calculations due to its relative simplicity compared to the other correlations.

In the correlations shown in Table 4.2, ϵ is the *absolute surface roughness* of the pipe and ϵ/D is known as the *relative roughness*. Table 4.3 lists typical values of the absolute surface roughness for different types of pipe. The values in this table were taken from Moody (1944).

In any fluid friction calculation, there are several variables that must be resolved including the fluid properties, pipe material, pipe length, pipe diameter, fluid flow rate, and pressure drop. Consider a design problem where the fluid is known (therefore

TABLE 4.2

Turbulent Friction Factor Correlations

Correlation	Equation
Chen	$f = \left[-2.0 \log \left\{ \frac{\epsilon/D}{3.7065} - \frac{5.0452}{Re} \log \left[\frac{1}{2.8257} \left(\frac{\epsilon}{D} \right)^{1.1098} + \frac{5.8506}{Re^{0.8981}} \right] \right\} \right]^{-2}$
Churchill	$f = 8 \left[\left(\frac{8}{Re} \right)^{12} + \frac{1}{(B+C)^{1.5}} \right]^{1/12}$ $B = \left[2.457 \ln \frac{1}{(7/Re)^{0.9} + (0.27\epsilon/D)} \right]^{16} \quad C = \left(\frac{37530}{Re} \right)^{16}$
Colebrook	$\frac{1}{\sqrt{f}} = -2 \log \left(\frac{\epsilon/D}{3.7} + \frac{2.51}{Re_D \sqrt{f}} \right)$
Haaland	$f = \left\{ -0.782 \ln \left[\frac{6.9}{Re} + \left(\frac{\epsilon/D}{3.7} \right)^{1.11} \right] \right\}^{-2}$
Swamee-Jain	$f = \frac{0.25}{\left[\log \left(\frac{\epsilon/D}{3.7} + \frac{5.74}{Re^{0.9}} \right) \right]^2}$

TABLE 4.3Absolute Roughness Values, ϵ , for Pipes

Pipe Material	ft	cm
Drawn tubing	0.000005	0.00015
Commercial steel or wrought iron	0.00015	0.0046
Asphalted cast iron	0.004	0.12
Galvanized iron	0.005	0.15
Cast iron	0.0085	0.26
Wood stave	0.0006 – 0.003	0.18 – 0.09
Concrete	0.001 – 0.01	0.031 – 0.31
Riveted steel	0.003 – 0.03	0.091 – 0.91

Source: Moody, L.F., *Trans. ASME*, 66, 8, 671–684, 1944.**TABLE 4.4**

Fluid Friction Calculations Where the Pipe (or Tube) Type, Length, and Fluid Are Specified

Problem Type	Pressure Drop	Fluid Flow Rate	Pipe Diameter
Type 1	Unknown	Known	Known
Type 2	Known	Unknown	Known
Type 3	Known	Known	Unknown

its properties can be determined), the type of pipe is specified, and the pipe length is known. This leaves three parameters; the pipe diameter, the fluid flow rate, and the pressure drop through the length of pipe. Knowing any two of these three parameters allows for a solution of the conservation of energy equation to find the third. This leads to three possible friction calculation problems. These three problem types depend on which parameters are known. The three problem types can be classified as “Type 1,” “Type 2,” and “Type 3” problems. Table 4.4 shows these types of problems and indicates which variables are known and unknown in the friction calculation. The following examples show the procedure for performing these three types of friction calculations manually.

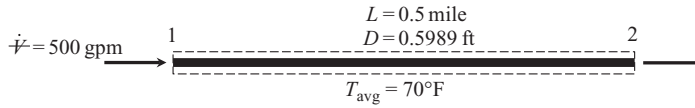
Example 4.2: A Type 1 Problem

Liquid heptane is being transported at volumetric flow rate of 495 gpm through an 8-nom sch 120 commercial steel pipe. The heptane is flowing in the pipe at an average temperature of 80°F. The pipe is 0.5 mile long. There is no elevation difference from the inlet to the outlet of the pipe. Determine the pressure drop through the pipe.

Solution

A sketch of the horizontal pipe and the system boundary to be analyzed is shown in Figure E4.2. The average temperature in the pipeline is given. At these conditions, the density and dynamic viscosity of the heptane can be found from Appendix B.3,

$$\rho = 42.332 \frac{\text{lbm}}{\text{ft}^3} \quad \mu = 0.92123 \frac{\text{lbm}}{\text{ft}\cdot\text{hr}} \left(\frac{\text{hr}}{3600\text{s}} \right) = 0.00025590 \text{ lbm/ft}\cdot\text{s}$$

**FIGURE E4.2**

Horizontal pipe for transporting heptane.

When expressing the conservation of energy equation in terms of length, it is more convenient to use the specific weight rather than the density. Given the density value above, the specific weight of the heptane can be found,

$$\gamma = \rho \frac{g}{g_c} = \left(42.332 \frac{\text{lbm}}{\text{ft}^3} \right) \left(\frac{32.174 \frac{\text{ft}}{\text{s}^2}}{32.174 \frac{\text{lbm-ft}}{\text{lbf-s}^2}} \right) = 42.332 \frac{\text{lbf}}{\text{ft}^3}$$

The inside diameter of the pipe can be found from Appendix C,

$$D = 0.59892 \text{ ft}$$

The length form of the conservation of energy equation can be written between the inlet and exit of the pipe as,

$$\frac{P_1}{\gamma} + \frac{V_1^2}{2g} + z_1 = \frac{P_2}{\gamma} + \frac{V_2^2}{2g} + z_2 + l_f$$

The heptane is flowing in a steady state and the pipe diameter is constant. Therefore, the velocity of the heptane does not change as it passes through the pipe. In addition, there is no elevation change from inlet to outlet. Therefore, the conservation of energy equation reduces to,

$$P_1 - P_2 = \gamma l_f$$

Substituting the head loss due to friction into this equation gives,

$$\Delta P = P_1 - P_2 = \gamma \left(f \frac{L}{D} \frac{V^2}{2g} \right)$$

The velocity of the heptane in the pipe can be found since the volumetric flow rate is given,

$$V = \frac{\dot{V}}{A} = \frac{4\dot{V}}{\pi D^2} = \frac{4 \left(495 \frac{\text{gal}}{\text{min}} \right) \left(\frac{2.228 \times 10^{-3} \text{ ft}^3 \cdot \text{min}}{\text{s-gal}} \right)}{\pi (0.5989 \text{ ft})^2} = 3.915 \frac{\text{ft}}{\text{s}}$$

The friction factor can be obtained from any of the correlations listed in Table 4.2. Using the Swamee-Jain correlation,

$$f = \frac{0.25}{\left[\log \left(\frac{\varepsilon/D}{3.7} + \frac{5.74}{\text{Re}^{0.9}} \right) \right]^2}$$

The Reynolds number and relative roughness need to be found,

$$\text{Re} = \frac{\rho V D}{\mu} = \frac{\left(42.332 \frac{\text{lbm}}{\text{ft}^3} \right) \left(3.915 \frac{\text{ft}}{\text{s}} \right) (0.5989 \text{ ft})}{0.00025590 \frac{\text{lbm}}{\text{ft-s}}} = 387,852$$

$$\frac{\varepsilon}{D} = \frac{\overset{\text{(Table 4.3)}}{0.00015 \text{ ft}}}{0.59892 \text{ ft}} = 2.505 \times 10^{-4}$$

Substituting these values into the Swamee-Jain correlation allows for the calculation of the friction factor,

$$f = \frac{0.25}{\left[\log \left(\frac{\varepsilon/D}{3.7} + \frac{5.74}{\text{Re}^{0.9}} \right) \right]^2} = \frac{0.25}{\left[\log \left(\frac{2.505 \times 10^{-4}}{3.7} + \frac{5.74}{387,852^{0.9}} \right) \right]^2} = 0.01630$$

Therefore, the pressure drop in the pipeline is,

$$\Delta P = \gamma f \frac{L}{D} \frac{V^2}{2g}$$

$$\Delta P = \left(42.332 \frac{\text{lbf}}{\text{ft}^3} \right) (0.01630) \frac{0.5 \text{ mile} \left(\frac{5280 \text{ ft}}{\text{mile}} \right)}{0.59892 \text{ ft}} \frac{\left(3.915 \frac{\text{ft}}{\text{s}} \right)^2}{2 \left(32.174 \frac{\text{ft}}{\text{s}^2} \right)} \left(\frac{\text{ft}^2}{144 \text{ in}^2} \right)$$

$$\Delta P = 5.0 \frac{\text{lbf}}{\text{in}^2} = \underline{\underline{5.0 \text{ psi}}}$$

From a design point of view, this type of calculation allows the engineer to start thinking about selecting a pump to overcome the calculated pressure drop. If the fluid flow rate must be met, then the pump must be able to offset this entire pressure drop.

The Type 1 problem is relatively straightforward. However, Type 2 and Type 3 problems require an iterative solution and become more complex from a computational perspective.

Example 4.3: A Type 2 Problem

Liquid water is flowing through a 1 std type M copper tube at 30°C. The tube is 50-m long. The inlet to the tube is 20-m higher than the outlet. As the water passes through

this tube, it experiences a pressure drop of 130 kPa. Determine the volumetric flow rate of water through the tube.

Solution

A sketch of the tube is shown in Figure E4.3 along with the system boundary to be analyzed. The properties of the water flowing through the tube can be found in Appendix B.3,

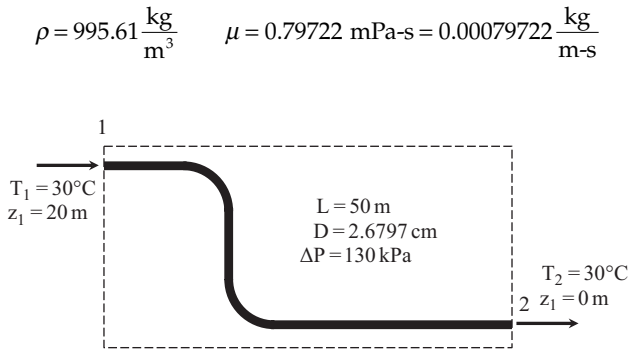


FIGURE E4.3

Copper tube used to transport water.

The specific weight of the water can be calculated once the density is known,

$$\gamma = \rho g = \left(995.61 \frac{\text{kg}}{\text{m}^3} \right) \left(9.807 \frac{\text{m}}{\text{s}^2} \right) \left(\frac{\text{N}\cdot\text{s}^2}{\text{kg}\cdot\text{m}} \right) = 9763.9 \frac{\text{N}}{\text{m}^3} = 9.7639 \frac{\text{kN}}{\text{m}^3}$$

The inside diameter of the tube can be found in Appendix D,

$$D = 2.6797 \text{ cm} = 0.026797 \text{ m}$$

Applying the conservation of energy in length form to the system boundary results in,

$$\frac{P_1}{\gamma} + z_1 = \frac{P_2}{\gamma} + z_2 + l_f$$

Rearranging this equation and substituting the head loss due to friction expression gives,

$$\frac{(P_1 - P_2)}{\gamma} = (z_2 - z_1) + f \frac{L}{D} \frac{V^2}{2g}$$

The unknowns in this equation are the friction factor and the velocity. However, the friction factor is related to the velocity through the Reynolds number. Therefore,

this solution is iterative. The iterative procedure used to solve a Type 2 problem is listed below.

1. Guess the friction factor (usually, $f = 0.02$ is a good starting value).
2. Calculate the velocity of the fluid from the conservation of energy equation.
3. Calculate the Reynolds number using the velocity found in Step 2.
4. Use the Reynolds number and the relative roughness to determine the friction factor using the Moody diagram or one of the correlations found in Table 4.2.
5. Compare the friction factor from Step 4 to the previous value of the friction factor.
6. If the two values of the friction factor do not match, use the newest value of the friction factor and repeat to Step 2 until closure.

Fortunately, this iteration usually closes quickly (within 1 to 2 iterations). Following this process, start by guessing the friction factor,

$$f = 0.02$$

Solving the conservation of energy equation for the velocity,

$$V = \sqrt{\frac{2gD}{Lf} \left[\frac{\Delta P}{\gamma} - (z_2 - z_1) \right]}$$

With the guessed value of f , the velocity is,

$$V = \sqrt{\frac{2 \left(9.807 \frac{\text{m}}{\text{s}^2} \right) (0.026797 \text{ m})}{(50 \text{ m})(0.02)} \left[\frac{130 \text{ kPa} \left(\frac{\text{kN}}{\text{kPa} \cdot \text{m}^2} \right)}{\left(9.7639 \frac{\text{kN}}{\text{m}^3} \right)} - (0 - 20) \text{ m} \right]}$$

$$V = 4.1845 \frac{\text{m}}{\text{s}}$$

Now, the Reynolds number corresponding to this velocity can be found,

$$\text{Re} = \frac{\rho V D}{\mu} = \frac{\left(995.61 \frac{\text{kg}}{\text{m}^3} \right) \left(4.1845 \frac{\text{m}}{\text{s}} \right) (0.026797 \text{ m})}{\left(0.00079722 \frac{\text{kg}}{\text{m} \cdot \text{s}} \right)} = 140,035$$

The relative roughness of the copper pipe is,

$$\frac{\varepsilon}{D} = \frac{\text{(Table 4.3 - drawn tubing)} \quad 0.00015 \text{ cm}}{2.6797 \text{ cm}} = 5.5976 \times 10^{-5}$$

Calculating the friction factor,

$$f = \frac{0.25}{\left[\log \left(\frac{\varepsilon/D}{3.7} + \frac{5.74}{\text{Re}^{0.9}} \right) \right]^2} = \frac{0.25}{\left[\log \left(\frac{5.5976 \times 10^{-5}}{3.7} + \frac{5.74}{140,035^{0.9}} \right) \right]^2} = 0.01708$$

This value of the friction factor is not the same as the guessed value (0.02). Therefore, the process needs to be repeated with the new value of the friction factor. The results are,

$$\begin{aligned}
 f &= 0.01708 \\
 V &= \sqrt{\frac{2gD}{Lf} \left[\frac{\Delta P}{\gamma} - (z_2 - z_1) \right]} = 4.528 \frac{\text{m}}{\text{s}} \\
 \text{Re} &= \frac{\rho VD}{\mu} = 151,533 \\
 \frac{\varepsilon}{D} &= 5.5976 \times 10^{-5} \\
 \therefore f &= 0.01683
 \end{aligned}$$

The friction factors are close, but not close enough to declare convergence. Another iteration results in,

$$\begin{aligned}
 f &= 0.01683 \\
 V &= \sqrt{\frac{2gD}{Lf} \left[\frac{\Delta P}{\gamma} - (z_2 - z_1) \right]} = 4.5616 \frac{\text{m}}{\text{s}} \\
 \text{Re} &= \frac{\rho VD}{\mu} = 152,654 \\
 \frac{\varepsilon}{D} &= 5.5976 \times 10^{-5} \\
 \therefore f &= 0.01681
 \end{aligned}$$

These two friction factors are very close. Therefore, the iteration can be declared complete and the volumetric flow rate of the water can be determined,

$$\dot{V} = AV = \left(\frac{\pi D^2}{4} \right) V = \left[\frac{\pi (0.026797 \text{ m}^2)}{4} \right] \left(4.564 \frac{\text{m}}{\text{s}} \right) \left(\frac{1000 \text{ L}}{\text{m}^3} \right) = \underline{\underline{2.57 \frac{\text{L}}{\text{s}}}}$$

This example demonstrates how the iterative procedure can be accomplished with a calculator. The iterative complexity of this calculation can easily be dealt with using computer software. For example, using a spreadsheet with solver capability, the final results are,

$$\begin{aligned}
 f &= 0.01681 \\
 V &= \sqrt{\frac{2gD}{Lf} \left[\frac{\Delta P}{\gamma} - (z_2 - z_1) \right]} = 4.5646 \frac{\text{m}}{\text{s}} \\
 \text{Re} &= \frac{\rho VD}{\mu} = 152,754 \\
 \frac{\varepsilon}{D} &= 5.5976 \times 10^{-5} \\
 \therefore \dot{V} &= \underline{\underline{2.57 \frac{\text{L}}{\text{s}}}}
 \end{aligned}$$

Notice that the computer solution matches the manual iteration very closely. This demonstrates that the iterative solution usually closes within a few iterations, making manual calculation feasible for Type 2 problems.

Example 4.4: A Type 3 Problem

Liquid ethanol is flowing at a rate of 800 gpm in a horizontal, galvanized iron pipe over a distance of 2.5 miles. The average temperature of the ethanol in the pipeline is 60°F. The pump selected for this system can overcome a pressure drop of 45 psi. Determine the nominal diameter required if the pipe is standard (std) sch 40.

Solution

A sketch of the pipeline and the system boundary to be analyzed is shown in Figure E4.4.

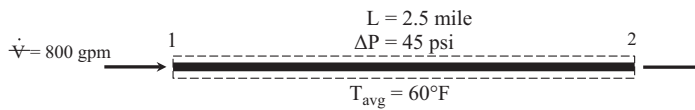


FIGURE E4.4

Galvanized iron pipe for transporting ethanol.

The ethanol properties can be found in Appendix B.3,

$$\rho = 49.514 \frac{\text{lbm}}{\text{ft}^3} \quad \mu = 3.1563 \frac{\text{lbm}}{\text{ft}\cdot\text{hr}} \left(\frac{\text{hr}}{3600 \text{ s}} \right) = 0.00087674 \frac{\text{lbm}}{\text{ft}\cdot\text{s}}$$

Given the density, the specific weight of the ethanol can be found,

$$\gamma = \rho \frac{g}{g_c} = \left(49.514 \frac{\text{lbm}}{\text{ft}^3} \right) \left(\frac{32.174 \frac{\text{ft}}{\text{s}^2}}{32.174 \frac{\text{lbm}\cdot\text{ft}}{\text{lbf}\cdot\text{s}^2}} \right) = 49.514 \frac{\text{lbf}}{\text{ft}^3}$$

Applying the conservation of energy in length form to the system identified above results in,

$$\frac{P_1}{\gamma} = \frac{P_2}{\gamma} + l_f$$

Rearranging this equation and substituting the expression for the head loss due to friction gives,

$$\frac{P_1 - P_2}{\gamma} = \frac{\Delta P}{\gamma} = f \frac{L}{D} \frac{V^2}{2g}$$

The velocity of the fluid is related to the volumetric flow rate,

$$V = \frac{\dot{V}}{A} = \frac{4\dot{V}}{\pi D^2}$$

Substituting this expression into the conservation of energy equation and simplifying gives,

$$\frac{\Delta P}{\gamma} = f \frac{8L\dot{V}^2}{\pi^2 D^5 g}$$

The unknowns in this equation are the friction factor and the diameter. However, the friction factor is related to the diameter through the Reynolds number. Therefore, this solution is iterative. The iterative procedure for a Type 3 problem is listed below.

1. Guess the friction factor (usually, $f = 0.02$ is a good starting value).
2. Calculate the diameter of the pipe from the conservation of energy equation.
3. Calculate the Reynolds number using the diameter found in Step 2.
4. Calculate the relative roughness using the diameter found in Step 2.
5. Use the Reynolds number and the relative roughness to determine the friction factor using one of the correlations found in Table 4.1.
6. Compare the friction factor from Step 5 to the previous value of the friction factor.
7. If the two values of the friction factor do not match, use the newest value of the friction factor and repeat to Step 2 until closure.

This iterative procedure usually closes quickly; within 1 to 2 iterations. Using the procedure outlined above, start by guessing the friction factor,

$$f = 0.02$$

Solving the conservation of energy equation for the diameter,

$$D = \left(\frac{8f\gamma L\dot{V}^2}{\pi^2 \Delta P g} \right)^{1/5}$$

Using the guessed value for the friction factor the diameter is,

$$D = \left[\frac{8(0.02) \left(49.514 \frac{\text{lbf}}{\text{ft}^3} \right) (2.5 \text{ mile}) \left(800 \frac{\text{gal}}{\text{min}} \right)^2 \left(\frac{5280 \text{ ft}}{\text{mile}} \right) \left(\frac{2.228 \times 10^{-3} \text{ ft}^3 \cdot \text{min}}{\text{s-gal}} \right)^2}{\pi^2 \left(45 \frac{\text{lbf}}{\text{in}^2} \right) \left(32.174 \frac{\text{ft}}{\text{s}^2} \right) \left(\frac{144 \text{ in}^2}{\text{ft}^2} \right)} \right]^{1/5}$$

$$D = 0.6944 \text{ ft}$$

The Reynolds number can be rewritten in terms of the volumetric flow rate,

$$\text{Re} = \frac{\rho V D}{\mu} = \frac{\rho D}{\mu} \left(\frac{4\dot{V}}{\pi D^2} \right) = \frac{4\rho\dot{V}}{\pi D \mu}$$

$$\text{Re} = \frac{4 \left(49.514 \frac{\text{lbm}}{\text{ft}^3} \right) \left(800 \frac{\text{gal}}{\text{min}} \right) \left(\frac{2.228 \times 10^{-3} \text{ ft}^3 \cdot \text{min}}{\text{s-gal}} \right)}{\pi (0.6944 \text{ ft}) \left(0.00087674 \frac{\text{lbm}}{\text{ft-s}} \right)} = 184,570$$

The relative roughness of the pipe is,

$$\frac{\varepsilon}{D} = \frac{\overset{\text{(Table 4.3)}}{0.005 \text{ ft}}}{0.6944 \text{ ft}} = 0.0072$$

Using the calculated values of the Reynolds number and the relative roughness, the friction factor can be found using any of the correlations listed in Table 4.1,

$$f = \frac{0.25}{\left[\log \left(\frac{\varepsilon/D}{3.7} + \frac{5.74}{\text{Re}^{0.9}} \right) \right]^2} = \frac{0.25}{\left[\log \left(\frac{0.0072}{3.7} + \frac{5.74}{184,570^{0.9}} \right) \right]^2} = 0.03460$$

This value of the friction factor is not the same as the guessed value (0.02). Therefore, the process must be repeated with the new value of the friction factor. The results are,

$$f = 0.03460$$

$$D = \left(\frac{8f\gamma L \dot{V}^2}{\pi^2 \Delta P g} \right)^{1/5} = 0.7749 \text{ ft}$$

$$\text{Re} = \frac{4\rho \dot{V}}{\pi D \mu} = 165,406$$

$$\frac{\varepsilon}{D} = 0.006453$$

$$\therefore f = 0.03353$$

Another iteration results in,

$$f = 0.03353$$

$$D = \left(\frac{8f\gamma L \dot{V}^2}{\pi^2 \Delta P g} \right)^{1/5} = 0.7700 \text{ ft}$$

$$\text{Re} = \frac{4\rho \dot{V}}{\pi D \mu} = 166,449$$

$$\frac{\varepsilon}{D} = 0.006494$$

$$\therefore f = 0.03359$$

For iterative calculation purposes, these two friction factor values are very close and the iteration can be considered closed. This last iteration indicates that the pipe diameter required is,

$$D = \underline{\underline{0.77 \text{ ft}}}$$

This value must now be translated to a nominal size. Since the pipe is schedule 40, Appendix C shows that this pipe diameter lies between 8-nom and 10-nom,

$$\begin{aligned} 8\text{-nom sch 40 (std): } D &= 0.66508 \text{ ft} \\ 10\text{-nom sch 40 (std): } D &= 0.83500 \text{ ft} \end{aligned}$$

If the smaller pipe diameter is selected, the pressure drop would be higher than 45 psi for a flow rate of 800 gpm. This means that the pump selected for this application would not be able to deliver the required 800 gpm through an 8-nom sch 40 pipe. Therefore, for this application, *select the 10-nom sch 40 (std) pipe*.

As with the previous example, this problem can also be solved using computer software. However, for a Type 3 problem this may not be necessary because the next larger discrete nominal pipe diameter will be chosen.

During the design and/or analysis of a fluid network, the engineer will typically be solving any of the Type 1, Type 2, or Type 3 problems as a subset of a larger collection of calculations. Therefore, it is desirable to take advantage of modern computing technology and perform these calculations using computer software.

4.4 Valves and Fittings

Valves and fittings are an integral part of a thermal energy system involving fluid transport. Valves can be used for flow control or to completely shut down the flow. Fittings may be classified as *branching*, *reducing*, *expanding*, or *deflecting*. Branching fittings are fittings that split or collect flows such as tees or wyes. Reducing or expanding fittings change the cross-sectional area of the flow such as reducers or bushings. Deflecting fittings change the direction of the flow such as elbows or return bends. Each of these components introduces additional head loss due to friction. The head loss due to valves and fittings is often called a *minor loss*. When determining total head loss in a fluid network, it is important to include these effects.

Friction effects in valves and fittings are dependent on how the valve or fitting is attached to the pipe (i.e., threaded, flanged, welded, or soldered). Table 4.5 shows some

TABLE 4.5
Standard Drawing Symbols for Joints




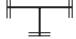








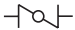
Joint Type	Drawing Symbol	Example	
Threaded		90° Elbow	
Flanged		Tee	
Welded		Concentric reducer	
Soldered		45° Elbow	

TABLE 4.6
Common Uses for Valves in Industrial Applications

Type of Valve	Drawing Symbol	Recommended Uses
Gate		Fully open or fully closed service; minimal line pressure drop; infrequent operation
Globe		Flow control (throttling), frequent operation; service with some line resistance
Check		Control the direction of flow and quick automatic reaction to flow change; should be used in conjunction with a gate valve
Ball		On or off service; flow control (throttling); when positive shut-off is necessary; when low profile is necessary
Butterfly		When positive shut-off is necessary; fully open or fully closed service

standard drawing symbols to signify pipe joints. Joints are generally threaded for pipes 2-nom and smaller. For pipes larger than 2-nom, joints are typically flanged or welded. Soldered joints usually pertain to systems utilizing tubing. Table 4.6 shows the standard drawing symbols and various uses of common valves used in industrial applications. A more comprehensive guide for valve selection can be found in the *Valve Selection Handbook* (Smith and Zappe 2004).

The great number of valve designs available to an engineer makes it difficult to thoroughly categorize them. However, it is possible to think of valves as either *low resistance* or *high resistance*. Low resistance valves have a straight through flow path. Valves of this type include gate valves, ball valves, plug valves, and butterfly valves. These types of valves are usually used for fully open or fully closed service. High resistance valves are used to control the flow of the fluid (e.g., a globe valve) or change the flow direction of a fluid (e.g., an angle valve). The American Society of Mechanical Engineers (ASME) has developed a valve and fitting class system. The suggested pairing of valve and fitting classes to pipe schedules is listed in Table 4.7.

In order to accommodate the friction losses in valves and fittings, the conservation of energy equation for an incompressible fluid flow can be modified to include a minor loss term,

$$\frac{P_1}{\gamma} + \frac{V_1^2}{2g} + z_1 = \frac{P_2}{\gamma} + \frac{V_2^2}{2g} + z_2 + l_f + l_m \quad (4.14)$$

TABLE 4.7
Valve and Fitting Class Pairings with Pipe Schedules

Valve or Fitting Class	Paired Pipe
Class 300 and lower	Schedule 40
Class 400 and 600	Schedule 80
Class 900	Schedule 120
Class 1500	Schedule 160
Class 2500 (½ to 6 inch)	xxs
Class 2500 (8 inch and up)	Schedule 160

The minor loss, l_m , is expressed as,

$$l_m = \sum_i \left(K_i \frac{V_i^2}{2g} \right) \quad (4.15)$$

In this equation, the K_i values are known as the *resistance* or *loss* coefficients for the valve or fitting being considered. The velocity head in Equation 4.15 is the velocity head associated with the valve or fitting which is considered to be the same as the velocity head in the pipe if the valve or fitting is the same nominal size. Combining Equation 4.15 with Equations 4.14 and 4.10 gives the conservation of energy equation between two points in a pipe network with fittings and valves,

$$\frac{P_1}{\gamma} + \frac{V_1^2}{2g} + z_1 = \frac{P_2}{\gamma} + \frac{V_2^2}{2g} + z_2 + \sum_i \left(f_i \frac{L_i}{D_i} \frac{V_i^2}{2g} \right) + \sum_i \left(K_i \frac{V_i^2}{2g} \right) \quad (4.16)$$

Equation 4.16 is often known as the *modified Bernoulli equation*. Notice that the head loss term due to pipe friction is written to accommodate several different diameter pipes in the system between points 1 and 2.

This edition of *Thermal Energy Systems: Design and Analysis* represents a significant change in how valve and fitting losses are calculated. In the first edition, K values were determined based on a publication from the Crane Company, known as “Crane Technical Paper 410” (The Crane Company 2017). While the Crane method (a 1K method) produces valid results in regions of fully turbulent flow, there is some concern in the industry regarding its application in lower Reynolds number regimes. Two methods are presented here; the 2K method (Hooper 1981), and the 3K method (Darby and Chhabra 2017).

4.4.1 The Hooper 2K Method

In the 2K method, the loss coefficient for the valve or fitting is computed using the following empirical equation,

$$K = \frac{K_1}{\text{Re}} + K_\infty \left(1 + \frac{1}{D} \right) \quad (4.17)$$

In Equation 4.17, Re is the Reynolds number of the flow, K_1 is the loss coefficient for the valve or fitting at $\text{Re} = 1$, K_∞ is the loss coefficient for a large fitting at an infinite Reynolds number, and D is the inside diameter of the pipe (in inches) connected to the fitting. Equation 4.17 shows that the loss coefficient, K , is a function of the Reynolds number of the flow and the pipe diameter. Table 4.8 (Hooper 1981) shows values for K_1 and K_∞ for various valves and fittings when using 2K method.

TABLE 4.8

Constants for the 2K Method

Fitting Type	K_1	K_∞
90° elbow		
Standard, threaded	800	0.40
Standard, flanged	800	0.25
Long radius, all types	800	0.20
90° mitered elbow		
1 weld (90° angle)	1000	1.15
2 welds (45° angle)	800	0.35
3 welds (30° angle)	800	0.30
4 welds (22½° angle)	800	0.27
5 welds (18° angle)	800	0.25
45° elbow		
Standard, all types	500	0.20
Long radius, all types	500	0.15
45° mitered elbow		
1 weld (45° angle)	500	0.25
2 welds (22½° angle)	500	0.15
180° bend		
Standard, threaded	1000	0.60
Standard, flanged or welded	1000	0.35
Long radius, all types	1000	0.30
Valves		
Gate, ball, or plug valve $\beta = d/D = 1.0$	300	0.10
Gate, ball, or plug valve $\beta = d/D = 0.90$	500	0.15
Gate, ball, or plug valve $\beta = d/D = 0.80$	1000	0.25
Globe, standard	1500	4.00
Globe, angle or Y-type	1000	2.00
Diaphragm, dam type	1000	2.00
Butterfly	800	0.25
Check, lift	2000	10.0
Check, swing	1500	1.50
Check, tilting disk	1000	0.50
Pipe Entrances from tanks: Equation 4.18		
Normal entrance with no pipe projection into tank	160	0.5
Pipe projecting into tank	160	1.0
Pipe Exits: Equation 4.18		
All pipe exits	0	1.0

The K value for pipe entrances from tanks and pipe exits are computed using a modified form of Equation 4.17 given by,

$$K = \frac{K_1}{\text{Re}} + K_\infty \quad (4.18)$$

Example 4.5

Figure E4.5 shows a pump and pipe system for transporting octane (40°C) to an elevated storage tank. The pipe used is 4-nom sch 10S stainless steel. The octane is flowing at a volumetric flow rate of 30 L/s. Determine the pressure loss due to the fittings and valve for this system using the 2K method.

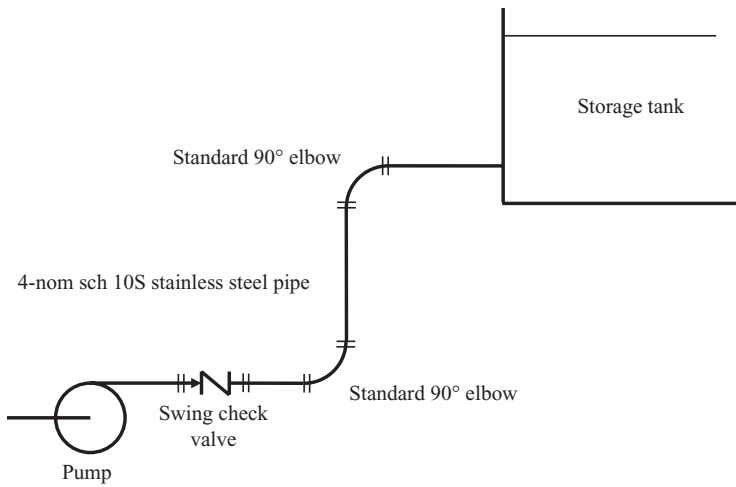


FIGURE E4.5

A pipe network between two large tanks.

Solution

The pressure loss due the valve and fittings can be expressed in terms of the head loss,

$$\frac{\Delta P}{\gamma} = l_m \rightarrow \Delta P = \gamma l_m$$

The head loss due to the valve and fittings is given by,

$$l_m = (K_{valve} + 2K_{elbow} + K_{exit}) \frac{V^2}{2g}$$

The K values for the elbows and check valve are given by Equation 4.17 and the K value for the pipe exit into the tank is given by Equation 4.18. The velocity of the octane can be calculated,

$$V = \frac{\dot{V}}{A} = \frac{4\dot{V}}{\pi D^2} = \frac{4 \left(30 \frac{\text{L}}{\text{s}} \right) \left(\frac{0.001 \text{ m}^3}{\text{L}} \right)}{\pi (0.10820 \text{ m})} = 3.2627 \frac{\text{m}}{\text{s}}$$

Appendix C

The Reynolds number of the flow is,

$$\text{Re} = \frac{\rho V D}{\mu} = \frac{\left(\overset{\text{Appendix B.3}}{686.04 \frac{\text{kg}}{\text{m}^3}} \right) \left(3.2627 \frac{\text{m}}{\text{s}} \right) (0.10820 \text{ m})}{\left(\underset{\text{Appendix B.3}}{0.42907 \text{ mPa}\cdot\text{s}} \right) \left(\frac{\text{Pa}}{1000 \text{ mPa}} \right) \left(\frac{\text{N}}{\text{m}^2 \cdot \text{Pa}} \right) \left(\frac{\text{kg}\cdot\text{m}}{\text{s}^2 \cdot \text{N}} \right)} = 564,450$$

The K values for the elbows and check valve can now be found using the K_1 and K_∞ values from Table 4.8,

$$K_{\text{elbow}} = \frac{K_1}{\text{Re}} + K_\infty \left(1 + \frac{1}{D} \right) = \frac{800}{564,450} + (0.25) \left(1 + \frac{1}{4.26} \right) = 0.3101$$

$$K_{\text{valve}} = \frac{K_1}{\text{Re}} + K_\infty \left(1 + \frac{1}{D} \right) = \frac{1500}{564,450} + (1.5) \left(1 + \frac{1}{4.26} \right) = 1.8548$$

Notice that D must be expressed in *inches* in this empirical relationship. $D = 4.26$ inches is the inside diameter of a 4-nom sch 10S pipe, taken from Appendix C. The K value for the pipe exit to the storage tank is,

$$K_{\text{exit}} = \frac{0}{564,450} + 1.0 = 1.0$$

Therefore, the total head loss due to the valve and fittings in this pipe network is,

$$l_m = \left(K_{\text{valve}} + 2K_{\text{elbow}} + K_{\text{exit}} \right) \frac{V^2}{2g} = \left[1.8548 + (2)(0.3101) + 1.0 \right] \frac{\left(3.2627 \frac{\text{m}}{\text{s}} \right)^2}{2 \left(9.807 \frac{\text{m}}{\text{s}^2} \right)} = 1.886 \text{ m}$$

This translates to a pressure loss of,

$$\Delta P = \gamma l_m = \rho g l_m = \left(686.04 \frac{\text{kg}}{\text{m}^3} \right) \left(9.807 \frac{\text{m}}{\text{s}^2} \right) (1.886 \text{ m}) \left(\frac{\text{N}\cdot\text{s}^2}{\text{kg}\cdot\text{m}} \right) \left(\frac{\text{Pa}\cdot\text{m}^2}{\text{N}} \right) \left(\frac{\text{kPa}}{1000 \text{ Pa}} \right) = \underline{12.7 \text{ kPa}}$$

In addition to the pressure loss due to the friction in the straight runs of pipe and the elevation change, the pump must also be sized properly to overcome the additional pressure loss due to the valve and fittings.

4.4.2 The Darby 3K Method

K values using the 3K method (Darby and Chhabra 2017) are calculated using the following empirical equation,

$$K = \frac{K_1}{\text{Re}} + K_\infty \left(1 + \frac{K_d}{D_{\text{nom}}^{0.3}} \right) \quad (4.19)$$

In Equation 4.19, Re is the Reynolds number of the flow, K_1 , K_∞ , and K_d are constants given in Table 4.9 (Darby and Chhabra 2017), and D_{nom} is the nominal diameter of the pipe attached to the valve or fitting, in inches.

Example 4.6

Determine the pressure loss due to the valve and fittings for the pipe system described in Example 4.5 using the 3K method.

Solution

The K values for the valve and fittings using the 3K method are computed using Equation 4.19 with the K_1 , K_∞ , and K_d constants from Table 4.10,

$$K_{elbow} = \frac{K_1}{Re} + K_\infty \left(1 + \frac{K_d}{D_{nom}^{0.3}} \right) = \frac{800}{564,450} + (0.091) \left(1 + \frac{4}{4^{0.3}} \right) = 0.3326$$

$$K_{valve} = \frac{K_1}{Re} + K_\infty \left(1 + \frac{K_d}{D_{nom}^{0.3}} \right) = \frac{1500}{564,500} + (0.46) \left(1 + \frac{4}{4^{0.3}} \right) = 1.6766$$

$$K_{exit} = \frac{K_1}{Re} + K_\infty \left(1 + \frac{K_d}{D_{nom}^{0.3}} \right) = \frac{0}{564,500} + 1.0 \left(1 + \frac{0}{4^{0.3}} \right) = 1.0$$

Therefore, the total head loss due to the valve and fittings in this pipe network using the 3K method is,

$$l_m = (K_{valve} + 2K_{elbow} + K_{exit}) \frac{V^2}{2g} = [1.6766 + (2)(0.3326) + 1.0] \frac{\left(3.2627 \frac{m}{s} \right)^2}{2 \left(9.807 \frac{m}{s^2} \right)} = 1.814 \text{ m}$$

This translates to a pressure loss of,

$$\Delta P = \gamma l_m = \rho g l_m = \left(686.04 \frac{kg}{m^3} \right) \left(9.807 \frac{m}{s^2} \right) (1.814 \text{ m}) \left(\frac{N \cdot s^2}{kg \cdot m} \right) \left(\frac{Pa \cdot m^2}{N} \right) \left(\frac{kPa}{1000 \text{ Pa}} \right) = \underline{\underline{12.2 \text{ kPa}}}$$

The results of Examples 4.5 and 4.6 indicate that both methods produce nearly the same result. While these methods require some computation, they are generally preferred over methods that use equivalent lengths and/or constant values of K . The 2K and 3K methods introduce the Reynolds number and the pipe diameter (inside or nominal) which make them applicable to all flow regimes (laminar, transition, and turbulent) and pipe diameters.

TABLE 4.9

Constants for the 3K Method

Fitting Type	K_1	K_∞	K_d
90° elbow			
Standard, threaded	800	0.140	4.0
Standard, flanged	800	0.091	4.0
Long radius, threaded	800	0.071	4.2
90° mitered elbow			
1 weld (90° angle)	1000	0.270	4.0
2 welds (45° angle)	800	0.068	4.1
3 welds (30° angle)	800	0.035	4.2
45° elbow			
Standard, all types	500	0.071	4.2
Long radius, all types	500	0.052	4.0
45° mitered elbow			
1 weld (45° angle)	500	0.086	4.0
2 welds (22½° angle)	500	0.052	4.0
180° bend			
Standard, threaded	1000	0.230	4.0
Standard, flanged or welded	1000	0.120	4.0
Long radius, all types	1000	0.100	4.0
Valves			
Gate valve $\beta = d/D = 1.0$	300	0.037	3.9
Globe valve, standard	1500	1.700	3.6
90° angle valve	1000	0.690	4.0
45° angle valve	950	0.250	4.0
Ball valve	300	0.017	3.6
Butterfly	1000	0.690	4.9
Check valve, lift	2000	2.850	3.8
Check valve, swing	1500	0.460	4.0
Pipe Entrances from tanks			
Flush, square with no pipe projection into tank	0	0.50	0
Flush, rounded with no pipe projection into tank			
$r/D = 0.02$	0	0.28	0
$r/D = 0.04$	0	0.24	0
$r/D = 0.06$	0	0.15	0
$r/D = 0.10$	0	0.09	0
$r/D \leq 0.15$	0	0.04	0
Chamfered	0	0.25	0
Pipe projecting inward into tank	0	0.78	0
Pipe Exits			
All pipe exits	0	1.0	0

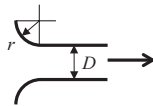
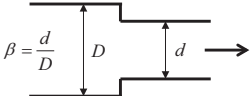
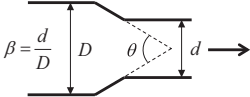

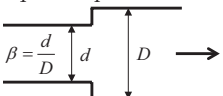
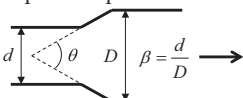
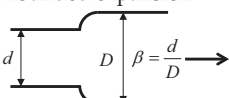


TABLE 4.10*K* Value Empirical Equations for Reducers and Expanders

Reducer or Expander	Empirical Equation for <i>K</i>
Square reduction 	$\text{Re}_D < 2500 \quad K = \left(1.2 + \frac{160}{\text{Re}_D} \right) \left(\frac{1}{\beta^4} - 1 \right)$ $\text{Re}_D > 2500 \quad K = (0.6 + 0.48 f_D) \left(\frac{1}{\beta^2} \right) \left(\frac{1}{\beta^2} - 1 \right)$
Tapered reduction 	For $\theta < 45^\circ$ multiply square reduction by $1.6 \sin(\theta/2)$ For $\theta > 45^\circ$ multiply square reduction by $\sqrt{\sin(\theta/2)}$
Rounded reduction 	$K = \left(0.1 + \frac{50}{\text{Re}_D} \right) \left(\frac{1}{\beta^4} - 1 \right)$
Square expansion 	$\text{Re}_d < 4000 \quad K = 2(1 - \beta^4)$ $\text{Re}_d < 4000 \quad K = (1 + 0.8 f_d)(1 - \beta^2)^2$
Tapered expansion 	For $\theta < 45^\circ$ multiply <i>K</i> for square expansion by $2.6 \sin(\theta/2)$ For $\theta > 45^\circ$ multiply square reduction by $\sqrt{\sin(\theta/2)}$
Rounded expansion 	Use <i>K</i> for square expansion

4.4.3 Reducers and Expansions

The head loss for pipe and tube expansions and contractions can be determined using Equation 4.15. The velocity used to calculate the head loss is the velocity of the fluid entering the fitting. The *K* values for pipe and tube reducers and expansions are a function of the geometry of the fitting and whether the fitting is square, tapered, or rounded. Expressions to compute the *K* values for various types of reducers and expanders are listed in Table 4.10 (Neutrium, Inc. 2012).

4.4.4 Check Valves

Check valves are used in fluid transport systems to provide flow in only one direction in the pipe network. If the fluid flow is reversed from its normal operation, the check valve will close thus preventing backflow. This is particularly useful when a system is used intermittently and backflow is not desired. A good example of this is pumping fluid to an elevated tank. A check valve in the discharge line of the pump will stop back flow from occurring when the pump is shut down. Two common types of check valves, the swing check valve and lift check valve, are shown in Figure 4.3.

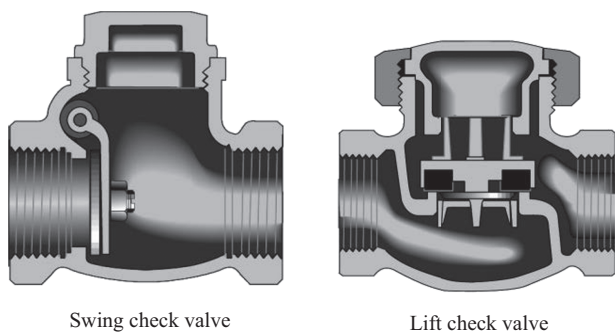
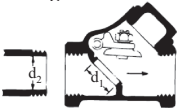
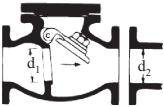





FIGURE 4.3 Swing and lift check valves. (Reprinted from The Crane Company, *Flow of Fluids Through Valves, Fittings, and Pipe*, Stamford, Connecticut, 2017. With permission.)

A check valve stops backflow by a seated disc inside the valve. When the flow is in the proper direction, the disc is moved off its seat. If the velocity of the flow is too small, the disc will lift, but it will not reach its stops. This results in noisy operation and premature wear of the moving parts in the valve. To alleviate this, experiments have been conducted to determine the minimum velocity required to completely move the disc to its stops,

TABLE 4.11
Values of C for Equation 4.20

Check Valve	C in Equation (4.20)
Swing	
	35
Swing, globe type	
	60 100 (UL Listed)
Lift	
	140
Lift, globe type	
	40
Tilting Disk	
	$80(\alpha = 5^\circ)$ $30(\alpha = 15^\circ)$

Note: The figures in this table are reprinted with permission from The Crane Company, *Flow of Fluids Through Valves, Fittings, and Pipe*, Stamford, Connecticut, 2017.

thereby eliminating noisy operation and rapid wear. The results of these experiments have been correlated to an empirical relationship given by,

$$V_{\min}[\text{ft/s}] = \frac{C}{\sqrt{\rho[\text{lbm/ft}^3]}} \quad (4.20)$$

In this equation, the velocity (V_{\min}) is in ft/s and the fluid density (ρ) is in lbm/ft³. The values of the constant, C , are taken from The Crane Company (2017) and are listed in Table 4.11.

Most problems encountered with check valves results from oversizing. It may seem feasible to select a check valve that has the same nominal diameter as the pipe. However, this may result in a situation where the valve disc is not fully lifted. This problem can be resolved by selecting a smaller diameter check valve and connecting it to the pipe using reducers.

Example 4.7

Consider the pump and pipe system shown in Figure E4.5. Determine if the check valve is properly sized. What is the minimum volumetric flow rate required to fully lift the valve?

Solution

The minimum velocity required to fully lift the valve is given by Equation 4.20. For the swing check valve,

$$V_{\min}[\text{ft/s}] = \frac{35}{\sqrt{\rho[\text{lbm/ft}^3]}}$$

Using this empirical relationship, the minimum velocity required is,

$$V_{\min}[\text{ft/s}] = \frac{35}{\sqrt{\left(686.04 \frac{\text{kg}}{\text{m}^3}\right) \left(0.062428 \frac{\text{kg}\cdot\text{ft}^3}{\text{m}^3\cdot\text{lbm}}\right)}} = 5.348 \frac{\text{ft}}{\text{s}} \left(\frac{\text{m}}{3.28084 \text{ ft}} \right) = \underline{\underline{1.63 \frac{\text{m}}{\text{s}}}}$$

Since the calculated velocity in the pipe is 3.26 m/s, the flow is sufficient to fully lift the valve and the valve is sized properly. The minimum volumetric flow rate required to fully lift the valve is,

$$\dot{V}_{\min} = \frac{\pi D^2}{4} V_{\min} = \frac{\pi (0.1082 \text{ m})^2}{4} \left(1.63 \frac{\text{m}}{\text{s}} \right) \left(\frac{\text{L}}{0.001 \text{ m}^3} \right) = \underline{\underline{15.0 \frac{\text{L}}{\text{s}}}}$$

4.4.5 Branch Fittings—Tees and Wyes

Tees and wyes are common branch fittings used in pipe networks. These types of fittings are used to either split flow (diverging) or combine flow (converging) as shown in Figure 4.4

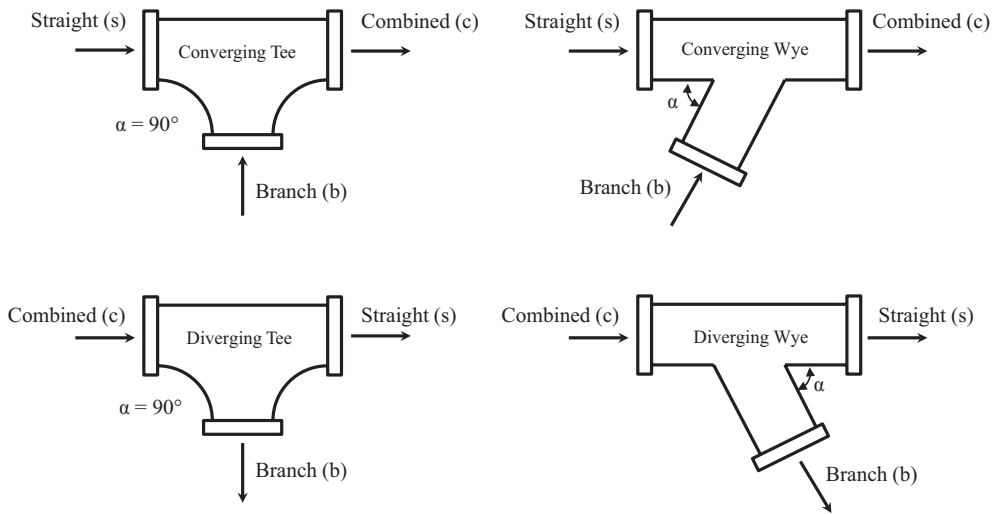


FIGURE 4.4
Converging and diverging tee and wye fittings.

There are two loss coefficients for tees and wyes. One of these loss coefficients is assigned to the flow that runs straight through the fitting, K_{run} . The other loss coefficient is for the flow that runs through the branch, K_{branch} . The value of the loss coefficient depends on the geometry of the fitting and the volumetric flow rate through each part of the fitting. Empirical expressions have been developed for these loss coefficients (Idelchik 2007). This work has been adopted and suggested in “Crane Technical Paper 410” (The Crane Company 2017).

For converging fittings, the following empirical expression has been developed,

$$K_{run} \text{ or } K_{branch} = C \left[1 + D \left(\frac{y_b}{\beta_b^2} \right)^2 - E(1 - y_b)^2 - F \left(\frac{y_b}{\beta_b} \right)^2 \right] \quad (4.21)$$

In this equation, C , D , E , and F are defined in Tables 4.12 and 4.13, y_b is the fraction of the volumetric flow passing through the branch of the fitting, and β_b is the branch diameter ratio,

$$y_b = \frac{\dot{V}_b}{\dot{V}_c} \quad (4.22)$$

$$\beta_b = \frac{D_b}{D_c} \quad (4.23)$$

In Equations 4.22 and 4.23, the subscript c is used to designate the combined flow, defined in Figure 4.4. To calculate the head loss across a branch or run, the velocity in the combined leg of the fitting is used to compute the velocity head.

TABLE 4.12

Loss Coefficient Constants for Converging Fittings: Equation 4.21

α	K_{branch}				K_{run}			
	C	D	E	F	C	D	E	F
30°	Table 4.13	1	2	1.74	1	0	1	1.74
45°	Table 4.13	1	2	1.41	1	0	1	1.41
60°	Table 4.13	1	2	1	1	0	1	1
90°	Table 4.13	1	2	0	$K_{run} = 1.55y_b - y_b^2$			

TABLE 4.13Values of C in Equation 4.21 for K_{branch}

β_{branch}^2	y_b	
	≤ 0.35	> 0.35
≤ 0.35	C = 1	C = 1
> 0.35	C = 0.9(1 - y_b)	C = 0.55

For diverging fittings, the expressions used to calculate the loss coefficients for the branch and run are,

$$K_{branch} = G \left[1 + H \left(\frac{y_b}{\beta_b^2} \right)^2 - J \left(\frac{y_b}{\beta_b^2} \right) \cos \alpha \right] \quad (4.24)$$

$$K_{run} = M y_b^2 \quad (4.25)$$

The values of G , H , J , and M are summarized in Tables 4.14, 4.15, and 4.16.

In a diverging or converging fitting, it is possible for the head loss in either the branch or the run to be negative. If this occurs, there is actually a head *gain* through that portion of the fitting. This can occur when the slower moving fluid in the fitting is accelerated to the velocity of the combined flow. Even though there may be head gain in a branch or run, the gain is offset by a higher head loss through the other leg of the fitting resulting in an overall head loss for the entire fitting.

Example 4.8

A 4-nom class 300 tee fitting with equal leg diameters has 300 gpm of water at 60°F flowing into the straight leg and 100 gpm of 60°F water converging in from the 90° branch leg. Determine the loss coefficients for the branch and run and the head loss across each flow path.

Solution

According to Table 4.7, a class-300 fitting should be paired with a schedule 40 pipe. Therefore, the inside diameter of the pipe connected to the fitting can be found in Appendix C,

$$D = 0.33550 \text{ ft}$$

TABLE 4.14

Branch Loss Coefficient Constants for
Diverging Fittings: Equation 4.24

α	G	H	J
0° to 60°	Table 4.15	1	2
90° with $\beta_{branch} \leq 2/3$	1	1	2
90° with $\beta_{branch} = 1$	$1 + 0.3y_b^2$	0.3	0

TABLE 4.15

Values of G in Equation 4.24 for K_{branch}

β_{branch}^2		
≤ 0.35	$G = 1.1 - 0.7y_b$ for $y_b \leq 0.6$	$G = 0.85$ for $y_b > 0.6$
> 0.35	$G = 1.0 - 0.6y_b$ for $y_b \leq 0.4$	$G = 0.60$ for $y_b > 0.4$

TABLE 4.16

Values of M in Equation 4.25 for K_{run}

β_{branch}^2	y_b	
	≤ 0.5	> 0.5
≤ 0.40	$M = 0.4$	$M = 0.4$
> 0.40	$M = 2(2y_b - 1)$	$M = 0.3(2y_b - 1)$

The loss coefficients for the branch and run of the tee can be found using Equation 4.21 and Table 4.12. Since the fitting has equal leg diameters,

$$\beta_{branch} = 1$$

The temperature of the water is the same for the straight and branch runs. Therefore, the volumetric flow rates are additive. The combined flow through the fitting is,

$$\dot{V}_c = \dot{V}_b + \dot{V}_s = (100 + 300) \text{ gpm} = 400 \text{ gpm}$$

The volumetric flow fraction through the branch is,

$$y_b = \frac{\dot{V}_b}{\dot{V}_c} = \frac{100 \text{ gpm}}{400 \text{ gpm}} = 0.25$$

Using Table 4.12 with the parameters calculated above, the values of the branch coefficients, C, D, E, and F can be found,

$$C = 0.9(1 - y_b) = 0.9(1 - 0.25) = 0.675$$

$$D = 1$$

$$E = 2$$

$$F = 0$$

Using these values, the loss coefficient for the branch can be found,

$$K_{branch} = C \left[1 + D \left(\frac{y_b}{\beta_b} \right)^2 - E(1 - y_b)^2 - F \left(\frac{y_b}{\beta_b} \right)^2 \right]$$

$$K_{branch} = (0.675) \left[1 + 1 \left(\frac{0.25}{1} \right)^2 - 2(1 - 0.25)^2 - 0 \right] = \underline{\underline{-0.0422}}$$

This indicates that there is actually a head *gain* in the branch due to the acceleration of the fluid to the velocity of the combined flow. The head loss associated with the branch flow can be found once the velocity in the combined leg is known,

$$V_c = \frac{4\dot{V}_c}{\pi D^2} = \frac{4 \left(400 \frac{\text{gal}}{\text{min}} \right) \left(2.228 \times 10^{-3} \frac{\text{ft}^3 \cdot \text{min}}{\text{s} \cdot \text{gal}} \right)}{\pi (0.33550 \text{ ft})^2} = 10.08 \frac{\text{ft}}{\text{s}}$$

Therefore, the head loss associated with the branch of the tee is,

$$l_{branch} = K_{branch} \frac{V_c^2}{2g} = (-0.0422) \frac{\left(10.08 \frac{\text{ft}}{\text{s}} \right)^2}{2 \left(32.174 \frac{\text{ft}}{\text{s}^2} \right)} = \underline{\underline{-0.067 \text{ ft}}}$$

According to Table 4.12, the loss coefficient for the run part of the tee is,

$$K_{run} = 1.55y_b - y_b^2 = 1.55(0.25) - (0.25)^2 = \underline{\underline{0.325}}$$

Therefore, the head loss associated with the run of the tee is,

$$l_{run} = K_{run} \frac{V_c^2}{2g} = (0.325) \frac{\left(10.08 \frac{\text{ft}}{\text{s}} \right)^2}{2 \left(32.174 \frac{\text{ft}}{\text{s}^2} \right)} = \underline{\underline{0.51 \text{ ft}}}$$

As expected, there is a net head loss associated with the fitting even though there is a head gain in the branch fluid.

4.5 Design and Analysis of Pipe Networks

In the design and analysis of fluid networks, the same three problem types that were discussed in Section 4.2 exist.

Type 1. Knowing the construction of the pipe network (i.e., the layout and all dimensions) and the required fluid flow rate, determine the pressure drop in the pipe network. This type of calculation is important in the selection of pumps to move the fluid.

Type 2. Knowing the construction of the pipe network and the pressure drop that a pump can overcome, determine the flow rate of the fluid through the network. This type of calculation allows the engineer to determine if a given pump has the capability to move the required amount of fluid through the network.

Type 3. Knowing the volumetric flow rate requirement and the pressure drop that the pump can overcome, determine the proper pipe diameter for the network.

In Section 4.3, these three types of problems have been applied to straight pipe lengths. The problems are no different in a complex pipe network. In addition to straight runs of pipe, there are valves and fittings as well.

Example 4.9

Liquid cyclohexane at 30°C is pumped at a volumetric flow rate of 10 L/s through a pipe network to a large storage tank as shown in Figure E4.9. Determine the pressure drop (kPa) from the pump discharge (A) to the pipe exit (B).

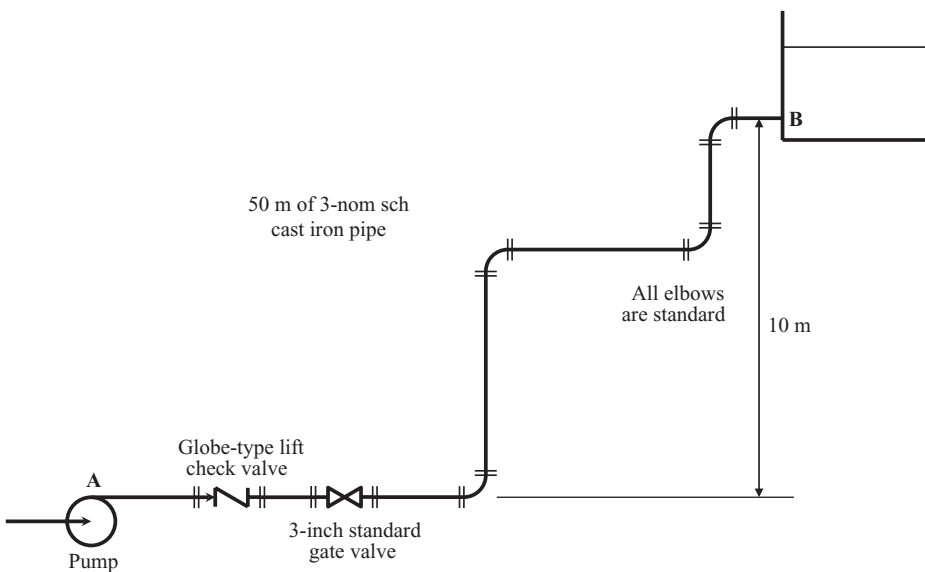


FIGURE E4.9

A pump and pipe network for transporting cyclohexane to a tank.

Solution

The pressure drop from A to B is equal to the pressure loss in the pipe network which includes the elevation head, the head loss due to friction, and the minor head loss due to the valves and fittings. Applying the conservation of energy equation between points A and B results in,

$$\frac{P_A}{\gamma} + z_A = \frac{P_B}{\gamma} + z_B + \left(f \frac{L}{D} + \sum K \right) \frac{V^2}{2g}$$

Rearranging this equation to solve for the pressure drop that the pump must overcome results in,

$$\frac{P_A - P_B}{\gamma} = \frac{\Delta P}{\gamma} = (z_B - z_A) + \left(f \frac{L}{D} + \sum K \right) \frac{V^2}{2g}$$

The properties of the cyclohexane can be found from Appendix B.3,

$$\gamma = \rho g = \left(769.15 \frac{\text{kg}}{\text{m}^3} \right) \left(9.807 \frac{\text{m}}{\text{s}^2} \right) \left(\frac{\text{N} \cdot \text{s}^2}{\text{kg} \cdot \text{m}} \right) = 7543.1 \frac{\text{N}}{\text{m}^3}$$

$$\mu = 0.81419 \text{ mPa} \cdot \text{s} \left[\left(\frac{\text{Pa} \cdot \text{s}}{1000 \text{ mPa} \cdot \text{s}} \right) \left(\frac{\text{kg}}{\text{Pa} \cdot \text{s} \cdot \text{m} \cdot \text{s}} \right) \right] = 0.00081419 \frac{\text{kg}}{\text{m} \cdot \text{s}}$$

The inside diameter of the pipe can be found in Appendix C and the roughness of the pipe can be found in Table 4.3,

$$D = 7.7927 \text{ cm} = 0.0077927 \text{ m} \quad \varepsilon = 0.26 \text{ cm} = 0.0026 \text{ m}$$

From the drawing, the elevations of points A and B as well as the length of straight pipe in the network are given,

$$z_A = 0 \text{ m} \quad z_B = 10 \text{ m} \quad L = 50 \text{ m}$$

To determine the friction factor, the Reynolds number and relative roughness are required. In order to determine the Reynolds number, the velocity of the cyclohexane in the pipe is needed. This velocity can be found by,

$$V = \frac{\dot{V}}{A} = \frac{4 \dot{V}}{\pi D^2} = \frac{4 \left(10 \frac{\text{L}}{\text{s}} \right) \left(\frac{\text{m}^3}{1000 \text{ L}} \right)}{\pi (0.0077927 \text{ m})^2} = 2.0967 \frac{\text{m}}{\text{s}}$$

The Reynolds number can now be found,

$$\text{Re} = \frac{\rho V D}{\mu} = \frac{\left(769.15 \frac{\text{kg}}{\text{m}^3} \right) \left(2.0967 \frac{\text{m}}{\text{s}} \right) (0.0077927 \text{ m})}{0.00081419 \frac{\text{kg}}{\text{m} \cdot \text{s}}} = 154,351$$

The relative roughness of the pipe can also be found,

$$\frac{\varepsilon}{D} = \frac{0.0026 \text{ m}}{0.0077927 \text{ m}} = 0.03336$$

Using the Reynolds number and the relative roughness, the friction factor can be found using any of the correlations in Table 4.2. Using the Swamee-Jain correlation,

$$f = \frac{0.25}{\left[\log \left(\frac{\varepsilon/D}{3.7} + \frac{5.74}{\text{Re}^{0.9}} \right) \right]^2} = \frac{0.25}{\left[\log \left(\frac{0.03336}{3.7} + \frac{5.74}{154,351^{0.9}} \right) \right]^2} = 0.06013$$

The only task left is to determine the total effect of the minor losses due to the valves and fittings. The check valve size is not given. However, the size can be specified by ensuring that the cyclohexane velocity in the pipe completely lifts the disc from its seat inside the valve. For a globe-type lift check valve, the minimum velocity required is,

$$V_{\min} [\text{ft/s}] = \frac{35}{\sqrt{\rho [\text{lbm/ft}^3]}}$$

For a 3-inch check valve, $\beta = 1$. Therefore,

$$V_{\min, 3\text{-inch}} = \frac{35}{\sqrt{\rho}} = \frac{35}{\sqrt{\left(769.15 \frac{\text{kg}}{\text{m}^3} \right) \left(0.062428 \frac{\text{lbm-m}^3}{\text{ft}^3 \cdot \text{kg}} \right)}} = 5.051 \frac{\text{ft}}{\text{s}} \left(\frac{0.3048 \text{ m}}{\text{ft}} \right) = 1.54 \frac{\text{m}}{\text{s}}$$

Notice that this calculation had to be done in English units before converting the velocity to the SI system. This result indicates that the pipe velocity is higher than the minimum velocity required to completely move the disc in the check valve. Therefore, a 3-inch check valve will work in this application and no reducers are needed to connect the check valve to the pipe. Therefore, the loss coefficients required are,

$$\sum K = K_{\text{check}} + K_{\text{gate}} + 4K_{\text{elbow}} + K_{\text{exit}}$$

Either the 2K or the 3K method of computing the loss coefficients can be used here. In this example, the 2K method will be used due to its relative simplicity compared to the 3K method. Using Equations 4.17 and 4.18 along with the constants from Table 4.8, the calculated loss coefficients are,

$$\begin{aligned} K_{\text{check}} &= \frac{K_1}{\text{Re}} + K_{\infty} \left(1 + \frac{1}{D} \right) = \frac{2000}{154,351} + 10 \left(1 + \frac{1}{3.068 \text{ in}} \right) = 13.2724 \\ K_{\text{gate}} &= \frac{K_1}{\text{Re}} + K_{\infty} \left(1 + \frac{1}{D} \right) = \frac{300}{154,351} + 0.10 \left(1 + \frac{1}{3.068 \text{ in}} \right) = 0.1345 \\ K_{\text{elbow}} &= \frac{K_1}{\text{Re}} + K_{\infty} \left(1 + \frac{1}{D} \right) = \frac{800}{154,351} + 0.25 \left(1 + \frac{1}{3.068 \text{ in}} \right) = 0.3367 \\ K_{\text{exit}} &= \frac{K_1}{\text{Re}} + K_{\infty} = \frac{0}{154,351} + 1.0 = 1.0 \end{aligned}$$

Therefore, the total loss coefficient is,

$$\sum K = 13.2724 + 0.1345 + 4(0.3367) + 1.0 = 15.754$$

Now, everything is known except the pressure drop from point A to B. Using the conservation of energy equation developed above,

$$\Delta P = \gamma \left[(z_B - z_A) + \left(f \frac{L}{D} + \sum K \right) \frac{V^2}{2g} \right]$$

$$\Delta P = \left(7543.1 \frac{\text{N}}{\text{m}^3} \right) \left\{ (10 - 0) \text{m} + \left[(0.06013) \left(\frac{50 \text{ m}}{0.077927 \text{ m}} \right) + 15.754 \right] \right\} \frac{\left(2.0967 \frac{\text{m}}{\text{s}} \right)^2}{2 \left(9.807 \frac{\text{m}}{\text{s}^2} \right)}$$

$$\Delta P = 110,712 \frac{\text{N}}{\text{m}^2} \left(\frac{\text{Pa} \cdot \text{m}^2}{\text{N}} \right) \left(\frac{\text{kPa}}{1000 \text{ Pa}} \right) = \underline{\underline{110.7 \text{ kPa}}}$$

This is the pressure that the pump must overcome to move the cyclohexane through the pipe network at the given flow rate of 10 L/s. Using the 3K method results in a total pressure loss of 106.4 kPa. The difference between the two methods, 4.3 kPa (~0.6 psi), is relatively small.

4.5.1 Parallel Pipe Networks

Often pipe or tube networks have parallel runs. Figure 4.5 shows a sketch of a pipe system with two parallel flow paths, labeled 1 and 2. The label “c” indicates combined flow. In order to analyze a system like this, a system boundary is sketched around the individual pipes in the network. Once the system boundary is identified, the conservation of mass and conservation of energy equations are applied.

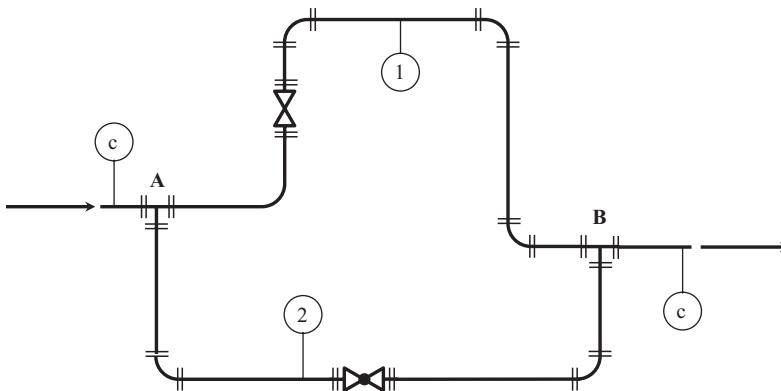


FIGURE 4.5
A parallel pipe network (plan view).

In Figure 4.5, if a system boundary was sketched around pipe 1 from A to B and a second system boundary around pipe 2 from A to B, it must be true that the pressure drop from A to B is the *same* through each parallel leg. Therefore,

$$(P_A - P_B)_1 = (P_A - P_B)_2 \quad (4.26)$$

If the diameters of each leg are constant, the conservation of energy between points A and B for each leg of the network can be written as,

$$\frac{P_A - P_B}{\gamma} = (z_B - z_A) + \left(f_1 \frac{L_1}{D_1} + \sum K_1 \right) \frac{V_1^2}{2g} + (K_{run,A} + K_{run,B}) \frac{V_c^2}{2g} \quad (4.27)$$

$$\frac{P_A - P_B}{\gamma} = (z_B - z_A) + \left(f_2 \frac{L_2}{D_2} + \sum K_2 \right) \frac{V_2^2}{2g} + (K_{branch,A} + K_{branch,B}) \frac{V_c^2}{2g} \quad (4.28)$$

Notice that the K values for the tees are separated out from the other fittings. This is because the minor losses of the branch and straight runs of the tee are associated with the combined velocity of the flow entering (or leaving) the tee. In Equations 4.27 and 4.28, V_c is the combined flow velocity. Since the pressure drop through each parallel leg is the same,

$$\begin{aligned} & \left(f_1 \frac{L_1}{D_1} + \sum K_1 \right) \frac{V_1^2}{2g} + (K_{run,A} + K_{run,B}) \frac{V_c^2}{2g} \\ &= \left(f_2 \frac{L_2}{D_2} + \sum K_2 \right) \frac{V_2^2}{2g} + (K_{branch,A} + K_{branch,B}) \frac{V_c^2}{2g} \end{aligned} \quad (4.29)$$

The following example illustrates how to apply these equations to a network with parallel flow paths.

Example 4.10

Figure E4.10 shows a parallel flow copper tubing network. Water at 80°F is flowing through the network such that the pressure drop from A to B is 0.2 psi. Determine the

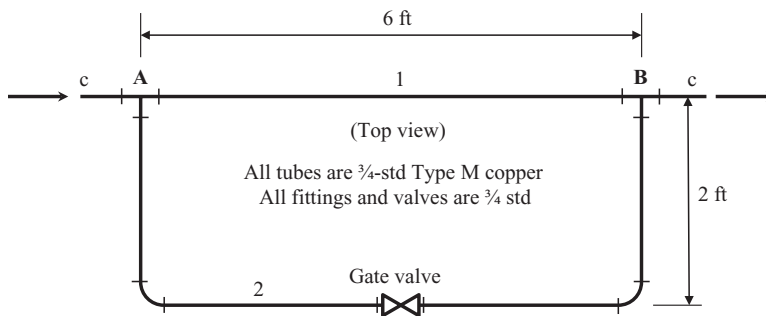


FIGURE E4.10

A parallel copper tubing network.

volumetric flow rate (gpm) through each leg of the parallel network and also determine the total volumetric flow (gpm) through the network.

Solution

The following data pertinent to the system can be found immediately,

$$\gamma = \rho \frac{g}{g_c} = \left(62.213 \frac{\text{lbm}}{\text{ft}^3} \right) \frac{g}{g_c} = 62.213 \frac{\text{lbf}}{\text{ft}^3}$$

Appendix B.3

$$\mu = \mu = \left(2.0737 \frac{\text{lbm}}{\text{ft-hr}} \right) \left(\frac{\text{hr}}{3600 \text{ s}} \right) = 0.00057603 \frac{\text{lbm}}{\text{ft-s}}$$

Appendix B.3

$$D = 0.06758 \text{ ft} \quad \varepsilon = 0.000005 \text{ ft} \quad \therefore \frac{\varepsilon}{D} = \frac{0.000005 \text{ ft}}{0.06758 \text{ ft}} = 0.000073986$$

Appendix D Table 4.3

$$L_1 = 6 \text{ ft} \quad L_2 = [6 + 2(2)]\text{ft} = 10 \text{ ft}$$

The conservation of energy equation applied to a system boundary surrounding parallel run 1 results in,

$$\frac{P_A - P_B}{\gamma} = f_1 \frac{L_1}{D} \frac{V_1^2}{2g} + (K_{run,A} + K_{run,B}) \frac{V_c^2}{2g}$$

Applying the conservation of energy equation to a system boundary surrounding parallel run 2 gives,

$$\frac{P_A - P_B}{\gamma} = \left(f_2 \frac{L_2}{D} + \sum K_2 \right) \frac{V_2^2}{2g} + (K_{branch,A} + K_{branch,B}) \frac{V_c^2}{2g}$$

The friction factors in each pipe require the calculation of the Reynolds number and the relative roughness. Since the volumetric flow rate in each pipe is not known, this becomes a Type 2 iterative solution.

In pipe 1, there are two minor losses associated with the tees. The tee at A is a diverging tee and the tee at B is converging. The losses are those associated with the value of K_{run} for each tee. In pipe 2, the minor losses include a diverging tee branch (A), two elbows, a gate valve, and a converging tee branch (B). The K values for the elbows and gate valve will be determined using the 3K method and values from Table 4.9. However, when calculating the K values for the tees, the value of y_b is unknown since the volumetric flow through each leg is to be determined. This compounds the iterative nature of this calculation.

Due to the highly iterative nature of this problem, it is most convenient to solve it using computer software. However, in this example, the first iteration will be shown to demonstrate how this solution strategy can be programmed into a variety of computer software programs.

Applying the conservation of energy equation to the pressure drop from A to B in leg 1 of the network,

$$\frac{(P_A - P_B)_1}{\gamma} = f \frac{L}{D} \frac{V_1^2}{2g} + (K_{run,A} + K_{run,B}) \frac{V_c^2}{2g}$$

Similarly, for leg 2 of the network,

$$\frac{(P_A - P_B)_2}{\gamma} = \left(f_2 \frac{L}{D} + 2K_{elbow} + K_{valve} \right) \frac{V_2^2}{2g} + (K_{branch,A} + K_{branch,B}) \frac{V_c^2}{2g}$$

For this parallel network of tubing, the pressure drop from A to B is the same through both legs,

$$\frac{(P_A - P_B)_1}{\gamma} = \frac{(P_A - P_B)_2}{\gamma}$$

In a typical Type 2 problem (e.g., Example 4.3), the iterative process begins by guessing the friction factor in the pipe and solving for the fluid velocity. However, in this problem, the fluid velocity in either conservation of energy equation (leg 1 or 2) cannot be explicitly solved for. An alternate solution is to guess the velocity in each tube, then compute the friction factors from the Reynolds numbers and relative roughness. Once this is done, the loss coefficients can be computed and the pressure drop from A to B through each leg can be found. If the two calculated pressure drops do not match, then the velocities must be adjusted until the pressure drops equalize.

To begin this iteration, the velocities in each tube will be estimated as follows,

$$V_1 = 3 \frac{\text{ft}}{\text{s}} \quad V_2 = 1.5 \frac{\text{ft}}{\text{s}}$$

This allows for the calculation of the Reynolds numbers and friction factors in each tube,

$$\begin{aligned} \text{Re}_1 &= \frac{\rho V_1 D}{\mu} = 21,896 & f_1 &= \frac{0.25}{\left[\log \left(\frac{\epsilon/D}{3.7} + \frac{5.74}{\text{Re}_1^{0.9}} \right) \right]} = 0.02543 \\ \text{Re}_2 &= \frac{\rho V_2 D}{\mu} = 10,948 & f_2 &= \frac{0.25}{\left[\log \left(\frac{\epsilon/D}{3.7} + \frac{5.74}{\text{Re}_2^{0.9}} \right) \right]} = 0.03035 \end{aligned}$$

Knowing the velocity in each tube allows for the calculation of the volumetric flow rate through each tube and the ratio of the branch flow to the combined flow,

$$\dot{V}_1 = \frac{\pi D^2}{4} V_1 = 4.8298 \text{ gpm} \quad \dot{V}_2 = \frac{\pi D^2}{4} V_2 = 2.4149 \text{ gpm} \quad \dot{V}_c = \dot{V}_1 + \dot{V}_2 = 7.2447 \text{ gpm}$$

$$y_b = \frac{\dot{V}_2}{\dot{V}_c} = 0.33333$$

The loss coefficients can now be determined for the fittings, valve, and tees. For the fittings and valve,

$$K_{elbow} = \frac{K_1}{\text{Re}_2} + K_\infty \left(1 + \frac{K_d}{D_{nom}^{0.3}} \right) = 0.82355$$

$$K_{valve} = \frac{K_1}{\text{Re}_2} + K_\infty \left(1 + \frac{K_d}{D_{nom}^{0.3}} \right) = 0.22171$$

The diameter of the tee ($\alpha = 90^\circ$) inlets and outlets are all the same. Therefore, $\beta_b = 1$. The K values of each tee can now be calculated,

$$K_{run,A} = My_b^2 = [2(2y_b - 1)]y_b^2 = -0.07407$$

$$K_{branch,A} = G \left[1 + H \left(\frac{y_b}{\beta_b^2} \right)^2 - J \left(\frac{y_b}{\beta_b^2} \right) \cos \alpha \right] = (1.0 - 0.6y_b) \left[1 + 0.3 \left(\frac{y_b}{\beta_b^2} \right)^2 \right] = 1.06778$$

$$K_{run,B} = 1.55y_b - y_b^2 = 0.40556$$

$$K_{branch,B} = C \left[1 + D \left(\frac{y_b}{\beta_b^2} \right)^2 - E(1 - y_b)^2 - F \left(\frac{y_b}{\beta_b^2} \right)^2 \right]$$

$$= 0.9(1 - y_b) \left[1 + \left(\frac{y_b}{\beta_b^2} \right)^2 - 2(1 - y_b)^2 \right] = 0.13333$$

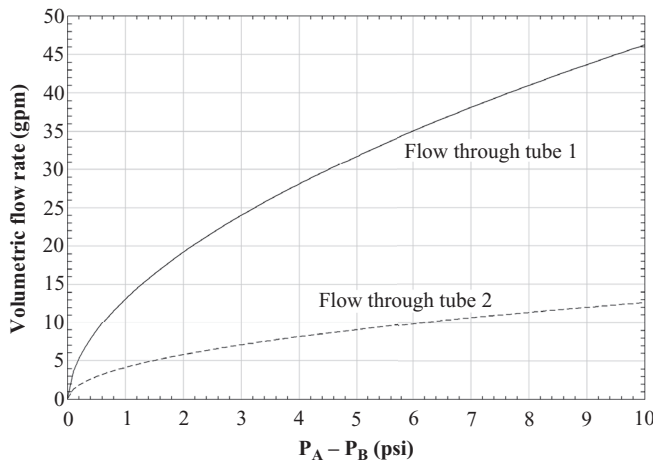
The velocity head for the friction loss in the tees is based on the combined flow velocity,

$$V_c = \frac{4\dot{V}_c}{\pi D^2} = 4.5 \frac{\text{ft}}{\text{s}}$$

At this point, everything is known to compute the pressure drop in each leg of the network,

$$(P_A - P_B)_1 = \gamma \left[f \frac{L}{D} \frac{V_1^2}{2g} + (K_{run,A} + K_{run,B}) \frac{V_c^2}{2g} \right] = 0.18150 \text{ psi}$$

$$(P_A - P_B)_2 = \gamma \left[\left(f_2 \frac{L}{D} + 2K_{elbow} + K_{valve} \right) \frac{V_2^2}{2g} + (K_{branch,A} + K_{branch,B}) \frac{V_c^2}{2g} \right] = 0.25938 \text{ psi}$$

**FIGURE 4.6**

Result of a parametric study for Example 4.10.

The actual pressure drop from A to B is given as 0.2 psi. Therefore, the velocities V_1 and V_2 need to be adjusted and the iterative calculation repeated until both pressure drops are equal to 0.2 psi.

The solution to this iterative set of equations is $\dot{V}_1 = 5.35$ gpm, $\dot{V}_2 = 1.88$ gpm, and $\dot{V}_c = 7.23$ gpm. This result indicates that leg 1, the straight run, carries more of the flow. This is expected because leg 1 has a lower head loss due to friction and fittings. In addition, the length of straight tube in leg 1 is smaller than in leg 2 resulting in a lower friction loss.

As Example 4.10 demonstrates, the solution of these types of problems involves multiple iterations of fairly complex calculations. Problems like these are best solved using computer software. Another feature of many computer software packages, especially equation solvers, is the ability to conduct parametric studies. Consider a case where you are interested in how the flow splits between the two legs of the parallel system shown in Example 4.10 as the pressure drop between points A and B varies. Using computer software, the problem can be solved for a range of $P_A - P_B$. The results can be plotted for a visual display of the behavior of the system as shown in Figure 4.6.

4.6 Economic Pipe Diameter

Many possible pipe diameters can be used to transport a fixed flow rate through a pipe. A small pipe has a low initial cost, but the pressure drop may be quite high resulting in a significant pumping cost to move the fluid through the pipe. On the other hand, a large pipe will have a significant first cost, but the pressure drop is smaller resulting in a low pumping cost. This thinking leads one to believe that there must be a pipe diameter that minimizes the total cost of the pipe system. This diameter is known as the *economic pipe diameter*, or *optimum pipe diameter*.

The expressions developed in this section are based on the work of Darby and Melson (1982) and further refined by Janna (2015). Even though many simplifying assumptions are

made as the method is developed, the resulting expressions provide a reasonable estimate to the economic diameter.

4.6.1 Cost of a Pipe System

There are many costs that are incurred in a pipe system. However, these costs can be grouped into two categories; capital (i.e., initial) costs, and annual costs. The capital cost of a pipe system includes the cost of the pipe itself and costs associated with installation, valves, fittings, pumps, insulation, hangers, and supports. The costs incurred annually are the cost of energy required to move the fluid through the pipe system, and any maintenance costs.

Since capital costs and annual costs occur at different times, economic interest factors must be considered to align all costs to a common point on the cash flow diagram for the pipe system. In the method presented here, costs are converted to annual costs. Interest is assumed to be compounded annually.

4.6.2 Determination of the Economic Diameter

The strategy used to determine the economic diameter is to develop a *cost function* that represents the total annual costs of the pipe system as a function of the pipe diameter,

$$AC_T = f(D) \quad (4.30)$$

The diameter that results in the lowest annual cost is the economic diameter. This diameter can be found by taking the derivative of Equation 4.30, setting it equal to zero, and solving for D .

The total annual cost of the pipe system is defined as,

$$AC_T = AC_P + AC_H + AC_M + AC_E \quad (4.31)$$

In this equation, AC_P is the annual cost of the pipe in the system including installation, AC_H is the annual cost of the hardware including valves, fittings, pumps, insulation, supports, etc., AC_M is the annual cost of maintenance for the system, and AC_E is the annual cost of the energy required to move the fluid through the system.

The initial cost of installed pipe per foot is determined from cost data collected in 1980 (Darby and Melson 1982). These data can be fit to the following equation,

$$\frac{IC_P}{L} = (1 + e)^{(yr-1980)} C_1 D^s \quad (4.32)$$

In this equation, C_1 and s are constants. C_1 represents the installed cost per foot of a 12-nom pipe based on 1980 dollars. The exponent s corresponds to various pipe classes. The values of C_1 and s are given in Table 4.17 (Janna 2015). The term in parenthesis involving the variables, e and yr , is a way to convert the constant C_1 from 1980 dollars to the current dollars. The variable e is an estimated average yearly escalation rate (expressed in decimal form) from 1980 to present that takes into account inflation. The variable, yr , is the current year. Equation 4.32 is valid for pipe diameters up to 36-inches.

TABLE 4.17Constants C_1 and s in Equation 4.32

Pipe Class (Max Working Pressure)	C_1 (\$/ft ^{$s+1$})	s
300# (720 psig)	22.50	1.14
400# (960 psig)	23.14	1.20
600# (1440 psig)	28.28	1.29
900# (2160 psig)	36.10	1.32
1500# (3600 psig)	53.39	1.35

Example 4.11

Determine the installed cost per foot of an 8-nom sch 40 (class 300#) pipe in 1980 and 2018 using an estimated yearly inflation rate of 2%.

Solution

The inside diameter of an 8-nom sch 40 pipe can be found in Appendix C,

$$D = 0.66508 \text{ ft}$$

Also, from Table 4.17,

$$s = 1.14 \quad C_1 = 22.50 \frac{\$}{\text{ft}^{2.14}}$$

Using Equation 4.32, in 1980, the installed pipe cost was,

$$\frac{IC_P}{L} = C_1 D^s = \left(22.50 \frac{\$}{\text{ft}^{2.14}} \right) (0.66508 \text{ ft})^{1.14} = \underline{\underline{14.13 \frac{\$}{\text{ft}}}}$$

Using the estimated inflation rate of 2%, the installed pipe cost in 2018 is,

$$\begin{aligned} \frac{IC_P}{L} &= (1+e)^{(yr-1980)} C_1 D^s \\ \frac{IC_P}{L} &= (1+0.02)^{(2018-1980)} \left(22.50 \frac{\$}{\text{ft}^{2.14}} \right) (0.66508 \text{ ft})^{1.14} = \underline{\underline{31.76 \frac{\$}{\text{ft}}}} \end{aligned}$$

This shows the estimated effect of inflation on the price of the installed pipe.

Knowing the initial cost per unit length of the pipe and installation, the annual cost can be determined by using the capital recovery interest factor from Chapter 2,

$$\frac{AC_P}{L} = \frac{IC_P}{L} \left(\frac{A}{P}, i, n \right) \quad (4.33)$$

For shorthand purposes, the variable crf will be used for the capital recovery factor. Using this notation, Equation 4.33 is written as,

$$\frac{AC_P}{L} = (crf) \frac{IC_P}{L} = (crf)(1+e)^{(yr-1980)} C_1 D^s \quad (4.34)$$

The fittings, valves, pumps, and other hardware used in a piping system are different for each design. For the economic diameter model, it is sufficient to estimate these costs as a multiple of the initial cost per unit length of the pipe and installation. This multiple, F , typically ranges from 5 to 7. Using this idea, the initial cost of the hardware per foot is given by,

$$\frac{IC_H}{L} = F \frac{IC_P}{L} = F(1+e)^{(yr-1980)} C_1 D^s \quad (4.35)$$

The annual cost per unit length of the hardware can be determined using the capital recovery factor,

$$\frac{AC_H}{L} = \frac{IC_H}{L} (crf) = (crf) F(1+e)^{(yr-1980)} C_1 D^s \quad (4.36)$$

Maintenance costs occur annually and are estimated to be a fraction of the initial cost per foot of the pipe and the hardware,

$$\frac{AC_M}{L} = b \left(\frac{IC_P}{L} + \frac{IC_H}{L} \right) \quad (4.37)$$

In this equation, b is the estimated percent (expressed as a decimal) of the initial costs that will be spent on annual maintenance. Typical values for b are 0.01–0.02 (1–2%).

Adding Equations 4.34, 4.36, and 4.37 together and algebraically rearranging results in,

$$\frac{AC_P}{L} + \frac{AC_H}{L} + \frac{AC_M}{L} = (crf + b)(1+F)(1+e)^{(yr-1980)} C_1 D^s \quad (4.38)$$

Multiplying both sides through by the length, L , gives,

$$AC_P + AC_H + AC_M = L(crf + b)(1+F)(1+e)^{(yr-1980)} C_1 D^s \quad (4.39)$$

These are the first three terms of Equation 4.31. The last term in Equation 4.31 is the annual cost of the energy required to move the fluid through the pipe system by the pumps. The annual cost of the energy can be written as,

$$AC_E = C_2 \dot{W}_p t \quad (4.40)$$

In this equation, C_2 is the cost of energy, \dot{W}_p is the electrical power input into the pump, and t is the annual operation time of the system. Due to inefficiencies, the power transmitted to the fluid is less than the power input to the pump. The efficiency of the pump can be defined as,

$$\eta_p = \frac{\dot{W}}{\dot{W}_p} \quad (4.41)$$

Solving Equation 4.41 for the power input to the pump and substituting into Equation 4.40 gives,

$$AC_E = \frac{C_2 \dot{W} t}{\eta_p} \quad (4.42)$$

The power delivered to the fluid can be determined by analyzing a general system boundary that represents a pipe system as shown in Figure 4.7. Assuming the pipe diameter is the same throughout the network and the fluid is incompressible, the conservation of energy equation applied to the system identified in Figure 4.7 results in,

$$\frac{\dot{W}}{\dot{m}} = (h_2 - h_1) + g(z_2 - z_1) \quad (4.43)$$

Assuming that the minor losses in the pipe system are negligible, Equation 4.43 can be rewritten as,

$$\frac{\dot{W}}{\dot{m}} = \frac{P_2 - P_1}{\rho} + g(z_2 - z_1) + f \frac{L}{D} \frac{V^2}{2} \quad (4.44)$$

The velocity of the fluid is related to the mass flow rate by,

$$V = \frac{\dot{m}}{\rho A} = \frac{4\dot{m}}{\pi \rho D^2} \quad (4.45)$$

Substituting Equation 4.45 into Equation 4.44 and solving for the power input to the fluid results in,

$$\dot{W} = \dot{m} \left[\frac{P_2 - P_1}{\rho} + g(z_2 - z_1) \right] + \frac{8fL\dot{m}^3}{\pi^2 \rho^2 D^5} \quad (4.46)$$

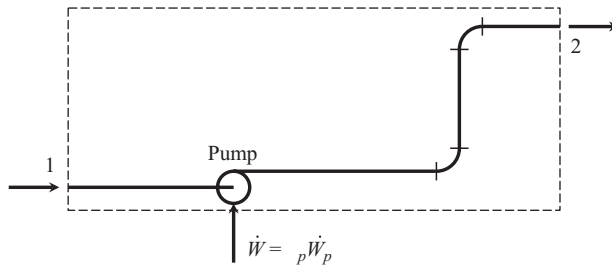


FIGURE 4.7
A pump and pipe network.

Substituting this result into Equation 4.42 gives the annual cost of the power required to move the fluid through the system,

$$AC_E = \frac{\dot{m}C_2 t}{\eta_p} \left[\frac{P_2 - P_1}{\rho} + g(z_2 - z_1) \right] + \frac{8C_2 t f L \dot{m}^3}{\eta_p \pi^2 \rho^2 D^5} \quad (4.47)$$

The total annual cost of the pipe network can now be determined by substituting Equations 4.47 and 4.39 into Equation 4.31,

$$AC_T = L(crf + b)(1 + F)(1 + e)^{(yr-1980)} C_1 D^s + \frac{\dot{m}C_2 t}{\eta_p} \left[\frac{P_2 - P_1}{\rho} + g(z_2 - z_1) \right] + \frac{8C_2 t f L \dot{m}^3}{\eta_p \pi^2 \rho^2 D^5} \quad (4.48)$$

The derivative of this equation with respect to the pipe diameter is,

$$\frac{d(AC_T)}{dD} = sL(crf + b)(1 + F)(1 + e)^{(yr-1980)} C_1 D^{s-1} - 5 \left(\frac{8C_2 t f L \dot{m}^3}{\eta_p \pi^2 \rho^2 D^6} \right) \quad (4.49)$$

Setting Equation 4.49 to zero and solving for the D gives,

$$D_{econ} = \left[\frac{40C_2 t f \dot{m}^3}{s(crf + b)(1 + F)(1 + e)^{(yr-1980)} C_1 \eta_p \pi^2 \rho^2} \right]^{\frac{1}{s+5}} \quad (4.50)$$

This is the economic diameter that minimizes the cost of the pipe system. Several observations can be made about the economic diameter,

- The derivative of the total annual cost function was taken with respect to the diameter, holding all other variables constant.
- The pipe length is not part of the economic diameter calculation.
- The only fluid property that is included directly is the density. However, the fluid's viscosity is also part of the problem through the friction factor.
- The pressure and elevation head losses through the pipe does not appear in the economic diameter calculation.
- The solution to the economic diameter equation is iterative because the friction factor is unknown.

The velocity of the fluid flowing in a pipe that has a diameter equal to the economic diameter is known as the *economic velocity*. This can be easily computed by,

$$V_{econ} = \frac{\dot{V}}{A} = \frac{4\dot{V}}{\pi D_{econ}^2} = \frac{4\dot{m}}{\pi \rho D_{econ}^2} \quad (4.51)$$

The following example demonstrates the calculation procedure used to determine the economic diameter using Equation 4.50.

Example 4.12

A commercial steel schedule 40 pipe is being used to transport liquid cyclohexane at 60°F to a heat exchanger at a flow rate of 1000 gpm. The fittings, valves, supports, and pump are estimated to cost 6.5 times the annual installed pipe cost per ft. Annual maintenance is estimated to be 2% of the installed pipe and hardware costs per ft. For this service, the pipe classification is determined to be 300#. The pump in the system runs 16 hours per day, 260 days per year. The efficiency of the pump, determined from performance curves, is 78%. The cost of energy is \$0.09/kW-h. The pipeline is expected to operate for 25 years with a minimum rate of return of 12%. Inflation is estimated to be 2.5% per year since 1980. The pipeline was put into service in 2013. Determine the economic diameter of the pipeline (ft) and the economic velocity of the cyclohexane (ft/s).

Solution

The two major complexities with economic diameter problems are (1) the iterative nature of the problem, and (2) keeping track of the units to ensure that the calculated D_{econ} is in ft. The iterative nature of the problem is easily dealt with by using computer software. The unit analysis presented here shows the conversions required to ensure that D is computed in the correct units. In Equation 4.49, the term in brackets must have units of $[\text{ft}^{(s+5)}]$.

The constants C_1 and s are determined from Table 4.16,

$$s = 1.14 \quad C_1 = 22.50 \frac{\$}{\text{ft}^{2.14}}$$

A time basis must be selected. It makes no difference what the basis is, but once a selection is made, careful conversion of all time-based parameters must be considered. In this example, the time basis selected is seconds. Therefore,

$$t = \left(16 \frac{\text{hr}}{\text{day}} \right) (260 \text{ day}) \left(\frac{3600 \text{ s}}{\text{hr}} \right) = 1.498 \times 10^7 \text{ s}$$

Also, when computing the mass flow rate, it must have units of $[\text{lbm/s}]$. This means that the volumetric flow rate and velocity must use seconds as a time basis as well. The volumetric flow rate is given in $[\text{gpm}]$. This must be converted to $[\text{ft}^3/\text{s}]$,

$$\dot{V} = 1000 \text{ gpm} \left(8.02083 \frac{\text{ft}^3}{\text{h-gpm}} \right) \left(\frac{\text{h}}{3600 \text{ s}} \right) = 2.2280 \frac{\text{ft}^3}{\text{s}}$$

Appendix A

Now, the mass flow rate can be found along with the its proper units,

$$\dot{m} = \rho \dot{V} = \left(48.867 \frac{\text{lbm}}{\text{ft}^3} \right) \left(2.2280 \frac{\text{ft}^3}{\text{s}} \right) = 108.87 \frac{\text{lbm}}{\text{s}}$$

Appendix B

The value of C_2 is given in $[\$/\text{kWh}]$. These units will need to be converted to $[\$/\text{ft-lbf}]$.

$$C_2 = \left(0.09 \frac{\$}{\text{kWh}} \right) \left(\frac{2.77778 \times 10^{-4} \text{ kWh}}{737.562 \text{ ft-lbf}} \right) = 3.3896 \times 10^{-8} \frac{\$}{\text{ft-lbf}}$$

Appendix A

This will introduce the proper length unit (ft), but it also unveils a new unit problem; the unit [lbf] has crept into the analysis. This means that both [lbm] and [lbf] are in the expression. To resolve this issue, g_c will have to be used.

The capital recovery factor is not dependent on the diameter of the pipe. Therefore, it can also be calculated. Using the capital recovery factor expression from Table 2.2,

$$crf = \left(\frac{A}{P}, 0.12, 25 \right) = \frac{0.12(1+0.12)^{25}}{(1+0.12)^{25} - 1} = 0.12750$$

The rest of the constants in Equation 4.50 are dimensionless. Using the units determined above, a unit analysis on the term in brackets in Equation 4.50 reveals,

$$\frac{40C_2 t \dot{m}^3}{s(crf + b)(1 + F)(1 + e)^{(yr-1980)} C_1 \eta_p \pi^2 \rho^2} [=] \frac{\left(\frac{\$}{\text{ft-lbf}} \right) (s) \left(\frac{\text{lbm}^3}{s^3} \right)}{\left(\frac{\$}{\text{ft}^{s+1}} \right) \left(\frac{\text{lbm}^2}{\text{ft}^6} \right) \left(g_c \frac{\text{lbm-ft}}{\text{lbf-s}^2} \right)} = \text{ft}^{s+5}$$

This analysis indicates that the units have worked out correctly and the force-mass conversion factor g_c must be included in the denominator of Equation 4.50 if the IP unit system is being used.

The friction factor is unknown at this point because the pipe diameter is unknown. Therefore, this is a Type 3 iterative solution. The iterative procedure is,

1. Guess the diameter of the pipe.
2. Determine the velocity in the pipe using the known volumetric flow rate and the diameter from Step 1.
3. Determine the Reynolds number of the flow using the velocity calculated in Step 2.
4. Calculate the relative roughness, ϵ/D using the diameter from Step 1.
5. Determine the friction factor using any of the correlations listed in Table 4.2.
6. Calculate the economic diameter using Equation 4.50.
7. If the diameter from (1) is not the same as the diameter from (7), repeat to Step 1 with the newly calculated diameter and repeat the process until closure.

This iterative process can be easily implemented into a variety of computer software packages.

To begin this solution, a diameter of 0.4 ft will be assumed. Following the iterative procedure outlined above,

Iteration 1	Iteration 2	Iteration 3
$D = 0.4 \text{ ft}$	$D = 0.48466 \text{ ft}$	$D = 0.48343 \text{ ft}$
$V = \frac{4\dot{V}}{\pi D^2} = 17.730 \frac{\text{ft}}{\text{s}}$	$V = \frac{4\dot{V}}{\pi D^2} = 12.077 \frac{\text{ft}}{\text{s}}$	$V = \frac{4\dot{V}}{\pi D^2} = 12.139 \frac{\text{ft}}{\text{s}}$
$\text{Re} = \frac{\rho V D}{\mu} = 498,946$	$\text{Re} = \frac{\rho V D}{\mu} = 411,791$	$\text{Re} = \frac{\rho V D}{\mu} = 412,838$
$\epsilon/D = 0.000375$	$\epsilon/D = 0.00030949$	$\epsilon/D = 0.00031028$
$f = 0.1694$	$f = 0.1668$	$f = 0.1668$
$D_{\text{calc}} = 0.48466 \text{ ft}$	$D_{\text{calc}} = 0.48343 \text{ ft}$	$D_{\text{calc}} = 0.48344 \text{ ft}$

The iterative process has closed to an economic diameter of $D_{econ} = 0.4834$ ft. This corresponds to an economic velocity of 12.14 ft/s.

The results of Example 4.12 indicate an economic diameter of 0.4834 ft. Referring to Appendix C, it is clear that this is not a standard pipe diameter. For schedule 40 pipe, it falls between 5-nom ($D = 0.42058$ ft) and 6-nom ($D = 0.50542$ ft). This selection is different compared to a pure type 3 problem. Here, *both* pipes will satisfy the volumetric flow rate. The next challenge is to determine which pipe size to specify. In order to do this, it is helpful to construct the *cost curves*.

4.6.3 Cost Curves

Once an economic diameter is calculated, a standard pipe needs to be selected. The selection of the proper size pipe can be aided by analysis of the *cost curves* for the system. The total annual cost of the system is given by Equation 4.48. This equation can be rearranged as follows,

$$\begin{aligned} AC_T - \frac{\dot{m}C_2t}{\eta_p} \left[\frac{P_2 - P_1}{\rho} + g(z_2 - z_1) \right] \\ = L(crf + b)(1 + F)(1 + e)^{(yr-1980)}C_1D^s + \frac{8C_2t\dot{m}^3}{\eta_p\pi^2\rho^2D^5} \end{aligned} \quad (4.52)$$

The left-hand side of Equation 4.52 is independent of the diameter of the pipe. Therefore, it can be replaced by a single variable, Ω , and rewritten as,

$$\Omega_T = L(crf + b)(1 + F)(1 + e)^{(yr-1980)}C_1D^s + \frac{8C_2t\dot{m}^3}{\eta_p\pi^2\rho^2D^5} \quad (4.53)$$

This is a total annual cost that includes the effect of the head losses due to pressure and elevation. Dividing this equation through by the length of the pipe results in,

$$\omega_T = \frac{\Omega_T}{L} = (crf + b)(1 + F)(1 + e)^{(yr-1980)}C_1D^s + \frac{8C_2t\dot{m}^3}{\eta_p\pi^2\rho^2D^5} \quad (4.54)$$

This is a representative cost per unit length of the installed pipe including the head loss effects. This value is *not* the installed cost per unit length; it includes the effect of the head loss through the pipe. The first term on the right hand side of Equation 4.54 is the annual cost per unit length of the pipe, hardware (including pumps, valves, and fittings), and maintenance. The second term is representative of the annual cost of the energy required to move the fluid through the system. Each of these terms is defined as follows,

$$\omega_H = (crf + b)(1 + F)(1 + e)^{(yr-1980)}C_1D^s \quad (4.55)$$

and,

$$\omega_E = \frac{8C_2t\dot{m}^3}{\eta_p\pi^2\rho^2D^5} \quad (4.56)$$

Substituting Equations 4.55 and 4.56 into Equation 4.54 results in,

$$\omega_T = \omega_H + \omega_E \quad (4.57)$$

Each of the terms in Equation 4.57 can be calculated as a function of the pipe diameter and plotted versus diameter. The resulting curves are known as the *cost curves* for the system. Figure 4.8 shows the cost curves for Example 4.12. The curves are drawn assuming that the friction factor is constant and equal to the value determined from the solution of Equation 4.50.

The cost curves clearly show the economic trade-off between the pipe size and the cost of energy required to transport the fluid. As the pipe diameter becomes larger, the capital cost of the pipeline increases (ω_H) whereas the energy costs decrease (ω_E). The trend is exactly opposite for small-diameter pipes. This trade-off results in an optimum point in the total cost curve. This optimum point occurs at the economic diameter.

The cost curves are helpful in visualizing how the pipe diameter influences the economics. In the case of Example 4.12, it was discovered that the economic diameter (0.4834 ft) falls between a 5-nom ($D = 0.42058$ ft) and 6-nom ($D = 0.50542$ ft) pipe. Using Figure 4.8, it can be seen that the annual cost per unit length of a 5-nom pipe is slightly larger than a 6-nom pipe. One may argue that *both* pipes are very close to the economic diameter and either pipe could be selected. While this argument has some validity, it may be wise to select the larger diameter to accommodate future expansion of the pipeline (e.g., increased volumetric flow rate). Therefore, the proper pipe to select for Example 4.11 is a 6-nom sch 40 commercial steel pipe.

Equation 4.54 provides an alternative way to find the economic diameter. Many equation-solving software packages have the capability to perform optimization or min/max studies. Using computer software to find the minimum cost point of the cost curves for Example 4.12 results in an economic diameter of $D_{econ} = 0.4844$ ft. The economic velocity corresponding to this diameter is $V_{econ} = 12.09$ ft/s. Notice that this solution is nearly identical to the solution of Example 4.12, but is not exactly the same. At first glance,

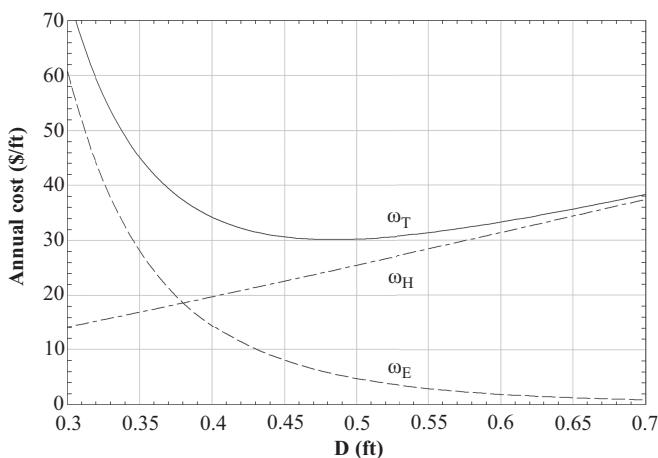


FIGURE 4.8

Cost curves for the pipe system described in Example 4.12.

this may seem strange. It would seem that the calculation of the economic diameter using Equation 4.50 should return the same result as performing a numerical minimization of Equation 4.54. The reason for the slight difference is because Equation 4.50 was derived assuming that the friction factor was not a function of the diameter. This, of course, is not true. The diameter of the pipe will influence the friction factor. However, looking at the results in Example 4.12 compared to the numerical minimization results, one can conclude that while the friction factor depends on the diameter of the pipe, the dependence is very weak. This suggests that the assumptions used to derive the economic diameter, Equation 4.50, are valid.

4.6.4 Economic Velocity Range

Calculation of the economic pipe diameter using Equation 4.50 requires the knowledge and/or estimates of several economic and system parameters. To complicate the calculation, an iterative solution is required to determine D_{econ} because the friction factor is required. An alternative to using Equation 4.50 is to determine the pipeline diameter using a Type 3 friction calculation and compute the corresponding fluid velocity. If this fluid velocity is within a reasonable range of economic velocities, then the selected diameter should be close to the economic diameter. This eliminates the need to use Equation 4.50. However, the reasonable range of economic velocities must be established. To establish a range of reasonable economic velocities the following range of economic parameters will be considered:

- Cost of energy: $\$0.05 / \text{kWh} \leq C_2 \leq \$0.15 / \text{kWh}$
- Hardware multiplier: $5 \leq F \leq 7$
- Maintenance fraction: $0.01 \leq b \leq 0.03$
- Yearly inflation rate: $0.01 \leq e \leq 0.02$
- Anticipated rate of return: $10\% \leq i \leq 20\%$
- System life: $25 \text{ yr} \leq n \leq 50 \text{ yr}$
- System installation year: 2018

In addition, the following range of system parameters will also be considered:

- Pipe material: Class 300 sch 40 commercial steel
- Fluid average temperature: 60°F
- Operating time: Continuously all year with 10% downtime for maintenance and repair
- Volumetric flow rate: $10 \text{ gpm} \leq \dot{V} \leq 2000 \text{ gpm}$
- Pump efficiency: $0.45 \leq \eta_p \leq 0.80$

Table 4.18 shows the resulting range of economic velocities for these ranges of system and economic parameters. It is important to understand that the use of Equation 4.50 is recommended for finding the economic diameter. However, Table 4.18 can provide a quick check to ensure that a selected pipe falls within a reasonable economic velocity range without having to solve Equation 4.50 directly.

TABLE 4.18

Economic Velocity Range for Several Fluids Calculated Using Equations 4.50 and 4.51 for a Range of Economic and System Parameters Summarized in Section 4.6.4

	$V_{\text{econ, min}}$ (ft/s)	$V_{\text{econ, max}}$ (ft/s)	$V_{\text{econ, min}}$ (m/s)	$V_{\text{econ, max}}$ (m/s)
<i>Common Liquids</i>				
Water	5.1	9.7	1.6	3.0
Acetone	5.6	10.6	1.7	3.2
Ammonia	6.2	11.6	1.9	3.5
Benzene	5.4	10.2	1.6	3.1
Toluene	5.4	10.2	1.6	3.1
<i>Hydrocarbon Liquids</i>				
Propane	6.6	12.3	2.0	3.8
Butane	6.3	11.8	1.9	3.6
Pentane	6.1	11.5	1.9	3.5
Hexane	5.9	11.2	1.8	3.4
Heptane	5.8	11.0	1.8	3.4
Octane	5.7	10.9	1.8	3.3
Nonane	5.7	10.8	1.7	3.3
Decane	5.6	10.6	1.7	3.2
Dodecane	5.5	10.4	1.7	3.2
Isobutane	6.3	11.9	1.9	3.6
Isopentane	6.1	11.5	1.9	3.5
Cyclohexane	5.5	10.4	1.7	3.2
<i>Alcohols</i>				
Methanol	5.6	10.5	1.7	3.2
Ethanol	5.4	10.3	1.7	3.1
<i>Liquid Refrigerants</i>				
R22	5.0	9.4	1.5	2.9
R123	4.6	8.8	1.4	2.7
R125	5.0	9.3	1.5	2.8
R134a	4.9	9.3	1.5	2.8
R410A	5.2	9.7	1.6	3.0
<i>Brines (20% Solution)</i>				
Sodium chloride	4.8	9.2	1.5	2.8
Calcium chloride	4.7	9.0	1.4	2.8
Magnesium chloride	4.7	8.9	1.4	2.7
Lithium chloride	4.8	9.1	1.5	2.8
Ethylene glycol	5.0	9.4	1.5	2.9
Propylene glycol	4.9	9.4	1.5	2.9
<i>Other Liquids</i>				
Carbon dioxide	5.7	10.7	1.7	3.2
Sulfur dioxide	4.8	9.0	1.5	2.7
Sulfur hexafluoride	4.8	8.9	1.4	2.7
Propylene	6.5	12.2	2.0	3.7

4.7 Pumps

In the design of a fluid piping system, one of the tasks of the engineer is to select a pump (or pumps) that provides the required flow rate through the piping system. There are a wide variety of pumps available designed for specific applications. However, they can be classified into one of two categories; *positive displacement* and *dynamic*. The main focus of this chapter will be on centrifugal pumps, a type of dynamic pump, because they are the most commonly used in industrial applications. Even among centrifugal pumps, there are many different types including end suction, submersible, split case, etc. These different pump designs are made to handle different types of fluids, system pressures, flows, and other conditions. The final selection of a pump must take into account all of these factors. Once the techniques of selecting a centrifugal pump are understood, they are easily transferrable to other types of pumps.

4.7.1 Types of Pumps

Pumps move fluid through a pipe system by transferring energy from an external source, usually an electric motor, to the fluid. The method of energy transfer classifies the pump. Table 4.19 displays the pump classification and the method of energy transfer to the fluid. For more detail on the different types of pumps available, the reader is encouraged to consult the *Pump Handbook* (Karassik et al. 2008).

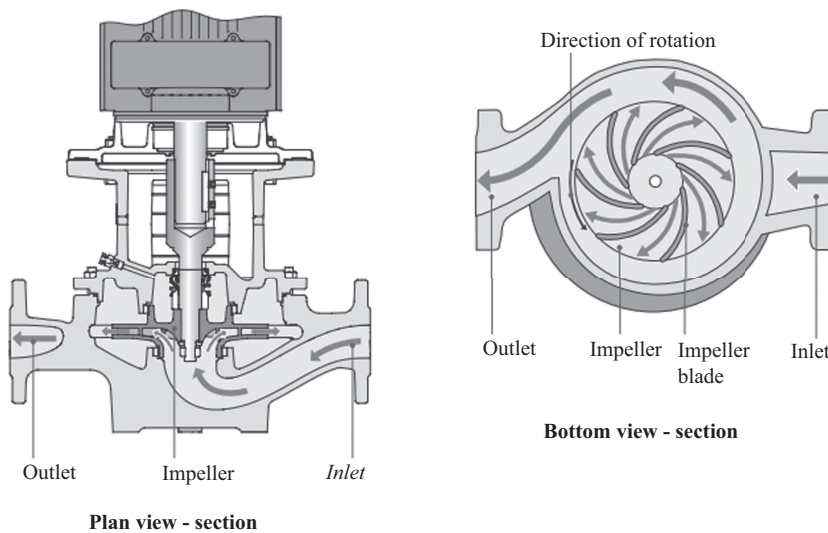
4.7.2 Dynamic Pump Operation

As indicated in Table 4.19, dynamic pumps transfer energy to the fluid using an impeller. As previously mentioned, there are many different types of dynamic pumps. An example of an inline centrifugal pump is shown in Figure 4.9. The purpose of the pump in a fluid system is to increase the fluid’s pressure such that elevation and friction effects are overcome and the fluid is delivered at the required flow rate. Therefore, the pressure rise across a pump is significant, but the changes in kinetic and potential energy of from the inlet to the outlet are often negligible.

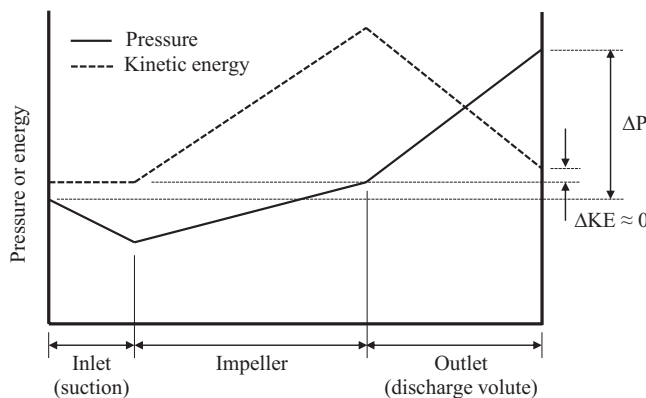
Figure 4.10 demonstrates how this is accomplished in a dynamic pump. As the fluid enters the pump through the suction port, there is a small drop in pressure due to friction

TABLE 4.19
Pump Classification and Methods of Energy Transfer to the Fluid

Positive Displacement	Dynamic
<i>Reciprocating Action</i> Energy transfer by pistons, plungers, diaphragms, bellows, etc.	<i>Centrifugal Action</i> Energy transfer by rotating impeller in the radial direction
<i>Rotary Action</i> Energy transfer by vanes, screws, or lobes	<i>Propeller Action</i> Energy transfer by rotating impeller in the axial direction
	<i>Mixed Action</i> Energy transfer by rotating impeller in a combined radial/axial direction

**FIGURE 4.9**

An inline centrifugal pump. (Reprinted from Grundfos Research and Technology, *The Centrifugal Pump*, Bjerringbro, Denmark, Grundfos, 2014.)

**FIGURE 4.10**

Operation of a dynamic pump.

and the kinetic energy stays constant because the suction line diameter is constant. As the fluid moves through the impeller, the fluid experiences a significant increase in velocity and the pressure begins to rise. The largest pressure increase in the pump occurs in the discharge passage of the pump. The discharge passage is called a *discharge volute*. The discharge volute is a liquid diffuser. The cross-sectional flow area of the volute increases in the direction of fluid flow. A thermodynamic analysis of the volute shows that as the fluid flows through the passage, its pressure increases. This pressure increase is offset by decrease in kinetic energy to satisfy the conservation of energy equation. When the fluid finally leaves the pump, its outlet velocity is very nearly the same as its velocity at the suction port, but the pressure has increased significantly.

4.7.2.1 Dynamic Pump Performance

In the design of a fluid system, one of the engineer's tasks is to select a pump to provide the required flow rate. To properly select a pump, the engineer must understand how a pump will perform when connected to the pipe system. Pump manufacturers provide *pump curves* that show how a given pump will perform. These pump curves are determined by the manufacturer based on experimental data. The pump is put on a test stand and the following parameters are measured: rotating shaft torque, impeller rotational speed, the suction and discharge pressures and elevations, the volumetric flow rate of the fluid, and the suction and discharge pipe specifications. With this information, the following performance parameters are calculated: the power input to the impeller, power input to the fluid, pressure head increase across the pump, and pump efficiency. These parameters are presented on the *pump head vs. capacity* axis. An example of a set of pump performance curves is shown in Figure 4.11.

The *capacity* of a pump is simply the volumetric flow rate delivered. The *pump head* can be determined by considering the head at the suction and discharge ports of a pump. On the suction side (subscript *s*), the total fluid head is,

$$H_s = \frac{P_s}{\gamma} + \frac{V_s^2}{2g} + z_s \quad (4.58)$$

Likewise, the fluid head on the discharge side of the pump (subscript *d*) is given by,

$$H_d = \frac{P_d}{\gamma} + \frac{V_d^2}{2g} + z_d \quad (4.59)$$

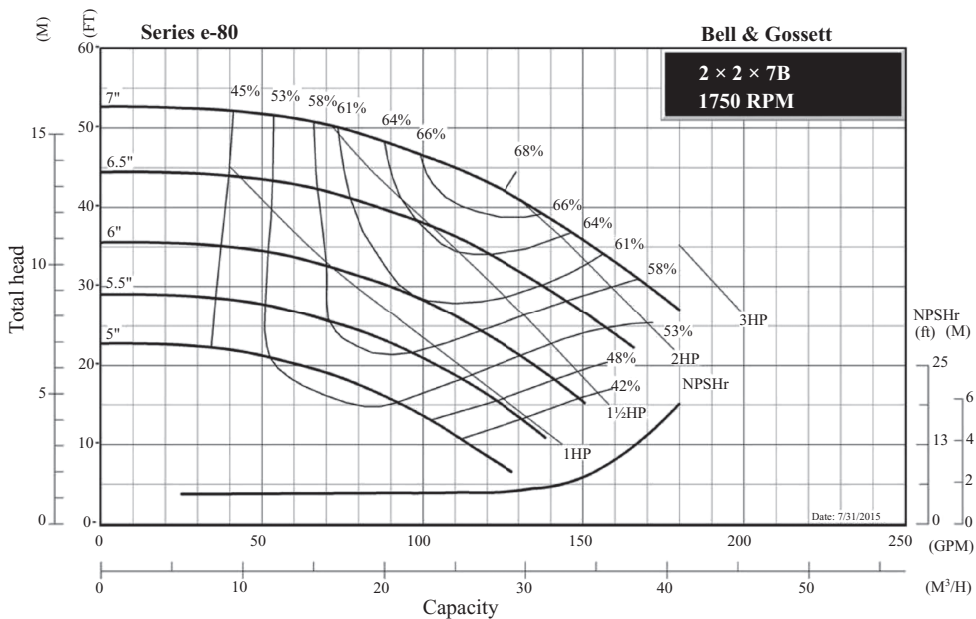


FIGURE 4.11

Centrifugal pump performance curves. (Reprinted from Xylem, Inc., *Series e-80: In-line mounted centrifugal pump performance curves—60 Hz*, Morton Grove, Illinois, USA, Bell & Gossett, 2016. With permission.)

The dynamic pump head delivered to the fluid is the difference between Equations 4.59 and 4.58,

$$H_p = H_d - H_s = \frac{P_d - P_s}{\gamma} + \frac{V_d^2 - V_s^2}{2g} + (z_d - z_s) \quad (4.60)$$

In most dynamic pumps, the change in velocity head and elevation head are very small compared to the pressure head delivered by the pump. The value calculated using Equation 4.60 is plotted against the capacity of the pump for several different impeller sizes as shown in Figure 4.11, labeled 5", 5.5", etc. Several impeller sizes are shown because the pump can be ordered with one of several different impeller sizes.

There are other curves on Figure 4.11 pertinent to the pump's performance. These include the pump efficiency and the power input to the pump. The pump head is related to the power input to the fluid by,

$$H_p = \frac{\dot{W}}{\dot{m}g} \quad (4.61)$$

The power term in Equation 4.61 is the power input to the *fluid*. This power value is sometimes referred to as the *water horsepower* or *hydraulic power*. Due to inefficiencies the power input to the pump is larger than the hydraulic power input to the fluid. This is quantified by the pump efficiency,

$$\eta_p = \frac{\dot{W}}{\dot{W}_p} \quad (4.62)$$

The power term in the denominator of Equation 4.62 is the power input to the pump's rotating shaft from an electric motor, an engine, or any other source. This power is often referred to as the *brake horsepower* input to the pump. On the pump performance curves shown in Figure 4.11, lines of constant pump efficiency and brake horsepower are displayed.

The curve near the bottom of the performance curves labeled "NPSHr" is read on the right-hand axis. This curve will be discussed in Section 4.7.6. The NPSHr curve is used to determine if cavitation will occur when the pump is installed in a pipe system.

Example 4.13

The pump shown in Figure 4.11 is fitted with a 6½-inch impeller. The pump is operating in a system and delivering 100 gpm. Determine (a) the head delivered by the pump, (b) the pressure rise across the pump assuming that the fluid is water at 70°F, (c) the brake horsepower input to the pump, and (d) the efficiency of the pump.

Solution

- From Figure 4.11, at a capacity of 100 gpm, this pump fitted with a 6½-inch impeller is imparting a total head of approximately 38 ft.
- In the upper right-hand corner of Figure 4.11, notice the label 2x2x7B. This means that the suction inlet is 2-nom, the discharge port is 2-nom and the

maximum impeller diameter that can be used in this pump is 7-in. Since the suction and discharge ports are the same size, the velocity is the same at both ports. If we also assume that the potential effects are negligible, then the pressure rise across the pump can be calculated using Equation 4.61,

$$H_p = \frac{P_d - P_s}{\gamma} + \frac{V_d^2 - V_s^2}{2g} + (z_d - z_s) = \frac{\Delta P}{\gamma}$$

$$\therefore \Delta P = \gamma H_p = \rho \frac{g}{g_c} H_p = \left(62.298 \frac{\text{lb}_f}{\text{ft}^3} \right) (38 \text{ ft}) \left(\frac{\text{ft}^2}{144 \text{ in}^2} \right) = 16.4 \text{ psi}$$

Appendix B.1

- c. The brake horsepower input to the pump can be read directly from Figure 4.11 as approximately 1.5 hp.
- d. The efficiency of the pump can also be read directly from Figure 4.12 as 64%.

Two interesting extremes can be observed on a pump performance curve. These are indicated on the plot on the left side of Figure 4.12 as the cutoff head, point (a), and the free delivery condition, point (b). The cutoff head represents the condition where the pump is not able to provide any flow to the system. A good example of this is a pump being used to move water from a stream to an irrigation ditch. If the elevation of the ditch is higher than the cutoff head, then the pump cannot provide the flow. In fact, there will be no flow at all. For this condition, the efficiency of the pump is zero,

$$\eta_{p,\text{cutoff}} = \frac{\dot{W}}{\dot{W}_{\text{bhp}}} = \frac{\dot{m}gH_p}{\dot{W}_{\text{bhp}}} = \frac{(0)gH_p}{\dot{W}_{\text{bhp}}} = 0 \quad (4.63)$$

The other extreme point, free delivery, occurs if the pump curves were extrapolated to the zero-head axis. In this case, the pump is providing no power input to the fluid and the fluid is passing through the pump as if it were a pipe. In this case, the efficiency is also zero,

$$\eta_{p,\text{free}} = \frac{\dot{W}}{\dot{W}_{\text{bhp}}} = \frac{\dot{m}gH_p}{\dot{W}_{\text{bhp}}} = \frac{\dot{m}g(0)}{\dot{W}_{\text{bhp}}} = 0 \quad (4.64)$$

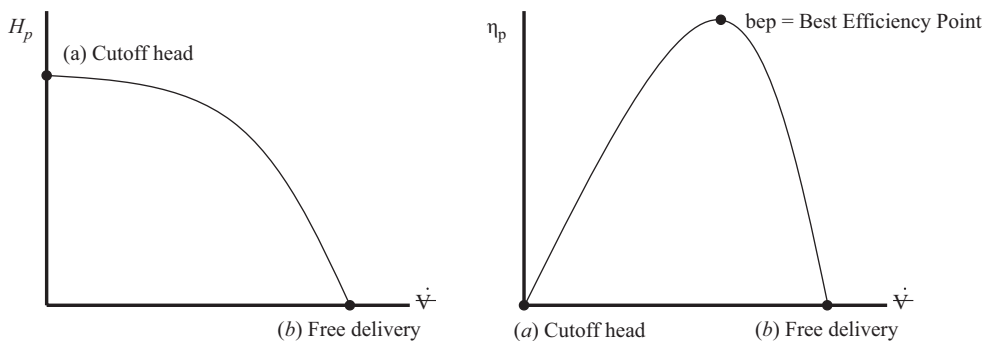


FIGURE 4.12
Pump curve extremes and the resulting pump efficiency.

For volume flow rates between these two extremes, the pump efficiency will increase, achieve a maximum, and then decrease as shown on the plot on the right side of Figure 4.12. The maximum point on the efficiency curve is called the *best efficiency point* (bep). In the selection of a pump for a system, it is good design practice to have the pump operating as near as possible to the bep.

4.7.3 Manufacturer's Pump Curves

There are hundreds of pump manufacturers and vendors who sell them. However, all manufacturers provide the same information about their pumps, similar to the performance curves shown in Figure 4.11. Most of these performance curves are published by the manufacturer in the form of a technical booklet. The booklet indicates what type of a pump the model is (end-suction, inline, etc.). For quick reference, these booklets also show performance maps that overlay the operating range of a specific model operating at a given speed, as shown in Figure 4.13. Knowing the system capacity requirement and head that the pump must overcome allows the engineer to quickly identify the proper model within a family of pumps. Once the model is identified, the detailed pump curves can be accessed for design work.

Appendix E contains complete technical booklets for the Bell and Gossett Series e-1531 (Xylem, Inc. 2015) end suction and Series e-80 inline (Xylem, Inc. 2016) centrifugal pumps. These examples are made available for solving various pump problems in this textbook. There are many other pump vendors. The reader is encouraged to consult the website www.pump-flo.com for a comprehensive list of vendors and pump curves.

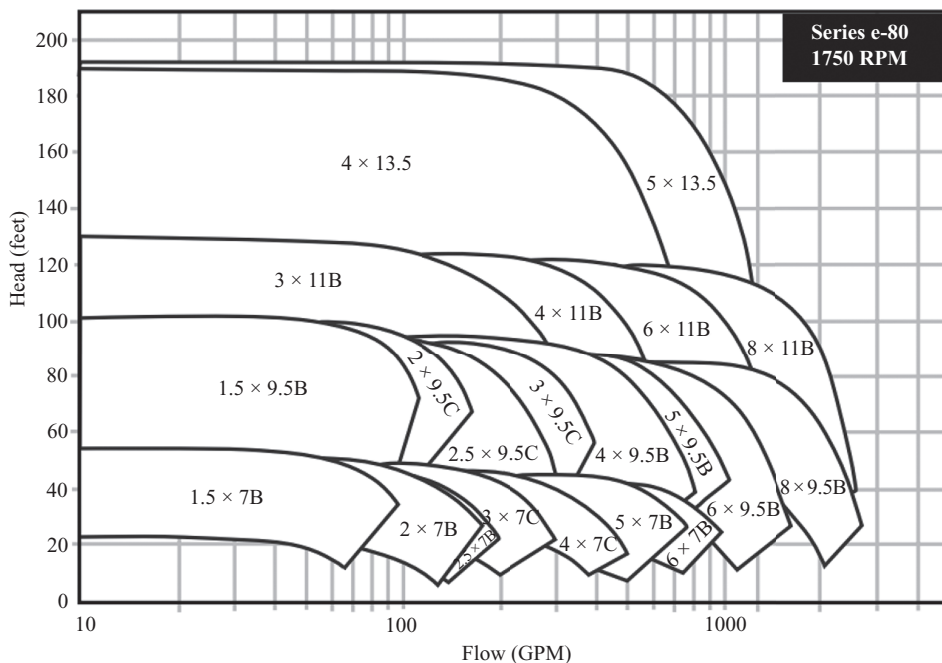


FIGURE 4.13

A performance map for a Bell & Gossett Series e-80 inline centrifugal pump. (Reprinted from Xylem, Inc., *Series e-80: In-line mounted centrifugal pump performance curves*—60 Hz, Morton Grove, Illinois, USA, Bell & Gossett, 2016. With permission.)

4.7.4 The System Curve

The pump selected for a specific application must deliver the proper flow rate while overcoming the elevation and friction effects in the pipe system. Therefore, knowledge of how the fluid flows through the pipe system as a function of elevation and friction effects must be fully understood. This cannot be accomplished until the system is completely designed. The design engineer must know the type of pipe, its diameter, total straight length, and number of fittings, in order to perform a full energy analysis of the network to determine the elevation and friction effects.

Systems are often designed to deliver a specified flow rate. For example, in a beverage bottling line where six 12-oz bottles are filled every 10 seconds, a fixed flow rate must be met. If the flow rate is higher, then the bottles will overflow. If the flow rate is smaller, the bottles will not fill completely. There are cases where a system is retrofitted which results in an increased or decreased flow rate compared to the initial design. In cases like this, replacing the pump may not be necessary, but it is important to know how the pump will respond to changes in the system flow rate. These factors make pump selection a very important step in the complete design of a fluid delivery system. Once a pipe system has been designed, the first step toward selecting a pump is to develop what is known as the *system curve*.

The system curve is a plot of the system head as a function of volumetric flow rate. The system head is analyzed between two points in a pipe system and is made up of any pressure, velocity, and elevation heads that may exist, as well as the total head loss due to friction.

4.7.4.1 System Curve for a Two-Tank System Open to the Atmosphere

Consider a two-tank system as shown in Figure 4.14. In this system, the two tanks are opened to the atmosphere and the liquid level in each tank is kept constant.

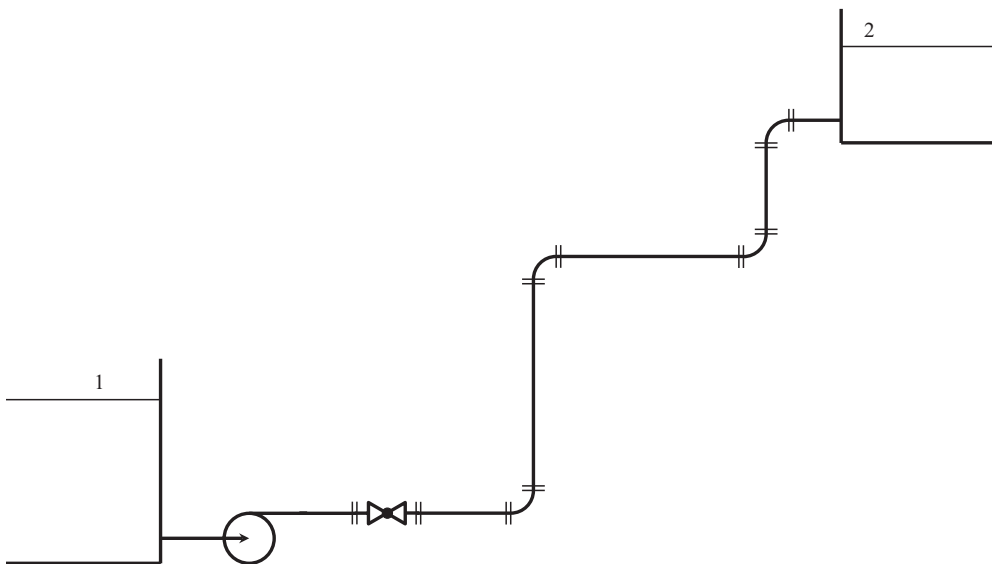


FIGURE 4.14

An example of a two-tank pipe and pump system.

Writing the conservation of energy equation between points 1 and 2 (the tank-free surfaces) results in,

$$\frac{P_1}{\gamma} + \frac{V_1^2}{2g} + z_1 + H_p = \frac{P_2}{\gamma} + \frac{V_2^2}{2g} + z_2 + \left(f \frac{L}{D} + \sum K \right) \frac{V^2}{2g} \quad (4.65)$$

Solving for the required pump head,

$$H_p = \frac{P_2 - P_1}{\gamma} + \frac{V_2^2 - V_1^2}{2g} + (z_2 - z_1) + \left(f \frac{L}{D} + \sum K \right) \frac{V^2}{2g} \quad (4.66)$$

Since the free surfaces of the tanks are both at atmospheric pressure, the change in the pressure head is zero. If the diameter of the pipes is constant throughout, then the velocity head difference is zero. Therefore, Equation 4.66 reduces to,

$$H_p = (z_2 - z_1) + \left(f \frac{L}{D} + \sum K \right) \frac{V^2}{2g} \quad (4.67)$$

The fluid velocity can be written in terms of volumetric flow rate. Making this substitution into Equation 4.67 results in,

$$H_p = (z_2 - z_1) + \left(f \frac{L}{D} + \sum K \right) \frac{8\dot{V}^2}{\pi^2 g D^4} \quad (4.68)$$

This equation indicates that the pump head required to overcome the friction effects and the elevation change is a *quadratic* function of the volumetric flow rate with an offset equal to the elevation difference between the tank surfaces. When this equation is plotted on a head-capacity axis the result is a parabola as shown in Figure 4.15. This parabola is known as the *system curve*. It shows the pump head required to overcome the various head losses in the system for different volumetric flow rates through the system.

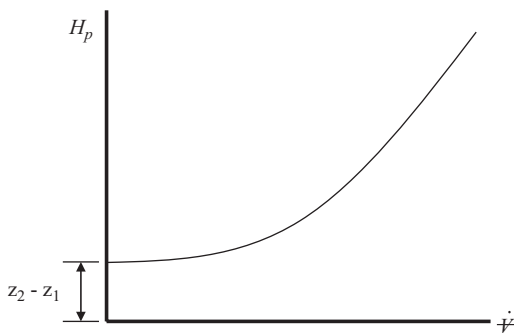


FIGURE 4.15

The system curve for a two-tank system open to the atmosphere.

Example 4.14

Consider the two-tank open system shown in Figure 4.14. The fluid being transported from the lower tank to the upper tank is water at an average temperature of 60°F. The elevation difference between free surfaces of the tanks is 15 ft. The pipe is 5-nom sch 40 commercial steel. The total length of straight pipe in the system is 40 ft and all fittings are regular. Draw the system curve up to 1000 gpm.

Solution

The analysis of this system is presented in Equations 4.65 through 4.68. The system curve is determined by solving Equation 4.68 for a range of volumetric flow rate values. This calculation is not iterative. However, since a parametric study must be conducted (i.e., varying the volumetric flow rate and calculating the resulting pump head), the use of computer software makes the problem easier. To demonstrate the calculation procedure, the pump head required at a volumetric flow of 500 gpm will be computed below.

The pump head is determined from Equation 4.68,

$$H_p = (z_2 - z_1) + \left(f \frac{L}{D} + \sum K \right) \frac{8 \dot{V}^2}{\pi^2 g D^4}$$

In order to solve this equation, the friction factor and the fitting loss coefficients need to be determined. These are both functions of the Reynolds number which required the pipe properties and the water properties,

$$\begin{aligned} D_{nom} &= 5 \text{ in} & D &= 0.42058 \text{ ft} & \varepsilon &= 0.00015 \text{ ft} & \frac{\varepsilon}{D} &= 0.00035665 \\ & & \text{Appendix C} & & \text{Table 4.3} & & & \\ \rho &= 62.364 \frac{\text{lbm}}{\text{ft}^3} & \mu &= \left(2.7120 \frac{\text{lbm}}{\text{ft-h}} \right) \left(\frac{\text{h}}{3600 \text{ s}} \right) = 0.00075333 \frac{\text{lbm}}{\text{ft-s}} \\ & \text{Appendix B.3} & \text{Appendix B.3} & & & & & \end{aligned}$$

Therefore, the Reynolds number of the flow is,

$$\text{Re} = \frac{\rho V D}{\mu} = \frac{4 \rho \dot{V}}{\pi D \mu} = 279,185$$

The friction factor can be calculated by,

$$f = \frac{0.25}{\left[\log \left(\frac{\varepsilon/D}{3.7} + \frac{5.74}{\text{Re}^{0.9}} \right) \right]^2} = 0.01756$$

The fitting loss coefficients will be computed using the 3K method,

$$K_{valve} = \frac{K_1}{\text{Re}} + K_{\infty} \left(1 + \frac{K_d}{D_{nom}^{0.3}} \right) = \frac{1500}{\text{Re}} + 1.7 \left(1 + \frac{3.6}{D_{nom}^{0.3}} \right) = 5.4816$$

$$K_{elbow} = \frac{K_1}{\text{Re}} + K_{\infty} \left(1 + \frac{K_d}{D_{nom}^{0.3}} \right) = \frac{800}{\text{Re}} + 0.091 \left(1 + \frac{4}{D_{nom}^{0.3}} \right) = 0.31846$$

$$K_{entrance} = 0.5$$

$$K_{exit} = 1$$

Therefore, the required pump head to overcome elevation and friction effects in the system is,

$$H_p = (z_2 - z_1) + \left(f \frac{L}{D} + \sum K \right) \frac{8 \dot{V}^2}{\pi^2 g D^4} = 24.918 \text{ ft}$$

The system curve is then determined by repeating these calculations over a range of volumetric flow rates up to 1000 gpm and plotting the results on H_p vs \dot{V} coordinates. Figure E4.14 shows the resulting system curve for this example.

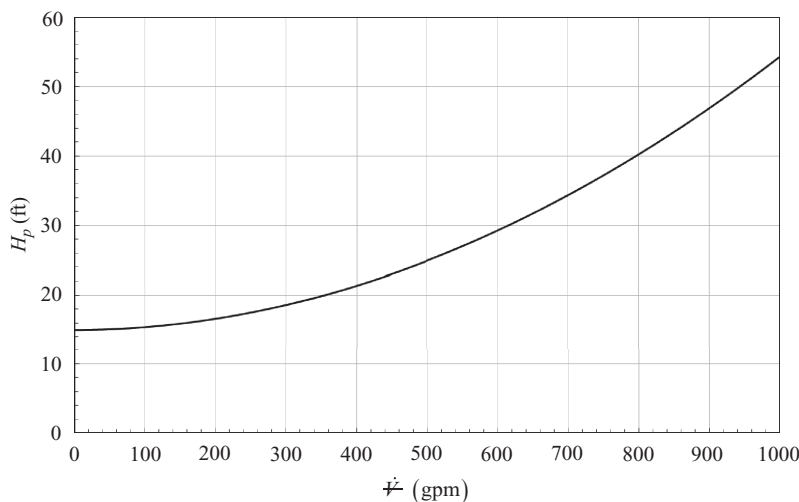


FIGURE E4.14

The system curve for the two-tank pump and pipe system.

4.7.4.2 System Curve for a Closed-Loop System

Another common system in mechanical engineering applications is a closed-loop piping system as shown in Figure 4.16. Closed-loop systems often have an *expansion tank* for each closed loop. The purpose of the expansion tank is to allow the system to operate in a steady state even when there are temperature variations which can cause the total fluid volume to increase or decrease.

Assuming that the net energy transfer between the working fluid and the heat exchangers is zero, the conservation of energy equation from the suction side of the pump (labeled “s” in Figure 4.17), all the way around the system and back to the suction side results in,

$$\frac{P_s}{\gamma} + \frac{V_s^2}{2g} + z_s + H_p = \frac{P_s}{\gamma} + \frac{V_s^2}{2g} + z_s + \left(f \frac{L}{D} + \sum K \right) \frac{V^2}{2g} \quad (4.69)$$

Solving Equation 4.69 for the pump head shows that the pump head is only dependent on the friction losses in the piping system,

$$H_p = \left(f \frac{L}{D} + \sum K \right) \frac{V^2}{2g} \quad (4.70)$$

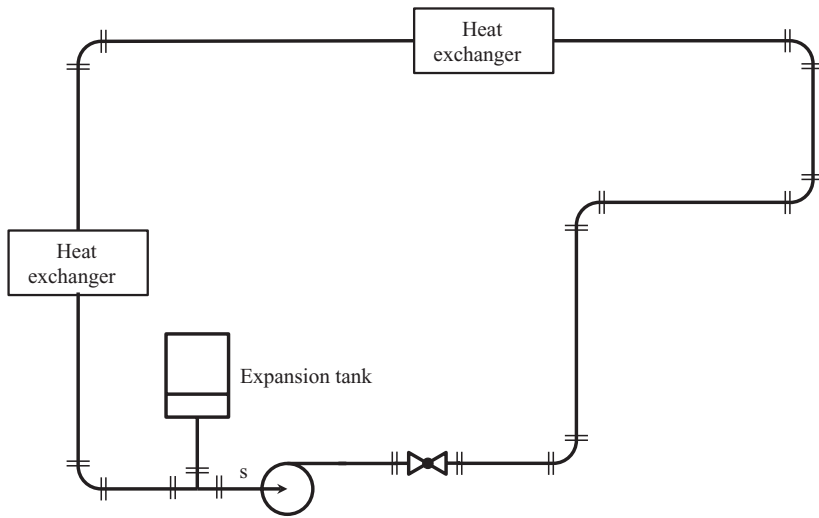


FIGURE 4.16
An example of a closed-loop system.

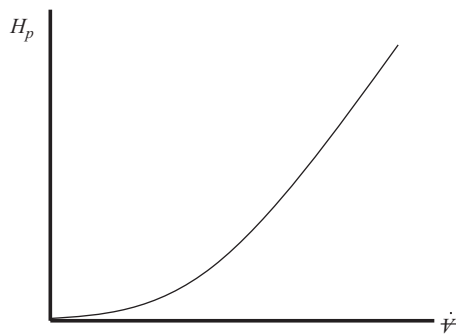


FIGURE 4.17
The system curve for a closed-loop system.

Introducing the volumetric flow rate gives,

$$H_p = \left(f \frac{L}{D} + \sum K \right) \frac{8 \dot{V}^2}{\pi^2 g D^4} \quad (4.71)$$

Equation 4.71 indicates that the pump head required to overcome the friction losses in the pipe system is a quadratic function of the volumetric flow rate. In the case of a closed-loop system, there is no offset in the curve. Figure 4.17 shows the *system curve* for a closed-loop system like the one described in Figure 4.16.

4.7.5 Pump Selection

Notice that the coordinates of the system curve are identical to the coordinates of a pump performance curve. Overlaying a pump performance curve on a system curve, as shown

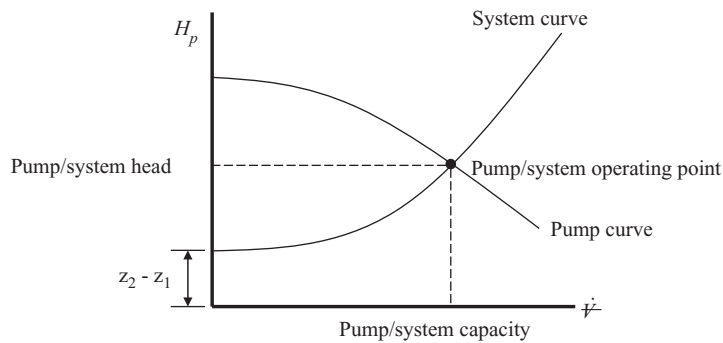


FIGURE 4.18
Operating point of a pump/pipe system.

in Figure 4.18, shows that there is a unique intersection of these two curves. This intersection is the *operating point* of the combined pump/pipe system.

To select the right pump, the system curve is overlaid on the pump curves. Then, the proper diameter impeller needs to be selected to deliver the required flow rate. As an example, consider the Bell & Gossett Series e-1531 2.5 BB pump from Appendix E operating at 3550 rpm. The performance curves for this model pump are repeated in Figure 4.19. Also included in Figure 4.19 is a system curve for a two-tank system similar to Figure 4.14 showing four operating points (A through D) corresponding to the intersection of the system curve with the impeller curve. Suppose that the flow

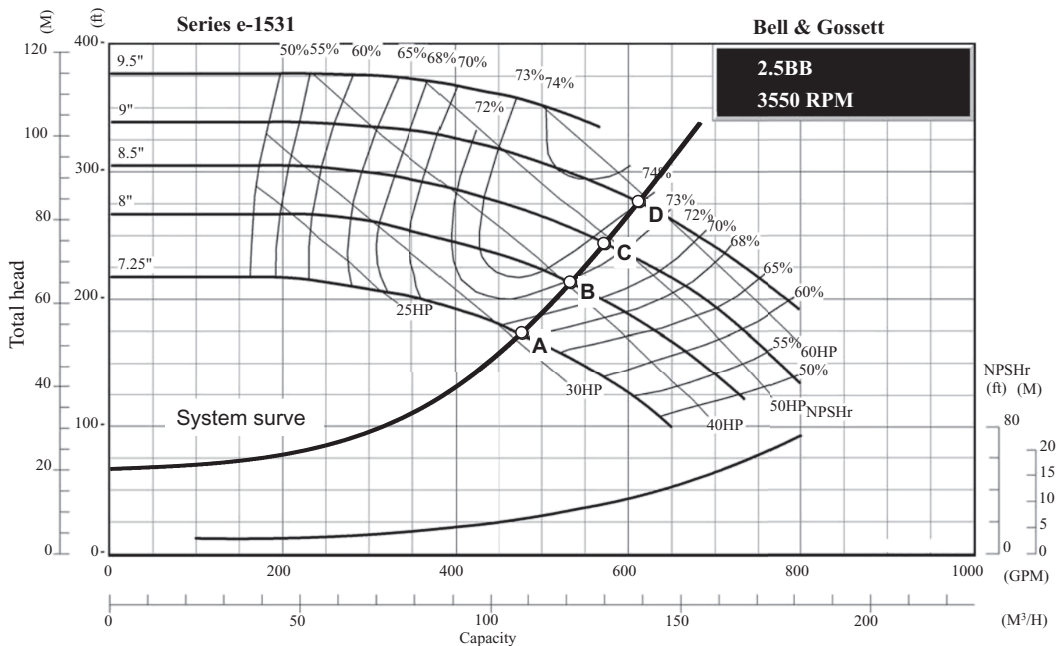


FIGURE 4.19
A system curve overlaid on pump performance curves.

requirement for the system is 550 gpm. From Figure 4.19, it can be seen that the operating points labeled C and D will provide more than the required 550 gpm. Operating points A and B do not provide 550 gpm. Therefore, the proper impeller size to choose is either the 8.5-inch (operating point C) or the 9-inch (operating point D). While the 9-inch impeller will meet the flow requirement, the power draw is higher compared to the 8.5-inch impeller. Unless there is projected future expansion of the system requiring an increased flow rate, the 8.5-inch impeller is a better selection. When matched with the system, the 8.5-inch impeller pump will provide approximately 570 gpm at a head of 245 ft. At this operating point, the pump will draw approximately 49 hp and operate with an efficiency of 72.5%. This flow rate is slightly larger than required. If the flow rate must be met exactly, a valve can be placed downstream of the pump discharge to adjust the flow.

When a valve is installed in the system, it adds a new friction loss that must be taken into account. The effect of the head loss through the valve shifts the system curve to the left due to the added resistance of the valve as shown in Figure 4.20. From this figure, it can be seen that adding a flow control valve allows the pump with the 8.5-inch impeller to deliver the required 550 gpm at 250 ft of head. At this operating point, the pump will draw approximately 47 hp and operate with an efficiency of 73.1%.

Notice that this pump selection produces an operating point that is very near the bep. In fact, if the flow control valve is installed and the system resistance increases, the power draw actually decreases and the pump efficiency increases compared to the original operating point. This demonstrates the importance of making certain that the pump selected is operating near, and perhaps slightly to the right of the bep.

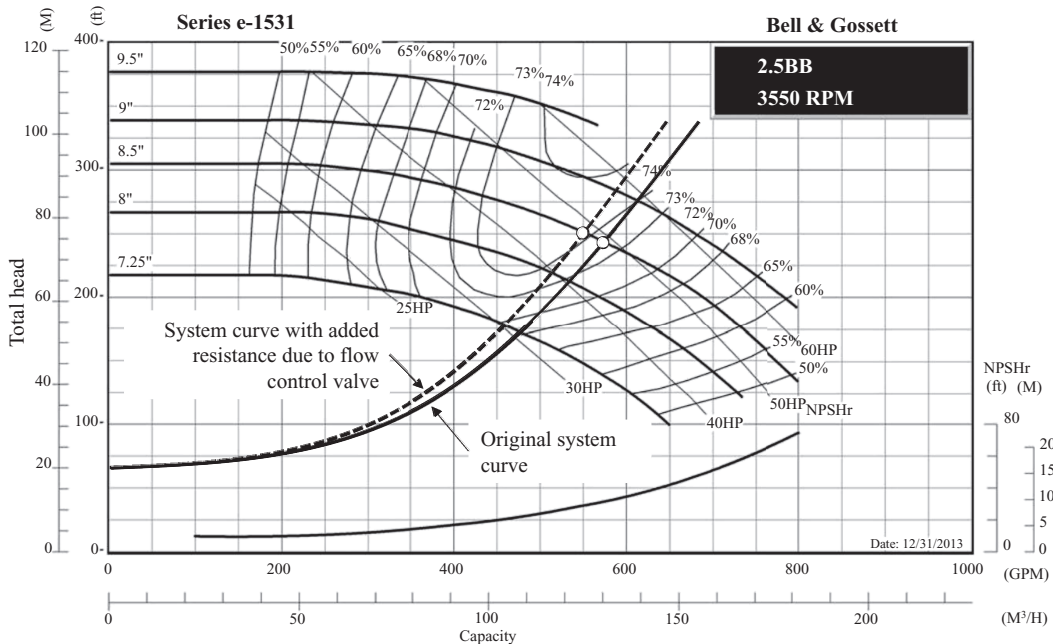


FIGURE 4.20

Achieving the required flow rate with a flow control valve.

Example 4.15

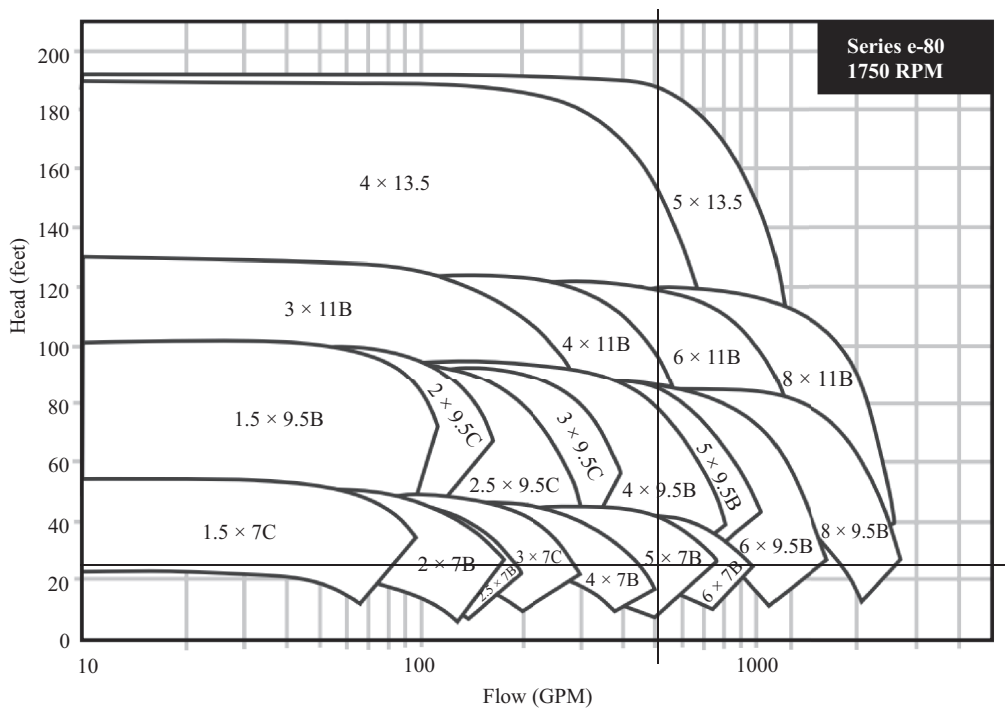
Select a pump from Appendix E that will be suitable for the pump and pipe system described in Example 4.14 for a required volumetric flow rate of 500 gpm.

Solution

The pump curves included in Appendix E are for a Bell & Gossett Series e-1531, an end suction pump, and a Series e-80, an inline pump. In this example, the Series e-80 pump will be considered. The specific model within this series can be found knowing the system curve as developed in Example 4.14. From the system curve, the head required at 500 gpm is 24.9 ft. This information allows the design engineer to begin identifying the specific pump model. Page 3 of the Series e-80 booklet shows three performance maps. These maps are for three different rotational speeds of the impeller.

As with any design problem, there are several solutions. Consider the performance map for the 1750 rpm family of pumps shown in Figure E4.15A. This map seems to indicate that a 5x7B pump may provide a solution.

Figure E4.15B shows a portion of the system curve from Example 4.14 superimposed on performance curves for a 5x7B pump operating 1770 rpm (Notice that the rotational speed of this particular model is 1770 rpm rather than 1750 rpm). This figure indicates

**FIGURE E4.15A**

Series e-80 1150 rpm pump performance map.

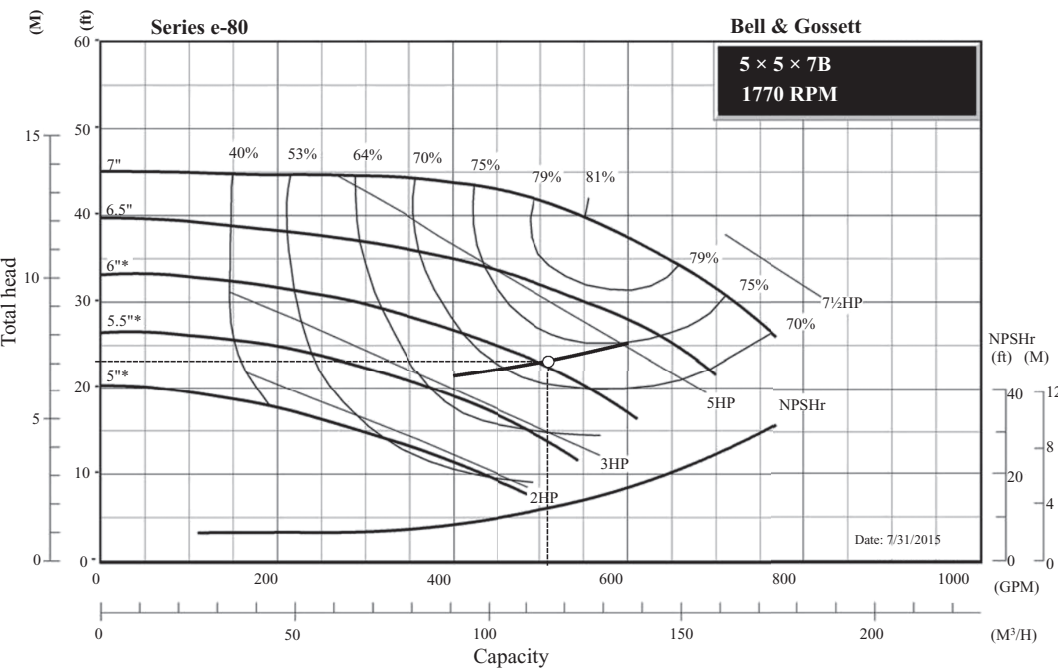


FIGURE E4.15B
The operating point of the system with a Series e-80 5x5x7B 6-inch impeller pump operating at 1170 rpm.

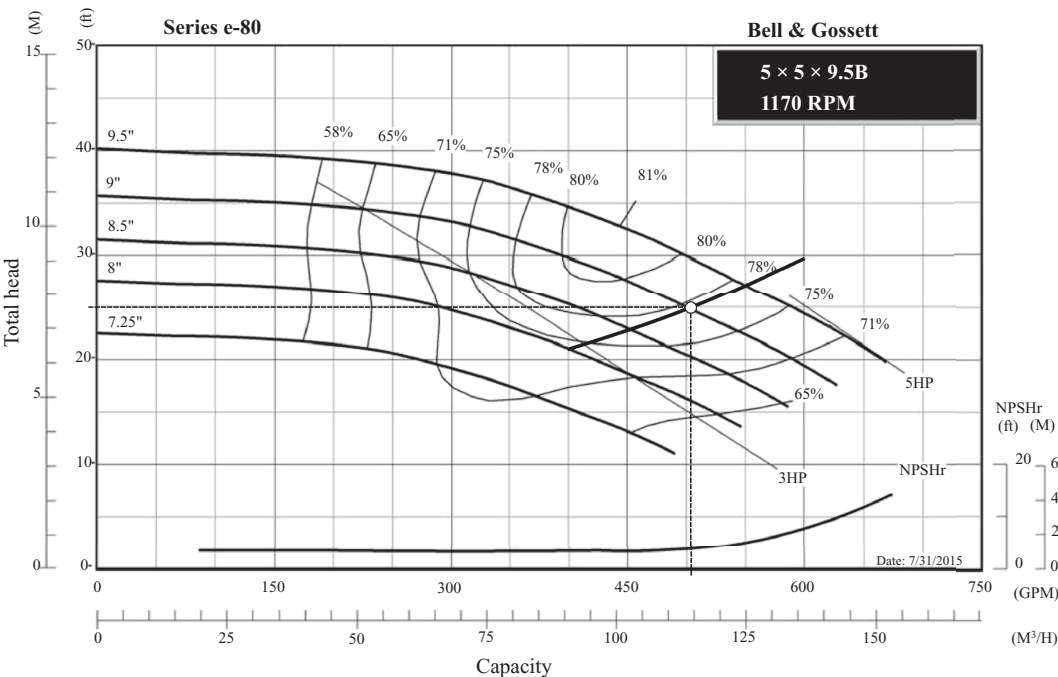


FIGURE E4.15C
The operating point of the system with a Series e-80 5x5x9B 9-inch impeller pump operating at 1170 rpm.

that a 6-inch impeller will deliver approximately 510 gpm at 23 ft of head. The pump will draw approximately 4 hp and operate with an efficiency of 72%. This is a nice choice for several reasons.

- Notice that this is a 5x5x7 pump. This means the suction and discharge ports are 5-nom which matches the pipe in the system exactly. Therefore, no reducing fittings are required to connect the pump to the pipeline.
- Look at the location of the pump/system operating point. It lies to the right of the best efficiency point. Therefore, if a valve needed to be installed to bring the flow down to 500 gpm the efficiency of the pump will increase.

Another possibility is to consider the Series e-80 pump operating at 1150 rpm. The performance map for the 1150 rpm pumps suggests that the 5x5x9.5B model, shown in Figure E4.15C, may also be a good solution. Overlaying the system curve on the 5x5x9.5B pump curves reveals another possible selection. From this figure, a 9-inch impeller operating at 1770 rpm will deliver 505 gpm at 25 ft of head. This pump will draw about 4.25 hp and operate with an efficiency of 77%.

Either pump, the 5x5x7B 6-inch impeller operating at 1770 rpm, or the 5x5x9.5B 9-inch impeller operating at 1170 rpm will work for the given application. However, there is a clear trade-off. The higher rpm pump is smaller, but it is operating at a lower efficiency than the lower rpm pump. The smaller pump may be cheaper because of size, but it may be more expensive to run from an energy cost point of view.

Other factors need to be taken into account before a final decision is made. For example, it is not clear from the given drawing, but there may be a limited amount of space to install the pump. Often times, space in a processing facility is at a premium. This may sway the decision toward the smaller diameter impeller pumps.

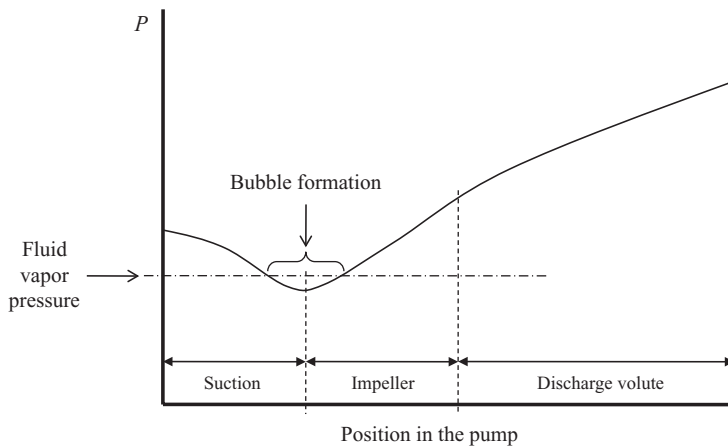
After a careful analysis, such as that conducted in Example 4.15, it may be entirely possible that there are *no* pumps in a technical booklet that satisfy the required flow rate and provide reasonable operating parameters. In this case, the engineer needs to search other pump models or other vendors for a solution. Many pump manufacturers have technical booklets with pump curves available on their websites. A comprehensive website that contains pump curves for *many* manufacturers can be found at www.pump-flo.com. This website features searching capability to find possible pumps for a given operating condition. The performance curves are somewhat interactive in that system curves can be automatically overlaid on the pump curves for quick visual validation that the pump may or may not be an acceptable solution.

4.7.6 Cavitation and the Net Positive Suction Head

Cavitation is a phenomenon that is to be avoided in liquid pump/pipe systems. In pumps, cavitation is prevented by designing the system so that the *net positive suction head available* (NPSHa) in the system is greater than the *net positive suction head required* (NPSHr) by the pump.

Figure 4.21 shows a qualitative pressure trace through a centrifugal pump. If the pressure of the fluid at any point drops below its vapor pressure, then bubbles will form. In a centrifugal pump, the lowest pressure occurs at the eye of the impeller. When the bubbles move to a higher-pressure region in the pump, they collapse. This bubble collapse causes a propagation of pressure waves which results in damage to the pump known as *cavitation erosion*. A pump that is experiencing cavitation makes a loud rattling noise and can experience vibration. In order to avoid cavitation, calculations involving the *net positive suction head* (NPSH) must be performed.

The NPSHa is the difference between the pressure head at the suction port of the pump and the vapor pressure head of the fluid. If this value is negative, the pump will experience

**FIGURE 4.21**

A pressure trace through a centrifugal pump showing bubble formation that leads to cavitation.

cavitation. In fact, it is entirely possible that the pump may experience cavitation with a positive NPSHa due to a pressure drop before the fluid gets to the eye of the impeller (see Figure 4.21). To determine whether or not cavitation will occur, pump manufacturers provide information on the NPSHr. This is determined experimentally and is reported on the pump performance curve as a function of capacity. Refer to any of the pump performance curves in Appendix E to see the NPSHr curves for various pumps. Notice that the NPSHr is read on the *right-hand* axis for the Bell & Gossett performance curves.

Cavitation will be prevented if the NPSHa is greater than the NPSHr. It is good design practice to add a safety factor (SF) and actually exceed the NPSHr,

$$\text{NPSHa} - \text{NPSHr} \geq \text{SF} \quad (4.72)$$

It is common practice to have the NPSHa exceed the NPSHr by $\text{SF} = 3 \text{ ft}$ ($\sim 1 \text{ m}$).

4.7.6.1 Calculating the NPSHa

The NPSHa is a characteristic of the suction side of the pipe system. In a system where fluid is being moved from a tank, there are two possible pumping scenarios as shown in Figure 4.22; *suction lift* and *flooded suction*. Of these two possibilities, the suction lift is prone to cavitation.

In either scenario, the conservation of energy equation written from the free surface of the tank (1) to the suction port of the pump (s) results in,

$$\frac{P_1}{\gamma} + z_1 = \frac{P_s}{\gamma} + \frac{V_s^2}{2g} + z_s + \left(f \frac{L}{D} + \sum K \right) \frac{V_s^2}{2g} \quad (4.73)$$

Solving this equation for the pressure head at the suction port of the pump,

$$\frac{P_s}{\gamma} = \frac{P_1}{\gamma} + (z_1 - z_s) - \left(f \frac{L}{D} + \sum K + 1 \right) \frac{V_s^2}{2g} \quad (4.74)$$

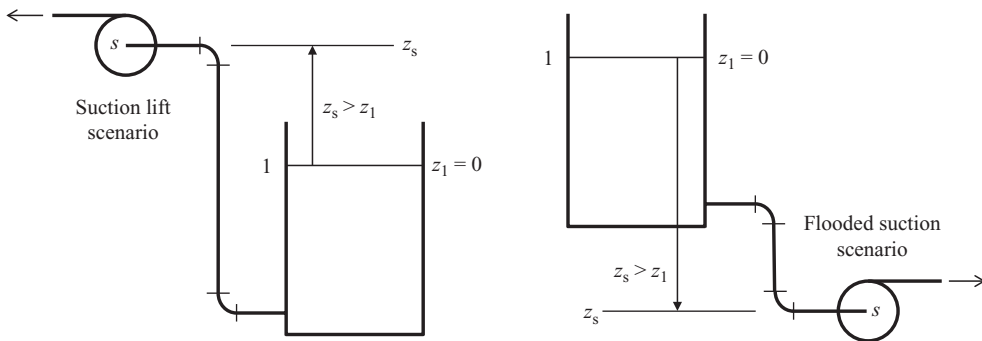


FIGURE 4.22
Suction lift and flooded suction configurations.

In Equation 4.74, the elevation difference is referenced to the surface of the fluid in the tank ($z_1 = 0$). This elevation difference is positive for a flooded suction application ($z_s < z_1$) and negative for a suction lift application ($z_s > z_1$). The NPSHa is the difference between the pressure head at the suction port and the fluid's vapor pressure head. Therefore, the NPSHa can be written as,

$$\text{NPSHa} = \frac{P_s}{\gamma} - \frac{P_v}{\gamma} = \frac{P_1}{\gamma} + (z_1 - z_s) - \left(f \frac{L}{D} + \sum K + 1 \right) \frac{V_s^2}{2g} - \frac{P_v}{\gamma} \quad (4.75)$$

Combining Equations 4.75 and 4.72 and solving for the elevation of the suction port of the pump results in,

$$z_s = z_1 + \frac{P_1 - P_v}{\gamma} - \left(f \frac{L}{D} + \sum K + 1 \right) \frac{V_s^2}{2g} - (\text{NPSHr} + \text{SF}) \quad (4.76)$$

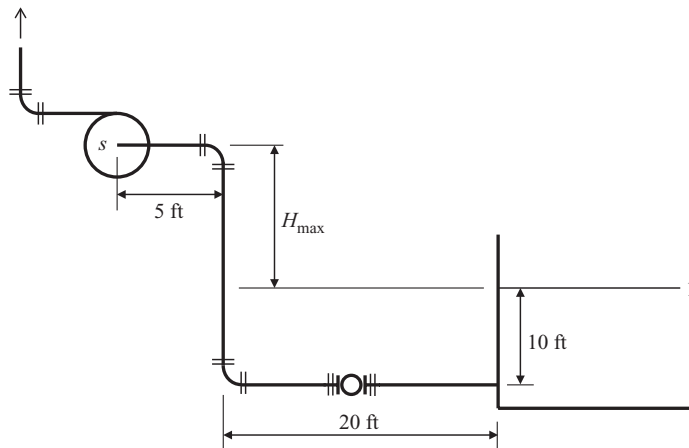
When forming Equation 4.76, the equality of Equation 4.72 was used. The value of z_s indicates the location of the pump with respect to the free surface of the liquid to prevent cavitation from occurring. In a suction lift scenario, if the pump is installed at an elevation higher than z_s , cavitation will most likely occur.

Example 4.16

Water at 100°F is being pumped vertically upward from an open holding tank by a Bell & Gossett Series e-1531 Model 2AD pump with a 6½-inch impeller operating at 3550 rpm as shown in Figure E4.16A. When the pump is installed in the pipe system, the head delivered by the pump is 150 ft. The suction pipe is 3-nom sch 40 commercial steel and the fittings and valve are standard. Atmospheric pressure is 14 psia. Determine the maximum height above the water surface in the tank that the pump can be installed to prevent cavitation.

Solution

By defining the tank surface to be the elevation reference ($z_1 = 0$ ft), the value of H_{\max} is equal to the difference between the elevation of the suction port of the pump, z_s , and the free surface of the water in the tank, z_1 . Therefore, Equation 4.76 can be written as,

**FIGURE E4.16A**

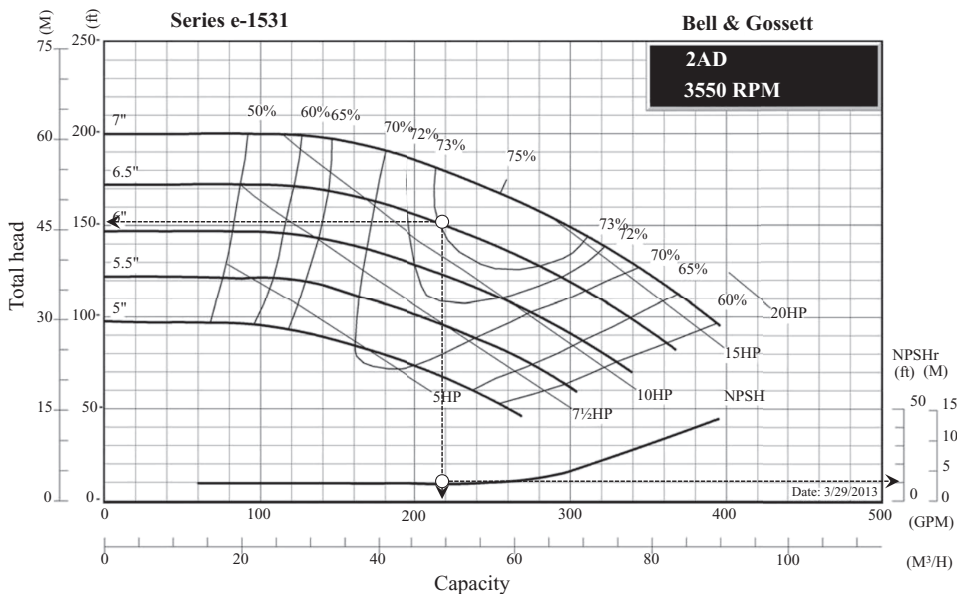
Water pumped upward from a large, open holding tank.

$$H_{\max} = \frac{P_1 - P_v}{\gamma} - \left(f \frac{L}{D} + \sum K + 1 \right) \frac{V_s^2}{2g} - (\text{NPSHr} + \text{SF})$$

The capacity and NPSHr can be found using the pump performance curve shown in Figure E4.16B. From this figure,

$$\dot{V} = 219 \text{ gpm} \quad \text{NPSHr} = 10 \text{ ft (read on the right-hand axis)}$$

The total length of straight pipe on the suction side of the pump is unknown since it depends on H_{\max} . From the sketch of the system, it can be seen that this relationship is,

**FIGURE E4.16B**

Pump performance curve and system operating parameters.

$$L = L' + H_{\max} \quad \text{where } L' = (20 + 10 + 5)\text{ft} = 35 \text{ ft}$$

Substituting this expression into the conservation of energy equation results in,

$$H_{\max} = \frac{P_1 - P_v}{\gamma} - \left[f \frac{(L' + H_{\max})}{D} + \sum K + 1 \right] \frac{V_s^2}{2g} - (\text{NPSHr} + \text{SF})$$

Solving this equation for H_{\max} ,

$$H_{\max} = \frac{\frac{P_1 - P_v}{\gamma} - \left(f \frac{L'}{D} + \sum K + 1 \right) \frac{V_s^2}{2g} - (\text{NPSHr} + \text{SF})}{\frac{f}{D} \frac{V_s^2}{2g} + 1}$$

The pipe diameters and properties of water at 100°F are,

$$\begin{aligned} D_{\text{nom}} &= 3 \text{ in} & D &= 0.25567 \text{ ft} & \varepsilon &= 0.00015 \text{ ft} & \frac{\varepsilon}{D} &= 0.00058669 \\ & & \text{Appendix C} & & \text{Table 4.3} & & & \\ P_v &= 0.95051 \text{ psia} & \rho &= 61.991 \frac{\text{lbm}}{\text{ft}^3} & \mu &= \left(1.6473 \frac{\text{lbm}}{\text{ft-h}} \right) \left(\frac{\text{h}}{3600 \text{ s}} \right) = 0.00045758 \frac{\text{lbm}}{\text{ft-s}} \\ & \text{Appendix B.1} & \text{Appendix B.1} & & \text{Appendix B.1} & & & \end{aligned}$$

The velocity of the water in the suction pipe is,

$$V_s = \frac{4\dot{V}}{\pi D^2} = 9.5041 \frac{\text{ft}}{\text{s}}$$

The Reynolds number of the flow is,

$$\text{Re} = \frac{\rho V_s D}{\mu} = 329,202$$

The friction factor can be calculated by,

$$f = \frac{0.25}{\left[\log \left(\frac{\varepsilon/D}{3.7} + \frac{5.74}{\text{Re}^{0.9}} \right) \right]} = 0.01870$$

The loss coefficients for the elbows and ball valve will be computed using the 3K method,

$$K_{\text{valve}} = \frac{K_1}{\text{Re}} + K_{\infty} \left(1 + \frac{K_d}{D_{\text{nom}}^{0.3}} \right) = \frac{300}{\text{Re}} + 0.017 \left(1 + \frac{3.6}{D_{\text{nom}}^{0.3}} \right) = 0.055674$$

$$K_{\text{elbow}} = \frac{K_1}{\text{Re}} + K_{\infty} \left(1 + \frac{K_d}{D_{\text{nom}}^{0.3}} \right) = \frac{800}{\text{Re}} + 0.091 \left(1 + \frac{4}{D_{\text{nom}}^{0.3}} \right) = 0.31803$$

$$K_{\text{entrance}} = 0.5 \text{ (flush, square with no pipe projection into the tank)}$$

The pump model is a Bell & Gossett 2AD. This means the suction port of the pump is a 2-nom diameter. Since the suction pipe is 3 nom, a reducer must be used to connect the suction pipe to the pump. Using Table 4.10 and assuming that the reducer is rounded,

$$K_{reducer} = \left(0.1 + \frac{50}{\text{Re}_D} \right) \left(\frac{1}{\beta^4} - 1 \right)$$

The Reynolds number is based on the large diameter pipe, which has been previously calculated. The value of β is the ratio of the small inside diameter to the large inside diameter,

$$\beta = \frac{d}{D} = \frac{\overset{2\text{-nom sch 40}}{0.17225 \text{ ft}}}{\underset{3\text{-nom sch 40}}{0.25567 \text{ ft}}} = 0.67372$$

Therefore, the loss coefficient for the reducer is,

$$K_{reducer} = \left(0.1 + \frac{50}{\text{Re}_D} \right) \left(\frac{1}{\beta^4} - 1 \right) = 0.38597$$

The sum of all the loss coefficients on the suction side of the system can now be found,

$$\sum K = K_{valve} + 3K_{elbow} + K_{entrance} + K_{reducer} = 1.8957$$

Three elbows are used; two shown on the system sketch and one is required to connect the piping to the pump since the Series e-1531 is an end-suction pump (refer to the photo of the pump on the Series e-1531 booklet in Appendix E). Now, all the unknowns have been identified and the value of H_{\max} can be found,

$$H_{\max} = \frac{\frac{P_1 - P_v}{\gamma} - \left(f \frac{L'}{D} + \sum K + 1 \right) \frac{V_s^2}{2g} - (\text{NPSHr} + \text{SF})}{\frac{f}{D} \frac{V_s^2}{2g} + 1} = 8.76 \text{ ft}$$

This calculation indicates that the pump can be located no higher than 8.76 ft above the surface of the water in the tank, otherwise cavitation will occur.

It may be tempting to neglect the effects of minor losses when calculating the NPSHa. While this may not be accurate, it will provide a quick estimate for an initial design. However, since the friction effects reduce z_{sv} as seen in Equation 4.76, the importance of the minor losses should not be neglected in the final design calculations.

4.7.7 Series and Parallel Pump Configurations

Multiple pump systems are used to provide pressure-boosting stations along a very long pipe line (e.g., the Alaskan Pipeline), or to provide redundancy in a system should one of the pumps fail. Pumps can be connected together in *series* or *parallel*. In multiple pump systems, the design engineer is interested in the *composite* performance of all the pumps operating together.

The most common application for pumps in *series* is for boosting pressure along a long pipeline. In a long pipeline, the friction losses may cause a single pump to be very large and cost prohibitive. Therefore, boosting the pressure with smaller pumps along the pipeline is a cost-effective way of transporting the fluid through the pipeline. Pumps in series

are *head additive*. This means that the composite performance of a series pump combination is equal to the sum of the head produced by each individual pump. This is illustrated in Figure 4.23 for the case of two identical pumps operating in series.

Parallel pump circuits are used to provide system redundancy in the case of a pump failure. Parallel pump systems are also helpful in using several smaller pumps to provide a large flow rate. Since the head across all pumps in a parallel circuit is the same, parallel pumps are *capacity additive*. This is demonstrated in Figure 4.24 for the case of two identical pumps in parallel.

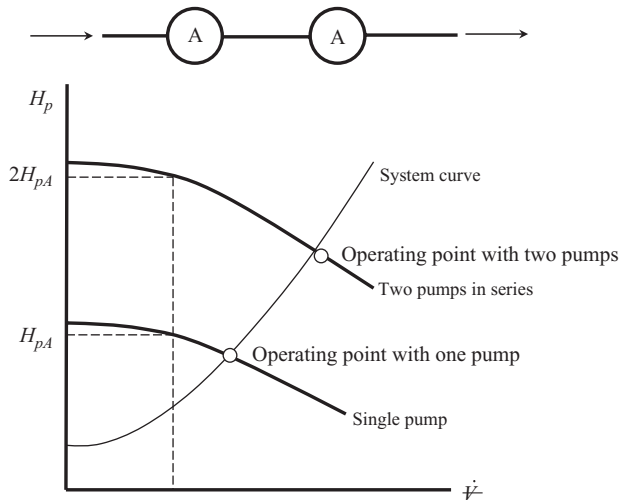


FIGURE 4.23
Performance curve for two identical pumps operating in series.

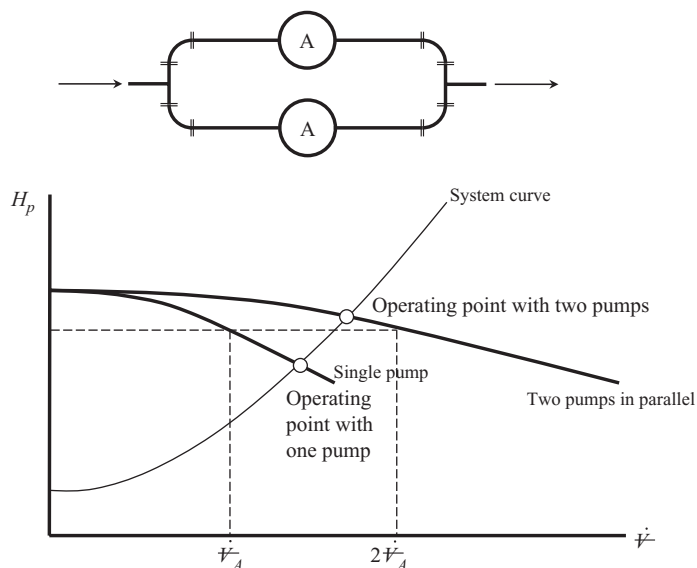


FIGURE 4.24
Performance curve for two identical pumps operating in parallel.

Example 4.17

Two Bell & Gossett Series 80-SC Model 1½ x 1½ x 7B pumps with 6½ -inch impellers are operating in parallel at 1150 rpm to deliver 20 m³/h (8.33 L/s) of water at 5.08 m of head with an elevation head increase of 3.5 m in the system. Determine (a) the system curve, (b) the composite pump curve, (c) the operating efficiency of each pump, and (d) if one of the pumps fails, determine the capacity, head, and efficiency of the remaining pump.

Solution

- a. There is not much information given about the system. However, two points are identified on the system curve; the operating point (20 m³/h @ 5.08 m), and the elevation offset (0 m³/h @ 3.5 m). Since the system curve is a parabola centered about the y -axis, the system curve can be determined using these two points. The pump head and capacity are related by,

$$H_p = \Delta z + b\dot{V}^2$$

The constant b can be determined since the operating point (20 m³/h @ 5.08 m) is known,

$$b = \frac{H_p - \Delta z}{\dot{V}^2} = \frac{(5.08 - 3.5)\text{m}}{(20 \text{ m}^3/\text{h})^2} = 0.00395 \frac{\text{m}}{(\text{m}^3/\text{h})^2}$$

This information can be used to construct the system curve by conducting a parametric study. The resulting system curve is shown in Figure E4.17A.

- b. The composite pump curve can be determined by reading data from the 6½-inch impeller curve, doubling the capacity at the same head, and plotting the results. This can be done for several points along the performance curve. These data can be overlaid on the system curve as shown in Figure E4.17B,

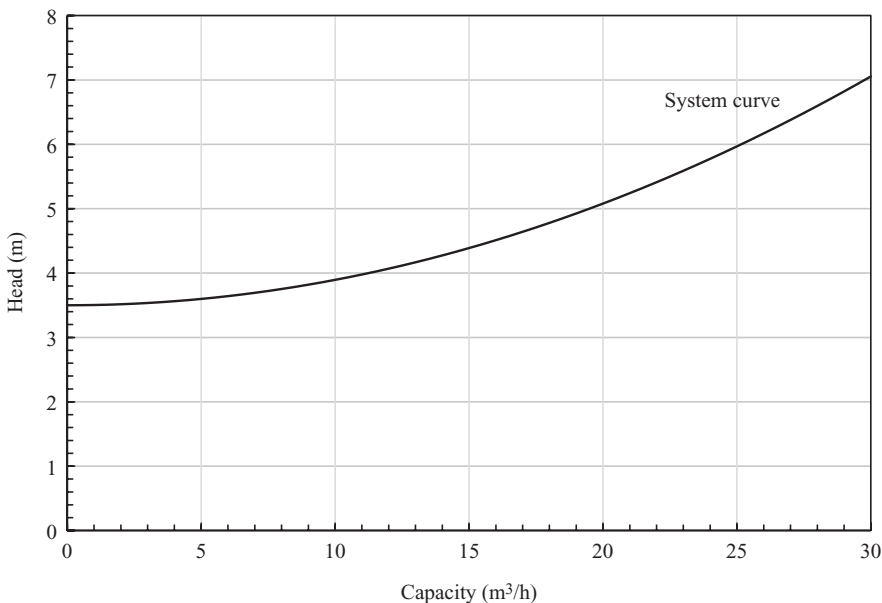
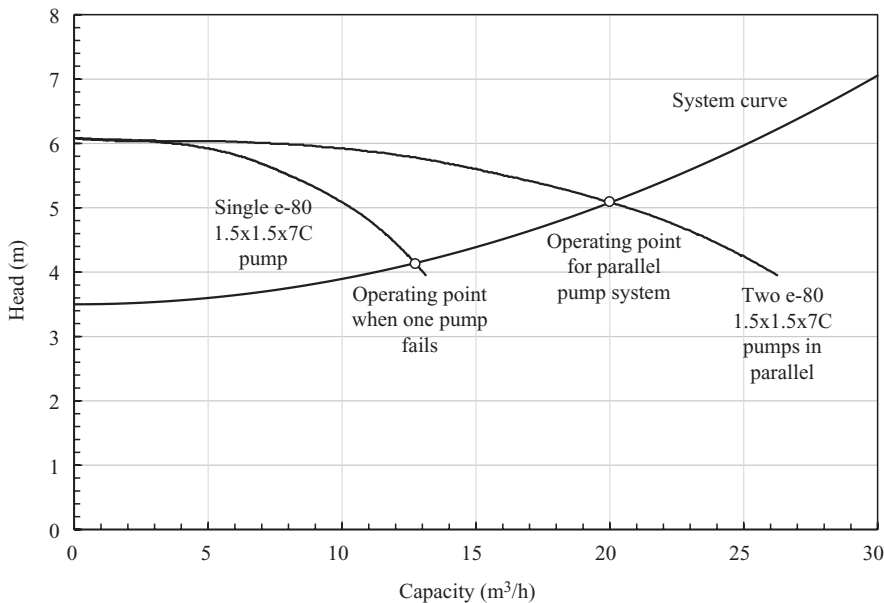


FIGURE E4.17A
System curve.

**FIGURE E4.17B**

Single pump and composite parallel pump curves with system curve.

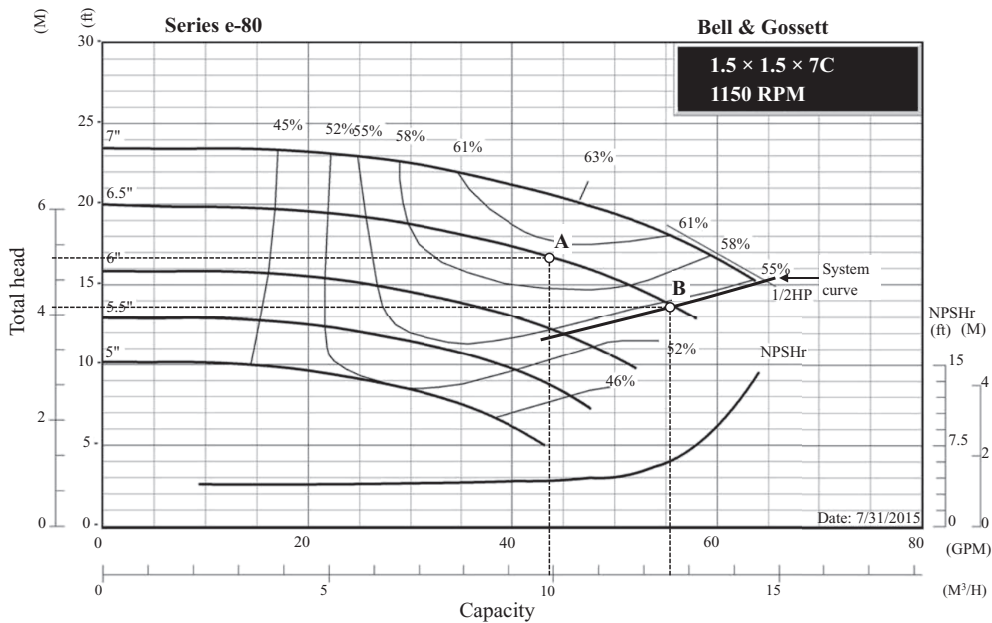
- c. The pump curves for this model pump from Appendix E are shown in Figure E4.17C. Since parallel pumps are capacity additive, each pump is providing half of the total capacity. Therefore,

$$\dot{V}_{\text{single pump}} = \frac{20 \text{ m}^3/\text{h}}{2} = 10 \text{ m}^3/\text{h}$$

The efficiency of each pump can be read directly from the performance curves at 10 m³/h for the 6½-inch impeller (point A). This point indicates that each pump will operate at an efficiency of approximately 60%. Notice that this point is the same point identified by 10 m³/h at 5.08 m of head. This must be true since the pressure head across each pump in the parallel circuit must be the same.

- d. When one of the pumps fails, the other pump's operating conditions change to match the system curve. Loss of a pump does not change the system curve. However, it does change the operating point as shown in Figure E4.17B. The pump curves in Figure 4.17C show a portion of the system curve. The intersection of the system curve with the pump curve for the 6½ inch impeller is the operating point when one of the pumps fails (point B). This operating point indicates that a single pump will deliver 12.7 m³/h at 4.11 m of head. It can also be seen that the efficiency of the pump drops to approximately 54.5%.

In Example 4.17, it can be seen that in a parallel pump circuit, the failure of one pump reduces the total capacity and the efficiency of the second pump. In the example, the efficiency dropped from 60% to 54.5%. This may seem like a small change. However, if the efficiency drops too low, it is possible that the pump's motor would overheat due to increased electrical current flowing through the copper windings. Careful design work must be considered to avoid this unfortunate consequence. It is always a good idea to determine the operating condition of the remaining pump(s) when one

**FIGURE E4.17C**

Performance curves for a Bell & Gossett 1.5x1.5x7C pump operating at 1150 rpm.

(or more) pumps in a parallel system fail to avoid possible overheating and burnout of a pump motor.

4.7.8 Affinity Laws

Pump curves from manufacturers are presented for a specified rotational operating speed of the pump. Many pumps use a single-speed motor because they are reasonably priced. However, as technology has improved over the years, the *variable speed* motor is becoming very attractive for use with pumps. Varying the rotational speed of the pump changes its performance. Given the pump curves at a single operating speed, the design engineer can use the *affinity laws* to predict its performance at a different operating speed. The affinity laws are also helpful if the impeller diameter is modified along with the rotational speed.

The affinity laws are derived using dimensional analysis and similitude. If all pumps of one type (e.g., centrifugal) behave similarly, then dimensional analysis should reveal how the pump parameters scale. In dimensional analysis, the Buckingham-Pi theorem is used to determine pertinent dimensionless groups. When analyzing centrifugal pumps using the Buckingham-Pi theorem, the performance parameters of the pump (head, power, and efficiency) are assumed to be a function of the fluid's density (ρ) and viscosity (μ), the rotational speed of the pump (ω), the impeller diameter (D) and the capacity delivered by the pump (\dot{V}). Application of the Buckingham-Pi theorem to this functional dependence reveals five dimensionless groups shown in Table 4.20.

The resulting functional dependence of these dimensionless groups are shown in the following equations,

$$\frac{gH_p}{\omega^2 D^2} = f_1 \left(\frac{\dot{V}}{\omega D^3}, \frac{\rho \omega D^2}{\mu} \right) \quad (4.77)$$

TABLE 4.20

Dimensionless Groups Related to Centrifugal Pump Performance

Dimensionless Group Name	Definition
Rotational Reynolds number	$\frac{\rho\omega D^2}{\mu}$
Volumetric flow coefficient	$\frac{\dot{V}}{\omega D^3}$
Head coefficient	$\frac{gH_p}{\omega^2 D^2}$
Power coefficient	$\frac{\dot{W}}{\rho\omega^3 D^5}$
Efficiency	η

$$\frac{\dot{W}}{\rho\omega^3 D^5} = f_2 \left(\frac{\dot{V}}{\omega D^3}, \frac{\rho\omega D^2}{\mu} \right) \quad (4.78)$$

$$\eta = f_3 \left(\frac{\dot{V}}{\omega D^3}, \frac{\rho\omega D^2}{\mu} \right) \quad (4.79)$$

Laboratory experiments indicate that the head coefficient, power coefficient, and efficiency are only weakly dependent on the rotational Reynolds number. Therefore, the Equations 4.77 through 4.79 can be written as,

$$\frac{gH_p}{\omega^2 D^2} \approx f_1 \left(\frac{\dot{V}}{\omega D^3} \right) \quad (4.80)$$

$$\frac{\dot{W}}{\rho\omega^3 D^5} \approx f_2 \left(\frac{\dot{V}}{\omega D^3} \right) \quad (4.81)$$

$$\eta \approx f_3 \left(\frac{\dot{V}}{\omega D^3} \right) \quad (4.82)$$

Equations 4.80 through 4.82 are known as the *affinity laws*. Given the performance data for a pump operating at a certain condition, the affinity laws can be used to predict the performance of the same pump at different conditions (e.g., changing the rotational speed or changing the impeller diameter). To apply the affinity laws, it is assumed that for geometrically similar pumps, the dimensionless groups shown in Equations 4.80 through 4.82 are equal at different operating conditions.

Example 4.18

The performance curves for a Bell & Gossett Series e-1531 2BD pump operating at 1750 rpm are shown in E4.18A. Consider this pump fitted with an 8-inch impeller pump delivering 1750 gpm of water.

- Determine the head, power draw, and efficiency of this pump from the pump curves.
- Using the affinity laws, determine the capacity, head, power draw, and efficiency if the impeller diameter is changed to 8.5-inch.
- Compare the results of the affinity law calculations to the actual values on the performance curves.

Solution

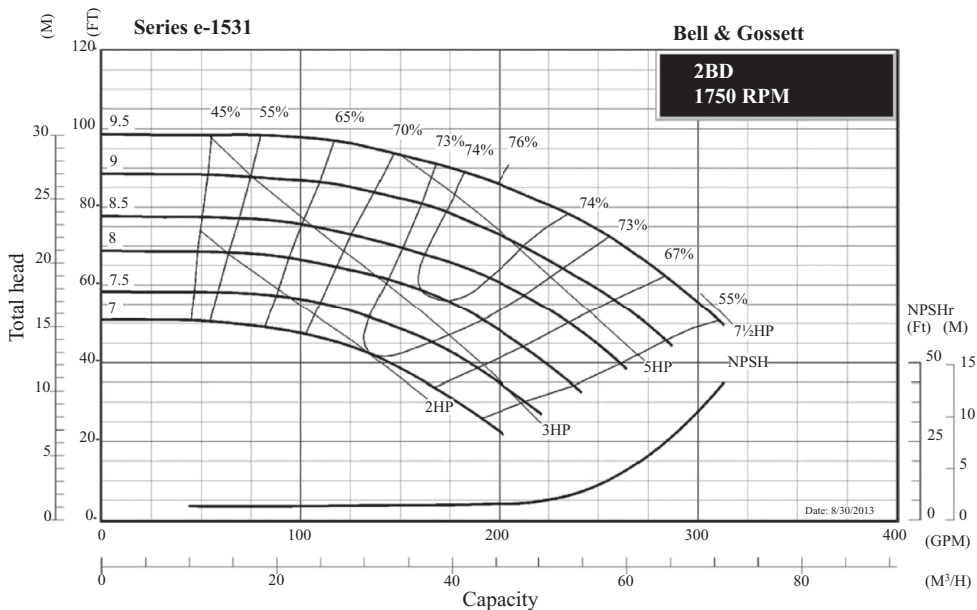
- At a capacity of 80 gpm, the 6-inch impeller pump, the head, power draw, and efficiency can be read from Figure E4.18A,

$$D_o = 8 \text{ in} \quad \dot{V}_o = 175 \text{ gpm} \quad H_o = 55.8 \text{ ft} \quad \dot{W}_o = 3.5 \text{ hp} \quad \eta = 74\%$$

The subscript “o” on these values indicates the original operating condition of the pump.

- To apply the affinity laws, it is assumed that the dimensionless groups in Equations 4.80 through 4.82 are the same for geometrically similar pumps. Changing only the impeller diameter should result in a new pump configuration that is geometrically similar to the original. Therefore, the new capacity of the pump can be determined by equating the volumetric flow coefficients,

$$\frac{\dot{V}_n}{\omega_n D_n^3} = \frac{\dot{V}_o}{\omega_o D_o^3}$$

**FIGURE E4.18A**

Performance curves for a Bell & Gossett Series e-1531 2BD pump operating at 1750 rpm.

In this equation the subscript “n” signifies the new operating condition. Solving this equation for the new capacity,

$$\dot{V}_n = \dot{V}_o \frac{\omega_n D_n^3}{\omega_o D_o^3} = \dot{V}_o \left(\frac{D_n}{D_o} \right)^3 = (175 \text{ gpm}) \left(\frac{8.5 \text{ in}}{8 \text{ in}} \right)^3 = 209.9 \text{ gpm}$$

Equating the head coefficients allows for predicting the new head delivered by the pump,

$$\frac{gH_{p,n}}{\omega_n^2 D_n^2} = \frac{gH_{p,o}}{\omega_o^2 D_o^2} \rightarrow H_{p,n} = H_{p,o} \left(\frac{D_n}{D_o} \right)^2 = (55.8 \text{ ft}) \left(\frac{8.5 \text{ in}}{8 \text{ in}} \right)^2 = 63.0 \text{ ft}$$

The power draw under these new operating conditions can be predicted by equating the power coefficients,

$$\frac{\dot{W}_n}{\rho \omega_n^3 D_n^5} = \frac{\dot{W}_o}{\rho \omega_o^3 D_o^5} \rightarrow \dot{W}_n = \dot{W}_o \left(\frac{D_n}{D_o} \right)^5 = (3.5 \text{ hp}) \left(\frac{8.5 \text{ in}}{8 \text{ in}} \right)^5 = 4.7 \text{ hp}$$

Since the efficiency is one of the five dimensionless groups in the affinity laws, the efficiency of the pump should not change,

$$\eta_n = \eta_o = 74\%$$

- c. Figure E4.18B shows the performance curves with the original operating condition and the new operating condition predicted by the affinity laws.

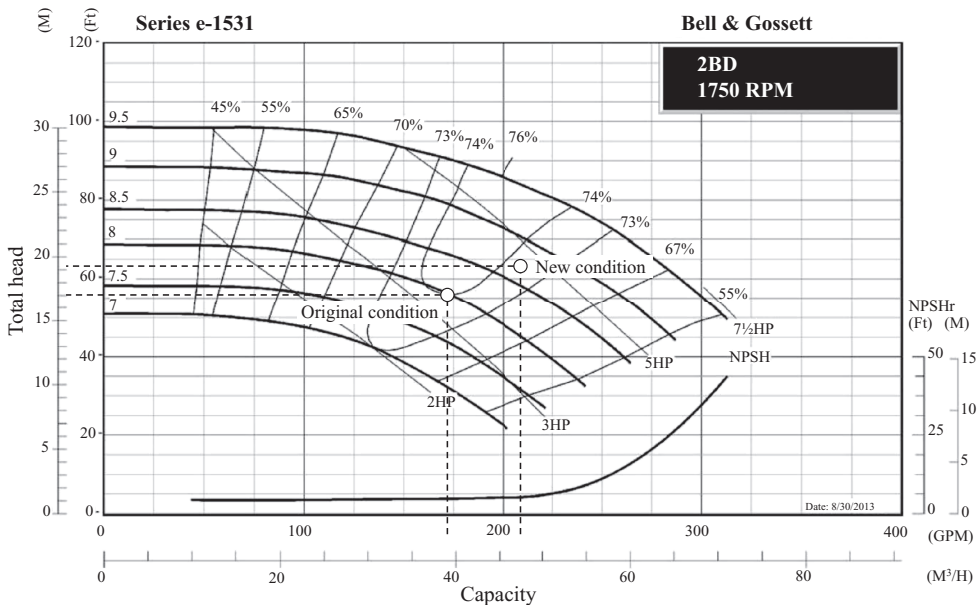
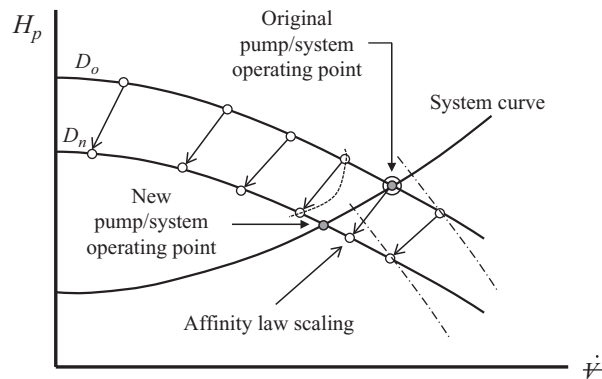


FIGURE E4.18B

Pump performance curve showing original and new operating conditions.

**FIGURE 4.25**

Demonstration of how the affinity laws scale pump performance but not the pump/pipe system operating point.

As seen in this figure, the affinity laws prediction is not exact (the new condition should be on the 8.5-inch impeller curve). This may be attributed to inaccurate reading of the original operating parameters from the pump curves. It can also be attributed to the assumption that the performance parameters are only weakly dependent on the rotational Reynolds number. Equations 4.80 through 4.82 are *approximate* based on this assumption.

As Example 4.18 demonstrates, there is no substitution for manufacturer's pump curves. However, the affinity laws can provide a reasonable approximation to pump performance. The affinity laws are particularly helpful to the design engineer when variable speed motors are used to drive a pump and pump curves are not available at a given operating speed.

A final comment is in order concerning the affinity laws. These laws scale the pump performance curves. The affinity laws *do not* scale pump/pipe system operating points. This is demonstrated in Figure 4.25. In this figure, only the pump impeller is changed and the affinity laws are used to predict the new pump performance curve. The operating speed of the pump is the same for the original and new condition. As shown in Figure 4.25, the original operating point, a point on the original pump performance curve, scales to a new performance point that is not necessarily consistent with the new pump/pipe system operating point. The only way to determine the new pump/pipe system operating point is to intersect the system curve with the new pump performance curve predicted from the affinity laws.

4.8 Design Practices for Pump/Pipe Systems

There are many factors that the design engineer must take into account when designing a pump/pipe system. Throughout this chapter, many of these design practices have been mentioned. In this section, a summary of some of the common design practices is presented. This is not intended to be all-inclusive. Nothing substitutes for experience. As the design engineer becomes more experienced in this area, he/she will no-doubt build upon these practices.

4.8.1 Economics

Economics is usually the bottom-line in industry. Hydraulic systems need to be designed to have minimum cost. This can be accomplished by carefully laying out the pipe system to minimize the friction losses while maintaining an economic diameter. Careful layout of the system includes wise placement of valves and fittings. While this may seem obvious, there may be physical limitations. Minimization of friction losses is one way to help reduce cost. Designing systems using the economic diameter is also a good way to minimize costs. As demonstrated in Section 4.6, the economic diameter is one that minimizes the total annual cost per foot of pipe. This includes the amortized capital costs *and* the cost of energy required to move the fluid through the system.

4.8.2 Environmental Impact

There are many ways to drive a pump. However, the predominant method is by using electric motors. According to the International Energy Agency (IEA), in 2011 electric motor driven systems (EMDS) accounted for 43% to 46% of all global electricity use (Waide and Brunner 2011). Electrical power generation using fossil fuels results in the emission of carbon dioxide due to the combustion of the fuel. The IEA estimates that without comprehensive energy policy measures, energy consumption attributed to EMDS is expected to rise to 13,360 TWh per year and carbon dioxide emissions to 8,570 Mt per year on a global scale. In 2011, end users of EMDS spent \$565 billion globally. By 2030, that could rise to nearly \$900 billion.

Not all EMDS are pump/motor combinations. However, there are millions of residential and commercial systems that utilize pumps to circulate fluids. The message here is that the real cost of a pump is not just economic; it becomes an environmental issue as well. Selecting the right pump helps minimize the depletion of the natural resources used to generate the electricity required to run the pump. This goes hand in hand with helping to reduce carbon dioxide emissions in the electrical generation process.

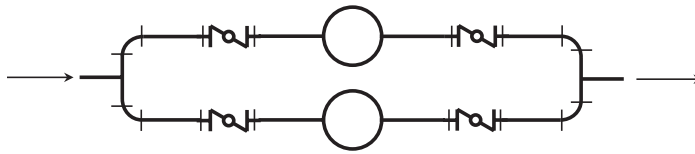
4.8.3 Noise and Vibration

In cases where pipes are located in an occupied environment, like an office, the fluid circulating through the pipes should cause no noise. In addition, excessive pressure drops in pipe systems can lead to vibration which should also be avoided. Recommended pressure drops to avoid noise and vibration are 25–30 psi per 1000 ft for liquids, 10–15 psi per 1000 ft for gases, and 4 psi per 100 ft for low-pressure steam.

4.8.4 Pump Placement and Flow Control

When placing a pump in a pipe network, it must be located to avoid cavitation. A net positive suction head analysis should be done for any pump installation to ensure that cavitation will be prevented.

Flow control can be accomplished by using control valves and/or using variable speed motors instead of single speed motors to drive the pump. If possible, it is recommended that valves be avoided for flow control because they introduce more friction resistance. This may not always be possible and a flow control valve must be specified. In this case,

**FIGURE 4.26**

Using valves to provide an opportunity to isolate a pump for repair or maintenance.

the valve is to be located at the *discharge* of the pump. Placing the valve in the suction line makes the pump more susceptible to cavitation.

Variable speed motors with digital control provide an attractive alternative to control valves. In the past, these types of systems may have been cost prohibitive. However, due to rapid improvements in technology, the cost of digitally-controlled variable speed motors is becoming more reasonable. This is a more environmentally-friendly alternative to flow control compared to a pressure drop across a control valve.

4.8.5 Valves

As discussed in the previous section, valves can be used for flow control. Another use of valves is to isolate sections of a system for repair and maintenance. An example is shown in Figure 4.26 where four butterfly valves are used. A butterfly valve is used here because it provides positive shut-off as discussed in Table 4.5. By shutting off the valves on either side of one of the pumps, it can be taken off-line for repair or maintenance while the other pump continues to circulate fluid through the system. The effect of taking one of the pumps offline can be determined using the procedures outlined in Section 4.7.7.

4.8.6 Expansion Tanks and Entrained Gases

As discussed in Section 4.7.4.2, expansion tanks are often incorporated in closed-loop systems. The expansion tank allows the system to operate in a steady state even when there are temperature variations which can cause the total fluid volume to increase or decrease. The expansion tank also creates a point of constant pressure in the system.

In many cases, particularly startup, there may be non-soluble gases (e.g., air) entrained in the liquid flowing through the system. These entrained gases can create noise as the liquid circulates through the pipes, and they also cause problems similar to cavitation in pumps. Entrained gases can be removed from a system by providing a high-elevation point in the system with bleed ports. In a closed-loop system, the strategic location of the expansion tank can provide an opportunity to bleed of entrained gases.

4.8.7 Other Sources for Design Practices

Listed above are only some of the more common design practices for pump/pipe system design. There are other sources that the design engineer can consult including, piping handbooks and guides, trade journals (for state-of-the-art information), company design practices, and experienced design engineers.

References

- Darby, R., and R. P. Chhabra. 2017. *Chemical Engineering Fluid Mechanics*. Boca Raton, Florida, USA: CRC Press.
- Darby, R., and J. D. Melson. 1982. "Direct Determination of Optimum Economic Pipe Diameter for Non-Newtonian Fluids." *Journal of Pipelines* 2: 11–21.
- Grundfos Research and Technology. 2014. *The Centrifugal Pump*. Bjerringbro, Denmark: Grundfos.
- Hooper, W. B. 1981. "The Two-K Method Predicts Head Losses in Pipe Fittings." *Chemical Engineering* 96–100.
- Idelchik, I. E. 2007. *Handbook of Hydraulic Resistance*. New York, NY: Begell House, Inc.
- Janna, W. S. 2015. *Design of Fluid-Thermal Systems*. Stamford, CT: Cengage Learning.
- Karassik, I. J., J. P. Messina, P. Cooper, and C. C. Heald. 2008. *Pump Handbook*. New York: McGraw-Hill.
- Moody, Lewis F. 1944. "Friction Factors for Pipe Flow." *Transactions of the A.S.M.E.* 671–684.
- Neutrium, Inc. 2012. *Pressure Loss from Fittings - Expansion and Reduction in Pipe Size*. November 2. https://neutrium.net/fluid_flow/pressure-loss-from-fittings-expansion-and-reduction-in-pipe-size/.
- Smith, P., and R. Zappe. 2004. *Valve Selection Handbook: Engineering Fundamentals for Selecting the Right Valve Design for Every Industrial Flow Application*. Oxford, UK: Gulf Professional Publishing.
- The Crane Company. 2017. *Flow of Fluids Through Valves, Fittings and Pipe*. Stamford, Connecticut: The Crane Company.
- Waide, P., and C. U. Brunner. 2011. *Energy-Efficiency Policy Opportunities for Electric Motor-Driven Systems*. Paris, France: International Energy Agency.
- Xylem, Inc. 2015. *Series e-1531: Closed coupled centrifugal pump curves - 60 Hz*. Morton Grove, Illinois, USA: Bell & Gossett.
- Xylem, Inc. 2016. *Series e-80: In-line mounted centrifugal pump performance curves—60 Hz*. Morton Grove, Illinois, USA: Bell & Gossett.
-

Problems

Piping and Tubing Standards

- 4.1 Consider an 8-nom commercial steel pipe carrying dodecane at 60°F. The volumetric flow rate of the dodecane is 800 gpm. Complete Table P4.1 showing the variation of the dodecane flow parameters inside the pipe as a function of the pipe schedule used.
- 4.2 Liquid Refrigerant 123 (R123) at 120°C is passing through a ½-std copper tube at a flow rate of 1200 kg/hr. Complete Table P4.2 showing the variation of the R-123 flow parameters inside the tube as a function of the type of tubing used.
- 4.3 Refrigerant R134a is flowing through a ¾-std type L copper tube in a refrigeration system. In this system, a desuperheater is used to heat water as shown in Figure P4.3. The R134a enters the desuperheater at 200 psia, 225°F. The desuperheater removes enough energy, \dot{Q}_{DSH} , such that the R134a enters the condenser as a saturated vapor with no appreciable loss in pressure. In the condenser, energy is transferred from the refrigerant at a rate of 60,000 Btu/h. This causes the R134a to leave the condenser as a saturated liquid with a negligible drop in pressure. Determine the velocity (ft/s) of the R134a as it (a) enters the condenser and (b) leaves the condenser.

TABLE P4.1
Dodecane Flow Parameters

Schedule	V (ft/s)	Re	f
20			
40			
80			
120			
160			

TABLE P4.2
R123 Flow Parameters

Type	V (m/s)	Re	f
K			
L			
M			

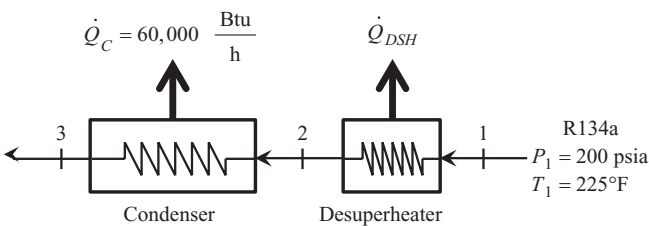


FIGURE P4.3
Condenser/desuperheater in a refrigeration system.

- 4.4 Compressed air at 500 kPa, 90°C is flowing through a 4-nom sch 40 commercial steel pipe at a volumetric flow rate of 375 m³/h. Determine the friction factor for this flow.
- 4.5 In a particular section of a fluid system, a 30% ethylene glycol mixture is flowing through a 6-nom xs cast iron pipe at a temperature of 0°C. In this section of piping, the velocity must be maintained in the range 1.5 m/s < V < 1.8 m/s. Determine the following,
- a. The range of volume flow rates corresponding to the velocity limits (L/s)
 - b. The range of friction factors corresponding to the velocity limits

Friction Calculations in Straight Pipes and Tubes

- 4.6 A 10-nom sch 40 horizontal commercial steel pipe is being used to transport octane. The pipe is 230 ft long. The octane is at 40°F and is flowing at 610 gpm. Determine the pressure drop of the octane as it flows through the pipe (psi).
- 4.7 Liquid propane is flowing through a 4 std type L copper tube. The tube is 200 m long and the outlet is 10 m higher than the inlet. The pressure drop through the tube is 90 kPa. The cyclohexane is at a temperature of -10°C. Determine the volumetric flow rate of the cyclohexane through the tube (L/s).

- 4.8 Water is flowing through a 2½-nom xs cast iron pipe at a rate of 4 L/s. The pipe is 75 m long and its outlet is 6 m higher than the inlet. The water is at a temperature of 25°C. Determine the pressure drop of the water through the pipe.
- 4.9 A 20% ethylene glycol solution is flowing through a 4-nom sch 80 commercial steel pipe. The pipe is 350 ft long and is horizontal. The pressure drop through the pipe is 4 psi. The ethylene glycol is at a temperature of 20°F.
- Determine the volumetric flow rate of the ethylene glycol (gpm)
 - Investigate the effect of the ethylene glycol temperature by plotting the volumetric flow rate (gpm) as a function of temperature for $20^{\circ}\text{F} \leq T \leq 100^{\circ}\text{F}$.
- 4.10 A fuel line supplying fuel to several large industrial diesel engines is made of type M copper tube. The tube is 40 ft long. The fuel is dispensed by gravity feed from a tank that is 12 ft above the engines. Diesel fuel (modeled as dodecane) at 80°F is being transported through the line. The required flow rate of the fuel is 300 gal/hr and the allowable pressure drop in the line is 1 psi. Specify the appropriate size (standard diameter) for this fuel line. The minor losses due to fittings can be considered negligible.
- 4.11 A horizontal pipeline is used to transport ethanol (ethyl alcohol) at 20°C over a distance of 3 km. The pipe is made of commercial steel. The required flow rate of the ethanol is 40 L/s. The pump connected to this pipeline can overcome a pressure drop of 200 kPa in the pipe. Specify the appropriate size (nominal diameter) of a schedule 40 pipe for this pipeline.
- 4.12 The Alaskan pipeline runs 798 miles from Prudhoe Bay to Valdez. Both cities are at sea level. The design specifications for the pipeline require a capacity of 2.4 million barrels per day (1 barrel = 42 gallons). The crude oil is maintained at 140°F in the pipeline. At this temperature, the oil has a density of 53.7 lbm/ft³ and a viscosity of 0.00257 lbm/ft-s. The pipe is made of commercial steel. Along the pipeline are pumping stations capable of boosting the oil pressure. Each pumping station can provide a pressure increase of 1100 psi.
- Construct a plot that shows the pipe diameter as a function of the number of pumping stations, N , for $1 \leq N \leq 30$
 - The Alaskan Pipeline is 48-inch nominal diameter and has 12 pumping stations. How does this compare to the plot that was generated in part (a) of this problem?
 - Use the plot generated in part (a) to discuss some of the issues that helped engineers arrive at the decision to construct a 48-inch pipeline with 12 pumping stations.
- 4.13 Fluid flow can cause excessive wear on the inside surface of a pipe, resulting in a much rougher surface over time. This increased surface roughness results in a larger pressure drop which requires more pumping energy to move the fluid compared to a new pipe. Consider an expensive 14-nom sch 120 pipe that has been in service for 50 years. The horizontal pipe is 300 m long and is transporting water at 20°C at a flow rate of 165 L/s. Due to wear, the absolute roughness of the pipe has become $\epsilon = 0.25$ cm.

The replacement of such a large, thick-walled pipe represents a significant cost. So, an alternative solution is being investigated. A ½-inch thick lining can be purchased that would reduce the absolute roughness to $\epsilon = 0.001$ cm.

It is anticipated that installing the lining will provide another 50 years of useful service for the pipe. The pump and motor combination that moves the water through the pipe has an efficiency of 54%, and the cost of energy is \$0.11/kWh. The pipeline runs continuously all year long. The mass flow rate of water carried by the original pipe must be the same as that carried through the lined pipe.

- Determine the annual savings in energy cost for a lined pipe compared to the old, rough pipe.
- If the cost of the liner and installation is \$197/m, determine the rate of return that results from the investment in the liner.
- Based on your analysis in part (b), is lining the pipe a good economic decision?

Valves and Fittings

- 4.14 A standard 90° elbow is being used in a 8-nom commercial steel pipe. The joint between the pipe and elbow is flanged. Under a *fully turbulent* flow condition, the loss coefficient for the elbow is found to be $K = 0.29$ using the method presented by the Crane Company (2017). Use the 2K method to calculate the K value of this elbow for the range of Reynolds numbers $10^4 < Re < 10^8$. Display your results on a plot showing K as a function of the Reynolds number [K vs. $\log(Re)$]. Comment on how the result compares to the value calculated using the Crane method.
- 4.15 Solve Problem 4.14 using the 3K method for calculating the K value of the elbow.
- 4.16 A piping system is made of 10-nom sch 80 commercial steel pipe. The pipe is transporting a 30% propylene glycol solution at a temperature of 40°C. Table P4.16 shows the number of fittings and valves in this pipe system. The joints are flanged. Determine the pressure loss (kPa) in this pipe system due to the fittings and valves using the 3K method.
- 4.17 The design of a pump and pipe system has been completed, except for the valves. The system is used to transport water at 120°F through 2 nom sch 40 commercial steel pipe at a required flow rate of 85 gpm. Without the valves, the pump selected has the capability to overcome an additional 18 psi of pressure drop due to the valves and still provide the required flow rate. The pipe/valve joints are threaded. Determine how many 2-inch globe valves can be installed in this pump and pipe system.

TABLE P4.16

Fittings and Valves in the Pipe System

Fitting or Valve	Number
45° standard elbow	4
90° standard elbow	10
180° standard bend	3
Gate valves	20
Globe valves	5
Ball valves	6
Check valve, lift-type	1
Pipe entrance, flush and square	1
Pipe exit	1

- 4.18 A $\frac{1}{2}$ -std type M copper tube system used to make a heat exchanger has 32 180° standard bends. The joints are soldered (assume this joint type can be treated as a welded joint). The fluid flowing through the tube is liquid Refrigerant 227ea (R227ea) at 160°F . The R227ea is flowing at a rate of 1500 lbm/h. Determine the pressure drop (psi) due to the bend fittings.
- 4.19 Air is passing through a round duct with an inside diameter of 2 ft in an air conditioning system. The air is at a temperature of 60°F and a pressure of 1 atm. The air is flowing at a rate of 5000 cfm. As the air passes through the duct system, it flows through three 90° mitered elbows with 3 miter joints. Determine the pressure loss due to the three mitered elbows. Express your answer in inches of water (in H_2O).
- 4.20 A tilting disc check valve is to be installed in a 4-nom sch 40 steel pipeline. For the valve being considered, the angle $\alpha = 5^\circ$. The fluid being transported through the pipeline is a 20% ethylene glycol solution at a 20°F . The volumetric flow rate of the ethylene glycol is 425 gpm.
- Specify the size and ASME class of the check valve required.
 - Determine the total pressure drop (psi) due to the check valve and any reducers required to connect to the 4-nom pipe.
- 4.21 Water at 80°C is flowing in a 6-nom sch 120 commercial steel pipe at a flow rate of 21 L/s. A globe-type lift check valve is to be installed in this pipe.
- Specify the size and ASME class of the check valve required.
 - Determine the total pressure drop (kPa) due to the check valve and any reducers required to connect to the 6-nom pipe.
- 4.22 A 6-nom class 400 wye fitting with equal leg diameters has 650 gpm of water flowing into the fitting at 60°F . 65% of the flow leaves the fitting through the straight run and the remaining flow leaves through the branch which is at an angle of 45° to the straight run. Determine the pressure loss (psi) for this wye fitting.
- 4.23 Hexane enters the branch portion of a tee at 6 L/s and the straight run portion at 10 L/s. The tee is a 3-nom class 300 fitting. All ports of the tee have the same diameter. Determine the head loss (m) in the branch and straight runs.

Design and Analysis of Pipe Networks

- 4.24 A gravity-feed piping system between two large tanks is used to transport a 20% magnesium chloride solution as shown in Figure P4.24. The magnesium chloride solution is at 80°F and the tanks are open to the atmosphere. The piping system is 3-nom sch 40 commercial steel. All fittings and valves are 3-nom and standard. The total straight length of pipe in the system is 60 ft. The elevation difference between the free surfaces of the tanks is 15 ft. Determine the volumetric flow rate (gpm) between the two tanks.
- 4.25 Figure P4.25 shows a pump and pipe network being used to transport heptane at 120°F to a large, elevated, closed storage tank. The tank is pressurized and maintained at 18 psia. The volumetric flow rate of the heptane is 500 gpm.
- Specify the nominal diameter of the check valve.
 - Determine the pump discharge pressure required (psia) to move the heptane through the discharge pipe.

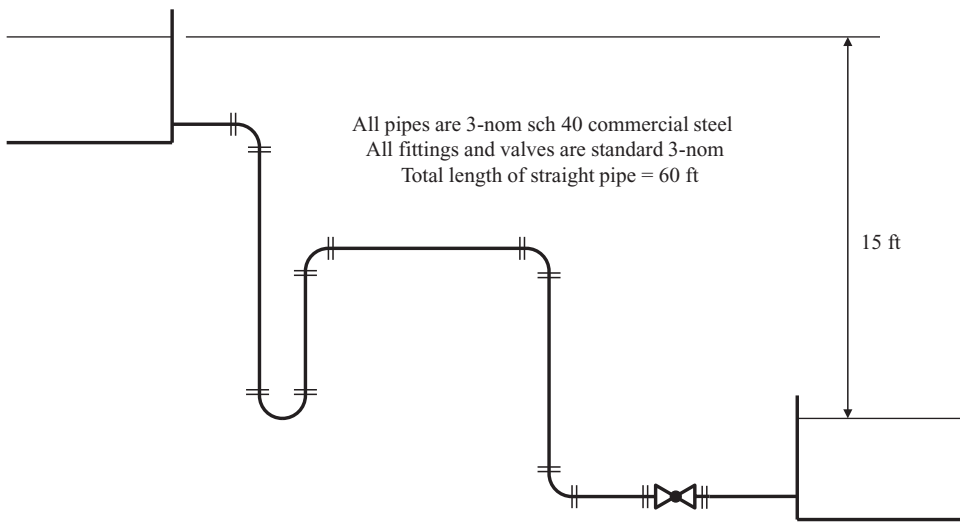


FIGURE P4.24
Two-tank gravity feed system.

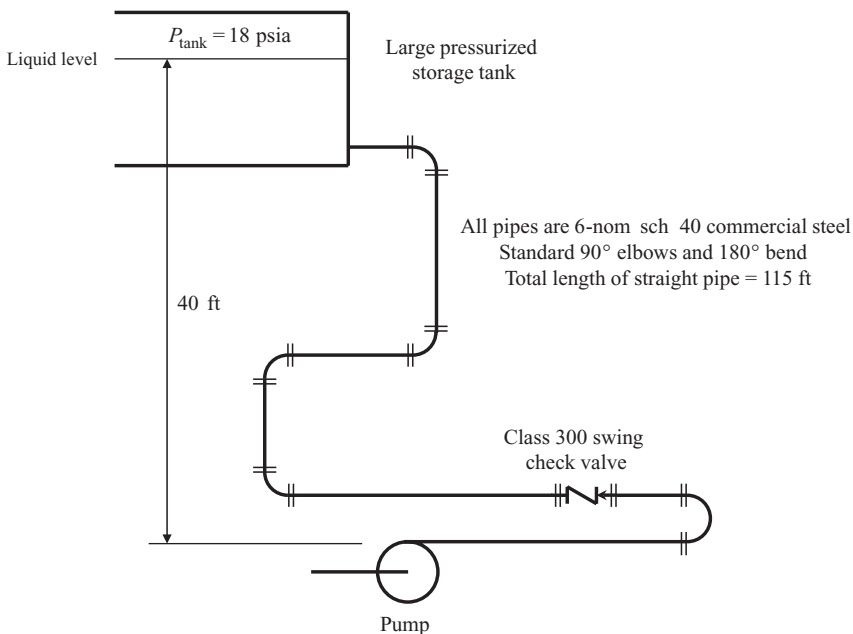
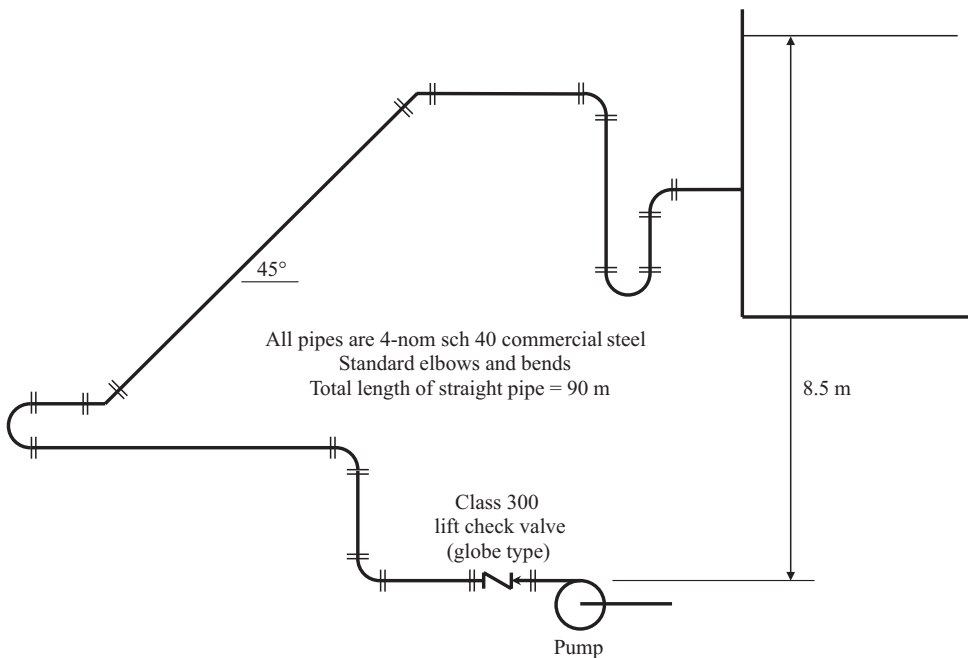


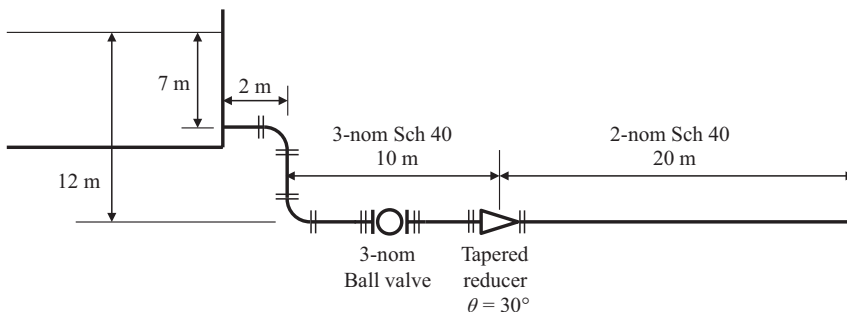
FIGURE P4.25
Pressurized storage tank system.

- c. Investigate the effect of the absolute roughness of the pipe. Construct a plot that shows the variation in pressure drop as a function of the absolute roughness for values ranging from 0 to 0.01 ft.
- 4.26 Water at 80°C is being pumped to a large reservoir 8.5 m above the discharge of the pump. The pipe network transporting the water is shown in Figure P4.26. The volumetric flow rate of the water is 10 L/s.

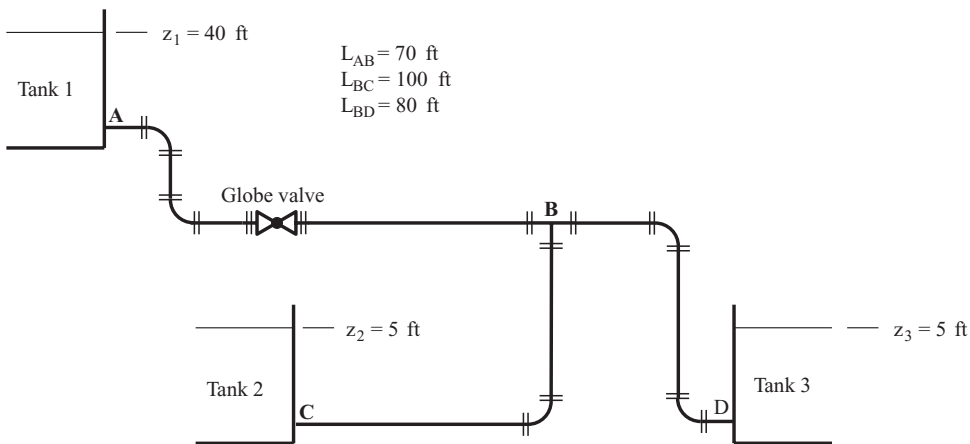
**FIGURE P4.26**

Pump and pipe network transporting water to a large reservoir.

- Specify the nominal diameter of the check valve.
 - Determine the pump head required to move the water through the system at the given flow rate (m).
- 4.27. A 15% calcium chloride solution at -5°C is being delivered from a large refrigerated storage tank with the gravity-feed pipe network shown in Figure P4.27. A 30° tapered reducer is used to reduce the pipe size from 3-nom sch 40 to 2-nom sch 40 as shown in the figure. All pipes are commercial steel and the elbows are standard. Determine,
- The volumetric flow rate of calcium chloride solution delivered by this system (L/s)
 - The velocity of the calcium chloride solution in each of the pipes (m/s)

**FIGURE P4.27**

Pipe system for transporting a calcium chloride solution.

**FIGURE P4.28**

Three tank gravity-feed system.

4.28. A large elevated tank (Tank 1) is being used to supply water at 60°F to two tanks at a lower elevation (Tanks 2 and 3) as shown in Figure P4.28. All pipes are 5-nom sch 40 commercial steel. The straight lengths of the piping in Sections AB, BC, and BD are indicated in the figure. The elevation of the free surface of the water in each tank is also indicated in the figure.

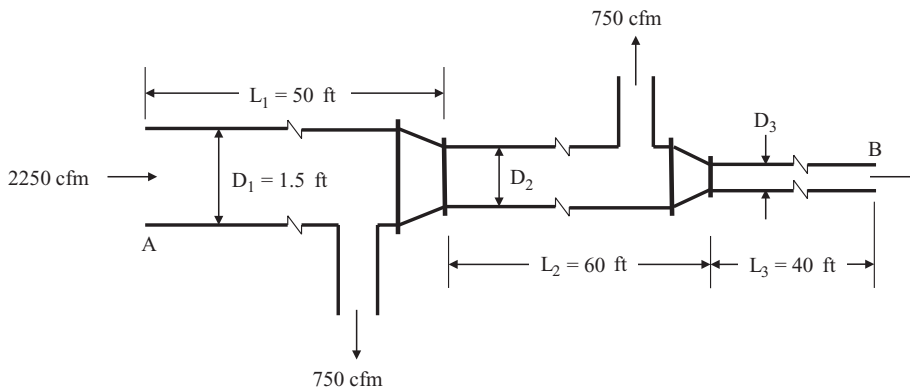
- Determine the volumetric flow rate (gpm) delivered to each lower tank (Tanks 2 and 3) for the conditions shown.
- The globe valve in this system is used for flow control. Determine the effect of partially closing the globe valve by constructing two plots; (1) the total volumetric flow from Tank 1, and (2) the volumetric flow delivered to each of the lower tanks (Tanks 2 and 3). Show each of these volume flows as a function of the globe valve constant, C , in the resistance coefficient equation,

$$K_{globe} = CK_{3K}$$

where K_{3K} is the K-value for a wide opened globe valve calculated using the 3K method and C varies between 1 (wide opened) and 100 (partially closed).

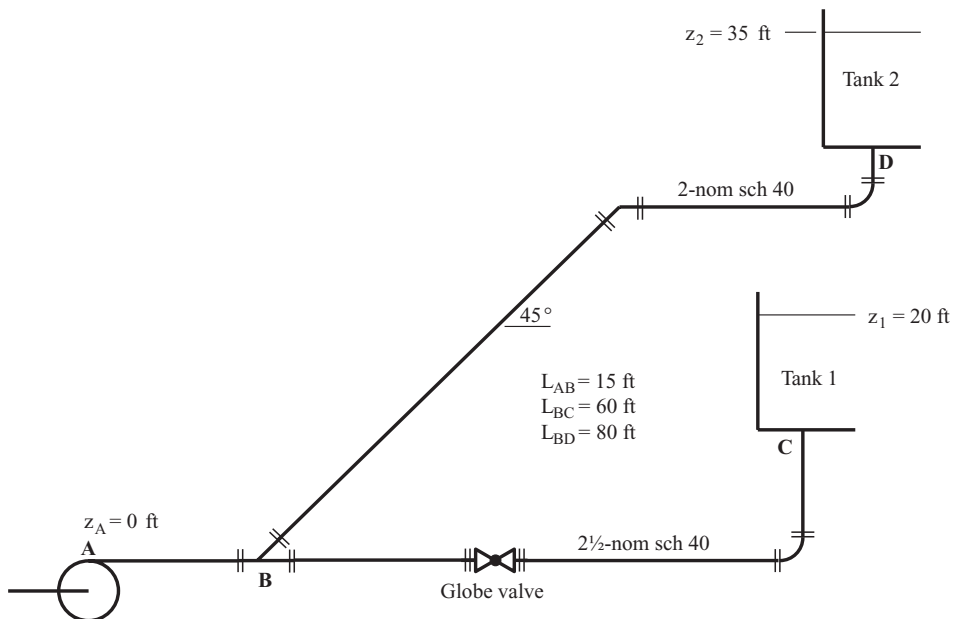
4.29. In order to properly size the fan required for a heating and air conditioning system, the pressure drop in the system must be determined. Consider the air distribution system shown in Figure P4.29. Dry air at 65°F, 1 atm enters the main duct of the system at 2250 cfm. There are two take-offs in the main duct where 750 cfm of air are used for individual room air conditioning. The remaining air travels down the main duct and is eventually distributed to a third room. All ducts are circular and the duct diameters are sized such that the velocity in each section of the main distribution duct is the same. The fittings that provide the required diameter reduction are 30° tapered reducers. The absolute roughness of a galvanized steel duct is 0.0005 ft. For this air distribution system, determine,

- The diameters of the second and third sections of the main duct (D_2 and D_3)
- The total pressure drop in the main duct from A to B, expressed in inches of water (in H_2O)

**FIGURE P4.29**

An air distribution system.

- 4.30 A pump is being used to deliver water at 70°F to two large, elevated tanks as shown in Figure P4.30. The pump is delivering a volumetric flow rate of 275 gpm. The pipes from A to B and B to C are 2½-nom sch 40 galvanized iron. The pipe from B to D is 2-nom sch 40 galvanized iron. The straight lengths of the piping in Sections AB, BC, and BD are indicated in the figure. The elevation of the free surface of the water in each tank is also indicated in the figure. Pumps draw water from the tanks which keep the water level constant in each tank. Determine the pressure required at the pump discharge (psig) and the volumetric flow rate (gpm) delivered to each tank.

**FIGURE P4.30**

Pipe system for distribution of water to two elevated tanks.

Economic Pipe Diameter

- 4.31 A commercial steel pipe is being designed to transport liquid benzene at 185°F to a heat exchanger at a flow rate of 850 gpm. The fittings, valves, supports, and pump are estimated to cost 6 times the installed pipe cost per ft. Annual maintenance is estimated to be 1.5% of the installed pipe and hardware initial costs per ft. For this service, the ASME pipe classification is determined to be 400 and a sch-80 pipe is required. The pump in the system runs 18 hours per day, 260 days per year. The efficiency of the pump is estimated to be 62%. The cost of electrical energy to run the pump is \$0.11/kWh. The pipeline is expected to have a 45-year life. An engineering economic analysis reveals that the rate of return due to the investment in the pipeline is 16%. Use an estimated escalation rate of 2% to account for yearly inflation.
- Determine the economic diameter and specify the standard pipe size that results in the minimum system cost if the design work was done for an installation that occurred in 2014.
 - Determine the economic velocity of the fluid (ft/s).
 - Construct the cost curves for this scenario assuming that the friction factor can be assumed constant at the value computed for the economic diameter from part (a). Your plot should look similar to Figure 4.8.
- 4.32 A commercial steel class 300 schedule 40 pipe is being used to transport 1000 gpm of liquid cyclohexane at 70°F. The fittings, valves, supports, and pump are estimated to cost 6.9 times the amortized installed pipe cost per ft. Annual maintenance is estimated to be 2% of the amortized installed pipe costs per ft. The pump in the system runs 12 hours per day, 260 days per year. The efficiency of the pump is estimated to be 68%. The cost of energy is \$0.09/kW-h. The pipeline is expected to have a 50-year life and a rate of return of 20%. Use an inflation rate of 1.5% to adjust the value of C_1 from Table 4.17 to 2012 dollars.
- Determine the economic diameter and specify the standard pipe size that results in the minimum system cost.
 - Determine the economic velocity of the fluid (ft/s).
 - Construct the cost curves for this scenario assuming that the friction factor can be assumed constant at the value computed for the economic diameter from part (a). Your plot should look similar to Figure 4.8.
- 4.33. A Bell & Gossett Series e-1531 model 5BD pump operating at 1770 rpm is being used to deliver 250 m³/h of a 10% methanol solution at 5°C through a pipe network. The impeller diameter is 8.5 inches. The pipe is class 300 sch 40 commercial steel. The pump and other fittings, valves and hardware for the pipe network cost 6.5 times the amortized pipe cost per ft. The pump runs 16 hr/day for 200 days each year. Annual maintenance is estimated to be 2% of the amortized installed pipe costs per ft. The cost of energy is \$0.12/kW-h. The pipeline is expected to have a 35-year life and a rate of return of 16%. Inflation costs are estimated to be 2.5%. The system was installed in 2017. Determine:
- The economic diameter (m)
 - The economic velocity of the fluid (m/s)
 - Specify a pipe that best suits this application (specify nominal diameter).

- 4.34 A production facility has a fluid transport system for liquid dimethyl carbonate. The pipeline transporting the dimethyl carbonate is made of class 400 sch 80 commercial steel. The properties of liquid dimethyl carbonate at 60°F are: $\rho = 67.152 \text{ lbm/ft}^3$, $\mu = 0.00043565 \text{ lbm/ft-s}$. Using the economic and system parameters given in Section 4.6.4, calculate the corresponding economic velocity range for dimethyl carbonate.

Dynamic Pump Performance

- 4.35 A centrifugal pump is being used to deliver 250 gpm of water at 60°F. The pump head is determined to be 25 ft and its efficiency is 70%. Determine the brake horsepower input to the pump and the hydraulic horsepower input to the water.
- 4.36 A centrifugal pump delivers 60 L/s of toluene at 40°C. The pump head is found to be 15 m and its efficiency is 48%. Determine the shaft power input to the pump (kW) and the power input to the toluene (kW).
- 4.37 A centrifugal pump is being used to transport 440 gpm of benzene at 80°F. The suction pipe inlet to the pump is 6-nom sch 40 and the pump discharge pipe is 5-nom sch 40. Pressure gauges on the suction and discharge ports of the pump indicate -4 psig and 55 psig, respectively. The elevation difference between the suction and discharge ports of the pump is 0.2 ft. At this condition, the pump has an efficiency of 60%. Determine the following,
- The head produced by this pump (ft)
 - The percentage of the total pump head that is used to increase the fluid's (i) pressure, (ii) velocity, and (iii) elevation
 - The power input required by the electric motor that drives this pump (kW)
 - The annual cost required to operate this pump if it runs for 16 hr/day for a total of 240 days and the cost of electrical energy is \$0.11/kWh
- 4.38 A centrifugal pump is being used to transport 45 m³/h of a 20% ethylene glycol solution at 0°C. The suction pipe inlet to the pump is 2½-nom sch 40 and the pump discharge pipe is 2-nom sch 40. Pressure gauges on the suction and discharge ports of the pump indicate -15 kPa and 250 kPa, respectively. The elevation difference between the suction and discharge ports of the pump is 0.08 m. At this condition, the pump has an efficiency of 68%. Determine the following:
- The head produced by this pump (m)
 - The percentage of the total pump head that is used to increase the fluid's (i) pressure, (ii) velocity, and (iii) elevation
 - The power input required by the electric motor that drives this pump (kW)
 - The annual cost required to operate this pump if it runs for 8 hr/day for a total of 260 days and the cost of electrical energy is \$0.12/kWh
- 4.39 Two pumps are being considered for a pipe system. Table P4.39 shows the economic and operating parameters of each pump. The fluid being transported in the system is a 30% propylene glycol solution. The propylene glycol is flowing at 300 gpm with an average temperature of 40°F. At this condition, the head required from the pump is 37 ft. The system operates continuously all year long with an estimated 10% downtime for maintenance and repair. The cost of electricity is \$0.11/kWh. The system is expected to last for 30 years and provide a rate of return of 18%. Determine which pump provides the best economic advantage for this application.

TABLE P4.39

Economic and Operating Parameters for Pumps A and B

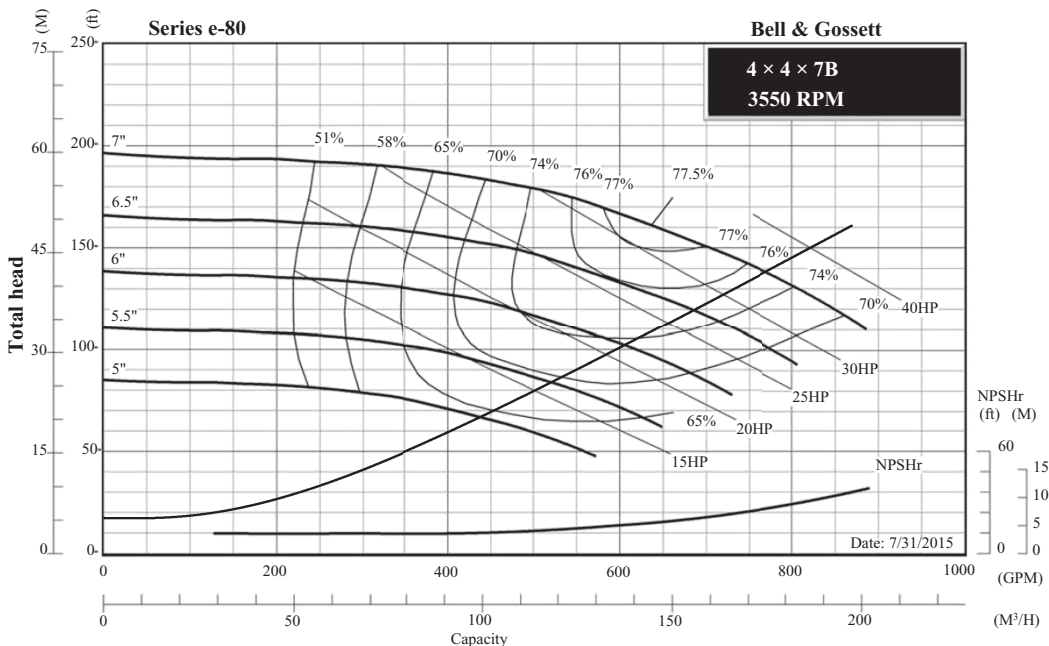
Pump	Initial Cost (\$)	Efficiency
A	\$4,700	0.66
B	\$5,500	0.71

4.40 A closed-loop pipe system similar to Figure 4.16 is being designed. At 280 gpm, the system curve indicates that the pump must deliver 120 ft. A 2.5x2.5x7B Bell & Gossett Series e-80 pump operating at 3550 rpm is to be specified for this application.

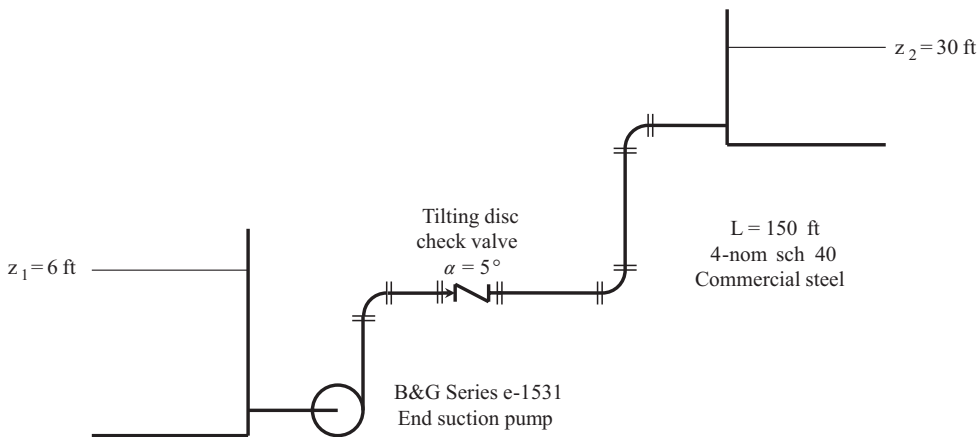
- Specify the impeller diameter for this application
- Specify the capacity (gpm), head (ft), brake horsepower input to the pump (hp), and efficiency of the pump you specified in part (a) when it is installed in the system.

4.41 Figure P4.41 shows a system curve overlaid on a set of Bell & Gossett Series e-1531 Model 4x4x7B at 3550 rpm pump curves. The flow requirement for the system is 150 m³/h.

- Specify the pump's impeller diameter for this application
For the impeller size specified in part (a), determine:
- The capacity (m³/h) and head (m) of the pump/pipe system?
- The power input to the pump (kW)
- The hydraulic power input to the fluid (kW)

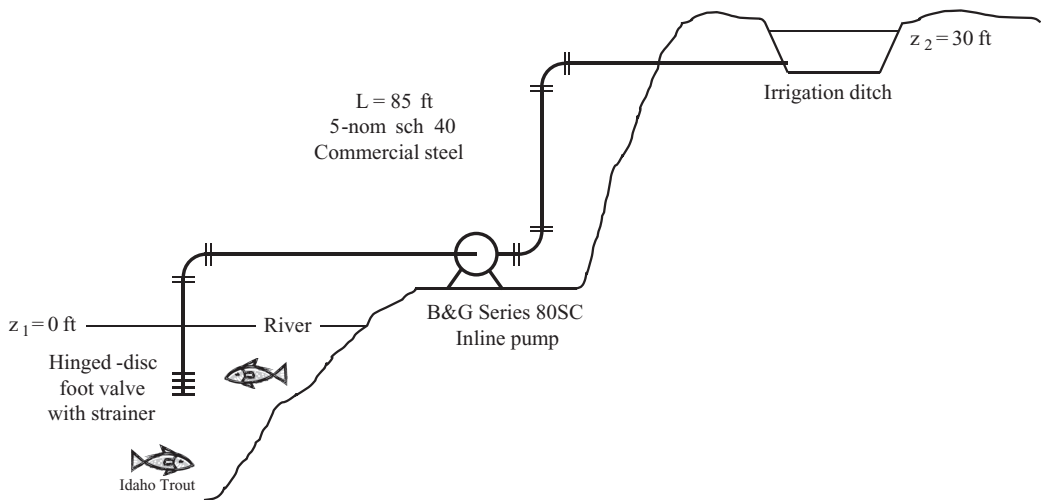
**FIGURE P4.41**

System curve overlaid on pump performance curves.

**FIGURE P4.42**

Two tank pump and pipe system.

- 4.42 A Bell & Gossett Series e-1531 end-suction pump is to be selected for the system shown in Figure P4.42. The system is designed to move water at 60°F from the lower tank to the upper tank. The system must deliver a minimum of 500 gpm of water from the lower tank to the upper tank when the pump is operating. A tilting disc check valve ($\alpha = 5^\circ$) is used to prevent the water from flowing backward when the pump is shut off. The total length of straight pipe in this system is 150 ft. The pipe is 4-nom sch 40 commercial steel.
- Plot the system curve up to 800 gpm.
 - Select a Series e-1531 Bell & Gossett pump for this system.
 - What is the operating point of the pump/pipe system based on the pump you selected in (b)? Specify the capacity (gpm), head (ft), brake horsepower input to the pump (hp), and efficiency of the pump.
- 4.43 Water from a river is to be pumped to an irrigation ditch as shown in Figure P4.43. The water temperature is 55°F . The irrigation requirement is 400 gpm. The elevation difference between the river and the surface of the water in the irrigation ditch is 30 ft. A hinged-disc foot valve with a strainer serves two functions; (1) it filters the water entering the suction pipe and, (2) it acts like a check valve when the pump is shut down. The pipeline contains 85 ft of 5-nom sch 40 commercial steel pipe. Model the foot valve as a swing check valve.
- Plot the system curve up to 600 gpm.
 - Select a Series e-80 Bell & Gossett inline pump for this system.
 - What is the operating point of the pump/pipe system based on the pump you selected in (b)? Specify the capacity (gpm), head (ft), brake horsepower input to the pump (hp), and efficiency of the pump.
- 4.44. A closed-loop pump/pipe system has a head requirement of 35 m at a flow rate of $60\text{ m}^3/\text{h}$. The pump is a Bell & Gossett Series e-1531 Model 2AD operating at 3550 rpm with a 6-inch impeller.
- Develop an equation for the system curve.

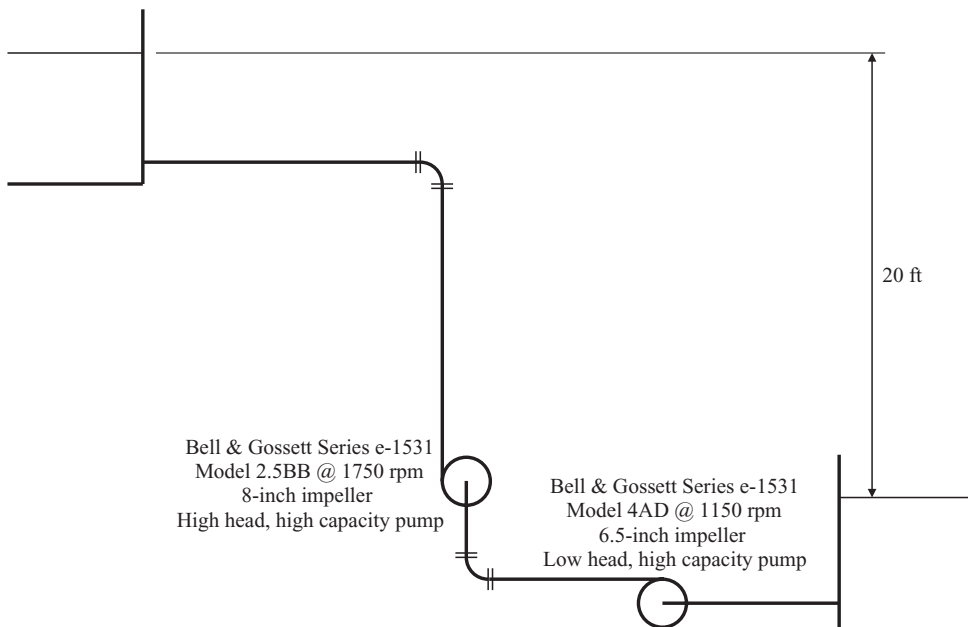
**FIGURE P4.43**

A pump/pipe irrigation system.

- b. Use a computer program to develop an equation for the 6-inch impeller using data read from the pump performance curve.
 - c. Determine the capacity (m^3/h) and head (m) of the pump/pipe system by simultaneously solving the pump curve and system equations.
 - d. Use the pump performance curve to determine the power draw (kW) and efficiency of the pump.
- 4.45 A two-tank pump/pipe system has a head requirement of 23.4 ft at a flow rate of 100 gpm. The elevation difference between the fluid surfaces in the tanks is 10 ft. The pump is a Bell & Gossett Series e-80 Model 2.5x2.5x9C operating at 1170 rpm with a 7.5-inch impeller.
- a. Develop an equation for the system curve.
 - b. Use a computer program to develop an equation for the 7.5-inch impeller using data read from the pump performance curve.
 - c. Determine the capacity (gpm) and head (ft) of the pump/pipe system by simultaneously solving the pump curve and system equations.
 - d. Use the pump performance curve to determine the power draw (hp) and efficiency of the pump.

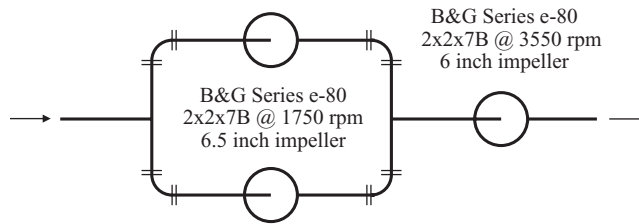
Series and Parallel Pump Configurations

- 4.46 Two Bell & Gossett Series e-80 3x3x7C pumps with 6.5-inch impellers are connected together in parallel. Both pumps are operating at 3550 rpm. This parallel pump combination is connected to a pipe system that has an elevation difference (outlet to inlet) of 40 ft. At a flow rate of 500 gpm, the head in the system is known to be 120 ft.
- a. Plot a pump performance curve that shows the performance of the individual pumps and the performance of both pumps operating in parallel.
 - b. Overlay the system curve on the plot you developed for part (a) and determine the operating point of this parallel pump/pipe system (head and capacity).

**FIGURE P4.47**

Series pump system used to transport a fluid to a large storage tank.

- c. What is the operating point of each individual pump (head and capacity) when they are both operating in parallel? What is the efficiency and power draw of each pump under this condition?
 - d. If one of the pumps fails, determine the operating point (head and capacity) along with the efficiency and power draw of the remaining operational pump.
- 4.47 Two pumps are used in series to move a fluid to an elevated storage tank as shown in Figure P4.47. The first pump is a Bell & Gossett Series e-1531 low head, high capacity pump (Model 4AD with a 6.5-inch impeller operating at 1150 rpm). The second pump is a Bell & Gossett Series e-1531 high head, high capacity pump (Model 2.5BB with an 8-inch impeller operating at 1750 rpm). At a flow of 240 gpm, the system head is 45 ft.
- a. Construct a plot showing the individual pump performance curves and the series pump configuration performance (head vs. capacity).
 - b. Overlay the system curve on the plot developed in part (a) and determine the operating point (capacity and head) of the series pump system.
 - c. If the Model 4AD pump fails, determine the operating point with the remaining 2.5BB pump (head, capacity, power draw, and efficiency).
 - d. If the Model 2.5BB pump fails, determine the operating point with the remaining 2.5BB pump (head, capacity, power draw, and efficiency).
- 4.48 Two Bell & Gossett Series e-1531 Model 6BD pumps are connected in parallel. One pump has a 9-inch impeller and the other pump has a 9.5-inch impeller. When both pumps are running in a system, the fluid flow rate is 3600 gpm.
- a. Construct a plot showing the individual pump performance curves and the series pump configuration performance (head vs. capacity).

**FIGURE P4.49**

Three pump parallel/series configuration.

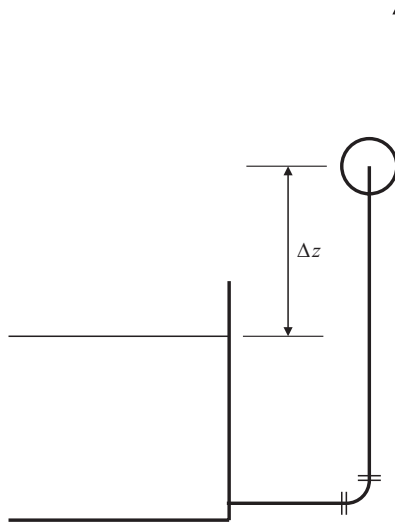
- b. Determine the operating point (capacity, head, power draw, and efficiency) of each pump in this parallel configuration.
- 4.49 Two Bell & Gossett Series e-80 2x2x7B pumps operating at 1750 rpm with 6.5-inch impellers are connected in parallel. A third pump, a Bell & Gossett Series e-80 2x2x7B pump operating at 3500 rpm with a 6-inch impeller is connected in series with the parallel pumps as shown in Figure P4.49. This composite pump combination is connected to a pipe system. For this pipe system, at a flow rate of 160 gpm, the head required is 140 ft. There is a 10 ft elevation difference from inlet to outlet.
- a. Construct a plot showing the individual parallel pump performance curves, the combined parallel pump curve, the individual series pump performance curve, and the composite pump performance curve.
 - b. Overlay the system curve on the plot developed in part (a) and determine the operating point (capacity and head) of the composite pump and pipe system.

Cavitation and the Net Positive Suction Head

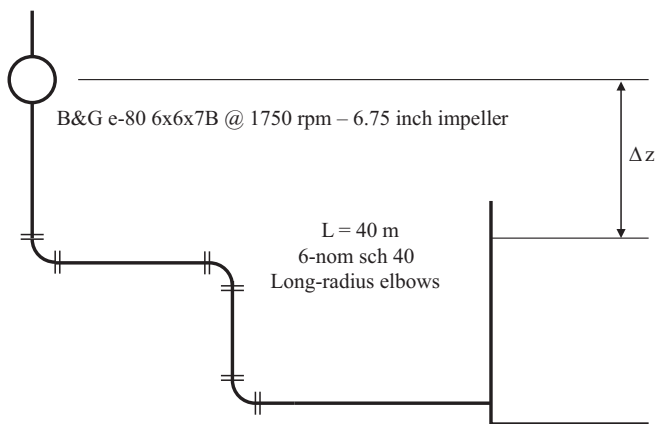
- 4.50 Water is being pumped through a pipe system at a temperature of 60°C. Determine the maximum absolute pressure at the eye of the pump's impeller that would cause cavitation.
- 4.51 The pressure at the eye of the impeller of a pump moving water at 120°F is 2 psia. Will cavitation occur in this pump?
- 4.52 A pressure gauge attached to the suction port of a centrifugal pump indicates a pressure of -8 psig. The pump is being used to transport water at 70°F. Atmospheric pressure is 14.696 psia. Will cavitation occur in this pump?
- 4.53 The pressure at the suction port of a pump transporting water at 30°C is 4.3 kPa (absolute). Will cavitation occur in this pump?
- 4.54 A Bell & Gossett Series e-80 5x5x7B centrifugal pump operating at 1770 rpm is fitted with a 6.5-inch impeller. The pump is being used to deliver water from a large tank as shown in Figure P4.54. The head at the operating point of the pump/pipe system is 30 ft. A suction-side pipe analysis reveals that the NPSHa can be calculated by,

$$\text{NPSHa} = 25.6 \text{ ft} - \Delta z$$

Determine the maximum value of Δz where cavitation will not occur.

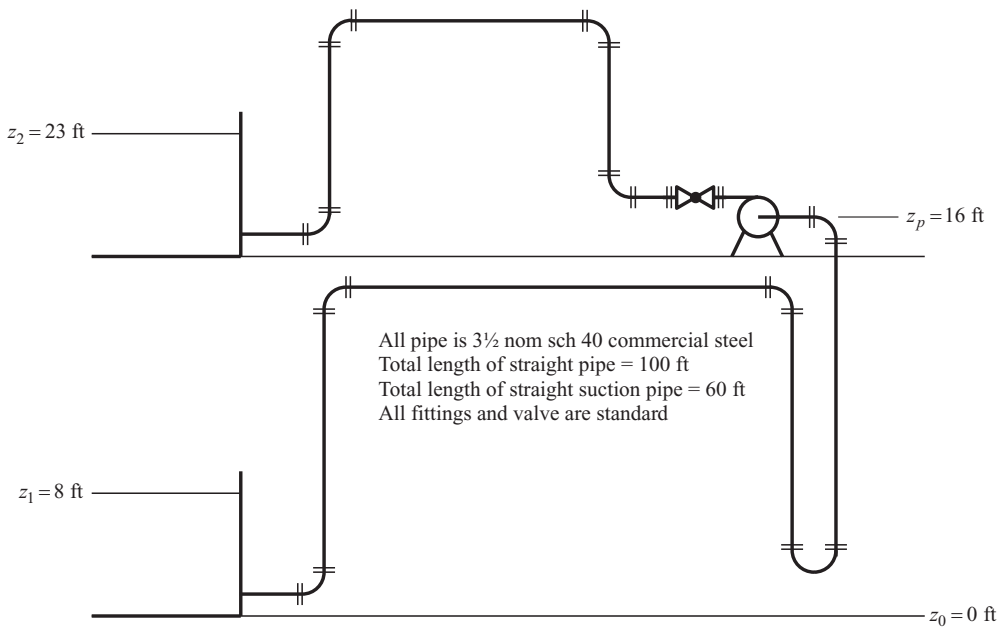
**FIGURE P4.54**

Suction side of a pump/pipe system used to deliver water from a storage tank.

**FIGURE P4.55**

Suction side of a pump/pipe system for transporting water.

- 4.55 A Bell & Gossett Series e-80 6x6x7B pump operating at 1750 rpm with a 6.75-inch impeller is being used to transport water from a large tank as shown in Figure P4.55. The water is at a temperature of 20°C and is being delivered at a rate of 160 m³/h. The suction line is 6-nom sch 40 commercial steel pipe that is 40 m long. Atmospheric pressure is 1 bar.
- Determine the maximum height above the water surface that the pump can be installed to prevent cavitation (m).
 - Investigate the effect of the water temperature by plotting the maximum height as a function of the water temperature for 10°C < T < 80°C.
- 4.56 Water is being transferred from a large tank on the ground floor to the second floor of an industrial processing facility as shown in Figure P4.56. A Bell & Gossett Series e-1531 Model 3BD pump operating at 1770 rpm with an 8-inch impeller has

**FIGURE P4.56**

A pump/pipe system used to transport water to the second floor of an industrial facility.

been selected for the system. The pipe is $3\frac{1}{2}$ nom sch 40 commercial steel. The total length of straight pipe in the system is 100 ft. The length of the suction line is 60 ft. Several elevations are indicated in Figure P4.56. Atmospheric pressure is 14.3 psia.

- Determine the pump/pipe system operating point (head, capacity, pump power draw, and pump efficiency)
- Due to maintenance and access issues, the proposed location for the pump is on the second floor of the building as shown in Figure P4.56. Should the pump be installed at this location?

Affinity Laws

- A centrifugal pump is tested in the laboratory. The pump has a 6-inch impeller and is operating at 3550 rpm. With water as the fluid, test results indicate that the pump delivers 280 gpm at 110 ft of head. Using the affinity laws, predict what the pump capacity and head would be if the rotational speed was reduced to 1770 rpm.
- A centrifugal pump is being tested with water at 60°F . The pump is operating at 1150 rpm and has a 7-inch impeller. Performance test results indicate that the pump delivers 80 gpm at a head of 32 ft with a power draw of 2.75 hp. Using the affinity laws, predict what the pump capacity, head, and power draw would be if the operational speed was increased to 1770 rpm and the fluid is,
 - Water at 140°F
 - Toluene at 140°F
 - Ethanol at 140°F

- 4.59 A point on the performance curve of a pump indicates that at an operational speed of 1150 rpm, a pump with a 6.5-inch impeller is capable of delivering 100 m³/h at 3.75 m of head. Use the affinity laws to predict what the pump capacity and head would be if the impeller speed remains the same, but the diameter is changed to 6 inches.
- 4.60 A centrifugal pump is capable of delivering 50 L/s of fluid at a head of 18 m while operating at 3550 rpm with a 7-inch impeller. At this condition, the pump power draw is 12 kW and the pump efficiency is 68%. Use the affinity laws to predict the pump capacity, head, power draw, and efficiency if the impeller is changed to a diameter of 9-inches and the operational speed is adjusted to 1150 rpm.
- 4.61 Table P4.61 shows performance data read from one of the Bell & Gossett pump curves in Appendix E.
- For each data point in Table P4.61, use the affinity laws to determine the new capacity and head of this pump if the operational speed is reduced to 1750 rpm using a variable speed motor.
 - In the Bell & Gossett Series e-1531 booklet, there is a set of performance curves for a Model 1.5BC pump operating at 1750 rpm. At each of the capacity values calculated from the affinity laws, determine the corresponding head from the 1.5BC 1750 rpm performance curve.
 - For each capacity value at 1750 rpm, you now have two head values; one calculated with the affinity laws and one read directly from the 1.5BC 1750 rpm pump performance curve. Compare these two head values by calculating the percent difference between the calculated value and the actual value using the following equation,

$$\%(\Delta H_p) = 100 \left(\frac{H_{p,actual} - H_{p,calc}}{H_{p,actual}} \right)$$

- Based on the results, comment on the validity of the affinity laws for this application.
- 4.62 A Bell & Gossett Series e-80 4x4x13.5 pump has a 12.5-inch impeller and is operating at 1750 rpm. The pump is installed in a closed-loop pipe system. An analysis of the pump/pipe system at 400 gpm indicates a required pump head of 75 ft.
- Determine the operating point of the pump/pipe system under these conditions.

TABLE P4.61

Performance Data for a Bell & Gossett
Series e-1531 Model 1.5BC Pump with an
8.5-inch Impeller Operating at 3525 rpm

Capacity (gpm)	Head (ft)
50.2	336
100	334
150	324
200	306
250	277

After several years of service, engineers have decided to refit the pump with a 12-inch impeller. The engineers also decide to install a variable speed drive for the pump. The new impeller is installed and the operating speed is reduced to 1480 rpm.

- b. Use the affinity laws to determine the new pump capacity and head for the operating point determined in part (a).
- c. Determine the operating point of the pump/pipe system under the new operating conditions (capacity and head).
- d. Explain why the points determined in parts (b) and (c) do not match.



Taylor & Francis

Taylor & Francis Group

<http://taylorandfrancis.com>

5

Energy Transport in Thermal Energy Systems

5.1 Introduction

Chapter 4 dealt with fluid transport in thermal energy systems. As a fluid moves through a pipe system, it is capable of transporting energy as a consequence of its thermodynamic state. In many thermal energy systems, fluids are used to transfer energy between different fluid streams. For example, in an air-conditioning system, a cold fluid circulating through tubes can be used to cool warm air passing over the outside of the tubes. The energy transfer accomplished in this process is *heat transfer*. The heat transfer is accomplished by *conduction* through a metal barrier separating the two fluids (e.g., a pipe or tube), and *convection* between the moving fluids and the metal interface. The device that accomplishes this heat transfer is a *heat exchanger*. Before embarking on a detailed discussion of heat exchangers, a brief review of heat conduction and convection, relative to heat exchangers, is presented.

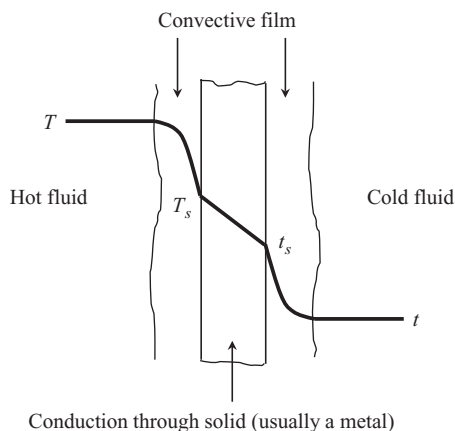
5.2 Heat Transfer Analysis of Heat Exchangers

The purpose of a heat exchanger is to transfer energy in the form of heat between two fluids. In a typical heat exchanger, this occurs by a combination of conduction and convection. Figure 5.1 shows the temperature profile between a hot fluid and a cold fluid in a heat exchanger. In Chapter 5, an uppercase T indicates the hot fluid temperature and a lowercase t is used for the cold fluid's temperature. The temperatures T and t represent the bulk (or average) temperature of the hot and cold fluids, respectively.

Through the convective film, the temperature changes in a nonlinear fashion and the heat transfer rate is governed by *Newton's law of cooling*. For the hot side of the heat exchanger shown in Figure 5.1, Newton's law of cooling is written as,

$$\dot{Q} = h_i A_i (T - T_s) \quad (5.1)$$

In this equation, A_i is the cross-sectional area through which the heat is being transferred, T_s is the surface temperature of the hot side of the solid material separating the hot and cold fluids, and h_i is the *convective heat transfer coefficient*. This is an unfortunate nomenclature conflict when h is used to represent enthalpy. However, this is common nomenclature in heat transfer analyses and will be used throughout this chapter.

**FIGURE 5.1**

Temperature profile between hot and cold fluids in a heat exchanger.

The convective heat transfer coefficient has units of $\text{W/m}^2\text{-K}$ or $\text{Btu/hr-ft}^2\text{-}^\circ\text{F}$. Its value is meant to help quantify the resistance to heat flow through the convective film. Most heat exchangers utilize *forced convection* to transfer the heat between the fluids. Typical convective heat transfer coefficients for forced liquid flow are typically between $100\text{--}20,000 \text{ W/m}^2\text{-K}$ ($18\text{--}3,500 \text{ Btu/hr-ft}^2\text{-}^\circ\text{F}$). Heat exchangers where one or both of the fluids are undergoing a phase change can experience much higher convective heat transfer coefficients; upwards of $100,000 \text{ W/m}^2\text{-K}$ ($18,000 \text{ Btu/hr-ft}^2\text{-}^\circ\text{F}$). Heat exchangers that take advantage of the high heat transfer coefficients offered by a phase change are commonly known as *boilers, evaporators, or condensers*.

The *heat flux* is determined by dividing both sides of Equation 5.1 by the area through which the heat is flowing. For example, the heat flux passing through the hot-side convective film is given by,

$$q_h'' = \frac{\dot{Q}}{A_h} = h_h(T - T_s) \quad (5.2)$$

If the heat transfer rate is occurring in a steady state, it is the same through all layers shown in Figure 5.1. Therefore, the convective heat transfer rate on the cold-fluid side is given by,

$$\dot{Q} = h_c A_c (t_s - t) \quad (5.3)$$

In this equation, A_c is the cross sectional area through which the heat is being transferred, t_s is the surface temperature of the cold side of the solid separating the two fluids, and h_c is the cold-side convective heat transfer coefficient. The heat flux through the cold-side convective film is,

$$q_c'' = \frac{\dot{Q}}{A_c} = h_c(t_s - t) \quad (5.4)$$

If the areas A_h and A_c are equal, the heat flux through the hot and cold convective films are also equal for a steady state heat transfer rate.

The heat transfer by conduction through the material separating the hot and cold fluids is governed by *Fourier's law*. For steady-state conduction through a planar surface, Fourier's law is written as,

$$\dot{Q} = kA \frac{(T_s - t_s)}{\Delta x} \quad (5.5)$$

In this equation, T_s is the temperature of the hot surface, t_s is the temperature of the cold surface, Δx is the thickness of the material, and k is the *thermal conductivity* of the material. Selected values of thermal conductivity can be found in Appendix B.8. If the material is cylindrical rather than planar (e.g., a tube or pipe), then Fourier's law is written in cylindrical coordinates as,

$$\dot{Q} = \frac{2\pi Lk(T_s - t_s)}{\ln(OD/ID)} \quad (5.6)$$

In Equation 5.6, ID and OD are the inside and outside diameters of the tube or pipe, respectively, and L is the length of the tube. Often times in conduction calculations involving tubes or pipes, the heat transfer rate per unit length is of interest. This can be determined by dividing Equation 5.6 by the tube length, L ,

$$q' = \frac{\dot{Q}}{L} = \frac{2\pi k(T_s - t_s)}{\ln(OD/ID)} \quad (5.7)$$

5.2.1 Thermal Resistance

The heat transfer rate can be thought of as being analogous to electrical current flow as shown in Figure 5.2. As indicated in the figure, the temperature difference driving the heat

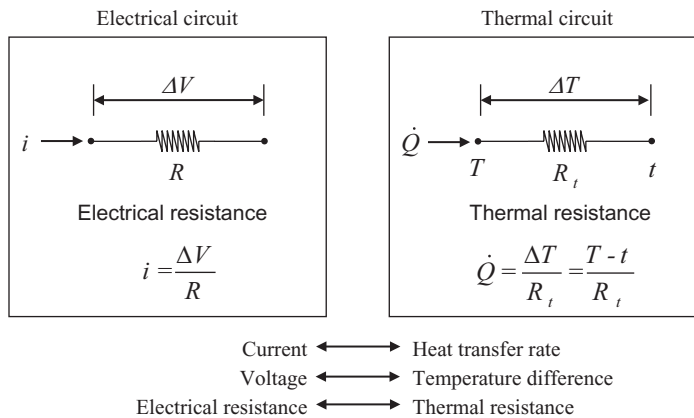


FIGURE 5.2

Heat transfer analogy to electrical current flow.

transfer is analogous to the voltage drop driving the electrical current, and the thermal resistance is analogous to the electrical resistance. The thermal resistance can be determined by algebraically rearranging the heat transfer rate equations to the form shown in the figure. For example, rearranging Newton's law of cooling to the form shown in Figure 5.2 for the thermal circuit results in,

$$\dot{Q} = hA(T - t) = \frac{T - t}{1/(hA)} \quad (5.8)$$

Therefore, the thermal resistance due to convection is,

$$R_{t,conv} = \frac{1}{hA} \quad (5.9)$$

Notice that the thermal resistance has units of K/W in the SI unit system and h-°F/Btu in the English unit system.

Table 5.1 shows a summary of the thermal resistance expressions for convection and conduction pertinent to heat exchangers. For certain geometries, it may be convenient to weight the resistance by either an area or a length as shown in Table 5.1. The double prime indicates an area-weighted resistance, whereas a single prime indicates a length-weighted resistance.

Thermal resistances are treated just like electrical resistances. For several thermal resistances in *series*, the total thermal resistance is given by,

$$R_{t,series} = \sum_i R_{t,i} \quad (5.10)$$

For thermal resistances in *parallel*, the total thermal resistance can be determined from,

$$\frac{1}{R_{t,parallel}} = \sum_i \frac{1}{R_{t,i}} \quad (5.11)$$

TABLE 5.1

Thermal Resistance Expressions for Conduction and Convection

Scenario	Thermal Resistance Expressions	
Conduction through a plane wall	$R_t = \frac{\Delta x}{kA}$	$R_t'' = AR_t = \frac{\Delta x}{k}$
Conduction through a cylindrical wall	$R_t = \frac{\ln(OD/ID)}{2\pi kL}$	$R_t' = LR_t = \frac{\ln(OD/ID)}{2\pi k}$
Convection on a plane wall	$R_t = \frac{1}{hA}$	$R_t'' = AR_t = \frac{1}{h}$
Convection on a cylindrical wall	$R_t = \frac{1}{\pi DLh}$	$R_t' = LR_t = \frac{1}{\pi Dh}$

Using the thermal resistance, the heat transfer rate, heat transfer rate per unit length of tube, and heat flux can be written as,

$$\dot{Q} = \frac{T - t}{R_t} \quad q' = \frac{\dot{Q}}{L} = \frac{T - t}{R'_t} \quad q'' = \frac{\dot{Q}}{A} = \frac{T - t}{R''_t} \quad (5.12)$$

Example 5.1

A 10-nom sch 10S AISI 316 stainless steel pipe is transporting acetone at an average temperature of 160°C. The pipe is bare and surrounded by air at 20°C. The convective heat transfer coefficients inside and outside the pipe are 1,200 W/m²-K and 75 W/m²-K, respectively. Neglecting any radiation effects, determine the,

- Heat transfer rate per unit length of the pipe
- Heat transfer rate per unit length of the pipe if the pipe is sch 80S.

Solution

A cross-sectional sketch of the pipe is shown in Figure E5.1. The thermal circuit that describes the heat flow is shown on the left-hand side of the sketch. Since the problem asks for the heat transfer per unit length of pipe, it is convenient to use the length-weighted resistance shown in Table 5.1.

- The heat transfer rate per unit length of pipe is given by,

$$q' = \frac{T - t}{R'_t}$$

The three resistances to heat flow are in series. Therefore, the total length-weighted resistance is,

$$R'_t = R'_{tc} + R'_{tp} + R'_{th}$$

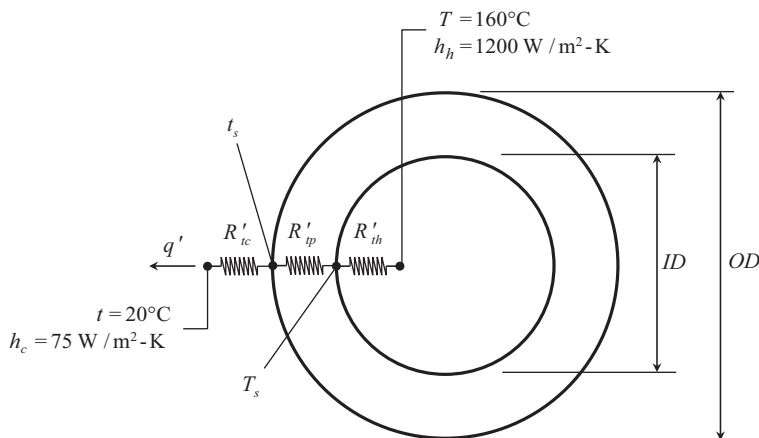


FIGURE E5.1
Pipe cross section.

Substituting the resistance expressions from Table 5.1,

$$R'_t = \frac{1}{\pi(ID)h_h} + \frac{\ln(OD/ID)}{2\pi k} + \frac{1}{\pi(OD)h_c}$$

For a 10-nom sch 10S pipe, the inside and outside diameters can be found in Appendix C,

$$OD = 0.27305 \text{ m} \quad ID = 0.26467 \text{ m}$$

The thermal conductivity is evaluated at the average pipe temperature. This temperature can be estimated by averaging the hot and cold fluid temperatures,

$$T_{avg} = \frac{T + t}{2} = \frac{(160 + 20)^\circ\text{C}}{2} = 90^\circ\text{C}$$

From Appendix B.8, the thermal conductivity of the pipe (AISI 316 stainless steel) at 90°C is,

$$k = 14.54 \text{ W/m-K}$$

In this example, each individual resistance will be calculated so a comparison can be made between the three values. The resistance of the inside convective film is,

$$R'_{th} = \frac{1}{\pi(ID)h_h} = \frac{1}{\pi(0.26467 \text{ m})\left(1200 \frac{\text{W}}{\text{m-K}}\right)} = 0.001002 \frac{\text{m-K}}{\text{W}}$$

The resistance due conduction through the pipe is,

$$R'_p = \frac{\ln(OD/ID)}{2\pi k} = \frac{\ln[(0.27305 \text{ m})/(0.26467 \text{ m})]}{2\pi\left(14.54 \frac{\text{W}}{\text{m-K}}\right)} = 0.0003413 \frac{\text{m-K}}{\text{W}}$$

The convective film resistance on the outside of the pipe is,

$$R'_{tc} = \frac{1}{\pi(OD)h_h} = \frac{1}{\pi(0.27305 \text{ m})\left(75 \frac{\text{W}}{\text{m-K}}\right)} = 0.01554 \frac{\text{m-K}}{\text{W}}$$

Summing these three resistances together gives the total length-weighted resistance for the pipe,

$$R'_t = (0.001002 + 0.0003413 + 0.01554) \frac{\text{m-K}}{\text{W}} = 0.01689 \frac{\text{m-K}}{\text{W}}$$

Now, the heat transfer rate per unit length of pipe can be found,

$$q' = \frac{T - t}{R'_t} = \frac{(160 - 20)\text{K}}{0.01689 \frac{\text{m-K}}{\text{W}}} = 8,290 \frac{\text{W}}{\text{m}} = \underline{\underline{8.29 \frac{\text{kW}}{\text{m}}}}$$

- b. Keeping all conditions the same, but moving to a 10-nom sch 80S pipe changes the inside diameter. Therefore, the inside convective film and the conduction resistances will change. The outside convective film resistance stays the same. For the 10-nom sch 80S pipe, the diameters are,

$$OD = 0.27305 \text{ m} \quad ID = 0.24765 \text{ m}$$

Performing similar calculations gives the heat transfer rate per unit length,

$$q' = \frac{T - t}{R'_t} = \frac{(160 - 20)\text{K}}{0.01768 \frac{\text{m-K}}{\text{W}}} = 7,917 \frac{\text{W}}{\text{m}} = \underline{\underline{7.917 \frac{\text{kW}}{\text{m}}}}$$

Table E5.1 summarizes the results of this calculation. This table shows several interesting things about this problem.

TABLE E5.1

Summary of Results

Schedule	OD(m)	ID(m)	$R'_{th} \left(\frac{\text{m-K}}{\text{W}} \right)$	$R'_{tp} \left(\frac{\text{m-K}}{\text{W}} \right)$	$R'_{tc} \left(\frac{\text{m-K}}{\text{W}} \right)$	$R'_t \left(\frac{\text{m-K}}{\text{W}} \right)$	$q' \left(\frac{\text{kW}}{\text{m}} \right)$
10S	0.27305	0.26467	0.001002	0.0003413	0.01554	0.01689	8.290
<i>Percent of Total Resistance</i>			5.94%	2.02%	92.04%		
80S	0.27305	0.24765	0.001071	0.001069	0.01554	0.01768	7.917
<i>Percent of Total Resistance</i>			6.06%	6.04%	87.90%		

- The change of inside diameter has a slight effect on the value of the hot-side convective resistance. The effect is small, but it can be seen that the inside diameter has an influence on the thermal resistance.
- The conduction resistance of the thicker pipe is about three times that of the thinner pipe. This may seem significant until the complete resistance picture is considered.
- The vast majority of the resistance to heat transfer is the convective film on the cold side (outside) of this tube. Even with the thicker tube, over 87% of the resistance is in the outside convective film.
- Due to the increase in pipe thickness, the heat transfer rate per unit length of pipe decreases by about 4.5%.

5.2.2 The Convective Heat Transfer Coefficient

In most heat exchangers, convection is achieved by forced flow. The flow can be inside of pipes or tubes, outside of pipes or tubes (finned or bare), or between two plates. Convective heat transfer coefficients can often be determined analytically for simple geometries and laminar flow conditions. However, for more complex geometries and especially for turbulent flow, the convective heat transfer coefficients are determined by experiment. The equations that result from experimental studies are called *correlations*.

Equations and correlations describing the convective heat transfer coefficient are often written in terms of the dimensionless quantities, Nusselt number (Nu), Reynolds number (Re), Prandtl number (Pr), or Peclet number. The Nusselt number is defined as,

$$\text{Nu} = \frac{hL_c}{k} \quad (5.13)$$

In this equation, h is the convective heat transfer coefficient, L_c is a *characteristic length* (in most heat exchanger calculations, this is some type of diameter), and k is the thermal conductivity of the fluid.

The Reynolds number is defined as in fluid flow calculations,

$$\text{Re} = \frac{\rho VL_c}{\mu} \quad (5.14)$$

In Equation 5.14, ρ is the fluid's density, V is the velocity of the fluid in the passage, L_c is the characteristic length of the passage, and μ is the dynamic viscosity of the fluid.

The Prandtl number is a dimensionless grouping of thermophysical properties of the fluid involving the isobaric heat capacity, c_p , dynamic viscosity, μ , and thermal conductivity, k ,

$$\text{Pr} = \frac{c_p \mu}{k} \quad (5.15)$$

This equation demonstrates that the Prandtl number is a fluid property. Values of the Prandtl number for a variety of substances can be found in the property tables in Appendix B.

The Peclet number is the product of the Reynolds number and Prandtl number,

$$\text{Pe} = \text{RePr} \quad (5.16)$$

It is common to express the Nusselt number as a function of the Reynolds number and the Prandtl number.

$$\text{Nu} = f(\text{Re}, \text{Pr}) \quad (5.17)$$

The functional relationship depends on the convection scenario defined by flow conditions (laminar or turbulent), geometry, and other factors. Once the function is known, the value of the convection heat transfer coefficient can be calculated. However, before an equation or correlation is used, it is important to understand the conditions that were used to derive the expression. These conditions place limits on the range of validity of the expression. The engineer must understand what these limits are. Applying the equation beyond its limit of validity may lead to errors in the analysis or design.

Correlations derived from experiment can be subject to significant uncertainty. Every effort should be made to use the most current correlation for the situation that is being

considered. There are many excellent resources available for convective heat transfer correlations, including *Heat Exchangers: Selection, Rating, and Thermal Design* (Kakac, Liu and Pramuanjaroenkij 2012), *The Heat Transfer Handbook* (Bejan and Kraus 2003) or *The Handbook of Heat Transfer* (Rohsenow, Hartnett and Cho 1998). The most up-to-date information concerning convective heat transfer correlations can be found in technical journals such as *The International Journal of Heat and Mass Transfer* and the *Journal of Heat Transfer* (a publication of the American Society of Mechanical Engineers).

5.2.2.1 Entry Length

As a fluid enters and flows through a tube, *hydrodynamic* and *thermal* boundary layers develop inside of the tube. The velocity profile develops in the hydrodynamic boundary layer while the temperature profile develops in the thermal boundary layer. The hydrodynamic and thermal boundary layers develop independently. The distance required for the boundary layers to fully develop is known as the *entry length*.

In engineering applications, two possibilities are often considered. The *combined entry* occurs when both layers develop together. Another possibility is *thermal entry*. This occurs when the thermal boundary layer develops in the presence of a fully developed hydrodynamic boundary layer. Thermal entry can occur when there is an unheated starting length in the tube, or if the Prandtl number of the fluid is high as is the case with many oils.

It can be shown that when the thermal boundary layer is fully developed, the heat transfer coefficient remains constant inside the rest of the tube. However, in the entry length, the heat transfer coefficient decreases until the boundary layer is fully developed. This behavior is shown in Figure 5.3. For laminar flow, characterized by $Re_D < 2300$, the thermal entry length can be estimated by,

$$x_{fd,thermal} = 0.05D Re_D Pr \quad (5.18)$$

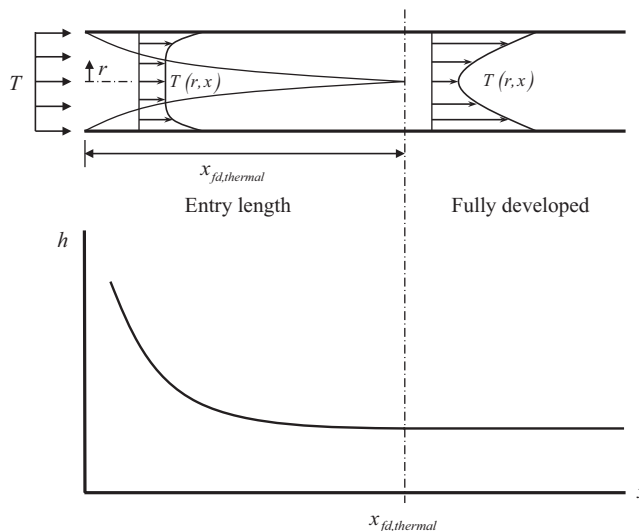


FIGURE 5.3

Thermal boundary layer development and convective heat transfer coefficient behavior for forced flow through a pipe or tube.

Beyond this point, the thermal boundary layer is fully developed and the heat transfer coefficient is constant. When the flow is turbulent ($Re_D > 2300$), the thermal entry length is characterized by,

$$x_{fd,thermal} = 10D \quad (5.19)$$

The remainder of this section lists equations and correlations for common convective heat transfer scenarios found in many different types of heat exchangers. More heat-exchanger-specific correlations are presented in subsequent sections of this chapter.

5.2.2.2 Forced External Cross Flow over a Cylindrical Surface

Churchill and Bernstein (1977) have developed the following correlation for forced external cross flow over a cylindrical surface,

$$Nu_D = \frac{hD}{k} = 0.3 + \frac{0.62 Re_D^{1/2} Pr^{1/3}}{\left[1 + (0.4/Pr)^{2/3}\right]^{1/4}} \left[1 + \left(\frac{Re_D}{282,000}\right)^{5/8}\right]^{4/5} \quad (5.20)$$

This correlation is valid for gases and liquids with $Re_D Pr \geq 0.2$. The fluid properties are evaluated at the *film temperature* (T_f). The film temperature is a reasonable estimate of the average temperature within the convective film. In the case of external flow, it is calculated using the *free-stream* (T_∞) temperature of the fluid and the *surface temperature* (T_s) of the material in contact with the fluid,

$$T_f = \frac{T_\infty + T_s}{2} \quad (5.21)$$

5.2.2.3 Forced Internal Laminar Flow—Combined Entry

The average Nusselt number over a tube of length, L , for forced internal laminar flow where the hydrodynamic and thermal boundary layers develop simultaneously is given by Shah and Bhatti (1987),

$$Nu_D = 0.664 \left(\frac{PeD}{L}\right)^{1/2} Pr^{-1/6} \quad (5.22)$$

This correlation is valid for $0.5 \leq Pr \leq 500$ and $PeD/L \geq 10^3$. The fluid properties are evaluated at the *average mean temperature*, T_m of the fluid over the tube length, L . The average mean temperature of the fluid can be estimated as the average between the mean inlet and outlet temperatures of the fluid entering and leaving the tube,

$$T_m = \frac{T_{m,in} + T_{m,out}}{2} \quad (5.23)$$

5.2.2.4 Forced Internal Laminar Flow—Thermal Entry

The average Nusselt number over a tube of length, L , for forced internal laminar flow in the situation where the thermal boundary layer is developing in the presence of a fully developed velocity profile is given by Gnielinski (1983),

$$\text{Nu}_D = \frac{hD}{k} = \left[3.66^3 + 1.61^3 \left(\frac{\text{Pe}D}{L} \right) \right]^{1/3} \quad (5.24)$$

Another correlation that can be used for this scenario is given by Hausen (1959),

$$\text{Nu}_D = \frac{hD}{k} = 3.66 + \frac{0.19(\text{Pe}D/L)^{0.8}}{1 + 0.117(\text{Pe}D/L)^{0.467}} \quad (5.25)$$

The fluid properties in Equations 5.24 and 5.25 are evaluated at the average mean temperature of the fluid given by Equation 5.23.

Equations 5.24 and 5.25 give similar results. These correlations can be used for laminar flow of liquids and gases in the range defined by $0.1 \leq \text{Pe}D/L \leq 10^4$.

5.2.2.5 Forced Internal Turbulent Flow

In many turbulent flow heat exchanger applications, the entry length is small compared to the total tube length and the entry effects can be neglected. For fully developed, turbulent flow, the recommended correlation is given below (Gnielinski 1976),

$$\text{Nu}_D = \frac{hD}{k} = \frac{(f/8)(\text{Re}_D - 1000)\text{Pr}}{1 + 12.7(f/8)^{1/2}(\text{Pr}^{2/3} - 1)} \quad (5.26)$$

This correlation is valid for $0.50 \leq \text{Pr} \leq 2000$ and $3000 \leq \text{Re}_D \leq 5 \times 10^6$. The fluid properties are evaluated at the average mean temperature of the fluid given by Equation 5.23.

In Equation 5.26, the friction factor, f , can be determined using any of the empirical expressions found in Chapter 4. Even though this correlation was developed for *smooth tubes*, Equation 5.26 can be used to obtain a reasonable estimate of the convective heat transfer coefficient with other values of surface roughness.

Example 5.2

A 40% methanol-water solution enters one of the tubes of a heat exchanger at a 30°C at a flow rate of 2.6 L/s. Heat is removed from the methanol-water solution as it passes through the heat exchanger and it leaves at -10°C . The heat exchanger is a single tube that is 1 std type L copper. Determine the convective heat transfer coefficient on the inside of the tube.

Solution

The inside diameter of the copper tube can be found in Appendix D,

$$D = 0.026035 \text{ m}$$

The relative roughness of copper tubing is listed in Table 4.3 (drawn tubing),

$$\varepsilon = 0.00015 \text{ cm} = 0.0000015 \text{ m}$$

In the heat transfer correlations, the properties are determined at the average temperature of the fluid,

$$T_m = \frac{T_{in} + T_{out}}{2} = \frac{(30 - 10)^\circ\text{C}}{2} = 10^\circ\text{C}$$

The properties of a 40% methanol water solution at this temperature are found in Appendix B.4,

$$\rho = 940.29 \frac{\text{kg}}{\text{m}^3} \quad \mu = 0.0025306 \frac{\text{kg}}{\text{m}\cdot\text{s}} \quad k = 0.38047 \frac{\text{W}}{\text{m}\cdot\text{K}} \quad \text{Pr} = 24.976$$

The velocity of the methanol-water in the tube can be found from the volumetric flow rate and the inside diameter of the tube,

$$V = \frac{4\dot{V}}{\pi D^2} = \frac{4\left(2.6 \frac{\text{L}}{\text{s}}\right)\left(\frac{\text{m}}{1000 \text{ L}}\right)}{\pi(0.026035 \text{ m})^2} = 4.8839 \frac{\text{m}}{\text{s}}$$

The Reynolds number corresponding to this flow rate is,

$$\text{Re} = \frac{\rho V D}{\mu} = \frac{\left(940.29 \frac{\text{kg}}{\text{m}^3}\right)\left(4.8839 \frac{\text{m}}{\text{s}}\right)(0.026035 \text{ m})}{0.0025306 \frac{\text{kg}}{\text{m}\cdot\text{s}}} = 47,246$$

This indicates the flow inside the tube is turbulent. Assuming that the entry length is negligible, the Gnielinski correlation (Equation 5.26) can be used to determine the Nusselt number. The friction factor can be determined using any of the correlations shown in Table 4.2. Using the Swamee-Jain correlation,

$$f = \frac{0.25}{\left[\log\left(\frac{\varepsilon/D}{3.7} + \frac{5.74}{\text{Re}^{0.9}}\right)\right]^2} = \frac{0.25}{\left[\log\left(\frac{0.0000015 \text{ m} / 0.026034 \text{ m}}{3.7} + \frac{5.74}{47,246^{0.9}}\right)\right]^2} = 0.021257$$

The Nusselt number can now be found,

$$\text{Nu}_D = \frac{hD_h}{k} = \frac{(f/8)(\text{Re}_D - 1000)\text{Pr}}{1 + 12.7(f/8)^{1/2}(\text{Pr}^{2/3} - 1)} = \frac{(0.021257/8)(47,246 - 1,000)(24.976)}{1 + 12.7(0.021257/8)^{1/2}(24.976^{2/3} - 1)} = 516.77$$

Therefore, the convective heat transfer coefficient on the inside of the tube is,

$$h = \frac{\text{Nu}_D k}{D} = \frac{(516.77) \left(0.38047 \frac{\text{W}}{\text{m}\cdot\text{K}} \right)}{0.026035 \text{ m}} = \underline{\underline{7557.3 \frac{\text{W}}{\text{m}^2\cdot\text{K}}}}$$

5.3 Fouling on Heat Exchanger Surfaces

Thermal resistances to heat transfer due to conduction and convection are part of any heat exchanger. Heat exchanger surfaces also collect unwanted materials which further inhibit heat transfer. This phenomenon is known as *fouling*. The effects of fouling can be significant and should be included in analysis and design calculations. Fouling is a complex physical phenomenon which can be modeled analytically. However, for design and analysis calculations, this approach is too complex. In lieu of the analytical treatment, typical fouling resistance values have been determined and tabulated. Table 5.2 lists some representative values for various fluids (Kakac, Liu and Paramuanjaroenkii 2012). The tabulated resistance values are area-weighted, which allows for the total resistance to be calculated once the surface area where the fouling occurs is known. These area-weighted fouling resistances are known as *fouling factors*,

$$R_f'' = AR_f \quad (5.27)$$

Fouling is a time-dependent phenomenon. A brand-new heat exchanger has clean surfaces and little or no fouling is present. After the heat exchanger is put into service, fouling will begin and continue until maintenance is performed to remove the fouling deposits. The fouling factors listed in Table 5.2 represent typical values after one year of normal service with no maintenance.

5.4 The Overall Heat Transfer Coefficient

Consider the tube cross section shown in Figure 5.4. In this heat exchange scenario, the total resistance to heat transfer is made up of five resistances. Starting on the inside of the tube and working outward, these resistances are,

1. The convective resistance on the inside of the tube
2. The fouling resistance on the inside of the tube
3. The conduction resistance through the tube wall separating the fluids
4. The fouling resistance on the outside of the tube
5. The convection resistance on the outside of the tube

The total thermal resistance can be expressed as,

$$R_t = R_i + R_{f,i} + R_w + R_{f,o} + R_o \quad (5.28)$$

TABLE 5.2

Representative Values of Fouling Factors for Heat Exchangers

Industrial Fluids	Fouling Factor R_f'	
	hr-ft ² -°F/Btu	m ² -K/W
<i>Oils</i>		
No. 2 Fuel Oil	0.002	0.000352
No. 6 Fuel Oil	0.005	0.000881
Engine Oil	0.005	0.000881
Vegetable Oils	0.003	0.000528
<i>Gases and Vapors</i>		
Engine Exhaust	0.010	0.001761
Steam	0.0005	0.000088
Refrigerants	0.002	0.000352
Compressed Air	0.010	0.001761
Ammonia	0.010	0.001761
Carbon Dioxide	0.010	0.001761
Coal Flue Gas	0.010	0.001761
Natural Gas Flue Gas	0.0005	0.000088
<i>Liquids</i>		
Ammonia	0.001	0.000176
Ammonia (oil bearing)	0.003	0.000528
Refrigerants	0.001	0.000176
Light Organic Liquids (e.g., hydrocarbons)	0.002	0.000352
Hydraulic Fluid	0.001	0.000176
Carbon Dioxide	0.001	0.000176
Methanol or Ethanol Solutions	0.002	0.000352
Ethylene Glycol Solutions	0.002	0.000352
Sodium or Calcium Chloride Solutions	0.003	0.000528
<i>Water^a</i>		
City or Well Water	0.002	0.000352
River Water	0.004	0.000705
Muddy or Silty Water	0.003	0.000528
Hard Water	0.005	0.000881
Distilled Water	0.0005	0.000088

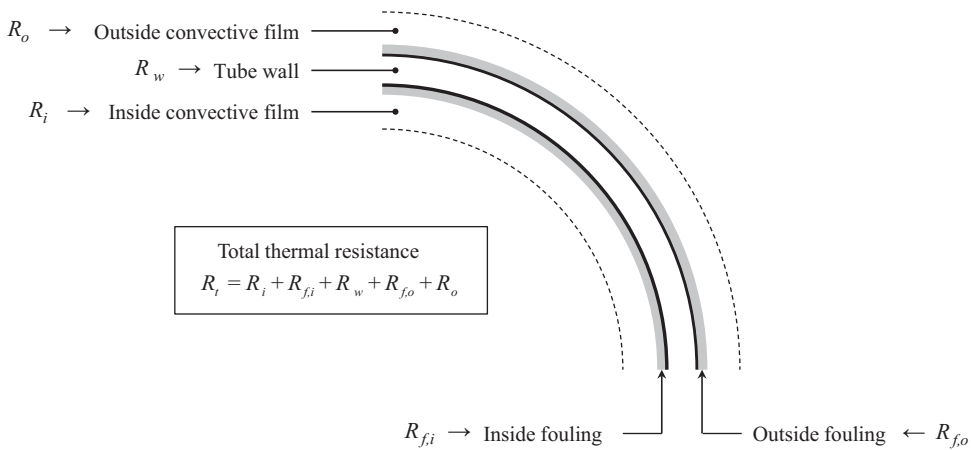
^a Extensive information is available for water fouling. The values shown here are worst-case values. Consult Kakac, Liu and Pramuanjaroenkij (2012) for more detail.

In heat exchanger calculations, it is more convenient to express the total resistance in terms of the *overall heat transfer coefficient*, U . The definition of the overall heat transfer coefficient is given by,

$$UA = \frac{1}{R_t} \quad (5.29)$$

In Equation 5.29, A represents the total heat transfer area in the heat exchanger. Making this substitution into the heat transfer rate expression given in Equation 5.12 results in,

$$\dot{Q} = UA(T - t) \quad (5.30)$$

**FIGURE 5.4**

Cross-sectional view of a tube showing resistances to heat transfer.

Equation 5.30 is similar in form to Newton's law of cooling. However, it takes into account *all* of the thermal resistance to heat transfer, not just the convection. Comparing Equation 5.30 to Newton's law of cooling, it can be seen that the units of U are identical to the units of the convective heat transfer coefficient, h . In heat exchanger design and analysis, the UA product of the heat exchanger is an important parameter that must be determined. Once the overall heat transfer coefficient is known, then the area of the heat exchanger can be determined.

Consider a circular tube without fins. In Equation 5.29, the area A can represent either the inside or outside surface area of the tube. If the outside area, A_o , is chosen, the value of U corresponds to U_o . Likewise, U_i is based on A_i . Since the inside and outside surface areas are different, the inside and outside U values will be different. However, Equation 5.29 indicates that the UA product is the same for both inside and outside surfaces. Therefore,

$$U_o A_o = U_i A_i \quad (5.31)$$

For a circular tube without fins, the total resistance is given by,

$$R_t = \frac{1}{h_i A_i} + \frac{R''_{f,i}}{A_i} + \frac{\ln(OD/ID)}{2\pi k L} + \frac{R''_{f,o}}{A_o} + \frac{1}{h_o A_o} \quad (5.32)$$

The overall heat transfer coefficient, based on the outside surface area can be found by substituting Equation 5.32 into Equation 5.29 and solving for $1/U_o$.

$$\frac{1}{U_o} = A_o R_t = \frac{1}{h_i} \left(\frac{A_o}{A_i} \right) + R''_{f,i} \left(\frac{A_o}{A_i} \right) + A_o \frac{\ln(OD/ID)}{2\pi k L} + R''_{f,o} + \frac{1}{h_o} \quad (5.33)$$

The areas are the inside (subscript *i*) and outside (subscript *o*) surface areas of the tube. Therefore, Equation 5.33 can be written as,

$$\frac{1}{U_o} = A_o R_t = \frac{1}{h_i} \left[\frac{\pi(OD)L}{\pi(ID)L} \right] + R''_{f,i} \left[\frac{\pi(OD)L}{\pi(ID)L} \right] + [\pi(OD)L] \frac{\ln(OD/ID)}{2\pi kL} + R''_{f,o} + \frac{1}{h_o} \quad (5.34)$$

In Equation 5.34, *OD* and *ID* correspond to the outside and inside diameters of the tube, respectively. Simplifying this equation gives,

$$\frac{1}{U_o} = A_o R_t = \frac{1}{h_i} \left(\frac{OD}{ID} \right) + R''_{f,i} \left(\frac{OD}{ID} \right) + \frac{OD}{2k} \ln \left(\frac{OD}{ID} \right) + R''_{f,o} + \frac{1}{h_o} \quad (5.35)$$

If the overall heat transfer coefficient was based on the *inside* diameter of the tube, then the resulting expression would be,

$$\frac{1}{U_i} = A_i R_t = \frac{1}{h_i} + R''_{f,i} + \frac{ID}{2k} \ln \left(\frac{OD}{ID} \right) + R''_{f,o} \left(\frac{ID}{OD} \right) + \frac{1}{h_o} \left(\frac{ID}{OD} \right) \quad (5.36)$$

Equations 5.35 and 5.36 demonstrate that the magnitude of U_o and U_i are different. However, as shown above, the UA product is the same for both surfaces. In heat exchanger calculations, it is common to base the overall heat transfer coefficient on the *outside diameter* of the tube or pipe.

Example 5.3

A 4-std type K copper tube is transporting an ethylene glycol solution. Superheated steam passes over the outside of the tube. The convective heat transfer coefficients are found to be 200 W/m²-K on the inside of the tube and 180 W/m²-K on the outside of the tube. Under these conditions, the average temperature of the tube is 150°C. The tube is 30 m long. Determine,

- The overall heat transfer coefficients based on the inside and outside surface areas for a fouled condition
- The UA product of the tube without fouling
- The UA product of the tube after one year of service

Solution

The data for the copper tube can be found in Appendix D (diameters) and Appendix B (thermal conductivity),

$$OD = 0.10478 \text{ m} \quad ID = 0.099187 \text{ m} \quad k = 391.4 \text{ W/m-K}$$

The fouling factors for the ethylene glycol solution on the inside of the tube and the superheated vapor steam on the outside of the tube are found in Table 5.2,

$$R''_{f,i} = 0.000352 \text{ m}^2\text{-K/W} \quad R''_{f,o} = 0.000088 \text{ m}^2\text{-K/W}$$

- a. Equations 5.35 and 5.36 can be used to find the overall heat transfer coefficients based on the outside and inside surface areas, respectively.

$$\begin{aligned} \frac{1}{U_{o,fouled}} &= \frac{1}{h_i} \left(\frac{OD}{ID} \right) + R''_{f,i} \left(\frac{OD}{ID} \right) + \frac{OD}{2k} \ln \left(\frac{OD}{ID} \right) + R''_{f,o} + \frac{1}{h_o} \\ \frac{1}{U_{o,fouled}} &= \frac{1}{200} \frac{\text{m}^2\text{-K}}{\text{W}} \left(\frac{0.10478 \text{ m}}{0.099187 \text{ m}} \right) + 0.000352 \frac{\text{m}^2\text{-K}}{\text{W}} \left(\frac{0.10478 \text{ m}}{0.099187 \text{ m}} \right) \\ &\quad + \frac{0.10478 \text{ m}}{2(391.4)} \frac{\text{m-K}}{\text{W}} \ln \left(\frac{0.10478 \text{ m}}{0.099187 \text{ m}} \right) + 0.000088 \frac{\text{m}^2\text{-K}}{\text{W}} + \frac{1}{180} \frac{\text{m}^2\text{-K}}{\text{W}} \\ \frac{1}{U_{o,fouled}} &= 0.01130 \frac{\text{m}^2\text{-K}}{\text{W}} \\ \therefore U_{o,fouled} &= \underline{\underline{88.46 \frac{\text{W}}{\text{m}^2\text{-K}}}} \end{aligned}$$

$$\begin{aligned} \frac{1}{U_{i,fouled}} &= \frac{1}{h_i} + R''_{f,i} + \frac{ID}{2k} \ln \left(\frac{OD}{ID} \right) + R''_{f,o} \left(\frac{ID}{OD} \right) + \frac{1}{h_o} \left(\frac{ID}{OD} \right) \\ \frac{1}{U_{i,fouled}} &= \frac{1}{200} \frac{\text{m}^2\text{-K}}{\text{W}} + 0.000352 \frac{\text{m}^2\text{-K}}{\text{W}} + \frac{0.099187 \text{ m}}{2(391.4)} \frac{\text{m-K}}{\text{W}} \ln \left(\frac{0.10478 \text{ m}}{0.099187 \text{ m}} \right) \\ &\quad + 0.000088 \frac{\text{m}^2\text{-K}}{\text{W}} \left(\frac{0.099187 \text{ m}}{0.10478 \text{ m}} \right) + \frac{1}{180} \frac{\text{m}^2\text{-K}}{\text{W}} \left(\frac{0.099187 \text{ m}}{0.10478 \text{ m}} \right) \\ \frac{1}{U_{i,fouled}} &= 0.01070 \frac{\text{m}^2\text{-K}}{\text{W}} \\ \therefore U_{i,fouled} &= \underline{\underline{93.45 \frac{\text{W}}{\text{m}^2\text{-K}}}} \end{aligned}$$

This calculation shows that the U value is dependent on which surface is chosen for A . However, in heat exchanger calculations, the UA product is more useful.

- b. To determine the UA product for a clean tube, the U values need to be recalculated without the fouling resistance. The results are,

$$\begin{aligned} \frac{1}{U_{o, clean}} &= \frac{1}{h_i} \left(\frac{OD}{ID} \right) + \frac{OD}{2k} \ln \left(\frac{OD}{ID} \right) + \frac{1}{h_o} \\ \frac{1}{U_{o, clean}} &= 0.01084 \frac{\text{m}^2\text{-K}}{\text{W}} \quad \therefore U_{o, clean} = \underline{\underline{92.21 \frac{\text{W}}{\text{m}^2\text{-K}}}} \end{aligned}$$

$$\frac{1}{U_{i, \text{clean}}} = \frac{1}{h_i} + \frac{ID}{2k} \ln \left(\frac{OD}{ID} \right) + \frac{1}{h_o} \left(\frac{ID}{OD} \right)$$

$$\frac{1}{U_{i, \text{clean}}} = 0.01027 \frac{\text{m}^2 \cdot \text{K}}{\text{W}} \quad \therefore \quad U_{i, \text{clean}} = \underline{\underline{97.41 \frac{\text{W}}{\text{m}^2 \cdot \text{K}}}}$$

Now, the UA products can be found for both conditions of a clean and fouled tube. For the clean tube,

$$(UA)_{o, \text{clean}} = U_{o, \text{clean}} A_o = U_{o, \text{clean}} [\pi(OD)L]$$

$$(UA)_{o, \text{clean}} = \left(92.21 \frac{\text{W}}{\text{m}^2 \cdot \text{K}} \right) [\pi(0.10478 \text{ m})(30 \text{ m})] = \underline{\underline{910.6 \frac{\text{W}}{\text{K}}}}$$

$$(UA)_{i, \text{clean}} = U_{i, \text{clean}} A_i = U_{i, \text{clean}} [\pi(ID)L]$$

$$(UA)_{i, \text{clean}} = \left(97.41 \frac{\text{W}}{\text{m}^2 \cdot \text{K}} \right) [\pi(0.099187 \text{ m})(30 \text{ m})] = \underline{\underline{910.6 \frac{\text{W}}{\text{K}}}}$$

As expected, the UA product is the same for both surfaces of the tube.

- c. After one year of service, the UA product based on the fouled value of the overall heat transfer coefficient is,

$$(UA)_{o, \text{fouled}} = \left(88.46 \frac{\text{W}}{\text{m}^2 \cdot \text{K}} \right) [\pi(0.10478 \text{ m})(30 \text{ m})] = \underline{\underline{873.6 \frac{\text{W}}{\text{K}}}}$$

$$(UA)_{i, \text{fouled}} = \left(93.45 \frac{\text{W}}{\text{m}^2 \cdot \text{K}} \right) [\pi(0.099187 \text{ m})(30 \text{ m})] = \underline{\underline{873.6 \frac{\text{W}}{\text{K}}}}$$

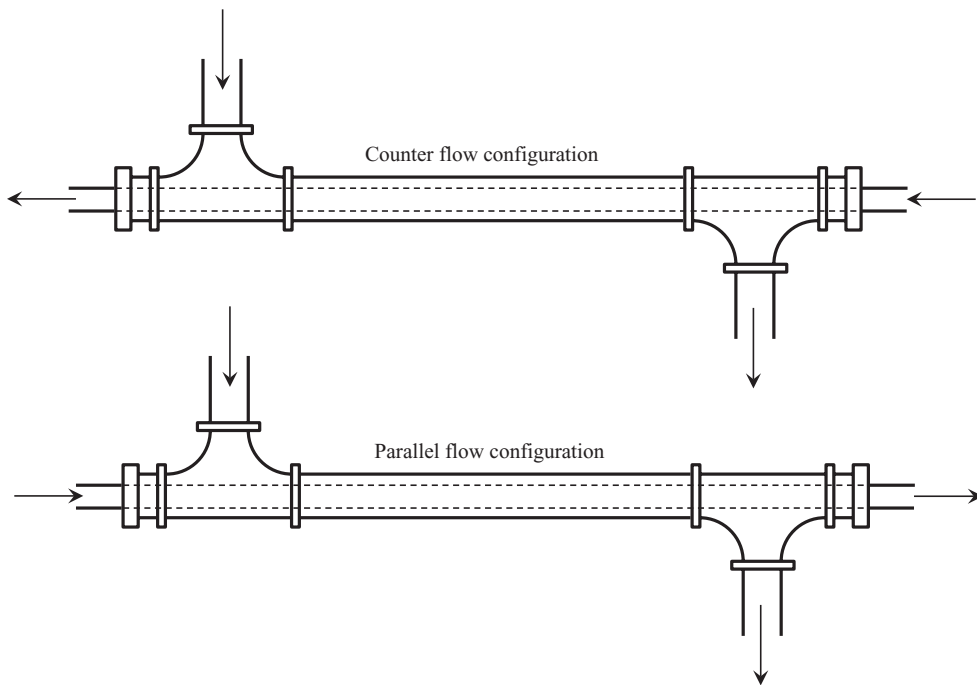
Since the UA product is directly proportional to the heat transfer rate, it can be seen in this case, that fouling reduces the heat transfer rate in this tube by approximately 4% after a year of normal service with no maintenance.

5.5 Heat Exchanger Types

There are many types of heat exchangers. The most common used in industry are *double pipe*, *shell and tube*, *plate and frame*, and *cross flow*. Detailed analysis and design procedures for each of these types of heat exchangers will be presented in subsequent sections of Chapter 5. In this section, a qualitative description of each of these types is presented.

5.5.1 Double Pipe Heat Exchanger

The *double pipe heat exchanger* (DPHX) is one of the simplest heat exchanger configurations. They can be purchased from many vendors. It is also possible to build a DPHX. The DPHX

**FIGURE 5.5**

Counter flow and parallel flow configurations for double pipe heat exchangers.

consists of two concentric pipes or tubes as shown in Figure 5.5. This figure indicates that there are two possible fluid flow configurations for DPHXs; counter flow and parallel flow. Each of these flow configurations results in different thermal performance.

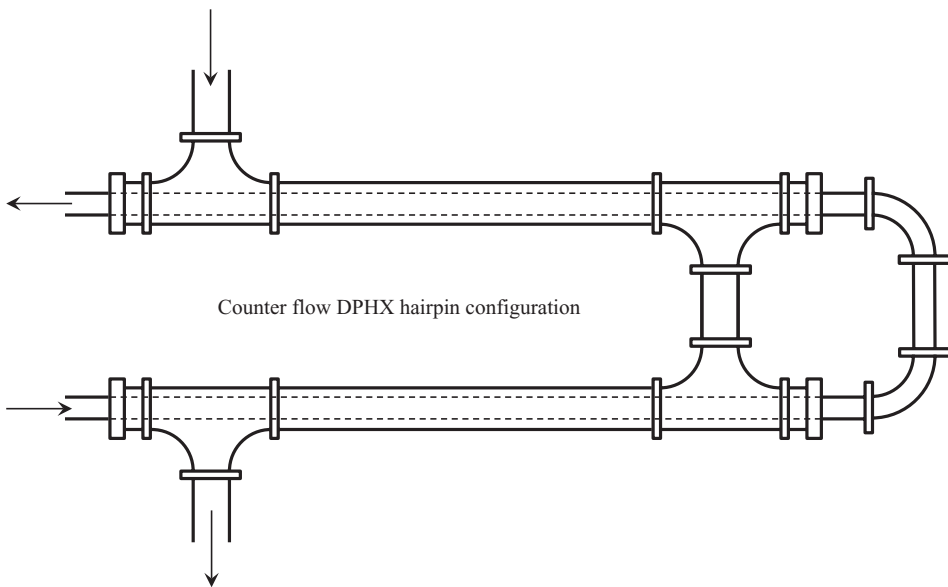
It is possible to connect DPHXs together in what is known as a *hairpin* configuration. The hairpin configuration is useful when a long heat exchanger length is required, but the installation footprint is small. Figure 5.6 shows a schematic of a counter flow hairpin DPHX. Notice that if several hairpins are added, this design allows the engineer to fit a rather large heat exchanger into a small footprint.

Double pipe heat exchangers are typically used in situations requiring low-to-moderate heat transfer rates.

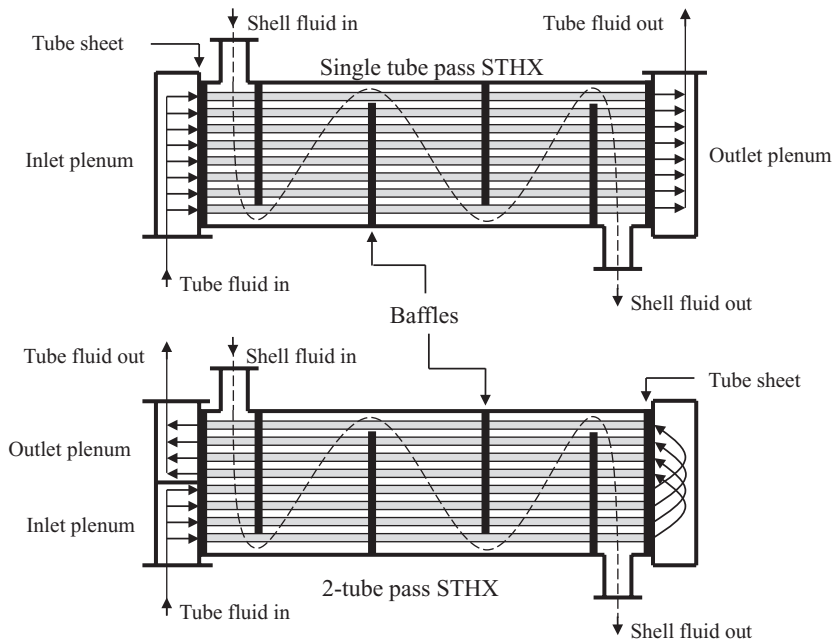
5.5.2 Shell and Tube Heat Exchanger

The *shell and tube heat exchanger* (STHX) provides a substantial amount of heat transfer area in a relatively small volume. It is a much more complex heat exchanger compared to the DPHX. As a result, the STHX is usually more expensive compared to the DPHX for the same heat transfer duty.

The STHX is made up of a large diameter shell that contains multiple tubes inside. The tubes can be arranged for several possible flow configurations. Figure 5.7 shows two possibilities; the *single tube pass* and the *2-tube pass* STHX. The shell-side fluid is distributed among the tubes by means of an *inlet plenum*. The shell-side fluid is collected and leaves the STHX through the *outlet plenum*. The plenums are connected to the heat exchanger at the *tube sheet*. The tube sheet is a shell-diameter piece of metal that has holes bored into it to provide a place to connect the tube bundle. Providing a place for the plenums to connect at

**FIGURE 5.6**

A counter flow hairpin double pipe heat exchanger.

**FIGURE 5.7**

Single tube pass and 2-Tube pass shell and tube heat exchangers.

the tube sheet allows for disassembly of the heat exchanger for tube maintenance. As the shell-side fluid flows across the tube bundles in the shell, its flow is diverted by means of *baffles*. The baffles provide heat transfer enhancement as well as structural support to hold the tube bundle in place.

Shell and tube heat exchangers are usually used in applications requiring large heat transfer rates. They are often used as condensers or evaporators where one of the fluids in the heat exchanger is undergoing a phase change.

5.5.3 Plate and Frame Heat Exchanger

The *plate and frame heat exchanger* (PFHX) was introduced in the 1930s. They are used extensively in the food processing industry and other industrial applications. In the PFHX, the hot and cold fluids circulate through a series of *plates* as shown in Figure 5.8. The plates are held together with a *frame*. *Gaskets* on the plates keep the fluids sealed inside the heat exchanger and also provide the desired flow path for the hot and cold fluids.

The plates are corrugated with a *chevron* pattern to enhance turbulence which increases the heat transfer rate. The metal plates are usually cold-stamped. Depending on the temperatures and pressures involved, the gaskets can be made of one of several materials including natural rubber styrene, resin-cured nitrile, silicone rubber, or neoprene. The plates are clamped together in the frame with long bolts as shown in Figure 5.8. Due to its relatively simple construction, it is easily taken apart for maintenance.

Plate and frame heat exchangers are typically used where low-to-moderate heat transfer rates are required.

5.5.4 Cross Flow Heat Exchanger

In a *cross flow heat exchanger* (CFHX) the hot and cold fluids never contact each other directly. However, the fluids can be categorized as *mixed* or *unmixed*. Figure 5.9 shows what is meant by mixed and unmixed fluids. A fluid is unmixed if it passes through the heat exchanger and its path is controlled by passages created by channels or fins. A fluid is mixed if it

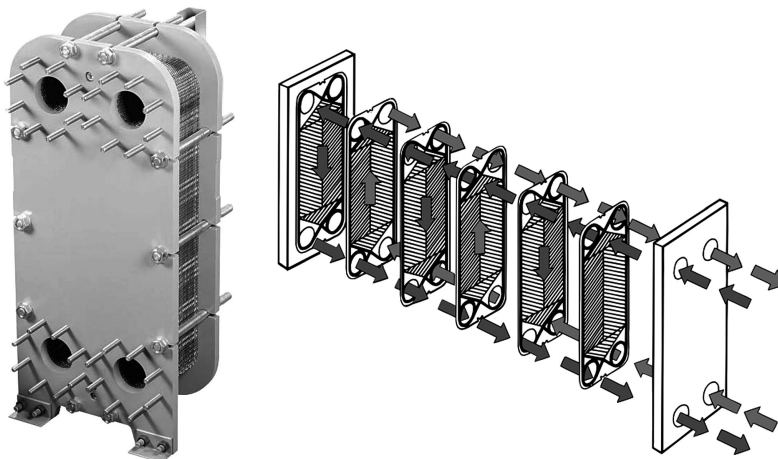


FIGURE 5.8

The plate and frame heat exchanger. (Reprinted from Xylem, Inc., *GPX Plate and Frame Heat Exchangers*, Buffalo, New York, USA, Bell & Gossett, 2011. With permission.)

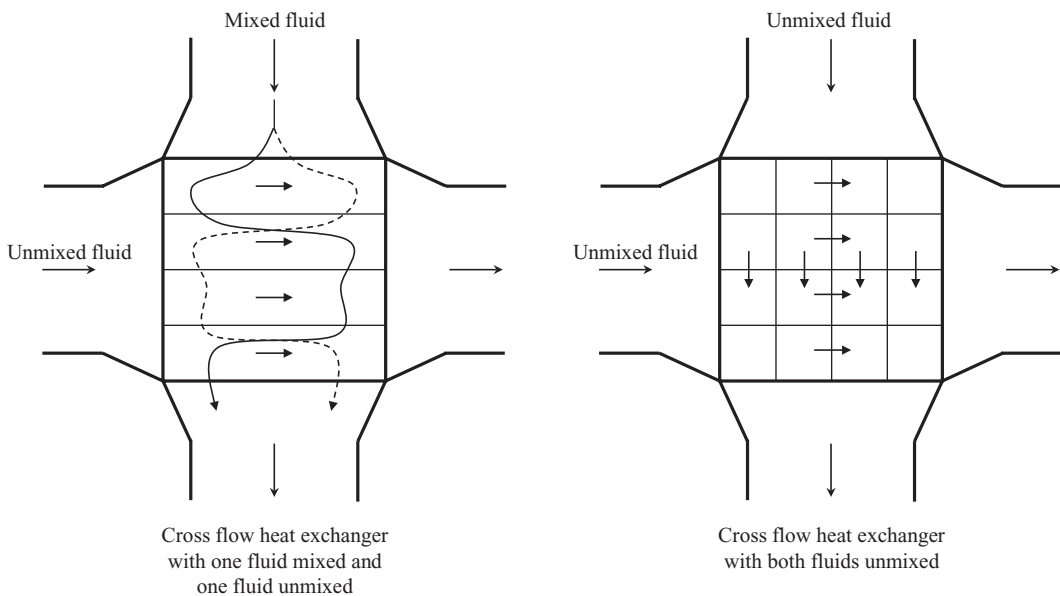


FIGURE 5.9
Cross flow heat exchangers showing mixed and unmixed fluids.

enters the heat exchanger and is free to wander about as it works its way through. An example of this is a fluid passing over a bank of tubes in cross flow. While the fluid's main path is "forward" through the heat exchanger, its path can be diverted and therefore "mixed." In both cases, the fluids are moving in cross flow to each other.

There are many configurations for cross flow heat exchangers. Perhaps one of the more common CFHXs is the finned-tube coil found in many heating and air conditioning systems. These heat exchangers range from very small to quite large. Therefore, the CFHX is used in systems where the heat transfer rate ranges from low to high.

5.6 Design and Analysis of Heat Exchangers

There are two types of problems encountered when considering heat exchangers in a thermal energy system; a *design* problem and an *analysis* problem. In a design problem, the heat exchanger has not yet been selected. It is being designed to meet a specific need. In analysis, the heat exchanger exists (e.g., from a vendor), and the analysis predicts its thermal performance.

As an example of a heat exchanger design problem, consider the case where the following information is known in an application: the mass flow rates of each fluid, the inlet temperature of each fluid, and the outlet temperature of either one of the fluids. A thermodynamic analysis can be used to determine the outlet temperature of the other fluid. However, a heat transfer analysis is required to determine the total heat transfer area, and thus the size, of the heat exchanger. In this case, the heat exchanger is being designed to meet a specific need.

By contrast, consider a case where a heat exchanger has been selected for an application and the following system parameters are known: the mass flow rates of each fluid, and the inlet temperatures of each fluid. In this case, an analysis of the existing heat exchanger is needed to determine the outlet temperatures of each fluid.

5.6.1 A Heat Exchanger Design Problem

Figure 5.10 shows a schematic of a heat exchanger. The type of heat exchanger is not important at this point. Included in the sketch are three different system boundaries specified with dashed lines.

Consider the design problem where the mass flow rates and inlet temperatures of the hot and cold fluids are known. In addition, the outlet temperature of the hot fluid is known. The design problem is to determine the total heat transfer area required and the cold fluid outlet temperature. Applying the conservation of energy equation to the system boundary surrounding the hot fluid results in,

$$\dot{Q} = \dot{m}_h(h_{hi} - h_{ho}) \quad (5.37)$$

In this equation, h is the hot fluid's enthalpy. If the fluid remains in the single phase (gas or liquid), Equation 5.37 can be re-written using the heat capacity of the substance,

$$\dot{Q} = \dot{m}_h c_{p,h,avg} (T_{hi} - T_{ho}) \quad (5.38)$$

In heat exchanger analysis, it is common to use the thermal capacity rate of the flow, which was introduced in Section 3.7.3, and is defined as,

$$\dot{C} = \dot{m}c_p \quad (5.39)$$

Using the thermal capacity rate, Equation 5.38 can be written as,

$$\dot{Q} = \dot{C}_h (T_{hi} - T_{ho}) \quad (5.40)$$

Likewise, for the system boundary surrounding the cold fluid,

$$\dot{Q} = \dot{C}_c (t_{co} - t_{ci}) \quad (5.41)$$

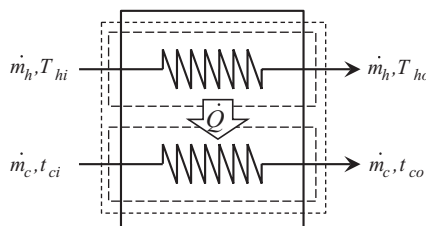


FIGURE 5.10

A heat exchanger with three different system boundaries.

Equations 5.40 and 5.41 can be combined to solve for the outlet temperature of the cold fluid,

$$t_{co} = t_{ci} + \frac{\dot{C}_h}{\dot{C}_c} (T_{hi} - T_{ho}) \quad (5.42)$$

This equation could have been derived using the larger system boundary in Figure 5.10 that encompasses both fluids. The heat transfer rate between the two fluids can be found from Equation 5.40 or 5.41. The analysis summarized in Equations 5.37 through 5.42 is purely thermodynamic. However, in the heat exchanger design problem, the parameter of interest is the *area* of the heat exchanger required to affect the hot and cold fluid temperature changes at the given flow rates. There is no indication of the area required in the thermodynamic analysis. This suggests that an equation is missing to complete the design. This equation comes from a heat transfer analysis.

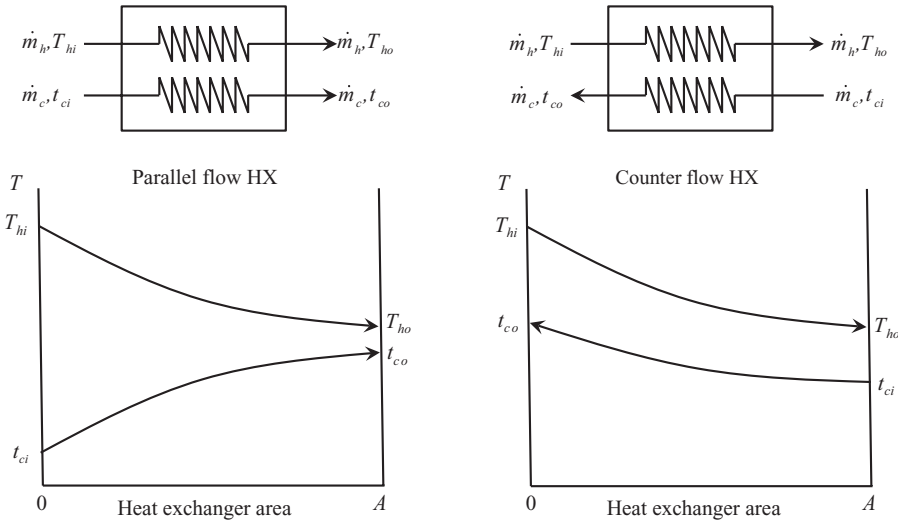
5.6.2 A Heat Exchanger Analysis Problem

Consider the same heat exchanger sketch shown in Figure 5.10. For an analysis problem, the heat exchanger is already selected. In other words, the heat exchange area is known. A typical analysis problem would be to predict the outlet fluid temperatures knowing the mass flow rates and inlet temperatures of each fluid. The thermodynamic analysis is the same as developed in Section 5.6.1. The equation for the cold fluid outlet temperature, Equation 5.42, cannot be solved because it is a function of the hot fluid outlet temperature, which is also an unknown. Therefore, Equation 5.42 is one equation with two unknowns. The same conclusion can be drawn as in the previous section. Something is missing that is required to complete the analysis. The missing equation comes from a heat transfer analysis of the heat exchanger.

5.6.3 Heat Exchanger Heat Transfer Analysis

As concluded in Sections 5.6.1 and 5.6.2, a thermodynamic analysis does not reveal anything about the *internal* performance of the heat exchanger. This is a limitation of thermodynamics because the heat exchanger is “black-boxed” by the system boundary. This does not diminish the importance of the thermodynamic analysis. As will be demonstrated, the thermodynamic analysis is an important part of the complete heat exchanger modeling strategy.

The heat transfer analysis required to complete the mathematical description involves the determination of the UA product of the heat exchanger and relating it to a temperature difference. Determination of U captures the effect of the heat transfer modes occurring within the heat exchanger. The size of the heat exchanger is contained in the area A . The question is, “How are these variables related to a temperature difference in a heat exchanger?” Equation 5.30 suggests that an equation analogous to Newton’s law of cooling may be helpful. This equation could be useful *if* the temperature difference between the hot and cold fluid is constant throughout the length of the heat exchanger. Unfortunately, this only occurs in a specialized heat exchanger under specific flow conditions. In reality, the temperature difference between the hot and cold fluids varies as a function of position within the heat exchanger. For example, consider the temperature profiles shown in Figure 5.11. This figure demonstrates the variation in the temperature difference ($T - t$) as a function of position within the heat exchanger for parallel and counter flow configurations.

**FIGURE 5.11**

Temperature profiles inside parallel and counter flow heat exchangers.

5.6.3.1 Logarithmic Mean Temperature Difference

In order to utilize an equation such as Equation 5.30, the temperature difference needs to be modified to account for the temperature variability shown in Figure 5.11. This is done using what is known as the *logarithmic mean temperature difference* (LMTD). Using the LMTD instead of a simple temperature difference, Equation 5.30 can be rewritten as,

$$\dot{Q} = UA(\text{LMTD}) \quad (5.43)$$

Figure 5.11 shows that the temperature profiles are a function of the *type* of heat exchanger (e.g., parallel flow or counter flow). This implies that the LMTD is dependent on the type of heat exchanger. To develop the LMTD for a parallel flow heat exchanger, a differential area within the heat exchanger will be analyzed as shown in Figure 5.12.

The conservation of energy equation applied to the hot and cold fluids in the differential element dA result in the following expressions,

$$d\dot{Q} = \dot{C}_h(-dT_h) = -\dot{C}_h dT_h \quad (5.44)$$

$$d\dot{Q} = \dot{C}_c dt_c \quad (5.45)$$

In order to have the same sign on the heat transfer rate, a negative sign is needed in Equation 5.44 because dT_h is negative. Equations 5.44 and 5.45 are the thermodynamic analysis of the differential area. The differential heat transfer rate can be expressed similar to Equation 5.30 as,

$$d\dot{Q} = U(T_h - t_c)dA = U(\Delta T)dA \quad (5.46)$$

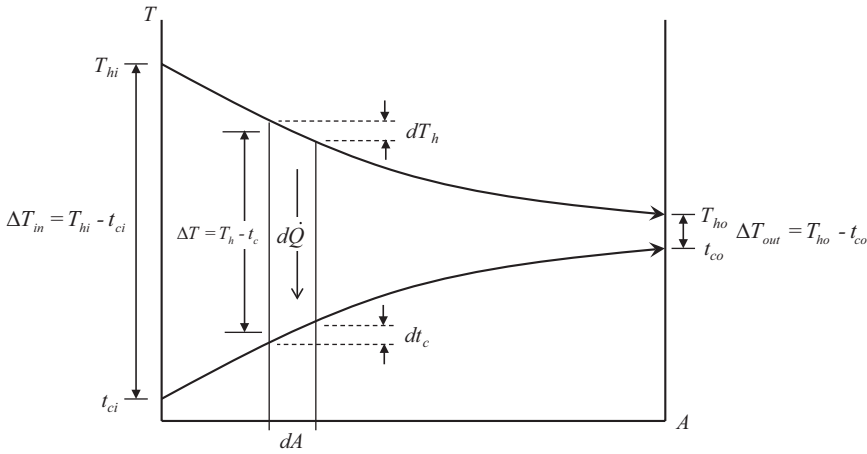


FIGURE 5.12
Differential analysis of a parallel flow heat exchanger.

The temperature difference in Equation 5.46 is the *local* temperature difference across the differential element. The differential of this temperature difference is written as,

$$d\Delta T = d(T_h - t_c) = dT_h - dt_c \quad (5.47)$$

Substituting Equations 5.44 and 5.45 into 5.47 results in,

$$d\Delta T = -d\dot{Q} \left(\frac{1}{\dot{C}_h} + \frac{1}{\dot{C}_c} \right) \quad (5.48)$$

Substituting Equation 5.46 into 5.48 and rearranging gives,

$$\frac{d\Delta T}{\Delta T} = -U \left(\frac{1}{\dot{C}_h} + \frac{1}{\dot{C}_c} \right) dA \quad (5.49)$$

This equation can be integrated from the inlet to the outlet of the heat exchanger,

$$\int_{in}^{out} \frac{d\Delta T}{\Delta T} = -U \left(\frac{1}{\dot{C}_h} + \frac{1}{\dot{C}_c} \right) \int_{in}^{out} dA \quad (5.50)$$

Performing the integration gives,

$$\ln \left(\frac{\Delta T_{out}}{\Delta T_{in}} \right) = -UA \left(\frac{1}{\dot{C}_h} + \frac{1}{\dot{C}_c} \right) \quad (5.51)$$

The thermodynamic energy balances, Equations 5.40 and 5.41 can be substituted into this equation resulting in,

$$\ln\left(\frac{\Delta T_{out}}{\Delta T_{in}}\right) = -\frac{UA}{\dot{Q}}[(T_{hi} - t_{ci}) - (T_{ho} - t_{co})] = -\frac{UA}{\dot{Q}}(\Delta T_{in} - \Delta T_{out}) \quad (5.52)$$

Solving this equation for the heat transfer rate reveals the form of the LMTD,

$$\dot{Q} = UA \left[\frac{\Delta T_{out} - \Delta T_{in}}{\ln(\Delta T_{out}/\Delta T_{in})} \right] \quad (5.53)$$

Comparing Equations 5.43 and 5.53, it can be seen that the LMTD is given by,

$$\text{LMTD} = \frac{\Delta T_{out} - \Delta T_{in}}{\ln(\Delta T_{out}/\Delta T_{in})} = \frac{\Delta T_{in} - \Delta T_{out}}{\ln(\Delta T_{in}/\Delta T_{out})} \quad (5.54)$$

Equation 5.54 shows that the LMTD is a function of the inlet and outlet temperatures of the hot and cold fluids. This equation was developed for the parallel flow heat exchanger. However, it is valid for counter flow heat exchangers as well. To apply Equation 5.54 to a counter flow heat exchanger, the inlet and outlet of the heat exchanger need to be defined. This may seem problematic since on one side where a fluid is entering, the other fluid exits as seen in Figure 5.11. This confusion is easily resolved by simply calling one end of the heat exchanger the *inlet* and the other end the *outlet*. Once the “ends” of the counter flow heat exchanger are specified, the temperature differences for the LMTD can be formed, as shown in Figure 5.13.

Example 5.4

A heat exchanger is being used to transfer heat between water and a 20% ethylene glycol solution. The ethylene glycol solution enters the heat exchanger at 150 gpm with a temperature of 20°F and exits at 40°F. The water enters the heat exchanger at 130 gpm

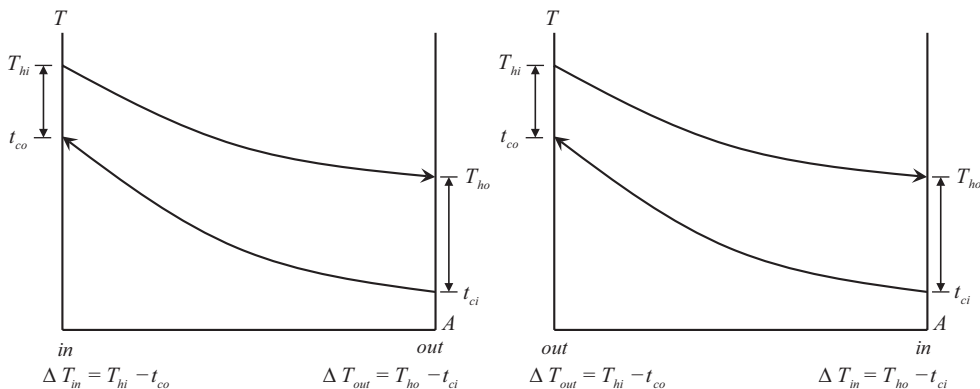


FIGURE 5.13

Possible definitions of ΔT_{out} and ΔT_{in} for a counter flow heat exchanger.

at a temperature of 80°F. A heat transfer analysis reveals that the overall heat transfer coefficient of the heat exchanger is 400 Btu/hr-ft²-°F. Determine the heat transfer area required for a,

- Parallel flow heat exchanger
- Counter flow heat exchanger

Solution

The area of the heat exchanger is unknown. Therefore, this is a heat exchanger design problem. The area can be determined using solving Equation 5.43,

$$A = \frac{\dot{Q}}{U(\text{LMTD})}$$

The heat transfer rate can be found from the cold fluid (the ethylene glycol solution),

$$\dot{Q} = \dot{C}_c(t_{co} - t_{ci})$$

The thermal capacity rate of the cold fluid is given by,

$$\dot{C}_c = \dot{m}_c c_{pc} = \rho_c \dot{V}_c c_{pc}$$

At this point, a decision needs to be made about what temperature should be used to evaluate the properties. Strictly speaking, the density should be evaluated at the inlet condition since the volumetric flow rate is given at that point and volumetric flow is not a conserved quantity. However, the variation in the liquid density is very small over the temperature range considered here. Therefore, volume flow rate can be considered conserved and the average value of the density will be used as well as the average value of the heat capacity. Interpolating in Appendix B.4, the properties of the 20% ethylene glycol mixture are found to be,

$$t_{c,avg} = \frac{t_{ci} + t_{co}}{2} = \frac{(20 + 40)^\circ\text{F}}{2} = 30^\circ\text{F} \quad \rho_c = 64.247 \frac{\text{lbm}}{\text{ft}^3} \quad c_{pc} = 0.92169 \frac{\text{Btu}}{\text{lbm-R}}$$

Therefore, the thermal capacity rate of the cold fluid and the heat transfer rate are,

$$\begin{aligned} \dot{C}_c &= \rho_c \dot{V}_c c_{pc} = \left(64.247 \frac{\text{lbm}}{\text{ft}^3} \right) \left(150 \frac{\text{gal}}{\text{min}} \right) \left(0.92169 \frac{\text{Btu}}{\text{lbm-R}} \right) \left(8.02083 \frac{\text{ft}^3}{\text{hr gal}} \right) = 71,244 \frac{\text{Btu}}{\text{hr-R}} \\ \therefore \dot{Q} &= \dot{C}_c(t_{co} - t_{ci}) = \left(71,244 \frac{\text{Btu}}{\text{hr-R}} \right) (40 - 20) \text{ R} = 1.4249 \times 10^6 \frac{\text{Btu}}{\text{hr}} \end{aligned}$$

Appendix A

The LMTD requires both sets of inlet and outlet temperatures. In this case, only three of the temperatures are known. The hot fluid outlet temperature is not

specified. However, it can be calculated by applying the conservation of energy to the hot fluid,

$$\dot{Q} = \dot{C}_h (T_{hi} - T_{ho}) \rightarrow T_{ho} = T_{hi} - \frac{\dot{Q}}{\dot{C}_h}$$

The hot fluid's thermal capacity rate is given by,

$$\dot{C}_h = \dot{m}_h c_{ph} = \rho_h \dot{V}_h c_{ph}$$

The hot fluid outlet temperature is unknown at this point. Therefore, as a first estimate, the known inlet temperature will be used to estimate the properties. From Appendix B.3, for water at 80°F,

$$\rho_h = 62.213 \frac{\text{lbm}}{\text{ft}^3} \quad c_{pc} = 0.99928 \frac{\text{Btu}}{\text{lbm-R}}$$

Therefore, the thermal capacity rate and outlet temperature of the hot fluid are,

$$\dot{C}_h = \rho_h \dot{V}_h c_{ph} = \left(62.213 \frac{\text{lbm}}{\text{ft}^3} \right) \left(130 \frac{\text{gal}}{\text{min}} \right) \left(0.99928 \frac{\text{Btu}}{\text{lbm-R}} \right) \left(8.02083 \frac{\text{ft}^3}{\text{hr}} \frac{\text{min}}{\text{gal}} \right) = 64,823 \frac{\text{Btu}}{\text{hr-R}}$$

Appendix A

$$\therefore T_{ho} = T_{hi} - \frac{\dot{Q}}{\dot{C}_h} = 80^\circ\text{F} - \frac{1.4249 \times 10^6 \frac{\text{Btu}}{\text{hr}}}{64,823 \frac{\text{Btu}}{\text{hr-}^\circ\text{F}}} = 58.0^\circ\text{F}$$

The value of the LMTD depends on the type of heat exchanger; parallel flow (PF) or counter flow (CF). For each of these configurations,

$$\text{LMTD}_{\text{PF}} = \frac{\Delta T_{\text{out}} - \Delta T_{\text{in}}}{\ln(\Delta T_{\text{out}}/\Delta T_{\text{in}})} = \frac{(T_{ho} - t_{co}) - (T_{hi} - t_{ci})}{\ln[(T_{ho} - t_{co})/(T_{hi} - t_{ci})]} = 35.4^\circ\text{R}$$

$$\text{LMTD}_{\text{CF}} = \frac{\Delta T_{\text{out}} - \Delta T_{\text{in}}}{\ln(\Delta T_{\text{out}}/\Delta T_{\text{in}})} = \frac{(T_{ho} - t_{ci}) - (T_{hi} - t_{co})}{\ln[(T_{ho} - t_{ci})/(T_{hi} - t_{co})]} = 39.0^\circ\text{R}$$

Now, the required heat exchanger can be found for each flow configuration,

$$A_{\text{PF}} = \frac{\dot{Q}}{U(\text{LMTD}_{\text{PF}})} = W \frac{1.4249 \times 10^6 \frac{\text{Btu}}{\text{hr}}}{\left(400 \frac{\text{Btu}}{\text{hr-ft-R}} \right) (34.9^\circ\text{R})} = \underline{102.1 \text{ ft}^2}$$

$$A_{\text{CF}} = \frac{\dot{Q}}{U(\text{LMTD}_{\text{CF}})} = \frac{1.4249 \times 10^6 \frac{\text{Btu}}{\text{hr}}}{\left(400 \frac{\text{Btu}}{\text{hr-ft-R}} \right) (39.0^\circ\text{R})} = \underline{91.3 \text{ ft}^2}$$

These values were calculated by evaluating the hot fluid properties at the inlet temperature (80°F). Based on the calculations above, the outlet temperature is 58.0°F which makes the average temperature of the hot fluid 69°F. To be more accurate, the properties of the hot fluid should be evaluated again at 69°F and the areas recalculated. Clearly, this is an iterative problem, well-suited for computer software. The solution, using computer software, showing the key variables is,

$$\begin{array}{ll}
 T_{ho} = 58.050^{\circ}\text{F} & T_{h,avg} = 69.025^{\circ}\text{F} \\
 \rho_h = 62.306 \frac{\text{lbm}}{\text{ft}^3} & c_{p,h} = 0.99932 \frac{\text{Btu}}{\text{lbm-R}} \\
 \dot{C}_h = 64,923 \frac{\text{Btu}}{\text{h-R}} & \dot{Q} = 1,425,043 \frac{\text{Btu}}{\text{h}} \\
 \text{LMTD}_{PF} = 34.924 \text{ R} & \text{LMTD}_{CF} = 39.017 \text{ R} \\
 A_{PF} = \underline{102.01 \text{ ft}^2} & A_{CF} = \underline{91.309 \text{ ft}^2}
 \end{array}$$

It is interesting to note that the iterative solution produced results that are nearly the same as the solution that was developed above. This is because the temperature difference in the hot fluid is relatively small, and the properties do not change much since it is a liquid. If the temperature difference is large enough to affect a significant change in properties, and computer software is not being used, then it is recommended that at least one iteration be performed.

5.6.4 The LMTD Heat Exchanger Model

In Section 5.6.3, it was shown that thermodynamics *and* heat transfer combine to form a mathematical model of a heat exchanger. Whether the heat exchanger problem is a design or analysis, the complete mathematical description of the heat exchanger is embodied in three equations. For a heat exchanger where both fluids remain in the single phase, the LMTD heat exchanger model can be written as,

$$\begin{aligned}
 \dot{Q} &= \dot{C}_h(T_{hi} - T_{ho}) \\
 \dot{Q} &= \dot{C}_c(t_{co} - t_{ci}) \\
 \dot{Q} &= UA(\text{LMTD})
 \end{aligned} \tag{5.55}$$

While this set of equations seems relatively simple, the complexity can quickly become overwhelming because of the need to determine the overall heat transfer coefficient, U . Subsequent sections of this chapter will present the detailed calculation of U for the various types of heat exchangers discussed in Section 5.5. An added level of complexity is the iterative nature of the problem due to unknown temperatures as shown in Example 5.5.

Example 5.5

Liquid hexane flows through a counter flow heat exchanger at 5 m³/h as shown in Figure E5.5. The hexane enters the heat exchanger at 90°C. Water, flowing at 5 m³/h, is used to cool the hexane. The water enters the heat exchanger at 15°C. The UA product of the heat exchanger is found to be 2.7 kW/K. Determine the outlet temperatures of the hot and cold fluids and the heat transfer rate between them.

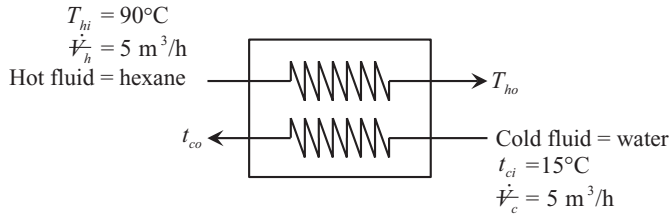


FIGURE E5.5
Counter flow heat exchanger using water to cool a flow of hexane.

Solution

This is a heat exchanger *analysis* problem. The heat exchanger is specified and has been analyzed using a heat transfer analysis. Therefore, the UA product for the heat exchanger is known. The solution to this problem is iterative because neither of the fluid outlet temperatures is known. In addition, the properties are evaluated at the average temperature of the fluid which introduces another level of iteration. Therefore, a problem like this is best solved using computer software. The equations required to solve this analysis problem are presented in the following development.

The temperatures T_{ho} and t_{co} are unknown. Therefore, using computer software, they will be guessed, either internally within the software or user-provided. Once these guesses are provided, the average temperature of each fluid can be determined,

$$T_{h,avg} = \frac{T_{hi} + T_{ho}}{2} \quad t_{c,avg} = \frac{t_{ci} + t_{co}}{2}$$

Since the fluids are both liquid, their properties can be estimated at the saturated liquid state,

$$\begin{aligned} \rho_h &= \rho(T_{h,avg}, x = 1) & c_{p,c} &= c_p(T_{h,avg}, x = 1) \\ \rho_c &= \rho(t_{c,avg}, x = 1) & c_{p,c} &= c_p(t_{c,avg}, x = 1) \end{aligned}$$

This set of equations indicates that the computer software used must be capable of calculating thermophysical properties as needed. The volumetric flow rate of each fluid is given. This allows for the calculation of the thermal capacity rate of each fluid,

$$\dot{C}_h = \rho_h \dot{V}_h c_{p,h} \quad \dot{C}_c = \rho_c \dot{V}_c c_{p,c}$$

Knowledge of the inlet and outlet temperatures also allows for the calculation of the LMTD for the heat exchanger,

$$\begin{aligned} \Delta T_{in} &= T_{hi} - t_{co} & \Delta T_{out} &= T_{ho} - t_{ci} \\ \text{LMTD} &= \frac{\Delta T_{in} - \Delta T_{out}}{\ln(\Delta T_{in}/\Delta T_{out})} \end{aligned}$$

To complete the analysis, the LMTD heat exchanger model must be satisfied,

$$\begin{aligned}\dot{Q} &= \dot{C}_h (T_{hi} - T_{ho}) \\ \dot{Q} &= \dot{C}_c (t_{co} - t_{ci}) \\ \dot{Q} &= UA(\text{LMTD})\end{aligned}$$

Solving this set of equations using computer software results in,

$$T_{ho} = 39.9^\circ\text{C} \quad t_{co} = 33.0^\circ\text{C} \quad \dot{Q} = 104.5 \text{ kW}$$

Each software package uses its own internal solver algorithms. Sometimes these algorithms are quite robust and can solve a complex set of equations. However, in some cases, algorithms may fail as they work to find a solution. The LMTD heat exchanger model can be particularly problematic for solvers because the LMTD contains a natural logarithm. To resolve this issue, it is often convenient to algebraically rearrange Equation 5.54 as,

$$\Delta T_{out} = \Delta T_{in} \exp\left(\frac{\Delta T_{out} - \Delta T_{in}}{\text{LMTD}}\right) \quad (5.56)$$

This rearrangement eliminates the natural logarithm and introduces an exponential. Equations of this type are less prone to failure using computer software.

As shown in this section, the analysis of a heat exchanger using the LMTD model is iterative because the outlet temperatures of the fluids are unknown. A further level of iteration is required to determine the thermophysical properties of the fluids (evaluated at the average temperature). Although this heat exchanger model is valid, many engineers prefer a method that can be solved using a calculator and not rely on computer software. The next section describes such a method.

5.6.5 The Effectiveness-NTU Heat Exchanger Model

The effectiveness-NTU (ϵ -NTU) method was developed to eliminate the iterative nature of the LMTD method. The *effectiveness*, ϵ , of a heat exchanger is defined in Section 3.7.3 and defined as the ratio of the actual heat transfer rate in the heat exchanger to the maximum possible heat transfer rate (i.e., when the pinch point temperature difference goes to zero),

$$\epsilon = \frac{\dot{Q}}{\dot{Q}_{\max}} \quad (5.57)$$

The maximum possible heat transfer rate would occur in an infinitely large heat exchanger. In this case, one of the fluids would experience the maximum possible temperature change, $(T_{hi} - t_{ci})$. Section 3.7.3.1 presents the analysis to show that the fluid with the minimum thermal capacity rate will experience this maximum temperature difference,

$$\dot{Q}_{\max} = \dot{C}_{\min} (T_{hi} - t_{ci}) \quad (5.58)$$

Therefore, the effectiveness of the heat exchanger can be written in one of two ways,

$$\varepsilon = \frac{\dot{C}_h(T_{hi} - T_{ho})}{\dot{C}_{\min}(T_{hi} - t_{ci})} = \frac{\dot{C}_c(t_{co} - t_{ci})}{\dot{C}_{\min}(T_{hi} - t_{ci})} \quad (5.59)$$

NTU is an acronym for the *number of transfer units*. The NTU is a dimensionless parameter defined by,

$$\text{NTU} = \frac{UA}{\dot{C}_{\min}} \quad (5.60)$$

For any heat exchanger, it has been shown that (Kays and London 1998),

$$\varepsilon = f(\text{NTU}, C_r) \quad \text{where} \quad C_r = \frac{\dot{C}_{\min}}{\dot{C}_{\max}} \quad (5.61)$$

The specific functional relationship is dependent on the type of heat exchanger (e.g., parallel flow, counter flow, etc.). The ε -NTU relationship for a particular heat exchanger can be derived from the LMTD model as shown in the following example.

Example 5.6

Determine the ε -NTU relationship for a parallel flow heat exchanger.

Solution

Consider the case where $\dot{C}_c = \dot{C}_{\min}$. For this scenario, Equation 5.59 can be written as,

$$\varepsilon = \frac{\dot{C}_c(t_{co} - t_{ci})}{\dot{C}_{\min}(T_{hi} - t_{ci})} = \frac{t_{co} - t_{ci}}{T_{hi} - t_{ci}}$$

The ratio of the thermal capacity rates can be written as,

$$C_r = \frac{\dot{C}_{\min}}{\dot{C}_{\max}} = \frac{\dot{Q}}{(t_{co} - t_{ci})} \frac{(T_{hi} - T_{ho})}{\dot{Q}} = \frac{T_{hi} - T_{ho}}{t_{co} - t_{ci}}$$

Solving this equation for the hot fluid outlet temperature gives,

$$T_{ho} = T_{hi} - C_r(t_{co} - t_{ci})$$

In the development of the LMTD for the parallel flow heat exchanger, Equation 5.51 states that,

$$\ln\left(\frac{\Delta T_{out}}{\Delta T_{in}}\right) = -UA\left(\frac{1}{\dot{C}_h} + \frac{1}{\dot{C}_c}\right)$$

For the parallel flow heat exchanger with cold fluid having the minimum thermal capacity rate for the cold fluid, this equation becomes,

$$\ln \left(\frac{T_{ho} - t_{co}}{T_{hi} - t_{ci}} \right) = -UA \left(\frac{1}{\dot{C}_{\max}} + \frac{1}{\dot{C}_{\min}} \right)$$

This equation can be algebraically rearranged to the following form,

$$\frac{T_{ho} - t_{co}}{T_{hi} - t_{ci}} = \exp \left[-\frac{UA}{\dot{C}_{\min}} \left(\frac{\dot{C}_{\min}}{\dot{C}_{\max}} + 1 \right) \right] = \exp[-NTU(1 + C_r)]$$

The ratio of temperature differences on the left-hand side of this equation can be algebraically manipulated after substituting the expression for T_{ho} from above,

$$\begin{aligned} \frac{T_{ho} - t_{co}}{T_{hi} - t_{ci}} &= \frac{[T_{hi} - C_r(t_{co} - t_{ci})] - t_{co} + (t_{ci} - t_{ci})}{T_{hi} - t_{co}} \\ &= \frac{(T_{hi} - t_{ci}) - C_r(t_{co} - t_{ci}) - (t_{co} - t_{ci})}{T_{hi} - t_{co}} \\ &= 1 - C_r \frac{t_{co} - t_{ci}}{T_{hi} - t_{co}} - \frac{t_{co} - t_{ci}}{T_{hi} - t_{co}} \end{aligned}$$

The temperature ratios on the right-hand side of this equation are the effectiveness of the heat exchanger. Therefore,

$$\frac{T_{ho} - t_{co}}{T_{hi} - t_{ci}} = 1 - \varepsilon C_r - \varepsilon = 1 - \varepsilon(1 + C_r)$$

Substitution of this equation into the equation that contains the NTU results in,

$$1 - \varepsilon(1 + C_r) = \exp[-NTU(1 + C_r)]$$

Solving this equation for the effectiveness gives the ε -NTU relationship,

$$\varepsilon = \frac{1 - \exp[-NTU(1 + C_r)]}{1 + C_r}$$

This equation was developed assuming that the cold fluid has the minimum thermal capacity rate. However, the same result would be found if the hot fluid has the minimum thermal capacity rate. Therefore, this expression reveals the functional relationship, Equation 5.61, for a parallel flow heat exchanger.

Example 5.6 demonstrates that the ε -NTU expressions are derived from the LMTD. ε -NTU expressions can be derived in a similar way for many other heat exchanger types. Table 5.3 shows the result of the ε -NTU relationships derived from the LMTD analysis for several different types of heat exchangers (Kays and London 1998). Some of these expressions can be complex to carry out with a calculator. However, plots of these equations can

TABLE 5.3 ε -NTU Relationships for Several Heat Exchanger Types

Heat Exchanger Type	ε -NTU Relationship
Counter flow	$\varepsilon = \frac{1 - \exp[-NTU(1 - C_r)]}{1 - C_r \exp[-NTU(1 - C_r)]} \quad C_r < 1$ $\varepsilon = \frac{NTU}{1 + NTU} \quad C_r = 1 \text{ (regenerative HX)}$
Parallel flow	$\varepsilon = \frac{1 - \exp[-NTU(1 + C_r)]}{1 + C_r}$
Shell and tube with one shell pass and an even number of tube passes	$\varepsilon = 2 \left\{ 1 + C_r + \sqrt{1 + C_r^2} \frac{1 + \exp \left[\frac{-NTU \sqrt{1 + C_r^2}}{1 - \exp \left[-NTU \sqrt{1 + C_r^2} \right]} \right]}{1 - \exp \left[-NTU \sqrt{1 + C_r^2} \right]} \right\}^{-1}$
Cross flow with both fluids unmixed	$\varepsilon = 1 - \exp \left[\left(\frac{1}{C_r} \right) (NTU)^{0.23} \left(\exp[-C_r (NTU)^{0.73}] - 1 \right) \right]$
Cross flow with \dot{C}_{\max} mixed and \dot{C}_{\min} unmixed	$\varepsilon = \frac{1}{C_r} \left\{ 1 - \exp \left[-C_r (1 - \exp(-NTU)) \right] \right\}$
Cross flow with \dot{C}_{\min} mixed, \dot{C}_{\max} unmixed	$\varepsilon = 1 - \exp \left\{ -\frac{1}{C_r} \left[1 - \exp(-C_r (NTU)) \right] \right\}$
Boilers, evaporators, and condensers $\dot{C}_r = 0$	$\varepsilon = 1 - \exp(-NTU)$

be drawn which make the ε -NTU calculation easier. Figures 5.16 through 5.19 show the ε -NTU plots for several heat exchanger types.

In Table 5.3, the ε -NTU relationship for the cross flow heat exchanger with both fluids unmixed is an empirical correlation. This empiricism was developed because the analytical ε -NTU relationship is an infinite series (Mason 1954). The functional form of the empirical relationship is taken from Bergman et al. (2011). The NTU exponents were determined by fitting the ε -NTU heat exchanger data from Kays and London (1998) for the ranges $0.25 \leq C_r \leq 1.0$ and $0.25 \leq NTU \leq 7$. The resulting NTU coefficients are slightly different than values shown in Bergman et al. (2011). This is because the NTU exponents provided in Bergman et al. (2011) are valid only for a value of $C_r = 1$.

Using the effectiveness and NTU concepts, the ε -NTU heat exchanger model can be summarized in the following set of equations,

$$\begin{aligned}
 \dot{Q} &= \dot{C}_h (T_{hi} - T_{ho}) \\
 \dot{Q} &= \dot{C}_c (t_{co} - t_{ci}) \\
 \varepsilon &= \frac{\dot{Q}}{\dot{Q}_{\max}} \quad \text{where } \varepsilon = f(NTU, C_r)
 \end{aligned} \tag{5.62}$$

Comparing the ε -NTU model to the LMTD model reveals that the LMTD equation is replaced by two equations; one defining the effectiveness of the heat exchanger and the other defining the ε -NTU relationship.

The following example demonstrates that the ε -NTU does not require an iterative solution for a heat exchanger analysis problem.

Example 5.7

Determine the fluid outlet temperatures and the heat transfer rate for the counter flow heat exchanger described in Example 5.5 using the ε -NTU model. Assume that the properties can be evaluated at the given fluid inlet temperatures. Compare the results to the LMTD model solution.

Solution

The effectiveness of a counter flow heat exchanger can be found using the ε -NTU equation found in Table 5.3 or from Figure 5.15. The effectiveness equation will be used here for more accuracy,

$$\varepsilon = \frac{1 - \exp[-NTU(1 - C_r)]}{1 - C_r \exp[-NTU(1 - C_r)]}$$

The NTU and C_r values are needed. They are defined as,

$$NTU = \frac{UA}{\dot{C}_{\min}} \quad C_r = \frac{\dot{C}_{\min}}{\dot{C}_{\max}}$$

In order to determine which fluids have the maximum and minimum thermal capacity rates, the properties of each fluid are required. Evaluating the properties at the inlet temperature of each fluid (Appendix B.3),

$$\text{Hot Fluid: hexane} \quad \rho_h = 591.12 \text{ kg/m}^3 \quad c_{ph} = 2.5628 \text{ kJ/kg-K}$$

$$\text{Cold Fluid: water} \quad \rho_c = 999.06 \text{ kg/m}^3 \quad c_{pc} = 4.1888 \text{ kJ/kg-K}$$

This allows for the calculation of the thermal capacity rate for each fluid,

$$\begin{aligned} \dot{C}_h &= \rho_h \dot{V} c_{ph} = \left(591.12 \frac{\text{kg}}{\text{m}^3} \right) \left(5 \frac{\text{m}^3}{\text{h}} \right) \left(2.5628 \frac{\text{kJ}}{\text{kg-K}} \right) \left(\frac{\text{h}}{3600 \text{ s}} \right) \\ \text{Hot Fluid: hexane} \quad &= 2.1041 \frac{\text{kW}}{\text{K}} \\ \dot{C}_c &= \rho_c \dot{V} c_{pc} = \left(999.06 \frac{\text{kg}}{\text{m}^3} \right) \left(5 \frac{\text{m}^3}{\text{h}} \right) \left(4.1888 \frac{\text{kJ}}{\text{kg-K}} \right) \left(\frac{\text{h}}{3600 \text{ s}} \right) \\ \text{Cold Fluid: water} \quad &= 5.8123 \frac{\text{kW}}{\text{K}} \end{aligned}$$

From this calculation, it can be seen that,

$$\dot{C}_{\min} = 2.1041 \frac{\text{kW}}{\text{K}} \quad \dot{C}_{\max} = 5.8123 \frac{\text{kW}}{\text{K}} \quad \therefore C_r = \frac{2.1041 \text{ kW/K}}{5.8123 \text{ kW/K}} = 0.36201$$

Once the minimum thermal capacity rate is found, the NTU can be calculated,

$$\text{NTU} = \frac{UA}{\dot{C}_{\min}} = \frac{2.7 \text{ kW/K}}{2.1041 \text{ kW/K}} = 1.2832$$

Now, the effectiveness of the heat exchanger can be found,

$$\varepsilon = \frac{1 - \exp[-\text{NTU}(1 - C_r)]}{1 - C_r \exp[-\text{NTU}(1 - C_r)]} = \frac{1 - \exp[-(1.2832)(1 - 0.36201)]}{1 - (0.36201)\exp[-(1.2832)(1 - 0.36201)]} = 0.66518$$

The maximum possible heat transfer rate can be found since both inlet temperatures are known and the value of the minimum thermal capacity rate has been found,

$$\dot{Q}_{\max} = \dot{C}_{\min} (T_{hi} - t_{ci}) = \left(2.1041 \frac{\text{kW}}{\text{K}} \right) (90 - 150) \text{ K} = 157.81 \text{ kW}$$

Knowing the effectiveness of the heat exchanger and the maximum possible heat transfer rate allows for the calculation of the actual heat transfer rate between the fluids,

$$\varepsilon = \frac{\dot{Q}}{\dot{Q}_{\max}} \rightarrow \dot{Q} = \varepsilon \dot{Q}_{\max} = (0.66518)(157.81 \text{ kW}) = \underline{104.97 \text{ kW}}$$

Once the heat transfer rate is found, the outlet temperatures can be determined using the conservation of energy equation applied to each fluid stream,

$$\begin{aligned} \dot{Q} &= \dot{C}_h (T_{hi} - T_{ho}) \rightarrow T_{ho} = T_{hi} - \frac{\dot{Q}}{\dot{C}_h} = 90^\circ\text{C} - \frac{104.97 \text{ kW}}{2.1041 \text{ kW/K}} = \underline{40.1^\circ\text{F}} \\ \dot{Q} &= \dot{C}_c (t_{co} - t_{ci}) \rightarrow t_{co} = t_{ci} + \frac{\dot{Q}}{\dot{C}_c} = 15^\circ\text{C} + \frac{104.97 \text{ kW}}{5.8123 \text{ kW/K}} = \underline{33.1^\circ\text{F}} \end{aligned}$$

Notice that this calculation was done without iteration. It can be easily done on a desktop using pencil, paper, and a calculator. Recall that this solution was done by evaluating the properties at the *inlet* temperature of the fluids. This set of equations can also be programmed into an equation solver and iteration on the properties can be accomplished if a more accurate result is desired. Table E5.7 shows the result of the calculations for this example problem.

Notice that the error introduced by using the inlet temperatures is very small for this analysis. The NTU method predicts a heat transfer rate that is 0.48% high, the hot and cold fluid outlet temperatures are over predicted by 0.2 and 0.1 degrees, respectively. This demonstrates that a reasonable solution can be obtained using the inlet fluid

temperatures in an ε -NTU analysis problem. The complete procedure can be done on a desktop using pencil, paper, and a calculator.

If more accuracy is desired, the ε -NTU analysis can be programmed into computer software to iterate on the properties. If this is done, the results are identical to the LMTD model as shown in Table E5.7. This is to be expected, since the ε -NTU method is derived directly from the LMTD analysis.

Table 5.3 shows the ε -NTU relations derived from the LMTD analysis. These equations are well suited for heat exchanger analysis problems. However, when performing heat exchanger design calculations, it may be more convenient to work with relationships of the form,

$$NTU = f(\varepsilon, C_r) \quad (5.63)$$

These NTU-explicit functions are shown in Table 5.4. These equations provide improved accuracy compared to reading ε -NTU plots such as those shown in Figures 5.14 through 5.17.

TABLE E5.7

Summary of Results

Parameter	LMTD Model	ε -NTU Model ^a	ε -NTU Model ^b
Heat Transfer Rate	104.5 kW	105.0 Btu/hr	104.5 kW
Hot Fluid Outlet Temperature	39.9°C	40.1°C	39.9°C
Cold Fluid Outlet Temperature	33.0°C	33.1°C	33.0°C

^a No iteration on properties; Solved "by hand" using the inlet temperatures to evaluate properties.

^b Solved in MS Excel to iterate on properties.

TABLE 5.4

NTU- ε Relationships for Several Heat Exchanger Types

Heat Exchanger Type	NTU- ε Relationship
Counter flow	$NTU = \frac{1}{C_r - 1} \ln \left(\frac{\varepsilon - 1}{\varepsilon C_r - 1} \right) \quad C_r < 1$ $NTU = \frac{\varepsilon}{1 - \varepsilon} \quad C_r = 1 \text{ (regenerative HX)}$
Parallel flow	$NTU = -\frac{\ln[1 - \varepsilon(1 + C_r)]}{1 + C_r}$
Shell and tube with one shell pass and an even number of tube passes	$NTU = -(1 + C_r^2)^{-1/2} \ln \left(\frac{\Gamma - 1}{\Gamma + 1} \right) \quad \Gamma = \frac{2/\varepsilon - (1 + C_r)}{\sqrt{(1 + C_r^2)}}$
Cross flow with \dot{C}_{\max} mixed and \dot{C}_{\min} unmixed	$NTU = -\ln \left[1 + \left(\frac{1}{C_r} \right) \ln(1 - \varepsilon C_r) \right]$
Cross flow with \dot{C}_{\min} mixed, \dot{C}_{\max} unmixed	$NTU = -\left(\frac{1}{C_r} \right) \ln[C_r \ln(1 - \varepsilon) + 1]$
Boilers, evaporators, and condensers $C_r = 0$	$NTU = -\ln(1 - \varepsilon)$

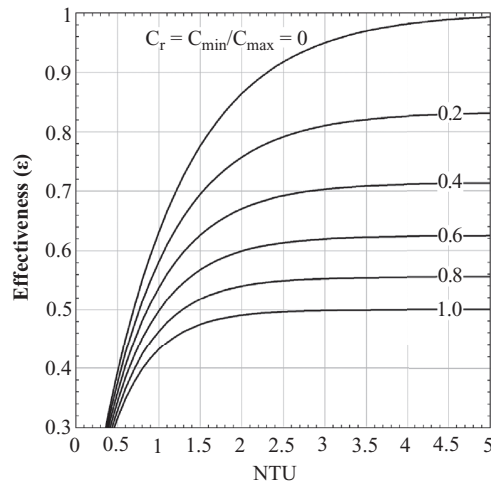


FIGURE 5.14
 ϵ -NTU plot for a parallel flow heat exchanger.

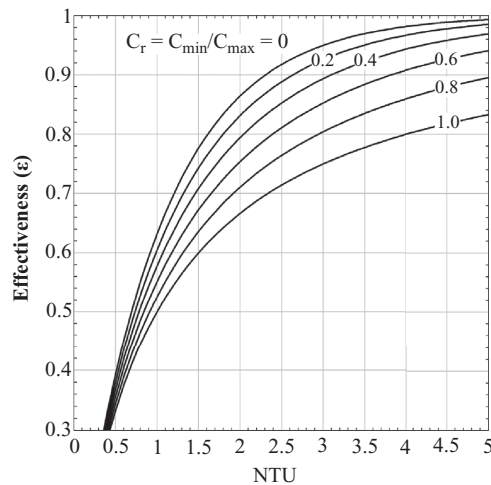


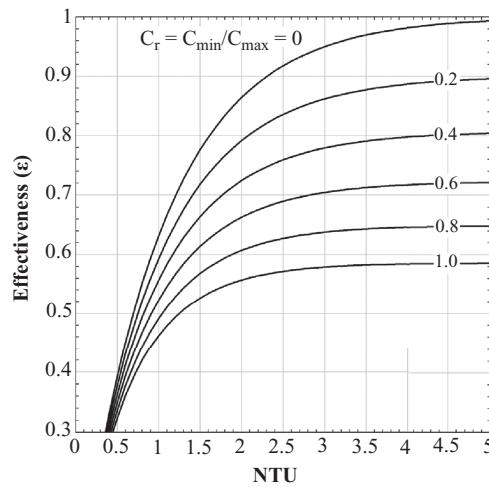
FIGURE 5.15
 ϵ -NTU plot for a counter flow heat exchanger.

5.7 Special Application Heat Exchangers

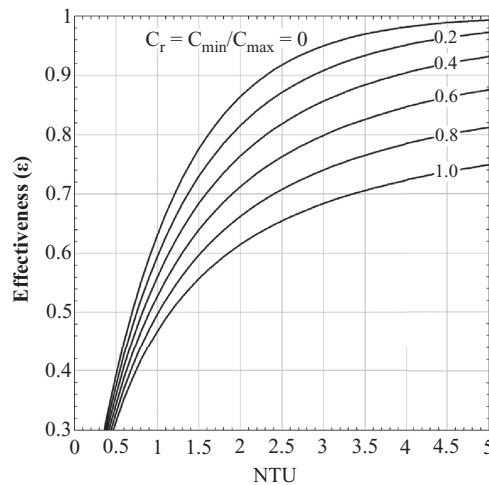
The LMTD and ϵ -NTU heat exchanger models in Sections 5.6.4 and 5.6.5 discussed above are valid for many different types of heat exchangers and working fluids. However, there are special cases where these models may be simplified.

5.7.1 The Counter Flow Regenerative Heat Exchanger

Tables 5.3 and 5.4 show two entries for ϵ -NTU and NTU- ϵ functions for counter flow heat exchangers. One equation is for $C_r < 1$ and the other equation is for $C_r = 1$. If $C_r = 1$ both

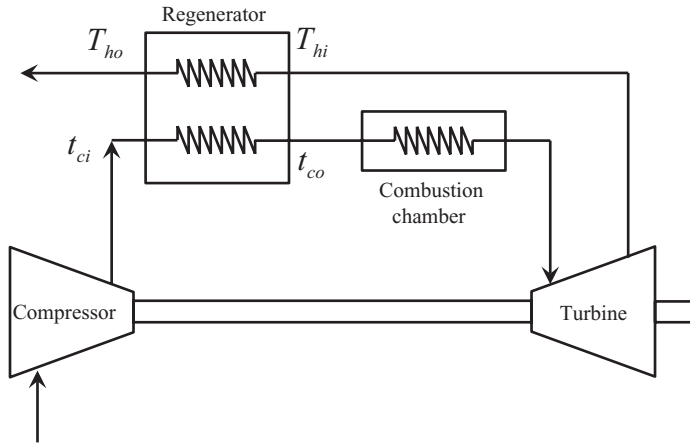
**FIGURE 5.16**

ϵ -NTU plot for a shell and tube heat exchanger and 2, 4, ..., n tube passes.

**FIGURE 5.17**

ϵ -NTU plot for a cross flow heat exchanger with both fluids unmixed.

fluids have the same thermal capacity rate. It is possible for this situation to occur with two different fluids, but it is rather coincidental. However, this situation can occur in a heat exchanger where both hot and cold fluids are the same and they have the same mass flow rate. A common type of heat exchanger where this can occur is a *regenerative* heat exchanger. An example of a regenerative heat exchanger used in a gas turbine cycle is shown in Figure 5.18. In this figure, the heat exchanger labeled “regenerator” is a counter flow regenerative heat exchanger. In the cycle shown in Figure 5.18, the purpose of the regenerator is to pre-heat the air entering the combustion chamber by utilizing otherwise-wasted hot turbine

**FIGURE 5.18**

A gas turbine cycle with a regenerative heat exchanger.

exhaust gases. The result is a reduction in fuel requirement for the same power output resulting in an increased thermal efficiency.

In the gas turbine cycle depicted in Figure 5.18, the fluid leaving the turbine is a mixture of combustion gases while air leaves the compressor. Therefore, the two fluids in the regenerator are different and they are at different temperatures. However, recall that the *air standard* gas turbine models are based on the assumption that the working fluid is air throughout and the flow rate of the fuel is considered negligible compared to the air flow rate. Furthermore, if the *cold air standard* model is used, the heat capacity of the air is assumed constant throughout the cycle. Therefore, if a cold air standard assumption is used to analyze the gas turbine shown in Figure 5.18, then the thermal capacity rates of the hot and cold fluids in the regenerator are identical which means that $C_r = 1$.

Using the ϵ -NTU heat exchanger model to analyze or design a counter flow regenerative heat exchanger is a relatively simple matter since ϵ -NTU and NTU- ϵ equations have been developed for the counter flow heat exchanger with $C_r = 1$, as shown in Tables 5.3 and 5.4. However, it is interesting to see how the LMTD model is impacted for this special situation.

Consider the regenerative heat exchanger in the gas turbine cycle shown in Figure 5.18. For the counter flow heat exchanger, the LMTD is defined as,

$$\text{LMTD} = \frac{\Delta T_{out} - \Delta T_{in}}{\ln(\Delta T_{out}/\Delta T_{in})} = \frac{(T_{hi} - t_{co}) - (T_{ho} - t_{ci})}{\ln[(T_{hi} - t_{co})/(T_{ho} - t_{ci})]} \quad (5.64)$$

The heat transfer rate between the two fluid streams is the same. Therefore,

$$\dot{C}_h(T_{hi} - T_{ho}) = \dot{C}_c(t_{co} - t_{ci}) \quad (5.65)$$

Since the heat capacity rates are constant in the cold air standard analysis of the gas turbine cycle, Equation 5.65 becomes,

$$T_{hi} - T_{ho} = t_{co} - t_{ci} \quad (5.66)$$

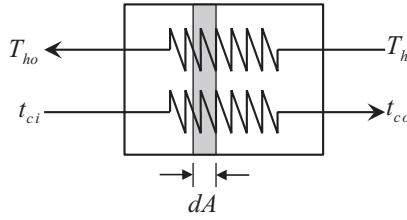


FIGURE 5.19
Differential analysis of a regenerative heat exchanger.

This equation can be algebraically rearranged to consider the temperature differences on each end of the regenerative heat exchanger,

$$T_{hi} - t_{co} = T_{ho} - t_{ci} \quad (5.67)$$

Equation 5.67 indicates that the temperature difference on each end of the heat exchanger is the same. Therefore, the LMTD becomes undefined (0/0). This means that the LMTD cannot be calculated for this type of a heat exchanger. However, to complete the heat exchanger model, a heat transfer equation analogous to Equation 5.53 is needed. To discover the form of the heat transfer equation needed, a differential area inside of the regenerative heat exchanger will be evaluated as shown in Figure 5.19. In the differential element, dA , the hot and cold fluid temperatures are specified as T and t , respectively.

For the differential area shown in Figure 5.19,

$$d\dot{Q} = \dot{C}dT \quad \text{and} \quad d\dot{Q} = \dot{C}dt \quad (5.68)$$

These are two thermodynamic equations for the heat transfer rate between the fluids; one for each fluid passing through the differential area. The heat transfer equation representing the heat transfer rate between the two fluids is,

$$d\dot{Q} = U(T - t)dA \quad (5.69)$$

Equations 5.68 and 5.69 can be combined into two new equations,

$$\frac{dT}{dA} = \frac{U}{\dot{C}}(T - t) \quad \text{and} \quad \frac{dt}{dA} = \frac{U}{\dot{C}}(T - t) \quad (5.70)$$

These equations suggest that the slopes of the temperature profiles are the same for both fluids. In addition, since the slopes through dA are identical, the temperature difference between the hot and cold fluids is the same on both sides of dA as it is within dA . Therefore, the derivatives in Equation 5.70 are *equal* and *constant*. This implies that the temperature profile of each fluid is linear and the profiles are parallel as shown in Figure 5.20. As a result, the temperature difference between the hot and cold fluids is constant throughout the heat exchanger.

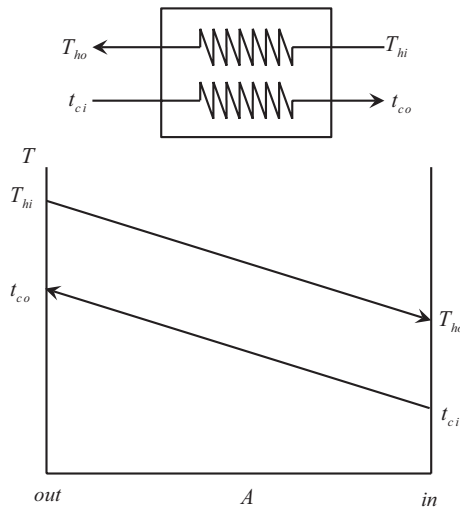


FIGURE 5.20
Temperature profiles in a counter flow regenerative heat exchanger.

Since the temperature difference is constant throughout this type of heat exchanger, an alternate model for the regenerative heat exchanger can be represented by the following three equations,

$$\begin{aligned}\dot{Q} &= \dot{C}(T_{hi} - T_{ho}) \\ \dot{Q} &= \dot{C}(t_{co} - t_{ci}) \\ \dot{Q} &= UA(T_{hi} - t_{co}) \quad \text{or} \quad \dot{Q} = UA(T_{ho} - t_{ci})\end{aligned}\tag{5.71}$$

Example 5.8

A stationary gas turbine cycle for electrical power generation is modified to include a regenerative heat exchanger as shown in Figure 5.18. Dry air, flowing at 100 lbm/s enters the regenerator at 600°F, 200 psia to be preheated before entering the combustion chamber. The preheating is accomplished with hot turbine exhaust at 1,000°F, 1 atm. The UA product of the regenerator is 48,000 Btu/hr-°R. Determine the outlet temperature of the hot and cold air streams from the regenerative heat exchanger. Assume dry air throughout the cycle and treat the heat capacity as a constant, evaluated at the average between the hot and cold inlet streams.

Solution

By treating the heat capacity as a constant value, the heat exchanger can be modeled using the set in Equation 5.71,

$$\begin{aligned}\dot{Q} &= \dot{C}(T_{hi} - T_{ho}) \\ \dot{Q} &= \dot{C}(t_{co} - t_{ci}) \\ \dot{Q} &= UA(T_{hi} - t_{co}) \quad \text{or} \quad \dot{Q} = UA(T_{ho} - t_{ci})\end{aligned}$$

Equating the heat transfer equation and the conservation of energy equation for the hot fluid, the outlet temperature of the hot fluid can be determined,

$$T_{ho} = \frac{(\dot{C} / UA)T_{hi} + t_{ci}}{(\dot{C} / UA) + 1}$$

The cold fluid outlet temperature can be found by equating the conservation of energy equations for the hot and cold fluids,

$$t_{co} = T_{hi} - T_{ho} + t_{ci}$$

The heat capacities of the hot and cold fluid streams evaluated at the inlet temperature are (interpolation in Appendix B.5),

$$c_{ph} = 0.26326 \frac{\text{Btu}}{\text{lbm-R}} \quad c_{pc} = 0.25167 \frac{\text{Btu}}{\text{lbm-R}}$$

The average heat capacity between the two inlet streams can be determined by,

$$c_{p,avg} = \frac{c_{p,h} + c_{p,c}}{2} = \frac{(0.26326 + 0.25167)\text{Btu/lbm-R}}{2} = 0.25747 \frac{\text{Btu}}{\text{lbm-R}}$$

Therefore, the thermal capacity rate of the air is,

$$\dot{C} = \dot{m}c_{p,avg} = \left(100 \frac{\text{lbm}}{\text{s}}\right) \left(0.25747 \frac{\text{Btu}}{\text{lbm-R}}\right) \left(\frac{3600 \text{ s}}{\text{h}}\right) = 92,689 \frac{\text{Btu}}{\text{h-R}}$$

Using these values, the hot fluid outlet temperature is,

$$T_{ho} = \frac{(\dot{C} / UA)T_{hi} + t_{ci}}{(\dot{C} / UA) + 1} = \frac{\left(\frac{98,267 \text{ Btu/h-R}}{48,000 \text{ Btu/h-R}}\right)(1000^\circ\text{F}) + 600^\circ\text{F}}{\left(\frac{98,267 \text{ Btu/h-R}}{48,000 \text{ Btu/h-R}}\right) + 1} = \underline{\underline{863.5^\circ\text{F}}}$$

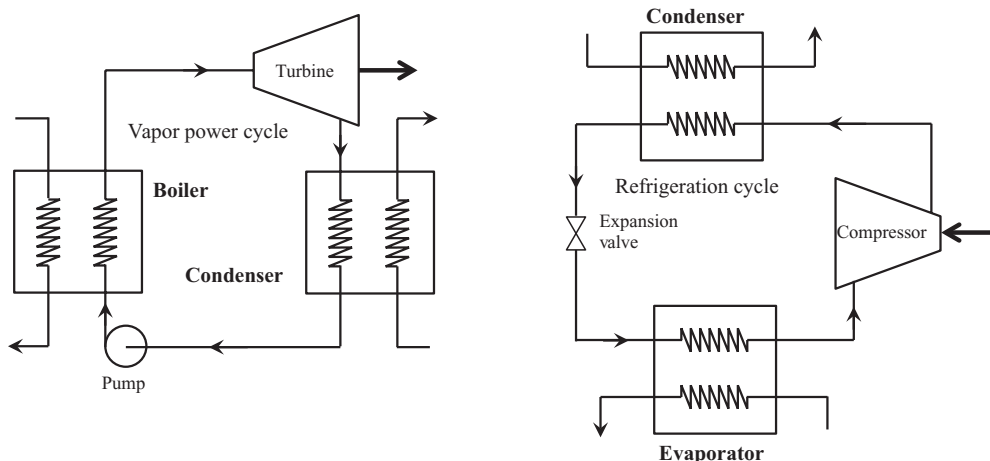
The cold fluid outlet temperature can now be calculated,

$$t_{co} = T_{hi} - T_{ho} + t_{ci} = (1000 - 863.5 + 600)^\circ\text{F} = \underline{\underline{736.5^\circ\text{F}}}$$

Notice the simplicity of this type of analysis compared to a situation where the thermal capacity rates of each fluid are different.

5.7.2 Heat Exchangers with Phase Change Fluids: Boilers, Evaporators, and Condensers

In many thermal energy systems, one of the working fluids passing through a heat exchanger experiences a phase change. Figure 5.21 is a schematic of two common thermal systems;

**FIGURE 5.21**

Vapor power and refrigeration cycles showing heat exchangers where a phase change occurs.

a vapor power cycle and a refrigeration cycle. In both of these cycles the working fluid undergoes two phase changes in the heat exchangers. In the vapor power cycle, liquid water is converted to steam in the *boiler* and condensed back to a liquid in the *condenser*. In the refrigeration cycle, the refrigerant is converted to a vapor in the *evaporator* and condensed back to a liquid in the *condenser*. These types of heat exchangers are generally categorized as either *boilers*, *evaporators* or *condensers*. The heat exchangers in Figure 5.21 are shown as counter flow heat exchangers for convenience in the sketch. In applications, the heat exchangers may have several different configurations such as shell and tube or cross flow.

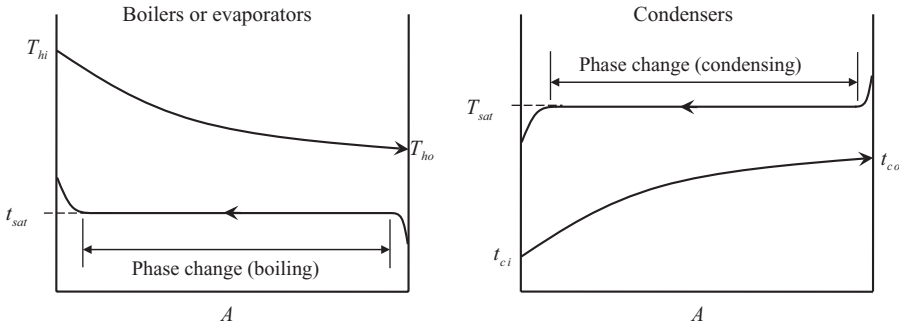
The ε -NTU model for analysis and design of heat exchangers is attractive due to its non-iterative nature. Recall that the ε -NTU method requires the determination of the thermal capacity rates for each fluid. In order to determine the thermal capacity rate of a fluid, the mass flow rate and heat capacity need to be known. However, for a pure fluid undergoing an isobaric phase change, the heat capacity is infinite. This can be verified by the following equation,

$$c_p = \left(\frac{\partial h}{\partial T} \right)_p \approx \left(\frac{\Delta h}{\Delta T} \right)_p = \frac{h_{fg}}{T_g - T_f} = \frac{h_{fg}}{0} = \infty \quad (5.72)$$

In Equation 5.72, T_g and T_f are the saturation temperatures of the saturated vapor and saturated liquid, respectively. For a pure fluid, these temperatures are the same. Also in Equation 5.72, h_{fg} is the enthalpy of vaporization of the fluid. The fact that the heat capacity of a phase-change fluid is infinite means that the thermal capacity rate of the phase change fluid must also be infinite. Therefore, the maximum heat capacity rate is always associated with the phase change fluid. This also implies that the ratio of the thermal capacity rates must be zero,

$$C_r = \frac{\dot{C}_{\min}}{\dot{C}_{\max}} = \frac{\dot{C}_{\min}}{\infty} = 0 \quad (5.73)$$

The last entries in Tables 5.3 and 5.4 show the ε -NTU and NTU- ε relationships for this case. Notice that the ε -NTU relationship is fairly simple and *independent of the heat exchanger configuration*.

**FIGURE 5.22**

Typical temperature profiles inside phase change heat exchangers.

Analysis and design using the LMTD method requires a careful analysis of the temperature profile within the heat exchanger. Figure 5.22 shows what typical temperature profiles look like for boilers, evaporators, and condensers where one fluid undergoes the phase change and the other fluid remains in the single phase. The figures are drawn for a pure fluid undergoing an isobaric phase change. In reality, there are pressure drops through heat exchangers. However, the magnitude of this pressure drop is relatively small. Therefore, Figure 5.22 is a good approximation to the actual behavior that is observed.

Figure 5.22 indicates that most of the heat exchange area in these types of heat exchangers is devoted to the phase change. Only a small percentage is used to subcool or superheat the fluid. Therefore, the LMTD is modified to use the *saturation temperature* of the phase change fluid for both the inlet and outlet temperatures. Using this idea, the LMTD of an evaporator (or boiler) can be written as,

$$\text{LMTD}_E = \frac{\Delta T_{in} - \Delta T_{out}}{\ln(\Delta T_{in}/\Delta T_{out})} = \frac{(T_{hi} - t_{sat}) - (T_{ho} - t_{sat})}{\ln(\Delta T_{in}/\Delta T_{out})} = \frac{T_{hi} - T_{ho}}{\ln(\Delta T_{in}/\Delta T_{out})} \quad (5.74)$$

Likewise, for a condenser, the LMTD is,

$$\text{LMTD}_C = \frac{\Delta T_{in} - \Delta T_{out}}{\ln(\Delta T_{in}/\Delta T_{out})} = \frac{(T_{sat} - t_{ci}) - (T_{sat} - t_{co})}{\ln(\Delta T_{in}/\Delta T_{out})} = \frac{t_{co} - t_{ci}}{\ln(\Delta T_{in}/\Delta T_{out})} \quad (5.75)$$

Equations 5.74 and 5.75 were developed for a counter flow heat exchanger. However, the temperature profiles shown in Figure 5.22 are the same for any type of evaporator or condenser. Therefore, Equations 5.74 and 5.75 are *independent of heat exchanger configuration*.

Once the calculation of the LMTD is determined for the heat exchanger, the complete LMTD model can be developed. For evaporators or boilers where the hot fluid remains in the single phase and the cold fluid is boiling, the LMTD model is given by,

$$\begin{aligned} \dot{Q} &= \dot{m}_h c_{ph} (T_{hi} - T_{ho}) \\ \dot{Q} &= \dot{m}_c (h_{co} - h_{ci}) \\ \dot{Q} &= UA(\text{LMTD}_E) \end{aligned} \quad (5.76)$$

Notice that the conservation of energy equation for the cold fluid is written in terms of the boiling fluid's enthalpy change. For the condenser where the hot fluid is undergoing the phase change and the cold fluid remains in the single phase, the LMTD model is,

$$\begin{aligned}\dot{Q} &= \dot{m}_h(h_{hi} - h_{ho}) \\ \dot{Q} &= \dot{m}_c c_{pc}(t_{c,o} - t_{c,i}) \\ \dot{Q} &= UA(\text{LMTD}_C)\end{aligned}\quad (5.77)$$

In applications where there is very little superheating and subcooling of the phase change fluid, the enthalpy difference can be approximated as the enthalpy of vaporization of the fluid.

Example 5.9

A 2-tube pass shell and tube heat exchanger is being used as water chiller as shown in Figure E5.9. The chiller is the evaporator of a refrigeration cycle utilizing R-123 as the working fluid. The R-123 flows at a rate of 5000 lbm/hr and leaves the condenser of the cycle as a saturated liquid at 200°F. The evaporating pressure is 5 psia and the pressure drop of the R-123 through the evaporator can be assumed to be negligible. The R-123 leaves the evaporator as a saturated vapor. Water enters the evaporator at 50°F with at a volumetric flow rate of 30 gpm. Determine the

- Evaporating temperature of the R-123 (°F)
- Capacity of the chiller (tons)
- Outlet temperature of the chilled water (°F)
- UA product of the chiller (Btu/hr-°F)

The properties of saturated R-123 are given in Table E5.9.

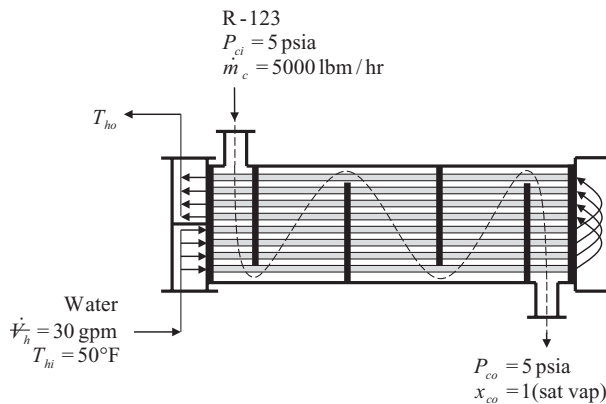


FIGURE E5.9

Two pass shell and tube heat exchanger for chilling water.

TABLE E5.9

Thermodynamic Properties of Saturated R-123

T (°F)	P (psia)	ρ (lbm/ft ³) Saturated Liquid	ρ (lbm/ft ³) Saturated Vapor	h (Btu/lbm) Saturated Liquid	h (Btu/lbm) Saturated Vapor
34.159	5	95.090	0.14725	86.554	164.41
200	97.891	79.228	2.5135	128.29	187.67

Solution

A schematic of the full refrigeration cycle is seen in Figure 5.21. The exit of the expansion valve in the refrigeration cycle is a two-phase mixture. The R-123 enters at this two-phase condition. It leaves the evaporator as a saturated vapor. Since the pressure is assumed to be constant on the R-123 side of the heat exchanger, the temperature must remain constant. This is the *evaporating* temperature asked for in part (a). Table E5.9 gives the value for the evaporating temperature,

$$t_{\text{evap}} = \underline{34.2^\circ\text{F}}$$

Parts (b) and (c) can be solved purely from the thermodynamic balances on each fluid. The heat transfer rate in the evaporator (also known as its *capacity*) can be found by,

$$\dot{Q} = \dot{m}_r (h_{\text{co}} - h_{\text{ci}})$$

The enthalpy of the refrigerant entering the evaporator is the same as the enthalpy leaving the condenser of the refrigeration cycle since the expansion process is *isenthalpic*. The enthalpy into the evaporator can be found at the saturated liquid state at 200°F. The enthalpy leaving the evaporator is a saturated vapor at 5 psia, therefore, its value can also be found. These enthalpy values are found in Table E5.9

$$h_{\text{co}} = 164.41 \text{ Btu/lbm} \quad h_{\text{ci}} = 128.29 \text{ Btu/lbm}$$

the capacity of the evaporator is,

$$\dot{Q} = \dot{m}_c (h_{\text{co}} - h_{\text{ci}}) = \left(5000 \frac{\text{lbm}}{\text{hr}} \right) (164.41 - 128.29) \frac{\text{Btu}}{\text{lbm}} \left(\frac{\text{ton-hr}}{12,000 \text{ Btu}} \right) = \underline{15.05 \text{ tons}}$$

Appendix A

Knowing the heat transfer rate allows for the calculation of the outlet temperature of the water,

$$\dot{Q} = \dot{m}_h c_{ph} (T_{hi} - T_{ho}) \rightarrow T_{ho} = T_{hi} - \frac{\dot{Q}}{(\rho_h \dot{V}_h) c_{ph}}$$

The density and heat capacity of the water should be evaluated at the average temperature of the water. However, the outlet temperature is not known. As an estimate, the inlet temperature will be used to evaluate the properties. From Appendix B.1,

$$\rho_h = 62.406 \text{ lbm/ft}^3 \quad c_{ph} = 1.0028 \text{ Btu/lbm-R}$$

Therefore, the outlet temperature of the chilled water is,

$$T_{ho} = 50^{\circ}\text{F} - \frac{(15.05 \text{ tons}) \left(\overset{\text{Appendix A}}{\left(12000 \frac{\text{Btu}}{\text{hr-ton}} \right)} \right)}{\left(62.406 \frac{\text{lbm}}{\text{ft}^3} \right) \left(30 \frac{\text{gal}}{\text{min}} \right) \left(1.0028 \frac{\text{Btu}}{\text{lbm-}^{\circ}\text{F}} \right) \left(\underset{\text{Appendix A}}{8.02083 \frac{\text{ft}^3 \cdot \text{min}}{\text{hr-gal}}} \right)} = 38.0^{\circ}\text{F}$$

This outlet temperature can be used to recalculate the properties of the water and determine a new outlet temperature,

$$T_{h,avg} = \frac{T_{hi} + T_{ho}}{2} = \frac{(50 + 38)^{\circ}\text{F}}{2} = 44^{\circ}\text{F}$$

$$\rho_h = 62.416 \text{ lbm/ft}^3 \quad c_{ph} = 1.0044 \text{ Btu/lbm-R}$$

$$T_{ho} = 50^{\circ}\text{F} - \frac{(15.05 \text{ tons}) \left(\overset{\text{Appendix A}}{\left(12000 \frac{\text{Btu}}{\text{hr-ton}} \right)} \right)}{\left(62.416 \frac{\text{lbm}}{\text{ft}^3} \right) \left(30 \frac{\text{gal}}{\text{min}} \right) \left(1.0044 \frac{\text{Btu}}{\text{lbm-}^{\circ}\text{F}} \right) \left(\underset{\text{Appendix A}}{8.02083 \frac{\text{ft}^3 \cdot \text{min}}{\text{hr-gal}}} \right)} = \underline{38.0^{\circ}\text{F}}$$

Since successive values of the water outlet temperature have not changed, the iterative process has converged and the outlet temperature has been found.

For part (d), the UA product of the evaporator can be found using either the LMTD model or the ε -NTU model. Both models will be used here to demonstrate the calculation process.

Using the LMTD model, the UA product is determined from the third equation in the heat exchanger model,

$$\dot{Q} = UA(\text{LMTD}_E) \rightarrow UA = \frac{\dot{Q}}{(\text{LMTD}_E)}$$

All fluid temperatures are known. Therefore, Equation 5.74 can be used to determine the LMTD for the chiller,

$$\text{LMTD}_E = \frac{T_{hi} - T_{ho}}{\ln(\Delta T_{in}/\Delta T_{out})} = \frac{(50 - 38)\text{R}}{\ln[(50 - 34.159)\text{R}/(38 - 34.159)\text{R}]} = 8.469 \text{ R}$$

Using this LMTD value, the UA product of the evaporator is,

$$UA = \frac{\dot{Q}}{(\text{LMTD}_E)} = \frac{15.05 \text{ tons}}{8.469 \text{ R}} \left(12000 \frac{\text{Btu}}{\text{hr-ton}} \right) = \underline{\underline{21,324 \frac{\text{Btu}}{\text{hr-R}}}}$$

Using the ε -NTU method, the UA product is calculated using Equation 5.60,

$$NTU = \frac{UA}{\dot{C}_{\min}} \rightarrow UA = \dot{C}_{\min}(NTU)$$

The NTU is calculated from the heat exchanger effectiveness given by Equation 5.57 and Table 5.5,

$$\varepsilon = \frac{\dot{Q}}{\dot{Q}_{\max}} \quad NTU = -\ln(1 - \varepsilon)$$

The maximum heat transfer rate is given by,

$$\dot{Q}_{\max} = \dot{C}_{\min}(T_{hi} - t_{co})$$

Since the chiller is a phase change heat exchanger, the minimum thermal capacity rate is associated with the fluid remaining in the single phase; the water.

$$\begin{aligned} \dot{C}_{\min} &= \rho_h \dot{V}_h c_{ph} = \left(62.416 \frac{\text{lbm}}{\text{ft}^3} \right) (30 \text{ gpm}) \left(1.0044 \frac{\text{Btu}}{\text{lbm-R}} \right) \left(\frac{8.02083 \text{ ft}^3}{\text{h-gpm}} \right) \\ &= 15,084.93 \frac{\text{Btu}}{\text{h-R}} \\ \dot{Q}_{\max} &= \dot{C}_{\min}(T_{hi} - t_{co}) = \left(15,084.93 \frac{\text{Btu}}{\text{h-R}} \right) (50 - 34.159)\text{R} = 238,960 \frac{\text{Btu}}{\text{h}} \end{aligned}$$

This results in an effectiveness of,

$$\varepsilon = \frac{\dot{Q}}{\dot{Q}_{\max}} = \frac{(15.05 \text{ ton}) \left(\frac{12,000 \text{ Btu}}{\text{ton-h}} \right)}{238,960 \frac{\text{Btu}}{\text{h}}} = 0.75577$$

The NTU for the chiller can now be found,

$$NTU = -\ln(1 - \varepsilon) = -\ln(1 - 0.75577) = 1.4097$$

Finally, the UA product can be calculated,

$$UA = \dot{C}_{\min}(NTU) = \left(15,084.93 \frac{\text{Btu}}{\text{h-R}} \right) (1.4097) = \underline{\underline{21,224 \frac{\text{Btu}}{\text{h-R}}}}$$

Notice that within round off error, both methods yield the same result for the UA product. The LMTD method, however, is easier to implement in this case.

In Example 5.9, the UA product of the heat exchanger was calculated. If this were a heat exchanger design problem, the overall heat transfer coefficient, U , would need to be

determined. Once U is known, then the total heat transfer area required can be found. From this information, the engineer can specify the number of tubes required in the shell.

Convective heat transfer coefficient correlations for boiling and condensing fluids can be quite complex. The boiling and condensing processes are dependent upon many things, including gravity effects. Because of this, many correlations are dependent on the *orientation* of the tube containing the boiling or condensing liquid. The reader is encouraged to refer to any of the excellent resources available, including *The Heat Transfer Handbook* (Bejan and Kraus 2003) or *The Handbook of Heat Transfer* (Rohsenow, Hartnett and Cho 1998). The most up-to-date information concerning boiling or and condensing convective heat transfer correlations can also be found in technical journals such as *The International Journal of Heat and Mass Transfer* and the *Journal of Heat Transfer*.

5.8 Double Pipe Heat Exchanger Design and Analysis

The double pipe heat exchanger was qualitatively discussed in Section 5.5.1. This section details the suggested procedures for design and analysis calculations including prediction of the heat exchanger's thermal and hydraulic performance. The thermal performance calculations result in determination of a heat exchanger area (a design problem) or outlet fluid temperatures from a given double pipe heat exchanger (an analysis problem).

5.8.1 Double Pipe Heat Exchanger Diameters

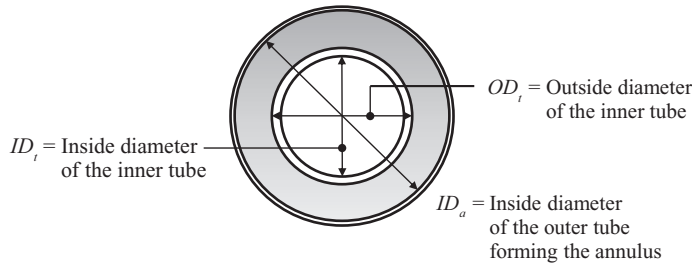
Design and analysis calculations for DPHXs are complicated by the fact that an annular space is created between the two tubes making up the heat exchanger, as shown in Figure 5.23. In a DPHX, the heat is transferred between the fluids flowing in the inner tube and the annulus. It is assumed that the outer tube is insulated so there is no heat gain/loss to/from the fluid in the annulus.

For hydraulic calculations involving the pressure drop through a DPHX, the Reynolds number and relative roughness of the flow in the inner tube is based on the inside diameter of tube. The Reynolds number and relative roughness of the fluid in the annulus is based on the *hydraulic diameter* of the annulus. The hydraulic diameter is defined as,

$$D_{hyd} = \frac{4(\text{cross sectional flow area})}{\text{wetted perimeter}} = \frac{4A}{P_{wetted}} \quad (5.78)$$

In the annulus, friction is present on both surfaces. Therefore, the wetted perimeter is the total circumference of the inner and outer tubes making up the annular space. Using the nomenclature in Figure 5.23, the hydraulic diameter of the annulus can be written as,

$$D_{hyd} = \frac{4\left(\frac{\pi}{4}\right)(ID_a^2 - OD_t^2)}{\pi(ID_a + OD_t)} = ID_a - OD_t \quad (5.79)$$

**FIGURE 5.23**

Cross-sectional view of a double pipe heat exchanger.

For heat transfer calculations, the Nusselt number and Reynolds number are based on the *equivalent* diameter for the flow in the annulus. Analogous to the hydraulic diameter, the equivalent diameter is defined as,

$$D_{equ} = \frac{4(\text{cross sectional flow area})}{\text{heat transfer perimeter}} = \frac{4A}{P_{heat}} \quad (5.80)$$

In the annular space, the heat transfer is occurring at the outer surface of the inner tube. It is assumed that no heat is transferred through the outer tube. Based on this definition, the equivalent diameter of the annulus can be written as,

$$D_{equ} = \frac{4\left(\frac{\pi}{4}\right)(ID_o^2 - OD_i^2)}{\pi(OD_i)} = \frac{(ID_o^2 - OD_i^2)}{OD_i} \quad (5.81)$$

Based on this discussion, it is seen that there is a single Reynolds number for the flow inside the inner tube with an inside diameter, D_i , given by,

$$Re_i = \frac{\rho V_i D_i}{\mu} \quad (5.82)$$

For the annulus, there are *two* Reynolds numbers. The Reynolds number based on the hydraulic diameter is used in friction calculations and is based on the hydraulic diameter,

$$Re_f = \frac{\rho V D_{hyd}}{\mu} \quad (5.83)$$

For heat transfer calculations in the annulus, the Reynolds number based on the equivalent diameter,

$$Re_Q = \frac{\rho V D_{equ}}{\mu} \quad (5.84)$$

Comparing Equations 5.83 and 5.84, it can be seen that for the flow of a fluid in an annulus,

$$\frac{\text{Re}_f}{\text{Re}_Q} = \frac{D_{hyd}}{D_{equ}} \quad (5.85)$$

Example 5.10

The outer pipe of a double pipe heat exchanger is 4-nom sch 40 commercial steel. The inside tube is 3 std type M copper. Water at an average temperature of 30°C is flowing in the annulus at a rate of 10 m³/h. Determine the Reynolds numbers of the annular flow for use in hydraulic analysis and heat transfer analysis.

Solution

Appendix B.3 lists the properties of water at 30°C,

$$\rho = 995.61 \frac{\text{kg}}{\text{m}^3} \quad \mu = 0.00079772 \frac{\text{kg}}{\text{m-s}}$$

The inside diameter of the outer tube forming the annulus can be determined from Appendix C,

$$\text{4-nom sch 40 commercial steel: } ID_a = 0.10226 \text{ m}$$

The inner tube is made of 3-std type M copper. The outside diameter of this tube can be found in Appendix D,

$$\text{3 std type M copper tube: } OD_t = 0.079375 \text{ m}$$

The hydraulic diameter of the annulus is given by Equation 5.79,

$$D_{hyd} = ID_a - OD_t = (0.10226 - 0.079375)\text{m} = 0.022885 \text{ m}$$

The equivalent diameter of the annulus is given by Equation 5.81

$$D_{equ} = \frac{(ID_a^2 - OD_t^2)}{OD_t} = \frac{(0.10226^2 - 0.079375^2)\text{m}^2}{0.079375 \text{ m}} = 0.052368 \text{ m}$$

Using the fluid properties and the hydraulic diameter, the Reynolds number for friction analysis is,

$$\text{Re}_f = \frac{\rho V D_{hyd}}{\mu} = \frac{4 \rho \dot{V}}{\pi D_{hyd} \mu} = \frac{4 \left(995.61 \frac{\text{kg}}{\text{m}^3} \right) \left(10 \frac{\text{m}^3}{\text{h}} \right) \left(\frac{\text{h}}{3600 \text{ s}} \right)}{\pi (0.022885 \text{ m}) \left(0.00079772 \frac{\text{kg}}{\text{m-s}} \right)} = \underline{192,884}$$

The Reynolds number used for heat transfer analysis can be determined using Equation 5.84 or 5.85,

$$\text{Re}_Q = \text{Re}_f \left(\frac{D_{equ}}{D_{hyd}} \right) = (192,884) \left(\frac{0.052368 \text{ m}}{0.022885 \text{ m}} \right) = \underline{441,379}$$

5.8.2 Overall Heat Transfer Coefficients for the Double Pipe Heat Exchanger

In DPHX calculations, it is common to base the overall heat transfer coefficient on the outside surface area of the inner tube. Therefore, Equation 5.35 is used to calculate the overall heat transfer coefficient of the heat exchanger. In most DPHX designs, the inner tube is a high thermal conductivity material such as copper. If this is the case, then the thermal resistance of the inner tube is very small compared to the convective and fouling resistances and is often omitted from the calculation.

It is also informative to determine the performance of the heat exchanger when it is brand new (no fouling) and after one year of service (fouling). For the case of a high thermal conductivity inner tube, two overall heat transfer coefficients can be calculated for these conditions,

$$\frac{1}{U_{o, clean}} = \frac{1}{h_i} \left(\frac{OD_t}{ID_t} \right) + \frac{1}{h_o} \quad (5.86)$$

and,

$$\frac{1}{U_{o, fouled}} = \frac{1}{h_i} \left(\frac{OD_t}{ID_t} \right) + R''_{f,i} \left(\frac{OD_t}{ID_t} \right) + R''_{f,o} + \frac{1}{h_o} \quad (5.87)$$

If the inner tube is not a high thermal conductivity material, then its conduction resistance must be included in Equation 5.86 and 5.87.

The recommended convective heat transfer coefficients in Equations 5.86 and 5.87 are given in Sections 5.2.2.3, 5.2.2.4, and 5.2.2.5. These correlations are summarized in Table 5.5. As discussed in Section 5.8.1, care must be taken to make sure that the proper diameter is being used when evaluating the Nusselt number and Reynolds number in the annulus.

5.8.3 Hydraulic Analysis of the Double Pipe Heat Exchanger

A heat exchanger is part of a larger thermal energy system. The fluids are moved through the heat exchanger by virtue of a pump (for liquid flows) or a compressor (for gas flows).

TABLE 5.5

Recommended Correlations for the Convective Heat Transfer Coefficient in DPHX Design and Analysis

Flow Regime and Condition	Correlation	Equation
Laminar (Re < 2300) Combined Entry Length	$Nu_D = 0.664 \left(\frac{PeD}{L} \right)^{1/2} Pr^{-1/6}$	(5.22)
Laminar (Re < 2300) Thermal Entry Length	$Nu_D = \frac{hD}{k} = \left[3.66^3 + 1.61^3 \left(\frac{PeD}{x} \right) \right]^{1/3}$ or $Nu_D = \frac{hD}{k} = 3.66 + \frac{0.19(PeD/x)^{0.8}}{1 + 0.117(PeD/x)^{0.467}}$	(5.24) (5.25)
Turbulent (Re > 2300)	$Nu_D = \frac{hD}{k} = \frac{(f/8)(Re_D - 1000)Pr}{1 + 12.7(f/8)^{1/2}(Pr^{2/3} - 1)}$	(5.26)

To properly size the pump or compressor, the pressure drop through the heat exchanger needs to be included in the development of the system curve.

5.8.3.1 Hydraulic Consequences of Fouling

Fouling is a phenomenon that not only affects heat transfer, but it can also result in an increased pressure drop due to a reduction in the flow area of the passage. Consider the flow through a tube. The pressure drop through a length of clean tube (subscript *c*) is given by,

$$\frac{\Delta P_c}{\gamma} = f_c \frac{L}{D_c} \frac{V_c^2}{2g} = \frac{8Lf_c \dot{V}^2}{\pi^2 g D_c^5} \quad (5.88)$$

Likewise, for the same tube under fouled conditions (subscript *f*),

$$\frac{\Delta P_f}{\gamma} = f_f \frac{L}{D_f} \frac{V_f^2}{2g} = \frac{8Lf_f \dot{V}^2}{\pi^2 g D_f^5} \quad (5.89)$$

Consider the case where the volumetric flow is the same for both the clean and fouled tube, the ratio of the pressure drop for the fouled tube to that of the clean tube is,

$$\frac{\Delta P_f}{\Delta P_c} = \frac{f_f}{f_c} \left(\frac{D_c}{D_f} \right)^5 \quad (5.90)$$

Equation 5.90 indicates that the pressure drop for the fouled pipe or tube is a function of the fifth-power of the diameter ratio. Since D_f is smaller than D_c , the ratio is greater than 1. Enhancing this ratio by the fifth power shows the potential impact fouling can have on the hydraulic performance in a pipe or tube.

In a double pipe heat exchanger, fouling occurs on the inside and outside surfaces of the inner tube and the inner surface of the outer tube. The effect of fouling on the pipe or tube diameter can be determined using the fouling factor, R_f'' , listed in Table 5.2. The fouling factor is a conductive thermal resistance due to fouling. Therefore, the thermal resistance expression for a tube in Table 5.1 can be used to determine the diameter of the fouled layer.

For the fouling layer on the inside of a tube, Table 5.1 shows that the total thermal conduction resistance due to the fouling layer is,

$$R_t = \frac{\ln(D_c/D_f)}{2\pi k_f L} \quad (5.91)$$

In Equation 5.91 and subsequent equations in this section, the subscripts “*c*” and “*f*” are used to denote a clean and fouled pipe or tube, respectively. Considering that the fouling film forms on the inside diameter of the clean pipe or tube, the fouling factor can be written as,

$$R_f'' = AR_t = (\pi D_c L) \frac{\ln(D_c/D_f)}{2\pi k_f L} = \frac{D_c}{2k_f} \ln \left(\frac{D_c}{D_f} \right) \quad (5.92)$$

Solving Equation 5.92 for the inside diameter of the fouled pipe or tube,

$$D_f = D_c \exp\left(-\frac{2k_f R_f''}{D_c}\right) \quad (5.93)$$

In Equations 5.92 and 5.93, k_f is the thermal conductivity of the fouling layer.

It is also possible to determine the increase in the outer diameter of the inner tube in a double pipe heat exchanger using the fouling factor, R_f'' , listed in Table 5.2. According to Table 5.1, the total thermal resistance due to the fouling layer is,

$$R_t = \frac{\ln(D_f/D_c)}{2\pi k_f L} \quad (5.94)$$

In the case of fouling on the outside of the tube, the fouling factor is expressed as,

$$R_f'' = AR_t = (\pi D_c L) \frac{\ln(D_f/D_c)}{2\pi k_f L} = \frac{D_c}{2k_f} \ln\left(\frac{D_f}{D_c}\right) \quad (5.95)$$

Solving Equation 5.95 for the outside diameter of the fouled tube results in,

$$D_f = D_c \exp\left(\frac{2k_f R_f''}{D_c}\right) \quad (5.96)$$

Equations 5.93 and 5.96 can be combined to form as a single equation,

$$D_f = D_c \exp\left(\pm \frac{2k_f R_f''}{D_c}\right) \quad (5.97)$$

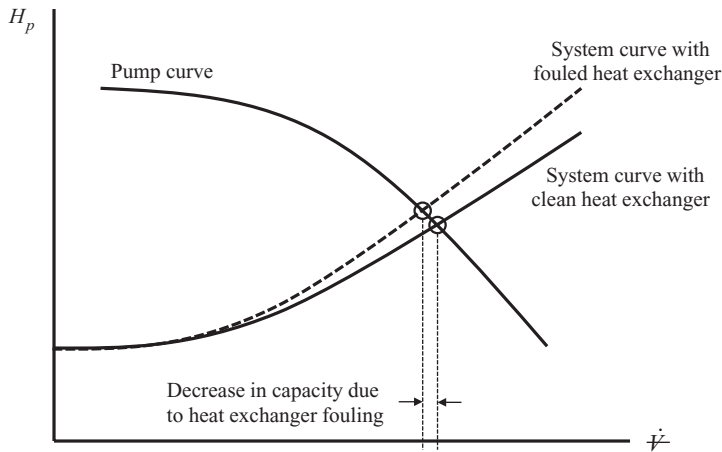
In Equation 5.97 the “+” sign is used to compute the fouled outside diameter of the tube and the “−” sign is used to calculate the inside fouled tube diameter. The diameter, D_c , represents the inside or outside diameter of the clean tube, depending on whether the fouling effect is being analyzed on the inside or outside of the tube. Values of the thermal conductivity of various common fouling materials, k_f , are listed in Table 5.6. For water flows, the most common fouling material is calcium carbonate.

As fouling progresses in the heat exchanger, flow passages experience a decrease in cross sectional area. This is analogous to a valve that is slowly being closed. This causes the volumetric flow in the system to decrease as the system seeks a new operating point

TABLE 5.6

Thermal Conductivity of Common Fouling Materials

Fouling Material	k_f (Btu/h-ft-°F)	k_f (W/m-K)
Calcium carbonate	1.70	2.94
Calcium phosphate	1.50	2.60
Calcium sulfate	1.35	2.34
Magnetic iron oxide	1.66	2.87

**FIGURE 5.24**

Effect of Fouling on the system curve and pump/system operating point.

with the pump, as shown in Figure 5.24. Recall that the fouling factors reported in Table 5.2 represent the fouling condition after one year of continuous service without interruption.

5.8.3.2 Pressure Drop through the Inner Tube

The pressure drop through the inner tube of the DPHX is related to the head loss due to friction through the tube,

$$\frac{\Delta P_t}{\gamma_t} = f_t \frac{L}{D_t} \frac{V_t^2}{2g} + l_m \quad (5.98)$$

A subscript “*t*” is used in Equation 5.98 to indicate the parameters inside the inner tube of the heat exchanger. L is the total length of the heat exchanger and l_m is the minor loss through the fittings that are used to make up a DPHX hairpin design. If the DPHX is a simple tube-in-tube design with no hairpins, then the minor loss in Equation 5.98 is zero. D_t is the inside diameter of the tube. If the pressure drop for a clean tube is being calculated, then this diameter is determined from pipe or tube data (Appendix C or Appendix D). If the pressure drop for a tube that is fouled is required, then the fouled inside diameter determined from Equation 5.97 is used in place of D_t in Equation 5.98.

5.8.3.3 Pressure Drop through the Annulus

In the annular space, an additional head loss is experienced by the fluid due to the fittings required to create the annulus (refer to Figure 5.5). This is accounted for by adding an additional velocity head to the friction loss. In addition, the hydraulic diameter of the annulus is used to determine the pressure drop,

$$\frac{\Delta P_a}{\gamma_a} = \left(f_a \frac{L}{D_{hyd}} + n \right) \frac{V_a^2}{2g} \quad (5.99)$$

In Equation 5.99, $n = 1$ for a single double pipe heat exchanger. If the heat exchanger is a hairpin design, n represents the total number of heat exchangers in the hairpin design. The hydraulic diameter can be found for a clean heat exchanger, or one that is fouled by applying Equation 5.97 to the outside surface of the inner tube and the inside surface of the outer tube that form the annulus. The friction factor for turbulent flow in an annulus can be found using the hydraulic diameter and any of the equations listed in Table 4.2. If the outer and inner pipes that make up the heat exchanger are different, the absolute roughness of the annular passage (required for friction factor calculation) can be estimated with an area weighted average,

$$\varepsilon_a = \frac{\varepsilon_{a,ID_a}[\pi(ID_a)L] + \varepsilon_t[\pi(OD_t)L]}{\pi(ID_a)L + \pi(OD_t)L} = \frac{\varepsilon_{a,ID_a}(ID_a) + \varepsilon_t(OD_t)}{ID_a + OD_t} \quad (5.100)$$

In this equation, ε_{ID_a} is the roughness of the outer pipe and ε_t is the roughness of the inner tube.

For laminar flow in an annulus, the friction factor is calculated using,

$$\frac{1}{f_a} = \frac{64}{\text{Re}_{D_{hyd}}} \left[\frac{1 + \kappa^2}{(1 - \kappa)^2} + \frac{1 + \kappa}{(1 - \kappa) \ln \kappa} \right] \text{ where } \kappa = \frac{OD_t}{ID_a} \quad (5.101)$$

A well-designed DPHX has pressure drops in either stream that are less than 10 psi (~70 kPa).

Example 5.11

A 4×2 counter flow double pipe heat exchanger has an outer pipe of 4-nom sch 40 commercial steel and an inner tube of 2-std type M copper as shown in Figure E5.11. Hot city water at an average temperature of 80°C flows in the tube at a flow rate of 10 L/s.

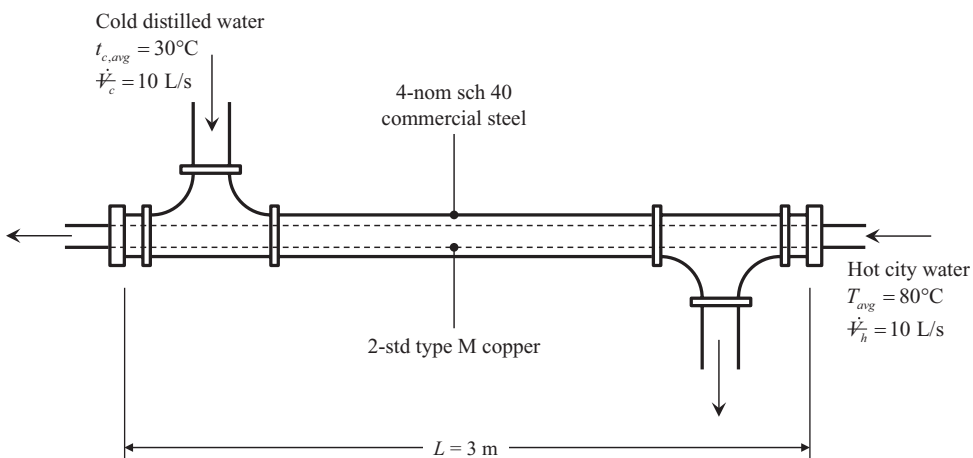


FIGURE E5.11

Counter flow water-to-water double pipe heat exchanger.

Cold distilled water flows in the annulus at a flow rate of 8 L/s and an average temperature of 30°C. The heat exchanger is a single DPHX with a length of 3 m. After one year of service, the volumetric flow rates in the tube and annulus are estimated to experience a 3% reduction due to fouling. The fouling layer is primarily calcium carbonate. Determine the pressure drop through the

- Tube under clean and fouled conditions
- Annulus under clean and fouled conditions

Solution

The properties of the hot and cold water can be determined from Appendix B.3,

$$\begin{aligned} T_{h,avg} &= 80^\circ\text{C} & \rho_h &= 971.77 \text{ kg/m}^3 & \gamma_h &= \rho_h g / g_c = 9530.1 \text{ N/m}^3 & \mu_h &= 0.00035404 \text{ kg/m-s} \\ t_{c,avg} &= 30^\circ\text{C} & \rho_c &= 995.61 \text{ kg/m}^3 & \gamma_c &= \rho_c g / g_c = 9763.9 \text{ N/m}^3 & \mu_c &= 0.00079722 \text{ kg/m-s} \end{aligned}$$

The pipe and tube data are determined from Appendix C, Appendix D, and Table 4.3,

$$\begin{aligned} \text{tube:} \quad ID_t &= 0.051029 \text{ m} & OD_t &= 0.053975 \text{ m} & \varepsilon_t &= 0.0000015 \text{ m} \\ \text{annulus:} \quad ID_a &= 0.10226 \text{ m} & \varepsilon_{a,ID_a} &= 0.000046 \text{ m} \end{aligned}$$

The fouling factors for flow in the tube and annulus, and the thermal conductivity of the fouling layer (calcium carbonate) are determined in Table 5.2 and Table 5.6,

$$R''_{f,t} = 0.000352 \text{ m}^2\text{-K/W} \quad R''_{f,a} = 0.000088 \text{ m}^2\text{-K/W} \quad k_f = 2.94 \text{ W/m-K}$$

- The pressure drop through the tube of the heat exchanger is given by Equation 5.98,

$$\frac{\Delta P_t}{\gamma_t} = f_t \frac{L}{D_t} \frac{V_t^2}{2g}$$

The minor loss term is zero since this heat exchanger is a single DPHX with no hairpins. For the case of a clean tube, the velocity in the tube is,

$$V_t = \frac{4\dot{V}_t}{\pi D_t^2} = \frac{4\left(10 \frac{\text{L}}{\text{s}}\right)\left(\frac{\text{m}^3}{1000 \text{ L}}\right)}{\pi(0.051029 \text{ m})^2} = 4.8896 \frac{\text{m}}{\text{s}}$$

The friction factor is determined from the Reynolds number,

$$\text{Re}_t = \frac{\rho_t V_t D_t}{\mu_t} = \frac{\left(971.77 \frac{\text{kg}}{\text{m}^3}\right)\left(4.8896 \frac{\text{m}}{\text{s}}\right)(0.051029 \text{ m})}{0.00035404 \frac{\text{kg}}{\text{m-s}}} = 684,869$$

$$f_t = \frac{0.25}{\left[\log \left(\frac{\varepsilon_t / D_t}{3.7} + \frac{5.74}{\text{Re}_t^{0.9}} \right) \right]^2} = \frac{0.25}{\left[\log \left(\frac{0.0000015 \text{ m}}{3.7(0.051029 \text{ m})} + \frac{5.74}{684,869^{0.9}} \right) \right]^2} = 0.012930$$

This leads to a pressure drop through the clean inner tube of,

$$\begin{aligned} \Delta P_t &= \gamma_t \left(f_t \frac{L}{D_t} \frac{V_t^2}{2g} \right) \\ &= \left(9530.1 \frac{\text{N}}{\text{m}^3} \right) (0.012930) \left(\frac{3 \text{ m}}{0.051029 \text{ m}} \right) \frac{\left(4.8896 \frac{\text{m}}{\text{s}} \right)^2}{2 \left(9.807 \frac{\text{m}}{\text{s}^2} \right)} \left(\frac{\text{kPa} \cdot \text{m}^2}{1000 \text{ N}} \right) = \underline{\underline{8.8 \text{ kPa}}} \end{aligned}$$

The inside diameter of a fouled tube can be determined form Equation 5.97,

$$\begin{aligned} D_{t,f} &= D_t \exp \left(- \frac{2k_f R''_{f,t}}{D_t} \right) \\ &= (0.051029 \text{ m}) \exp \left[- \frac{2 \left(2.94 \frac{\text{W}}{\text{m} \cdot \text{K}} \right) \left(0.000352 \frac{\text{m}^2 \cdot \text{K}}{\text{W}} \right)}{0.051029 \text{ m}} \right] = 0.049001 \text{ m} \end{aligned}$$

The volumetric flow rate under fouled conditions is estimated to be 3% lower than for the clean condition. Therefore,

$$\dot{V}_{t,f} = (1 - 0.03)(10 \text{ L/s}) = 9.7 \text{ L/s}$$

The velocity in the tube under fouled conditions is,

$$V_{t,f} = \frac{4 \dot{V}_{t,f}}{\pi D_{t,f}^2} = \frac{4 \left(9.7 \frac{\text{L}}{\text{s}} \right) \left(\frac{\text{m}^3}{1000 \text{ L}} \right)}{\pi (0.049001 \text{ m})^2} = 5.1437 \frac{\text{m}}{\text{s}}$$

The friction factor in the fouled tube is determined form the Reynolds number,

$$\text{Re}_{t,f} = \frac{\rho_t V_{t,f} D_{t,f}}{\mu_t} = \frac{\left(971.77 \frac{\text{kg}}{\text{m}^3} \right) \left(5.1437 \frac{\text{m}}{\text{s}} \right) (0.049001 \text{ m})}{0.00035404 \frac{\text{kg}}{\text{m} \cdot \text{s}}} = 691,822$$

$$f_{t,f} = \frac{0.25}{\left[\log \left(\frac{\epsilon_t / D_{t,f}}{3.7} + \frac{5.74}{\text{Re}_{t,f}^{0.9}} \right) \right]^2} = \frac{0.25}{\left[\log \left(\frac{0.0000015 \text{ m}}{3.7(0.049001 \text{ m})} + \frac{5.74}{691,822^{0.9}} \right) \right]^2} = 0.012932$$

Notice that in the calculation of the friction factor, the roughness of the pipe is assumed to be unchanged. Now, the pressure drop in the fouled tube can be calculated,

$$\begin{aligned} \Delta P_{t,f} &= \gamma_t \left(f_{t,f} \frac{L}{D_{t,f}} \frac{V_{t,f}^2}{2g} \right) \\ &= \left(9530.1 \frac{\text{N}}{\text{m}^3} \right) (0.012932) \left(\frac{3 \text{ m}}{0.049001 \text{ m}} \right) \frac{\left(5.1437 \frac{\text{m}}{\text{s}} \right)^2}{2 \left(9.807 \frac{\text{m}}{\text{s}^2} \right)} \left(\frac{\text{kPa} \cdot \text{m}^2}{1000 \text{ N}} \right) = \underline{10.2 \text{ kPa}} \end{aligned}$$

b. The pressure drop in the annulus is determined from Equation 5.99,

$$\frac{\Delta P_a}{\gamma_a} = \left(f_a \frac{L}{D_{hyd}} + 1 \right) \frac{V_a^2}{2g}$$

The value of $n = 1$ in Equation 5.99 since the heat exchanger is a single DPHX design. For the clean annulus, the hydraulic diameter is given by,

$$D_{hyd} = ID_a - OD_t = (0.10226 - 0.053975) \text{ m} = 0.048285 \text{ m}$$

The velocity in the clean annulus is,

$$V_a = \frac{4\dot{V}_a}{\pi D_{hyd}^2} = \frac{4 \left(8 \frac{\text{L}}{\text{s}} \right) \left(\frac{\text{m}^3}{1000 \text{ L}} \right)}{\pi (0.048285 \text{ m})^2} = 4.3689 \frac{\text{m}}{\text{s}}$$

The friction factor is determined from the Reynolds number,

$$\text{Re}_a = \frac{\rho_a V_a D_{hyd}}{\mu_a} = \frac{\left(995.61 \frac{\text{kg}}{\text{m}^3} \right) \left(4.3689 \frac{\text{m}}{\text{s}} \right) (0.048285 \text{ m})}{0.00079722 \frac{\text{kg}}{\text{m} \cdot \text{s}}} = 579,031$$

To evaluate the friction factor, the roughness of the annular passage is required. Using the area-weighting scheme shown in Equation 5.100,

$$\varepsilon_a = \frac{\varepsilon_{a,ID_a}(ID_a) + \varepsilon_t(OD_t)}{ID_a + OD_t}$$

$$\varepsilon_a = \frac{(0.000046 \text{ m})(0.10226 \text{ m}) + (0.0000015 \text{ m})(0.053975 \text{ m})}{(0.10226 + 0.053975) \text{ m}} = 0.0000306 \text{ m}$$

Therefore, the friction factor is,

$$f_a = \frac{0.25}{\left[\log \left(\frac{\varepsilon/D_{hyd}}{3.7} + \frac{5.74}{\text{Re}_a^{0.9}} \right) \right]^2} = \frac{0.25}{\left[\log \left(\frac{0.0000306 \text{ m}}{3.7(0.048285 \text{ m})} + \frac{5.74}{579,031^{0.9}} \right) \right]^2} = 0.018458$$

This leads to a pressure drop through the clean annulus of,

$$\Delta P_a = \gamma_a \left(f_a \frac{L}{D_{hyd}} + 1 \right) \frac{V_a^2}{2g}$$

$$= \left(9763.9 \frac{\text{N}}{\text{m}^3} \right) \left[(0.018458) \left(\frac{3 \text{ m}}{0.048285 \text{ m}} \right) + 1 \right] \frac{\left(\frac{4.3689 \frac{\text{m}}{\text{s}}}{2 \left(9.807 \frac{\text{m}}{\text{s}^2} \right)} \right)^2 \left(\frac{\text{kPa} \cdot \text{m}^2}{1000 \text{ N}} \right)}{1} = \underline{\underline{19.9 \text{ kPa}}}$$

When the annulus becomes fouled, the hydraulic diameter is affected by the fouling deposit on both surface of the passage. The inside diameter of the outer pipe decreases and is given by,

$$ID_{a,f} = ID_a \exp \left(- \frac{2k_f R''_{f,a}}{ID_a} \right)$$

$$= (0.10226 \text{ m}) \exp \left[- \frac{2 \left(2.94 \frac{\text{W}}{\text{m} \cdot \text{K}} \right) \left(0.000088 \frac{\text{m}^2 \cdot \text{K}}{\text{W}} \right)}{0.10226 \text{ m}} \right] = 0.10174 \text{ m}$$

The outside diameter of the inner tube of the heat exchanger increases as a result of fouling,

$$OD_{t,f} = OD_t \exp \left(- \frac{2k_f R''_{f,a}}{OD_t} \right)$$

$$= (0.053975 \text{ m}) \exp \left[- \frac{2 \left(2.94 \frac{\text{W}}{\text{m} \cdot \text{K}} \right) \left(0.000088 \frac{\text{m}^2 \cdot \text{K}}{\text{W}} \right)}{0.053975 \text{ m}} \right] = 0.054495 \text{ m}$$

The hydraulic diameter of the annulus under fouled conditions can now be calculated,

$$D_{hyd,f} = ID_{a,f} - OD_{t,f} = (0.10174 - 0.054495)\text{m} = 0.047249 \text{ m}$$

The velocity of the water in the fouled annulus is,

$$V_{a,f} = \frac{4\dot{V}_{a,f}}{\pi D_{hyd,f}^2} = \frac{4\left(8\frac{\text{L}}{\text{s}}\right)(1 - 0.03)\left(\frac{\text{m}^3}{1000 \text{ L}}\right)}{\pi(0.047249 \text{ m})^2} = 4.4258 \frac{\text{m}}{\text{s}}$$

Notice that the velocity is computed using the estimated 3% decrease in volumetric flow rate due to fouling. The Reynolds number and resulting friction factor for the fouled annulus are,

$$\text{Re}_{a,f} = \frac{\rho_a V_{a,f} D_{hyd,f}}{\mu_a} = \frac{\left(995.61 \frac{\text{kg}}{\text{m}^3}\right)\left(4.4258 \frac{\text{m}}{\text{s}}\right)(0.047249 \text{ m})}{0.00079722 \frac{\text{kg}}{\text{m-s}}} = 573,976$$

$$\begin{aligned} \varepsilon &\approx \frac{\varepsilon_a(ID_{a,f}) + \varepsilon_t(OD_{t,f})}{ID_{a,f} + OD_{t,f}} \\ &= \frac{(0.000046 \text{ m})(0.10174 \text{ m}) + (0.0000015 \text{ m})(0.054495 \text{ m})}{(0.10174 + 0.054495)\text{m}} = 0.0000305 \text{ m} \end{aligned}$$

$$f_{a,f} = \frac{0.25}{\left[\log\left(\frac{\varepsilon/D_{hyd,f}}{3.7} + \frac{5.74}{\text{Re}_{a,f}^{0.9}}\right)\right]^2} = \frac{0.25}{\left[\log\left(\frac{0.0000305 \text{ m}}{3.7(0.047249 \text{ m})} + \frac{5.74}{573,976^{0.9}}\right)\right]^2} = 0.018524$$

Therefore, the pressure drop through the annulus when it becomes fouled is,

$$\begin{aligned} \Delta P_{a,f} &= \gamma_a \left(f_{a,f} \frac{L}{D_{hyd,f}} + 1 \right) \frac{V_{a,f}^2}{2g} \\ &= \left(9763.9 \frac{\text{N}}{\text{m}^3} \right) \left[(0.018524) \left(\frac{3 \text{ m}}{0.047249 \text{ m}} \right) + 1 \right] \frac{\left(4.4258 \frac{\text{m}}{\text{s}} \right)^2}{2 \left(9.807 \frac{\text{m}}{\text{s}^2} \right)} \left(\frac{\text{kPa-m}^2}{1000 \text{ N}} \right) = \underline{\underline{20.7 \text{ kPa}}} \end{aligned}$$

As expected, the pressure drop for both the inner tube and the annulus increase under fouled conditions.

Based on the results in Example 5.11, one may argue that the effect of fouling is fairly small and therefore insignificant. In Example 5.11, both fluids have fairly small fouling factors (see Table 5.2). The flow in the annulus has a particularly small fouling factor because the fluid is distilled water. Given other conditions, the effect of fouling on the hydraulic performance of the heat exchanger can be significant. As an example, the plate and frame heat exchangers used in dairy applications for pasteurization of milk are usually maintained daily (sometimes more often) to remove the fouling layer on the milk side. Even though a regular maintenance schedule can reduce the effect of fouling, it is good to know how much the hydraulic performance of the heat exchanger is impacted in a worst-case scenario.

5.8.4 Fluid Placement in a Double Pipe Heat Exchanger

There are two criteria that dictate which fluid flows in the tube and which goes through the annulus. The *hydraulic* criterion is consistent with keeping the pressure drop to a minimum. To meet this criterion, the fluid with the higher mass flow rate should go through the passage with the larger cross-sectional area. However, the *fouling* criterion sometimes competes with the hydraulic criterion. The idea with the fouling criterion is to extend the life of the heat exchanger by making it easy to mechanically clean. In the DPHX, it is far easier to mechanically clean the inside tube. Therefore, according to this criterion, the fluid with the higher fouling factor should go through the tube. As mentioned above, both of these criteria may not necessarily be met simultaneously. In instances like this, it is up to the design engineer to make the decision based on which criterion is most important in the heat exchanger application.

5.8.5 Double Pipe Heat Exchanger Design Considerations

Several design considerations for DPHXs have already been discussed. They are included here along with others. The list below is by no means all-inclusive. However, the major design considerations are summarized.

- The pressure drop through either side of the heat exchanger (tube or annulus) should be no more than 10 psi (~70 kPa). This will help minimize the cost of moving the fluid through the heat exchanger.
- An optimum DPHX design is one where the fluids in the tube and annulus are within the recommended economic velocity range (shown in Table 4.18) or calculated using a reasonable range of economic and system parameters for the specific application.
- Fluid placement should be based on either the hydraulic criterion (minimizing the pressure drop) or the fouling criterion (easy mechanical cleaning of the heat exchanger).
- The inner tube in a DPHX should be of high thermal conductivity (copper is a good choice). In cases where copper cannot be used, an economically feasible material can be chosen. If the material does not have a large thermal conductivity, the conduction thermal resistance of the material should be included in the calculation of the overall heat transfer coefficients (for both clean and fouled situations).
- The material for the outer tube of the DPHX does not need to be made of an expensive material like copper. In fact, a low thermal conductivity material is more desirable for the outer tube.

- The outer tube of the DPHX should be insulated to avoid stray heat losses to the environment surrounding the heat exchanger.
- When different materials are used for the inner and outer tubes, the absolute roughness values are likely to be different. When calculating the friction factor in the annulus, using the highest value for the absolute roughness will tend to overestimate the pressure drop and leads to a more conservative design. Using an area weighted average as demonstrated in Example 5.11 may give a more reasonable estimate of the pressure drop.
- The flow direction (parallel or counter) is an important consideration. The counter flow DPHX has the advantage of being smaller than the parallel flow configuration for the same thermal performance. However, in a counter flow heat exchanger, it is possible for the outlet fluid temperatures to “cross.” That is, it is possible for the cold fluid outlet temperature to be hotter than the hot fluid outlet temperature. In cases where this is not desirable, a parallel flow heat exchanger should be used.
- With a regular maintenance schedule for cleaning the heat exchanger, the hydraulic consequences of fouling are usually small, especially if the pressure drops for a clean heat exchanger are well below the suggested maximum threshold. However, some fluids have higher than normal fouling factors which may lead to a substantial increase in pressure drop due to fouling.

5.8.6 Computer Software for Design and Analysis of Heat Exchangers

The complete design or analysis of any heat exchanger involves simultaneous consideration of the heat transfer performance along with the hydraulic performance. These types of calculations can be highly iterative if the LMTD method is chosen for the heat exchanger model. However, where possible, the ε -NTU method eliminates iteration except for the fluid properties. In turbulent flow, the friction factor is required to evaluate the convective heat transfer coefficient. This is another iterative calculation. Clearly, heat exchanger design and analysis calculations can become very complex and iterative on several levels, making them well-suited for computer software.

Computer software for heat exchanger design and analysis must have

- A robust solver engine that is capable of handling complex multiple non-linear equations and arriving at a global solution
- A method to compute thermophysical properties of the fluids involved

As the complete set of equations gets larger and the iterations more complex, the chance of non-convergence increases with any solver engine. This requires the engineer to select wise starting guesses for the variables in the model. This may require some hand calculations to get rough estimates of temperatures, and other unknown parameters. Often, solving a heat exchanger design or analysis problems requires several runs of the program.

The software packages described in Chapter 1, Section 1.2 are capable of calculation of thermophysical properties in real-time. It is also possible to program the property formulation equations into the software package of choice. Literature sources, such as the *Journal of Physical and Chemical Reference Data*, often can be used to find modern property formulations, complete with the equations required for property calculation.

5.8.7 Double Pipe Heat Exchanger Design Example

In this section, the steps required to design a double pipe heat exchanger will be presented for the following scenario:

In an industrial process, 10,000 lbm/hr of toluene must be cooled from 96°F to 75°F. A supply of city water at 65°F is available at a flow rate of 12,500 lbm/hr to provide the cooling needed.

While each design problem has its own subtle nuances, the following general procedure should work for most DPHX design problems. In the DPHX design problem, the goals are to specify the inner and outer tubes and determine the required heat exchanger length to provide the heat transfer rate that will meet the thermal and hydraulic requirements of the heat exchanger. In this case, the toluene must be cooled from 96°F to 75°F, with city water available at 65°F. The flow rates of each fluid stream are known. Therefore, the properties of both hot and cold fluids can be determined.

5.8.7.1 Fluid Properties

The average temperature of the toluene (hot fluid) can be determined immediately,

$$T_{h,avg} = \frac{T_{hi} + T_{ho}}{2} = \frac{(96 + 75)^{\circ}\text{F}}{2} = 85.5^{\circ}\text{F}$$

The properties of the toluene can be determined at this temperature, either by interpolation in Table B.3 or using computer software. In this example, computer software (REFPROP) is used to determine fluid properties. The resulting properties are,

Fluid	T (°F)	ρ (lbm/ft ³)	γ (lbf/ft ³)	c_p (Btu/ lbm-R)	μ (lbm/ft-s)	k (Btu/h-ft-F)	Pr
Toluene (hot)	85.5	53.548	53.548	0.41022	0.00035060	0.074618	6.9388

Applying the conservation of energy equation to each fluid stream in the heat exchanger,

$$\begin{aligned}\dot{C}_h(T_{hi} - T_{ho}) &= \dot{C}_c(t_{co} - t_{ci}) \\ \therefore t_{co} &= t_{ci} + \frac{\dot{C}_h}{\dot{C}_c}(T_{hi} - T_{ho}) = t_{ci} + \frac{\dot{m}_h c_{ph,avg}}{\dot{m}_c c_{pc,avg}}(T_{hi} - T_{ho})\end{aligned}$$

This equation indicates that the average heat capacity of each fluid is required. The average heat capacity of the toluene has been determined. However, the average heat capacity of the water is unknown since the outlet temperature is unknown. Therefore, this part of the process is iterative. Using the water inlet temperature, 65°F, the heat

capacity is 1.0004 Btu/lbm-R. Using this value to estimate the outlet temperature of the water results in,

$$t_{co} = 65^{\circ}\text{F} + \frac{(10,000 \text{ lbm/h})(0.40957 \text{ Btu/lbm-R})}{(12,500 \text{ lbm/h})(1.0004 \text{ Btu/lbm-R})} (96 - 75)^{\circ}\text{F} = 71.9^{\circ}\text{F}$$

The average temperature of the cold water can now be found,

$$t_{c,avg} = \frac{t_{ci} + t_{co}}{2} = \frac{(65 + 71.9)^{\circ}\text{F}}{2} = 68.5^{\circ}\text{F}$$

At the estimated average temperature of 68.5°F, the heat capacity of the water is 1.0000 Btu/lbm-R. Recalculating the outlet temperature with this new heat capacity value gives,

$$t_{co} = 65^{\circ}\text{F} + \frac{(10,000 \text{ lbm/h})(0.40957 \text{ Btu/lbm-R})}{(12,500 \text{ lbm/h})(1.0000 \text{ Btu/lbm-R})} (96 - 75)^{\circ}\text{F} = 71.9^{\circ}\text{F}$$

Since successive values of the outlet temperature are the same, the outlet temperature, and more importantly, the average temperature of the water, has been found. Therefore, the properties of the hot and cold fluids in the heat exchanger are,

Fluid	T (°F)	ρ (lbm/ft ³)	γ (lbf/ft ³)	c_p (Btu/ lbm-R)	μ (lbm/ft-s)	k (Btu/h-ft-F)	Pr
Toluene (hot)	85.5	53.548	53.548	0.41022	0.00035060	0.074618	6.9388
Water (cold)	68.4	62.310	62.310	1.0000	0.00066900	0.34598	6.9615

Notice that the thermal conductivity of the toluene is an order of magnitude smaller than the water. This suggests that it is more difficult to transfer heat to/from toluene. As a result, the heat exchanger might be larger than expected.

5.8.7.2 Fluid Placement

The water flow is larger than the toluene. Therefore, it would be prudent to locate the water flow in the passage with the larger cross-sectional area. However, fouling should also be considered. The fouling factors for each fluid can be found in Table 5.2.

Hot Fluid = Toluene (organic fluid)	$R''_{hi} = 0.002 \text{ hr} - \text{ft}^2 - ^{\circ}\text{F/Btu}$
Cold Fluid = City Water	$R''_{fc} = 0.002 \text{ hr} - \text{ft}^2 - ^{\circ}\text{F/Btu}$

Since the fouling factors are the same for each fluid, the hydraulic criterion will be used to place the fluids. Initially, the toluene will be placed in the tube and the water in the annulus. Once the tube sizes are determined, a check will be done to ensure that the hydraulic criterion is satisfied. From this point forward in the design process, the hot fluid variables

will be assigned the subscript “*t*” to indicate that it is in the tube. Likewise, the subscript “*a*” will be used for the fluid in the annulus.

Fluid	Placement
Hot Fluid = Toluene	tube
Cold Fluid = City Water	annulus

5.8.7.3 Determination of Pipe and/or Tube Sizes

Keeping the velocities in the tube and annulus in the economic range should result in a heat exchanger that is close to cost-optimized. From Table 4.18, the estimated economic velocity ranges for the hot and cold fluids are,

Hot fluid = Toluene	5.4–10.2 ft/s
Cold fluid = City Water	5.1–9.7 ft/s

The inner tube will be selected first. Using an average economic velocity for the toluene, an estimated inside diameter of the inner tube can be found,

$$\dot{m}_t = \rho_t \left(\frac{\pi D_{t,est}^2}{4} \right) V_{t,econ}$$

$$\therefore D_{t,est} = \sqrt{\frac{4\dot{m}_t}{\pi \rho_t V_{t,econ}}} = \sqrt{\frac{4 \left(10,000 \frac{\text{lbm}}{\text{hr}} \right) \left(\frac{\text{hr}}{3600 \text{ s}} \right)}{\pi \left(53.548 \frac{\text{lbm}}{\text{ft}^3} \right) \left(\frac{5.4 + 10.2}{2} \right) \frac{\text{ft}}{\text{s}}}} = 0.092021 \text{ ft}$$

All of the heat transfer takes place through the inner tube. Therefore, a high thermal conductivity material will be selected. The inner tube will be specified as type M copper. The estimated diameter falls between the following type M copper tubes (data taken from Appendix D),

Type M Standard Size	Inside Diameter (ft)
1	0.087917
1¼	0.10758

Calculating the velocities that would be experienced inside each of these tubes results in,

Type M Standard Size	Inside Diameter (ft)	Fluid Velocity (ft/s)
1	0.087917	8.5375
1¼	0.10758	5.7018

Both of these velocities are within the economic range. However, the larger-diameter tube will be selected because it will result in smaller pressure drop on the tube side of the heat exchanger. Therefore, the specification for the inner tube is,

Tube	Specification	ID (ft)	OD (ft)	V (ft/s)
Inner	1¼-std type M copper	0.10758	0.11458	5.7018

Now that the inner tube is specified, the outer tube can be selected. The estimated inside diameter of the outer tube, based on the average economic velocity of the water, is,

$$\dot{m}_a = \rho_a \left[\frac{\pi}{4} (ID_{a,est}^2 - OD_t^2) \right] V_{a,econ} \rightarrow ID_{a,est} = \sqrt{OD_t^2 + \frac{4\dot{m}_a}{\pi \rho_a V_{a,econ}}}$$

$$\therefore ID_{a,est} = \sqrt{(0.11548 \text{ ft})^2 + \frac{4 \left(12,500 \frac{\text{lbm}}{\text{hr}} \right) \left(\frac{\text{hr}}{3600 \text{ s}} \right)}{\pi \left(62.310 \frac{\text{lbm}}{\text{ft}^3} \right) \left(\frac{5.1 + 9.7}{2} \right) \frac{\text{ft}}{\text{s}}}} = 0.15072 \text{ ft}$$

The outer pipe in the heat exchanger will be specified as sch 40 commercial steel. The estimated diameter falls between a 1½ nom and 2 nom sch 40 pipe. Calculating the resulting velocity in the annulus formed by the outer pipe and inner tube results in,

Tube	Specification	ID _a (ft)	V _a (ft/s)
Outer	1½-nom sch 40 steel	0.13417	14.562
Outer	2-nom sch 40 steel	0.17225	4.2895

This analysis indicates that the outer tube should be 2-nom. The final tube sizes for the 2 × 1¼ double pipe heat exchanger are given below.

Tube/Pipe	Specification	ID (ft)	OD (ft)	A (ft²)	V (ft/s)
Inner	1¼-std type M copper	0.10758	0.11458	0.0090898	5.7018
Outer	2-std type M copper	0.17225	—	0.012991 ^a	4.2895 ^a

^a Flow area and velocity in the annulus formed by the outer pipe and inner tube.

Notice that the cross-sectional area of the annulus is larger than the cross-sectional area of the tube. Therefore, the hydraulic criterion is met by the fluid placement suggested in Section 5.8.7.2. However, the economic velocity is slightly lower than the estimated minimum value for water from Table 4.18.

5.8.7.4 Calculation of Annulus Diameters

$$D_{hyd} = ID_a - OD_t = 0.057667 \text{ ft} \quad D_{equ} = \frac{(ID_a^2 - OD_t^2)}{OD_t} = 0.14436 \text{ ft}$$

5.8.7.5 Calculation of Reynolds Numbers

$$\text{Re}_t = \frac{\rho_t V_t (ID_t)}{\mu_t} = 93,770 \quad \text{Re}_{a,heat} = \frac{\rho_a V_a (D_{equ})}{\mu_a} = 23,039$$

$$\text{Re}_{a,fric} = \frac{\rho_a V_a (D_{hyd})}{\mu_a} = 57,673$$

5.8.7.6 Calculation of Friction Factors

$$f_t = \frac{0.25}{\left[\log \left(\frac{\epsilon_t / ID_t}{3.7} + \frac{5.74}{\text{Re}_t^{0.9}} \right) \right]^2} = 0.018376 \quad f_a = \frac{0.25}{\left[\log \left(\frac{\epsilon_a / D_{hyd}}{3.7} + \frac{5.74}{\text{Re}_{a,fric}^{0.9}} \right) \right]^2} = 0.028650$$

The absolute roughness of the annulus is estimated using an area weighted value following the procedure shown in Example 5.11.

5.8.7.7 Calculation of Nusselt Numbers

The Reynolds numbers indicate that both flows are turbulent. Table 5.5 indicates that Equation 5.26 is the recommended correlation for the Nusselt number,

$$\text{Nu}_t = \frac{(f_t/8)(\text{Re}_t - 1000) \text{Pr}_t}{1 + 12.7(f_t/8)^{1/2}(\text{Pr}_t^{2/3} - 1)} = 567.46 \quad \text{Nu}_a = \frac{(f_a/8)(\text{Re}_{a,heat} - 1000) \text{Pr}_a}{1 + 12.7(f_a/8)^{1/2}(\text{Pr}_a^{2/3} - 1)} = 469.27$$

5.8.7.8 Calculation of Convective Heat Transfer Coefficients

$$\text{Nu}_t = \frac{h_t (ID_t)}{k_t} \quad h_t = \frac{\text{Nu}_t k_t}{ID_t} = 393.59 \frac{\text{Btu}}{\text{hr} - \text{ft}^2 - ^\circ\text{F}}$$

$$\text{Nu}_a = \frac{h_a (D_{equ})}{k_a} \quad h_a = \frac{\text{Nu}_a k_a}{D_{equ}} = 1124.7 \frac{\text{Btu}}{\text{hr} - \text{ft}^2 - ^\circ\text{F}}$$

5.8.7.9 Calculation of Overall Heat Transfer Coefficients

$$\frac{1}{U_{o, \text{clean}}} = \frac{1}{h_t} \left(\frac{OD_t}{ID_t} \right) + \frac{1}{h_a} \rightarrow U_{o, \text{clean}} = 278.15 \frac{\text{Btu}}{\text{hr} - \text{ft}^2 - ^\circ\text{F}}$$

$$\frac{1}{U_{o, \text{fouled}}} = \frac{1}{h_t} \left(\frac{OD_t}{ID_t} \right) + R''_{f,i} \left(\frac{OD_t}{ID_t} \right) + R''_{f,o} + \frac{1}{h_a} \rightarrow U_{o, \text{fouled}} = 129.44 \frac{\text{Btu}}{\text{hr} - \text{ft}^2 - ^\circ\text{F}}$$

5.8.7.10 Application of the Heat Exchanger Model

At this point, most of the major parameters required in the heat exchanger model have been calculated. A decision now needs to be made concerning the heat exchanger model (LMTD or ε -NTU). For the design problem, either method turns out to be non-iterative. In this solution, the ε -NTU method will be used. The ε -NTU heat exchanger model is,

$$\begin{aligned}\dot{Q} &= \dot{C}_h(T_{hi} - T_{ho}) \\ \dot{Q} &= \dot{C}_c(t_{co} - t_{ci}) \\ \varepsilon &= \frac{\dot{Q}}{\dot{Q}_{\max}} \quad \text{where} \quad \dot{Q}_{\max} = \dot{C}_{\min}(T_{hi} - t_{ci}) \\ \varepsilon &= f(\text{NTU}, C_r) \quad \text{where} \quad \text{NTU} = \frac{U_o A_o}{\dot{C}_{\min}} \quad \text{and} \quad C_r = \frac{\dot{C}_{\min}}{\dot{C}_{\max}}\end{aligned}$$

The thermal capacity rates of each fluid are,

$$\begin{aligned}\dot{C}_h &= \dot{m}_h c_{ph,avg} = 4,102.2 \frac{\text{Btu}}{\text{hr} - \text{R}} & \dot{C}_c &= \dot{m}_c c_{pc,avg} = 12,501 \frac{\text{Btu}}{\text{hr} - \text{R}} \\ \dot{C}_{\min} &= 4,102.2 \frac{\text{Btu}}{\text{hr} - \text{R}} & \dot{C}_{\max} &= 12,501 \frac{\text{Btu}}{\text{hr} - \text{R}} & C_r &= \frac{4,102.2 \text{ Btu/hr} - \text{R}}{12,501 \text{ Btu/hr} - \text{R}} = 0.32816\end{aligned}$$

The heat exchanger effectiveness can now be calculated,

$$\begin{aligned}\dot{Q} &= \dot{C}_h(T_{hi} - T_{ho}) = \dot{C}_c(t_{co} - t_{ci}) = 86,145 \frac{\text{Btu}}{\text{hr}} \\ \dot{Q}_{\max} &= \dot{C}_{\min}(T_{hi} - t_{ci}) = 127,167 \frac{\text{Btu}}{\text{hr}} \\ \therefore \varepsilon &= \frac{\dot{Q}}{\dot{Q}_{\max}} = 0.67742\end{aligned}$$

In order to calculate the NTU, the type of heat exchanger needs to be specified. The cold fluid outlet temperature is only slightly lower than the hot fluid outlet temperature. If the fluid flow configuration is parallel, the heat exchanger may have an excessive length. Therefore, a counter flow arrangement will be specified. Using the expression for the NTU- ε relationship in Table 5.4,

$$\text{NTU}_{\text{CF}} = \frac{1}{C_r - 1} \ln \left(\frac{\varepsilon - 1}{\varepsilon C_r - 1} \right) = 1.3098$$

5.8.7.11 Heat Exchanger Length

The overall heat transfer coefficients for a clean and fouled heat exchanger were calculated in Section 5.8.7.9. These two values can be used to calculate two heat exchanger lengths,

$$\text{NTU}_{\text{CF}} = \frac{U_{o,\text{clean}} A_{o,\text{clean}}}{\dot{C}_{\min}} \rightarrow A_{o,\text{clean}} = \frac{\dot{C}_{\min} (\text{NTU})}{U_{o,\text{clean}}} = 19.317 \text{ ft}^2$$

$$A_{o,\text{clean}} = \pi(OD_t) L_{\text{clean}} \rightarrow L_{\text{clean}} = \frac{A_{o,\text{clean}}}{\pi(OD_t)} = \underline{\underline{53.7 \text{ ft}}}$$

For a heat exchanger that is fouled,

$$\text{NTU}_{\text{CF}} = \frac{U_{o,\text{fouled}} A_{o,\text{fouled}}}{\dot{C}_{\min}} \rightarrow A_{o,\text{fouled}} = \frac{\dot{C}_{\min} (\text{NTU})}{U_{o,\text{fouled}}} = 41.509 \text{ ft}^2$$

$$A_{o,\text{fouled}} = \pi(OD_t) L_{\text{fouled}} \rightarrow L_{\text{fouled}} = \frac{A_{o,\text{fouled}}}{\pi(OD_t)} = \underline{\underline{115.3 \text{ ft}}}$$

This analysis indicates that the heat exchanger length is somewhere in the range specified by,

$$54 \text{ ft (clean)} < L < 115 \text{ ft (fully fouled)}$$

An initial observation is that fouling of the heat exchanger has a significant impact on its thermal performance. The fully fouled length represents the required heat exchanger length to meet the specified thermal performance after one year of continuous service with no maintenance. There are many fouling models, but if one assumes that the fouling occurs linearly over a year the incremental heat exchanger length per month due to fouling is,

$$\Delta L = \frac{L_{\text{fouled}} - L_{\text{clean}}}{12 \text{ months}} = \frac{(115 - 54) \text{ ft}}{12 \text{ months}} = 5.083 \frac{\text{ft}}{\text{mo}}$$

Selecting a quarterly maintenance schedule (every three months), the heat exchanger length is,

$$L = L_{\text{clean}} + M \Delta L = 54 \text{ ft} + (3 \text{ mo}) \left(5.083 \frac{\text{ft}}{\text{mo}} \right) = 69.2 \text{ ft}$$

In this equation, M is the number of months between maintenance cleanings. This length is too long for a single DPHX. Therefore, a hairpin design is chosen with each hairpin measuring 10 ft. Therefore, the DPHX will contain 7 hairpins, each with a length of 10 ft for a total heat exchanger length of 70 ft. Accompanying this specification is the requirement of a quarterly maintenance schedule.

5.8.7.12 Calculation of Pressure Drops through the Heat Exchanger

The pressure drop through the tube-side of the DPHX is determined from Equation 5.98,

$$\frac{\Delta P_t}{\gamma_t} = f_t \frac{L}{D_t} \frac{V_t^2}{2g} + l_m$$

The minor loss represents the friction loss due to the fittings required to make the hairpin design. In this case, a 180° long radius bend will be used to estimate the minor loss. Using the 3K method (Table 4.9), the K value for a single bend is,

$$K = \frac{K_1}{\text{Re}_t} + K_\infty \left(1 + \frac{K_d}{D_{t,nom}^{0.3}} \right) = \frac{1000}{93,770} + (0.1) \left(1 + \frac{4.0}{1.25^{0.3}} \right) = 0.12002$$

Therefore, the head loss due to the 6 bends required to connect 7 hairpins together is,

$$l_m = 6K \frac{V_t^2}{2g}$$

Combining the minor loss expression with Equation 5.98 results in a pressure drop through the inner tube of,

$$\Delta P_t = \gamma_t \left(f_t \frac{L}{D_t} + 6K \right) \frac{V_t^2}{2g} = 2.4 \text{ psi}$$

The pressure drop through the annulus is given by Equation 5.99,

$$\begin{aligned} \frac{\Delta P_a}{\gamma_a} &= \left(f_a \frac{L}{D_{hyd}} + n \right) \frac{V_a^2}{2g} \\ \therefore \Delta P_a &= \gamma_a \left(f_a \frac{L}{D_{hyd}} + 6 \right) \frac{V_a^2}{2g} = 5.2 \text{ psi} \end{aligned}$$

These calculated pressure drops are for a clean heat exchanger. As demonstrated in Section 5.8.3.1, these values are expected to increase slightly as fouling occurs. It is possible to estimate the percent reduction in flow in each passage, determine the fouled diameters, and recalculate the pressure drop. However, since both the tube and annulus pressure drops are well below the 10 psi threshold, it would seem highly unlikely that fouling would have a significant impact on the hydraulic performance, especially since a quarterly maintenance schedule is being suggested.

5.8.7.13 Preliminary Design Specifications of the Heat Exchanger

Based on the design calculations in this section, a set of preliminary design specifications for the heat exchanger is shown in Table 5.7. The heat exchanger length specified in this design is somewhere between a clean heat exchanger and one that is fully fouled. In order

to fully specify the design, a thorough analysis will need to be conducted to ensure that the heat exchanger performs as required. The next section considers the analysis of the heat exchanger designed in this section.

5.8.8 Double Pipe Heat Exchanger Analysis Example

In this section, the double pipe heat exchanger designed in Section 5.8.7 will be analyzed to ensure proper thermal and hydraulic performance. The goal of the analysis is to determine the outlet temperatures of the hot and cold fluid streams along with the pressure drop through each passage in the heat exchanger given the heat exchanger specifications determined during the design phase. The preliminary design specifications for the heat exchanger determined in Section 5.8.7 are listed in Table 5.7.

The average temperature of each fluid stream is unknown since the outlet temperatures are unknown. Therefore, iteration will be required to determine the fluid properties. An additional level of iteration is introduced in the heat exchanger model. All equations in the heat exchanger model must be simultaneously satisfied. If the LMTD model is selected, all three equations shown in Equation set 5.55 include the unknown fluid outlet temperatures. The complexity of the LMTD iteration can be reduced by using the ε -NTU heat exchanger model, summarized in Equation set 5.62. The iterative nature of the heat exchanger analysis problem is well-suited for a computer solution. A suggested procedure for setting up the required analysis equations is outlined in the remainder of this section and applied to the analysis of the double pipe heat exchanger designed in Section 5.8.7.

5.8.8.1 Initial Guess of the Fluid Outlet Temperatures

This step is dependent on the computer software being used to solve the problem. Some software sets unknown variables to a default value. Other software, such as spreadsheets, will require user input for unknown variables.

5.8.8.2 Fluid Properties

The hot and cold fluid properties required are shown in Section 5.8.7.1. These properties are evaluated at the average fluid temperatures.

5.8.8.3 Calculation of Annulus Diameters

Since the heat exchanger has been specified, the diameters of the inner and outer tube are known. Therefore, the annulus diameters can be calculated as shown in Section 5.8.7.3.

TABLE 5.7
Double Pipe Heat Exchanger Design Specifications

Inner tube	1¼-std type M copper
Outer pipe	2-nom sch 40 steel
Flow configuration	counter flow
Hot fluid—toluene	in the tube
Cold fluid—city water	in the annulus
Total length	70 ft
Number of hairpins	7
Maintenance schedule	every 3 months

5.8.8.4 Calculation of Fluid Velocities

The velocity of each fluid is required for the calculation of the Reynolds number and the pressure drop through each passage. The velocities in the tube and annulus are determined by,

$$V_t = \frac{4\dot{m}_t}{\rho_t \pi D_t^2} \quad V_a = \frac{4\dot{m}_a}{\rho_a \pi (ID_a^2 - OD_t^2)}$$

5.8.8.5 Calculation of Reynolds Numbers

Once the fluid properties and velocities are known, the Reynolds numbers for the tube and annulus can be determined using the equations shown in Section 5.8.7.5.

5.8.8.6 Calculation of Friction Factors

The friction factors in the tube and annulus are determined using the equations shown in Section 5.8.7.6. If the outer pipe and inner tube are of different materials, then the absolute roughness of the annulus can be estimated using an area weighted value following the procedure shown in Example 5.11.

5.8.8.7 Calculation of Nusselt Numbers

The expression used for the Nusselt number calculation depends on the flow regime. The recommended correlations for DPHX calculations are shown in Table 5.5. The flows in the DPHX designed in Section 5.8.7 are turbulent. Therefore, for this analysis, the equations shown in Section 5.8.7.8 can be used.

5.8.8.8 Calculation of Convective Heat Transfer Coefficients

The convective heat transfer coefficients can be determined from the Nusselt numbers using the equations shown in Section 5.8.7.8.

5.8.8.9 Calculation of Overall Heat Transfer Coefficients

At this point, it is suggested that both clean and fouled situations be considered. The value of interest is for the fouled heat exchanger. Under fouled conditions, the heat exchanger must deliver the fluids at the required temperature(s). However, knowing how the heat exchanger will perform when it is clean is also of interest. For the clean heat exchanger,

$$\frac{1}{U_{o,clean}} = \frac{1}{h_t} \left(\frac{OD_t}{ID_t} \right) + \frac{1}{h_a}$$

For the fouled heat exchanger, the maintenance period must be taken into account. Assuming that fouling occurs linearly, the fouling factors shown in Table 5.2 can be adjusted as follows,

$$R''_{f,adjusted} = \frac{R''_f}{(12/M)} \quad (5.102)$$

In Equation 5.102, M is the number of months the heat exchanger operates before it is maintained. Notice that if the maintenance period is yearly, $M = 12$ (months), then the adjusted

value of the fouling factor is the same as shown in Table 5.2. Using this thinking, the fouled overall heat transfer coefficient for the fouled heat exchanger can be calculated by,

$$\frac{1}{U_{o,fouled}} = \frac{1}{h_t} \left(\frac{OD_t}{ID_t} \right) + \frac{R''_{f,i}}{(12/M)} \left(\frac{OD_t}{ID_t} \right) + \frac{R''_{f,o}}{(12/M)} + \frac{1}{h_a}$$

5.8.8.10 Calculation of the UA Values

Once the overall heat transfer coefficient is known, the UA value for the heat exchanger can be determined for clean and fouled conditions,

$$(UA)_{clean} = U_{o,clean} [\pi(OD_t)L] \quad (UA)_{fouled} = U_{o,fouled} [\pi(OD_t)L]$$

5.8.8.11 Application of the Heat Exchanger Model

The LMTD model or the ε -NTU model can now be used to determine the fluid outlet temperatures for both clean and fouled conditions. The model selected is one of personal preference. However, recall that the ε -NTU model removes the iteration required in the LMTD method.

5.8.8.12 Calculation of the Pressure Drops

The equations shown in Section 5.8.7.12 can be used to determine the pressure drop in the tube and annulus. These values represent the pressure drop under a clean condition. If necessary, the pressure drops can be estimated under a fouled condition.

5.8.8.13 Heat Exchanger Specifications and Performance

Following the procedure outlined in Sections 5.8.8.1 through 5.8.8.12, the heat exchanger outlet temperatures and pressure drops can be determined. In the solution presented here, the ε -NTU method was used for the heat exchanger model. Table 5.8 combines the information from Table 5.7 along with the thermal and hydraulic performance of the heat exchanger.

Recall that the heat exchanger is designed to cool 10,000 lbm/h of toluene from 96°F to 75°F. Table 5.8 indicates that when the heat exchanger is clean, the outlet temperature of the toluene is 72.4°F. After three months of operation, the heat exchanger fouling causes the toluene outlet temperature to rise to 74.9°F. Based on this analysis, the heat exchanger's thermal performance is as expected as long as maintenance is done to clean it out after three months of operation.

Table 5.8 shows that the pressure drops in the tube and annulus are 2.4 psi and 5.2 psi, respectively. These values were computed for a clean heat exchanger. These values can be expected to increase slightly over the three-month period between maintenance cleanings. Since the maintenance schedule is more frequent than yearly, the anticipated impact on the pressure drop is assumed to be minimal.

5.9 Shell and Tube Heat Exchanger Design and Analysis

STHXs are typically used where large heat transfer rates are needed. They are often used as condensers or evaporators. The shell is usually made up of wrought iron pipe ranging

TABLE 5.8

Summary of the Double Pipe Heat Exchanger Design and Analysis Results

<i>Heat exchanger specifications</i>	
Inner tube	1¼-std type M copper
Outer pipe	2-nom sch 40 steel
Flow configuration	counter flow
Total length	70 ft
Number of hairpins	7
Maintenance schedule	every 3 months
<i>Fluid placement</i>	
Hot fluid—toluene	in the tube
Cold fluid—city water	in the annulus
<i>Thermal Performance</i>	
Hot fluid mass flow rate	10,000 lbm/hr
Hot fluid inlet temperature	96°F
Cold fluid mass flow rate	12,500 lbm/hr
Cold fluid inlet temperature	65°F
<i>Clean Heat Exchanger</i>	
Hot fluid outlet temperature	72.4°F
Cold fluid outlet temperature	72.7°F
Heat transfer rate	96,769 Btu/h
UA product	6,997 Btu/h-°F
<i>Fouled Heat Exchanger</i>	
Hot fluid outlet temperature	74.9°F
Cold fluid outlet temperature	71.9°F
Heat transfer rate	86,695 Btu/h
UA product	5,445 Btu/h-°F
<i>Hydraulic Performance</i>	
Hot fluid (tube) pressure drop	2.4 psi
Cold fluid (annulus) pressure drop	5.2 psi

from 8-nom to 39-nom. The schedule depends on the pressure inside of the shell. Other materials can be used if corrosion can be caused by the shell fluid.

The tubes are specified differently compared to copper water tubing. They are standardized to the Birmingham Wire Gage (BWG) specification and often called *condenser tubes*. Table 5.9 shows the dimensional data for several STHX tubes using the BWG specification (Kakac, Liu and Pramuanjaroenkij 2012). When specifying a tube, the outside diameter and BWG are specified. For example, a 1-in 12 BWG tube has an outside diameter of 1-inch and an inside diameter of 0.782-in. The tubes usually come in standard lengths of 8, 12, and 16 feet.

The tubes are typically laid out in one of two configurations; square-pitch or triangular-pitch as shown in Figure 5.25. The pitch, P_T , is defined as the tube center-to-center distance. The tube clearance, C , is the distance between tubes.

TABLE 5.9
BWG Specification for Tubes in a Shell and Tube Heat Exchanger

OD (in)	BWG	ID (in)	ID (cm)	OD (in)	BWG	ID (in)	ID (cm)
3/4	10	0.482	1.224	1 1/4	7	0.890	2.261
	11	0.510	1.295		8	0.920	2.337
	12	0.532	1.351		10	0.982	2.494
	13	0.560	1.422		11	1.010	2.565
	14	0.584	1.483		12	1.032	2.621
	15	0.606	1.539		13	1.060	2.692
	16	0.620	1.575		14	1.084	2.753
	17	0.634	1.610		16	1.120	2.845
	18	0.652	1.656		18	1.152	2.926
	20	0.680	1.727		20	1.180	2.997
1	8	0.670	1.702	1 1/2	10	1.232	3.129
	10	0.732	1.859		12	1.282	3.256
	11	0.760	1.930		14	1.334	3.388
	12	0.782	1.986		16	1.370	3.480
	13	0.810	2.057				
	14	0.834	2.118				
	15	0.856	2.174				
	16	0.870	2.210				
	18	0.902	2.291				
	20	0.930	2.362				

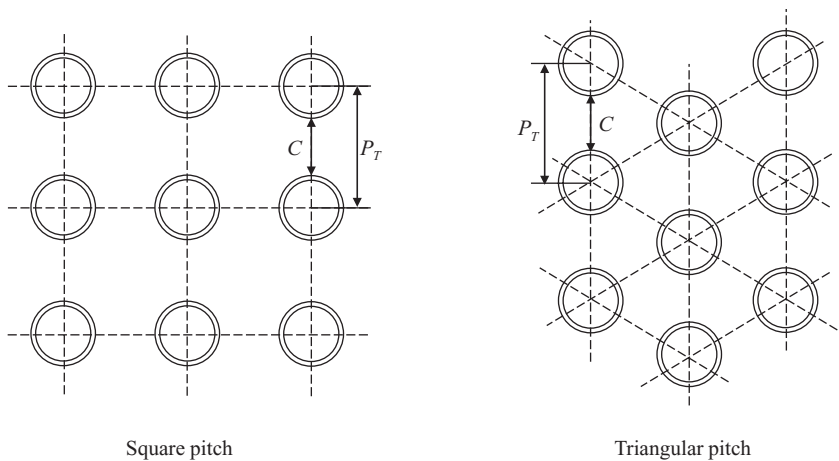


FIGURE 5.25
Tube layout for square and triangular pitch patterns.

The maximum number of tubes that can fit inside of a given shell depends on the tube size, tube pitch, and number of tube passes in the shell. Table 5.10 shows an abbreviated table of the maximum tube counts for various shell sizes and tube passes (indicated as 1P, 2P, or 4P) to retain the structural integrity of the tube sheet (Kakac, Liu and Pramuanjaroenkij 2012). A more comprehensive table of tube counts and BWG tubing dimensions can be found in Kakac, Liu, and Pramuanjaroenkij (2012).

TABLE 5.10
Tube Counts in Shell and Tube Heat Exchangers

Shell Diam (in)	3/4-in Tubes						1-in Tubes					
	1-in Triangular Pitch			1-in Square Pitch			1 1/4-in Triangular Pitch			1 1/4-in Square Pitch		
	1P	2P	4P	1P	2P	4P	1P	2P	4P	1P	2P	4P
8	37	30	24	32	26	20	21	16	16	21	16	14
10	61	52	40	52	52	40	32	32	26	32	32	26
12	92	82	76	81	76	68	55	52	48	48	45	40
13 1/4	109	106	86	97	90	82	68	66	58	61	56	52
15 1/4	151	138	122	137	124	116	91	86	80	81	76	68
17 1/4	203	196	178	177	166	158	131	118	106	112	112	96
19 1/4	262	250	226	224	220	204	163	152	140	138	132	128
21 1/4	316	302	278	277	270	246	199	188	170	177	166	158
23 1/4	384	376	352	341	324	308	241	232	212	213	208	192
25	470	452	422	413	394	370	294	282	256	260	252	238
27	559	534	488	481	460	432	349	334	302	300	288	278
29	630	604	556	553	526	480	397	376	338	341	326	300
31	745	728	678	657	640	600	472	454	430	406	398	380
33	856	830	774	749	718	688	538	522	486	465	460	432
35	970	938	882	845	824	780	608	592	562	522	518	488
37	1074	1044	1012	934	914	886	674	664	632	596	574	562
39	1206	1176	1128	1049	1024	982	766	736	700	665	644	624

Shell Diam (in)	1 1/4-in Tubes						1 1/2-in Tubes					
	1 9/16-in Triangular Pitch			1 9/16-in Square Pitch			1 7/8-in Triangular Pitch			1 7/8-in Square Pitch		
	1P	2P	4P	1P	2P	4P	1P	2P	4P	1P	2P	4P
10	20	18	14	16	12	10	–	–	–	–	–	–
12	32	30	26	30	24	22	18	14	14	16	16	12
13 1/4	38	36	32	32	30	30	27	22	18	22	22	16
15 1/4	54	51	45	44	40	37	26	34	32	29	29	24
17 1/4	69	66	62	56	53	51	48	44	42	29	39	34
19 1/4	95	91	86	78	73	71	61	58	55	50	48	45
21 1/4	117	112	105	96	90	86	76	78	70	32	60	57
23 1/4	140	136	130	127	112	106	95	91	86	78	74	70
25	170	164	155	140	135	127	115	110	105	94	90	86
27	202	196	185	166	160	151	136	131	125	112	108	102
29	235	228	217	193	188	178	160	154	147	131	127	120
31	275	270	255	226	220	209	184	177	172	151	146	141
33	315	305	297	258	252	244	215	206	200	176	170	164
35	357	348	335	293	287	275	246	238	230	202	196	188
37	407	390	380	334	322	311	275	268	260	224	220	217
39	449	436	425	370	362	348	307	299	290	252	246	237

Baffles are used to provide support for the tubes inside the shell. The baffles are also designed to influence the flow of the shell fluid. The distance between baffles is known as the *baffle spacing* or *baffle pitch* and given the symbol, B . The optimum baffle spacing for segmental baffles is somewhere between 0.4 and 0.6 of the shell diameter.

There are several different types of baffle designs. Unfortunately, many of the baffle designs are proprietary. Manufacturers test their own designs or use an independent contractor to evaluate their designs. To maintain a competitive edge, the results are usually kept confidential. The design of the baffle influences the convective heat transfer coefficient on the shell side of the heat exchanger. In this presentation, the performance of the *segmental cut baffle* is given. This is a common type of baffle used in many STHXs. Figure 5.26 shows a sketch of what a segmental cut baffle looks like and how they are typically placed within the shell.

The number of *passes* in a STHX corresponds to the number of passes the tube fluid makes. Figure 5.27 shows the schematic of a 1-shell 1-pass (1-1 or 1P) and a 1-shell 2-pass (1-2 or 2P) STHX. 1-4, 1-6, and 1-8 STHX are also available. It is also possible to connect shells together to make a multi-shell STHX. For example, a 2-4 STHX has 2 shell passes with 2 tube passes in each shell for a total of 4 tube passes.

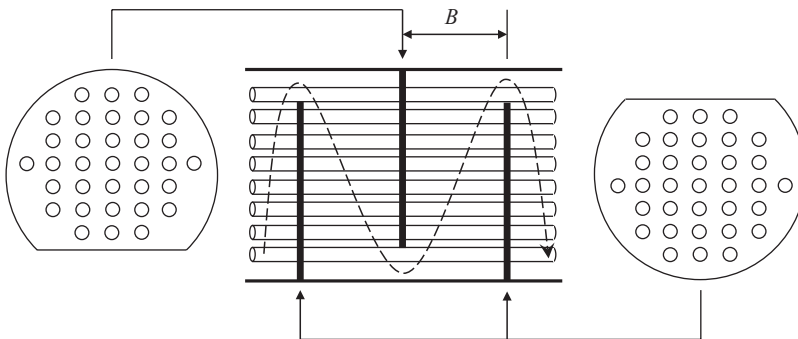


FIGURE 5.26
Segmental cut baffles in a shell and tube heat exchanger.

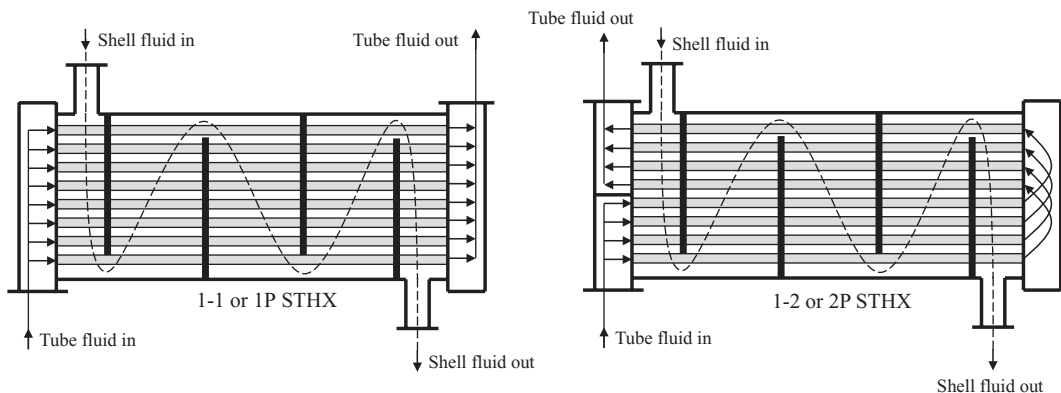


FIGURE 5.27
Single- and multi-pass shell and tube heat exchangers.

5.9.1 LMTD for Shell and Tube Heat Exchangers

At some point during the design and/or analysis process of any heat exchanger, the heat exchanger model must be invoked. Two models were presented in Section 5.6.4 (the LMTD model) and Section 5.6.5 (the ε -NTU model). Due to the complex temperature profiles that occur inside of a STHX, the LMTD is difficult to quantify. To simplify this problem, it is common practice to use the fluid temperatures in and out of the heat exchanger to calculate the LMTD for a counter flow heat exchanger and then modify this value using a correction factor. Then, the heat transfer equation in the LMTD model becomes,

$$\dot{Q} = UA(F)(\text{LMTD}_{\text{CF}}) \quad (5.103)$$

In this equation, LMTD_{CF} is the LMTD for a counter flow heat exchanger. The correction factor, F , depends on the configuration of the heat exchanger. For a STHX with 1 shell pass and 2 or more tube passes, F is given by,

$$F = \frac{\sqrt{R^2 + 1} \ln \left(\frac{1 - P}{1 - PR} \right)}{(R - 1) \ln \left[\frac{2 - P(R + 1 - \sqrt{R^2 + 1})}{2 - P(R + 1 + \sqrt{R^2 + 1})} \right]} \quad (5.104)$$

In Equation 5.104, P and R are defined as,

$$R = \frac{\dot{C}_c}{\dot{C}_h} = \frac{T_{hi} - T_{ho}}{t_{co} - t_{ci}} \quad (5.105)$$

$$P = \frac{t_{co} - t_{ci}}{T_{hi} - t_{ci}} \quad (5.106)$$

The value of F is a modifier to the LMTD for a counter flow heat exchanger. Therefore, the closer F is to 1, the better the heat exchanger is performing. In fact, if F is less than 0.75, the heat exchanger is operating inefficiently leading to higher operating cost to produce the desired heat transfer rate. It is common practice to design STHXs that maintain $F \geq 0.75$.

5.9.2 Tube Side Analysis of Shell and Tube Heat Exchangers

Shell and tube heat exchangers are meant for high heat transfer and mass flow rates. Therefore, it is unlikely that the flow inside the tubes is laminar. However, it is good practice to check the Reynolds number of the flow. For turbulent flow, the Gnielinski correlation (Equation 5.26) is recommended. The Reynolds number is based on the velocity of the flow through one tube. The effect of all tubes together is accounted for when the total outside surface area of the tube bundle is calculated. The velocity through one of the tubes is calculated from the total mass flow rate by,

$$V_t = \frac{\dot{m}_t}{\rho_t A_t} \quad (5.107)$$

In this equation, the mass flow rate and the cross-sectional area are *total* values. The total cross-sectional area available in the tubes can be found by,

$$A_t = \frac{N_t}{N_p} \left[\frac{\pi (ID_t^2)}{4} \right] \quad (5.108)$$

Here, N_t is the total number of tubes in the heat exchanger and N_p is the number of tube passes. Using these expressions, the Reynolds number of the flow inside *one* of the tubes is,

$$Re_t = \frac{\rho_t V_t (ID_t)}{\mu_t} \quad (5.109)$$

The pressure drop of the tube-side fluid consists of two parts; the pressure drop as the fluid flows through the tubes, and the pressure drop associated with the abrupt expansion and contraction experienced at the tube sheet and losses associated with any return bends. The pressure drop through the tubes can be found by,

$$\frac{\Delta P_{tubes}}{\gamma_t} = N_p \left(f_t \frac{L_t}{ID_t} \frac{V_t^2}{2g} \right) \quad (5.110)$$

The pressure drop due to the minor losses in the tube sheet and return bends is given by,

$$\frac{\Delta P_m}{\gamma_t} = 4N_p \frac{V_t^2}{2g} \quad (5.111)$$

In this equation, the value “4” was determined experimentally. Adding Equations 5.110 and 5.111 together results in the total pressure drop of the tube-side fluid,

$$\Delta P_t = \Delta P_{tubes} + \Delta P_m = \gamma_t N_p \left(f_t \frac{L_t}{ID_t} + 4 \right) \frac{V_t^2}{2g} \quad (5.112)$$

5.9.3 Shell Side Analysis of Shell and Tube Heat Exchangers

Analysis of the shell-side fluid is more complicated due to the complex flow path taken as it passes through the heat exchanger. A suitable correlation for the convective heat transfer coefficient between the shell fluid and the outside surface of the tubes for a STHX with segmental baffles is suggested by McAdams (Fraas 1989) and given by,

$$Nu_s = 0.36 Re_s^{0.55} Pr_s^{1/3} \left(\frac{\mu}{\mu_w} \right)^{0.14} \quad (5.113)$$

This correlation is valid for Reynolds numbers from 2,000 to 1,000,000. The properties are evaluated at the average temperature of the shell fluid, except for μ_w , which is evaluated

at the wall temperature of the tubes. The tube wall temperature can be estimated by averaging the average of the hot and cold fluid temperatures,

$$T_w = \frac{1}{2} \left(\frac{T_{hi} + T_{ho}}{2} + \frac{t_{ci} + t_{co}}{2} \right) \quad (5.114)$$

In cases where the tube wall temperature estimated using Equation 5.114 is reasonably close to the shell fluid's average temperature, the ratio of the dynamic viscosities raised to the 0.14 power in Equation 5.113 is very close to 1. In cases like this, Equation 5.113 can be simplified to,

$$\text{Nu}_s = 0.36 \text{Re}_s^{0.55} \text{Pr}_s^{1/3} \quad (5.115)$$

In Equations 5.113 and 5.115, the Nusselt and Reynolds numbers are based on the equivalent diameter of the shell,

$$\text{Nu}_s = \frac{h_s D_e}{k_s} \quad \text{and} \quad \text{Re}_s = \frac{\rho_s V_s D_e}{\mu_s} \quad (5.116)$$

For the shell-side, the equivalent diameter is dependent on the tube pitch. Figure 5.28 shows square and triangular pitch layouts with hypothetical flow passages shaded in dark grey. Using the definition of the equivalent diameter and the variables indicated in Figure 5.28, an expression can be derived for the equivalent diameter of the shell.

For a STHX with square pitch tubes,

$$D_e = \frac{4(\text{cross sectional area})}{\text{heat transfer perimeter}} = \frac{4 \left[P_T^2 - \frac{\pi(OD_t^2)}{4} \right]}{\pi(OD_t)} = \frac{4P_T^2}{\pi(OD_t)} - OD_t \quad (5.117)$$

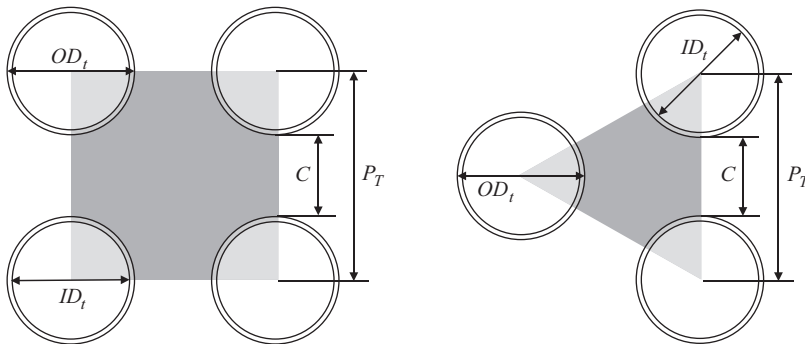


FIGURE 5.28

Square and triangular pitch layouts used to determine the equivalent diameter of the shell.

Likewise, for triangular pitch tubes,

$$D_e = \frac{4(\text{cross sectional area})}{\text{heat transfer perimeter}} = \frac{4 \left[\frac{P_T^2 \sqrt{3}}{4} - \frac{\pi}{8} (OD_t^2) \right]}{\frac{\pi}{2} (OD_t)} = \frac{2\sqrt{3} (P_T^2)}{\pi (OD_t)} - OD_t \quad (5.118)$$

Equations 5.117 and 5.118 can be written as a single equation,

$$D_e = \frac{XP_T^2}{\pi (OD_t)} - OD_t \quad \begin{cases} X = 4 \text{ for square pitch} \\ X = 2\sqrt{3} \text{ for triangular pitch} \end{cases} \quad (5.119)$$

The shell-side fluid velocity varies as it travels around the labyrinth of tubes and baffles that make up the tube bundle. However, a constant value of velocity is preferred to calculate the Reynolds number given in Equation 5.116. In order to do this, a characteristic shell-side flow area is defined as,

$$A_s = \frac{D_s CB}{P_T} \quad (5.120)$$

In this equation, D_s is the actual shell diameter, C is the tube clearance (see Figure 5.28), P_T is the tube pitch, and B is the baffle spacing. Using this as the characteristic flow area in the shell, the shell-fluid velocity can be found by,

$$V_s = \frac{\dot{m}_s}{\rho_s A_s} \quad (5.121)$$

The pressure drop of the shell fluid is difficult to model analytically. Therefore, an empirical expression based on experimental data is preferred. The empiricism is cast in the form of a head loss term and is expressed as (Kern 1950),

$$\frac{\Delta P_s}{\gamma_s} = \frac{f_s}{\phi_s} (N_b + 1) \frac{D_s}{D_e} \frac{V_s^2}{2g} \quad (5.122)$$

In this equation, N_b is the number of baffles in the heat exchanger, $\phi_s = (\mu/\mu_w)^{0.14}$, and f_s is the shell-side friction factor which is determined by the empirical relationship,

$$f_s = \exp[0.576 - 0.19 \ln(\text{Re}_s)] \quad (5.123)$$

Equation 5.123 is valid for $400 \leq \text{Re}_s \leq 1,000,000$. Equation 5.122 is formulated to include minor losses at the inlet and outlet of the shell. As was seen with the shell-side Nusselt number, if the estimated tube wall temperature is reasonably close to the shell side average temperature, then Equation 5.122 can be estimated as,

$$\frac{\Delta P_s}{\gamma_s} = f_s(N_b + 1) \frac{D_s}{D_e} \frac{V_s^2}{2g} \quad (5.124)$$

Similar to double pipe heat exchangers, the pressure drop on either side (tube or shell) should be no greater than 10 psi (~70 kPa).

5.9.4 Shell and Tube Heat Exchanger Design Considerations

The list below discusses some of the major design considerations for shell and tube heat exchangers. The list is not intended to be all-inclusive. However, most of the major points are addressed here.

5.9.4.1 Tube Side Considerations

- Higher flow rates through the tubes result in higher heat transfer rates. However, the downside is the pressure drop across the tubes will increase.
- Multiple tube passes will increase the heat transfer rate between the fluids. However, the pressure drop will increase faster than the heat transfer rate. There is a tradeoff between heat transfer enhancement and increased pumping power that must be considered.

5.9.4.2 Shell Side Considerations

- The optimum baffle spacing is somewhere between 0.4 and 0.6 of the shell diameter. Keeping the baffle spacing in this range makes the shell fluid flow in more of a cross flow pattern across the tubes and keeps the value of the LMTD correction factor, F , high. This increases the heat transfer rate between the two fluids.
- The heat transfer rate can be increased by increasing the number of baffles. However, the drawback is that the pressure drop increases faster than the heat transfer rate. Higher heat transfer rates are desirable. However, the higher pressure drop means more pumping power is required to move the fluid through the shell side.

5.9.4.3 General Considerations

- As with the double pipe heat exchanger, there are two criteria for fluid placement; hydraulic and fouling. It may be more desirable to place the fluid with the higher fouling factor through the tubes. The reason for this is that the tubes are easy to clean mechanically. If the fluid fouling factors are approximately the same, then use the hydraulic criterion and route the higher mass flow rate fluid through the side with the larger flow area.
- In a design problem, the heat exchanger should be kept as small as possible while maintaining the desired performance. This is an economic issue, both from capital cost and operating cost perspectives.
- The economics of the heat exchanger are somewhat reflected in the value of the LMTD correction factor, F . This value should be greater than or equal to 0.75.
- It is desirable to keep the velocity in the tubes in the economic range.

- The heat exchanger should deliver the required heat transfer rate when completely fouled. Recall that the fouling factors represent fouling after one year of service.
- The pressure drop on each side of the heat exchanger should not exceed 10 psi (~70 kPa).

5.9.5 Shell and Tube Heat Exchanger Design

Many STHX parameters are specified in the design process, such as shell diameter, tube specifications, baffle type, baffle spacing, tube pitch, and so on. The process can be highly iterative due to the large number of design parameters involved. Unless you work for a STHX heat exchanger manufacturer, you would probably not be tasked with designing a STHX. It is more likely that you will communicate your requirements with an applications engineer who works for the heat exchanger manufacturer, and the manufacturer would design and build the heat exchanger. This is an important process because the cost of STHXs can be quite high due to their size and internal complexity. It is more likely that an engineer would be tasked with *analyzing* a STHX to determine if its thermal and hydraulic performance meets specific requirements for the heat exchange application.

5.9.6 Shell and Tube Heat Exchanger Analysis

Given the manufacturer's specifications for the construction of a shell and tube heat exchanger, an analysis procedure can be used to determine if the heat exchanger would be suitable for a given application. This section details the analysis procedure for the following example:

In an industrial process, it is necessary to heat a flow of cyclohexane from 15°C to 45°C. The cyclohexane is flowing at 35 kg/s. The heating is to be done with hot distilled water which is available at 53°C. The water flow rate can be varied, but the maximum flow rate available is 42 kg/s. Since the flow rates are very large, a shell and tube heat exchanger will be used for the heating process. Manufacturer's design specifications for a particular STHX are shown in Table 5.11. Analyze this heat exchanger and determine if it is able to provide the required thermal and hydraulic performance.

5.9.6.1 Initial Guess of the Fluid Outlet Temperatures

Even though the desired outlet temperature of the cold fluid is known, in the analysis it is treated as an unknown. The following initial guesses will be made for the fluid outlet temperatures,

$$T_{ho} = 45^{\circ}\text{C} \quad t_{co} = 45^{\circ}\text{C}$$

This step is dependent on the computer software being used to solve the problem. Some software sets unknown variables to a default value. Other software, such as spreadsheets, will require user input for unknown variables.

TABLE 5.11

Manufacturer's Design Specifications for a Shell and Tube Heat Exchanger

Parameter	Value
Shell diameter	27 in
Number of shell passes	1
Tube specification	¾-inch 16 BWG
Tube pitch	1-inch triangular
Number of tube passes	2
Heat exchanger length	6 m
Number of segmental baffles	15

5.9.6.2 Fluid Properties

Given the estimates of the outlet fluid temperatures, the fluid properties can be evaluated at the average temperature. The resulting properties are,

Fluid	T (°C)	ρ (kg/m ³)	γ (N/m ³)	c_p (kJ/kg-K)	μ (kg/m-s)	k (W/m-K)	Pr
water	49	988.44	9693.7	4.1813	0.00055580	0.63944	3.6344
cyclohexane	30	769.15	7543.1	1.8826	0.00081889	0.11667	13.213

5.9.6.3 Shell and Tube Parameters

Dimensional data for the tubes can be determined from Table 5.9. For a ¾ 16-BWG tube,

$$ID_t = 0.015748 \text{ m} \quad OD_t = (0.75 \text{ in}) \left(\frac{0.00254 \text{ m}}{\text{in}} \right) = 0.001905 \text{ m}$$

The number of tubes in the shell can be determined from Table 5.10,

$$N_t = 534$$

The absolute roughness of the tubes can be determined from Table 4.3,

$$\varepsilon_t = 0.000005 \text{ m (copper)}$$

The clearance between the tubes in the tube bundle is,

$$C = P_T - OD_t = 0.0063500 \text{ m}$$

For the shell, the parameters required are the equivalent diameter, Equation 5.119, and the baffle spacing,

$$D_e = \frac{2\sqrt{3}(P_T^2)}{\pi(OD_t)} - OD_t = 0.018293 \text{ m} \quad B = \frac{L}{N_b + 1} = 0.375 \text{ m}$$

5.9.6.4 Fluid Velocities

The flow area through one of the tubes is,

$$A_t = \frac{N_t}{N_p} \left(\frac{\pi ID_t^2}{4} \right) = 0.052006 \text{ m}^2 \quad (N_p = 2 \text{ pass})$$

The characteristic flow area for the shell is given by Equation 5.120,

$$A_s = \frac{D_s CB}{P_T} = 0.064294 \text{ m}^2$$

Before the fluid velocities can be calculated, a decision needs to be made concerning the fluid placement. The fluid with the higher mass flow rate is the water (hot fluid). The hydraulic criterion suggests that the water should be placed in the shell (largest flow area). The fouling factors of each fluid can be found in Table 5.2,

$$R''_{fh} = 0.000088 \frac{\text{m}^2\text{-K}}{\text{W}} \text{ (distilled water)}$$

$$R''_{fc} = 0.000352 \frac{\text{m}^2\text{-K}}{\text{W}} \text{ (cyclohexane - organic liquid)}$$

These values indicate that the cyclohexane should be placed in the tubes. In this case, the hydraulic criterion and the fouling criterion are complimentary. Therefore, the water (hot fluid) will be placed in the shell and the cyclohexane (cold fluid) in the tubes.

Now, the velocities of each fluid can be determined,

$$V_t = \frac{\dot{m}_t}{\rho_t A_t} = 0.87499 \frac{\text{m}}{\text{s}} \quad V_s = \frac{\dot{m}_s}{\rho_s A_s} = 0.33044 \frac{\text{m}}{\text{s}}$$

5.9.6.5 Calculation of Reynolds Numbers

$$\text{Re}_t = \frac{\rho_t V_t (ID_t)}{\mu_t} = 12,942 \quad \text{Re}_s = \frac{\rho_s V_s D_e}{\mu_s} = 10,750$$

5.9.6.6 Calculation of Friction Factors

$$f_t = \frac{0.25}{\left[\log \left(\frac{\varepsilon / ID_t}{3.7} + \frac{5.74}{\text{Re}_t^{0.9}} \right) \right]^2} = 0.029513 \quad f_s = \exp \left[0.576 - 0.19 \ln (\text{Re}_s) \right] = 0.30492$$

5.9.6.7 Calculation of Nusselt Numbers

$$\text{Nu}_t = \frac{(f_t/8)(\text{Re}_t - 1000)\text{Pr}_t}{1 + 12.7(f_t/8)^{1/2}(\text{Pr}_t^{2/3} - 1)} = 128.23 \quad \text{Nu}_s = 0.36 \text{Re}_s^{0.55} \text{Pr}_s^{1/3} = 91.284$$

Here, the shell-side Nusselt number is estimated using Equation 5.115, assuming that $(\mu/\mu_w)^{0.14}$ is nearly 1. This will be checked later.

5.9.6.8 Calculation of Convective Heat Transfer Coefficients

$$\text{Nu}_t = \frac{h_t(\text{ID}_t)}{k_t} \rightarrow h_t = \frac{\text{Nu}_t k_t}{\text{ID}_t} = 950.00 \frac{\text{W}}{\text{m}^2 \cdot \text{K}}$$

$$\text{Nu}_s = \frac{h_s D_e}{k_s} \rightarrow h_s = \frac{\text{Nu}_s k_s}{D_e} = 3190.8 \frac{\text{W}}{\text{m}^2 \cdot \text{K}}$$

5.9.6.9 Calculation of the Overall Heat Transfer Coefficients

Both clean and fouled values of the overall heat transfer coefficient will be calculated. For a clean heat exchanger,

$$\frac{1}{U_{o,\text{clean}}} = \frac{1}{h_t} \left(\frac{\text{OD}_t}{\text{ID}_t} \right) + \frac{1}{h_s} \rightarrow U_{o,\text{clean}} = 630.22 \frac{\text{W}}{\text{m}^2 \cdot \text{K}}$$

For the fouled heat exchanger, a maintenance period needs to be identified. The STHX is a large, complex heat exchanger that may require substantial time to take offline, open up, clean, reassemble, and bring back online. To begin, a yearly maintenance scheme will be considered. For yearly maintenance, $M = 12$ in the following equation,

$$\frac{1}{U_{o,\text{fouled}}} = \frac{1}{h_t} \left(\frac{\text{OD}_t}{\text{ID}_t} \right) + \frac{R''_{f,i}}{(12/M)} \left(\frac{\text{OD}_t}{\text{ID}_t} \right) + \frac{R''_{f,o}}{(12/M)} + \frac{1}{h_s} \rightarrow U_{o,\text{fouled}} = 488.95 \frac{\text{W}}{\text{m}^2 \cdot \text{K}}$$

5.9.6.10 Calculation of the UA Values

Once the overall heat transfer coefficient is known, the UA value for the heat exchanger can be determined for clean and fouled conditions,

$$(UA)_{\text{clean}} = U_{o,\text{clean}} [N_t \pi (\text{OD}_t) L] = 241.69 \frac{\text{kW}}{\text{K}}$$

$$(UA)_{\text{fouled}} = U_{o,\text{fouled}} [N_t \pi (\text{OD}_t) L] = 187.51 \frac{\text{kW}}{\text{K}}$$

5.9.6.11 Application of the Heat Exchanger Model

The LMTD model or the ε -NTU model can now be used to determine the fluid outlet temperatures for both clean and fouled conditions. The model selected is one of personal preference. However, recall that the ε -NTU model removes the iteration required in the LMTD method. In addition, the LMTD model requires the calculation of the LMTD correction factor, F , using Equation 5.104, which contains a natural logarithm term. Since there is a natural logarithm term in the LMTD itself, the combination of these two natural logarithms can cause easily cause non-convergence problems with solvers. Because of this, the ε -NTU method will be used here. The ε -NTU heat exchanger model is given by,

$$\begin{aligned}\dot{Q} &= \dot{C}_h(T_{hi} - T_{ho}) \\ \dot{Q} &= \dot{C}_c(t_{co} - t_{ci}) \\ \varepsilon &= \frac{\dot{Q}}{\dot{Q}_{\max}} \quad \text{where} \quad \dot{Q}_{\max} = \dot{C}_{\min}(T_{hi} - t_{ci}) \\ \varepsilon &= f(\text{NTU}, C_r) \quad \text{where} \quad \text{NTU} = \frac{U_o A_o}{\dot{C}_{\min}} \quad \text{and} \quad C_r = \frac{\dot{C}_{\min}}{\dot{C}_{\max}}\end{aligned}$$

The thermal capacity rates of the fluids are,

$$\begin{aligned}\dot{C}_h &= \dot{m}_h c_{ph,avg} = 175.61 \frac{\text{kW}}{\text{K}} & \dot{C}_c &= \dot{m}_c c_{pc,avg} = 65.890 \frac{\text{kW}}{\text{K}} \\ \dot{C}_{\min} &= 65.890 \frac{\text{kW}}{\text{K}} & \dot{C}_{\max} &= 175.61 \frac{\text{kW}}{\text{K}} & C_r &= \frac{65.890 \text{ kW/K}}{175.61 \text{ kW/K}} = 0.37520\end{aligned}$$

The NTU for a single shell pass STHX is given in Table 5.4,

$$\text{NTU} = -(1 + C_r^2)^{-1/2} \ln \left(\frac{\Gamma - 1}{\Gamma + 1} \right) = 3.6681 \quad \text{where} \quad \Gamma = \frac{2/\varepsilon - (1 + C_r)}{\sqrt{(1 + C_r^2)}}$$

Solving the heat exchanger model will reveal the fluid outlet temperatures. The numbers shown in Sections 5.9.6.2 through this point in the analysis are the results when the fluid outlet temperatures guessed in Section 5.9.6.1. The solution of the heat exchanger model will automatically update and iterate on the fluid properties as well. The resulting solutions for a clean and fouled heat exchanger are.

Heat Exchanger Condition	T_{ho} (°C)	t_{co} (°C)
Clean	41.5	45.6
Fouled	41.8	44.8

The requirement of this heat exchanger is to heat the cyclohexane (the cold fluid) to a temperature of 45°C. When the heat exchanger is clean, this will occur. However, under fouled conditions, the outlet temperature of the cold fluid is only 44.8°F. By changing the maintenance schedule to once every 6 months ($M = 6$), the following result is obtained,

Heat Exchanger Condition	T_{ho} (°C)	t_{co} (°C)
Clean	41.5	45.6
Fouled	41.7	45.2

This result indicates that cleaning the heat exchanger twice each year instead of annually, results in the heat exchanger meeting the thermal requirements even under fouled conditions.

5.9.6.12 Calculation of Pressure Drops

At this point, the heat exchanger model has converged and there is no further iteration required. The pressure drop through the tubes is given by Equation 5.112,

$$\Delta P_t = \Delta P_{tubes} + \Delta P_m = \gamma_t N_p \left(f_t \frac{L_t}{ID_t} + 4 \right) \frac{V_t^2}{2g} = 15.6 \text{ kPa}$$

Assuming that $(\mu/\mu_w)^{0.14}$ is nearly 1, the pressure drop through the shell is given by Equation 5.124,

$$\frac{\Delta P_s}{\gamma_s} = f_s (N_b + 1) \frac{D_s}{D_e} \frac{V_s^2}{2g} = 9.9 \text{ kPa}$$

These are the pressure drops for a clean heat exchanger and are well below the 10 psi (~70 kPa) threshold. It is unlikely that the shell side pressure drop will increase much due to fouling since the fluid in the shell, distilled water, has such a low fouling factor. Fouling for the tube can be estimated by calculating the fouled inside diameter,

$$ID_{t,f} = ID_{t,c} \exp \left(- \frac{2k_f \frac{R_f''}{(M/12)}}{ID_{t,c}} \right) = 0.012594 \text{ m}$$

In this equation, $M = 6$ (months), and k_f was estimated to be 2.5 W/m-K (the fouling thermal conductivities listed in Table 5.6 are between 2 and 3 W/m-K).

The velocity inside a fouled tube is determined as,

$$V_{t,f} = \frac{\dot{m}_t(1-0.02)}{\rho_t A_{t,f}} = 1.3410 \frac{\text{m}}{\text{s}} \quad \text{where} \quad A_{t,f} = \frac{N_t}{N_p} \left(\frac{\pi ID_{t,f}^2}{4} \right) = 0.033259 \text{ m}^2$$

This value was computed by estimating a reduction in mass flow rate in the tubes of 2% due to the added flow resistance introduced by the fouling layer.

The Reynolds number and friction factor for the fouled tube is,

$$\text{Re}_{t,f} = \frac{\rho_t V_{t,f} (ID_{t,f})}{\mu_t} = 15,888 \quad f_{t,f} = \frac{0.25}{\left[\log \left(\frac{\varepsilon / ID_{t,f}}{3.7} + \frac{5.74}{\text{Re}_{t,f}^{0.9}} \right) \right]^2} = 0.028235$$

This leads to a pressure drop through the fouled tubes of,

$$\Delta P_{t,f} = \Delta P_{tubes} + \Delta P_m = \gamma_t N_p \left(f_{t,f} \frac{L_t}{ID_{t,f}} + 4 \right) \frac{V_{t,f}^2}{2g} = 42.7 \text{ kPa}$$

This calculation indicates that the fouled tube pressure drop is below the 10 psi (~70 kPa) threshold.

5.9.6.13 Design and Analysis Checks

The shell calculations (Nusselt number and pressure drop) were done assuming that the ratio $(\mu/\mu_w)^{0.14}$ in Equations 5.113 and 5.122 was close to 1. Now that the outlet fluid temperatures have been found, the viscosity ratio can be calculated. The average of the average fluid temperatures is,

$$T_w = \frac{1}{2} \left(\frac{T_{hi} + T_{ho}}{2} + \frac{t_{ci} + t_{co}}{2} \right) = 38.718^\circ\text{C}$$

The viscosity of the shell side fluid (water) at this temperature is,

$$\mu_w = 0.00066877 \frac{\text{kg}}{\text{m} \cdot \text{s}}$$

This leads to a viscosity ratio raised to the 0.14 power of,

$$\left(\frac{\mu}{\mu_w} \right)^{0.14} = 0.98$$

This value is close enough to 1 to justify the calculations in Sections 5.9.6.7 and 5.9.7.12.

Finally, the value of the LMTD correction factor, F , can be calculated. Even though the LMTD method was not used, the LMTD correction factor will indicate how close to true counter flow the STHX is performing. Using Equations 5.104 through 5.106,

$$R = \frac{\dot{C}_c}{\dot{C}_h} = \frac{T_{hi} - T_{ho}}{t_{co} - t_{ci}} = 0.37533 \quad P = \frac{t_{co} - t_{ci}}{T_{hi} - t_{ci}} = 0.79500$$

$$\therefore F = \frac{\sqrt{R^2 + 1} \ln \left(\frac{1 - P}{1 - PR} \right)}{(R - 1) \ln \left[\frac{2 - P(R + 1 - \sqrt{R^2 + 1})}{2 - P(R + 1 + \sqrt{R^2 + 1})} \right]} = 0.61520$$

Even though this value is below the recommended minimum value of 0.75, the heat exchanger is performing as required, both thermally and hydraulically. The lower value of F suggests that the STHX could be better designed resulting in a smaller heat exchanger.

5.9.6.14 Summary of Results

The results of this analysis are given in Table 5.12

5.10 Plate and Frame Heat Exchanger Design and Analysis

The PFHX was briefly introduced in Section 5.5.3. An example of a PFHX is shown in Figure 5.8. The heat exchanger is made up of a series of plates bolted together. The fluids pass between the plates by virtue of gaskets. Some common metals used to manufacture the plates are shown in Table 5.13 along with the material's thermal conductivity at a temperature of 150°F (66°C). The gaskets are used to direct the fluid flow throughout the heat exchanger as well as sealing. They are designed so a gasket failure ends up leaking fluid to the atmosphere which eliminates possible mixing of the hot and cold fluids.

PFHXs are typically used where low to moderate heat transfer rates are required. The PFHX has a distinct advantage of a fairly small footprint compared to other types of heat exchangers for the same heat transfer duty. The maximum fluid pressures in the heat exchanger are dictated by the gaskets and plate material. Typical maximum operating pressures can be from 10 bar to 25 bar (145 psig to 360 psig). The maximum fluid temperature is dictated by the gasket material. Depending on the type of gasket material, the maximum fluid temperature can range from 150°C to 260°C (300°F to 500°F).

There are many possible flow configurations for PFHXs. In addition, there are many plate chevron patterns available. Therefore, the design of PFHXs turns out to be very specialized. Much of the data for plates and flow configurations is considered proprietary. Manufacturers of PFHXs have developed their own design procedures applicable to their

TABLE 5.12

Results of the STHX Analysis of Section 5.9.6

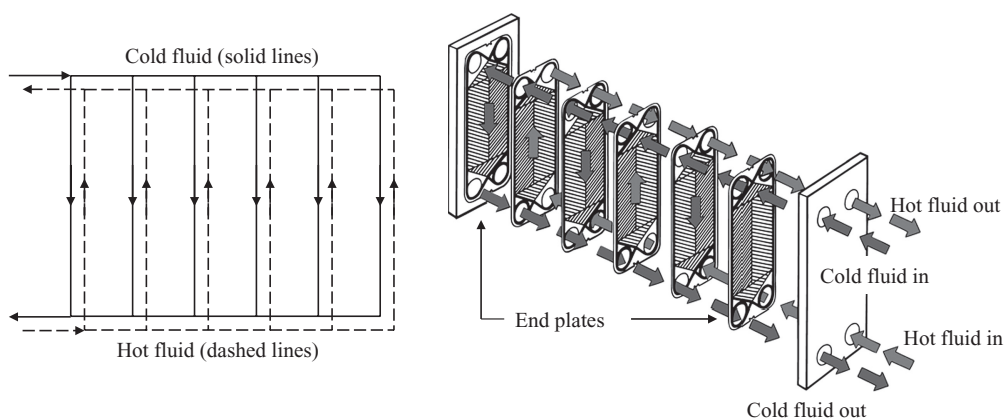
Parameter	Value	
<i>Manufacturer's Specifications</i>		
Shell diameter	27 in	
Number of shell passes	1	
Tube specification	¾-inch 16 BWG	
Tube pitch	1-inch triangular	
Number of tube passes	2	
Heat exchanger length	6 m	
Number of segmental baffles	15	
<i>Fluid Placement</i>		
Hot fluid—distilled water	in the shell	
Cold fluid—cyclohexane	in the tubes	
<i>Thermal Performance</i>		
Hot fluid mass flow rate	42 kg/s	
Hot fluid inlet temperature	53°C	
Cold fluid mass flow rate	35 kg/s	
Cold fluid inlet temperature	15°C	
Desired cold fluid outlet temperature	45°C	
	<i>Clean</i>	<i>Fouled</i>
Hot fluid outlet temperature	41.5°C	41.7°C
Cold fluid outlet temperature	45.6°C	45.2°C
Heat transfer rate	2,014.9 kW	1,991.1 kW
UA product	241.74 kW/K	211.01 kW/K
LMTD correction factor, <i>F</i>		0.6152
<i>Hydraulic Performance</i>		
	<i>Clean</i>	<i>Fouled</i>
Shell pressure drop	9.9 kPa	~10 kPa
Tube pressure drop	15.6 kPa	~40 kPa
<i>Other</i>		
Maintenance schedule	every 6 months	

TABLE 5.13

Common Materials Used for Plates in Plate and Frame Heat Exchangers

Material	Thermal Conductivity at 150°F (66°C)	
	Btu/hr-ft-°F	W/m-K
AISI 304 Stainless Steel	8.99	15.6
AISI 316 Stainless Steel	8.16	14.1
Titanium	12.3	21.3
90/10 Copper-nickel	31.5	54.6
70/30 Copper-nickel	17.9	31.0

Note: Values were calculated using Engineering Equation Solver (EES).

**FIGURE 5.29**

A 1/1-U configuration plate and frame heat exchanger. (Reprinted from Xylem, Inc., *GPX Plate and Frame Heat Exchangers*, Buffalo, New York, USA, Bell & Gossett, 2011. With permission.)

TABLE 5.14

Recommended Fouling Factors for Plate and Frame Heat Exchangers

Fluid	Fouling Factor	
	hr-ft ² -°F/Btu	m ² -K/W
Demineralized or distilled water	0.00001	0.0000017
Soft water	0.00002	0.0000034
Hard water	0.00005	0.0000086
Steam	0.00001	0.0000017
Lubricating oils	0.00002 – 0.00005	0.0000034 – 0.0000086
Organic solvents	0.00001 – 0.00006	0.0000017 – 0.0000103
General process fluids	0.00001 – 0.00006	0.0000017 – 0.0000103

heat exchangers. When purchasing a PFHX from a vendor, the engineer generally specifies the duty requirements of the heat exchanger (inlet and outlet temperature requirements, flow rates, etc.) and an engineer from the company will perform the design calculations and specify a PFHX to meet the requirement.

In this section, the 1/1-U configuration (also known as a *single-pass counter flow* arrangement) will be analyzed. Figure 5.29 shows a schematic of the 1/1-U configuration along with the hot and cold fluid flow paths.

Fouling effects for a PFHX are often less severe compared to the DPHX and STHX. This is due to several factors including, enhanced turbulence due to the chevron pattern of the plate, very smooth plate surfaces with fewer mineral deposition sites, and other factors. Table 5.14 lists the recommended values of fouling factors for PFHXs (Kakac, Liu, and Pramuanjaroenkij 2012). The values in this table were taken from a more comprehensive table in Kakac, Liu, and Pramuanjaroenkij (2012).

5.10.1 Plate and Frame Heat Exchanger Dimensions

Figure 5.30 shows the plate dimensions of a chevron-stamped plate and the dimensions dealing with the cross section of a single plate and the flow passage created by two plates.

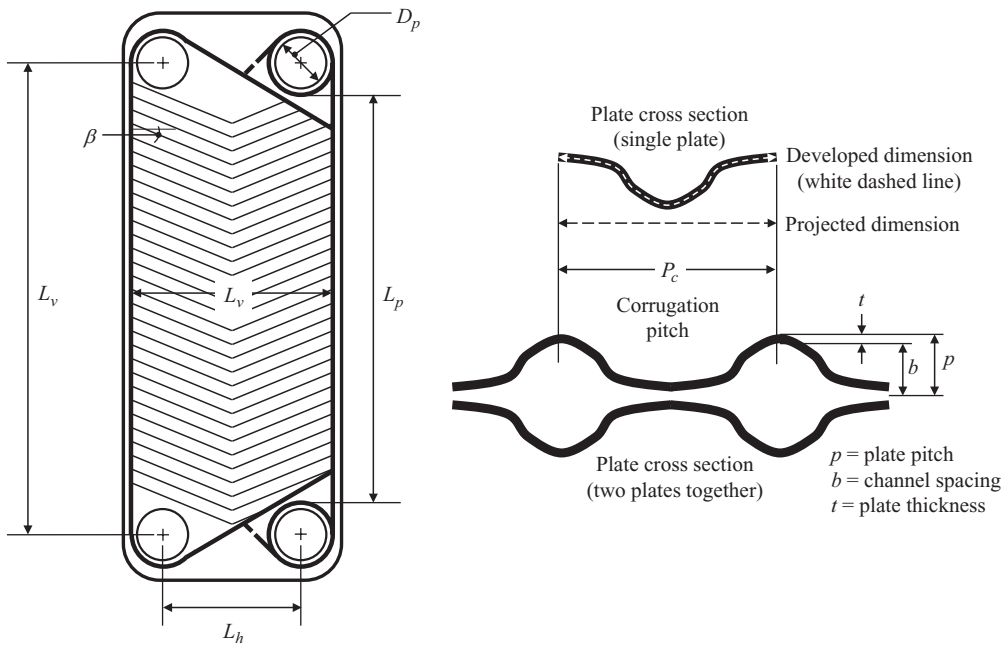
**FIGURE 5.30**

Plate dimensions and cross-sectional views perpendicular to the flow channel.

Chevron patterns in the plate are made by corrugation of the plate. Therefore, the effective area, A_e , seen by the fluid is greater than the projected area, A_p , of the plate. The ratio of the effective area to the projected area is known as the plate *enlargement factor*, Φ , and is defined as,

$$\Phi = \frac{A_e}{A_p} = \frac{A_e}{L_p L_w} \quad (5.125)$$

Enlargement factors usually vary between 1.15 and 1.25. Manufacturers of PFHXs may provide the plate enlargement factor as part of the heat exchanger's specification. If this information is not available, an estimate of 1.17 can be used as a typical average (Edwards, Changel, and Parrott 1974). The plate dimensions L_p and L_w are defined in Figure 5.30. If the actual plate dimensions are unknown, they can be estimated using the port-to-port distance and the port diameter,

$$L_p \approx L_v - D_p \quad (5.126)$$

$$L_w \approx L_h + D_p \quad (5.127)$$

The cross section of two plates together, shown in Figure 5.30, indicates that the channel spacing is defined as,

$$b = p - t \quad (5.128)$$

As indicated in Figure 5.30, p is the plate pitch, and t is the plate thickness. The channel spacing defined by Equation 5.128 is considered the average channel spacing. If the plate pitch is not specified by a manufacturer, it can be determined from the compressed plate pack length of the heat exchanger, L_c (which can usually be determined from engineering drawings), by,

$$p = \frac{L_c}{N_t} \quad (5.129)$$

In Equation 5.129, N_t is the total number of plates in the heat exchanger.

The hydraulic diameter of the passages formed between two plates is determined using the conventional definition given in Equation 5.78. Applying this equation to the flow passage formed by two plates, the hydraulic diameter can be written as,

$$D_{hyd} = \frac{4bL_w}{2(b + \Phi L_w)} \quad (5.130)$$

The channel spacing, b , is much smaller than the plate width, L_w . Therefore, Equation 5.130 is typically written as,

$$D_{hyd} \approx \frac{2b}{\Phi} \quad (5.131)$$

5.10.2 Thermal Performance of a Plate and Frame Heat Exchangers

The overall heat transfer coefficient for a PFHX can be found knowing the total thermal resistance and the effective heat transfer area,

$$U = \frac{1}{AR_t} \quad (5.132)$$

For the PFHX, the total thermal resistance can be written as,

$$R_t = \frac{1}{h_h A_h} + \frac{R''_{fh}}{A_h} + \frac{x_p}{k_p A_p} + \frac{R''_{fc}}{A_c} + \frac{1}{h_c A_c} \quad (5.133)$$

Notice that the thermal resistance for a plane wall is used to model the conduction resistance through the plate (subscript p). Since the heat transfer is occurring through a plate, all of the areas listed in Equations 5.132 and 5.133 are the same. Multiplying Equation 5.133

through by the plate area and substituting into Equation 5.132 results in an expression for the overall heat transfer coefficient for a PFHX,

$$\frac{1}{U_o} = \frac{1}{h_h} + R''_{fh} + \frac{\Delta x_p}{k_p} + R''_{fc} + \frac{1}{h_c} \quad (5.134)$$

The subscript “o” is used to be consistent with other types of heat exchangers previously analyzed. Since the areas are the same on both sides of the plate, U is the same on both sides. The UA product of the PFHX can be found by multiplying U_o by the effective plate area seen by either fluid in the heat exchanger,

$$UA = U_o (N_e A_e) \quad (5.135)$$

The effective area, A_e , is defined in Equation 5.125. The variable N_e is the number of effective plates in the heat exchanger. In the PFHX design, the two end plates do not transfer heat. They are used to provide a gasket seal at the inlet and outlet of the heat exchanger. Therefore,

$$N_e = N_t - 2 \quad (5.136)$$

Design methods and data for PFHXs are largely proprietary. PFHX manufacturers have developed their own specialized design methods for the heat exchangers that they sell. As a result, there is little information available regarding heat transfer coefficient correlations. The heat transfer and hydraulic performance of a PFHX is highly dependent on the plate design; in particular, the chevron pattern. However, a correlation that can be used to estimate the heat transfer coefficient with reasonable accuracy has been developed by Kumar (1984) and is given by,

$$\text{Nu}_{D_{hyd}} = \frac{h D_{hyd}}{k} = C_h \text{Re}^n \text{Pr}^{1/3} \left(\frac{\mu}{\mu_w} \right)^{0.17} \quad (5.137)$$

This correlation can be used to estimate Nusselt numbers for a wide range of chevron angles and Reynolds numbers. The fluid properties are evaluated at the average temperature between the inlet and outlet of the heat exchanger, except μ_w which is evaluated at the average plate temperature. An estimate of the average plate temperature, similar to Equation 5.114 can be used. If the average plate temperature is relatively close to the average fluid temperature, then Equation 5.137 can be written as,

$$\text{Nu}_{D_{hyd}} = \frac{h D_{hyd}}{k} = C_h \text{Re}^n \text{Pr}^{1/3} \quad (5.138)$$

The values of the constants C_h and n are given in Table 5.15 (Kumar 1984).

The Reynolds number in Equations 5.137 and 5.138 is based on the mass flow rate through the individual channels that the fluid traverses in the heat exchanger,

$$\text{Re} = \frac{\rho V_{ch} D_{hyd}}{\mu} = \frac{G_{ch} D_{hyd}}{\mu} \quad (5.139)$$

TABLE 5.15

Constants in Nusselt Number and Pressure Loss Equations for Plate and Frame Heat Exchangers

Chevron Angle	Nusselt Number, Equation 5.137			Pressure Drop, Equation 5.144		
	Re	C_h	n	Re	K_p	m
$\leq 30^\circ$	≤ 10	0.718	0.349	≤ 10	200	1
	> 10	0.348	0.663	10–100	77.6	0.589
				> 100	11.96	0.183
45°	< 10	0.718	0.349	< 15	188	1
	10–100	0.400	0.598	15–300	73.16	0.652
	> 100	0.300	0.663	> 300	5.764	0.206
50°	< 20	0.630	0.333	< 20	136	1
	20–300	0.291	0.591	20–300	45	0.631
	> 300	0.130	0.732	> 300	3.088	0.161
60°	< 20	0.562	0.326	< 40	96	1
	20–400	0.306	0.529	40–400	12.96	0.457
	> 400	0.108	0.703	> 400	3.04	0.215
$\geq 65^\circ$	< 20	0.562	0.326	< 50	96	1
	20–500	0.331	0.503	50–500	11.2	0.451
	> 500	0.087	0.718	> 500	2.556	0.213

In Equation 5.139, G_{ch} is known as the *mass velocity* through the channels. In general, the mass velocity is the mass flow rate per unit area perpendicular to the direction of flow. For the PFHX, this can be expressed as,

$$G_{ch} = \frac{\dot{m}}{N_{cp} b L_w} \quad (5.140)$$

In this equation, N_{cp} is the number of channel passes is determined by,

$$N_{cp} = \frac{N_t - 1}{2N_p} \quad (5.141)$$

Here, N_t is the total number of plates in the heat exchanger, and N_p is the total number of passes the fluid makes as it passes through the heat exchanger. For a 1-1/U arrangement, the number of passes for each fluid is $N_p = 1$.

5.10.3 Hydraulic Performance of a Plate and Frame Heat Exchanger

The pressure drop of the fluids through a PFHX is dependent on two friction losses; friction through the plates, and the loss through the inlet and outlet ports of the heat exchanger,

$$\Delta P = \Delta P_{plates} + \Delta P_{ports} \quad (5.142)$$

The pressure drop through the plates is formulated similar to the friction loss through a pipe, except the hydraulic diameter of the passage is used,

$$\Delta P_{plates} = f \frac{L_v N_p}{D_{hyd}} \frac{G_{ch}^2}{2\rho} \left(\frac{\mu}{\mu_w} \right)^{-0.17} \quad (5.143)$$

In this equation, L_v is the vertical port-to-port distance as shown in Figure 5.30. The friction factor in Equation 5.143 is a function of the plate design. Kumar (1984) suggests that the friction factor for flow between plates be calculated using the following correlation,

$$f = \frac{K_p}{Re^m} \quad (5.144)$$

The values of K_p and m are listed in Table 5.15 for a range of chevron angles and Reynolds numbers. If the average plate temperature is relatively close to the average fluid temperature, then Equation 5.144 can be written as,

$$\Delta P_{plates} = f \frac{L_v N_p}{D_{hyd}} \frac{G_{ch}^2}{2\rho} \quad (5.145)$$

The pressure drop through the inlet and outlet ports of the heat exchanger are treated as a minor loss with a loss coefficient of 1.4,

$$\Delta P_{ports} = 1.4 N_p \frac{G_{port}^2}{2\rho} \quad (5.146)$$

The port mass velocity is determined from the total flow rate of the fluid and the inside diameter of the port,

$$G_{port} = \frac{\dot{m}}{\rho A_{port}} = \frac{4\dot{m}}{\pi D_p^2} \quad (5.147)$$

In this equation, D_p is the port diameter as shown in Figure 5.30.

The maximum allowable pressure drop for each fluid in a PFHX can be estimated as 30 kPa (4.35 psi) per NTU, where the NTU value of the heat exchanger can be calculated from using Equation 5.60.

5.10.4 Plate and Frame Heat Exchanger Analysis

As mentioned in Section 5.10.2, the design of PFHXs is often proprietary. Therefore, a more common problem is to analyze a manufacturer's heat exchanger to determine if it suits the requirements of a given application. In this section, the analysis procedure will be presented for the following problem,

Distilled water, flowing at 120,000 lbm/h enters a 1-1/U counterflow plate and frame heat exchanger at a temperature of 190°F. The desired outlet temperature of the distilled water is 110°F. The cooling is provided using city (hard) water available at 50°F with a flow rate of 100,000 lbm/h. After consulting with the manufacturer, a heat exchanger with specifications given in Table 5.16 is suggested. Verify that this heat exchanger will perform as required.

TABLE 5.16

Manufacturer's Design Specifications for a Plate and Frame Heat Exchanger

Parameter	Value
Plate material	AISI 304 Stainless Steel
Chevron angle	$\beta = 50^\circ$
Number of passes	$N_p = 1$
Number of plates	$N_t = 50$
Plate thickness	$t = 0.04$ in
Vertical port distance	$L_v = 3.8$ ft
Horizontal port distance	$L_h = 0.9$ ft
Plate width	$L_w = 16$ in
Enlargement factor	$\Phi = 1.18$
Compressed plate pack length	$L_c = 8$ in
Port diameters	$D_p = 3$ in

To verify this design, the heat exchanger will be analyzed to determine its thermal and hydraulic performance.

5.10.4.1 Initial Guess of the Fluid Outlet Temperatures

Even though the desired outlet temperature of the hot fluid is known, in the analysis it is treated as an unknown. The following initial guesses will be made for the fluid outlet temperatures,

$$T_{ho} = 110^\circ\text{F} \quad t_{co} = 150^\circ\text{F}$$

This step is dependent on the computer software being used to solve the problem. Some software sets unknown variables to a default value. Other software, such as spreadsheets, will require user input for unknown variables.

5.10.4.2 Fluid Properties

Given the estimates of the outlet fluid temperatures, the fluid properties can be evaluated at the average temperature. The resulting properties are,

Fluid	T (°F)	ρ (lbm/ft ³)	γ (lbf/ft ³)	c_p (Btu/lbm-R)	μ (lbm/ft-s)	k (Btu/h-ft-°F)	Pr
distilled water	150	61.193	61.193	1.0009	0.00028858	0.37929	2.7414
city water	100	61.991	61.991	0.9989	0.00045757	0.36164	4.5501

5.10.4.3 Calculation of the Hydraulic Diameter of the Channel

The plate pitch, p , is not given by the manufacturer. However, it can be estimated from the compressed plate pack length as given by Equation 5.129,

$$p = \frac{L_c}{N_t} = \frac{8 \text{ in}}{50} \left(\frac{\text{ft}}{12 \text{ in}} \right) = 0.013333 \text{ ft}$$

The average channel spacing can now be found using Equation 5.128,

$$b = p - t = 0.013333 \text{ ft} - 0.04 \text{ in} \left(\frac{\text{ft}}{12 \text{ in}} \right) = 0.01000 \text{ ft}$$

Therefore, the hydraulic diameter, estimated from Equation 5.131, is,

$$D_{hyd} = \frac{2b}{\Phi} = \frac{2(0.01000 \text{ ft})}{1.18} = 0.016949 \text{ ft}$$

5.10.4.4 Calculation of the Fluid Mass Velocities

The mass velocity of each fluid is determined using Equation 5.140. In order to use this equation, the number of channel passes must be determined using Equation 5.141,

$$N_{cp} = \frac{N_t - 1}{2N_p} = \frac{50 - 1}{2(1)} = 24.5$$

This result is a physical impossibility (there cannot be 0.5 channel passes). However, it accounts for the fact that one of the fluids makes an extra traverse through a set of plates due to the even number of plates. If the number of plates were odd, both fluids have the same number of plate passes. Using the extra half-pass for even-plate heat exchangers divides the extra plate pass equally between the hot and cold fluids. This is considered to be a reasonable estimate when calculating the mass velocity of each fluid. Once the number of channel passes is determined, the mass velocity of each fluid can be found,

$$G_{ch,h} = \frac{\dot{m}_h}{N_{cp} b L_w} = 102.04 \frac{\text{lbm}}{\text{ft}^2 \cdot \text{s}} \quad G_{ch,c} = \frac{\dot{m}_c}{N_{cp} b L_w} = 85.034 \frac{\text{lbm}}{\text{ft}^2 \cdot \text{s}}$$

5.10.4.5 Calculation of Reynolds Numbers

$$\text{Re}_h = \frac{G_{ch,h} D_{hyd}}{\mu_h} = 5,993 \quad \text{Re}_c = \frac{G_{ch,c} D_{hyd}}{\mu_c} = 3,150$$

5.10.4.6 Calculation of Nusselt Numbers

The Nusselt number of each fluid can be found using Equation 5.138,

$$\text{Nu}_{D_{\text{hyd}}} = \frac{h D_{\text{hyd}}}{k} = C_h \text{Re}^n \text{Pr}^{1/3}$$

Using this equation assumes that the value of $(\mu/\mu_w)^{0.17}$ is near 1. This will be checked as one of the last steps in the analysis process. The values of the constants C_h and n are determined from Table 5.15. This leads to Nusselt numbers of,

$$\text{Nu}_{D_{\text{hyd}},h} = (0.130) \text{Re}_h^{0.732} \text{Pr}_h^{1/3} = 105.97 \quad \text{Nu}_{D_{\text{hyd}},c} = (0.130) \text{Re}_c^{0.732} \text{Pr}_c^{1/3} = 78.35$$

5.10.4.7 Calculation of Convective Heat Transfer Coefficients

$$h_h = \frac{\text{Nu}_{D_{\text{hyd}},h} k_h}{D_{\text{hyd}}} = 2,371 \frac{\text{Btu}}{\text{h-ft}^2 \cdot ^\circ\text{F}} \quad h_c = \frac{\text{Nu}_{D_{\text{hyd}},c} k_c}{D_{\text{hyd}}} = 1,672 \frac{\text{Btu}}{\text{h-ft}^2 \cdot ^\circ\text{F}}$$

5.10.4.8 Calculation of the Overall Heat Transfer Coefficients

Both clean and fouled values of the overall heat transfer coefficient will be calculated. For a clean heat exchanger,

$$\frac{1}{U_{o,\text{clean}}} = \frac{1}{h_h} + \frac{t}{k_p} + \frac{1}{h_c} \rightarrow U_{o,\text{clean}} = 719.08 \frac{\text{Btu}}{\text{h-ft}^2 \cdot ^\circ\text{F}}$$

For the fouled heat exchanger, a maintenance period needs to be identified. Since fouling is reduced in a PFHX due to the plate design, and the fouling factors for the hot- and cold-water flows are very low (Table 5.14), a yearly maintenance scheme will be considered. For yearly maintenance, $M = 12$ in the following equation,

$$\frac{1}{U_{\text{fouled}}} = \frac{1}{h_h} + \frac{R''_{fh}}{(12/M)} + \frac{t}{k_p} + \frac{R''_{fc}}{(12/M)} + \frac{1}{h_c} \rightarrow U_{o,\text{fouled}} = 689.34 \frac{\text{Btu}}{\text{h-ft}^2 \cdot ^\circ\text{F}}$$

Notice that the reduction in the overall heat transfer coefficient is not as pronounced as compared to the double pipe and shell-and-tube heat exchangers.

5.10.4.9 Calculation of the UA Values

The effective heat transfer area of each plate can be found from Equation 5.125,

$$A_e = \Phi L_p L_w = \Phi (L_o - D_p) L_w = 5.5853 \text{ ft}^2$$

Once the overall heat transfer coefficient is known, the UA value for the heat exchanger can be determined for clean and fouled conditions,

$$(UA)_{clean} = U_{clean} A_e = 192,782 \frac{\text{Btu}}{\text{h} \cdot ^\circ\text{F}} \quad (UA)_{fouled} = U_{fouled} A_e = 184,809 \frac{\text{Btu}}{\text{h} \cdot ^\circ\text{F}}$$

5.10.4.10 Application of the Heat Exchanger Model

If the heat exchanger being analyzed is a true counter flow or parallel flow design, the LMTD or ε -NTU model can be used. If the flow pattern is multi-pass, then the LMTD model is used by calculating the LMTD for a counter flow heat exchanger and then modifying it with a correction factor. For the heat exchanger being analyzed here, the LMTD model will be used. At this point, no iteration has been done. Therefore, the following values use the average fluid properties shown in Section 5.10.4.2.

The thermal capacity rates of the hot and cold fluids are,

$$\dot{C}_h = \dot{m}_h c_{ph} = 120,108 \frac{\text{Btu}}{\text{h} \cdot \text{R}} \quad \dot{C}_c = \dot{m}_c c_{pc} = 99,893 \frac{\text{Btu}}{\text{h} \cdot \text{R}}$$

The LMTD of the heat exchanger can now be found,

$$\begin{aligned} \Delta T_{in} &= T_{hi} - t_{co} = 40 \text{ R} & \Delta T_{out} &= T_{ho} - t_{ci} = 60 \text{ R} \\ \therefore LMTD &= \frac{\Delta T_{out} - \Delta T_{in}}{\ln(\Delta T_{out} / \Delta T_{in})} = 49.326 \text{ R} \end{aligned}$$

The LMTD heat exchanger model, Equation set 5.55 can now be applied. For the clean heat exchanger,

$$\begin{aligned} \dot{Q}_h &= \dot{C}_h (T_{hi} - T_{ho}) = 9,608,660 \text{ Btu/h} \\ \dot{Q}_c &= \dot{C}_c (t_{co} - t_{ci}) = 9,989,257 \text{ Btu/h} \\ \dot{Q} &= (UA)_{clean} (LMTD) = 9,509,183 \text{ Btu/h} \end{aligned}$$

The three heat transfer rates must be equal. This means that, iteration is required to determine the outlet temperatures and the average fluid properties. For the fouled heat exchanger, the first two equations from the conservation of energy are the same. However, the heat transfer equation now represents the fouled heat exchanger. Therefore, the LMTD model for the fouled heat exchanger is,

$$\begin{aligned} \dot{Q}_h &= \dot{C}_h (T_{hi} - T_{ho}) = 9,608,660 \text{ Btu/h} \\ \dot{Q}_c &= \dot{C}_c (t_{co} - t_{ci}) = 9,989,257 \text{ Btu/h} \\ \dot{Q} &= (UA)_{fouled} (LMTD) = 9,115,881 \text{ Btu/h} \end{aligned}$$

As with the clean heat exchanger model, iteration is required to determine the fluid outlet temperatures and average fluid properties. Using computer software to solve the clean and fouled heat exchanger LMTD models provides the following results,

Heat Exchanger Condition	T_{ho} (°F)	t_{co} (°F)	Heat Transfer Rate (Btu/h)
Clean	109.2	147.2	9,709,109
Fouled	110.4	145.7	9,558,751

Notice that the fouled fluid outlet temperature is slightly higher than the required value of 110°F. This may be considered sufficient for the given application. If not, adding an additional plate to the heat exchanger results in the following outlet temperatures,

Heat Exchanger Condition	T_{ho} (°F)	t_{co} (°F)	Heat Transfer Rate (Btu/h)
Clean	108.3	148.2	9,812,306
Fouled	109.6	146.7	9,662,004

5.10.4.11 Calculation of Pressure Drops

At this point, the heat transfer model has converged. No further iteration is required for the pressure drop calculations. For the 50-plate heat exchanger under fouled conditions, the pressure drop through the plates is given by Equation 5.145,

$$\Delta P_{plates} = f \frac{L_v N_p}{D_{hyd}} \frac{G_{ch}^2}{2\rho}$$

Using this equation assumes that the value of $(\mu/\mu_w)^{-0.17}$ is near 1. This will be checked as one of the last steps in the analysis process. The friction factor for each fluid is determined using Equation 5.144 with the values of K_p and m determined from Table 5.15,

$$f_h = \frac{K_p}{\text{Re}_h^m} = \frac{3.088}{\text{Re}_h^{0.161}} = 0.96023 \quad f_c = \frac{K_p}{\text{Re}_c^m} = \frac{3.088}{\text{Re}_c^{0.161}} = 1.10195$$

Therefore, the pressure drop for each fluid as it passes through the heat exchanger is,

$$\Delta P_{plates,h} = f_h \frac{L_v N_p}{D_{hyd}} \frac{G_{ch,h}^2}{2\rho_h} = 3.95 \text{ psi} \quad \Delta P_{plates,c} = f_c \frac{L_v N_p}{D_{hyd}} \frac{G_{ch,c}^2}{2\rho_c} = 3.11 \text{ psi}$$

The port pressure drop for each fluid is given by Equation 5.146,

$$\Delta P_{ports} = 1.4 N_p \frac{G_{port}^2}{2\rho}$$

The port mass velocity for each fluid is given by Equation 5.147,

$$G_{port,h} = \frac{4\dot{m}_h}{\pi D_p^2} = 679.06 \frac{\text{lbm}}{\text{ft}^2 \cdot \text{s}} \quad G_{port,c} = \frac{4\dot{m}_c}{\pi D_p^2} = 565.88 \frac{\text{lbm}}{\text{ft}^2 \cdot \text{s}}$$

Therefore, the port losses for each fluid are,

$$\Delta P_{ports,h} = 1.4N_p \frac{G_{port,h}^2}{2\rho_h} = 1.14 \text{ psi} \quad \Delta P_{ports,c} = 1.4N_p \frac{G_{port,c}^2}{2\rho_c} = 0.78 \text{ psi}$$

The total pressure drop for each fluid can now be computed,

$$\Delta P_h = \Delta P_{plates,h} + \Delta P_{ports,h} = 5.1 \text{ psi} \quad \Delta P_c = \Delta P_{plates,c} + \Delta P_{ports,c} = 3.9 \text{ psi}$$

Since the fouling factors are so low for the hot and cold water in the heat exchanger, the effect of additional pressure drop due to fouling will be considered negligible in this application. There are, however, some applications that require frequent cleaning of the plates due to high fouling factors. For example, in the dairy industry, plate and frame heat exchangers used for pasteurization of milk must be cleaned daily (sometimes more often) due to the very high fouling factor of milk.

5.10.4.12 Checks

The first check will be on the values of $(\mu/\mu_w)^{0.17}$ (for the Nusselt number calculation) and $(\mu/\mu_w)^{-0.17}$ for the plate pressure drop expression. In the analysis, these values were assumed to be close to 1. Since the heat transfer model is solved and the outlet temperatures are known, the average plate temperature can be estimated by,

$$T_w = \frac{1}{2} \left(\frac{T_{hi} + T_{ho}}{2} + \frac{t_{ci} + t_{co}}{2} \right) = 124.03^\circ\text{F}$$

The viscosity of water at this temperature is,

$$\mu_w = 0.00036039 \frac{\text{lbm}}{\text{ft} \cdot \text{s}}$$

This leads to a viscosity ratio of,

$$\begin{aligned} \left(\frac{\mu_h}{\mu_w} \right)^{0.17} &= 0.96 & \left(\frac{\mu_c}{\mu_w} \right)^{0.17} &= 1.05 \\ \left(\frac{\mu_h}{\mu_w} \right)^{-0.17} &= 1.04 & \left(\frac{\mu_c}{\mu_w} \right)^{-0.17} &= 0.96 \end{aligned}$$

These values indicate that the approximations, Equations 5.138 and 5.145 are valid.

The second check will be to determine if the fluid pressure drops are with the recommended maximum value,

$$\Delta P_{\max} = (4.35 \text{ psi})\text{NTU} = (4.35 \text{ psi}) \frac{(UA)_{\text{fouled}}}{\dot{C}_{\min}} = 8.0 \text{ psi}$$

Here, the UA product for the fouled heat exchanger is used because it is smaller compared to a clean heat exchanger. The calculated pressure drops of the hot and cold fluids are smaller than this maximum value. Therefore, the hydraulic performance of the heat exchanger meets the requirement.

Another interesting parameter that can be calculated is the effectiveness of the heat exchanger,

$$\varepsilon = \frac{\dot{Q}}{\dot{Q}_{\max}} = \frac{\dot{Q}}{\dot{C}_{\min}(T_{hi} - t_{ci})} = 0.6835$$

This value tends to indicate that the heat exchanger is thermally performing well.

5.10.4.13 Summary of Analysis Results

Table 5.17 shows a summary of the analysis of the PFHX with the specifications given in Table 5.16 as recommended by the manufacturer.

5.11 Cross Flow Heat Exchanger Design and Analysis

There are many different types of CFHXs. This precludes a detailed presentation in this book. The reader is encouraged to consult Kays and London (1998) or Thulukkanam (2013) for a thorough treatment of many types of cross flow heat exchangers.

One particular cross flow heat exchanger that is used extensively in many industrial applications is the finned-tube heat exchanger. Fins can be placed on the outside of the tubes as individual fins (e.g., circular fins), or the fins can be formed of a continuous thin plate that has holes bored for the tubes to pass through. This type of heat exchanger is used in many heating, ventilating, and air-conditioning applications. In these applications, air is heated or cooled by circulating it outside the finned tubes. Hot or cold water is usually in the tubes to provide heating or cooling to the air. It is also possible to use a finned tube heat exchanger as an evaporator or condenser in a refrigeration system. In either case, the refrigerant flows in the tubes and air is circulated outside the finned tubes. Figure 5.31 shows a sketch of a continuous plane finned tube CFHX. Air passages are created by the fins. However, the air can move through the tube bank in a rather arbitrary fashion as it flows through the fins. Therefore, according to the definitions in Section 5.5.4, the fluid in the tubes is unmixed, and the air passing over the tubes is considered mixed.

TABLE 5.17

Results of the PHFX Analysis of Section 5.10.4

Parameter	Value	
<i>Manufacturer's Specifications</i>		
Plate material	AISI 304 Stainless Steel	
Chevron angle	50°	
Number of passes	1	
Number of plates	50	
Plate thickness	0.04 in	
Vertical port distance	3.8 ft	
Horizontal port distance	0.9 ft	
Plate width	16 in	
Enlargement factor	1.25	
Compressed plate pack length	8 in	
Port diameters	3 in	
<i>Thermal Performance</i>		
Hot fluid mass flow rate	120,000 lbm/h	
Hot fluid inlet temperature	190°F	
Desired hot fluid outlet temperature	110°F	
Cold fluid mass flow rate	100,000 lbm/h	
Cold fluid inlet temperature	50°F	
	<i>Clean</i>	<i>Fouled</i>
Hot fluid outlet temperature	109.2°F	110.4°F ^a
Cold fluid outlet temperature	147.2°F	145.7°F
Heat transfer rate	9,709,109 Btu/h	9,588,751 Btu/h
UA product	192,099 Btu/h-°F	184,008 Btu/h-°F
<i>Hydraulic Performance</i>		
	<i>Hot fluid</i>	<i>Cold fluid</i>
Plate pressure drop	3.95 psi	3.11 psi
Port pressure drop	1.14 psi	0.78 psi
Total pressure drop	5.1 psi	3.9 psi
<i>Other</i>		
Maintenance schedule	every 12 months	

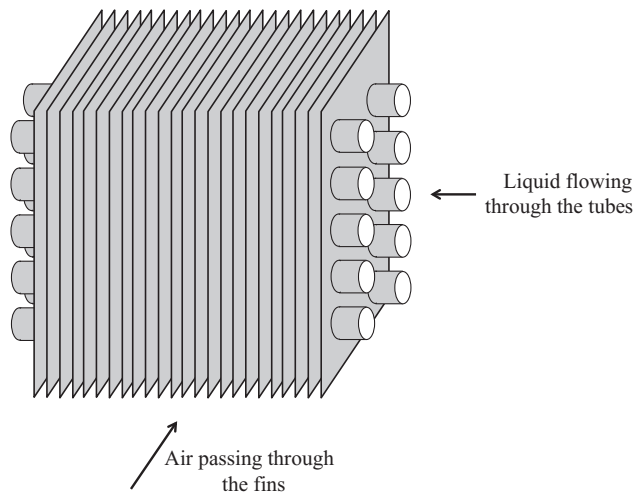
^a With a 51-plate heat exchanger, the hot fluid outlet temperature is 109.6°F.

When calculating the thermal resistance for a finned tube heat exchanger, Equation 5.32 is modified to include the effect of the fins as follows,

$$R_t = \frac{1}{h_i A_i} + \frac{R''_{f,i}}{A_i} + \frac{\ln(OD/ID)}{2\pi kL} + \frac{R''_{f,o}}{\eta_o A_o} + \frac{1}{\eta_o h_o A_o} \quad (5.148)$$

In Equation 5.148, η_o is the surface efficiency of the fin array, which is defined by,

$$\eta_o = 1 - \frac{N_f A_f}{A_t} (1 - \eta_f) \quad (5.149)$$

**FIGURE 5.31**

Example of a continuous plane finned tube cross flow heat exchanger.

In Equation 5.149, N_f is the total number of fins in the, A_f is the surface area of a single fin, A_t is the total area on the air-side which includes the fin area and the unfinned tube area exposed to the air flow, and η_f is the individual fin efficiency. There are several expressions for the fin efficiency that can be found in various heat transfer texts and handbooks. The fin efficiency expressions are dependent on the fin geometry and they also are a function of the convective heat transfer coefficient on the outside of the finned tube.

The design and analysis procedures for the CFHX are similar to the methods developed in the previous sections for other types of heat exchangers. The LMTD and ε -NTU models can be used to model the performance of the CFHX. When using the LMTD method, the LMTD is calculated for a counter flow heat exchanger, and then modified using a correction factor, similar to the shell and tube heat exchanger. The correction factor is dependent on whether the fluids are mixed or unmixed. In lieu of the LMTD correction factor, the ε -NTU method can be easily implemented using the equations shown in Tables 5.3 and 5.4.

The convective heat transfer coefficient inside the tubes of the heat exchanger can be determined from the appropriate correlation based on the flow regime inside the tube (Sections 5.2.2.3 through 5.2.2.5). The convective heat transfer coefficient on the outside of the finned tubes is usually determined using the *Colburn factor*, j , which is defined as,

$$j = \frac{\text{Nu}_D}{\text{Re}_D \text{Pr}^{1/3}} \quad (5.150)$$

The correlations developed for j depend on the type of heat exchanger and whether there is water condensing out of the air stream which is possible during a dehumidification process.

For dry, clean plane finned-tubes, Wang et al. (1996) have demonstrated that the Colburn factor can be found using,

$$j = 0.394 \text{Re}_{D_c}^{-0.392} \left(\frac{th}{D_c} \right)^{-0.0449} N^{-0.0897} \left(\frac{F_p}{D_c} \right)^{-0.212} \quad (5.151)$$

In this equation, th is the fin thickness, D_c is the collar diameter of the fins (the diameter of the holes punched in the plate that accepts the tubes), F_p is the fin pitch (spacing), and N is the number of rows of tubes in the heat exchanger. This correlation is valid for $800 \leq Re_{D_c} \leq 7500$. The properties are evaluated at the average temperature of the air passing over the finned tubes in the heat exchanger. Wang et al. (1996) report that 97% of the experimental data collected to develop Equation 5.151 are represented to within $\pm 10\%$.

Wang et al. (1996) also developed an expression for the friction factor on the finned-tube side of the heat exchanger. This expression is similar to Equation 5.151 and given by,

$$f = 1.039 Re_{D_c}^{-0.418} \left(\frac{th}{D_c} \right)^{-0.104} N^{-0.0935} \left(\frac{F_p}{D_c} \right)^{-0.197} \quad (5.152)$$

88% of the experimental data collected to develop this equation are represented to within $\pm 10\%$. This value of the friction factor is used in a pressure drop correlation, which is developed for the configuration of the finned tube heat exchanger.

There are many other expressions for the Colburn factor and the friction factor for other types of CFHXs. In addition, contact resistance and fouling effects on the finned-tube side can become quite complex.

Even though the design and analysis procedure is very similar to other heat exchangers discussed in this chapter, the determination of the outside convective heat transfer coefficient (using the Colburn factor), the thermal resistance of the heat exchanger, and the pressure drop on the fin side can be quite complex. In lieu of the complex analysis required for CFHXs, it may be possible to extract heat transfer performance information from manufacturer's data. For example, many finned tube coil manufacturers provide performance curves that indicate the heat transfer rate within one of their finned tube coils for specific fluid flow rates and fluid temperature conditions. The calculation of the UA product using this type of data is demonstrated in the following example.

Example 5.12

Manufacturer's performance curves for a particular finned tube CFHX utilizing water and dry air as the working fluids indicate that at a water flow rate of 80 gpm, the heat transferred between the air and the water is 49,860 Btu/hr. These results were developed experimentally for the following conditions: (1) the air flows through the heat exchanger at 1,000 cfm at essentially atmospheric pressure and (2) the temperature difference between the inlet temperatures of the hot water and the cold air is 50°F . If the air temperature entering the heat exchanger is 68°F , estimate the fluid outlet temperatures and the UA product for this finned tube CFHX.

Solution

The water inlet temperature can be found since the inlet temperature difference in the heat exchanger is specified,

$$T_{wi} - t_{ai} = \Delta T \rightarrow T_{wi} = t_{ai} + \Delta T = (68 + 50)^\circ\text{F} = 118^\circ\text{F}$$

The outlet temperatures of the fluids are not known at this point. Therefore, the properties will be estimated using the inlet temperatures. Subsequent iteration will allow for the calculation of the outlet temperatures. The water properties can be found in Appendix B.3 and the air properties are in Appendix B.5. Interpolation is required.

Alternatively, computer software can be used to find the fluid properties. At the inlet temperatures given, the fluid properties are,

Fluid	T (°F)	ρ (lbm/ft ³)	c_p (Btu/lbm-R)	μ (lbm/ft-s)	k (Btu/h-ft-°F)	Pr
water	118.00	61.740	0.99927	0.00038136	0.36890	3.7190
air	68.000	0.075180	0.24054	0.000012261	0.014745	0.72007

Using these properties, the outlet temperatures of the fluids can be found since the heat transfer rate is known,

$$\begin{aligned}\dot{Q} &= \dot{C}_w(T_{wi} - T_{wo}) \rightarrow T_{wo} = T_{wi} - \frac{\dot{Q}}{\dot{C}_w} \\ \dot{C}_w &= \dot{m}_w c_{pw} = (\rho_w \dot{V}_w) c_{pw} = \left(61.740 \frac{\text{lbm}}{\text{ft}^3}\right) \left(80 \text{ gpm}\right) \left(0.99927 \frac{\text{Btu}}{\text{hr-R}}\right) \left(8.02083 \frac{\text{ft}^3}{\text{hr-gpm}}\right) \\ \dot{C}_w &= 39,588 \frac{\text{Btu}}{\text{hr-R}} \\ \therefore T_{wo} &= 118^\circ\text{F} - \frac{49,860 \text{ Btu/hr}}{39,588 \text{ Btu/hr-R}} = 116.74^\circ\text{F}\end{aligned}$$

Likewise, for the air,

$$\begin{aligned}\dot{Q} &= \dot{C}_a(t_{ao} - t_{ai}) \rightarrow t_{ao} = t_{ai} + \frac{\dot{Q}}{\dot{C}_a} \\ \dot{C}_a &= \dot{m}_a c_{pa} = (\rho_a \dot{V}_a) c_{pa} = \left(0.075180 \frac{\text{lbm}}{\text{ft}^3}\right) \left(1000 \frac{\text{ft}^3}{\text{min}}\right) \left(0.24054 \frac{\text{Btu}}{\text{hr-R}}\right) \left(60 \frac{\text{min}}{\text{hr}}\right) \\ \dot{C}_a &= 1,085.0 \frac{\text{Btu}}{\text{hr-R}} \\ \therefore t_{ao} &= 68^\circ\text{F} + \frac{49,860 \text{ Btu/hr}}{1,085.0 \text{ Btu/hr-R}} = 113.95^\circ\text{F}\end{aligned}$$

These outlet temperatures can now be used to recalculate the fluid properties and new outlet temperatures. This process is repeated until successive outlet temperatures are sufficiently close. The result of the iteration is,

$$T_{wo} = 116.7^\circ\text{F} \quad t_{ao} = 116.0^\circ\text{F}$$

The resulting fluid properties, evaluated at the average temperature are,

Fluid	T (°F)	ρ (lbm/ft ³)	c_p (Btu/lbm-R)	μ (lbm/ft-s)	k (Btu/h-ft-°F)	Pr
water	117.37	61.750	0.99925	0.00038367	0.36866	3.7438
air	92.014	0.071899	0.24065	0.000012695	0.015310	0.71833

At this point, the fluid outlet temperatures are known. The UA product of the heat exchanger can now be determined by solving the heat transfer equation in the heat exchanger model. Using the ε -NTU method, the heat transfer equation in the is represented,

$$\varepsilon = \dot{Q}/\dot{Q}_{\max}$$

$$\dot{Q}_{\max} = \dot{C}_{\min}(T_{wi} - t_{ai})$$

$$NTU = f(\varepsilon, C_r)$$

$$NTU = \frac{UA}{\dot{C}_{\min}}$$

The thermal capacity rates were calculated above, therefore it is a simple matter to pick out the maximum and minimum values,

$$\dot{C}_{\min} = 1,038.1 \text{ Btu/hr-R} \quad \dot{C}_{\max} = 39,593 \text{ Btu/hr-R}$$

$$\therefore C_r = \frac{\dot{C}_{\min}}{\dot{C}_{\max}} = \frac{1,038.1 \text{ Btu/hr-R}}{39,593 \text{ Btu/hr-R}} = 0.026220$$

The maximum heat transfer rate can now be found,

$$\dot{Q}_{\max} = \dot{C}_{\min}(T_{wi} - t_{ai}) = \left(1,038.1 \frac{\text{Btu}}{\text{hr-R}}\right)(50)\text{R} = 51,907 \frac{\text{Btu}}{\text{hr}}$$

The effectiveness of this heat exchanger is,

$$\varepsilon = \frac{\dot{Q}}{\dot{Q}_{\max}} = \frac{49,860 \text{ Btu/hr}}{51,907 \text{ Btu/hr}} = 0.96056$$

In the finned-tube CFHX, the fluid in the tubes (water in this example) is unmixed and the fluid passing through the fins (air) is mixed. Furthermore, from the previous calculations, the hot fluid (water) has the higher thermal capacity rate. Using the proper expression for the NTU from Table 5.4,

$$NTU = -\left(\frac{1}{C_r}\right) \ln[C_r \ln(1 - \varepsilon) + 1]$$

$$NTU = -\left(\frac{1}{0.026220}\right) \ln[(0.026220) \ln(1 - 0.96056) + 1] = 3.3782$$

Therefore, the heat exchanger's UA product can be estimated,

$$UA = \dot{C}_{\min}(NTU) = \left(1038.1 \frac{\text{Btu}}{\text{hr-R}}\right)(3.3782) = \underline{\underline{3,507.0 \frac{\text{Btu}}{\text{hr-R}}}}$$

This UA value computed above can be used in an analysis of the heat exchanger (e.g., predicting outlet temperatures for known inlet conditions and flow rates) for different conditions than tested by the manufacturer. In reality, the U value of the heat exchanger will change as the flow rates and fluid temperatures change. However, if the expected change is minimal, the predicted outlet temperature using the estimated UA should be reasonably close to the expected outlet temperatures.

The previous example shows how manufacturer's performance data can be used to estimate the performance of a CFHX at other conditions. This type of calculation eliminates the need to determine the overall heat transfer coefficient using the complicated Colburn factor. However, if more detail is required, appropriate sources for the Colburn factor should be consulted and an in-depth analysis conducted.

References

- Bejan, A., and A. D. Kraus. 2003. *Heat Transfer Handbook*. John Wiley.
- Bergman, T. L., A. S. Lavine, F. P. Incropera, and D. P. DeWitt. 2011. *Fundamentals of Heat and Mass Transfer*. Hoboken, NJ: John Wiley & Sons.
- Churchill, S. W., and M. Bernstein. 1977. "Correlating Equation for Forced-Convection from Gases and Liquids to a Circular-Cylinder in Cross-Flow." *Journal of Heat Transfer - Transactions of the ASME* 99 (2): 300–306.
- Edwards, J.F., A.A. Chungal, and D.L. Parrott. 1974. "Heat transfer and pressure drop characteristics of a plate heat exchanger using Newtonian and non-Newtonian liquids." *Chem. Eng.* 286–293.
- Fraas, A. P. 1989. *Heat Exchanger Design*. New York: John Wiley & Sons.
- Gnielinski, V. 1983. "Forced convection ducts." In *Heat Exchanger Design Handbook*, by E.U. Schlunder, 2.5.1–2.5.3. Washington, DC, USA: Hemisphere.
- Gnielinski, V. 1976. "New Equations for Heat and Mass-Transfer in Turbulent Pipe and Channel Flow." *International Chemical Engineering* 16 (2): 359–368.
- Hausen, H. 1959. "Neue Gleichungen für die Wärmeübertragung bei freier oder erzwungener Strömung." *Allg. Warmetech* 75.
- Kakac, S., H. Liu, and A. Pramuanjaroenkij. 2012. *Heat Exchangers: Selection, Rating, and Thermal Design*. Boca Raton, FL: CRC Press.
- Kays, W. M., and A. L. London. 1998. *Compact Heat Exchangers*. New York: Kreiger Publishing.
- Kern, D. Q. 1950. *Process Heat Transfer*. New York: McGraw-Hill.
- Kumar, H. 1984. "The plate heat exchanger: Construction and design." *Inst. Chem. Symp. Series*. University of Leeds. 1275–1286.
- Mason, J. L. 1954. "Heat Transfer in Cross-Flow." *Proc. Appl. Mechanics*. 2nd U.S. Nat. Congress. 801.
- Rohsenow, W. M., J. P. Hartnett, and Y. I. Cho. 1998. *Handbook of Heat Transfer*. New York: McGraw-Hill.
- Shah, R. K., and M. S. Bhatti. 1987. "Laminar convective heat transfer in ducts." In *Handbook of Single-Phase Convective Heat Transfer*, by S. Kakac, R. K. Shah and W. Aung, Chapter 3. New York: John Wiley & Sons.
- Thulukkanam, K. 2013. *Heat Exchanger Design Handbook*. Boca Raton, Florida: CRC Press, Taylor & Francis Group.
- Wang, C., Y. Chang, Y. Hsieh, and Y. Lin. 1996. "Sensible Heat and Friction Characteristics of Plate Fin-and-Tube Heat Exchangers having Plate Fins." *Int. J. Refrig.* 19 (4): 223–230.

Problems

Heat Transfer Analysis of Heat Exchangers

- 5.1 The plates in a plate and frame heat exchanger are made of Inconel 600 ($k = 16 \text{ W/m-K}$) and are 1.5 mm thick. Consider one of the plates in this heat exchanger. The convective heat transfer coefficients on hot and cold side of the plate are $2,250 \text{ W/m}^2\text{-K}$ and $1,600 \text{ W/m}^2\text{-K}$, respectively. The average temperature difference between the hot and cold fluids is 10 K. Determine the following:
 - a. The average heat flux from the hot fluid to the cold fluid, including the conductive resistance of the plate
 - b. The average heat flux from the hot fluid to the cold fluid, assuming that the conductive resistance of the plate is negligible
 - c. The percent error in the heat flux by assuming the conductive resistance of the plate can be ignored
- 5.2 The plates in a plate and frame heat exchanger are made of Monel 200 ($k = 38.1 \text{ Btu/hr-ft-}^\circ\text{F}$) and are 0.04-in thick. Consider one of the plates in this heat exchanger. The convective heat transfer coefficients on hot and cold side of the plate are $180 \text{ Btu/hr-ft}^2\text{-}^\circ\text{F}$ and $200 \text{ Btu/hr-ft}^2\text{-}^\circ\text{F}$, respectively. The average heat flux through the plate is $1,200 \text{ Btu/h-ft}^2$. Determine the average temperature difference between the hot and cold fluids.
- 5.3 A 2½-nom sch 40S stainless steel pipe ($k = 16.5 \text{ W/m-K}$) is being used in a heat exchanger application. The pipe is 1-m long. The convective heat transfer coefficients on the inside and outside of the pipe are $1,590 \text{ W/m}^2\text{-K}$ and $1,980 \text{ W/m}^2\text{-K}$, respectively. The fouling factor on each side of the pipe is $0.0002 \text{ m}^2\text{-K/W}$. Determine the UA product for the pipe under the following conditions,
 - a. When it is first put into service (i.e., clean)
 - b. After being in service for one year without maintenance (i.e., fouled)
- 5.4 The convective heat transfer coefficients on the inside and outside of a ½-std type L copper tube are $150 \text{ Btu/hr-ft}^2\text{-}^\circ\text{F}$ and $450 \text{ Btu/hr-ft}^2\text{-}^\circ\text{F}$, respectively. The tube is 4-ft long. An ethylene glycol solution flows on the outside of the tube and Refrigerant-22 is on the inside. The average temperature of the copper tube is 100°F . Determine the UA product for this tube for the following conditions,
 - a. When it is first put into service (i.e., clean)
 - b. After being in service for one year without maintenance (i.e., fouled)
 - c. Repeat parts (a) and (b), assuming that the thermal resistance of the copper tube is negligible.
- 5.5 Liquid propane is flowing through a 6-nom galvanized iron pipe at a flow rate of 3 kg/s. The average temperature of the propane in the pipe is 0°C .
 - a. Determine the convective heat transfer coefficient inside the pipe.
 - b. Determine the convective heat transfer coefficient for the C2–C10 hydrocarbons, ethane, propane [Part (a)], butane, pentane, hexane, heptane, octane, nonane, and decane, for the same conditions as described in the problem. Plot the convective heat transfer coefficient vs. the number of carbon atoms in the fluid. Can you suggest an explanation for the trend seen in the plot?

(Note: The properties of the hydrocarbon fluids listed in this part of the problem can be found in Appendix B.3, except butane. If you are not using computer software to compute properties, omit butane from your calculation.)

- 5.6 Due to extreme pressures for a particular application, a 10-ft long pipe is made of 2-nom sch 160 pipe ($k_{\text{pipe}} = 70 \text{ Btu/hr-ft-}^\circ\text{F}$). The convective heat transfer coefficients inside and outside of the pipe are have been determined to be $h_i = 1248 \text{ Btu/hr-ft}^2\text{-}^\circ\text{F}$ and $h_o = 652 \text{ Btu/hr-ft}^2\text{-}^\circ\text{F}$, respectively. The fouling factors on each side of the pipe are $0.002 \text{ hr-ft}^2\text{-}^\circ\text{F/Btu}$. Determine the UA value of this pipe for both clean and fouled conditions.
- 5.7 Jojoba oil is flowing through a $\frac{3}{4}$ -nom stainless steel pipe at a flow rate of $1,850 \text{ lbm/h}$. After the velocity profile in the pipe is fully developed, the oil enters a heater, as shown in Figure P5.7. The length of the heater section is 5 ft. The properties of the jojoba oil at the average temperature in the heater section are given in Table P5.7. Determine the convective heat transfer coefficient inside the heater section of the pipe.

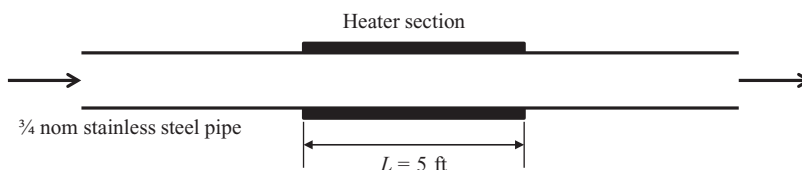


FIGURE P5.7
Heater section of the pipe used to heat jojoba oil.

TABLE P5.7

Thermophysical Properties of Jojoba Oil at the Average Temperature in the Heater

ρ (lbm/ft ³)	c_p (Btu/lbm-R)	μ (lbm/ft-s)	k (Btu/h-ft- $^\circ\text{F}$)
68.671	0.30339	0.012095	0.077424

- 5.8 A 15% magnesium chloride solution is flowing through a 5-nom sch 40 commercial steel pipe at a rate of $325,000 \text{ lbm/h}$. The average temperature of the magnesium chloride solution as it flows through the pipe is 10°F . Determine the convective heat transfer coefficient inside the pipe.
- 5.9 Water is flowing inside of a 3-std type K copper tube at a flow rate of 1.2 kg/s . The average temperature of the water is 50°C . Cold, dry air at a temperature of 5°C and atmospheric pressure flows outside of the tube in cross flow with a velocity of 85 m/s . Determine the UA product for this tube under clean conditions.
- 5.10 An innovative engineering student has been contemplating whether or not it would be feasible to capture some of the waste heat that leaves the stack of a wood burning stove to preheat water. The proposal is to insert a 6-ft long copper coil made of $\frac{1}{2}$ -std type K tubing into a 4-inch (ID) stovepipe. Cold water flows at a rate of 2 gpm through the tube. The average mean temperature of the tube is estimated to be 100°F . The hot combustion gases (which can be modeled as air), flow over the outside of the copper coil in cross flow at free stream temperature of 450°F . The flow

rate of the combustion gases through the stovepipe is the result of an induced draft effect. This volumetric flow rate can be estimated using the following expression,

$$\dot{V}_{gas} = 0.68 A_{chimney} \sqrt{2gh \left(\frac{T_{gas} - T_{amb}}{T_{gas}} \right)}$$

In this equation, $A_{chimney}$ is the cross-sectional area of the stove pipe, h is the total height of the stovepipe, T_{gas} is the free-stream combustion gas temperature, and T_{amb} is the outside ambient temperature. Notice that T_{gas} in the denominator of the term in the square root must be on the *absolute* temperature scale. Consider the situation where the outdoor temperature is -5°F and the total height of the stovepipe is 8 ft. In order to model this heat exchanger, the UA product must be determined. Let's help the innovative engineering student by estimating the UA product for the heat exchanger under clean conditions.

- 5.11 A building in a processing facility has been retrofitted for a new process. There is a need for hot water in this new process. The original design of the building did not include a hot water line. Adjacent to this building is another building that has a hot water line that can be used. The proposal is to run a 1-nom sch 40 commercial steel pipe ($k = 54 \text{ W/m-K}$) above-ground from one building to the other. The total length of pipe exposed to the outdoor air is 5 m. The hot water flows in the pipe at a rate of 1 kg/s and has a yearly average temperature of 52°C . The hot water is made using electricity which has a cost of $\$0.08/\text{kWh}$. The average monthly weather data for the location is given in Table P5.11. Estimate the yearly cost of electrical energy lost due to the convective heat transfer from the exposed outdoor pipe.

TABLE P5.11

Average Monthly Weather Data

Month	Average Outdoor Temperature ($^{\circ}\text{C}$)	Average Wind Speed (m/s)
Jan	-0.3	15.3
Feb	2.5	16.0
Mar	6.9	4.1
Apr	10.3	5.2
May	15.3	14.2
Jun	19.7	8.1
Jul	24.2	8.4
Aug	23.4	5.7
Sep	18.3	3.6
Oct	11.7	10.7
Nov	4.4	11.8
Dec	-0.6	9.1

Design and Analysis of Heat Exchangers

- 5.12 A heat exchanger is being used to cool 48,000 lbm/hr of oil from 150°F to 102°F by using 32,000 lbm/hr of water at an inlet temperature of 70°F . The overall heat transfer coefficient is determined to be $145 \text{ Btu/hr-ft}^2\text{-}^{\circ}\text{F}$. The average heat capacities of the oil and water can be taken as 0.5 Btu/lbm-R and 1.0 Btu/lbm-R ,

- respectively. Determine the heat transfer area required for counter flow and parallel flow configurations.
- 5.13 A counter flow double pipe heat exchanger is being used to cool hot oil from 320°F to 285°F using cold water. The water, which flows through the inner tube, enters the heat exchanger at 70°F and leaves at 175°F. The inner tube is $\frac{3}{4}$ -std type L copper. The overall heat transfer coefficient based on the outside diameter of the inner tube is 140 Btu/hr-ft²-°F. Design conditions call for a total heat transfer duty (heat transfer rate between the two fluids) of 20,000 Btu/hr. Determine the required length of this heat exchanger (ft).
- 5.14 A flow of cold water enters a parallel flow heat exchanger at 20°C and leaves at 100°C. The cold water is being heated by a hot water flow that enters the heat exchanger at 160°C and leaves at 120°C. The overall heat transfer coefficient for this heat exchanger is 324 W/m²-K. The heat exchanger must transfer heat between the water streams at a rate of 20 kW. Determine the heat exchanger area required (m²).
- 5.15 A counter flow heat exchanger is being used to cool a flow of hot water using a cold 20% ethylene glycol solution. The hot water enters at 80°F with a volumetric flow rate of 500 gpm. The ethylene glycol solution enters the heat exchanger at 30°F and leaves at 60°F. The ethylene glycol solution is flowing at a volumetric flow rate of 300 gpm. The overall heat transfer coefficient for the heat exchanger is found to be 520 Btu/hr-ft²-°F. Determine,
- The outlet temperature of the water (°F)
 - The heat transfer rate between the water and ethylene glycol solution (Btu/h)
 - The required heat transfer area of the heat exchanger (ft²)
- 5.16 Solve Problem 5.15 for a parallel flow heat exchanger.
- 5.17 Solve Problem 5.15 for a shell and tube heat exchanger with one shell pass and two tube passes.
- 5.18 Solve Problem 5.15 for a cross flow heat exchanger where the water flow is mixed and the ethylene glycol solution flow is unmixed.
- 5.19 Solve Problem 5.15 for a cross flow heat exchanger where the ethylene glycol solution flow is mixed and the water flow is unmixed.
- 5.20 A counter flow heat exchanger is utilizing a cold 20% magnesium chloride solution to cool a flow of hexane. The hexane enters the heat exchanger at 26°C and the magnesium chloride solution enters at 0°C. The volumetric flow rates of the hexane and magnesium chloride solution are 30 L/s and 26 L/s, respectively. The heat exchanger has an overall heat transfer coefficient of 1,280 W/m²-K. The required heat transfer rate between the fluids is 700 kW. Determine,
- The outlet temperature of the hexane (°C)
 - The outlet temperature of the magnesium chloride solution
 - The required heat transfer area of the heat exchanger (m²)
- 5.21 Solve Problem 5.20 for a parallel flow heat exchanger.
- 5.22 Solve Problem 5.20 for a shell and tube heat exchanger with 1 shell pass and 2 tube passes.
- 5.23 Solve Problem 5.20 for a cross flow heat exchanger where the hexane flow is mixed and the magnesium chloride solution flow is unmixed.

- 5.24 Solve Problem 5.20 for a cross flow heat exchanger where the magnesium chloride solution flow is mixed and the hexane flow is unmixed.
- 5.25 Liquid heptane enters a counter flow heat exchanger at 45°F. The heptane is heated using a flow of hot water entering the heat exchanger at 150°F. The volumetric flow rates of the heptane and water are 280 gpm and 200 gpm, respectively. The UA product of the heat exchanger is found to be 25,675 Btu/hr-ft²-°F. Determine the outlet temperatures of both fluids (°F) and the heat transfer rate between them (Btu/hr).
- 5.26 Solve Problem 5.25 for a parallel flow heat exchanger.
- 5.27 Solve Problem 5.25 for a shell and tube heat exchanger with 1 shell pass and 2 tube passes.
- 5.28 Solve Problem 5.25 for a cross flow heat exchanger where both fluids are unmixed.
- 5.29 A counter flow heat exchanger is being used to heat a flow of liquid toluene. The toluene enters the heat exchanger at 5°C with a volumetric flow rate of 10 L/s. Hot water is being used to heat the toluene. The water enters the heat exchanger at 70°C and a volumetric flow rate of 18 L/s. The UA product of the heat exchanger is 25 kW/K. Determine the outlet temperatures of both fluids (°F) and the heat transfer rate between them (kW).
- 5.30 Solve Problem 5.29 for a parallel flow heat exchanger.
- 5.31 Solve Problem 5.29 for a shell and tube heat exchanger with 1 shell pass and 4 tube passes.
- 5.32 Solve Problem 5.29 for a cross flow heat exchanger where the water flow is mixed and the toluene flow is unmixed.

Special Application Heat Exchangers

- 5.33 The series of heat exchangers shown in Figure P5.33 is designed to raise a liquid's temperature so a desired chemical reaction can take place in the reactor. The specific heat of the liquid can be assumed constant at an average value of 3.2 kJ/kg-K. The liquid flow rate is 1.4 kg/s. The temperature of the liquid entering HX 1 is 300 K and the temperature leaving the reactor is 390 K. The UA value of HX 1 is 2.88 kW/K. Saturated vapor steam is supplied to HX 2 at 375 K and saturated liquid condensate leaves at 375 K. The UA values of HX 2 and HX 3 are 4.7 kW/K and 9.6 kW/K, respectively. Determine the values of the unknown temperatures (K) in the system and the heat transfer rates in each of the three heat exchangers.

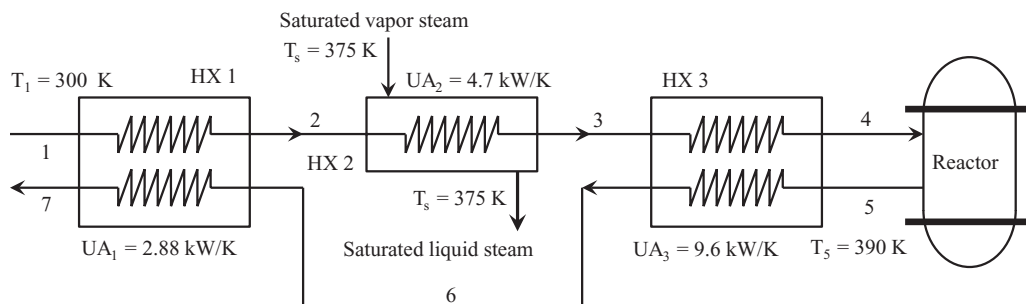


FIGURE P5.33

Heat exchangers used to control a chemical reaction.

- 5.34 A gas turbine cycle utilizes a regenerative heat exchanger as shown in Figure P5.34. Air enters the compressor at atmospheric conditions, 1 atm and 70°F with a mass flow rate of 15,000 lbm/hr. The exhaust pressure of the compressor is 7 atm. The compressor is operating with an isentropic efficiency of 77%. The regenerator pre-heats the air entering the combustion chamber, thus reducing the fuel requirement and increasing the thermal efficiency of the cycle. The regenerator in the cycle has a UA product of 25,000 Btu/hr-°F. Combustion gases (which can be modeled as dry air, $M = 28.965$ lbm/lbmol) leave the combustion chamber at 2300°F. The combustion gases then pass through the turbine which has an isentropic efficiency of 72%. Assume that the pressure drops in all heat exchangers and connecting piping are negligible. Use the ideal gas law to model the properties of air. Even though the temperature varies significantly in this cycle, the average heat capacity evaluated between the highest and lowest temperatures in the cycle ($c_{p,avg} = 0.26856$ Btu/lbm-R) can be used for analysis of the components. Determine the following:
- The net power delivered by the cycle (hp)
 - The heat transfer rate required at the combustion chamber
 - The thermal efficiency of the cycle
 - Investigate the effect of the size of the regenerator by plotting the thermal efficiency of the cycle as a function of the regenerator UA value for the range $0 \text{ Btu/hr-°F} \leq UA \leq 50,000 \text{ Btu/hr-°F}$. What is the significance of $UA = 0 \text{ Btu/hr-°F}$?

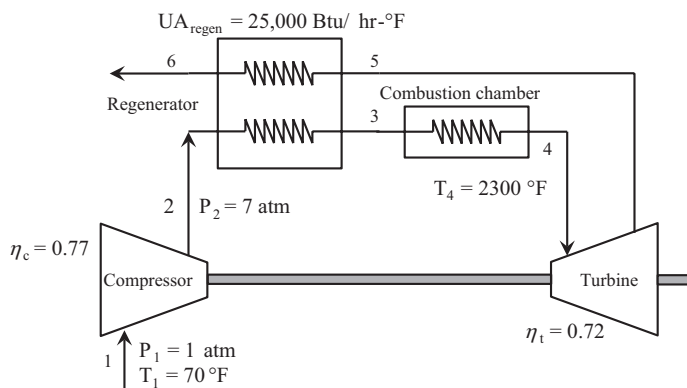


FIGURE P5.34

Gas turbine cycle with regenerative heat exchanger.

- 5.35 A shell and tube heat exchanger is being used as a steam condenser. Cold water flows in the tubes at a rate of 0.8 kg/s. The water enters the heat exchanger at 15°C and leaves at 63°C. The steam enters the shell side of the heat exchanger as a saturated vapor at 200 kPa and fully condenses to a saturated liquid. The pressure drop on the shell side is negligible. Determine the following:
- Mass flow rate of the condensing steam (kg/s)
 - Heat transfer rate between the water and the condensing steam (kW)
 - UA product of the heat exchanger (kW/K)

Consider a situation where the cold-water inlet temperature to the heat exchanger is adjusted to 20°C while its flow rate (0.8 kg/s) remains constant and the steam fully condenses at 120 kPa. For this scenario, estimate the following:

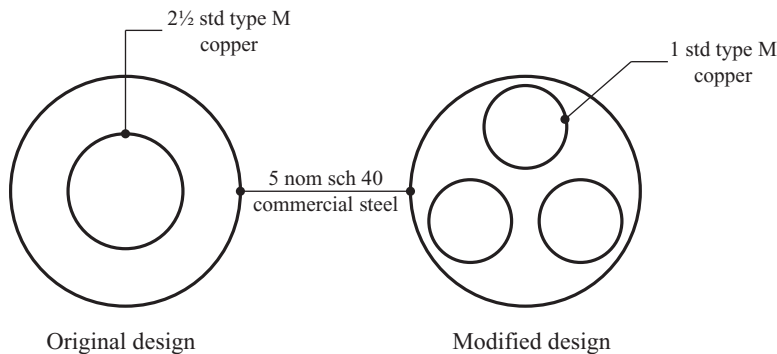
- d. Outlet temperature of the cold water ($^{\circ}\text{C}$)
 - e. Heat transfer rate between the water and the condensing steam (kW)
- 5.36 The evaporator of a vapor compression refrigeration cycle utilizing R-123 as the refrigerant is being used to chill water. The evaporator is a shell and tube heat exchanger with the water flowing through the tubes. The water enters the heat exchanger at a temperature of 54°F . The approach temperature difference of the evaporator is 3°R . The evaporating pressure of the refrigeration cycle is 4.8 psia and the condensing pressure is 75 psia. The refrigerant is flowing through the cycle with a flow rate of 18,000 lbm/hr. The R-123 leaves the evaporator as a saturated vapor and leaves the condenser as a saturated liquid. Determine the following:
- a. The outlet temperature of the chilled water
 - b. The volumetric flow rate of the chilled water (gpm)
 - c. The UA product of the evaporator ($\text{Btu/h}\cdot^{\circ}\text{F}$)
 - d. The heat transfer rate between the refrigerant and the water (tons)

Double Pipe Heat Exchangers

- 5.37 The outer pipe in a double pipe heat exchanger is 4-nom sch 40 commercial steel. The inner tube is 2-std type K copper. The fluid inside the inner tube is flowing at a volumetric rate of 20 gpm and the fluid in the annulus flows at 40 gpm. For this heat exchanger determine,
- a. The hydraulic diameter of the annulus (ft)
 - b. The equivalent diameter of the annulus (ft)
 - c. The velocity of the fluid in the inner tube (ft/s)
 - d. The velocity of the fluid in the annulus (ft/s)
- 5.38 A double pipe heat exchanger is made of a 6-nom sch 80 outer pipe and a 4-std type K copper inner tube. The fluid in the annular space is liquid water that has a volumetric flow rate of 20 L/s and an average temperature of 30°C . The fluid in the inner tube is a 40% ethylene glycol solution at an average temperature of 0°C and flowing at 15 L/s. Determine the Reynolds numbers of the flow in the pipe and the annulus for:
- a. Friction calculations
 - b. Heat transfer calculations
- 5.39 A double pipe heat exchanger is made of an 8-nom sch 20 commercial steel outer pipe and a 4-std type M copper inner tube. The fluid in the annular space is liquid water that has a volumetric flow rate of $120\text{ m}^3/\text{h}$ and an average temperature of 50°C . The fluid in the inner tube is liquid ammonia at an average temperature of -20°C and flowing at $60\text{ m}^3/\text{h}$. Determine the friction factor in the
- a. Tube
 - b. Annulus
- 5.40 A counter flow double pipe heat exchanger has an outer pipe of 4-nom sch 40 commercial steel and an inner tube of 2-std type M copper. Hard water at an average temperature of 120°F flows in the tube at a flow rate of 80 gpm. City water flows in the annulus at a flow rate of 75 gpm and an average temperature of 50°F . The heat exchanger is a single DPHX with a length of 6 ft. After one year of service,

the volumetric flow rates in the tube and annulus are estimated to experience a 2.5% reduction due to fouling. The fouling layer is primarily calcium carbonate. Determine the pressure drop and the power required (watts) to move the water through the:

- a. Inner tube for clean and fouled conditions
 - b. Annulus for clean and fouled conditions
 - c. Determine the increased power requirement (watts) due to fouling to move the water through the tube.
 - d. Determine the increased power requirement (watts) due to fouling to move the water through the annulus.
 - e. Based on your answers in Parts (c) and (d), is fouling a concern from a hydraulic point of view?
- 5.41 Determine the UA product for the double pipe heat exchanger described in Problem 5.40 for both clean and fouled conditions.
- 5.42 A double pipe heat exchanger is constructed with a 5-nom sch 40 commercial steel outer pipe and a 2½-std type M copper inner tube. The heat exchanger is 2-m long. Water flows in the tube at an average temperature of 30°C and a flow rate of 5 kg/s. A 30% ethanol-water solution flows in the annulus with an average temperature of 5°C and a mass flow rate of 12 kg/s. For a clean heat exchanger, determine the,
- a. UA product of the heat exchanger (W/K)
 - b. Pressure drop through the tube and annulus (kPa)
- In an effort to increase the heat transfer rate with a heat exchanger of the same footprint, it is proposed to replace the single 2½-std type M inner tube with three 1-std type M tubes in a triangular arrangement as shown in Figure P5.42. The water flow rate is split evenly between the three tubes. For this modified design, determine the
- c. UA product of the heat exchanger (W/K)
 - d. Percent increase in the UA product in the modified design compared to the original design
 - e. Pressure drop through the tubes and annulus (kPa)
 - f. Percent increase in the pressure drop through the inner tubes and annulus in the modified design compared to the original design
- 5.43 A double pipe heat exchanger is made of a 6-nom sch 40 commercial steel outer pipe and a 5-nom sch 40S stainless steel inner pipe. The fluid in the annular space is cyclohexane that has a volumetric flow rate of 50,000 lbm/h and an average temperature of 180°F. The fluid in the inner tube is river water at an average temperature of 60°F and flowing at 125,000 lbm/h. The thermal conductivity of the inner pipe is 9.5 Btu/h-ft-°F. Determine the overall heat transfer coefficient, based on the outside diameter of the inner pipe for a clean heat exchanger.
- 5.44 Design a double pipe heat exchanger to cool a flow of liquid benzene from 85°F to 60°F. The mass flow rate of the benzene is 12,500 lbm/h. City water at 50°F is available to provide the required cooling. The water supply flow rate is available up to 16,000 lbm/h. Once the design process is complete, analyze the heat exchanger to determine its thermal and hydraulic performance. Report your results in a table similar to Table 5.8. Justify your selections by providing all calculations required

**FIGURE P5.42**

Original and modified heat exchanger designs.

to design and analyze the heat exchanger (e.g., computer code, spreadsheets, and/or hand calculations).

- 5.45 A flow of 6 kg/s of octane is to be cooled from 70°C to 64°C. A flow of distilled water at 4 kg/s is available at 60°C to accomplish the cooling. Design a double pipe heat exchanger to meet this goal. Once the design is complete, analyze the heat exchanger to determine its thermal and hydraulic performance. Report your results in a table similar to Table 5.8. Justify your selections by providing all calculations required to design and analyze the heat exchanger (e.g., computer code, spreadsheets, and/or hand calculations).
- 5.46 Design and analyze a double pipe heat exchanger with requirements specified by your instructor. Report your results in a table similar to Table 5.8. Justify your selections by providing all calculations required to design and analyze the heat exchanger (e.g., computer code, spreadsheets, and/or hand calculations).
- 5.47 A counter flow double pipe heat exchanger has hot distilled water at 80°C entering the annulus at a flow rate of 1 kg/s. Cold distilled water at 50°C enters the inner tube at a flow rate of 0.9 kg/s. The heat exchanger consists of 9 hairpins, each with a length of 2 m. The outer pipe is 2-nom sch 40 commercial steel and the inner tube is 1-std type M copper. After one year of continuous service, determine the
- Outlet temperatures of the hot and cold-water flows
 - Heat transfer rate (kW) between the hot and cold water
 - Pressure drop through the inner tube (kPa)
 - Pressure drop through the annulus (kPa)

When computing the pressure drops, ignore the effect of diameter changes due to fouling.

- 5.48 A parallel flow double pipe heat exchanger is constructed using a 3/4-nom sch 5S stainless steel outer pipe and a 1/2-std type M copper tube. Ethanol enters the tube at 900 lbm/h and a temperature of 80°F. Water flows through the annulus at 1,200 lbm/h and it enters the heat exchanger at 140°F. The heat exchanger is 6-ft long with no hairpins. For a clean heat exchanger, determine the
- Outlet temperatures of the hot and cold fluid flows
 - Heat transfer rate (Btu/h) between the hot and cold fluids

- c. Pressure drop through the inner tube (psi)
- d. Pressure drop through the annulus (psi)

Shell and Tube Heat Exchangers

- 5.49 A shell and tube heat exchanger has two tube passes inside of a 29-in shell. The tubes are 1-in 16 BWG tubes on a $1\frac{1}{4}$ -in square pitch and the heat exchanger contains the maximum amount of tubes allowable. Water at an average temperature of 80°F is flowing through the tubes. The total flow rate of the water is 750,000 lbm/hr. Determine the
- a. Clearance, C , between the tubes (in)
 - b. The number of tubes in the heat exchanger
 - c. The Reynolds number of the flow inside one of the tubes
 - d. Determine the answers to (a) through (c) if the tube pitch is $1\frac{1}{4}$ in triangular instead of square.
- 5.50 A shell and tube heat exchanger is has 1 shell with 2 tube passes. A 30% methanol solution is flowing through the shell at a rate of 90 kg/s. The shell has a diameter of 12 in. The tubes are $\frac{3}{4}$ -in on a 1-in triangular pitch. The heat exchanger is 2-m long and there are 3 baffles per meter of length. Determine the
- a. The tube clearance (mm)
 - b. The number of tubes in the heat exchanger
 - c. The Reynolds number of the methanol solution flowing through the shell
- 5.51 A shell and tube heat exchanger is made of a single shell with four tube passes. The hot fluid enters the heat exchanger at 96°F and leaves at 82°F. The cold fluid enters at 49°F and leaves at 83°F. Determine the LMTD for this heat exchanger. Comment on the economic viability of this heat exchanger.
- 5.52 The condenser of a steam power plant is a shell and tube design with cooling water flowing through the tubes. The condenser has 4 tube passes inside of a 39-inch shell. The tubes are $1\frac{1}{2}$ -in 12 BWG tubes on a $1\frac{7}{8}$ -in triangular pitch. The cooling water enters the heat exchanger at a flow rate of 300 kg/s at an average temperature of 30°C. Determine the Reynolds number of the water flow inside of one of the tubes of this heat exchanger.
- 5.53 The tubes in a shell and tube heat exchanger are 10 ft long. The liquid in the tubes is ammonia at an average temperature of 110°F. The flow rate of the ammonia entering the heat exchanger is 120,000 lbm/hr. The heat exchanger tubes are 1-in 14 BWG tubes on a $1\frac{1}{4}$ -in triangular pitch. The shell diameter is 12-in. Determine the pressure drop (psi) through the tube side of the heat exchanger for a single-pass, 2-pass, and 4-pass tube configuration.
- 5.54 The evaporator of a refrigeration cycle is being used to chill water. The water flows in the tubes while the refrigerant boils in the shell. The water enters the heat exchanger at a flow rate of 50 L/s. The average temperature of the water through the heat exchanger is 6°C. The shell of the heat exchanger has a diameter of $21\frac{1}{4}$ -in. The tubes in the heat exchanger have a length of 3.5 m and are $\frac{3}{4}$ -in 16 BWG tubes on a 1-in square pitch. Determine the pressure drop (kPa) on the tube side of the heat exchanger for a single-pass, 2-pass, and 4-pass tube design.

- 5.55 A shell and tube heat exchanger has a single shell and 4 tube passes. The shell diameter is 25-in. The shell contains 10 baffles with a spacing of 0.36 m. Liquid ammonia flows through the shell with a flow rate of 70 kg/s and an average temperature of 90°C. The tubes are 1¼-in 13 BWG tubes on a 1 9/16-in square pitch. Determine the
- Shell-side convective heat transfer coefficient ($\text{W/m}^2\text{-K}$)
 - Shell-side pressure drop (kPa)
- 5.56 Water is flowing at a rate of 240,000 lbm/hr through the shell-side of a shell and tube heat exchanger. The average temperature of the water is 40°F. The shell has a diameter of 17¼-in and there is one tube pass. The shell contains 12 baffles with a spacing of 10 in. The tubes are ¾-in 15 BWG tubes on a 1-in triangular pitch. Determine the following,
- The shell-side convective heat transfer coefficient ($\text{Btu/hr-ft}^2\text{-}^\circ\text{F}$)
 - The shell-side pressure drop (psi)
- 5.57 Liquid pentane is flowing in the shell of a shell and tube heat exchanger at a rate of 350,000 lbm/hr and an average temperature of 20°F. The shell has a diameter of 27 in and a length of 16 ft. The tubes in the heat exchanger are ¾-in 15 BWG tubes on a 1-in triangular pitch. The purpose of this problem is to investigate how the number of baffles impacts the heat transfer and the pressure drop on the shell side of the heat exchanger. Calculate the shell-side convective heat transfer coefficient and pressure drop for the case where the heat exchanger has 10 baffles. Repeat the calculation for 20 baffles. Then determine the
- Ratio of the shell-side convective heat transfer coefficient for the 20-baffle heat exchanger to the 10-baffle heat exchanger
 - Ratio of the shell-side pressure drop for the 20-baffle heat exchanger to the 10-baffle heat exchanger
 - If the optimum baffle spacing is somewhere between $0.4D_s$ and $0.6D_s$, how many baffles would you recommend for this heat exchanger? What are the values of the shell-side convective heat transfer coefficient and pressure drop for the number of baffles you recommended?
- 5.58 A shell and tube heat exchanger is made up of a single 27-in shell and 2 tube passes. The tubes are 1½ 14 BWG with a 1 7/8-in in triangular pitch. City water passes through the shell of the heat exchanger. The water enters at 70°C with a mass flow rate of 20 kg/s. Liquid hexane passes through the tubes at a flow rate of 45 kg/s. The hexane enters the heat exchanger at 20°C. The heat exchanger is 5 m long and there are 3 baffles per meter. Determine the
- Fluid outlet temperatures and the pressure drop (kPa) for each fluid stream for a clean heat exchanger.
 - Fluid outlet temperatures and the pressure drop (kPa) for each fluid stream for a clean heat exchanger if a square tube pitch is used instead of triangular.
- 5.59 A shell and tube heat exchanger is being used to cool 150,000 lbm/h of benzene in a detergent manufacturing process. The benzene enters the heat exchanger at 125°F and its outlet temperature must not exceed 90°F. City water, flowing at 180,000 lbm/h enters the heat exchanger at 65°F to provide the required cooling. The heat exchanger is a single shell 2-tube pass configuration with a 17¼ inch

shell. The tubes are $\frac{3}{4}$ -in 18 BWG on a 1-in triangular pitch. The heat exchanger is 16 ft long and contains 10 baffles. The benzene is routed through the tubes and the water flows in the shell. If maintenance does not occur on the heat exchanger until a year of service is complete, determine the

- a. Benzene and water outlet temperatures
 - b. Pressure drops for each of the fluids (psi)
 - c. If the benzene outlet temperature calculated in Part (a) is higher than the maximum allowed temperature of 90°F, what maintenance period would you recommend (months between cleanings)? Assume that the fouling occurs linearly in time.
 - d. What is the benzene outlet temperature for the maintenance period suggested in Part (c)?
- 5.60 Liquid carbon dioxide enters the tubes of a shell and tube heat exchanger at a temperature of 0°C and a flow rate of 30 kg/s. The carbon dioxide is heated with a flow of city water that enters the shell side of the heat exchanger at a temperature of 40°C and a flow rate of 31 kg/s. The heat exchanger is a single shell, two-tube pass configuration with a 25 in shell. The tubes are $\frac{3}{4}$ -in 10 BWG laid out on a 1-in triangular pitch. The heat exchanger is 2 m long and contains 2 baffles per meter of length. Determine
- a. The outlet temperatures and pressure drops of each fluid in the heat exchanger for the case of a brand new heat exchanger just put into service
 - b. The outlet temperatures of each fluid after the heat exchanger has been in continuous service for one year without maintenance
 - c. If the outlet temperature of the carbon dioxide must be 20°C or higher, is this heat exchanger sufficient for the required duty?

Plate and Frame Heat Exchangers

- 5.61 Table P5.61 shows manufacturer's data for a particular plate and frame heat exchanger. Determine the,
- a. Average channel spacing (mm)
 - b. Flow area for one channel between two plates (m²)
 - c. Channel hydraulic diameter (cm)
 - d. Projected plate area (m²)
 - e. Effective surface area per plate (m²)
- 5.62 Table P5.62 shows manufacturer's data for a particular plate and frame heat exchanger. Determine the
- a. Average channel spacing (in)
 - b. Flow area for one channel between two plates (in²)
 - c. Channel hydraulic diameter (in)
 - d. Projected plate area (ft²)
 - e. Effective surface area per plate (ft²)
- 5.63 A 1-1/U counter flow plate and frame heat exchanger has 39 total plates. The plates are made from titanium and stamped with a 45° chevron pattern. Each plate has a

TABLE P5.61

Manufacturer's Data for a Plate and Frame Heat Exchanger

Parameter	Value
Chevron angle	50°
Enlargement factor	1.19
Port diameters	15 cm
Plate thickness	0.6 mm
Vertical port-to-port distance	1.45 m
Horizontal port-to-port distance	0.65 m
Plate pitch	3.5 mm

TABLE P5.62

Manufacturer's Data for a Plate and Frame Heat Exchanger

Parameter	Value
Chevron angle	60°
Enlargement factor	1.17
Port diameters	2 in
Plate thickness	0.025 in
Vertical port-to-port distance	25.2 in
Horizontal port-to-port distance	5.51 in
Compressed plate pack length	5 ft
Number of plates	400

length of $L_p = 32$ in and a width of $L_w = 17$ in. The plate thickness is 0.04 in and the plate pitch is 0.14 in. The plate enlargement factor is 1.16. All port diameters are 2.5 in. The hot fluid, hard water, flows at 120,000 lbm/hr with an average temperature of 145°F. The cold fluid is hard water flowing at 150,000 lbm/hr and an average temperature of 50°F. Determine the

- Conduction resistance between the two fluids due to the plate (hr-ft²-°F/Btu). How does this compare with the fouling factor on each side of the plate?
 - Pressure drop of the hot and cold water flows due to friction effects of the plates (psi)
 - Pressure drop of the hot and cold water flows due to port losses (psi)
- 5.64 In a distillery, a plate and frame heat exchanger with a 1-1/U counter flow plate arrangement is being used to cool down a flow of pure ethanol using cold water. The plates are stamped with a 50° chevron pattern. The plate width is 248 mm and the effective heat transfer area of each plate is 0.32 m². The plates have an enlargement factor of 1.25. They are 0.6 mm thick and the plate pitch is 3.2 mm. The ethanol enters the heat exchanger at a flow rate of 10.3 kg/s at an average temperature of 80°C. The cold water flows at a rate of 9.8 kg/s with an average temperature of 15°C. The diameter of the hot and cold ports on the heat exchanger is 55 mm. The heat exchanger has 116 plates. Determine the total pressure drop of each fluid as it passes through this heat exchanger (kPa).
- 5.65 Cold distilled water is being used to cool a 30% ethylene glycol solution in a 1-1/U counter flow plate and frame heat exchanger. The ethylene glycol solution

flows at 14.5 kg/s and enters the heat exchanger at 32°C. The water enters the heat exchanger at a flow rate of 18.2 kg/s with a temperature of 15°C. The plates are AISI 316 stainless steel and have a 60° chevron pattern. The plates have a vertical port distance of 1.1 m and a horizontal port distance of 0.3 m. The plate width is 0.4 m. Each plate has a thickness of 0.8 mm and the plate pitch is 3.5 mm. There are 187 total plates in the heat exchanger. The port diameters are 63.5 mm. The fouling factor for the ethylene glycol solution can be taken as $5 \times 10^{-7} \text{ m}^2\text{-K/W}$. For the case of yearly maintenance on the heat exchanger, determine the,

- a. Outlet temperature of each fluid (°C)
 - b. Pressure drop of each fluid as it passes through the heat exchanger (kPa)
 - c. Estimated maximum allowable pressure drop for either fluid (kPa)
 - d. Effectiveness of the heat exchanger
- 5.66 A 1-1/U counter flow plate and frame heat exchanger is being used to warm a flow of cold acetone. The acetone enters the heat exchanger at 25°F with a flow rate of 315,000 lbm/h. Soft water at 50°F and a flow rate of 220,000 lbm/h is used to provide the required heat transfer. The heat exchanger has 236 plates made of AISI 316 stainless steel, stamped with a 45° chevron pattern. The plate thickness is 0.04 in and the plate pitch is 0.14 in. The vertical and horizontal port distances are 35 in and 18 in, respectively. The plate width is 21.5 in. The port diameters are 3 in. The fouling factor of acetone is estimated as $3 \times 10^{-5} \text{ h-ft}^2\text{-F/Btu}$. If the maintenance schedule for this heat exchanger is yearly, determine the,
- a. Outlet temperature of each fluid (°F)
 - b. Pressure drop of each fluid as it passes through the heat exchanger (psi)
 - c. Heat transfer duty (e.g., the heat transfer rate between the fluids) (Btu/h)
- 5.67 Distilled water is being cooled by a 20% propylene glycol solution in a 1-1/U counter flow plate and frame heat exchanger. The water enters the heat exchanger at 50°F at a flow rate of 86,000 lbm/h. For safety reasons, the water outlet temperature should never be colder than 35°F. The propylene glycol solution enters the heat exchanger at 28°F with a flow rate of 73,000 lbm/h. The port distances on the heat exchanger are $L_v = 35 \text{ in}$ and $L_h = 18 \text{ in}$. The plate width is $L_w = 21.5 \text{ in}$. The plate thickness is 0.04 in with a plate pitch of 0.12 in. The chevron angle is 30° and the plate enlargement factor is 1.17. All ports have a 2 in diameter. The fouling factor of the propylene glycol solution can be estimated as $2 \times 10^{-5} \text{ h-ft}^2\text{-°F/Btu}$.
- a. Determine the maximum number of plates the heat exchanger can have while ensuring that the water outlet temperature never drops below 35°F.
 - b. Determine the thermal and hydraulic performance of the heat exchanger with the specified number of plates. Summarize your findings in a table similar to Table 5.17.
- 5.68 A 1/1-U counter flow plate and frame heat exchanger is being used to cool liquid ammonia using a chilled 15% magnesium chloride solution. The ammonia enters the heat exchanger at 32°C with a flow rate of 5 kg/s. The ammonia must not cooled any lower than 14°C. The calcium chloride solution enters the heat exchanger at -8°C at a flow rate of 4.2 kg/s. The plates of the heat exchanger are made from AISI 304 stainless steel. The plate thickness is 0.6 mm and the plate pitch is 3.5 mm. The vertical port distance is 0.9 m and the horizontal port distance is 0.25 m. The port

diameters are 42 mm. The plate enlargement factor is 1.16. The fouling factors for ammonia and the magnesium chloride solution can be taken as $2 \times 10^{-6} \text{ m}^2\text{-K/W}$ and $3.2 \times 10^{-6} \text{ m}^2\text{-K/W}$, respectively.

- a. Determine the maximum number of plates that can be in this heat exchanger.
 - b. Determine the thermal and hydraulic performance of the heat exchanger with the specified number of plates. Summarize your results in a table similar to Table 5.17.
- 5.69 A plate and frame heat exchanger with a 1-1/U configuration has water (fouling factor = $0.00005 \text{ h-ft}^2\text{-}^\circ\text{F/Btu}$) for both hot and cold fluids. The heat exchanger has 125 plates. The horizontal port distance is 15 in and the vertical port distance is 27 in. The plates are 0.04 in thick and stamped with a 65° chevron pattern. The plate pitch is 0.15 in and the plate enlargement factor is 1.17. The port diameters are 1.5 in. The plates are made from AISI 316 stainless steel. Hot water enters the heat exchanger at 135°F with a flow rate of 72,000 lbm/h. The cold water, flowing at a rate of 68,000 lbm/h, enters the heat exchanger at 55°F . Determine the thermal and hydraulic performance of this heat exchanger. Report your answers in a table similar to Table 5.17.

Cross Flow Heat Exchangers

- 5.70 Hot air is used to heat cold water from 35°C to 95°C in a finned-tube heat exchanger similar to the one shown in Figure 5.31. The water flows in the tubes at a flow rate of 1.9 kg/s. The air, at 1 atm, enters the heat exchanger at 210°C and leaves at 100°C . The overall heat transfer coefficient for the heat exchanger is $185 \text{ W/m}^2\text{-K}$. Determine the air-side area required for this heat exchanger.
- 5.71 A cross flow heat exchanger similar to the one shown in Figure 5.31 is being used to recover heat from a flow of hot air that enters the heat exchanger at 200°F with a mass flow rate of 14,400 lbm/h. Cool water, flowing in the tubes, enters the heat exchanger at 50°F and leaves at 80°F while flowing at 12,000 lbm/h. Determine the
- a. Heat transfer rate recovered from the hot air flow (Btu/h)
 - b. The exit temperature of the air ($^\circ\text{F}$)
 - c. UA product for this heat exchanger (Btu/h- $^\circ\text{F}$)
- Consider a situation where the mass flow rates of the air and water are the same, and the entering air temperature is the same. However, the entering water temperature is now 60°F rather than 50°F . Based on your previous analysis, estimate the
- d. Temperature of the air and water leaving the heat exchanger ($^\circ\text{F}$)
 - e. Heat transfer rate recovered from the hot air flow (Btu/h)
- 5.72 Water enters a heat exchanger at 85°C with a flow rate of 2.5 kg/s. Dry atmospheric air enters the heat exchanger at 20°C at a flow rate of 12 kg/s. It is desired to select a cross flow heat exchanger for this task such that the air leaves the heat exchanger at a temperature near, but not less than, 60°C . The design engineer is considering three possible cross flow heat exchangers that have been identified as viable solutions to accomplish this task;

HXI: both fluids unmixed ($UA_{\text{I}} = 23.5 \text{ kW/K}$)

HXII: \dot{C}_{\min} mixed with \dot{C}_{\max} unmixed ($UA_{\text{II}} = 32.0 \text{ kW/K}$)

HXIII: \dot{C}_{\max} mixed with \dot{C}_{\min} unmixed ($UA_{\text{III}} = 32.8 \text{ kW/K}$)

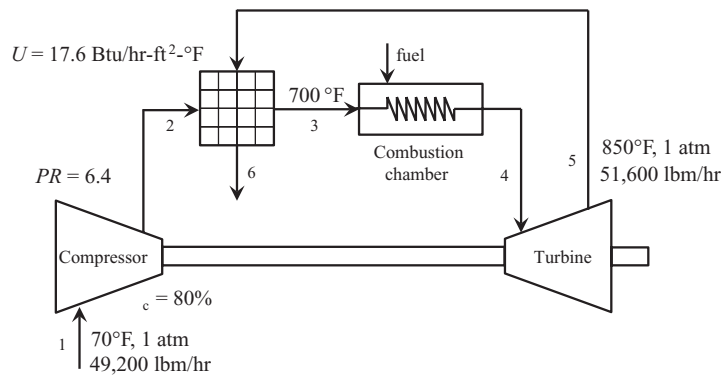
- a. Calculate the outlet temperature of the air for the three heat exchangers. Is the minimum outlet temperature of 60°C satisfied?
 - b. Calculate the effectiveness of each of the heat exchangers. Is there an advantage to one configuration over the others?
 - c. Which heat exchanger would you recommend, and why?
- 5.73 In Example 5.12, the UA product for a cross flow finned tube heat exchanger was calculated. In that example, it was stated that, "... the U value of the heat exchanger will change as the flow rates and fluid temperatures change. However, if the expected change is minimal, the predicted outlet temperature using the estimated UA should be reasonably close to the expected outlet temperatures." The purpose of this exercise is to determine the validity of this statement using manufacturer's data for a finned tube air heating coil for residential applications. The manufacturer's data for this cross flow, finned tube coil is given in Table P5.73. Air flows through the fins and water flows through the tubes of the heat exchanger. Given this data determine the
- a. UA product for each of the three air flow rates. Can a simple relationship be developed for the UA product as a function of the air flow rate? If so, determine this relationship.
- If the manufacturer only provided data for the 1,200-cfm air flow case, determine the
- b. Percent error in the UA product that would occur at 1,000 cfm and 1,400 cfm compared to the UA product calculated at 1,200 cfm. Is the variation in the UA product for this heat exchanger significant over the range of air flows given for the application?
- 5.74 To increase the thermal efficiency of a gas turbine cycle, the combustion air is often preheated using the hot gases exhausting the turbine. Consider the case where this is being accomplished using a cross flow (unmixed-unmixed) heat exchanger as shown in Figure P5.74. Hot combustion gases exit the turbine at a mass flow rate of 51,600 lbm/hr with a temperature of 850°F. Air enters the compressor at 1 atm, 70°F at a mass flow rate of 49,200 lbm/hr. The pressure ratio across the compressor is $PR = 6.4$ and the isentropic efficiency of the compressor is 80%. The overall heat transfer coefficient for the heat exchanger has been found to be $U = 17.6 \text{ Btu/hr-ft}^2\text{-}^\circ\text{F}$. If the combustion air is to be preheated to 700°F, determine the total heat exchange area required for this heat exchanger (ft^2). Assume that the pressure drops through the connecting lines and the heat exchangers are negligible and that the working fluid can be modeled as air throughout the cycle.

TABLE P5.73

Manufacturer's Performance Data for a Cross Flow Finned Tube Air Heating Coil

Air Flow Entering Coil (cfm)	Water Flow Entering Coil (gpm)	Heat Transfer Duty ^a (Btu/h)
1000	6	66,000
1200	6	72,000
1400	6	77,500

^a Entering air temperature = 68°F, entering water temperature = 180°F.

**FIGURE P5.74**

Gas turbine cycle with combustion air preheater.

6

Simulation, Evaluation, and Optimization of Thermal Energy Systems

6.1 Introduction

Before the advent of modern computing technology, thermal energy systems were designed using a combination of lengthy hand calculations, graphs, and plots that represent component performance and experience. The resulting system may not have been an optimum economic design, but it was a workable solution. Modern engineering practice requires the engineer to consider the environmental impact of his/her designs in addition to thermal performance and cost effectiveness. This implies that the system should be designed to meet some sort of optimum condition. Modern computing technology allows this to occur through a series of processes known as *simulation*, *evaluation*, and *optimization*.

Simulation is the development and solution of a mathematical model that predicts the operating condition of a thermal energy system. Evaluation involves the use of a simulation model to study the effect of changing one or more variables in the simulation. Together, simulation and evaluation provide the design engineer with the means to study several thermal energy systems using computer software and allow the designer to feel confident that the selected thermal system will operate as predicted by the simulation. Optimization considers what configuration the thermal energy system should take to operate at an optimum condition. This optimum condition may be the system configuration with minimum cost, the system with maximum thermal efficiency, or the system with the minimum exergy destruction, to name a few. To perform a successful optimization, the mathematical model making up the simulation must be developed first.

6.2 Thermal Energy System Simulation

The simulation problem may be stated in general terms as follows:

GIVEN:

- Thermal energy system configuration (system specifications)
- Thermal energy system performance parameters (e.g., temperatures, flow rates, or heat transfer rates)
- Component performance equations

FIND: The operating point of the thermal energy system.

SOLUTION: The general solution strategy is as follows:

- Write a system of n equations with n unknowns that completely describes the system. This system of equations will include fluid properties, application of appropriate fundamental laws from thermodynamics, fluid mechanics, and/or heat transfer, and equations describing component performance.
- Solve the resulting system of equations. The resulting solution is the operating point of the thermal energy system for the given conditions.

The resulting set of equations is an $n \times n$ system. Therefore, computer software can be used to determine the solution. Some software requires reasonable initial guesses of the unknown variables. This can become quite challenging as the simulations become more complex.

6.2.1 Simulation Example: A Pump and Pipe System

To demonstrate the simulation procedure, a familiar example will be presented. In this section, a simulation will be written and solved for a pump and pipe system. Consider the following problem,

A pump and pipe system used to transfer irrigation water in a farming application is shown in Figure 6.1 below. The pipe system is made of 4-nom sch 40 commercial steel pipe with regular fittings. A globe valve is used in the system for flow control. With the globe valve wide-opened, this system must provide a minimum of 400 gpm of water at 60°F. The pump selected to meet this requirement is a Bell & Gossett Series e-80 4 × 4 × 9½ pump with a 9-inch impeller operating at 1170 rpm. Determine the operating point (volumetric flow rate and head) of the system.

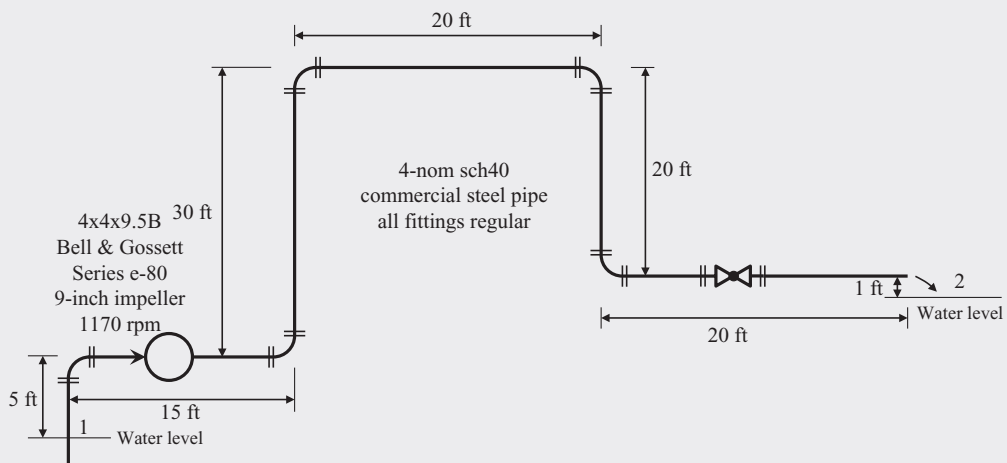


FIGURE 6.1

A pump and pipe network.

In Chapter 4, these types of problems are solved by determining the system curve and superimposing it on a pump curve to select the pump and determine the operating point graphically. To write a simulation for this system, all component and system parameters need to be represented by equations. When formulating the $n \times n$ equation set that makes up the simulation, it is important to keep track of equations and unknowns. Once an $n \times n$ system is determined, it can be solved.

The conservation of energy equation applied to a system boundary surrounding the system from point 1 to point 2 is,

$$z_1 + H_p = z_2 + \left(f \frac{L}{D} + 5K_e + K_v + K_{exit} \right) \frac{V^2}{2g} \quad (6.1)$$

This is the first equation of the simulation. Unfortunately, many of the variables are unknown at this point. To help keep track of the known and unknown values, it is helpful to build the simulation equations in tabular form. The goal is to continue adding equations until the number of equations is equal to the number of unknowns. Some of the unknown values in this first equation are easily determined. For example, the total pipe length and elevations can be found using the dimensions in the system sketch. These “easy-to-find” variables do not need to be included in the equation set. Following this strategy, the first equation in the simulation is shown in Table 6.1. Notice that the elevations, pipe length, pipe diameter, and the acceleration due to gravity (g) are not counted as unknowns. These are values that are easily determined. Keeping these easy-to-find variables out of the simulation makes a much less complicated set of equations in the end.

TABLE 6.1

First Equation of the Pump/Pipe Simulation

Equation	New Unknowns	Equations \times Unknowns
$z_1 + H_p = z_2 + \left(f \frac{L}{D} + K_{ent} + 5K_e + K_v + K_{exit} \right) \frac{V^2}{2g}$	$H_p, f, K_{ent}, K_e, K_v, K_{exit}, V$	1×7

The resistance coefficients for the elbows, valve, and exit can be found using the Darby 3K method. These equations are summarized in Table 6.2. Notice that one more *new* unknown is introduced in this set of equations, the Reynolds number of the flow. The absolute roughness of the pipe, ϵ , is not counted as an unknown because it can be easily found in Table 4.3.

TABLE 6.2

Resistance Coefficient Equations for the Pump/Pipe Simulation

Equation	New Unknowns	Equations × Unknowns
$K_{ent} = \frac{K_{1,ent}}{\text{Re}} + K_{\infty,ent} \left(1 + \frac{K_{d,ent}}{D_{nom}^{0.3}} \right)$	Re	2×8
$K_e = \frac{K_{1,e}}{\text{Re}} + K_{\infty,e} \left(1 + \frac{K_{d,e}}{D_{nom}^{0.3}} \right)$		3×8
$K_v = \frac{K_{1,v}}{\text{Re}} + K_{\infty,v} \left(1 + \frac{K_{d,v}}{D_{nom}^{0.3}} \right)$		4×8
$K_{exit} = \frac{K_{1,exit}}{\text{Re}} + K_{\infty,exit} \left(1 + \frac{K_{d,exit}}{D_{nom}^{0.3}} \right)$		5×8

The friction factor in the conservation of energy equation can be determined by any of the correlations presented in Chapter 4. Using the Swamee-Jain correlation, another set of equations can be added to the simulation set as shown in Table 6.3. The density and dynamic viscosity of the water are not treated as unknowns here because they can easily be evaluated since the temperature is known and the water can be treated as an incompressible substance.

TABLE 6.3

Friction Equations for the Pump/Pipe Simulation

Equation	New Unknowns	Equations × Unknowns
$f = 0.25 \left[\log \left(\frac{\epsilon / D}{3.7} + \frac{5.74}{\text{Re}^{0.9}} \right) \right]^{-2}$		6×8
$\text{Re} = \frac{\rho V D}{\mu}$		7×8
$V = \frac{4 \dot{V}}{\pi D^2}$	\dot{V}	8×9

At this point, there appears to be at least one more equation that needs to be added to complete the simulation. The behavior of the *system* has been fully identified with the equations shown in Tables 6.1, 6.2, and 6.3. What is missing is the *performance* of the pump in the system. Therefore, to complete the simulation, an equation needs to be developed that describes how the pump head varies with capacity. This information is determined from the manufacturer's pump curves.

The pump curve is a 2-dimensional equation. Equations of this type can be determined using a variety of software packages. To determine the equation, a series of *x-y* data need to be read from the pump performance curve. Figure 6.2 shows the result of fitting several data points from the 9-inch impeller pump curve from Appendix E using a spreadsheet

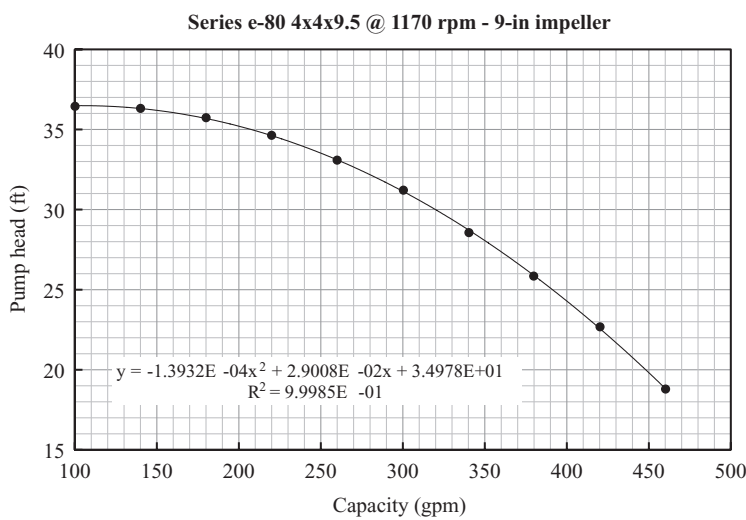


FIGURE 6.2
Determination of an empirical equation to represent the pump performance.

program with curve fitting capability. From the curve-fitting exercise, the pump performance can be written as,

$$H_p = a_1 \dot{V}^2 + a_2 \dot{V} + a_3 \tag{6.2}$$

The coefficients resulting from the curve-fitting exercise are given in Table 6.4. Since the equation developed for the pump curve is empirical, it is important to make certain that the coefficients are assigned the proper units. The units of the coefficients can be determined by considering the functional form being fit.

The pump performance curve, Equation 6.2, is the final equation needed to complete the simulation of the system. The complete set of equations that make up the simulation of the pump and pipe system are shown in Table 6.5. The coefficients of the pump curve equation are not counted as unknowns since they have been determined by the curve-fitting exercise. Notice that after adding the pump curve equation, the number of equations equals the number of unknowns. This means that the simulation is complete and is ready to be solved.

Solving the simulation shown in Table 6.5 results in an operating point defined by $H_p = 24$ ft and $\dot{V} = 404$ gpm. It is interesting to see the other operating parameters of the system such as the Reynolds number of the flow, or the velocity of the fluid in the pipe.

TABLE 6.4
Coefficients of Equation 6.2 Resulting from Curve Fitting the Pump Performance Data from Appendix E

Coefficient	Value and Units
a_1	-1.3932×10^{-4} ft/gpm ²
a_2	2.9008×10^{-2} ft/gpm
a_3	3.4978×10^1 ft

TABLE 6.5

Complete Equation Set for the Pump/Pipe System Simulation

Equation	New Unknowns	Equations \times Unknowns
$z_1 + H_p = z_2 + \left(f \frac{L}{D} + K_{ent} + 5K_e + K_v + K_{exit} \right) \frac{V^2}{2g}$	$H_p, f, K_{ent}, K_e, K_v, K_{exit}, V$	1×7
$K_{ent} = \frac{K_{1,ent}}{\text{Re}} + K_{\infty,ent} \left(1 + \frac{K_{d,ent}}{D_{nom}^{0.3}} \right)$	Re	2×8
$K_e = \frac{K_{1,e}}{\text{Re}} + K_{\infty,e} \left(1 + \frac{K_{d,e}}{D_{nom}^{0.3}} \right)$		3×8
$K_v = \frac{K_{1,v}}{\text{Re}} + K_{\infty,v} \left(1 + \frac{K_{d,v}}{D_{nom}^{0.3}} \right)$		4×8
$K_{exit} = \frac{K_{1,exit}}{\text{Re}} + K_{\infty,exit} \left(1 + \frac{K_{d,exit}}{D_{nom}^{0.3}} \right)$		5×8
$f = 0.25 \left[\log \left(\frac{\epsilon/D}{3.7} + \frac{5.74}{\text{Re}^{0.9}} \right) \right]^{-2}$		6×8
$\text{Re} = \frac{\rho V D}{\mu}$		7×8
$V = \frac{4\dot{V}}{\pi D^2}$	\dot{V}	8×9
$H_p = a_1 \dot{V}^2 + a_2 \dot{V} + a_3$		9×9

However, the parameters of main interest from the simulation are the capacity (gpm) and head (ft).

To determine the power draw and the pump efficiency, this point needs to be identified on the pump performance curve as shown in the Figure 6.3. This figure indicates that the pump will draw approximately 3.5 hp and operate with a fairly high efficiency of about 70%.

As demonstrated in this familiar example, the process of constructing a system simulation requires the mathematical representation of the performance of the thermal energy system and the performance of the components that make up the thermal energy system. For the pipes and fittings, the conservation of energy equation is required. For the pump, the manufacturer's performance information needs to be converted to an empirical equation through a data fitting exercise. The simulation results provide the operating point of the pump and pipe system.

A simulation is the mathematical solution of a set of equations. For the pump and pipe system in this problem, the graphical representation of the simulation is shown in Figure 6.4. The simulation equations are solving for the intersection of two 2-dimensional equations; the system curve and the pump performance curve. Often, engineering components are 3-dimensional in their performance. For example, manufacturers of refrigeration

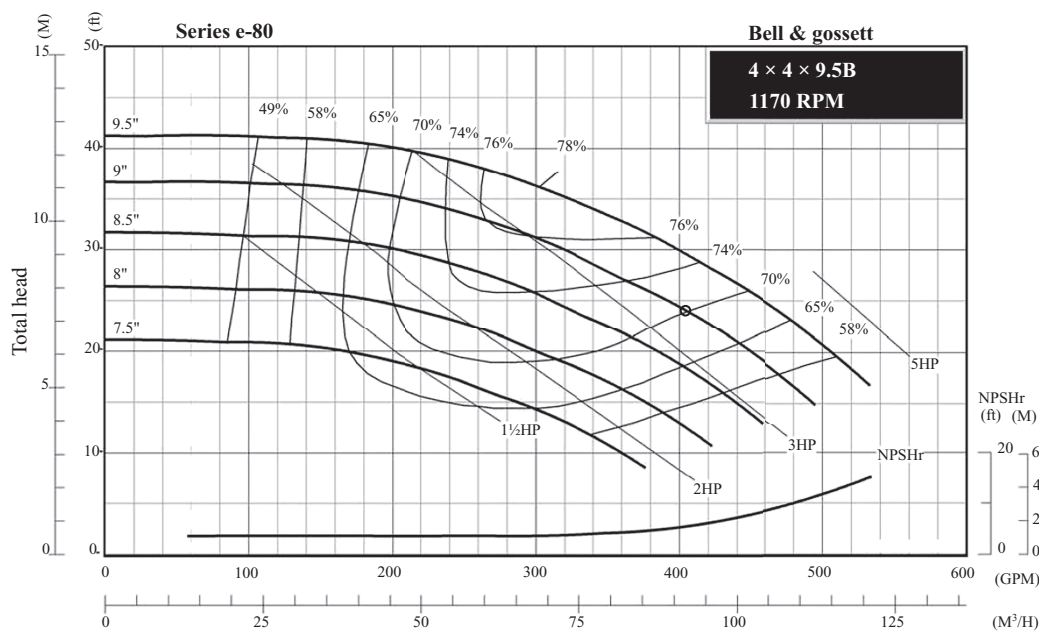


FIGURE 6.3
Determination of pump efficiency and power draw from the pump performance curve.

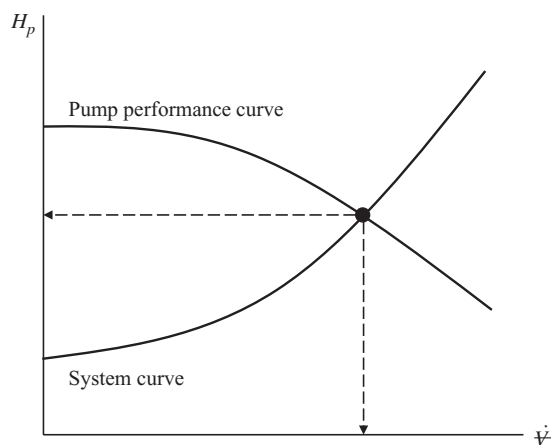


FIGURE 6.4
Graphical representation of the simulation.

compressors report the power draw by the compressor as a function of the evaporating and condensing temperatures in the refrigeration cycle,

$$\dot{W} = f(T_c, t_e) \tag{6.3}$$

As systems and component performance become more complex, the graphical solution is impossible to envision. The solution of the simulation set is in *n*-dimensional space where

n is the number of equations and unknowns. However, writing the simulation equations as shown in this section will lead to a set of equations that can be solved using software.

6.2.2 Modeling Thermal Energy System Equipment

In Section 6.2.1, data read from the pump performance curve were fit to a 2-dimensional function. However, many thermal system components behave three dimensionally. Consider a cooling tower being used to cool condenser water in a refrigeration plant. The water is cooled by direct contact with cool, moist atmospheric air. A sketch of a cooling tower is shown in Figure 6.5. Manufacturers of cooling towers often present cooling tower performance data showing the *outlet water temperature* (T_{out}) as a function of the *wet bulb temperature* (T_{wb}) of the entering ambient air and the *range* (R). The range is the difference between the inlet and outlet temperatures of the water. Table 6.6 shows an example of typical manufacturer's performance data for a cooling tower such as the one shown in Figure 6.5. Referring to Table 6.6; when the wet bulb temperature is 20°C and the range is 10°C, the temperature of the water leaving the tower is 25.9°C. Therefore, the temperature of the water entering the cooling tower is $25.9 + 10 = 35.9^\circ\text{C}$.

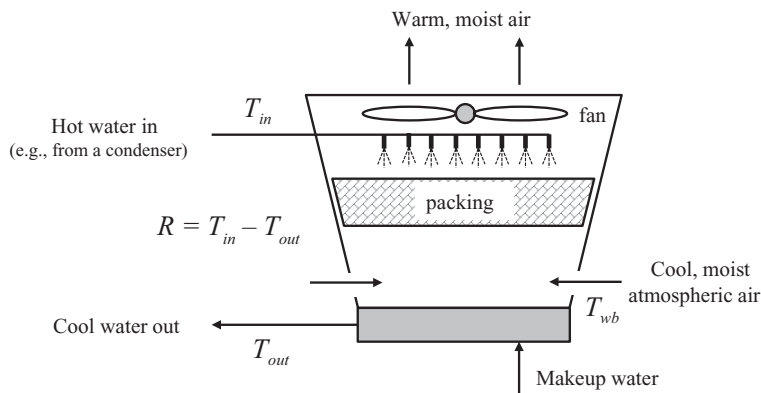


FIGURE 6.5
Cooling tower used for cooling water.

TABLE 6.6

Cooling Tower Performance Data: Outlet Water Temperature, T_{out} ($^\circ\text{C}$) as a Function of the Inlet Air Wet Blub temperature, T_{wb} ($^\circ\text{C}$), and the Range, $R = T_{in} - T_{out}$

Range,	Wet Bulb Temperature, T_{wb} ($^\circ\text{C}$)						
R ($^\circ\text{C}$)	20	21	22	23	24	25	26
10	25.90	26.42	26.92	27.50	28.11	28.72	29.40
12	26.24	26.69	27.20	27.76	28.34	28.96	29.62
14	26.62	27.04	27.54	28.05	28.64	29.23	29.91
16	27.00	27.43	27.89	28.40	28.94	29.56	30.20
18	27.45	27.81	28.30	28.77	29.29	29.88	30.54
20	27.92	28.29	28.70	29.18	29.69	30.27	30.89
22	28.40	28.73	29.14	29.60	30.10	30.70	31.30

Table 6.6 represents the real *performance* of the cooling tower. The data are 3-dimensional. Therefore, the mathematical representation of these data is an equation of the form,

$$T_{out} = f(R, T_{wb}) \quad (6.4)$$

In order to convert the numerical performance data from Table 6.6 into a mathematical equation, the functional form of the equation must be determined. Most thermal equipment behaves very predictably, and usually does not exhibit any strange fluctuating behavior. For cases like this, a simple polynomial function is usually sufficient. The order of the polynomial may be more difficult to determine. Most thermal components with 3-dimensional performance characteristics can be modeled with an equation of the form,

$$y(x, z) = a_1 + a_2x + a_3z + a_4xz + a_5x^2 + a_6z^2 + a_7x^2z + a_8xz^2 + a_9x^2z^2 \quad (6.5)$$

Using this functional form, the cooling tower outlet water temperature data in Table 6.6 can be represented by the following equation,

$$T_{out} = a_1 + a_2R + a_3T_{wb} + a_4RT_{wb} + a_5R^2 + a_6T_{wb}^2 + a_7R^2T_{wb} + a_8RT_{wb}^2 + a_9R^2T_{wb}^2 \quad (6.6)$$

Given this functional form, the task is to find the coefficients $a_1 - a_9$ that best represent the performance data. There are several methods that can be used to determine the coefficients. Two popular methods are the *exact fitting* method (Section 6.2.2.1) and the *least squares* method (Section 6.2.2.2).

6.2.2.1 Exact Fitting Method

The idea behind the exact fitting method is to select a set of data points and determine an equation that passes through these points *exactly*. The set of points may be all, or a subset of the manufacturer's performance data, depending on the functional form chosen to represent the data. When a data set is fit exactly, a performance equation is written for every data point. Therefore, if the equation chosen to represent the data has n terms, then n data points are needed to determine the unknown coefficients, a_1, a_2, \dots, a_n in the function. Using this reasoning and the functional form proposed in Equation 6.6, nine data points are needed to determine the coefficients a_1 through a_9 for the cooling tower example. Table 6.6 contains 49 data points. With some clever data selection, nine data points can be extracted from Table 6.6 that covers the full performance range. Table 6.7 shows a subset of the performance data of Table 6.6 that represent the full performance range.

TABLE 6.7

Cooling Tower Performance Data: Nine Selected Data Points Representing the Full Range of Performance Data in Table 6.6

R (°C)	T_{wb} (°C)		
	20	23	26
10	25.90	27.50	29.40
16	27.00	28.40	30.20
22	28.40	29.60	31.30

Using the data subset from Table 6.7, nine equations can be written using the functional form shown in Equation 6.6. The resulting set of nine equations has nine unknowns, the coefficients a_1 through a_9 ,

$$\begin{aligned}
 a_1 + 10a_2 + 20a_3 + 200a_4 + 100a_5 + 400a_6 + 2000a_7 + 4000a_8 + 40000a_9 &= 25.9 \\
 a_1 + 10a_2 + 23a_3 + 230a_4 + 100a_5 + 529a_6 + 2300a_7 + 5290a_8 + 52900a_9 &= 27.5 \\
 a_1 + 10a_2 + 26a_3 + 260a_4 + 100a_5 + 676a_6 + 2600a_7 + 6760a_8 + 67600a_9 &= 29.4 \\
 a_1 + 16a_2 + 20a_3 + 320a_4 + 256a_5 + 400a_6 + 5120a_7 + 6400a_8 + 102400a_9 &= 27.0 \\
 a_1 + 16a_2 + 23a_3 + 368a_4 + 256a_5 + 529a_6 + 5888a_7 + 8464a_8 + 135424a_9 &= 28.4 \\
 a_1 + 16a_2 + 26a_3 + 416a_4 + 256a_5 + 676a_6 + 6656a_7 + 10816a_8 + 173056a_9 &= 30.2 \\
 a_1 + 22a_2 + 20a_3 + 440a_4 + 484a_5 + 400a_6 + 9680a_7 + 8800a_8 + 193600a_9 &= 28.4 \\
 a_1 + 22a_2 + 23a_3 + 506a_4 + 484a_5 + 529a_6 + 11132a_7 + 11638a_8 + 256036a_9 &= 29.6 \\
 a_1 + 22a_2 + 26a_3 + 572a_4 + 484a_5 + 676a_6 + 12584a_7 + 14872a_8 + 327184a_9 &= 31.3
 \end{aligned} \tag{6.7}$$

In this set of equations, the units have purposely been left out for clarity. However, each number and coefficient must have a consistent set of units. This will be addressed after the coefficients are determined. Equation set 6.7 can be solved using computer software as a 9×9 system of equations or using matrix methods. Spreadsheet programs often include the ability to conduct matrix algebra. In matrix form, Equation set 6.7 can be written as,

$$[\mathbf{A}][\mathbf{a}] = [\mathbf{b}] \tag{6.8}$$

The $[\mathbf{A}]$ matrix is square ($n \times n$) and contains data. The $[\mathbf{b}]$ matrix is a column vector that also contains data. Solving Equation 6.8 for the column vector of unknown coefficients can be done by pre-multiplying each side of Equation 6.8 by the inverse of the $[\mathbf{A}]$ matrix,

$$[\mathbf{a}] = [\mathbf{A}]^{-1}[\mathbf{b}] \tag{6.9}$$

This matrix algebra allows for the calculation of the unknown coefficients in the column vector $[\mathbf{a}]$. For the cooling tower problem, the resulting coefficients of Equation 6.6 using this exact fitting technique are given in Table 6.8.

TABLE 6.8

Coefficients of Equation 6.6 Resulting from the Exact Fitting of the Nine Data Points in Table 6.7

Coefficient	Value and Units
a_1	$1.525185 \times 10^1 \text{ }^\circ\text{C}$
a_2	7.231481×10^{-1}
a_3	3.259259×10^{-1}
a_4	$-5.092593 \times 10^{-2} \text{ }^\circ\text{C}^{-1}$
a_5	$4.166667 \times 10^{-3} \text{ }^\circ\text{C}^{-1}$
a_6	$7.407407 \times 10^{-3} \text{ }^\circ\text{C}^{-1}$
a_7	$4.440892 \times 10^{-16} \text{ }^\circ\text{C}^{-2}$
a_8	$9.259259 \times 10^{-4} \text{ }^\circ\text{C}^{-2}$
a_9	$-3.469447 \times 10^{-18} \text{ }^\circ\text{C}^{-3}$

Notice that the units of each coefficient are included in Table 6.8. Since performance equations are often empirical (resulting from a curve fit to data) it is important to make certain that coefficients have units that are consistent with the data that were used. In this example, the coefficients must have units that make each term in Equation 6.6 dimensionally homogeneous. In other words, each term of Equation 6.6 must have units of °C.

Once the coefficients are determined, it is always a good idea to make certain that the resulting equation compares favorably to the equipment performance data. The best way to verify the equation is to compute either the deviation or the percent deviation between the data and the values computed from the equation. The deviation between the performance data and the calculated value is,

$$\Delta y = y_{data} - y_{calc} \quad (6.10)$$

The percent deviation is defined as,

$$\% \Delta y = 100 \left(\frac{\Delta y}{y_{data}} \right) = 100 \left(\frac{y_{data} - y_{calc}}{y_{data}} \right) \quad (6.11)$$

When the y -values become very small, the percent deviation calculation can be misleading. In those cases, the difference, Equation 6.10, is favored over the percent deviation, Equation 6.11. Using the coefficients from Table 6.8 in Equation 6.6, the percent deviations in water outlet temperature are calculated and displayed in the plot shown in Figure 6.6. A plot of this type is called a *deviation plot*.

In the deviation plot shown in Figure 6.6, the nine selected data points for the exact fit have a 0% deviation. The other data are within $\pm 0.1\%$ of the published performance data.

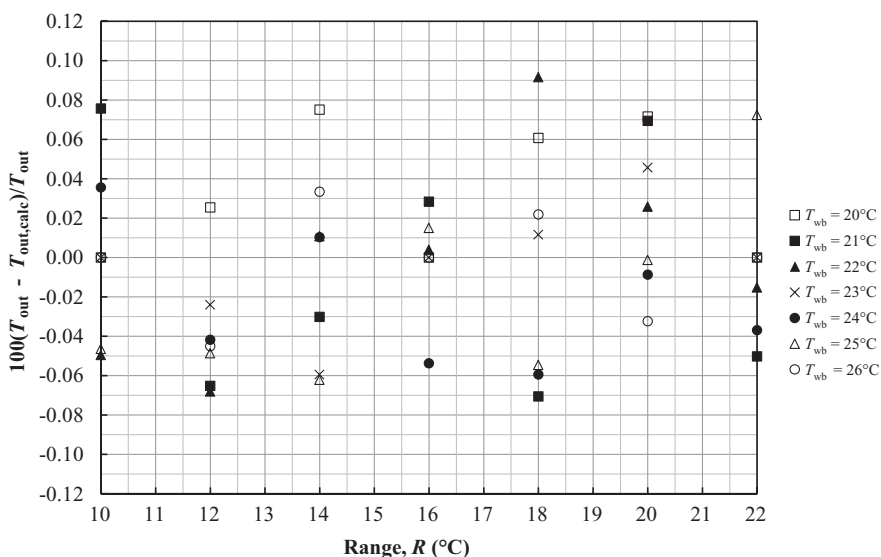


FIGURE 6.6

Deviation plot showing the percent deviation between water outlet temperatures calculated with Equation 6.6 and the manufacturer's performance data.

Based on the percent deviation analysis, the equation developed can be said to be accurate to within $\pm 0.1\%$ over the entire range of the manufacturer's performance data.

In Table 6.8, the a_7 and a_9 coefficients are several orders of magnitude smaller than the rest of the coefficients. Therefore, it appears that they may be insignificant in this equation. To test this thinking, the terms containing the coefficients a_7 and a_9 can be removed from Equation 6.6 to produce the following equation,

$$T_{out} = a_1 + a_2R + a_3T_{wb} + a_4RT_{wb} + a_5R^2 + a_6T_{wb}^2 + a_8RT_{wb}^2 \quad (6.12)$$

The coefficients of this equation are the same as Table 6.8 with the a_7 and a_9 coefficients eliminated. Table 6.9 shows the coefficients of Equation 6.12. To verify that the terms containing the a_7 and a_9 coefficients can be eliminated, the deviation plot can be recalculated using Equation 6.12. Figure 6.7 shows the resulting deviation plot. Notice that there is no perceivable difference between Figures 6.6 and 6.7. Therefore, the equation that represents the manufacturer's performance data for the cooling tower water outlet temperature can be represented by Equation 6.12 with the coefficients from Table 6.9.

The procedure for developing empirical equations from manufacturer's performance data was shown above using data for a cooling tower. However, the procedure is the same for a wide variety of common components in thermal energy systems. The exact fitting method is so popular and easy to implement that some manufacturers supply what is known as "9-point data" that can be used in an exact fitting application using Equation 6.5 to fit the data. For example, Table 6.10 shows a manufacturer's 9-point data for a refrigeration compressor.

From these data, four equations can be developed using the functional form of Equation 6.5; one for the capacity the compressor is able to provide (Btu/h), one for the power input to the compressor (Watts), one for the current input to the compressor (Amps), and one for

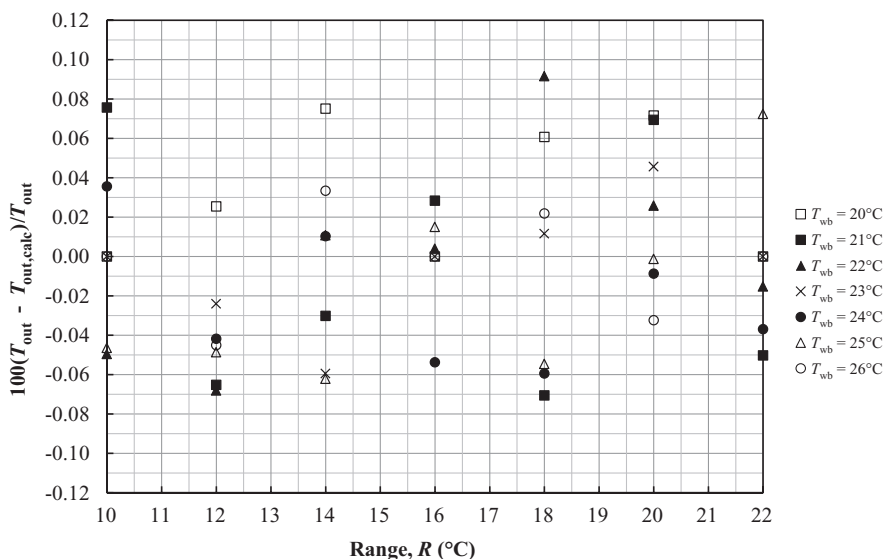


FIGURE 6.7

Deviation plot showing the percent deviation between water outlet temperatures calculated with Equation 6.12 and the manufacturer's performance data.

TABLE 6.9

Coefficients of Equation 6.12 Resulting from the Elimination of the a_7 and a_9 Terms from Equation 6.6

Coefficient	Value and Units
a_1	$1.525185 \times 10^1 \text{ }^\circ\text{C}$
a_2	7.231481×10^{-1}
a_3	3.259259×10^{-1}
a_4	$-5.092593 \times 10^{-2} \text{ }^\circ\text{C}^{-1}$
a_5	$4.166667 \times 10^{-3} \text{ }^\circ\text{C}^{-1}$
a_6	$7.407407 \times 10^{-3} \text{ }^\circ\text{C}^{-1}$
a_8	$9.259259 \times 10^{-4} \text{ }^\circ\text{C}^{-2}$

TABLE 6.10

An Example of 9-Point Data for a Refrigeration Compressor Supplied by a Manufacturer

Condensing Temperature	Evaporating Temperature			Units
	-30°F	-10°F	10°F	
130°F	500	1031	1864	Btu/h
	141	213	302	Watts
	2.07	2.51	3.16	Amps
	3.54	4.84	6.17	EER
120°F	542	1080	1923	Btu/h
	143	210	292	Watts
	2.08	2.49	3.08	Amps
	3.78	5.14	6.59	EER
110°F	583	1135	1958	Btu/h
	144	207	280	Watts
	2.09	2.47	2.99	Amps
	4.04	5.49	7.00	EER

the compressor's EER. (energy efficiency ratio). All of these parameters can be correlated as a function of the evaporating temperature and the condensing temperature.

$$\text{Btu/h, or Watts, or Amps, or EER} = f(T_{\text{evap}}, T_{\text{cond}}) \quad (6.13)$$

6.2.2.2 Method of Least Squares

Another method that is commonly used to fit component performance data is the method of least squares. In this method, the unknown coefficients are determined by performing an optimization. The goal is to *minimize* the sum of the squares of the residuals (SSQR) between the data and the correlated equation. In general, the function to be minimized is,

$$\text{SSQR}(a_1, a_2, \dots, a_n) = \sum_{i=1}^m (y_{i,\text{calc}} - y_{i,\text{data}})^2 \quad (6.14)$$

The function y_{calc} contains the unknown coefficients $a_1 - a_n$. The minimization is accomplished by taking the partial derivative of the SSQR function with respect to each unknown coefficient and setting it equal to zero,

$$\frac{\partial(SSQR)}{\partial a_k} = 0 \quad k = 1, n \quad (6.15)$$

The resulting set of equations is an $n \times n$ system that contains the n unknown coefficients. In addition, the n equations contain the component performance data.

Applying the method of least squares to the cooling tower example, we are interested in determining the coefficients of Equation 6.12 that minimize the sum of the squares of the residuals. Mathematically, this can be expressed as,

$$\min SSQR(a_1, a_2, a_3, a_4, a_5, a_6, a_8) = \sum_{i=1}^9 (T_{i,calc} - T_{i,data})^2 \quad (6.16)$$

Performing the partial differentiation and setting each derivative equal to zero results in the following set of equations:

$$\frac{\partial(SSQR)}{\partial a_1} = 2 \left\{ \sum_{i=1}^n \left[(a_1 + a_2 R_i + a_3 T_{wb,i} + a_4 R_i T_{wb,i} + a_5 R_i^2 + a_6 T_{wb,i}^2 + a_7 R_i T_{wb,i}^2) - T_i \right] \right\} = 0$$

$$\frac{\partial(SSQR)}{\partial a_2} = 2 \left\{ \sum_{i=1}^n \left[(a_1 + a_2 R_i + a_3 T_{wb,i} + a_4 R_i T_{wb,i} + a_5 R_i^2 + a_6 T_{wb,i}^2 + a_7 R_i T_{wb,i}^2) - T_i \right] R_i \right\} = 0$$

$$\frac{\partial(SSQR)}{\partial a_3} = 2 \left\{ \sum_{i=1}^n \left[(a_1 + a_2 R_i + a_3 T_{wb,i} + a_4 R_i T_{wb,i} + a_5 R_i^2 + a_6 T_{wb,i}^2 + a_7 R_i T_{wb,i}^2) - T_i \right] T_{wb,i} \right\} = 0$$

$$\frac{\partial(SSQR)}{\partial a_4} = 2 \left\{ \sum_{i=1}^n \left[(a_1 + a_2 R_i + a_3 T_{wb,i} + a_4 R_i T_{wb,i} + a_5 R_i^2 + a_6 T_{wb,i}^2 + a_7 R_i T_{wb,i}^2) - T_i \right] R_i T_{wb,i} \right\} = 0$$

$$\frac{\partial(SSQR)}{\partial a_5} = 2 \left\{ \sum_{i=1}^n \left[(a_1 + a_2 R_i + a_3 T_{wb,i} + a_4 R_i T_{wb,i} + a_5 R_i^2 + a_6 T_{wb,i}^2 + a_7 R_i T_{wb,i}^2) - T_i \right] R_i^2 \right\} = 0$$

$$\frac{\partial(SSQR)}{\partial a_6} = 2 \left\{ \sum_{i=1}^n \left[(a_1 + a_2 R_i + a_3 T_{wb,i} + a_4 R_i T_{wb,i} + a_5 R_i^2 + a_6 T_{wb,i}^2 + a_7 R_i T_{wb,i}^2) - T_i \right] T_{wb,i}^2 \right\} = 0$$

$$\frac{\partial(SSQR)}{\partial a_8} = 2 \left\{ \sum_{i=1}^n \left[(a_1 + a_2 R_i + a_3 T_{wb,i} + a_4 R_i T_{wb,i} + a_5 R_i^2 + a_6 T_{wb,i}^2 + a_7 R_i T_{wb,i}^2) - T_i \right] R_i T_{wb,i}^2 \right\} = 0$$

These equations are known as the *normal equations*. In this example, there are seven normal equations with seven unknowns (the coefficients a_1 through a_6 , and a_8). The equation set that results from the partial differentiation can be solved using equation solving software or matrix methods as described by Equations 6.8 and 6.9. Here, the matrix method will be demonstrated.

Rewriting these equations in matrix form $[A][a] = [b]$ results in,

$$\begin{bmatrix} \sum 1 & \sum R_i & \sum T_{wb,i} & \sum R_i T_{wb,i} & \sum R_i^2 & \sum T_{wb,i}^2 & \sum R_i T_{wb,i}^2 \\ \sum R_i & \sum R_i^2 & \sum R_i T_{wb,i} & \sum R_i^2 T_{wb,i} & \sum R_i^3 & \sum R_i T_{wb,i}^2 & \sum R_i^2 T_{wb,i}^2 \\ \sum T_{wb,i} & \sum R_i T_{wb,i} & \sum T_{wb,i}^2 & \sum R_i T_{wb,i}^2 & \sum R_i^2 T_{wb,i} & \sum T_{wb,i}^3 & \sum R_i T_{wb,i}^3 \\ \sum R_i T_{wb,i} & \sum R_i^2 T_{wb,i} & \sum R_i T_{wb,i}^2 & \sum R_i^2 T_{wb,i}^2 & \sum R_i^3 T_{wb,i} & \sum R_i T_{wb,i}^3 & \sum R_i^2 T_{wb,i}^3 \\ \sum R_i^2 & \sum R_i^3 & \sum R_i^2 T_{wb,i} & \sum R_i^3 T_{wb,i} & \sum R_i^4 & \sum R_i^2 T_{wb,i}^2 & \sum R_i^3 T_{wb,i}^2 \\ \sum T_{wb,i}^2 & \sum R_i T_{wb,i}^2 & \sum T_{wb,i}^3 & \sum R_i T_{wb,i}^3 & \sum R_i^2 T_{wb,i}^2 & \sum T_{wb,i}^4 & \sum R_i T_{wb,i}^4 \\ \sum R_i T_{wb,i}^2 & \sum R_i^2 T_{wb,i}^2 & \sum R_i T_{wb,i}^3 & \sum R_i^2 T_{wb,i}^3 & \sum R_i^3 T_{wb,i}^2 & \sum R_i T_{wb,i}^4 & \sum R_i^2 T_{wb,i}^4 \end{bmatrix} \begin{bmatrix} a_1 \\ a_2 \\ a_3 \\ a_4 \\ a_5 \\ a_6 \\ a_8 \end{bmatrix} = \begin{bmatrix} \sum T_i \\ \sum T_i R_i \\ \sum T_i T_{wb,i} \\ \sum T_i R_i T_{wb,i} \\ \sum T_i R_i^2 \\ \sum T_i T_{wb,i}^2 \\ \sum T_i R_i T_{wb,i}^2 \end{bmatrix}$$

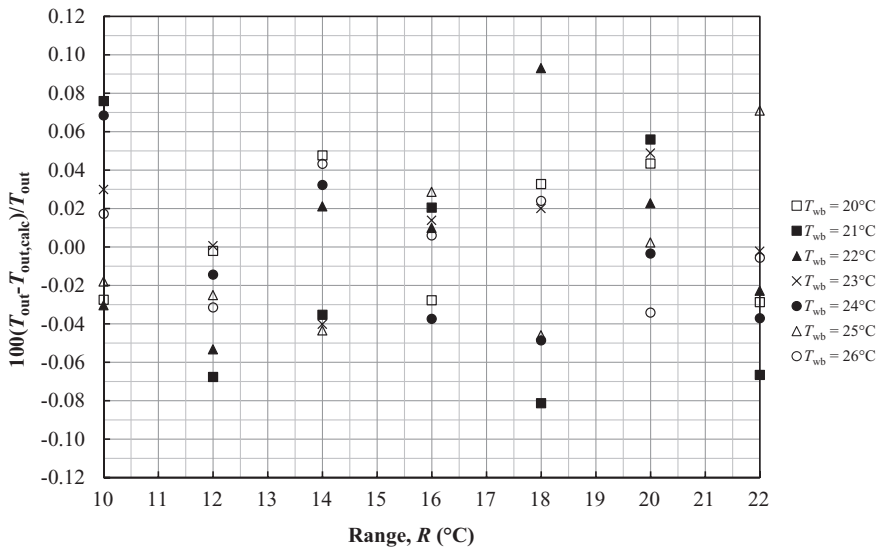
The summations in the $[A]$ matrix and $[b]$ vector can be calculated using the performance data shown in Table 6.6. The result is a matrix equation where the $[A]$ matrix and $[b]$ vector are made up completely of numbers, and the $[a]$ vector contains the unknown coefficients. When using the least squares technique, *all* of the performance data can be included in the analysis. This is an advantage over the exact fitting method. However, the tradeoff is that the calculation becomes more complex due to the additional burden of calculating all of the summation terms in the $[A]$ and $[b]$ matrices. While forming these matrices requires some calculation, it should be noted in this example that the $[A]$ matrix is symmetric. Therefore, only the diagonal and either the upper or lower triangle need to be calculated. Using the matrix algebra shown in Equation 6.9, the coefficients of Equation 6.12 can be found. Table 6.11 shows the resulting coefficients determined using all of the data in Table 6.6. Figure 6.8 shows the deviation plot comparing Equation 6.12 using the least squares coefficients from Table 6.11 to the manufacturer's performance data for the cooling tower. As Figure 6.8 indicates, all of the performance data is represented to within $\pm 0.10\%$. Even though the coefficients are different, the results are very similar to the exact fitting method.

The method of least squares has several advantages over exact fitting.

TABLE 6.11

Coefficients of Equation 6.12 Resulting from a Least Squares Analysis of the Cooling Tower Performance Data Presented in Table 6.6

Coefficient	Value and Units
a_1	$1.608918 \times 10^1 \text{ }^\circ\text{C}$
a_2	6.976531×10^{-1}
a_3	2.546769×10^{-1}
a_4	$-4.873724 \times 10^{-2} \text{ }^\circ\text{C}^{-1}$
a_5	$4.170918 \times 10^{-3} \text{ }^\circ\text{C}^{-1}$
a_6	$8.894558 \times 10^{-3} \text{ }^\circ\text{C}^{-1}$
a_8	$8.801020 \times 10^{-4} \text{ }^\circ\text{C}^{-2}$

**FIGURE 6.8**

Deviation plot showing the percent deviation between water outlet temperatures calculated with Equation 6.12 and the manufacturer's performance data.

- All of the performance data of the component being modeled can be used. This can be an advantage when it is difficult to find a representative subset of data for the exact fitting method.
- The functional form is not limited to a form like Equation 6.5. Virtually any functional form can be used when a minimization of the SSQR is being conducted.

6.2.3 Simulation Example: Modeling of an Air Conditioning System

Section 6.2.1 demonstrated how simulation techniques can be used to determine the operating point of a pump and pipe network. In this section, a more complex thermal energy system will be simulated; an air conditioning system. In this system, dry air at 28°C with a mass flow rate of 4 kg/s flows through a counter flow heat exchanger as shown in Figure 6.9. Cold water enters the other side of the heat exchanger at 6°C. The UA product for the heat exchanger is 7 kW/K. The suction pressure entering the pump is 80 kPa (gage) and the pressure of the water leaving the heat exchanger is 90 kPa (gage). The performance data for the pump have been correlated to the following function,

$$P_2 - P_1 = a_1 + a_2 \dot{m}_w^2 \quad (6.17)$$

In Equation 6.17, the constants are $a_1 = 120$ kPa, and $a_2 = -15.4$ kPa-s²/kg². These coefficients result in a pressure drop expressed in kPa. The mass flow rate of the water must be in kg/s in Equation 6.17.

The heat exchanger manufacturer has provided data that shows how the water pressure drop varies with the mass flow rate. These data have been correlated to the following empirical function,

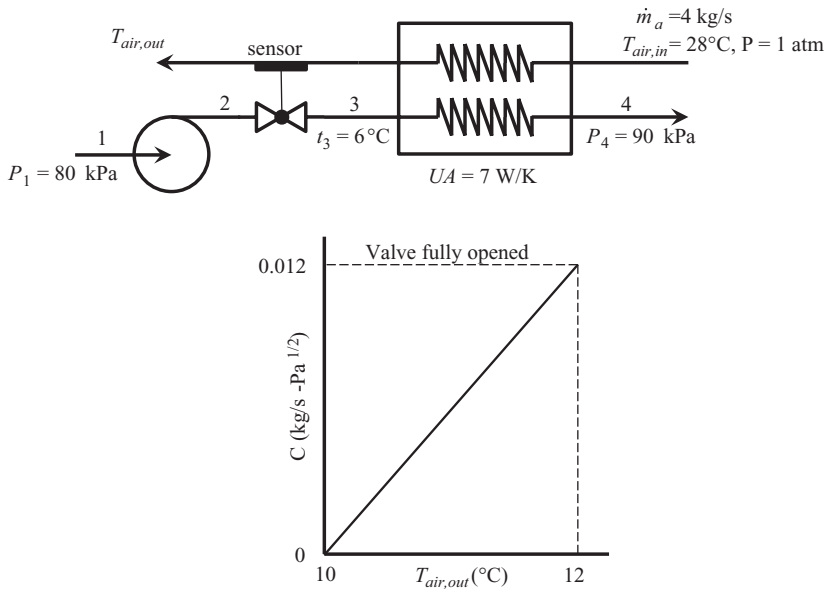


FIGURE 6.9
An air conditioning system.

$$P_3 - P_4 = a_3 \dot{m}_w^2 \quad (6.18)$$

In this equation, $a_3 = 9.26$ kPa \cdot s 2 /kg 2 and the water flow rate is in kg/s. The resulting pressure drop calculated with this equation is in kPa.

The air temperature leaving the heat exchanger is used to adjust the control valve (a globe valve). A sensor placed on the air outlet line senses the air temperature and adjusts the valve to maintain the air outlet temperature somewhere between 10°C and 12°C . The pressure drop through the valve is related to the water flow rate by the following empirical relationship,

$$\dot{m}_w = C \sqrt{P_2 - P_3} \quad (6.19)$$

In Equation 6.19, C has units of kg/s \cdot Pa $^{1/2}$. Therefore, the pressure drop in this equation must be expressed in Pa. C is not a constant. It is a function of the air outlet temperature. The valve manufacturer's performance data for the control valve is shown in the plot accompanying the system sketch in Figure 6.13. The linear relationship shown on this plot can be represented by,

$$C = a_4 T_{air,out} + a_5 \quad (6.20)$$

In Equation 6.20, $a_4 = 0.006$ kg/s \cdot Pa $^{1/2}\cdot$ $^\circ\text{C}$ and $a_5 = -0.06$ kg/s \cdot Pa $^{1/2}$.

The task is to simulate this thermal energy system and determine the water mass flow rate, the outlet temperatures of the fluids leaving the heat exchanger, the heat transfer rate

between the two fluids, the pressures on each side of the control valve, and the value of C for the control valve.

The component performance equations, extracted from manufacturer's performance data, are summarized above. In order to fully describe the air conditioning system's operating point, the counter flow heat exchanger needs to be modeled. Using the LMTD method, the heat exchanger model is given by,

$$\begin{aligned}\dot{Q}_{HX} &= \dot{m}_a c_{pa} (T_{air,in} - T_{air,out}) \\ \dot{Q}_{HX} &= \dot{m}_w c_{pw} (t_4 - t_3) \\ \dot{Q}_{HX} &= UA(LMTD)\end{aligned}\quad (6.21)$$

The LMTD is defined as,

$$LMTD = \frac{\Delta T_{out} - \Delta T_{in}}{\ln(\Delta T_{out} / \Delta T_{in})} \quad (6.22)$$

For a counter flow heat exchanger, the temperature differences are defined by,

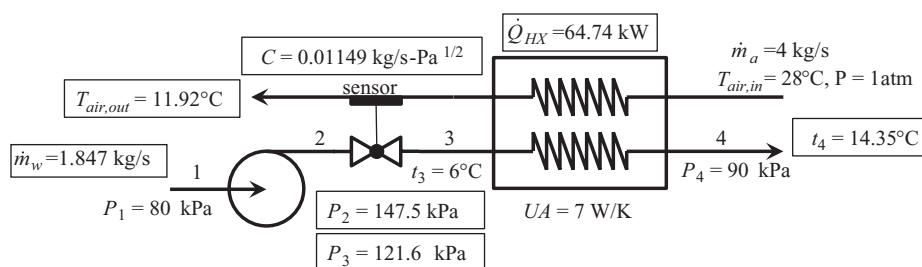
$$\begin{aligned}\Delta T_{in} &= T_{air,in} - t_4 \\ \Delta T_{out} &= T_{air,out} - t_3\end{aligned}\quad (6.23)$$

Using the strategy developed in Section 6.2.1, equations developed above can be formulated into a simulation as shown in Table 6.12. The simulation indicates that there are 14 unknowns. Among these unknowns are the desired operating parameters of the air conditioning system.

TABLE 6.12

Simulation Equations for the Air Conditioning System Shown in Figure 6.9

Component	Equation	New Unknowns	Equations \times Unknowns
Pump	$P_2 - P_1 = a_1 + a_2 \dot{m}_w^2$	P_2, \dot{m}_w	1×2
Cooling Coil	$P_3 - P_4 = a_3 \dot{m}_w^2$	P_3	2×3
	$\dot{Q}_{HX} = \dot{m}_a c_{pa} (T_{air,in} - T_{air,out})$	$\dot{Q}_{HX}, T_{air,out}, c_{pa}$	3×6
	$\dot{Q}_{HX} = \dot{m}_w c_{pw} (t_4 - t_3)$	t_4, c_{pw}	4×8
	$\dot{Q}_{HX} = UA(LMTD)$	$LMTD$	5×9
	$\Delta T_{out} = \Delta T_{in} \exp \left[\frac{\Delta T_{out} - \Delta T_{in}}{LMTD} \right]$	$\Delta T_{in}, \Delta T_{out}$	6×11
Valve	$\Delta T_{in} = T_{air,in} - t_4$		7×11
	$\Delta T_{out} = T_{air,out} - t_3$		8×11
	$\dot{m}_w = C \sqrt{P_2 - P_3}$	C	9×12
Properties	$C = a_4 T_{air,out} + a_5$		10×12
	$C_{pa} = c_p (T_{a,avg}, P_{atm})$	$T_{a,avg}$	11×13
	$T_{a,avg} = (T_{air,in} + T_{air,out}) / 2$		12×13
	$c_{pw} = c_p (t_{w,avg}, x = 0)$	$t_{w,avg}$	13×14
	$t_{w,avg} = (t_3 + t_4) / 2$		14×14

**FIGURE 6.10**

Operating conditions of the air conditioning system determined by solving the system simulation equations.

The results of the solution of the simulation equations are shown in Figure 6.10. In this figure, the calculated values from the simulation are shown in boxes. The simulation results tell the engineer much about the operating point of the thermal energy system. For example, with the equipment specified, a flow rate of 1.85 kg/s of water at 6°C is needed to cool the air to 11.9°C . In addition, the heat transfer rate between the water and air is 64.7 kW. The solution indicates that the control valve is operating in a nearly wide-opened condition as evidenced by the air outlet temperature and the value of the valve coefficient, C (see Figure 6.9).

6.2.4 Advantages and Pitfalls of Thermal Energy System Simulation

The advent of modern computing technology has significantly changed the way thermal energy system design and analysis is done. Modern software has allowed the engineer to completely model the thermal energy system to any level of complexity desired. The results of the simulation reveal the system operating conditions to a level of certainty consistent with the assumptions made in building the simulation equation set. The more complex the model becomes, the more realistic the results should be. However, the drawback with complex systems of equations is that they are more difficult to solve.

When using computer software, it is important to understand the numerical algorithm used by the software as it seeks a solution to the simulation equations. Any numerical solution of an $n \times n$ system of equations requires an initial guess for the unknown variables. This initial guess seeds the method. The engineer must be familiar with how these initial guesses are established with the software being used. In many cases, it is worth the time to do some quick calculations and determine reasonable values for some of the unknown variables and use them to seed the numerical algorithm. It can be very frustrating knowing that the simulation set is correct, but the numerical algorithm will not converge. Wise selection of the initial guesses can help alleviate this frustration.

Even with wise initial guesses for the seed of the numerical algorithm, the simulation set may still not converge. When this happens, the following actions are suggested.

- Take as much of the complexity out of the equation set as possible. For example, consider temporarily specifying an unknown variable and see if the equation set can be solved. This will reveal many things. If the answers seem reasonable, they can be used as initial guesses as the complexity is built back into the simulation.

- One of the more common errors in building a complex equation set is overlooking the unit analysis. The units *must* work out correctly. Make sure that *all* the equations in the simulation set are dimensionally homogeneous. Make sure that proper unit conversions are applied. An equation set that has inconsistent units is incorrect and unable to contribute to a meaningful solution for the simulation.
- When dealing with heat exchangers, there will be several temperature differences established. Make sure that these temperatures differences are consistent with the heat exchanger model as discussed in Chapter 5. For example, a heat exchanger with single phase fluids can be modeled using the LMTD method by the following equation set,

$$\begin{aligned}\dot{Q} &= \dot{m}_h c_{ph} (T_{hi} - T_{ho}) \\ \dot{Q} &= \dot{m}_c c_{pc} (t_{co} - t_{ci}) \\ \dot{Q} &= UA(LMTD)\end{aligned}\tag{6.24}$$

In this equation set, the subscript *h* represents the hot fluid, and *c* is the cold fluid. The temperature differences of the hot and cold fluids must be arranged such that the heat transfer rate has the same algebraic sign for both fluids. In addition, the temperature differences needed to define the LMTD need to be written consistent with the flow configuration of the heat exchanger (e.g., parallel or counter flow).

- Make sure that the performance equations developed for various components are being applied within the region of validity of the empirical equation that you are using. If an empirical equation is being used outside of the bounds of its validity, there is no guarantee that it represents the component's performance. While the equation may extrapolate smoothly, this does not mean it follows the component behavior. It is good practice to avoid any extrapolation of empirical equations. It is also good practice to avoid extrapolation of thermophysical property formulations used in the simulation.

These are just a few suggestions that may be helpful in arriving at the successful convergence of a complex simulation. While not very reassuring, it is also a good idea to adopt the credo of the Apollo 13 ground team; "Failure is not an option!"

6.3 Thermal Energy System Evaluation

Simulation is a first step to a much more design-oriented activity called *evaluation*. Once a simulation is developed and successfully solved, the engineer can use the simulation to conduct *parametric studies*. The result of a parametric study tells the engineer how the system will behave if one or more of its operating conditions are changed.

Consider the air conditioning system that was simulated in Section 6.2.3. Without changing the equipment, there are several meaningful evaluations that can be conducted once

the original simulation is complete. For example, what would happen to the outlet air temperature and the water flow rate if

- The inlet air temperature changes?
- The air flow rate changes?
- The water temperature entering the heat exchanger changes?

These three parametric studies can be conducted using computer software and the results plotted to gain a visual understanding of how the system will respond to the parametric variable(s). However, before embarking on these three parametric studies, special attention needs to be given to the water flow rate. In Section 6.2.3, the solution to the simulation revealed that the control valve was nearly wide opened. Since the control valve is operating over such a narrow range of outlet air temperatures, it is entirely possible that when the parameters discussed above are varied, the valve may end up in a wide opened state. There are several ways to accomplish this in a computer program using logic statements or developing routines that represent the physical behavior of the valve.

The parametric studies discussed in this section assume that one of the parameters in the system is varied while others remain constant. Figures 6.11, 6.12, and 6.13 show the results of the parametric studies cited above. These figures indicate that over the range of the parameter being varied, the control valve ends up in a wide opened position for all three scenarios. This is indicated by the mass flow rate of the water suddenly becoming constant. This behavior influences the outlet temperature of the air. The control valve in this system was obviously selected to maintain outlet air temperatures between 10°C and 12°C. The results of the parametric studies indicate operating limits to maintain the desired range of outlet temperatures. For example, Figure 6.12 reveals that if the air flow rate is higher than about 4.1 kg/s, the control valve ends up wide opened and the outlet air temperature increases. If the application requires strict control of the air outlet temperature, these parametric studies are of great importance to the engineer. If the application

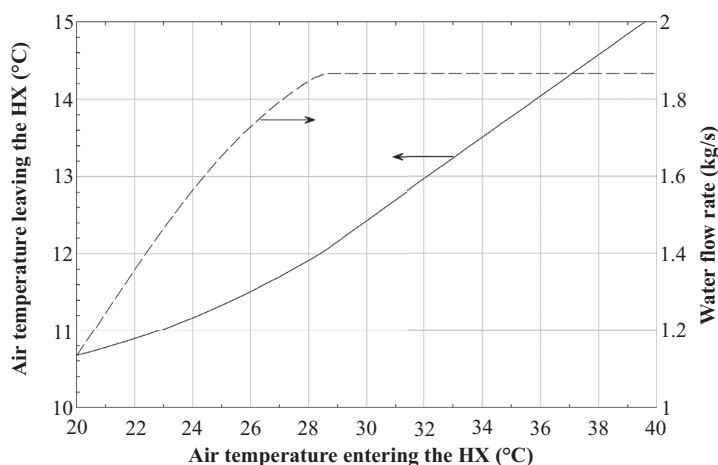
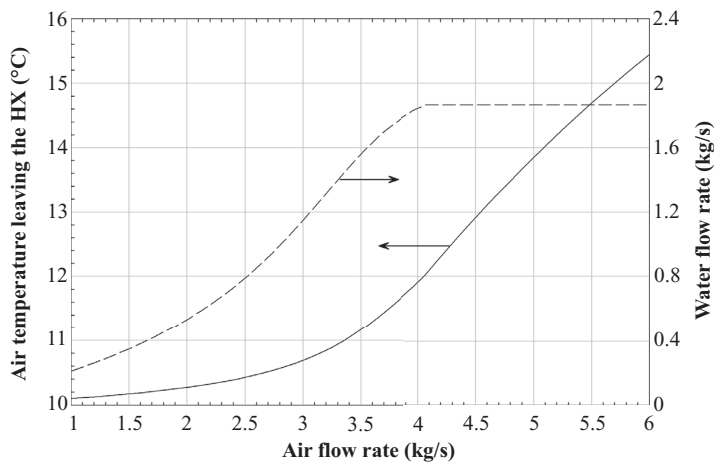
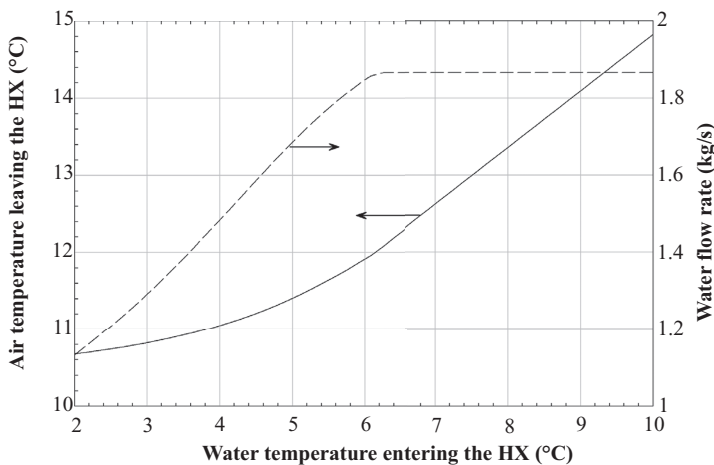


FIGURE 6.11

Outlet air temperature and water flow rate as a function of the inlet air temperature for the air conditioning system shown in Figure 6.9.

**FIGURE 6.12**

Outlet air temperature and water flow rate as a function of the air flow rate for the air conditioning system shown in Figure 6.9.

**FIGURE 6.13**

Outlet air temperature and water flow rate as a function of the water temperature entering the heat exchanger for the air conditioning system shown in Figure 6.9.

allows for the air outlet temperature to exceed 12°C, the parametric studies are still useful in predicting how the system will respond.

This section demonstrates that the evaluation of thermal energy systems requires a successful simulation. In some instances, the simulation equations need to be modified to allow for limiting behavior of equipment (e.g., the control valve in the air conditioning example). The evaluation allows the engineer to perform a series of “what if” scenarios to predict how the system will respond to changes in operating parameter(s).

6.4 Thermal Energy System Optimization

Optimization is the process of finding conditions that give a minimum or maximum value of a function. Optimization has always been an expected role of engineers. However, on small projects, the cost of engineering time may not justify an optimization analysis. As the system grows in complexity, the optimization of the system becomes more difficult. In these cases, it may be possible to consider optimization of subsystems and then combine these optimized subsystems.

In thermal system design, the engineer is interested in minimizing or maximizing a system parameter. For example, minimizing total system cost, minimizing system irreversibility, minimizing pressure drop, maximizing profit, or maximizing thermal efficiency. Component modeling and system simulation are preliminary steps to optimizing thermal energy systems.

6.4.1 Mathematical Statement of Optimization

Optimization is the process of finding conditions that result in the minimum or maximum value of a function. In the purest mathematical sense, optimization refers to the *minimization* of a function. A function can always be maximized by minimizing the negative of the function. The function minimized is called the *objective function*. Sometimes the objective function is referred to as the *cost function* since it is often written to represent total system cost. The variables involved in the objective function are called the *design variables*.

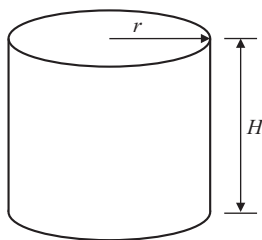
The formal mathematical statement of optimization is written as:

$$\begin{aligned}
 &\text{minimize} && y(x_1, x_2, \dots, x_n) \\
 &\text{subject to} && \Phi_i(x_1, x_2, \dots, x_n) = 0 \quad i = 1, 2, \dots, p \\
 &&& \Psi_j(x_1, x_2, \dots, x_n) \leq 0 \quad j = 1, 2, \dots, q
 \end{aligned} \tag{6.25}$$

The Φ_i functions are known as *equality constraints* and the Ψ_j functions are called *inequality constraints*. The variables x_1 through x_n are known as the *design variables*. In the optimization problem, the values being sought are the design variables x_1 through x_n that minimize the objective function. Notice that the objective function and the constraints are functions of only design variables.

Example 6.1

Formulate the optimization statement required to design a minimum cost cylindrical storage tank closed at both ends to contain a specified volume. The cost of the tank depends directly on the area of the material used to construct the tank.

**FIGURE E6.1**

Cylindrical storage tank primary dimensions.

Solution

Since the cost is directly proportional to the area of the material used, the objective function is written to represent the total surface area of the enclosed cylindrical tank. Figure E6.1 shows a sketch of the tank and the primary dimensions, r , the tank radius, and H , the tank height.

The total surface area of the tank is given by,

$$A = 2\pi rH + 2\pi r^2$$

The design variables are the radius of the tank, r , and the height of the tank, H . There is one equality constraint in this problem; the tank must have a specified volume. Therefore,

$$V = \pi r^2 H$$

Using these relationships, the formal mathematical statement of this optimization problem can be written in the form of Equation 6.25 as,

$$\begin{aligned} \text{minimize} \quad & A(r, H) = 2\pi rH + 2\pi r^2 \\ \text{subject to} \quad & \Phi(r, H) = \pi r^2 H - V = 0 \end{aligned}$$

Notice that the constraint is written such that it is exactly equal to zero. The constraint equation also contains the design variables r and H . The tank volume is not a variable. It is a specified constant.

6.4.2 Closed-Form Solution of an Optimization Problem

Consider the cylindrical tank problem in Example 6.1. The formal optimization statement was found to be,

$$\begin{aligned} \text{minimize} \quad & A(r, H) = 2\pi rH + 2\pi r^2 \\ \text{subject to} \quad & \Phi(r, H) = \pi r^2 H - V = 0 \end{aligned} \tag{6.26}$$

This problem can be converted to an *unconstrained optimization* by using the single constraint to eliminate one of the design variables from the problem. For example, in Equation set 6.26, the constraint can be solved for the tank height, H ,

$$H = \frac{V}{\pi r^2} \quad (6.27)$$

Equation 6.27 can be substituted into the objective function to give,

$$A = 2\pi \left(\frac{V}{\pi r} + r^2 \right) \quad (6.28)$$

Notice that Equation 6.28 is only a function of one variable, r . The minimum value of the tank surface area, A , can be found by taking the derivative of A with respect to r and setting it equal to zero. This procedure results in,

$$r^* = \left(\frac{V}{2\pi} \right)^{1/3} \quad (6.29)$$

In Equation 6.29, an asterisk is used to indicate an optimum value. This is consistent nomenclature found in optimization literature. Once r^* is found, the value of H^* can be found from Equation 6.27,

$$H^* = \frac{V}{\pi(r^*)^2} = \frac{V}{\pi} \left(\frac{2\pi}{V} \right)^{2/3} = \left(\frac{4V}{\pi} \right)^{1/3} \quad (6.30)$$

Notice that the *second derivative* of A with respect to r is,

$$\frac{d^2 A}{dr^2} = \frac{2V}{\pi r^3} + r > 0 \quad (6.31)$$

Equation 6.31 is an indication that the values of r^* and H^* produce a *minimum* value of A since the second derivative is positive.

The solution of unconstrained optimization problems using the method shown here is easily done for simple objective functions and equality constraints. However, as the optimization problem becomes more complex and multidimensional, the method may be more difficult to implement. Although the mathematics is sound, the implementation may be too complex. The next section presents a mathematical theorem that can be applied to more complex optimization problems.

6.4.3 Method of Lagrange Multipliers

As optimization problems become multidimensional and more complex, they cannot be solved in a simple, closed-form solution as shown in Section 6.4.2. However, a method

exists that can be used to solve more complex optimization problems with equality constraints. The method is known as the *method of Lagrange multipliers*. Implementation of this method relies on the *Lagrange multiplier theorem*.

Consider the problem of minimizing a multivariate objective function $f(\mathbf{x})$ subject to equality constraint functions $\Phi_i(\mathbf{x})$ where $i = 1, 2, \dots, p$. Let \mathbf{x}^* be a solution that represents a local minimum for the problem. For these conditions, the Lagrange multiplier theorem states that there exists Lagrange multipliers, λ_j where $j = 1, 2, \dots, p$ such that,

$$\nabla L(\mathbf{x}^*, \lambda) = 0 \quad (6.32)$$

In Equation 6.32, the function, L , is called the *Lagrange function* or the *Lagrangian*, and is defined as,

$$L(\mathbf{x}, \lambda) = f(\mathbf{x}) + \sum_{j=1}^p \lambda_j \Phi_j(\mathbf{x}) \quad (6.33)$$

To demonstrate how this theorem can be applied to an optimization problem, consider the cylindrical tank design problem from Example 6.1. The optimization problem was to minimize the area (and thus the cost) of a cylindrical storage tank. The formal optimization problem is given by Equation set 6.26. To solve the optimization problem using the method of Lagrange multipliers, the Lagrange function needs to be constructed. From the Lagrange multiplier theorem, the Lagrange function for this problem is,

$$L = 2\pi rH + 2\pi r^2 + \lambda(\pi r^2 H - V) \quad (6.34)$$

Notice that since there is only one equality constraint, there is one Lagrange multiplier. Applying the Lagrange multiplier theorem, the gradient of the Lagrange function is found and set equal to zero,

$$\begin{aligned} \nabla L(r, H, \lambda) = 0 \quad \rightarrow \quad & \frac{\partial L}{\partial r} = 2\pi H + 4\pi r + 2\pi\lambda rH = 0 \\ & \frac{\partial L}{\partial H} = 2\pi r + \lambda\pi r^2 = 0 \\ & \frac{\partial L}{\partial \lambda} = \pi r^2 H - V = 0 \end{aligned} \quad (6.35)$$

These three equations can be simplified to,

$$\begin{aligned} H + 2r + \lambda rH &= 0 \\ 2r + \lambda r^2 &= 0 \\ \pi r^2 H - V &= 0 \end{aligned} \quad (6.36)$$

From the second equation in Equation set 6.36, it can be seen that,

$$\lambda = -\frac{2}{r^*} \quad (6.37)$$

Substituting Equation 6.37 into the first equation in Equation set 6.36 gives,

$$H^* = 2r^* \quad (6.38)$$

From the third equation in Equation set 6.36,

$$H^* = \frac{V}{\pi(r^*)^2} \quad (6.39)$$

Substituting Equation 6.39 into Equation 6.38 and solving for r gives,

$$r^* = \left(\frac{V}{2\pi} \right)^{1/3} \quad (6.40)$$

Finally, substituting Equation 6.40 into Equation 6.38 gives,

$$H^* = 2r^* = 2 \left(\frac{V}{2\pi} \right)^{1/3} = \left(\frac{4V}{\pi} \right)^{1/3} \quad (6.41)$$

Notice that Equations 6.40 and 6.41 are the same results as developed in Equations 6.29 and 6.30. In addition to the optimum solution of r^* and H^* , the Lagrange multiplier can also be found. From Equation 6.37,

$$\lambda = -\frac{2}{r^*} = -2 \left(\frac{2\pi}{V} \right)^{1/3} = -\left(\frac{16\pi}{V} \right)^{1/3} \quad (6.42)$$

The Lagrange multiplier is useful in what is known as *post-optimality studies* which will be discussed later in this section. The application of the Lagrange multiplier theorem allows for the solution of complex optimization problems that contain several design variables and equality constraints.

Example 6.2

A shell and tube heat exchanger is being designed. In order to transfer the required amount of heat between the fluids in the heat exchanger, it has been determined that 100 m of tubing is required. The pitch of the tubes is such that 200 tubes can fit in a cross-sectional area of 1 m² inside the shell of the heat exchanger. The cost of 100 m of tubing is \$2,120. The cost of the shell is a function of the shell diameter and tube length given by the empirical relationship,

$$C_{shell} = 2590 D_s^{2.5} L_{HX}$$

The heat exchanger will take up space on the floor which represents an additional cost. The cost of floor space has been determined to be,

$$C_{\text{floor}} = 750D_s L_{HX}$$

In these cost equations, the shell diameter, D_s , and heat exchanger length, L_{HX} , are in meters. Determine the heat exchanger length and shell diameter that minimize the initial cost of the heat exchanger. What is the minimum initial cost?

Solution

The first step is to form the objective function. Based on the information given, the total initial cost of the heat exchanger is made up of the cost of the tubes, shell, and floor space. Therefore, the objective function to be minimized is,

$$\begin{aligned} C_{HX} &= 2120 + C_{\text{shell}} + C_{\text{floor}} \\ C_{HX} &= 2120 + 2590D_s^{2.5}L_{HX} + 750D_s L_{HX} \end{aligned}$$

There is one constraint in this problem; the number of tubes in the shell is limited by the pitch that only allows for 200 tubes per m^2 of cross sectional area of the shell. This can be written as,

$$\begin{aligned} \frac{\pi D_s^2}{4} L_{HX} \left(200 \frac{\text{tubes}}{\text{m}^2} \right) &= 100 \text{ m} \\ 50\pi D_s^2 L_{HX} &= 100 \end{aligned}$$

Therefore, the formal optimization statement is,

$$\begin{aligned} \text{minimize} \quad & C_{HX} = 2120 + 2590D_s^{2.5}L_{HX} + 750D_s L_{HX} \\ \text{subject to} \quad & 50\pi D_s^2 L_{HX} - 100 = 0 \end{aligned}$$

The design variables are the shell diameter, D_s , and the length of the heat exchanger, L_{HX} . Using the method of Lagrange multipliers, the Lagrange function is,

$$L = 2120 + 2590D_s^{2.5}L_{HX} + 750D_s L_{HX} + \lambda(50\pi D_s^2 L_{HX} - 100)$$

The gradient of the Lagrange function is,

$$\nabla L = \begin{cases} \frac{\partial L}{\partial D_s} = 6475D_s^{1.5}L_{HX} + 750L_{HX} + 100\lambda\pi D_s L_{HX} \\ \frac{\partial L}{\partial L_{HX}} = 2590D_s^{2.5} + 750D_s + 50\lambda\pi D_s^2 \\ \frac{\partial L}{\partial \lambda} = 50\pi D_s^2 L_{HX} - 100 \end{cases}$$

Setting this gradient equal to zero results in three equations with three unknowns; the two design variables, D_s and L_{HX} , and the Lagrange multiplier, λ ,

$$\begin{aligned} 6475D_s^{1.5}L_{HX} + 750L_{HX} + 100\lambda\pi D_s L_{HX} &= 0 \\ 2590D_s^{2.5} + 750D_s + 50\lambda\pi D_s^2 &= 0 \\ 50\pi D_s^2 L_{HX} - 100 &= 0 \end{aligned}$$

This set of equations can be solved using computer software. The solution is,

$$\begin{aligned} D_s &= \underline{0.69840 \text{ m}} \\ L_{HX} &= \underline{1.3187 \text{ m}} \\ \lambda &= -20.616 \end{aligned}$$

The minimum initial cost associated with this solution can be determined using the values of the design variables in the objective function,

$$C_{HX} = \underline{\$4,181.59}$$

The shell diameter calculated is not a standard size. The next larger standard shell size should be specified for the heat exchanger (29-inch). The resulting cost will be slightly higher than the optimum value.

In order to apply the method of Lagrange multipliers, the mathematical optimization statement must be formulated as shown in Equation set 6.26. Only design variables are involved in the objective function and constraint(s). This formalism is necessary to determine the Lagrange function. In Example 6.2, the design variables are easily incorporated into the objective function and constraint. However, there may be situations where some analysis is required to write the objective function and constraint(s) as functions of only design variables. This is demonstrated in Example 6.3.

Example 6.3

Circular ducts are being used to deliver air to different rooms in an air conditioning system as shown in Figure E6.3 (top view). A total volumetric flow rate of 6,000 cfm

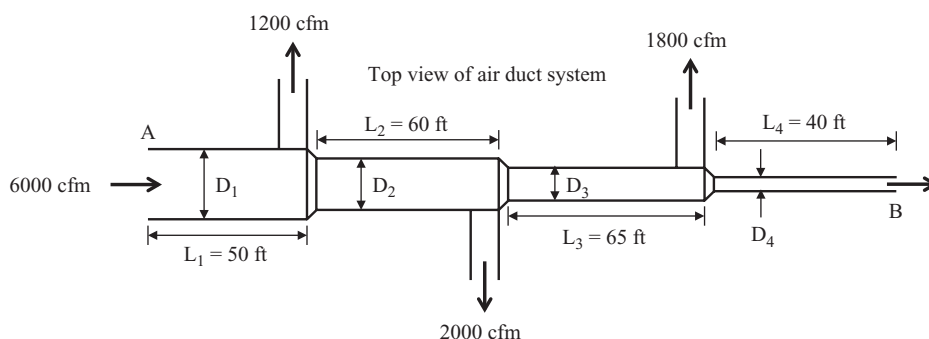


FIGURE E6.3
Circular duct air distribution system.

enters the main duct. As air is drawn off the main duct and delivered to different rooms, the diameter of the main duct is reduced to keep the velocity of the air at an appropriate speed for proper distribution into the other rooms. A total of 850 ft² of sheet metal is available to build the main duct. It can be assumed that the friction factor in the duct is constant at $f = 0.02$. The specific weight of the air can also be assumed to be constant at 0.075 lbf/ft³. The lengths of the main duct sections (50 ft, 60 ft, 65 ft, and 40 ft) are fixed by the construction of the space where the duct is to be installed. Using the method of Lagrange multipliers, determine the diameters of the main air duct, D_1 , D_2 , D_3 , and D_4 such that the pressure drop between points A and B is minimized.

Solution

The first step is to construct the objective function. The goal is to minimize the pressure drop from point A to B in the system. Therefore, the objective function will be of the form,

$$\min \rightarrow \Delta P_{AB} = \Delta P_1 + \Delta P_2 + \Delta P_3 + \Delta P_4$$

The design variables are the four duct diameters, D_1 , D_2 , D_3 , and D_4 . However, the objective function does not contain these variables. Further analysis is required to write the objective function in terms of the design variables.

The pressure drops in the individual sections of the main duct can be determined from the conservation of energy applied between the beginning and end of each section. Neglecting minor losses due to the decreasing diameter from section to section, the individual pressure drops can be written as,

$$\begin{aligned} \frac{\Delta P_{AB}}{\gamma} &= \frac{\Delta P_1}{\gamma} + \frac{\Delta P_2}{\gamma} + \frac{\Delta P_3}{\gamma} + \frac{\Delta P_4}{\gamma} \\ \frac{\Delta P_{AB}}{\gamma} &= f \frac{L_1}{D_1} \frac{V_1^2}{2g} + f \frac{L_2}{D_2} \frac{V_2^2}{2g} + f \frac{L_3}{D_3} \frac{V_3^2}{2g} + f \frac{L_4}{D_4} \frac{V_4^2}{2g} \end{aligned}$$

The velocity of the air in each section of the main duct is related to the diameter of the duct and the volumetric flow rate by,

$$V = \frac{\dot{V}}{A} = \frac{4\dot{V}}{\pi D^2} \quad \therefore \quad V^2 = \frac{16\dot{V}^2}{\pi^2 D^4}$$

Using this expression, the individual pressure losses can be written as,

$$\Delta P = \gamma f \frac{L}{D} \frac{V^2}{2g} = \left(\frac{8\gamma f L \dot{V}^2}{\pi^2 g} \right) \frac{1}{D^5} = \frac{K}{D^5}$$

In this equation, K is a constant value that can be calculated for each section of the main duct. Therefore, the objective function can be written as,

$$\min \rightarrow \Delta P_{AB} = \frac{K_1}{D_1^5} + \frac{K_2}{D_2^5} + \frac{K_3}{D_3^5} + \frac{K_4}{D_4^5}$$

This form of the objective function contains the four *design variables*, D_1 , D_2 , D_3 , and D_4 .

There is one equality constraint in this problem; the total number of square feet of sheet metal available to construct the main duct. This constraint can be written as,

$$\pi D_1 L_1 + \pi D_2 L_2 + \pi D_3 L_3 + \pi D_4 L_4 = 850 \text{ ft}^2$$

In order to use the Lagrange multiplier theorem, the optimization problem must be written in its formal mathematical form specified by the Equation set 6.26. Therefore, the formal mathematical statement of the optimization problem is,

$$\begin{aligned} \text{minimize} \quad & \Delta P_{AB} = \frac{K_1}{D_1^5} + \frac{K_2}{D_2^5} + \frac{K_3}{D_3^5} + \frac{K_4}{D_4^5} \\ \text{subject to} \quad & \pi D_1 L_1 + \pi D_2 L_2 + \pi D_3 L_3 + \pi D_4 L_4 - 850 \text{ ft}^2 = 0 \end{aligned}$$

The Lagrange Function can now be formed according to Equation 6.33,

$$L(D_1, D_2, D_3, D_4, \lambda) = \frac{K_1}{D_1^5} + \frac{K_2}{D_2^5} + \frac{K_3}{D_3^5} + \frac{K_4}{D_4^5} + \lambda(\pi D_1 L_1 + \pi D_2 L_2 + \pi D_3 L_3 + \pi D_4 L_4 - 850 \text{ ft}^2)$$

Setting the gradient of the Lagrange function equal to zero results in,

$$\begin{aligned} \frac{\partial L}{\partial D_1} &= -\frac{5K_1}{D_1^6} + \lambda \pi L_1 = 0 \\ \frac{\partial L}{\partial D_2} &= -\frac{5K_2}{D_2^6} + \lambda \pi L_2 = 0 \\ \frac{\partial L}{\partial D_3} &= -\frac{5K_3}{D_3^6} + \lambda \pi L_3 = 0 \\ \frac{\partial L}{\partial D_4} &= -\frac{5K_4}{D_4^6} + \lambda \pi L_4 = 0 \\ \frac{\partial L}{\partial \lambda} &= \pi D_1 L_1 + \pi D_2 L_2 + \pi D_3 L_3 + \pi D_4 L_4 - 850 \text{ ft}^2 = 0 \end{aligned}$$

This is a system of five equations with five unknowns. The solution to these equations results in the diameters D_1 , D_2 , D_3 , and D_4 along with the Lagrange multiplier, λ . Once these diameters are known, the minimum pressure drop can be calculated from the objective function.

The solution to this set of equations results in the following values for the design variables and the Lagrange multiplier,

$$\begin{aligned} D_1 &= 1.5189 \text{ ft} \\ D_2 &= 1.4100 \text{ ft} \\ D_3 &= 1.1782 \text{ ft} \\ D_4 &= 0.83589 \text{ ft} \\ \lambda &= 0.048978 \end{aligned}$$

Substituting the calculated design variables into the objective function reveals that the minimum pressure drop from A to B is

$$\Delta P_{AB} = 8.3262 \frac{\text{lbf}}{\text{ft}^2}$$

As demonstrated Examples 6.2 and 6.3, the method of Lagrange multipliers is fairly easy to implement for multivariate optimization problems with equality constraints. The method ultimately results in a system of n equations and n unknowns representing the gradient of the Lagrange function. The next section will address the significance of the Lagrange multipliers.

6.4.3.1 Significance of the Lagrange Multipliers

The Lagrange multipliers are determined as a consequence of solving the equations resulting from setting the gradient of the Lagrange function to zero. In Examples 6.2 and 6.3, the Lagrange multipliers were determined, but their units were conveniently omitted. The Lagrange multipliers, however, must have units that make the Lagrange function dimensionally homogeneous.

In Example 6.2, the Lagrange function was written as,

$$L = 2120 + 2590D_s^{2.5}L_{HX} + 750D_sL_{HX} + \lambda(50\pi D_s^2L_{HX} - 100) \quad (6.43)$$

The units of each term in this function are [\$]. Therefore, the Lagrange multiplier, λ , must have units of [\$/\$m]. The Lagrange multiplier in Example 6.2 is correctly expressed as $\lambda = -20.616$ \$/\$m. But the question still remains; “What do these units mean?”

Each Lagrange multiplier in an optimization problem is associated with a constraint. In Example 6.2, the Lagrange multiplier is associated with the constraint pertaining to the total length of tubing available to form the tube bundle inside the shell of the heat exchanger. Recall that the units of the Lagrange multiplier for Example 6.2 is [\$/\$m]. This indicates that the value of the Lagrange multiplier has some relationship between the heat exchanger initial cost (objective function) and the length of tubing available (constraint). To reveal this relationship, consider Example 6.2 again with 101 m of tubing available instead of 100. Solving the optimization problem for this case results in, $D_s = 0.69480$ m, $L_{HX} = 1.3319$ m, which results in a minimized heat exchanger cost of $C_{HX} = \$4,202.20$. By making an additional 1 m of tubing available, the heat exchanger cost increases by $\$4,202.20 - \$4,181.59 = \$20.61$. Referring back to Example 6.2, the Lagrange multiplier was determined to be $\lambda = -20.616$ \$/\$m. This exercise reveals the significance of the Lagrange multiplier; it indicates the change in the minimized objective function per unit change in the constraint,

$$\frac{\partial f^*}{\partial \Phi_k} = -\lambda_k \quad (6.44)$$

This is particularly helpful in the case of an optimization with multiple constraints. The constraint with the largest absolute value of the Lagrange multiplier will have the largest impact on the minimized objective function.

6.4.4 Formulation and Solution of Optimization Problems Using Software

Optimization of a thermal energy system can often be much more complex than Examples 6.2 and 6.3. For most thermal energy system optimization problems, the development of the objective function is usually straightforward. The difficulty comes in the formulation of the constraints. In most cases, the constraints are related to the system simulation. In other words, an objective function can be minimized for a thermal system, but the optimum configuration of the system must obey the physical behavior of the system (i.e., the simulation). Due to the complexity of such problems, the solutions are determined numerically using software. Most computing software includes the capability to find minimum or maximum conditions subject to constraints. There are many different types of optimization algorithms. The method used to find optimum solutions depends on the software.

Whatever method is used in the software, it is most likely based on determining a search vector and searching along that vector until a minimum value is found, then repeating the process until closure. Often, determination of the search vector is achieved by considering the gradient of the objective function at a point. Knowing that the gradient vector points in the direction of increasing objective function value helps establish the proper search direction (in this case, in the direction opposite of the gradient vector). Once the search direction is established, a search technique is used to find the minimum value along the search direction. This process is demonstrated with a 3-dimensional function, $y(x,z)$, as shown in Figure 6.14.

The function shown in Figure 6.14 is a three-dimensional “bowl” with the minimum point identified as $y^*(x^*, z^*)$. An initial guess of the optimum point is required. At that point, the gradient vector of the objective function is computed, ∇y_1 , which establishes the first search direction. The minimum value of the objective function is determined along the first search direction using a numerical method such as Newton’s method. At this

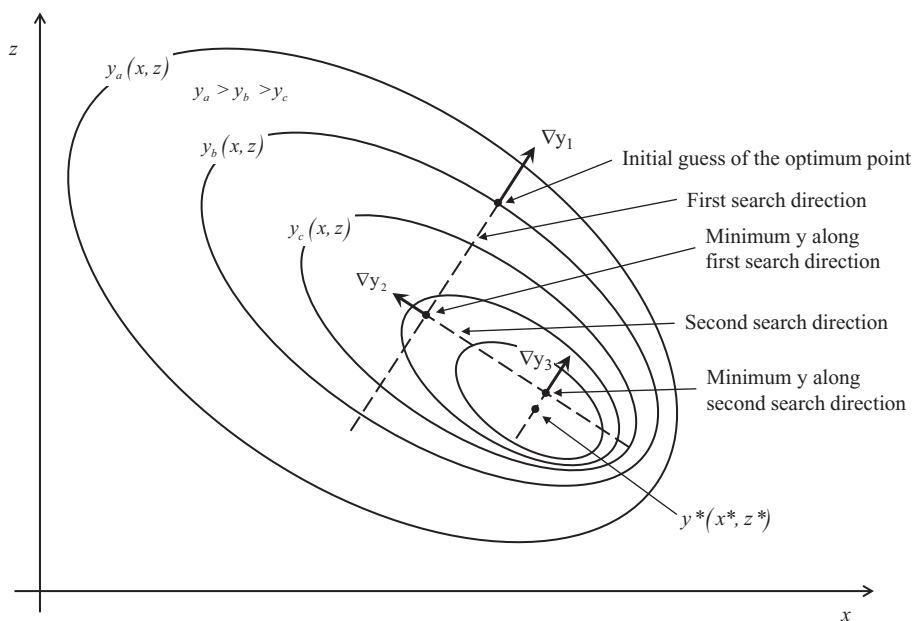


FIGURE 6.14

A 3-dimensional function showing a search algorithm.

new minimum, a second search direction is established by calculating the gradient of the objective function, ∇y_2 . The second search direction is traversed until a new minimum is found, and the process repeats until the minimum of the objective function is found.

There are different gradient-type algorithms, depending on how the search direction is established and how the minimum is found along the search direction. Numerical algorithms that incorporate a gradient-type search determine the derivatives of the gradient vector numerically. Some software allows for the selection of how these numerical derivatives are calculated (i.e., backward, central, or forward differences). Most numerical algorithms also allow the user to specify convergence tolerances as well. The user should have an understanding of the numerical method used and the options available to tweak the algorithm.

Figure 6.14 shows that an initial guess is required to seed the algorithm. In the case of the 3-dimensional function shown, the two design variables must be guessed. Often, users of numerical optimization algorithms can experience significant frustration due to non-convergence. One possible cause of non-convergence is due to the algorithm being seeded with poor initial guesses for the design variables. In complex optimization problems with many design variables, it is very helpful to predict final values for design variables and use them as the seed to start the optimization algorithm. As an example, consider a fluid flowing through a heat exchanger. If the inlet temperature of the fluid is known, and the heat is being transferred from the fluid, then the outlet temperature of the fluid must be smaller than the inlet temperature. So, when specifying the initial value for the outlet temperature, specify it to be something less than the inlet temperature. There are many instances where very sensible engineering guesses can be made for design variables. Using sensible and physically correct initial values for any of the unknown design variables will go a long way in successful convergence of the optimization algorithm.

Once a solution has been found to an optimization problem, it is helpful to update the initial guesses for the design variables to the solution and run the optimization again. It may even be helpful to change the optimization algorithm if the software allows the user to choose from several optimization algorithms. If the same solution can be found using several different methods, then the user can be confident that the correct solution has indeed been found. The message here is that it may take *several* runs of an optimization algorithm to ensure that the final solution is the correct optimum solution.

Section 6.4 is not meant to be an all-encompassing treatise on optimization. There are complete courses and books that deal with this subject. It is a mathematically rigorous topic. Mathematics provides the framework for the development of the numerical algorithms that are available in various software packages. The goal in any of these numerical methods is to find the global minimum of the objective function quickly in the most computationally efficient way.

Problems

Modeling Thermal Energy System Equipment

- 6.1 Develop an empirical equation that represents the pump head (ft) as a function of capacity (gpm) for a Bell & Gossett Series e-80 $2 \times 2 \times 7B$ pump with a $6\frac{1}{2}$ -inch impeller operating at 1750 rpm. The equation should be valid from 40 to 160 gpm. Estimate the percent accuracy in the calculated pump head from the correlated equation by developing a deviation plot.

- 6.2 Develop an empirical equation that represents the pump efficiency (%) as a function of capacity (gpm) for a Bell & Gossett Series e-80 $2 \times 2 \times 7$ B pump with a 6½-inch impeller operating at 1750 rpm. The equation should be valid from 40 to 160 gpm. Estimate the percent accuracy in the calculated pump efficiency from the correlated equation by developing a deviation plot.
- 6.3 Develop an empirical equation that represents the net positive suction head required (m) as a function of capacity (m^3/h) for a Bell & Gossett Series e-1531 2.5BB pump with a 9-inch impeller operating at 3550 rpm. The equation should be valid from 50 to 180 m^3/h . Estimate the percent accuracy in the calculated NPSHr from the correlated equation by developing a deviation plot.
- 6.4 Use the exact fitting technique to develop an empirical equation for the capacity (Btu/h) of the refrigeration compressor described by the 9-point performance data shown in Table 6.10. What is the range of validity of this equation?
- 6.5 Use the exact fitting technique to develop an empirical equation for the power draw (W) of the refrigeration compressor described by the 9-point performance data shown in Table 6.10. What is the range of validity of this equation?
- 6.6 Use the exact fitting technique to develop an empirical equation for the current draw (amps) of the refrigeration compressor described by the 9-point performance data shown in Table 6.10. What is the range of validity of this equation?
- 6.7 Use the exact fitting technique to develop an empirical equation for the E.E.R. of the refrigeration compressor described by the 9-point performance data shown in Table 6.10. What is the range of validity of this equation?
- 6.8 A vortex tube is a device that splits a flow of air into two streams, one hot and one cold, without any moving parts. If you are not familiar with vortex tubes, read about them online. They are sometimes used in industrial applications for spot cooling. The cooling performance data for a particular vortex tube are shown in Table P6.8. This table shows the temperature difference between the incoming air flow and the cold air leaving the tube as a function of the inlet pressure of the air into the tube and the mass flow rate of the cold air stream, represented as a percent of the incoming flow. Use the exact fitting technique to develop an empirical equation that can be used to predict the temperature difference between the inlet air and the cold exit air over the range of the data provided. Estimate the accuracy of the empirical equation by developing a deviation plot that shows all of the available data.

TABLE P6.8Temperature Drop ($^{\circ}\text{R}$) of the Cold Air in a Vortex Tube

Inlet Pressure (psig)	Cold Fraction (%)				
	30	40	50	60	70
40	85.0	80.0	73.0	62.5	51.5
60	100.0	93.0	84.0	73.0	59.5
80	110.0	102.0	92.0	80.0	65.5
100	118.0	110.0	99.0	86.0	70.0
120	124.0	116.0	104.0	90.5	74.0

- 6.9 Solve Problem 6.8 using the method of least squares.
- 6.10 Manufacturer's data for the mass flow rate of Refrigerant-22 flowing through a compressor is shown in Table P6.10 as a function of the evaporating and condensing temperatures. Use the method of least squares to determine an empirical equation that can be used to predict the R22 mass flow rate as a function of the evaporating and condensing temperatures. Estimate the accuracy of the equation by generating a deviation plot that shows all the data in Table P6.10.
- 6.11 The manufacturer of a refrigeration compressor reports the compressor power draw and evaporating capacity as a function of the evaporating and condensing temperatures in the refrigeration cycle. The data for the compressor are shown in Tables P6.11A and 6.11B. Using these data, determine the COP_C for a refrigeration system using this compressor at evaporating and condensing temperatures of

TABLE P6.10

Mass Flow Rate (lbm/h) of R22 Flowing through a Refrigeration Compressor

Condensing Temperature (°F)	Evaporating Temperature (°F)				
	-25	-20	-15	-10	-5
80	617	715	824	946	1084
90	594	693	800	919	1052
100	567	667	775	892	1022
110	531	636	746	863	991
120	486	597	711	831	959

TABLE P6.11A

Power Draw (kW) of a Refrigeration Compressor

Condensing Temperature (°F)	Evaporating Temperature (°F)				
	-25	-20	-15	-10	-5
80	8.00	8.46	8.88	9.29	9.73
90	8.38	8.96	9.47	9.94	10.41
100	8.61	9.35	9.99	10.56	11.08
110	8.64	9.59	10.40	11.10	11.72
120	8.44	9.63	10.64	11.51	12.27

TABLE P6.11B

Refrigeration Evaporator Capacity (Btu/h) of a Refrigeration Compressor

Condensing Temperature (°F)	Evaporating Temperature (°F)				
	-25	-20	-15	-10	-5
80	50,925	58,918	67,765	77,663	88,807
90	47,222	54,946	63,349	72,628	82,997
100	43,254	50,838	58,927	67,716	77,402
110	38,886	46,460	54,364	62,794	71,946
120	33,984	41,678	49,527	57,728	66,475

−12°F and 92.5°F, respectively. Develop the required equation(s) using either the exact fitting method or the method of least squares.

Thermal Energy System Simulation and Evaluation

- 6.12 A Bell & Gossett Series e-80 2x2x7B inline pump with a 6½ inch impeller operating at 1750 rpm is being used to transfer water at 60°F between two large tanks as shown in Figure P6.12. All fittings are standard and the globe valve is fully opened.
- Write and solve a simulation for this system and determine its operating point; head (ft), capacity (gpm), and pump efficiency.
 - Investigate how the operating parameters are affected by the pump speed over the range $1500 \leq \text{rpm} \leq 3500$ in 100 rpm increments. Develop two plots. In the first plot show the head (ft) vs. capacity (gpm). In the second plot, show the efficiency vs. capacity (gpm). For both plots, show the operating points with a symbol. Label several of the symbols with the corresponding pump operating speed (rpm).
- 6.13 A centrifugal pump and a gear pump are operating in series in a closed loop to deliver a 20% ethylene glycol solution at an average temperature of 10°C through a long pipe system. In the capacity range up to $2 \text{ m}^3/\text{s}$, the pump performance equations expressed in terms of pressure increase as a function of capacity are given by,

$$\text{centrifugal pump: } \Delta P = 50 + 0.2\dot{V} - 10\dot{V}^2$$

$$\text{gear pump: } \Delta P = 30 - 10\dot{V}$$

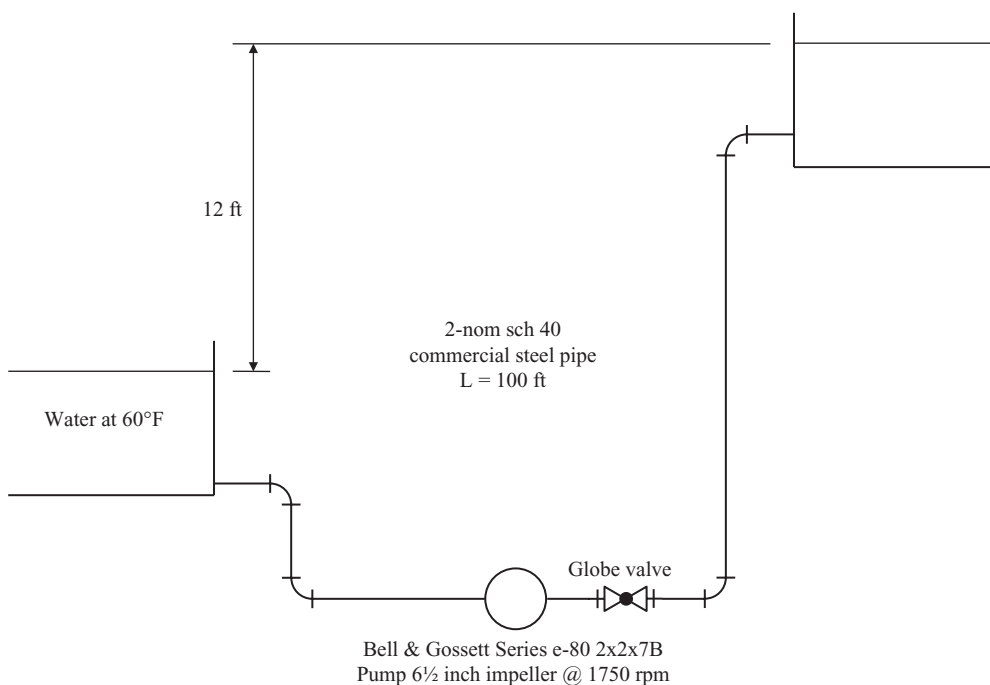


FIGURE P6.12

A pump and pipe system used to transfer water between two large tanks.

A detailed friction analysis reveals that the pressure drop through the closed loop system is given by,

$$\Delta P = 20\dot{V}^2$$

In the equations above, the pressure changes are in kPa and the capacity is in m^3/s .

- On the same plot, show the system curve, the performance curves for each pump, and the performance curve of the combined series pumps in terms of head (m) as a function of capacity (m^3/s). Draw the curves from 0 to 2 m^3/s .
 - Write a simulation of the system and determine its operating point.
 - If the economic velocity of the ethylene glycol solution for this system is 2.9 m/s, specify the standard schedule steel pipe required for this application.
- 6.14 A liquid nitrogen cooler is shown in Figure P6.14. The goal of this system is to cool the liquid nitrogen flow at State 1. This is accomplished by diverting a portion of the liquid through an expansion valve. When the liquid passes through the valve, it flashes into saturated liquid and saturated vapor in the flash tank. The saturated vapor is drawn off the top and the saturated liquid is used to cool the liquid flow using an in-tank heat exchanger. For the conditions shown in Figure P6.14, determine the mass flow rate (lbm/hr) and temperature ($^{\circ}\text{F}$) of the liquid nitrogen at State 4, and the mass flow rate (lbm/hr) of the saturated vapor at State 3.
- 6.15 One way to liquefy a gas is to flash it through a valve. However, this requires that the inlet conditions to the valve be at a state where an expansion will cause the gas to flash into a saturated mixture of liquid and vapor. Consider a situation where helium gas is at 10 bar and the desired pressure of the liquid is 1 bar. In order to produce liquid helium, the inlet state to the throttling process must lie between the two states identified as *a* and *b* on the *P-h* diagram shown in Figure P6.15A. For an inlet pressure of 10 bar, this temperature range is $2.53 \text{ K} \leq T \leq 7.60 \text{ K}$ for helium.

One possible way to achieve this low temperature at the entrance to the valve is shown in Figure P6.15B. This system is known as a liquefaction system.

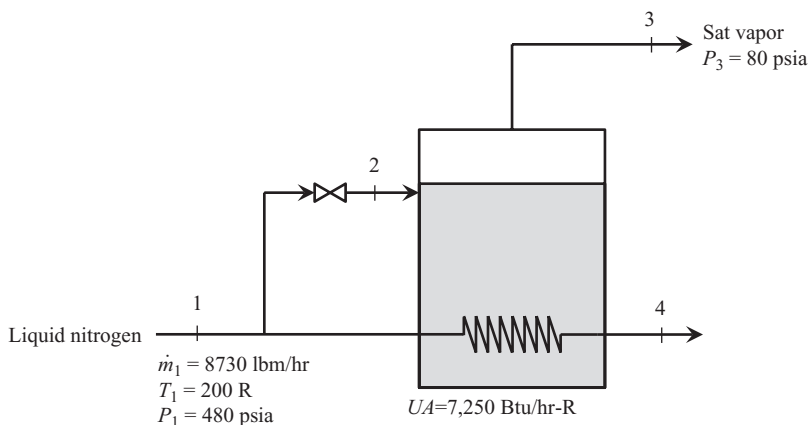
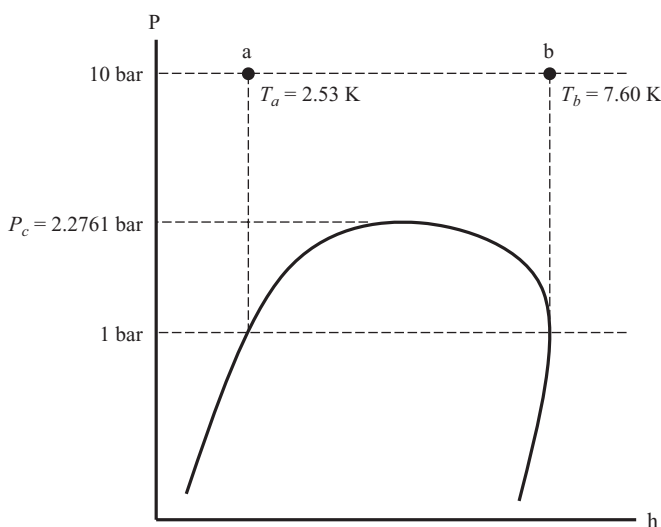
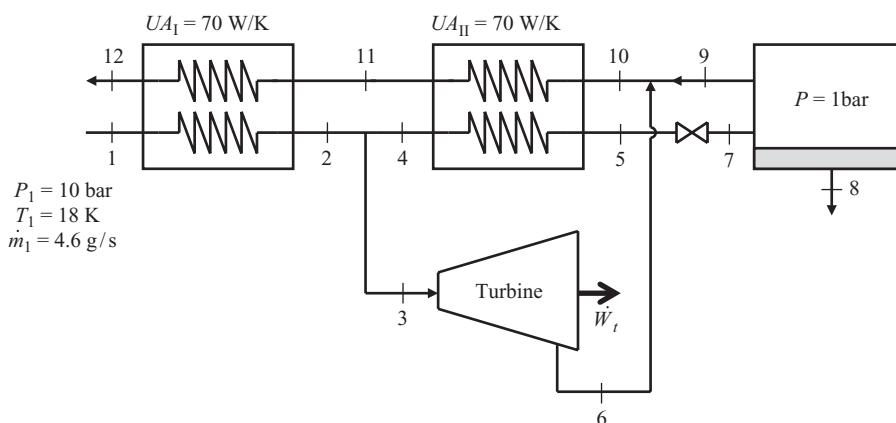


FIGURE P6.14

Liquid nitrogen cooler.

**FIGURE P6.15A**

Pressure-enthalpy diagram for helium.

**FIGURE P6.15B**

Helium liquefaction system.

In this system, the helium gas is supplied at 10 bar, 18 K at a flow rate of 4.6 g/s. This gas is cooled further using two heat exchangers. The cooling of the gas is accomplished by mixing the cold saturated vapor leaving the separator and the cold gas at the exhaust of a small turbine operating between the high and low pressures of the system. The UA product of each heat exchanger is 70 W/K. The separator operates at a pressure of 1 bar. Manufacturer's performance data for the turbine relate the turbine temperatures and mass flow rate with two empirical equations,

$$T_6 = a_1 + a_2 T_3$$

$$\dot{m} = b_1 + b_2 T_3$$

In these turbine performance equations $a_1 = 4.6$ K, $a_2 = 0.1$, $b_1 = 3.75$ g/s, and $b_2 = -0.125$ g/s-K. Write and solve a simulation for this helium liquefaction system and determine the,

- Unknown temperatures in the cycle (K)
- Heat transfer rate in each heat exchanger (W)
- Liquid helium mass flow rate leaving the separator (g/s)
- Power delivered by the turbine (W)

Evaluate the system to determine how the inlet helium flow rate at State 2 influences the liquid helium production rate and the turbine output power. Plot the following parameters as a function of the inlet helium mass flow rate for the range $3.4 \leq \dot{m}_1 \leq 5.0$ g/s,

- Liquid helium mass flow rate leaving the separator (g/s)
 - Quality of the helium leaving the valve at State 7
 - Turbine output power (W)
- 6.16 Process steam boilers often incorporate a continuous blowdown scheme to eliminate impurities that can accumulate over time. One way to accomplish this is shown in Figure P6.16A. In this system, the boiler is operating at 300 psia. Saturated vapor steam leaves the boiler as the high-pressure process steam flow at a flow rate of 1,000,000 lbm/hr. Saturated liquid water, containing the impurities, exits the boiler at 300 gpm. The dirty water is then flashed into a separator through a valve. The separator pressure is 65 psia. Saturated vapor leaves the separator as the low-pressure process steam flow. The high pressure and low-pressure process steam flows make their way through the plant and eventually

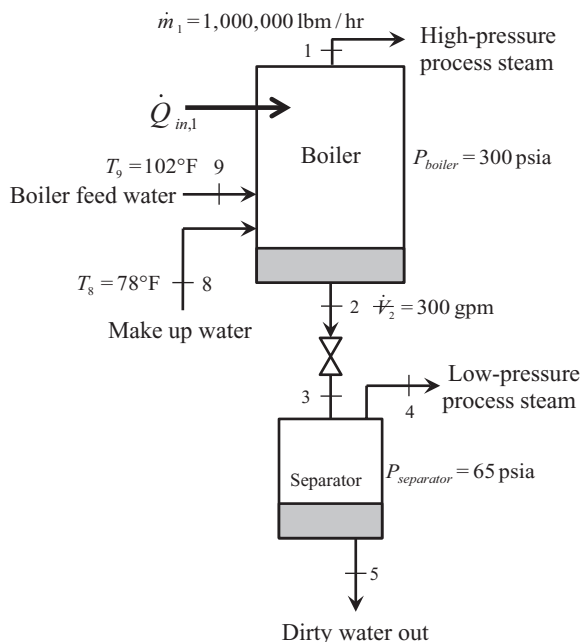


FIGURE P6.16A
Boiler blowdown system.

condense, combine and return to the boiler as a liquid boiler feed water at 102°F. The saturated liquid at the separator exit is discarded. In order to maintain steady operation, makeup water must replace the discarded dirty water. This makeup water enters the boiler at 78°F. Simulate this system and determine the

- Mass flow rate (lbm/hr) of the low-pressure process steam
- Volumetric flow rate (gpm) of the discarded dirty water
- Temperature of the discarded dirty water
- Boiler heat transfer rate required to maintain continuous, steady state operation (Btu/hr)

The result of your simulation should reveal that the temperature of the discarded dirty water is quite hot. It is proposed that this hot, dirty water be used to preheat the makeup water going into the boiler in an attempt to reduce fuel cost. This can be accomplished by adding a heat exchanger as shown in Figure P6.16B. It is reasonable to treat the heat exchanger as a counter flow regenerative heat exchanger. The mass flow rates of the water on each side are the same (the makeup water must replace the discarded dirty water). However, the heat capacities of the water on each side of the heat exchanger are slightly different. In reality, this difference is very small. Therefore, assuming that the thermal capacitance rates of each flow are equal is a reasonable approximation. A heat capacity value of 1.01 Btu/lbm-R is a reasonable estimate of

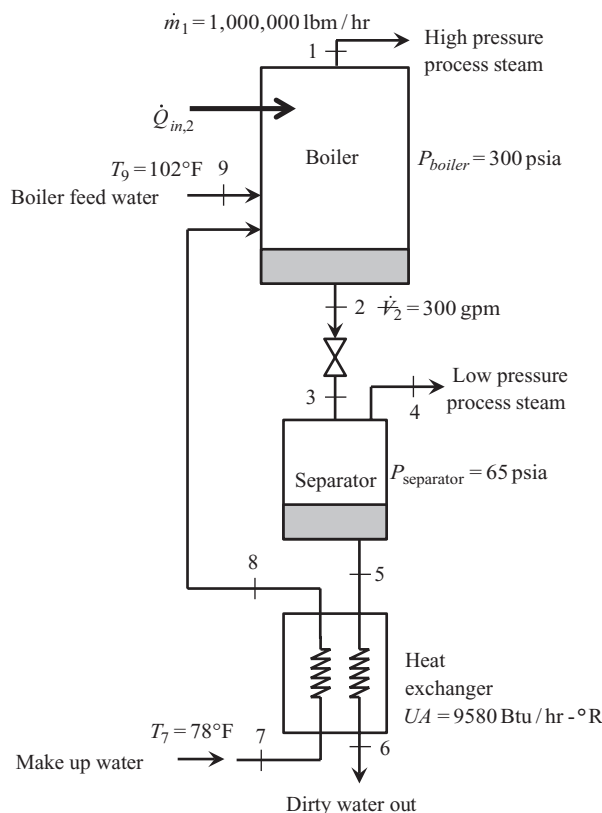


FIGURE P6.16B

Boiler blowdown system with regenerative heat exchanger.

c_p for the water passing through the heat exchanger. The UA product of the heat exchanger is 9,580 Btu/hr-R. Simulate this modified system and determine the:

- e. Temperature of the discarded dirty water
- f. Temperature rise of the makeup water as it flows through the heat exchanger
- g. Boiler heat transfer rate required to maintain continuous, steady state operation (Btu/hr)

This particular system operates continuously throughout the year. The heat transfer rate is provided by the combustion of natural gas that costs \$0.70/therm. (A therm is 100,000 Btu). Determine:

- h. The annual energy cost savings realized by incorporating the regenerative heat exchanger as shown in Figure P6.16B.
- i. If management requires a minimum rate of return of 25%, and the heat exchanger is expected to have a 50-year life, how much money can be spent on the heat exchanger? Does the heat exchanger appear to be a viable investment?

Investigate the effect of the separator pressure on the operating parameters of the boiler blowdown system described in Figure P6.16B. For this evaluation, vary the separator pressure from 20 psia to 100 psia and plot the following curves:

- j. Annual energy cost savings as a function of the separator pressure
- k. Mass flow rate of the low-pressure process steam (lbm/hr) and the volumetric flow rate of the dirty water (gpm) leaving the separator as a function of the separator pressure.
- l. Comment on the results of the parametric studies from Parts (j) and (k)

Optimization of Thermal Energy Systems

- 6.17 The initial cost of a thermal energy system is \$650,000. The uniform annual income derived from the system, before maintenance costs, is \$215,000. There are no maintenance costs in the first year. However, in the second year of operation, maintenance costs are \$12,000. The maintenance costs increase by \$12,000 in each subsequent year. The expected rate of return from this system is 15%. The goal of this problem is to determine the life of the system that maximizes the uniform annual profit.

- a. Formulate the objective function for this problem. There should be one design variable; the life of the thermal energy system, n .
- b. What is the break-even point for this scenario (i.e., at what time is the uniform annual profit zero?)

To solve the unconstrained problem requires the derivative of the objective function with respect to n . However, this derivative can be quite complex to determine since n is involved in economic interest factors. As an alternative, your instructor may assign Part (c), Part (d), or both:

- c. Plot the uniform annual profit vs. n and estimate the value of n that maximizes the uniform annual profit. It will be difficult to select a thermal energy system that has an expected life *exactly* equal to the optimum value. Is it better for the thermal energy system to have a longer life or shorter life compared to the optimum value? Explain your reasoning.
- d. Use optimization software to determine the value of n .

- 6.18 A retrofit HVAC project includes installing rectangular air ducts in braced floor joists. The dimensions of the joist and floor joist are shown in Figure P6.18. The duct is to be designed such that the pressure drop through the duct is minimized. This occurs when the duct has the maximum cross-sectional area.
- Write the formal optimization statement in the form of Equation set 6.26.
 - Solve the optimization problem by combining the constraint with the objective function and solving the resulting unconstrained problem.
 - Solve the optimization problem using the method of Lagrange multipliers.
- 6.19 Hot water is being transported in an insulated type K copper tube as shown in Figure P6.19. Due to space restrictions in the installation, the outside diameter of the insulation is to be minimized. The annual cost of the insulated pipe is limited to \$80,000. The annual cost of the insulated pipe has two components; the cost of the heat loss, C_{heat} , and the cost of the pumping energy required to move the fluid through the tube, C_{pump} . The expressions for these costs are,

$$C_{heat} = \frac{a_1}{t_{ins}} \quad \text{and} \quad C_{pump} = \frac{a_2}{ID_t^5}$$

In these equations, $a_1 = 3000$ \$-m and $a_2 = 16$ \$-m⁵.

- Write the formal optimization statement in the form of Equation set 6.26.
- Solve the optimization problem using the method of Lagrange multipliers and determine the tube diameter (m) and insulation thickness (m) that results in the minimum outside diameter of the insulation.

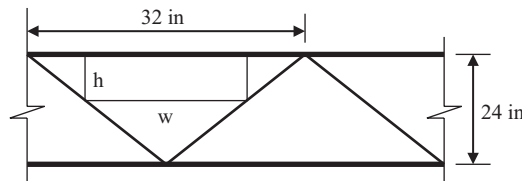


FIGURE P6.18

Air duct in a retrofit HVAC project.

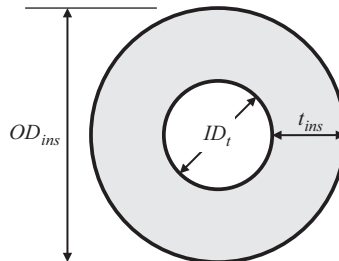


FIGURE P6.19

Insulated copper tube transporting hot water.

The solution of the optimization problem from Part (b) results in the inside tube diameter and insulation thickness that minimize the outside diameter of the insulation. However, the copper tube inside diameter calculated in Part (b) is likely not a standard size. The next part of this problem deals with specifying the *standard* copper tube diameter for this application. One possibility is to consider the optimum outside insulation diameter calculated in Part (b) as a condition that must be met. For this case,

- c. Use the copper tube data in Appendix D to specify the standard tubing size for this case.
- d. What is the corresponding insulation thickness (m) associated with the copper tube diameter specified in Part (c)?
- e. What is the annual cost associated with the tubing size specified in Part (c) and the insulation thickness specified in Part (d)?

A second possibility is to specify that the annual cost constraint must be met. For this case,

- f. Use the copper tube data in Appendix D to specify the standard tubing size for this case.
- g. What is the corresponding insulation thickness associated with the copper tube diameter specified in Part (f)?
- h. What is the outside diameter of the insulation with the tubing size specified in part (f) and the insulation thickness specified in Part (g)?

From these exercises, it should be clear that using standard size tubing the optimum solution determined in Part (b) cannot be achieved. However, the fact remains that a standard tube size must be specified.

- i. Which solution seems more viable, Parts (c) – (e) or Parts (f) – (h)? Explain your reasoning.

- 6.20 A flow of hot air is cooled in a heat exchanger with chilled water in a closed-loop system. The water is chilled in a refrigeration system as shown in Figure P6.20.

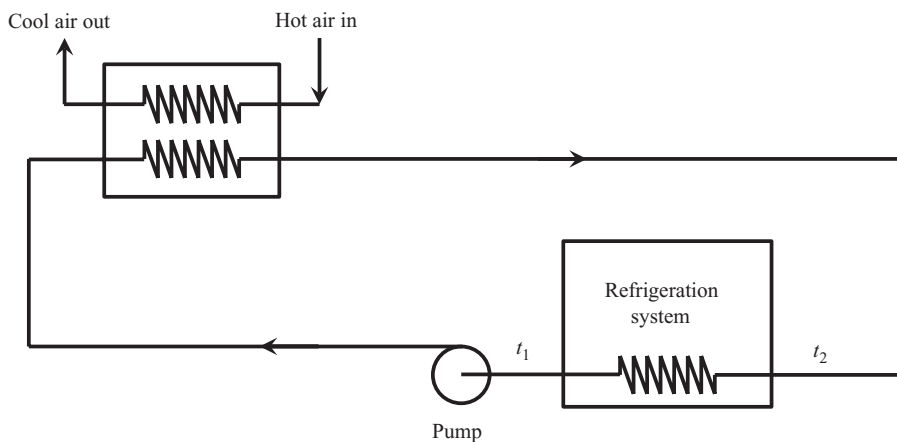


FIGURE P6.20

Chilled water system for cooling a flow of hot air.

The total length of pipe transporting the water is 4000 ft. The friction factor in the pipe is 0.018.

The heat transfer rate at the evaporator of the refrigeration system is 350 tons. In order to maintain this heat transfer duty, the average temperature between the chilled water supply and the warm return water must be,

$$T_{avg} = \frac{t_1 + t_2}{2} = 50^\circ\text{F}$$

In order to overcome the friction effects in the pipe, the pump must provide a head of 70 ft, which can be considered independent of the mass flow rate of the water.

It is desired to design this system such that the cost is minimized. The cost can be considered to be made up of three components. The initial cost of the pipe is,

$$IC_{pipe} = b_1 D$$

In this equation, $b_1 = 91,450$ \$/ft and D is the inside diameter of the pipe. The annual cost of the pumping power required to circulate the water is,

$$AC_{pump} = b_2 \dot{m}$$

In this equation, $b_2 = 0.06$ \$-hr/lbm and \dot{m} is the mass flow rate of the water. The annual cost of operating the refrigeration system used to produce the chilled water is,

$$AC_{chiller} = b_3 + b_4 t_1$$

Here, $b_3 = 41,300$ \$, $b_4 = -800$ \$/°F, and t_1 is the chilled water temperature leaving the refrigeration system. This thermal energy system is expected to last 40 years and provide a rate of return of 18%.

- Formulate the optimization problem and constraint(s).
- Use the method of Lagrange multipliers to solve the optimization problem formulated in Part (a) and determine the inside diameter of the pipe that minimizes the total cost of the thermal energy system. What is the minimum present worth of the thermal energy system cost at the calculated diameter?
- How does the velocity of the water in the pipe compare to the economic velocity computed in Table 4.18?

Without resolving the optimization problem, use the Lagrange multipliers to estimate the value of the objective function if the

- Pump head was 71 ft instead of 70 ft
 - Heat transfer rate at the evaporator of the chiller was 351 kW instead of 350 kW
- It is unlikely that the diameter specified in Part (b) is a standard pipe size. If sch 40 commercial steel pipe is being used in this system,
- Specify the nominal pipe size for this application. Justify your selection.

- 6.21 A flow rate of 32,000 cfm of gas at a temperature of 120°F and a pressure of 25 psia is to be compressed to 2500 psia. Under these conditions, the gas behaves according to the ideal gas law. The choice of compressor type is influenced by the fact that centrifugal compressors can handle high-volume flow rates but develop only low-pressure ratios per stage. A reciprocating compressor, on the other hand, is suited to low volume flow rates but can develop high pressure ratios. To combine the advantages of each, the compression will be done using a low-stage centrifugal compressor and a high-stage reciprocating compressor. Between the compressor stages, an intercooler is used to return the gas temperature to 120°F. A sketch of this dual-stage compressor system is shown in Figure P6.21. The first cost of each compressor, expressed in terms of volume flow rates and pressure ratios are given by the following equations,

$$IC_c = a_1 \dot{V}_1 + a_2 \frac{P_2}{P_1} \quad (\text{centrifugal compressor})$$

$$IC_r = b_1 \dot{V}_3 + b_2 \frac{P_4}{P_3} \quad (\text{reciprocating compressor})$$

In the above equations, $a_1 = 0.035$ \$/cfm, $a_2 = 1700$ \$, $b_1 = 0.095$ \$/cfm, and $b_2 = 900$ \$. Using the method of Lagrange multipliers, determine the

- Minimum first cost of the compressors
 - Pressure ratios across each compressor to achieve this optimum condition
- 6.22 A cascade refrigeration cycle is shown in Figure P6.22. The purpose of a refrigeration cycle of this type is to achieve very low temperature refrigeration while saving energy costs. Energy costs are reduced because the work required for the two-stage cascade system is lower than the compression for a single stage operating between the same source and sink conditions. In the interstage heat exchanger, the refrigerant in the low-pressure stage leaves at T_c . The refrigerant enters the interstage heat exchanger from the high-pressure stage at T_c . The overall heat transfer coefficient in the interstage heat exchanger is $U = 800$ W/m²-K and the total heat transferred between the two stages is 160 kW.

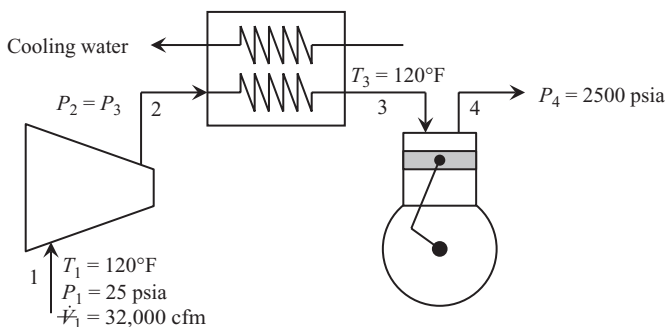
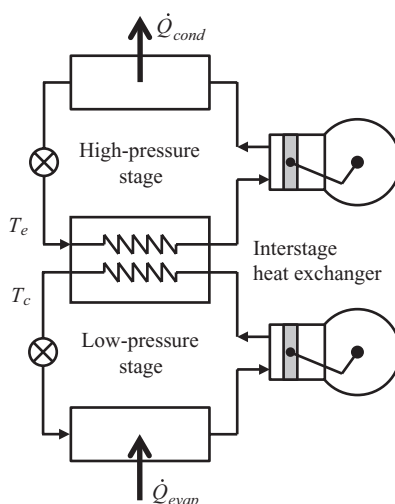


FIGURE P6.21

Two stage compression with intercooling.

**FIGURE P6.22**

Cascade refrigeration system.

A cost analysis reveals that the initial cost of the interstage heat exchanger is related to the heat transfer area by,

$$IC_{HX} = a_1 A$$

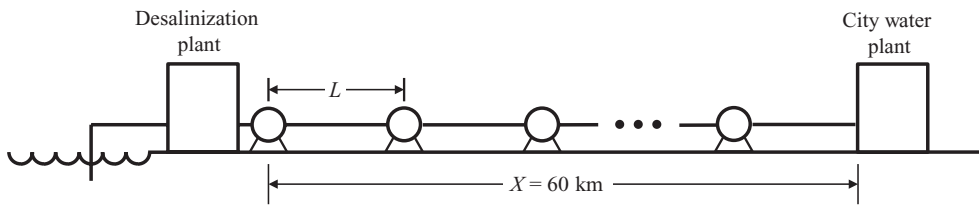
where $a_1 = 100$ \$/m². The cost of energy required by the compressor of each stage is a function of the refrigerant temperatures in the interstage heat exchanger. An economic analysis conducted over the expected life of the system shows that the present value of the lifetime energy costs for each stage is given by,

$$PV_L = a_2 + a_3 T_c \quad (\text{low pressure stage})$$

$$PV_H = a_4 + a_5 T_e^2 \quad (\text{high pressure stage})$$

In these cost equations, $a_2 = 127,000$ \$, $a_3 = 150$ \$/K, $a_4 = 189,000$ \$, and $a_5 = -0.3$ \$/K². Notice that the temperatures must be on the kelvin (K) scale.

- Using the method of Lagrange multipliers, determine the minimum cost of this cascade refrigeration system
 - What are the values of the design variables that result in the minimum cost calculated in Part (a)?
 - Using the value(s) of the Lagrange multiplier(s), estimate the minimum cost of the system if the heat transfer rate between the fluids in the interstage heat exchanger was increased to 170 kW.
- 6.23 Ocean water is processed in a desalinization plant on the coast and transported by a pipeline to a city water plant 60 km inland as shown in Figure P6.23. Fresh water flows in the horizontal pipeline at a rate of 570 m³/h. The friction factor in the pipe can be assumed to be 0.019.

**FIGURE P6.23**

Pump and pipe network transporting water to an inland city.

The initial cost of each pump can be expressed as a function of the pressure increase that must be provided to overcome the friction loss over a distance, L , the distance between the pumping stations, as

$$C_{\text{pump}} = a_1 + a_2 \Delta P^{1.2}$$

In this equation, $a_1 = 5000$ \$, and $a_2 = 0.00032$ \$/Pa^{1.2}. The initial cost of the pipe can be expressed as a function of diameter by,

$$C_{\text{pipe}} = a_3 D^{1.5}$$

where $a_3 = 5,120,000$ \$/m^{1.5}.

- Formulate the objective function and constraint(s).
- Using the method of Lagrange multipliers, solve the optimization problem formulated in Part (a) and determine the number of pumps required to minimize the initial cost of the system.

The solution of Part (b) is the mathematical optimum. Therefore, the number of pumps is likely not an integer, nor is the diameter of the pipe a standard diameter. Assuming that schedule 40 commercial steel pipe is used,

- Specify the nominal diameter (inches) and number of pumps for this application. What is the total system initial cost for the number of pumps and pipe diameter you specified? How does this value compare with the total system initial cost determined in Part (b)?

Appendix A: Conversion Factors and Constants

The conversion factors between SI and IP units in this appendix were calculated from a publication of the National Institute of Standards and Technology (NIST) (Thompson and Taylor 2008).

Metric Symbols and Names		
Prefix Symbol	Prefix Name	
E	exa	10^{18}
P	peta	10^{15}
T	tera	10^{12}
G	giga	10^9
M	mega	10^6
k	kilo	10^3
h	hecto	10^2
da	deka	10^1
d	deci	10^{-1}
c	centi	10^{-2}
m	milli	10^{-3}
μ	micro	10^{-6}
n	nano	10^{-9}
p	pico	10^{-12}
f	femto	10^{-15}
a	atto	10^{-18}

SI Conversions

$1\ x = 10^{-1}\ \text{dax} = 10^{-2}\ \text{hx} = 10^{-3}\ \text{kx} = 10^{-6}\ \text{Mx} = 10^{-9}\ \text{Gx} = 10^{-12}\ \text{Tx} = 10^{-15}\ \text{Px} = 10^{-18}\ \text{Ex}$

$1\ x = 10^1\ \text{dx} = 10^2\ \text{cx} = 10^3\ \text{mx} = 10^6\ \mu\text{x} = 10^9\ \text{nx} = 10^{12}\ \text{px} = 10^{15}\ \text{fx} = 10^{18}\ \text{ax}$

x represents any of the base SI units such as meter (m), liter (L), gram (g), watt (W), etc.

Length Conversions

$1\ \text{m} = 3.28084\ \text{ft} = 1.09361\ \text{yd}$

$1\ \text{in} = 2.54\ \text{cm}$

$1\ \text{ft} = 12\ \text{in}$

$1\ \text{yd} = 3\ \text{ft}$

$1\ \text{mi} = 5,280\ \text{ft}$

Volume Conversions

$1\ \text{L} = 0.001\ \text{m}^3 = 0.264172\ \text{gal} = 0.0353147\ \text{ft}^3$

$1\ \text{ft}^3 = 7.480519\ \text{gal}$

Mass Conversions

$1\ \text{kg} = 2.2046\ \text{lbm} = 6.85218 \times 10^{-3}\ \text{slug}$

$1\ \text{ton [US, short]} = 0.907185\ \text{metric ton} = 907.18474\ \text{kg} = 2,000\ \text{lbm}$

Force Conversions

$$1 \text{ N} = 10^5 \text{ dyne} = 0.224809 \text{ lbf} = 7.233014 \text{ poundal}$$

$$1 \text{ ton-force [US, short]} = 0.907185 \text{ metric ton-force} = 8896.4432 \text{ N} = 2,000 \text{ lbf}$$

Pressure Conversions

$$1 \text{ kPa} = 0.01 \text{ bar} = 0.145038 \text{ lbf/in}^2$$

$$1 \text{ atm} = 101.325 \text{ kPa} = 14.696 \text{ lbf/in}^2 = 2116.22 \text{ lbf/ft}^2 = 29.9213 \text{ in Hg [0°C]} \\ = 406.783 \text{ in water [4°C]} = 760 \text{ torr}$$

Dynamic Viscosity Conversions

$$1 \text{ N-s/m}^2 = 1 \text{ Pa-s} = 10 \text{ poise} = 1 \text{ kg/m-s} = 0.0208854 \text{ lbf-s/ft}^2 = 0.671969 \text{ lbm/ft-s}$$

Kinematic Viscosity Conversions

$$1 \text{ m}^2/\text{s} = 10^4 \text{ stokes} = 10.7639 \text{ ft}^2/\text{s} = 38,750 \text{ ft}^2/\text{h}$$

Energy Conversions

$$1 \text{ kJ} = 2.77778 \times 10^{-4} \text{ kWh} = 0.947817 \text{ Btu} = 737.562 \text{ ft-lbf}$$

$$1 \text{ therm [US]} = 1.0548 \times 10^4 \text{ kJ} = 29.3001 \text{ kWh} = 9.99761 \times 10^4 \text{ Btu}$$

$$1 \text{ therm [Europe]} = 1.05506 \times 10^4 \text{ kJ} = 29.3071 \text{ kWh} = 10^5 \text{ Btu}$$

$$1 \text{ quad} = 1.00024 \times 10^{10} \text{ therm [US]} = 10^{10} \text{ therm [Europe]} = 1.05506 \times 10^{15} \text{ kJ} \\ = 2.93071 \times 10^{10} \text{ kWh} = 10^{15} \text{ Btu}$$

Specific Energy Conversions

$$1 \text{ kJ/kg} = 0.429923 \text{ Btu/lbm} = 334.553 \text{ ft-lbf/lbm} = 10^3 \text{ m}^2/\text{s}^2 = 1.07639 \times 10^4 \text{ ft}^2/\text{s}^2$$

Energy Transfer Rate Conversions

$$1 \text{ kW} = 3412.14 \text{ Btu/hr} = 737.562 \text{ ft-lbf/s} = 1.341 \text{ hp} = 0.284345 \text{ ton [refrigeration]}$$

Specific Entropy and Specific Heat Capacity Conversions

$$1 \text{ kJ/kg-K} = 0.238846 \text{ Btu/lbm-R} = 185.863 \text{ ft-lbf/lbm-R}$$

Density Conversions

$$1 \text{ kg/m}^3 = 1 \text{ g/L} = 0.062428 \text{ lbm/ft}^3 = 1.94032 \times 10^{-3} \text{ slug/ft}^3$$

Specific Volume Conversions

$$1 \text{ m}^3/\text{kg} = 1 \text{ L/g} = 16.0185 \text{ ft}^3/\text{lbm} = 515.378 \text{ ft}^3/\text{slug}$$

Mass Flow Rate Conversions

$$1 \text{ kg/s} = 2.20462 \text{ lbm/s} = 0.0682518 \text{ slug/s}$$

Volumetric Flow Rate Conversions

$$1 \text{ m}^3/\text{s} = 1,000 \text{ L/s} = 35.3147 \text{ ft}^3/\text{s}$$

$$1 \text{ gpm [liq]} = 6.30902 \times 10^{-5} \text{ m}^3/\text{s} = 0.0630902 \text{ L/s} = 8.02083 \text{ ft}^3/\text{hr}$$

Thermal Conductivity Conversion

$$1 \text{ W/m-K} = 0.577789 \text{ Btu/hr-ft}^2\text{-}^\circ\text{F}$$

Heat Transfer Coefficient Conversion

$$1 \text{ W/m}^2\text{-K} = 0.176110 \text{ Btu/hr-ft}^2\text{-}^\circ\text{F}$$

Thermal Resistance Conversion

1 m²-K/W = 5.67826 hr-ft²-°F/Btu

Time Conversions

1 h = 60 min = 3,600 s

Temperature Conversions

From	To °C	To °F	To K	To °R
°C	°C = °C	°F = 1.8°C + 32	K = °C + 273.15	°R = 1.8(°C + 273.15)
°F	°C = (°F - 32)/1.8	°F = °F	K = (°F + 459.67)/1.8	°R = °F + 459.67
K	°C = K - 273.15	°F = 1.8K - 459.67	K = K	°R = 1.8K
°R	°C = (°R - 491.67)/1.8	°F = °R - 459.67	K = °R/1.8	°R = °R

Constants

Acceleration due to gravity on Earth at sea level	$g = 9.807 \frac{\text{m}}{\text{s}^2} = 32.174 \frac{\text{ft}}{\text{s}^2}$
Conversion factor in Newton’s second law	$g_c = 1[\text{SI system}] = 32.174 \frac{\text{lbm}\cdot\text{ft}}{\text{lbf}\cdot\text{s}^2}$
Universal gas constant (4 significant figures)	$R = 8.314 \frac{\text{J}}{\text{mol}\cdot\text{K}} = 1545. \frac{\text{ft}\cdot\text{lbf}}{\text{lbmol}\cdot^\circ\text{R}}$

Reference

Thompson, Ambler, and Barry N. Taylor. 2008. *Guide for the Use of the International System of Units (SI)*. Special Publication 811, Gaithersburg, MD: National Institute of Standards and Technology.



Taylor & Francis

Taylor & Francis Group

<http://taylorandfrancis.com>

Appendix B: Thermophysical Properties

This appendix contains thermophysical properties of several fluids. In all cases, the most modern formulations as of the time of this writing have been used to compute the properties. Tables are presented in both SI and IP units.

Appendix	Page
Appendix B.1	
Thermophysical Properties of Saturated Water (SI Units)	460
Thermophysical Properties of Saturated Water (IP Units)	462
Appendix B.2	
Thermophysical Properties of Single Phase Water (SI Units)	464
Thermophysical Properties of Single Phase Water (IP Units)	468
Appendix B.3	
Thermophysical Properties of Liquids at Saturation (SI Units)	472
Thermophysical Properties of Liquids at Saturation (IP Units)	483
Appendix B.4	
Thermophysical Properties of Ethylene Glycol–Water Solutions (SI Units)	494
Thermophysical Properties of Ethylene Glycol–Water Solutions (IP Units)	495
Thermophysical Properties of Propylene Glycol–Water Solutions (SI Units)	496
Thermophysical Properties of Propylene Glycol–Water Solutions (IP Units)	497
Thermophysical Properties of Methanol–Water Solutions (SI Units)	498
Thermophysical Properties of Methanol–Water Solutions (IP Units)	499
Thermophysical Properties of Ethanol–Water Solutions (SI Units)	500
Thermophysical Properties of Ethanol–Water Solutions (IP Units)	501
Thermophysical Properties of Calcium Chloride–Water Solutions (SI Units)	502
Thermophysical Properties of Calcium Chloride–Water Solutions (IP Units)	503
Thermophysical Properties of Magnesium Chloride–Water Solutions (SI Units)	504
Thermophysical Properties of Magnesium Chloride–Water Solutions (IP Units)	505
Thermophysical Properties of Sodium Chloride–Water Solutions (SI Units)	506
Thermophysical Properties of Sodium Chloride–Water Solutions (IP Units)	507
Appendix B.5	
Thermophysical Properties of Dry Air (SI Units)	508
Thermophysical Properties of Dry Air (IP Units)	511
Appendix B.6	
Thermophysical Properties of Saturated R134a (SI Units)	514
Thermophysical Properties of Saturated R134a (IP Units)	516
Appendix B.7	
Thermophysical Properties of Single Phase R134a (SI Units)	518
Thermophysical Properties of Single Phase R134a (IP Units)	521
Appendix B.8	
Thermophysical Properties of Metals (SI Units)	524
Thermophysical Properties of Metals (IP Units)	525

APPENDIX B.1

Thermophysical Properties of Saturated Water (SI Units)

<i>T</i> °C	<i>P</i> kPa	ρ_f kg/m ³	v_g m ³ /kg	<i>u_f</i> kJ/kg	<i>u_g</i> kJ/kg	<i>h_f</i> kJ/kg	<i>h_g</i> kJ/kg	<i>s_f</i> kJ/kg-K	<i>s_g</i> kJ/kg-K	<i>T</i> °C
0.01	0.61165	999.79	205.99	0.0	2374.9	0.00061178	2500.9	0.0	9.1555	0.01
10	1.2282	999.65	106.30	42.020	2388.6	42.021	2519.2	0.15109	8.8998	10
20	2.3393	998.16	57.757	83.912	2402.3	83.914	2537.4	0.29648	8.6660	20
30	4.2470	995.61	32.878	125.73	2415.9	125.73	2555.5	0.43675	8.4520	30
40	7.3849	992.18	19.515	167.53	2429.4	167.53	2573.5	0.57240	8.2555	40
50	12.352	988.00	12.027	209.33	2442.7	209.34	2591.3	0.70381	8.0748	50
60	19.946	983.16	7.6672	251.16	2455.9	251.18	2608.8	0.83129	7.9081	60
70	31.201	977.73	5.0395	293.03	2468.9	293.07	2626.1	0.95513	7.7540	70
80	47.414	971.77	3.4052	334.96	2481.6	335.01	2643.0	1.0756	7.6111	80
90	70.182	965.30	2.3591	376.97	2494.0	377.04	2659.5	1.1929	7.4781	90
99.974	101.325	958.37	1.6732	418.95	2506.0	419.06	2675.5	1.3069	7.3544	99.974
100	101.42	958.35	1.6718	419.06	2506.0	419.17	2675.6	1.3072	7.3541	100
110	143.38	950.95	1.2093	461.26	2517.7	461.42	2691.1	1.4188	7.2381	110
120	198.67	943.11	0.89121	503.60	2528.9	503.81	2705.9	1.5279	7.1291	120
130	270.28	934.83	0.66800	546.09	2539.5	546.38	2720.1	1.6346	7.0264	130
140	361.54	926.13	0.50845	588.77	2549.6	589.16	2733.4	1.7392	6.9293	140
150	476.16	917.01	0.39245	631.66	2559.1	632.18	2745.9	1.8418	6.8371	150
160	618.23	907.45	0.30678	674.79	2567.8	675.47	2757.4	1.9426	6.7491	160
170	792.19	897.45	0.24259	718.20	2575.7	719.08	2767.9	2.0417	6.6650	170
180	1002.8	887.00	0.19384	761.92	2582.8	763.05	2777.2	2.1392	6.5840	180
190	1255.2	876.08	0.15636	806.00	2589.0	807.43	2785.3	2.2355	6.5059	190
200	1554.9	864.66	0.12721	850.47	2594.2	852.27	2792.0	2.3305	6.4302	200
210	1907.7	852.72	0.10429	895.39	2598.3	897.63	2797.3	2.4245	6.3563	210
220	2319.6	840.22	0.086092	940.82	2601.2	943.58	2800.9	2.5177	6.2840	220
230	2797.1	827.12	0.071503	986.81	2602.9	990.19	2802.9	2.6101	6.2128	230
240	3346.9	813.37	0.059705	1033.4	2603.1	1037.6	2803.0	2.7020	6.1423	240
250	3976.2	798.89	0.050083	1080.8	2601.8	1085.8	2800.9	2.7935	6.0721	250
260	4692.3	783.63	0.042173	1129.0	2598.7	1135.0	2796.6	2.8849	6.0016	260
270	5503.0	767.46	0.035621	1178.1	2593.7	1185.3	2789.7	2.9765	5.9304	270
280	6416.6	750.28	0.030153	1228.3	2586.4	1236.9	2779.9	3.0685	5.8579	280
290	7441.8	731.91	0.025555	1279.9	2576.5	1290.0	2766.7	3.1612	5.7834	290
300	8587.9	712.14	0.021660	1332.9	2563.6	1345.0	2749.6	3.2552	5.7059	300
310	9865.1	690.67	0.018335	1387.9	2547.1	1402.2	2727.9	3.3510	5.6244	310
320	11284.	667.09	0.015471	1445.3	2526.0	1462.2	2700.6	3.4494	5.5372	320
330	12858.	640.77	0.012979	1505.8	2499.2	1525.9	2666.0	3.5518	5.4422	330
340	14601.	610.67	0.010781	1570.6	2464.4	1594.5	2621.8	3.6601	5.3356	340
350	16529.	574.71	0.0088024	1642.1	2418.1	1670.9	2563.6	3.7784	5.2110	350
360	18666.	527.59	0.0069493	1726.3	2351.8	1761.7	2481.5	3.9167	5.0536	360
370	21044.	451.43	0.0049544	1844.1	2230.3	1890.7	2334.5	4.1112	4.8012	370
373.946	22064.	322.00	0.0031056	2015.7	2015.7	2084.3	2084.3	4.4070	4.4070	373.946

Thermophysical Properties of Saturated Water (SI Units)

T °C	P kPa	c _{pf} kJ/kg-K	c _{pg} kJ/kg-K	μ _f mPa-s	μ _g mPa-s	k _f W/m-K	k _g W/m-K	Pr _f	Pr _g	T °C
0.01	0.61165	4.2199	1.8844	1.7914	0.0089458	0.55560	0.016761	13.606	1.0058	0.01
10	1.2282	4.1955	1.8947	1.3060	0.0092384	0.57871	0.017412	9.4682	1.0053	10
20	2.3393	4.1844	1.9059	1.0016	0.0095441	0.59795	0.018087	7.0092	1.0057	20
30	4.2470	4.1801	1.9180	0.79722	0.0098602	0.61434	0.018786	5.4245	1.0067	30
40	7.3849	4.1796	1.9314	0.65272	0.010185	0.62844	0.019509	4.3411	1.0083	40
50	12.352	4.1815	1.9468	0.54650	0.010516	0.64057	0.020261	3.5674	1.0105	50
60	19.946	4.1851	1.9648	0.46602	0.010854	0.65096	0.021043	2.9961	1.0134	60
70	31.201	4.1902	1.9862	0.40353	0.011195	0.65972	0.021860	2.5630	1.0172	70
80	47.414	4.1969	2.0120	0.35404	0.011539	0.66697	0.022717	2.2278	1.0220	80
90	70.182	4.2053	2.0429	0.31417	0.011885	0.67277	0.023618	1.9638	1.0280	90
99.974	101.325	4.2156	2.0799	0.28166	0.012231	0.67720	0.024568	1.7533	1.0355	99.974
100	101.42	4.2157	2.0800	0.28158	0.012232	0.67721	0.024570	1.7529	1.0355	100
110	143.38	4.2283	2.1244	0.25461	0.012580	0.68035	0.025579	1.5824	1.0447	110
120	198.67	4.2435	2.1770	0.23203	0.012927	0.68224	0.026652	1.4432	1.0559	120
130	270.28	4.2615	2.2389	0.21294	0.013273	0.68295	0.027795	1.3287	1.0691	130
140	361.54	4.2826	2.3109	0.19664	0.013618	0.68253	0.029016	1.2339	1.0846	140
150	476.16	4.3071	2.3939	0.18261	0.013961	0.68102	0.030321	1.1549	1.1022	150
160	618.23	4.3354	2.4883	0.17043	0.014304	0.67873	0.031721	1.0886	1.1220	160
170	792.19	4.3678	2.5944	0.15977	0.014645	0.67552	0.033221	1.0331	1.1437	170
180	1002.8	4.4050	2.7129	0.15038	0.014985	0.67128	0.034832	0.98682	1.1671	180
190	1255.2	4.4474	2.8443	0.14204	0.015325	0.66609	0.036563	0.94839	1.1922	190
200	1554.9	4.4958	2.9895	0.13458	0.015666	0.66001	0.038426	0.91675	1.2188	200
210	1907.7	4.5512	3.1503	0.12787	0.016009	0.65306	0.040435	0.89109	1.2472	210
220	2319.6	4.6146	3.3289	0.12177	0.016354	0.64526	0.042606	0.87083	1.2778	220
230	2797.1	4.6876	3.5285	0.11619	0.016705	0.63663	0.044960	0.85554	1.3110	230
240	3346.9	4.7719	3.7537	0.11106	0.017062	0.62717	0.047525	0.84498	1.3476	240
250	3976.2	4.8701	4.0105	0.10628	0.017429	0.61689	0.050336	0.83908	1.3887	250
260	4692.3	4.9856	4.3075	0.10181	0.017810	0.60578	0.053446	0.83792	1.4354	260
270	5503.0	5.1230	4.6563	0.097585	0.018208	0.59383	0.056926	0.84187	1.4893	270
280	6416.6	5.2889	5.0731	0.093550	0.018630	0.58103	0.060878	0.85156	1.5525	280
290	7441.8	5.4931	5.5821	0.089657	0.019083	0.56732	0.065456	0.86811	1.6274	290
300	8587.9	5.7504	6.2197	0.085855	0.019580	0.55265	0.070900	0.89334	1.7176	300
310	9865.1	6.0848	7.0449	0.082094	0.020135	0.53692	0.077587	0.93034	1.8283	310
320	11284.	6.5373	8.1589	0.078310	0.020773	0.52002	0.086156	0.98446	1.9672	320
330	12858.	7.1863	9.7526	0.074428	0.021532	0.50176	0.097740	1.0660	2.1485	330
340	14601.	8.2080	12.236	0.070331	0.022477	0.48193	0.11452	1.1978	2.4015	340
350	16529.	10.116	16.692	0.065803	0.023739	0.46047	0.14127	1.4456	2.8049	350
360	18666.	15.004	27.356	0.060306	0.025638	0.43916	0.19144	2.0604	3.6635	360
370	21044.	45.155	96.598	0.052263	0.029659	0.44542	0.34946	5.2982	8.1982	370
373.946	22064	—	—	—	—	—	—	—	—	373.946

APPENDIX B.1 (CONTINUED)

Thermophysical Properties of Saturated Water (IP Units)

<i>T</i> °F	<i>P</i> psia	ρ_f lbm/ft ³	v_g ft ³ /lbm	<i>u_f</i> Btu/lbm	<i>u_g</i> Btu/lbm	<i>h_f</i> Btu/lbm	<i>h_g</i> Btu/lbm	<i>s_f</i> Btu/ lbm-R	<i>s_g</i> Btu/ lbm-R	<i>T</i> °F
32.018	0.088713	62.415	3299.7	0.0	1021.7	0.0002632	1075.9	0.0	2.1882	32.018
40	0.12173	62.423	2443.3	8.0373	1024.3	8.0377	1079.4	0.016215	2.1604	40
50	0.17814	62.406	1702.8	18.077	1027.6	18.078	1083.8	0.036110	2.1271	50
60	0.25640	62.364	1206.0	28.096	1030.9	28.096	1088.2	0.055576	2.0954	60
70	0.36336	62.298	867.11	38.100	1034.2	38.101	1092.5	0.074644	2.0653	70
80	0.50747	62.213	632.38	48.095	1037.4	48.097	1096.8	0.093340	2.0366	80
90	0.69904	62.110	467.40	58.086	1040.6	58.088	1101.1	0.11168	2.0093	90
100	0.95051	61.991	349.83	68.076	1043.9	68.078	1105.4	0.12969	1.9832	100
120	1.6950	61.710	202.95	88.057	1050.3	88.062	1114.0	0.16477	1.9346	120
140	2.8930	61.377	122.82	108.05	1056.6	108.06	1122.3	0.19868	1.8901	140
160	4.7472	60.998	77.184	128.07	1062.7	128.08	1130.6	0.23152	1.8493	160
180	7.5195	60.578	50.169	148.12	1068.8	148.14	1138.6	0.26336	1.8118	180
200	11.538	60.120	33.609	168.21	1074.7	168.24	1146.5	0.29429	1.7772	200
211.95	14.696	59.829	26.802	180.24	1078.1	180.28	1151.0	0.31236	1.7578	211.95
220	17.201	59.626	23.133	188.35	1080.4	188.40	1154.1	0.32436	1.7451	220
240	24.986	59.097	16.314	208.55	1085.8	208.63	1161.3	0.35366	1.7153	240
260	35.447	58.535	11.759	228.83	1091.0	228.95	1168.2	0.38225	1.6874	260
280	49.222	57.940	8.6431	249.21	1095.9	249.37	1174.7	0.41017	1.6612	280
300	67.029	57.312	6.4658	269.69	1100.5	269.91	1180.7	0.43750	1.6365	300
320	89.667	56.650	4.9142	290.30	1104.7	290.60	1186.3	0.46428	1.6131	320
340	118.02	55.955	3.7884	311.06	1108.5	311.45	1191.3	0.49058	1.5908	340
360	153.03	55.225	2.9580	331.99	1111.8	332.50	1195.6	0.51643	1.5694	360
380	195.74	54.458	2.3361	353.11	1114.6	353.77	1199.3	0.54190	1.5489	380
400	247.26	53.652	1.8638	374.45	1116.9	375.30	1202.2	0.56703	1.5289	400
420	308.76	52.804	1.5006	396.04	1118.6	397.12	1204.4	0.59187	1.5096	420
440	381.48	51.912	1.2177	417.91	1119.6	419.27	1205.6	0.61648	1.4905	440
460	466.75	50.971	0.99506	440.11	1119.9	441.81	1205.9	0.64092	1.4718	460
480	565.95	49.976	0.81791	462.69	1119.4	464.78	1205.1	0.66524	1.4531	480
500	680.55	48.920	0.67555	485.69	1118.0	488.27	1203.1	0.68952	1.4344	500
520	812.10	47.795	0.56007	509.21	1115.5	512.35	1199.8	0.71384	1.4155	520
540	962.24	46.590	0.46553	533.32	1111.9	537.14	1194.8	0.73829	1.3962	540
560	1132.7	45.290	0.38742	558.14	1106.8	562.77	1188.0	0.76299	1.3762	560
580	1325.5	43.876	0.32227	583.85	1099.9	589.44	1179.0	0.78812	1.3552	580
600	1542.5	42.318	0.26739	610.67	1091.0	617.42	1167.4	0.81388	1.3329	600
620	1786.2	40.572	0.22062	638.96	1079.3	647.11	1152.3	0.84062	1.3085	620
640	2059.2	38.566	0.18017	669.30	1063.9	679.19	1132.6	0.86888	1.2812	640
660	2364.9	36.152	0.14439	702.84	1042.8	714.96	1106.1	0.89974	1.2491	660
680	2707.3	32.936	0.11132	742.67	1011.8	757.89	1067.6	0.93611	1.2078	680
700	3093.0	27.283	0.074795	802.01	948.82	823.00	991.66	0.99065	1.1361	700
705.103	3200.1	20.102	0.049747	867.19	867.19	896.67	896.67	1.0533	1.0533	705.103

Thermophysical Properties of Saturated Water (IP Units)

T °F	P psia	c_{pf} Btu/ lbm-R	c_{pg} Btu/ lbm-R	μ_f lbm/ft-h	μ_g lbm/ft-h	k_f Btu/h-ft-R	k_g Btu/ h-ft-R	Pr_f	Pr_g	T °F
32.018	0.088713	1.0086	0.45037	4.3335	0.021641	0.32123	0.0096906	13.606	1.0058	32.018
40	0.12173	1.0055	0.45144	3.7382	0.021951	0.32750	0.0098562	11.477	1.0054	40
50	0.17814	1.0028	0.45284	3.1593	0.022349	0.33460	0.010067	9.4682	1.0053	50
60	0.25640	1.0010	0.45431	2.7120	0.022756	0.34101	0.010282	7.9609	1.0054	60
70	0.36336	0.99991	0.45583	2.3585	0.023172	0.34685	0.010502	6.7991	1.0058	70
80	0.50747	0.99928	0.45742	2.0737	0.023595	0.35220	0.010725	5.8837	1.0063	80
90	0.69904	0.99898	0.45910	1.8407	0.024025	0.35711	0.010953	5.1490	1.0070	90
100	0.95051	0.99893	0.46087	1.6473	0.024462	0.36164	0.011186	4.5501	1.0079	100
120	1.6950	0.99934	0.46485	1.3471	0.025350	0.36964	0.011665	3.6419	1.0102	120
140	2.8930	1.0003	0.46959	1.1273	0.026256	0.37637	0.012167	2.9961	1.0134	140
160	4.7472	1.0016	0.47535	0.96150	0.027173	0.38194	0.012693	2.5215	1.0176	160
180	7.5195	1.0035	0.48240	0.83323	0.028099	0.38644	0.013248	2.1637	1.0232	180
200	11.538	1.0059	0.49105	0.73199	0.029031	0.38992	0.013836	1.8883	1.0304	200
211.95	14.696	1.0076	0.49712	0.68135	0.029589	0.39154	0.014204	1.7533	1.0355	211.95
220	17.201	1.0088	0.50162	0.65069	0.029964	0.39244	0.014461	1.6727	1.0394	220
240	24.986	1.0125	0.51446	0.58443	0.030897	0.39406	0.015129	1.5017	1.0507	240
260	35.447	1.0170	0.52991	0.52969	0.031829	0.39480	0.015845	1.3645	1.0644	260
280	49.222	1.0224	0.54828	0.48395	0.032757	0.39473	0.016615	1.2534	1.0809	280
300	67.029	1.0287	0.56982	0.44529	0.033681	0.39387	0.017445	1.1630	1.1002	300
320	89.667	1.0362	0.59471	0.41228	0.034602	0.39242	0.018340	1.0886	1.1220	320
340	118.02	1.0449	0.62308	0.38384	0.035519	0.39032	0.019308	1.0275	1.1462	340
360	153.03	1.0550	0.65510	0.35910	0.036433	0.38750	0.020355	0.97764	1.1726	360
380	195.74	1.0666	0.69098	0.33738	0.037348	0.38401	0.021490	0.93713	1.2009	380
400	247.26	1.0802	0.73111	0.31814	0.038266	0.37988	0.022722	0.90465	1.2312	400
420	308.76	1.0959	0.77608	0.30095	0.039190	0.37514	0.024064	0.87920	1.2639	420
440	381.48	1.1143	0.82680	0.28545	0.040126	0.36980	0.025528	0.86010	1.2996	440
460	466.75	1.1358	0.88459	0.27133	0.041081	0.36387	0.027137	0.84693	1.3391	460
480	565.95	1.1612	0.95129	0.25835	0.042063	0.35735	0.028915	0.83950	1.3839	480
500	680.55	1.1916	1.0295	0.24629	0.043083	0.35025	0.030901	0.83792	1.4354	500
520	812.10	1.2285	1.1231	0.23496	0.044156	0.34254	0.033152	0.84264	1.4958	520
540	962.24	1.2740	1.2374	0.22419	0.045303	0.33422	0.035751	0.85459	1.5680	540

APPENDIX B.2

Thermophysical Properties of Single Phase Water (SI Units)

<i>T</i> °C	ρ kg/m ³	<i>v</i> m ³ /kg	<i>u</i> kJ/kg	<i>h</i> kJ/kg	<i>s</i> kJ/kg-K	<i>c_p</i> kJ/kg-K	μ mPa-s	<i>k</i> W/m-K	Pr	<i>T</i> °C
P = 1 kPa (0.001 MPa)										
50	0.0067072	149.09	2445.3	2594.4	9.2430	1.8761	0.010537	0.020232	0.97716	50
100	0.0058075	172.19	2516.4	2688.6	9.5139	1.8914	0.012336	0.024160	0.96574	100
150	0.0051210	195.27	2588.4	2783.7	9.7531	1.9139	0.014252	0.028482	0.95766	150
200	0.0045797	218.35	2661.7	2880.0	9.9682	1.9403	0.016240	0.033149	0.95056	200
250	0.0041419	241.44	2736.3	2977.7	10.165	1.9692	0.018270	0.038120	0.94381	250
300	0.0037805	264.52	2812.4	3077.0	10.346	1.9996	0.020325	0.043361	0.93729	300
350	0.0034772	287.59	2890.1	3177.7	10.514	2.0312	0.022390	0.048845	0.93107	350
400	0.0032189	310.67	2969.4	3280.1	10.672	2.0636	0.024456	0.054544	0.92525	400
450	0.0029963	333.74	3050.4	3384.1	10.821	2.0969	0.026515	0.060439	0.91991	450
500	0.0028025	356.82	3133.0	3489.8	10.963	2.1309	0.028562	0.066508	0.91510	500
600	0.0024816	402.97	3303.4	3706.3	11.226	2.2006	0.032605	0.079104	0.90704	600
700	0.0022266	449.12	3480.8	3930.0	11.468	2.2716	0.036564	0.092212	0.90074	700
800	0.0020191	495.27	3665.4	4160.7	11.694	2.3424	0.040428	0.10573	0.89562	800
900	0.0018470	541.42	3856.9	4398.4	11.906	2.4114	0.044194	0.11959	0.89114	900
1000	0.0017019	587.58	4055.3	4642.8	12.106	2.4776	0.047860	0.13371	0.88686	1000
1100	0.0015780	633.71	4260.0	4893.8	12.295	2.5403	0.051428	0.14803	0.88250	1100
1200	0.0014708	679.90	4470.9	5150.8	12.476	2.5989	0.054901	0.16252	0.87790	1200
1400	0.0012950	772.20	4909.1	5681.3	12.813	2.7035	0.061575	0.19183	0.86779	1400
1600	0.0011567	864.53	5366.6	6231.1	13.124	2.7922	0.067916	0.22138	0.85658	1600
P = 100 kPa (0.01 MPa)										
50	988.03	0.0010121	209.32	209.42	0.70377	4.1813	0.54652	0.64062	3.5671	50
100	0.58967	1.6959	2506.2	2675.8	7.3610	2.0766	0.012234	0.024564	1.0342	100
150	0.51636	1.9366	2582.9	2776.6	7.6148	1.9846	0.014192	0.028843	0.97655	150
200	0.46031	2.1724	2658.2	2875.5	7.8356	1.9754	0.016204	0.033436	0.95735	200
250	0.41560	2.4062	2733.9	2974.5	8.0346	1.9893	0.018249	0.038340	0.94690	250
300	0.37895	2.6389	2810.6	3074.5	8.2172	2.0124	0.020313	0.043530	0.93908	300
350	0.34832	2.8709	2888.7	3175.8	8.3866	2.0399	0.022384	0.048975	0.93230	350
400	0.32230	3.1027	2968.3	3278.6	8.5452	2.0698	0.024453	0.054649	0.92617	400
450	0.29992	3.3342	3049.4	3382.8	8.6946	2.1015	0.026515	0.060527	0.92061	450
500	0.28046	3.5656	3132.2	3488.7	8.8361	2.1344	0.028564	0.066586	0.91562	500
600	0.24827	4.0279	3302.8	3705.6	9.0998	2.2029	0.032608	0.079173	0.90727	600
700	0.22272	4.4899	3480.4	3929.4	9.3424	2.2731	0.036568	0.092282	0.90076	700
800	0.20194	4.9520	3665.0	4160.2	9.5681	2.3434	0.040433	0.10581	0.89549	800
900	0.18472	5.4136	3856.6	4398.0	9.7800	2.4122	0.044198	0.11967	0.89091	900
1000	0.17020	5.8754	4055.0	4642.6	9.9800	2.4782	0.047864	0.13380	0.88656	1000
1100	0.15780	6.3371	4259.8	4893.5	10.170	2.5407	0.051432	0.14813	0.88216	1100
1200	0.14708	6.7990	4470.7	5150.6	10.350	2.5993	0.054904	0.16262	0.87754	1200
1400	0.12950	7.7220	4908.9	5681.2	10.688	2.7038	0.061578	0.19194	0.86742	1400
1600	0.11567	8.6453	5366.5	6231.0	10.998	2.7923	0.067918	0.22149	0.85623	1600

APPENDIX B.2 (CONTINUED)

Thermophysical Properties of Single Phase Water (SI Units)

<i>T</i> °C	ρ kg/m ³	<i>v</i> m ³ /kg	<i>u</i> kJ/kg	<i>h</i> kJ/kg	<i>s</i> kJ/kg-K	<i>c_p</i> kJ/kg-K	μ mPa-s	<i>k</i> W/m-K	Pr	<i>T</i> °C
P = 500 kPa (0.05 MPa)										
50	988.21	0.0010119	209.26	209.76	0.70358	4.1804	0.54660	0.64083	3.5657	50
100	958.54	0.0010433	418.94	419.47	1.3069	4.2148	0.28169	0.67744	1.7526	100
150	917.02	0.0010905	631.65	632.19	1.8418	4.3070	0.18262	0.68103	1.1549	150
200	2.3528	0.42503	2643.3	2855.8	7.0610	2.1429	0.016060	0.034648	0.99325	200
250	2.1078	0.47443	2723.8	2961.0	7.2724	2.0788	0.018164	0.039254	0.96191	250
300	1.9135	0.52260	2803.2	3064.6	7.4614	2.0670	0.020265	0.044223	0.94720	300
350	1.7539	0.57016	2883.0	3168.1	7.6346	2.0763	0.022359	0.049512	0.93764	350
400	1.6199	0.61732	2963.7	3272.3	7.7955	2.0957	0.024444	0.055079	0.93005	400
450	1.5056	0.66419	3045.6	3377.7	7.9465	2.1206	0.026516	0.060886	0.92352	450
500	1.4066	0.71093	3129.0	3484.5	8.0892	2.1490	0.028571	0.066902	0.91776	500
600	1.2436	0.80412	3300.4	3702.5	8.3543	2.2121	0.032623	0.079455	0.90823	600
700	1.1149	0.89694	3478.5	3927.0	8.5977	2.2793	0.036585	0.092568	0.90085	700
800	1.0104	0.98971	3663.6	4158.4	8.8240	2.3479	0.040450	0.10612	0.89497	800
900	0.92399	1.0823	3855.4	4396.6	9.0362	2.4155	0.044215	0.12001	0.88997	900
1000	0.85121	1.1748	4054.0	4641.4	9.2364	2.4807	0.047880	0.13416	0.88535	1000
1100	0.78910	1.2673	4259.0	4892.6	9.4263	2.5427	0.051447	0.14852	0.88079	1100
1200	0.73545	1.3597	4470.0	5149.8	9.6071	2.6008	0.054918	0.16304	0.87608	1200
1400	0.64745	1.5445	4908.4	5680.6	9.9448	2.7048	0.061590	0.19238	0.86593	1400
1600	0.57828	1.7293	5366.1	6230.7	10.255	2.7931	0.067928	0.22195	0.85481	1600
P = 1000 kPa (1 MPa)										
50	988.43	0.0010117	209.18	210.19	0.70335	4.1793	0.54670	0.64109	3.5639	50
100	958.77	0.0010430	418.80	419.84	1.3065	4.2136	0.28183	0.67772	1.7522	100
150	917.31	0.0010901	631.41	632.50	1.8412	4.3054	0.18274	0.68137	1.1547	150
200	4.8539	0.20602	2622.2	2828.3	6.6955	2.4281	0.015876	0.036312	1.0616	200
250	4.2965	0.23275	2710.4	2943.1	6.9265	2.2106	0.018058	0.040464	0.98657	250
300	3.8762	0.25798	2793.6	3051.6	7.1246	2.1425	0.020205	0.045122	0.95939	300
350	3.5398	0.28250	2875.7	3158.2	7.3029	2.1248	0.022329	0.050201	0.94512	350
400	3.2615	0.30661	2957.9	3264.5	7.4669	2.1293	0.024433	0.055627	0.93526	400
450	3.0262	0.33045	3040.9	3371.3	7.6200	2.1452	0.026518	0.061343	0.92732	450
500	2.8240	0.35411	3125.0	3479.1	7.7641	2.1677	0.028581	0.067303	0.92052	500
600	2.4931	0.40111	3297.5	3698.6	8.0310	2.2237	0.032642	0.079811	0.90945	600
700	2.2330	0.44783	3476.2	3924.1	8.2755	2.2871	0.036607	0.092929	0.90098	700
800	2.0227	0.49439	3661.7	4156.1	8.5024	2.3534	0.040473	0.10650	0.89433	800
900	1.8490	0.54083	3853.9	4394.8	8.7150	2.4196	0.044237	0.12043	0.88881	900
1000	1.7030	0.58720	4052.7	4639.9	8.9155	2.4839	0.047901	0.13462	0.88385	1000
1100	1.5784	0.63355	4257.9	4891.4	9.1056	2.5452	0.051466	0.14901	0.87908	1100
1200	1.4710	0.67981	4469.0	5148.9	9.2866	2.6028	0.054936	0.16355	0.87427	1200
1400	1.2948	0.77232	4907.7	5680.0	9.6245	2.7062	0.061605	0.19294	0.86408	1400
1600	1.1564	0.86475	5365.5	6230.3	9.9351	2.7940	0.067940	0.22253	0.85305	1600

APPENDIX B.2 (CONTINUED)

Thermophysical Properties of Single Phase Water (SI Units)

<i>T</i> °C	ρ kg/m ³	<i>v</i> m ³ /kg	<i>u</i> kJ/kg	<i>h</i> kJ/kg	<i>s</i> kJ/kg-K	<i>c_p</i> kJ/kg-K	μ mPa-s	<i>k</i> W/m-K	Pr	<i>T</i> °C
P = 5000 kPa (5 MPa)										
50	990.16	0.0010099	208.59	213.64	0.70150	4.1702	0.54751	0.64317	3.5500	50
100	960.63	0.0010410	417.64	422.85	1.3034	4.2045	0.28290	0.67999	1.7493	100
150	919.56	0.0010875	629.55	634.98	1.8368	4.2926	0.18376	0.68408	1.1531	150
200	867.26	0.0011531	847.91	853.68	2.3251	4.4761	0.13546	0.66287	0.91469	200
250	800.09	0.0012499	1079.5	1085.7	2.7910	4.8562	0.10658	0.61802	0.83747	250
300	22.053	0.045345	2699.0	2925.7	6.2110	3.1722	0.019794	0.054298	1.1564	300
350	19.242	0.051970	2809.5	3069.3	6.4516	2.6608	0.022157	0.056664	1.0404	350
400	17.290	0.057837	2907.5	3196.7	6.6483	2.4610	0.024406	0.060565	0.99174	400
450	15.792	0.063323	3000.6	3317.2	6.8210	2.3717	0.026582	0.065367	0.96444	450
500	14.581	0.068582	3091.7	3434.7	6.9781	2.3323	0.028703	0.070782	0.94579	500
600	12.706	0.078703	3273.3	3666.8	7.2605	2.3216	0.032821	0.082832	0.91991	600
700	11.297	0.088519	3457.7	3900.3	7.5136	2.3515	0.036804	0.095933	0.90215	700
800	10.188	0.098155	3646.9	4137.7	7.7458	2.3986	0.040669	0.10969	0.88929	800
900	9.2861	0.10769	3841.8	4380.2	7.9618	2.4528	0.044423	0.12386	0.87967	900
1000	8.5364	0.11715	4042.6	4628.3	8.1648	2.5091	0.048074	0.13832	0.87209	1000
1100	7.9018	0.12655	4249.3	4882.0	8.3566	2.5649	0.051625	0.15295	0.86574	1100
1200	7.3571	0.13592	4461.6	5141.2	8.5388	2.6186	0.055080	0.16770	0.86008	1200
1400	6.4687	0.15459	4902.0	5675.0	8.8784	2.7168	0.061724	0.19738	0.84960	1400
1600	5.7739	0.17319	5361.1	6227.1	9.1900	2.8016	0.068037	0.22712	0.83927	1600
P = 10,000 kPa (10 MPa)										
50	992.31	0.0010077	207.86	217.94	0.69920	4.1592	0.54854	0.64574	3.5331	50
100	962.93	0.0010385	416.23	426.62	1.2996	4.1935	0.28425	0.68279	1.7458	100
150	922.32	0.0010842	627.27	638.11	1.8313	4.2773	0.18502	0.68744	1.1512	150
200	870.94	0.0011482	844.31	855.80	2.3174	4.4491	0.13670	0.66697	0.91191	200
250	805.70	0.0012412	1073.4	1085.8	2.7792	4.7934	0.10799	0.62346	0.83023	250
300	715.29	0.0013980	1329.4	1343.3	3.2488	5.6807	0.086433	0.55506	0.88459	300
350	44.564	0.022440	2699.6	2924.0	5.9459	4.0117	0.022177	0.069107	1.2874	350
400	37.827	0.026436	2833.1	3097.4	6.2141	3.0953	0.024553	0.068716	1.1060	400
450	33.578	0.029781	2944.5	3242.3	6.4219	2.7473	0.026802	0.071561	1.0289	450
500	30.478	0.032811	3047.0	3375.1	6.5995	2.5830	0.028966	0.075923	0.98547	500
600	26.057	0.038377	3242.0	3625.8	6.9045	2.4576	0.033117	0.087077	0.93470	600
700	22.937	0.043598	3434.0	3870.0	7.1693	2.4370	0.037098	0.10000	0.90406	700
800	20.564	0.048629	3628.2	4114.5	7.4085	2.4571	0.040946	0.11390	0.88328	800
900	18.675	0.053548	3826.5	4362.0	7.6290	2.4952	0.044679	0.12834	0.86867	900
1000	17.126	0.058391	4029.9	4613.8	7.8349	2.5411	0.048306	0.14307	0.85798	1000
1100	15.827	0.063183	4238.5	4870.3	8.0288	2.5898	0.051835	0.15797	0.84979	1100
1200	14.719	0.067939	4452.3	5131.7	8.2126	2.6384	0.055269	0.17295	0.84314	1200
1400	12.924	0.077375	4895.0	5668.7	8.5543	2.7301	0.061876	0.20297	0.83229	1400
1600	11.528	0.086745	5355.6	6223.1	8.8671	2.8110	0.068161	0.23288	0.82276	1600

APPENDIX B.2 (CONTINUED)

Thermophysical Properties of Single Phase Water (SI Units)

T °C	ρ kg/m ³	v m ³ /kg	u kJ/kg	h kJ/kg	s kJ/kg-K	c_p kJ/kg-K	μ mPa-s	k W/m-K	Pr	T °C
P = 50,000 kPa (50 MPa)										
50	1008.7	0.00099138	202.46	252.03	0.68100	4.0816	0.55737	0.66526	3.4197	50
100	980.27	0.0010201	405.93	456.94	1.2705	4.1156	0.29480	0.70446	1.7223	100
150	942.70	0.0010608	610.98	664.02	1.7912	4.1741	0.19471	0.71324	1.1395	150
200	896.97	0.0011149	819.45	875.19	2.2628	4.2827	0.14600	0.69787	0.89596	200
250	842.41	0.0011871	1034.2	1093.5	2.7013	4.4666	0.11782	0.66278	0.79399	250
300	776.48	0.0012879	1259.6	1324.0	3.1218	4.7801	0.098674	0.61003	0.77319	300
350	693.25	0.0014425	1503.9	1576.1	3.5431	5.3746	0.083217	0.54007	0.82816	350
400	577.79	0.0017307	1787.8	1874.4	4.0029	6.7899	0.068075	0.44839	1.0309	400
450	402.04	0.0024873	2160.3	2284.7	4.5896	9.5716	0.050974	0.31973	1.5260	450
500	257.07	0.0038900	2528.1	2722.6	5.1762	7.2889	0.040922	0.20590	1.4486	500
600	163.72	0.0061080	2947.1	3252.5	5.8245	4.1028	0.039185	0.15037	1.0692	600
700	129.59	0.0077166	3228.7	3614.6	6.2178	3.2857	0.041453	0.14796	0.92050	700
800	110.22	0.0090728	3472.2	3925.8	6.5225	2.9831	0.044392	0.15755	0.84055	800
900	97.121	0.010296	3702.0	4216.8	6.7819	2.8556	0.047518	0.17090	0.79399	900
1000	87.405	0.011441	3927.3	4499.4	7.0131	2.8041	0.050694	0.18585	0.76486	1000
1100	79.785	0.012534	4152.2	4778.9	7.2244	2.7902	0.053869	0.20147	0.74606	1100
1200	73.583	0.013590	4378.6	5058.1	7.4207	2.7961	0.057017	0.21726	0.73377	1200
1400	63.977	0.015631	4839.2	5620.8	7.7788	2.8344	0.063187	0.24858	0.72047	1400
1600	56.788	0.017609	5312.1	6192.6	8.1015	2.8845	0.069157	0.27902	0.71494	1600
P = 100,000 kPa (100 MPa)										
50	1027.4	0.00097333	196.59	293.92	0.65865	4.0071	0.57007	0.68738	3.3232	50
100	999.76	0.0010002	395.09	495.11	1.2375	4.0385	0.30772	0.72981	1.7028	100
150	964.85	0.0010364	594.29	697.93	1.7475	4.0781	0.20615	0.74335	1.1310	150
200	923.74	0.0010826	795.14	903.40	2.2064	4.1460	0.15651	0.73314	0.88509	200
250	876.66	0.0011407	999.06	1113.1	2.6277	4.2499	0.12813	0.70539	0.77194	250
300	823.17	0.0012148	1207.6	1329.1	3.0219	4.3987	0.10961	0.66281	0.72739	300
350	762.34	0.0013118	1422.8	1554.0	3.3979	4.6070	0.095916	0.60850	0.72618	350
400	692.93	0.0014431	1646.8	1791.1	3.7639	4.8942	0.084622	0.54536	0.75942	400
450	614.16	0.0016282	1881.9	2044.7	4.1271	5.2577	0.074632	0.47655	0.82340	450
500	528.28	0.0018929	2126.9	2316.2	4.4900	5.5688	0.065842	0.40661	0.90175	500
600	374.21	0.0026723	2597.9	2865.1	5.1581	5.1682	0.054338	0.29451	0.95355	600
700	282.04	0.0035456	2976.1	3330.7	5.6639	4.1810	0.050714	0.24292	0.87286	700
800	230.64	0.0043358	3281.7	3715.3	6.0406	3.5764	0.050780	0.23223	0.78201	800
900	198.32	0.0050424	3551.4	4055.6	6.3440	3.2643	0.052275	0.23619	0.72247	900
1000	175.75	0.0056899	3804.0	4373.0	6.6038	3.1013	0.054397	0.24654	0.68426	1000
1100	158.82	0.0062964	4048.8	4678.4	6.8347	3.0158	0.056827	0.25983	0.65957	1100
1200	145.50	0.0068729	4290.3	4977.6	7.0450	2.9731	0.059419	0.27445	0.64368	1200
1400	125.53	0.0079662	4772.5	5569.1	7.4216	2.9516	0.064813	0.30474	0.62775	1400
1600	111.03	0.0090066	5260.0	6160.6	7.7555	2.9673	0.070273	0.33451	0.62337	1600

APPENDIX B.2 (CONTINUED)

Thermophysical Properties of Single Phase Water (IP Units)

T °F	ρ lbm/ft ³	v ft ³ /lbm	u Btu/ lbm	h Btu/ lbm	s Btu/ lbm-R	c_p Btu/ lbm-R	μ lbm/ft-h	k Btu/h- ft-R	Pr	T °F
P = 1 psia										
50	62.407	0.016024	18.077	18.080	0.036110	1.0028	3.1593	0.33460	9.4680	50
100	61.991	0.016131	68.076	68.078	0.12969	0.99893	1.6473	0.36164	4.5501	100
150	0.0027581	362.57	1061.1	1128.2	2.0166	0.45401	0.026783	0.012389	0.98147	150
200	0.0025476	392.53	1078.2	1150.9	2.0523	0.45400	0.029226	0.013665	0.97098	200
250	0.0023673	422.42	1095.4	1173.6	2.0856	0.45569	0.031760	0.015011	0.96413	250
300	0.0022111	452.26	1112.7	1196.5	2.1167	0.45826	0.034363	0.016422	0.95889	300
350	0.0020743	482.09	1130.2	1219.5	2.1460	0.46136	0.037018	0.017895	0.95440	350
400	0.0019534	511.93	1147.8	1242.6	2.1737	0.46480	0.039713	0.019424	0.95030	400
500	0.0017497	571.53	1183.6	1289.5	2.2253	0.47234	0.045185	0.022641	0.94264	500
600	0.0015844	631.15	1220.2	1337.1	2.2725	0.48040	0.050719	0.026048	0.93541	600
700	0.0014477	690.75	1257.6	1385.6	2.3162	0.48881	0.056274	0.029622	0.92862	700
800	0.0013328	750.30	1295.9	1434.9	2.3570	0.49751	0.061820	0.033344	0.92238	800
900	0.0012347	809.91	1335.1	1485.1	2.3953	0.50644	0.067337	0.037198	0.91678	900
1000	0.0011501	869.49	1375.2	1536.2	2.4316	0.51557	0.072810	0.041168	0.91184	1000
1200	0.0010115	988.63	1458.1	1641.1	2.4989	0.53427	0.083584	0.049410	0.90378	1200
1400	0.00090272	1107.8	1544.8	1749.9	2.5608	0.55312	0.094089	0.057982	0.89756	1400
1600	0.00081506	1226.9	1635.2	1862.4	2.6182	0.57164	0.10430	0.066814	0.89238	1600
1800	0.00074291	1346.1	1729.2	1978.5	2.6720	0.58942	0.11422	0.075848	0.88760	1800
2000	0.00068251	1465.2	1826.7	2098.1	2.7227	0.60617	0.12384	0.085037	0.88278	2000
P = 50 psia										
50	62.417	0.016021	18.074	18.222	0.036103	1.0024	3.1586	0.33473	9.4593	50
100	62.001	0.016129	68.059	68.208	0.12966	0.99872	1.6473	0.36174	4.5481	100
150	61.202	0.016339	118.03	118.18	0.21519	1.0007	1.0391	0.37939	2.7408	150
200	60.128	0.016631	168.18	168.33	0.29424	1.0057	0.73217	0.39001	1.8880	200
250	58.825	0.017000	218.66	218.82	0.36801	1.0146	0.55589	0.39458	1.4293	250
300	0.11398	8.7735	1104.0	1185.2	1.6736	0.52898	0.033860	0.017166	1.0434	300
350	0.10608	9.4268	1123.7	1211.0	1.7064	0.50488	0.036643	0.018547	0.99746	350
400	0.099374	10.063	1142.8	1235.9	1.7363	0.49418	0.039432	0.019989	0.97486	400
500	0.088446	11.306	1180.3	1284.9	1.7902	0.48788	0.045029	0.023058	0.95278	500
600	0.079809	12.530	1217.8	1333.8	1.8387	0.48982	0.050637	0.026357	0.94105	600
700	0.072765	13.743	1255.8	1383.0	1.8830	0.49504	0.056237	0.029857	0.93243	700
800	0.066891	14.950	1294.4	1432.8	1.9243	0.50188	0.061812	0.033532	0.92515	800
900	0.061910	16.152	1333.9	1483.4	1.9629	0.50965	0.067348	0.037358	0.91879	900
1000	0.057628	17.353	1374.1	1534.8	1.9993	0.51801	0.072832	0.041313	0.91323	1000
1200	0.050638	19.748	1457.3	1640.2	2.0670	0.53578	0.083617	0.049547	0.90420	1200
1400	0.045169	22.139	1544.2	1749.1	2.1290	0.55414	0.094125	0.058127	0.89730	1400
1600	0.040770	24.528	1634.7	1861.8	2.1865	0.57236	0.10434	0.066973	0.89168	1600
1800	0.037155	26.914	1728.9	1978.0	2.2403	0.58995	0.11425	0.076023	0.88661	1800
2000	0.034129	29.301	1826.4	2097.7	2.2911	0.60658	0.12387	0.085227	0.88162	2000

APPENDIX B.2 (CONTINUED)

Thermophysical Properties of Single Phase Water (IP Units)

T °F	ρ lbm/ft ³	v ft ³ /lbm	u Btu/ lbm	h Btu/ lbm	s Btu/ lbm-R	c_p Btu/ lbm-R	μ lbm/ft-h	k Btu/h- ft-R	Pr	T °F
P = 100 psia										
50	62.427	0.016019	18.070	18.367	0.036096	1.0021	3.1578	0.33486	9.4504	50
100	62.010	0.016126	68.042	68.340	0.12963	0.99852	1.6474	0.36185	4.5461	100
150	61.211	0.016337	118.00	118.30	0.21514	1.0006	1.0393	0.37950	2.7401	150
200	60.138	0.016628	168.14	168.44	0.29418	1.0055	0.73239	0.39012	1.8877	200
250	58.835	0.016997	218.61	218.92	0.36793	1.0144	0.55611	0.39471	1.4292	250
300	57.320	0.017446	269.65	269.97	0.43744	1.0285	0.44543	0.39396	1.1629	300
350	0.21774	4.5926	1116.2	1201.2	1.6205	0.56717	0.036253	0.019273	1.0669	350
400	0.20260	4.9358	1137.2	1228.6	1.6532	0.53117	0.039143	0.020603	1.0091	400
500	0.17897	5.5875	1176.7	1280.1	1.7100	0.50566	0.044871	0.023499	0.96555	500
600	0.16086	6.2166	1215.2	1330.3	1.7598	0.50008	0.050555	0.026680	0.94760	600
700	0.14632	6.8343	1253.8	1380.4	1.8049	0.50166	0.056202	0.030102	0.93661	700
800	0.13431	7.4455	1292.9	1430.8	1.8466	0.50646	0.061806	0.033728	0.92809	800
900	0.12418	8.0528	1332.6	1481.7	1.8855	0.51298	0.067360	0.037523	0.92089	900
1000	0.11551	8.6573	1373.1	1533.4	1.9222	0.52053	0.072855	0.041461	0.91467	1000
1200	0.10141	9.8610	1456.5	1639.2	1.9900	0.53734	0.083651	0.049688	0.90464	1200
1400	0.090407	11.061	1543.6	1748.4	2.0522	0.55517	0.094163	0.058276	0.89705	1400
1600	0.081577	12.258	1634.2	1861.2	2.1098	0.57309	0.10438	0.067137	0.89096	1600
1800	0.074327	13.454	1728.5	1977.6	2.1637	0.59049	0.11429	0.076202	0.88561	1800
2000	0.068266	14.649	1826.1	2097.4	2.2145	0.60699	0.12390	0.085420	0.88045	2000
P = 500 psia										
50	62.509	0.015998	18.040	19.521	0.036035	0.99967	3.1519	0.33589	9.3806	50
100	62.086	0.016107	67.906	69.397	0.12939	0.99688	1.6481	0.36270	4.5299	100
150	61.286	0.016317	117.78	119.29	0.21477	0.99912	1.0410	0.38033	2.7346	150
200	60.217	0.016607	167.82	169.35	0.29369	1.0041	0.73420	0.39100	1.8853	200
250	58.921	0.016972	218.18	219.75	0.36733	1.0127	0.55787	0.39568	1.4278	250
300	57.416	0.017417	269.09	270.71	0.43671	1.0265	0.44713	0.39504	1.1618	300
350	55.697	0.017954	320.85	322.51	0.50275	1.0471	0.37259	0.39008	1.0002	350
400	53.737	0.018609	373.86	375.58	0.56634	1.0776	0.31922	0.38074	0.90352	400
500	1.0070	0.99305	1140.8	1232.8	1.4938	0.75528	0.043633	0.027913	1.1806	500
600	0.86300	1.1587	1192.2	1299.5	1.5601	0.61119	0.049968	0.029628	1.0308	600
700	0.76664	1.3044	1237.2	1357.9	1.6128	0.56516	0.055986	0.032249	0.98116	700
800	0.69398	1.4410	1280.0	1413.4	1.6588	0.54763	0.061813	0.035402	0.95617	800
900	0.63592	1.5725	1322.3	1467.9	1.7003	0.54182	0.067503	0.038923	0.93966	900
1000	0.58791	1.7009	1364.5	1522.0	1.7387	0.54179	0.073082	0.042711	0.92705	1000
1200	0.51227	1.9521	1450.3	1631.1	1.8088	0.55014	0.083954	0.050850	0.90828	1200
1400	0.45479	2.1988	1538.8	1742.4	1.8721	0.56361	0.094481	0.059495	0.89505	1400
1600	0.40933	2.4430	1630.4	1856.6	1.9304	0.57901	0.10468	0.068465	0.88532	1600
1800	0.37236	2.6856	1725.4	1974.0	1.9848	0.59483	0.11457	0.077649	0.87770	1800
2000	0.34163	2.9271	1823.5	2094.5	2.0359	0.61029	0.12417	0.086978	0.87123	2000

APPENDIX B.2 (CONTINUED)

Thermophysical Properties of Single Phase Water (IP Units)

T °F	ρ lbm/ft ³	v ft ³ /lbm	u Btu/ lbm	h Btu/ lbm	s Btu/ lbm-R	c_p Btu/ lbm-R	μ lbm/ft-h	k Btu/h- ft-R	Pr	T °F
P = 1000 psia										
50	62.611	0.015972	18.002	20.959	0.035953	0.99668	3.1448	0.33717	9.2960	50
100	62.179	0.016083	67.738	70.716	0.12908	0.99488	1.6490	0.36375	4.5102	100
150	61.380	0.016292	117.50	120.51	0.21430	0.99737	1.0431	0.38137	2.7279	150
200	60.315	0.016580	167.42	170.49	0.29309	1.0023	0.73645	0.39211	1.8824	200
250	59.028	0.016941	217.66	220.80	0.36659	1.0106	0.56006	0.39688	1.4262	250
300	57.536	0.017380	268.42	271.64	0.43581	1.0239	0.44924	0.39638	1.1605	300
350	55.835	0.017910	319.98	323.30	0.50167	1.0437	0.37467	0.39155	0.99874	350
400	53.903	0.018552	372.73	376.16	0.56501	1.0727	0.32133	0.38242	0.90138	400
500	49.097	0.020368	484.35	488.12	0.68811	1.1829	0.24789	0.35176	0.83364	500
600	1.9444	0.51430	1154.9	1250.1	1.4466	0.87452	0.049460	0.034841	1.2415	600
700	1.6435	0.60846	1213.2	1325.8	1.5151	0.67947	0.055917	0.035556	1.0686	700
800	1.4531	0.68818	1262.5	1389.9	1.5681	0.61243	0.061984	0.037838	1.0033	800
900	1.3134	0.76138	1308.6	1449.6	1.6137	0.58384	0.067812	0.040895	0.96813	900
1000	1.2037	0.83077	1353.4	1507.2	1.6546	0.57136	0.073468	0.044434	0.94469	1000
1200	1.0381	0.96330	1442.4	1620.8	1.7275	0.56706	0.084400	0.052406	0.91325	1200
1400	0.91658	1.0910	1532.8	1734.8	1.7924	0.57450	0.094924	0.061089	0.89269	1400
1600	0.82230	1.2161	1625.7	1850.9	1.8516	0.58655	0.10510	0.070176	0.87844	1600
1800	0.74652	1.3395	1721.5	1969.5	1.9066	0.60032	0.11495	0.079497	0.86808	1800
2000	0.68402	1.4619	1820.3	2091.0	1.9581	0.61444	0.12451	0.088954	0.86004	2000
P = 5000 psia										
50	63.398	0.015773	17.663	32.267	0.035073	0.97578	3.0972	0.34678	8.7151	50
100	62.905	0.015897	66.454	81.172	0.12661	0.98038	1.6578	0.37181	4.3712	100
150	62.101	0.016103	115.39	130.29	0.21067	0.98445	1.0602	0.38941	2.6801	150
200	61.067	0.016375	164.46	179.63	0.28844	0.98904	0.75427	0.40070	1.8618	200
250	59.840	0.016711	213.76	229.23	0.36092	0.99576	0.57722	0.40628	1.4147	250
300	58.437	0.017112	263.41	279.26	0.42903	1.0059	0.46567	0.40679	1.1515	300
350	56.864	0.017586	313.61	329.90	0.49358	1.0204	0.39064	0.40277	0.98971	350
400	55.111	0.018145	364.60	381.40	0.55530	1.0407	0.33728	0.39528	0.88798	400
500	50.968	0.019620	470.26	488.42	0.67300	1.1070	0.26573	0.36906	0.79703	500
600	45.573	0.021943	584.81	605.12	0.78857	1.2468	0.21578	0.32888	0.81798	600
700	37.345	0.026777	722.26	747.05	0.91627	1.7091	0.16854	0.26995	1.0671	700
800	16.845	0.059365	987.53	1042.5	1.1589	3.5565	0.092113	0.13975	2.3442	800
900	9.6243	0.10390	1156.7	1252.9	1.3207	1.3753	0.080067	0.078107	1.4098	900
1000	7.6172	0.13128	1244.8	1366.4	1.4014	0.97056	0.082413	0.069232	1.1554	1000
1200	5.8191	0.17185	1373.0	1532.1	1.5081	0.73986	0.090913	0.069994	0.96098	1200
1400	4.8761	0.20508	1482.4	1672.3	1.5879	0.67338	0.10021	0.076960	0.87679	1400
1600	4.2545	0.23505	1586.7	1804.3	1.6553	0.65105	0.10952	0.085970	0.82941	1600
1800	3.7994	0.26320	1690.1	1933.8	1.7153	0.64576	0.11871	0.095731	0.80076	1800
2000	3.4456	0.29023	1794.4	2063.1	1.7702	0.64813	0.12772	0.10577	0.78267	2000

APPENDIX B.2 (CONTINUED)

Thermophysical Properties of Single Phase Water (IP Units)

<i>T</i> °F	ρ lbm/ft ³	<i>V</i> ft ³ /lbm	<i>u</i> Btu/ lbm	<i>h</i> Btu/ lbm	<i>s</i> Btu/ lbm-R	<i>c_p</i> Btu/ lbm-R	μ lbm/ft-h	<i>k</i> Btu/h- ft-R	Pr	<i>T</i> °F
P = 10,000 psia										
50	64.320	0.015547	17.169	45.959	0.033492	0.95587	3.0602	0.35740	8.1847	50
100	63.757	0.015685	64.981	94.024	0.12345	0.96555	1.6726	0.38110	4.2377	100
150	62.945	0.015887	113.02	142.44	0.20631	0.97080	1.0821	0.39889	2.6335	150
200	61.940	0.016145	161.19	191.09	0.28299	0.97503	0.77624	0.41092	1.8418	200
250	60.770	0.016455	209.49	239.96	0.35441	0.98029	0.59800	0.41750	1.4041	250
300	59.453	0.016820	258.01	289.15	0.42139	0.98778	0.48528	0.41915	1.1436	300
350	57.997	0.017242	306.86	338.79	0.48466	0.99820	0.40939	0.41646	0.98127	350
400	56.402	0.017730	356.20	389.03	0.54487	1.0121	0.35557	0.41019	0.87735	400
500	52.766	0.018952	457.04	492.14	0.65829	1.0534	0.28452	0.38803	0.77240	500
600	48.409	0.020657	562.35	600.60	0.76574	1.1217	0.23787	0.35461	0.75241	600
700	43.048	0.023230	675.11	718.12	0.87164	1.2404	0.20120	0.31139	0.80149	700
800	36.171	0.027646	800.78	851.97	0.98223	1.4572	0.16758	0.25864	0.94415	800
900	27.645	0.036173	943.79	1010.8	1.1034	1.6854	0.13616	0.19772	1.1607	900
1000	20.204	0.049495	1082.7	1174.3	1.2196	1.5138	0.11578	0.14614	1.1993	1000
1200	13.230	0.075586	1278.2	1418.1	1.3768	0.99601	0.10692	0.10838	0.98253	1200
1400	10.390	0.096246	1417.1	1595.3	1.4778	0.80717	0.11064	0.10492	0.85121	1400
1600	8.7826	0.11386	1537.5	1748.3	1.5560	0.73348	0.11720	0.11052	0.77781	1600
1800	7.7049	0.12979	1651.1	1891.4	1.6224	0.70193	0.12467	0.11899	0.73545	1800
2000	6.9124	0.14467	1762.4	2030.3	1.6813	0.68897	0.13250	0.12859	0.70987	2000
P = 50,000 psia										
50	69.921	0.014302	12.552	144.97	0.011806	0.89599	3.3971	0.40763	7.4669	50
100	69.082	0.014476	56.431	190.46	0.096932	0.91626	1.9333	0.43420	4.0797	100
150	68.207	0.014661	100.56	236.30	0.17539	0.91668	1.2939	0.45876	2.5855	150
200	67.288	0.014861	144.50	282.10	0.24759	0.91519	0.95800	0.47848	1.8324	200
250	66.320	0.015078	188.23	327.83	0.31442	0.91446	0.75881	0.49278	1.4082	250
300	65.301	0.015314	231.78	373.56	0.37668	0.91474	0.63029	0.50200	1.1485	300
350	64.236	0.015568	275.19	419.32	0.43502	0.91580	0.54212	0.50683	0.97957	350
400	63.130	0.015840	318.49	465.15	0.48994	0.91739	0.47878	0.50799	0.86463	400
500	60.813	0.016444	404.83	557.08	0.59110	0.92130	0.39540	0.50178	0.72599	500
600	58.383	0.017128	490.83	649.41	0.68262	0.92533	0.34399	0.48727	0.65324	600
700	55.867	0.017900	576.40	742.13	0.76623	0.92887	0.30928	0.46731	0.61474	700
800	53.294	0.018764	661.43	835.16	0.84317	0.93153	0.28383	0.44417	0.59526	800
900	50.691	0.019727	745.75	928.40	0.91440	0.93309	0.26377	0.41917	0.58716	900
1000	48.087	0.020796	829.19	1021.7	0.98064	0.93339	0.24703	0.39400	0.58521	1000
1200	43.011	0.023250	992.82	1208.1	1.1003	0.92856	0.21988	0.34803	0.58664	1200
1400	38.339	0.026083	1150.8	1392.3	1.2051	0.91135	0.19946	0.31288	0.58097	1400
1600	34.300	0.029155	1301.8	1571.8	1.2968	0.88186	0.18538	0.29140	0.56101	1600
1800	30.952	0.032308	1445.8	1744.9	1.3770	0.84961	0.17679	0.28077	0.53496	1800
2000	28.212	0.035446	1583.8	1911.9	1.4479	0.82212	0.17234	0.27774	0.51012	2000

APPENDIX B.3

Thermophysical Properties of Liquids at Saturation (SI Units)

<i>T</i> °C	<i>P</i> _{sat} kPa	ρ kg/m ³	<i>h</i> _{fg} kJ/kg	<i>c</i> _p kJ/ kg·K	μ mPa·s	ν mm ² /s	<i>k</i> W/m·K	α mm ² /s	Pr	<i>T</i> °C
Water										
5	0.87258	999.92	2489.0	4.2055	1.5183	1.5184	0.56772	0.13501	11.247	5
10	1.2282	999.65	2477.2	4.1955	1.3060	1.3064	0.57871	0.13798	9.4682	10
15	1.7058	999.06	2465.4	4.1888	1.1376	1.1387	0.58874	0.14068	8.0940	15
20	2.3393	998.16	2453.5	4.1844	1.0016	1.0035	0.59795	0.14317	7.0092	20
25	3.1699	997.00	2441.7	4.1816	0.89004	0.89271	0.60646	0.14547	6.1369	25
30	4.2470	995.61	2429.8	4.1801	0.79722	0.80074	0.61434	0.14762	5.4245	30
35	5.6290	993.99	2417.9	4.1795	0.71912	0.72347	0.62165	0.14964	4.8348	35
40	7.3849	992.18	2406.0	4.1796	0.65272	0.65786	0.62844	0.15154	4.3411	40
45	9.5950	990.17	2394.0	4.1804	0.59575	0.60167	0.63474	0.15334	3.9236	45
50	12.352	988.00	2381.9	4.1815	0.54650	0.55314	0.64057	0.15505	3.5674	50
60	19.946	983.16	2357.7	4.1851	0.46602	0.47400	0.65096	0.15820	2.9961	60
70	31.201	977.73	2333.0	4.1902	0.40353	0.41272	0.65972	0.16103	2.5630	70
80	47.414	971.77	2308.0	4.1969	0.35404	0.36432	0.66697	0.16354	2.2278	80
90	70.182	965.30	2282.5	4.2053	0.31417	0.32546	0.67277	0.16573	1.9638	90
100	101.42	958.35	2256.4	4.2157	0.28158	0.29382	0.67721	0.16762	1.7529	100
150	476.16	917.01	2113.7	4.3071	0.18261	0.19914	0.68102	0.17243	1.1549	150
200	1554.9	864.66	1939.7	4.4958	0.13458	0.15565	0.66001	0.16978	0.91675	200
250	3976.2	798.89	1715.2	4.8701	0.10628	0.13304	0.61689	0.15855	0.83908	250
300	8587.9	712.14	1404.6	5.7504	0.085855	0.12056	0.55265	0.13495	0.89334	300
Ammonia										
−60	21.893	713.62	1441.8	4.3031	0.39129	0.54832	0.75700	0.24652	2.2242	−60
−50	40.836	702.09	1415.9	4.3599	0.32887	0.46841	0.72228	0.23596	1.9851	−50
−40	71.692	690.15	1388.6	4.4137	0.28124	0.40751	0.68811	0.22590	1.8040	−40
−30	119.43	677.83	1359.7	4.4645	0.24407	0.36008	0.65463	0.21632	1.6646	−30
−20	190.08	665.14	1329.1	4.5138	0.21441	0.32235	0.62196	0.20716	1.5560	−20
−10	290.71	652.06	1296.7	4.5636	0.19022	0.29172	0.59014	0.19832	1.4710	−10
0	429.38	638.57	1262.2	4.6165	0.17009	0.26636	0.55920	0.18969	1.4042	0
10	615.05	624.64	1225.5	4.6757	0.15303	0.24499	0.52912	0.18117	1.3523	10
20	857.48	610.20	1186.4	4.7448	0.13832	0.22668	0.49986	0.17265	1.3130	20
30	1167.2	595.17	1144.4	4.8282	0.12545	0.21078	0.47135	0.16403	1.2850	30
40	1555.4	579.44	1099.3	4.9318	0.11404	0.19681	0.44354	0.15521	1.2680	40
50	2034.0	562.86	1050.5	5.0635	0.10379	0.18440	0.41632	0.14607	1.2624	50
60	2615.6	545.24	997.30	5.2351	0.094483	0.17329	0.38959	0.13649	1.2696	60
70	3313.5	526.31	938.90	5.4648	0.085933	0.16328	0.36324	0.12629	1.2928	70
80	4142.0	505.67	873.97	5.7837	0.077979	0.15421	0.33710	0.11526	1.3379	80
90	5116.7	482.75	800.58	6.2501	0.070468	0.14597	0.31102	0.10308	1.4161	90
100	6255.3	456.63	715.63	6.9912	0.063231	0.13847	0.28477	0.089202	1.5523	100
110	7578.3	425.61	613.39	8.3621	0.056028	0.13164	0.25813	0.072528	1.8151	110
120	9112.5	385.49	480.31	11.940	0.048340	0.12540	0.23124	0.050238	2.4961	120

APPENDIX B.3 (CONTINUED)

Thermophysical Properties of Liquids at Saturation (SI Units)

<i>T</i> °C	<i>P</i> _{sat} kPa	<i>ρ</i> kg/m ³	<i>h</i> _{fg} kJ/kg	<i>c</i> _p kJ/ kg·K	<i>μ</i> mPa·s	<i>ν</i> mm ² /s	<i>k</i> W/m·K	<i>α</i> mm ² /s	Pr	<i>T</i> °C
Propane										
−100	2.8994	643.74	480.44	2.0538	0.42569	0.66127	0.16437	0.12432	5.3190	−100
−80	13.049	622.76	462.41	2.1059	0.31590	0.50726	0.15206	0.11595	4.3750	−80
−60	42.693	601.08	443.63	2.1720	0.24359	0.40526	0.13981	0.10709	3.7844	−60
−40	111.12	578.43	423.36	2.2558	0.19255	0.33288	0.12795	0.098058	3.3948	−40
−30	167.83	566.64	412.41	2.3054	0.17232	0.30411	0.12221	0.093552	3.2508	−30
−20	244.52	554.45	400.77	2.3608	0.15473	0.27906	0.11662	0.089096	3.1322	−20
−10	345.28	541.80	388.30	2.4230	0.13928	0.25706	0.11121	0.084712	3.0346	−10
−5	406.04	535.27	381.72	2.4570	0.13223	0.24704	0.10857	0.082551	2.9926	−5
0	474.46	528.59	374.87	2.4932	0.12559	0.23759	0.10597	0.080412	2.9547	0
5	551.12	521.75	367.73	2.5318	0.11930	0.22866	0.10343	0.078295	2.9205	5
10	636.60	514.73	360.28	2.5733	0.11335	0.22021	0.10093	0.076198	2.8899	10
20	836.46	500.06	344.31	2.6662	0.10229	0.20455	0.096073	0.072059	2.8387	20
30	1079.0	484.39	326.70	2.7767	0.092188	0.19032	0.091409	0.067961	2.8004	30
40	1369.4	467.46	307.07	2.9127	0.082844	0.17722	0.086923	0.063839	2.7760	40
50	1713.3	448.87	284.86	3.0893	0.074066	0.16501	0.082598	0.059565	2.7702	50
60	2116.8	427.97	259.23	3.3375	0.065654	0.15341	0.078398	0.054887	2.7950	60
70	2586.8	403.62	228.62	3.7350	0.057364	0.14212	0.074277	0.049271	2.8845	70
80	3131.9	373.29	189.80	4.5445	0.048787	0.13069	0.070213	0.041389	3.1577	80
90	3764.1	328.83	132.77	7.6233	0.038819	0.11805	0.067139	0.026783	4.4077	90
Pentane										
−80	0.10043	717.29	440.72	1.9990	0.78523	1.0947	0.15551	0.10846	10.093	−80
−40	2.7187	681.58	412.64	2.0792	0.41915	0.61496	0.13791	0.097314	6.3193	−40
−20	9.0283	663.44	398.87	2.1384	0.33262	0.50136	0.12935	0.091172	5.4990	−20
−10	15.191	654.22	391.89	2.1727	0.29997	0.45851	0.12520	0.088078	5.2057	−10
0	24.448	644.87	384.81	2.2099	0.27220	0.42210	0.12113	0.084997	4.9660	0
10	37.835	635.37	377.56	2.2500	0.24825	0.39071	0.11716	0.081953	4.7675	10
20	56.558	625.70	370.11	2.2929	0.22732	0.36331	0.11329	0.078964	4.6010	20
30	81.993	615.82	362.40	2.3385	0.20883	0.33911	0.10951	0.076044	4.4594	30
40	115.67	605.70	354.38	2.3870	0.19232	0.31752	0.10584	0.073207	4.3373	40
50	159.25	595.30	346.01	2.4382	0.17744	0.29806	0.10227	0.070459	4.2303	50
60	214.54	584.59	337.22	2.4925	0.16391	0.28038	0.098799	0.067805	4.1350	60
70	283.46	573.51	327.94	2.5501	0.15150	0.26416	0.095426	0.065249	4.0486	70
80	368.01	562.01	318.11	2.6113	0.14005	0.24919	0.092149	0.062789	3.9687	80
90	470.34	550.01	307.63	2.6770	0.12939	0.23524	0.088964	0.060421	3.8934	90
100	592.65	537.42	296.40	2.7482	0.11940	0.22216	0.085868	0.058139	3.8212	100
120	906.71	510.00	271.14	2.9137	0.10100	0.19803	0.079923	0.053785	3.6819	120
140	1330.5	478.31	240.75	3.1340	0.084073	0.17577	0.074275	0.049548	3.5474	140
160	1887.9	439.49	202.15	3.4903	0.067854	0.15439	0.068887	0.044908	3.4379	160
180	2609.9	385.55	146.99	4.4391	0.051042	0.13239	0.063884	0.037326	3.5468	180

APPENDIX B.3 (CONTINUED)

Thermophysical Properties of Liquids at Saturation (SI Units)

<i>T</i> °C	<i>P</i> _{sat} kPa	ρ kg/m ³	<i>h</i> _{fg} kJ/kg	<i>c</i> _p kJ/ kg·K	μ mPa·s	ν mm ² /s	<i>k</i> W/m·K	α mm ² /s	Pr	<i>T</i> °C
Hexane										
−50	0.20366	721.49	412.78	1.9903	0.81257	1.1262	0.14730	0.10257	10.980	−50
−40	0.46089	712.71	406.50	2.0189	0.68420	0.96000	0.14312	0.099466	9.6516	−40
−30	0.96456	703.92	400.26	2.0493	0.58487	0.83087	0.13912	0.096439	8.6156	−30
−20	1.8855	695.11	394.03	2.0817	0.50631	0.72839	0.13528	0.093491	7.7911	−20
−10	3.4719	686.25	387.79	2.1161	0.44302	0.64556	0.13160	0.090626	7.1233	−10
0	6.0652	677.34	381.52	2.1525	0.39118	0.57753	0.12809	0.087857	6.5735	0
10	10.114	668.35	375.18	2.1909	0.34813	0.52088	0.12472	0.085177	6.1152	10
20	16.187	659.27	368.74	2.2312	0.31192	0.47313	0.12149	0.082595	5.7283	20
30	24.973	650.07	362.17	2.2733	0.28112	0.43245	0.11839	0.080115	5.3979	30
40	37.292	640.74	355.45	2.3172	0.25467	0.39746	0.11542	0.077741	5.1126	40
60	76.424	621.60	341.38	2.4100	0.21169	0.34056	0.10984	0.073325	4.6445	60
80	142.54	601.63	326.24	2.5094	0.17836	0.29647	0.10471	0.069357	4.2745	80
100	246.29	580.60	309.70	2.6161	0.15178	0.26141	0.099987	0.065829	3.9711	100
120	399.76	558.16	291.35	2.7318	0.12999	0.23289	0.095627	0.062714	3.7136	120
140	616.32	533.84	270.63	2.8612	0.11165	0.20915	0.091587	0.059963	3.4879	140
160	910.70	506.85	246.68	3.0142	0.095730	0.18887	0.087815	0.057480	3.2859	160
180	1299.6	475.83	218.02	3.2169	0.081352	0.17097	0.084245	0.055037	3.1065	180
200	1803.4	437.73	181.55	3.5578	0.067525	0.15426	0.080798	0.051882	2.9733	200
220	2450.9	382.16	127.74	4.6726	0.052142	0.13644	0.077711	0.043519	3.1352	220
Heptane										
−60	0.010397	750.18	419.34	2.0026	1.5345	2.0455	0.14821	0.098656	20.734	−60
−40	0.077005	733.56	405.97	2.0420	0.99774	1.3601	0.14210	0.094868	14.337	−40
−20	0.39420	717.02	393.11	2.0922	0.70470	0.98282	0.13591	0.090599	10.848	−20
0	1.5223	700.45	380.59	2.1526	0.52712	0.75255	0.12973	0.086037	8.7468	0
10	2.7467	692.11	374.39	2.1863	0.46334	0.66946	0.12666	0.083705	7.9978	10
20	4.7222	683.72	368.21	2.2221	0.41085	0.60090	0.12363	0.081374	7.3844	20
30	7.7770	675.27	362.01	2.2597	0.36706	0.54358	0.12063	0.079052	6.8762	30
40	12.326	666.72	355.77	2.2992	0.33007	0.49507	0.11766	0.076757	6.4498	40
60	28.039	649.32	343.04	2.3827	0.27127	0.41778	0.11186	0.072299	5.7785	60
80	57.090	631.36	329.77	2.4717	0.22681	0.35924	0.10624	0.068077	5.2770	80
100	106.23	612.67	315.71	2.5658	0.19210	0.31354	0.10082	0.064136	4.8887	100
120	183.60	593.03	300.58	2.6653	0.16422	0.27693	0.095614	0.060493	4.5778	120
140	298.61	572.12	284.03	2.7714	0.14126	0.24690	0.090607	0.057145	4.3206	140
160	461.74	549.53	265.61	2.8874	0.12184	0.22171	0.085784	0.054064	4.1009	160
180	684.66	524.57	244.66	3.0201	0.10495	0.20007	0.081105	0.051193	3.9082	180
200	980.41	496.14	220.14	3.1853	0.089771	0.18094	0.076509	0.048413	3.7375	200
220	1364.2	462.01	190.09	3.4269	0.075454	0.16332	0.071899	0.045413	3.5963	220
240	1855.1	416.64	149.97	3.9284	0.060780	0.14588	0.067211	0.041064	3.5525	240
260	2479.4	335.09	82.509	7.2271	0.041997	0.12533	0.064864	0.026785	4.6792	260

APPENDIX B.3 (CONTINUED)

Thermophysical Properties of Liquids at Saturation (SI Units)

<i>T</i> °C	<i>P</i> _{sat} kPa	ρ kg/m ³	<i>h</i> _{fg} kJ/kg	<i>c</i> _p kJ/ kg·K	μ mPa·s	ν mm ² /s	<i>k</i> W/m·K	α mm ² /s	Pr	<i>T</i> °C
Octane										
−40	0.012988	750.20	404.85	2.0404	1.4814	1.9747	0.14666	0.095817	20.609	−40
−20	0.083067	734.17	391.98	2.0866	0.98686	1.3442	0.13930	0.090930	14.783	−20
10	0.75269	710.22	373.52	2.1752	0.61684	0.86853	0.12914	0.083592	10.390	10
0	0.38526	718.21	379.58	2.1433	0.71102	0.98999	0.13242	0.086020	11.509	0
10	0.75269	710.22	373.52	2.1752	0.61684	0.86853	0.12914	0.083592	10.390	10
20	1.3916	702.20	367.53	2.2090	0.54141	0.77102	0.12595	0.081198	9.4956	20
40	4.1263	686.04	355.65	2.2821	0.42907	0.62543	0.11987	0.076565	8.1687	40
60	10.450	669.61	343.76	2.3610	0.35007	0.52281	0.11410	0.072172	7.2439	60
80	23.298	652.79	331.67	2.4445	0.29170	0.44686	0.10860	0.068058	6.5659	80
100	46.824	635.45	319.17	2.5318	0.24674	0.38829	0.10335	0.064237	6.0447	100
120	86.423	617.43	306.03	2.6225	0.21086	0.34151	0.098299	0.060708	5.6255	120
140	148.66	598.53	292.02	2.7169	0.18135	0.30300	0.093434	0.057457	5.2734	140
160	241.17	578.48	276.85	2.8161	0.15645	0.27045	0.088722	0.054463	4.9657	160
180	372.53	556.91	260.16	2.9223	0.13494	0.24230	0.084137	0.051699	4.6867	180
200	552.24	533.27	241.43	3.0403	0.11596	0.21745	0.079653	0.049129	4.4262	200
220	790.84	506.68	219.89	3.1805	0.098855	0.19510	0.075248	0.046695	4.1783	220
240	1100.3	475.51	194.21	3.3681	0.083037	0.17463	0.070916	0.044279	3.9438	240
260	1495.1	436.27	161.58	3.6869	0.067831	0.15548	0.066742	0.041493	3.7471	260
280	1995.0	378.16	113.81	4.6731	0.051845	0.13710	0.063640	0.036012	3.8071	280
Nonane										
−40	0.0023016	765.37	401.57	2.0099	2.3580	3.0808	0.14782	0.096089	32.062	−40
−20	0.018188	749.46	389.10	2.0606	1.3789	1.8399	0.14066	0.091083	20.200	−20
0	0.10056	733.69	377.09	2.1212	0.94012	1.2814	0.13410	0.086167	14.871	0
20	0.42095	717.95	365.44	2.1896	0.69754	0.97158	0.12807	0.081466	11.926	20
40	1.4136	702.14	354.04	2.2639	0.54552	0.77694	0.12249	0.077060	10.082	40
60	3.9784	686.18	342.75	2.3425	0.44174	0.64376	0.11732	0.072986	8.8203	60
80	9.7038	669.98	331.42	2.4245	0.36631	0.54675	0.11250	0.069256	7.8947	80
100	21.057	653.42	319.91	2.5090	0.30880	0.47260	0.10798	0.065864	7.1754	100
120	41.500	636.39	308.02	2.5957	0.26328	0.41372	0.10373	0.062796	6.5883	120
140	75.519	618.75	295.58	2.6843	0.22615	0.36550	0.099707	0.060031	6.0884	140
160	128.59	600.34	282.38	2.7753	0.19509	0.32497	0.095872	0.057543	5.6475	160
180	207.09	580.92	268.17	2.8694	0.16856	0.29015	0.092184	0.055303	5.2467	180
200	318.26	560.20	252.65	2.9685	0.14545	0.25964	0.088598	0.053277	4.8735	200
220	470.16	537.72	235.40	3.0761	0.12497	0.23240	0.085061	0.051424	4.5193	220
240	671.82	512.80	215.80	3.1993	0.10646	0.20760	0.081502	0.049678	4.1788	240
260	933.60	484.23	192.78	3.3544	0.089332	0.18448	0.077827	0.047915	3.8503	260
280	1268.1	449.57	164.28	3.5893	0.072933	0.16223	0.073892	0.045792	3.5427	280
300	1692.7	402.26	124.95	4.1366	0.056076	0.13940	0.069525	0.041783	3.3364	300
320	2238.0	289.18	37.983	25.073	0.031260	0.10810	0.078846	0.010875	9.9406	320

APPENDIX B.3 (CONTINUED)

Thermophysical Properties of Liquids at Saturation (SI Units)

<i>T</i> °C	<i>P</i> _{sat} kPa	<i>ρ</i> kg/m ³	<i>h</i> _{fg} kJ/kg	<i>c</i> _p kJ/ kg·K	<i>μ</i> mPa·s	<i>ν</i> mm ² /s	<i>k</i> W/m·K	<i>α</i> mm ² /s	Pr	<i>T</i> °C
Decane										
−20	0.0039896	761.59	386.87	2.0404	1.9189	2.5196	0.14144	0.091021	27.682	−20
0	0.026319	745.90	375.18	2.1040	1.2731	1.7068	0.13604	0.086682	19.690	0
20	0.12780	730.33	363.83	2.1742	0.91238	1.2493	0.13074	0.082337	15.173	20
40	0.48671	714.78	352.74	2.2494	0.68976	0.96499	0.12557	0.078101	12.356	40
60	1.5248	699.16	341.82	2.3282	0.54215	0.77543	0.12053	0.074047	10.472	60
80	4.0763	683.38	330.95	2.4096	0.43875	0.64203	0.11563	0.070222	9.1428	80
100	9.5701	667.35	320.02	2.4929	0.36304	0.54401	0.11090	0.066658	8.1612	100
120	20.184	650.97	308.87	2.5775	0.30554	0.46935	0.10633	0.063370	7.4065	120
140	38.944	634.13	297.37	2.6632	0.26046	0.41074	0.10195	0.060367	6.8041	140
160	69.756	616.67	285.32	2.7499	0.22415	0.36349	0.097764	0.057651	6.3050	160
180	117.39	598.44	272.55	2.8380	0.19419	0.32449	0.093789	0.055223	5.8761	180
200	187.42	579.21	258.83	2.9284	0.16891	0.29162	0.090036	0.053082	5.4937	200
220	286.20	558.65	243.88	3.0228	0.14712	0.26335	0.086512	0.051229	5.1407	220
240	420.86	536.33	227.30	3.1245	0.12795	0.23857	0.083224	0.049664	4.8038	240
260	599.39	511.52	208.51	3.2397	0.11070	0.21641	0.080176	0.048381	4.4730	260
280	830.94	483.02	186.56	3.3828	0.094727	0.19611	0.077367	0.047349	4.1419	280
300	1126.4	448.49	159.62	3.5932	0.079368	0.17697	0.074807	0.046421	3.8123	300
320	1500.1	402.23	123.34	4.0398	0.063558	0.15801	0.072646	0.044707	3.5345	320
340	1974.8	317.26	57.874	8.5345	0.043216	0.13622	0.075060	0.027721	4.9138	340
Dodecane										
0	0.0017553	764.28	376.34	2.1375	2.2663	2.9652	0.14146	0.086590	34.245	0
20	0.011684	749.36	364.36	2.1964	1.4866	1.9838	0.13647	0.082916	23.926	20
40	0.057945	734.56	352.90	2.2626	1.0596	1.4425	0.13172	0.079254	18.201	40
60	0.22694	719.77	341.84	2.3340	0.79919	1.1103	0.12715	0.075689	14.670	60
80	0.73371	704.91	331.08	2.4091	0.62760	0.89033	0.12274	0.072276	12.319	80
100	2.0269	689.88	320.52	2.4870	0.50761	0.73580	0.11845	0.069041	10.657	100
120	4.9161	674.60	310.04	2.5666	0.41956	0.62193	0.11427	0.065998	9.4235	120
140	10.699	658.97	299.50	2.6475	0.35230	0.53462	0.11017	0.063151	8.4658	140
160	21.267	642.88	288.77	2.7292	0.29915	0.46533	0.10614	0.060495	7.6921	160
180	39.168	626.21	277.70	2.8118	0.25594	0.40871	0.10217	0.058026	7.0435	180
200	67.635	608.82	266.11	2.8952	0.21992	0.36122	0.098248	0.055738	6.4807	200
220	110.58	590.53	253.82	2.9800	0.18926	0.32049	0.094367	0.053626	5.9765	220
240	172.59	571.10	240.61	3.0669	0.16267	0.28484	0.090527	0.051685	5.5110	240
260	258.91	550.25	226.23	3.1575	0.13925	0.25306	0.086729	0.049919	5.0694	260
280	375.49	527.53	210.32	3.2545	0.11830	0.22425	0.082981	0.048334	4.6396	280
300	529.05	502.35	192.41	3.3630	0.099309	0.19769	0.079303	0.046941	4.2115	300
320	727.34	473.69	171.72	3.4942	0.081853	0.17280	0.075730	0.045753	3.7767	320
340	979.60	439.82	146.96	3.6770	0.065539	0.14901	0.072340	0.044731	3.3313	340
360	1297.7	396.77	115.18	4.0295	0.049828	0.12558	0.069335	0.043367	2.8958	360

APPENDIX B.3 (CONTINUED)

Thermophysical Properties of Liquids at Saturation (SI Units)

<i>T</i> °C	<i>P</i> _{sat} kPa	<i>ρ</i> kg/m ³	<i>h</i> _{fg} kJ/kg	<i>c</i> _{<i>p</i>} kJ/ kg·K	<i>μ</i> mPa·s	<i>ν</i> mm ² /s	<i>k</i> W/m·K	<i>α</i> mm ² /s	Pr	<i>T</i> °C
Methanol										
−80	0.0025173	887.13	1296.9	2.2124	5.8336	6.5758	0.25568	0.13027	50.479	−80
−60	0.028074	867.24	1276.4	2.2267	2.9632	3.4169	0.24074	0.12467	27.408	−60
−40	0.20096	847.70	1254.6	2.2652	1.7755	2.0945	0.22826	0.11887	17.620	−40
−20	1.0283	828.52	1231.0	2.3224	1.1615	1.4019	0.21794	0.11326	12.378	−20
10	7.4384	800.28	1191.2	2.4496	0.68284	0.85325	0.20571	0.10493	8.1314	10
0	4.0562	809.65	1205.1	2.4011	0.80548	0.99485	0.20941	0.10772	9.2356	0
10	7.4384	800.28	1191.2	2.4496	0.68284	0.85325	0.20571	0.10493	8.1314	10
20	13.032	790.93	1176.6	2.5047	0.58498	0.73962	0.20233	0.10214	7.2416	20
40	35.518	772.10	1145.0	2.6340	0.44145	0.57176	0.19637	0.096555	5.9216	40
60	84.713	752.79	1109.6	2.7880	0.34372	0.45659	0.19119	0.091094	5.0123	60
80	181.11	732.58	1069.2	2.9658	0.27424	0.37435	0.18651	0.085844	4.3608	80
100	353.73	710.95	1022.1	3.1689	0.22275	0.31332	0.18212	0.080837	3.8760	100
120	640.81	687.29	966.15	3.4024	0.18306	0.26635	0.17782	0.076041	3.5027	120
140	1090.2	660.83	898.89	3.6783	0.15129	0.22894	0.17346	0.071360	3.2082	140
160	1759.6	630.42	817.72	4.0224	0.12497	0.19823	0.16893	0.066617	2.9757	160
180	2715.8	594.32	723.80	4.4939	0.10251	0.17248	0.16421	0.061482	2.8053	180
200	4027.0	549.21	621.13	5.2742	0.082795	0.15075	0.15957	0.055089	2.7365	200
220	5787.7	484.87	467.93	7.5369	0.064314	0.13264	0.15743	0.043078	3.0791	220
240	8182.6	310.87	73.259	390.28	0.038619	0.12423	0.26891	0.0022164	56.049	240
Ethanol										
−80	0.00040787	875.68	1014.2	1.9428	3.8662	4.4150	0.19801	0.11639	37.933	−80
−60	0.0061203	857.77	997.73	1.9811	2.2846	2.6634	0.18843	0.11088	24.020	−60
−40	0.055632	840.37	981.23	2.0479	1.5075	1.7938	0.18060	0.10494	17.094	−40
−20	0.34589	823.28	964.14	2.1414	2.9166	3.5427	0.17418	0.098800	35.857	−20
10	3.1485	797.86	936.24	2.3236	1.4638	1.8347	0.16657	0.089848	20.420	10
0	1.6017	806.34	945.94	2.2571	1.8177	2.2542	0.16888	0.092789	24.294	0
10	3.1485	797.86	936.24	2.3236	1.4638	1.8347	0.16657	0.089848	20.420	10
20	5.8759	789.34	926.01	2.3961	1.1931	1.5115	0.16445	0.086949	17.384	20
40	17.880	772.01	903.52	2.5590	0.81899	1.0609	0.16065	0.081318	13.046	40
60	46.734	753.99	877.53	2.7438	0.58416	0.77476	0.15726	0.076015	10.192	60
80	107.81	734.85	847.02	2.9481	0.43008	0.58527	0.15408	0.071124	8.2289	80
100	224.17	714.02	810.92	3.1739	0.32453	0.45451	0.15096	0.066616	6.8229	100
120	427.30	690.78	768.09	3.4249	0.24908	0.36058	0.14777	0.062460	5.7729	120
140	756.55	664.23	717.34	3.6958	0.19300	0.29057	0.14444	0.058839	4.9383	140
160	1257.6	633.44	657.70	3.9678	0.15017	0.23707	0.14105	0.056118	4.2245	160
180	1980.7	597.60	588.18	4.2485	0.11713	0.19600	0.13779	0.054273	3.6113	180
200	2980.6	554.99	505.72	4.6872	0.091299	0.16450	0.13490	0.051859	3.1722	200
220	4320.5	497.13	397.54	6.0630	0.069103	0.13900	0.13288	0.044087	3.1529	220
240	6094.7	333.83	122.67	63.991	0.037405	0.11205	0.17769	0.0083181	13.470	240

APPENDIX B.3 (CONTINUED)

Thermophysical Properties of Liquids at Saturation (SI Units)

<i>T</i> °C	<i>P</i> _{sat} kPa	ρ kg/m ³	<i>h</i> _{fg} kJ/kg	<i>c</i> _p kJ/ kg·K	μ mPa·s	ν mm ² /s	<i>k</i> W/m·K	α mm ² /s	Pr	<i>T</i> °C
Acetone										
−80	0.015650	897.33	634.81	1.9969	1.6933	1.8870	0.19740	0.11016	17.130	−80
−60	0.13085	876.00	615.66	2.0099	1.0035	1.1455	0.18978	0.10779	10.628	−60
−40	0.72172	854.82	596.79	2.0281	0.68472	0.80102	0.18183	0.10488	7.6375	−40
−20	2.9169	833.58	577.95	2.0540	0.50851	0.61003	0.17366	0.10143	6.0144	−20
10	15.454	801.21	549.13	2.1087	0.35657	0.44504	0.16130	0.095471	4.6615	10
0	9.2991	812.10	558.87	2.0883	0.39775	0.48978	0.16540	0.097527	5.0220	0
10	15.454	801.21	549.13	2.1087	0.35657	0.44504	0.16130	0.095471	4.6615	10
20	24.662	790.19	539.22	2.1311	0.32192	0.40739	0.15720	0.093349	4.3642	20
40	56.582	767.66	518.73	2.1822	0.26705	0.34787	0.14907	0.088987	3.9093	40
60	115.67	744.28	497.07	2.2417	0.22586	0.30346	0.14109	0.084564	3.5886	60
80	215.48	719.79	473.88	2.3102	0.19410	0.26966	0.13332	0.080171	3.3636	80
100	372.30	693.84	448.71	2.3895	0.16904	0.24363	0.12578	0.075864	3.2115	100
110	477.84	680.19	435.21	2.4341	0.15842	0.23291	0.12210	0.073749	3.1581	110
120	604.83	666.00	420.97	2.4828	0.14883	0.22347	0.11850	0.071660	3.1184	120
140	934.13	635.64	389.81	2.5969	0.13213	0.20786	0.11148	0.067534	3.0779	140
160	1383.8	601.79	353.96	2.7457	0.11791	0.19594	0.10471	0.063371	3.0919	160
180	1980.9	562.85	311.35	2.9628	0.10534	0.18715	0.098144	0.058852	3.1800	180
200	2757.9	515.54	257.85	3.3565	0.093515	0.18139	0.091688	0.052986	3.4234	200
220	3757.4	449.93	182.00	4.6149	0.080823	0.17964	0.085422	0.041139	4.3665	220
Benzene										
10	0.0060742	889.31	444.41	1.6954	0.76992	0.86575	0.14637	0.097079	8.9180	10
20	0.010030	878.84	437.15	1.7204	0.66038	0.75141	0.14289	0.094507	7.9509	20
30	0.015919	868.31	429.95	1.7476	0.57090	0.65749	0.13952	0.091944	7.1510	30
40	0.024388	857.69	422.79	1.7766	0.49715	0.57964	0.13624	0.089410	6.4829	40
50	0.036204	846.96	415.62	1.8071	0.43583	0.51458	0.13305	0.086932	5.9194	50
60	0.052249	836.12	408.41	1.8388	0.38446	0.45982	0.12992	0.084500	5.4416	60
70	0.073517	825.12	401.13	1.8717	0.34109	0.41338	0.12683	0.082125	5.0336	70
80	0.10111	813.97	393.75	1.9054	0.30423	0.37376	0.12378	0.079809	4.6832	80
90	0.13623	802.63	386.23	1.9401	0.27268	0.33973	0.12076	0.077553	4.3806	90
100	0.18016	791.10	378.54	1.9756	0.24551	0.31034	0.11777	0.075356	4.1183	100
110	0.23428	779.33	370.65	2.0120	0.22196	0.28481	0.11480	0.073214	3.8900	110
120	0.30002	767.32	362.51	2.0494	0.20142	0.26250	0.11184	0.071124	3.6908	120
140	0.47249	742.43	345.39	2.1277	0.16752	0.22564	0.10597	0.067083	3.3636	140
160	0.71033	716.12	326.81	2.2127	0.14084	0.19667	0.10013	0.063189	3.1124	160
180	1.0272	687.98	306.31	2.3087	0.11937	0.17350	0.094325	0.059386	2.9216	180
200	1.4378	657.34	283.22	2.4238	0.10170	0.15471	0.088562	0.055586	2.7833	200
220	1.9582	623.05	256.47	2.5756	0.086833	0.13937	0.082853	0.051631	2.6993	220
240	2.6067	582.87	224.10	2.8102	0.073968	0.12690	0.077243	0.047156	2.6911	240
260	3.4064	531.50	181.64	3.3008	0.062322	0.11726	0.071954	0.041014	2.8589	260

APPENDIX B.3 (CONTINUED)

Thermophysical Properties of Liquids at Saturation (SI Units)

<i>T</i> °C	<i>P</i> _{sat} kPa	<i>ρ</i> kg/m ³	<i>h</i> _{fg} kJ/kg	<i>c</i> _{<i>p</i>} kJ/ kg·K	<i>μ</i> mPa·s	<i>ν</i> mm ² /s	<i>k</i> W/m·K	<i>α</i> mm ² /s	Pr	<i>T</i> °C
Cyclohexane										
10	6.3407	787.96	401.90	1.7893	1.1414	1.4486	0.11984	0.084994	17.044	10
20	10.343	778.60	395.65	1.8357	0.95778	1.2301	0.11772	0.082363	14.935	20
30	16.240	769.15	389.38	1.8826	0.81419	1.0586	0.11559	0.079827	13.261	30
40	24.642	759.61	383.06	1.9299	0.69989	0.92139	0.11345	0.077391	11.906	40
50	36.267	749.95	376.67	1.9777	0.60744	0.80997	0.11132	0.075056	10.791	50
60	51.936	740.17	370.19	2.0260	0.53155	0.71815	0.10920	0.072821	9.8618	60
70	72.566	730.25	363.59	2.0748	0.46845	0.64149	0.10709	0.070682	9.0757	70
80	99.166	720.19	356.85	2.1242	0.41537	0.57676	0.10500	0.068637	8.4031	80
90	132.83	709.96	349.94	2.1745	0.37025	0.52151	0.10294	0.066679	7.8212	90
100	174.73	699.54	342.84	2.2257	0.33154	0.47393	0.10090	0.064806	7.3131	100
110	226.10	688.92	335.50	2.2782	0.29803	0.43261	0.098900	0.063012	6.8654	110
120	288.24	678.07	327.90	2.3323	0.26882	0.39644	0.096936	0.061295	6.4677	120
130	362.51	666.96	319.98	2.3881	0.24316	0.36458	0.095014	0.059653	6.1117	130
140	450.30	655.55	311.72	2.4461	0.22047	0.33632	0.093137	0.058082	5.7904	140
160	672.31	631.60	293.91	2.5703	0.18221	0.28849	0.089538	0.055153	5.2307	160
180	966.43	605.71	273.93	2.7097	0.15116	0.24956	0.086170	0.052501	4.7534	180
200	1345.7	577.00	251.01	2.8735	0.12526	0.21709	0.083070	0.050102	4.3330	200
220	1824.4	544.05	223.93	3.0833	0.10296	0.18924	0.080297	0.047868	3.9534	220
240	2419.0	504.04	190.40	3.4051	0.082864	0.16440	0.078017	0.045457	3.6166	240
Toluene										
−60	0.0054177	941.08	466.17	1.4936	2.7659	2.9390	0.15229	0.10835	27.126	−60
−40	0.042077	922.37	452.76	1.5274	1.5984	1.7329	0.14761	0.10477	16.540	−40
−20	0.22511	903.83	440.01	1.5723	1.0598	1.1725	0.14253	0.10030	11.691	−20
0	0.90575	885.35	427.75	1.6257	0.76681	0.86611	0.13720	0.095323	9.0860	0
20	2.9189	866.82	415.81	1.6855	0.58660	0.67674	0.13171	0.090150	7.5067	20
40	7.8923	848.12	404.01	1.7501	0.46600	0.54945	0.12615	0.084992	6.4648	40
60	18.540	829.15	392.16	1.8184	0.38047	0.45887	0.12065	0.080020	5.7344	60
80	38.868	809.79	380.07	1.8896	0.31717	0.39166	0.11522	0.075300	5.2014	80
100	74.246	789.93	367.57	1.9632	0.26869	0.34015	0.10995	0.070901	4.7975	100
120	131.37	769.40	354.43	2.0390	0.23046	0.29953	0.10489	0.066860	4.4800	120
140	218.12	748.04	340.46	2.1175	0.19950	0.26670	0.10010	0.063196	4.2203	140
160	343.44	725.61	325.40	2.1993	0.17383	0.23957	0.095618	0.059918	3.9983	160
180	517.19	701.83	308.96	2.2859	0.15207	0.21667	0.091490	0.057027	3.7995	180
200	750.13	676.28	290.75	2.3803	0.13323	0.19700	0.087750	0.054512	3.6138	200
220	1054.0	648.38	270.24	2.4874	0.11658	0.17980	0.084424	0.052347	3.4347	220
240	1441.7	617.21	246.61	2.6175	0.10155	0.16454	0.081531	0.050466	3.2603	240
260	1928.2	581.17	218.52	2.7945	0.087639	0.15080	0.079082	0.048693	3.0969	260
280	2531.6	537.13	183.35	3.0901	0.074250	0.13823	0.077109	0.046457	2.9755	280
300	3275.7	476.60	134.38	3.8919	0.060238	0.12639	0.076019	0.040984	3.0839	300

APPENDIX B.3 (CONTINUED)

Thermophysical Properties of Liquids at Saturation (SI Units)

<i>T</i> °C	<i>P</i> _{sat} kPa	ρ kg/m ³	<i>h</i> _{fg} kJ/kg	<i>c</i> _p kJ/ kg·K	μ mPa·s	ν mm ² /s	<i>k</i> W/m·K	α mm ² /s	Pr	<i>T</i> °C
R22										
−100	2.0102	1571.3	268.26	1.0612	0.89602	0.57023	0.14312	0.085832	6.6436	−100
−90	4.8130	1544.9	262.53	1.0612	0.73051	0.47286	0.13778	0.084043	5.6264	−90
−80	10.372	1518.2	256.84	1.0624	0.60936	0.40137	0.13259	0.082203	4.8826	−80
−70	20.469	1491.2	251.12	1.0655	0.51759	0.34711	0.12752	0.080264	4.3245	−70
−60	37.505	1463.7	245.33	1.0710	0.44603	0.30474	0.12258	0.078197	3.8970	−60
−50	64.530	1435.6	239.39	1.0793	0.38879	0.27082	0.11774	0.075990	3.5639	−50
−40	105.23	1406.8	233.24	1.0905	0.34197	0.24308	0.11299	0.073646	3.3007	−40
−30	163.89	1377.2	226.81	1.1049	0.30289	0.21994	0.10836	0.071209	3.0886	−30
−20	245.31	1346.5	220.02	1.1227	0.26971	0.20030	0.10378	0.068654	2.9175	−20
−10	354.79	1314.7	212.79	1.1439	0.24106	0.18336	0.099250	0.065992	2.7785	−10
0	497.99	1281.5	205.05	1.1692	0.21598	0.16853	0.094743	0.063230	2.6654	0
10	680.95	1246.7	196.69	1.1993	0.19371	0.15538	0.090247	0.060359	2.5743	10
20	910.02	1209.9	187.60	1.2356	0.17370	0.14356	0.085742	0.057353	2.5031	20
30	1191.9	1170.7	177.64	1.2807	0.15547	0.13280	0.081205	0.054161	2.4520	30
40	1533.6	1128.5	166.60	1.3389	0.13867	0.12288	0.076604	0.050696	2.4239	40
50	1942.7	1082.3	154.19	1.4191	0.12296	0.11361	0.071900	0.046812	2.4269	50
60	2427.5	1030.4	139.94	1.5392	0.10799	0.10481	0.067040	0.042270	2.4795	60
70	2997.4	969.74	123.00	1.7434	0.093339	0.096252	0.061948	0.036643	2.6268	70
80	3663.8	893.74	101.57	2.1814	0.078270	0.087576	0.056583	0.029024	3.0174	80
R32										
−110	1.4525	1363.8	438.66	1.5647	0.66291	0.48607	0.23063	0.10808	4.4975	−110
−100	3.8130	1339.0	429.48	1.5600	0.55456	0.41415	0.22432	0.10739	3.8564	−100
−90	8.8687	1313.9	420.20	1.5586	0.47122	0.35864	0.21740	0.10616	3.3782	−90
−80	18.654	1288.4	410.71	1.5606	0.40512	0.31444	0.20999	0.10444	3.0108	−80
−70	36.067	1262.4	400.92	1.5663	0.35146	0.27842	0.20222	0.10227	2.7223	−70
−60	64.955	1235.7	390.73	1.5758	0.30715	0.24856	0.19421	0.099731	2.4923	−60
−50	110.14	1208.4	380.06	1.5895	0.27004	0.22347	0.18604	0.096860	2.3072	−50
−40	177.41	1180.2	368.79	1.6077	0.23861	0.20219	0.17779	0.093707	2.1576	−40
−30	273.44	1151.0	356.83	1.6311	0.21173	0.18396	0.16954	0.090311	2.0370	−30
−20	405.75	1120.6	344.03	1.6607	0.18852	0.16824	0.16135	0.086700	1.9405	−20
−10	582.63	1088.8	330.25	1.6980	0.16830	0.15458	0.15324	0.082891	1.8648	−10
0	813.10	1055.3	315.30	1.7450	0.15049	0.14261	0.14525	0.078879	1.8079	0
10	1106.9	1019.7	298.92	1.8056	0.13463	0.13204	0.13741	0.074632	1.7692	10
20	1474.6	981.38	280.78	1.8859	0.12033	0.12262	0.12970	0.070075	1.7498	20
30	1927.5	939.62	260.41	1.9973	0.10723	0.11412	0.12210	0.065062	1.7541	30
40	2478.3	893.04	237.09	2.1629	0.094988	0.10637	0.11458	0.059318	1.7931	40
50	3141.2	839.26	209.62	2.4385	0.083217	0.099156	0.10703	0.052300	1.8959	50
60	3933.2	773.31	175.51	3.0007	0.071369	0.092290	0.099377	0.042826	2.1550	60
70	4876.8	680.93	127.78	4.8653	0.058172	0.085431	0.092046	0.027784	3.0748	70

APPENDIX B.3 (CONTINUED)

Thermophysical Properties of Liquids at Saturation (SI Units)

<i>T</i> °C	<i>P</i> _{sat} kPa	<i>ρ</i> kg/m ³	<i>h</i> _{fg} kJ/kg	<i>c</i> _{<i>p</i>} kJ/kg·K	<i>μ</i> mPa·s	<i>ν</i> mm ² /s	<i>k</i> W/m·K	<i>α</i> mm ² /s	Pr	<i>T</i> °C
R123										
−100	0.011610	1754.5	220.49	0.92605	3.7133	2.1164	0.11303	0.069566	30.423	−100
−80	0.12548	1709.6	212.07	0.92359	2.0932	1.2244	0.10738	0.068005	18.004	−80
−60	0.80750	1665.1	204.21	0.93199	1.3834	0.83082	0.10200	0.065730	12.640	−60
−40	3.5752	1620.0	196.63	0.94805	0.98641	0.60891	0.096071	0.062555	9.7340	−40
−30	6.7480	1597.0	192.87	0.95776	0.84796	0.53097	0.092972	0.060783	8.7354	−30
−20	11.997	1573.8	189.11	0.96816	0.73539	0.46728	0.089848	0.058969	7.9242	−20
−10	20.247	1550.1	185.30	0.97903	0.64240	0.41441	0.086742	0.057156	7.2506	−10
0	32.645	1526.1	181.44	0.99023	0.56459	0.36995	0.083686	0.055377	6.6807	0
10	50.567	1501.6	177.49	1.0017	0.49878	0.33216	0.080707	0.053654	6.1909	10
20	75.610	1476.6	173.44	1.0135	0.44260	0.29974	0.077821	0.051998	5.7645	20
30	109.58	1451.0	169.27	1.0257	0.39427	0.27172	0.075037	0.050416	5.3896	30
40	154.47	1424.8	164.94	1.0385	0.35240	0.24733	0.072359	0.048906	5.0574	40
60	285.89	1370.0	155.73	1.0663	0.28386	0.20720	0.067311	0.046078	4.4967	60
80	489.09	1311.2	145.54	1.0996	0.23054	0.17582	0.062621	0.043431	4.0484	80
100	785.53	1246.9	134.01	1.1433	0.18809	0.15084	0.058190	0.040818	3.6955	100
120	1199.0	1174.4	120.53	1.2072	0.15336	0.13059	0.053884	0.038006	3.4360	120
140	1756.3	1088.3	104.02	1.3178	0.12382	0.11378	0.049522	0.034532	3.2949	140
160	2490.1	975.68	81.886	1.5836	0.096802	0.099215	0.044842	0.029023	3.4185	160
180	3450.6	765.91	40.596	4.5486	0.064292	0.083942	0.039715	0.011400	7.3635	180
R125										
−100	3.0883	1688.7	189.96	1.0351	1.1336	0.67133	0.11573	0.066213	10.139	−100
−90	7.2856	1656.2	185.18	1.0450	0.89075	0.53782	0.11103	0.064151	8.3836	−90
−80	15.468	1623.4	180.37	1.0581	0.72062	0.44389	0.10630	0.061885	7.1729	−80
−70	30.076	1589.9	175.47	1.0736	0.59524	0.37438	0.10157	0.059500	6.2921	−70
−60	54.318	1555.7	170.41	1.0912	0.49932	0.32097	0.096846	0.057052	5.6259	−60
−50	92.164	1520.5	165.14	1.1107	0.42375	0.27870	0.092188	0.054591	5.1052	−50
−40	148.30	1484.0	159.59	1.1323	0.36278	0.24446	0.087570	0.052114	4.6908	−40
−30	228.06	1446.1	153.71	1.1565	0.31258	0.21615	0.083016	0.049637	4.3546	−30
−20	337.33	1406.4	147.41	1.1840	0.27051	0.19233	0.078538	0.047162	4.0782	−20
−10	482.52	1364.5	140.60	1.2161	0.23469	0.17199	0.074145	0.044681	3.8494	−10
−5	570.72	1342.6	136.97	1.2344	0.21867	0.16287	0.071982	0.043432	3.7501	−5
0	670.52	1319.8	133.16	1.2547	0.20372	0.15435	0.069840	0.042174	3.6599	0
5	782.88	1296.2	129.14	1.2773	0.18970	0.14636	0.067720	0.040902	3.5782	5
10	908.75	1271.5	124.90	1.3029	0.17651	0.13882	0.065619	0.039610	3.5048	10
20	1205.2	1218.3	115.57	1.3666	0.15221	0.12494	0.061473	0.036923	3.3837	20
30	1568.5	1158.4	104.81	1.4575	0.13008	0.11230	0.057382	0.033988	3.3041	30
40	2008.5	1088.4	92.024	1.6052	0.10940	0.10052	0.053317	0.030518	3.2937	40
50	2536.8	1001.1	75.924	1.9102	0.089205	0.089107	0.049261	0.025760	3.4591	50
60	3170.3	872.09	52.112	3.1392	0.067051	0.076885	0.045865	0.016753	4.5892	60

APPENDIX B.3 (CONTINUED)

Thermophysical Properties of Liquids at Saturation (SI Units)

<i>T</i> °C	<i>P</i> _{sat} kPa	ρ kg/m ³	<i>h</i> _{fg} kJ/kg	<i>c</i> _p kJ/ kg·K	μ mPa·s	ν mm ² /s	<i>k</i> W/m·K	α mm ² /s	Pr	<i>T</i> °C
R134a										
−100	0.55940	1582.4	261.49	1.1842	1.8824	1.1896	0.14323	0.076431	15.564	−100
−80	3.6719	1529.0	249.67	1.1981	1.0203	0.66728	0.13154	0.071806	9.2927	−80
−70	7.9814	1501.9	243.82	1.2096	0.80910	0.53873	0.12603	0.069373	7.7656	−70
−60	15.906	1474.3	237.95	1.2230	0.66051	0.44800	0.12071	0.066943	6.6923	−60
−50	29.451	1446.3	231.98	1.2381	0.55089	0.38089	0.11557	0.064541	5.9016	−50
−40	51.209	1417.7	225.86	1.2546	0.46703	0.32943	0.11059	0.062175	5.2983	−40
−30	84.378	1388.4	219.53	1.2729	0.40095	0.28879	0.10576	0.059846	4.8255	−30
−20	132.73	1358.3	212.92	1.2930	0.34758	0.25590	0.10107	0.057547	4.4469	−20
−10	200.60	1327.1	205.97	1.3156	0.30355	0.22873	0.096491	0.055267	4.1386	−10
0	292.80	1294.8	198.60	1.3410	0.26653	0.20585	0.092013	0.052992	3.8845	0
10	414.61	1261.0	190.74	1.3704	0.23487	0.18626	0.087618	0.050705	3.6734	10
20	571.71	1225.3	182.28	1.4049	0.20737	0.16923	0.083284	0.048381	3.4979	20
30	770.20	1187.5	173.10	1.4465	0.18313	0.15422	0.078992	0.045989	3.3533	30
40	1016.6	1146.7	163.02	1.4984	0.16145	0.14079	0.074716	0.043483	3.2378	40
50	1317.9	1102.3	151.81	1.5661	0.14177	0.12861	0.070427	0.040795	3.1527	50
60	1681.8	1052.9	139.12	1.6602	0.12361	0.11741	0.066091	0.037811	3.1051	60
70	2116.8	996.25	124.37	1.8039	0.10651	0.10691	0.061672	0.034316	3.1153	70
80	2633.2	928.24	106.42	2.0648	0.089846	0.096791	0.057147	0.029815	3.2464	80
100	3972.4	651.18	34.385	17.592	0.047429	0.072835	0.058884	0.0051403	14.169	100
R227ea										
−100	0.28879	1803.4	164.26	0.95223	1.8003	0.99829	0.090519	0.052712	18.939	−100
−90	0.82377	1774.7	160.44	0.96521	1.4397	0.81121	0.088723	0.051794	15.662	−90
−80	2.0645	1745.7	156.67	0.97846	1.1758	0.67357	0.086772	0.050802	13.259	−80
−70	4.6422	1716.0	152.92	0.99209	0.97631	0.56894	0.084685	0.049743	11.438	−70
−60	9.5257	1685.8	149.15	1.0062	0.82125	0.48717	0.082480	0.048623	10.019	−60
−50	18.087	1654.8	145.35	1.0211	0.69788	0.42172	0.080159	0.047438	8.8900	−50
−40	32.140	1623.1	141.46	1.0369	0.59775	0.36827	0.077740	0.046191	7.9729	−40
−30	53.960	1590.5	137.47	1.0539	0.51512	0.32387	0.075236	0.044886	7.2154	−30
−20	86.272	1556.9	133.33	1.0722	0.44597	0.28645	0.072659	0.043527	6.5808	−20
−10	132.23	1522.1	129.00	1.0921	0.38741	0.25452	0.070021	0.042121	6.0425	−10
0	195.36	1486.0	124.44	1.1141	0.33731	0.22699	0.067335	0.040672	5.5810	0
10	279.57	1448.2	119.58	1.1386	0.29406	0.20305	0.064613	0.039186	5.1817	10
20	389.08	1408.4	114.37	1.1663	0.25640	0.18205	0.061868	0.037665	4.8334	20
30	528.42	1366.2	108.72	1.1983	0.22334	0.16347	0.059114	0.036109	4.5271	30
40	702.45	1320.9	102.52	1.2364	0.19403	0.14690	0.056364	0.034514	4.2563	40
50	916.39	1271.4	95.639	1.2837	0.16778	0.13196	0.053634	0.032861	4.0158	50
60	1175.9	1216.5	87.846	1.3463	0.14393	0.11832	0.050941	0.031104	3.8039	60
80	1858.3	1078.2	67.813	1.5960	0.10076	0.093454	0.045838	0.026638	3.5083	80
100	2821.6	786.76	26.802	7.1411	0.051620	0.065611	0.048251	0.0085882	7.6397	100

APPENDIX B.3 (CONTINUED)

Thermophysical Properties of Liquids at Saturation (IP Units)

<i>T</i> °F	<i>P_{sat}</i> psia	<i>ρ</i> lbm/ft³	<i>h_{fg}</i> Btu/ lbm	<i>c_p</i> Btu/ lbm-R	<i>μ</i> lbm/ ft-h	<i>ν</i> ft²/h	<i>k</i> Btu/ h-ft-F	<i>α</i> ft²/h	Pr	<i>T</i> °F
Water										
40	0.12173	62.423	1071.4	1.0055	3.7382	0.059885	0.32750	0.0052180	11.477	40
60	0.25640	62.364	1060.1	1.0010	2.7120	0.043487	0.34101	0.0054626	7.9609	60
80	0.50747	62.213	1048.7	0.99928	2.0737	0.033333	0.35220	0.0056652	5.8837	80
100	0.95051	61.991	1037.4	0.99893	1.6473	0.026572	0.36164	0.0058400	4.5501	100
120	1.6950	61.710	1025.9	0.99934	1.3471	0.021829	0.36964	0.0059939	3.6419	120
140	2.8930	61.377	1014.3	1.0003	1.1273	0.018367	0.37637	0.0061304	2.9961	140
160	4.7472	60.998	1002.5	1.0016	0.96150	0.015763	0.38194	0.0062513	2.5215	160
180	7.5195	60.578	990.51	1.0035	0.83323	0.013755	0.38644	0.0063570	2.1637	180
200	11.538	60.120	978.24	1.0059	0.73199	0.012175	0.38992	0.0064479	1.8883	200
220	17.201	59.626	965.65	1.0088	0.65069	0.010913	0.39244	0.0065241	1.6727	220
240	24.986	59.097	952.68	1.0125	0.58443	0.0098893	0.39406	0.0065854	1.5017	240
260	35.447	58.535	939.27	1.0170	0.52969	0.0090492	0.39480	0.0066319	1.3645	260
280	49.222	57.940	925.34	1.0224	0.48395	0.0083526	0.39473	0.0066637	1.2534	280
300	67.029	57.312	910.84	1.0287	0.44529	0.0077696	0.39387	0.0066806	1.1630	300
350	134.63	55.594	871.56	1.0497	0.37105	0.0066743	0.38899	0.0066656	1.0013	350
400	247.26	53.652	826.94	1.0802	0.31814	0.0059298	0.37988	0.0065548	0.90465	400
500	680.55	48.920	714.86	1.1916	0.24629	0.0050346	0.35025	0.0060084	0.83792	500
600	1542.5	42.318	549.97	1.5100	0.19352	0.0045731	0.30510	0.0047746	0.95780	600
700	3093.0	27.283	168.65	15.579	0.12315	0.0045137	0.26673	0.00062754	7.1927	700
Ammonia										
−60	5.5439	43.911	610.41	1.0406	0.81034	0.018454	0.41982	0.0091881	2.0085	−60
−40	10.398	43.085	597.39	1.0549	0.68035	0.015791	0.39785	0.0087536	1.8040	−40
−20	18.279	42.229	583.54	1.0684	0.58167	0.013774	0.37637	0.0083423	1.6511	−20
−10	23.723	41.790	576.27	1.0749	0.54092	0.012944	0.36584	0.0081443	1.5893	−10
0	30.397	41.344	568.77	1.0814	0.50466	0.012207	0.35547	0.0079505	1.5353	0
10	38.487	40.890	561.02	1.0880	0.47221	0.011548	0.34525	0.0077602	1.4881	10
20	48.194	40.429	553.01	1.0948	0.44297	0.010957	0.33519	0.0075727	1.4469	20
40	73.322	39.482	536.14	1.1094	0.39232	0.0099368	0.31553	0.0072034	1.3795	40
60	107.63	38.498	518.02	1.1263	0.34981	0.0090865	0.29647	0.0068370	1.3290	60
80	153.13	37.472	498.50	1.1469	0.31343	0.0083642	0.27797	0.0064681	1.2931	80
100	212.01	36.396	477.36	1.1727	0.28174	0.0077410	0.25999	0.0060912	1.2708	100
120	286.60	35.256	454.34	1.2063	0.25371	0.0071961	0.24244	0.0057004	1.2624	120
140	379.36	34.038	429.05	1.2512	0.22856	0.0067148	0.22525	0.0052889	1.2696	140
160	492.95	32.719	400.97	1.3133	0.20568	0.0062862	0.20833	0.0048481	1.2966	160
180	630.24	31.264	369.32	1.4034	0.18452	0.0059021	0.19156	0.0043660	1.3518	180
200	794.38	29.620	332.88	1.5432	0.16458	0.0055565	0.17478	0.0038239	1.4531	200
220	989.03	27.693	289.46	1.7884	0.14525	0.0052451	0.15784	0.0031868	1.6459	220
240	1218.7	25.281	234.42	2.3459	0.12550	0.0049643	0.14058	0.0023704	2.0943	240
260	1489.7	21.599	151.20	5.2730	0.10163	0.0047054	0.12501	0.0010976	4.2869	260

APPENDIX B.3 (CONTINUED)

Thermophysical Properties of Liquids at Saturation (IP Units)

<i>T</i> °F	<i>P_{sat}</i> psia	<i>ρ</i> lbm/ft ³	<i>h_{fg}</i> Btu/ lbm	<i>c_p</i> Btu/ lbm-R	<i>μ</i> lbm/ ft-h	<i>ν</i> ft ² /h	<i>k</i> Btu/ h-ft-F	<i>α</i> ft ² /h	Pr	<i>T</i> °F
Propane										
−100	2.8959	38.432	196.29	0.50817	0.69836	0.018172	0.085541	0.0043801	4.1487	−100
−80	5.4971	37.677	191.78	0.51717	0.60569	0.016076	0.081613	0.0041884	3.8382	−80
−60	9.7038	36.904	187.08	0.52746	0.52948	0.014347	0.077757	0.0039946	3.5917	−60
−40	16.117	36.110	182.13	0.53916	0.46580	0.012899	0.073978	0.0037997	3.3948	−40
−30	20.363	35.704	179.55	0.54557	0.43775	0.012260	0.072123	0.0037026	3.3113	−30
−20	25.424	35.291	176.88	0.55240	0.41184	0.011670	0.070295	0.0036059	3.2364	−20
−10	31.399	34.870	174.12	0.55967	0.38786	0.011123	0.068495	0.0035098	3.1692	−10
0	38.389	34.440	171.26	0.56740	0.36558	0.010615	0.066724	0.0034145	3.1088	0
10	46.498	34.002	168.28	0.57565	0.34483	0.010142	0.064984	0.0033201	3.0546	10
20	55.834	33.553	165.18	0.58446	0.32545	0.0096998	0.063277	0.0032267	3.0061	20
30	66.509	33.093	161.94	0.59391	0.30730	0.0092862	0.061602	0.0031343	2.9628	30
40	78.636	32.620	158.55	0.60406	0.29026	0.0088981	0.059961	0.0030430	2.9241	40
60	107.71	31.631	151.26	0.62693	0.25902	0.0081886	0.056781	0.0028633	2.8599	60
80	144.04	30.573	143.16	0.65428	0.23093	0.0075533	0.053737	0.0026864	2.8117	80
100	188.62	29.425	134.07	0.68826	0.20530	0.0069768	0.050825	0.0025096	2.7801	100
120	242.54	28.157	123.68	0.73302	0.18148	0.0064452	0.048030	0.0023271	2.7697	120
140	307.01	26.718	111.52	0.79768	0.15882	0.0059446	0.045328	0.0021269	2.7950	140
160	383.40	25.010	96.711	0.90722	0.13652	0.0054588	0.042682	0.0018812	2.9018	160
180	473.45	22.798	77.172	1.1629	0.11313	0.0049621	0.040092	0.0015122	3.2815	180
Pentane										
−100	0.028105	44.408	187.53	0.48012	1.6733	0.037680	0.088220	0.0041377	9.1065	−100
−60	0.18117	43.172	180.82	0.49038	1.1748	0.027213	0.082545	0.0038990	6.9794	−60
−20	0.79033	41.923	174.24	0.50444	0.88765	0.021173	0.076965	0.0036394	5.8177	−20
0	1.4761	41.290	170.93	0.51286	0.78590	0.019034	0.074248	0.0035062	5.4285	0
20	2.5941	40.648	167.59	0.52217	0.70209	0.017272	0.071596	0.0033731	5.1206	20
40	4.3250	39.996	164.17	0.53235	0.63171	0.015795	0.069007	0.0032410	4.8733	40
60	6.8884	39.331	160.66	0.54337	0.57161	0.014533	0.066487	0.0031110	4.6716	60
80	10.541	38.651	157.03	0.55521	0.51951	0.013441	0.064038	0.0029841	4.5042	80
100	15.575	37.954	153.24	0.56787	0.47375	0.012482	0.061661	0.0028609	4.3630	100
120	22.316	37.237	149.27	0.58135	0.43306	0.011630	0.059356	0.0027419	4.2416	120
140	31.117	36.495	145.07	0.59572	0.39650	0.010865	0.057123	0.0026275	4.1350	140
160	42.357	35.725	140.63	0.61106	0.36331	0.010170	0.054960	0.0025176	4.0394	160
180	56.440	34.922	135.88	0.62752	0.33290	0.0095327	0.052865	0.0024124	3.9516	180
200	73.792	34.079	130.77	0.64533	0.30477	0.0089433	0.050835	0.0023115	3.8691	200
220	94.860	33.187	125.25	0.66489	0.27854	0.0083929	0.048867	0.0022146	3.7898	220
240	120.12	32.238	119.22	0.68677	0.25384	0.0078740	0.046958	0.0021209	3.7125	240
260	150.07	31.215	112.58	0.71197	0.23036	0.0073799	0.045103	0.0020295	3.6363	260
280	185.26	30.097	105.17	0.74217	0.20781	0.0069045	0.043299	0.0019384	3.5619	280
300	226.28	28.855	96.751	0.78060	0.18586	0.0064412	0.041542	0.0018443	3.4924	300

APPENDIX B.3 (CONTINUED)

Thermophysical Properties of Liquids at Saturation (IP Units)

<i>T</i> °F	<i>P</i> _{sat} psia	ρ lbm/ft ³	<i>h</i> _{fg} Btu/ lbm	<i>c</i> _p Btu/ lbm-R	μ lbm/ ft-h	ν ft ² /h	<i>k</i> Btu/ h-ft-F	α ft ² /h	Pr	<i>T</i> °F
Hexane										
-40	0.066846	44.493	174.88	0.48252	1.6551	0.037200	0.082748	0.0038543	9.6516	-40
-20	0.15120	43.883	171.90	0.49063	1.3915	0.031710	0.080182	0.0037242	8.5147	-20
0	0.31475	43.272	168.92	0.49932	1.1880	0.027454	0.077735	0.0035978	7.6307	0
20	0.60983	42.656	165.94	0.50860	1.0272	0.024080	0.075405	0.0034757	6.9283	20
40	1.1102	42.036	162.92	0.51848	0.89771	0.021356	0.073184	0.0033579	6.3599	40
60	1.9140	41.410	159.87	0.52893	0.79169	0.019119	0.071064	0.0032445	5.8925	60
80	3.1465	40.775	156.76	0.53993	0.70361	0.017256	0.069041	0.0031360	5.5025	80
100	4.9606	40.130	153.57	0.55145	0.62949	0.015686	0.067110	0.0030325	5.1726	100
120	7.5373	39.474	150.27	0.56348	0.56638	0.014348	0.065268	0.0029343	4.8898	120
140	11.084	38.805	146.86	0.57600	0.51209	0.013197	0.063509	0.0028414	4.6445	140
160	15.835	38.120	143.31	0.58900	0.46495	0.012197	0.061830	0.0027538	4.4291	160
180	22.046	37.416	139.59	0.60251	0.42363	0.011322	0.060227	0.0026716	4.2379	180
200	29.995	36.692	135.68	0.61655	0.38711	0.010550	0.058696	0.0025946	4.0663	200
240	52.315	35.165	127.18	0.64654	0.32535	0.0092521	0.055832	0.0024557	3.7676	240
280	85.383	33.502	117.48	0.68018	0.27469	0.0081993	0.053205	0.0023348	3.5117	280
320	132.09	31.642	106.12	0.72042	0.23158	0.0073188	0.050773	0.0022273	3.2859	320
360	195.73	29.468	92.254	0.77557	0.19307	0.0065518	0.048484	0.0021214	3.0884	360
400	280.44	26.695	73.881	0.87985	0.15573	0.0058334	0.046281	0.0019704	2.9605	400
440	392.55	21.925	42.687	1.5500	0.10942	0.0049907	0.044983	0.0013236	3.7706	440
Heptane										
-40	0.011169	45.794	174.65	0.48804	2.4136	0.052705	0.082160	0.0036761	14.337	-40
-20	0.028779	45.221	171.55	0.49440	1.9731	0.043634	0.080174	0.0035861	12.168	-20
0	0.067277	44.647	168.51	0.50154	1.6465	0.036879	0.078182	0.0034915	10.562	0
20	0.14459	44.073	165.52	0.50942	1.3974	0.031706	0.076194	0.0033937	9.3428	20
40	0.28883	43.497	162.55	0.51800	1.2027	0.027651	0.074215	0.0032939	8.3946	40
60	0.54133	42.917	159.59	0.52723	1.0474	0.024405	0.072256	0.0031934	7.6424	60
80	0.95943	42.332	156.63	0.53704	0.92123	0.021762	0.070320	0.0030932	7.0355	80
100	1.6189	41.741	153.65	0.54739	0.81713	0.019576	0.068408	0.0029940	6.5384	100
120	2.6156	41.143	150.64	0.55821	0.73002	0.017744	0.066525	0.0028966	6.1257	120
140	4.0667	40.536	147.58	0.56948	0.65623	0.016189	0.064672	0.0028016	5.7785	140
160	6.1110	39.918	144.44	0.58115	0.59303	0.014856	0.062854	0.0027094	5.4831	160
180	8.9083	39.287	141.22	0.59320	0.53833	0.013702	0.061070	0.0026205	5.2290	180
200	12.639	38.643	137.88	0.60561	0.49056	0.012695	0.059323	0.0025349	5.0080	200
240	23.715	37.300	130.81	0.63161	0.41109	0.011021	0.055941	0.0023745	4.6415	240
280	41.140	35.866	123.02	0.65947	0.34741	0.0096863	0.052703	0.0022282	4.3471	280
320	66.970	34.306	114.27	0.69011	0.29473	0.0085914	0.049598	0.0020950	4.1009	320
360	103.51	32.563	104.17	0.72573	0.24964	0.0076664	0.046596	0.0019717	3.8882	360
400	153.38	30.537	92.083	0.77192	0.20937	0.0068561	0.043646	0.0018516	3.7028	400
440	219.70	28.006	76.670	0.84730	0.17101	0.0061061	0.040670	0.0017139	3.5627	440

APPENDIX B.3 (CONTINUED)

Thermophysical Properties of Liquids at Saturation (IP Units)

<i>T</i> °F	<i>P</i> _{sat} psia	ρ lbm/ft ³	<i>h</i> _{fg} Btu/ lbm	<i>c</i> _p Btu/ lbm-R	μ lbm/ ft-h	ν ft ² /h	<i>k</i> Btu/ h-ft-F	α ft ² /h	Pr	<i>T</i> °F
Octane										
−40	0.0018837	46.833	174.17	0.48766	3.5837	0.076519	0.084798	0.0037129	20.609	−40
−20	0.0055233	46.277	171.06	0.49347	2.8270	0.061090	0.082394	0.0036081	16.931	−20
10	0.022631	45.445	166.54	0.50371	2.0852	0.045884	0.078961	0.0034494	13.302	10
0	0.014494	45.722	168.03	0.50010	2.2942	0.050177	0.080084	0.0035024	14.327	0
10	0.022631	45.445	166.54	0.50371	2.0852	0.045884	0.078961	0.0034494	13.302	10
20	0.034556	45.169	165.06	0.50750	1.9051	0.042178	0.077858	0.0033965	12.418	20
40	0.075796	44.615	162.14	0.51559	1.6122	0.036137	0.075711	0.0032913	10.979	40
60	0.15458	44.060	159.26	0.52432	1.3861	0.031459	0.073635	0.0031875	9.8695	60
80	0.29575	43.502	156.41	0.53362	1.2074	0.027755	0.071629	0.0030857	8.9948	80
100	0.53487	42.941	153.57	0.54342	1.0634	0.024765	0.069687	0.0029864	8.2925	100
140	1.5156	41.802	147.89	0.56429	0.84686	0.020259	0.065968	0.0027967	7.2439	140
180	3.6689	40.634	142.10	0.58652	0.69221	0.017035	0.062446	0.0026202	6.5015	180
220	7.8351	39.424	136.08	0.60986	0.57597	0.014610	0.059094	0.0024578	5.9442	220
260	15.127	38.158	129.70	0.63421	0.48483	0.012706	0.055886	0.0023093	5.5020	260
300	26.912	36.818	122.80	0.65973	0.41075	0.011156	0.052800	0.0021737	5.1322	300
340	44.782	35.379	115.21	0.68689	0.34869	0.0098559	0.049816	0.0020499	4.8079	340
380	70.537	33.800	106.66	0.71682	0.29525	0.0087351	0.046912	0.0019362	4.5114	380
420	106.19	32.020	96.787	0.75204	0.24802	0.0077457	0.044069	0.0018301	4.2324	420
460	154.03	29.921	84.895	0.79907	0.20502	0.0068520	0.041277	0.0017265	3.9688	460
Nonane										
0	0.0032413	46.678	166.81	0.49399	3.1784	0.068092	0.080889	0.0035080	19.410	0
20	0.0085364	46.130	163.93	0.50192	2.5540	0.055365	0.078764	0.0034017	16.276	20
40	0.020490	45.584	161.10	0.51048	2.1159	0.046417	0.076736	0.0032976	14.076	40
60	0.045350	45.038	158.32	0.51957	1.7935	0.039821	0.074798	0.0031964	12.458	60
80	0.093468	44.492	155.57	0.52912	1.5473	0.034776	0.072943	0.0030985	11.224	80
100	0.18090	43.943	152.85	0.53905	1.3535	0.030802	0.071168	0.0030044	10.252	100
120	0.33117	43.392	150.15	0.54933	1.1973	0.027592	0.069466	0.0029143	9.4680	120
140	0.57702	42.837	147.45	0.55988	1.0686	0.024946	0.067831	0.0028282	8.8203	140
160	0.96206	42.277	144.75	0.57068	0.96072	0.022724	0.066259	0.0027463	8.2746	160
180	1.5422	41.712	142.04	0.58169	0.86887	0.020830	0.064744	0.0026684	7.8063	180
200	2.3866	41.139	139.29	0.59288	0.78961	0.019194	0.063284	0.0025946	7.3976	200
240	5.2152	39.967	133.67	0.61574	0.65938	0.016498	0.060508	0.0024587	6.7099	240
280	10.284	38.752	127.77	0.63919	0.55625	0.014354	0.057901	0.0023376	6.1407	280
320	18.650	37.478	121.48	0.66331	0.47194	0.012593	0.055431	0.0022298	5.6475	320
360	31.574	36.126	114.66	0.68837	0.40117	0.011105	0.053066	0.0021339	5.2040	360
400	50.501	34.671	107.12	0.71500	0.34036	0.0098169	0.050770	0.0020480	4.7934	400
440	77.069	33.070	98.592	0.74449	0.28692	0.0086761	0.048498	0.0019698	4.4045	440
480	113.14	31.255	88.656	0.77979	0.23879	0.0076399	0.046191	0.0018952	4.0312	480
520	160.92	29.090	76.507	0.82907	0.19398	0.0066681	0.043759	0.0018144	3.6751	520

APPENDIX B.3 (CONTINUED)

Thermophysical Properties of Liquids at Saturation (IP Units)

<i>T</i> °F	<i>P</i> _{sat} psia	<i>ρ</i> lbm/ft ³	<i>h</i> _{fg} Btu/ lbm	<i>c</i> _p Btu/ lbm-R	<i>μ</i> lbm/ ft-h	<i>ν</i> ft ² /h	<i>k</i> Btu/ h-ft-F	<i>α</i> ft ² /h	Pr	<i>T</i> °F
Decane										
20	0.0021136	46.891	163.07	0.49761	3.4953	0.074542	0.079690	0.0034153	21.826	20
40	0.0055546	46.349	160.31	0.50649	2.8439	0.061359	0.077969	0.0033214	18.474	40
60	0.013350	45.809	157.60	0.51581	2.3643	0.051611	0.076268	0.0032278	15.990	60
80	0.029661	45.270	154.92	0.52553	2.0004	0.044189	0.074587	0.0031352	14.095	80
100	0.061481	44.730	152.28	0.53557	1.7176	0.038399	0.072931	0.0030443	12.613	100
120	0.11984	44.190	149.66	0.54589	1.4930	0.033787	0.071297	0.0029556	11.431	120
160	0.38867	43.101	144.46	0.56720	1.1624	0.026970	0.068105	0.0027858	9.6811	160
200	1.0579	41.997	139.25	0.58915	0.93350	0.022228	0.065020	0.0026279	8.4584	200
240	2.5007	40.868	133.96	0.61153	0.76704	0.018769	0.062055	0.0024830	7.5590	240
280	5.2711	39.706	128.49	0.63423	0.64101	0.016144	0.059220	0.0023516	6.8652	280
320	10.117	38.498	122.75	0.65724	0.54224	0.014085	0.056525	0.0022340	6.3050	320
360	17.978	37.229	116.62	0.68067	0.46247	0.012422	0.053979	0.0021301	5.8316	360
400	29.972	35.881	109.97	0.70482	0.39624	0.011043	0.051592	0.0020400	5.4133	400
440	47.388	34.425	102.63	0.73033	0.33983	0.0098717	0.049370	0.0019637	5.0271	440
480	71.689	32.816	94.332	0.75847	0.29050	0.0088523	0.047318	0.0019011	4.6565	480
520	104.55	30.980	84.663	0.79213	0.24604	0.0079417	0.045437	0.0018515	4.2893	520
560	147.94	28.773	72.848	0.83907	0.20434	0.0071018	0.043728	0.0018112	3.9210	560
600	204.41	25.852	57.070	0.93080	0.16257	0.0062886	0.042242	0.0017555	3.5822	600
640	277.88	20.758	29.815	1.5759	0.11196	0.0053935	0.042489	0.0012988	4.1526	640
Dodecane										
20	0.00012516	48.025	163.68	0.50667	6.4766	0.13486	0.082783	0.0034021	39.640	20
40	0.00039939	47.505	160.74	0.51383	4.9462	0.10412	0.081134	0.0033239	31.325	40
60	0.0011435	46.987	157.88	0.52166	3.9163	0.083348	0.079534	0.0032447	25.687	60
80	0.0029764	46.473	155.09	0.53006	3.1881	0.068601	0.077976	0.0031655	21.672	80
100	0.0071236	45.960	152.36	0.53894	2.6532	0.057729	0.076457	0.0030867	18.702	100
120	0.015827	45.447	149.69	0.54822	2.2481	0.049466	0.074971	0.0030091	16.439	120
160	0.064528	44.419	144.48	0.56772	1.6833	0.037896	0.072089	0.0028587	13.256	160
200	0.21282	43.382	139.40	0.58814	1.3143	0.030297	0.069306	0.0027163	11.154	200
240	0.59151	42.328	134.39	0.60917	1.0572	0.024977	0.066602	0.0025830	9.6696	240
280	1.4302	41.248	129.36	0.63060	0.86840	0.021053	0.063961	0.0024590	8.5618	280
320	3.0846	40.134	124.23	0.65230	0.72368	0.018032	0.061370	0.0023442	7.6921	320
360	6.0544	38.975	118.93	0.67424	0.60869	0.015618	0.058820	0.0022383	6.9773	360
400	10.990	37.759	113.34	0.69644	0.51453	0.013627	0.056304	0.0021411	6.3644	400
440	18.694	36.470	107.35	0.71908	0.43543	0.011939	0.053818	0.0020522	5.8178	440
480	30.113	35.086	100.84	0.74248	0.36750	0.010474	0.051361	0.0019716	5.3126	480
520	46.344	33.579	93.618	0.76728	0.30804	0.0091736	0.048937	0.0018994	4.8298	520
560	68.646	31.905	85.457	0.79471	0.25509	0.0079953	0.046554	0.0018361	4.3545	560
600	98.476	29.992	75.980	0.82747	0.20712	0.0069058	0.044237	0.0017825	3.8743	600
640	137.58	27.714	64.523	0.87289	0.16283	0.0058753	0.042035	0.0017376	3.3812	640

APPENDIX B.3 (CONTINUED)

Thermophysical Properties of Liquids at Saturation (IP Units)

<i>T</i> °F	<i>P</i> _{sat} psia	<i>ρ</i> lbm/ft ³	<i>h</i> _{fg} Btu/ lbm	<i>c</i> _p Btu/ lbm-R	<i>μ</i> lbm/ ft-h	<i>ν</i> ft ² /h	<i>k</i> Btu/ h-ft-F	<i>α</i> ft ² /h	Pr	<i>T</i> °F
Methanol										
−60	0.010240	53.595	545.05	0.53570	5.6283	0.10502	0.13582	0.0047305	22.200	−60
−40	0.029147	52.920	539.76	0.54140	4.2952	0.081164	0.13198	0.0046063	17.620	−40
−20	0.074839	52.252	534.21	0.54842	3.3650	0.064400	0.12852	0.0044849	14.359	−20
0	0.17575	51.591	528.38	0.55688	2.6909	0.052158	0.12541	0.0043651	11.949	0
20	0.38182	50.936	522.26	0.56697	2.1891	0.042979	0.12261	0.0042459	10.122	20
40	0.77490	50.284	515.80	0.57884	1.8081	0.035958	0.12010	0.0041262	8.7146	40
60	1.4810	49.636	509.00	0.59260	1.5140	0.030502	0.11783	0.0040060	7.6140	60
80	2.6843	48.986	501.81	0.60827	1.2834	0.026198	0.11577	0.0038854	6.7427	80
100	4.6412	48.332	494.19	0.62582	1.1000	0.022759	0.11389	0.0037654	6.0443	100
120	7.6946	47.670	486.07	0.64519	0.95221	0.019975	0.11216	0.0036467	5.4777	120
140	12.287	46.995	477.38	0.66634	0.83148	0.017693	0.11054	0.0035299	5.0123	140
160	18.970	46.303	468.02	0.68924	0.73155	0.015799	0.10901	0.0034157	4.6254	160
180	28.414	45.588	457.88	0.71393	0.64776	0.014209	0.10755	0.0033044	4.2999	180
200	41.417	44.845	446.83	0.74048	0.57661	0.012858	0.10613	0.0031961	4.0230	200
220	58.901	44.067	434.72	0.76909	0.51546	0.011697	0.10474	0.0030905	3.7848	220
240	81.922	43.248	421.37	0.80005	0.46226	0.010689	0.10336	0.0029873	3.5780	240
260	111.67	42.378	406.61	0.83383	0.41544	0.0098032	0.10198	0.0028859	3.3969	260
280	149.46	41.448	390.21	0.87115	0.37378	0.0090180	0.10057	0.0027853	3.2377	280
300	196.77	40.446	371.97	0.91311	0.33632	0.0083153	0.099139	0.0026844	3.0976	300
Ethanol										
−60	0.0024978	53.063	426.09	0.47970	4.5422	0.085601	0.10682	0.0041966	20.398	−60
−40	0.0080688	52.463	422.13	0.48947	3.6467	0.069511	0.10442	0.0040663	17.094	−40
−20	0.023196	51.868	418.09	0.50119	2.9977	0.057795	0.10227	0.0039340	14.691	−20
0	0.060275	51.278	413.94	0.51461	6.6755	0.13018	0.10034	0.0038023	34.238	0
20	0.14341	50.690	409.63	0.52965	5.1161	0.10093	0.098600	0.0036725	27.483	20
40	0.31583	50.103	405.12	0.54636	3.9875	0.079587	0.097034	0.0035447	22.452	40
60	0.64976	49.514	400.37	0.56480	3.1563	0.063745	0.095613	0.0034190	18.645	60
80	1.2585	48.919	395.30	0.58504	2.5342	0.051803	0.094314	0.0032954	15.720	80
100	2.3102	48.317	389.85	0.60702	2.0616	0.042669	0.093114	0.0031748	13.440	100
120	4.0428	47.702	383.95	0.63065	1.6975	0.035587	0.091991	0.0030579	11.638	120
140	6.7782	47.070	377.52	0.65578	1.4131	0.030022	0.090924	0.0029456	10.192	140
160	10.936	46.417	370.50	0.68234	1.1880	0.025593	0.089895	0.0028383	9.0171	160
180	17.042	45.736	362.80	0.71035	1.0073	0.022023	0.088888	0.0027360	8.0496	180
200	25.740	45.022	354.34	0.73995	0.86037	0.019110	0.087887	0.0026381	7.2437	200
220	37.789	44.267	345.04	0.77137	0.73935	0.016702	0.086879	0.0025443	6.5644	220
240	54.064	43.462	334.81	0.80472	0.63835	0.014688	0.085854	0.0024547	5.9833	240
260	75.549	42.598	323.57	0.83980	0.55303	0.012983	0.084804	0.0023706	5.4766	260
280	103.32	41.663	311.22	0.87602	0.48018	0.011525	0.083730	0.0022941	5.0239	280
300	138.53	40.648	297.70	0.91243	0.41748	0.010271	0.082639	0.0022282	4.6095	300

APPENDIX B.3 (CONTINUED)

Thermophysical Properties of Liquids at Saturation (IP Units)

<i>T</i> °F	<i>P</i> _{sat} psia	<i>ρ</i> lbm/ft ³	<i>h</i> _{fg} Btu/ lbm	<i>c</i> _p Btu/ lbm-R	<i>μ</i> lbm/ ft-h	<i>ν</i> ft ² /h	<i>k</i> Btu/ h-ft-F	<i>α</i> ft ² /h	Pr	<i>T</i> °F
Acetone										
−80	0.015336	54.834	265.77	0.47999	2.5517	0.046534	0.11023	0.0041880	11.111	−80
−60	0.042370	54.099	261.25	0.48211	2.0210	0.037357	0.10770	0.0041294	9.0466	−60
−40	0.10468	53.365	256.74	0.48473	1.6564	0.031039	0.10513	0.0040641	7.6375	−40
−20	0.23507	52.629	252.25	0.48793	1.3930	0.026468	0.10252	0.0039922	6.6298	−20
0	0.48635	51.891	247.74	0.49173	1.1945	0.023019	0.099880	0.0039143	5.8806	0
20	0.93747	51.147	243.19	0.49617	1.0397	0.020327	0.097227	0.0038312	5.3057	20
40	1.6993	50.397	238.58	0.50123	0.91570	0.018170	0.094572	0.0037439	4.8532	40
60	2.9197	49.637	233.88	0.50691	0.81429	0.016405	0.091942	0.0036541	4.4895	60
80	4.7864	48.866	229.09	0.51320	0.72995	0.014938	0.089316	0.0035615	4.1943	80
100	7.5294	48.082	224.16	0.52011	0.65889	0.013703	0.086708	0.0034672	3.9523	100
120	11.421	47.282	219.09	0.52763	0.59838	0.012655	0.084126	0.0033721	3.7529	120
140	16.776	46.464	213.84	0.53578	0.54638	0.011759	0.081576	0.0032769	3.5886	140
160	23.947	45.624	208.39	0.54459	0.50136	0.010989	0.079062	0.0031820	3.4535	160
180	33.325	44.760	202.71	0.55413	0.46211	0.010324	0.076588	0.0030879	3.3434	180
200	45.337	43.867	196.76	0.56446	0.42764	0.0097487	0.074157	0.0029949	3.2551	200
220	60.441	42.940	190.50	0.57573	0.39718	0.0092496	0.071772	0.0029032	3.1860	220
240	79.129	41.975	183.87	0.58810	0.37006	0.0088162	0.069433	0.0028127	3.1344	240
260	101.92	40.965	176.82	0.60184	0.34575	0.0084402	0.067142	0.0027233	3.0992	260
280	129.38	39.901	169.28	0.61733	0.32378	0.0081144	0.064898	0.0026347	3.0799	280
Benzene										
50	0.88098	55.518	191.19	0.40522	1.8625	0.033548	0.084629	0.0037618	8.9180	50
60	1.1701	55.155	189.45	0.40847	1.7085	0.030977	0.083503	0.0037065	8.3576	60
70	1.5342	54.792	187.72	0.41189	1.5713	0.028677	0.082399	0.0036511	7.8545	70
80	1.9875	54.427	186.00	0.41547	1.4485	0.026614	0.081312	0.0035958	7.4014	80
100	3.2264	53.692	182.57	0.42305	1.2394	0.023085	0.079188	0.0034863	6.6215	100
120	5.0327	52.949	179.15	0.43108	1.0695	0.020199	0.077131	0.0033792	5.9774	120
140	7.5780	52.197	175.70	0.43949	0.93004	0.017818	0.075115	0.0032744	5.4416	140
160	11.059	51.434	172.22	0.44822	0.81451	0.015836	0.073133	0.0031723	4.9920	160
180	15.696	50.658	168.68	0.45723	0.71797	0.014173	0.071178	0.0030730	4.6121	180
200	21.731	49.868	165.07	0.46650	0.63665	0.012767	0.069245	0.0029766	4.2891	200
220	29.424	49.062	161.35	0.47602	0.56760	0.011569	0.067328	0.0028829	4.0130	220
240	39.054	48.238	157.53	0.48581	0.50852	0.010542	0.065424	0.0027918	3.7760	240
260	50.916	47.393	153.56	0.49591	0.45760	0.0096555	0.063530	0.0027031	3.5720	260
280	65.316	46.525	149.44	0.50638	0.41339	0.0088853	0.061644	0.0026165	3.3958	280
300	82.575	45.631	145.12	0.51732	0.37473	0.0082123	0.059765	0.0025318	3.2437	300
350	140.44	43.252	133.31	0.54772	0.29669	0.0068597	0.055094	0.0023256	2.9496	350
400	223.84	40.584	119.45	0.58637	0.23752	0.0058525	0.050468	0.0021207	2.7597	400
450	339.09	37.421	102.20	0.64615	0.19058	0.0050928	0.045911	0.0018988	2.6821	450
500	494.06	33.181	78.143	0.78891	0.15076	0.0045437	0.041602	0.0015893	2.8589	500

APPENDIX B.3 (CONTINUED)

Thermophysical Properties of Liquids at Saturation (IP Units)

<i>T</i> °F	<i>P</i> _{sat} psia	ρ lbm/ft ³	<i>h</i> _{fg} Btu/ lbm	<i>c</i> _p Btu/ lbm-R	μ lbm/ ft-h	ν ft ² /h	<i>k</i> Btu/ h-ft-F	α ft ² /h	Pr	<i>T</i> °F
Cyclohexane										
50	0.91964	49.191	172.90	0.42766	2.7613	0.056134	0.069286	0.0032935	17.044	50
60	1.2130	48.867	171.41	0.43380	2.5005	0.051170	0.068608	0.0032365	15.810	60
70	1.5801	48.541	169.91	0.43998	2.2741	0.046850	0.067926	0.0031805	14.730	70
80	2.0346	48.214	168.41	0.44620	2.0764	0.043067	0.067242	0.0031256	13.779	80
100	3.2667	47.554	165.40	0.45874	1.7494	0.036789	0.065871	0.0030196	12.184	100
120	5.0461	46.885	162.35	0.47141	1.4921	0.031825	0.064501	0.0029183	10.905	120
140	7.5326	46.207	159.26	0.48422	1.2859	0.027828	0.063137	0.0028218	9.8618	140
160	10.908	45.519	156.10	0.49719	1.1179	0.024558	0.061783	0.0027300	8.9958	160
180	15.374	44.819	152.87	0.51035	0.97905	0.021845	0.060443	0.0026425	8.2666	180
200	21.150	44.106	149.54	0.52376	0.86289	0.019564	0.059122	0.0025593	7.6444	200
220	28.473	43.378	146.10	0.53750	0.76458	0.017626	0.057822	0.0024800	7.1074	220
240	37.595	42.634	142.53	0.55164	0.68055	0.015963	0.056548	0.0024044	6.6389	240
260	48.779	41.870	138.81	0.56627	0.60805	0.014522	0.055302	0.0023324	6.2262	260
280	62.300	41.085	134.91	0.58151	0.54498	0.013265	0.054088	0.0022640	5.8591	280
300	78.445	40.273	130.80	0.59747	0.48967	0.012159	0.052910	0.0021989	5.5295	300
350	132.25	38.093	119.36	0.64176	0.37720	0.0099022	0.050136	0.0020508	4.8284	350
400	209.28	35.591	105.58	0.69668	0.29040	0.0081593	0.047654	0.0019219	4.2454	400
450	315.14	32.508	87.953	0.77863	0.21894	0.0067351	0.045573	0.0018005	3.7406	450
500	456.95	28.069	62.163	0.99724	0.15299	0.0054505	0.044553	0.0015916	3.4244	500
Toluene										
-20	0.016122	56.938	191.70	0.37074	3.0366	0.053332	0.083735	0.0039668	13.445	-20
0	0.038601	56.296	188.70	0.37712	2.4643	0.043774	0.082073	0.0038658	11.323	0
20	0.084886	55.655	185.76	0.38410	2.0510	0.036852	0.080366	0.0037594	9.8027	20
40	0.17336	55.014	182.87	0.39160	1.7408	0.031642	0.078625	0.0036496	8.6702	40
60	0.33188	54.371	180.02	0.39955	1.5005	0.027597	0.076861	0.0035381	7.7999	60
80	0.60025	53.726	177.19	0.40787	1.3096	0.024375	0.075081	0.0034263	7.1140	80
100	1.0326	53.077	174.37	0.41652	1.1548	0.021757	0.073295	0.0033154	6.5622	100
120	1.6995	52.422	171.55	0.42544	1.0271	0.019593	0.071522	0.0032069	6.1097	120
140	2.6890	51.762	168.71	0.43461	0.92039	0.017781	0.069755	0.0031008	5.7344	140
160	4.1083	51.094	165.84	0.44398	0.83003	0.016245	0.068004	0.0029978	5.4191	160
180	6.0835	50.418	162.92	0.45355	0.75270	0.014929	0.066275	0.0028983	5.1511	180
200	8.7594	49.731	159.95	0.46328	0.68588	0.013792	0.064574	0.0028028	4.9208	200
250	19.628	47.959	152.16	0.48837	0.55293	0.011529	0.060488	0.0025825	4.4643	250
300	38.941	46.085	143.65	0.51466	0.45367	0.0098441	0.056700	0.0023905	4.1179	300
350	70.260	44.068	134.14	0.54280	0.37610	0.0085345	0.053280	0.0022274	3.8315	350
400	117.64	41.846	123.22	0.57426	0.31293	0.0074781	0.050286	0.0020926	3.5736	400
450	185.66	39.317	110.24	0.61261	0.25941	0.0065980	0.047760	0.0019829	3.3275	450
500	279.67	36.281	94.010	0.66791	0.21201	0.0058434	0.045723	0.0018869	3.0969	500
550	406.48	32.240	71.683	0.78551	0.16689	0.0051763	0.044238	0.0017468	2.9633	550

APPENDIX B.3 (CONTINUED)

Thermophysical Properties of Liquids at Saturation (IP Units)

<i>T</i> °F	<i>P</i> _{sat} psia	<i>ρ</i> lbm/ft ³	<i>h</i> _{fg} Btu/ lbm	<i>c</i> _p Btu/ lbm-R	<i>μ</i> lbm/ ft-h	<i>ν</i> ft ² /h	<i>k</i> Btu/ h-ft-F	<i>α</i> ft ² /h	Pr	<i>T</i> °F
R22										
-160	0.15206	99.188	117.07	0.25370	2.5230	0.025437	0.084860	0.0033723	7.5428	-160
-140	0.43595	97.362	114.31	0.25361	1.9732	0.020266	0.081366	0.0032953	6.1501	-140
-120	1.0821	95.521	111.58	0.25374	1.5938	0.016686	0.077983	0.0032174	5.1860	-120
-100	2.3879	93.656	108.86	0.25435	1.3198	0.014092	0.074699	0.0031358	4.4938	-100
-80	4.7824	91.759	106.10	0.25562	1.1141	0.012141	0.071503	0.0030484	3.9828	-80
-60	8.8364	89.818	103.28	0.25770	0.95452	0.010627	0.068382	0.0029544	3.5971	-60
-40	15.263	87.824	100.34	0.26064	0.82725	0.0094194	0.065326	0.0028538	3.3007	-40
-20	24.906	85.765	97.259	0.26452	0.72317	0.0084320	0.062356	0.0027486	3.0678	-20
0	38.728	83.627	93.981	0.26938	0.63619	0.0076075	0.059421	0.0026378	2.8841	0
20	57.795	81.394	90.462	0.27531	0.56207	0.0069055	0.056514	0.0025220	2.7381	20
40	83.255	79.050	86.651	0.28249	0.49778	0.0062970	0.053623	0.0024013	2.6224	40
60	116.33	76.569	82.488	0.29125	0.44111	0.0057609	0.050733	0.0022749	2.5323	60
80	158.33	73.920	77.897	0.30221	0.39038	0.0052810	0.047828	0.0021410	2.4667	80
100	210.61	71.057	72.774	0.31656	0.34424	0.0048446	0.044886	0.0019955	2.4278	100
120	274.65	67.902	66.962	0.33669	0.30157	0.0044413	0.041877	0.0018317	2.4246	120
140	352.08	64.325	60.202	0.36788	0.26124	0.0040613	0.038761	0.0016380	2.4795	140
160	444.75	60.070	52.007	0.42434	0.22184	0.0036930	0.035480	0.0013919	2.6533	160
180	554.98	54.518	41.219	0.56415	0.18075	0.0033155	0.032021	0.0010411	3.1846	180
200	686.20	44.680	22.417	1.7777	0.12739	0.0028510	0.030671	0.00038615	7.3832	200
R32										
-160	0.29498	84.626	187.40	0.37351	1.5079	0.017819	0.13218	0.0041817	4.2611	-160
-140	0.81582	82.899	183.00	0.37259	1.2458	0.015028	0.12796	0.0041428	3.6275	-140
-120	1.9662	81.143	178.52	0.37268	1.0468	0.012901	0.12335	0.0040789	3.1628	-120
-100	4.2348	79.352	173.90	0.37381	0.89067	0.011224	0.11844	0.0039928	2.8111	-100
-80	8.3124	77.517	169.09	0.37605	0.76518	0.0098711	0.11333	0.0038877	2.5391	-80
-60	15.105	75.628	164.03	0.37948	0.66248	0.0087597	0.10809	0.0037663	2.3258	-60
-40	25.731	73.675	158.66	0.38425	0.57722	0.0078347	0.10280	0.0036311	2.1576	-40
-20	41.511	71.645	152.92	0.39056	0.50555	0.0070564	0.097498	0.0034844	2.0251	-20
10	78.179	68.419	143.44	0.40366	0.41745	0.0061013	0.089635	0.0032455	1.8799	10
0	63.947	69.521	146.73	0.39873	0.44461	0.0063953	0.092239	0.0033275	1.9220	0
10	78.179	68.419	143.44	0.40366	0.41745	0.0061013	0.089635	0.0032455	1.8799	10
20	94.715	67.285	140.00	0.40928	0.39217	0.0058285	0.087051	0.0031611	1.8438	20
40	135.65	64.908	132.60	0.42304	0.34648	0.0053380	0.081956	0.0029847	1.7885	40
60	188.74	62.351	124.37	0.44150	0.30607	0.0049088	0.076959	0.0027957	1.7559	60
80	256.18	59.556	115.07	0.46741	0.26970	0.0045285	0.072054	0.0025884	1.7495	80
100	340.37	56.429	104.36	0.50655	0.23623	0.0041864	0.067211	0.0023513	1.7804	100
120	444.04	52.796	91.607	0.57339	0.20445	0.0038725	0.062372	0.0020604	1.8795	120
140	570.47	48.276	75.508	0.71719	0.17265	0.0035763	0.057458	0.0016595	2.1550	140
160	724.09	41.654	51.946	1.2879	0.13661	0.0032797	0.052872	0.00098555	3.3278	160

APPENDIX B.3 (CONTINUED)

Thermophysical Properties of Liquids at Saturation (IP Units)

<i>T</i> °F	<i>P</i> _{sat} psia	<i>ρ</i> lbm/ft ³	<i>h</i> _{fg} Btu/ lbm	<i>c</i> _p Btu/ lbm-R	<i>μ</i> lbm/ ft-h	<i>ν</i> ft ² /h	<i>k</i> Btu/ h-ft-F	<i>α</i> ft ² /h	Pr	<i>T</i> °F
R123										
−100	0.035558	105.80	90.085	0.22115	4.3594	0.041203	0.061080	0.0026105	15.784	−100
−80	0.097215	104.26	88.219	0.22242	3.4880	0.033456	0.059337	0.0025589	13.075	−80
−60	0.23604	102.70	86.394	0.22429	2.8595	0.027843	0.057486	0.0024956	11.157	−60
−40	0.51854	101.13	84.592	0.22659	2.3862	0.023595	0.055546	0.0024240	9.7340	−40
−20	1.0463	99.538	82.797	0.22918	2.0183	0.020276	0.053554	0.0023476	8.6371	−20
0	1.9630	97.921	80.993	0.23196	1.7253	0.017620	0.051547	0.0022694	7.7640	0
20	3.4599	96.275	79.167	0.23488	1.4876	0.015452	0.049559	0.0021916	7.0504	20
40	5.7781	94.596	77.306	0.23788	1.2918	0.013656	0.047614	0.0021159	6.4542	40
60	9.2084	92.880	75.397	0.24098	1.1285	0.012150	0.045729	0.0020431	5.9470	60
80	14.090	91.121	73.427	0.24417	0.99087	0.010874	0.043914	0.0019737	5.5095	80
100	20.805	89.314	71.380	0.24751	0.87379	0.0097833	0.042175	0.0019079	5.1279	100
120	29.776	87.452	69.243	0.25104	0.77340	0.0088437	0.040511	0.0018453	4.7926	120
140	41.464	85.525	66.997	0.25485	0.68668	0.0080290	0.038918	0.0017855	4.4967	140
160	56.360	83.523	64.623	0.25906	0.61124	0.0073182	0.037389	0.0017280	4.2351	160
180	74.986	81.430	62.095	0.26383	0.54515	0.0066947	0.035915	0.0016717	4.0046	180
200	97.892	79.228	59.383	0.26939	0.48684	0.0061447	0.034486	0.0016158	3.8030	200
250	177.80	73.043	51.498	0.28962	0.36675	0.0050210	0.031016	0.0014662	3.4246	250
300	298.53	65.107	40.935	0.33495	0.27023	0.0041505	0.027465	0.0012594	3.2956	300
350	474.41	51.322	22.169	0.68304	0.17314	0.0033736	0.023429	0.00066835	5.0476	350
R125										
−140	0.66539	104.52	80.808	0.24833	2.4531	0.023469	0.065708	0.0025315	9.2709	−140
−120	1.6245	102.26	78.519	0.25143	1.9097	0.018675	0.062678	0.0024378	7.6607	−120
−100	3.5260	99.957	76.196	0.25532	1.5317	0.015324	0.059637	0.0023368	6.5575	−100
−80	6.9483	97.598	73.802	0.25982	1.2546	0.012855	0.056599	0.0022320	5.7594	−80
−60	12.640	95.166	71.302	0.26491	1.0435	0.010965	0.053600	0.0021261	5.1572	−60
−40	21.509	92.645	68.659	0.27062	0.87759	0.0094727	0.050631	0.0020194	4.6908	−40
−30	27.460	91.343	67.272	0.27376	0.80737	0.0088388	0.049163	0.0019661	4.4957	−30
−20	34.610	90.010	65.835	0.27710	0.74397	0.0082654	0.047708	0.0019128	4.3212	−20
−10	43.111	88.642	64.341	0.28070	0.68643	0.0077439	0.046267	0.0018595	4.1645	−10
0	53.120	87.233	62.785	0.28459	0.63396	0.0072674	0.044840	0.0018062	4.0236	0
10	64.803	85.780	61.159	0.28884	0.58587	0.0068299	0.043429	0.0017528	3.8966	10
20	78.331	84.276	59.454	0.29353	0.54160	0.0064265	0.042034	0.0016992	3.7821	20
30	93.882	82.714	57.657	0.29876	0.50064	0.0060527	0.040654	0.0016451	3.6791	30
40	111.64	81.084	55.756	0.30466	0.46257	0.0057048	0.039289	0.0015905	3.5868	40
60	154.57	77.575	51.567	0.31927	0.39359	0.0050737	0.036603	0.0014779	3.4331	60
80	208.77	73.620	46.712	0.34009	0.33205	0.0045104	0.033963	0.0013565	3.3250	80
100	276.09	68.989	40.907	0.37392	0.27557	0.0039944	0.031349	0.0012152	3.2869	100
120	358.72	63.183	33.537	0.44460	0.22128	0.0035022	0.028740	0.0010231	3.4231	120
140	459.81	54.443	22.419	0.75028	0.16220	0.0029793	0.026518	0.00064920	4.5892	140

APPENDIX B.3 (CONTINUED)

Thermophysical Properties of Liquids at Saturation (IP Units)

<i>T</i> °F	<i>P</i> _{sat} psia	ρ lbm/ft ³	<i>h</i> _{fg} Btu/ lbm	<i>c</i> _p Btu/ lbm-R	μ lbm/ ft-h	ν ft ² /h	<i>k</i> Btu/ h-ft-F	α ft ² /h	Pr	<i>T</i> °F
R134a										
-100	0.90296	94.327	105.73	0.28813	2.1068	0.022335	0.073917	0.0027197	8.2123	-100
-80	1.9927	92.424	102.93	0.29156	1.6681	0.018048	0.070465	0.0026149	6.9020	-80
-60	4.0020	90.486	100.09	0.29549	1.3586	0.015014	0.067144	0.0025112	5.9789	-60
-40	7.4272	88.504	97.167	0.29987	1.1298	0.012765	0.063942	0.0024093	5.2983	-40
-20	12.898	86.469	94.133	0.30474	0.95425	0.011036	0.060845	0.0023091	4.7793	-20
-10	16.632	85.427	92.562	0.30738	0.88102	0.010313	0.059333	0.0022595	4.5643	-10
0	21.171	84.368	90.949	0.31019	0.81544	0.0096654	0.057842	0.0022103	4.3730	0
10	26.628	83.288	89.288	0.31318	0.75635	0.0090812	0.056372	0.0021612	4.2019	10
20	33.124	82.186	87.575	0.31637	0.70280	0.0085514	0.054920	0.0021122	4.0485	20
30	40.784	81.059	85.803	0.31980	0.65400	0.0080682	0.053485	0.0020633	3.9104	30
40	49.741	79.904	83.967	0.32350	0.60930	0.0076254	0.052065	0.0020142	3.7859	40
60	72.105	77.499	80.072	0.33193	0.53011	0.0068403	0.049263	0.0019150	3.5719	60
80	101.39	74.937	75.823	0.34217	0.46178	0.0061623	0.046497	0.0018134	3.3983	80
100	138.85	72.171	71.134	0.35510	0.40175	0.0055666	0.043748	0.0017070	3.2610	100
120	185.86	69.137	65.876	0.37227	0.34805	0.0050342	0.040996	0.0015928	3.1605	120
140	243.92	65.728	59.853	0.39679	0.29904	0.0045496	0.038212	0.0014652	3.1051	140
160	314.73	61.764	52.727	0.43619	0.25315	0.0040986	0.035369	0.0013129	3.1219	160
180	400.34	56.857	43.791	0.51557	0.20831	0.0036638	0.032456	0.0011072	3.3091	180
200	503.59	49.761	30.883	0.80623	0.15953	0.0032059	0.029881	0.00074482	4.3043	200
R227ea										
-100	0.51957	107.75	66.325	0.23602	2.5088	0.023284	0.049372	0.0019414	11.993	-100
-80	1.1861	105.66	64.528	0.23973	2.0625	0.019520	0.047977	0.0018940	10.306	-80
-60	2.4513	103.52	62.713	0.24365	1.7183	0.016598	0.046498	0.0018434	9.0039	-60
-40	4.6615	101.33	60.859	0.24783	1.4460	0.014271	0.044948	0.0017899	7.9729	-40
-20	8.2640	99.063	58.947	0.25235	1.2261	0.012377	0.043336	0.0017336	7.1394	-20
-10	10.754	97.901	57.962	0.25475	1.1315	0.011557	0.042511	0.0017045	6.7805	-10
0	13.806	96.719	56.954	0.25728	1.0454	0.010808	0.041673	0.0016747	6.4536	0
10	17.500	95.513	55.919	0.25993	0.96673	0.010121	0.040826	0.0016445	6.1549	10
20	21.926	94.282	54.855	0.26272	0.89472	0.0094898	0.039970	0.0016137	5.8809	20
30	27.177	93.023	53.757	0.26567	0.82857	0.0089071	0.039105	0.0015824	5.6290	30
40	33.350	91.733	52.622	0.26879	0.76763	0.0083681	0.038234	0.0015506	5.3966	40
60	48.878	89.046	50.219	0.27569	0.65924	0.0074033	0.036477	0.0014859	4.9825	60
80	69.382	86.188	47.604	0.28371	0.56583	0.0065651	0.034709	0.0014195	4.6250	80
100	95.801	83.107	44.722	0.29332	0.48445	0.0058292	0.032941	0.0013513	4.3137	100
120	129.15	79.730	41.491	0.30542	0.41262	0.0051752	0.031184	0.0012806	4.0411	120
140	170.55	75.942	37.792	0.32178	0.34817	0.0045847	0.029453	0.0012053	3.8039	140
160	221.26	71.540	33.419	0.34674	0.28899	0.0040396	0.027771	0.0011195	3.6084	160
180	282.77	66.102	27.960	0.39447	0.23250	0.0035172	0.026208	0.0010051	3.4994	180
200	357.11	58.315	20.226	0.55566	0.17333	0.0029723	0.025248	0.00077918	3.8147	200

APPENDIX B.4

Thermophysical Properties of Ethylene Glycol–Water Solutions (SI Units)

<i>Conc</i> mass %	<i>T</i> _{freeze} °C	<i>T</i> °C	ρ kg/m ³	c_p kJ/kg-K	μ mPa-s	ν mm ² /s	<i>k</i> W/m-K	α mm ² /s	Pr	<i>T</i> °C
10	−3.357	0	1013.6	4.0374	2.3449	2.3134	0.52328	0.12787	18.092	0
		20	1010.6	4.0459	1.2745	1.2612	0.55289	0.13523	9.3265	20
		40	1004.3	4.0619	0.80135	0.79789	0.57833	0.14176	5.6283	40
		60	995.23	4.0831	0.56338	0.56608	0.59961	0.14756	3.8363	60
		80	983.55	4.1071	0.42808	0.43524	0.61678	0.15269	2.8505	80
		100	969.62	4.1316	0.33982	0.35047	0.62987	0.15723	2.2290	100
		120	953.75	4.1543	0.27241	0.28562	0.63890	0.16125	1.7712	120
		140	936.25	4.1727	0.21315	0.22766	0.64390	0.16482	1.3813	140
		160	917.44	4.1847	0.15735	0.17151	0.64490	0.16798	1.0211	160
		180	897.63	4.1878	0.10594	0.11802	0.64194	0.17077	0.69113	180
20	−7.949	0	1029.1	3.8608	3.1776	3.0878	0.48414	0.12186	25.340	0
		20	1024.1	3.8962	1.6624	1.6233	0.50766	0.12723	12.759	20
		40	1016.4	3.9328	1.0133	0.99691	0.52908	0.13236	7.5318	40
		60	1006.2	3.9693	0.69688	0.69258	0.54832	0.13729	5.0448	60
		80	993.76	4.0048	0.52381	0.52710	0.56533	0.14205	3.7106	80
		100	979.32	4.0379	0.41676	0.42556	0.58004	0.14668	2.9012	100
		120	963.11	4.0675	0.33995	0.35297	0.59241	0.15122	2.3341	120
		140	945.40	4.0926	0.27534	0.29124	0.60235	0.15568	1.8708	140
		160	926.42	4.1118	0.21448	0.23152	0.60982	0.16009	1.4462	160
		180	906.43	4.1240	0.15563	0.17169	0.61475	0.16445	1.0440	180
30	−14.58	0	1045.0	3.6581	4.2976	4.1126	0.44592	0.11665	35.255	0
		20	1038.0	3.7183	2.1664	2.0870	0.46490	0.12045	17.327	20
		40	1028.8	3.7754	1.2856	1.2496	0.48303	0.12436	10.048	40
		60	1017.5	3.8287	0.86604	0.85118	0.50018	0.12840	6.6293	60
		80	1004.3	3.8777	0.63884	0.63613	0.51624	0.13257	4.7986	80
		100	989.41	3.9215	0.49766	0.50299	0.53106	0.13687	3.6749	100
		120	973.15	3.9596	0.39488	0.40577	0.54452	0.14131	2.8715	120
		140	955.71	3.9913	0.30780	0.32207	0.55649	0.14589	2.2076	140
		160	937.30	4.0158	0.22732	0.24253	0.56684	0.15059	1.6105	160
		180	918.16	4.0326	0.15342	0.16709	0.57544	0.15542	1.0751	180
40	−23.81	0	1060.4	3.4342	5.8107	5.4798	0.40990	0.11256	48.682	0
		20	1051.9	3.5190	2.8191	2.6801	0.42530	0.11490	23.326	20
		40	1041.4	3.5978	1.6351	1.5702	0.44050	0.11757	13.355	40
		60	1029.1	3.6697	1.0821	1.0515	0.45535	0.12057	8.7209	60
		80	1015.4	3.7338	0.77997	0.76814	0.46966	0.12388	6.2008	80
		100	1000.5	3.7893	0.58440	0.58413	0.48326	0.12748	4.5823	100
		120	984.55	3.8353	0.43445	0.44126	0.49598	0.13135	3.3594	120
		140	967.93	3.8708	0.30586	0.31599	0.50764	0.13549	2.3322	140
		160	950.85	3.8952	0.19464	0.20470	0.51806	0.13988	1.4634	160
		180	933.57	3.9073	0.10686	0.11447	0.52708	0.14449	0.79220	180

APPENDIX B.4 (CONTINUED)

Thermophysical Properties of Ethylene Glycol–Water Solutions (IP Units)

<i>Conc</i> mass %	<i>T</i> _{freeze} °F	<i>T</i> °F	ρ lbm/ft ³	<i>c_p</i> Btu/ lbm-R	μ lbm/ft-h	ν ft ² /h	<i>k</i> Btu/ h-ft-R	α ft ² /h	Pr	<i>T</i> °F
10	25.96	40	63.254	0.96455	4.8833	0.077202	0.30636	0.0050213	15.375	40
		60	63.148	0.96569	3.4822	0.055143	0.31586	0.0051796	10.646	60
		80	62.980	0.96742	2.6033	0.041336	0.32462	0.0053279	7.7583	80
		100	62.752	0.96964	2.0286	0.032328	0.33264	0.0054668	5.9135	100
		120	62.467	0.97227	1.6382	0.026224	0.33991	0.0055966	4.6857	120
		140	62.130	0.97520	1.3629	0.021936	0.34645	0.0057180	3.8363	140
		160	61.744	0.97834	1.1614	0.018809	0.35225	0.0058314	3.2255	160
		180	61.311	0.98159	1.0078	0.016437	0.35733	0.0059374	2.7684	180
		200	60.836	0.98486	0.88538	0.014554	0.36167	0.0060365	2.4109	200
		220	60.321	0.98805	0.78291	0.012979	0.36529	0.0061290	2.1176	220
20	17.69	20	64.305	0.91942	9.9238	0.15432	0.27494	0.0046502	33.186	20
		40	64.189	0.92396	6.5582	0.10217	0.28286	0.0047692	21.423	40
		60	64.017	0.92866	4.5782	0.071516	0.29041	0.0048849	14.640	60
		80	63.791	0.93346	3.3577	0.052635	0.29758	0.0049975	10.532	80
		100	63.513	0.93833	2.5729	0.040509	0.30438	0.0051074	7.9315	100
		120	63.187	0.94320	2.0487	0.032422	0.31079	0.0052148	6.2173	120
		140	62.815	0.94804	1.6858	0.026838	0.31681	0.0053200	5.0447	140
		160	62.400	0.95279	1.4258	0.022849	0.32243	0.0054232	4.2132	160
		180	61.944	0.95741	1.2326	0.019899	0.32765	0.0055247	3.6018	180
		200	61.450	0.96185	1.0833	0.017629	0.33246	0.0056248	3.1341	200
30	5.764	20	65.345	0.86878	13.630	0.20858	0.25390	0.0044724	46.638	20
		40	65.153	0.87695	8.7872	0.13487	0.26012	0.0045528	29.624	40
		60	64.912	0.88493	6.0095	0.092578	0.26622	0.0046344	19.976	60
		80	64.626	0.89271	4.3327	0.067042	0.27216	0.0047175	14.211	80
		100	64.297	0.90023	3.2728	0.050901	0.27795	0.0048020	10.600	100
		120	63.927	0.90749	2.5741	0.040267	0.28357	0.0048880	8.2379	120
		140	63.518	0.91445	2.0950	0.032984	0.28900	0.0049755	6.6291	140
		160	63.074	0.92109	1.7536	0.027802	0.29424	0.0050646	5.4894	160
		180	62.596	0.92737	1.5001	0.023965	0.29926	0.0051553	4.6485	180
		200	62.086	0.93328	1.3034	0.020993	0.30407	0.0052477	4.0005	200
40	-10.86	0	66.554	0.80118	32.251	0.48458	0.22892	0.0042932	112.87	0
		20	66.345	0.81319	18.763	0.28282	0.23387	0.0043348	65.244	20
		40	66.091	0.82484	11.758	0.17791	0.23882	0.0043808	40.611	40
		60	65.795	0.83610	7.8733	0.11966	0.24376	0.0044311	27.006	60
		80	65.460	0.84693	5.5885	0.085373	0.24868	0.0044855	19.033	80
		100	65.088	0.85729	4.1714	0.064089	0.25355	0.0045440	14.104	100
		120	64.682	0.86715	3.2483	0.050219	0.25836	0.0046063	10.902	120
		140	64.245	0.87647	2.6178	0.040746	0.26310	0.0046723	8.7208	140
		160	63.780	0.88522	2.1660	0.033960	0.26773	0.0047421	7.1614	160
		180	63.289	0.89337	1.8253	0.028841	0.27226	0.0048153	5.9894	180

APPENDIX B.4 (CONTINUED)

Thermophysical Properties of Propylene Glycol–Water Solutions (SI Units)

<i>Conc</i> mass %	<i>T</i> _{freeze} °C	<i>T</i> °C	ρ kg/m ³	<i>c_p</i> kJ/kg-K	μ mPa-s	ν mm ² /s	<i>k</i> W/m-K	α mm ² /s	Pr	<i>T</i> °C
10	−2.867	0	1009.3	4.0590	2.7446	2.7192	0.51549	0.12583	21.611	0
		20	1006.2	4.0763	1.4323	1.4234	0.54381	0.13258	10.736	20
		40	999.42	4.1011	0.88380	0.88431	0.56879	0.13877	6.3724	40
		60	989.81	4.1303	0.61366	0.61998	0.59018	0.14436	4.2947	60
		80	978.22	4.1610	0.45625	0.46641	0.60775	0.14931	3.1238	80
		100	965.50	4.1901	0.34567	0.35802	0.62128	0.15357	2.3313	100
		120	952.50	4.2147	0.25395	0.26661	0.63053	0.15706	1.6975	120
		140	940.08	4.2317	0.17216	0.18314	0.63528	0.15969	1.1468	140
		160	929.07	4.2380	0.10249	0.11032	0.63528	0.16134	0.68374	160
		180	920.33	4.2308	0.050990	0.055403	0.63031	0.16188	0.34226	180
20	−7.173	0	1020.1	3.9359	4.3124	4.2275	0.47112	0.11734	36.028	0
		20	1014.8	3.9768	2.0301	2.0005	0.49221	0.12197	16.402	20
		40	1006.4	4.0190	1.1693	1.1619	0.51228	0.12666	9.1737	40
		60	995.59	4.0612	0.77776	0.78120	0.53100	0.13133	5.9484	60
		80	983.18	4.1016	0.56382	0.57347	0.54808	0.13591	4.2195	80
		100	969.86	4.1389	0.42044	0.43350	0.56320	0.14030	3.0897	100
		120	956.38	4.1714	0.30437	0.31826	0.57607	0.14440	2.2040	120
		140	943.47	4.1976	0.20190	0.21400	0.58636	0.14806	1.4453	140
		160	931.86	4.2159	0.11581	0.12428	0.59376	0.15114	0.82230	160
		180	922.28	4.2248	0.054220	0.058789	0.59798	0.15347	0.38307	180
30	−12.79	0	1031.6	3.8026	7.1171	6.8994	0.42845	0.10923	63.166	0
		20	1023.8	3.8570	2.9650	2.8961	0.44443	0.11255	25.732	20
		40	1013.4	3.9104	1.5731	1.5523	0.46056	0.11622	13.357	40
		60	1001.2	3.9623	0.99458	0.99343	0.47657	0.12014	8.2692	60
		80	987.60	4.0122	0.70106	0.70987	0.49215	0.12420	5.7153	80
		100	973.42	4.0595	0.51549	0.52957	0.50703	0.12831	4.1273	100
		120	959.27	4.1036	0.36996	0.38567	0.52089	0.13232	2.9145	120
		140	945.79	4.1441	0.24246	0.25636	0.53346	0.13611	1.8835	140
		160	933.65	4.1803	0.13577	0.14542	0.54445	0.13950	1.0425	160
		180	923.48	4.2118	0.060780	0.065816	0.55356	0.14232	0.46245	180
40	−20.57	0	1042.4	3.6416	11.879	11.397	0.38784	0.10218	111.54	0
		20	1032.3	3.7067	4.3838	4.2467	0.40026	0.10461	40.597	20
		40	1020.1	3.7708	2.1408	2.0987	0.41321	0.10743	19.536	40
		60	1006.3	3.8339	1.2827	1.2746	0.42651	0.11055	11.530	60
		80	991.63	3.8958	0.87425	0.88163	0.43998	0.11389	7.7411	80
		100	976.62	3.9567	0.62846	0.64351	0.45345	0.11735	5.4838	100
		120	961.88	4.0164	0.44177	0.45928	0.46673	0.12081	3.8016	120
		140	948.00	4.0749	0.28154	0.29698	0.47964	0.12416	2.3919	140
		160	935.59	4.1324	0.15082	0.16120	0.49201	0.12726	1.2667	160
		180	925.25	4.1886	0.062967	0.068054	0.50367	0.12996	0.52365	180

APPENDIX B.4 (CONTINUED)

Thermophysical Properties of Propylene Glycol–Water Solutions (IP Units)

<i>Conc</i> mass %	<i>T_{freeze}</i> °F	<i>T</i> °F	ρ lbm/ft ³	c_p Btu/ lbm-R	μ lbm/ft-h	ν ft ² /h	<i>k</i> Btu/ h-ft-R	α ft ² /h	Pr	<i>T</i> °F
10	26.84	40	62.989	0.97019	5.6489	0.089682	0.30164	0.0049359	18.169	40
		60	62.880	0.97250	3.9391	0.062645	0.31074	0.0050815	12.328	60
		80	62.697	0.97541	2.9024	0.046293	0.31924	0.0052202	8.8681	80
		100	62.448	0.97879	2.2407	0.035880	0.32714	0.0053520	6.7041	100
		120	62.144	0.98253	1.7970	0.028917	0.33440	0.0054767	5.2800	120
		140	61.792	0.98649	1.4845	0.024024	0.34100	0.0055941	4.2946	140
		160	61.402	0.99057	1.2525	0.020399	0.34692	0.0057038	3.5763	160
		180	60.983	0.99463	1.0702	0.017549	0.35214	0.0058056	3.0227	180
		200	60.544	0.99854	0.91815	0.015165	0.35663	0.0058991	2.5708	200
		220	60.094	1.0022	0.78427	0.013051	0.36038	0.0059837	2.1810	220
20	19.09	20	63.741	0.93695	14.166	0.22225	0.26805	0.0044882	49.518	20
		40	63.627	0.94218	8.6458	0.13588	0.27496	0.0045866	29.626	40
		60	63.442	0.94760	5.6941	0.089752	0.28173	0.0046863	19.152	60
		80	63.195	0.95316	4.0069	0.063406	0.28833	0.0047869	13.246	80
		100	62.892	0.95878	2.9830	0.047431	0.29473	0.0048878	9.7039	100
		120	62.542	0.96441	2.3262	0.037195	0.30090	0.0049888	7.4557	120
		140	62.153	0.96997	1.8815	0.030272	0.30681	0.0050892	5.9483	140
		160	61.732	0.97541	1.5627	0.025315	0.31242	0.0051884	4.8790	160
		180	61.287	0.98067	1.3197	0.021534	0.31770	0.0052860	4.0737	180
		200	60.827	0.98568	1.1221	0.018447	0.32264	0.0053812	3.4280	200
30	8.979	20	64.517	0.90387	24.607	0.38140	0.24453	0.0041932	90.955	20
		40	64.306	0.91112	13.832	0.21510	0.24959	0.0042599	50.494	40
		60	64.036	0.91834	8.5131	0.13294	0.25472	0.0043315	30.692	60
		80	63.713	0.92549	5.6713	0.089012	0.25989	0.0044075	20.196	80
		100	63.345	0.93257	4.0431	0.063826	0.26507	0.0044872	14.224	100
		120	62.938	0.93953	3.0495	0.048453	0.27024	0.0045701	10.602	120
		140	62.500	0.94637	2.4060	0.038496	0.27536	0.0046554	8.2691	140
		160	62.037	0.95305	1.9630	0.031643	0.28040	0.0047425	6.6722	160
		180	61.557	0.95957	1.6376	0.026602	0.28534	0.0048307	5.5069	180
		200	61.065	0.96589	1.3808	0.022612	0.29015	0.0049192	4.5967	200
40	−5.023	0	65.489	0.85571	93.754	1.4316	0.21805	0.0038910	367.92	0
		20	65.245	0.86451	43.200	0.66211	0.22178	0.0039320	168.39	20
		40	64.945	0.87323	22.389	0.34474	0.22565	0.0039789	86.642	40
		60	64.595	0.88188	12.884	0.19945	0.22964	0.0040313	49.477	60
		80	64.202	0.89045	8.1254	0.12656	0.23373	0.0040885	30.955	80
		100	63.770	0.89894	5.5440	0.086937	0.23791	0.0041501	20.948	100
		120	63.308	0.90735	4.0397	0.063809	0.24215	0.0042154	15.137	120
		140	62.822	0.91568	3.1029	0.049392	0.24643	0.0042839	11.530	140
		160	62.318	0.92394	2.4801	0.039798	0.25075	0.0043550	9.1385	160
		180	61.802	0.93211	2.0362	0.032947	0.25508	0.0044281	7.4406	180

APPENDIX B.4 (CONTINUED)

Thermophysical Properties of Methanol–Water Solutions (SI Units)

<i>Conc</i> mass %	<i>T</i> _{freeze} °C	<i>T</i> °C	ρ kg/m ³	<i>c</i> _{<i>p</i>} kJ/kg-K	μ mPa-s	ν mm ² /s	<i>k</i> W/m-K	α mm ² /s	Pr	<i>T</i> °C
10	−6.548	−5	984.45	4.2513	3.1070	3.1561	0.50195	0.11993	26.315	−5
		0	984.39	4.2408	2.5348	2.5750	0.50955	0.12206	21.097	0
		5	984.05	4.2301	2.1026	2.1367	0.51700	0.12420	17.204	5
		10	983.46	4.2192	1.7709	1.8007	0.52430	0.12636	14.251	10
		15	982.62	4.2083	1.5122	1.5389	0.53144	0.12852	11.974	15
		20	981.54	4.1975	1.3073	1.3319	0.53840	0.13068	10.192	20
		25	980.23	4.1871	1.1426	1.1657	0.54519	0.13283	8.7754	25
		30	978.70	4.1771	1.0083	1.0302	0.55179	0.13497	7.6326	30
		35	976.96	4.1677	0.89694	0.91809	0.55819	0.13709	6.6969	35
		40	975.02	4.1590	0.80327	0.82385	0.56439	0.13918	5.9193	40
20	−15.09	−15	974.91	4.0064	6.4493	6.6153	0.44563	0.11409	57.983	−15
		−10	974.30	4.0296	5.0298	5.1625	0.45117	0.11492	44.923	−10
		−5	973.51	4.0502	3.9961	4.1048	0.45665	0.11582	35.442	−5
		0	972.52	4.0681	3.2301	3.3214	0.46209	0.11680	28.437	0
		5	971.35	4.0832	2.6531	2.7313	0.46748	0.11787	23.173	5
		10	970.00	4.0953	2.2115	2.2798	0.47283	0.11903	19.154	10
		15	968.48	4.1043	1.8684	1.9292	0.47813	0.12029	16.038	15
		20	966.79	4.1101	1.5979	1.6528	0.48339	0.12165	13.586	20
		30	962.90	4.1114	1.2063	1.2527	0.49378	0.12473	10.044	30
		40	958.37	4.0980	0.94179	0.98270	0.50402	0.12833	7.6574	40
30	−25.69	−25	968.53	3.6331	12.405	12.808	0.39857	0.11327	113.08	−25
		−20	967.11	3.6871	9.3562	9.6744	0.40231	0.11283	85.747	−20
		−15	965.56	3.7381	7.1951	7.4518	0.40604	0.11249	66.241	−15
		−10	963.90	3.7859	5.6353	5.8463	0.40975	0.11228	52.068	−10
		−5	962.12	3.8301	4.4897	4.6665	0.41345	0.11220	41.593	−5
		0	960.22	3.8705	3.6346	3.7851	0.41715	0.11224	33.723	0
		10	956.08	3.9382	2.4870	2.6013	0.42458	0.11276	23.068	10
		20	951.48	3.9865	1.7888	1.8800	0.43210	0.11392	16.503	20
		30	946.42	4.0127	1.3399	1.4157	0.43976	0.11580	12.226	30
		40	940.90	4.0144	1.0355	1.1006	0.44762	0.11851	9.2868	40
40	−38.70	−35	962.74	3.2421	20.860	21.668	0.35960	0.11521	188.07	−35
		−30	960.50	3.3122	15.400	16.034	0.36196	0.11378	140.92	−30
		−25	958.19	3.3800	11.597	12.103	0.36430	0.11249	107.60	−25
		−20	955.83	3.4451	8.8989	9.3101	0.36663	0.11134	83.622	−20
		−10	950.91	3.5659	5.5182	5.8030	0.37127	0.10949	53.001	−10
		0	945.73	3.6712	3.6395	3.8484	0.37595	0.10828	35.541	0
		10	940.29	3.7578	2.5306	2.6913	0.38074	0.10775	24.976	10
		20	934.57	3.8224	1.8385	1.9673	0.38571	0.10797	18.220	20
		30	928.56	3.8618	1.3834	1.4898	0.39093	0.10902	13.666	30
		40	922.27	3.8728	1.0684	1.1585	0.39646	0.11100	10.437	40

Thermophysical Properties of Methanol–Water Solutions (IP Units)

<i>Conc</i> mass %	<i>T</i> _{freeze} °F	<i>T</i> °F	ρ lbm/ft ³	c_p Btu/ lbm-R	μ lbm/ft-h	ν ft ² /h	<i>k</i> Btu/ h-ft-R	α ft ² /h	Pr	<i>T</i> °F
10	20.21	25	61.458	1.0148	7.1729	0.11671	0.29100	0.0046658	25.015	25
		30	61.456	1.0134	6.4062	0.10424	0.29344	0.0047115	22.125	30
		35	61.448	1.0120	5.7513	0.093596	0.29586	0.0047575	19.674	35
		40	61.436	1.0106	5.1892	0.084466	0.29824	0.0048036	17.584	40
		50	61.395	1.0077	4.2839	0.069776	0.30293	0.0048964	14.250	50
		60	61.336	1.0048	3.5972	0.058648	0.30751	0.0049895	11.754	60
		70	61.258	1.0020	3.0665	0.050058	0.31196	0.0050825	9.8491	70
		80	61.163	0.99924	2.6486	0.043304	0.31629	0.0051752	8.3676	80
		90	61.051	0.99664	2.3134	0.037892	0.32048	0.0052670	7.1943	90
		100	60.924	0.99424	2.0393	0.033473	0.32452	0.0053576	6.2478	100
20	4.842	5	60.862	0.95690	15.601	0.25634	0.25748	0.0044211	57.982	5
		10	60.842	0.96004	13.557	0.22282	0.25926	0.0044385	50.201	10
		20	60.792	0.96578	10.417	0.17135	0.26280	0.0044761	38.282	20
		30	60.727	0.97073	8.1806	0.13471	0.26630	0.0045173	29.821	30
		40	60.648	0.97486	6.5550	0.10808	0.26976	0.0045627	23.688	40
		50	60.555	0.97812	5.3497	0.088345	0.27320	0.0046124	19.154	50
		60	60.449	0.98047	4.4393	0.073440	0.27660	0.0046669	15.736	60
		70	60.329	0.98185	3.7392	0.061979	0.27997	0.0047264	13.113	70
		80	60.197	0.98223	3.1912	0.053012	0.28331	0.0047915	11.064	80
		100	59.895	0.97980	2.4013	0.040092	0.28991	0.0049400	8.1158	100
30	−14.24	−10	60.435	0.87211	27.255	0.45099	0.23101	0.0043830	102.89	−10
		0	60.333	0.88613	20.093	0.33304	0.23341	0.0043658	76.283	0
		10	60.221	0.89926	15.163	0.25179	0.23579	0.0043541	57.828	10
		20	60.101	0.91137	11.694	0.19458	0.23817	0.0043483	44.749	20
		30	59.972	0.92237	9.2030	0.15346	0.24055	0.0043486	35.288	30
		40	59.833	0.93215	7.3781	0.12331	0.24293	0.0043556	28.311	40
		50	59.686	0.94060	6.0164	0.10080	0.24532	0.0043697	23.068	50
		60	59.530	0.94762	4.9821	0.083690	0.24773	0.0043914	19.058	60
		80	59.191	0.95694	3.5550	0.060060	0.25260	0.0044596	13.468	80
		100	58.817	0.95926	2.6467	0.044999	0.25761	0.0045659	9.8556	100
40	−37.67	−35	60.163	0.76676	58.136	0.96631	0.20716	0.0044908	215.18	−35
		−30	60.087	0.77623	48.741	0.81117	0.20793	0.0044580	181.96	−30
		−25	60.009	0.78555	41.127	0.68535	0.20869	0.0044269	154.82	−25
		−20	59.930	0.79473	34.921	0.58269	0.20944	0.0043974	132.51	−20
		0	59.604	0.82953	19.247	0.32291	0.21243	0.0042964	75.158	0
		20	59.258	0.86052	11.545	0.19484	0.21541	0.0042244	46.122	20
		40	58.891	0.88663	7.4465	0.12645	0.21844	0.0041835	30.225	40
		60	58.504	0.90679	5.1014	0.087197	0.22157	0.0041765	20.878	60
		80	58.095	0.91995	3.6671	0.063122	0.22485	0.0042072	15.003	80
		100	57.664	0.92502	2.7325	0.047386	0.22834	0.0042808	11.069	100

APPENDIX B.4 (CONTINUED)

Thermophysical Properties of Ethanol–Water Solutions (SI Units)

<i>Conc</i> mass %	<i>T</i> _{freeze} °C	<i>T</i> °C	ρ kg/m ³	<i>c_p</i> kJ/kg-K	μ mPa-s	ν mm ² /s	<i>k</i> W/m-K	α mm ² /s	Pr	<i>T</i> °C
10	−4.388	0	984.99	4.4017	3.3170	3.3676	0.50270	0.11595	29.044	0
		5	984.67	4.3764	2.6376	2.6787	0.50927	0.11818	22.667	5
		10	984.02	4.3506	2.1531	2.1881	0.51577	0.12048	18.162	10
		15	983.07	4.3257	1.7975	1.8284	0.52219	0.12280	14.890	15
		20	981.84	4.3033	1.5287	1.5570	0.52852	0.12509	12.447	20
		25	980.37	4.2850	1.3194	1.3459	0.53476	0.12730	10.572	25
		30	978.67	4.2722	1.1513	1.1764	0.54089	0.12937	9.0939	30
		35	976.77	4.2666	1.0118	1.0359	0.54689	0.13123	7.8939	35
		40	974.70	4.2696	0.89217	0.91532	0.55276	0.13282	6.8914	40
20	−11.13	45	972.49	4.2829	0.78623	0.80846	0.55848	0.13408	6.0295	45
		−10	977.60	4.3827	9.5644	9.7836	0.43871	0.10240	95.547	−10
		−5	976.83	4.3774	6.9767	7.1422	0.44324	0.10366	68.902	−5
		0	975.77	4.3694	5.2493	5.3796	0.44782	0.10504	51.217	0
		5	974.42	4.3595	4.0621	4.1687	0.45243	0.10650	39.142	5
		10	972.82	4.3488	3.2237	3.3137	0.45706	0.10803	30.673	10
		15	970.98	4.3382	2.6161	2.6943	0.46169	0.10960	24.582	15
		20	968.92	4.3287	2.1648	2.2342	0.46631	0.11118	20.095	20
		25	966.65	4.3211	1.8212	1.8841	0.47091	0.11274	16.712	25
30	−20.14	30	964.20	4.3165	1.5534	1.6111	0.47546	0.11424	14.102	30
		40	958.81	4.3200	1.1640	1.2140	0.48440	0.11695	10.381	40
		−20	973.10	4.0715	25.213	25.910	0.38499	0.097171	266.65	−20
		−15	971.36	4.0998	17.304	17.814	0.38802	0.097434	182.83	−15
		−10	969.42	4.1242	12.258	12.644	0.39113	0.097830	129.25	−10
		−5	967.28	4.1451	8.9429	9.2453	0.39431	0.098343	94.012	−5
		0	964.96	4.1632	6.7046	6.9480	0.39754	0.098956	70.213	0
		5	962.46	4.1789	5.1538	5.3548	0.40081	0.099655	53.733	5
		10	959.79	4.1926	4.0530	4.2227	0.40411	0.10042	42.049	10
40	−29.53	20	954.01	4.2161	2.6599	2.7881	0.41071	0.10211	27.305	20
		30	947.72	4.2376	1.8618	1.9645	0.41722	0.10389	18.910	30
		40	940.99	4.2610	1.3652	1.4508	0.42353	0.10563	13.735	40
		−25	965.29	3.6450	35.834	37.122	0.34154	0.097071	382.43	−25
		−20	962.30	3.7020	24.550	25.512	0.34361	0.096455	264.50	−20
		−15	959.22	3.7551	17.312	18.048	0.34574	0.095987	188.03	−15
		−10	956.04	3.8045	12.542	13.118	0.34791	0.095653	137.14	−10
		−5	952.78	3.8503	9.3164	9.7782	0.35012	0.095441	102.45	−5
		0	949.43	3.8926	7.0833	7.4605	0.35235	0.095339	78.252	0
		10	942.51	3.9672	4.3572	4.6229	0.35681	0.095427	48.445	10
		20	935.32	4.0293	2.8757	3.0746	0.36120	0.095843	32.080	20
		30	927.89	4.0799	2.0062	2.1621	0.36541	0.096525	22.399	30
		40	920.26	4.1199	1.4573	1.5836	0.36934	0.097417	16.256	40

APPENDIX B.4 (CONTINUED)

Thermophysical Properties of Ethanol–Water Solutions (IP Units)

<i>Conc</i> mass %	<i>T_{freeze}</i> °F	<i>T</i> °F	ρ lbm/ft ³	c_p Btu/ lbm-R	μ lbm/ft-h	ν ft ² /h	<i>k</i> Btu/h- ft-R	α ft ² /h	Pr	<i>T</i> °F
10	24.10	25	61.491	1.0557	9.7894	0.15920	0.28749	0.0044287	35.947	25
		30	61.492	1.0526	8.4768	0.13785	0.28961	0.0044744	30.809	30
		35	61.486	1.0493	7.4106	0.12052	0.29172	0.0045215	26.656	35
		40	61.474	1.0460	6.5363	0.10633	0.29383	0.0045697	23.268	40
		50	61.430	1.0391	5.2087	0.084790	0.29800	0.0046686	18.162	50
		60	61.363	1.0325	4.2671	0.069538	0.30212	0.0047685	14.583	60
		70	61.275	1.0267	3.5750	0.058343	0.30618	0.0048667	11.988	70
		80	61.168	1.0222	3.0470	0.049813	0.31017	0.0049604	10.042	80
		90	61.045	1.0195	2.6281	0.043052	0.31407	0.0050462	8.5316	90
20	11.97	100	60.907	1.0192	2.2821	0.037468	0.31788	0.0051209	7.3165	100
		15	61.025	1.0467	22.304	0.36549	0.25377	0.0039731	91.991	15
		20	61.000	1.0460	18.682	0.30626	0.25522	0.0040000	76.565	20
		30	60.931	1.0441	13.493	0.22145	0.25816	0.0040580	54.570	30
		40	60.841	1.0415	10.097	0.16596	0.26111	0.0041206	40.276	40
		50	60.731	1.0387	7.7984	0.12841	0.26408	0.0041864	30.672	50
		60	60.603	1.0359	6.1912	0.10216	0.26706	0.0042541	24.015	60
		70	60.457	1.0334	5.0328	0.083246	0.27002	0.0043219	19.261	70
		80	60.296	1.0316	4.1725	0.069200	0.27297	0.0043884	15.769	80
30	-4.256	90	60.121	1.0308	3.5141	0.058450	0.27588	0.0044518	13.130	90
		100	59.934	1.0312	2.9947	0.049966	0.27875	0.0045102	11.078	100
		0	60.702	0.97557	51.388	0.84656	0.22321	0.0037693	224.59	0
		10	60.575	0.98254	34.433	0.56844	0.22519	0.0037836	150.24	10
		20	60.431	0.98844	23.956	0.39642	0.22721	0.0038038	104.22	20
		30	60.274	0.99344	17.253	0.28624	0.22928	0.0038290	74.754	30
		40	60.102	0.99770	12.822	0.21334	0.23137	0.0038586	55.291	40
		50	59.918	1.0014	9.8045	0.16363	0.23349	0.0038915	42.049	50
		60	59.722	1.0046	7.6896	0.12876	0.23561	0.0039271	32.787	60
40	-21.16	70	59.515	1.0076	6.1669	0.10362	0.23772	0.0039644	26.138	70
		80	59.298	1.0104	5.0420	0.085027	0.23982	0.0040027	21.243	80
		100	58.839	1.0164	3.5273	0.059948	0.24392	0.0040787	14.698	100
		-20	60.402	0.85934	118.81	1.9670	0.19644	0.0037845	519.76	-20
		-10	60.200	0.87522	76.166	1.2652	0.19773	0.0037529	337.13	-10
		0	59.990	0.88993	50.674	0.84472	0.19908	0.0037290	226.53	0
		10	59.773	0.90353	34.901	0.58389	0.20046	0.0037118	157.31	10
		20	59.549	0.91605	24.819	0.41678	0.20187	0.0037007	112.62	20
		30	59.318	0.92753	18.176	0.30642	0.20330	0.0036950	82.929	30
		40	59.081	0.93801	13.674	0.23145	0.20473	0.0036942	62.651	40
		60	58.591	0.95612	8.3032	0.14171	0.20758	0.0037054	38.245	60
		80	58.082	0.97071	5.4435	0.093721	0.21034	0.0037306	25.122	80
		100	57.557	0.98208	3.7746	0.065581	0.21292	0.0037667	17.411	100

APPENDIX B.4 (CONTINUED)

Thermophysical Properties of Calcium Chloride–Water Solutions (SI Units)

<i>Conc</i> mass %	<i>T</i> _{freeze} °C	<i>T</i> °C	ρ kg/m ³	<i>c_p</i> kJ/kg-K	μ mPa-s	ν mm ² /s	<i>k</i> W/m-K	α mm ² /s	Pr	<i>T</i> °C
5	−2.361	0	1043.1	3.8720	1.9790	1.8971	0.55904	0.13841	13.707	0
		5	1041.7	3.8734	1.6917	1.6240	0.56753	0.14066	11.546	5
		10	1040.8	3.8764	1.4659	1.4084	0.57601	0.14276	9.8652	10
		15	1040.2	3.8809	1.2855	1.2358	0.58444	0.14477	8.5364	15
		20	1039.6	3.8866	1.1392	1.0958	0.59281	0.14671	7.4687	20
		25	1038.8	3.8932	1.0185	0.98048	0.60108	0.14863	6.5967	25
		30	1037.4	3.9005	0.91727	0.88422	0.60924	0.15057	5.8725	30
		35	1035.2	3.9083	0.83087	0.80265	0.61726	0.15257	5.2608	35
		40	1031.9	3.9164	0.75577	0.73243	0.62512	0.15469	4.7349	40
10	−5.840	45	1027.2	3.9244	0.68928	0.67102	0.63280	0.15698	4.2747	45
		−5	1089.8	3.5602	2.6193	2.4034	0.54737	0.14108	17.036	−5
		0	1088.3	3.5688	2.2273	2.0466	0.55523	0.14296	14.316	0
		5	1087.4	3.5781	1.9163	1.7623	0.56312	0.14473	12.176	5
		10	1086.8	3.5879	1.6668	1.5336	0.57102	0.14644	10.473	10
		15	1086.4	3.5981	1.4642	1.3478	0.57894	0.14811	9.1002	15
		20	1085.9	3.6086	1.2981	1.1954	0.58687	0.14977	7.9817	20
		25	1085.0	3.6192	1.1603	1.0693	0.59480	0.15147	7.0599	25
		30	1083.6	3.6298	1.0447	0.96412	0.60273	0.15324	6.2916	30
15	−11.05	35	1081.4	3.6403	0.94679	0.87553	0.61065	0.15512	5.6441	35
		40	1078.1	3.6505	0.86283	0.80030	0.61857	0.15716	5.0921	40
		−10	1137.8	3.2651	3.5905	3.1557	0.53586	0.14424	21.878	−10
		−5	1136.3	3.2792	3.0425	2.6774	0.54333	0.14581	18.362	−5
		0	1135.4	3.2929	2.6052	2.2945	0.55080	0.14732	15.575	0
		5	1134.8	3.3063	2.2529	1.9852	0.55829	0.14880	13.342	5
		10	1134.4	3.3193	1.9664	1.7335	0.56581	0.15027	11.536	10
		15	1133.9	3.3319	1.7315	1.5270	0.57335	0.15176	10.062	15
		20	1133.2	3.3440	1.5371	1.3564	0.58093	0.15330	8.8479	20
20	−18.26	25	1132.1	3.3556	1.3749	1.2145	0.58856	0.15493	7.8389	25
		30	1130.4	3.3667	1.2384	1.0956	0.59623	0.15667	6.9930	30
		40	1124.6	3.3868	1.0238	0.91041	0.61175	0.16062	5.6681	40
		−15	1188.4	3.0056	5.1425	4.3271	0.52391	0.14667	29.502	−15
		−10	1186.9	3.0232	4.3363	3.6534	0.53117	0.14803	24.680	−10
		−5	1185.7	3.0399	3.6963	3.1173	0.53841	0.14937	20.870	−5
		0	1184.8	3.0558	3.1830	2.6866	0.54564	0.15071	17.826	0
		5	1183.9	3.0709	2.7673	2.3374	0.55287	0.15207	15.371	5
		10	1183.0	3.0851	2.4273	2.0519	0.56011	0.15347	13.370	10
20	−18.26	15	1181.9	3.0985	2.1468	1.8164	0.56737	0.15493	11.724	15
		20	1180.6	3.1110	1.9131	1.6205	0.57466	0.15647	10.357	20
		30	1176.5	3.1336	1.5504	1.3178	0.58936	0.15986	8.2431	30
		40	1169.8	3.1527	1.2852	1.0986	0.60431	0.16385	6.7047	40

APPENDIX B.4 (CONTINUED)

Thermophysical Properties of Calcium Chloride–Water Solutions (IP Units)

<i>Conc</i> mass %	<i>T_{freeze}</i> °F	<i>T</i> °F	ρ lbm/ft ³	c_p Btu/ lbm-R	μ lbm/ft-h	ν ft ² /h	<i>k</i> Btu/h- ft-R	α ft ² /h	Pr	<i>T</i> °F
5	27.75	30	65.147	0.92477	4.9670	0.076243	0.32191	0.0053433	14.269	30
		35	65.086	0.92485	4.5362	0.069695	0.32464	0.0053932	12.923	35
		40	65.040	0.92506	4.1615	0.063984	0.32737	0.0054411	11.759	40
		45	65.004	0.92540	3.8339	0.058980	0.33009	0.0054874	10.748	45
		50	64.977	0.92585	3.5462	0.054576	0.33281	0.0055323	9.8651	50
		60	64.935	0.92705	3.0669	0.047230	0.33822	0.0056185	8.4061	60
		70	64.892	0.92860	2.6862	0.041394	0.34359	0.0057018	7.2598	70
		80	64.824	0.93042	2.3776	0.036678	0.34888	0.0057845	6.3408	80
		90	64.707	0.93242	2.1222	0.032797	0.35408	0.0058688	5.5884	90
		100	64.518	0.93453	1.9061	0.029544	0.35918	0.0059572	4.9593	100
10	21.49	25	68.010	0.85075	6.1057	0.089776	0.31727	0.0054835	16.372	25
		30	67.958	0.85190	5.5799	0.082108	0.31980	0.0055239	14.864	30
		35	67.917	0.85310	5.1182	0.075359	0.32233	0.0055630	13.546	35
		40	67.887	0.85434	4.7113	0.069398	0.32486	0.0056011	12.390	40
		50	67.848	0.85694	4.0320	0.059428	0.32993	0.0056746	10.473	50
		60	67.818	0.85965	3.4935	0.051513	0.33501	0.0057464	8.9644	60
		70	67.779	0.86243	3.0607	0.045157	0.34010	0.0058182	7.7614	70
		80	67.711	0.86525	2.7083	0.039998	0.34519	0.0058920	6.7884	80
		90	67.593	0.86805	2.4173	0.035763	0.35028	0.0059700	5.9905	90
		100	67.405	0.87081	2.1739	0.032250	0.35537	0.0060543	5.3269	100
15	12.11	15	71.018	0.78022	8.5229	0.12001	0.31010	0.0055964	21.444	15
		20	70.966	0.78208	7.7686	0.10947	0.31249	0.0056303	19.443	20
		30	70.892	0.78576	6.5175	0.091936	0.31729	0.0056959	16.141	30
		40	70.848	0.78933	5.5360	0.078139	0.32209	0.0057596	13.567	40
		50	70.816	0.79279	4.7570	0.067174	0.32692	0.0058229	11.536	50
		60	70.783	0.79613	4.1319	0.058375	0.33176	0.0058873	9.9154	60
		70	70.731	0.79932	3.6250	0.051251	0.33663	0.0059543	8.6075	70
		80	70.644	0.80236	3.2097	0.045435	0.34154	0.0060255	7.5404	80
		90	70.508	0.80522	2.8660	0.040647	0.34648	0.0061026	6.6605	90
		100	70.307	0.80790	2.5786	0.036676	0.35146	0.0061876	5.9274	100
20	−0.8660	0	74.257	0.71545	13.744	0.18509	0.30037	0.0056539	32.736	0
		10	74.136	0.72022	11.300	0.15243	0.30504	0.0057130	26.681	10
		20	74.046	0.72474	9.4197	0.12721	0.30969	0.0057709	22.044	20
		30	73.976	0.72902	7.9534	0.10751	0.31434	0.0058286	18.446	30
		40	73.914	0.73306	6.7962	0.091947	0.31898	0.0058870	15.619	40
		50	73.851	0.73684	5.8720	0.079511	0.32362	0.0059471	13.370	50
		60	73.776	0.74038	5.1254	0.069472	0.32829	0.0060101	11.559	60
		70	73.678	0.74367	4.5154	0.061286	0.33297	0.0060769	10.085	70
		80	73.547	0.74671	4.0117	0.054545	0.33768	0.0061488	8.8709	80
		100	73.141	0.75205	3.2358	0.044240	0.34723	0.0063126	7.0083	100

APPENDIX B.4 (CONTINUED)

Thermophysical Properties of Magnesium Chloride–Water Solutions (SI Units)

<i>Conc</i> mass %	<i>T</i> _{freeze} °C	<i>T</i> °C	ρ kg/m ³	<i>c</i> _{<i>p</i>} kJ/kg-K	μ mPa-s	ν mm ² /s	<i>k</i> W/m-K	α mm ² /s	Pr	<i>T</i> °C
5	−2.999	0	1043.8	3.8744	2.2022	2.1099	0.55226	0.13656	15.450	0
		5	1043.2	3.8786	1.8527	1.7760	0.56160	0.13880	12.795	5
		10	1042.3	3.8833	1.5858	1.5214	0.57057	0.14096	10.793	10
		15	1041.3	3.8885	1.3774	1.3228	0.57921	0.14305	9.2467	15
		20	1040.0	3.8939	1.2107	1.1641	0.58757	0.14509	8.0231	20
		25	1038.6	3.8993	1.0741	1.0342	0.59570	0.14710	7.0309	25
		30	1037.0	3.9047	0.95932	0.92513	0.60364	0.14908	6.2054	30
		35	1035.2	3.9098	0.86025	0.83096	0.61145	0.15106	5.5007	35
		40	1033.5	3.9145	0.77246	0.74746	0.61915	0.15305	4.8837	40
10	−8.283	45	1031.6	3.9185	0.69275	0.67153	0.62682	0.15506	4.3306	45
		−5	1089.9	3.5633	3.3696	3.0916	0.53090	0.13670	22.616	−5
		0	1089.0	3.5731	2.7921	2.5640	0.54025	0.13884	18.467	0
		5	1087.9	3.5826	2.3499	2.1601	0.54949	0.14099	15.321	5
		10	1086.6	3.5917	2.0031	1.8435	0.55860	0.14313	12.880	10
		15	1085.1	3.6004	1.7246	1.5893	0.56755	0.14527	10.941	15
		20	1083.5	3.6088	1.4955	1.3803	0.57633	0.14740	9.3643	20
		25	1081.7	3.6169	1.3025	1.2041	0.58492	0.14951	8.0539	25
		30	1079.7	3.6247	1.1361	1.0522	0.59330	0.15159	6.9410	30
15	−16.79	35	1077.6	3.6323	0.98975	0.91844	0.60144	0.15365	5.9774	35
		40	1075.4	3.6395	0.85876	0.79853	0.60933	0.15568	5.1294	40
		−15	1137.4	3.2601	6.2748	5.5168	0.50140	0.13522	40.799	−15
		−10	1136.6	3.2732	5.1741	4.5521	0.50986	0.13704	33.217	−10
		−5	1135.7	3.2858	4.3202	3.8042	0.51850	0.13895	27.378	−5
		0	1134.5	3.2981	3.6455	3.2133	0.52726	0.14091	22.803	0
		5	1133.2	3.3100	3.1027	2.7380	0.53609	0.14293	19.157	5
		10	1131.7	3.3218	2.6581	2.3488	0.54495	0.14497	16.203	10
		15	1130.0	3.3333	2.2877	2.0245	0.55377	0.14702	13.771	15
20	−28.71	20	1128.2	3.3448	1.9742	1.7499	0.56251	0.14907	11.739	20
		30	1124.1	3.3677	1.4700	1.3077	0.57951	0.15308	8.5428	30
		40	1119.6	3.3910	1.0802	0.96486	0.59555	0.15686	6.1509	40
		−25	1187.5	2.9861	12.758	10.744	0.47376	0.13360	80.416	−25
		−20	1187.1	2.9996	10.421	8.7787	0.48133	0.13517	64.945	−20
		−15	1186.3	3.0133	8.5696	7.2235	0.48918	0.13684	52.787	−15
		−10	1185.3	3.0269	7.0933	5.9844	0.49727	0.13860	43.178	−10
		−5	1184.0	3.0407	5.9089	4.9906	0.50554	0.14042	35.541	−5
		0	1182.5	3.0545	4.9529	4.1885	0.51395	0.14229	29.436	0
20	−28.71	10	1178.9	3.0822	3.5428	3.0051	0.53098	0.14612	20.565	10
		20	1174.9	3.1100	2.5924	2.2065	0.54796	0.14996	14.713	20
		30	1170.6	3.1376	1.9379	1.6554	0.56448	0.15368	10.771	30
		40	1166.4	3.1651	1.4777	1.2669	0.58015	0.15714	8.0620	40

APPENDIX B.4 (CONTINUED)

Thermophysical Properties of Magnesium Chloride–Water Solutions (IP Units)

<i>Conc</i> mass %	<i>T_{freeze}</i> °F	<i>T</i> °F	ρ lbm/ft ³	c_p Btu/ lbm-R	μ lbm/ft-h	ν ft ² /h	<i>k</i> Btu/h- ft-R	α ft ² /h	Pr	<i>T</i> °F
5	26.60	30	65.165	0.92517	5.5504	0.085174	0.31786	0.0052723	16.155	30
		35	65.149	0.92568	5.0187	0.077034	0.32091	0.0053213	14.477	35
		40	65.128	0.92624	4.5647	0.070088	0.32390	0.0053692	13.054	40
		45	65.102	0.92685	4.1743	0.064119	0.32681	0.0054162	11.838	45
		50	65.072	0.92749	3.8363	0.058955	0.32967	0.0054623	10.793	50
		60	64.997	0.92886	3.2828	0.050507	0.33521	0.0055523	9.0966	60
		70	64.906	0.93030	2.8498	0.043907	0.34055	0.0056399	7.7852	70
		80	64.803	0.93175	2.5008	0.038591	0.34573	0.0057259	6.7397	80
		90	64.689	0.93316	2.2102	0.034167	0.35079	0.0058112	5.8794	90
		100	64.567	0.93445	1.9602	0.030360	0.35577	0.0058965	5.1487	100
10	17.09	20	68.057	0.85027	8.7128	0.12802	0.30494	0.0052696	24.295	20
		25	68.029	0.85160	7.8063	0.11475	0.30795	0.0053156	21.587	25
		30	67.997	0.85290	7.0324	0.10342	0.31096	0.0053618	19.289	30
		35	67.962	0.85417	6.3670	0.093685	0.31394	0.0054079	17.324	35
		40	67.923	0.85542	5.7907	0.085254	0.31690	0.0054542	15.631	40
		50	67.834	0.85783	4.8458	0.071436	0.32275	0.0055465	12.880	50
		60	67.731	0.86015	4.1052	0.060611	0.32849	0.0056385	10.749	60
		70	67.616	0.86237	3.5074	0.051872	0.33411	0.0057300	9.0527	70
		80	67.488	0.86450	3.0104	0.044606	0.33959	0.0058206	7.6636	80
		100	67.199	0.86851	2.2142	0.032950	0.35006	0.0059980	5.4936	100
15	1.773	5	71.005	0.77865	15.179	0.21378	0.28970	0.0052399	40.798	5
		10	70.980	0.78040	13.614	0.19180	0.29240	0.0052787	36.335	10
		15	70.951	0.78211	12.261	0.17281	0.29514	0.0053186	32.492	15
		20	70.919	0.78379	11.085	0.15630	0.29791	0.0053595	29.163	20
		30	70.842	0.78707	9.1507	0.12917	0.30352	0.0054434	23.729	30
		40	70.752	0.79026	7.6386	0.10796	0.30918	0.0055298	19.524	40
		50	70.648	0.79338	6.4302	0.091018	0.31487	0.0056175	16.202	50
		60	70.532	0.79644	5.4439	0.077183	0.32053	0.0057059	13.527	60
		80	70.266	0.80252	3.9261	0.055876	0.33161	0.0058807	9.5015	80
		100	69.959	0.80867	2.8039	0.040079	0.34210	0.0060470	6.6278	100
20	-19.68	-15	74.138	0.71249	32.314	0.43586	0.27279	0.0051642	84.399	-15
		-10	74.128	0.71428	28.829	0.38891	0.27517	0.0051970	74.833	-10
		0	74.089	0.71788	23.092	0.31167	0.28010	0.0052664	59.182	0
		10	74.027	0.72150	18.649	0.25192	0.28522	0.0053402	47.174	10
		20	73.944	0.72515	15.181	0.20531	0.29049	0.0054176	37.896	20
		30	73.843	0.72881	12.454	0.16866	0.29587	0.0054977	30.678	30
		40	73.727	0.73248	10.294	0.13962	0.30132	0.0055796	25.024	40
		60	73.461	0.73984	7.1856	0.097815	0.31226	0.0057454	17.025	60
		80	73.170	0.74720	5.1536	0.070433	0.32301	0.0059081	11.921	80
		100	72.876	0.75451	3.7905	0.052012	0.33325	0.0060606	8.5820	100

APPENDIX B.4 (CONTINUED)

Thermophysical Properties of Sodium Chloride–Water Solutions (SI Units)

<i>Conc</i> mass %	<i>T</i> _{freeze} °C	<i>T</i> °C	ρ kg/m ³	<i>c_p</i> kJ/kg-K	μ mPa-s	ν mm ² /s	<i>k</i> W/m-K	α mm ² /s	Pr	<i>T</i> °C
5	−3.054	0	1038.1	3.9121	1.8918	1.8223	0.55832	0.13747	13.256	0
		5	1037.4	3.9157	1.6223	1.5638	0.56748	0.13970	11.194	5
		10	1036.4	3.9196	1.4046	1.3552	0.57641	0.14189	9.5512	10
		15	1035.3	3.9237	1.2279	1.1860	0.58511	0.14404	8.2339	15
		20	1034.0	3.9281	1.0837	1.0481	0.59357	0.14615	7.1718	20
		25	1032.5	3.9327	0.96578	0.93542	0.60180	0.14822	6.3112	25
		30	1030.7	3.9376	0.86897	0.84306	0.60980	0.15025	5.6111	30
		35	1028.8	3.9428	0.78943	0.76730	0.61757	0.15224	5.0400	35
		40	1026.7	3.9483	0.72409	0.70523	0.62511	0.15420	4.5735	40
10	−6.553	45	1024.5	3.9540	0.67059	0.65457	0.63241	0.15612	4.1926	45
		−5	1078.0	3.6780	2.4367	2.2604	0.54719	0.13801	16.378	−5
		0	1076.8	3.6883	2.0715	1.9238	0.55567	0.13992	13.750	0
		5	1075.4	3.6979	1.7784	1.6537	0.56406	0.14184	11.659	5
		10	1073.9	3.7068	1.5417	1.4356	0.57236	0.14378	9.9847	10
		15	1072.3	3.7150	1.3498	1.2587	0.58058	0.14574	8.6369	15
		20	1070.6	3.7226	1.1933	1.1146	0.58871	0.14772	7.5457	20
		25	1068.7	3.7294	1.0654	0.99689	0.59675	0.14972	6.6583	25
		30	1066.7	3.7356	0.96053	0.90047	0.60470	0.15175	5.9339	30
15	−10.90	35	1064.6	3.7411	0.87452	0.82148	0.61256	0.15381	5.3410	35
		40	1062.3	3.7459	0.80405	0.75689	0.62033	0.15589	4.8553	40
		−10	1119.6	3.4952	3.2795	2.9292	0.53646	0.13709	21.367	−10
		−5	1118.0	3.5075	2.7510	2.4607	0.54432	0.13881	17.727	−5
		0	1116.2	3.5188	2.3318	2.0890	0.55219	0.14059	14.859	0
		5	1114.4	3.5289	1.9972	1.7921	0.56006	0.14241	12.584	5
		10	1112.5	3.5380	1.7286	1.5537	0.56793	0.14429	10.768	10
		15	1110.5	3.5460	1.5118	1.3613	0.57581	0.14622	9.3097	15
		20	1108.5	3.5529	1.3360	1.2053	0.58370	0.14821	8.1320	20
20	−16.46	25	1106.3	3.5588	1.1930	1.0784	0.59159	0.15026	7.1769	25
		30	1104.0	3.5635	1.0766	0.97510	0.59948	0.15237	6.3995	30
		40	1099.3	3.5699	0.90447	0.82279	0.61528	0.15679	5.2478	40
		−15	1162.7	3.3533	4.6494	3.9989	0.52535	0.13475	29.677	−15
		−10	1160.7	3.3642	3.8326	3.3019	0.53274	0.13643	24.203	−10
		−5	1158.7	3.3742	3.1960	2.7582	0.54019	0.13816	19.963	−5
		0	1156.7	3.3833	2.6960	2.3308	0.54768	0.13995	16.655	0
		5	1154.5	3.3915	2.3006	1.9927	0.55521	0.14179	14.053	5
		10	1152.3	3.3988	1.9860	1.7234	0.56280	0.14370	11.993	10
20	−16.46	15	1150.1	3.4052	1.7342	1.5079	0.57043	0.14566	10.352	15
		20	1147.8	3.4106	1.5319	1.3347	0.57810	0.14768	9.0379	20
		30	1142.9	3.4189	1.2375	1.0827	0.59359	0.15191	7.1272	30
		40	1137.8	3.4234	1.0467	0.91998	0.60927	0.15642	5.8816	40

APPENDIX B.4 (CONTINUED)

Thermophysical Properties of Sodium Chloride–Water Solutions (IP Units)

<i>Conc</i> mass %	<i>T_{freeze}</i> °F	<i>T</i> °F	ρ lbm/ft ³	c_p Btu/ lbm-R	μ lbm/ft-h	ν ft ² /h	k Btu/h- ft-R	α ft ² /h	Pr	<i>T</i> °F
5	26.50	30	64.818	0.93419	4.7417	0.073155	0.32140	0.0053077	13.783	30
		35	64.794	0.93466	4.3433	0.067032	0.32437	0.0053561	12.515	35
		40	64.767	0.93513	3.9902	0.061608	0.32730	0.0054040	11.400	40
		45	64.737	0.93563	3.6766	0.056794	0.33019	0.0054514	10.418	45
		50	64.703	0.93615	3.3978	0.052515	0.33304	0.0054983	9.5510	50
		60	64.623	0.93725	2.9280	0.045309	0.33862	0.0055907	8.1043	60
		70	64.529	0.93842	2.5533	0.039568	0.34403	0.0056812	6.9647	70
		80	64.420	0.93968	2.2531	0.034975	0.34927	0.0057699	6.0617	80
		90	64.296	0.94101	2.0119	0.031292	0.35435	0.0058567	5.3429	90
		100	64.157	0.94242	1.8181	0.028338	0.35926	0.0059418	4.7691	100
10	20.21	25	67.280	0.87901	5.6809	0.084436	0.31725	0.0053644	15.740	25
		30	67.238	0.88037	5.1909	0.077202	0.31997	0.0054055	14.282	30
		35	67.193	0.88169	4.7575	0.070803	0.32268	0.0054467	12.999	35
		40	67.146	0.88295	4.3735	0.065134	0.32537	0.0054881	11.868	40
		50	67.044	0.88533	3.7296	0.055630	0.33071	0.0055716	9.9846	50
		60	66.931	0.88751	3.2193	0.048098	0.33598	0.0056560	8.5039	60
		70	67.146	0.88295	4.3735	0.065134	0.32537	0.0054881	11.868	40
		80	66.677	0.89125	2.4871	0.037301	0.34633	0.0058280	6.4003	80
		90	66.534	0.89282	2.2260	0.033457	0.35141	0.0059157	5.6556	90
		100	66.381	0.89419	2.0166	0.030380	0.35643	0.0060048	5.0592	100
15	12.39	15	69.882	0.83515	7.7761	0.11127	0.31047	0.0053197	20.917	15
		20	69.826	0.83679	7.0482	0.10094	0.31299	0.0053566	18.844	20
		25	69.768	0.83836	6.4090	0.091862	0.31551	0.0053942	17.030	25
		30	69.709	0.83985	5.8466	0.083872	0.31804	0.0054324	15.439	30
		40	69.584	0.84259	4.9128	0.070602	0.32309	0.0055106	12.812	40
		50	69.453	0.84501	4.1816	0.060207	0.32815	0.0055913	10.768	50
		60	69.315	0.84712	3.6053	0.052014	0.33321	0.0056746	9.1660	60
		70	69.170	0.84891	3.1488	0.045523	0.33827	0.0057608	7.9022	70
		80	69.018	0.85038	2.7857	0.040362	0.34333	0.0058497	6.8998	80
		100	68.693	0.85238	2.2662	0.032990	0.35347	0.0060368	5.4648	100
20	2.379	5	72.582	0.80091	11.247	0.15496	0.30354	0.0052216	29.677	5
		10	72.516	0.80238	10.088	0.13912	0.30591	0.0052575	26.461	10
		20	72.379	0.80513	8.2035	0.11334	0.31068	0.0053313	21.260	20
		30	72.238	0.80761	6.7665	0.093670	0.31548	0.0054076	17.322	30
		40	72.091	0.80982	5.6611	0.078528	0.32031	0.0054866	14.313	40
		50	71.939	0.81177	4.8042	0.066782	0.32518	0.0055684	11.993	50
		60	71.782	0.81345	4.1354	0.057611	0.33008	0.0056529	10.191	60
		70	71.619	0.81486	3.6108	0.050416	0.33501	0.0057404	8.7826	70
		80	71.452	0.81600	3.1979	0.044755	0.33998	0.0058310	7.6754	80
		100	71.102	0.81749	2.6177	0.036816	0.35001	0.0060216	6.1139	100

APPENDIX B.5

Thermophysical Properties of Dry Air (SI Units)

<i>T</i> °C	ρ kg/m ³	<i>v</i> m ³ /kg	<i>u</i> kJ/kg	<i>h</i> kJ/kg	<i>s</i> kJ/kg-K	<i>c_p</i> kJ/kg-K	μ mPa-s	<i>k</i> W/m-K	Pr	<i>T</i> °C
P = 1 kPa (0.001 MPa)										
0	0.012751	78.425	195.14	273.57	8.0991	1.0039	0.017241	0.023970	0.72210	0
10	0.012301	81.294	202.31	283.61	8.1352	1.0043	0.017740	0.024723	0.72064	10
20	0.011881	84.168	209.49	293.65	8.1700	1.0047	0.018232	0.025467	0.71928	20
30	0.011489	87.040	216.66	303.70	8.2037	1.0052	0.018717	0.026202	0.71803	30
40	0.011122	89.912	223.85	313.76	8.2364	1.0057	0.019195	0.026929	0.71687	40
50	0.010778	92.782	231.04	323.82	8.2680	1.0063	0.019667	0.027649	0.71581	50
60	0.010454	95.657	238.23	333.88	8.2987	1.0070	0.020132	0.028361	0.71485	60
70	0.010150	98.522	245.43	343.96	8.3285	1.0078	0.020592	0.029066	0.71397	70
80	0.0098624	101.40	252.64	354.04	8.3574	1.0086	0.021046	0.029763	0.71319	80
90	0.0095908	104.27	259.86	364.13	8.3856	1.0095	0.021494	0.030454	0.71250	90
100	0.0093338	107.14	267.09	374.23	8.4130	1.0105	0.021937	0.031139	0.71190	100
150	0.0082309	121.49	303.41	424.90	8.5405	1.0167	0.024076	0.034469	0.71010	150
200	0.0073611	135.85	340.08	475.93	8.6544	1.0247	0.026103	0.037664	0.71013	200
250	0.0066576	150.20	377.19	527.39	8.7578	1.0342	0.028034	0.040743	0.71163	250
300	0.0060768	164.56	414.81	579.37	8.8527	1.0450	0.029883	0.043721	0.71424	300
350	0.0055892	178.92	452.99	631.91	8.9406	1.0566	0.031658	0.046612	0.71760	350
400	0.0051740	193.27	491.76	685.03	9.0226	1.0685	0.033370	0.049425	0.72142	400
600	0.0039889	250.70	652.80	903.49	9.3065	1.1153	0.039708	0.060071	0.73722	600
800	0.0032455	308.12	822.50	1130.6	9.5405	1.1544	0.045453	0.070012	0.74948	800
P = 101.325 kPa (1 atm)										
0	1.2927	0.77357	194.91	273.29	6.7722	1.0059	0.017258	0.024009	0.72307	0
10	1.2469	0.80199	202.09	283.35	6.8084	1.0061	0.017756	0.024760	0.72151	10
20	1.2043	0.83036	209.28	293.41	6.8433	1.0064	0.018247	0.025503	0.72007	20
30	1.1644	0.85881	216.46	303.48	6.8771	1.0067	0.018731	0.026237	0.71875	30
40	1.1272	0.88715	223.66	313.55	6.9098	1.0072	0.019209	0.026963	0.71752	40
50	1.0922	0.91558	230.85	323.62	6.9414	1.0077	0.019680	0.027681	0.71641	50
60	1.0594	0.94393	238.06	333.70	6.9721	1.0083	0.020145	0.028392	0.71539	60
70	1.0284	0.97238	245.27	343.79	7.0020	1.0089	0.020604	0.029096	0.71448	70
80	0.99926	1.0007	252.48	353.88	7.0310	1.0097	0.021058	0.029793	0.71366	80
90	0.97170	1.0291	259.71	363.98	7.0592	1.0105	0.021505	0.030483	0.71293	90
100	0.94563	1.0575	266.94	374.09	7.0866	1.0115	0.021948	0.031167	0.71229	100
150	0.83378	1.1994	303.28	424.81	7.2142	1.0174	0.024085	0.034494	0.71038	150
200	0.74562	1.3412	339.97	475.86	7.3282	1.0252	0.026111	0.037686	0.71033	200
250	0.67433	1.4830	377.09	527.35	7.4317	1.0347	0.028042	0.040763	0.71177	250
300	0.61549	1.6247	414.73	579.35	7.5266	1.0454	0.029889	0.043740	0.71434	300
350	0.56611	1.7664	452.92	631.90	7.6145	1.0568	0.031664	0.046629	0.71767	350
400	0.52406	1.9082	491.70	685.04	7.6965	1.0688	0.033375	0.049441	0.72147	400
600	0.40403	2.4751	652.75	903.54	7.9804	1.1154	0.039712	0.060083	0.73723	600
800	0.32875	3.0418	822.46	1130.7	8.2145	1.1545	0.045456	0.070021	0.74948	800

APPENDIX B.5 (CONTINUED)

Thermophysical Properties of Dry Air (SI Units)

<i>T</i> °C	ρ kg/m ³	<i>v</i> m ³ /kg	<i>u</i> kJ/kg	<i>h</i> kJ/kg	^{<i>s</i>} kJ/ kg-K	^{<i>c</i>_p} kJ/ kg-K	μ mPa-s	<i>k</i> W/m-K	Pr	<i>T</i> °C
P = 500 kPa (0.05 MPa)										
0	6.3933	0.15641	193.99	272.20	6.3106	1.0140	0.017324	0.024169	0.72679	0
10	6.1638	0.16224	201.22	282.34	6.3470	1.0135	0.017820	0.024915	0.72487	10
20	5.9505	0.16805	208.44	292.47	6.3822	1.0132	0.018308	0.025651	0.72312	20
30	5.7516	0.17386	215.67	302.60	6.4162	1.0130	0.018790	0.026380	0.72151	30
40	5.5658	0.17967	222.90	312.73	6.4490	1.0129	0.019265	0.027102	0.72004	40
50	5.3917	0.18547	230.12	322.86	6.4809	1.0130	0.019734	0.027816	0.71871	50
60	5.2283	0.19127	237.36	332.99	6.5117	1.0132	0.020198	0.028522	0.71750	60
70	5.0746	0.19706	244.59	343.12	6.5417	1.0136	0.020655	0.029222	0.71641	70
80	4.9298	0.20285	251.84	353.26	6.5708	1.0140	0.021106	0.029915	0.71543	80
90	4.7931	0.20863	259.09	363.41	6.5992	1.0146	0.021553	0.030602	0.71457	90
100	4.6638	0.21442	266.35	373.55	6.6267	1.0153	0.021994	0.031282	0.71380	100
150	4.1101	0.24330	302.78	424.43	6.7547	1.0202	0.024124	0.034595	0.71141	150
200	3.6745	0.27215	339.54	475.61	6.8690	1.0274	0.026146	0.037777	0.71106	200
250	3.3228	0.30095	376.72	527.20	6.9726	1.0364	0.028072	0.040844	0.71230	250
300	3.0326	0.32975	414.40	579.27	7.0677	1.0467	0.029916	0.043814	0.71472	300
350	2.7892	0.35853	452.63	631.89	7.1557	1.0580	0.031688	0.046697	0.71796	350
400	2.5821	0.38728	491.44	685.08	7.2378	1.0697	0.033397	0.049504	0.72168	400
600	1.9910	0.50226	652.58	903.72	7.5219	1.1159	0.039728	0.060131	0.73728	600
800	1.6202	0.61721	822.34	1130.9	7.7561	1.1548	0.045468	0.070060	0.74947	800
P = 1000 kPa (1 MPa)										
0	12.821	0.077997	192.84	270.84	6.1073	1.0241	0.017412	0.024386	0.73125	0
10	12.353	0.080952	200.12	281.07	6.1441	1.0228	0.017904	0.025122	0.72888	10
20	11.920	0.083893	207.40	291.29	6.1796	1.0217	0.018388	0.025851	0.72674	20
30	11.516	0.086836	214.67	301.50	6.2139	1.0208	0.018867	0.026572	0.72479	30
40	11.140	0.089767	221.94	311.71	6.2470	1.0202	0.019339	0.027287	0.72303	40
50	10.788	0.092696	229.21	321.91	6.2790	1.0197	0.019806	0.027994	0.72143	50
60	10.458	0.095621	236.48	332.10	6.3101	1.0195	0.020266	0.028695	0.71999	60
70	10.148	0.098542	243.76	342.30	6.3403	1.0194	0.020721	0.029389	0.71870	70
80	9.8561	0.10146	251.03	352.49	6.3696	1.0194	0.021170	0.030077	0.71754	80
90	9.5808	0.10438	258.31	362.69	6.3980	1.0196	0.021614	0.030759	0.71650	90
100	9.3208	0.10729	265.60	372.88	6.4257	1.0200	0.022053	0.031434	0.71559	100
150	8.2092	0.12181	302.15	423.97	6.5542	1.0237	0.024175	0.034728	0.71264	150
200	7.3368	0.13630	339.00	475.30	6.6688	1.0301	0.026190	0.037894	0.71192	200
250	6.6333	0.15075	376.25	527.01	6.7727	1.0385	0.028111	0.040950	0.71292	250
300	6.0537	0.16519	413.99	579.18	6.8680	1.0485	0.029951	0.043910	0.71517	300
350	5.5677	0.17961	452.26	631.87	6.9561	1.0594	0.031720	0.046784	0.71828	350
400	5.1542	0.19402	491.11	685.13	7.0383	1.0709	0.033426	0.049585	0.72192	400
600	3.9749	0.25158	652.36	903.94	7.3227	1.1166	0.039749	0.060192	0.73733	600
800	3.2354	0.30908	822.19	1131.3	7.5569	1.1552	0.045484	0.070110	0.74945	800

APPENDIX B.5 (CONTINUED)

Thermophysical Properties of Dry Air (SI Units)

<i>T</i> °C	ρ kg/m ³	<i>v</i> m ³ /kg	<i>u</i> kJ/kg	<i>h</i> kJ/kg	<i>s</i> kJ/ kg·K	<i>c_p</i> kJ/ kg·K	μ mPa·s	<i>k</i> W/m·K	Pr	<i>T</i> °C
P = 5000 kPa (5 MPa)										
0	65.195	0.015339	183.56	260.26	5.6122	1.1079	0.018284	0.026560	0.76270	0
10	62.539	0.015990	191.34	271.29	5.6519	1.0985	0.018731	0.027191	0.75670	10
20	60.116	0.016635	199.06	282.23	5.6899	1.0905	0.019175	0.027824	0.75150	20
30	57.893	0.017273	206.73	293.10	5.7263	1.0836	0.019616	0.028458	0.74695	30
40	55.844	0.017907	214.37	303.91	5.7614	1.0778	0.020054	0.029093	0.74295	40
50	53.949	0.018536	221.98	314.66	5.7952	1.0728	0.020489	0.029727	0.73942	50
60	52.189	0.019161	229.56	325.37	5.8278	1.0685	0.020921	0.030361	0.73629	60
70	50.550	0.019782	237.12	336.03	5.8594	1.0649	0.021349	0.030993	0.73351	70
80	49.018	0.020401	244.66	346.67	5.8899	1.0618	0.021773	0.031623	0.73104	80
90	47.583	0.021016	252.19	357.27	5.9195	1.0591	0.022194	0.032251	0.72885	90
100	46.235	0.021629	259.71	367.85	5.9483	1.0569	0.022612	0.032877	0.72691	100
150	40.552	0.024660	297.22	420.51	6.0807	1.0509	0.024645	0.035963	0.72016	150
200	36.165	0.027651	334.78	473.04	6.1980	1.0509	0.026594	0.038974	0.71708	200
250	32.663	0.030616	372.59	525.67	6.3038	1.0550	0.028464	0.041910	0.71652	250
300	29.796	0.033562	410.78	578.58	6.4004	1.0618	0.030263	0.044772	0.71771	300
350	27.403	0.036492	449.42	631.88	6.4895	1.0704	0.031999	0.047568	0.72006	350
400	25.372	0.039414	488.57	685.64	6.5725	1.0801	0.033678	0.050302	0.72314	400
600	19.597	0.051028	650.67	905.81	6.8586	1.1216	0.039929	0.060729	0.73743	600
800	15.978	0.062586	821.01	1133.9	7.0937	1.1583	0.045621	0.070539	0.74915	800
P = 10,000 kPa (10 MPa)										
0	131.34	0.0076138	172.15	248.29	5.3747	1.2099	0.019810	0.029882	0.80213	0
10	125.47	0.0079700	180.58	260.28	5.4178	1.1896	0.020156	0.030327	0.79062	10
20	120.19	0.0083202	188.89	272.09	5.4588	1.1725	0.020512	0.030797	0.78091	20
30	115.40	0.0086655	197.09	283.74	5.4979	1.1579	0.020876	0.031287	0.77264	30
40	111.04	0.0090058	205.20	295.26	5.5352	1.1455	0.021245	0.031791	0.76552	40
50	107.04	0.0093423	213.23	306.66	5.5711	1.1348	0.021618	0.032307	0.75937	50
60	103.35	0.0096759	221.21	317.96	5.6055	1.1256	0.021994	0.032833	0.75400	60
70	99.949	0.010005	229.12	329.17	5.6387	1.1176	0.022372	0.033367	0.74931	70
80	96.788	0.010332	237.00	340.31	5.6707	1.1106	0.022750	0.033906	0.74519	80
90	93.844	0.010656	244.83	351.39	5.7016	1.1046	0.023129	0.034451	0.74156	90
100	91.093	0.010978	252.63	362.41	5.7315	1.0993	0.023507	0.034999	0.73835	100
150	79.629	0.012558	291.30	416.88	5.8686	1.0819	0.025385	0.037767	0.72719	150
200	70.903	0.014104	329.73	470.77	5.9889	1.0747	0.027221	0.040543	0.72156	200
250	64.000	0.015625	368.21	524.46	6.0968	1.0738	0.029006	0.043296	0.71940	250
300	58.380	0.017129	406.93	578.22	6.1949	1.0771	0.030739	0.046013	0.71953	300
350	53.704	0.018621	446.00	632.21	6.2853	1.0830	0.032422	0.048690	0.72116	350
400	49.746	0.020102	485.52	686.55	6.3691	1.0907	0.034058	0.051326	0.72373	400
600	38.510	0.025967	648.63	908.30	6.6574	1.1275	0.040193	0.061484	0.73704	600
800	31.469	0.031777	819.57	1137.3	6.8934	1.1620	0.045819	0.071133	0.74847	800

APPENDIX B.5 (CONTINUED)

Thermophysical Properties of Dry Air (IP Units)

<i>T</i> °F	ρ lbm/ft ³	<i>v</i> ft ³ /lbm	<i>u</i> Btu/lbm	<i>h</i> Btu/lbm	<i>s</i> Btu/ lbm-R	<i>c_p</i> Btu/ lbm-R	μ lbm/ft-h	<i>k</i> Btu/h- ft-R	Pr	<i>T</i> °F
P = 1 psia										
20	0.0056259	177.75	81.890	114.81	1.7973	0.23993	0.040896	0.013568	0.72320	20
40	0.0054006	185.16	85.317	119.60	1.8071	0.24001	0.042249	0.014054	0.72150	40
60	0.0051928	192.57	88.746	124.41	1.8165	0.24011	0.043580	0.014535	0.71992	60
80	0.0050003	199.99	92.176	129.21	1.8256	0.24023	0.044891	0.015009	0.71848	80
100	0.0048216	207.40	95.609	134.01	1.8343	0.24036	0.046181	0.015478	0.71716	100
150	0.0044261	225.93	104.21	146.04	1.8549	0.24080	0.049323	0.016626	0.71438	150
200	0.0040906	244.46	112.83	158.10	1.8739	0.24137	0.052356	0.017741	0.71232	200
250	0.0038023	263.00	121.48	170.18	1.8916	0.24209	0.055289	0.018828	0.71092	250
300	0.0035521	281.52	130.18	182.31	1.9081	0.24296	0.058131	0.019888	0.71014	300
350	0.0033327	300.06	138.92	194.48	1.9236	0.24396	0.060889	0.020924	0.70993	350
400	0.0031389	318.58	147.71	206.71	1.9383	0.24510	0.063571	0.021938	0.71022	400
600	0.0025464	392.71	183.54	256.26	1.9901	0.25061	0.073644	0.025804	0.71522	600
800	0.0021421	466.83	220.56	307.00	2.0339	0.25692	0.082877	0.029428	0.72356	800
1000	0.0018486	540.95	258.86	359.02	2.0722	0.26322	0.091471	0.032869	0.73251	1000
1200	0.0016259	615.04	298.37	412.26	2.1064	0.26905	0.099566	0.036168	0.74065	1200
1400	0.0014510	689.18	338.98	466.60	2.1373	0.27422	0.10726	0.039355	0.74741	1400
1600	0.0013101	763.30	380.56	521.90	2.1655	0.27873	0.11464	0.042452	0.75271	1600
1800	0.0011942	837.38	422.98	578.05	2.1916	0.28263	0.12175	0.045477	0.75669	1800
2000	0.0010971	911.49	466.13	634.92	2.2157	0.28601	0.12865	0.048442	0.75957	2000
P = 14.696 psia (1 atm)										
20	0.082729	12.088	81.794	114.69	1.6127	0.24041	0.040934	0.013589	0.72417	20
40	0.079406	12.594	85.226	119.50	1.6225	0.24044	0.042285	0.014075	0.72236	40
60	0.076341	13.099	88.659	124.31	1.6319	0.24050	0.043615	0.014555	0.72070	60
80	0.073504	13.605	92.094	129.12	1.6410	0.24059	0.044924	0.015029	0.71918	80
100	0.070870	14.110	95.531	133.93	1.6498	0.24070	0.046212	0.015496	0.71779	100
150	0.065047	15.373	104.14	145.97	1.6704	0.24107	0.049352	0.016642	0.71487	150
200	0.060109	16.636	112.77	158.04	1.6894	0.24160	0.052382	0.017757	0.71271	200
250	0.055869	17.899	121.43	170.14	1.7071	0.24228	0.055313	0.018842	0.71123	250
300	0.052189	19.161	130.13	182.27	1.7236	0.24312	0.058153	0.019902	0.71040	300
350	0.048964	20.423	138.87	194.45	1.7391	0.24410	0.060910	0.020937	0.71014	350
400	0.046114	21.685	147.67	206.68	1.7538	0.24522	0.063590	0.021950	0.71040	400
600	0.037409	26.732	183.50	256.25	1.8056	0.25068	0.073659	0.025814	0.71531	600
800	0.031469	31.777	220.54	307.01	1.8495	0.25697	0.082888	0.029436	0.72360	800
1000	0.027158	36.822	258.84	359.04	1.8878	0.26326	0.091480	0.032876	0.73253	1000
1200	0.023886	41.866	298.35	412.28	1.9220	0.26907	0.099575	0.036174	0.74066	1200
1400	0.021318	46.909	338.97	466.62	1.9529	0.27424	0.10727	0.039360	0.74741	1400
1600	0.019248	51.953	380.55	521.93	1.9811	0.27875	0.11465	0.042457	0.75271	1600
1800	0.017545	56.996	422.97	578.08	2.0071	0.28265	0.12176	0.045481	0.75669	1800
2000	0.016118	62.042	466.12	634.96	2.0312	0.28602	0.12865	0.048446	0.75957	2000

APPENDIX B.5 (CONTINUED)

Thermophysical Properties of Dry Air (IP Units)

<i>T</i> °F	ρ lbm/ft ³	<i>v</i> ft ³ /lbm	<i>u</i> Btu/lbm	<i>h</i> Btu/lbm	<i>s</i> Btu/ lbm-R	<i>c_p</i> Btu/ lbm-R	μ lbm/ft-h	<i>k</i> Btu/h-ft-R	Pr	<i>T</i> °F
P = 50 psia										
20	0.28191	3.5472	81.544	114.39	1.5281	0.24165	0.041035	0.013646	0.72664	20
40	0.27050	3.6969	84.990	119.22	1.5380	0.24157	0.042381	0.014130	0.72455	40
60	0.25997	3.8466	88.436	124.05	1.5475	0.24153	0.043706	0.014607	0.72266	60
80	0.25025	3.9960	91.882	128.88	1.5566	0.24152	0.045011	0.015079	0.72093	80
100	0.24123	4.1454	95.329	133.71	1.5654	0.24155	0.046296	0.015545	0.71937	100
150	0.22131	4.5185	103.96	145.79	1.5861	0.24177	0.049427	0.016687	0.71611	150
200	0.20445	4.8912	112.61	157.89	1.6051	0.24218	0.052450	0.017798	0.71369	200
250	0.18999	5.2634	121.28	170.01	1.6228	0.24277	0.055375	0.018881	0.71203	250
300	0.17745	5.6354	129.99	182.17	1.6394	0.24354	0.058210	0.019937	0.71104	300
350	0.16647	6.0071	138.75	194.37	1.6549	0.24446	0.060963	0.020970	0.71067	350
400	0.15677	6.3788	147.56	206.62	1.6696	0.24553	0.063639	0.021981	0.71084	400
600	0.12716	7.8641	183.42	256.23	1.7215	0.25087	0.073697	0.025839	0.71553	600
800	0.10697	9.3484	220.47	307.03	1.7654	0.25710	0.082919	0.029458	0.72371	800
1000	0.092317	10.832	258.78	359.08	1.8037	0.26335	0.091506	0.032894	0.73258	1000
1200	0.081199	12.315	298.31	412.33	1.8379	0.26914	0.099596	0.036190	0.74068	1200
1400	0.072472	13.798	338.93	466.69	1.8688	0.27429	0.10729	0.039375	0.74741	1400
1600	0.065440	15.281	380.52	522.01	1.8971	0.27879	0.11466	0.042470	0.75269	1600
1800	0.059652	16.764	422.95	578.16	1.9231	0.28268	0.12178	0.045493	0.75667	1800
2000	0.054805	18.247	466.10	635.04	1.9472	0.28605	0.12867	0.048457	0.75954	2000
P = 100 psia										
20	0.56507	1.7697	81.190	113.96	1.4798	0.24342	0.041182	0.013732	0.73001	20
40	0.54191	1.8453	84.655	118.83	1.4898	0.24317	0.042521	0.014212	0.72756	40
60	0.52061	1.9208	88.119	123.69	1.4993	0.24298	0.043840	0.014686	0.72534	60
80	0.50096	1.9962	91.582	128.55	1.5085	0.24285	0.045138	0.015154	0.72334	80
100	0.48275	2.0715	95.044	133.40	1.5173	0.24276	0.046418	0.015617	0.72153	100
150	0.44263	2.2592	103.70	145.54	1.5381	0.24275	0.049537	0.016753	0.71780	150
200	0.40874	2.4465	112.38	157.68	1.5572	0.24299	0.052550	0.017858	0.71503	200
250	0.37972	2.6335	121.08	169.84	1.5750	0.24346	0.055466	0.018936	0.71310	250
300	0.35458	2.8202	129.81	182.03	1.5916	0.24412	0.058294	0.019989	0.71192	300
350	0.33258	3.0068	138.58	194.26	1.6072	0.24496	0.061040	0.021019	0.71139	350
400	0.31317	3.1932	147.40	206.53	1.6219	0.24597	0.063711	0.022027	0.71143	400
600	0.25398	3.9373	183.30	256.21	1.6738	0.25114	0.073752	0.025876	0.71582	600
800	0.21365	4.6806	220.38	307.05	1.7177	0.25728	0.082964	0.029488	0.72385	800
1000	0.18440	5.4230	258.71	359.13	1.7561	0.26347	0.091543	0.032921	0.73265	1000
1200	0.16221	6.1648	298.25	412.41	1.7903	0.26923	0.099628	0.036213	0.74070	1200
1400	0.14479	6.9066	338.89	466.78	1.8212	0.27436	0.10732	0.039395	0.74741	1400
1600	0.13075	7.6482	380.48	522.11	1.8495	0.27884	0.11469	0.042489	0.75268	1600
1800	0.11919	8.3900	422.92	578.28	1.8755	0.28272	0.12180	0.045510	0.75664	1800
2000	0.10951	9.1316	466.08	635.17	1.8996	0.28609	0.12869	0.048472	0.75951	2000

APPENDIX B.5 (CONTINUED)

Thermophysical Properties of Dry Air (IP Units)

<i>T</i> °F	ρ lbm/ft ³	<i>v</i> ft ³ /lbm	<i>u</i> Btu/lbm	<i>h</i> Btu/lbm	<i>s</i> Btu/ lbm-R	<i>c_p</i> Btu/ lbm-R	μ lbm/ft-h	<i>k</i> Btu/h-ft-R	Pr	<i>T</i> °F
P = 500 psia										
20	2.8692	0.34853	78.338	110.61	1.3635	0.25808	0.042567	0.014566	0.75420	20
40	2.7410	0.36483	81.971	115.75	1.3740	0.25627	0.043831	0.015002	0.74876	40
60	2.6247	0.38100	85.585	120.86	1.3841	0.25477	0.045081	0.015436	0.74406	60
80	2.5187	0.39703	89.183	125.94	1.3937	0.25352	0.046317	0.015869	0.73997	80
100	2.4215	0.41297	92.767	131.00	1.4029	0.25248	0.047540	0.016299	0.73639	100
150	2.2104	0.45241	101.69	143.57	1.4244	0.25057	0.050537	0.017365	0.72921	150
200	2.0349	0.49142	110.57	156.07	1.4441	0.24943	0.053450	0.018415	0.72399	200
250	1.8864	0.53011	119.45	168.53	1.4623	0.24884	0.056284	0.019446	0.72025	250
300	1.7589	0.56854	128.33	180.96	1.4792	0.24870	0.059041	0.020459	0.71769	300
350	1.6481	0.60676	137.22	193.40	1.4951	0.24890	0.061727	0.021455	0.71610	350
400	1.5508	0.64483	146.16	205.86	1.5100	0.24938	0.064346	0.022434	0.71530	400
600	1.2563	0.79599	182.38	256.08	1.5625	0.25324	0.074235	0.026196	0.71764	600
800	1.0570	0.94607	219.66	307.26	1.6067	0.25869	0.083349	0.029752	0.72469	800
1000	0.91278	1.0956	258.14	359.58	1.6453	0.26447	0.091861	0.033145	0.73298	1000
1200	0.80344	1.2446	297.79	413.03	1.6796	0.26997	0.099897	0.036409	0.74074	1200
1400	0.71761	1.3935	338.51	467.53	1.7106	0.27493	0.10755	0.039568	0.74728	1400
1600	0.64842	1.5422	380.17	522.96	1.7389	0.27928	0.11489	0.042644	0.75246	1600
1800	0.59143	1.6908	422.66	579.20	1.7650	0.28308	0.12198	0.045651	0.75637	1800
2000	0.54368	1.8393	465.86	636.16	1.7891	0.28637	0.12885	0.048601	0.75922	2000
P = 1000 psia										
20	5.8129	0.17203	74.767	106.62	1.3089	0.27683	0.044832	0.015841	0.78343	20
40	5.5294	0.18085	78.629	112.12	1.3201	0.27279	0.045941	0.016200	0.77360	40
60	5.2762	0.18953	82.443	117.54	1.3308	0.26946	0.047056	0.016567	0.76539	60
80	5.0482	0.19809	86.219	122.90	1.3409	0.26669	0.048175	0.016939	0.75846	80
100	4.8416	0.20654	89.963	128.21	1.3505	0.26436	0.049292	0.017316	0.75253	100
150	4.3992	0.22731	99.218	141.31	1.3730	0.26000	0.052071	0.018269	0.74104	150
200	4.0375	0.24768	108.37	154.23	1.3933	0.25711	0.054812	0.019229	0.73291	200
250	3.7351	0.26773	117.46	167.04	1.4120	0.25524	0.057506	0.020186	0.72713	250
300	3.4776	0.28755	126.52	179.77	1.4294	0.25411	0.060148	0.021138	0.72308	300
350	3.2554	0.30718	135.58	192.46	1.4456	0.25354	0.062737	0.022081	0.72036	350
400	3.0612	0.32667	144.64	205.13	1.4607	0.25341	0.065274	0.023015	0.71870	400
600	2.4780	0.40355	181.26	255.98	1.5139	0.25572	0.074929	0.026648	0.71903	600
800	2.0858	0.47943	218.79	307.57	1.5585	0.26035	0.083898	0.030121	0.72518	800
1000	1.8027	0.55472	257.45	360.17	1.5972	0.26566	0.092312	0.033456	0.73301	1000
1200	1.5881	0.62968	297.22	413.82	1.6317	0.27085	0.10028	0.036677	0.74053	1200
1400	1.4196	0.70442	338.04	468.48	1.6628	0.27560	0.10788	0.039804	0.74693	1400
1600	1.2837	0.77900	379.78	524.03	1.6911	0.27982	0.11518	0.042854	0.75204	1600
1800	1.1717	0.85346	422.34	580.37	1.7172	0.28350	0.12223	0.045840	0.75593	1800
2000	1.0778	0.92782	465.59	637.40	1.7414	0.28672	0.12907	0.048773	0.75876	2000

APPENDIX B.6

Thermophysical Properties of Saturated R134a (SI Units)

T °C	P kPa	ρ_f kg/m ³	v_g m ³ /kg	u_f kJ/kg	u_g kJ/kg	h_f kJ/kg	h_g kJ/kg	s_f kJ/kg-K	s_g kJ/kg-K	T °C
-103.3	0.38956	1591.1	35.496	71.455	321.11	71.455	334.94	0.41262	1.9639	-103.3
-95	0.93899	1569.1	15.435	81.287	325.29	81.288	339.78	0.46913	1.9201	-95
-90	1.5241	1555.8	9.7698	87.225	327.87	87.226	342.76	0.50201	1.8972	-90
-85	2.3990	1542.5	6.3707	93.180	330.49	93.182	345.77	0.53409	1.8766	-85
-80	3.6719	1529.0	4.2682	99.158	333.15	99.161	348.83	0.56544	1.8580	-80
-75	5.4777	1515.5	2.9312	105.16	335.85	105.17	351.91	0.59613	1.8414	-75
-70	7.9814	1501.9	2.0590	111.19	338.59	111.20	355.02	0.62619	1.8264	-70
-65	11.380	1488.2	1.4765	117.26	341.35	117.26	358.16	0.65568	1.8130	-65
-60	15.906	1474.3	1.0790	123.35	344.15	123.36	361.31	0.68462	1.8010	-60
-55	21.828	1460.4	0.80236	129.48	346.96	129.50	364.48	0.71305	1.7902	-55
-50	29.451	1446.3	0.60620	135.65	349.80	135.67	367.65	0.74101	1.7806	-50
-45	39.117	1432.1	0.46473	141.86	352.65	141.89	370.83	0.76852	1.7720	-45
-40	51.209	1417.7	0.36108	148.11	355.51	148.14	374.00	0.79561	1.7643	-40
-35	66.144	1403.1	0.28402	154.40	358.38	154.44	377.17	0.82230	1.7575	-35
-30	84.378	1388.4	0.22594	160.73	361.25	160.79	380.32	0.84863	1.7515	-30
-25	106.40	1373.4	0.18162	167.11	364.12	167.19	383.45	0.87460	1.7461	-25
-20	132.73	1358.3	0.14739	173.54	366.99	173.64	386.55	0.90025	1.7413	-20
-15	163.94	1342.8	0.12067	180.02	369.85	180.14	389.63	0.92559	1.7371	-15
-10	200.60	1327.1	0.099590	186.55	372.69	186.70	392.66	0.95065	1.7334	-10
-5	243.34	1311.1	0.082801	193.13	375.51	193.32	395.66	0.97544	1.7300	-5
0	292.80	1294.8	0.069309	199.77	378.31	200.00	398.60	1.0000	1.7271	0
5	349.66	1278.1	0.058374	206.48	381.08	206.75	401.49	1.0243	1.7245	5
10	414.61	1261.0	0.049442	213.25	383.82	213.58	404.32	1.0485	1.7221	10
15	488.37	1243.4	0.042090	220.09	386.52	220.48	407.07	1.0724	1.7200	15
20	571.71	1225.3	0.035997	227.00	389.17	227.47	409.75	1.0962	1.7180	20
25	665.38	1206.7	0.030912	233.99	391.77	234.55	412.33	1.1199	1.7162	25
30	770.20	1187.5	0.026642	241.07	394.30	241.72	414.82	1.1435	1.7145	30
35	886.98	1167.5	0.023033	248.25	396.76	249.01	417.19	1.1670	1.7128	35
40	1016.6	1146.7	0.019966	255.52	399.13	256.41	419.43	1.1905	1.7111	40
45	1159.9	1125.1	0.017344	262.91	401.40	263.94	421.52	1.2139	1.7092	45
50	1317.9	1102.3	0.015089	270.43	403.55	271.62	423.44	1.2375	1.7072	50
55	1491.5	1078.3	0.013140	278.09	405.55	279.47	425.15	1.2611	1.7050	55
60	1681.8	1052.9	0.011444	285.91	407.38	287.50	426.63	1.2848	1.7024	60
65	1889.8	1025.6	0.0099604	293.92	408.99	295.76	427.82	1.3088	1.6993	65
70	2116.8	996.25	0.0086527	302.16	410.33	304.28	428.65	1.3332	1.6956	70
75	2364.1	964.09	0.0074910	310.68	411.32	313.13	429.03	1.3580	1.6909	75
80	2633.2	928.24	0.0064483	319.55	411.83	322.39	428.81	1.3836	1.6850	80
85	2925.8	887.16	0.0054990	328.93	411.67	332.22	427.76	1.4104	1.6771	85
90	3244.2	837.83	0.0046134	339.06	410.45	342.93	425.42	1.4390	1.6662	90
101.06	4059.3	511.90	0.0019535	381.71	381.71	389.64	389.64	1.5621	1.5621	101.06

Thermophysical Properties of Saturated R134a (SI Units)

T °C	P kPa	c_{pf} kJ/kg-K	c_{pg} kJ/kg-K	μ_f mPa-s	μ_g mPa-s	k_f W/m-K	k_g W/m-K	Pr_f	Pr_g	T °C
-103.3	0.38956	1.1838	0.58530	2.1536	0.0068294	0.14524	0.0030801	17.553	1.2978	-103.3
-95	0.93899	1.1861	0.60524	1.5720	0.0071588	0.14022	0.0037452	13.298	1.1569	-95
-90	1.5241	1.1892	0.61730	1.3410	0.0073562	0.13727	0.0041459	11.618	1.0953	-90
-85	2.3990	1.1933	0.62943	1.1624	0.0075528	0.13438	0.0045469	10.322	1.0456	-85
-80	3.6719	1.1981	0.64165	1.0203	0.0077484	0.13154	0.0049479	9.2927	1.0048	-80
-75	5.4777	1.2036	0.65401	0.90473	0.0079430	0.12876	0.0053493	8.4569	0.97112	-75
-70	7.9814	1.2096	0.66654	0.80910	0.0081364	0.12603	0.0057509	7.7656	0.94303	-70
-65	11.380	1.2161	0.67932	0.72879	0.0083286	0.12335	0.0061529	7.1854	0.91952	-65
-60	15.906	1.2230	0.69239	0.66051	0.0085194	0.12071	0.0065554	6.6923	0.89982	-60
-55	21.828	1.2304	0.70582	0.60182	0.0087089	0.11812	0.0069586	6.2688	0.88336	-55
-50	101.325	1.2381	0.71969	0.55089	0.0088970	0.11557	0.0073625	5.9016	0.86968	-50.000
-45	39.117	1.2462	0.73406	0.50633	0.0090837	0.11306	0.0077675	5.5807	0.85845	-45
-40	51.209	1.2546	0.74900	0.46703	0.0092690	0.11059	0.0081736	5.2983	0.84939	-40
-35	66.144	1.2635	0.76458	0.43213	0.0094531	0.10816	0.0085812	5.0482	0.84228	-35
-30	84.378	1.2729	0.78087	0.40095	0.0096361	0.10576	0.0089906	4.8255	0.83693	-30
-25	106.40	1.2827	0.79792	0.37292	0.0098181	0.10340	0.0094022	4.6261	0.83322	-25
-20	132.73	1.2930	0.81580	0.34758	0.0099995	0.10107	0.0098164	4.4469	0.83101	-20
-15	163.94	1.3040	0.83458	0.32456	0.010181	0.098767	0.010234	4.2851	0.83022	-15
-10	200.60	1.3156	0.85435	0.30355	0.010362	0.096491	0.010655	4.1386	0.83079	-10
-5	243.34	1.3279	0.87520	0.28428	0.010543	0.094241	0.011082	4.0056	0.83267	-5
0	292.80	1.3410	0.89723	0.26653	0.010726	0.092013	0.011514	3.8845	0.83584	0
5	349.66	1.3552	0.92059	0.25011	0.010911	0.089806	0.011954	3.7741	0.84031	5
10	414.61	1.3704	0.94546	0.23487	0.011099	0.087618	0.012402	3.6734	0.84612	10
15	488.37	1.3869	0.97206	0.22066	0.011291	0.085444	0.012862	3.5815	0.85335	15
20	571.71	1.4049	1.0007	0.20737	0.011488	0.083284	0.013335	3.4979	0.86211	20
25	665.38	1.4246	1.0316	0.19489	0.011693	0.081134	0.013825	3.4219	0.87256	25
30	770.20	1.4465	1.0655	0.18313	0.011907	0.078992	0.014336	3.3533	0.88493	30
35	886.98	1.4709	1.1028	0.17200	0.012132	0.076853	0.014874	3.2920	0.89953	35
40	1016.6	1.4984	1.1445	0.16145	0.012373	0.074716	0.015446	3.2378	0.91679	40
45	1159.9	1.5298	1.1917	0.15139	0.012633	0.072575	0.016062	3.1912	0.93728	45
50	1317.9	1.5661	1.2461	0.14177	0.012917	0.070427	0.016734	3.1527	0.96180	50
55	1491.5	1.6089	1.3099	0.13253	0.013232	0.068267	0.017481	3.1234	0.99154	55
60	1681.8	1.6602	1.3868	0.12361	0.013587	0.066091	0.018326	3.1051	1.0282	60
65	1889.8	1.7234	1.4822	0.11496	0.013996	0.063894	0.019305	3.1007	1.0745	65
70	2116.8	1.8039	1.6051	0.10651	0.014475	0.061672	0.020471	3.1153	1.1350	70
75	2364.1	1.9115	1.7714	0.098169	0.015053	0.059421	0.021903	3.1579	1.2174	75
80	2633.2	2.0648	2.0122	0.089846	0.015773	0.057147	0.023735	3.2464	1.3372	80
85	2925.8	2.3064	2.3971	0.081372	0.016711	0.054880	0.026205	3.4198	1.5287	85
90	3244.2	2.7559	3.1207	0.072450	0.018023	0.052755	0.029819	3.7848	1.8862	90
101.06	4059.3	-	-	-	-	-	-	-	-	101.06

APPENDIX B.6 (CONTINUED)

Thermophysical Properties of Saturated R134a (IP Units)

T °F	P psia	ρ_f lbm/ ft ³	v_g ft ³ /lbm	u_f Btu/ lbm	u_g Btu/ lbm	h_f Btu/ lbm	h_g Btu/ lbm	s_f Btu/ lbm-R	s_g Btu/ lbm-R	T °F
-153.94	0.056501	99.330	568.59	30.741	138.15	30.74068	144.10	0.098618	0.46939	-153.94
-140	0.12879	98.051	260.63	34.687	139.82	34.687	146.04	0.11124	0.45957	-140
-130	0.22105	97.128	156.50	37.525	141.05	37.525	147.46	0.11998	0.45345	-130
-120	0.36529	96.200	97.480	40.372	142.31	40.373	148.90	0.12849	0.44800	-120
-110	0.58332	95.267	62.763	43.232	143.58	43.233	150.36	0.13679	0.44316	-110
-100	0.90296	94.327	41.637	46.105	144.88	46.107	151.84	0.14489	0.43886	-100
-90	1.3588	93.379	28.381	48.994	146.19	48.997	153.33	0.15281	0.43505	-90
-80	1.9927	92.424	19.825	51.900	147.52	51.904	154.84	0.16057	0.43168	-80
-70	2.8545	91.460	14.161	54.825	148.86	54.830	156.35	0.16817	0.42869	-70
-60	4.0020	90.486	10.321	57.768	150.22	57.776	157.86	0.17563	0.42606	-60
-50	5.5014	89.501	7.6621	60.732	151.58	60.744	159.38	0.18296	0.42373	-50
-40	7.4272	88.504	5.7839	63.718	152.95	63.733	160.90	0.19016	0.42169	-40
-30	9.8624	87.494	4.4330	66.725	154.32	66.746	162.41	0.19724	0.41989	-30
-20	12.898	86.469	3.4449	69.756	155.69	69.784	163.92	0.20421	0.41831	-20
-10	16.632	85.427	2.7109	72.812	157.06	72.848	165.41	0.21109	0.41693	-10
-5	18.794	84.900	2.4154	74.350	157.75	74.391	166.15	0.21449	0.41631	-5
0	21.171	84.368	2.1579	75.894	158.43	75.940	166.89	0.21786	0.41572	0
5	23.777	83.830	1.9330	77.445	159.11	77.497	167.62	0.22122	0.41518	5
10	26.628	83.288	1.7357	79.002	159.79	79.062	168.35	0.22456	0.41467	10
20	33.124	82.186	1.4094	82.140	161.14	82.214	169.79	0.23117	0.41374	20
30	40.784	81.059	1.1543	85.307	162.49	85.401	171.20	0.23771	0.41293	30
40	49.741	79.904	0.95280	88.507	163.81	88.623	172.59	0.24418	0.41222	40
50	60.134	78.719	0.79198	91.742	165.12	91.883	173.94	0.25059	0.41159	50
60	72.105	77.499	0.66246	95.013	166.41	95.185	175.26	0.25695	0.41103	60
70	85.805	76.240	0.55724	98.324	167.67	98.532	176.53	0.26327	0.41052	70
80	101.39	74.937	0.47104	101.68	168.91	101.93	177.75	0.26955	0.41005	80
90	119.01	73.583	0.39988	105.08	170.11	105.38	178.92	0.27580	0.40959	90
100	138.85	72.171	0.34070	108.53	171.26	108.89	180.02	0.28204	0.40914	100
110	161.07	70.693	0.29111	112.04	172.37	112.46	181.05	0.28827	0.40867	110
120	185.86	69.137	0.24928	115.62	173.41	116.12	181.99	0.29451	0.40815	120
130	213.41	67.488	0.21374	119.27	174.38	119.85	182.83	0.30077	0.40757	130
140	243.92	65.728	0.18332	123.00	175.26	123.69	183.54	0.30708	0.40689	140
150	277.61	63.832	0.15709	126.84	176.02	127.64	184.10	0.31346	0.40606	150
160	314.73	61.764	0.13428	130.79	176.64	131.74	184.46	0.31995	0.40503	160
170	355.53	59.469	0.11424	134.91	177.05	136.02	184.57	0.32659	0.40371	170
180	400.34	56.857	0.096375	139.24	177.19	140.54	184.33	0.33350	0.40196	180
190	449.52	53.755	0.080115	143.88	176.89	145.43	183.55	0.34082	0.39951	190
200	503.59	49.761	0.064663	149.07	175.80	150.95	181.83	0.34896	0.39577	200
210	563.35	43.197	0.047695	155.85	172.50	158.26	177.48	0.35960	0.38830	210
213.91	588.75	31.957	0.031292	199.73	199.73	212.84	212.84	2.2312	2.2312	213.91

Thermophysical Properties of Saturated R134a (IP Units)

T °F	P psia	c_{pf} Btu/ lbm-R	c_{pg} Btu/ lbm-R	μ_f lbm/ ft-h	μ_g lbm/ft-h	k_f Btu/h- ft-R	k_g Btu/h- ft-R	Pr_f	Pr_g	T °F
-153.94	0.056501	0.28294	0.13989	5.2097	0.016521	0.083976	0.0017808	17.553	1.2978	-153.94
-140	0.12879	0.28342	0.14434	3.8752	0.017265	0.081262	0.0021396	13.516	1.1646	-140
-130	0.22105	0.28423	0.14754	3.2441	0.017795	0.079365	0.0023971	11.618	1.0953	-130
-120	0.36529	0.28532	0.15076	2.7699	0.018324	0.077511	0.0026546	10.196	1.0406	-120
-110	0.58332	0.28663	0.15401	2.4011	0.018849	0.075695	0.0029123	9.0923	0.99679	-110
-100	0.90296	0.28813	0.15731	2.1068	0.019371	0.073917	0.0031702	8.2123	0.96119	-100
-90	1.3588	0.28978	0.16066	1.8669	0.019890	0.072174	0.0034283	7.4957	0.93207	-90
-80	1.9927	0.29156	0.16409	1.6681	0.020404	0.070465	0.0036867	6.9020	0.90815	-80
-70	2.8545	0.29347	0.16761	1.5009	0.020915	0.068789	0.0039455	6.4031	0.88852	-70
-60	4.0020	0.29549	0.17126	1.3586	0.021422	0.067144	0.0042049	5.9789	0.87250	-60
-50	5.5014	0.29762	0.17506	1.2362	0.021924	0.065529	0.0044649	5.6143	0.85959	-50
-40	7.4272	0.29987	0.17902	1.1298	0.022423	0.063942	0.0047258	5.2983	0.84939	-40
-30	9.8624	0.30224	0.18316	1.0366	0.022917	0.062381	0.0049877	5.0222	0.84160	-30
-20	12.898	0.30474	0.18752	0.95425	0.023409	0.060845	0.0052509	4.7793	0.83597	-20
-10	16.632	0.30738	0.19211	0.88102	0.023897	0.059333	0.0055158	4.5643	0.83232	-10
-5	18.794	0.30876	0.19449	0.84736	0.024141	0.058585	0.0056489	4.4659	0.83118	-5
0	21.171	0.31019	0.19695	0.81544	0.024384	0.057842	0.0057827	4.3730	0.83049	0
5	23.777	0.31166	0.19947	0.78515	0.024628	0.057105	0.0059170	4.2851	0.83022	5
10	26.628	0.31318	0.20206	0.75635	0.024871	0.056372	0.0060521	4.2019	0.83038	10
20	33.124	0.31637	0.20749	0.70280	0.025358	0.054920	0.0063247	4.0485	0.83190	20
30	40.784	0.31980	0.21325	0.65400	0.025849	0.053485	0.0066013	3.9104	0.83502	30
40	49.741	0.32350	0.21939	0.60930	0.026345	0.052065	0.0068828	3.7859	0.83975	40
50	60.134	0.32753	0.22597	0.56816	0.026849	0.050658	0.0071706	3.6734	0.84612	50
60	72.105	0.33193	0.23306	0.53011	0.027366	0.049263	0.0074662	3.5719	0.85424	60
70	85.805	0.33678	0.24076	0.49477	0.027900	0.047876	0.0077718	3.4804	0.86428	70
80	101.39	0.34217	0.24918	0.46178	0.028456	0.046497	0.0080902	3.3983	0.87646	80
90	119.01	0.34823	0.25851	0.43086	0.029042	0.045122	0.0084249	3.3252	0.89112	90
100	138.85	0.35510	0.26897	0.40175	0.029668	0.043748	0.0087809	3.2610	0.90876	100
110	161.07	0.36302	0.28090	0.37421	0.030344	0.042374	0.0091648	3.2059	0.93004	110
120	185.86	0.37227	0.29476	0.34805	0.031088	0.040996	0.0095857	3.1605	0.95595	120
130	213.41	0.38331	0.31125	0.32305	0.031920	0.039610	0.010056	3.1262	0.98793	130
140	243.92	0.39679	0.33145	0.29904	0.032869	0.038212	0.010596	3.1051	1.0282	140
150	277.61	0.41380	0.35714	0.27581	0.033977	0.036800	0.011231	3.1013	1.0805	150
160	314.73	0.43619	0.39137	0.25315	0.035304	0.035369	0.012004	3.1219	1.1510	160
170	355.53	0.46753	0.44004	0.23078	0.036950	0.033918	0.012986	3.1810	1.2521	170
180	400.34	0.51557	0.51594	0.20831	0.039084	0.032456	0.014300	3.3091	1.4101	180
190	449.52	0.60118	0.65317	0.18506	0.042038	0.031026	0.016198	3.5858	1.6951	190
200	503.59	0.80623	0.98353	0.15953	0.046641	0.029881	0.019362	4.3043	2.3692	200
210	563.35	2.1134	3.0079	0.12573	0.056626	0.031242	0.027923	8.5051	6.0999	210
213.91	588.75	-	-	-	-	-	-	-	-	213.91

APPENDIX B.7

Thermophysical Properties of Single Phase R134a (SI Units)

T °C	ρ kg/m ³	v m ³ /kg	u kJ/kg	h kJ/kg	s kJ/kg-K	c_p kJ/kg-K	μ mPa-s	k W/m-K	Pr	T °C
P = 10 kPa (0.01 MPa)										
-100	1582.4	0.00063195	75.360	75.366	0.43539	1.1842	1.8827	0.14323	15.566	-100
-80	1529.0	0.00065402	99.157	99.163	0.56544	1.1981	1.0204	0.13155	9.2932	-80
-60	0.58001	1.7241	344.41	361.65	1.8400	0.68454	0.0085303	0.0065526	0.89115	-60
-40	0.52903	1.8903	356.77	375.67	1.9029	0.71847	0.0093211	0.0081541	0.82130	-40
-20	0.48655	2.0553	369.85	390.40	1.9635	0.75455	0.010105	0.0097557	0.78156	-20
0	0.45051	2.2197	383.66	405.85	2.0222	0.79068	0.010883	0.011357	0.75764	0
20	0.41950	2.3838	398.19	422.02	2.0793	0.82629	0.011655	0.012959	0.74314	20
40	0.39253	2.5476	413.42	438.90	2.1350	0.86123	0.012422	0.014561	0.73474	40
60	0.36884	2.7112	429.36	456.47	2.1894	0.89548	0.013185	0.016163	0.73048	60
80	0.34786	2.8747	445.97	474.72	2.2425	0.92905	0.013942	0.017764	0.72916	80
100	0.32916	3.0380	463.25	493.63	2.2946	0.96198	0.014696	0.019366	0.72998	100
120	0.31236	3.2014	481.18	513.19	2.3457	0.99429	0.015445	0.020968	0.73239	120
140	0.29721	3.3646	499.75	533.39	2.3958	1.0260	0.016190	0.022570	0.73600	140
160	0.28346	3.5278	518.95	554.23	2.4450	1.0572	0.016931	0.024172	0.74054	160
180	0.27092	3.6911	538.77	575.68	2.4934	1.0879	0.017669	0.025774	0.74579	180
200	0.25945	3.8543	559.20	597.74	2.5411	1.1181	0.018403	0.027376	0.75161	200
220	0.24892	4.0174	580.23	620.40	2.5880	1.1478	0.019133	0.028977	0.75787	220
240	0.23921	4.1804	601.85	643.65	2.6342	1.1771	0.019860	0.030579	0.76448	240
260	0.23022	4.3437	624.05	667.48	2.6798	1.2060	0.020583	0.032181	0.77137	260
P = 50 kPa (0.05 MPa)										
-100	1582.5	0.00063191	75.353	75.384	0.43535	1.1842	1.8838	0.14324	15.574	-100
-80	1529.1	0.00065398	99.148	99.181	0.56539	1.1981	1.0208	0.13156	9.2960	-80
-60	1474.4	0.00067824	123.34	123.38	0.68458	1.2230	0.66074	0.12072	6.6936	-60
-40	2.7023	0.37006	355.55	374.05	1.7665	0.74790	0.0092706	0.0081729	0.84835	-40
-20	2.4699	0.40487	368.97	389.21	1.8288	0.77053	0.010071	0.0097718	0.79410	-20
0	2.2780	0.43898	382.98	404.92	1.8885	0.80114	0.010860	0.011372	0.76508	0
20	2.1157	0.47266	397.64	421.27	1.9463	0.83373	0.011641	0.012972	0.74815	20
40	1.9759	0.50610	412.97	438.28	2.0024	0.86677	0.012414	0.014573	0.73837	40
60	1.8541	0.53935	428.98	455.94	2.0571	0.89974	0.013181	0.016174	0.73326	60
80	1.7469	0.57244	445.64	474.26	2.1105	0.93240	0.013943	0.017775	0.73138	80
100	1.6516	0.60547	462.96	493.24	2.1627	0.96466	0.014699	0.019376	0.73181	100
120	1.5664	0.63841	480.93	512.85	2.2139	0.99647	0.015451	0.020977	0.73394	120
140	1.4897	0.67128	499.53	533.09	2.2641	1.0278	0.016198	0.022579	0.73736	140
160	1.4202	0.70413	518.75	553.96	2.3134	1.0587	0.016941	0.024180	0.74175	160
180	1.3569	0.73697	538.59	575.44	2.3619	1.0892	0.017680	0.025782	0.74689	180
200	1.2992	0.76970	559.03	597.52	2.4096	1.1192	0.018415	0.027383	0.75263	200
220	1.2461	0.80250	580.08	620.20	2.4565	1.1488	0.019146	0.028985	0.75882	220
240	1.1973	0.83521	601.71	643.47	2.5028	1.1779	0.019874	0.030586	0.76538	240
260	1.1521	0.86798	623.92	667.32	2.5484	1.2067	0.020598	0.032188	0.77223	260

APPENDIX B.7 (CONTINUED)

Thermophysical Properties of Single Phase R134a (SI Units)

<i>T</i> °C	<i>P</i> kg/m ³	<i>v</i> m ³ /kg	<i>u</i> kJ/kg	<i>h</i> kJ/kg	<i>s</i> kJ/ kg·K	<i>c_p</i> kJ/ kg·K	<i>μ</i> mPa·s	<i>k</i> W/m·K	Pr	<i>T</i> °C
P = 100 kPa (0.1 MPa)										
−100	1582.5	0.00063191	75.344	75.407	0.43529	1.1842	1.8852	0.14326	15.583	−100
−80	1529.2	0.00065394	99.137	99.202	0.56533	1.1980	1.0214	0.13158	9.2995	−80
−60	1474.5	0.00067820	123.33	123.40	0.68451	1.2229	0.66109	0.12074	6.6956	−60
−40	1417.8	0.00070532	148.09	148.16	0.79554	1.2545	0.46727	0.11061	5.2996	−40
−20	5.0401	0.19841	367.81	387.65	1.7677	0.79505	0.010028	0.0097966	0.81382	−20
0	4.6232	0.21630	382.10	403.73	1.8288	0.81542	0.010832	0.011392	0.77529	0
20	4.2784	0.23373	396.94	420.31	1.8874	0.84352	0.011623	0.012990	0.75474	20
40	3.9860	0.25088	412.40	437.49	1.9441	0.87396	0.012404	0.014589	0.74307	40
60	3.7336	0.26784	428.49	455.28	1.9991	0.90521	0.013177	0.016189	0.73683	60
80	3.5130	0.28466	445.23	473.70	2.0528	0.93667	0.013944	0.017789	0.73421	80
100	3.3181	0.30138	462.61	492.74	2.1053	0.96806	0.014704	0.019389	0.73414	100
120	3.1444	0.31803	480.61	512.42	2.1566	0.99923	0.015458	0.020990	0.73592	120
140	2.9885	0.33462	499.25	532.71	2.2070	1.0301	0.016208	0.022590	0.73907	140
160	2.8476	0.35117	518.50	553.62	2.2564	1.0606	0.016953	0.024191	0.74328	160
180	2.7198	0.36767	538.36	575.13	2.3049	1.0908	0.017694	0.025792	0.74828	180
200	2.6031	0.38416	558.83	597.25	2.3527	1.1205	0.018430	0.027393	0.75391	200
220	2.4961	0.40062	579.89	619.95	2.3997	1.1499	0.019163	0.028994	0.76002	220
240	2.3977	0.41707	601.53	643.24	2.4460	1.1790	0.019892	0.030595	0.76651	240
260	2.3069	0.43348	623.76	667.11	2.4916	1.2076	0.020617	0.032197	0.77331	260
P = 500 kPa (0.5 MPa)										
−100	1583.0	0.00063171	75.271	75.587	0.43487	1.1839	1.8967	0.14338	15.660	−100
−80	1529.8	0.00065368	99.048	99.375	0.56487	1.1976	1.0260	0.13172	9.3278	−80
−60	1475.2	0.00067787	123.22	123.56	0.68400	1.2223	0.66384	0.12090	6.7113	−60
−40	1418.7	0.00070487	147.96	148.31	0.79496	1.2536	0.46928	0.11080	5.3099	−40
−20	1359.4	0.00073562	173.38	173.75	0.89964	1.2918	0.34910	0.10126	4.4535	−20
0	1295.6	0.00077184	199.66	200.05	0.99959	1.3399	0.26730	0.092142	3.8869	0
20	23.744	0.042116	390.55	411.61	1.7339	0.96352	0.011504	0.013250	0.83654	20
40	21.526	0.046455	407.40	430.63	1.7967	0.94679	0.012349	0.014788	0.79066	40
60	19.808	0.050485	424.40	449.64	1.8555	0.95652	0.013169	0.016353	0.77026	60
80	18.406	0.054330	441.78	468.95	1.9118	0.97514	0.013970	0.017931	0.75974	80
100	17.225	0.058055	459.65	488.68	1.9661	0.99794	0.014758	0.019516	0.75464	100
120	16.211	0.061687	478.04	508.88	2.0189	1.0230	0.015535	0.021105	0.75301	120
140	15.324	0.065257	496.98	529.60	2.0703	1.0494	0.016303	0.022697	0.75376	140
160	14.540	0.068776	516.47	550.86	2.1205	1.0765	0.017062	0.024290	0.75622	160
180	13.840	0.072254	536.54	572.67	2.1697	1.1041	0.017816	0.025885	0.75992	180
200	13.209	0.075706	557.17	595.03	2.2180	1.1318	0.018563	0.027480	0.76456	200
220	12.637	0.079133	578.38	617.94	2.2654	1.1596	0.019306	0.029077	0.76992	220
240	12.116	0.082535	600.14	641.41	2.3121	1.1873	0.020043	0.030674	0.77583	240
260	11.638	0.085925	622.47	665.43	2.3580	1.2149	0.020776	0.032271	0.78217	260

APPENDIX B.7 (CONTINUED)

Thermophysical Properties of Single Phase R134a (SI Units)

<i>T</i> °C	ρ kg/m ³	<i>v</i> m ³ /kg	<i>u</i> kJ/kg	<i>h</i> kJ/kg	<i>s</i> kJ/ kg·K	<i>c_p</i> kJ/ kg·K	μ mPa·s	<i>k</i> W/m·K	Pr	<i>T</i> °C
P = 1000 kPa (1 MPa)										
−100	1583.6	0.00063147	75.180	75.811	0.43435	1.1835	1.9111	0.14354	15.757	−100
−80	1530.5	0.00065338	98.937	99.591	0.56430	1.1971	1.0317	0.13190	9.3634	−80
−60	1476.1	0.00067746	123.09	123.76	0.68337	1.2216	0.66729	0.12110	6.7310	−60
−40	1419.9	0.00070427	147.79	148.50	0.79425	1.2526	0.47179	0.11102	5.3228	−40
−20	1360.8	0.00073486	173.18	173.91	0.89881	1.2901	0.35116	0.10152	4.4625	−20
0	1297.5	0.00077071	199.39	200.16	0.99860	1.3372	0.26915	0.092451	3.8929	0
20	1227.7	0.00081453	226.69	227.50	1.0952	1.4006	0.20893	0.083611	3.4999	20
40	49.004	0.020406	399.45	419.86	1.7135	1.1340	0.012370	0.015410	0.91026	40
60	43.350	0.023068	418.46	441.53	1.7806	1.0535	0.013232	0.016749	0.83229	60
80	39.372	0.025399	437.00	462.40	1.8414	1.0387	0.014065	0.018226	0.80156	80
100	36.295	0.027552	455.65	483.21	1.8988	1.0438	0.014878	0.019755	0.78613	100
120	33.792	0.029593	474.62	504.21	1.9536	1.0579	0.015674	0.021307	0.77820	120
140	31.692	0.031554	494.00	525.55	2.0065	1.0768	0.016458	0.022873	0.77477	140
160	29.889	0.033457	513.84	547.30	2.0579	1.0986	0.017231	0.024448	0.77430	160
180	28.314	0.035318	534.19	569.51	2.1080	1.1222	0.017996	0.026028	0.77590	180
200	26.922	0.037144	555.05	592.20	2.1570	1.1470	0.018753	0.027612	0.77897	200
220	25.678	0.038944	576.45	615.39	2.2050	1.1724	0.019504	0.029199	0.78315	220
240	24.557	0.040722	598.37	639.10	2.2522	1.1983	0.020250	0.030788	0.78815	240
260	23.539	0.042483	620.84	663.32	2.2985	1.2244	0.020990	0.032378	0.79379	260
P = 4000 kPa (4 MPa)										
−100	1587.2	0.00063004	74.643	77.163	0.43123	1.1813	2.0024	0.14449	16.371	−100
−80	1534.9	0.00065151	98.286	100.89	0.56090	1.1941	1.0671	0.13295	9.5843	−80
−60	1481.5	0.00067499	122.29	124.99	0.67962	1.2174	0.68828	0.12228	6.8525	−60
−40	1426.6	0.00070097	146.82	149.62	0.79005	1.2465	0.48695	0.11235	5.4027	−40
−20	1369.3	0.00073030	171.97	174.89	0.89400	1.2810	0.36351	0.10304	4.5191	−20
0	1308.6	0.00076418	197.86	200.91	0.99291	1.3227	0.28014	0.094232	3.9322	0
20	1242.9	0.00080457	224.65	227.87	1.0881	1.3756	0.21952	0.085770	3.5207	20
40	1169.4	0.00085514	252.65	256.07	1.1812	1.4485	0.17257	0.077471	3.2266	40
60	1082.4	0.00092387	282.39	286.09	1.2740	1.5642	0.13383	0.069049	3.0317	60
80	967.24	0.0010339	315.32	319.46	1.3713	1.8145	0.098907	0.059942	2.9940	80
100	677.84	0.0014753	364.80	370.70	1.5117	9.4035	0.050372	0.054130	8.7507	100
120	200.28	0.0049930	445.13	465.10	1.7616	1.6841	0.019036	0.026830	1.1949	120
140	165.99	0.0060245	471.28	495.38	1.8368	1.4047	0.019013	0.026158	1.0210	140
160	146.16	0.0068418	495.07	522.43	1.9008	1.3151	0.019427	0.026800	0.95331	160
180	132.37	0.0075546	518.11	548.33	1.9592	1.2798	0.019992	0.027871	0.91801	180
200	121.91	0.0082028	540.97	573.78	2.0142	1.2682	0.020626	0.029134	0.89781	200
220	113.54	0.0088075	563.91	599.14	2.0667	1.2692	0.021295	0.030500	0.88616	220
240	106.60	0.0093809	587.07	624.60	2.1173	1.2776	0.021986	0.031925	0.87988	240
260	100.71	0.0099295	610.55	650.27	2.1664	1.2908	0.022690	0.033386	0.87726	260

APPENDIX B.7 (CONTINUED)

Thermophysical Properties of Single Phase R134a (IP Units)

<i>T</i> °F	ρ lbm/ ft ³	<i>v</i> ft ³ /lbm	<i>u</i> Btu/ lbm	<i>h</i> Btu/ lbm	<i>s</i> Btu/ lbm-R	<i>c_p</i> IBtu/ lbm-R	μ lbm/ ft-h	<i>k</i> Btu/h- ft-R	Pr	<i>T</i> °F
P = 10 psia										
-140	98.056	0.010198	34.681	34.700	0.11122	0.28341	3.8788	0.081275	13.526	-140
-120	96.206	0.010394	40.366	40.386	0.12847	0.28530	2.7720	0.077524	10.201	-120
-100	94.333	0.010601	46.099	46.118	0.14487	0.28811	2.1082	0.073930	8.2158	-100
-80	92.430	0.010819	51.894	51.914	0.16055	0.29154	1.6690	0.070478	6.9042	-80
-60	90.491	0.011051	57.763	57.783	0.17562	0.29547	1.3592	0.067154	5.9802	-60
-40	88.507	0.011299	63.715	63.736	0.19015	0.29986	1.1300	0.063946	5.2988	-40
-20	0.22293	4.4857	155.93	164.23	0.42382	0.18409	0.023458	0.0052444	0.82346	-20
0	0.21215	4.7136	159.21	167.94	0.43206	0.18683	0.024538	0.0057575	0.79625	0
20	0.20251	4.9380	162.57	171.71	0.44009	0.19039	0.025608	0.0062710	0.77747	20
40	0.19380	5.1600	166.00	175.56	0.44795	0.19433	0.026669	0.0067847	0.76387	40
60	0.18587	5.3801	169.52	179.49	0.45565	0.19846	0.027724	0.0072985	0.75384	60
80	0.17860	5.5991	173.13	183.50	0.46323	0.20268	0.028772	0.0078124	0.74642	80
100	0.17192	5.8167	176.82	187.59	0.47068	0.20695	0.029814	0.0083264	0.74101	100
150	0.15731	6.3569	186.44	198.21	0.48884	0.21768	0.032397	0.0096116	0.73371	150
200	0.14507	6.8932	196.60	209.36	0.50641	0.22833	0.034953	0.010897	0.73238	200
250	0.13464	7.4272	207.29	221.04	0.52348	0.23883	0.037485	0.012183	0.73484	250
300	0.12564	7.9592	218.50	233.24	0.54009	0.24914	0.039994	0.013468	0.73982	300
350	0.11778	8.4904	230.23	245.95	0.55629	0.25926	0.042484	0.014754	0.74652	350
400	0.11086	9.0204	242.46	259.16	0.57212	0.26919	0.044955	0.016040	0.75444	400
P = 40 psia										
-140	98.073	0.010196	34.664	34.740	0.11117	0.28337	3.8898	0.081314	13.555	-140
-120	96.225	0.010392	40.347	40.424	0.12842	0.28525	2.7787	0.077566	10.219	-120
-100	94.353	0.010598	46.078	46.156	0.14481	0.28805	2.1129	0.073974	8.2275	-100
-80	92.454	0.010816	51.870	51.951	0.16049	0.29147	1.6726	0.070525	6.9128	-80
-60	90.518	0.011048	57.736	57.818	0.17555	0.29538	1.3621	0.067205	5.9868	-60
-40	88.537	0.011295	63.685	63.769	0.19008	0.29975	1.1325	0.064001	5.3041	-40
-20	86.500	0.011561	69.726	69.811	0.20414	0.30461	0.95626	0.060898	4.7832	-20
0	84.392	0.011849	75.869	75.957	0.21781	0.31008	0.81672	0.057882	4.3752	0
20	82.196	0.012166	82.130	82.220	0.23115	0.31632	0.70324	0.054936	4.0492	20
40	0.82467	1.2126	164.41	173.39	0.41770	0.21102	0.026421	0.0068500	0.81392	40
60	0.78319	1.2768	168.15	177.60	0.42597	0.21085	0.027537	0.0073558	0.78932	60
80	0.74687	1.3389	171.92	181.83	0.43396	0.21249	0.028635	0.0078640	0.77376	80
100	0.71456	1.3995	175.74	186.11	0.44173	0.21501	0.029720	0.0083736	0.76312	100
150	0.64672	1.5463	185.60	197.05	0.46046	0.22302	0.032385	0.0096512	0.74834	150
200	0.59215	1.6888	195.92	208.43	0.47839	0.23211	0.034997	0.010932	0.74308	200
250	0.54690	1.8285	206.73	220.27	0.49569	0.24161	0.037571	0.012214	0.74321	250
300	0.50855	1.9664	218.03	232.59	0.51246	0.25126	0.040112	0.013497	0.74673	300
350	0.47552	2.1030	229.82	245.40	0.52878	0.26091	0.042627	0.014781	0.75248	350
400	0.44671	2.2386	242.10	258.68	0.54470	0.27051	0.045118	0.016065	0.75974	400

APPENDIX B.7 (CONTINUED)

Thermophysical Properties of Single Phase R134a (IP Units)

<i>T</i> °F	ρ lbm/ ft ³	v ft ³ /lbm	u Btu/ lbm	h Btu/ lbm	s Btu/ lbm-R	c_p Btu/ lbm-R	μ lbm/ ft-h	k Btu/h- ft-R	Pr	<i>T</i> °F
P = 100 psia										
-140	98.106	0.010193	34.631	34.819	0.11106	0.28329	3.9119	0.081392	13.616	-140
-120	96.261	0.010388	40.310	40.502	0.12831	0.28516	2.7921	0.077649	10.254	-120
-100	94.395	0.010594	46.036	46.232	0.14470	0.28794	2.1223	0.074063	8.2509	-100
-80	92.500	0.010811	51.823	52.023	0.16037	0.29133	1.6798	0.070619	6.9300	-80
-60	90.570	0.011041	57.684	57.888	0.17542	0.29521	1.3680	0.067306	6.0001	-60
-40	88.596	0.011287	63.626	63.835	0.18994	0.29953	1.1375	0.064109	5.3148	-40
-20	86.567	0.011552	69.659	69.873	0.20399	0.30434	0.96071	0.061015	4.7919	-20
0	84.471	0.011838	75.793	76.012	0.21765	0.30973	0.82078	0.058010	4.3823	0
20	82.288	0.012152	82.041	82.267	0.23096	0.31586	0.70705	0.055076	4.0549	20
40	79.995	0.012501	88.422	88.653	0.24401	0.32299	0.61239	0.052195	3.7895	40
60	77.560	0.012893	94.957	95.195	0.25684	0.33153	0.53181	0.049344	3.5731	60
80	75.074	0.013329	101.59	101.83	0.26911	0.34021	0.46783	0.046819	3.3994	80
100	72.379	0.013816	108.35	108.6	0.28171	0.35324	0.40568	0.043981	3.2583	100
150	64.521	0.015503	125.09	125.33	0.31973	0.39758	0.32906	0.037215	2.88617	150
200	56.665	0.019704	151.82	152.06	0.38068	0.46071	0.035677	0.031295	2.32352	200
250	49.974	0.023362	173.47	173.71	0.42968	0.5043	0.038376	0.02489	1.80025	250
300	43.223	0.026734	195.33	195.57	0.46754	0.53667	0.041016	0.013723	1.29107	300
350	37.044	0.029930	222.53	222.77	0.49460	0.56095	0.043610	0.014974	1.08909	350
400	31.325	0.033005	240.12	240.36	0.51105	0.57829	0.046168	0.016236	0.9134	400
P = 200 psia										
-140	98.161	0.010187	34.574	34.952	0.11089	0.28316	3.9492	0.081522	13.717	-140
-120	96.322	0.010382	40.247	40.631	0.12812	0.28500	2.8146	0.077786	10.312	-120
-100	94.463	0.010586	45.966	46.358	0.14450	0.28775	2.1381	0.074209	8.2903	-100
-80	92.576	0.010802	51.745	52.145	0.16016	0.29110	1.6919	0.070775	6.9588	-80
-60	90.656	0.011031	57.596	58.005	0.17520	0.29492	1.3778	0.067473	6.0225	-60
-40	88.694	0.011275	63.527	63.945	0.18970	0.29918	1.1459	0.064288	5.3327	-40
-20	86.679	0.011537	69.548	69.975	0.20374	0.30389	0.96813	0.061209	4.8066	-20
0	84.600	0.011820	75.667	76.104	0.21737	0.30916	0.82755	0.058220	4.3945	0
20	82.438	0.012130	81.897	82.346	0.23066	0.31512	0.71340	0.055306	4.0647	20
40	80.173	0.012473	88.253	88.715	0.24367	0.32200	0.61849	0.052450	3.7970	40
60	77.775	0.012858	94.758	95.234	0.25646	0.33016	0.53783	0.049630	3.5779	60
80	75.199	0.013298	101.44	101.93	0.26911	0.34021	0.46783	0.046819	3.3994	80
100	72.379	0.013816	108.35	108.6	0.28171	0.35324	0.40568	0.043981	3.2583	100
150	64.521	0.015503	125.09	125.33	0.31973	0.39758	0.032906	0.037215	2.88617	150
200	56.665	0.019704	151.82	152.06	0.38068	0.46071	0.035677	0.031295	2.32352	200
250	49.974	0.023362	173.47	173.71	0.42968	0.5043	0.038376	0.02489	1.80025	250
300	43.223	0.026734	195.33	195.57	0.46754	0.53667	0.041016	0.013723	1.29107	300
350	37.044	0.029930	222.53	222.77	0.49460	0.56095	0.043610	0.014974	1.08909	350
400	31.325	0.033005	240.12	240.36	0.51105	0.57829	0.046168	0.016236	0.9134	400

APPENDIX B.7 (CONTINUED)

Thermophysical Properties of Single Phase R134a (IP Units)

<i>T</i> °F	ρ lbm/ ft ³	<i>v</i> ft ³ /lbm	<i>u</i> Btu/ lbm	<i>h</i> Btu/ lbm	<i>s</i> Btu/ lbm-R	<i>c_p</i> Btu/ lbm-R	μ lbm/ ft-h	<i>k</i> Btu/h- ft-R	Pr	<i>T</i> °F
P = 300 psia										
-140	98.215	0.010182	34.519	35.084	0.11071	0.28303	3.9870	0.081651	13.820	-140
-120	96.383	0.010375	40.185	40.761	0.12794	0.28484	2.8374	0.077923	10.372	-120
-100	94.531	0.010579	45.896	46.484	0.14431	0.28756	2.1540	0.074355	8.3302	-100
-80	92.652	0.010793	51.668	52.267	0.15995	0.29087	1.7040	0.070930	6.9880	-80
-60	90.742	0.011020	57.510	58.122	0.17498	0.29464	1.3877	0.067638	6.0450	-60
-40	88.791	0.011262	63.430	64.056	0.18947	0.29883	1.1543	0.064466	5.3509	-40
-20	86.790	0.011522	69.438	70.078	0.20349	0.30346	0.97555	0.061400	4.8215	-20
0	84.727	0.011803	75.542	76.198	0.21710	0.30861	0.83430	0.058428	4.4068	0
20	82.586	0.012109	81.754	82.427	0.23036	0.31441	0.71971	0.055533	4.0748	20
40	80.347	0.012446	88.089	88.780	0.24334	0.32106	0.62454	0.052701	3.8048	40
60	77.984	0.012823	94.565	95.277	0.25608	0.32888	0.54379	0.049910	3.5833	60
80	75.456	0.013253	101.21	101.95	0.26868	0.33837	0.47385	0.047137	3.4015	80
100	72.705	0.013754	108.06	108.83	0.28120	0.35045	0.41198	0.044351	3.2554	100
150	64.004	0.015624	126.70	127.57	0.31323	0.41087	0.27778	0.036943	3.0895	150
200	5.6254	0.17777	188.60	198.48	0.42765	0.29406	0.036742	0.011841	0.91248	200
250	4.8155	0.20766	201.12	212.66	0.44838	0.27752	0.039297	0.012810	0.85135	250
300	4.2834	0.23346	213.48	226.45	0.46716	0.27546	0.041881	0.013951	0.82694	300
350	3.8902	0.25706	226.01	240.29	0.48480	0.27847	0.044452	0.015153	0.81688	350
400	3.5807	0.27928	238.82	254.34	0.50164	0.28385	0.047000	0.016384	0.81429	400
P = 500 psia										
-140	98.323	0.010171	34.408	35.350	0.11036	0.28277	4.0646	0.081908	14.033	-140
-120	96.503	0.010362	40.062	41.021	0.12757	0.28454	2.8838	0.078195	10.494	-120
-100	94.665	0.010564	45.759	46.737	0.14392	0.28720	2.1861	0.074644	8.4113	-100
-80	92.803	0.010776	51.515	52.513	0.15955	0.29043	1.7286	0.071238	7.0472	-80
-60	90.910	0.011000	57.339	58.358	0.17455	0.29411	1.4076	0.067966	6.0909	-60
-40	88.981	0.011238	63.239	64.280	0.18901	0.29817	1.1712	0.064817	5.3877	-40
-20	87.007	0.011493	69.223	70.287	0.20299	0.30264	0.99041	0.061778	4.8518	-20
0	84.975	0.011768	75.299	76.388	0.21656	0.30758	0.84779	0.058837	4.4319	0
20	82.874	0.012067	81.477	82.594	0.22978	0.31308	0.73228	0.055979	4.0955	20
40	80.684	0.012394	87.769	88.916	0.24269	0.31931	0.63655	0.053190	3.8214	40
60	78.385	0.012758	94.192	95.373	0.25536	0.32652	0.55554	0.050453	3.5953	60
80	75.943	0.013168	100.77	101.99	0.26784	0.33508	0.48564	0.047750	3.4080	80
100	73.315	0.013640	107.53	108.79	0.28022	0.34562	0.42416	0.045055	3.2537	100
150	65.353	0.015302	125.62	127.04	0.31142	0.39105	0.29395	0.038102	3.0169	150
200	14.981	0.066751	176.38	182.56	0.39695	0.87921	0.045954	0.018648	2.1666	200
250	9.6166	0.10399	195.27	204.90	0.42975	0.34167	0.043033	0.014239	1.0326	250
300	7.9775	0.12535	209.28	220.89	0.45153	0.30615	0.044669	0.014739	0.92787	300
350	6.9964	0.14293	222.69	235.93	0.47070	0.29738	0.046832	0.015695	0.88735	350
400	6.3051	0.15860	236.08	250.76	0.48848	0.29691	0.049162	0.016798	0.86896	400

APPENDIX B.8

Thermophysical Properties of Metals (SI Units)

<i>T</i> °C	ρ kg/m ³	<i>c</i> kJ/kg-K	<i>k</i> W/m-K	ρ kg/m ³	<i>c</i> kJ/kg-K	<i>k</i> W/m-K	ρ kg/m ³	<i>c</i> kJ/kg-K	<i>k</i> W/m-K
Aluminum			Brass			Bronze			
30	2701	0.9044	236.1	8530	0.3781	116.7	8799	0.4213	52.00
90	2690	0.9320	238.5	8530	0.3886	129.3	8771	0.4453	52.00
150	2678	0.9587	239.1	8544	0.3985	138.4	8742	0.4698	52.81
210	2665	0.9839	236.7	8581	0.4075	142.0	8712	0.4953	54.91
270	2652	1.0090	234.3	8618	0.4165	145.6	8682	0.5208	57.01
330	2640	1.0350	231.8	8655	0.4255	149.2	8652	0.5463	59.11
Chromium			Copper			Iron			
30	7160	0.4501	93.61	8932	0.3854	400.7	7869	0.4484	79.86
90	7151	0.4711	91.93	8904	0.3926	395.9	7851	0.4742	73.44
150	7141	0.4907	89.72	8876	0.3993	391.4	7833	0.4966	67.79
210	7129	0.5081	86.66	8847	0.4053	387.2	7813	0.5137	63.35
270	7118	0.5255	83.60	8818	0.4113	383.0	7793	0.5308	58.91
330	7106	0.5426	80.55	8789	0.4173	378.8	7772	0.5491	54.52
Iron-Armco			AISI 1010 Carbon Steel			AISI 302 Stainless Steel			
30	7867	0.4484	72.48	7831	0.4354	63.74	8052	0.4825	15.27
90	7815	0.4742	68.28	7814	0.4618	60.62	8031	0.5008	16.53
150	7782	0.4966	64.24	7797	0.4874	57.55	8008	0.5174	17.61
210	7782	0.5137	60.46	7777	0.5117	54.58	7983	0.5315	18.42
270	7781	0.5308	56.68	7757	0.5360	51.61	7958	0.5456	19.23
330	7779	0.5491	52.93	7737	0.5610	48.65	7932	0.5594	20.04
AISI 304 Stainless Steel			AISI 316 Stainless Steel			AISI 347 Stainless Steel			
30	7899	0.4782	14.95	8237	0.4691	13.46	7975	0.4826	14.32
90	7877	0.5010	15.97	8214	0.4907	14.54	7954	0.5014	15.24
150	7854	0.5199	16.97	8190	0.5093	15.56	7931	0.5183	16.16
210	7829	0.5325	17.93	8164	0.5231	16.49	7907	0.5321	17.09
270	7805	0.5451	18.89	8139	0.5369	17.42	7882	0.5459	18.02
330	7780	0.5574	19.84	8113	0.5504	18.35	7857	0.5594	18.95
Lead			Nickel			Inconel X-750			
30	11337	0.1291	35.26	8899	0.4453	90.37	8509	0.4401	11.76
90	11277	0.1309	34.48	8876	0.4699	84.07	8490	0.4605	12.84
150	11214	0.1332	33.70	8853	0.4974	78.51	8470	0.4773	13.91
210	11147	0.1362	32.92	8829	0.5295	74.13	8448	0.4884	14.96
270	11081	0.1392	32.14	8805	0.5616	69.75	8426	0.4995	16.01
330	11014	0.1422	31.36	8781	0.5910	65.63	8405	0.5106	17.06
Silver			Titanium			Zirconium			
30	10498	0.2351	248.9	4500	0.5229	21.85	6570	0.2787	22.67
90	10462	0.2375	426.5	4492	0.5403	20.95	6563	0.2919	22.01
150	10424	0.2403	423.6	4485	0.5556	20.28	6556	0.3025	21.50
210	10386	0.2436	419.6	4477	0.5676	19.98	6548	0.3091	21.23
270	10348	0.2469	415.7	4469	0.5796	19.68	6540	0.3157	20.96
330	10309	0.2502	411.7	4461	0.5917	19.40	6533	0.3223	20.71

APPENDIX B.8 (CONTINUED)

Thermophysical Properties of Metals (IP Units)

T °F	ρ lbm/ft³	c Btu/lbm-R	k Btu/hr-ft-°F	ρ lbm/ft³	c Btu/lbm-R	k Btu/hr-ft-°F	ρ lbm/ft³	c Btu/lbm-R	k Btu/hr-ft-°F
Aluminum			Brass			Bronze			
100	168.5	0.2169	136.6	532.5	0.09062	68.35	549.0	0.1014	30.05
200	167.9	0.2230	137.9	532.5	0.09294	75.09	547.4	0.1067	30.05
300	167.2	0.2289	138.2	533.4	0.09513	79.92	545.8	0.1121	30.49
400	166.4	0.2344	136.9	535.5	0.09712	81.85	544.0	0.1177	31.61
500	165.7	0.2400	135.6	537.6	0.09911	83.77	542.3	0.1234	32.74
600	165.0	0.2456	134.3	539.8	0.1011	85.70	540.6	0.1290	33.86
Chromium			Copper			Iron			
100	446.9	0.1082	53.96	557.4	0.09227	231.2	491.1	0.1079	45.66
200	446.4	0.1128	53.06	555.8	0.09386	228.6	490.1	0.1136	42.23
300	445.8	0.1171	51.87	554.2	0.09535	226.2	489.0	0.1185	39.21
400	445.1	0.1210	50.23	552.5	0.09668	223.9	487.8	0.1223	36.84
500	444.5	0.1248	48.60	550.8	0.09800	221.7	486.7	0.1261	34.46
600	443.8	0.1287	46.96	549.1	0.09933	219.4	485.5	0.1299	32.09
Iron-Armco			AISI 1010 Carbon Steel			AISI 302 Stainless Steel			
100	490.7	0.1079	41.56	488.7	0.1048	36.59	502.5	0.1158	8.917
200	487.7	0.1136	39.32	487.8	0.1106	34.92	501.3	0.1193	9.590
300	485.8	0.1185	37.16	486.7	0.1163	33.29	499.9	0.1235	10.170
400	485.8	0.1223	35.14	485.6	0.1217	31.70	498.5	0.1266	10.600
500	485.8	0.1261	33.11	484.5	0.1270	30.11	497.0	0.1298	11.030
600	485.7	0.1299	31.09	483.3	0.1324	28.52	495.6	0.1329	11.470
AISI 304 Stainless Steel			AISI 316 Stainless Steel			AISI 347 Stainless Steel			
100	492.9	0.1149	8.716	514.0	0.1127	7.856	497.7	0.1158	8.345
200	491.7	0.1200	9.262	512.7	0.1175	8.434	496.5	0.1200	8.834
300	490.3	0.1241	9.795	511.3	0.1216	8.980	495.2	0.1237	9.326
400	488.9	0.1269	10.31	509.8	0.1246	9.477	493.7	0.1268	9.824
500	487.5	0.1297	10.82	508.3	0.1277	9.975	492.3	0.1298	10.32
600	486.1	0.1325	11.34	506.9	0.1307	10.47	490.9	0.1329	10.82
Lead			Nickel			Inconel X-750			
100	707.2	0.0309	20.31	555.4	0.1071	51.74	531.0	0.1057	6.874
200	703.8	0.0313	19.90	554.1	0.1126	48.37	529.9	0.1103	7.452
300	700.1	0.0318	19.48	552.7	0.1187	45.41	528.8	0.1139	8.023
400	696.3	0.0325	19.06	551.3	0.1258	43.07	527.5	0.1164	8.585
500	692.4	0.0331	18.64	549.9	0.1329	40.72	526.3	0.1189	9.146
600	688.6	0.0338	18.23	548.5	0.1400	38.38	525.0	0.1213	9.708
Silver			Titanium			Zirconium			
100	655.1	0.0562	247.6	280.8	0.1254	12.56	410.1	0.06697	13.05
200	653.0	0.0568	246.3	280.4	0.1293	12.08	409.7	0.06989	12.69
300	650.8	0.0574	244.7	280.0	0.1327	11.72	409.3	0.07223	12.42
400	648.6	0.0581	242.6	279.5	0.1353	11.56	408.8	0.07369	12.28
500	646.4	0.0588	240.6	279.1	0.1380	11.40	408.4	0.07515	12.13
600	644.2	0.0596	238.5	278.6	0.1406	11.24	407.9	0.07661	11.99



Taylor & Francis

Taylor & Francis Group

<http://taylorandfrancis.com>

Appendix C: Standard Pipe Dimensions

This appendix shows standard pipe dimensions for steel, iron, and stainless steel (SS) pipes. The data shown here are a subset of a much more comprehensive table published by The Crane Company (2017).

Reference

The Crane Company. *Flow of Fluids Through Valves, Fittings and Pipe*. Stamford, Connecticut: The Crane Company, 2017.

Nominal Diameter	Outside Diameter			Schedule		Inside Diameter		
	in	ft	cm	Steel (Iron)	SS	in	ft	cm
1/8	0.405	0.033750	1.0287		10S	0.307	0.025583	0.77978
				40 (std)	40S	0.269	0.022417	0.68326
				80 (xs)	80S	0.215	0.017917	0.54610
1/4	0.540	0.045000	1.3716		10S	0.410	0.034167	1.0414
				40	40S	0.364	0.030333	0.92456
				80	80S	0.302	0.025167	0.76708
3/8	0.675	0.056250	1.7145	10	10S	0.545	0.045417	1.3843
				40 (std)	40S	0.493	0.041083	1.2522
				80 (xs)	80S	0.423	0.035250	1.0744
1/2	0.840	0.070000	2.1336		5S	0.710	0.059167	1.8034
					10S	0.674	0.056167	1.7120
				40 (std)	40S	0.622	0.051833	1.5799
				80 (xs)	80S	0.546	0.045500	1.3868
				160		0.466	0.038833	1.1836
				(xxs)		0.252	0.021000	0.64008
3/4	1.050	0.087500	2.6670		5S	0.920	0.076667	2.3368
					10S	0.884	0.073667	2.2454
				40 (std)	40S	0.824	0.068667	2.0930
				80 (xs)	80S	0.742	0.061833	1.8847
				160		0.612	0.051000	1.5545
				(xxs)		0.434	0.036167	1.1024
1	1.315	0.10958	3.3401		5S	1.185	0.098750	3.0099
					10S	1.097	0.091417	2.7864
				40 (std)	40S	1.049	0.087417	2.6645
				80 (xs)	80S	0.957	0.079750	2.4308
				160		0.815	0.067917	2.0701
				(xxs)		0.599	0.049917	1.5215

(Continued)

Nominal Diameter	Outside Diameter			Schedule		Inside Diameter		
	in	ft	cm	Steel (Iron)	SS	in	ft	cm
1 1/4	1.660	0.13833	4.2164		5S	1.530	0.12750	3.8862
					10S	1.442	0.12017	3.6627
				40 (std)	40S	1.380	0.11500	3.5052
				80 (xs)	80S	1.278	0.10650	3.2461
				160		1.160	0.096667	2.9464
				(xxs)		0.896	0.074667	2.2758
1 1/2	1.900	0.15833	4.8260		5S	1.770	0.14750	4.4958
					10S	1.682	0.14017	4.2723
				40 (std)	40S	1.610	0.13417	4.0894
				80 (xs)	80S	1.500	0.12500	3.8100
				160		1.338	0.11150	3.3985
				(xxs)		1.100	0.091667	2.7940
2	2.375	0.19792	6.0325		5S	2.245	0.18708	5.7023
					10S	2.157	0.17975	5.4788
				40 (std)	40S	2.067	0.17225	5.2502
				80 (xs)	80S	1.939	0.16158	4.9251
				160		1.687	0.14058	4.2850
				(xxs)		1.503	0.12525	3.8176
2 1/2	2.875	0.23958	7.3025		5S	2.709	0.22575	6.8809
					10S	2.635	0.21958	6.6929
				40 (std)	40S	2.469	0.20575	6.2713
				80 (xs)	80S	2.323	0.19358	5.9004
				160		2.125	0.17708	5.3975
				(xxs)		1.771	0.14758	4.4983
3	3.500	0.29167	8.8900		5S	3.334	0.27783	8.4684
					10S	3.260	0.27167	8.2804
				40 (std)	40S	3.068	0.25567	7.7927
				80 (xs)	80S	2.900	0.24167	7.3660
				160		2.624	0.21867	6.6650
				(xxs)		2.300	0.19167	5.8420
3 1/2	4.000	0.33333	10.160		5S	3.834	0.31950	9.7384
					10S	3.760	0.31333	9.5504
				40 (std)	40S	3.548	0.29567	9.0119
				80 (xs)	80S	3.364	0.28033	8.5446
4	4.500	0.37500	11.430		5S	4.334	0.36117	11.008
					10S	4.260	0.35500	10.820
				40 (std)	40S	4.026	0.33550	10.226
				80 (xs)	80S	3.826	0.31883	9.7180
				120		3.624	0.30200	9.2050
				160		3.438	0.28650	8.7325
				(xxs)		3.152	0.26267	8.0061

(Continued)

Nominal Diameter	Outside Diameter			Schedule		Inside Diameter		
	in	ft	cm	Steel (Iron)	SS	in	ft	cm
5	5.563	0.46358	14.130		5S	5.345	0.44542	13.576
					10S	5.295	0.44125	13.449
				40 (std)	40S	5.047	0.42058	12.819
				80 (xs)	80S	4.813	0.40108	12.225
				120		4.563	0.38025	11.590
				160		4.313	0.35942	10.955
				(xxs)		4.063	0.33858	10.320
6	6.625	0.55208	16.828	5	5S	6.407	0.53392	16.274
				10	10S	6.357	0.52975	16.147
				40 (std)	40S	6.065	0.50542	15.405
				80 (xs)	80S	5.761	0.48008	14.633
				120		5.501	0.45842	13.973
				160		5.187	0.43225	13.175
				xxs		4.897	0.40808	12.438
8	8.625	0.71875	21.908		5S	8.407	0.70058	21.354
					10S	8.329	0.69408	21.156
				20		8.125	0.67708	20.638
				30		8.071	0.67258	20.500
				40 (std)	40S	7.981	0.66508	20.272
				60		7.813	0.65108	19.845
				80 (xs)	80S	7.625	0.63542	19.368
				100		7.437	0.61975	18.890
				120		7.187	0.59892	18.255
				140		7.001	0.58342	17.783
				(xxs)		6.875	0.57292	17.463
				160		6.813	0.56775	17.305
10	10.750	0.89583	27.305		5S	10.482	0.87350	26.624
					10S	10.420	0.86833	26.467
				20		10.250	0.85417	26.035
				30		10.136	0.84467	25.745
				40 (std)	40S	10.020	0.83500	25.451
				60 (std)	80S	9.750	0.81250	24.765
				80		9.562	0.79683	24.287
				100		9.312	0.77600	23.652
				120		9.062	0.75517	23.017
				140 (xxs)		8.750	0.72917	22.225
				160		8.500	0.70833	21.590

(Continued)

Nominal Diameter	Outside Diameter			Schedule		Inside Diameter		
	in	ft	cm	Steel (Iron)	SS	in	ft	cm
12	12.75	1.0625	32.385		5S	12.438	1.0365	31.593
					10S	12.390	1.0325	31.471
				20		12.250	1.0208	31.115
				30		12.090	1.0075	30.709
				(std)	40S	12.000	1.0000	30.480
				40		11.983	0.99858	30.437
				(xs)	80S	11.750	0.97917	29.845
				60		11.626	0.96883	29.530
				80		11.374	0.94783	28.890
				100		11.062	0.92183	28.097
				120 (xxs)		10.750	0.89583	27.305
				140		10.500	0.87500	26.670
				160		10.126	0.84383	25.720
14	14	1.1667	35.560		5S	13.688	1.1407	34.768
					10S	13.624	1.1353	34.605
				10		13.500	1.1250	34.290
				20		13.376	1.1147	33.975
				30 (std)		13.250	1.1042	33.655
				40		13.124	1.0937	33.335
				(xs)		13.000	1.0833	33.020
				60		12.812	1.0677	32.542
				80		12.500	1.0417	31.750
				100		12.124	1.0103	30.795
				120		11.812	0.98433	30.002
				140		11.500	0.95833	29.210
				160		11.188	0.93233	28.418
16	16	1.3333	40.640		5S	15.670	1.3058	39.802
					10S	15.624	1.3020	39.685
				10		15.500	1.2917	39.370
				20		15.376	1.2813	39.055
				30 (std)		15.250	1.2708	38.735
				40 (xs)		15.000	1.2500	38.100
				60		14.688	1.2240	37.308
				80		14.312	1.1927	36.352
				100		13.938	1.1615	35.403
				120		13.562	1.1302	34.447
				140		13.124	1.0937	33.335
				160		12.182	1.0152	30.942

(Continued)

Nominal Diameter	Outside Diameter			Schedule		Inside Diameter		
	in	ft	cm	Steel (Iron)	SS	in	ft	cm
18	18	1.5000	45.720		5S	17.670	1.4725	44.882
					10S	17.624	1.4687	44.765
					10	17.500	1.4583	44.450
					20	17.376	1.4480	44.135
					(std)	17.250	1.4375	43.815
					30	17.124	1.4270	43.495
					(xs)	17.000	1.4167	43.180
					40	16.876	1.4063	42.865
					60	16.500	1.3750	41.910
					80	16.124	1.3437	40.955
					100	15.688	1.3073	39.848
					120	15.250	1.2708	38.735
					140	14.876	1.2397	37.785
					160	14.438	1.2032	36.673
20	20	1.6667	50.800		5S	19.624	1.6353	49.845
					10S	19.564	1.6303	49.693
					10	19.500	1.6250	49.530
					20 (std)	19.250	1.6042	48.895
					30 (xs)	19.000	1.5833	48.260
					40	18.812	1.5677	47.782
					60	18.376	1.5313	46.675
					80	17.938	1.4948	45.563
					100	17.438	1.4532	44.293
					120	17.000	1.4167	43.180
					140	16.500	1.3750	41.910
					160	16.062	1.3385	40.797
22	22	1.8333	55.880		5S	21.624	1.8020	54.925
					10S	21.564	1.7970	54.773
					10	21.500	1.7917	54.610
					20 (std)	21.250	1.7708	53.975
					30 (xs)	21.000	1.7500	53.340
					60	20.250	1.6875	51.435
					80	19.750	1.6458	50.165
					100	19.250	1.6042	48.895
					120	18.750	1.5625	47.625
					140	18.250	1.5208	46.355
					160	17.750	1.4792	45.085

(Continued)

Nominal Diameter	Outside Diameter			Schedule		Inside Diameter		
	in	ft	cm	Steel (Iron)	SS	in	ft	cm
24	24	2.0000	60.960		5S	23.564	1.9637	59.853
				10	10S	23.500	1.9583	59.690
				20 (std)		23.250	1.9375	59.055
				(xs)		23.000	1.9167	58.420
				30		22.876	1.9063	58.105
				40		22.624	1.8853	57.465
				60		22.062	1.8385	56.037
				80		21.562	1.7968	54.767
				100		20.938	1.7448	53.183
				120		20.376	1.6980	51.755
				140		19.876	1.6563	50.485
				160		19.312	1.6093	49.052
26	26	2.1667	66.040	10		25.376	2.1147	64.455
				(std)		25.250	2.1042	64.135
				20 (xs)		25.000	2.0833	63.500
28	28	2.3333	71.120	10		27.376	2.2813	69.535
				(std)		27.250	2.2708	69.215
				20 (xs)		27.000	2.2500	68.580
				30		26.750	2.2292	67.945
30	30	2.5000	76.200		5S	29.500	2.4583	74.930
				10	10S	29.376	2.4480	74.615
				(std)		29.250	2.4375	74.295
				20 (xs)		29.000	2.4167	73.660
				30		28.750	2.3958	73.025
32	32	2.6667	81.280	10		31.376	2.6147	79.695
				(std)		31.250	2.6042	79.375
				20 (xs)		31.000	2.5833	78.740
				30		30.750	2.5625	78.105
				40		30.624	2.5520	77.785
34	34	2.8333	86.360	10		33.376	2.7813	84.775
				(std)		33.250	2.7708	84.455
				20 (xs)		33.000	2.7500	83.820
				30		32.750	2.7292	83.185
				40		32.624	2.7187	82.865
36	36	3.0000	91.440	10		35.376	2.9480	89.855
				(std)		35.250	2.9375	89.535
				20 (xs)		35.000	2.9167	88.900
				30		34.750	2.8958	88.265
				40		34.500	2.8750	87.630

Appendix D: Standard Copper Tubing Dimensions

This appendix shows dimensional data for Type K, L, and M standard copper tubing. The data were taken from *The Copper Tube Handbook* (2010).

Reference

The Copper Tube Handbook. New York: Copper Development Association, Inc., 2010.

Standard Size	Outside Diameter			Type	Inside Diameter		
	in	ft	cm		in	ft	cm
1/4	0.375	0.031250	0.95250	K	0.305	0.025417	0.77470
				L	0.315	0.026250	0.80010
3/8	0.500	0.041667	1.2700	K	0.402	0.033500	1.0211
				L	0.430	0.035833	1.0922
				M	0.450	0.037500	1.1430
1/2	0.625	0.052083	1.5875	K	0.527	0.043917	1.3386
				L	0.545	0.045417	1.3843
				M	0.569	0.047417	1.4453
5/8	0.750	0.062500	1.9050	K	0.652	0.054333	1.6561
				L	0.666	0.055500	1.6916
3/4	0.875	0.072917	2.2225	K	0.745	0.062083	1.8923
				L	0.785	0.065417	1.9939
				M	0.811	0.067583	2.0599
1	1.125	0.093750	2.8575	K	0.995	0.082917	2.5273
				L	1.025	0.085417	2.6035
				M	1.055	0.087917	2.6797
1 1/4	1.375	0.11458	3.4925	K	1.245	0.10375	3.1623
				L	1.265	0.10542	3.2131
				M	1.291	0.10758	3.2791
1 1/2	1.625	0.13542	4.1275	K	1.481	0.12342	3.7617
				L	1.505	0.12542	3.8227
				M	1.527	0.12725	3.8786
2	2.125	0.17708	5.3975	K	1.959	0.16325	4.9759
				L	1.985	0.16542	5.0419
				M	2.009	0.16742	5.1029

(Continued)

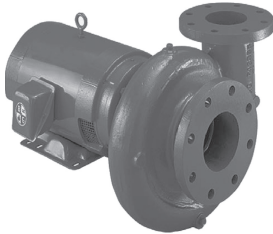
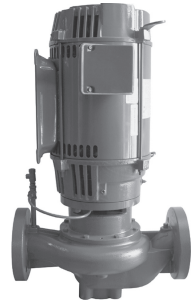
Standard Size	Outside Diameter			Type	Inside Diameter		
	in	ft	cm		in	ft	cm
2 1/2	2.625	0.21875	6.6675	K	2.435	0.20292	6.1849
				L	2.465	0.20542	6.2611
				M	2.495	0.20792	6.3373
3	3.125	0.26042	7.9375	K	2.907	0.24225	7.3838
				L	2.945	0.24542	7.4803
				M	2.981	0.24842	7.5717
3 1/2	3.625	0.30208	9.2075	K	3.385	0.28208	8.5979
				L	3.425	0.28542	8.6995
				M	3.459	0.28825	8.7859
4	4.125	0.34375	10.478	K	3.857	0.32142	9.7968
				L	3.905	0.32542	9.9187
				M	3.935	0.32792	9.9949
5	5.125	0.42708	13.018	K	4.805	0.40042	12.205
				L	4.875	0.40625	12.383
				M	4.907	0.40892	12.464
6	6.125	0.51042	15.558	K	5.741	0.47842	14.582
				L	5.845	0.48708	14.846
				M	5.881	0.49008	14.938
8	8.125	0.67708	20.638	K	7.583	0.63192	19.261
				L	7.725	0.64375	19.622
				M	7.785	0.64875	19.774
10	10.125	0.84375	25.718	K	9.449	0.78742	24.000
				L	9.625	0.80208	24.448
				M	9.701	0.80842	24.641
12	12.125	1.0104	30.798	K	11.315	0.94292	28.740
				L	11.565	0.96375	29.375
				M	11.617	0.96808	29.507

Appendix E: Pump Curves

This appendix contains complete technical booklets for the Bell & Gossett Series e-80 inline centrifugal pumps and Series e-1531 end suction centrifugal pumps. This information is included here for purposes of learning how to use the pump curves. Permission has been granted by Xylem, Inc. to include these pump curves in this textbook.

Series e-80

IN-LINE MOUNTED CENTRIFUGAL PUMP PERFORMANCE CURVES – 60 HZ



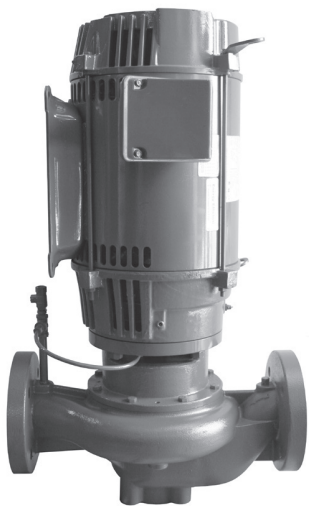
Series e-1531

CLOSED COUPLED CENTRIFUGAL PUMP PERFORMANCE CURVES – 60 HZ

References

- Xylem, Inc. 2015. *Series e-1531: Closed coupled centrifugal pump curves - 60 Hz*. Morton Grove, Illinois, USA: Bell & Gossett.
- Xylem, Inc. 2016. *Series e-80: In-line mounted centrifugal pump performance curves - 60 Hz*. Morton Grove, Illinois, USA: Bell & Gossett.

CURVES
B-193B



Series e-80

IN-LINE MOUNTED CENTRIFUGAL PUMP PERFORMANCE CURVES – 60 HZ

Series e-80

TABLE OF CONTENTS

Useful Pump Formulas 2

Selection Charts 3

1800 RPM PUMP CURVES

7" - Size Curves 4-7

9.5" - Size Curves 7-11

11" - Size Curves 11-13

13.5" - Size Curves 13-14

1200 RPM PUMP CURVES

7" - Size Curves 15-18

9.5" - Size Curves 18-22

11" - Size Curves 22-24

13.5" - Size Curves 24-25

3600 RPM PUMP CURVES

7" - Size Curves 26-29

9.5" - Size Curves 29-31

11" - Size Curves 31

USEFUL PUMP FORMULAS

Pressure (PSI) = $\frac{\text{Head (Feet)} \times \text{Specific Gravity}}{2.31}$

Head (Feet) = $\frac{\text{Pressure (PSI)} \times 2.31}{\text{Specific Gravity}}$

Vacuum (Inches of Mercury) = $\frac{\text{Dynamic Suction Lift (Feet)} \times .883}{\text{x Specific Gravity}}$

Horsepower (Brake) = $\frac{\text{GPM} \times \text{Head (Feet)} \times \text{Specific Gravity}}{3960 \times \text{Pump Efficiency}}$

Horsepower (Water) = $\frac{\text{GPM} \times \text{Head (Feet)} \times \text{Specific Gravity}}{3960}$

Efficiency (Pump) = $\frac{\text{Horsepower (Water)}}{\text{Horsepower (Brake)}} \times 100 \text{ Per Cent}$

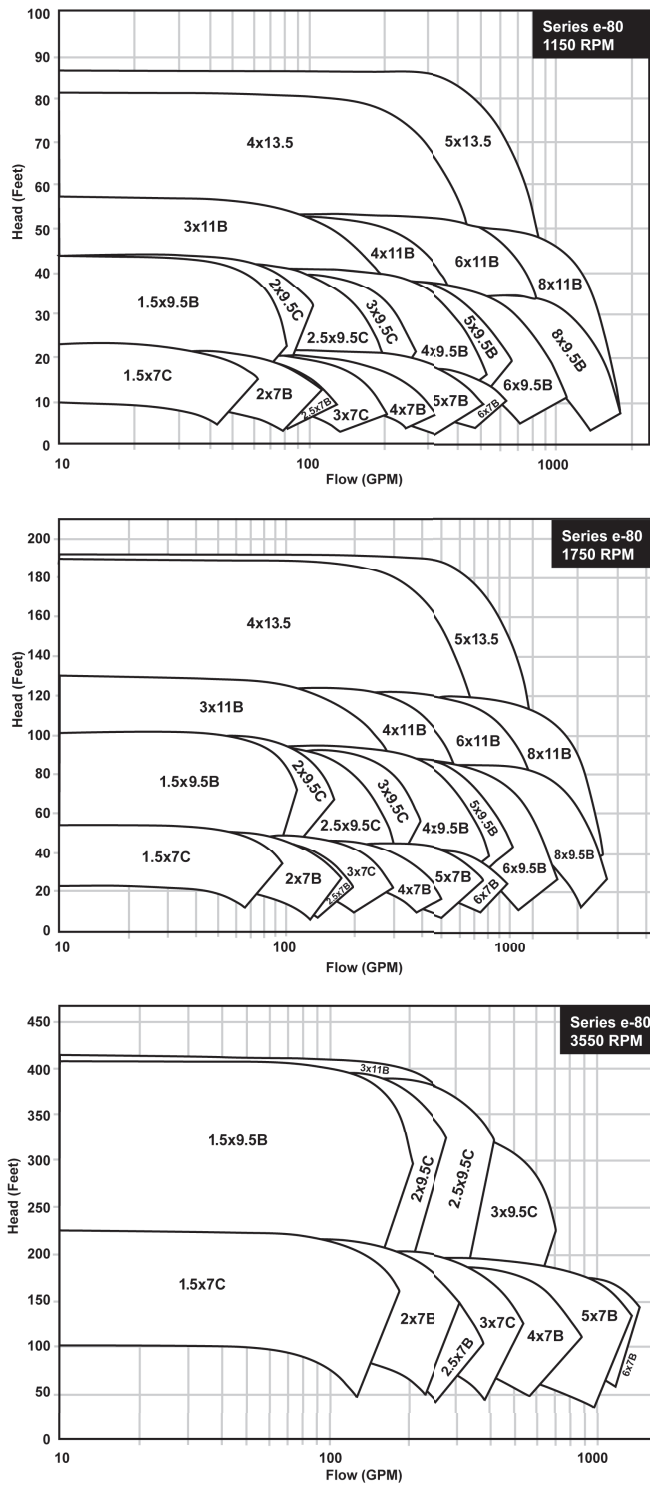
NPSH (Available) = Positive Factors – Negative Factors

Affinity Laws: Effect of change of speed or impeller diameter on centrifugal pumps.

	GPM Capacity	Ft. Head	BHP
Impeller Diameter Change	$Q_2 = \frac{D_2}{D_1} Q_1$	$H_2 = \left(\frac{D_2}{D_1}\right)^2 H_1$	$P_2 = \left(\frac{D_2}{D_1}\right)^3 P_1$
Speed Change	$Q_2 = \frac{RPM_2}{RPM_1} Q_1$	$H_2 = \left(\frac{RPM_2}{RPM_1}\right)^2 H_1$	$P_2 = \left(\frac{RPM_2}{RPM_1}\right)^3 P_1$

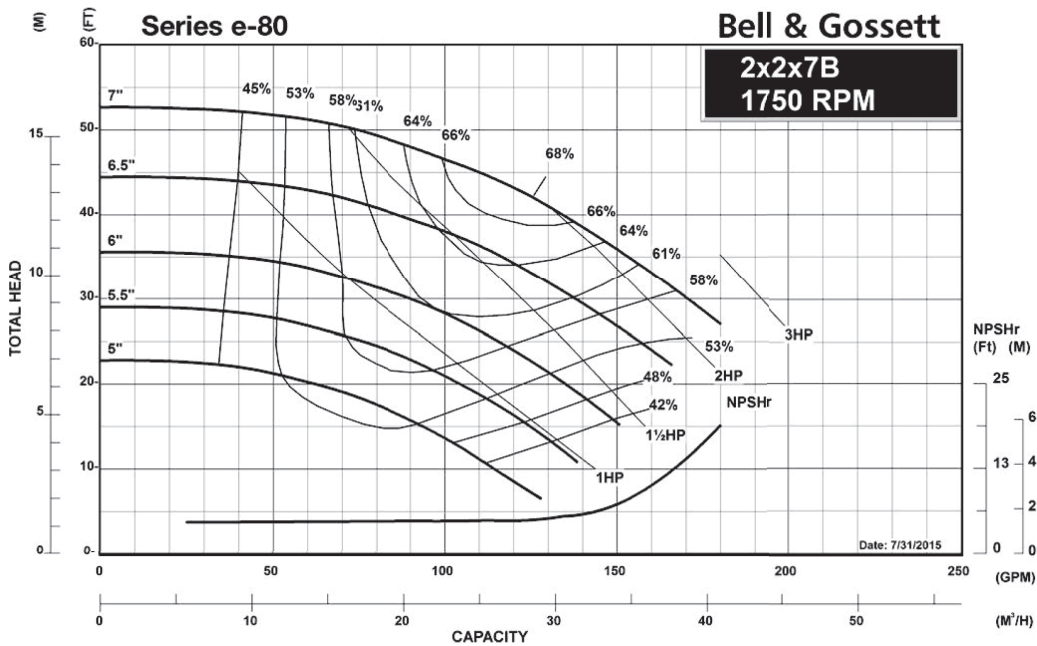
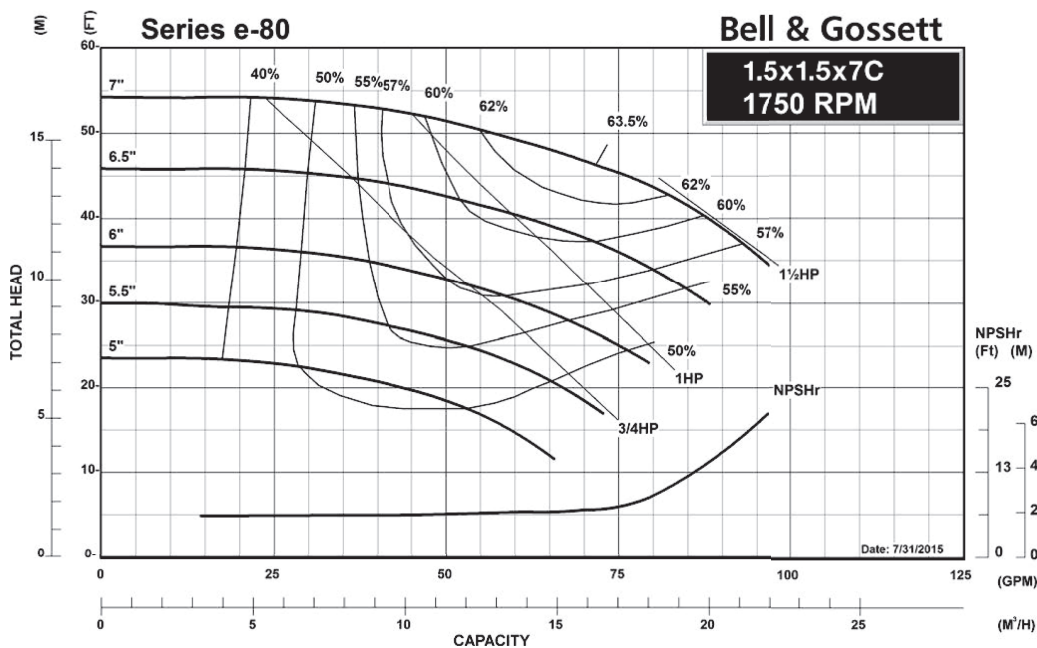
Where Q = GPM, H = Head, P = BHP, D = Impeller Dia., RPM = Pump Speed

Series e-80 Selection Charts



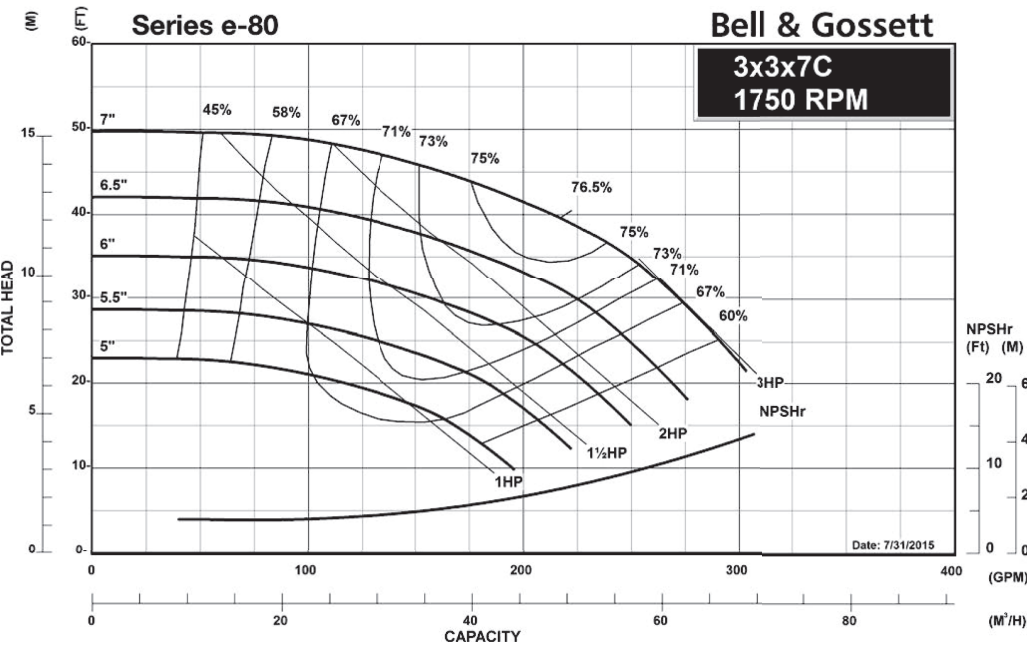
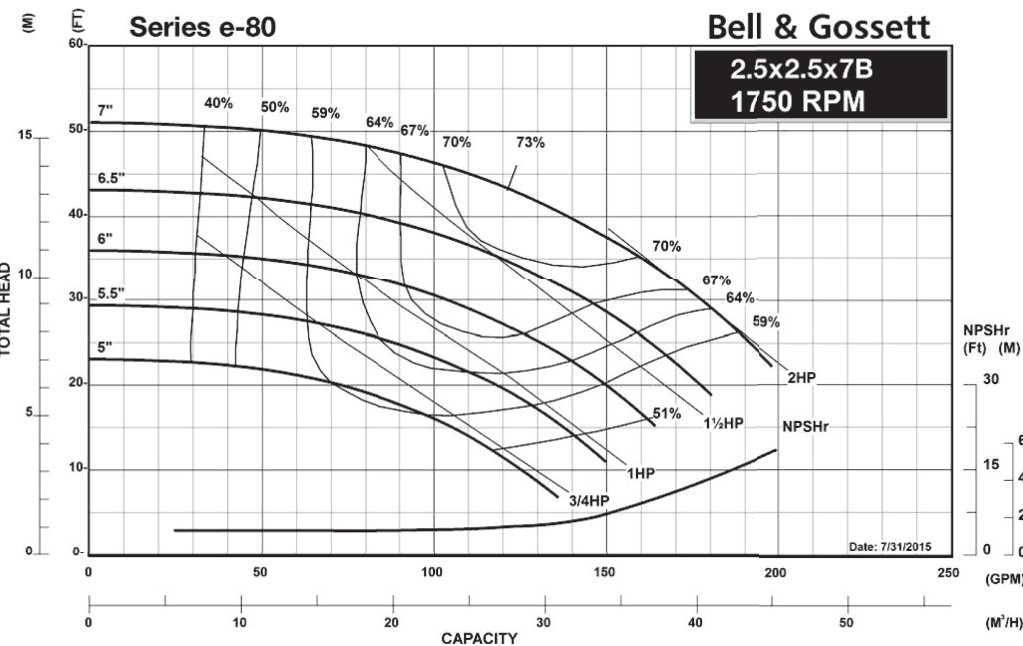
Series e-80

1800 RPM PUMP CURVES



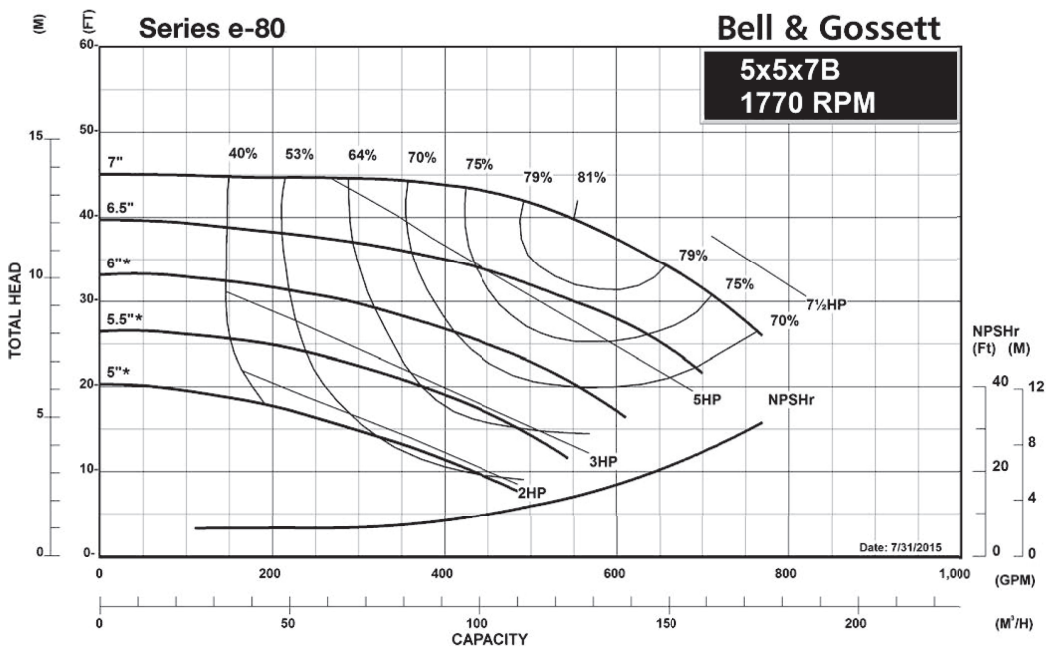
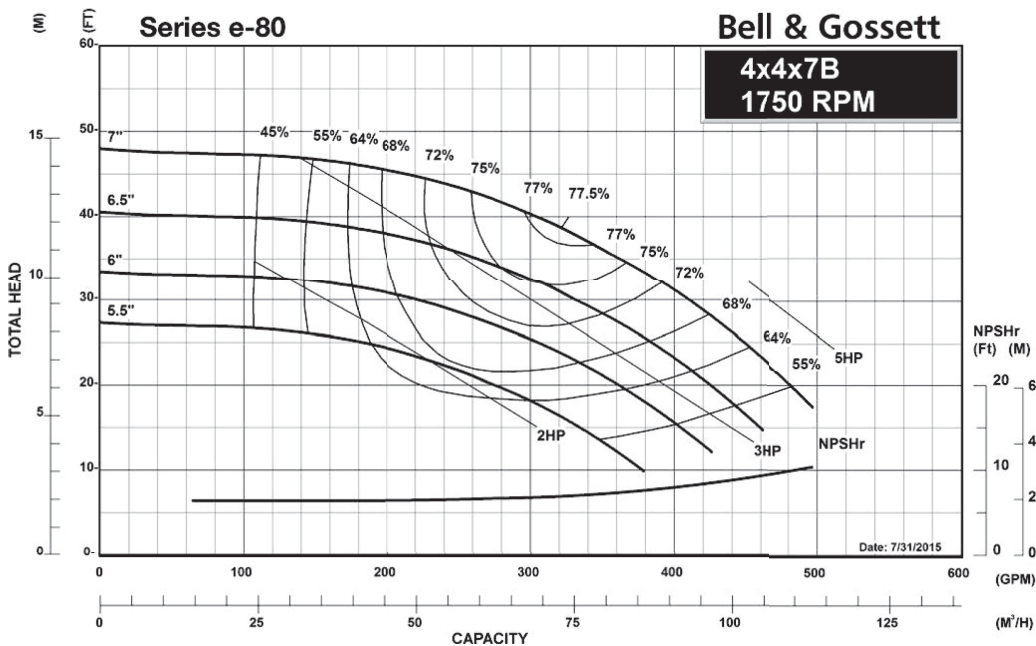
Series e-80

1800 RPM PUMP CURVES



Series e-80

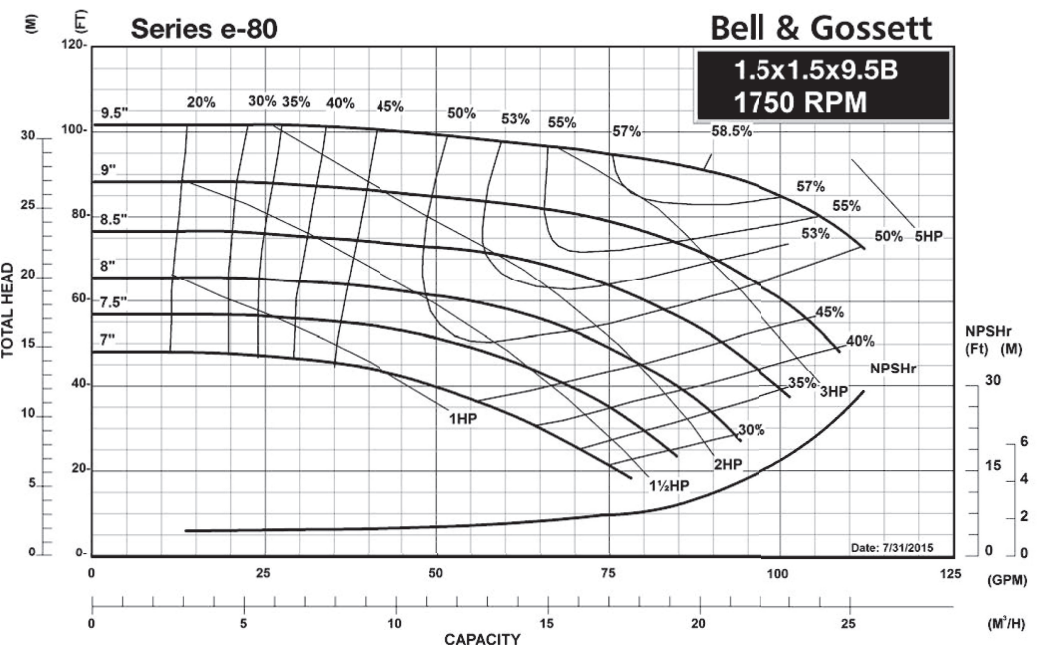
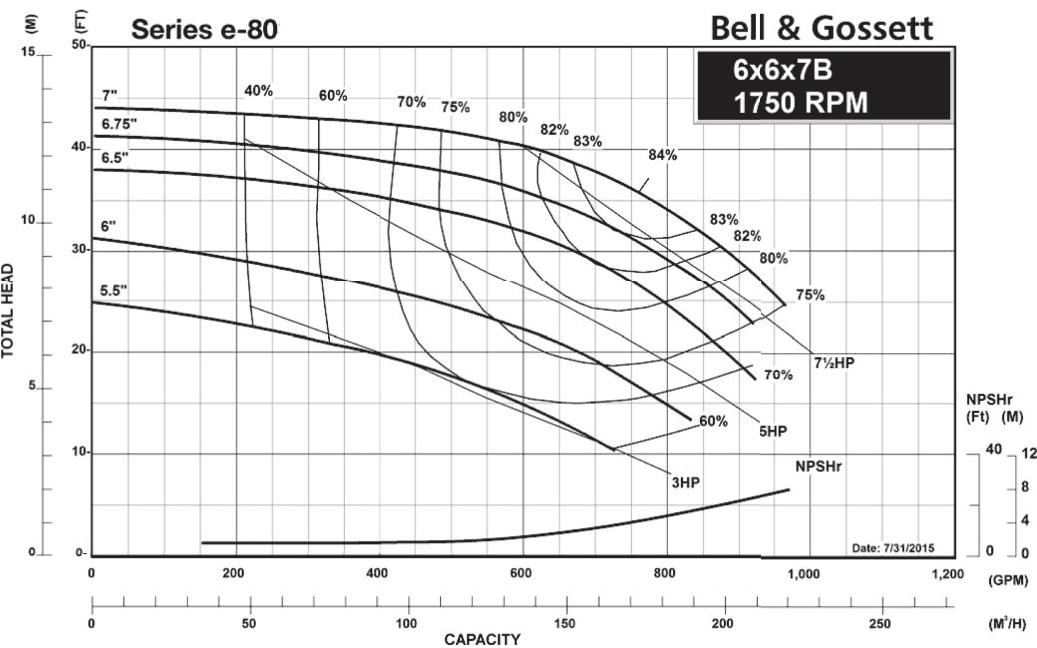
1800 RPM PUMP CURVES



*6" and below requires oversized diameter and angle trim. See manual.

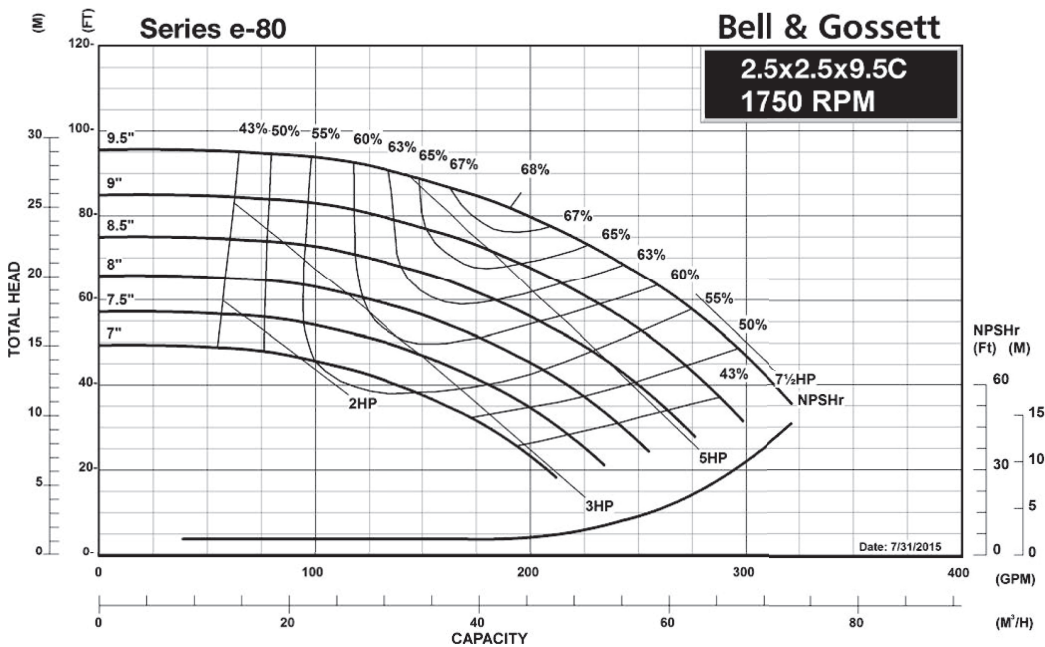
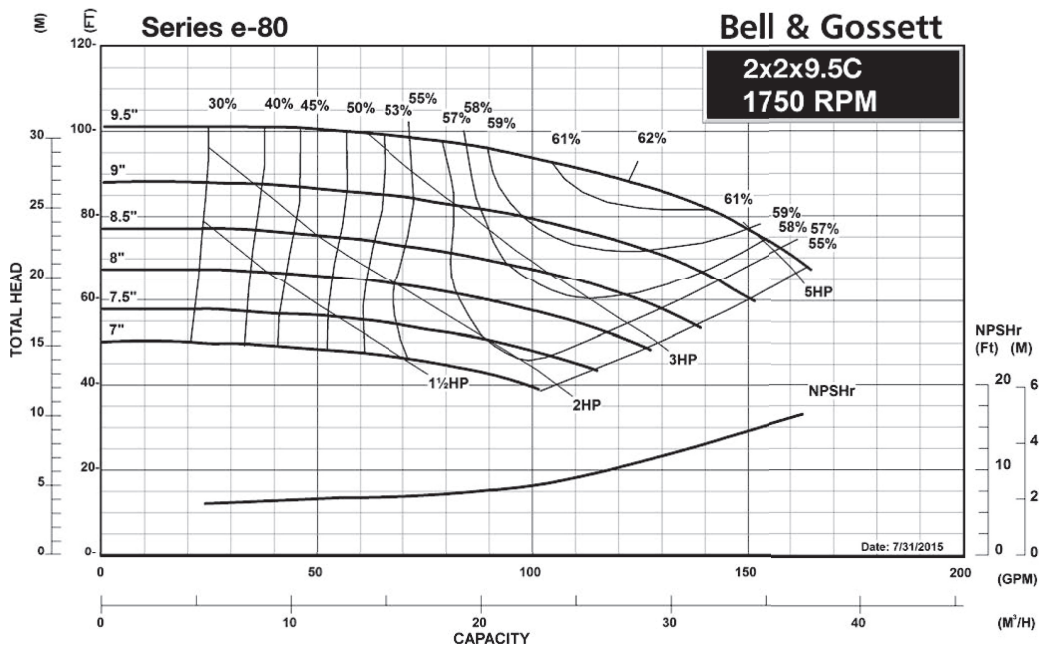
Series e-80

1800 RPM PUMP CURVES



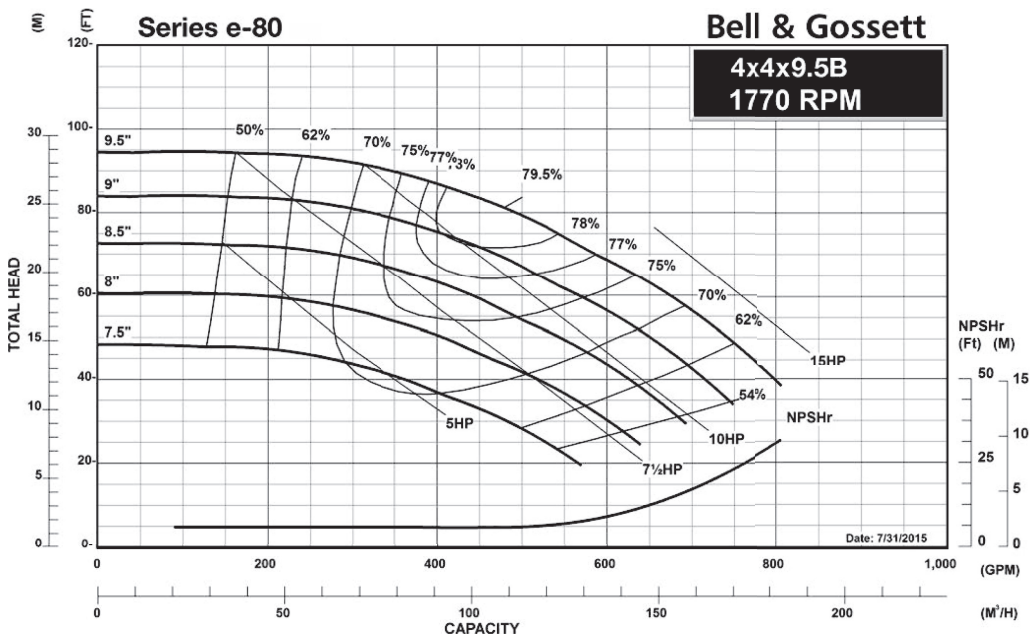
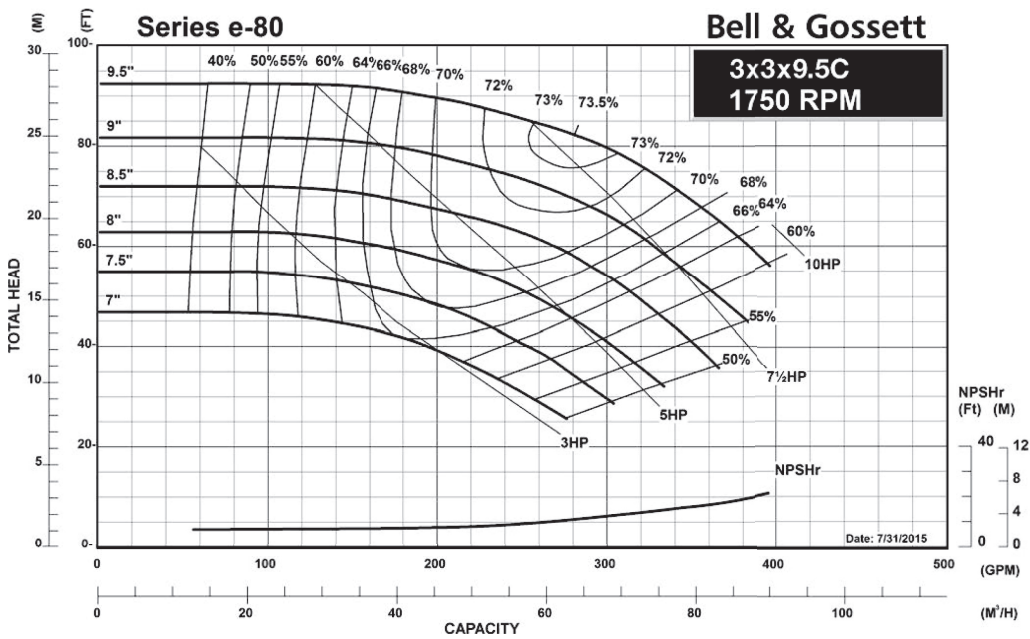
Series e-80

1800 RPM PUMP CURVES



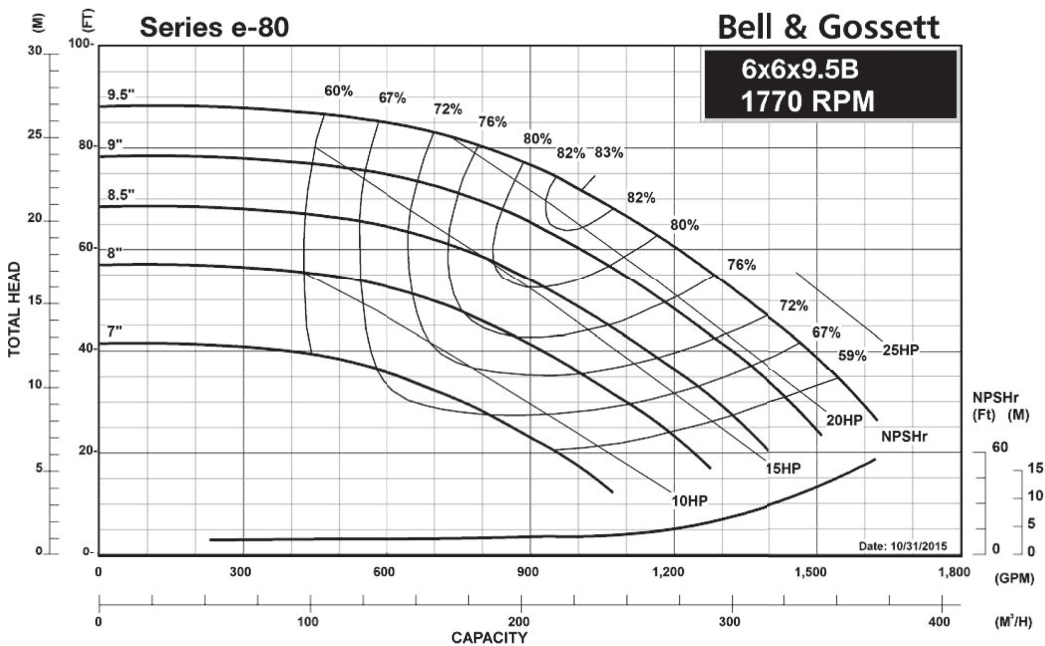
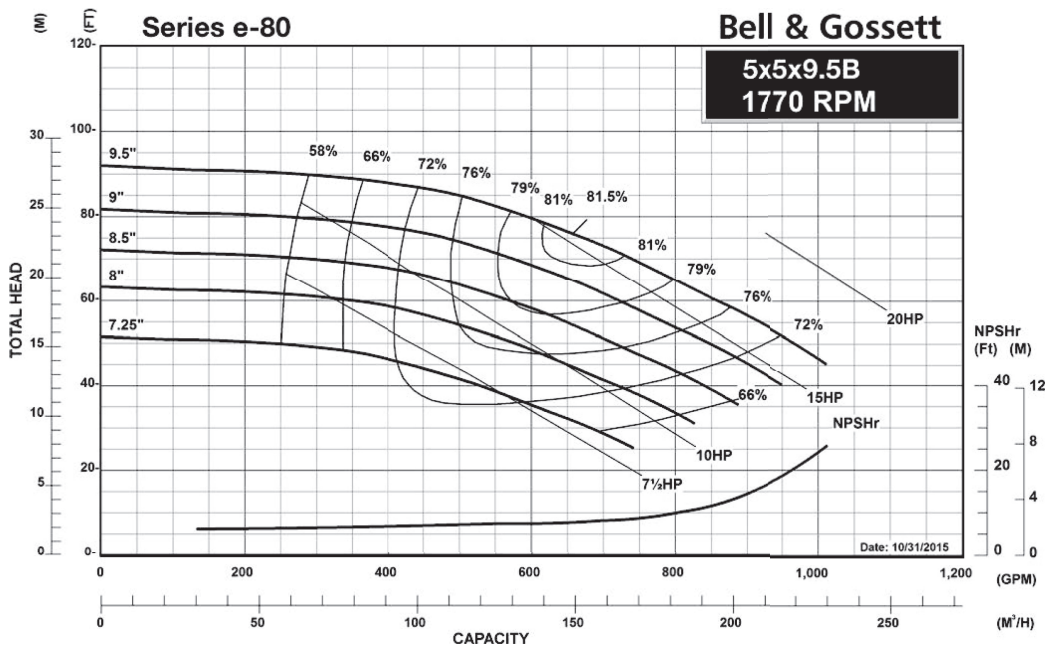
Series e-80

1800 RPM PUMP CURVES



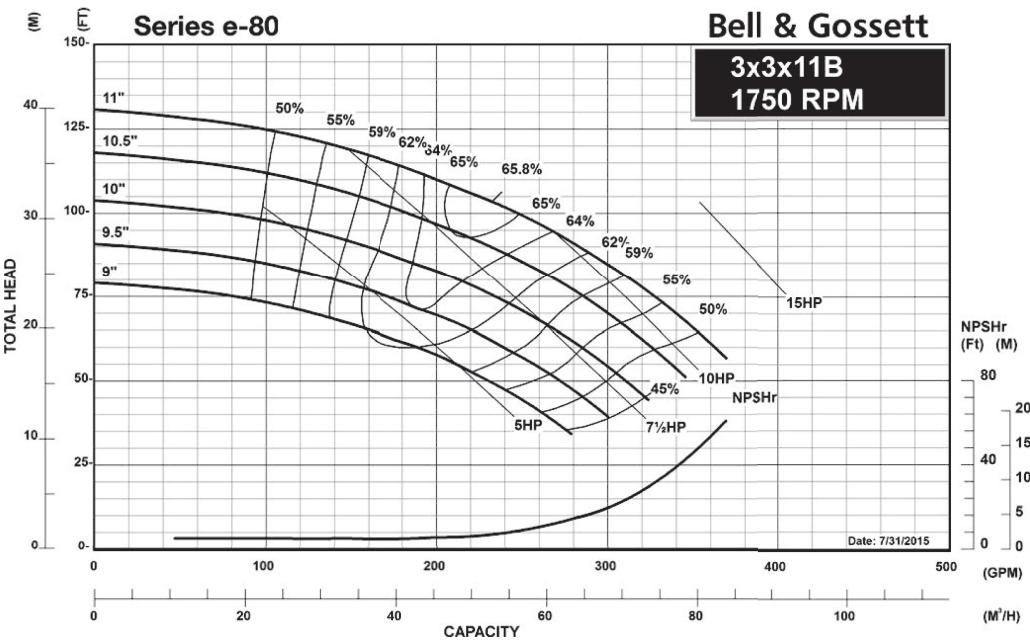
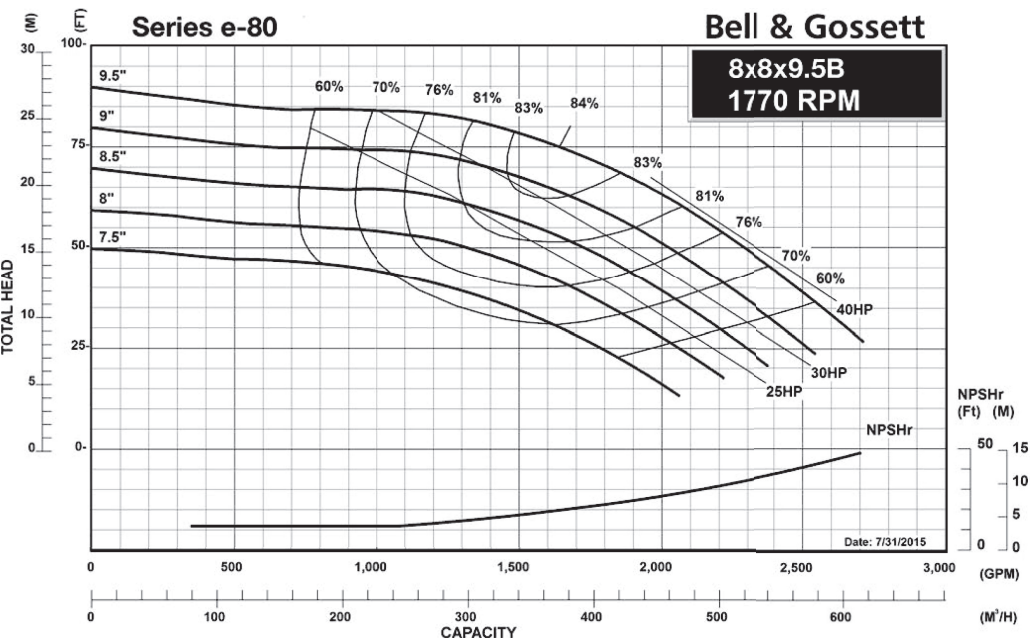
Series e-80

1800 RPM PUMP CURVES



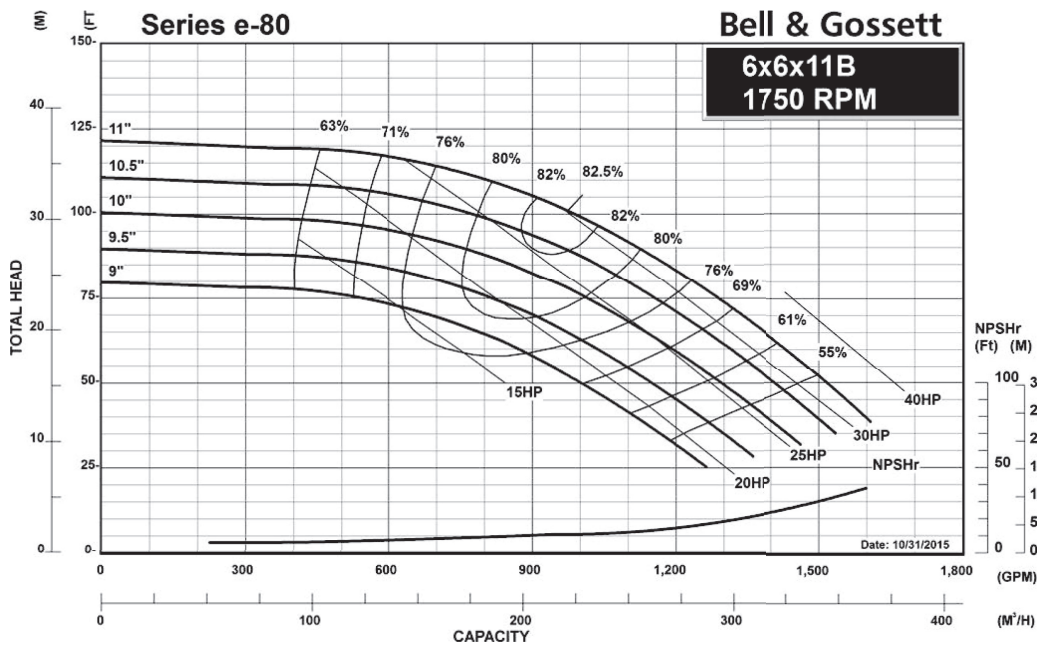
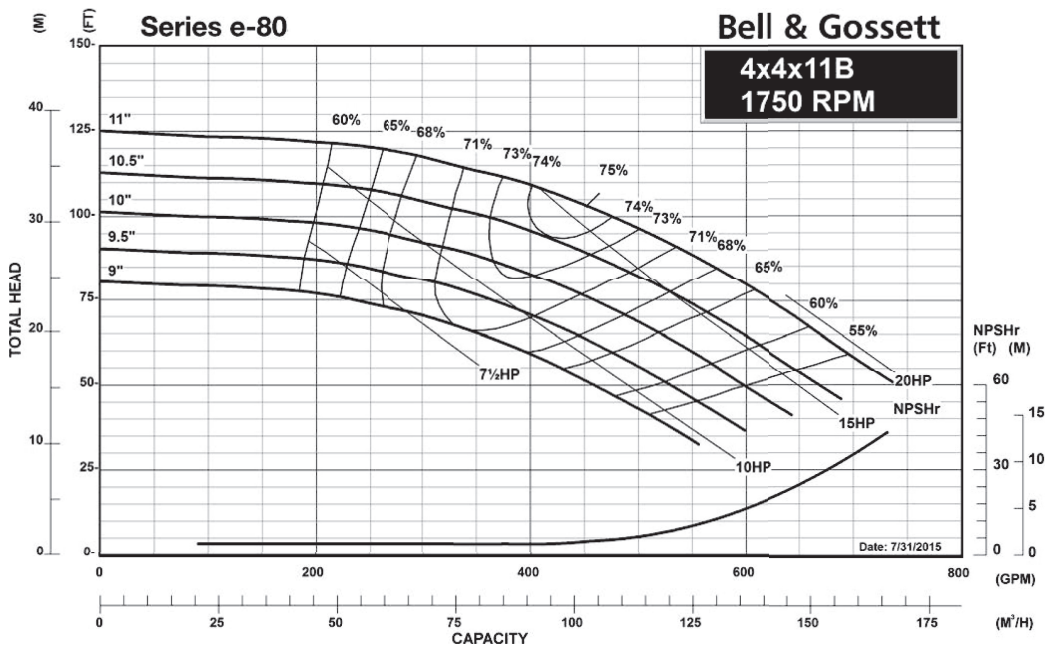
Series e-80

1800 RPM PUMP CURVES



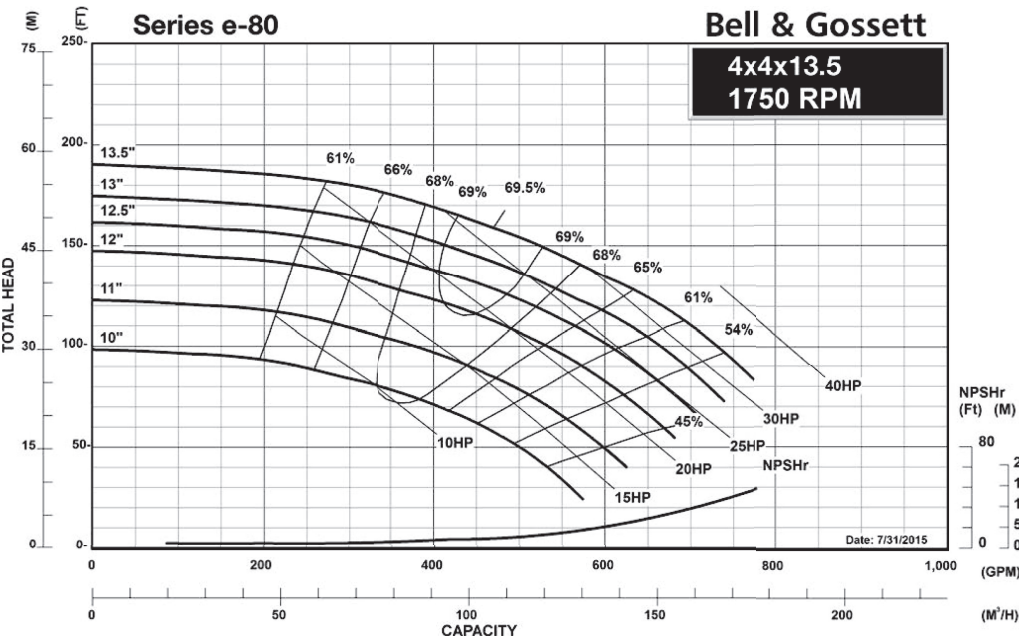
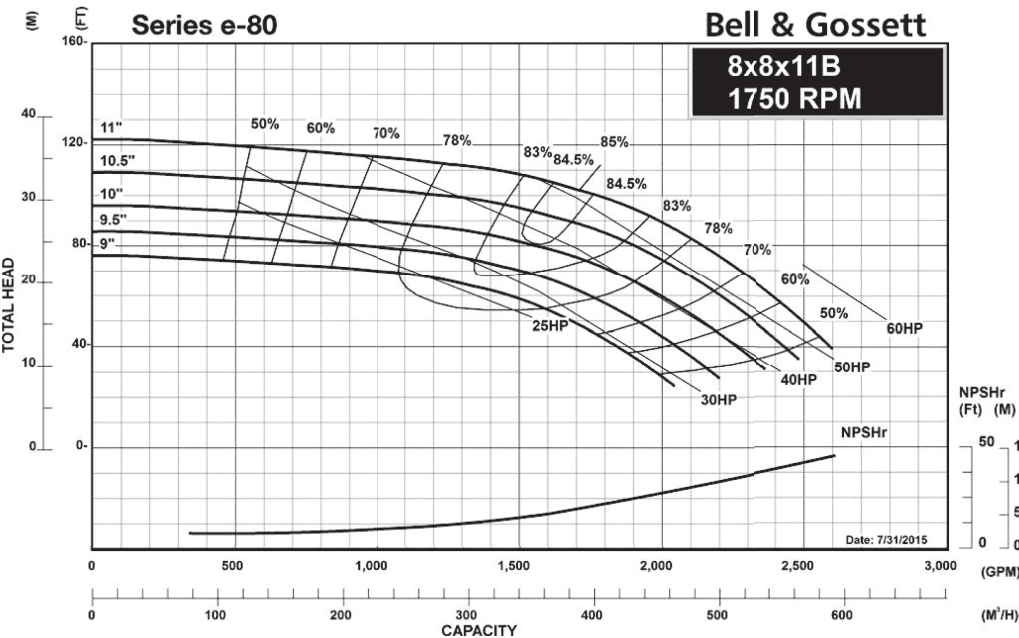
Series e-80

1800 RPM PUMP CURVES



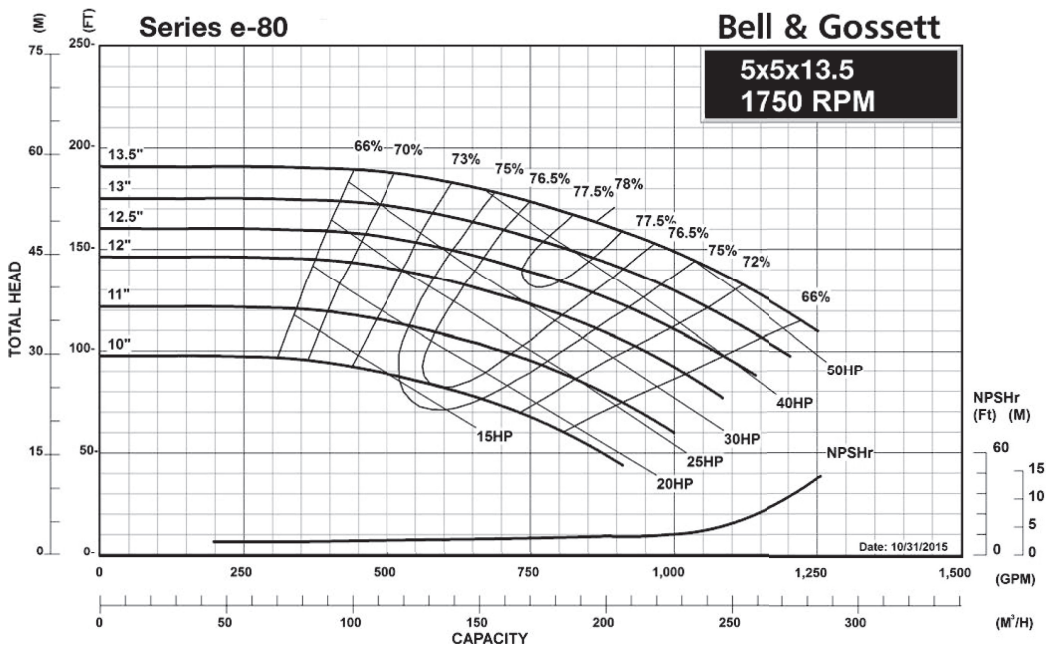
Series e-80

1800 RPM PUMP CURVES



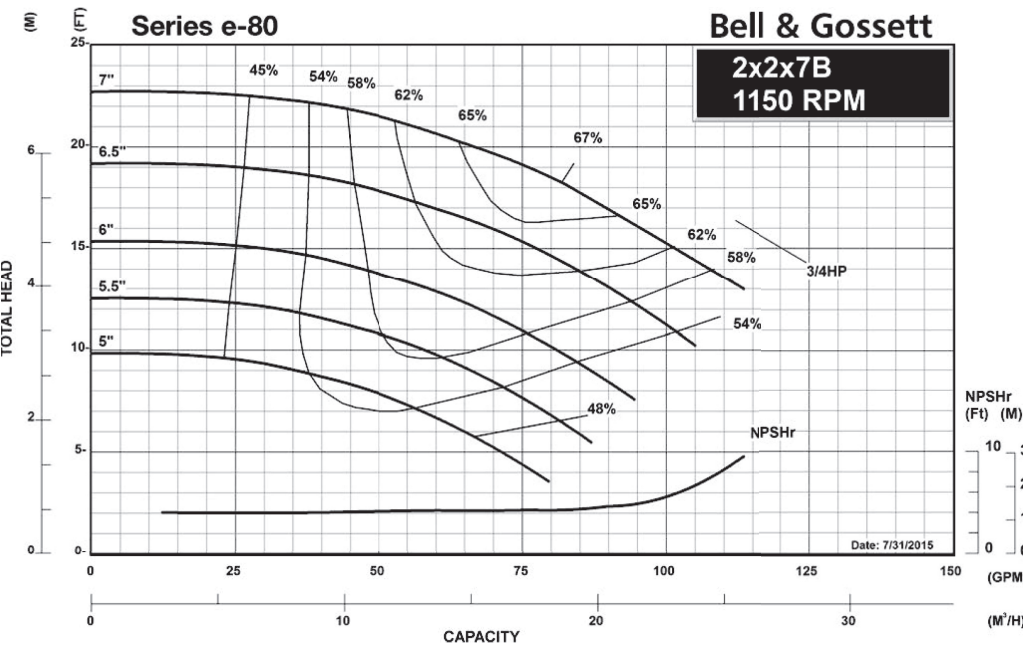
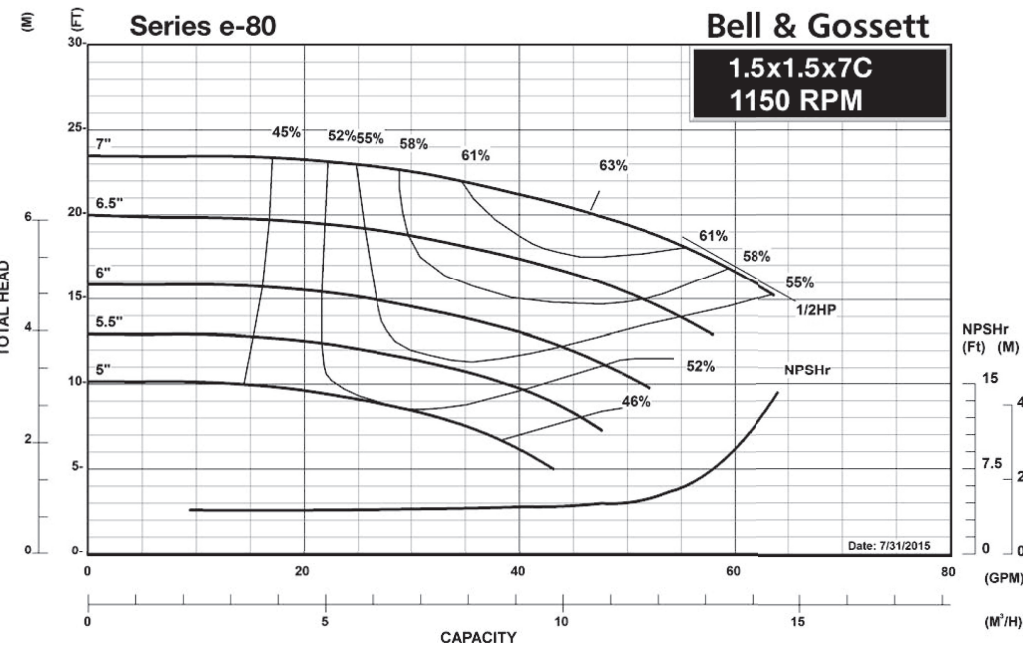
Series e-80

1800 RPM PUMP CURVES



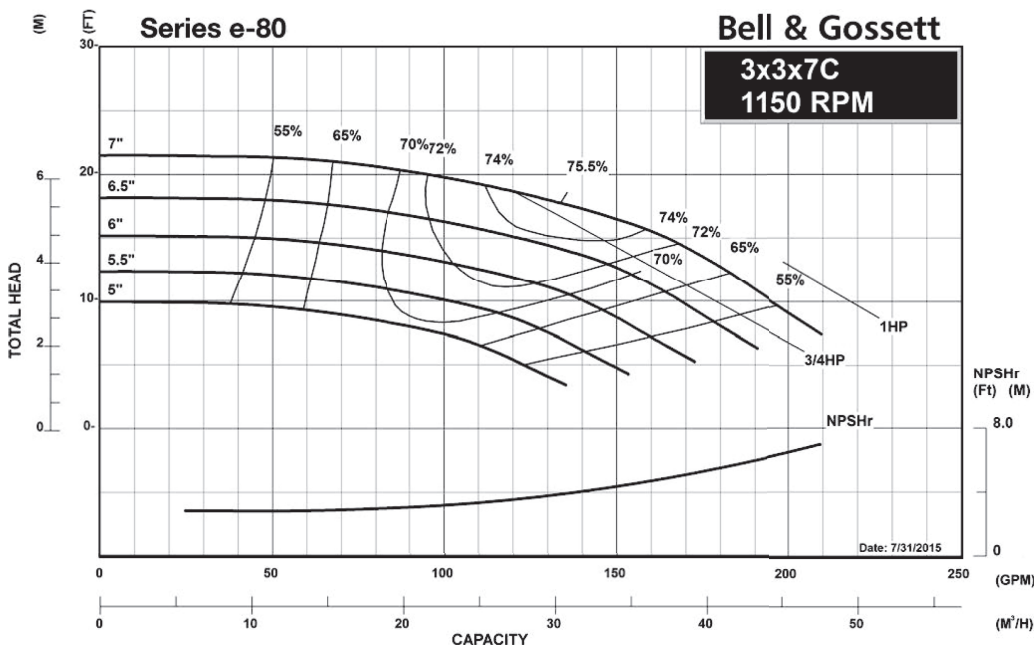
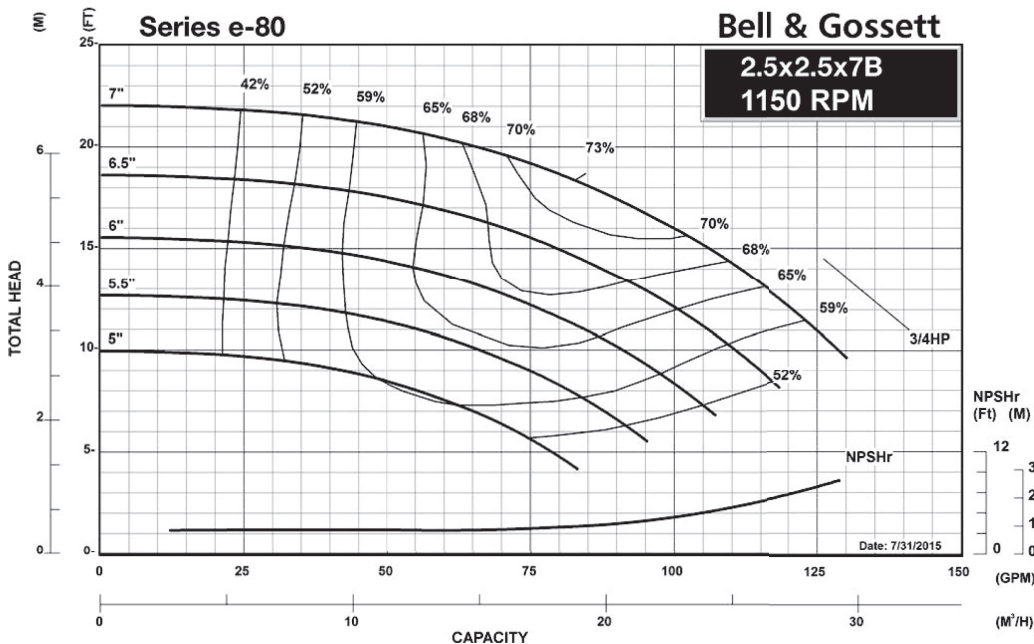
Series e-80

1200 RPM PUMP CURVES



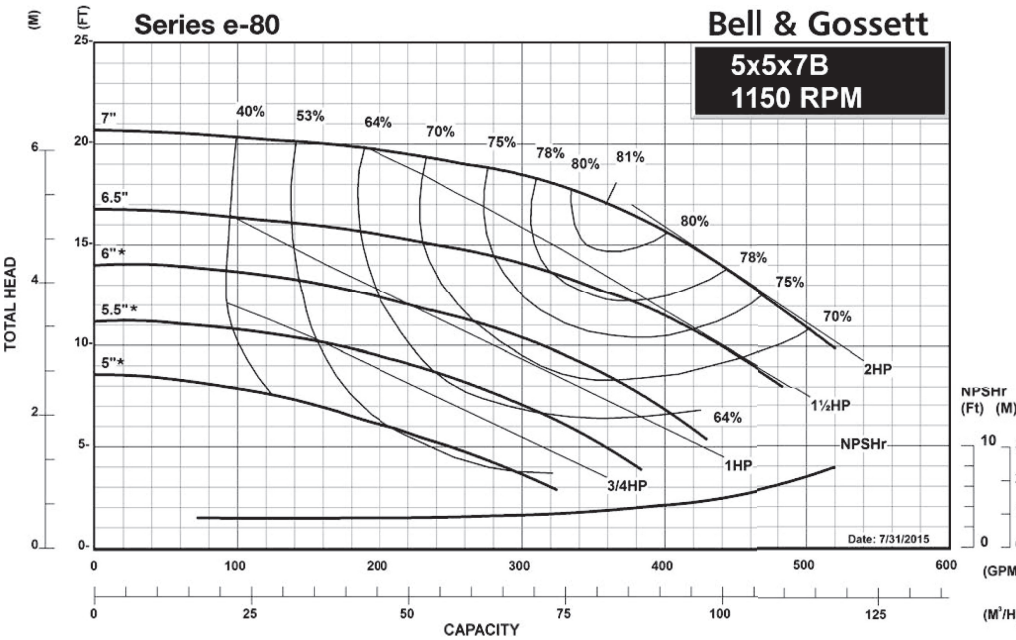
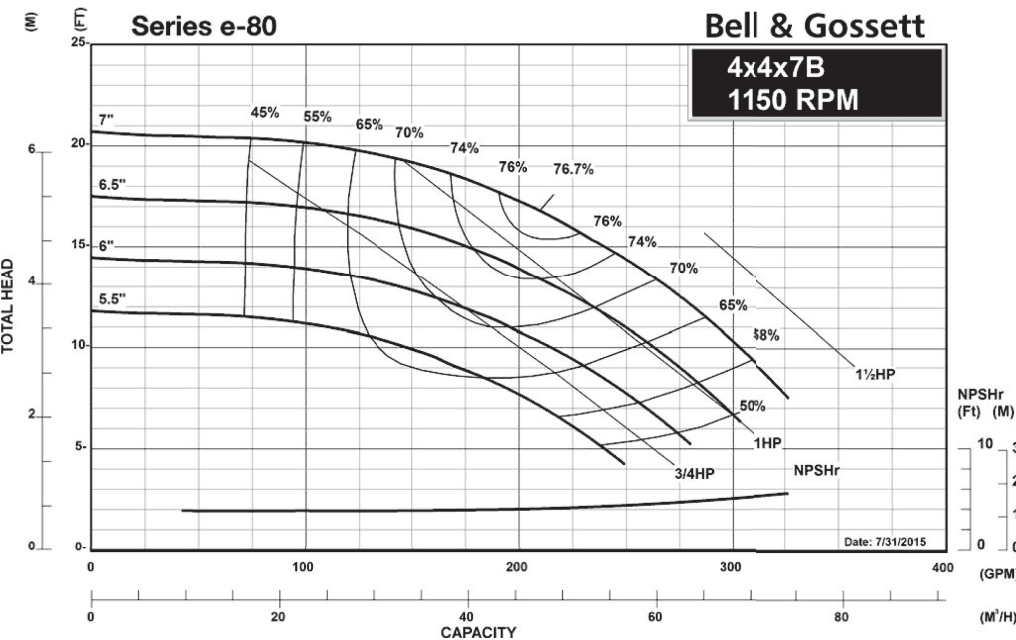
Series e-80

1200 RPM PUMP CURVES



Series e-80

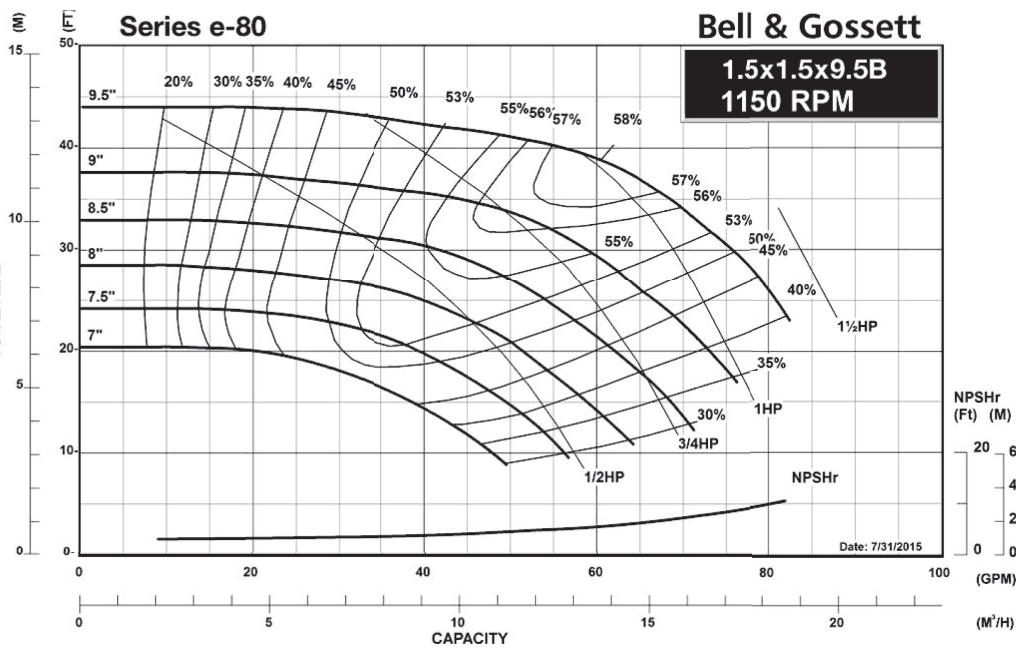
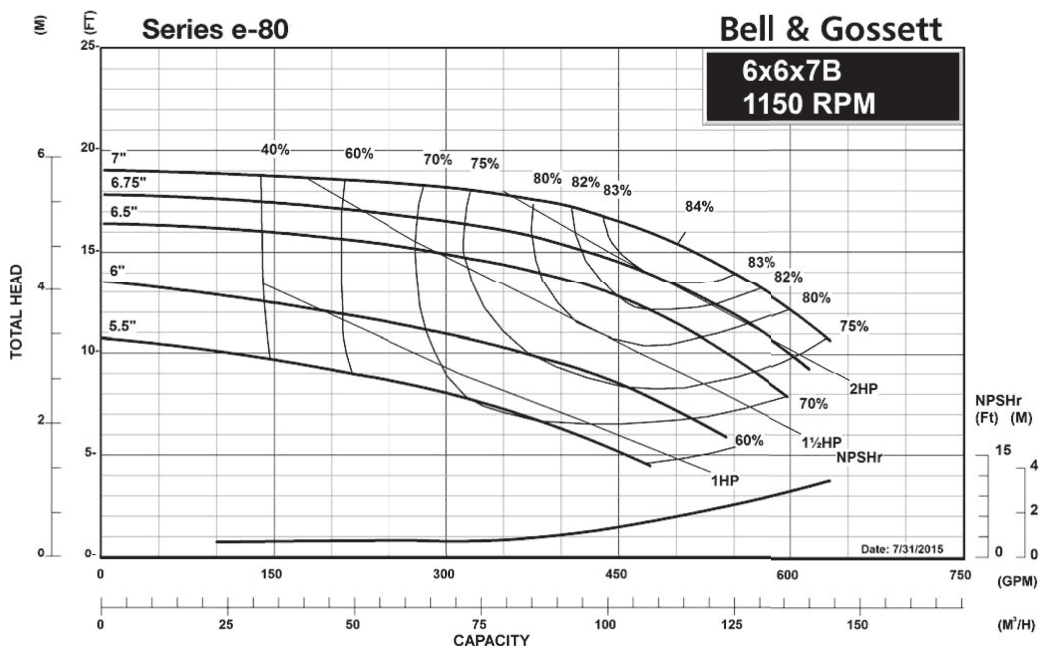
1200 RPM PUMP CURVES



*6" and below requires oversized diameter and angle trim. See manual.

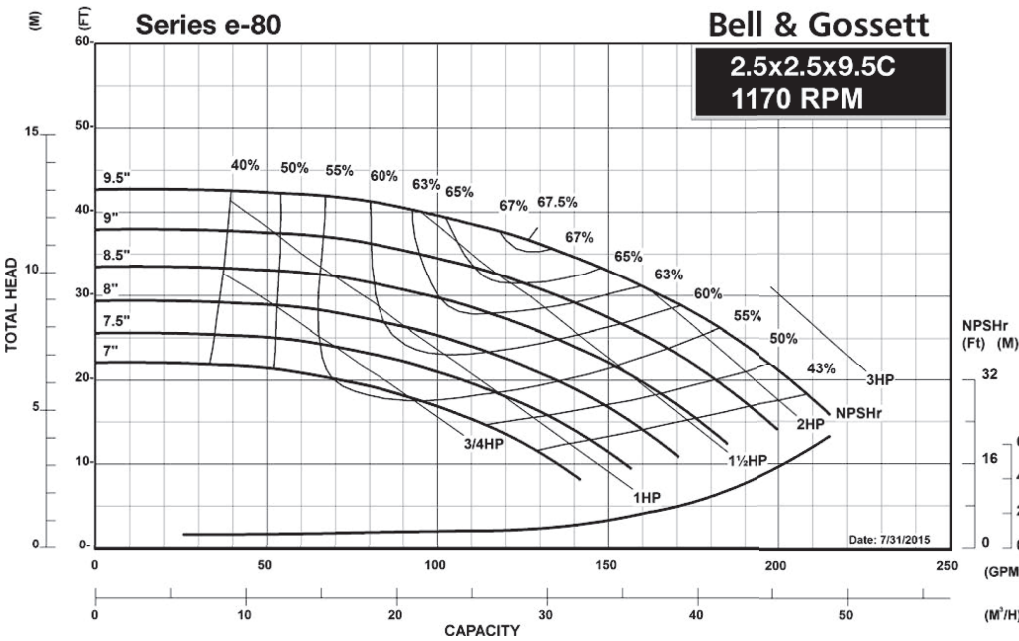
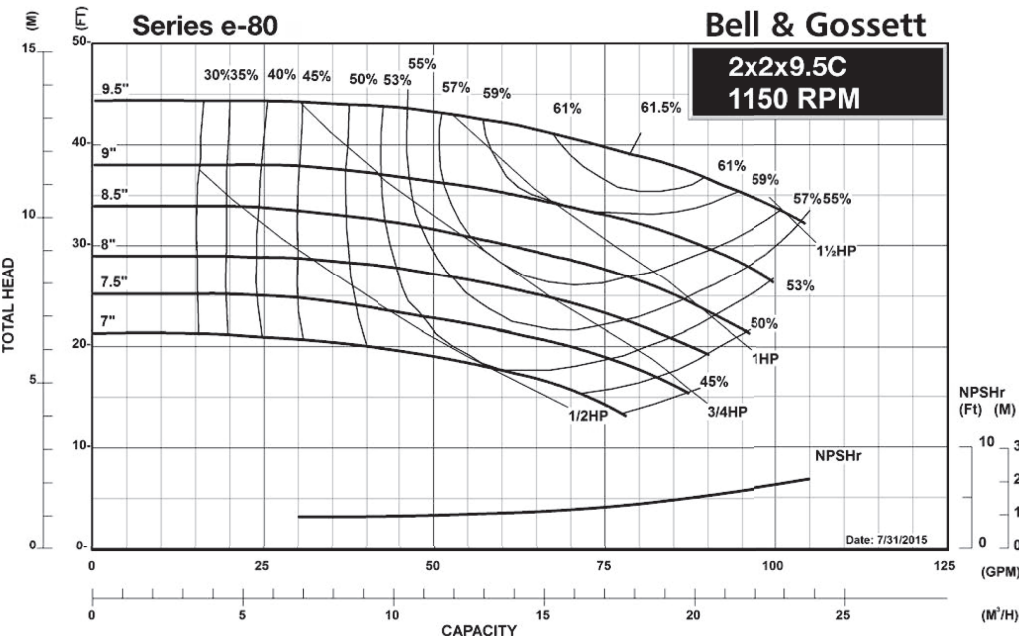
Series e-80

1200 RPM PUMP CURVES



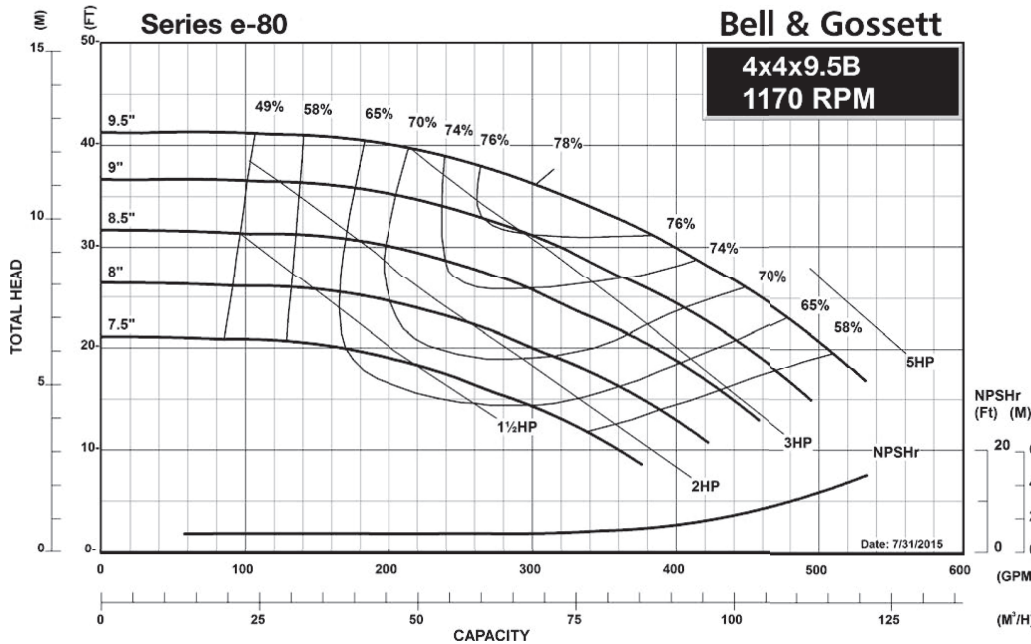
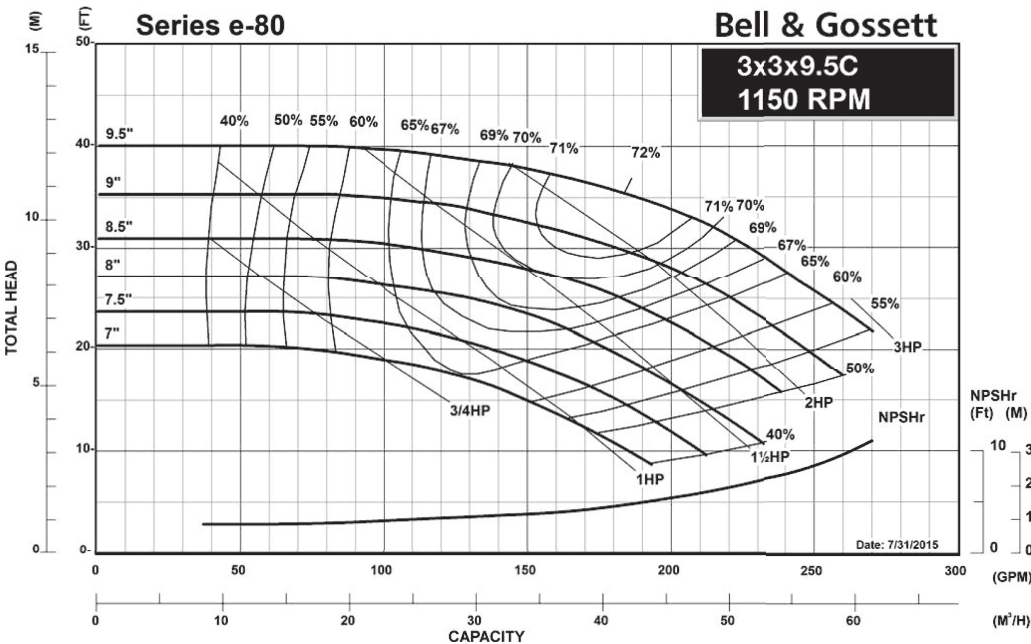
Series e-80

1200 RPM PUMP CURVES



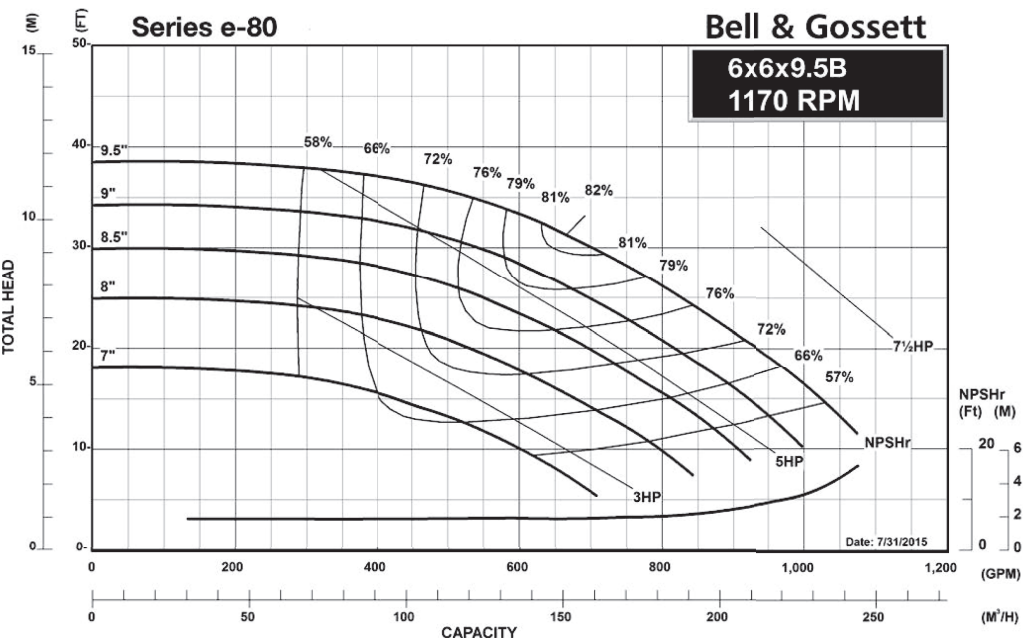
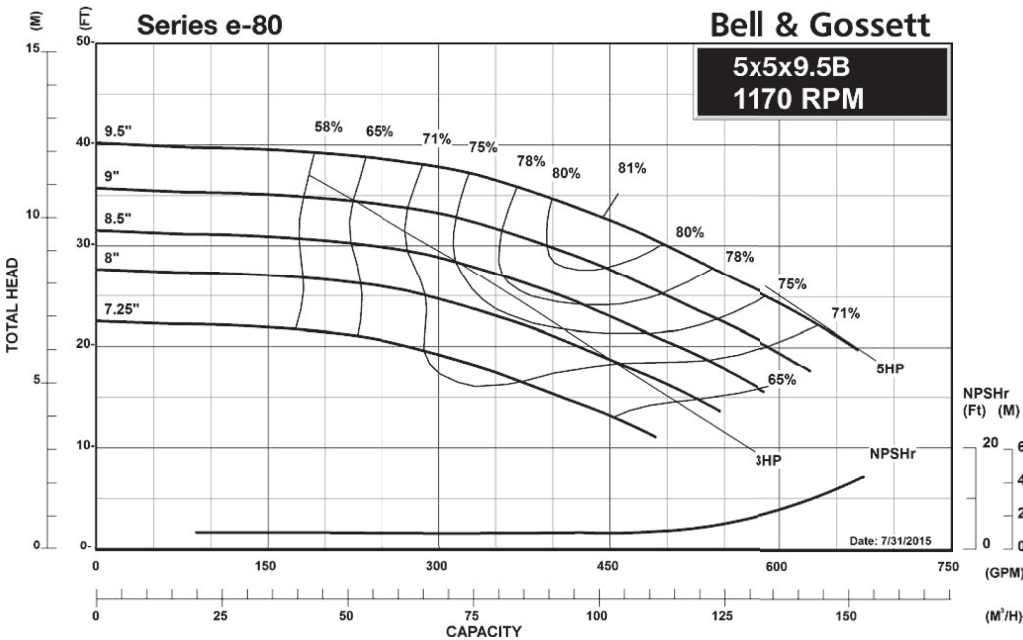
Series e-80

1200 RPM PUMP CURVES



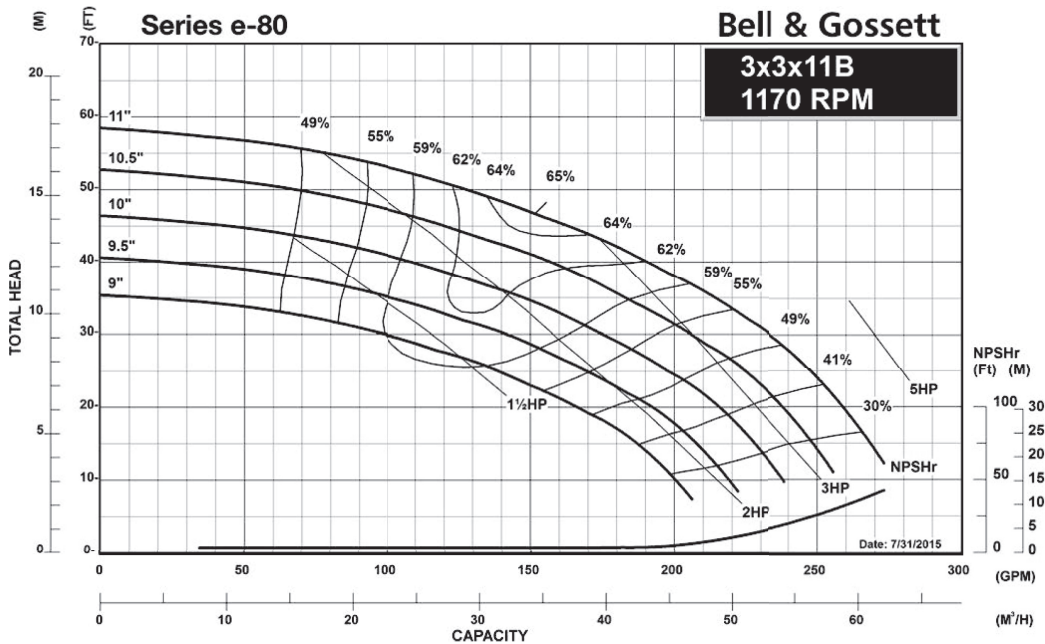
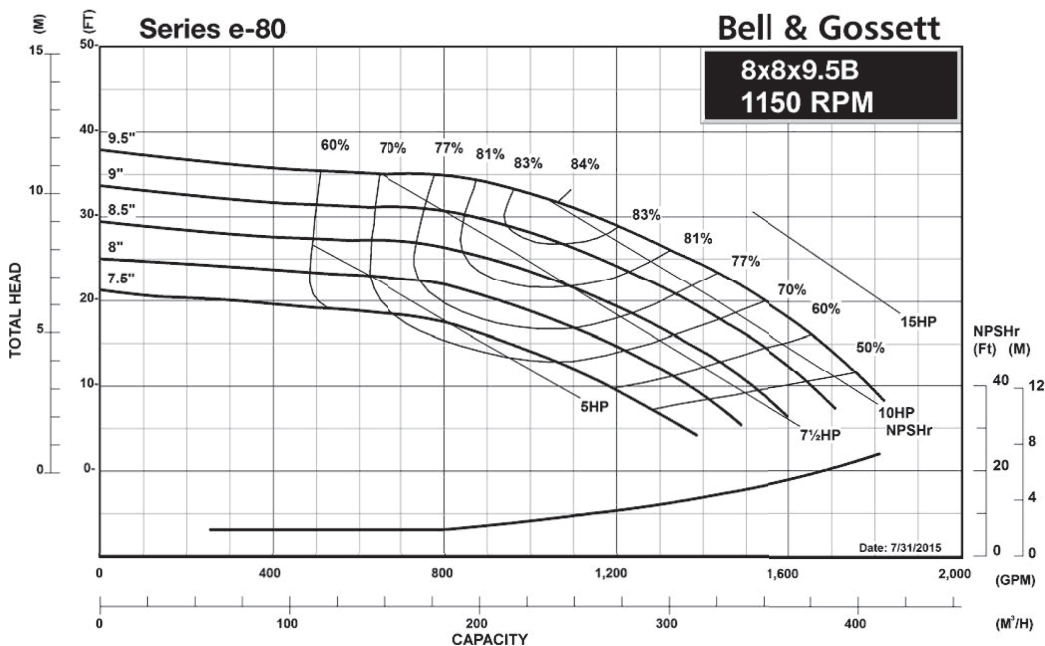
Series e-80

1200 RPM PUMP CURVES



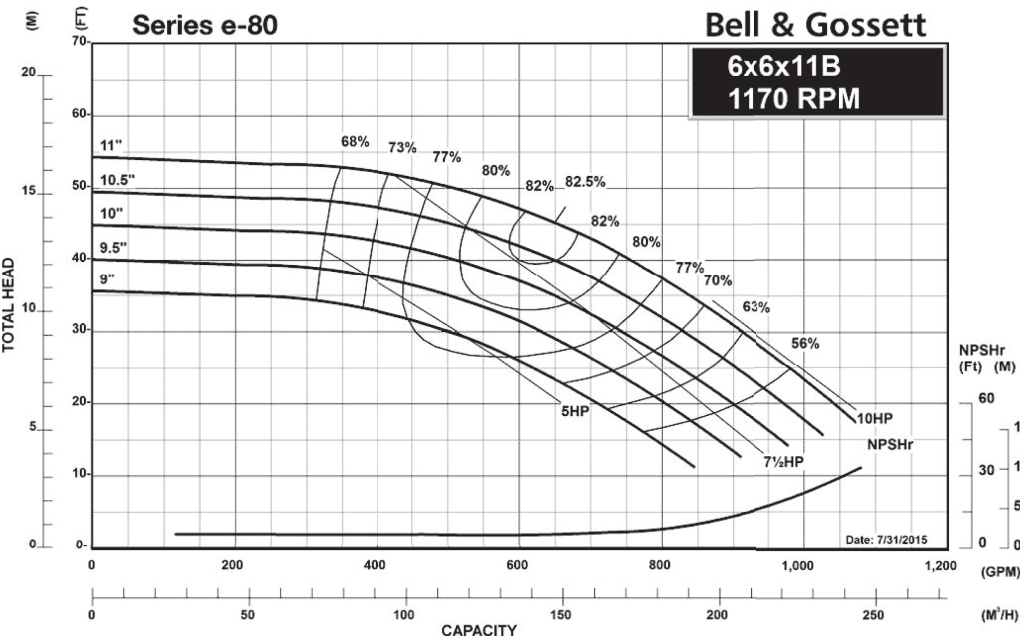
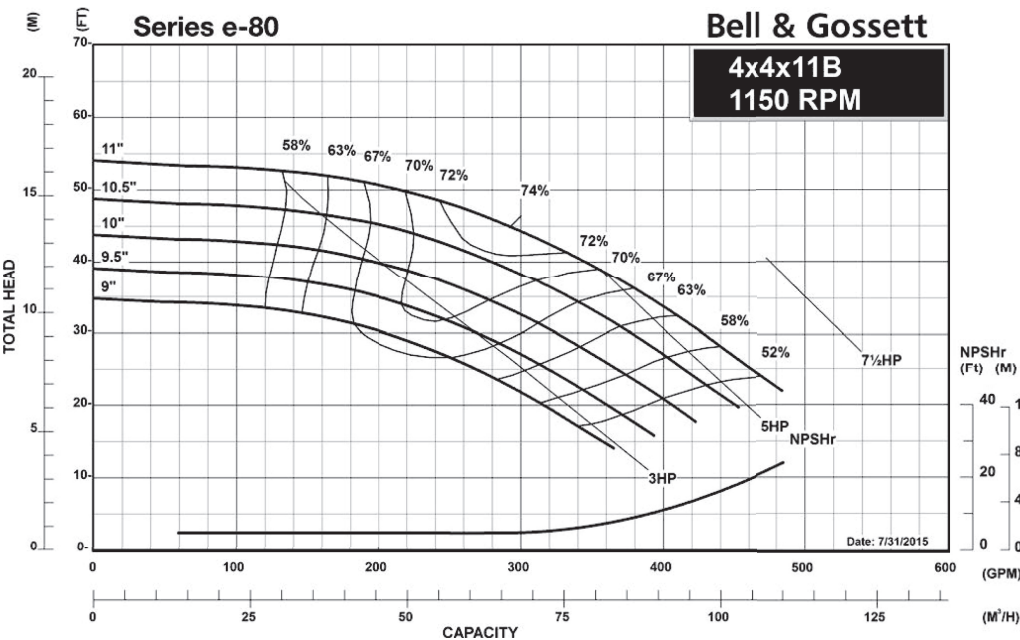
Series e-80

1200 RPM PUMP CURVES



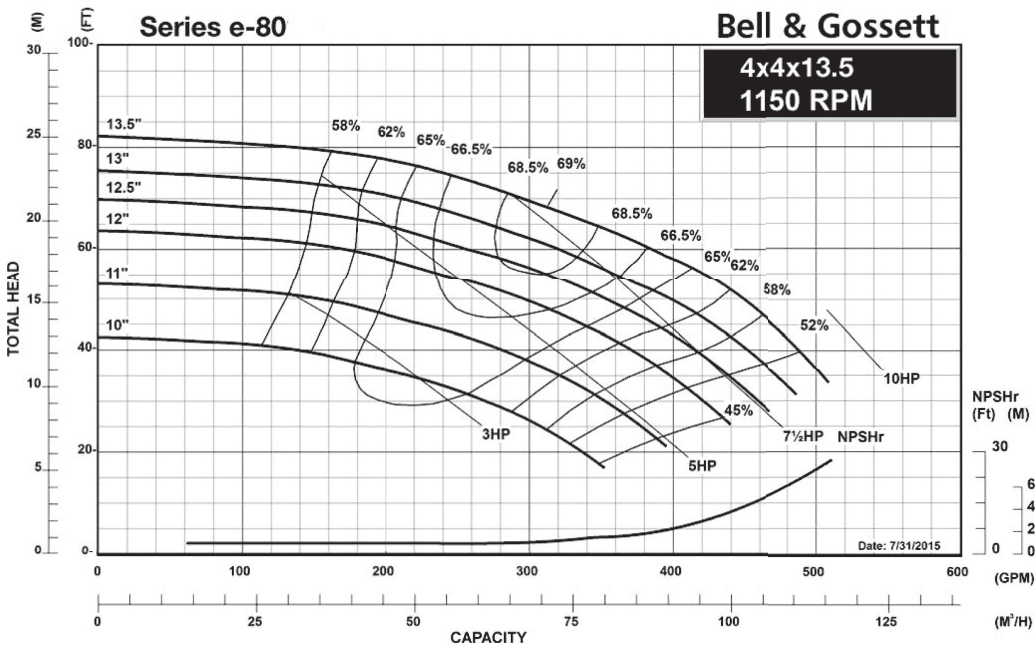
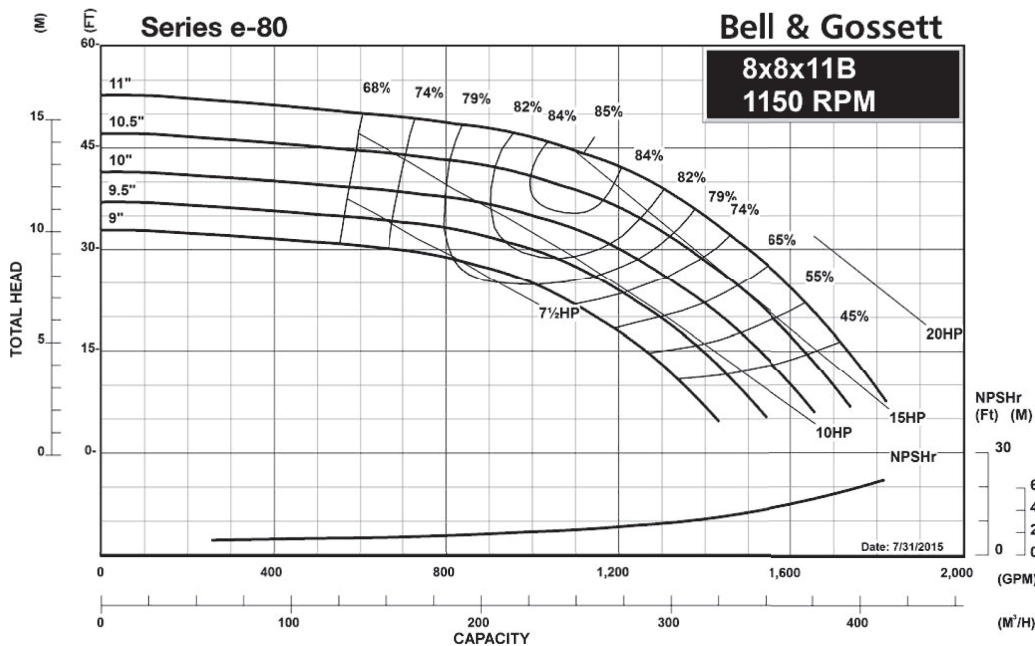
Series e-80

1200 RPM PUMP CURVES



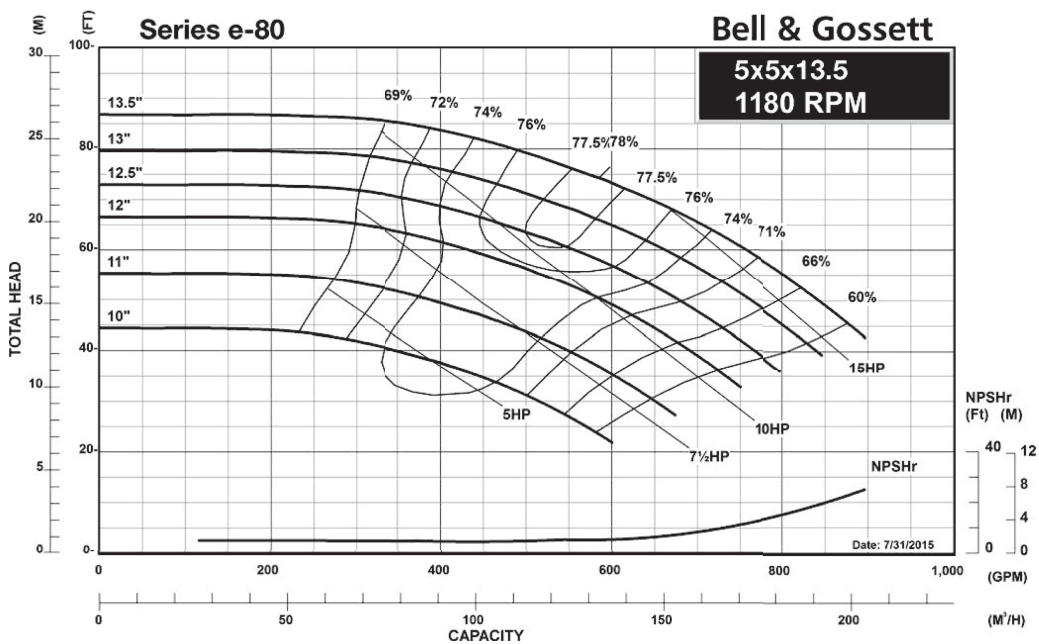
Series e-80

1200 RPM PUMP CURVES



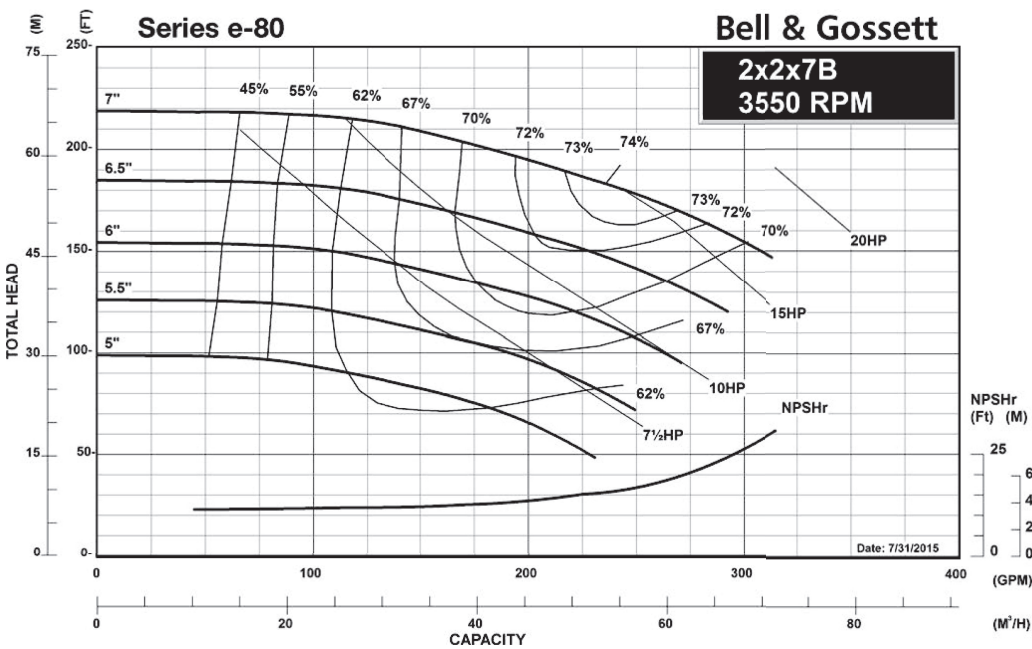
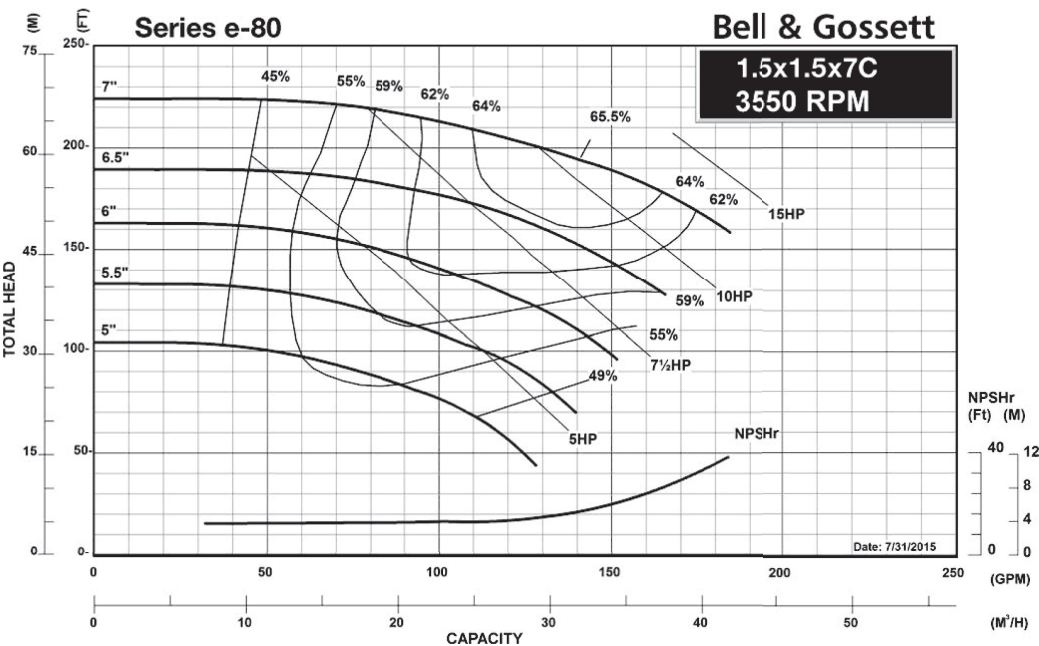
Series e-80

1200 RPM PUMP CURVES



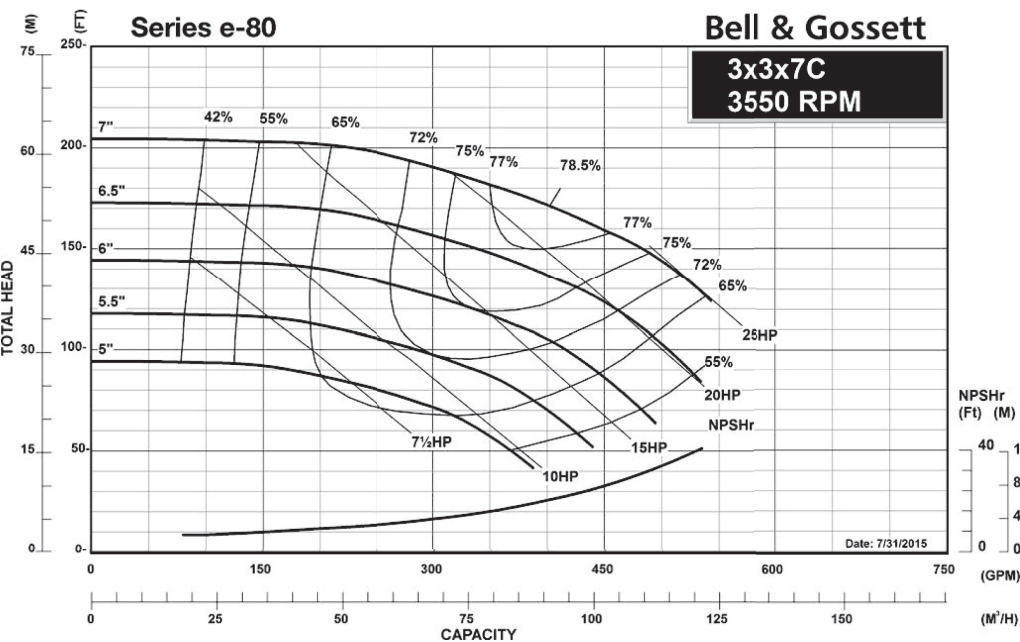
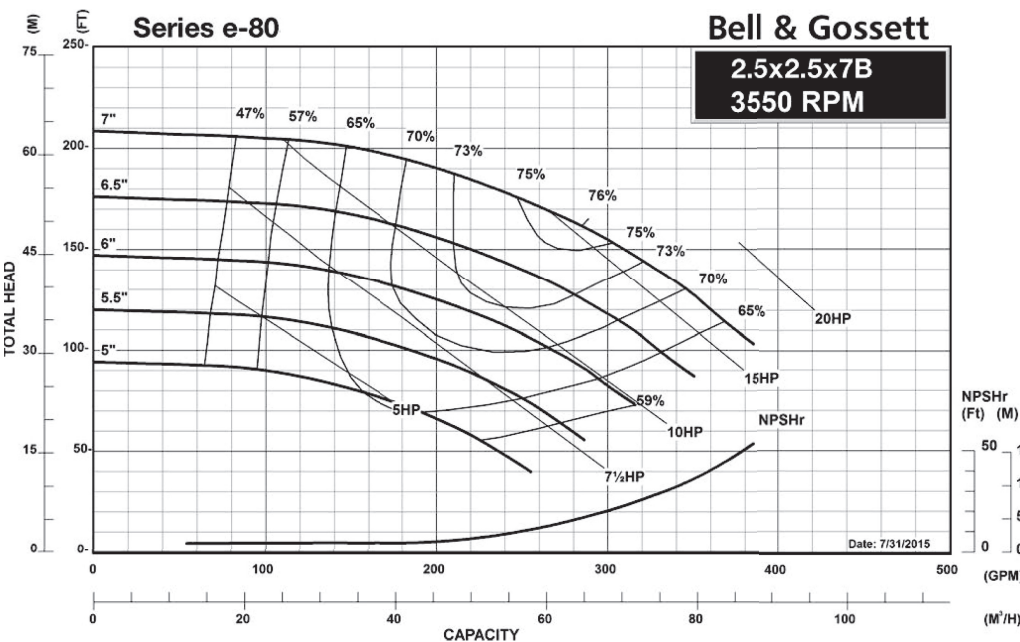
Series e-80

3600 RPM PUMP CURVES



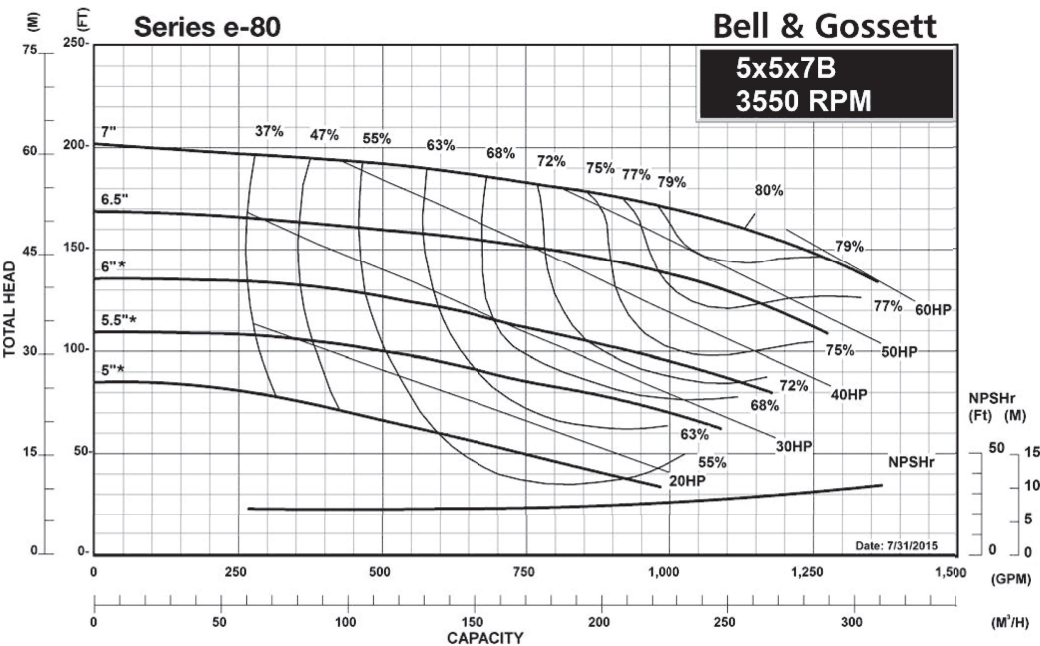
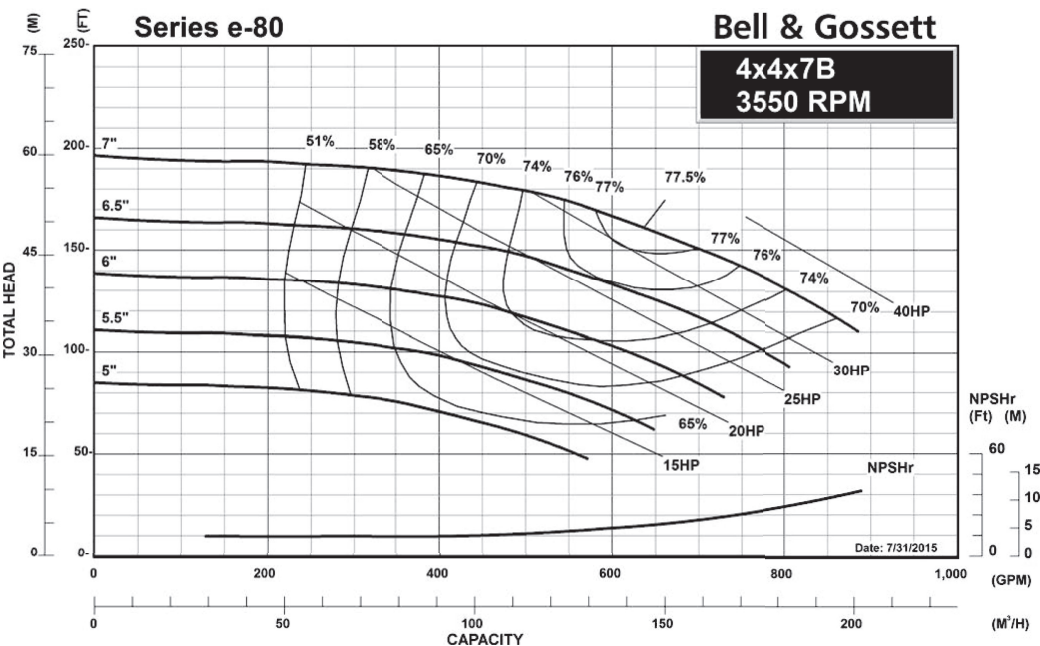
Series e-80

3600 RPM PUMP CURVES



Series e-80

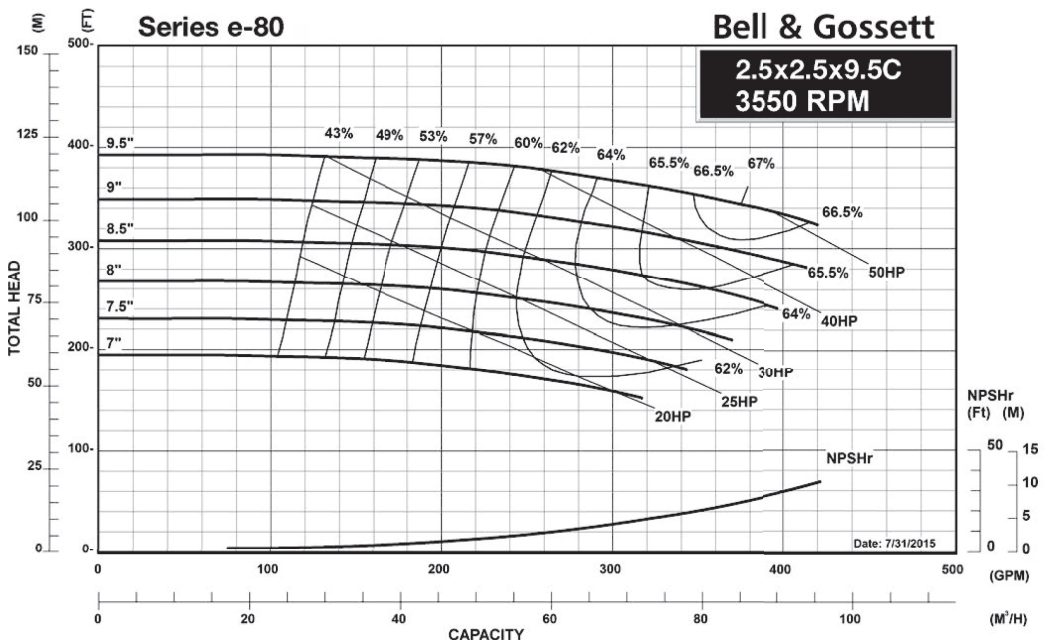
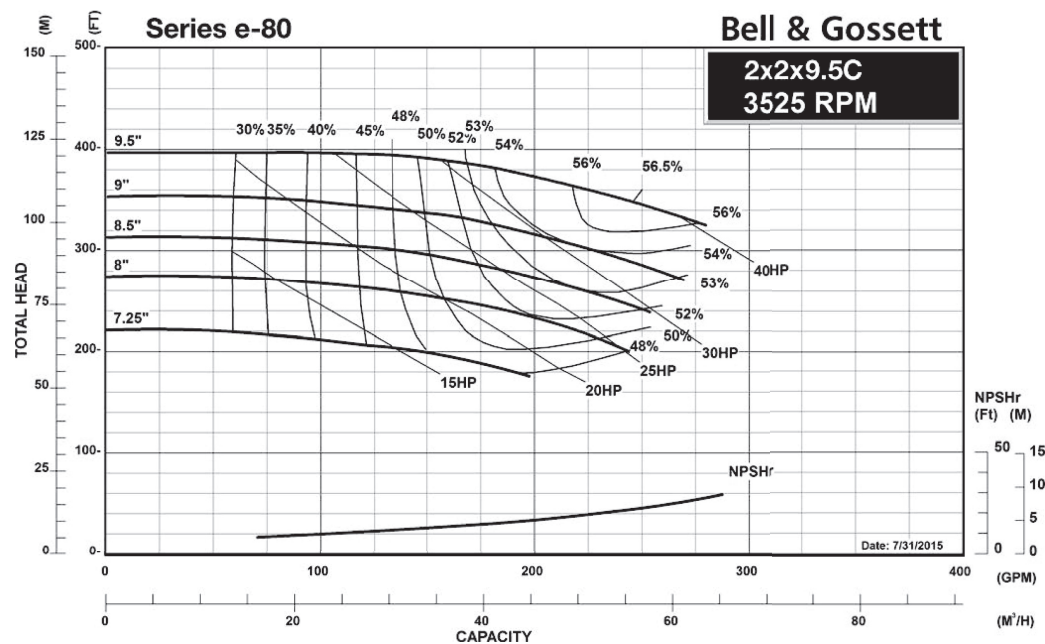
3600 RPM PUMP CURVES



*6" and below requires oversized diameter and angle trim. See manual.

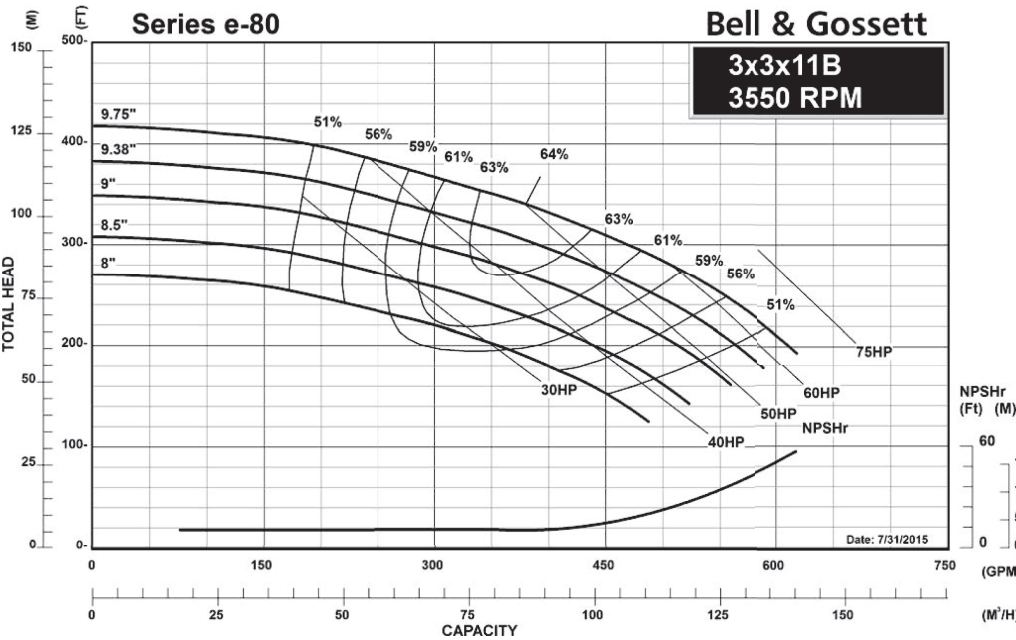
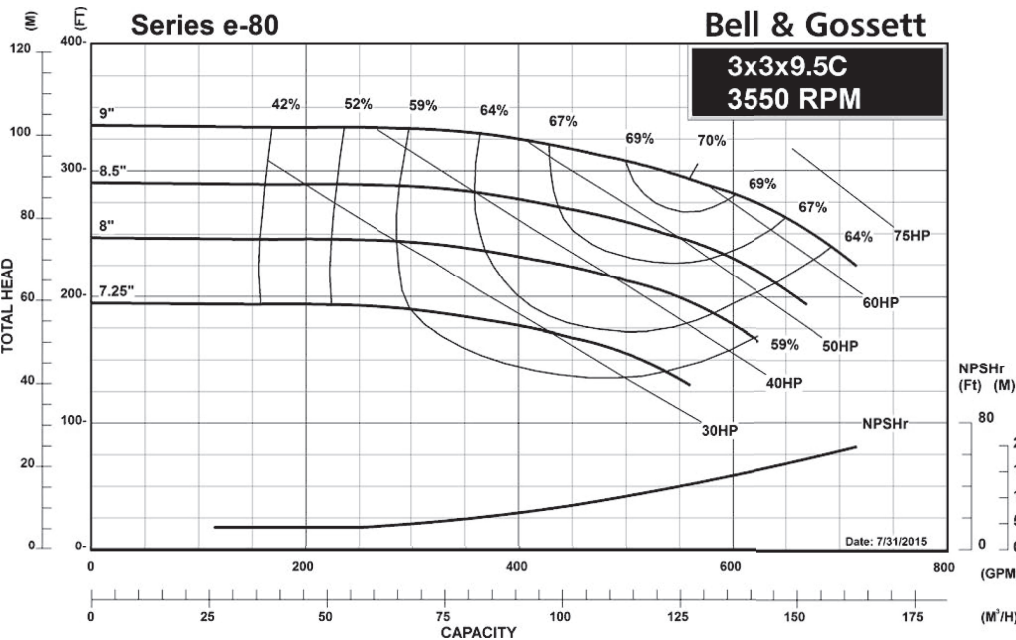
Series e-80

3600 RPM PUMP CURVES



Series e-80

3600 RPM PUMP CURVES



Xylem |'zīləm|

- 1) The tissue in plants that brings water upward from the roots;
- 2) a leading global water technology company.

We're a global team unified in a common purpose: creating innovative solutions to meet our world's water needs. Developing new technologies that will improve the way water is used, conserved, and re-used in the future is central to our work. We move, treat, analyze, and return water to the environment, and we help people use water efficiently, in their homes, buildings, factories and farms. In more than 150 countries, we have strong, long-standing relationships with customers who know us for our powerful combination of leading product brands and applications expertise, backed by a legacy of innovation.

For more information on how Xylem can help you, go to www.xyleminc.com



Xylem Inc.
8200 N. Austin Avenue
Morton Grove, Illinois 60053
Phone: (847) 966-3700
Fax: (847) 965-8379
www.bellgossett.com

Bell & Gossett is a trademark of Xylem Inc. or one of its subsidiaries.
© 2016 Xylem Inc. B-193B June 2016

CURVES
B-263A



Series e-1531

CLOSED COUPLED CENTRIFUGAL PUMP PERFORMANCE CURVES – 60 HZ

 **Bell & Gossett**
a xylem brand

Series e-1531 – Table of Contents

Useful Pump Formulas 2

Selection Charts 3

1800 RPM PUMP CURVES

A - Size Curves 4

B - Size Curves 8

1200 RPM PUMP CURVES

A - Size Curves 12

B - Size Curves 16

3600 RPM PUMP CURVES

A - Size Curves 20

B - Size Curves 24

USEFUL PUMP FORMULAS

Pressure (PSI) = $\frac{\text{Head (Feet)} \times \text{Specific Gravity}}{2.31}$

Head (Feet) = $\frac{\text{Pressure (PSI)} \times 2.31}{\text{Specific Gravity}}$

Vacuum (Inches of Mercury) = $\frac{\text{Dynamic Suction Lift (Feet)} \times .883}{\text{Specific Gravity}}$

Horsepower (Brake) = $\frac{\text{GPM} \times \text{Head (Feet)} \times \text{Specific Gravity}}{3960 \times \text{Pump Efficiency}}$

Horsepower (Water) = $\frac{\text{GPM} \times \text{Head (Feet)} \times \text{Specific Gravity}}{3960}$

Efficiency (Pump) = $\frac{\text{Horsepower (Water)}}{\text{Horsepower (Brake)}} \times 100 \text{ Per Cent}$

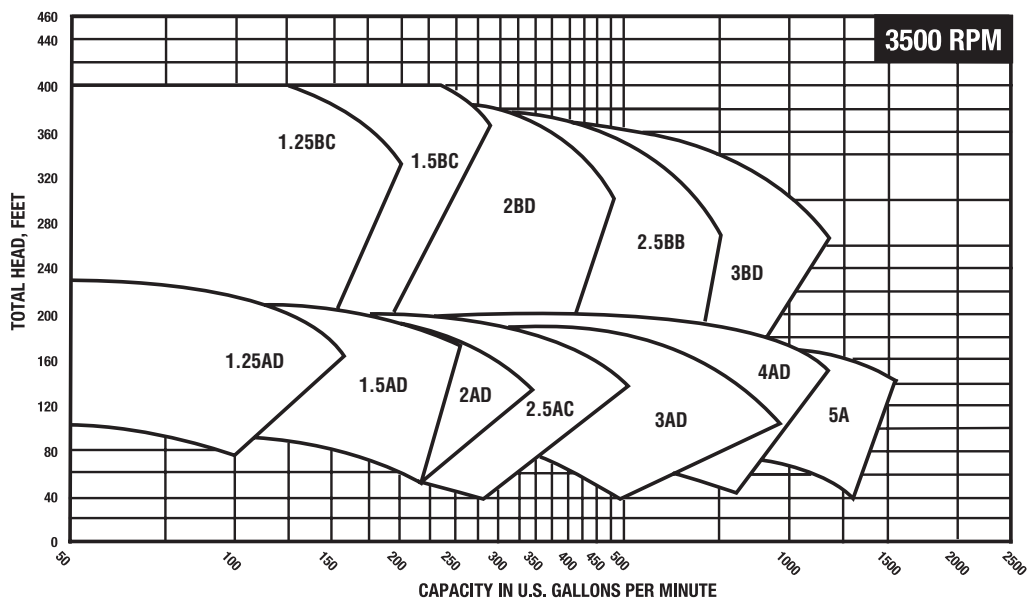
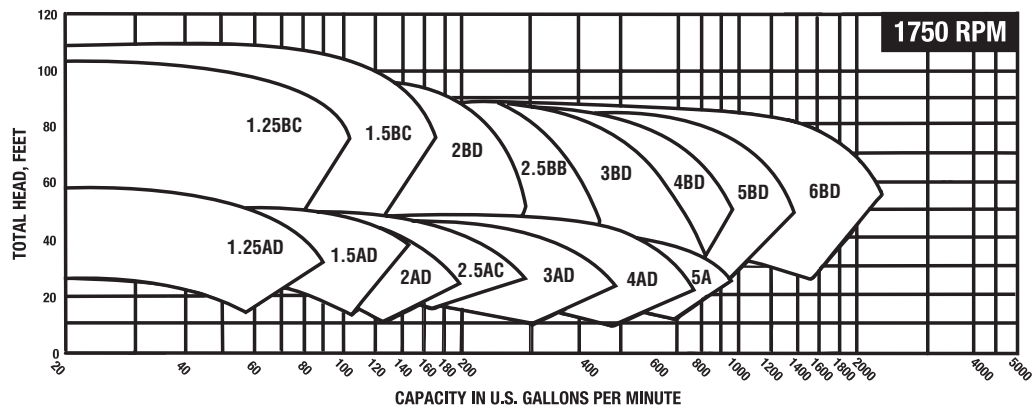
NPSH (Available) = Positive Factors – Negative Factors

Affinity Laws: Effect of change of speed or impeller diameter on centrifugal pumps.

	GPM Capacity	Ft. Head	BHP
Impeller Diameter Change	$Q_2 = \frac{D_2}{D_1} Q_1$	$H_2 = \left(\frac{D_2}{D_1}\right)^2 H_1$	$P_2 = \left(\frac{D_2}{D_1}\right)^3 P_1$
Speed Change	$Q_2 = \frac{RPM_2}{RPM_1} Q_1$	$H_2 = \left(\frac{RPM_2}{RPM_1}\right)^2 H_1$	$P_2 = \left(\frac{RPM_2}{RPM_1}\right)^3 P_1$

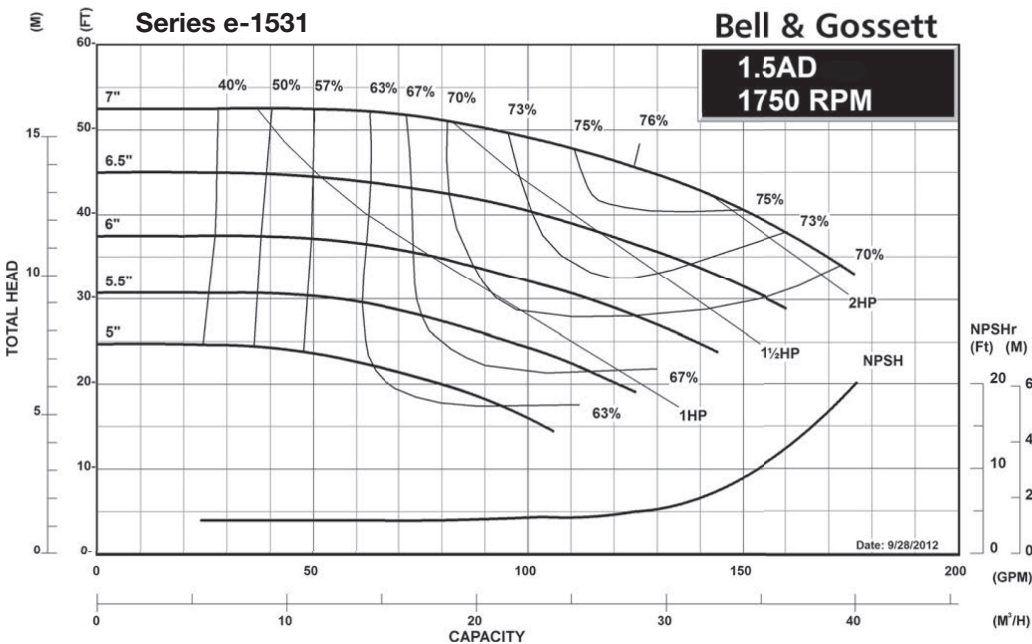
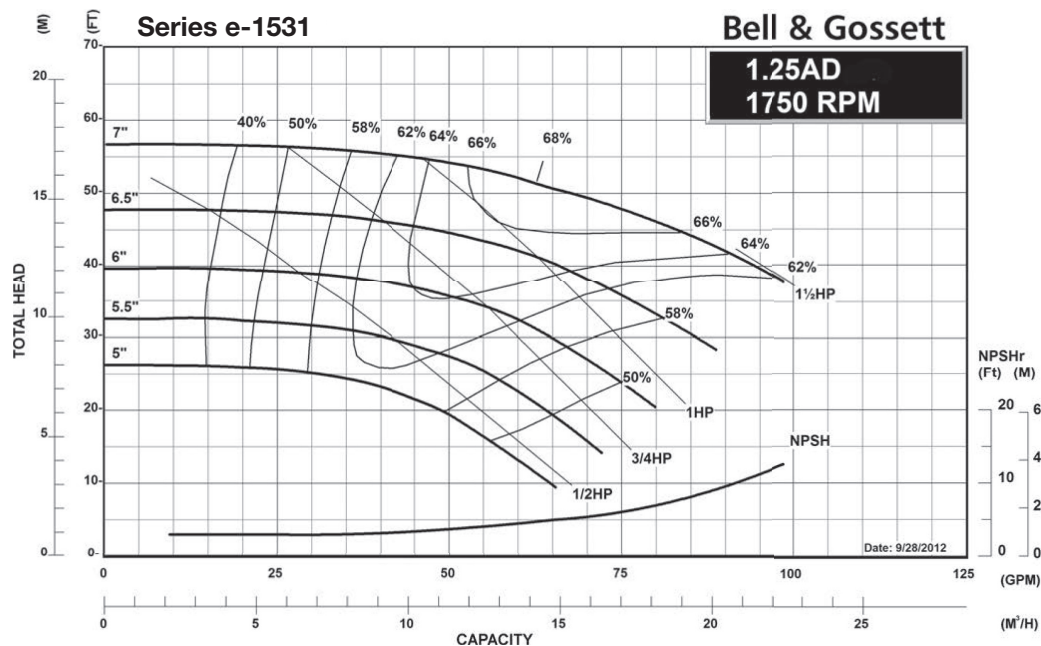
Where Q = GPM, H = Head, P = BHP, D = Impeller Dia., RPM = Pump Speed

Series e-1531 Selection Charts



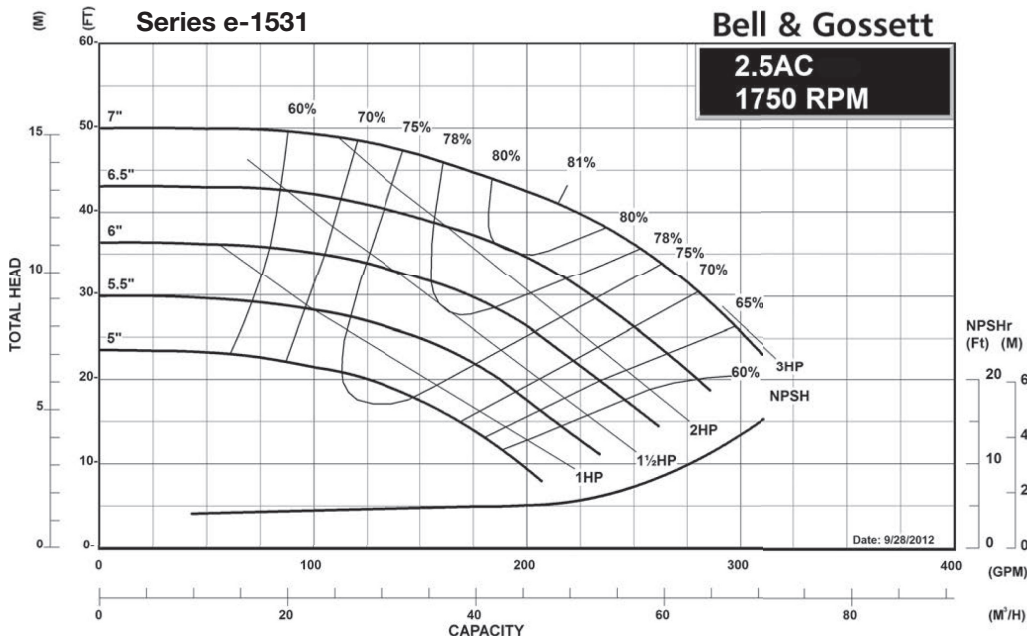
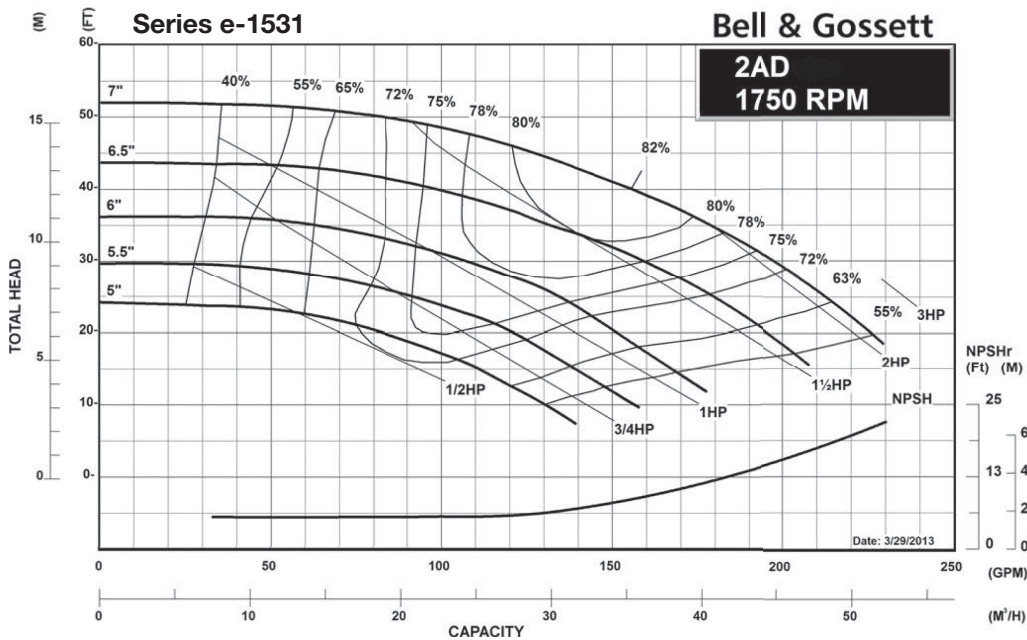
SERIES e-1531

1800 RPM SYNCHRONOUS SPEED



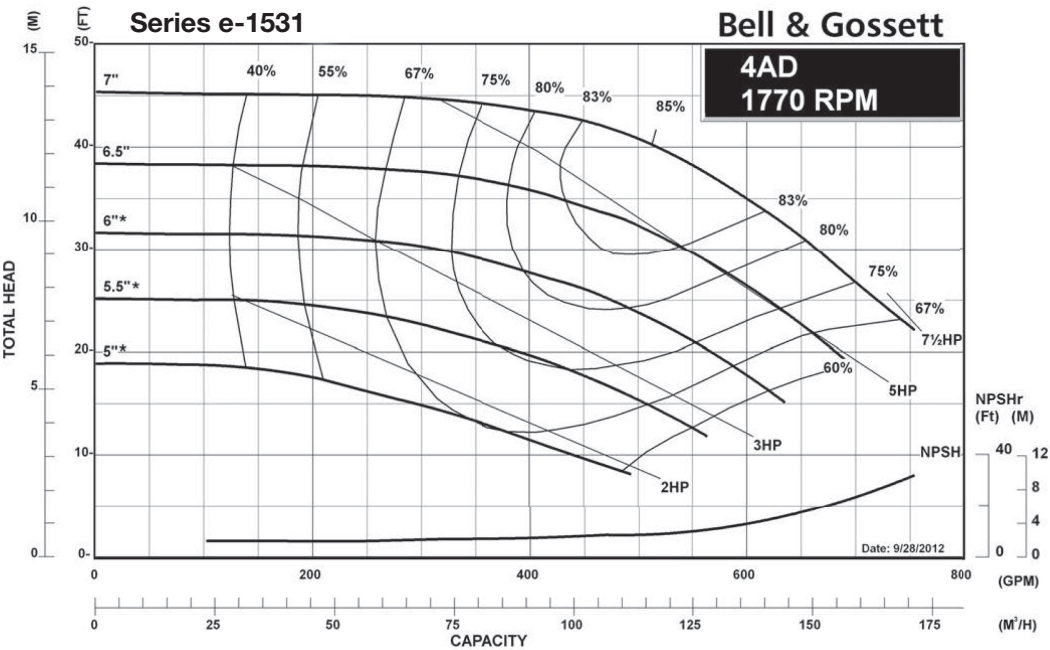
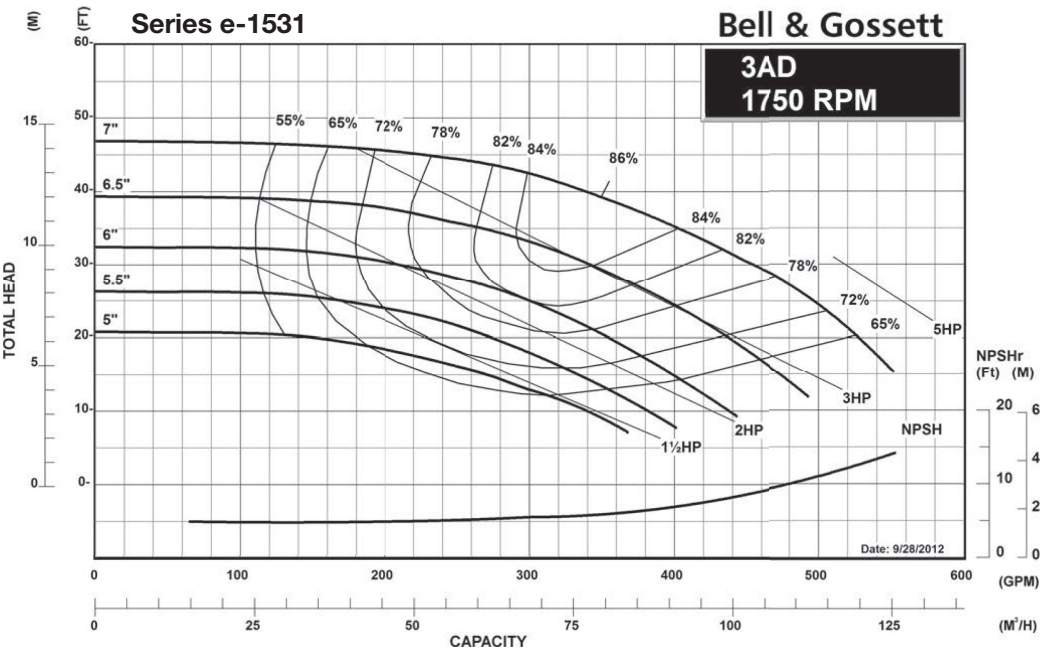
SERIES e-1531

1800 RPM SYNCHRONOUS SPEED



SERIES e-1531

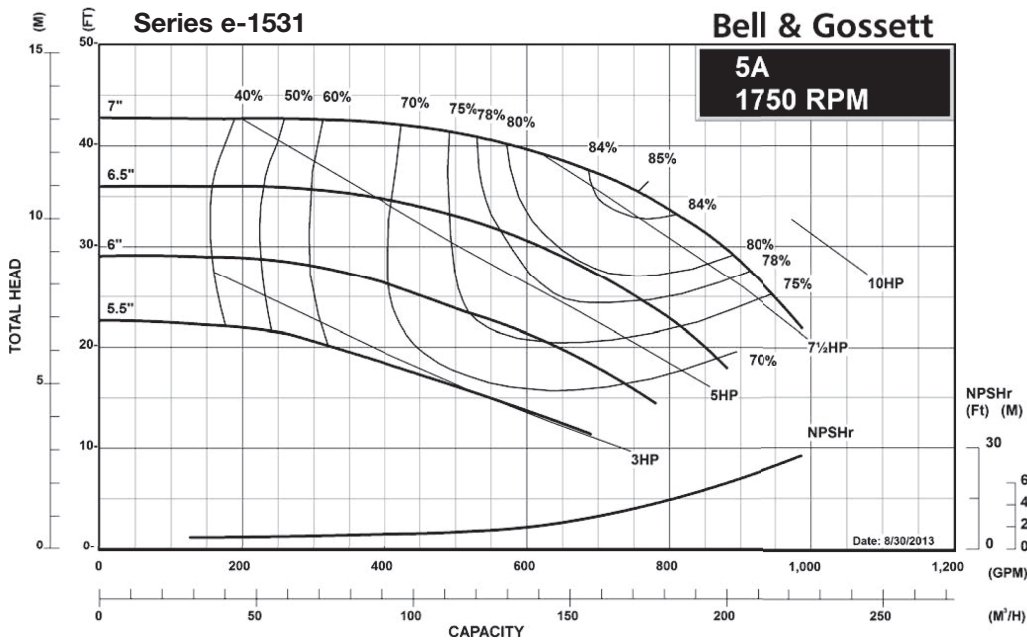
1800 RPM SYNCHRONOUS SPEED



* 6" and below requires oversized diameter and angle trim. See manual.

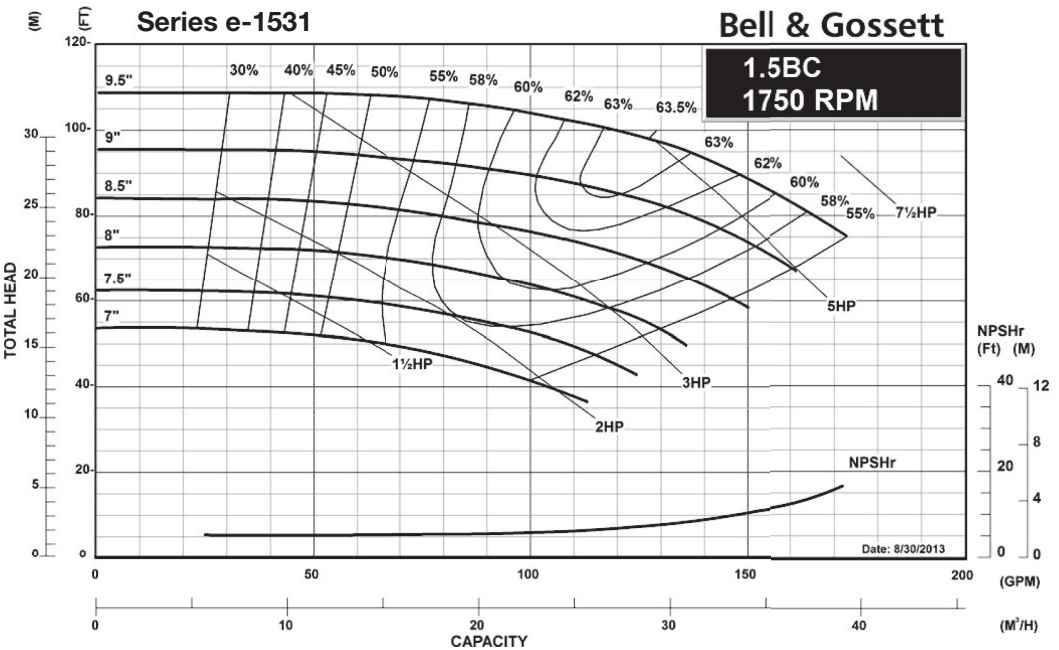
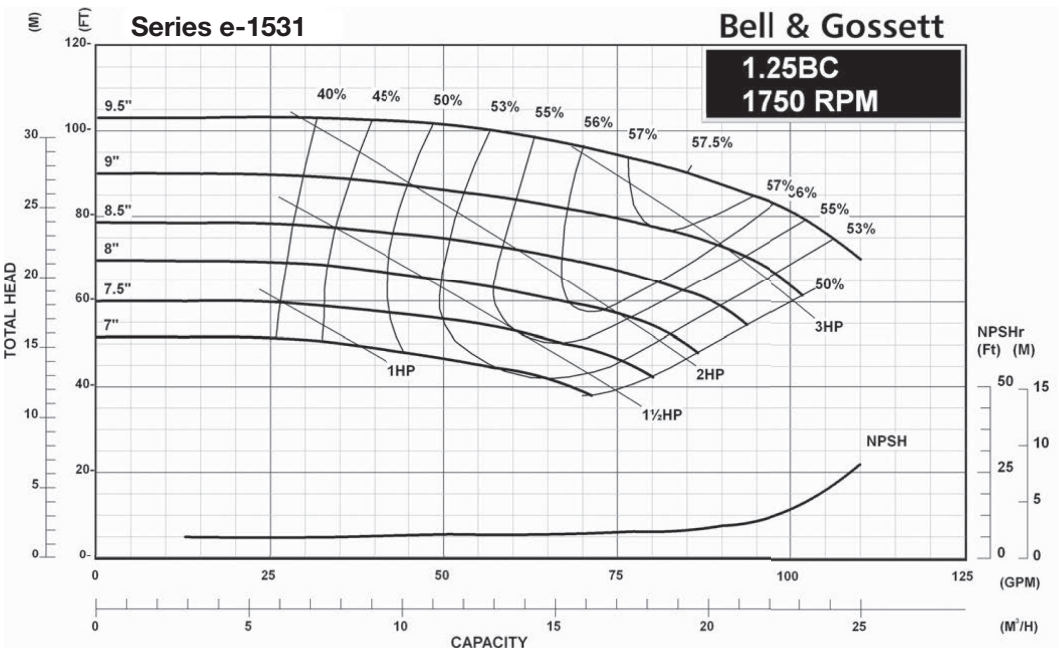
SERIES e-1531

1800 RPM SYNCHRONOUS SPEED



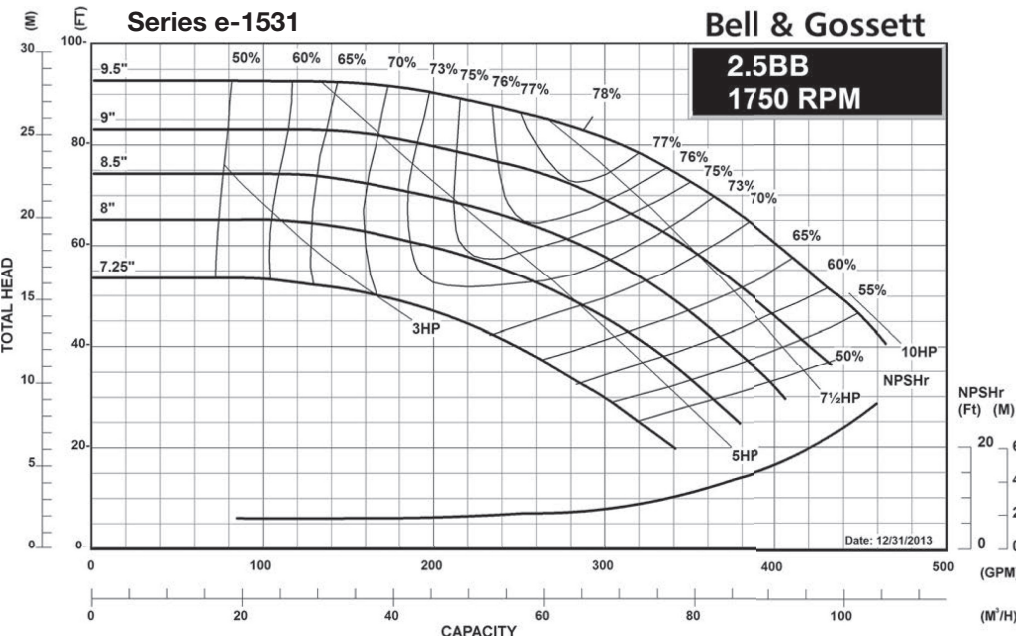
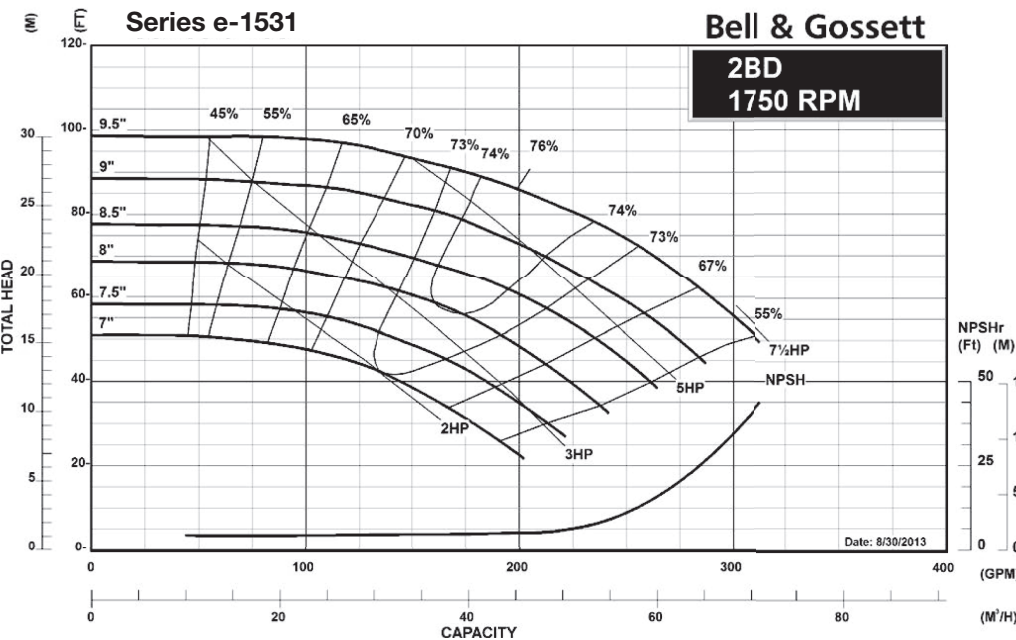
SERIES e-1531

1800 RPM SYNCHRONOUS SPEED



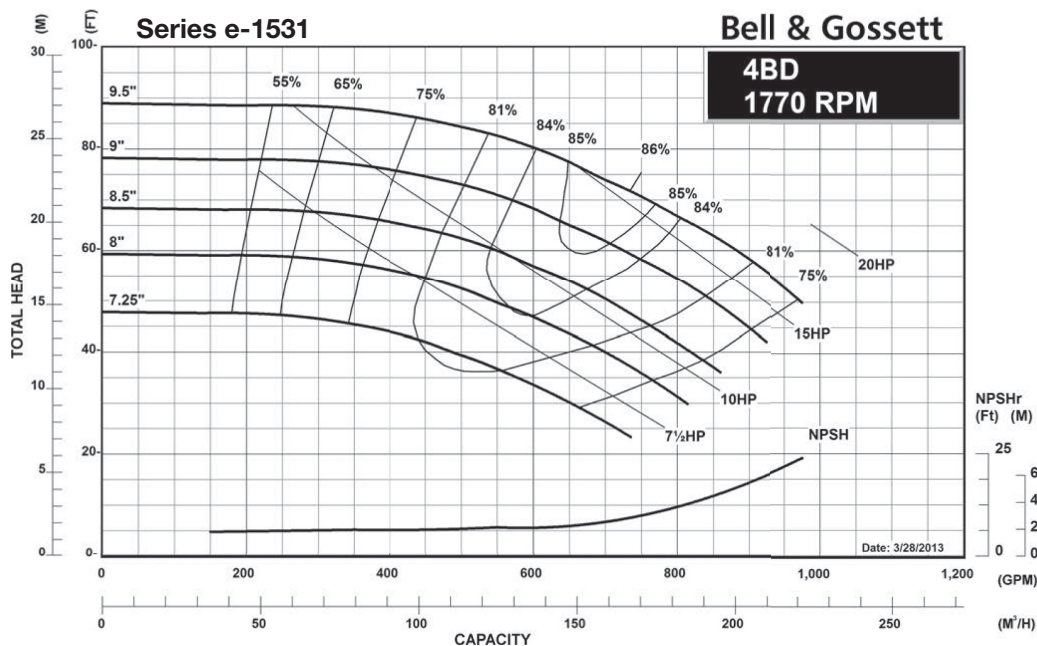
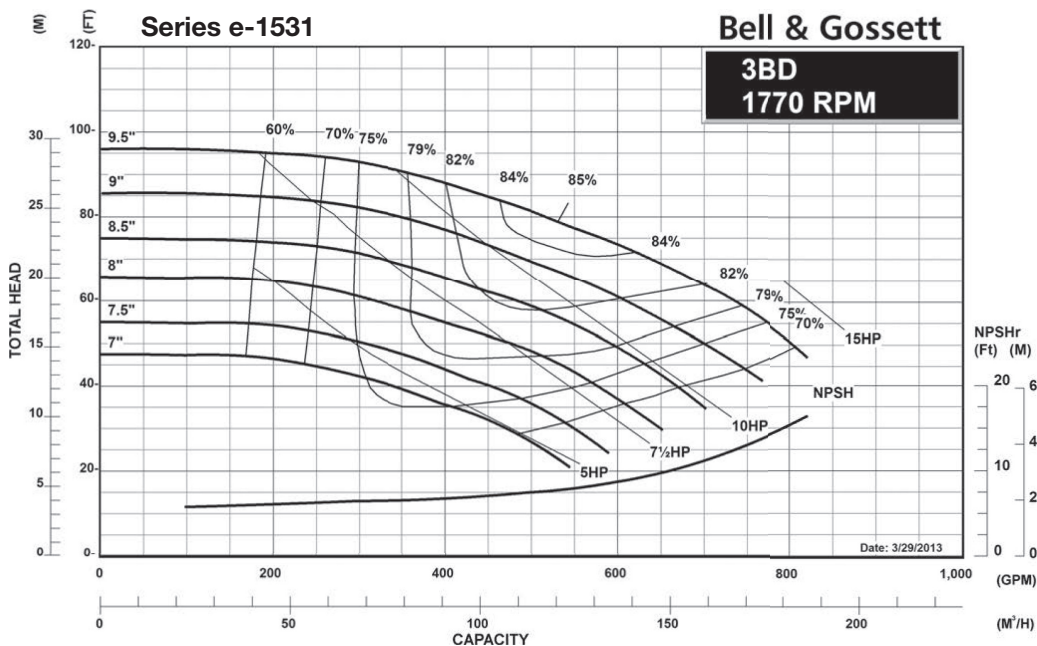
SERIES e-1531

1800 RPM SYNCHRONOUS SPEED



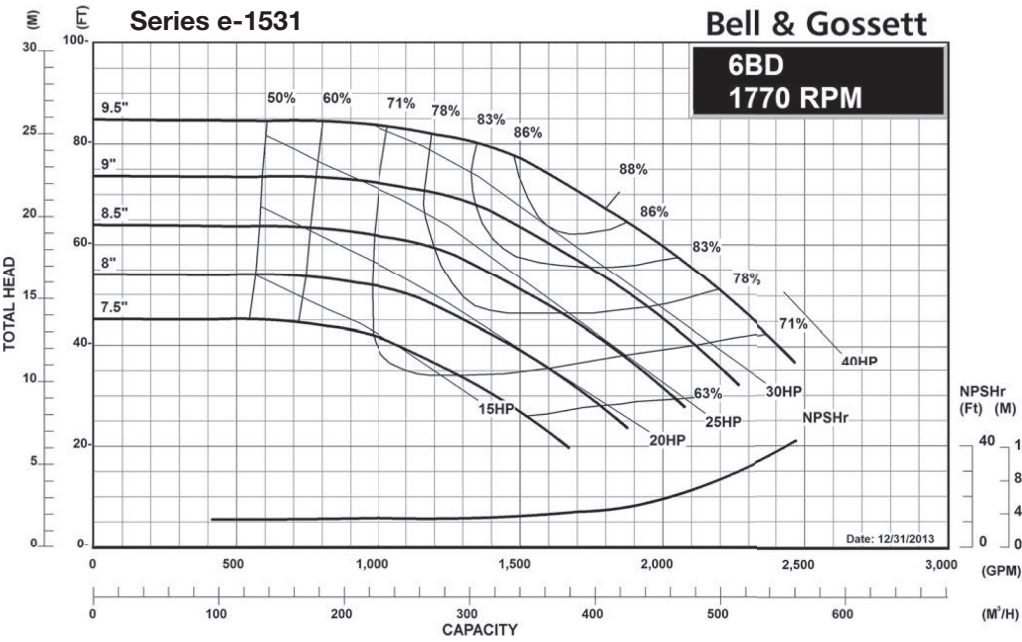
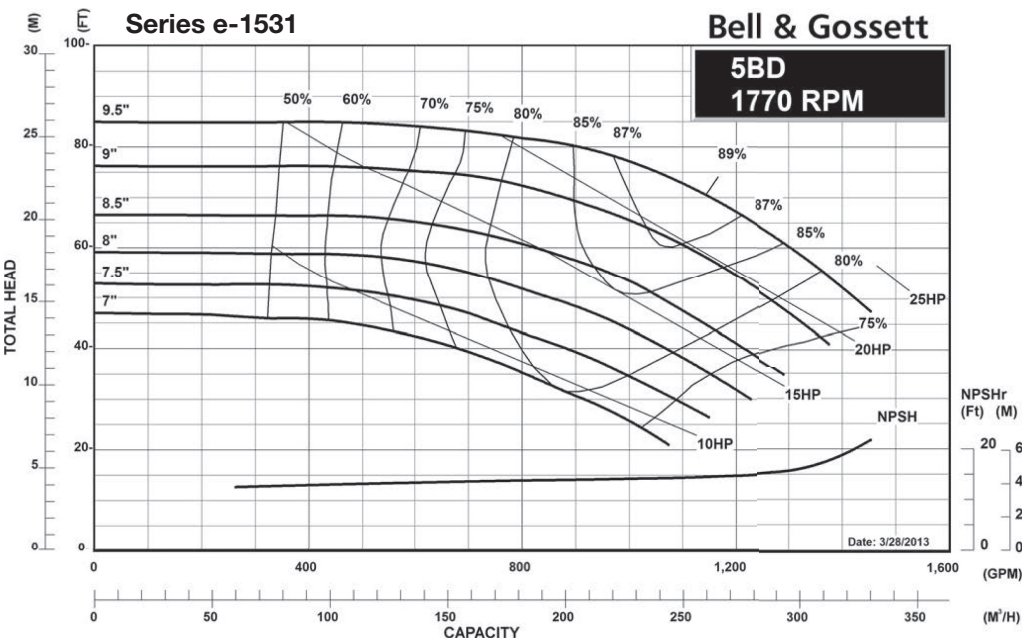
SERIES e-1531

1800 RPM SYNCHRONOUS SPEED



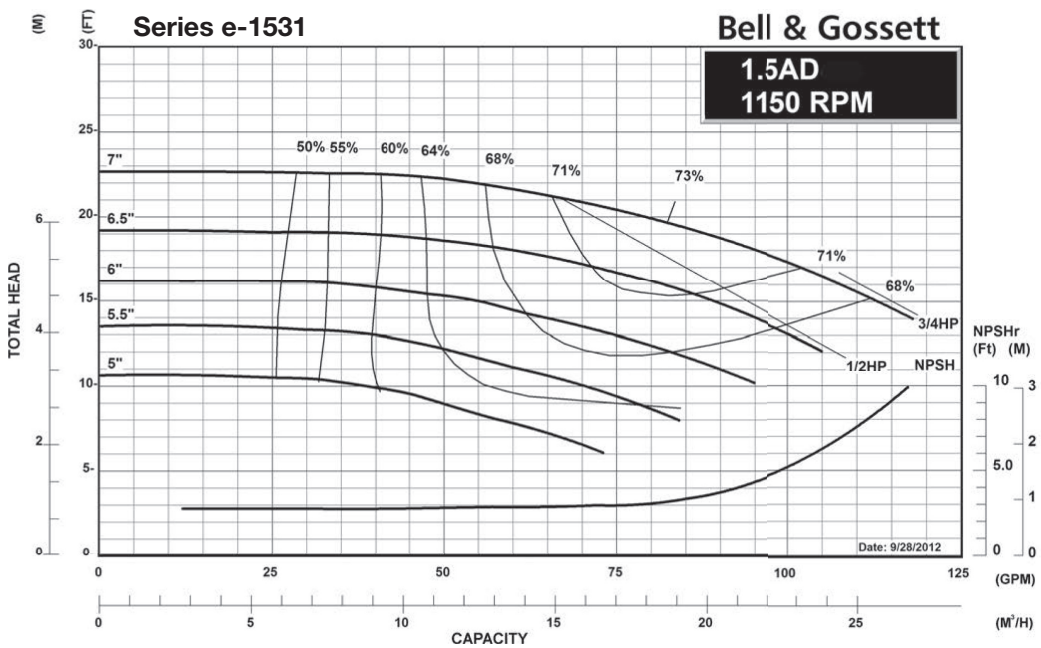
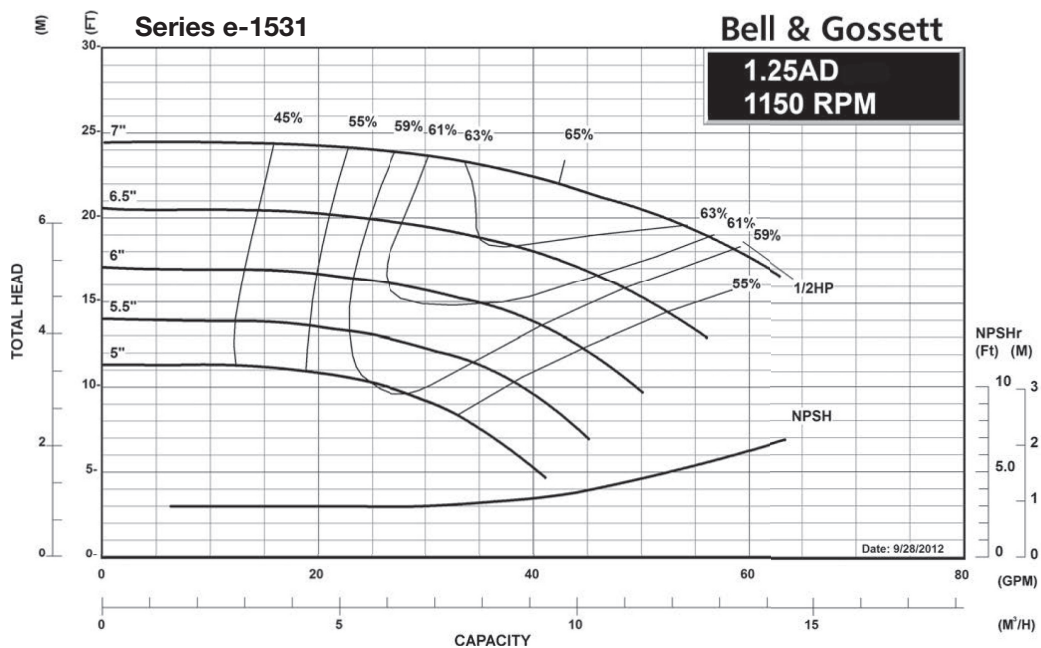
SERIES e-1531

1800 RPM SYNCHRONOUS SPEED



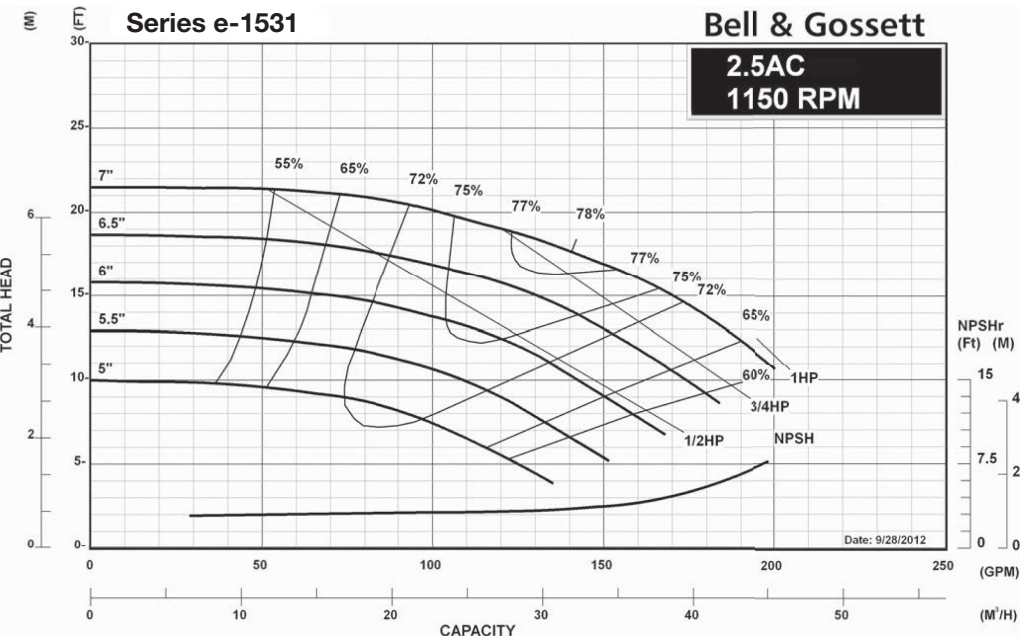
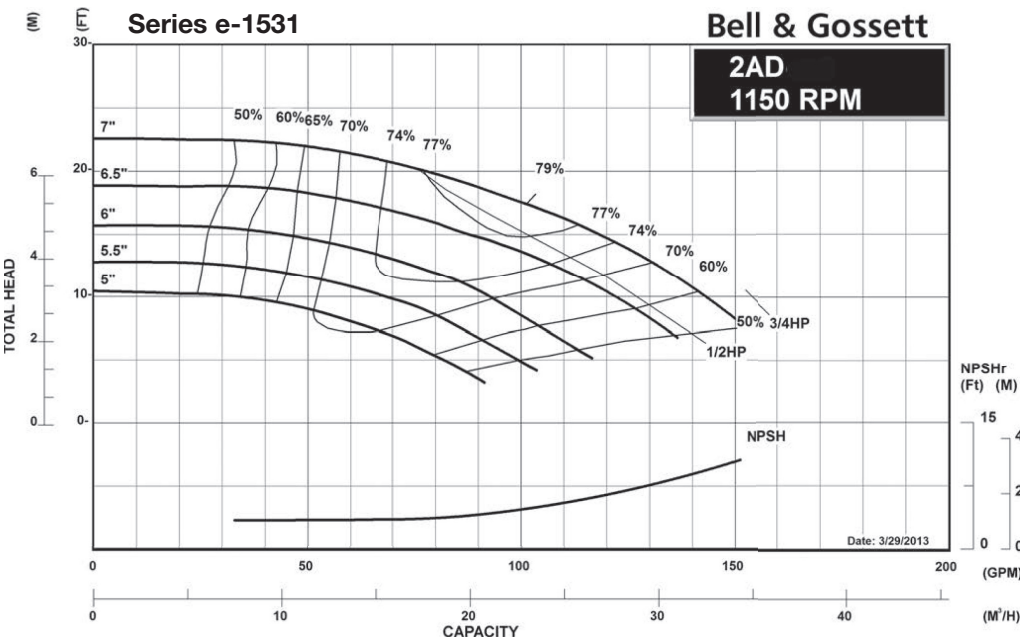
SERIES e-1531

1200 RPM SYNCHRONOUS SPEED



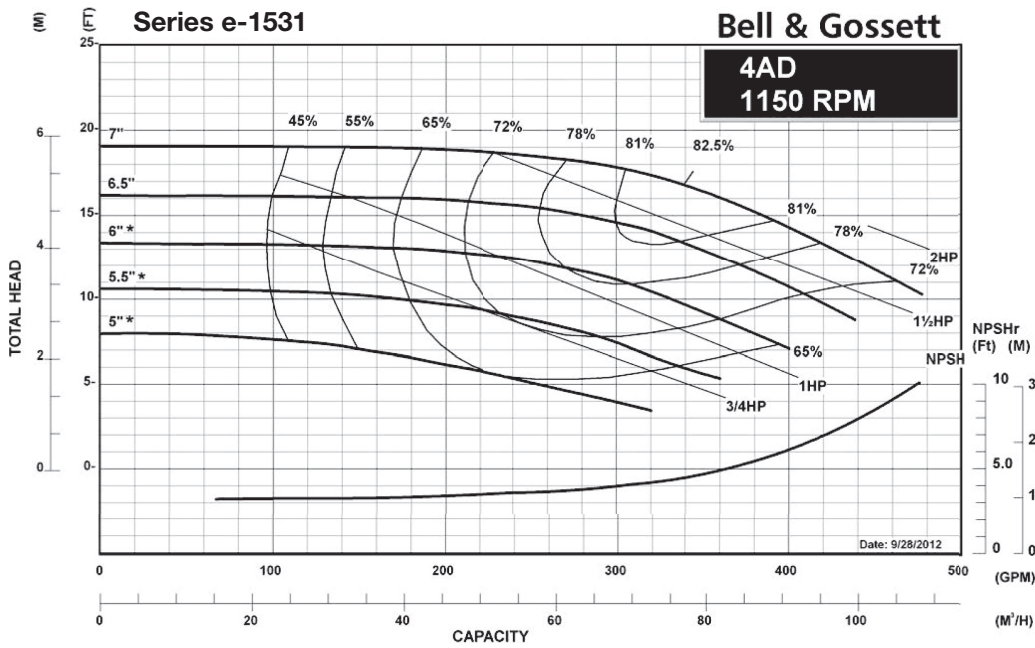
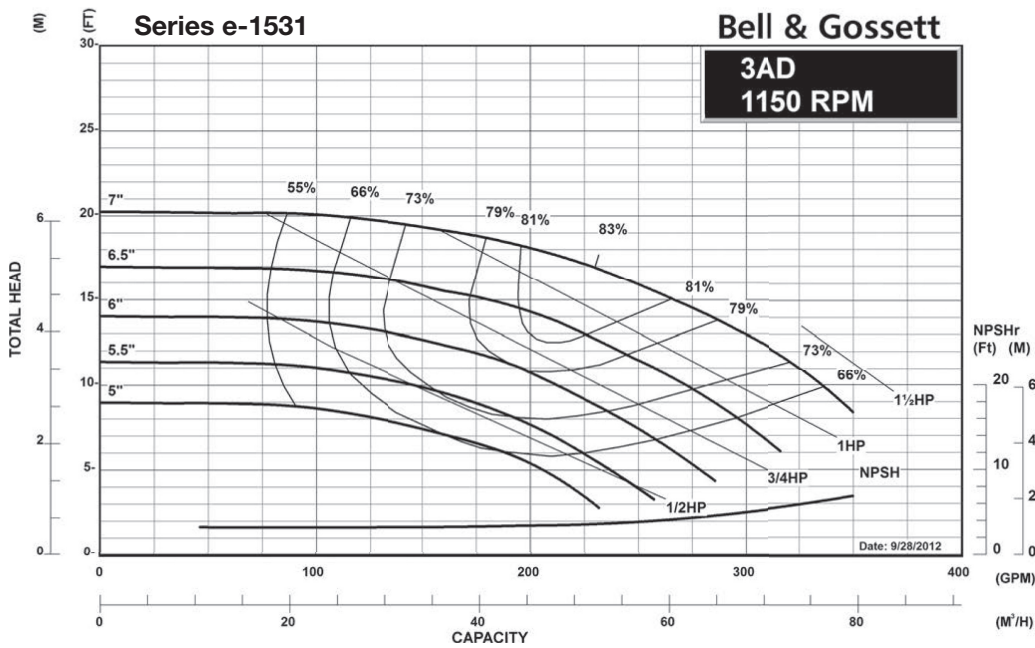
SERIES e-1531

1200 RPM SYNCHRONOUS SPEED



SERIES e-1531

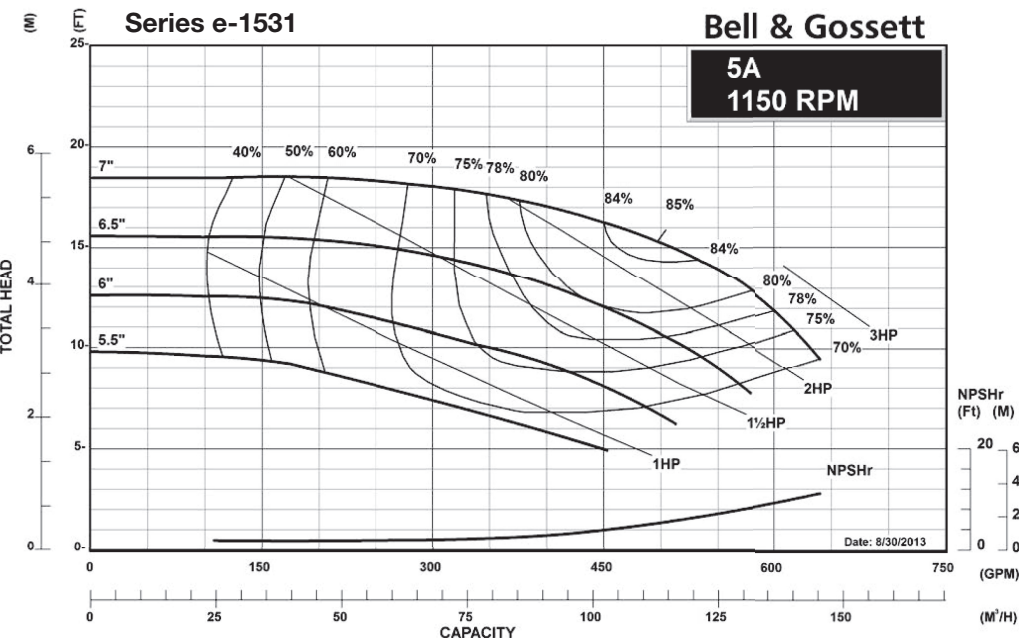
1200 RPM SYNCHRONOUS SPEED



* 6" and below requires oversized diameter and angle trim. See manual.

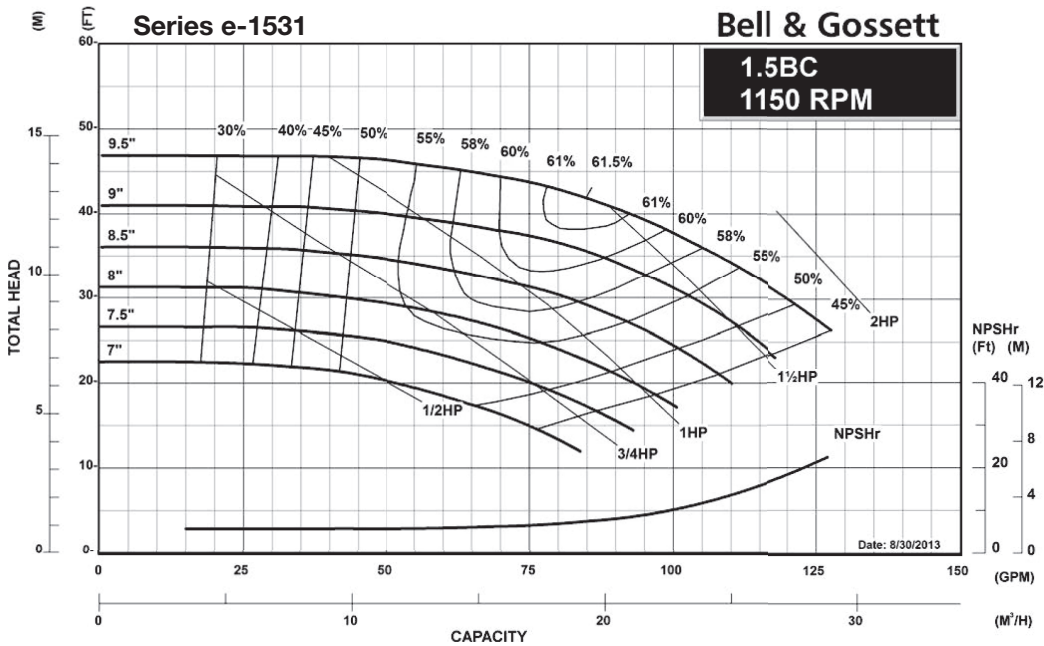
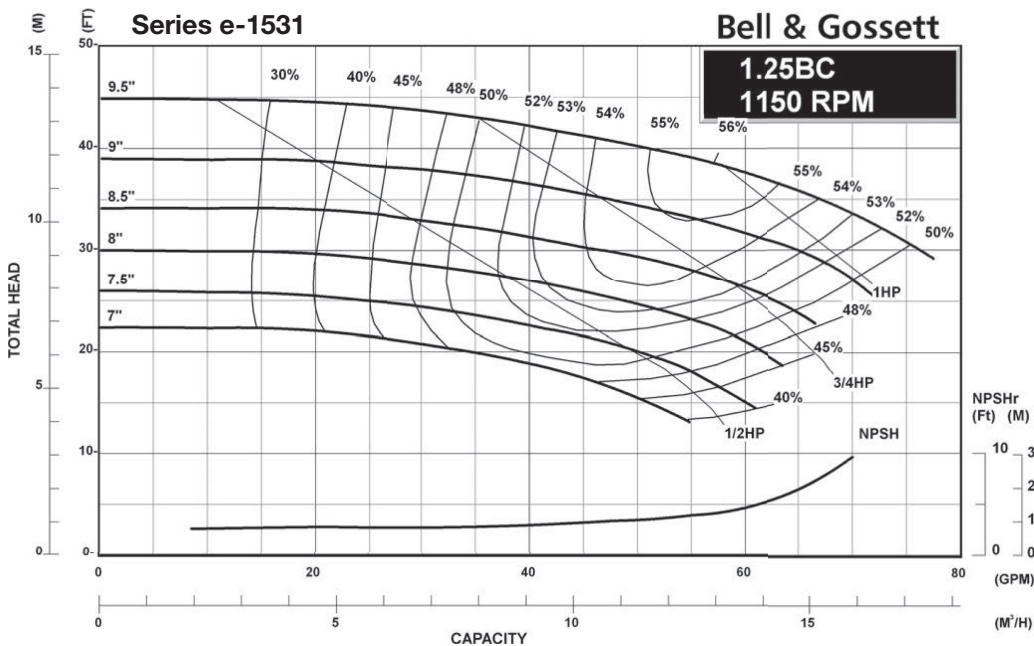
SERIES e-1531

1200 RPM SYNCHRONOUS SPEED



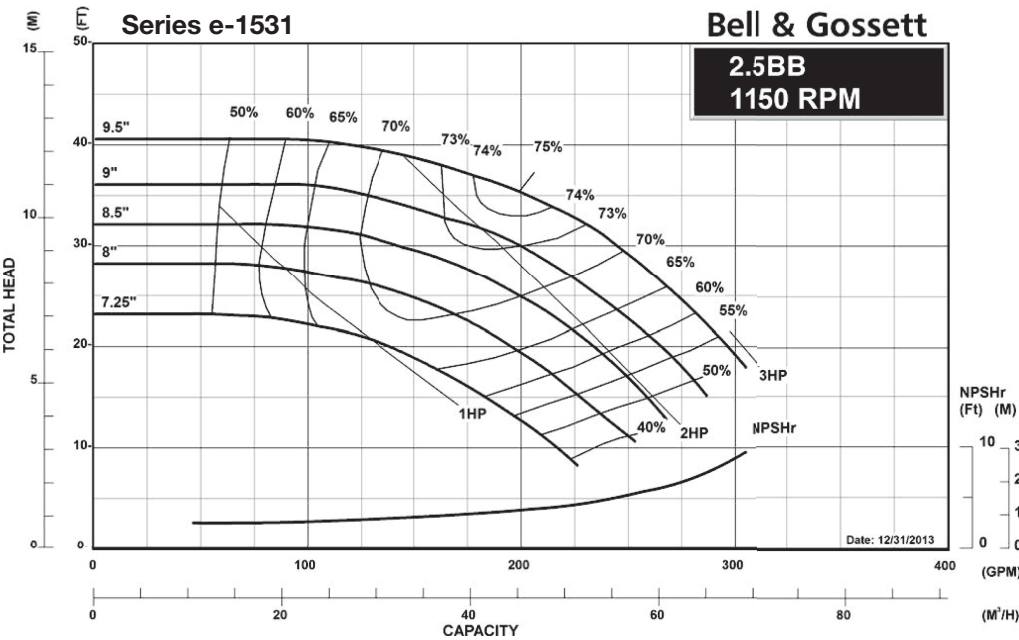
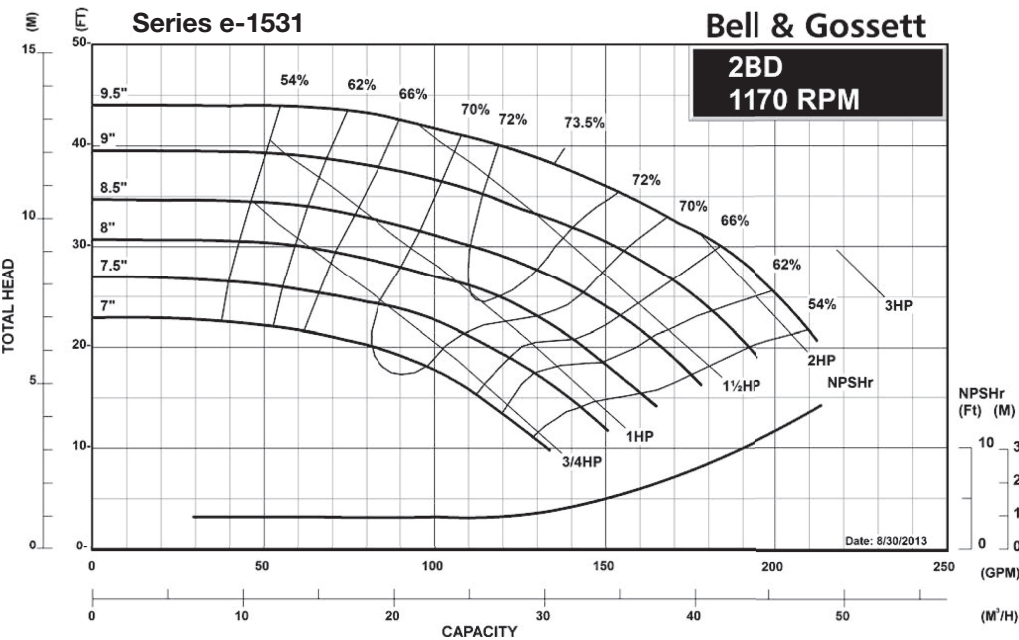
SERIES e-1531

1200 RPM SYNCHRONOUS SPEED



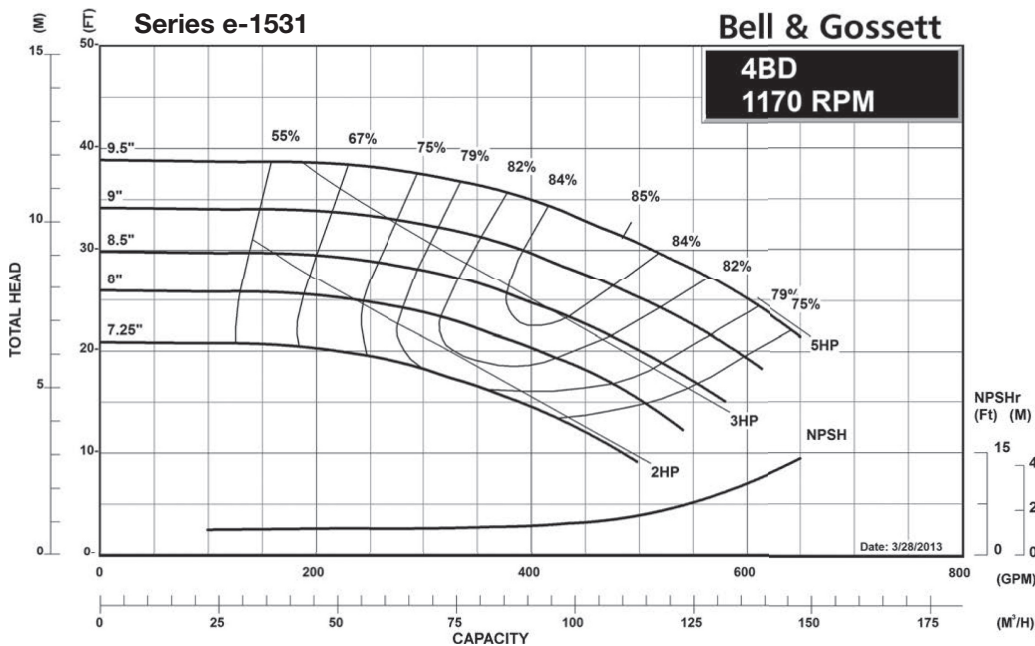
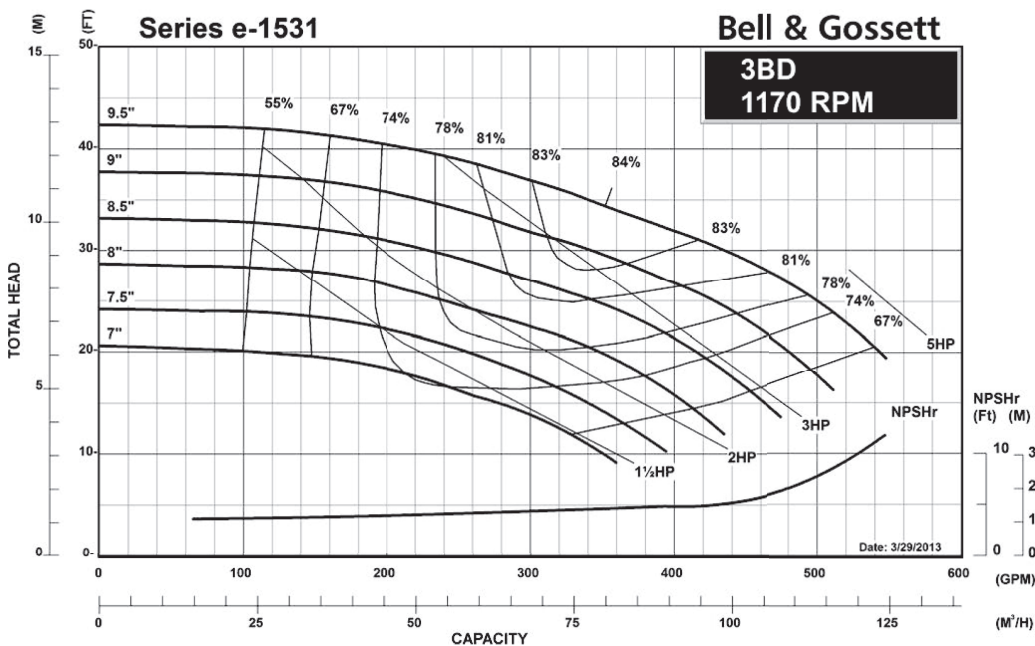
SERIES e-1531

1200 RPM SYNCHRONOUS SPEED



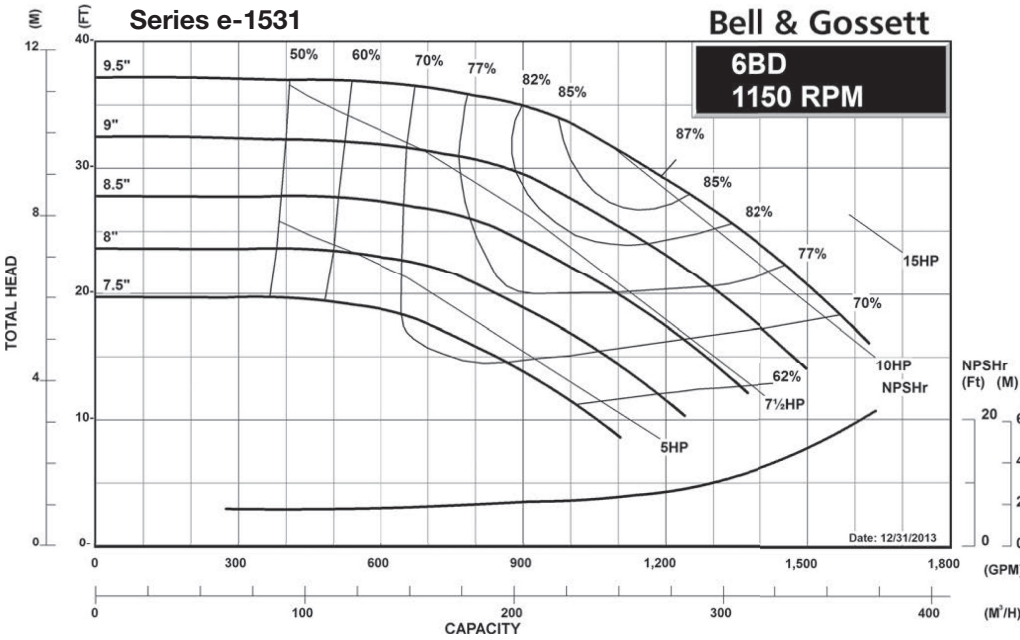
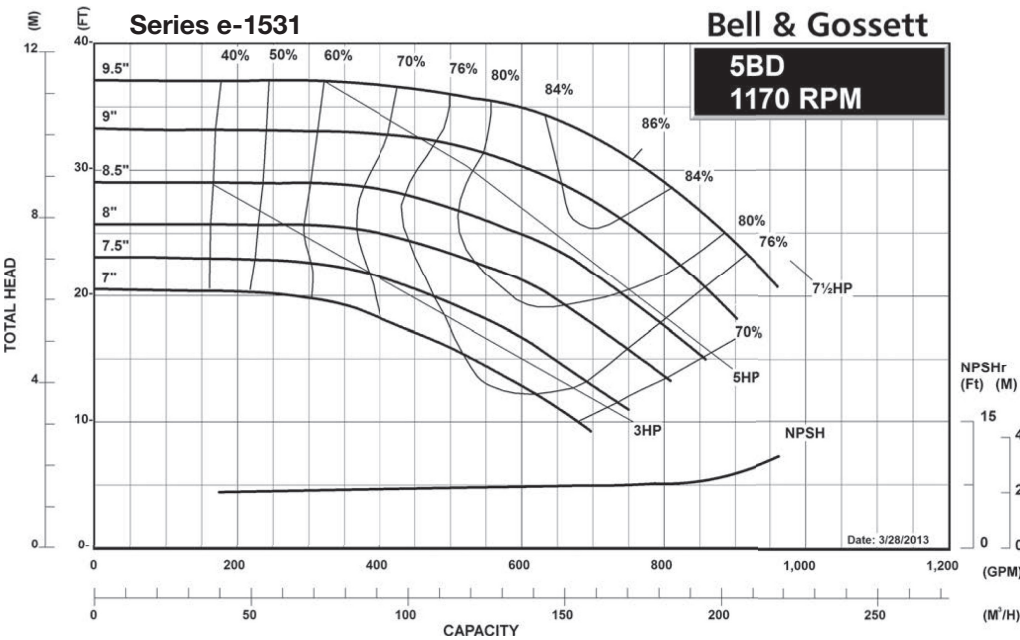
SERIES e-1531

1200 RPM SYNCHRONOUS SPEED



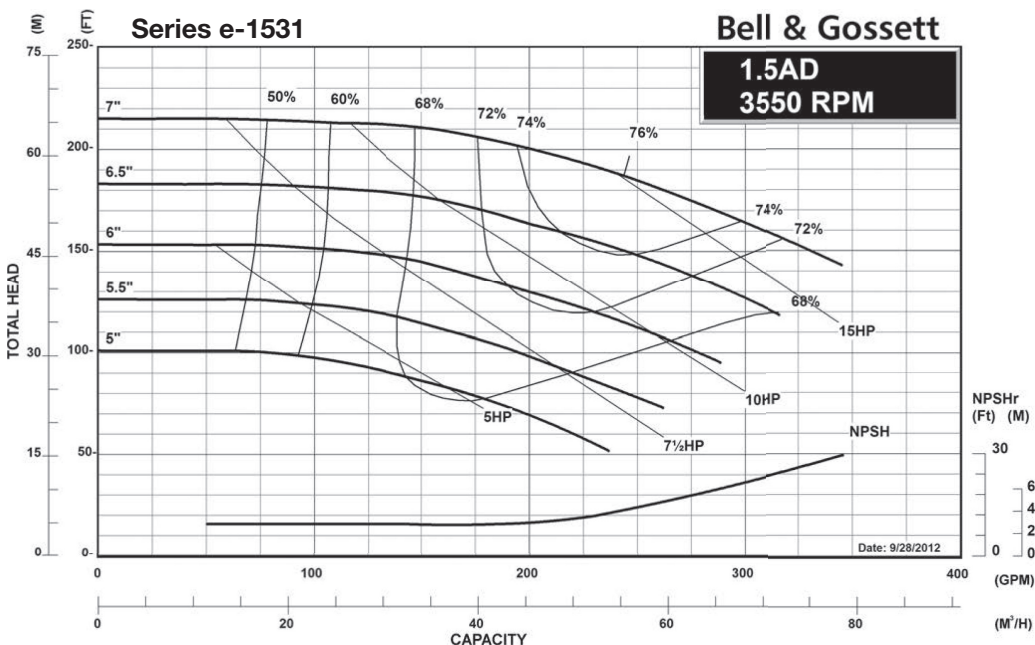
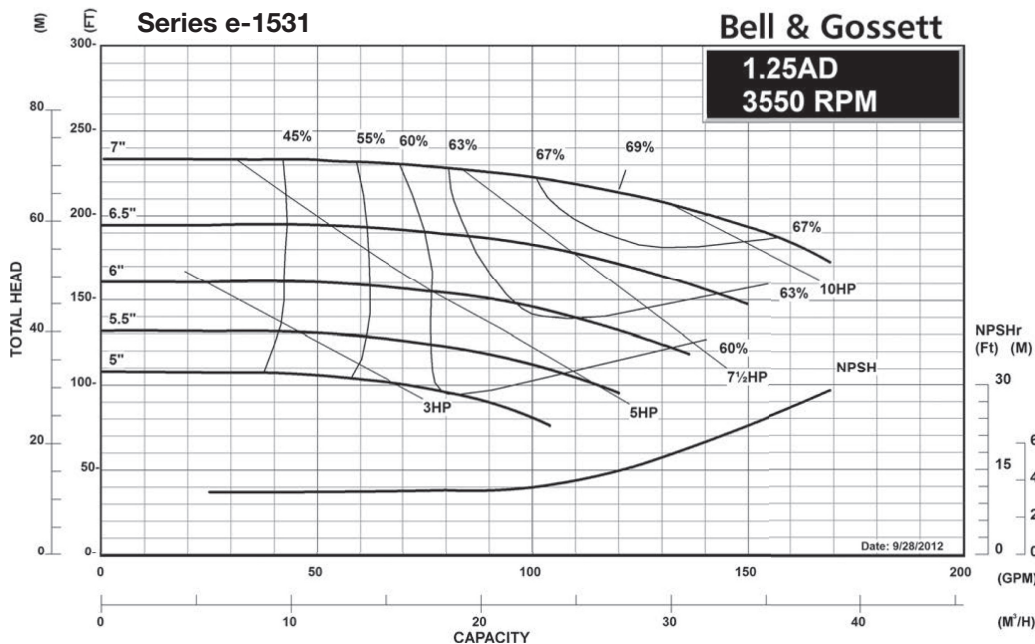
SERIES e-1531

1200 RPM SYNCHRONOUS SPEED



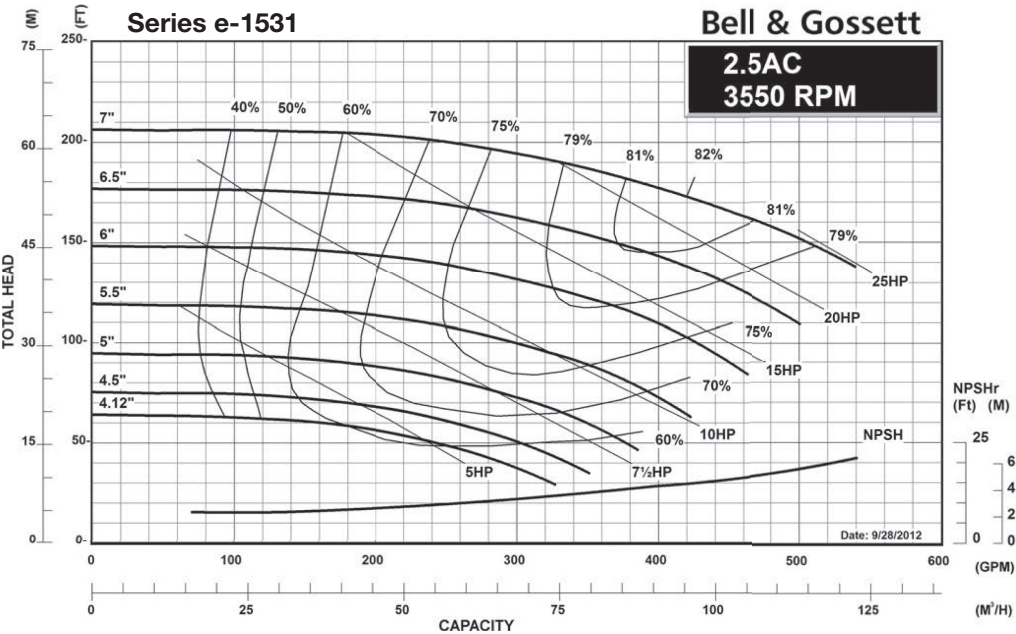
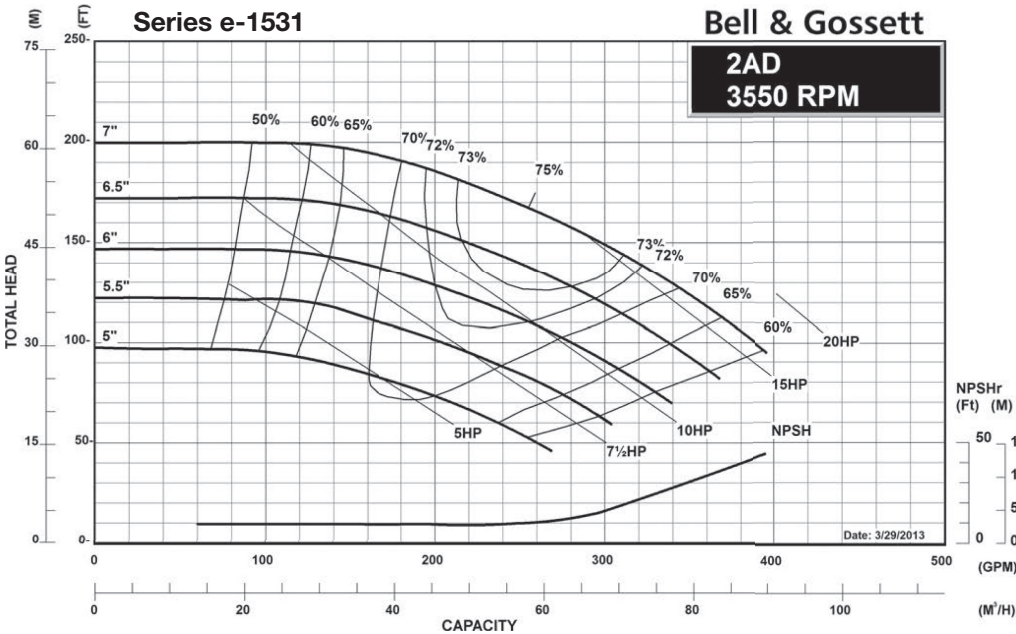
SERIES e-1531

3600 RPM SYNCHRONOUS SPEED



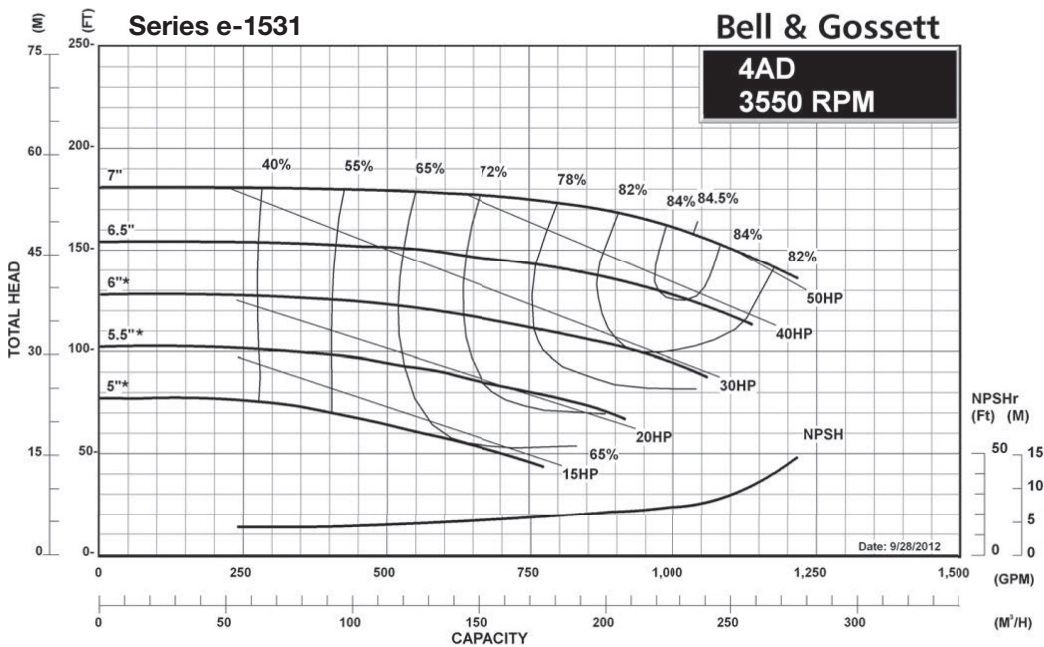
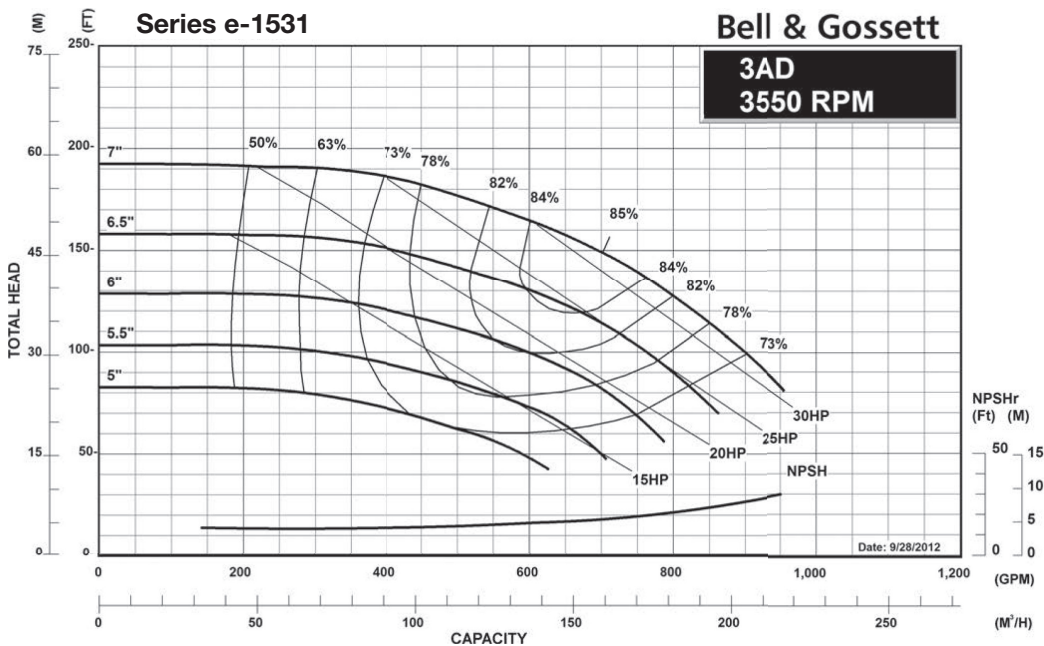
SERIES e-1531

3600 RPM SYNCHRONOUS SPEED



SERIES e-1531

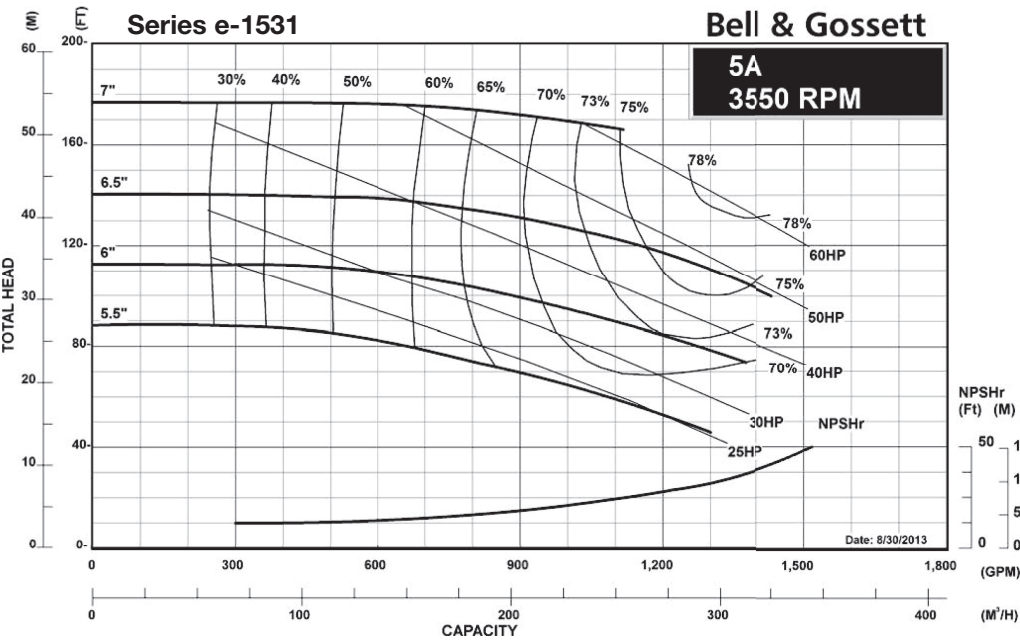
3600 RPM SYNCHRONOUS SPEED



* 6" and below requires oversized diameter and angle trim. See manual.

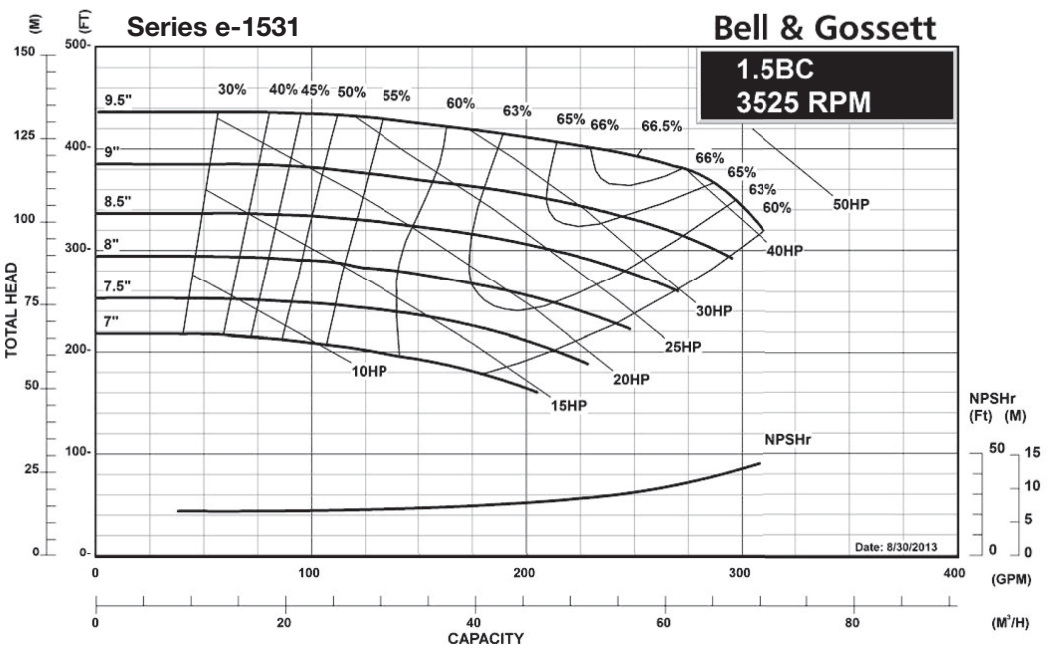
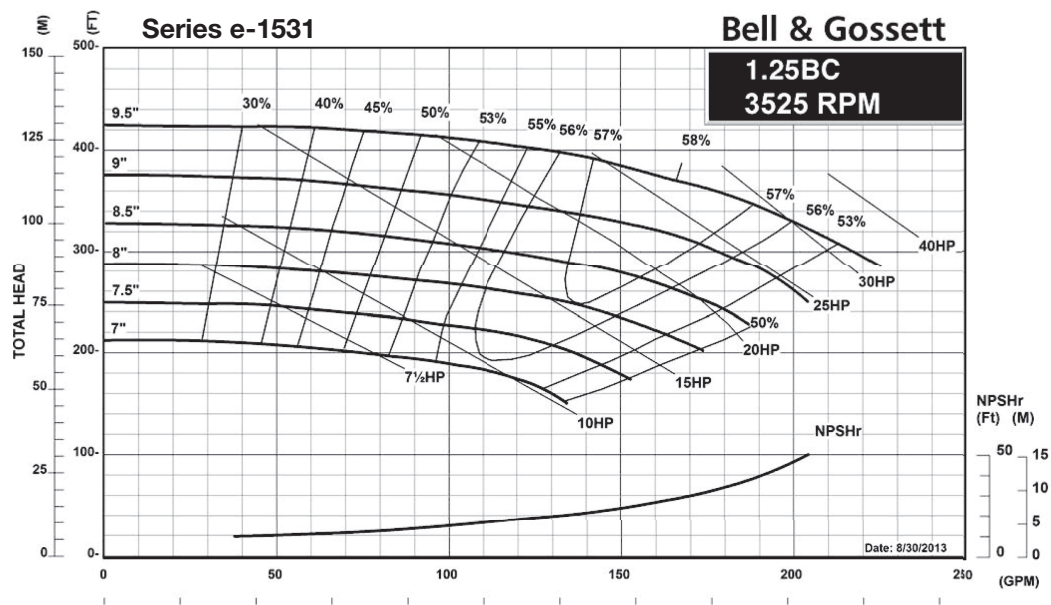
SERIES e-1531

3600 RPM SYNCHRONOUS SPEED



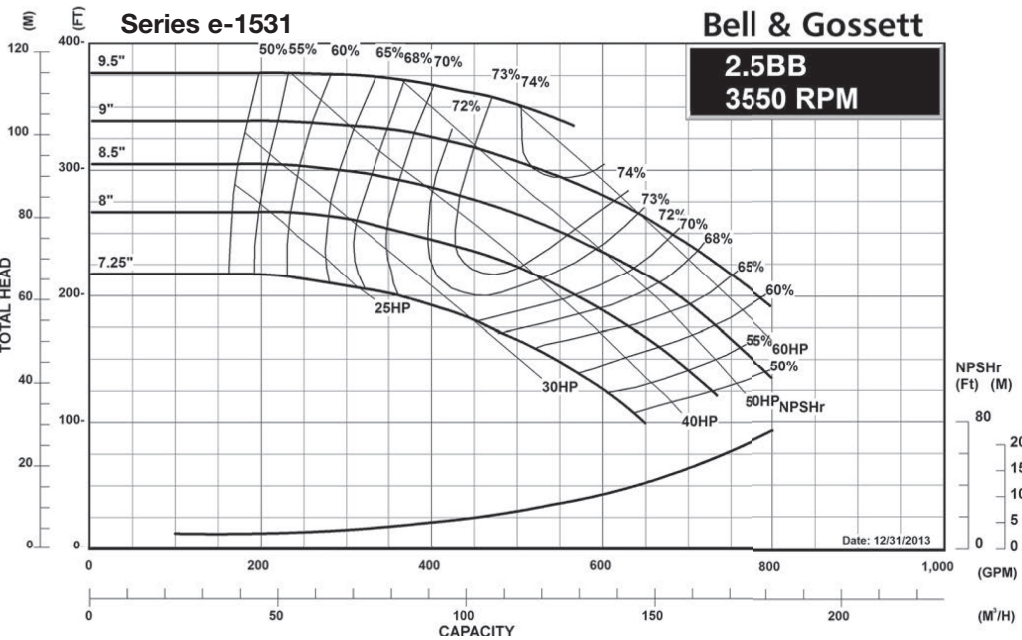
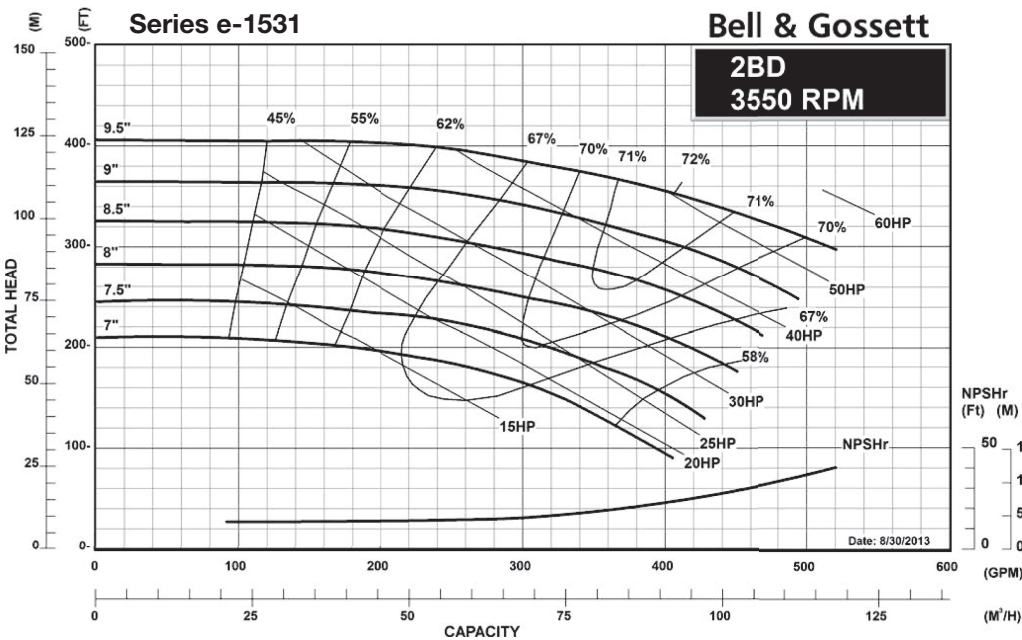
SERIES e-1531

3600 RPM SYNCHRONOUS SPEED



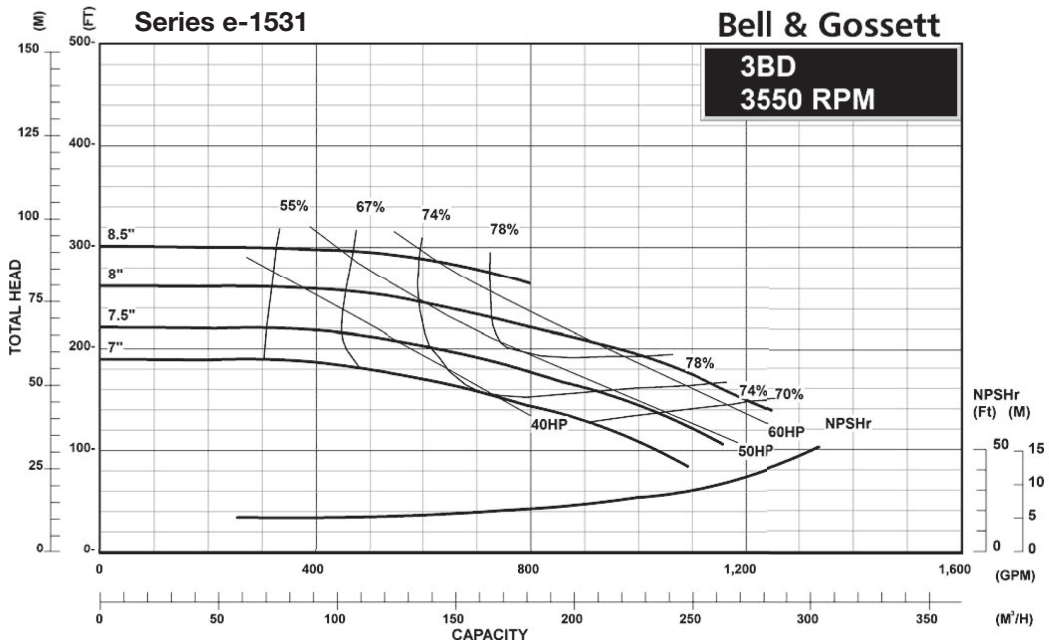
SERIES e-1531

3600 RPM SYNCHRONOUS SPEED



SERIES e-1531

3600 RPM SYNCHRONOUS SPEED



Xylem |'zīləm|

- 1) The tissue in plants that brings water upward from the roots;
- 2) a leading global water technology company.

We're a global team unified in a common purpose: creating innovative solutions to meet our world's water needs. Developing new technologies that will improve the way water is used, conserved, and re-used in the future is central to our work. We move, treat, analyze, and return water to the environment, and we help people use water efficiently, in their homes, buildings, factories and farms. In more than 150 countries, we have strong, long-standing relationships with customers who know us for our powerful combination of leading product brands and applications expertise, backed by a legacy of innovation.

For more information on how Xylem can help you, go to www.xyleminc.com

xylem
Let's Solve Water

Xylem Inc.
8200 N. Austin Avenue
Morton Grove, Illinois 60053
Phone: (847) 966-3700
Fax: (847) 965-8379
www.bellgossett.com

Bell & Gossett is a trademark of Xylem Inc. or one of its subsidiaries.
© 2015 Xylem Inc. B-263A October 2015



Taylor & Francis

Taylor & Francis Group

<http://taylorandfrancis.com>

Index

A

Accelerated Cost Recovery System (ACRS), 65
American Society of Mechanical Engineers (ASME), 30, 191
Amortization schedule, 52
Analysis of thermal energy systems, 79–173
 absolute scale, 95
 absolute temperatures, 130
 brine chilling system for ice rink
 manufacture, analysis of, 143–148
 caloric theory, 116
 Carnot efficiency, 130
 combined law, 120
 compressors, pumps, and fans, 98–99, 123
 conservation of energy, 86–94
 conservation of mass, 82–86
 conserved and balanced quantities, 81–82
 cooling coefficient of performance, 128
 counter flow heat exchanger, effectiveness of, 109–113
 cycle energy performance parameters, 127–131
 dead state, 118
 description of exergy, 117–118
 diffusers, 100–103
 energy efficiency ratio, 128
 energy and exergy analysis of thermal energy cycles, 126–137
 energy/exergy conundrum, 136–137
 engine and radiator system, analysis of, 138–143
 entropy, 81
 entropy balance (second law of thermodynamics), 94–116
 entropy generation, 94, 95
 exergetic cycle efficiency, 132–137
 exergetic efficiencies of flow devices, 123–126
 exergy accounting and exergy flow diagrams, 122–123
 exergy balance (combined law), 116–126
 exergy conservation, 118
 extensive property, 79
 first law of thermodynamics, 86
 flow work, 87
 fluid friction, 102

 gas turbine system for power delivery, analysis of, 149–157
 generalized balance law, 81–82
 heat exchanger effectiveness, 103–116
 heat exchangers, 123–126
 heating coefficient of performance, 129
 heat pump cycle, 129
 intensive property, 79
 internal energy, 86
 isentropic efficiencies of flow devices, 97–103
 kinetic energy, 86
 law of conservation of energy, 86
 maximum thermal efficiency of a cycle, 129–131
 nomenclature, 79–80
 nozzles, 99–100
 parallel flow heat exchanger, effectiveness of, 113–115
 phlogiston theory, 116
 pinch point temperature difference, 104, 115
 potential energy, 86
 problems, 157–173
 procedure, 80–81
 refrigeration and heat pump cycles, 134–135
 reversible, 96–97, 130
 significance, 135–136
 steady flow condition, 83
 storage term, 82
 system boundary, 81
 thermal capacity rate, 109
 thermodynamic definition of exergy, 118
 total values, 79
 transformational property, 116
 turbines, 97–98, 123
Annual cost (AC) analysis, 61–63
Artificial ice, 143
Available energy, 117

B

Bernoulli's equation, 179
Best efficiency point (bep), 230
Bingham plastic, 25
Birmingham Wire Gage (BWG) specification, 353
Brake horsepower (pumps), 228

Branch fittings (tees and wyes), 200–204
 Brine chilling system for ice rink manufacture,
 analysis of, 143–148
 artificial ice, 143
 chiller effectiveness, 148
 saturated condensing pressure, 144
 saturated evaporating temperature, 143
 Buckingham-Pi theorem, 249

C

Caloric theory, 116
 Capital outlay (CO) items, 64
 Capital recovery factor, 49
 Carnot efficiency, 130
 Cash flow diagram, 42–43
 CFHX, *see* Cross flow heat exchanger (CFHX)
 Check valves, 198–200
 Coefficient of performance (COP), 144
 Colburn factor, 385
 Combined law, *see* Exergy balance (combined law)
 Compound amount factor, 46–47
 Convective heat transfer coefficient, 277
 Conversion factors and constants, 455–457
 Cooling coefficient of performance, 128
 CoolProp database, 3
 Copper tubing dimensions, standard, *see*
 Standard copper tubing dimensions
 Counter flow heat exchanger, effectiveness of,
 109–113
 Counter flow regenerative heat exchanger, 315–320
 Cross flow heat exchanger (CFHX), 297–298
 Colburn factor, 385
 design and analysis, 383–389
 mixed fluid, 297
 unmixed fluid, 297

D

Darby 3K method (valves and fittings), 195–198
 Darcy-Weisbach friction factor, 179
 Dead state, 118
 Depreciation and taxes, 64–70
 accelerated depreciation schemes, 65
 after-tax cash flow, 64–65
 capital outlay items, 64
 straight-line depreciation, 65
 sum of the years' digits, 65–70
 Dilatant substance, 25
 DLL, *see* Dynamic link library (DLL)
 Double pipe heat exchanger (DPHX), 294–295
 analysis example, 350–352
 application of heat exchanger model, 347, 352

 calculation of annulus diameters, 346, 350
 calculation of convective heat transfer
 coefficients, 346, 351
 calculation of fluid velocities, 351
 calculation of friction factors, 346, 351
 calculation of Nusselt numbers, 346, 351
 calculation of overall heat transfer
 coefficients, 346, 351–352
 calculation of pressure drops, 352
 calculation of pressure drops through heat
 exchanger, 349
 calculation of Reynolds numbers, 346, 351
 calculation of UA values, 352
 computer software for design and analysis,
 341
 design and analysis, 327–352
 design considerations, 340–341
 design example, 342–350
 design specifications of heat exchanger,
 349–350
 determination of pipe and/or tube sizes,
 344–345
 diameters, 327–329
 fluid placement, 340, 343–344
 fluid properties, 342–343, 350
 hairpin configuration, 295
 heat exchanger length, 348
 heat exchanger specifications and
 performance, 352
 hydraulic analysis, 330–340
 hydraulic consequences of fouling,
 331–333
 initial guess of fluid outlet temperatures,
 350
 overall heat transfer coefficients, 330
 pressure drop through annulus, 333–340
 pressure drop through inner tube, 333
 results of design and analysis, 353
 Dynamic link library (DLL), 3

E

Economic decision making, 56–64
 annual cost analysis, 61–63
 present worth analysis, 57–61
 selection of alternatives, 64
 Economic pipe diameter, 213–224
 cost curves, 221–223
 cost of a pipe system, 214
 determination, 214–221
 economic velocity, 218
 economic velocity range, 223–224
 optimum pipe diameter, 213

- Effectiveness-NTU heat exchanger model, 308–315
- Electric motor driven systems (EMDS), 254
- Energy efficiency ratio (EER), 128
- Energy transport in thermal energy systems, 277–406
 - “black-boxed” heat exchanger, 300
 - convective heat transfer coefficient, 277, 284–289
 - correlations, 284
 - counter flow regenerative heat exchanger, 315–320
 - cross flow heat exchanger, 297–298
 - cross flow heat exchanger design and analysis, 383–389
 - design and analysis of heat exchangers, 298–315
 - double pipe heat exchanger, 294–295
 - double pipe heat exchanger design and analysis, 327–352
 - effectiveness-NTU heat exchanger model, 308–315
 - entry length, 285–286
 - film temperature, 286
 - forced convection, 278
 - forced external cross flow over a cylindrical surface, 286
 - forced internal laminar flow (combined entry), 286
 - forced internal laminar flow (thermal entry), 287
 - forced internal turbulent flow, 287–289
 - fouling on heat exchanger surfaces, 289
 - Fourier’s law, 279
 - free-stream temperature, 286
 - heat exchanger, 277
 - heat exchanger analysis problem, 300
 - heat exchanger design problem, 299–300
 - heat exchanger heat transfer analysis, 300–306
 - heat exchangers with phase change fluids (boilers, evaporators, and condensers), 320–327
 - heat exchanger types, 294–298
 - heat flux, 278
 - heat transfer, 277
 - heat transfer analysis of heat exchangers, 277–289
 - LMTD heat exchanger model, 306–308
 - logarithmic mean temperature difference, 301–306
 - Newton’s law of cooling, 277
 - Nusselt number, 284
 - overall heat transfer coefficient, 289–294
 - Peclet number, 284
 - plate and frame heat exchanger, 297
 - plate and frame heat exchanger design and analysis, 369–383
 - Prandtl number, 284
 - problems, 390–406
 - Reynolds number, 284
 - shell and tube heat exchanger, 295–297
 - shell and tube heat exchanger design and analysis, 352–369
 - smooth tubes, 287
 - special application heat exchangers, 315–327
 - surface temperature, 286
 - thermal conductivity, 279
 - thermal resistance, 279–283
- Engineering economics, 41–77
 - accelerated depreciation schemes, 65
 - after-tax cash flow, 64–65
 - amortization schedule, 52
 - annual cost analysis, 61–63
 - capital outlay items, 64
 - capital recovery factor, 49
 - cash flow diagram, 42–43
 - compound amount factor, 46–47
 - depreciation and taxes, 64–70
 - discrete interest factors, 50
 - economic decision making, 56–64
 - gradient present worth factor, 49
 - interest factor, 45
 - minimum acceptable rate of return, 44
 - nomenclature, 41
 - nominal and effective interest rates, 51
 - present worth analysis, 57–61
 - present worth factor, 46
 - problems, 70–77
 - selection of alternatives, 64
 - simple interest, 44
 - Single Payment Compound Amount Factor, 44–45
 - straight-line depreciation, 65
 - sum of the years’ digits, 65–70
 - time value of money, 43–50
 - time value of money examples, 51–55
 - uniform series present worth factor, 48
 - uniform series sinking fund factor, 48
 - using software to calculate interest factors, 55–56
- Engineering Equation Solver (EES), 2
- Engine and radiator system, analysis of, 138–143
 - assumptions, 139
 - parametric study, 141

- schematic, 138
- unconstrained optimum, 142
- workable solutions, 142
- Evaluation of thermal energy systems,
 - see* Simulation, evaluation, and optimization of thermal energy systems
- Exergetic cycle efficiency, 132–137
 - energy/exergy conundrum, 136–137
 - power cycles, 132–133
 - refrigeration and heat pump cycles, 134–135
 - significance, 135–136
- Exergy balance (combined law), 116–126
 - absolute scale, 121
 - available energy, 117
 - caloric theory, 116
 - combined law, 120
 - compressors, pumps, and fans, 123
 - dead state, 118
 - description of exergy, 117–118
 - ethical responsibility, 118
 - exergetic efficiencies of flow devices, 123–126
 - exergy accounting and exergy flow diagrams, 122–123
 - exergy balance, 118–122
 - exergy conservation, 118
 - flow exergy, 119
 - free energy, 117
 - heat exchangers, 123–126
 - irreversibility, 119
 - phlogiston theory, 116
 - thermodynamic definition of exergy, 118
 - transformational property, 116
 - turbines, 123
 - useful energy, 117

F

- First law of thermodynamics, 86
- Fittings (fluid transport), *see* Valves and fittings (fluid transport)
- Flow exergy, 119
- Flow work, 87
- Fluids, working, *see* Working fluids, properties of
- Fluid transport in thermal energy systems, 175–275
 - absolute surface roughness, 180
 - affinity laws, 249–253
 - Bernoulli's equation, 179
 - branch fittings (tees and wyes), 200–204
 - cavitation and the net positive suction head, 240–245

- check valves, 198–200
- cost curves, 221–223
- cost of a pipe system, 214
- Darby 3K method, 195–198
- Darcy-Weisbach friction factor, 179
- design and analysis of pipe networks, 204–213
- design practices for pump/pipe systems, 253–255
- dynamic pump operation, 225–230
- dynamic pump performance, 227–230
- economic pipe diameter, 213–224
- economic velocity, 218
- economic velocity range, 223–224
- electric motor driven systems, 254
- expansion tanks and entrained gases, 255
- fluid flow fundamentals, 177–190
- head loss due to friction in pipes and tubes, 179
- Hooper 2K method, 192–195
- length form, 178
- manufacturer's pump curves, 230
- modified Bernoulli equation, 192
- Moody friction factor, 179
- parallel pipe networks, 208–213
- piping and tubing standards, 175–177
- problems, 256–275
- pumps, 225–253
- reducers and expansions, 198
- relative roughness, 180
- Reynolds number, 180
- specific energy form, 178
- specific weight, 178
- Swamee-Jain correlation, 180
- system curve, 231–235
- valves and fittings, 190–204
- variable speed motor, 249
- Fourier's law, 1, 25, 279
- Free energy, 117

G

- Gas turbine system for power delivery, analysis
 - of, 149–157
 - air-fuel ratio, 151
 - assumptions, 150
 - exergy destruction rate, 155
 - gasifier turbine, 149
 - isentropic efficiency, 152
 - regenerator, 157
 - specific fuel consumption, 153
- Generalized balance law, 82
- Gradient present worth factor, 49

H

Heat exchanger; *see also* Energy transport in thermal energy systems
 double pipe, *see* Double pipe heat exchanger (DPHX)
 plate and frame, *see* Plate and frame heat exchanger (PFHX)
 shell and tube, *see* Shell and tube heat exchanger (STHX)
 Heat exchanger effectiveness, 103–116
 counter flow heat exchanger, effectiveness of, 109–113
 parallel flow heat exchanger, effectiveness of, 113–115
 pinch point temperature difference, 104
 significance of PPTD and effectiveness, 115–116
 thermal capacity rate, 109
 Heating coefficient of performance, 129
 High resistance valves, 191
 Hooper 2K method (valves and fittings), 192–195
 Horsepower per ton (HPT), 144
 Hydraulic power (pumps), 228

I

Internal energy, 86
 International Association for the Properties of Water and Steam (IAPWS), 10
 International Energy Agency (IEA), 254
 Isentropic efficiency, 97

K

Kinetic energy, 86

L

Lagrange multiplier theorem, 432
 Law of conservation of energy, 86
 LMTD heat exchanger model, 306–308
 Logarithmic mean temperature difference (LMTD), 301–306
 Low resistance valves, 191

M

Minimum acceptable rate of return (MARR), 44
 Modified Accelerated Cost Recovery System (MACRS), 65
 Money, time value of, *see* Time value of money
 Moody friction factor, 179

N

National Institute for Standards and Technology (NIST), 6
 Net positive suction head (NPSH), cavitation and (fluid transport), 240–245
 calculation, 241
 flooded suction, 241
 net positive suction head available (NPSHa), 240
 net positive suction head required (NPSHr), 240
 safety factor, 241
 suction lift, 241
 Newtonian fluids, 24
 Newton's law of cooling, 1, 277
 Newton's law of viscosity, 22
 Newton's second law of motion, 4
 Non-Newtonian fluids, 25
 Number of transfer units (NTU), 309
 Nusselt number, 284

O

Optimization of thermal energy systems, *see* Simulation, evaluation, and optimization of thermal energy systems
 Optimum designs, 29–30
 Optimum economic diameter, 30

P

Parallel flow heat exchanger, effectiveness of, 113–115
 Peclet number, 284
 Phlogiston theory, 116
 Pinch point temperature difference (PPTD), 104, 115
 Pipe diameter, *see* Economic pipe diameter
 Pipe dimensions, standard, *see* Standard pipe dimensions
 Pipe networks, design and analysis of, 204–213
 Piping and tubing standards, 175–177
 copper tubing, common uses of, 177
 nominal diameter, 175
 schedule number, 175
 standard diameter, 176
 Plate and frame heat exchanger (PFHX), 297
 analysis, 376–383
 application of the heat exchanger model, 380–381

- calculation of convective heat transfer
 - coefficients, 379
 - calculation of fluid mass velocities, 378
 - calculation of hydraulic diameter of the channel, 378
 - calculation of Nusselt numbers, 379
 - calculation of overall heat transfer
 - coefficients, 379
 - calculation of pressure drops, 381–382
 - calculation of Reynolds numbers, 378
 - calculation of UA values, 379–380
 - checks, 382–383
 - design and analysis, 369–383
 - dimensions, 371–373
 - fluid properties, 377
 - hydraulic performance, 375–376
 - initial guess of fluid outlet temperatures, 377
 - mass velocity, 375
 - plate enlargement factor, 372
 - results of analysis, 384
 - single-pass counter flow arrangement, 371
 - thermal performance, 373–375
 - Potential energy, 86
 - Prandtl number, 284
 - Present worth (PW) analysis, 57–61
 - Present worth factor, 46
 - Problems
 - analysis of thermal energy systems, 157–173
 - energy transport in thermal energy systems, 390–406
 - engineering economics, 70–77
 - fluid transport in thermal energy systems, 256–275
 - simulation, evaluation, and optimization, 440–454
 - thermal energy systems, introduction to, 31–40
 - Pseudoplastic substance, 25
 - Pump curves, 535–593
 - Bell & Gossett Series e-80, 537–566
 - Bell & Gossett Series e-1531, 568–593
 - Pump/pipe systems, design practices for (fluid transport), 253–255
 - economics, 254
 - electric motor driven systems, 254
 - environmental impact, 254
 - expansion tanks and entrained gases, 255
 - miscellaneous sources, 255
 - noise and vibration, 254
 - pump placement and flow control, 254–255
 - valves, 255
 - Pumps (fluid transport), 225–253
 - affinity laws, 249–253
 - best efficiency point, 230
 - brake horsepower, 228
 - Buckingham-Pi theorem, 249
 - cavitation and the net positive suction head, 240–245
 - closed-loop system, system curve for, 234–235
 - discharge volute, 226
 - dynamic pump operation, 225–230
 - dynamic pump performance, 227–230
 - hydraulic power, 228
 - manufacturer's pump curves, 230
 - operating point, 236
 - pump capacity, 227
 - pump curves, 227
 - pump head, 227
 - pump selection, 235–240
 - quadratic function of volumetric flow rate, 232
 - series and parallel pump configurations, 245–248
 - system curve, 231–235
 - two-tank system open to the atmosphere, system curve for, 231–234
 - types, 225
 - variable speed motor, 249
 - water horsepower, 228
- R**
- REFPROP database, 2–3
 - Reynolds number, 180, 284
 - Rheopectic substance, 25
- S**
- Saturated condensing pressure (SCP), 144
 - Saturated evaporating temperature (SET), 143
 - Shear thickening fluids, classification of, 25
 - Shear-thinning fluids, classification of, 25
 - Shell and tube heat exchanger (STHX), 295–297
 - analysis, 362–369
 - application of heat exchanger model, 366–367
 - baffle spacing, 356
 - calculation of convective heat transfer coefficients, 365
 - calculation of friction factors, 364
 - calculation of Nusselt numbers, 365
 - calculation of overall heat transfer coefficients, 365
 - calculation of pressure drops, 367–368
 - calculation of Reynolds numbers, 364
 - calculation of UA values, 365
 - condenser tubes, 353

- design, 362
 - design and analysis, 352–369
 - design and analysis checks, 368–369
 - design considerations, 361–362
 - fluid properties, 363
 - fluid velocities, 364
 - general design considerations, 361–362
 - initial guess of fluid outlet temperatures, 362
 - inlet plenum, 295
 - LMTD, 357
 - outlet plenum, 295
 - results of analysis, 370
 - segmental cut baffle, 356
 - shell side analysis, 358–361
 - shell side considerations, 361
 - shell and tube parameters, 363
 - tube side analysis, 357–358
 - tube side considerations, 361
 - Shomate equation, 19
 - Simulation, evaluation, and optimization of
 - thermal energy systems, 407–454
 - closed-form solution of optimization
 - problem, 430–431
 - cost function, 429
 - design variables, 429, 437
 - deviation plot, 417
 - equality constraints, 429
 - evaluation, 407, 426–428
 - exact fitting method, 415–419
 - formulation and solution of optimization
 - problems using software, 439–440
 - inequality constraints, 429
 - mathematical statement of optimization,
 - 429–430
 - method of Lagrange multipliers, 431–438
 - method of least squares, 419
 - modeling thermal energy system
 - equipment, 414–422
 - 9-point data, 419
 - normal equations, 421
 - objective function, 429
 - optimization, 407, 429–440
 - outlet water temperature, 414
 - parametric studies, 426
 - post-optimality studies, 433
 - problems, 440–454
 - significance of Lagrange multipliers, 438
 - simulation, 407–426
 - simulation advantages and pitfalls, 425–426
 - simulation example (modeling of air
 - conditioning system), 422–425
 - simulation example (pump and pipe
 - system), 408–414
 - sum of the squares of the residuals, 419
 - wet bulb temperature, 414
 - Single Payment Compound Amount Factor,
 - 44–45
 - Software, 2–3
 - approach, 3
 - to calculate interest factors, 55–56
 - CoolProp, 3
 - for DPHX design and analysis, 431
 - Engineering Equation Solver, 2
 - REFPROP, 2–3
 - simulation, evaluation, and optimization of
 - thermal energy systems, 439–440
 - Standard copper tubing dimensions,
 - 533–534
 - user-written libraries, 3
 - Standard pipe dimensions, 527–532
 - STHX, *see* Shell and tube heat exchanger (STHX)
 - Straight-line depreciation (SLD), 65
 - Sum of the squares of the residuals (SSQR), 419
 - Sum of the years' digits (SYD), 65–70
 - Swamee-Jain correlation, 180
- ## T
- Thermal energy systems, introduction to, 1–40
 - CoolProp, 3
 - dynamic viscosity, 22–23
 - engineering design and analysis, 26–31
 - engineering design and environmental
 - impact, 30–31
 - Engineering Equation Solver, 2
 - equation of state, 9
 - estimation of liquid properties, 13–16
 - evaluation of thermodynamic properties,
 - 10–21
 - Fourier's law of conduction, 25
 - Gibbs equations, 10
 - Helmholtz energy, 10
 - ideal gas model, 16–21
 - important thermodynamic property
 - relationships, 9–10
 - incompressible substance model, 11–13
 - independent property pairs, 8
 - isochoric heat capacity, 9
 - kinematic viscosity, 23–24
 - Newtonian and non-Newtonian fluids, 24–25
 - optimum designs, 29–30
 - problems, 31–40
 - real fluid model, 10
 - REFPROP, 2–3
 - software, 2–3
 - Tds equations, 10

- thermal conductivity, 22, 25–26
- thermal energy system design and analysis, 1–2
- thermal energy system topics, 3–4
- thermodynamic properties, 7–10
- transport properties, 22–26
- two-phase region, thermodynamic properties in, 8–9
- units and unit systems, 4–6
- user-written libraries, 3
- workable designs, 27–28
- working fluids, properties of, 6–26
- Thermophysical properties, 459–525
 - calcium chloride–water solutions (IP units), 503
 - calcium chloride–water solutions (SI units), 502
 - dry air (IP units), 511–513
 - dry air (SI units), 508–510
 - ethanol–water solutions (IP units), 501
 - ethanol–water solutions (SI units), 500
 - ethylene glycol–water solutions (IP units), 495
 - ethylene glycol–water solutions (SI units), 494
 - liquids at saturation (IP units), 483–493
 - liquids at saturation (SI units), 472–482
 - magnesium chloride–water solutions (IP units), 505
 - magnesium chloride–water solutions (SI units), 504
 - metals (IP units), 525
 - metals (SI units), 524
 - methanol–water solutions (IP units), 499
 - methanol–water solutions (SI units), 498
 - propylene glycol–water solutions (IP units), 497
 - propylene glycol–water solutions (SI units), 496
 - saturated R134a (IP units), 516–517
 - saturated R134a (SI units), 514–515
 - saturated water (IP units), 462–463
 - saturated water (SI units), 460–461
 - single phase R134a (IP units), 521–523
 - single phase R134a (SI units), 518–520
 - single phase water (IP units), 468–471
 - single phase water (SI units), 464–467
 - sodium chloride–water solutions (IP units), 507
 - sodium chloride–water solutions (SI units), 506
- Thixotropic substance, 25
- Time value of money, 43–50
 - discrete interest factors, 50
 - equivalent uniform series that represents a future value (uniform series sinking fund factor), 48
 - equivalent uniform series that represents a present value (capital recovery factor), 49
 - examples, 51–55
 - future value of a present sum (Single Payment Compound Amount Factor), 44–45
 - future value of a uniform series (compound amount factor), 46–47
 - interest factor, 45
 - minimum acceptable rate of return, 44
 - present value of a future sum (present worth factor), 46
 - present value of a uniform linearly increasing series (gradient present worth factor), 49
 - present value of a uniform series (uniform series present worth factor), 48
 - simple interest, 44
- U
 - Uniform series present worth factor, 48
 - Uniform series sinking fund factor, 48
 - Units and unit systems, 4–6
 - Universal gas constant, 16
 - Useful energy, 117
 - User-written libraries, 3
 - U.S. Internal Revenue Service (IRS), 64
- V
 - Valves and fittings (fluid transport), 190–204
 - branch fittings (tees and wyes), 200–204
 - branching fittings, 190
 - check valves, 198–200
 - Darby 3K method, 195–198
 - deflecting fittings, 190
 - expanding fittings, 190
 - high resistance valves, 191
 - Hooper 2K method, 192–195
 - low resistance valves, 191
 - minor loss, 190
 - modified Bernoulli equation, 192
 - reducers and expansions, 198
 - reducing fittings, 190
 - resistance or loss coefficients, 192

W

Water horsepower (pumps), 228
Workable designs, 27–28
Working fluids, properties of, 6–26
 absolute viscosity, 22
 Bingham plastic, 25
 dilatant substance, 25
 dynamic viscosity, 22–23
 equation of state, 9
 estimation of liquid properties, 13–16
 evaluation of thermodynamic properties,
 10–21
 Fourier's law of conduction, 25
 Gibbs equations, 10
 Helmholtz energy, 10
 ideal gas model, 16–21
 important thermodynamic property
 relationships, 9–10
 incompressible substance model, 11–13
 independent property pairs, 8
 isobars, 7
 isochoric heat capacity, 9
 kinematic viscosity, 23–24
 molar quantities, 16
 Newtonian and non-Newtonian fluids,
 24–25
 Newton's law of viscosity, 22
 pseudoplastic substance, 25

 quality of the fluid, 8
 real fluid model, 10
 reference state, 11
 rheology, 25
 rheopectic substance, 25
 saturated liquid specific volume, 8
 saturated vapor specific volume, 8
 shearing stress, 22
 shear thickening fluids, classification of, 25
 shear-thinning fluids, classification of, 25
 Shomate equation, 19
 single phase points, 7
 state postulate, 7
 Tds equations, 10
 thermal conductivity, 22, 25–26
 thermodynamic properties, 7–10
 thixotropic substance, 25
 transport properties, 22–26
 two-phase region, thermodynamic
 properties in, 8–9
 universal gas constant, 16
 vapor pressure, 8

X

Xylem pump curves, *see* Pump curves